https://ntrs.nasa.gov/search.jsp?R=19720008127 2020-03-11T18:47:15+00:00Z

Space Shuttle Program

MSC-03328

CASE FILE COPY

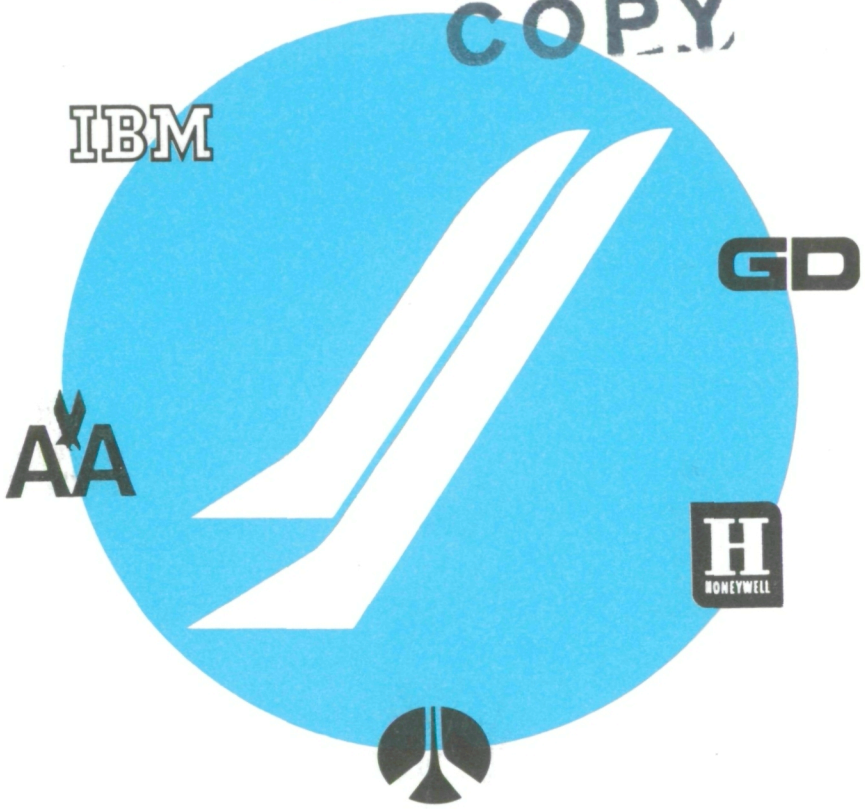

Phase B Extension TECHNICAL REPORT

Volume II

Contract NAS9-10960, Exhibit F
SD 71-342
12 November 1971

NOV 1971
RECEIVED
NASA STI FACILITY
INPUT BRANCH

Space Division • North American Rockwell 12214 Lakewood Boulevard, Downey, California 90241

SD 71-342
MSC-03328

SPACE SHUTTLE
PHASE B EXTENSION
TECHNICAL REPORT

Volume II

Approved by

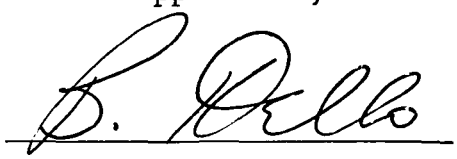

B. Hello
Vice President and Program Manager
Space Shuttle Program

Contract NAS9-10960
Exhibit F
12 November 1971

Space Division • North American Rockwell 12214 LAKEWOOD BOULEVARD • DOWNEY, CALIFORNIA 90241

Page intentionally left blank

FOREWORD

This report is submitted to NASA in accordance with contract NAS9-10960. The report documents the results of studies to define Space Shuttle programs that satisfy specific funding constraints and minimize technical risk. The studies were performed under the direction of the Space Division of North American Rockwell, Downey, California. Other members of the study team were Convair Aerospace Division of General Dynamics and Aerospace Division/Honeywell, Inc.

The report is provided in two volumes. Volume I presents the results of the effort accomplished during the months of July and August, 1971, when the following studies were made: external hydrogen tanks versus external hydrogen/oxygen tanks; variations on payload bay size; single engine orbiter impact; evaluation of various interim boosters and phased development programs; and low technology orbiter designs.

Volume II reports the results of the effort for September and October, 1971, during which the space shuttle systems were defined using a low technology orbiter combined with either an F-1 flyback booster or a pressure-fed booster.

Page intentionally left blank

CONTENTS

Page

VOLUME II

Page intentionally left blank

ILLUSTRATIONS

TABLES

4.0 PHASE B EXTENSION - PHASE 2 STUDY ACTIVITY

This section describes those analyses, trade studies, and system definitions performed between September 12 and October 31, 1971 constituting Part 2 of the Phase B extension.

During this part of the study, this contractor was directed to define Shuttle system programs encompassing the following concepts:

EOHT Orbiter		
Mark I	Mark II	Booster
J-2, J-2S, or HiPc engines	HiPc engines	1. Pressure fed, ocean recoverable (storable or LO_2/propane propellants) 2. LO_2-RP F-1 propulsion, flyback recovery

One booster and a block change orbiter (Mark I to Mark II) was to be examined in each program considered. The objectives of this part of the study were to:

1. Select orbiter main engines and development approach
2. Confirm the LO_2/LH_2 tank concept selection
3. Select either a LO_2/RP flyback booster or a pressure-fed booster for the program
4. Define the program approach

Sizing and optimizations based on cost and system capability were performed for all concepts. Program cost comparisons are reported herein and a recommendation for further design definition is made. Subsystem concepts, vehicle arrangements, and flight characteristics are reported for these recommended systems.

4.1 MISSION AND SYSTEM REQUIREMENTS

4.1.1 Program Approach

Figure 4-1 illustrates the program philosophy which was followed in establishing the vehicle system requirements and performance evaluations during the second part of the Phase B extension study. This approach was also considered in performing the various system cost trade studies reported herein.

Two categories of booster design were considered: (1) LO_2-RP propellant, F-1 engine main propulsion system (MPS), winged flyback recovery, and (2) a pressure-fed, ocean recoverable, refurbishable booster system.

The booster-orbiter combination for each concept was sized to meet the Mark II payload requirements, as well as the total system requirements described in the next section (4.1.2). This yielded an orbiter propellant tank of a given size. Inasmuch as it was planned to use only one tank design in the program, the tank structural requirements were established for the most stringent loads, whether Mark I or Mark II. The requirement for higher LO_2 tank pressure for the J-2 or J-2S engines compared to the HiPc engine required that the LO_2 tank be designed for the Mark I system.

The orbiter airframe requirements are also established by the most stringent of the Mark I and Mark II requirements. However, calculations indicate that there is negligible weight penalty involved irrespective of the requirements (i.e., Mark I versus Mark II).

The Mark I system, configured initially to the requirements in Section 4.1.2, is modified to the Mark II configuration through the addition of kits, updated thermal protection system (TPS), and the addition of HiPc engines.

4.1.2 Basic Requirements and Changes from Phase 1

Table 4-1 describes the basic ground rules for the Phase 2 segment of this study. The table is divided into a "requirements" section and a "subsystem baseline" section. The requirements reflect the program approach. Key issues to be noted in the requirements are as follows:

1. The Mark II payload and reference mission are unchanged. However, the Mark I payload and mission requirement is stipulated as 10K lb minimum payload to 100-nm orbit with 90-degree inclination. A desire for 25K lb payload to polar orbit has been stated. The maximum down payload for any mission would be 25K lb.

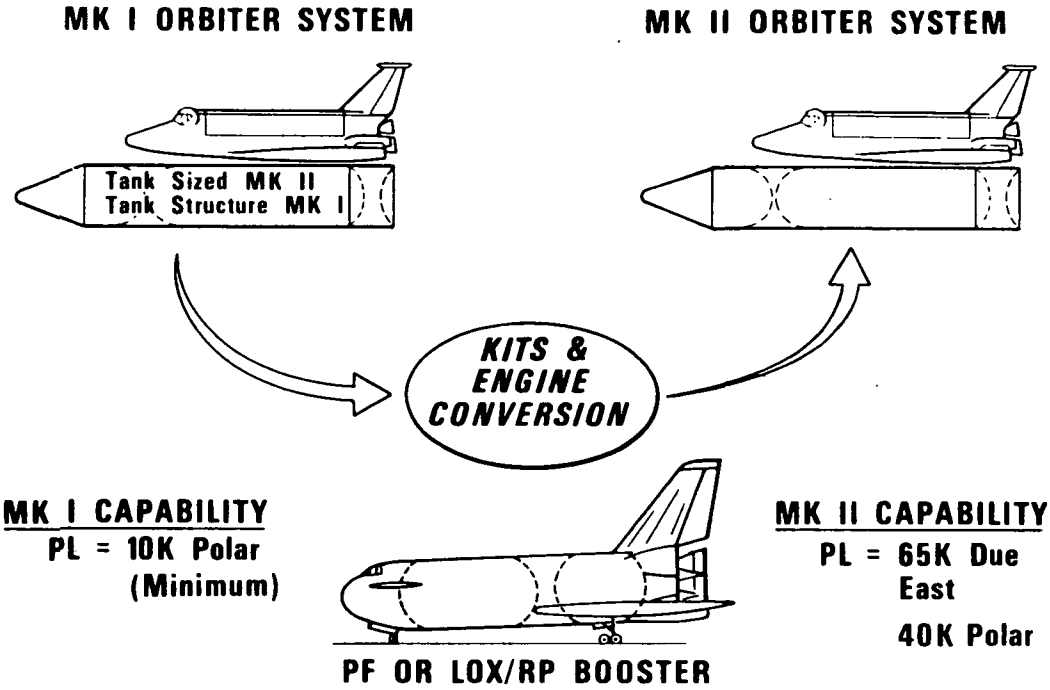

Figure 4-1. Mark I/II Vehicle Design Approach

Table 4-1. Ground Rules

Item	Mark I	Mark II
REQUIREMENTS		
PAYLOAD UP (LB)	10K LB POLAR MIN 25K DESIRED	40K LB POLAR 25K LB LOGS (WITH ABES) 65K LB DUE EAST
PAYLOAD DOWN (LB)	25K LB	40K LB
OMS ΔV LOADED (FPS)	900 DUE EAST 650 POLAR	650 POLAR 1500 LOGS 900 DUE EAST
OMS ΔV TANK SIZE (FPS)	1000 (SAME TANK AS MK II)	1000/FOR DUE EAST MISSION KIT TO 2000 FPS (IN CARGO BAY)
CARGO BAY	15 X 60 FT PAYLOAD ENVELOPE	15 X 60 (MOD IF DESIRED FOR WING CARRY THROUGH)
CROSS RANGE (N MI)	SAME AS MK II (AERO CAPABILITY)	RETURN TO LAUNCH SITE, SINGLE ORBIT, POLAR MISSION
ABORT	INTACT RECOVERY ON LAND	INTACT RECOVERY ON LAND
DESIGN TOUCHDOWN VELOCITY	150 KNOTS	PERFORMANCE TO BE COMPUTED
WEIGHT CONTINGENCY	10% ORBITER & BOOSTER 2% TANK	10% ORBITER & BOOSTER 2% TANK
STAGING VELOCITY (FPS)	6K ± 1K	6K ± 1K
MAX DYNAMIC PRESS (PSF)	650	650
MANIPULATORS	YES	YES
DOCKING CAPABILITY	YES	YES

Table 4-1. Ground Rules (Cont)

Item	Mark I	Mark II
ON-ORBIT MISSION ORIENTATION CONSTRAINTS	AS REQUIRED	NONE PERMITTED, EXCEPT RADIATOR LOOKING AT SUN
TURNAROUND	1 MONTH	2 WEEKS
REDUNDANCY	SUBSYSTEMS - FS CRIT SUBSYS - FO/FS	
BOOSTER IMPACT	NO P.F.B. LAND IMPACT PERMITTED	
SUBSYSTEM BASELINE		
OMS ENGINE	PODS 2 X LEMAE (RETRO FIT WITH 2 X REGEN COOLED)	2 X REGEN COOLED (USE TRANSTAGE FOR SIZING)
MAIN PROPULSION	4 X J-2S F_{VAC} = 265K LB ϵ = 40:1	4 X HiPc (F = 265K) ϵ = 90:1 FIXED NOZZLE
MPS FEED	SIZE LINE FOR MK I	USE MK I FEED LINE
ABES	B-1 ENGS (2) - PROVISIONS IN CARGO BAY - GO AROUND ALL ENGINES OPERATING	B-1 ENGS - PROVISIONS IN CARGO BAY - GO AROUND ALL ENGINES OPERATING
STRUCTURE	ALUM (STRESS TO MK I REQMTS & MAX PAYLOAD)	ALUM (LOCAL BEEF-UP FROM MK I)
WING SIZE	150 KNOTS TOUCH DOWN	USE MK I WING - REDUCE SINK SPEED
TANK	SIZE TANK FOR MK II - STRESS FOR MK I MPS HEAVY WALL MONOCOQUE	SAME AS MK I
ACPS	HYPERGOLIC - COMMON HDWE WITH MK II	HYPERGOLIC - SIZE FOR MK II MISSIONS
APU	MONOPROPELLANT - COMMON HDWE WITH MK II	MONOPROPELLANT
HYDRAULIC POWER	3000 PSI - COMMON HDWE WITH MK II	3000 PSI
AVIONICS	ORBITER AVIONICS PROVIDES BOOST GUIDANCE & CONTROL - AIRCRAFT AVIONICS FOR FLT TEST/SPACECRAFT AVIONICS FOR ORBITAL MISSIONS	ORBITER AVIONICS PROVIDES BOOST GUIDANCE & CONTROL-AIRCRAFT AVIONICS FOR FLT TEST/SPACECRAFT AVIONICS FOR ORBITAL MISSIONS
TPS TYPE	ABLATOR - 350 F BACKFACE/ NOM TRAJ (MARTIN) 200 N MI & 1100 N MI X-RANGE	RSI/NOM TRAJ - 1100 N MI X-RANGE
BOOSTER	BASELINES: REUSABLE LOX/RP HEAT SINK, 5XF-1 ENGINES, PRESS FED LOX/PROPANE, STORABLE	REUSABLE LOX/RP HEAT SINK, 5XF-1 ENGINES
INTEGRATED VEH CONFIG	TANDEM, OPPOSING ORBITER/ BOOSTER VERTICALS	TANDEM, OPPOSING ORBITER/ BOOSTER VERTICALS
BOOSTER/ORBITER INTERFACE	INTERSTAGE WITH UNIFORM DISTRIBUTED LOAD	INTERSTAGE WITH UNIFORM DISTRIBUTED LOAD
BOOSTER/ORBITER SEPARATION	DUAL PLANE-INTERSTAGE REMAINS WITH ORBITER TANK & IS SUBSEQUENTLY DROPPED	DUAL PLANE - INTERSTAGE REMAINS WITH ORBITER TANK & IS SUBSEQUENTLY DROPPED

2. The OMS ΔV requirement for Mark I is assumed to be the same as for Mark II polar or due east missions. However, the tank sizing has been modified from previous ground rules. Specifically, in both Mark I and Mark II, the tank will be sized to provide 1000 fps ΔV for the heaviest vehicle system (i.e., vehicle plus maximum payload). Where velocity capability in excess of 1000 fps is required, a tank kit will be utilized to provide the additional propellants.

3. The orbiter configuration will incorporate aerodynamic capability for return to launch site from a polar mission. The Mark II vehicle will incorporate thermal protection to provide structural capability during such a maneuver. Data will be prepared for the Mark I system to reflect payload capability with a TPS adequate for a low cross range (200 nm) entry and also for the high cross range maneuver. The abort requirement will be modified from "once-around" to intact recovery on a land mass.

4. The vehicle wing size will be based on a Mark I vehicle with maximum down payload (25K lb) and 200 nm cross range TPS to achieve a tail scrape angle tounchdown velocity of 150 knots. The Mark II touchdown velocity resulting from this approach will be accepted. It is estimated that this velocity will be between 160 and 170 knots.

5. A dry weight contingency of ten percent will be carried on the orbiter and booster exclusive of GFE (e.g., main engines and air breathing engines). However, the orbiter tank contingency will be two percent. This value is justified by inspection of the basic HO tank design concept, namely, a simple heavy wall monocoque LH_2 tank in tandem with a lighter weight monocoque LO_2 tank, where the LH_2 tank carries the boost loads into the orbiter. The ability of the analysts to predict the weight of this type of structure is mature enough to justify the low contingency.

6. By NASA direction, the staging velocity is limited to 6000 $\pm$ 1000 fps. Maximum dynamic pressure is limited to 650 fps.

7. Docking capability is required in both Mark I and Mark II vehicles.

In general, the subsystem baseline is the same as that recommended as a low technology system at the completion of Phase 1 except for the following items.

1. The OMS engine system will be pod mounted for improved maintainability. Storable propellants will be utilized. LEMA engines will be used in Mark I, with a new engine to be developed for Mark II.

2. Four J-2S engines are baselined for Mark I with four HiPc engines of equal thrust for Mark II. The HiPc engines will be of fixed expansion ratio equal to 90:1.

3. The MPS feed lines will be larger in diameter for the J-2S engines than for the HiPc engines. Therefore, these larger lines will be incorporated into the design and retained in Mark II.

4. By direction, two air breathing engines (designated GE F101) will be utilized in the ABES system to be stored in the cargo bay when required for specific missions.

5. The orbiter vehicle structure will be all aluminum for the baseline. However, trade studies to determine an optimum blend of aluminum and other material will be conducted.

6. The HO tank will be sized for the Mark II requirements. However, the tank structure will reflect the pressurization requirements imposed by the J-2 or J-2S engines used in Mark I.

7. The ACPS system will be hypergolic and pod mounted, sized for Mark II requirements.

8. The APU will be monopropellant.

9. The hydraulic system will operate at 3000 psi (compared to 4000 psi in Phase 1).

10. The general approach to the avionics design will separate spacecraft and aircraft functions. The aircraft functions only will be required for horizontal flight test.

11. The Mark I TPS system will feature ablative insulation. Mark II will feature an RSI type of system. In each case, the back face temperature will be limited to 350 F. Nominal entry trajectories will be the basis for determining insulation requirements:

    The baseline orbiter-booster position will feature opposing verticals to minimize the rolling moment due to yaw angle, and to ensure that the orbiter plume impinges on the booster belly. The interface between the booster and orbiter will be through an interstage between the booster nose and the HO tank aft skirt. A double plane separation will be baselined.

4.1.3 Requirements and Capability Analysis

4.1.3.1 Mission Payload, Inclination, and Altitude Requirements versus Capabilities

The flight rates for the shuttle through 1990 are defined in Technical Directive NR-4[1] and presented here in Table 4-2. This model, intended as a ground rule for schedule and cost analyses, does not specify the missions in terms of shuttle payload, inclination, and altitude. One question to be answered in this section is, are there meaningful missions and payloads desired in the U.S. Space Program that the reduced-capability Mark I can fly at the rates of the model?

The Fleming Model[2,3] was judged to be the best expression of the desires of the U.S. Space Program in the operational time period of the shuttle. The flight rates of this model over the years is shown in Table 4-3. They are greater than the flight rates of Table 4-2 and, hence, may provide the meaningful missions for the Mark I shuttle if the Mark I can fly enough of them.

The lack of complete data on DOD missions is noted on Table 4-3. Some assumptions were made relative to the DOD missions in order to use them in the analysis that follows.

1. All DOD missions at 28.5°/30° inclination in the April 1971 Fleming Model include a propulsive stage as part of the shuttle payload. Therefore, a shuttle altitude of 100 by 100 nm could logically be assumed.

2. Of the 93 DOD missions at 90° inclination, 21 missions identify propulsive stages in their payloads and justify an assumption of a shuttle altitude of 100 by 100 nm. Fifty-six missions have a payload of 28 K lb, which could easily include an integral propulsive capability. These were assumed to have a shuttle altitude of 100 by 100 nm. The remaining 16 missions were assumed at 100 by 100 nm for lack of any other data.

---

[1] Study Schedule Ground Rules and Program Mission Model, Technical Directive Number NR-4 (September 24, 1971).

[2] Fleming Model (April 1971) informally published.

[3] NASA/DOD Earth Orbit Shuttle Traffic Models based on End-to-End Loading of Payloads, MSC Internal Note No. 71-FM-259 (MSC-04491) (July 8, 1971).

Table 4-2. TD NR-4 Traffic Model[1]

	Calendar Years														
	78	79	80	81	82	83	84	85	86	87	88	89	90	91	Totals
Concurrent Total[2]	2	12	15	15	22	30	42	60	60	60	60	60	7		445
USAF	-	--	--	--	--	--	6	18	20	20	20	20	3		107
NASA Total	2	12	15	15	22	30	36	42	40	40	40	40	4		338
Mark I	2	12	15	15	22	25	20	12	--	--	--	--	-		123
Mark II	-	--	--	--	--	5	16	30	40	40	40	40	4		215
Phased Total	1	3	3	3	3	6	42	60	60	60	60	60	60	39	460
USAF	-	--	--	--	--	--	6	18	20	20	20	20	20	14	138
NASA Total	1	3	3	3	3	6	36	42	40	40	40	40	40	25	322
Mark I	1	3	3	3	3	4	20	12	--	--	--	--	--	--	49
Mark II	-	--	--	--	--	2	16	30	40	40	40	40	40	25	273

[1] No payload, inclination, and altitude data were provided.

[2] Both systems of current study would be concurrent programs.

Table 4-3. Fleming Model[1]

	Calendar Years														
	78	79	80	81	82	83	84	85	86	87	88	89	90	91	Totals
NASA (MSC Internal Note No. 71-FM-259)	(3)[2]	6 (4)	21	34	31	30	33	50	46	46	44	48	41		437
DOD[3] (Fleming Model, April 1971)	(1)	2 (2)	12	16	28	27	22	25	29	29	27	25	30		275
Total	4	14	33	50	59	57	55	75	75	75	71	73	71		712

[1] Based on evolution of Space Program requirements

Tug available in 1985 (earth-based)
Modular Space Station emplacement in 1981
Other payloads include satellites, propulsive stages with payloads, and research application modules
DOD missions

Used NR Phase B shuttle capability

[2] First 10 missions are not defined in model.

[3] DOD mission data is incomplete; No shuttle altitudes given through 1987 and no payload, inclination, or altitude data given for last 3 years (classified).

The mission model (in the reference cited in footnote 3) which is characterized by tug availability in 1985 and end-to-end loading of payloads on the tug was used to generate the NASA missions data in this section. This model is a modification of the informally distributed Fleming Model. The Fleming Model is the direct basis of the DOD mission data in this section.

The choice of tug availability in 1985 rather than 1979 (both were considered in the reference cited in footnote 3) was felt to be more consistent with the desire to keep annual funding down during the Shuttle development program. End-to-end loading of tug payloads rather than side-by-side loading as considered in a companion report to the reference cited in footnote 3 was chosen because it simplifies the operations of the tug. It keeps the cg of the tug with its payloads always near the longitudinal axis, whether it is maneuvering with 3, 2, or 1 payload attached in its phasing maneuvers to emplace its payloads. It always has its full, effective gimbaling available for use as necessary.

Figure 4-2 shows a distribution of the NASA missions by Shuttle orbit inclination. The 80 percent of NASA missions launchable from KSC allow for the impact of ballistic type boosters in the ocean. The remaining 20 percent can be launched from WTR with a ballistic type booster. A manned reusable booster with expendable LH_2 and LO_2 tanks might also be judged to be constrained to over-water launches due to the need to dispose of its LH_2 and LO_2 tanks during an intact ascent abort.

Also shown in Figure 4-2 is a distribution of the NASA flights by altitude. Associated with each altitude bar is an OMS ΔV budget. These OMS ΔV budgets for the several altitudes are based upon the theoretical value plus 25 percent. Deorbit from the mission altitude is considered to be direct. All OMS propellants aboard are considered to be available for deorbit; i.e., no failure of an OMS tank or plumbing can deny use of OMS propellant for deorbit. No allowance of OMS propellants is made for down-phasing maneuvers to bring the ground track for a once-a-day landing opportunity to within the cross-range of the orbiter. In other words, it is assumed that the orbiter's cross-range will permit the needed landing opportunities without expenditure of OMS ΔV.

Figure 4-2 shows that two thirds of the flights can be flown with the 1000 fps ΔV capability of the integral OMS tanks. Another 25 percent can be flown with a kit in the cargo bay to provide for 380 fps of ΔV, leaving only 11 percent requiring still additional ΔV to total 1880 fps. A 1000-fps ΔV kit size has been identified to satisfy the additional ΔV needs. From the available, unclassified DOD mission data, Figure 4-3 was developed to show a distribution with inclination. It indicates the need for WTR launches for 60 percent of the missions if over-water launch trajectories are required for the chosen shuttle configuration.

a) DISTRIBUTION BY INCLINATION

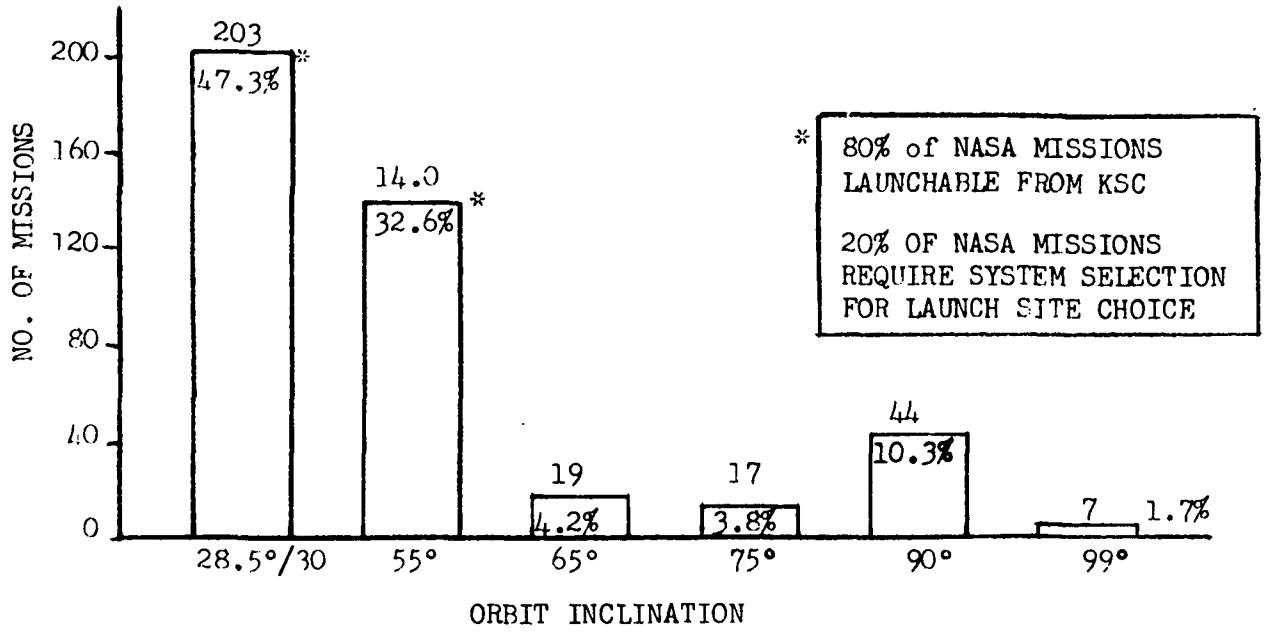

b) DISTRIBUTION BY ALTITUDE

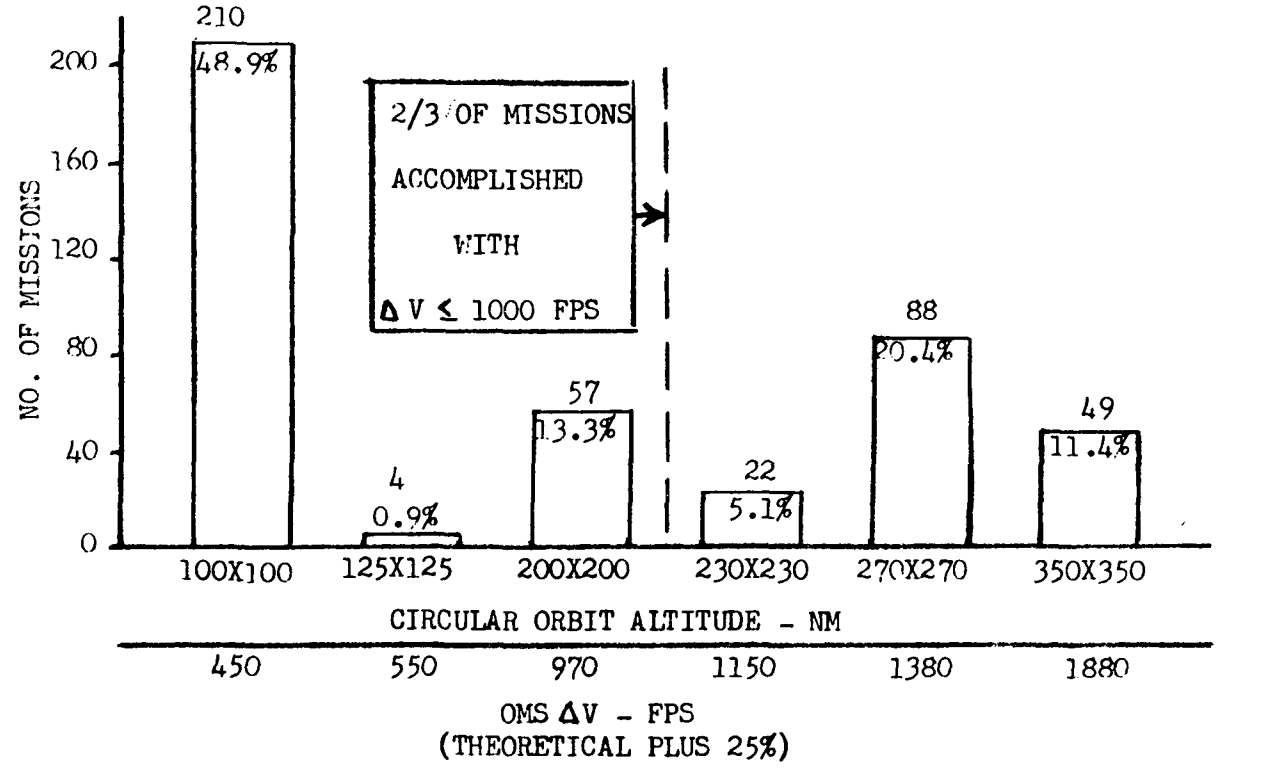

Note: MSC Internal Note 71-FM-259, 8 July 1971 (Tug available 1985), 1978 through 1990

Figure 4-2. NASA Shuttle Flights

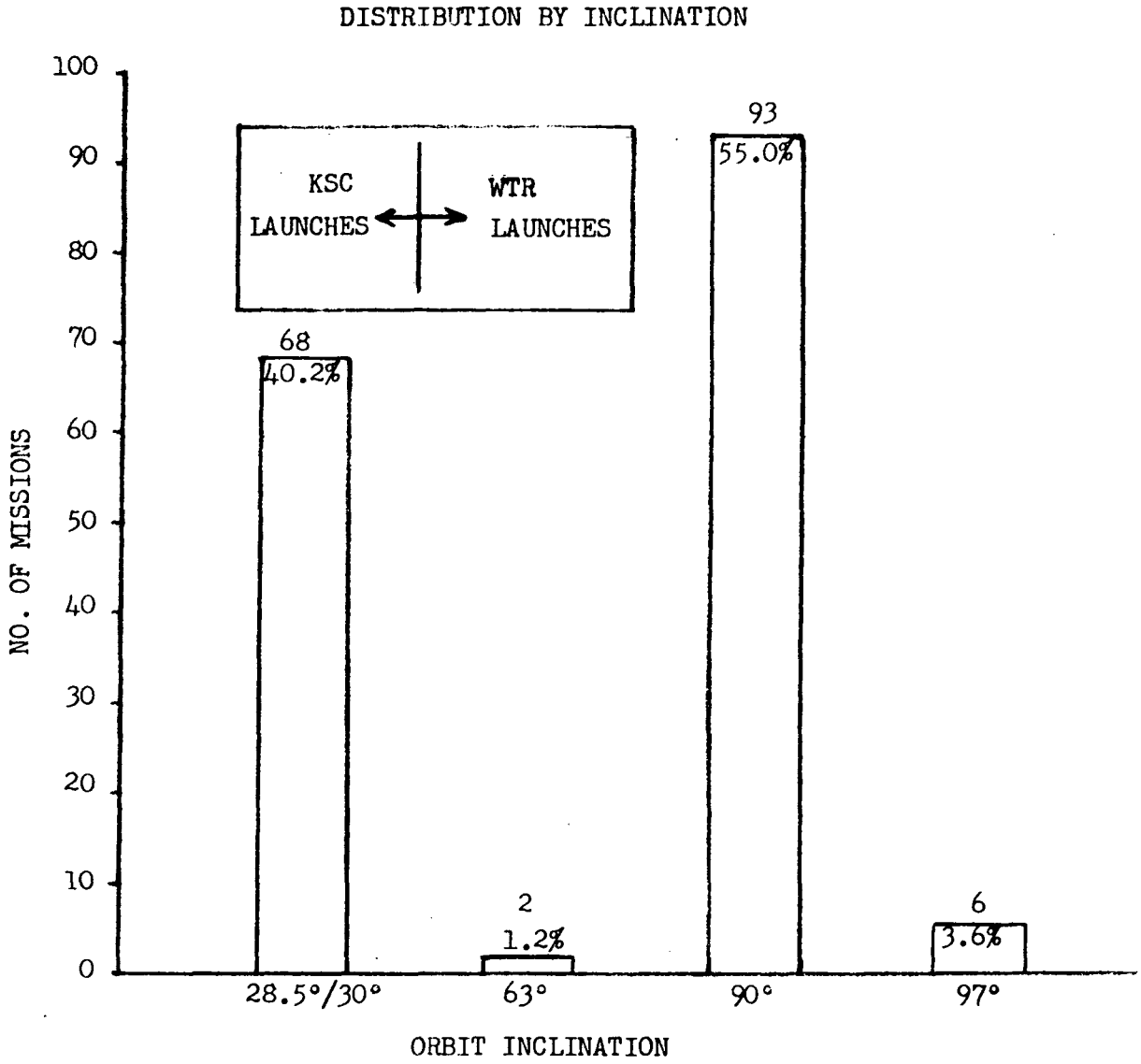

Figure 4-3. DOD Shuttle Flights

From Figures 4-2 and 4-3, it is seen that more than 90 percent of NASA and DOD missions are flown at three inclinations, 28.5/30 degrees, 55 degrees, and 90 degrees. To determine the capability of Mark I and Mark II to fly these missions, the payload vs altitude requirements at these inclinations are mapped so that the payload versus altitude capability curves of the shuttle can be superimposed on them. This provides an immediate identification of missions within and beyond the current shuttle capabilities.

Figure 4-4 is provided to explain the several superimposed curves and minimize notes on the payload versus altitude.

Figures 4-5, 4-6, and 4-7 show these mission requirements versus shuttle capability for the due east, 55 degree inclination, and polar missions, respectively.

Table 4-4 summarizes the capabilities by showing the missions that can be flown. Since the Fleming Model was tailored to the Phase B shuttle capability, it would be expected that the Mark II orbiters would show only a slight, if any, deficiency. That very slight deficiency shown is due to the different sizing ground rules of the Phase B extension study. Only about seven percent of the total missions, NASA and DOD, cannot be flown by the Mark I orbiter. It is of special interest to note that the Mark I without ABES could fly the Space Station assembly and support missions (20K lb to 270 by 270 nm at 55 degree inclination) were they to occur prior to the availability of Mark II orbiters in sufficient numbers.

Based on the data presented, it is quite apparent that the Mark I shuttle will be able to fly meaningful missions and payloads for the U.S. Space Program throughout its life in the inventory.

Important aspects of the requirements versus capability comparison which are not evaluated here include:

1. The installation of the 1000 fps OMS kit in the cargo bay as planned would decrease the usable volume of the cargo bay. Thus, missions requiring more than 1000 fps (above approximately 200 nm) should be reviewed for size compatibility with this reduced cargo bay size.

2. For any missions judged to require the ABES, the size compatibility of their payloads with the cargo bay as effectively reduced by the presence of the ABES should be checked. For example, if Space Station crew exchange missions require ABES, the cargo bay would be reduced by inclusion of ABES and the OMS ΔV kit.

CURVES

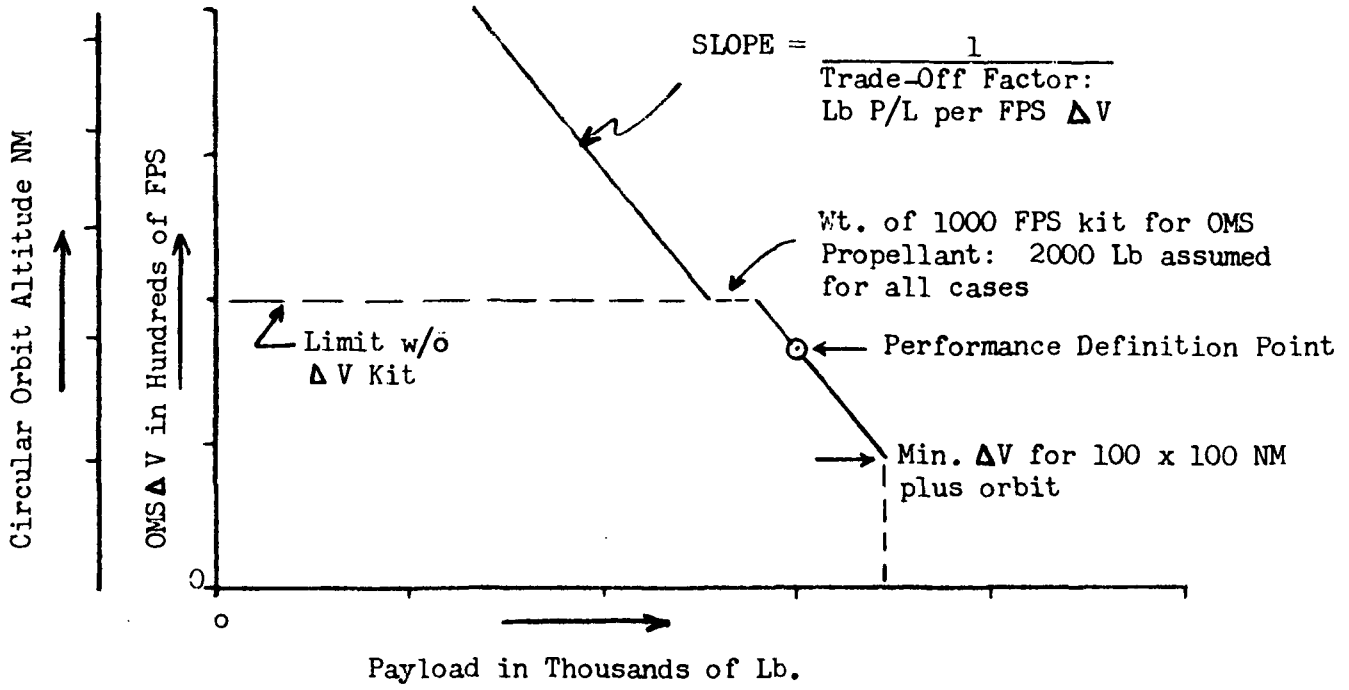

All curves are without ABES. "W/ABES" curves would be to left by amount of Wt. of ABES with fuel as needed for mission.

OMS ΔV = Theoretical plus 25%

Performance Definition Points:

⊙ - Manned Reusable Booster

⊗ - Unmanned Pressure-Fed Booster

TRADE-OFF FACTORS - LB/FPS
MANNED REUSABLE BOOSTER

SHUTTLE SYSTEM	28.5°/30° ORBIT	55° ORBIT	90° ORBIT
Mark I	17.6	16.1	15.1
Mark II	20.1	18.3	17.1

Figure 4-4. Legend for ΔV Versus Payload Tradeoff

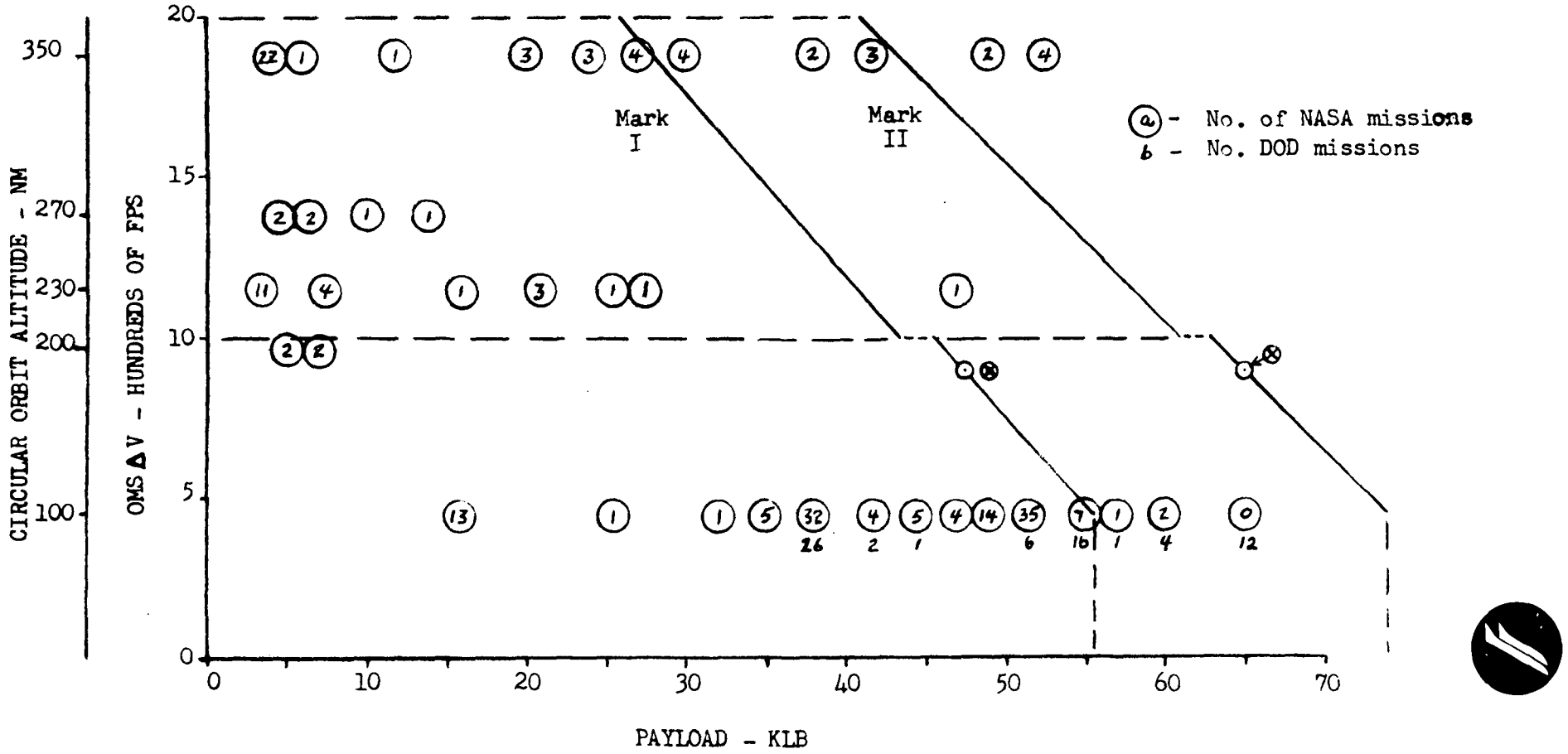

Figure 4-5. Due East Missions

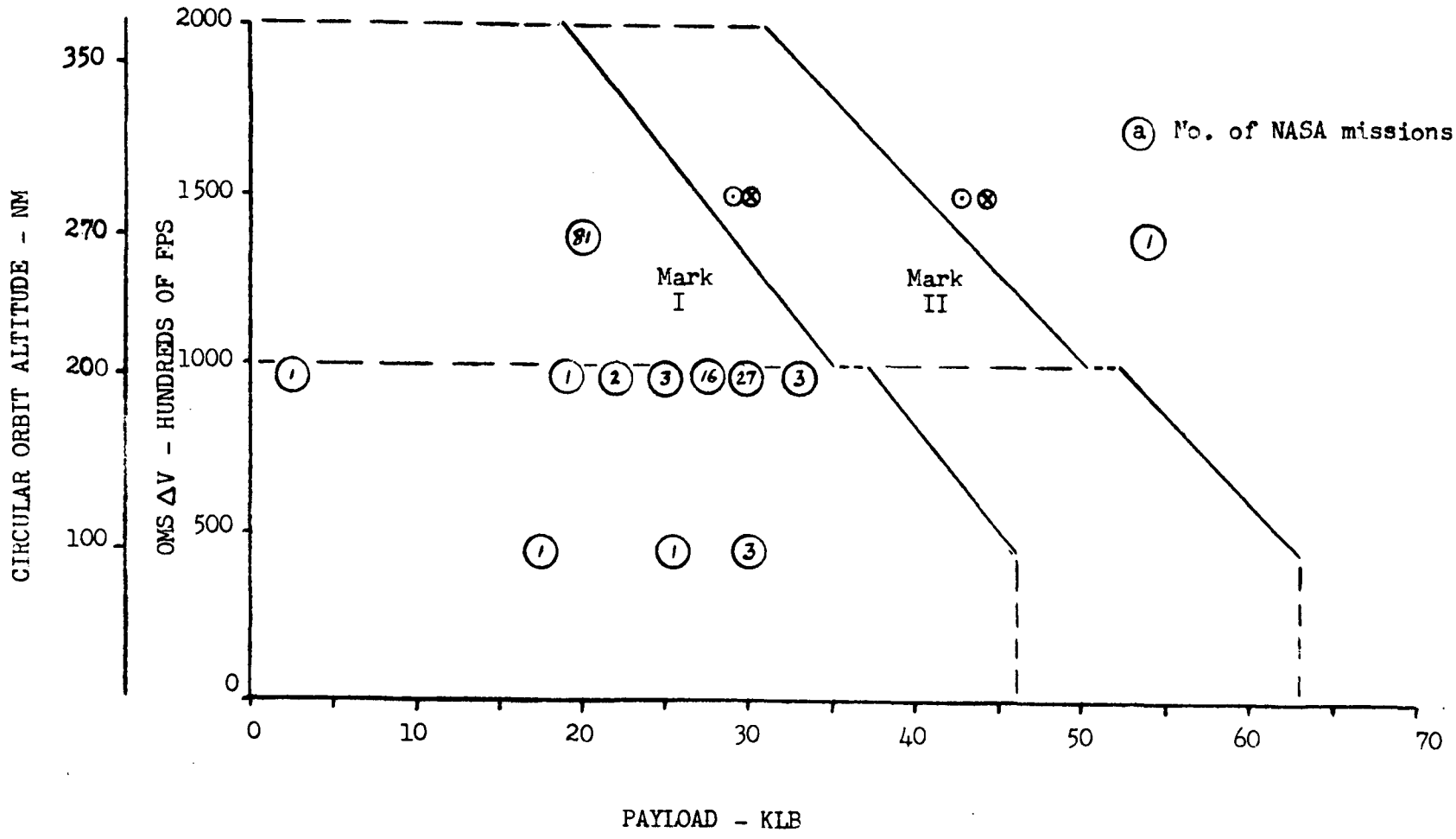

Figure 4-6. 55-Degree Inclination Missions

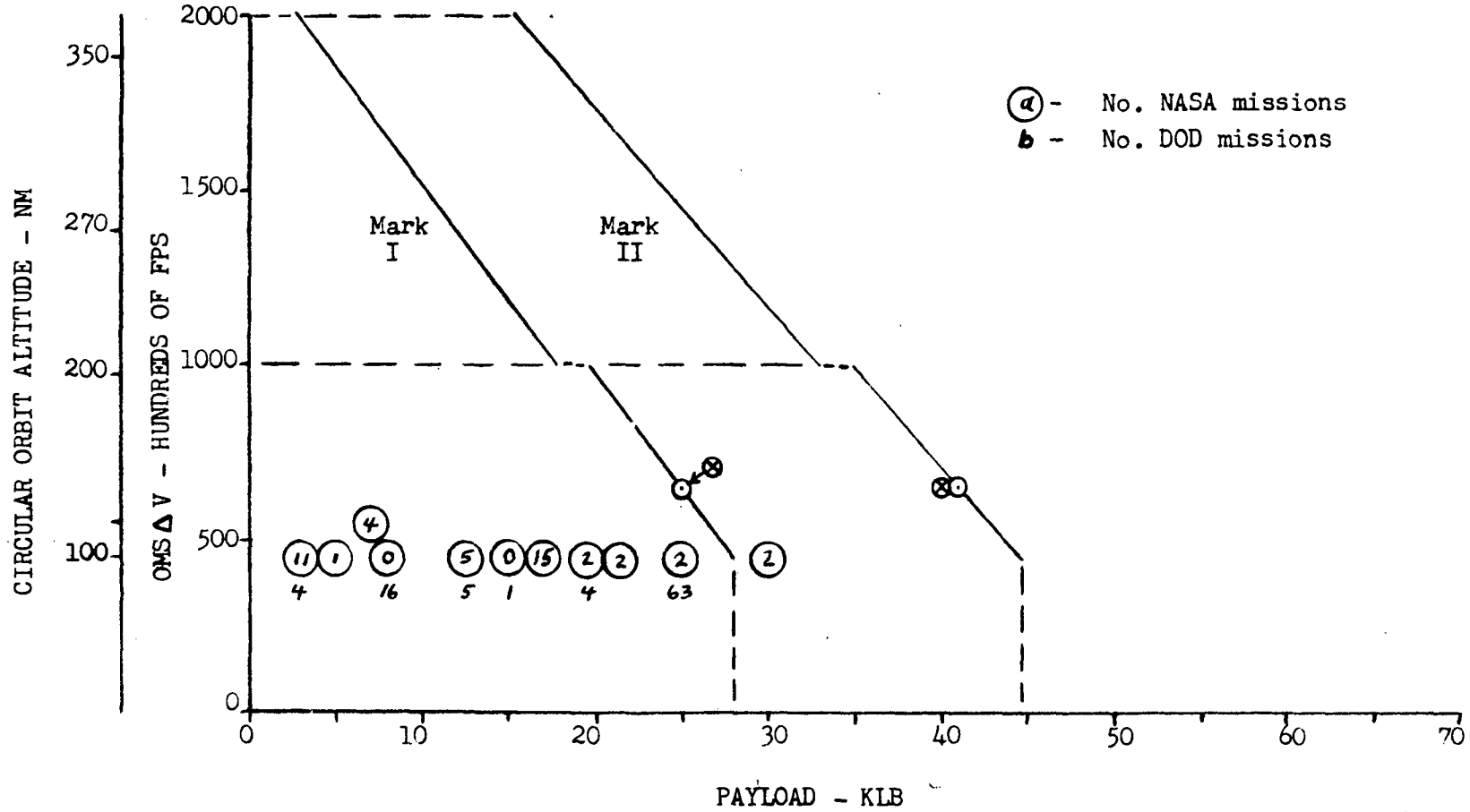

Figure 4-7. Polar Missions

Table 4-4. Capability Summary

	Due East Missions	55-Degree Inclination Missions	Polar Missions	All Incl Missions
Number of Missions	273	140	137	550
Mark I - No ABES				
Number of missions within capability	237	139	135	511
Percent of missions within capability	87%	99+%	98+%	93%
Mark II - No ABES				
Number of missions within capability	267	139	137	543
Percent of missions within capability	98%	99+%	100%	98+%
OMS kit used as required.				
OMS kit required on 152 missions (28%).				
Mark I flies 97+% of NASA missions prior to Mark II availability (1983).				

3. Those missions that cannot be flown by Mark I prior to the availability of Mark II and those thereafter that cannot be flown by Mark II should be looked at critically in regard to (a) their importance in the Space Program, (b) their possible redesign to come within capability, and (c) the feasibility of accomplishing them by two shuttle flights if warranted.

4.1.3.2 Orbiter Docking Requirements

To conduct an effective program involving the shuttle, space station, research application module (RAM), and large unmanned satellites during the 1978-1985 period, a docking system on the Mark I orbiter will be required. This capability will allow the effective transfer of personnel and cargo from one vehicle to another and provide for the servicing and maintenance of orbiting vehicles and satellites. As an additional benefit, the docking system will allow the docking of the orbiter with the U.S.S.R. orbital vehicles.

Use of the space station is predicted upon the assembly and the resultant logistic support provided by the orbiter. A docking port is required by the orbiter to conduct personnel and cargo transfer. With a space station IOC date of 1982[1], the Mark I orbiter will require a docking capability by this date.

To increase the operational effectiveness of the orbiter conducting near-earth observations and scientific experimentation, an attached RAM will be utilized. This module will be removed from the cargo bay and attached to the outside of the orbiter to provide unobstructed operation of its sensors. To provide a stable base of attachment and allow easy access to the module by the orbiter crew, a docking port is required. With a RAM IOC date of 1979[2], a Mark I docking port is needed to support this mission.

One of the principal functions of the orbiter is to service and maintain near-earth orbital satellites. This function will accomplish an extended useful satellite life through the conductance of repair and refurbishment. For the larger satellites, the satellite servicing and maintenance function can be best accomplished by the orbiter crew having direct access to the interior of the satellite. This will minimize the hazards to the crew and maximize the accessibility of the internal parts of the satellite for repair. To accomplish the transfer of the crewman to the satellite a docking port will be required on the orbiter. Large satellites will be introduced into use in 1978 when the Large Space Telescope satellite is placed in orbit. The servicing of this satellite at six-month intervals has been assigned to the orbiter beginning with its sixth mission (1979) as specified by NASA ("First Ten Payload Candidate Missions," NASA Headquarters, dated 18 August 1971).

During the initial phases of the Shuttle Program (1978-1982), when the probability of failure occurring on-orbit is greatest, it is desirable for the second orbiter to have the capability to rendezvous and dock with the stranded orbiter. This should not necessarily be looked upon as a crew rescue capability, but one of investigation and retrieval after the fact. The crew rescue requirement cannot be established since the orbiters available (two) the scheduled mission frequency (up to 22 per year) the turnaround time (one month) and the permanent on-orbit delta-V capability (1000 fps) are incompatible with timely crew rescue.

---

[1]Modular Space Station, Systems Requirement Book, SD 71-205 (1971).

[2]Preliminary Technical Data Document Vol. 1, GDC DE-268 (August 28, 1971).
Section 4.1, Requirements Analysis and Definition Appendix X, Derived System Requirements.

There is a concerted effort by the United States and USSR[1] to manufacture and utilize compatible space systems to facilitate the conducting of integrated near-earth space operations between Salyut and Apollo and to provide for international space rescue. To effectively accomplish these goals, a standardized docking system is being developed to be installed on all orbiting vehicles. During the time period of interest, based upon all indications, the USSR will be active in a number of manned near earth orbit programs. If it is desirous to participate in or support these programs and to facilitate the accomplishment of the impending international agreements, a docking system should be installed on the Mark I orbiter.

4.1.3.3 Manipulator Requirements

In order to generate requirements for payload deployment and retrieval for Generation I vehicles, a mission model for the first twelve flights was assembled (Table 4-5). These missions were based on the expressions of the customer on the first ten flights[2,3] plus 2 initial flights for systems testing.

The overall objectives for the twelve flights are to accomplish the flight test of the shuttle system and to demonstrate, as completely as possible, the on-orbit operational task capabilities of the system. To determine the particular requirements noted above, only the on-orbit tasks need be considered here.

Table 4-5 shows the weights and volumes for all the payloads. Table 4-6 presents the flight program of on-orbit operational task demonstrations derived from the missions in Table 4-5. From the table it can be seen that this model requires an orbiter with manipulators (or any other payload-handling device that will accomplish retrieval of large payloads such as the returning OOS). This program accomplishes all of the capability demonstrations envisioned in the customer's program[2,3]. The progression of capabilities achieved is shown in Figure 4-8 and Table 4-6.

If a manipulator arm was not available, the effects of not having retrieval capability would be felt in flights 3, 4, 6, 9, and 10. Flight 3 could not deploy the passive Meteoroid and Exposure Model because Flight 4 cannot retrieve it. Both flights 3 and 4 deploy and retrieve (on the same flight) the 128-lb contamination monitoring module by EVA. Flight 6 could not retrieve the OAO-1 (Orbital Astronomical Observatory) of the desired

---

[1] International Rendezvous and Docking Mission Study, CCA 4162 500-300 (July 29, 1971).

[2] First Ten Shuttle Missions, Memorandum for the Record from R. H. Lindley, OMSF, NASA Hdqtrs (September 4, 1970).

[3] Typical Shuttle Mission Profiles and Attitude Timelines, Vol. III, First Ten Missions, MSC Internal Note No. 70-FM-104 (December 11, 1970).

Table 4-5. Payload Characteristics

Flight Number	Mission Duration (Days)	Orbital Parameters	Payload	
			Wt (lb) / Vol (cu ft)	Description
1	TBD	100 x 100 nm 28.5° incl	5,000 / NA	Development flight instrumentation
2	TBD	100 x 100 nm 28.5° incl	5,000 / NA	Development flight for shuttle
3	5	256 x 256 nm 28.5° incl	8,720 / 3,872	Development flt instrumentation, EVA equipment, meteoroid and exposure module, contam monitoring module
4	6	245 x 245 nm 28.5° incl	17,500 / 5,590	DFI, EVA equipment, materials sample collection box, RAM, contam monitoring module, satellites: SATS-F, SATS-G, SESP-1001 (DOD)
5	7	199 x 196 nm (launch SATS) 208 x 207 nm (rendezvous w/Skylab A) 50° incl	14,600 / 4,181	DFI, EVA equipment, sample return box, manned support module, satellites: SAS-E, EPS-C, SATS-H
6	4	420 x 420 nm (plumb in OMS props) 35° incl	9,430 / 580	DFI, Container for OAO-1, satellite to be retrieved
7	4	256 x 256 nm 28.5° incl	30,950 / 2,390	DFI, satellites: HEAQ, SESP-1000 (DOD)
8	4	132 x 132 nm 28.5° incl	43,860 / 1,110	DFI, Agena w/ATS-H satellite Agena w/earth resources sat.
9 (DOD)	7	115 x 115 nm 28.5° incl	49,360(1) / 9,000(2)	DFI, OOS w/Mission "T" Experiment
10 (DOD)	5	125 x 125 nm 30° incl	48,460(1) / 6,500	DFI, OOS w/payload "P"
11	7	118 x 118 nm 55° incl	19,060 / 5,000	DFI, RAM, seven sets of exp equipment non-astronaut personnel, TBD
12	3	200 x 200 nm 28.5° incl	36,310 / 7,700(2)	Cosmic Ray Module No. 1 Cosmic Ray Module No. 2

(1) Low OMS ΔV propellants budget allows excess of 45K payload.

(2) Exceeds 15 by 60 feet; volume of 7018 cubic feet.

program. Flights 9 and 10 would require substitute missions for the DOD OOS (Orbit-to-Orbit Shuttle) missions.

It may thus be concluded that there is an early (Generation I) requirement for a set of manipulator arms (or the equivalent).

Table 4-6. Initial Shuttle Missions

Full Capability Orbiter
(15 FT X 60 FT Cargo Bay; Manipulators Installed)

ON-ORBIT TASKS	1978	1979			1980			1981			1982	
	FLIGHT NO.											
	1	2	3	4	5	6	7	8	9	10	11	12
C/O & OPERATE MANIPULATORS	SOLELY FLT TEST	SOLELY FLT TEST	X	X	X	X	X	X	X	X		X
EVA			X	X	X							
DEPLOY & RETRIEVE PASSIVE MODULES			X	X								
C/O & DEPLOY SATELLITES				X	X		X	X	X	X		X
RENDEZVOUS				X	X	X			X	X		
C/O & OPERATE PAYLOAD MODULES				X	X						X	
RETRIEVE SATELLITES						X						
C/O & DEPLOY PROPULSIVE STAGES								X				
C/O & DEPLOY TUG									X	X		
RETRIEVE TUG									X	X		
SUPPORT NON-ASTRONAUT PERSONNEL											X	
ONBOARD SCIENTIFIC EXPERIMENTS											X	

← SCIENTIFIC MISSIONS BASED ON MSC REPT 70 FM195 →

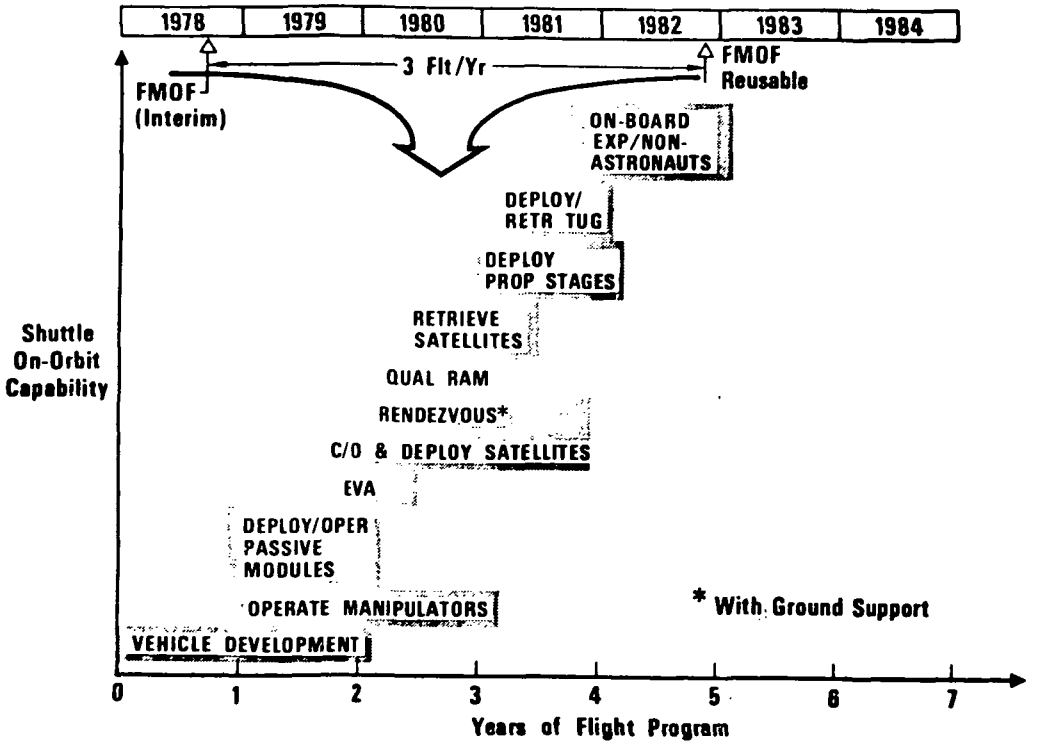

Figure 4-8. Phased Development of On-Orbit Capabilities

4.1.4 Proposed Mission Timeline for ACPS Sizing

A due-east mission was timelined as shown in Table 4-7 for the purpose of generating ACPS propellant budget requirements. Table 4-8 is a brief mission profile with a summary of on-orbit ACPS and OMS fuel allocation as they are distributed throughout this mission. The rules applied in developing the timeline is shown below. The selection of the due-east mission is based on the following rationale.

1. Approximately 60 percent of the missions of the TD 2533 traffic model are due-east launches.

2. Mission involves a deployment of a payload into earth orbit, representative of the on-orbit operations required for placement of satellites, propulsive units with their satellite payloads, and tugs (OOS's). These placements are 77 percent of the shuttle payloads (TD 2533).

3. Mission involves a rendezvous as do the missions for Space Station support, tug (or OOS) retrieval, satellite retrieval, and service or maintenance of satellites or free-flying RAM's.

4. Mission involves waiting-in-orbit which characterizes all tug (or OOS) missions and is comparable to the station-keeping function in space station support missions.

5. Mission involves retrieval, a capability necessary to on-orbit service; maintenance; life extension; and return-to-earth of expensive satellites. Retrieval in these aspects is considered one of the keys of shuttle cost effectiveness over the long haul.

6. Mission does not involve a long period of tight attitude deadband operations, characterizing the sortie type, sensor-pointing missions. These operations, however, are not likely to exceed 10 to 15 percent of the shuttle missions. Furthermore, tight deadband requirements upon the orbiter has not yet been firmly established.

4.1.4.1 Ground Rules

Ground rules governing the duration of limit cycle (attitude stabilization) attitude maneuvers and translational maneuvers were established for

Table 4-7. Mission Timeline

Function Subfunction Event	Start G.E.T. (d h m s)	Δ Time to Next Event (d h m s)	OMS ΔV (fps)	ACPS Propell. Consump. (lb)	Resultant Ha/Hp (nm)	Remarks
Liftoff	00:00:00:00	00:00:00:00				Launch from KSC
Perform Mated Ascent	00:00:00:00	00:00:02:20				
Perform initial ascent maneuver Perform roll maneuver Perform pitch maneuver Maintain ascent profile						
Perform Orbiter/Booster Staging	00:00:02:20	00:00:00:03				
Sense booster oxidizer depletion Perform separation						
Achieve Initial Earth Orbit	00:00:02:23	00:00:06:00				
Stabilize orbiter on ascent trajectory Control trajectory to injection Perform injection maneuver						
Insertion	00:00:08:23	00:00:00:00			100/50	
Maintain Orbiter MPS Engine	00:00:08:23	00:00:02:00				Assume HU, NF and XYH at Insertion
Cutoff attitude Hold attitude DB ± 0.5°/3-axis				0.06		*Insertion to deployment = 730.18#*
Conduct MPS Post-Burn Procedures						
Maneuver on Orbiter LH_2 + LO_2 Tank	00:00:10:23	00:00:10:00		114.40		ACPS propellant consumption computed with external tank attached to orbiter at this point
Separation Attitude						
Hold attitude DB ± 1°/3-axis Hold attitude DB ± 0.5°/3-axis	00:00:20:23	00:00:01:00		0.15 0.03		
Jettison External Tank						

Table 4-7. Mission Timeline (Cont)

Function Subfunction Event	Start G. E. T. (d h m s)	Δ Time to Next Event (d h m s)	OMS ΔV (fps)	ACPS Propell. Consump. (lb)	Resultant Ha/Hp (nm)	Remarks
Separation Maneuver = 3 fps -Z direction	00:00:21:23	00:00:10:30		486.00		
Maneuver to line-of-sight altitude with external tank				35.59		Deorbit external LH_2 + LO_2 tank
Hold attitude DB ± 10°/3-axis				0.14		Deorbit ΔV = 300 fps, 486# includes cross-coupling effects
Ignition and Deorbit External Tank						
Maintain Orbiter Attitude	00:00:31:53	00:00:09:05		0.03		
Hold attitude DB ± 45°/3-axis						
Open Cargo Bay Doors						Add 1m 23s to G. E. T. from this point on
Maneuver on OMS Burn Attitude and Hold;	00:00:39:35	00:00:10:00		38.10		Inertial Hold on OMS burn attitude
Horizontal, inplane, posigrade, HU.						
Hold attitude DB ± 1°/3-axis				1.43		
Hold attitude DB ± 0.5°/3-axis	00:00:49:35	00:00:01:00		0.29		Refine DB
First Hohmann Burn	00:00:50:35	00:00:00:41	121.7			
OMS provides ΔV Attitude controlled to ±0.5°/3-axis						
Insertion-Maintain OMS Engine Cutoff Att.	00:00:51:16	00:00:02:00		0.57	117/100	
Hold attitude DB ± 0.5°/3-axis						
Maneuver to HU, NF and Pitch	00:00:52:16	00:00:30:32		12.57		Maneuver rate = 1°/S/P
Hold attitude DB ± 10°/3-axis				0.43		
Conduct OMS Post-Burn Procedures						
Maneuver on OMS Burn Attitude and Hold;	00:01:23:48	00:00:10:00		38.10		Inertial hold on OMS burn attitude
Horizontal, inplane, posigrade, HU.						
Hold attitude DB ± 1°/3-axis				1.43		
Hold attitude DB ± 0.5°/3-axis	00:01:33:48	00:00:01:00		0.29		

Table 4-7. Mission Timeline (Cont)

Function Subfunction Event	Start G.E.T. (d h m s)	Δ Time to Next Event (d h m s)	OMS ΔV (fps)	ACPS Propell. Consump. (lb)	Resultant Ha/Hp (nm)	Remarks
Second Hohmann Burn	00:01:34:48	00:00:00:12	30.6			Circularization burn
OMS provides ΔV. Attitude controlled to ±0.5 °/3-axis						
Insertion-Maintain OMS Engine Cutoff Att.	00:01:35:00	00:00:02:00		0.57	117/117	
Hold attitude DB ± 0.5°/3-axis						
						Deployment 712.21#
Maintain HU, NF and XYH	00:01:37:00	00:00:48:00		0.15		Local horizontal, orbital rate
Hold attitude DB ± 45°/3-axis						
Conduct OMS Post-Burn Procedures						
Pre-Deployment Checkout of Payload						
Activate Manipulator Arms and Attach to Payload						
Maneuver on Release Attitude and Hold	00:02:25:00	00:00:25:00		81.15		Inertial hold
Hold attitude DB ± 10°/3-axis				0.36		Redefine DB
Deploy Payload from Cargo Bay						Payload; recoverable propulsive stage and satellite
Final Checkout and Orient Payload						
Activate Payload Subsystems						
Coast to Release Point and Close DB	00:02:50:00	00:00:10:00		81.15		Refine DB
Hold attitude DB ± 1°/3-axis				1.43		
Hold attitude DB ± 0.5°/3-axis	00:03:00:00	00:00:01:00		0.29		
Release Payload						
Retract Manipulator Arms						
Separate to Safe Distance	00:03:01:00	00:00:10:00		230.00		Total ACPS ΔV = 5 fps
Hold attitude DB ± 0.5/3-axis				2.86		out-of-plane translation

Table 4-7. Mission Timeline (Cont)

Function Subfunction Event	Start G.E.T. (d h m s)	Δ Time to Next Event (d h m s)	OMS ΔV (fps)	ACPS Propell. Consump. (lb)	Resultant Ha/Hp (nm)	Remarks
Maneuver on Line-of-Sight to Payload	00:03:11:00	00:00:57:00		81.15		Monitor payload functioning. Crew maintains visual sight-of-target
Hold attitude DB ± 10°/3-axis				0.81		
Monitor Payload Functioning						
Return to Original Plane	00:04:08:00	00:00:10:00		230.00		Total ACPS ΔV = 5 fps In-plane translation
Hold attitude DB ± 0.5°/3-axis				2.86		
Maintain HU, NF						
Hold attitude DB ± 45°/3-axis	00:04:18:00	05:10:31:00		24.86		Wait in Orbit 24.86# Phasing 112.09#
Maneuver on OMS Burn Attitude and Hold	05:14:49:00	00:00:10:00		38.10		Perform phasing and rendezvous maneuvers with recoverable stage
Horizontal, inplane, posigrade, HU						
Hold attitude DB ± 1°/3-axis				1.43		
Hold attitude DB ± 0.5°/3-axis	05:14:59:00	00:00:01:00		0.29		
Third Hohmann Burn	05:15:00:00	00:00:00:17	42.8			Orbiter trails target by 6.8° at burn
OMS provides ΔV Attitude-controlled to ±0.5°/3-axis						
Insertion-Maintain OMS Engine Cutoff Att.	05:15:00:17	00:00:02:00			141/117	
Hold attitude DB ± 0.5°/3-axis				0.57		
Maneuver to HU, NF and Pitch	05:15:02:17	00:00:41:24		12.57		1°/S/P
Hold attitude DB ± 10°/3-axis				5.86		
Conduct Post-Burn Procedure						
Maneuver to OMS Burn Attitude and Hold	05:15:43:41	00:00:10:00		38.10		Inertial hold on burn attitude; posigrade
Hold attitude DB ± 1°/3-axis				1.43		
Hold attitude DB ± 0.5°/3-axis	05:15:53:41	00:00:01:00		0.29		
Fourth Hohmann Burn	05:15:54:41	00:00:00:42	127.0			Corrective combination burn
OMS provides ΔV Attitude controlled to ±0.5°/3-axis						

Table 4-7. Mission Timeline (Cont)

Function Subfunction Event	Start G.E.T. (d h m s)	Δ Time to Next Event (d h m s)	OMS ΔV (fps)	ACPS Propell. Consump. (lb)	Resultant Ha/Hp (nm)	Remarks
Insertion-Maintain OMS Engine Cutoff Att.	05:15:55:23	00:00:02:00		0.57	160/135	Hp is the 4th OMS burn point which is 10 minutes past 141 nm
Hold attitude DB ± 0.5°/3-axis						
Maneuver to HU, NF and Pitch	05:15:57:23	00:00:21:21		12.57		1°/S/P
Hold attitude DB ± 10°/3-axis				0.31		
Conduct Post Burn Procedures						
Maneuver to OMS Burn Attitude and Hold	05:16:18:44	00:00:10:00		81.15		Rendezvous 948.15# Inertial hold (yaw to correct for out-of-plane errors)
Horizontal, posigrade, HU						
Hold attitude DB ± 1°/3-axis				1.43		
Hold attitude DB ± 0.5°/3-axis	05:16:28:44	00:00:01:00		0.29		
Fifth Hohmann Burn	05:16:29:44	00:00:00:18	47.0			Coelliptic circularization
OMS provides ΔV Attitude controlled to ±0.5°/3-axis						
Insertion-Maintain OMS Engine Cutoff Attitude	05:16:30:02	00:00;02:00			160/160	
Hold attitude DB ± 0.5°/3-axis				0.57		
Maneuver to Line-of-Sight Attitude with Target	05:16:32:02	00:01:43:46		80.07		Line-of-Sight attitude 1°/S/P and Y
Hold attitude DB ± 10°/3-axis				1.49		
Conduct Post-Burn Procedures						
Maneuver on TPI Attitude, Posigrade, Pitched up	05:18:15:48	00:00:10:00		81.15		Inertial hold
Hold attitude DB ± 1°/3-axis				1.43		
Hold attitude DB ± 0.5°/3-axis	05:18:25:48	00:00:01:00		0.29		
TPI ΔV	05:18:26:48	00:00:00:10	21.0		171/160	171 nm will not be attained
OMS provides ΔV Attitude controlled to ± 0.5°/3-axis						
Maintain Attitude	05:18:26:58	00:00:21:35				
Hold attitude DB ± 10°/3-axis				0.31		

Table 4-7. Mission Timeline (Cont)

Function Subfunction Event	Start G.E.T. (d h m s)	Δ Time to Next Event (d h m s)	OMS ΔV (fps)	ACPS Propell. Consump. (lb)	Resultant Ha/Hp (nm)	Remarks
Maneuver on TPF Attitude	05:18:48:33	00:00:10:00		81.15		Crew maintains visual sight of target
Hold attitude DB ± 1.0°/3-axis				1.43		
Hold attitude DB ± 0.5°/3-axis	05:18:58:33	00:00:01:00		0.29		
TPF Maneuvers	05:18:59:33	00:00:20:00		611.39	170/170	Braking gates (3)
ACPS provides ΔV						ACPS ΔV = 28 fps (theoretical value) (20 minutes allowed for maneuvers)
Attitude controlled to ±0.5°/3-axis				5.72		
Maintain Target Attitude and Translate on Target to 500 ft at 1 fps	05:19:19:33	00:00:30:27		162.45		Retrieval 334.24# Target attitude assumes a fixed inertial attitude
Hold attitude DB ± 10°/3-axis				0.44		
Activate Manipulator Arms						
Maneuver Below Target and Close In on Target to 50 ft at 1 fps	05:19:50:00	00:00:10:00		81.15 87.34		Normal and axial maneuvers
Hold attitude DB ± 1.0°/3-axis				1.43		Payload in arm's reach of manipulator arms
Hold attitude DB ± 0.5°/3-axis	05:20:00:00	00:00:05:00		1.43		
Retrieve Payload With Manipulator Arms						Payload: recoverable propulsive stage
Secure Payload and Manipulator Arms to Cargo Bay						
Maintain Attitude	05:20:05:00	00:23:51:00				Deorbit 48.36# Local horizontal, orbital rate
Hold attitude DB ± 45°/3-axis				4.54		
Maneuver on Deorbit Burn Attitude and Hold Retrograde, In-plane, HU	06:19:56:00	00:00:20:00		38.10		Inertial hold on deorbit attitude
Hold attitude DB ± 0.5°/3-axis				5.72		

Table 4-7. Mission Timeline (Cont)

Function Subfunction Event	Start G. E. T. (d h m s)	Δ Time to Next Event (d h m s)	OMS ΔV (fps)	ACPS Propell. Consump. (lb)	Resultant Ha/Hp (nm)	Remarks
Close Cargo Bay Doors						
Deorbit Burn	06:20:16:00	00:00:01:45	250.0		170/TBD	
OMS provides ΔV Attitude controlled to ±1.0°/3-axis						
						Preentry 61.93# 1°/S/Y
Maneuver to Entry Attitude	06:20:17:45	00:00:16:35		23.02		
Yaw to NF Hold attitude DB ± 10°/3-axis				0.24		
Conduct OMS Post-Burn Procedures						
Pitch Up 30° Above Local Horizontal	06:20:34:20	00:00:02:00		38.10		Refine DB
Hold attitude DB ± 0.5/3-axis				0.57		
						Entry 1500.00#
Entry (400 Kft)	06:20:36:20	00:01:00:00		1500.00		Entry Parameters: V_e = 25,780 fps γ_e = -1.1° Unpowered landing
Maneuver as required to maintain proper cross range and temperature limits of the orbiter						
Land	06:21:36:20					
		Total	640.1	4472.02		

Table 4-8. Summary of OMS and ACPS Fuel Allocation

Due-East Mission	Mission Phase	Fuel Allocation	
		ACPS (lb)	OMS (fps)
Inclination: 28.5°	Liftoff at KSC		
Payload: recoverable propulsive stage with satellite max wt = 65 Klb	Insertion (50 x 100 nm)		
	External tank separation	730	
	Hohmann burn No. 1 (100 x 117 nm)		122
	Hohmann burn No. 2 (117 x 117 nm)		
	Deployment of payload	712	
	Wait in orbit	25	
	Phasing	112	
	Hohmann burn No. 3 (117 x 141 nm)		43
	Rendezvous	948	
	Hohmann burn No. 4 (135 x 160 nm)		127
	Hohmann burn No. 5 (160 x 160 nm)		47
	TPI		21
	Retrieval of recoverable propulsive stage	334	
	Deorbit	48	
	Deorbit burn		333
	Preentry	62	
	Entry	1500	
Totals		4472	723

the various timeline events to give consistency and uniformity in the preparation of ACPS propellant budget for the due-east mission. These rules are listed below:

1. Prior to every Hohmann transfer burn, the DB (dead band) is held to ±1.0°/3-axis for 10 minutes followed by a DB hold of ±0.5°/3-axis one minute before the OMS burn.

2. During all OMS burns, the orbiter is stabilized to ±0.5°/3-axis.

3. Maintain OMS engine cutoff attitude and hold DB to ±0.5°/3-axis for two minutes after every Hohmann transfer burn.

4. During phasing or orbital coast in a circular orbit, hold DB to ±45°/3-axis to keep the orbiter in a manageable attitude. (Free drift may replace the ±45°/3-axis hold.)

5. Twenty minutes prior to the deorbit burn, the DB is closed to ±0.5°/3-axis and held throughout the entire deorbit maneuver phase into the final OMS burn.

6. Prior to every deployment, the DB is held to ±1.0°/3°-axis for 10 minutes followed by a DB hold of ±0.5/3-axis at the time of payload release (DB may be more or less stringent than stated, depending upon the payload deployment requirements).

7. Separation to a safe distance after having deployed a payload requires out-of-phase translation of 5 fps (total). Ten minutes is allowed for this operation. Return to the original orbit is the reverse operation and the same delta V and time is assumed. The DB hold for these operations is ±0.5°/3-axis throughout the whole operation.

8. Effects of cross-coupling are included for orientation maneuvers performed during deployment, rendezvous, and retrieval phases of the mission.

9. For entry maneuvers, a total of 1500 pounds of ACPS propellant consumption is assumed.

10. Computations for ACPS propellant rates are based on the VC70-0176 orbiter.

4.2 CONFIGURATION EVALUATION

4.2.1 Orbiter Configuration Concepts

As a result of the Phase 1 studies, NASA direction at the start of Phase 2, and review of NASA MSC-040A configuration, orbiter configurations were updated to support the Phase 2 studies. Changes that affected the orbiter configuration were:

1. Consideration of J-2 and J-2S engines for the Mark I orbiter and staging velocity of 6000 ± 1000 fps, which necessitated consideration of four- and five-main-engine installations

2. One-for-one replacement of the Mark I main engines with space shuttle main engines (SSME's).

3. Use of ablator TPS for Mark I orbiters and RSI TPS for Mark II orbiters

4. Maximum use of aluminum structure

5. Retrofit of Mark I orbiters to meet Mark II technical requirements

6. OMS ΔV tankage sized to provide 1000 fps on due-east mission

Initial activities were directed toward (1) review of the NASA MSC -040A configuration and recommended configuration improvements and (2) definition of orbiter configuration and weights to support the integrated vehicle sizing analyses.

The -040A configuration is illustrated in Figure 4-9 with some of the design considerations. Preliminary analysis indicated that modification to the body camber and wing configuration (incidence versus twist) may be desirable for aerodynamic trim capability. However, the configuration has not modified, pending further analysis and wind tunnel results. The -040A configuration did not identify the manipulator arm stowed location. Manipulator arm stowage is provided within a fairing on top of the cargo bay doors. The main and nose gear were modified to provide a free-fall gear. Equally important, the main gear is rotated into the wing to preclude reduction in the body structure depth available to carry loads. Earlier NR orbiter configurations did not provide the bubble canopy shape. The -040A canopy shape was adopted to improve rearward visibility. The wing RCS pod location caused exhaust plume impingement on upward deflected elevons (entry) and was moved to the wing tip. Subsequent NASA -040A configurations also

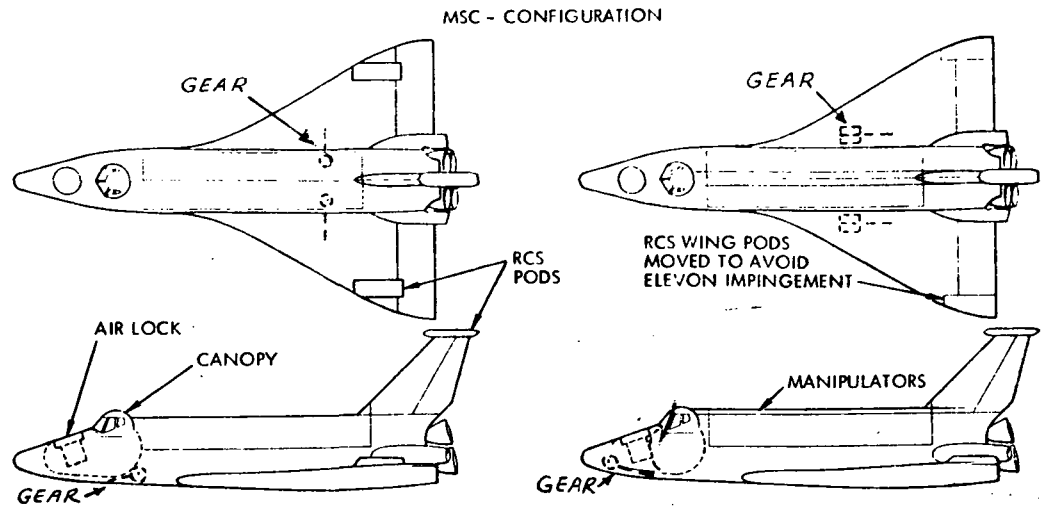

CONSIDERATIONS:

● BODY & WING SHAPE	● -040A MAINTAINED
● MANIPULATOR LOCATION	● MANIPULATOR LOCATED ON TOP OF CARGO DOORS
● MAIN & NOSE GEAR	● MOVED TO FREEFALL LOCATION, NO CUT OUT IN BODY STRUCTURE
● CANOPY SHAPE	● -040A CANOPY MAINTAINED
● RCS POD LOCATION	● MOVED WING PODS TO WING TIP
● AIRLOCK LOCATION	● MOVED AIRLOCK OUTSIDE PRESSURE VESSEL

Figure 4-9. Orbiter Configuration Concept

show this location. The air lock in -040A is located within the cabin pressure vessel and, therefore, must be designed for collapse pressure of 14.7 psia. The air lock is assumed to be outside the cabin pressure vessel pending the results of several candidate cabin arrangements. The configuration shown on the right side of Figure 4-9 was baselined for initial sizing activity.

In support of the integrated vehicle sizing activity, preliminary orbiter configurations and weight estimates were made for J-2 and J-2S Mark I orbiters, four- and five-engine orbiters, and appropriate Mark II systems. The four-engine system was previously shown. The five-engine system uses the same basic orbiter design with the aft fuselage modified to install three bottom engines side by side and two top engines side by side. Both the four- and five-engine systems can be trimmed, with the c.g. of the five-engine orbiter predicted to be approximately one percent further aft than the four-engine system. An orbiter weight summary used for vehicle sizing is shown in Table 4-9. The final orbiter dry weight prediction is shown in Section 4.4.3.13.

Table 4-9. Orbiter Weight for Integrated Vehicle Sizing Analysis

System		Orbiter Dry Weight (lb)	
No. of Engines	Engine Type	Mark I	Mark II
4	J-2	108, 516	
4	230K SSME		113,944
5	J-2	115,469	
5	230K SSME		119,912
4	J-2S	110,303	
4	265K SSME		116,169
5	J-2S	117,686	
5	265K SSME		123,274

4.2.2 Booster Configuration Concepts

Two booster concepts were considered in Part II of the study. These were a flyback booster and a pressure-fed booster. This section will discuss the initial configurations and configuration trades which led to the selected baselines described in Sections 4.4.5 and 4.4.6 of this report.

4.2.2.1 Flyback Booster Concepts

This section of the report presents data on the initial flyback booster configurations and trade study results leading to selection of the B-18E-3 baseline configuration discussed in Section 4.4.5. The study was initiated by selecting five basic booster types for preliminary layouts, as shown in Figure 4-10 below. These concepts were selected as a logical configuration family incorporating varying degrees of Saturn S-1C commonality. And, they had a good chance of being balanced.

Initial Booster Concepts

1. B-18D — Maximum use of S-1C components, mounted on a swept wing with tip fins, and with ten centrally located ABRES engines. The wing can be readily located to achieve optimum balance.

2. B-18E — Maximum use of S-1C components, a delta wing/ canard arrangement, and ten ABES engines located in the nose for balance.

3. B-18F-1 — Maximum use of S-1C components except for tapered LO_2 tank, a delta wing/canard arrangement, with ten ABES engines located in wing and intertank areas. The tapered LO_2 tank was used to lengthen the nose for balance.

4. B-18G — A minimum size (four F-1, $\epsilon = 10$) version with delta wing/canard arrangement, seven ABES engines in wing and intertank area, and a 26-foot diameter body. The higher fineness ratio body has been shown in previous studies to provide a good balance capability.

5. B-18G-1 — Identical to B-18G except for using $\epsilon = 16$ expansion ratio nozzles, S-1C engine spacing, and eight ABES engines.

Synthesis Input. Synthesis input data was then generated including weight/coefficient inputs, aerodynamic boost drag, flyback L/D, landing theoretical wing loading, propulsion weights, I_{sp}, recommended throttle schedule, geometry, and sensitivity factors.

Designation & Dwg No.	Configuration	Swing (theo) ft^2	ABES Engines	Main Engine	ϵ	Body Config	Remarks
B-18D 76Z0652	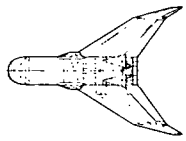	8000	(10) Aft in wing and side body pods	(5) F-1 S-IC Spacing	16:1	33-ft dia Thrust struct, hold down, intertank, LO_2/RP tanks. Same as S-IC	Max S-IC commonality. Wing below tanks. Tip fins. No canard. (5) S-IC LO_2 lines
B-18E 76Z0646	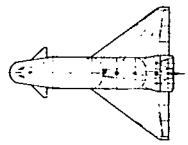	8000	(10) Fwd in nose	(5) F-1 S-IC Spacing	16:1	33-ft dia Thrust struct, hold down, intertank, LO_2/RP tanks. Same as S-IC	Max S-IC commonality. Wing thru RP tank. Canard. (5) S-IC LO_2 lines.
B-18 F-1 76Z0622	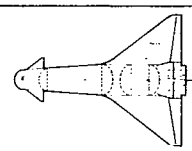	8000	(10) Aft in wing and intertank	(5) F-1 S-IC Spacing	16:1	33-ft dia Thrust struct, and RP tank dia. Same as S-IC Longer intertank. Tapered LO_2 tank	Partial S-IC commonality Wing thru RP tank. Canard. (5) longer LO_2 lines (taper for balance).
B-18G 76Z0653	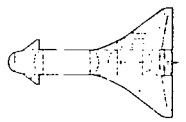	5330	(7) Aft in wing and intertank	(4) F-1 Min Spacing	10:1	26-ft dia	All new structure Low/midwing through RP tank. Canard. (4) longer LO_2 lines. min wt/cost potential.
B-18 G-1 76Z0654	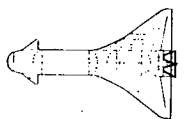	5330	(8) Aft in wing and inter-tank	(4) F-1 S-IC Spacing	16:1	26-ft dia	Identical to B-18G except for ϵ = 16 engine nozzles and spacing

Figure 4-10. Initial Booster Concepts

The orbiter used for all runs was NR Case 1 with a gross weight of 1.029 million pounds. Ascent engines are J2S uprated at 327,500 pounds thrust and 447.3 sec I_{sp} vacuum. (This orbiter was later superseded by NR, after vehicle comparisons were completed.)

Final Booster Concepts. Data from the final synthesis runs were used to resize the initial five booster concepts. Configurations B-18D, B-18E, and B-18F-1B have the same body diameter and tank volume as Saturn S-1C; hence, the body size was held constant. The increased wing area is depicted by a reference line on the original drawings, as shown in Figures 4-11, 4-12, and 4-13.

Configurations B-18G and B-18G-1 are shown in Figures 4-14 and 4-15, respectively. These configurations were redrawn using the final synthesis data. Since they were allowed to grow geometrically, the body diameter and length are changed slightly (i.e., 26-foot to 26.5-foot diameter). A large increase in theoretical wing area was required, however, from the initial 5330 ft^2 to 7206 ft^2 for the B-18G and 7464 ft^2 for the B-18G-1 in order to retain the desired landing wing loading of 66.5 lb/ft^2.

Performance Comparison. A performance comparison of the basic configuration types is shown in Table 4-10. B-18D, B-18E, and B-18F-1B have the same tank volumes as S-1C; therefore, propellants are "off-loaded" to the weight required for the mission. B-18D, the heaviest vehicle, has the lowest L/D and requires the largest number of flyback engines, twelve. B-18E and B-18F-1B are very similar in performance and weight; however, B-18E has the greatest S-1C commonality.

The B-18G tanks are sized by the mission requirements. This "hot rod" version is slimmer and lighter than the other vehicles, requiring only four ascent and seven flyback engines, but it has the least S-1C commonality.

Expansion Ratio Comparison – B-18G vs B-18G-1. The effect of increasing the ascent engine expansion ratio (ϵ) from 10 on the B-18G to 16 on the B-18G-1 is shown in Table 4-11. $\epsilon = 16$ is the current F-1 engine value. This engine has a higher I_{sp}, but is larger in diameter and heavier due to the larger expansion nozzle. The result is a higher dry weight for B-18G-1 but lower propellant weight, resulting in a lower booster gross weight. The larger base area on B-18G-1 decreases the L/D, requiring an additional flyback engine.

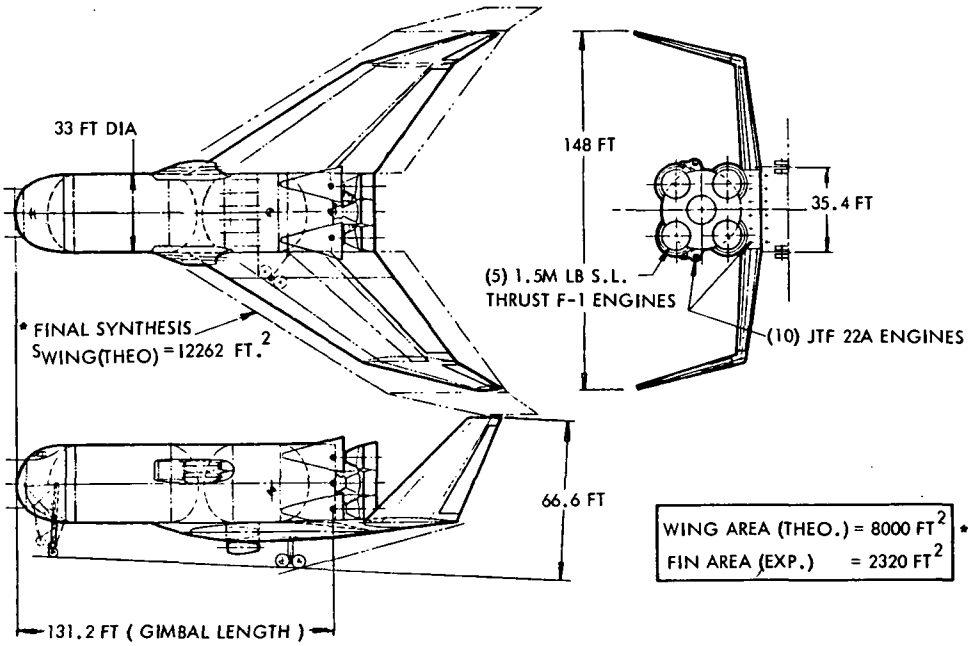

Figure 4-11. B-18D LO_2/RP Booster, Drawing 76Z0652 (Ref)

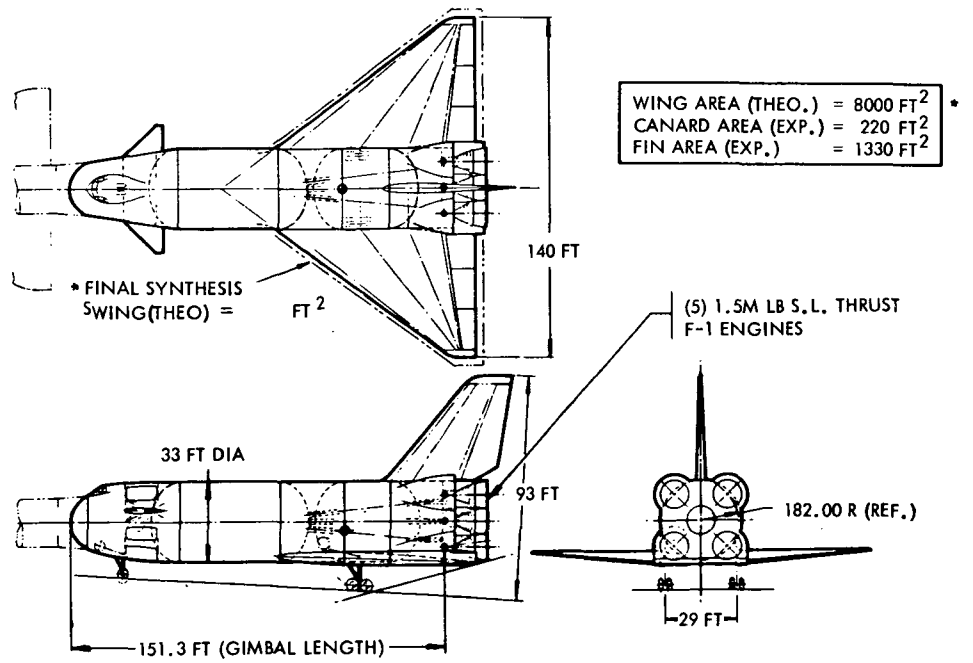

Figure 4-12. B-18E LO_2/RP Booster, Drawing 76Z0646 (Ref)

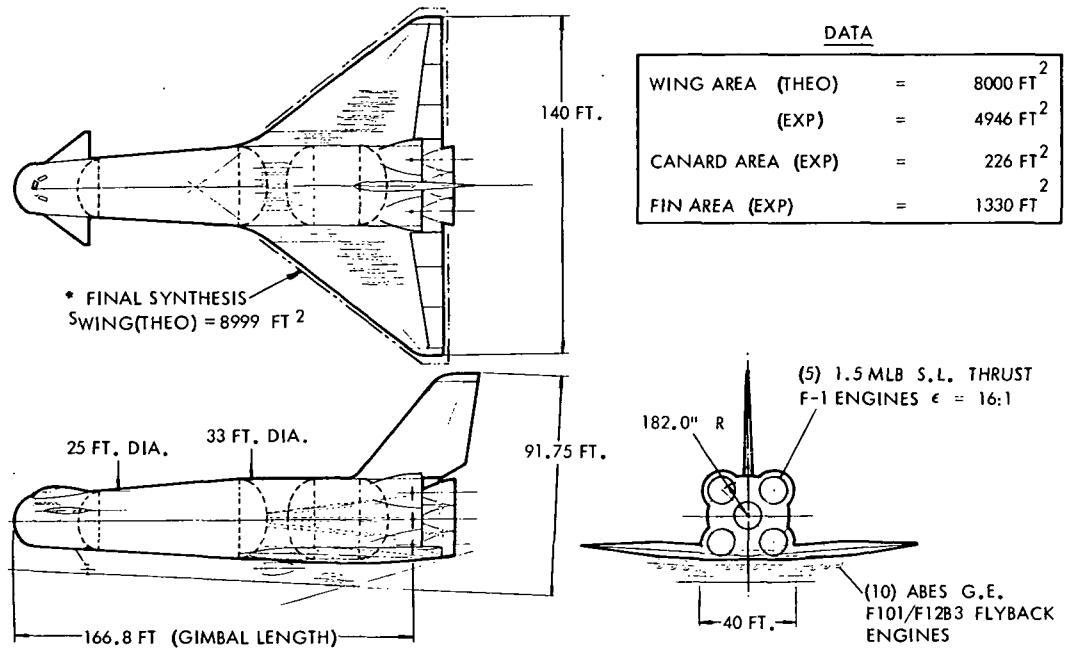

Figure 4-13. B-18F-1B LO_2/RP Booster, Drawing 76Z0622A (Ref)

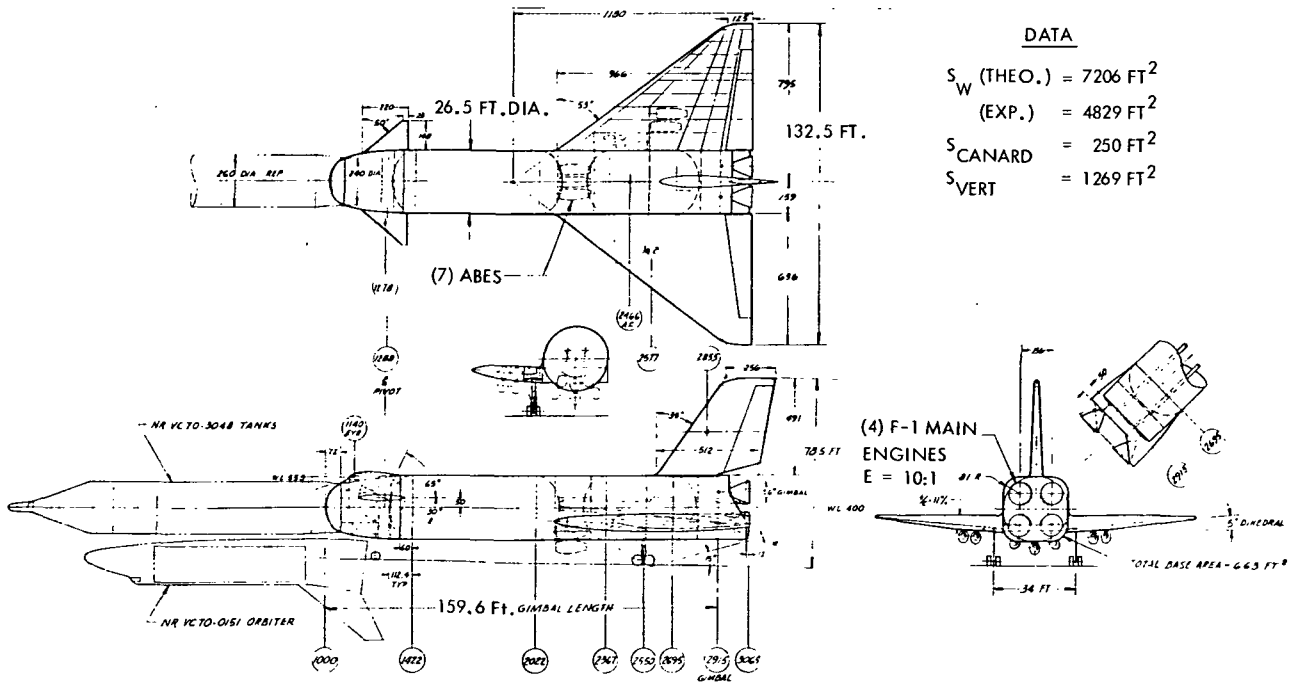

Figure 4-14. B-18G LO_2/RP Booster, Drawing 76Z0653 Sht 2 (Ref)

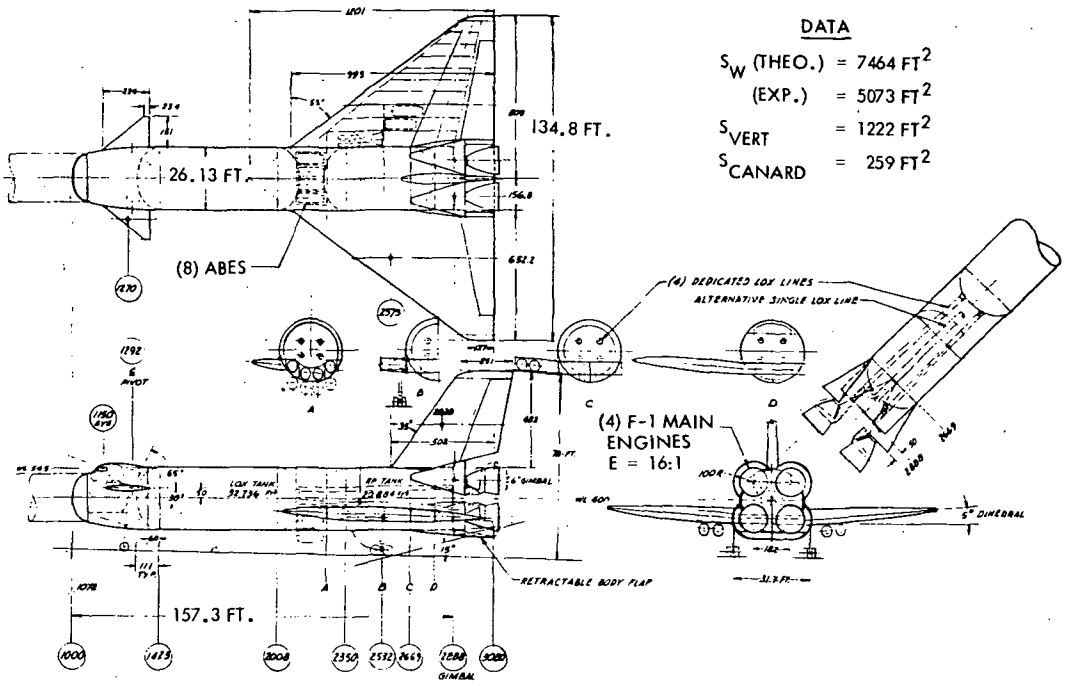

Figure 4-15. B-18G-1 LO_2/RP Booster, Drawing 76Z0654A (Ref)

Table 4-10. Performance Comparison

	B-18D	B-18E	B-18F-1B	B-18G
ORBITER				
GROSS WEIGHT		1.029 M		
PROPELLANT WEIGHT-ASCENT		779 K		
NUMBER OF ENGINES		4		
THRUST		327,500		
ISP_{VAC}		447.3		
BOOSTER				
GROSS WEIGHT	4.578 M	4.127 M	4.121 M	3.875 M
PROPELLANT WEIGHT-ASCENT	3.764 M	3.434 M	3.430 M	3.328 M
LANDING WEIGHT	715 K	600 K	603 K	479 K
DRY WEIGHT	683 K	572 K	572 K	452 K
LENGTH	131.5	151.3	166.8	159.4
DIAMETER	33	33	33	26.5
WING THEORETICAL AREA	12326	8974	9000	7198
ASCENT ENGINES – NUMBER	5	5	5	4
– EXPANSION RATIO	16	16	16	10
– ISP SL/VAC	265.4/304.1	265.4/304.1	265/304.1	264.7/289.3
– ENGINE SL THRUST	1.402 M	1.289 M	1.288 M	1.532 M
– T/W LIFTOFF	1.25	1.25	1.25	1.25
FLYBACK L/D (INCL. BASE DRAG)	5.3	5.40	5.75	6.5
AIR-BREATHING ENGINES – NUMBER	12	10	10	7
GLOW	5.607 M	5.156 M	5.150 M	4.903 M

Table 4-11. Expansion Ratio Comparison

COMPARISON ITEM	B-18G (ϵ = 16)	B-18F-1 (ϵ = 16)
GEOMETRY		
LENGTH	159.6 FT.	157.3 FT.
DIAMETER	26.5 FT.	26.1 FT.
WING THEORITICAL AREA	7206 FT^2	7464 FT^2
CANARD AREA	250 FT^2	250 FT^2
PROPULSION-ASCENT		
NO. OF ENGINES	4	4
EXPANSION RATIO (e)	10	16
ISP SL/VAC	264.7/289.3 SEC	265.4/304.1 SEC
ENGINE THRUST/T/W	1.538 M LB/1.25	1.492 M LB/1.25
MAXIMUM q	645 PSF	653 PSF
PROPULSION - AIR BREATHING		
NO. OF ENGINES	7	8
L/D (INCL. BASE DRAG)	6.5	5.9
FLYBACK FUEL	27712 LB	31170 LB
WEIGHTS		
GROSS WEIGHT (BOOSTER)	3.891 M LB	3.744 M LB
PROPELLANT WEIGHT	3.343 M LB	3.177 M LB
LANDING WEIGHT	479 K LB	496 K LB
DRY WEIGHT	452 K LB	470 K LB
FAIRINGS	13511 LB	20286 LB
ASCENT ENGINES	66900 LB	74460 LB
PROPULSION - FLYBACK	30923 LB	35310 LB
GLOW	4.920 M LB	4.772 M LB
OLOW	1.029 M LB	1.029 M LB

Initial Booster Arrangement Selection. Review of the performance comparison of the basic configuration types resulted in the decisions shown in Figure 4-16:

Eliminated: B-18D because of excess weight and requirement for tip fins.

B-18F-1B because the complexity of a tapered LO_2 tank did not indicate sufficient performance and balance advantages.

Retained: B-18E because of high S-1C commonality, and potential low cost.

B-18G because of small size and fewer engines resulting in minimum weight and low cost potential.

Note: No further work has been done on B-18G because of marginal engine-out capability and minimum S-1C commonality.

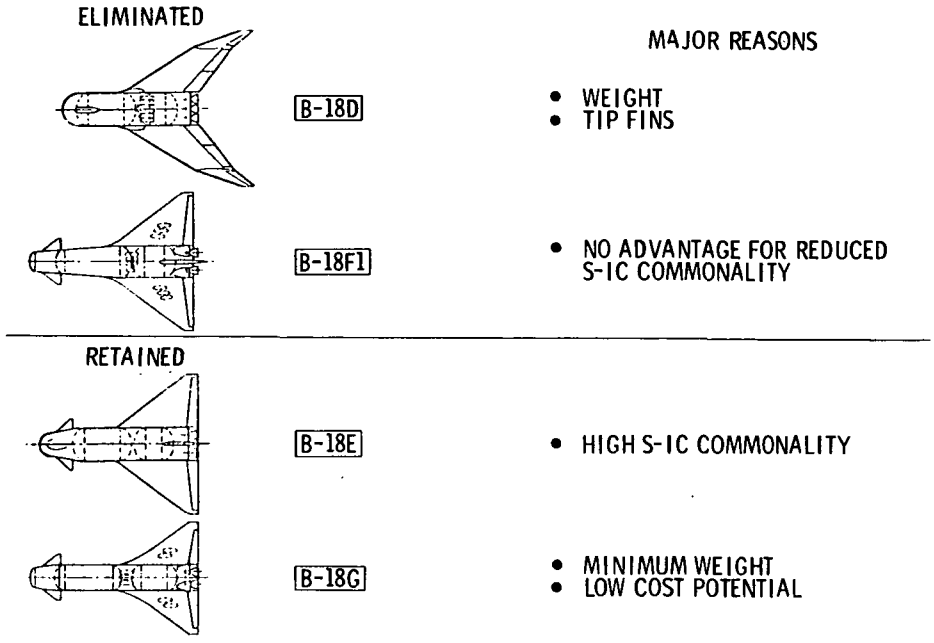

Figure 4-16. Initial Booster Arrangement Selection

Expansion of the B-18E Series. After selecting the B-18E arrangement, a series of vehicles was developed to determine an optimum configuration. The four versions are shown in Figure 4-17. The basic fuselage geometry was held constant to retain the high Saturn S-1C commonality. Variations were made in location of the ABES engines; wing planform, area, and location; with and without canards; and use of ballast as required to balance.

B-18E Series – Performance Comparison. A tabulation of the performance parameters taken from the synthesis runs for B-18E and its derivatives B-18E-1, B-18E-2, and B-18E-3 is shown in Table 4-12. The results reflect vehicle differences in wing areas, canards, flyback engines, flyback L/D, and structural weights. The B-18E in this comparison was updated from the B-18E compared in Table 4-10.

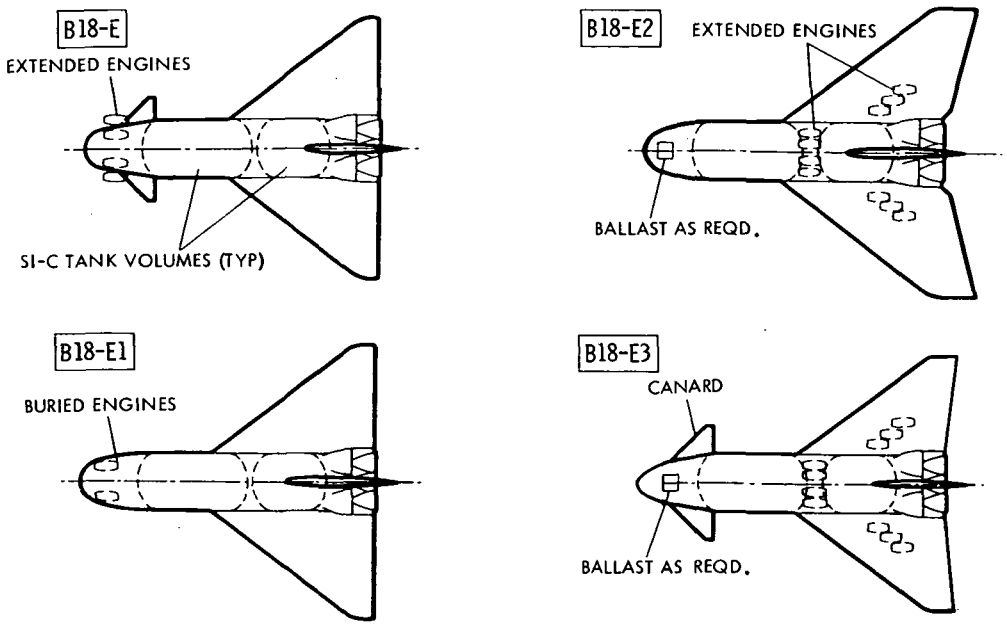

Figure 4-17. B-18E Series Configurations

Table 4-12. Performance Comparison

BOOSTER DESIGNATION	B-18E	B-18E-1	B-18E-2	B-18E-3
GLOW MLB	5.252	5.330	5.413	5.202
BLOW MLB	4.223	4.301	4.383	4.173
OLOW MLB	1.029	1.029	1.029	1.029
BOOST. DRY STRUC. WT. KLB	594	603	632	587
BOOST. LAND. WT. KLB	622	632	662	616
BOOST. ASCENT PROPEL. WT. MLB	3.506	3.571	3.630	3.466
V_{STAGE} FPS	6,451	6,450	6,450	6,450
Q_{MAX} PSF	659	655	654	661
Q_{STAGE} PSF	68	68	67	69
BOOST. S_{WING} THEO. FT^2	9,303	10,679	11,174	8,549
BOOST. S_{CANARD} EXP. FT^2	370	0	0	543
BOOST. $S_{VERT.}$ EXP. FT^2	1,200	1,700	2,200	1,700
$W_{LANDING}/S_{WING}$ THEO. PSF	66.9	59.2	59.2	72
NO. A/B ENGINES	10	11*	10	10
L/D CRUISE	5.40	5.38	5.97	5.65
SFC	.72	.76	.71	.71
V_{CRUISE} KTS	281	281	281	281
WT. FLYBACK JP KLB	43.4	46.8	41.1	40.4
WT. BALLAST KLB	5	0	20	4

*BURIED ENGINE THRUST VECTOR EFFECT INCL. BOOSTER CONT. = 10% ORB. CONT. = 5%

Selection of the Baseline Configuration. Results of the trade study are shown in Figure 4-18. Key factors in making the final selection are summarized here:

B-18E – A larger wing than desired was necessary because the canard area was limited by physical clearance from the extendable ABES engines in the nose.

B-18E-1 – The buried ABES engines in nose require complex engine inlets and exhausts dictating a no-canard configuration and consequently a large wing area. Also, the thrust vector loss requires use of 11 ABES engines.

B-18E-2 – Moving ABES engines aft, and eliminating canard, requires the largest wing area of all study configurations. The resultant balance problem caused the largest ballast requirement and the highest landing weight.

B-18E-3 – Tradeoff with optimum canard and wing area resulted in the lowest landing weight and low ballast requirement, while allowing ABES engines to be located aft in wings and intertank area. This was the selected configuration.

The selected B-18E-3 baseline booster configuration is discussed in detail in Section 4.4.5 of this report.

	WEIGHT	ABES AFT	CANARD	BALLAST
E 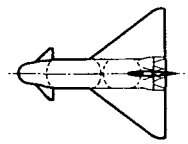	622 K		YES	5 K ✓
E1 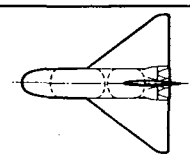	632 K		NO	0 ✓
E2 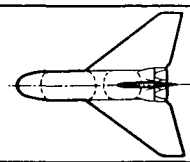	662 K	✓	NO	20 K
E3 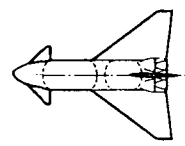	616 K ✓	✓	YES (SAVES 46 K LBS)	4 K ✓ } SELECTED

Figure 4-18. Baseline Booster Selection

4.2.2.2 Pressure-Fed Booster Trade Studies

The other booster concept that was considered was a pressure-fed booster. The pressure-fed booster concept attempts to reduce costs by employing a relatively simple design approach with a minimum number of components. The engine turbo machinery is eliminated and replaced by a large pressurization system to provide the required pressures at the engines. As presently envisioned for the space shuttle, the booster would be recovered from the ocean and refurbished for reuse.

Several trade studies were made leading to the selection of the baseline pressure fed booster described in Section 4.4.6. The principal trades are (1) number of stages, (2) number of stage elements, (3) number of engines, (4) expendable versus recoverable and (5) propellant selection, described below. It should be noted that performance and costs shown in these studies are not necessarily compatible with the current baseline, but they are internally consistant so that the comparisons are valid.

Number of Stages. A single-stage booster was compared to a two-stage booster for the baseline 40 k polar mission utilizing a common 1.7 M lb orbiter. The stage parameters are summarized in Figure 4-19. The individual elements of the two-stage/three-element vehicle were identical in size to minimize development. The final evaluation of the number of stages is shown in Table 4-13. Although the total hardware weight is the same for both

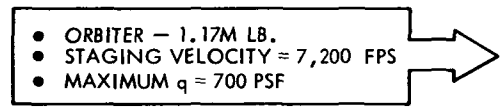

ONE-STAGE		TWO-STAGE		
		1ST	TOTAL	2ND
OLOW	1.173		1.173	
SLOW		3.534		1.753
BLOW	6.132		5.279	
GLOW	7.305		6.452	
B HARDWARE	0.586	0.40	0.586	0.186
THRUST	9.495	8.388		4.194
THRUST/ENGINE	1.356	1.048		1.048

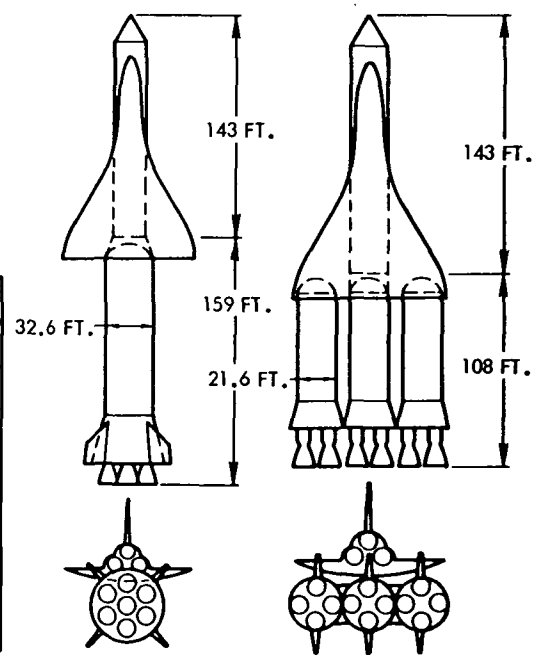

Figure 4-19. Number of Stages

Table 4-13. Number of Stages

	ONE-STAGE	THREE-ELEMENT TWO-STAGE
QUANTITY OF HARDWARE	1 ELEMENT	3 ELEMENTS
RECOVERY	LARGE SINGLE UNIT	3 SMALLER UNITS AT DIFFERENT IMPACT AREAS
COST ($M)		
DDT&E	450	628
PRODUCTION (10% ATTRITION)	2,145	5,025
OPERATIONS	950	870
TOTAL PROGRAM	3,545	6,523

concepts, the total program cost for the two-stage booster system is nearly double the cost of the single stage because of higher cost of producing the larger number of elements.

Number of Elements. A single-stage/single-element booster was compared to a single-stage/three-element booster. The results of the comparison are shown in Table 4-14. The booster total hardware weight nearly doubles for the three-element vehicle (900 k lb vs. 515 k lb) and the GLOW increases by 1.1 M lb. Production cost differential would be even higher than indicated for the 1 vs. 2 stage comparison.

Number of Engines. The number of engines impacts the vehicle and the program in various ways as described in Figure 4-20. Use of multiple engines eliminates the need for throttling as discrete cutoff is used to meet trajectory constraints, and eliminates the need for a separate vehicle roll control system as main engine TVC can be used. A baseline of seven engines is selected because it provides the maximum packaging efficiency (minimum base area) and reduces the ΔV loss from discrete shutdown of engines for Q and g limiting.

Expendable versus Recoverable. A study was conducted to determine the cost effectiveness of recovering the pressure-fed booster. The results of the study are shown in Figure 4-21. Although operations and DDT&E costs are higher for a recoverable system, the reduction in recurring production is offsetting and the total program cost is approximately $500 million less for the recoverable booster.

Table 4-14. Single Stage Booster Summary

Propellant	N_2O_4 / UDMH	N_2O_4 / UDMH
Stages	1	1
No Elements	1	3
Thrust Total	9.098	10.603
Booster Mass Fract.	0.874	0.871
Weights		
Element Hrdwre	0.515	0.300
Total Hrdwre	0.515	0.900
Total Element	5.83	2.325
Total Stage	5.83	6.983
Orbiter	1.133	1.133
Payload	0.040	0.04
Glow	6.998	8.156

	SINGLE	MULTIPLE
DEVELOPMENT REQUIREMENTS		
THROTTLING	REQUIRED	NOT REQUIRED
ENGINE SIZE	LARGE	LESS
ROLL CONTROL SYSTEM	REQUIRED	NOT REQUIRED

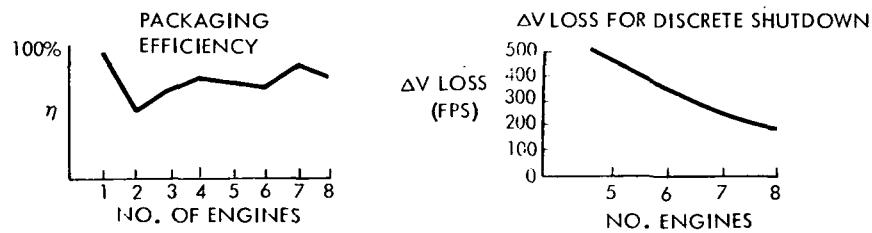

• 7 ENGINES SELECTED FOR BASELINE

Figure 4-20. Number of Engines

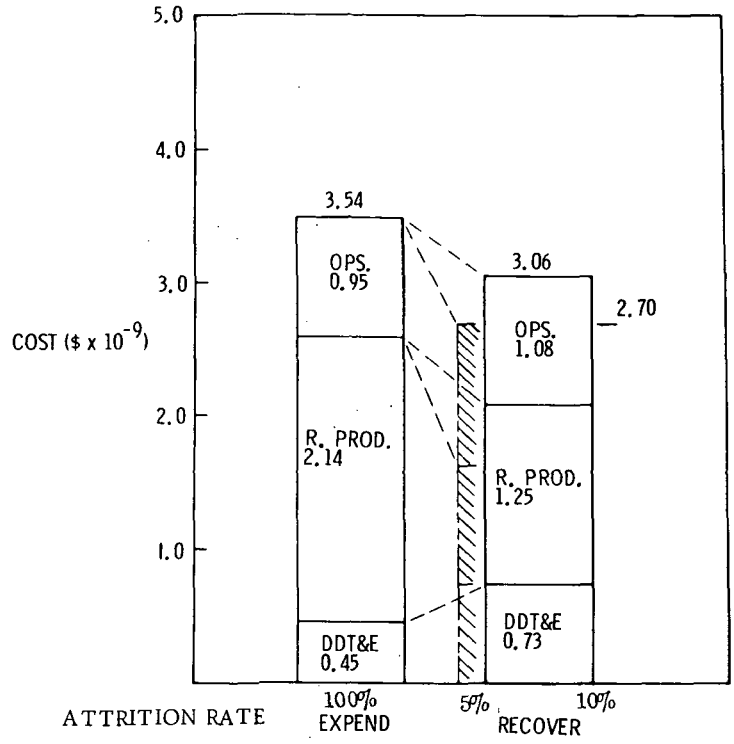

Figure 4-21. Expendable/Recoverable Comparison

Propellant Selection. A study was made to select the most cost effective propellant combination. The final contending combinations were N_2O_4/UDMH (storable), O_2/RP, and O_2/C_3H_8. Total program costs were lowest for O_2/RP and higher for N_2O_4/UDMH, although differences were minor (approximately 2.5 percent total spread). Table 4-15 summarizes the selection study. Recommendation was to continue study of O_2/RP and O_2/C_3H_8, with the final selection to be predicated on engine considerations to be determined by engine contractors. In the meantime, O_2/C_3H_8 was chosen for the baseline.

Table 4-15. Propellant Selection Summary

- STORABLES CAN BE ELIMINATED FROM FURTHER STUDY
  - HIGHEST TOTAL PROGRAM COSTS
  - HIGHLY TOXIC
- BOTH O_2/C_3H_8 & O_2/RP SHOULD BE STUDIED FURTHER
  - O_2/RP 6% LOWER HARDWARE WEIGHT
  - O_2/C_3H_8 MAY HAVE ENGINE & OPERATIONAL ADVANTAGES
  - TOTAL PROGRAM COSTS ARE ESSENTIALLY EQUAL

→ FINAL SELECTION DEPENDENT UPON ENGINE CONSIDERATIONS
- COOLING
- I_{sp}
- LITVC

4.2.3 LO_2-RP System Analysis and Trades

Design of the integrated booster/orbiter mated vehicle is concerned with the functions performed by these two flight vehicles while mated. Design of each of these vehicles is required to provide for functions necessary during ascent: trajectory, shaping, guidance, control, and separation. The design of each vehicle is also influenced by the environment experienced during ascent: loads, heating, vibration, and acoustics. The integrated vehicle design process involves analyses and trade studies that apportion functional requirements between the orbiter and booster while evaluating and minimizing adverse environmental factors on the total system.

At the start of Phase 2 of the Phase B extension, an integrated vehicle configuration consisting of a four-engine F-1 LO_2/RP reusable booster and an early orbiter configuration with four J-2S engines was established for detailed control, loads, and separation analyses. This configuration is represented by drawing VC70-3058 (Figure 4-22). The mass properties and inertias for this configuration are given in Table 4-16. In parallel with the detailed dynamic analyses for this configuration, the performance and ascent trajectory were evaluated for a spectrum of boosters (four and five F-1) and orbiters (J-2, J-2S Mark I orbiters and J-2S and HiPc Mark II orbiters).

4.2.3.1 Sizing and Propulsion Comparisons

The booster/orbiter integrated vehicle is sized to meet the design mission requirements by means of a digital simulation program that combines vehicle weight/size scaling relationships and trajectory performance evaluations. Results define the propellant quantities of the booster and orbiter, weights of each vehicle, and a nominal trajectory. Solutions are obtained for a range of booster/orbiter sizes through selection of a range of staging velocities.

The major ground rules for the LO_2-RP sizing are:

1. The vehicle is sized to meet Mark II mission requirements, and a subsequent evaluation is made to see if minimum Mark I requirements are met.

2. The orbiter does not require once-around abort capability for one orbiter engine out at staging.

3. The staging velocity limits are 6000 ± 1000 fps.

4. The nominal dynamic pressure should be limited to 650 psf.

Table 4-16. Mated Vehicle Mass Properties

W_{PL} = 40000	Weight (lb)	*Center of Gravity			Moment of Inertia (10^6 slug ft^2)		
		$\bar{X}_o$	$\bar{Y}_o$	$\bar{Z}_o$	Pitch	Roll	Yaw
Orbiter	181084	1028.8	0	377.6	5.93	0.73	6.20
Tank/adapter (inert)	58652	705.3	0	125.0	2.20	0.15	2.20
Orbiter (less propellant)	239736	949.7	0	315.8	9.75	1.50	9.40
Reserve fluids	5265	296.4	0	125.0			
In-flight losses	5123	296.4	0	125.0			
Ascent propellant	778992	296.4	0	125.0			
Orbital gross wt at liftoff	1029116	448.6	0	169.4	38.07	2.94	36.28
Orbiter burnout	462000	2772.0	0	182.0	34.28	3.08	34.33
Combination burnout	1491116	1168.5	0	173.3	443.46	6.03	441.71
Booster propellant	3088000	2327.3	0	115.0			
Combination liftoff	4579116	1950.0	0	134.0	2982.06	6.77	2979.57

Stations shown are orbiter stations

X_o at nose = 200

Z_o at frl of orbiter = 400

Booster stations

$X_B = X_o - 370$

Z_B at C_L thrust = $Z_{o_{frl}} - 285$

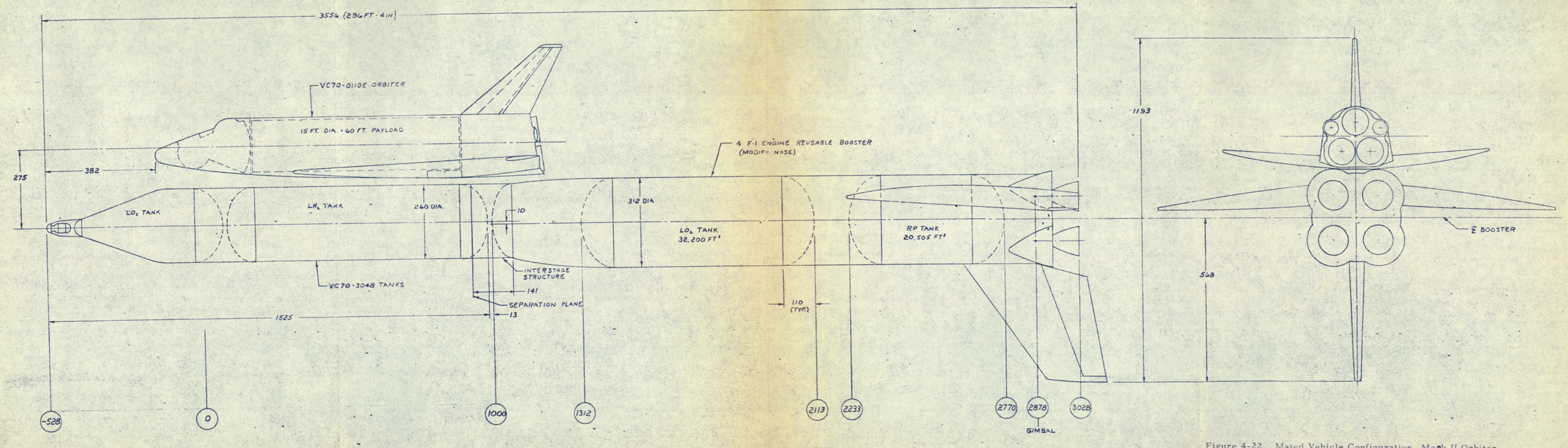

Figure 4-22. Mated Vehicle Configuration, Mark II Orbiter, 4F-1 Reusable Booster

5. The Mark II orbiter thrust level for the HiPc engines is matched to that of the Mark II engine (J-2 or J-2S), and both Mark I and Mark II orbiters have the same number of engines.

The matrix of orbiter/booster configurations studied is given in Table 4-17. The two booster configurations are a four F-1 engine version with optimized tankage (B-18-G configuration as described in Section 4.2.2) and a five F-1 engine version that uses S-1C tankage (B-18-E configuration). These boosters were combined with four basic orbiter configurations: four- and five-engine orbiters with HiPc engines of 230 K and 265 K vacuum thrust level (J-2 and J-2S thrust levels for Mark I). An additional orbiter using four J-2S engines for Mark II was introduced near the end of the study.

Results of staging velocity tradeoffs are shown in Figures 4-23 and 4-24 for the 4 x 265 K HiPc orbiter and four F-1 and five F-1 boosters. Figure 4-25 shows the staging velocity trade for the Mark II J-2S orbiter. Figure 4-26 shows the staging velocity trade for the 5 x 265 K HiPc orbiter and the five F-1 booster. The performance for these configurations is best for staging velocities of approximately 6000 fps. For lower staging velocities, the increased orbiter propellant load results in a significant increase in orbiter tank dry weight. Also, at these lower staging velocities the dynamic pressure is high, which is undesirable for separation and orbiter ascent performance. At the high end of the staging velocity range, the orbiter tank weight is favorably reduced, but the gross liftoff weight (GLOW) and booster dry weight increases because of the increased booster propellant load. These cases are then forced to a low thrust-to-weight ratio for the four F-1 case, but the five F-1 booster has a margin in this respect except for the use of J-2S orbiters for Mark II (Figure 4-25).

After the 6000 fps staging velocity was selected for further trades on orbiter propulsion, the data of Figure 4-27 were obtained. These data show the GLOW and total system empty weight for seven cases of four- and five-orbiter engines of the two thrust levels, 230 K lb and 265 K lb. The 4 x 230-K lb case would not run for the four F-1 booster. Figure 4-28 shows the Mark I polar mission performance for these seven cases. The cases with J-2 engine for Mark I with a 230 K HiPc Mark II show a substantial performance degradation over the J-2S version of orbiter. The comparison between four or five J-2S engines reveals that the five-engine system shows a Mark II performance improvement (lower GLOW with approximately the same dry weight). There is a significant reduction in performance for the Mark I five-engine orbiters. The increased orbiter thrust-to-weight ratio (T/W) reduces Mark II similar size for the five-engine orbiter. However, the increased T/W for the Mark I polar mission does not give a corresponding gain; thus, a payload reduction results. For these reasons and the orbiter base design and trim considerations, the four-engine orbiter with J-2S thrust level is superior technically. The five F-1 booster is selected

Table 4-17. LO_2/RP Reusable Booster Matrix

Case	Orbiter	Orbiter Prop.				Booster	
		Eng	No	MR	TH	B-18-	F-1
B-4-4	Mark II	HiPc	4	6	265	G	4
	Mark I	J-2S	4	6.0			
	Mark I	J-2S	4	5.5			
F-4-5	Mark II	HiPc	4	6	265	E	5
	Mark I	J-2S	4	5.5			
C-5-4	Mark II	HiPc	5	6	230	G	4
	Mark I	J-2	5	5.5			
E-5-5	Mark II	HiPc	5	6	230	E	5
	Mark I	J-2	5	5.5			
D-5-4	Mark II	HiPc	5	6	265	G	4
	Mark I	J-2S	5	5.5			
F-5-5	Mark II	HiPc	5	6	265	E	5
	Mark I	J-2S	5	5.5			
A-4-4	Mark II	HiPc	4	6	230	G	4
	Mark I	J-2	4	5.5			
E-4-5	Mark II	HiPc	4	6	230	E	5
	Mark I	J-2	4	5.5			
K-4-5	Mark II	J-2S	4	5.5	265	E	5
	Mark I	J-2S	4	5.5			
M-1	Mark II		4	5.5	265	G	4
	Mark I	J-2S		5.5			
-2	Mark II		4	5.25	260		
	Mark I	J-2S		5.25			
-3	Mark II		4	5.0	255		
	Mark I	J-2S		5.0			
N-1	Mark II	HiPc	4	6	296.7	G & E	4/5
-2	Mark II	HiPc	4	6	330		
-3	Mark II	HiPc	4	6	360		

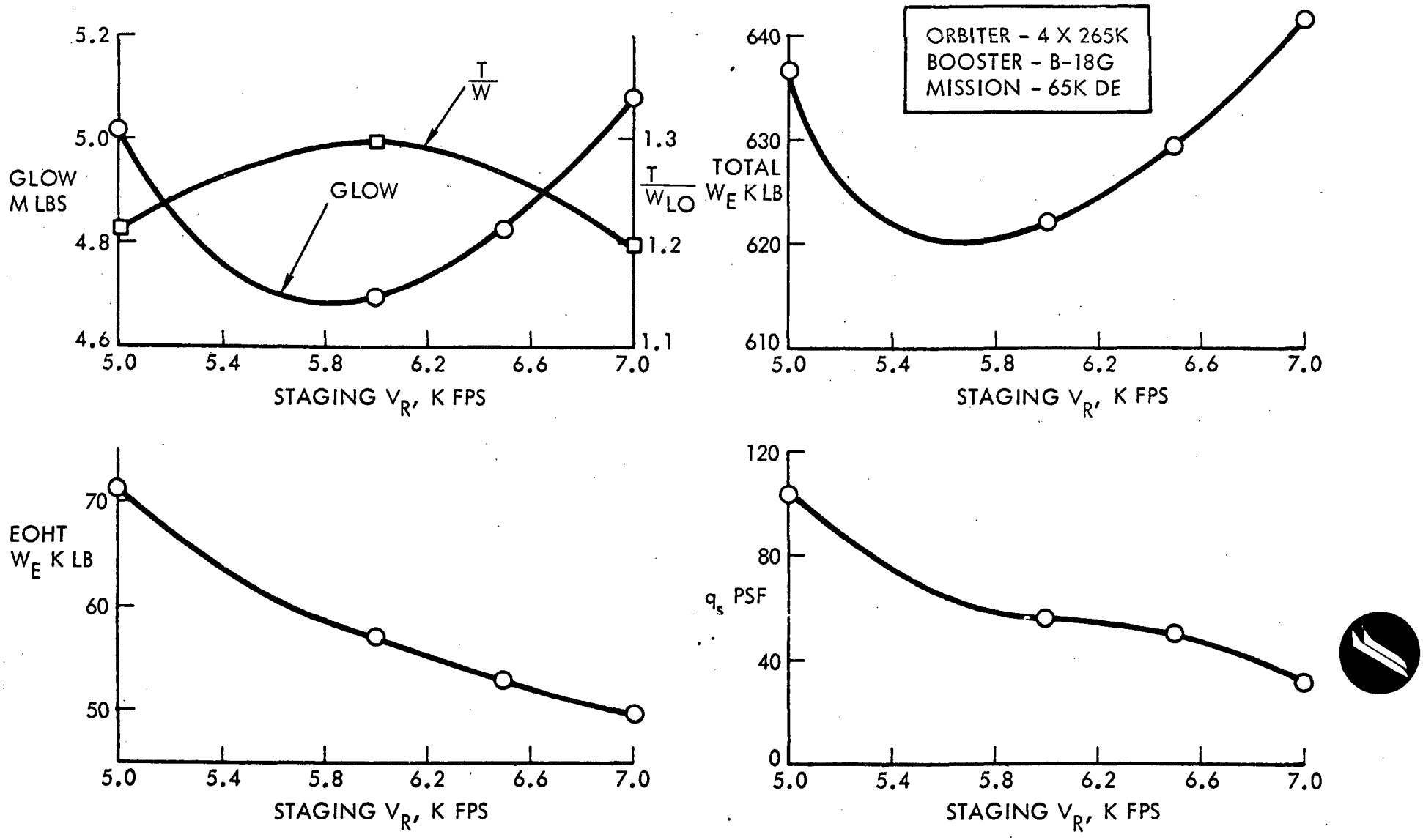

Figure 4-23. Mark II Sizing, 4F-1 Booster

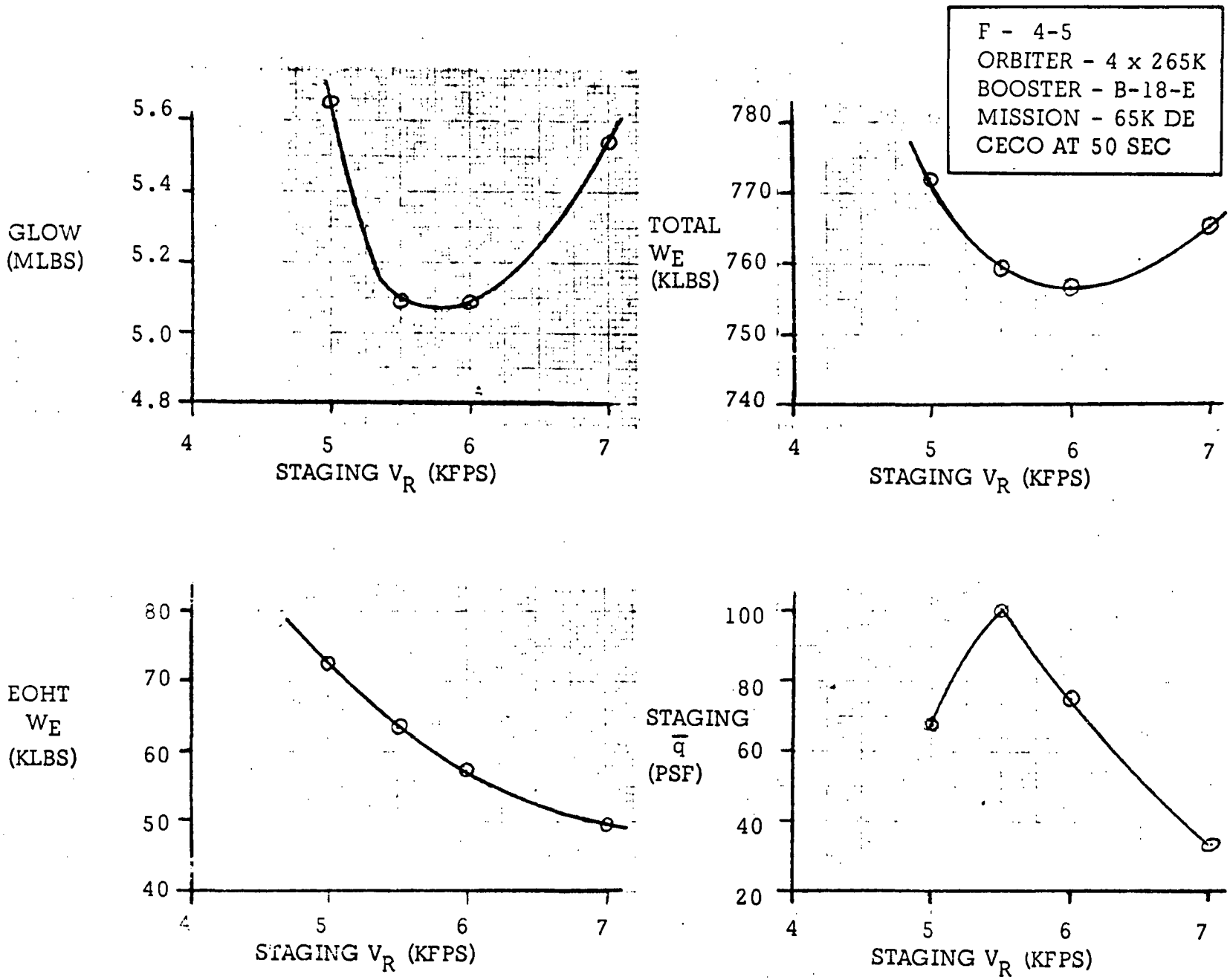

Figure 4-24. Mark II Sizing, 5F-1 Booster Staging Velocity Trade, J-2S/HiPc Orbiter

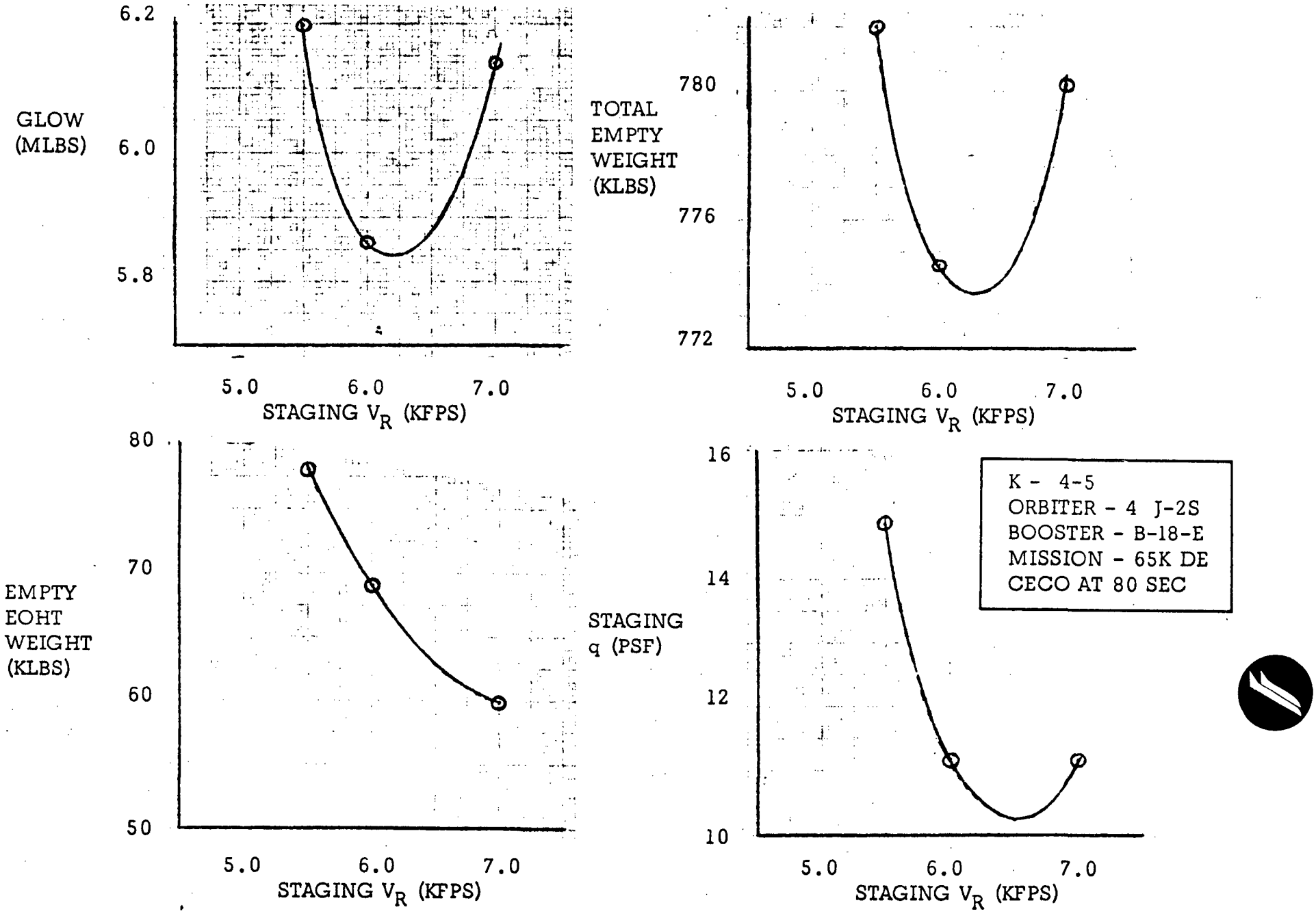

Figure 4-25. Mark II Sizing, 5F-1 Booster Staging Velocity Trade, J-2S Orbiter

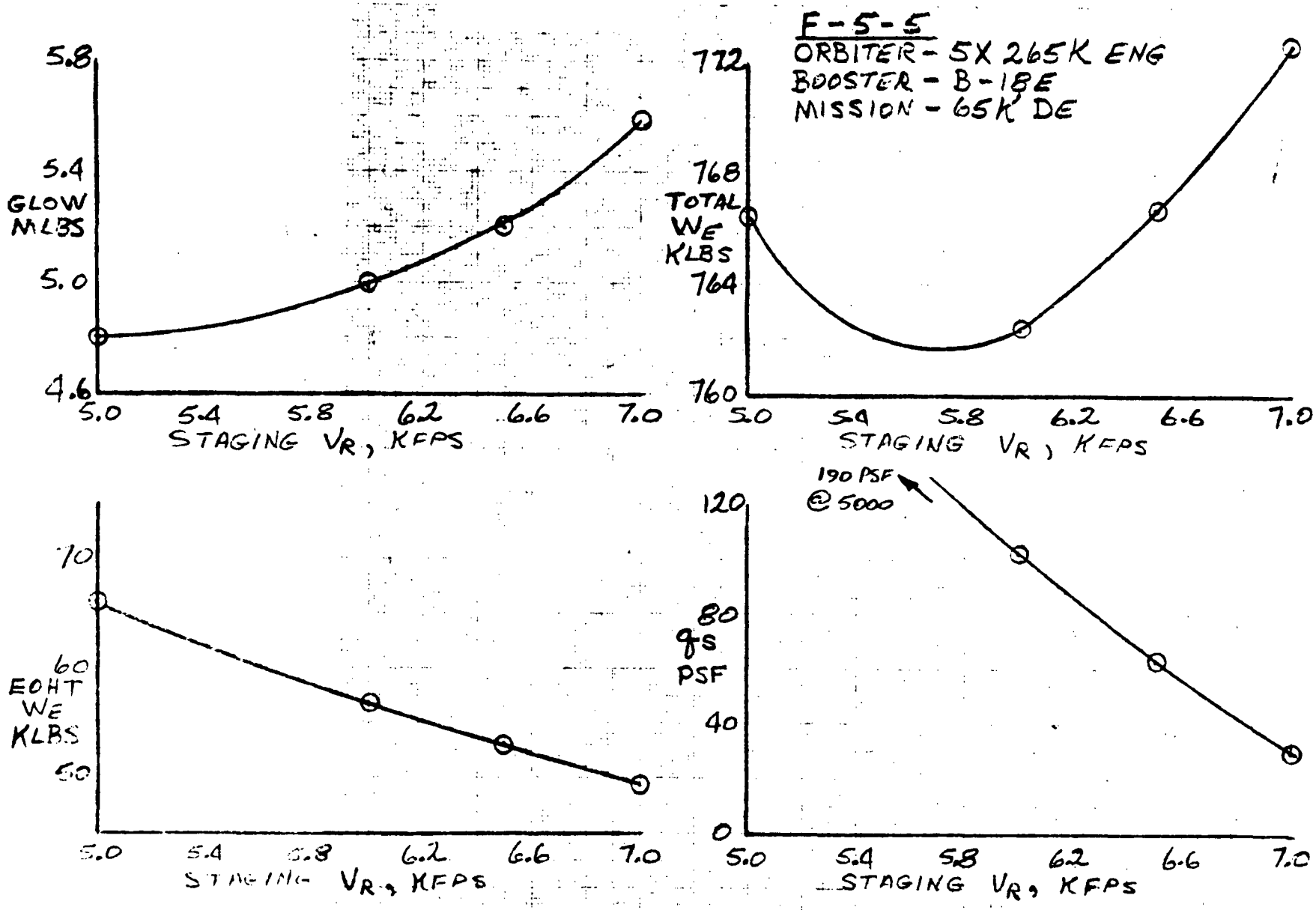

Figure 4-26. Mark II Sizing, 5F-1 Booster

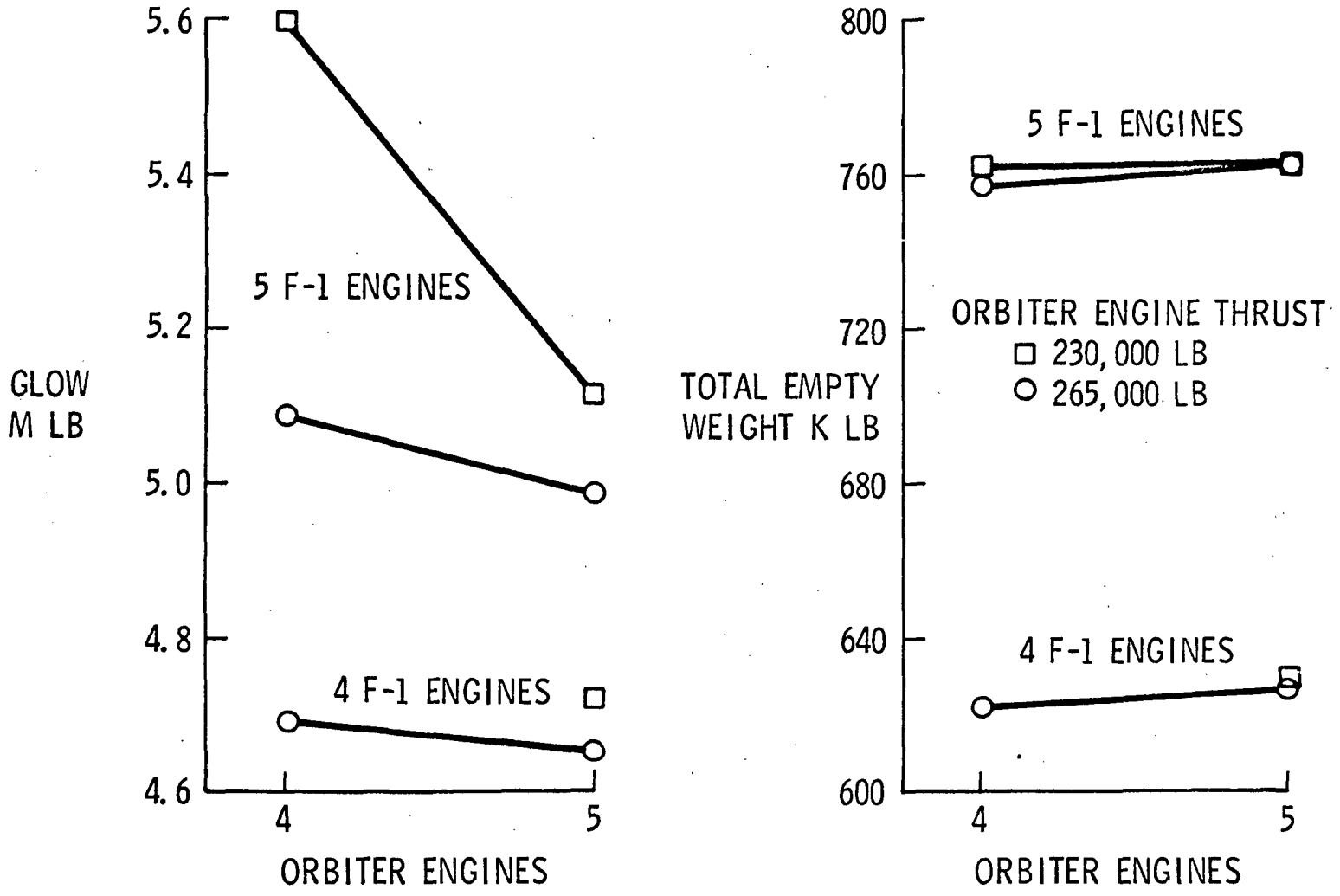

Figure 4-27. Mark II Sizing, 65K Due East Mission, Staging V_R = 6000 fps

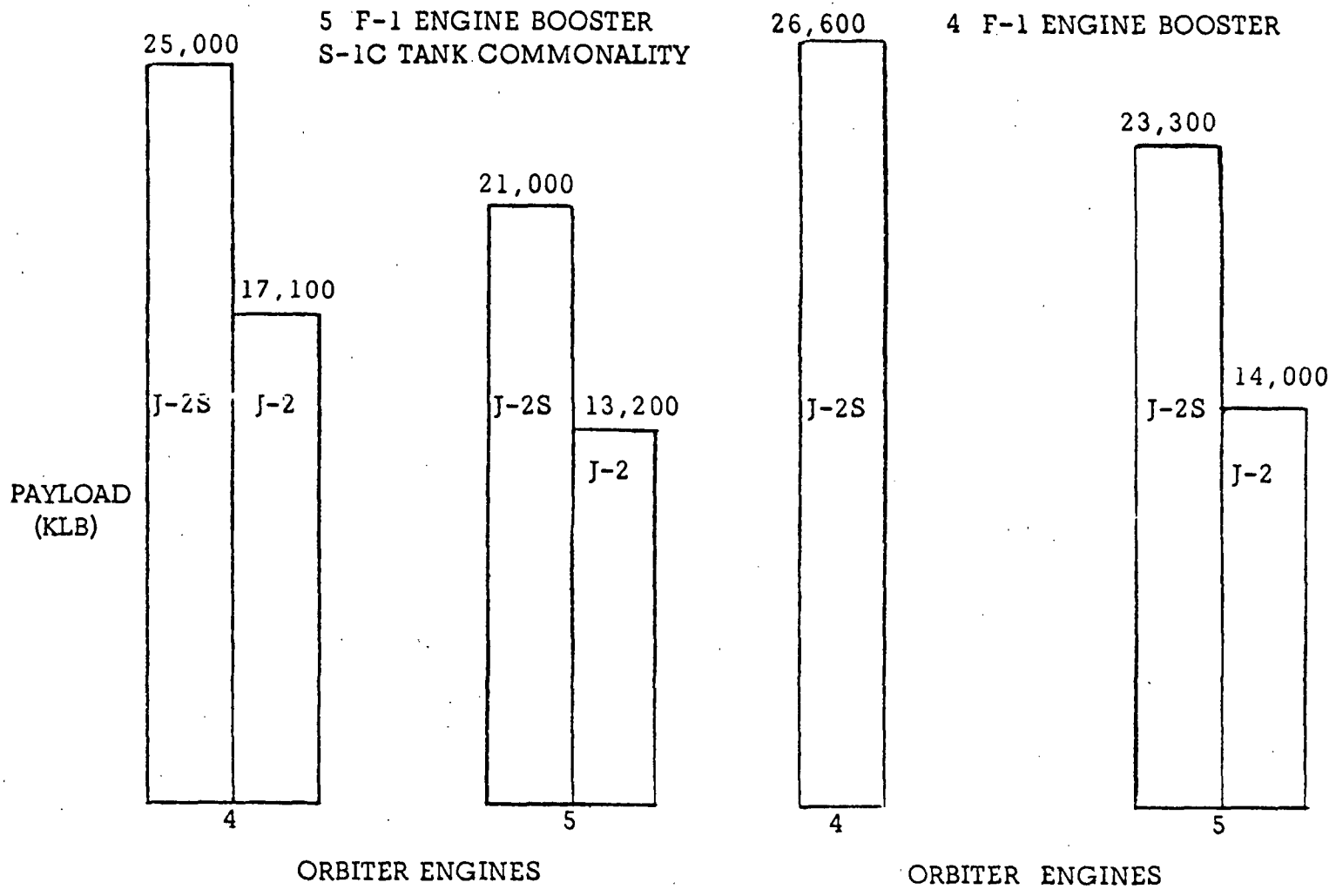

Figure 4-28. Mark I Polar Mission Payload Capability

over the four F-1 because of its increased commonality with the S-1C, pad abort capability with engine out, and built-in performance margins. The cost aspects of these configurations are discussed in Section 4.2.3.7. The booster performance of the foregoing sizing data was based on an early input that the F-1 engine would have throttling capability of 300 K at sea level. Figure 4-29 shows the throttling schemes used. The J-2S Mark II sizing, where the vehicle gross weights were increased substantially, was achieved without throttling. The requirement for throttling and its impact on orbiter/booster ascent loads ($q\alpha$, $q\beta$) are subjects of continuing investigation.

A trade study of orbiter MPS mixture ratios and thrust level was conducted and is represented in Figures 4-30 through 4-32. The orbiter mixture ratio is best at 6.0 because the orbiter external LO_2 hydrogen tank uses a heavy wall monocoque construction in the hydrogen tank. Thus, the increase in hydrogen volume for lower mixture ratios costs more in tank weight than the I_{SP} performance improvement will offset. Also, the data indicated that increasing the thrust level of the HiPc engines provided negligible benefit in terms of dry weight.

4.2.3.2 Aerodynamic Characteristics (LO_2/RP System)

The LO_2/RP system launch vehicle concept is an orbiter/EOHT second stage mounted tandem to a first-stage booster. The booster is a winged configuration manned for entry, flyback, and horizontal landing after separation at end boost.

The matrix of launch vehicle alternatives considered were boosters with four F-1 engines and five F-1 engines and orbiters with four and five engines of the J-2S and HiPc types. The size and shape of the various orbiters are the same and were determined from the HiPc engine performance. However, the five-engine booster design is larger than the four-engine booster configuration and, as a result, the launch vehicles with five engine boosters have approximately 15 percent higher drag than the launch vehicles with four-engine boosters.

Presented in Figures 4-33 and 4-34 are curves showing, respectively, the forebody axial force coefficient versus Mach number and the power-on booster base axial force versus altitude for the four- and five-booster engines launch configurations. The aerodynamic data for these configurations are based on predictions made by NR and GDC in-house and DATCOM methods and correlated with available wind tunnel test data to account for differences between the configuration tested and the configuration to which the data apply.

All configurations are static longitudinally and directionally stable throughout the boost Mach range, and engine gimbal provides sufficient thrust vector control for roll stability.

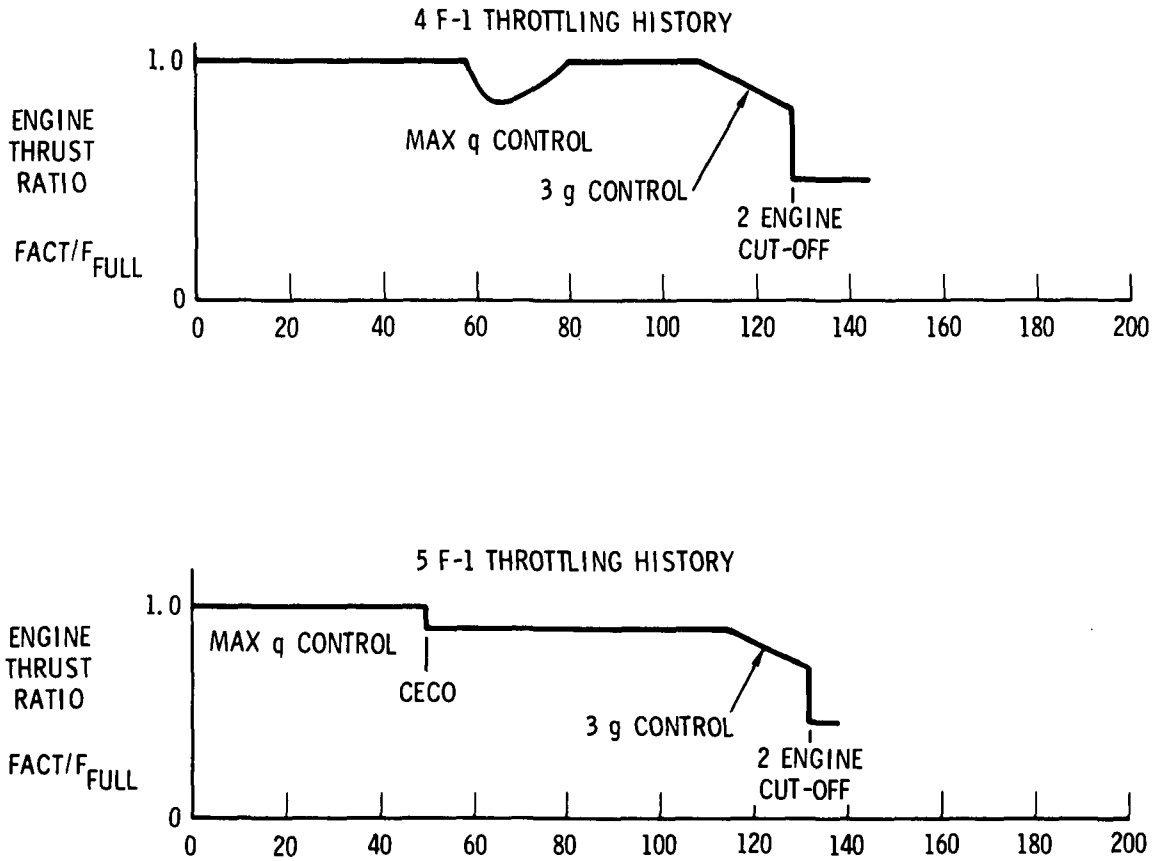

Figure 4-29. Throttling History

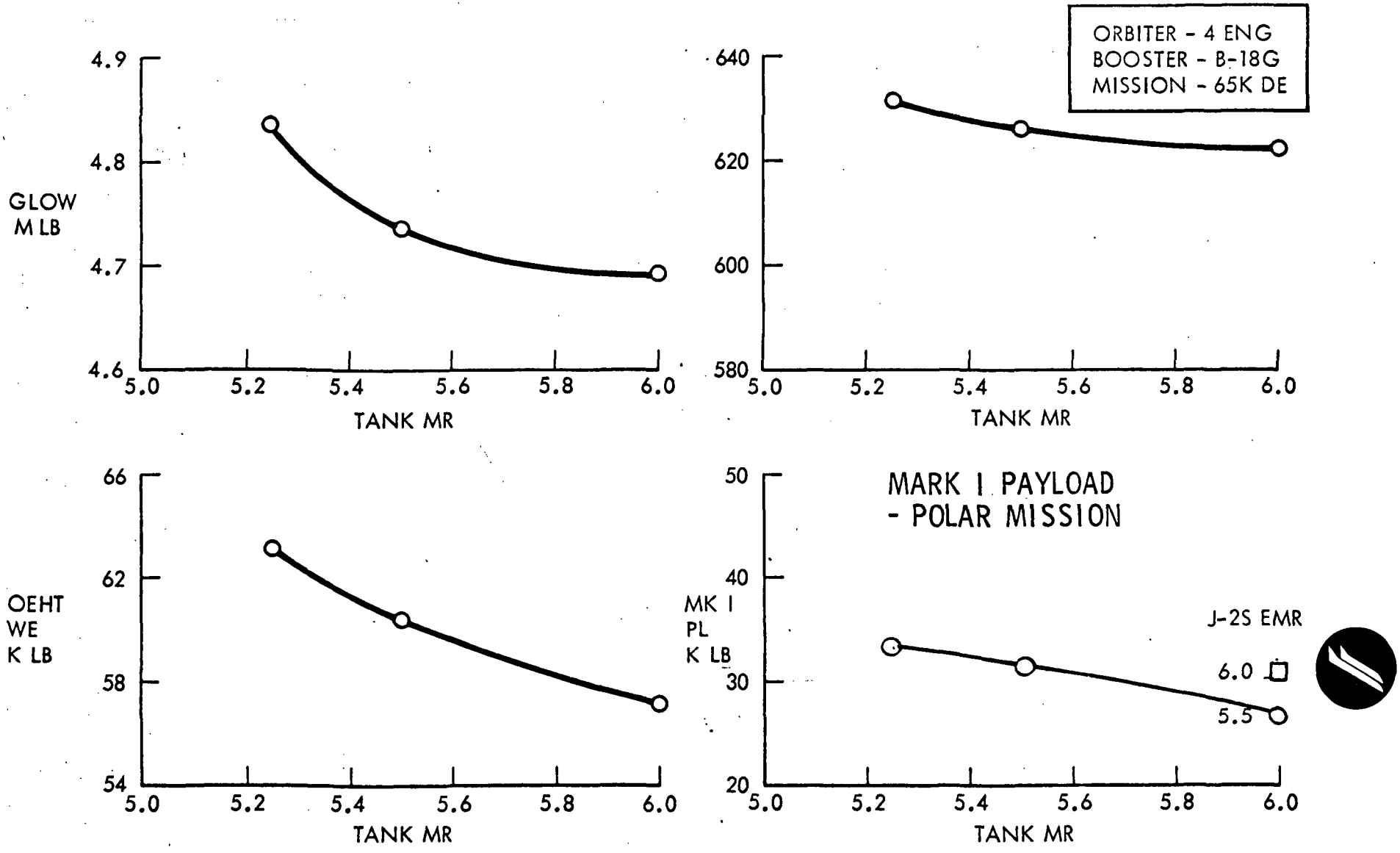

Figure 4-30. Orbiter Mixture Ratio Trade

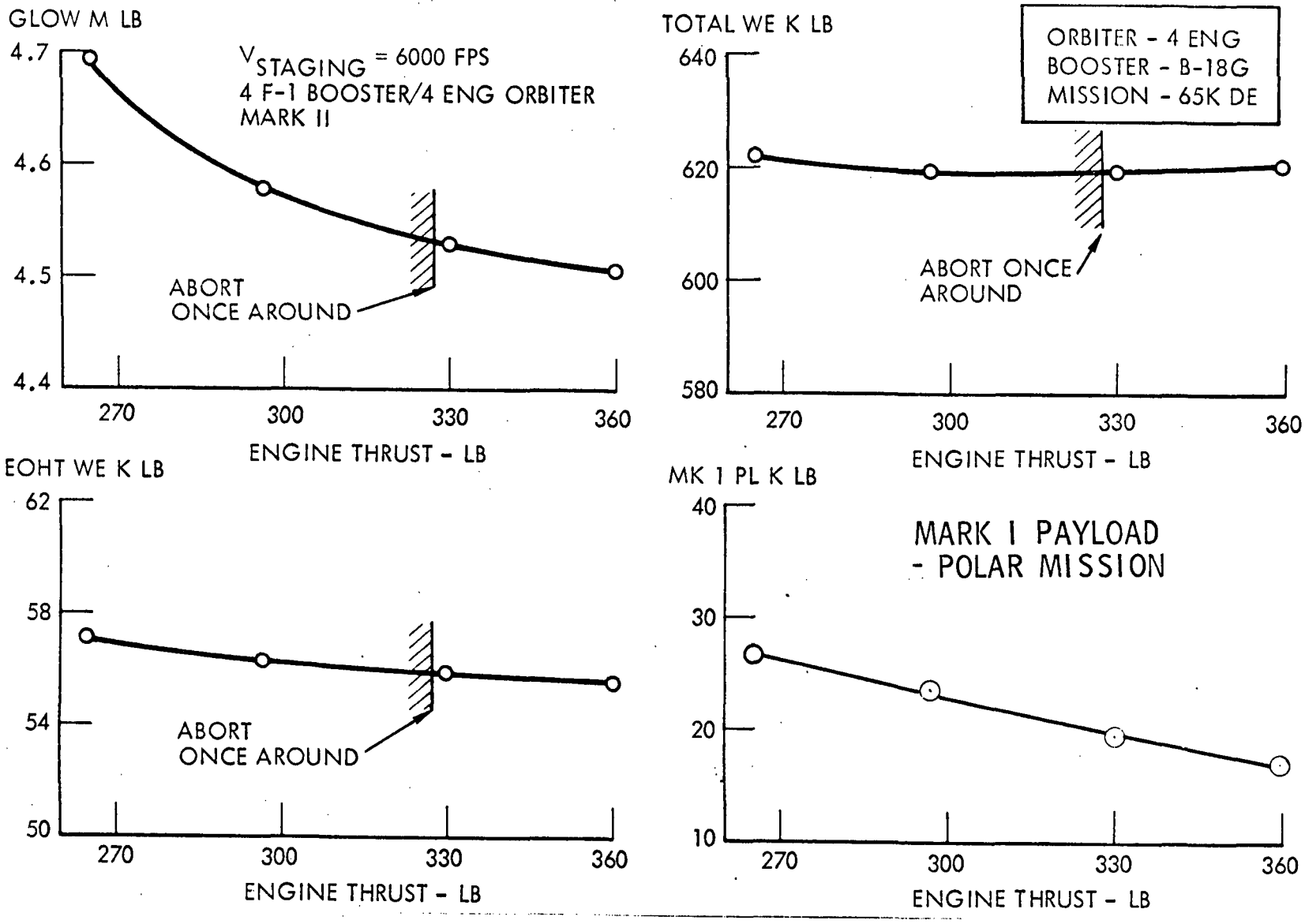

Figure 4-31. HiPc Engine Thrust Level Trade

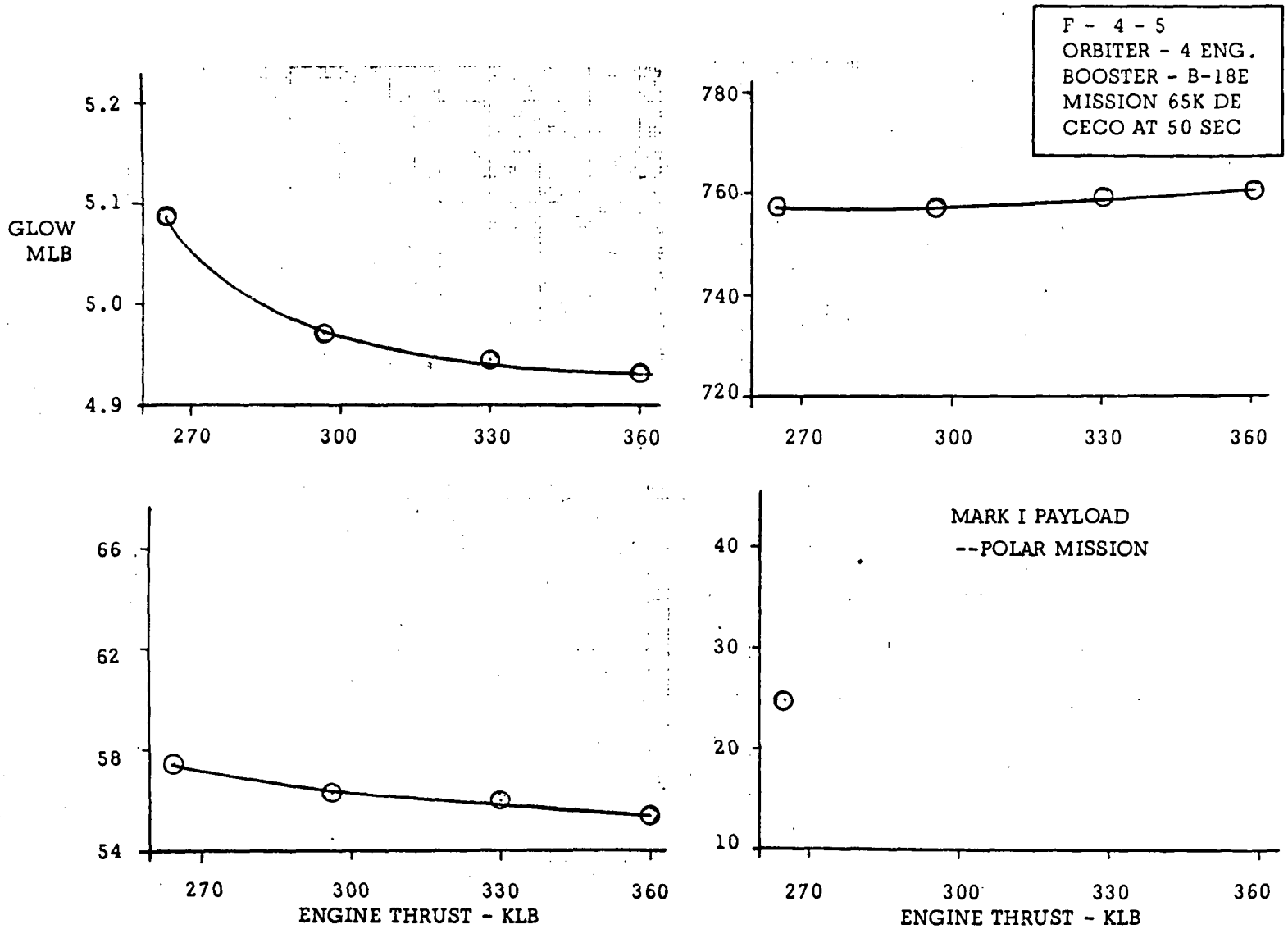

Figure 4-32. HiPc Engine Thrust Level Trade, Staging V_R = 6000 fps

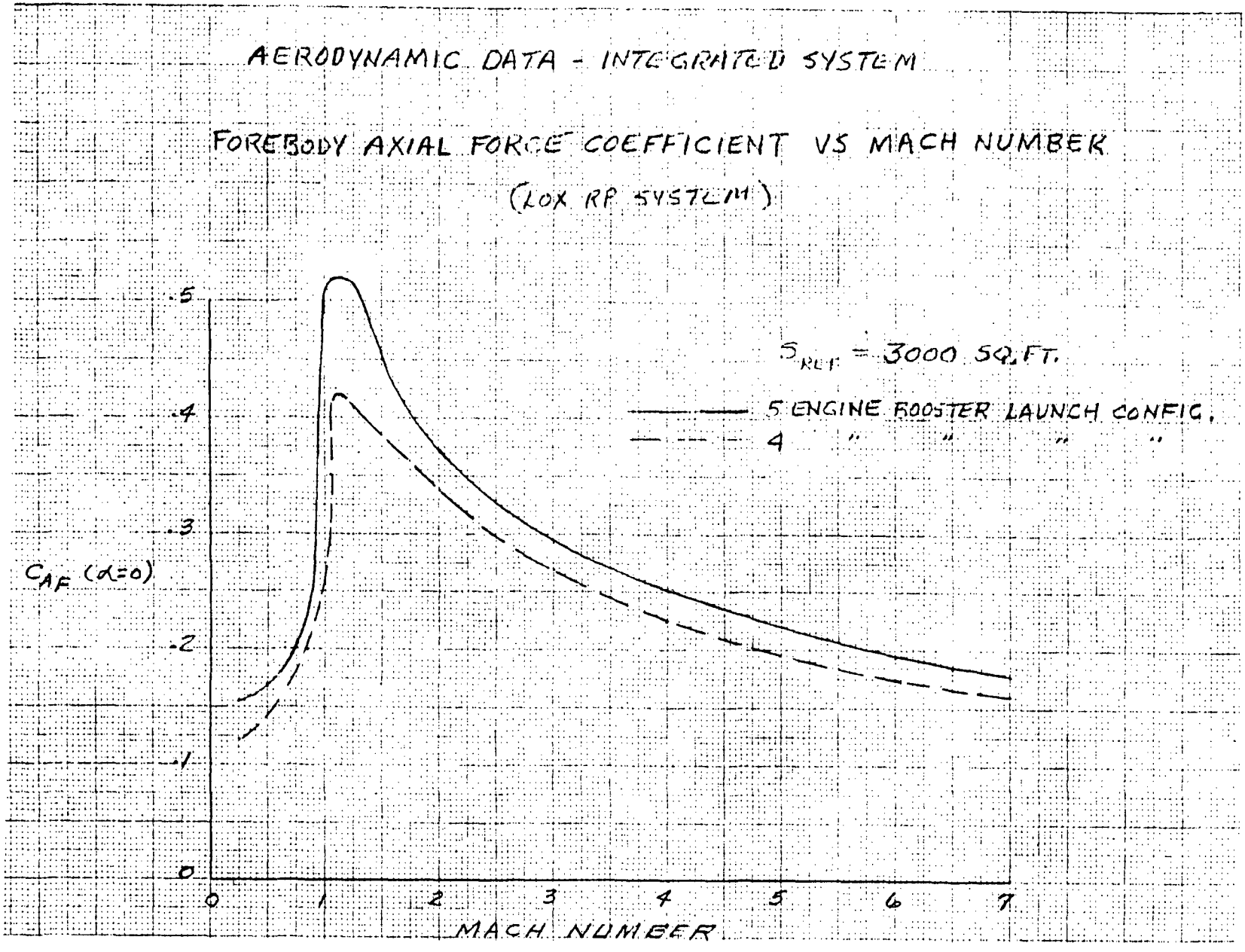

Figure 4-33. Axial Force Characteristics

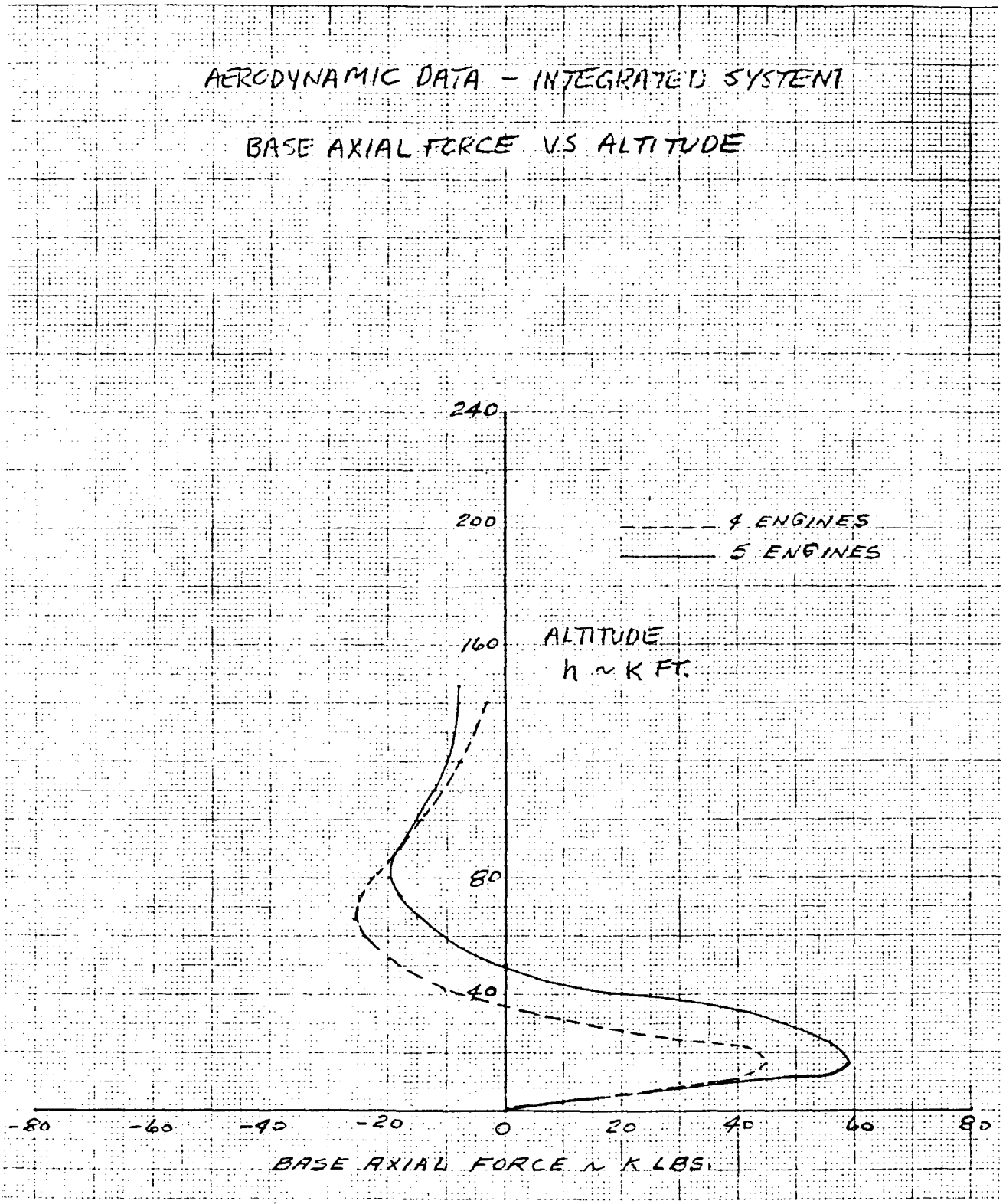

Figure 4-34. Power-On Base Force Characteristics

4.2.3.3 Ascent Trajectory, Control, and Separation Trade Studies

The ascent trajectory model in the sizing simulation uses a gravity turn for booster ascent and optimum pitch plane steering during orbiter flight. Earlier Phase B configurations had exhibited a significant performance effect when a more realistic booster ascent was assumed incorporating c. g. offset and aerodynamic moment trim (lifting trajectory). The tandem mated configuration c. g. offset is equivalent to only a degree of thrust vector deflection on the average. Thus, the performance effect is expected to be small. A check of these effects is made with an earlier tandem mount LO_2-LH_2 flyback booster with similar c. g. relationships. These results indicate a 1200-lb increase in payload (polar mission) for the lifting-trajectory case ($\alpha = 0$) over the gravity-turn case then the booster was flown in an inverted attitude (booster down, orbiter up). When the $\alpha = 0$ lifting trajectory was run with the booster in an upright attitude (booster up, orbiter down), the payload capability was 500 pounds less than the gravity turn. Similar results obtained by a Honeywell control simulation indicate performance is possibly less sensitive than shown here.

The preferred ascent orientation of the booster and orbiter is determined by considerations other than performance. While the booster-up, orbiter-down orientation is less efficient (payload degradation of 1700 pounds or less), there are four other considerations that favor this orientation:

1. Orbiter abort — For abort during booster ascent, the orbiter would fly with the thrust vector cant (control toward the tank to follow the c. g.) oriented to lift the trajectory.

2. Orbiter ascent — During orbiter ascent, optimum steering results in orbiter thrust vector orientations of approximately +10 degrees. The orbiter will achieve this condition at zero degrees in the inverted position or 20 degrees in the orbiter-up position. The reduction in orbiter angle of attack of 20 degrees after staging will tend to balance the booster penalty for this orientation.

3. Orbiter separation — The orbiter/booster separation concept is to maneuver the orbiter tail away from the booster. For the inverted orientation, this results in maneuvering the orbiter toward positive angles of attack which are correct for orbiter ascent flight.

4. Booster entry — The booster orientation is correct for the required positive angle of attack entry after apogee.

While roll maneuvers could be used to accomplish some of the required orientations, a booster-up, orbiter-down ascent is recommended, especially in the case of the 5 x F-1 engine booster since ascent propellant can be increased without increasing tank size.

Booster control requirements were determined for the preferred LO_2-RP system. Two ground rules were imposed: to use the F-1 engine and the F-1 engine actuator without modification. This results in a 6-degree gimbal limit in pitch and yaw with a 5-degree-per-second rate capability. A third ground rule was to design the integrated vehicle to a structural loading criterion characterized by the shuttle Phase B criteria of maximum $\bar{q}\alpha$ and $\bar{q}\beta$ of 2800 and 2400 psf-degree, respectively. The impact of greater $\bar{q}\alpha$, $\bar{q}\beta$ design limits on orbiter and booster is being investigated. Five conditions were evaluated to determine the gimbal requirements for thrust vector control. They are to (1) track the c. g. of both the integrated boost vehicle and the booster alone (in case of abort); (2) trim the vehicle in the event of an engine failure; (3) trim the vehicle in the event of an actuator failure; (4) allow for control of dynamic overshoots, bending, and slosh response; and (5) set vehicle trim requirements at maximum $\bar{q}\alpha$ and $\bar{q}\beta$. Results of control studies are presented in Section 4.4.1.4.

Two engine-location patterns were examined: a diamond and a square. The diamond pattern (all engines located in either the Y or Z axes) is preferable for control system mechanization in that if an engine fails, the gimbal command algorithm is a simpler mechanization. The square pattern (engine location 45 degrees from the Y or Z axes) is preferable from a base configuration (area) standpoint, commonality with the S-1C configuration, and for landing clearance. Thus the square pattern was selected as the baseline.

Three basic booster/orbiter separation and interface configurations were studied: (1) an expendable interstage that is dropped at staging; (2) a reusable interstage that returns with the booster; and (3) a fixed interstage that stays with the orbiter external tank (Figure 4-35). For the expendable interstage, two booster designs were considered: a sharp nose and blunt nose design. For the reusable interstage, several concepts were evaluated. These are shown in Figure 4-36. Table 4-18 presents the weight tradeoffs for the interstage, orbiter tank, and booster. The study results converted to a common basis of increased in-system GLOW for constant performance are shown in Figures 4-37 through 4-39. It is seen that the blunt nose booster-expendable interstage provides the maximum GLOW advantage. The reusable interstage has attractive operational features in that no parts are dropped at staging. However, the load distribution effects on the orbiter tank of the 4- or 6-point concentrated load cost more in tank weight than the retention of a uniform load interstage with the tank. The expendable interstage is selected as baseline with the operational mode of retaining the interstage with the orbiter until the interstage impact point is acceptable. Further studies of reusable interstage concepts will consider a requirement that the load distribution be uniform on both the booster and orbiter sides of the interface.

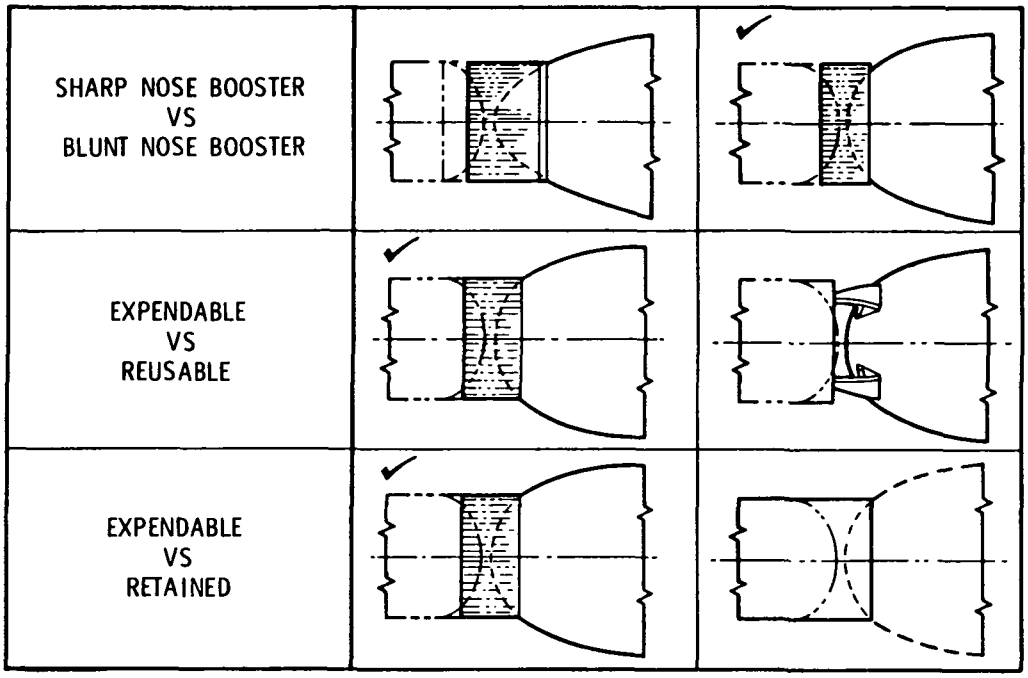

Figure 4-35. Expendable Versus Reusable Adapter

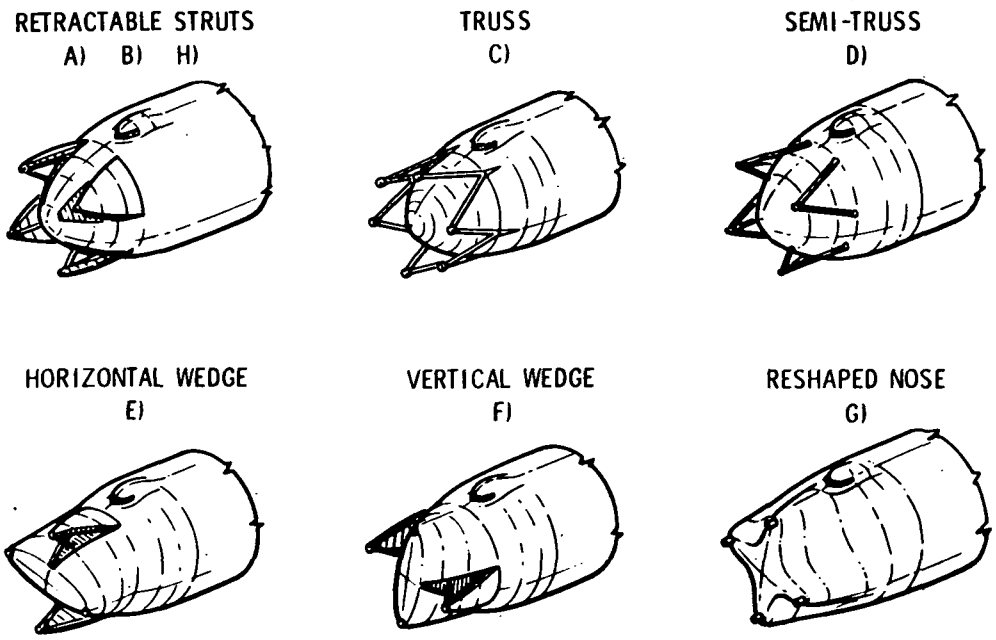

Figure 4-36. Reusable Adapter Concepts

Table 4-18. Weight Tradeoffs

CONCEPT	LOAD AT ORBITER INTERFACE	LOAD AT BOOSTER INTERFACE	INTERSTAGE WEIGHT (LB)	WEIGHT EFFECT ON ORBITER TANK (WEIGHT OF SKIRT + 100 IN. OF TANK)	WEIGHT EFFECT ON BOOSTER
1. EXPENDABLE ADAPTER					
A) BOOSTER EJECT	UNIFORM	UNIFORM (SHARP NOSE)	4,780	4,900	13,693
B) BOOSTER EJECT	UNIFORM	UNIFORM (BLUNT NOSE)	3,230	4,900	11,827
C) ORBITER EJECT	UNIFORM	UNIFORM (SHARP NOSE)	4,780	4,900	13,693
D) ORBITER EJECT	UNIFORM	UNIFORM (BLUNT NOSE)	3,230	4,900	11,827
2. REUSABLE ADAPTER					
A) RETRACTABLE STRUTS (SHORT)	4 POINT	SEMI-UNIFORM		11,356	22,319
B) RETRACTABLE STRUT (LONG)	4 POINT	SEMI-UNIFORM		11,356	29,565
C) FIXED TRUSS	6 POINT	6 POINT		12,000	42,629
D) FIXED SEMI-TRUSS	4 POINT	12 POINT		11,356	38,219
E) HORIZONTAL WEDGE	4 POINT	SEMI-UNIFORM		11,356	25,990
F) VERTICAL WEDGE	4 POINT	SEMI-UNIFORM		12,775	23,448
G) RESHAPED NOSE	4 POINT	UNIFORM		12,775	49,984
H) RETRACTABLE STRUT BLUNT NOSE	4 POINT	SEMI-UNIFORM		11,356	18,084
3. RETAINED INTERSTAGE					
A) ORBITER RETAIN	UNIFORM	UNIFORM (SHARP NOSE)		9,680	13,693
B) ORBITER RETAIN	UNIFORM	UNIFORM (BLUNT NOSE)		8,130	11,827

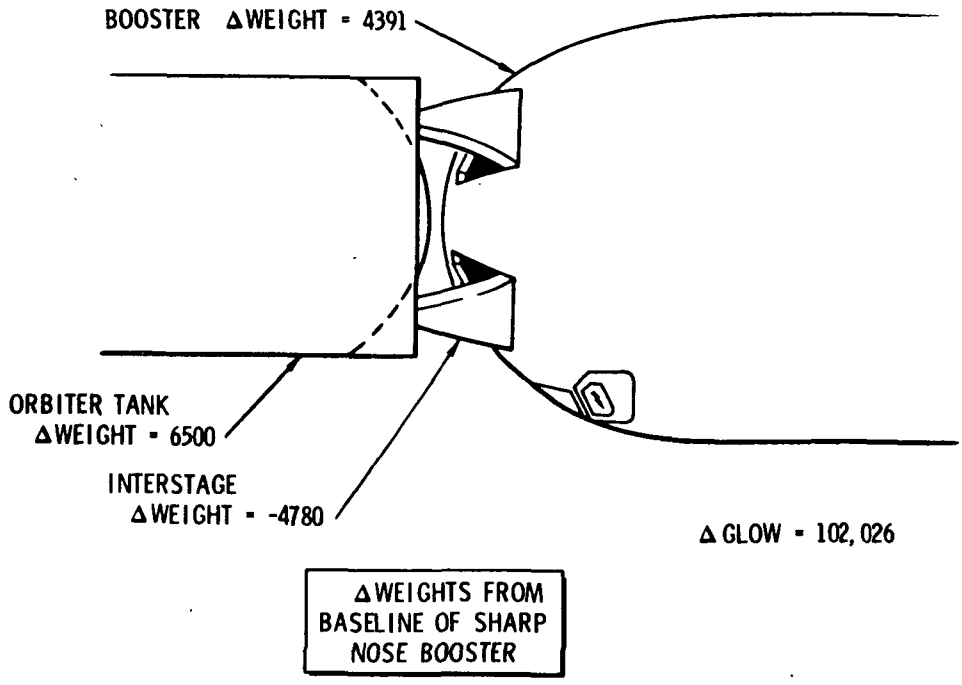

Figure 4-37. Reusable Adapter Retractable Strut - Blunt Nose

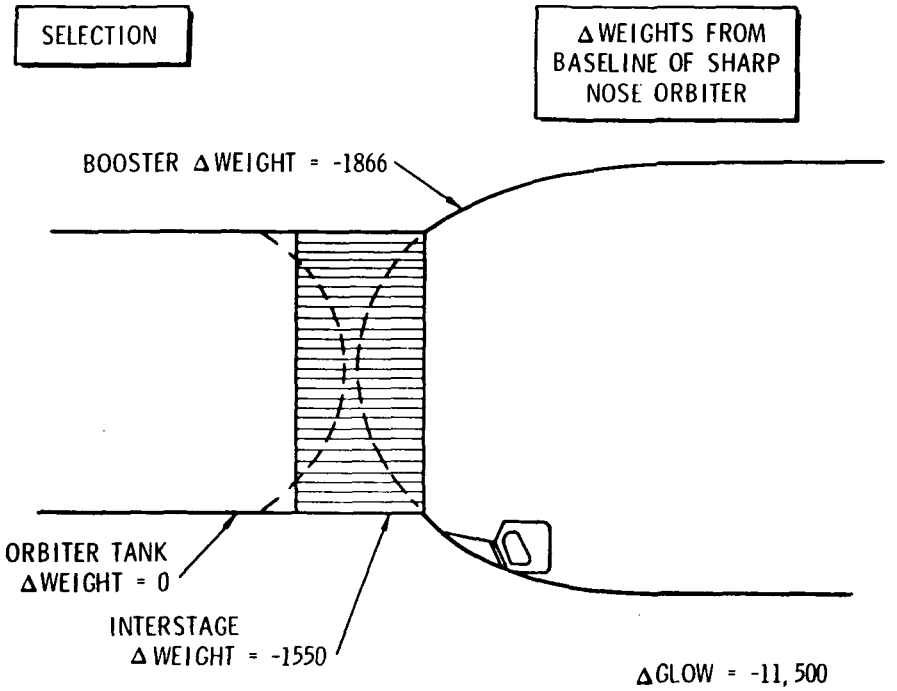

Figure 4-38. Expendable Adapter Orbiter Dual Plane Separation

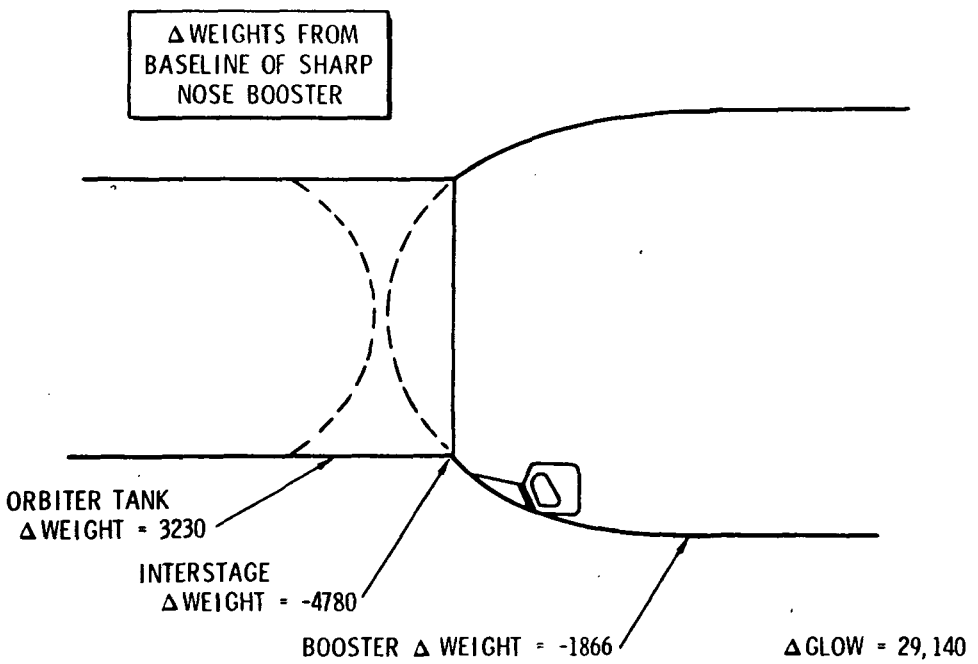

Figure 4-39. Expendable Adapter Interstage Retained With Orbiter Tank

In connection with orbiter tank configuration tradeoff studies, the tank/booster separation characteristics of the baseline design (LO_2 forward, hydrogen aft) was compared with that of a LO_2 aft, hydrogen forward tank (see description in Section 3.6). Figure 4-40 shows comparative separation clearance paths. Separation of the LO_2 aft design is considered marginal at best because of the distance while the booster nose is forward of the orbiter tail. Figure 4-41 depicts the separation trajectory of the baseline concept relative to the booster nose. Study is continuing in this area to improve clearances and to develop local design details.

4.2.3.4 Abort Modes

Abort situations during mated flight present three major performance requirements: (1) separation of the orbiter from the disabled booster (the failure is assumed to be in the booster system); (2) intact recovery of the booster; and (3) intact recovery of the orbiter. Because of the tandem arrangement of the booster and orbiter propellant tank, the first of these may present significant problems. The basic requirement for desirable separation is that the orbiter plus tank have a higher plus-x (or lower minus-x) acceleration than the booster. Since gravity acts equally on both vehicles, the required relative acceleration must be produced by the thrust and aerodynamic force differences. However, the booster engines cannot be totally shut down because they are required to deplete the remaining propellant and they do not have restart capability.

Consider, for example, an abort situation at approximately T + 20 seconds. Immediate ignition of the orbiter engines and advancing the throttles to 109 percent EPL would provide the orbiter plus tank with a load factor (T-D/W) of approximately 0.8. After shutdown of three of the booster's five engines and 20 percent throttling of the remaining two, the booster load factor would be approximately 0.65. A separation acceleration of approximately 0.15 g's (4.8 ft/sec^2) would therefore exist, and theoretically the vehicles could be separated and flown back to the launch site. Now consider an abort situation at approximately T + 40 seconds. Because of the increased drag, the orbiter-plus-tanks load factor has reduced to 0.65 and, because of reduced weight, the booster load factor has increased to 0.78. A relative acceleration to provide separation is not available at this time (or until normal separation) without (1) shutting down more booster engines; (2) using retro rockets on the booster; or (3) using additional posigrade rockets on the orbiter. Abort separation studies are continuing to evaluate these possibilities.

Intact recovery of the reusable booster after a mated ascent abort is dependent upon the failure that justified the abort. However, if controlled flight is possible under rocket power, the procedure consists of burning the remaining propellant in a manner that does not exceed design conditions or

TANK CONFIGURATION NO. 1 & NO. 7

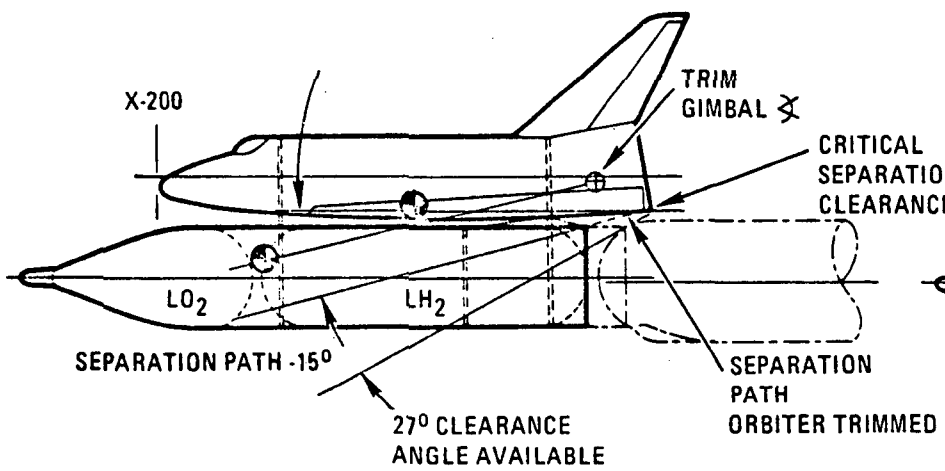

- SEPARATION DOES NOT REQUIRE ORBITAL PITCH MANEUVER

TANK CONFIGURATION NO. 12B

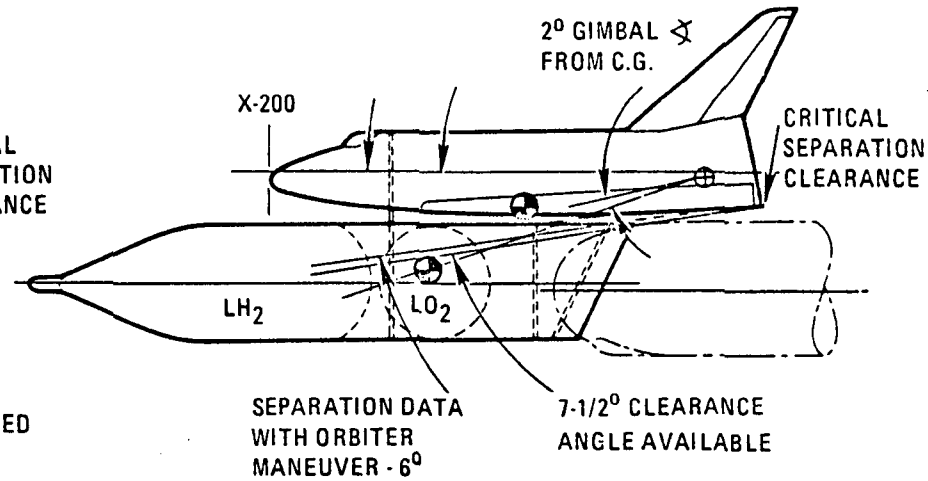

- SEPARATION REQUIRES ORBITAL NOSE DOWN MANEUVER

Figure 4-40. Booster Separation

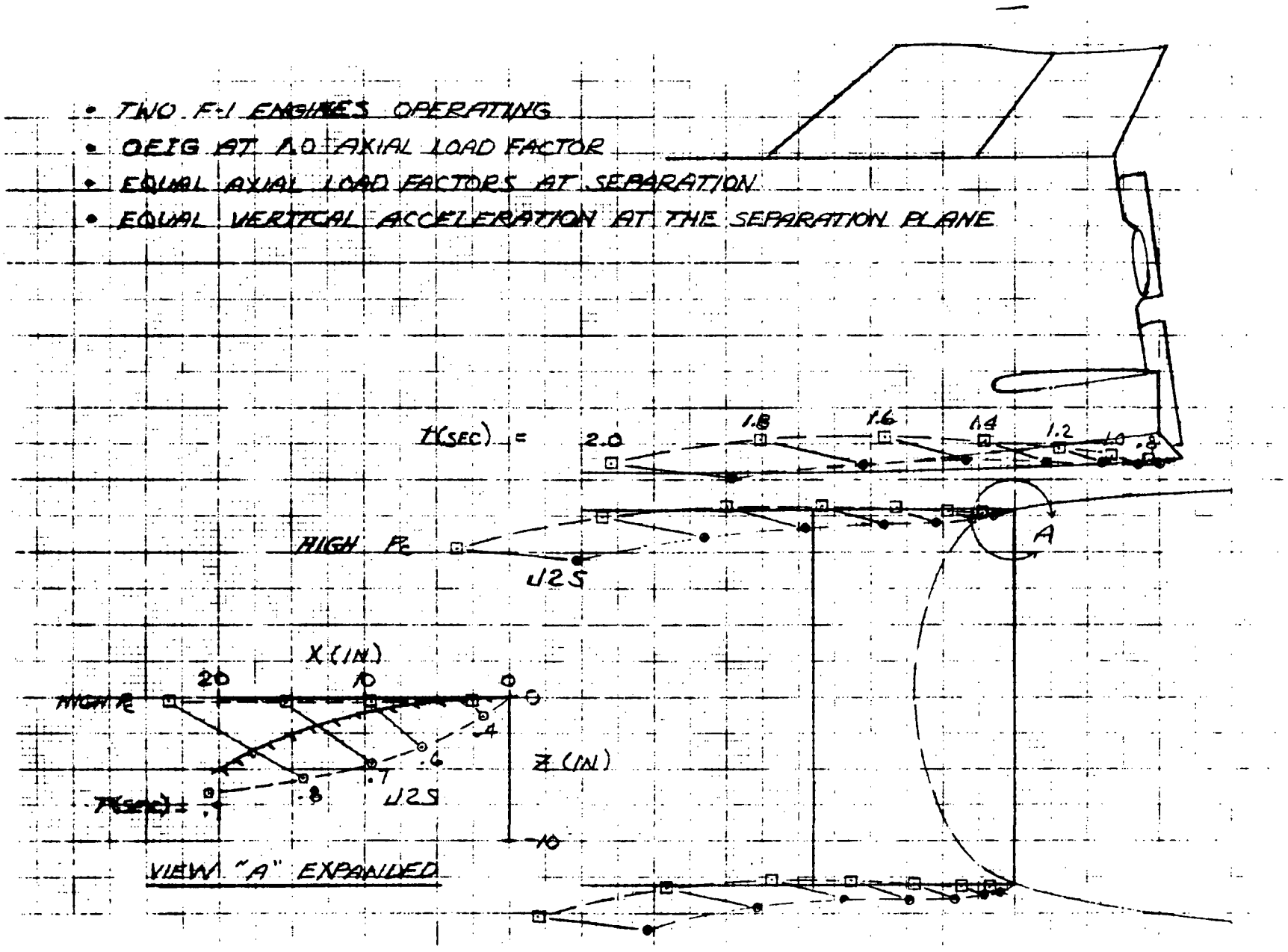

Figure 4-41. Separation Dynamics

produce excessive range and then flying back to the launch site with the air-breathing engine system (ABES).

The orbiter abort modes, procedures, sequences, etc., corresponding to the various LO_2-RP systems differ somewhat from those previously defined for HiPc LO_2/LH_2 systems. The differences are primarily because of basic sizing and configuration ground rules. The no-once-around-abort sizing ground rule is, of course, the most influential. This ground rule change results in the requirement for either return-to-launch-site or downrange abort modes at staging and for sometime thereafter and generally results in orbiter initial T/W's of less than 1.0. The orbiter engine size also contributes to the low T/W's. Conversely, the low initial orbiter T/W's eliminate the once-around abort capability with one engine out at staging.

Most of the available orbiter abort flight modes are adversely affected by low orbiter T/W's. That is, the time span of the no-abort regime immediately after liftoff is increased, the return-to-launch-site abort regime is shortened, the downrange abort regime is lengthened, and the beginning of the once-around abort regime is later. The orbiter T/W can be increased either by increasing the number or thrust level of the engines or by decreasing the propellant load (higher staging velocity). However, as discussed in Section 4.2.3.1, other considerations led to an orbiter configuration with an initial T/W of less than 1.0 and, consequently, lower abort capabilities.

The return-to-launch-site and downrange abort modes require use of the orbiter MPS to provide thrust for shaping the trajectory so that the orbiter can glide to a normal approach and landing at the launch site or another site after propellant depletion. Theoretically, aerodynamic lift can be used to assist the engines in extending the flight range and, therefore, lengthen the return-to-launch-site abort regime. However, the L/D and trim characteristics of the EOHT configurations, in addition to their relatively low normal load-carrying capabilities, have indicated that essentially exoatmospheric flight is more desirable. Thrust is used to maintain altitude, turn the velocity vector, and change the velocity magnitude.

A single alternate landing site may be selected for all downrange aborts initiated during launches within a finite launch azimuth range if the downrange abort mode is required. This site must be between approximately 1000 and 7000 nm downrange from the launch site and within approximately 1500 nm of the normal mission first pass ground track. For a due-east launch, several sites on the west coast of Africa between 30°N latitude and 30°S latitude would be available. For north polar and 55° inclination launches, sites would be available in the northern continental U.S. or southeast Canada.

4.2.3.5 Facilities Requirements

No trade analyses were performed in this area during this study period.

4.2.3.6 Test Requirements and Operations

The test philosophy for the LO_2/RP F-1 booster is the same as for the baseline presented for the Phase B booster.

No major trade studies were performed in this contract phase involving test requirements or operations. Results of the analyses performed derived the baseline LO_2/RP F-1 booster test program as described under Section 4.4.5.

4.2.3.7 Program Cost Comparisons

The total program costs for concurrent orbiter and booster development were evaluated for staging velocity mixture ratio, thrust level, and propulsion system trades. The program costs were developed for a concurrent program (flyback booster and orbiter development is concurrent) and a phased program (expendable S-IC used for 15 flights). These programs are shown in Figures 4-42 and 4-43. Figures 4-44 and 4-45 show results of the staging velocity trade studies for four and five F-1 boosters. While the four F-1 booster was lower in cost, the five F-1 was selected because of abort margins (See 4.2.3.1). The figures also show that use of the J-2S engine for Mark I and Mark II results in measurable cost benefits. The cost trends with staging velocity are heavily influenced by orbiter expendable tank weight. For low staging velocities, the larger size orbiter tank results in increased total program cost. This is especially true for the 5 x F-1 booster vehicle, which uses S-1C size tankage. Thus the booster weight variation with staging velocity is only that resulting from TPS and recovery elements (wing, landing gear, etc). A preliminary selection of a 6000 fps staging velocity was made. However, further studies have shown advantages of higher staging velocities, leaving this issue for further consideration. The cost comparison of four and five F-1 boosters and four- and five-engine orbiters with two thrust levels (230 K and 265 K) is presented in Figure 4-46. There is no significant advantage to the use of the 230 K (J-2 Mark I) engine over use of the 265 K (J-2S Mark I) engine. Also, there is no significant cost advantage for the use of five engines in place of four in the orbiter. Selection of a four-engine orbiter with the 265 K thrust level made on a technical basis is compatible with the cost tradeoffs.

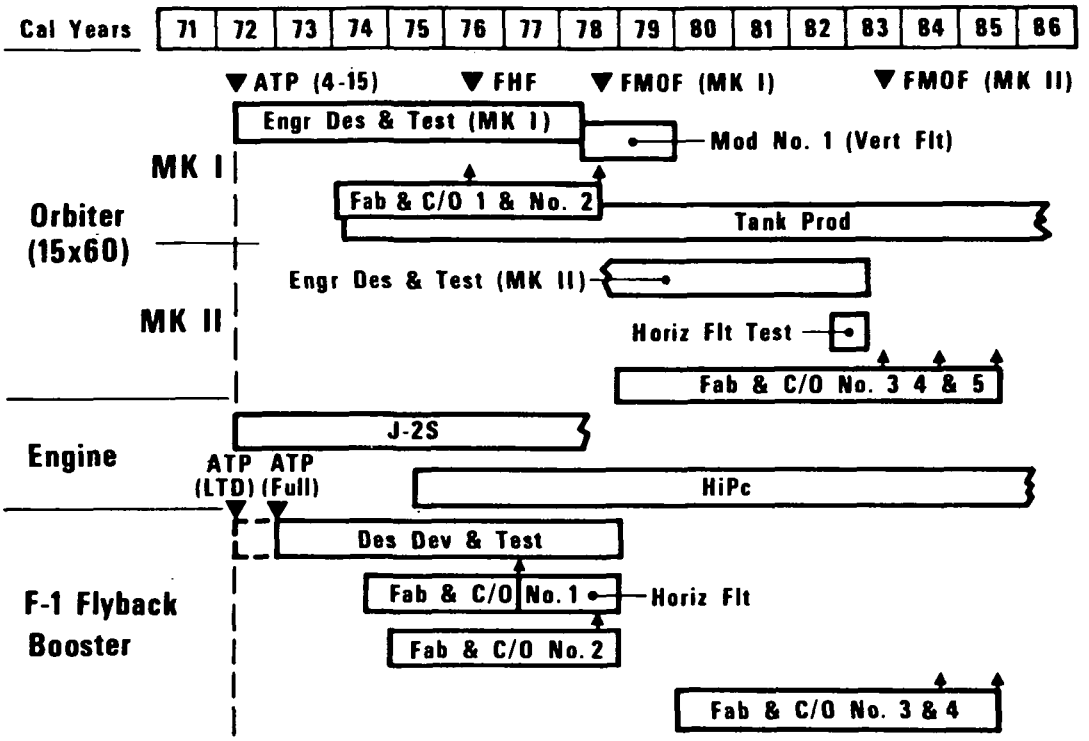

Figure 4-42. Program Schedule F-1 Flyback Booster

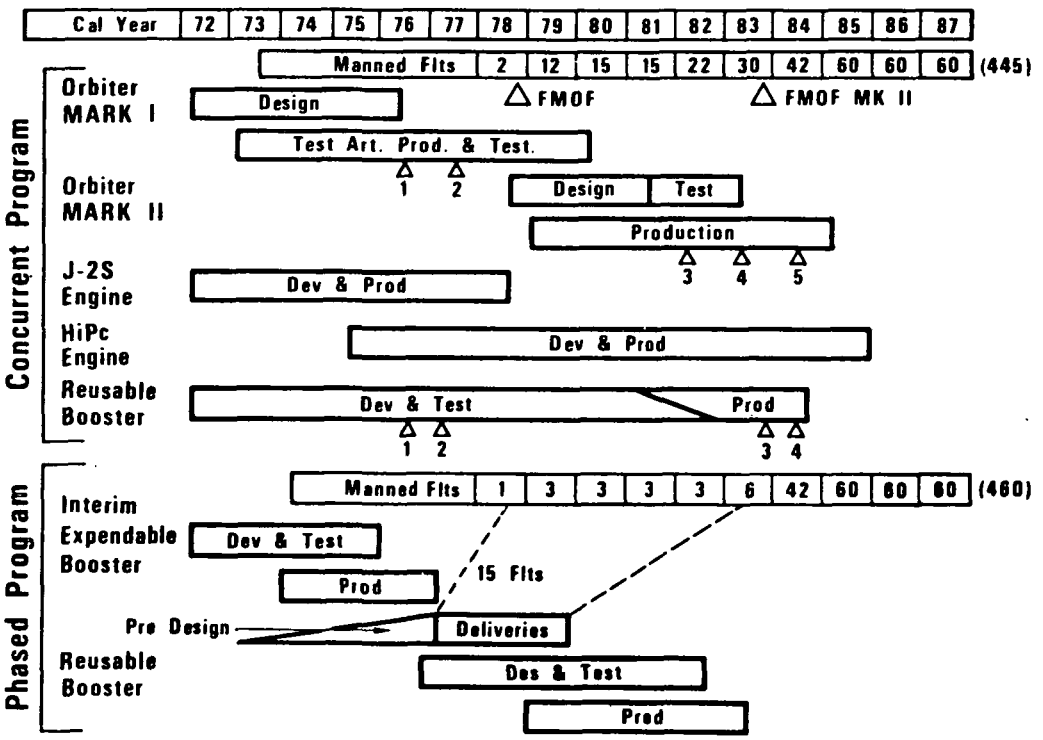

Figure 4-43. Concurrent Versus Phased Program Comparison

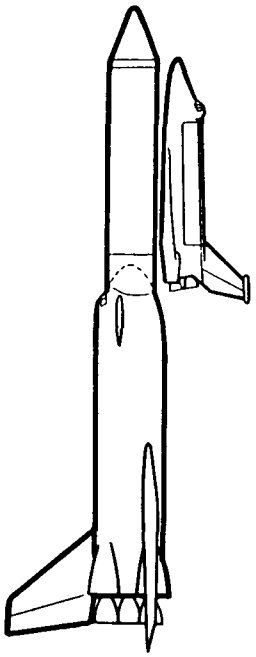

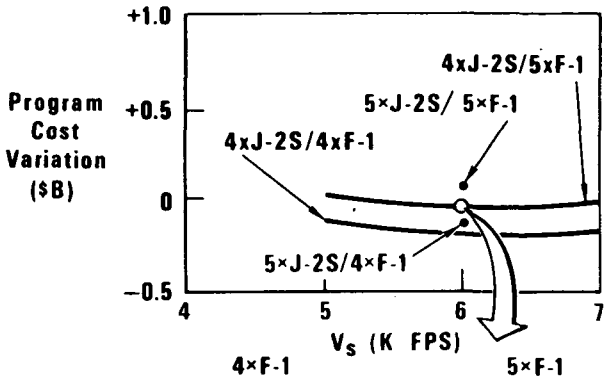

ITEM	MARK I	MARK II	MARK I	MARK II
GLOW $\bar{M}$ Lb	4.58	4.69	4.98	5.09
BLOW $\bar{M}$ Lb	3.58	3.58	3.97	3.97
OLOW $\bar{M}$ Lb	1.00	1.11	1.01	1.12
PL K Lb	27 (Polar)	65 (East)	25 (Polar)	65 (East)
ABORT	X	X	✓	✓
V_S (FPS)	6,300	6,000	6,200	6,000

Figure 4-44. F-1 Flyback Booster/J-2S to HiPc Orbiter

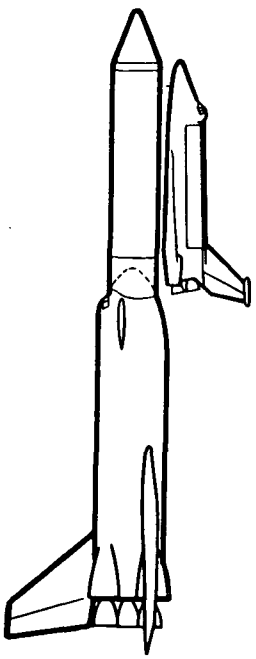

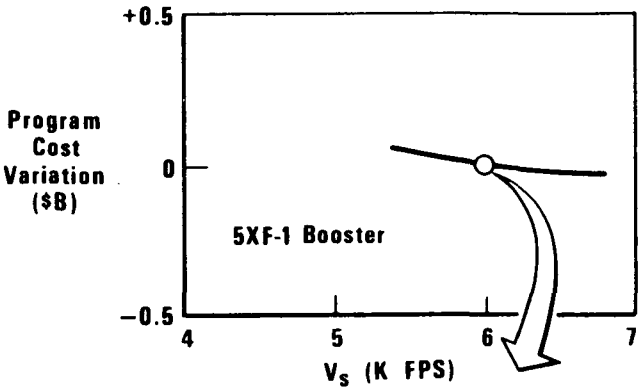

ITEM	MARK I	MARK II
GLOW M Lb	5.82	5.86
BLOW M Lb	4.59	4.59
OLOW M Lb	1.23	1.27
PL K Lb	49Polar	65 East
V_S (FPS)	6,100	6,000

Figure 4-45. F-1 Flyback Booster/J-2S to J-2S Orbiter

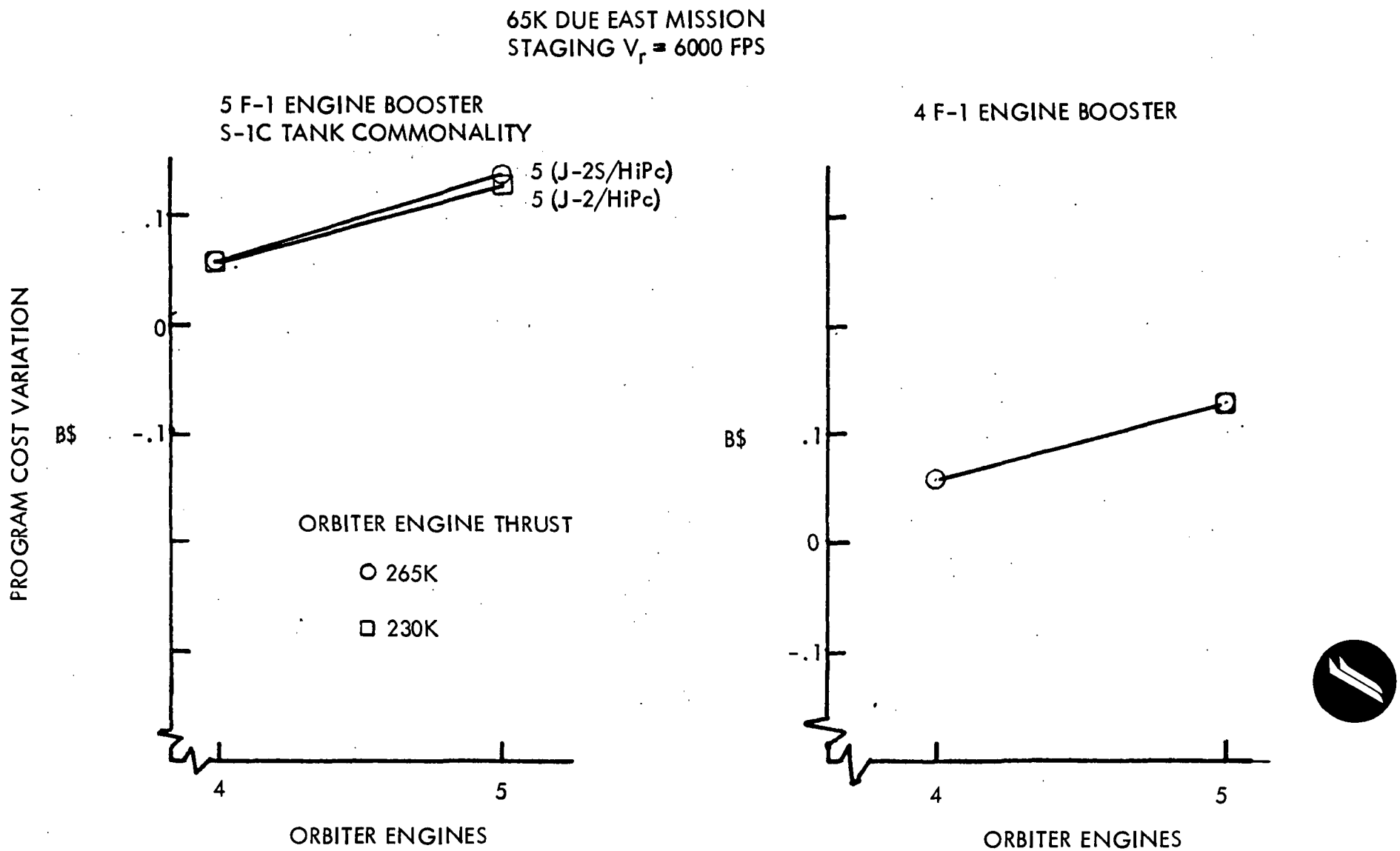

Figure 4-46. Total Program Cost Estimate

The cost comparisons of the mixture ratio and thrust level trade discussed in Section 4.2.3.1 are given in Figure 4-47. The conclusions are: The tank mixture ratio should be retained at 6.0. The improved engine performance at lower MR's is offset by the decrease in propellant bulk density and higher tank weight and cost. Also, it is seen that increased orbiter engine thrust provides no cost benefits because the higher thrust engines cost more to develop and because the higher weight of the high-thrust engines result in higher weight orbiters to maintain a constant landing speed.

In summary, the four J-2S/four HiPc orbiters combined with a five F-1 booster (S-1C size tanks) was selected for definition. However, a four J-2S Mark I and Mark II orbiter would be more attractive from a cost and risk point of view and would provide increased payload capability in the Mark I System. Consideration should be given to this system.

The cost sensitivity to total program cost to the life factor of the F-1 booster engines is shown in Figure 4-48. The baseline costs are for a 10-flight-per-engine life capability. An increase to 20 flights per engine would reduce total program costs by approximately $200 million.

The comparison of peak annual funding for concurrent versus phased development is shown in Figure 4-49. Use of the S-IC as an interim booster with delay of the flyback booster development results in the same magnitude of annual funding peak with the control gain being shifted for the phased program to 1980 from 1975.

The total program cost for the concurrent program, utilizing HiPc orbiter engines for Mark II and three different orbiter engines for Mark I is shown in Figure 4-50. The total program cost is least for a HiPc Mark I orbiter program. A J-2 or J-2S Mark I orbiter is approximately equal in total program cost: $200 million increase over the HiPc configuration. The peak annual funding requirement of these three configurations is almost equal, being within a minus $20 million and plus $50 million of the $1.23 billion figure for the J-2S configuration.

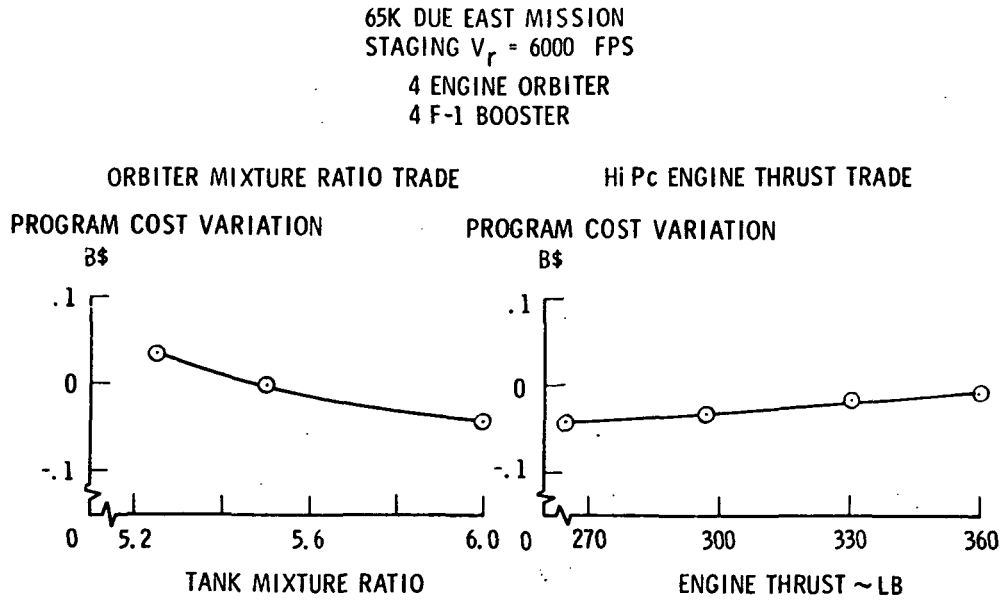

Figure 4-47. Total Program Cost Estimate

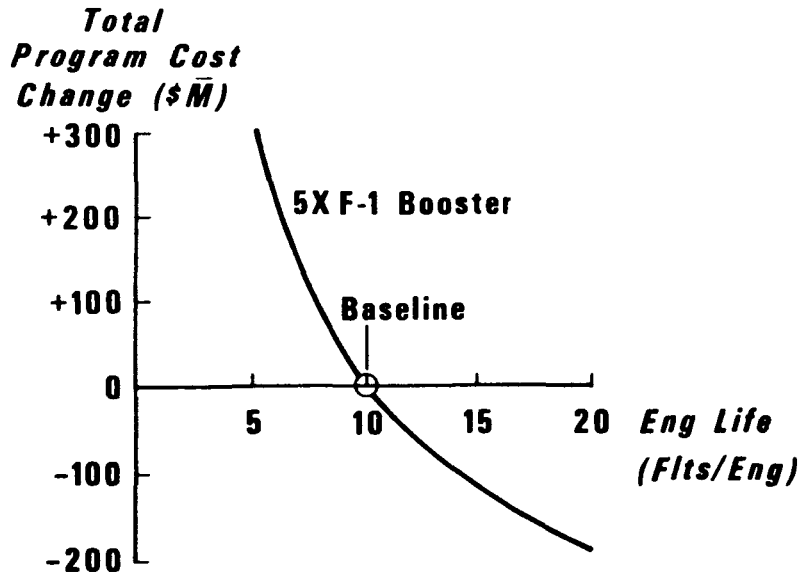

Figure 4-48. Program Cost Sensitivity, F-1 Engine Life

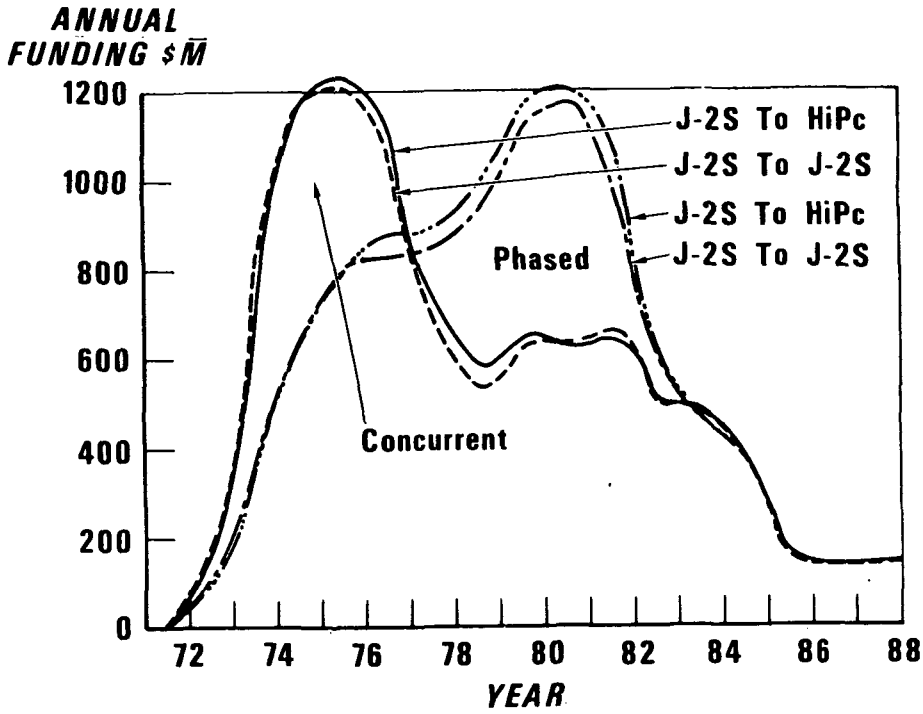

Figure 4-49. F-1 Flyback, Concurrent Versus Phased Development

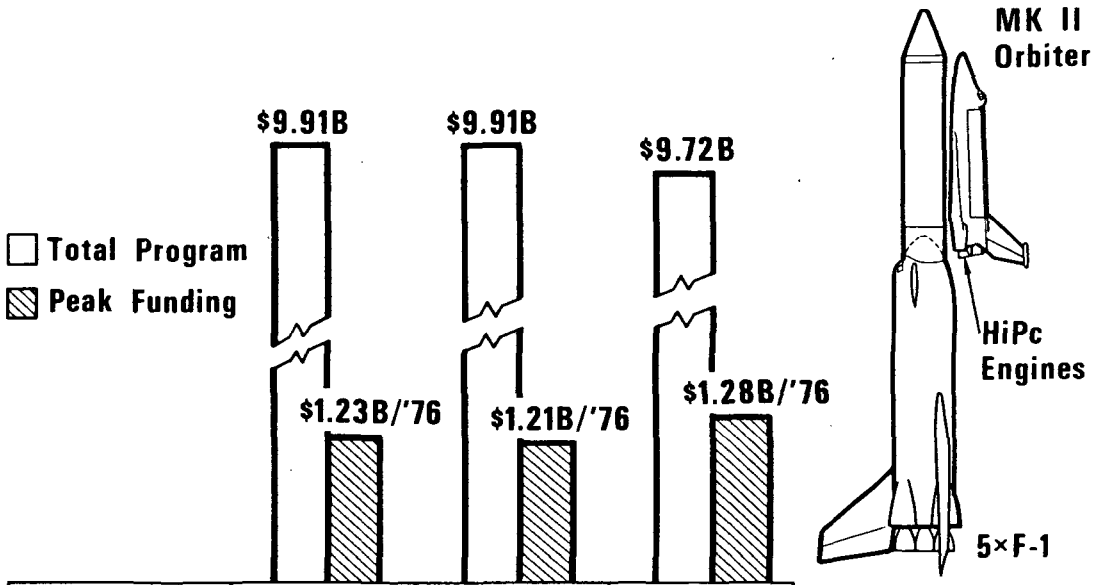

MARK I	J-2S	J-2	HiPc
GLOW M Lb	4.98	5.48	5.09
PL (Polar) K Lb	25	17	49

F-1 FLYBACK
5.09
40

Figure 4-50. Mark I Options

4.2.4 Pressure-Fed Booster System Analysis and Trades

4.2.4.1 Sizing and Propulsion Requirements

At the beginning of the second half of the Phase B extension period, sizing of the pressure-fed booster (PFB) was in progress. Initial weight scaling data were defined for LO_2/RP, LO_2/propane, and N_2O_4/UDMH propellant combinations. System sizing computer calculations were made for a matrix of combinations of boosters and orbiters with various engine arrangements. Table 4-19 is the matrix. Since the staging velocity range was specified at 6000 ± 1000 fps, at least three sizing runs were needed to define the trends for each configuration. Since both 40,000-pound polar payload and 65,000-pound due-east payload were required, sizing was carried out for both cases on combinations of greatest interest.

In general, it was found that when five engines are used on the orbiter, the empty and gross weight values are larger for 65,000-pound due-east payload than for 40,000-pound polar for all staging velocities above about 4500 fps. The reverse is true for staging velocities below 4500 fps. For subsequent updated resizing for staging velocities above 4500 fps, only due-east sizing was conducted.

For four-engine orbiters, the pattern is generally similar. For staging velocities below about 5500 to 6000 fps, polar sizing seems to govern, whereas at greater staging velocity due east sizing appears to predominate. Since staging velocities equal to or lower than 6000 fps are preferred for the four-engine orbiter, polar sizing was carried out in updated sizing studies.

Thus, with the initial booster weight scaling data, 33 integrated vehicle sizing runs were made. Representative cases were selected for initial parametric program cost analysis. Preliminary results indicated that a PFB with LO_2/propane propellants staging from the orbiter at about 6000 fps would be an attractive low-cost system. Selected was a Mark II orbiter with four high-pressure engines each with 265,000 pounds of thrust. The initial cost estimates for the 5 x 265,000-pound HiPc orbiter also appeared attractive, but the four-engine orbiter is less complex and had similar projected cost. N_2O_4/UDMH propellants were not selected because of cost and toxicity factors. The program cost comparison is given in Figure 4-51. The initial selected system is shown in Figure 4-52.

Early scaling data for the PFB were based on the concept of an aluminum booster with engine chamber pressure of 300 psia and engines equipped with ablative nozzles.

Table 4-19. PFB/Orbiter Sizing and Propulsion Matrix

Case	Engine		Booster Propellant	Booster Weight Scaling*					
				Initial		Interim Revision		Final Revision	
	Mark I	Mark II		**40K-P	***65K-E	**40K-P	***65K-E	**40K-P	***65K-E
G	5 x J-2	5 x HiPc (230)	LO_2/C_3H_8	X (3)					X (4)
H	5 x J-2S	5 x HiPc (265)	LO_2/C_3H_8	X (5)	X (4)	X (3)			
I	4 x J-2S	4 x HiPc (265)	LO_2/C_3H_8	X (3)	X (3)	X (4)		X (4)	
J	5 x J-2S	5 x HiPc (265)	N_2O_4/UDMH	X (3)	X (3)				
K	4 x J-2S	4 x HiPc (265)	N_2O_4/UDMH		X (3)				
L	4 x J-2S	4 x HiPc (265)	LO_2/RP-1	X (3)	X (3)	X (3)		X (2)	
M	4 x J-2S	5 x HiPc (265)	LO_2/RP-1			X (3)	X (3)		X (5)
N	4 x J-2S	4 x J-2S (265)	LO_2/C_3H_8					X (3)	
O	4 x J-2	4 x HiPc (230)	LO_2/C_3H_8					X (2)	

*Number in parentheses in each box ( ) indicates number of discrete staging velocities considered -- typically 5,000, 6,000 and 7,000 fps.
**Orbiter tank sized for 40,000-pound polar payload
***Orbiter tank sized for 65,000-pound due-east payload

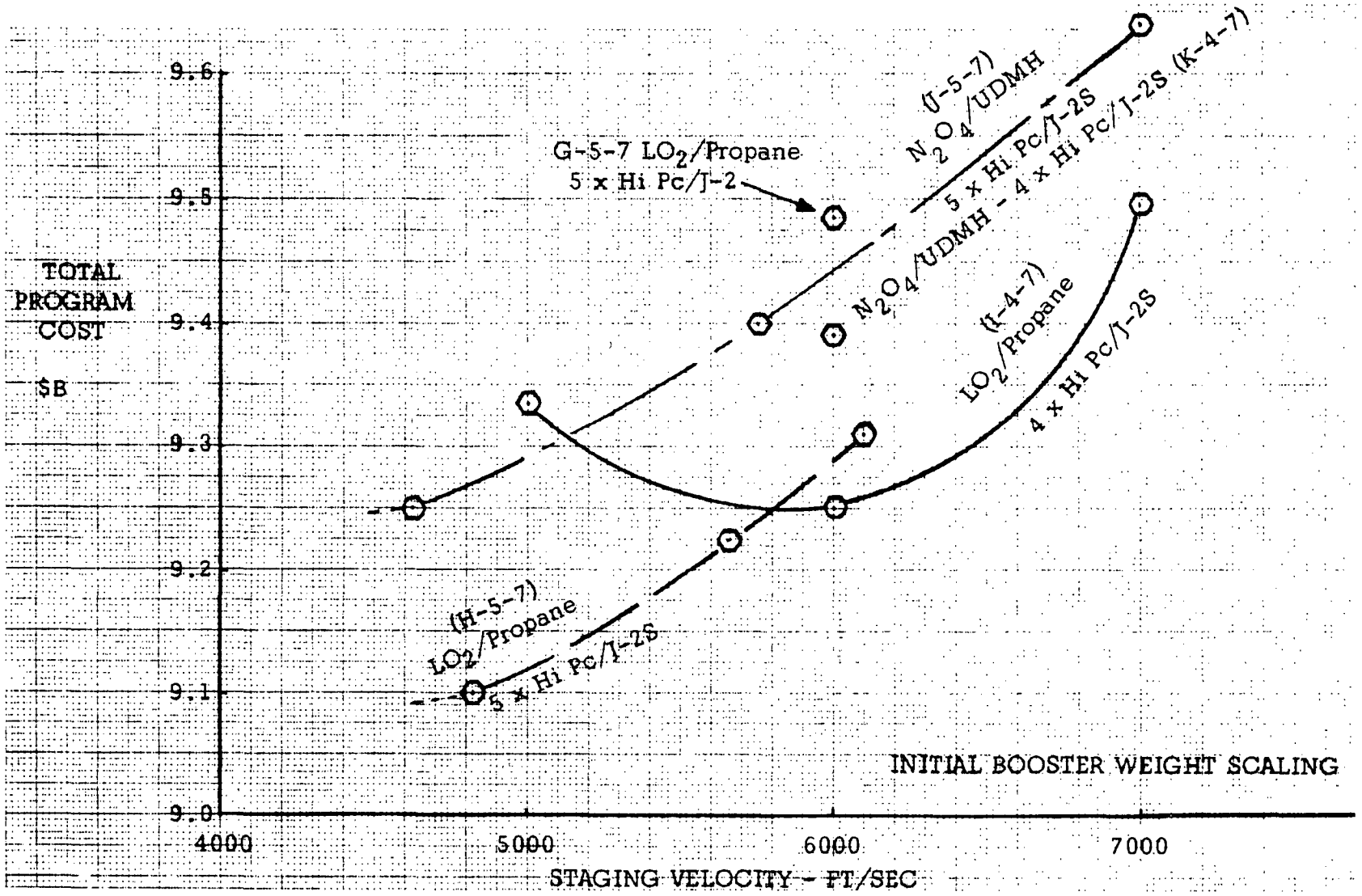

Figure 4-51. Program Cost Comparison, Pressure-Fed Boosters, HO/Orbiters

I-4-7 LO_2/PROPANE PRESSURE-FED BOOSTER
MK II ORBITER 4 x 265 KLB Hi Pc ENGINES

SYSTEM PARAMETERS			
CARGO BAY		15 X 60 Ft	
PAYLOAD (KLB)		40 POLAR	
OMS ΔV (FPS)		650 POLAR	
SYSTEM GLOW	(MLB)	5.423	
T/W @ LO		1.3	
STAGE GROSS WT	(MLB)	4.361	1.061
MAIN PROP WT	(MLB)*	3.725	.816
OMS PROP WT	(KLB)		11
FLYBACK FUEL	(KLB)	--	
FLYBACK RANGE	(NMI)	--	
STAGE DRY WT	(KLB)	590	
ORB EXT TANKS	(KLB)		56
STAGE LANDING WT	(KLB)	630	160
MAX Q	(PSF)	650	
STAGING V_R	(FPS)	6000	
γ_R		18	
MAIN ENGINE F_{SL}	(KLB)	1006	
F_{VAC}	(KLB)	1222	265
NO. OF MAIN ENG.		7	4

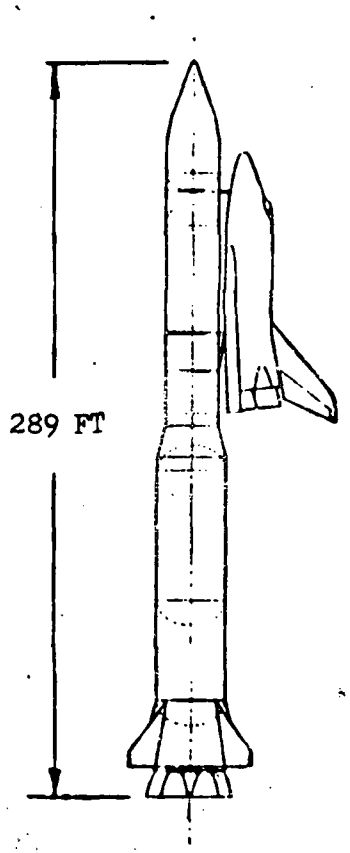

*INCLUDES TVC PROPELLANTS

INITIAL BOOSTER WT SCALING

Figure 4-52. Integrated System Description

A change in concept by General Dynamics led to revised weight scaling data. Inconel 718 was chosen for the tankage; the combustion chamber pressure was reduced to 250 psia; and film-cooled nozzles were used in the engines. Reduced booster weights were indicated in an interim scaling evaluation. The comparison now included the PFB with LO_2/RP-1 propellants. Approximate resized vehicles thus were calculated, and cost estimates were made to determine if the new booster information would likely cause a change in the previously selected system. No significant change was indicated, and the selection was retained. Since program cost estimates are similar, the choice of LO_2/propane or LO_2/RP-1 probably will hinge on engine development considerations.

As illustrated in the right-hand column of Table 4-19, the final revision of weight scaling data has been incorporated into the vehicle sizing runs listed. The program cost figures for these systems have been updated.

The cost tradeoff data for a J-2S/HiPc orbiter (Mark I to Mark II) are included in Figure 4-53. Also shown for the selected vehicle are results of detailed calculations with the new scaling data. Minor adjustments were made to the flight profile of the selected system to ensure meeting all the various system criteria. The resulting trajectory was established as the baseline flight profile.

Figure 4-54 shows a PFB/orbiter system in which the system is sized to carry out Mark II payload requirements with four J-2S engines in the orbiter at 265,000 pounds of thrust each. The estimated cost figure for this configuration would support this vehicle as an alternate choice to the selected 4 by J-2S/HiPc system.

Figure 4-55 gives results for a PFB and an orbiter equipped with five J-2 engines (Mark I) and 5 x 230,000-pound HiPc engines for Mark II. As indicated, for five engines, the staging velocity of some 5500 fps appears desirable. Also, due-east sizing was used since previous studies indicated that for orbiters with five engines such sizing would dominate. As with other vehicles with a J-2 or J-2S Mark I orbiter and a HiPc Mark II orbiter, the EOHT tank is sized for a mixture ratio of 6:1 for Mark II and is somewhat off-loaded for operating at 5.5:1 ratio with the J-2 engine. The greatly reduced specific impulse of the J-2 engine results in a Mark I polar orbit payload of approximately 12,000 pounds, which slightly exceeds the minimum requirement.

The basic issues for comparison for the several concepts evaluated with the pressure-fed booster included total program cost and peak annual funding. Figure 4-56 illustrates the annual funding requirements for both concurrent and phased programs in which the J-2S/HiPc orbiter is compared with the J-2S/J-2S orbiter. If a phased program is used to reduce the initial

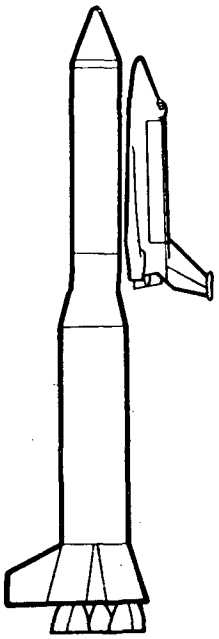

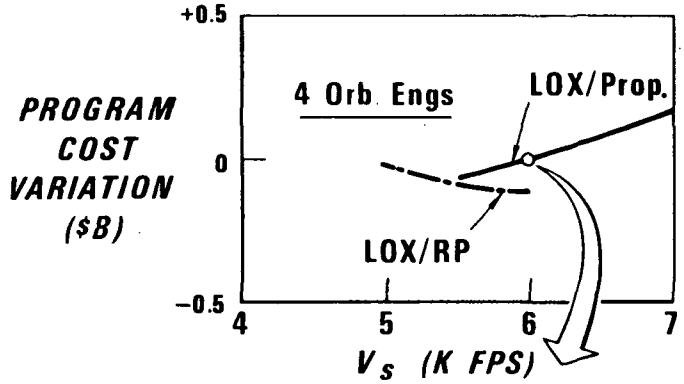

ITEM	MARK I	MARK II
GLOW $\bar{M}$ Lb	5.173	5.253
BLOW $\bar{M}$ Lb	4.198	4.198
OLOW $\bar{M}$ Lb	0.975	1.055
PL K Lb	25 Polar	40 Polar
V_S (FPS)	6,280	5,970

Figure 4-53. PFB J-2S to HiPc Orbiter (No Orbiter Engines)

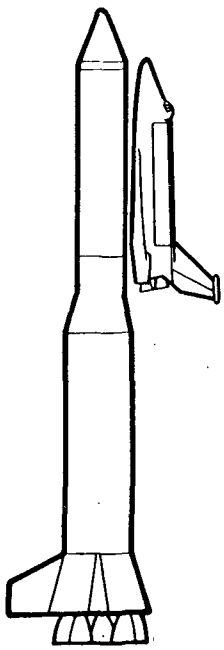

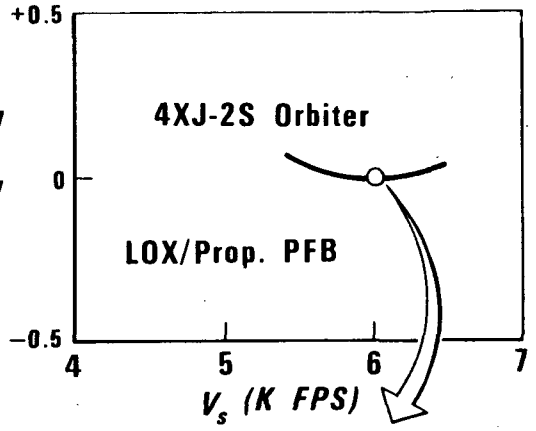

ITEM	MARK I	MARK II
GLOW $\bar{M}$ Lb	5.901	5.901
BLOW $\bar{M}$ Lb	4.699	4.699
OLOW $\bar{M}$ Lb	1.202	1.202
PL K Lb	49 Polar	40 Polar
V_S (FPS)	6000	6000

Figure 4-54. PFB J-2S to J-2S Orbiter

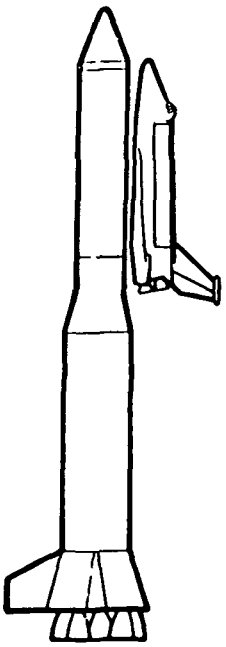

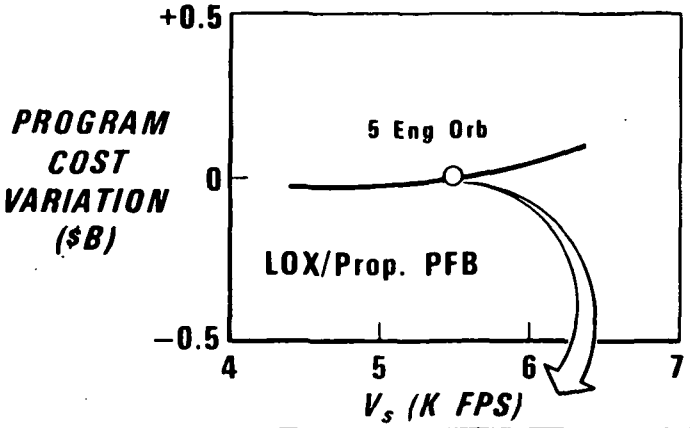

ITEM	MARK I	MARK II
GLOW $\bar{M}$ Lb	5.010	5.138
BLOW $\bar{M}$ Lb	3.971	3.970
OLOW $\bar{M}$ Lb	1.039	1.167
PL K Lb	12 Polar	65 East
V_S (FPS)	~5,700	5,500

Figure 4-55. PFB J-2 to HiPc Orbiter (5-Engine Orbiter)

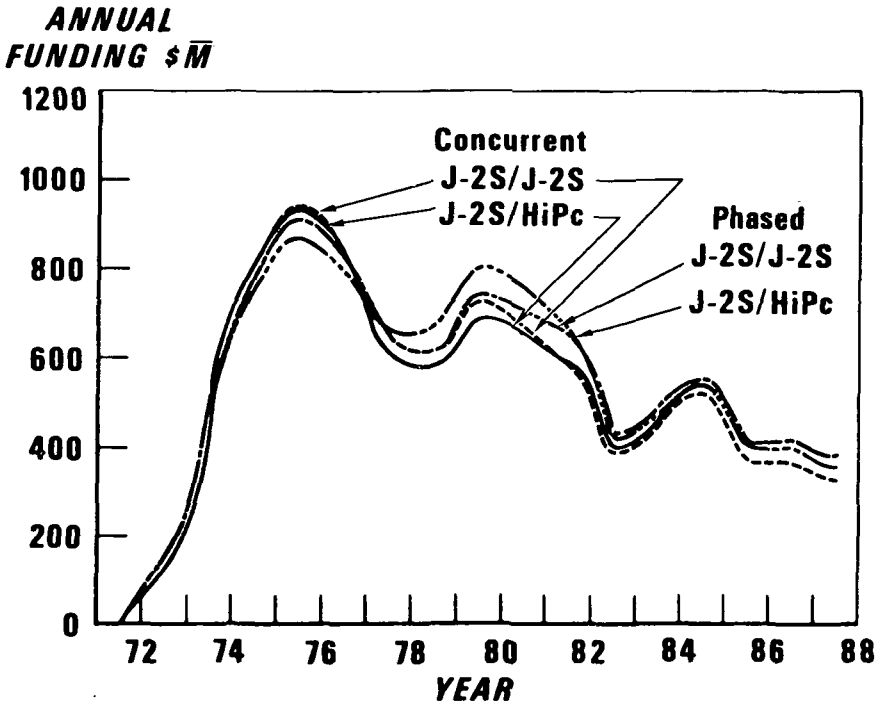

Figure 4-56. PFB, Concurrent Versus Phased Development

peak funding, then some four to five years later the peak funding will be increased by an amount slightly exceeding the previous reduction. The phased program, therefore, would result in a slightly greater program cost.

For a system consisting of a recoverable LO_2/propane pressure-fed booster combined with a 4 x HiPc Mark II orbiter, three Mark I options are shown in Figure 4-57. For a Mark I orbiter with J-2S engines, a lower peak annual funding is indicated than for a Mark I orbiter with HiPc engines. However, the total program cost for the J-2S Mark I orbiter is shown to be slightly higher than the Mark I orbiter with HiPc engines. It may be further observed that the J-2 engine offers no advantage over the J-2S in peak annual funding and results in a somewhat larger total program cost. Furthermore, the J-2 case is for five J-2 engines, which would add complexity to the orbiter in comparison with a four-engine design. Therefore, the combination of the J-2S Mark I and a HiPc Mark II orbiter program still appears attractive as a selected system.

Figure 4-58 displays the program schedule for a concurrent program that includes a reusable pressure-fed booster. A phased program schedule is shown in Figure 4-43 of this report. The concurrent schedule illustrated here gives the key development milestones for the selected system that has been described. Included are the requirements for development of the orbiter, the orbiter engine, and the pressure-fed booster. The following paragraphs discuss the technical aspects of the pressure-fed booster/orbiter system.

4.2.4.2 Aerodynamic Characteristics (PFB System)

The PFB system launch vehicle concept consists of an orbiter/EOHT second stage mounted in tandem to a first-stage booster. The booster is an unmanned configuration. The initial configurations featured aft-mounted cruciform fins on a flared skirt. The flared skirt and fin arrangement are sized to provide the desired stability characteristics for the launch configuration during boost and for the booster during entry. The empty booster will be decelerated to acceptable impact velocities with a parachute recovery system for water impact. The floating booster will be retrieved for refurbishment and reuse.

The launch vehicles considered were an orbiter/EOHT mated with pressure-fed boosters that use LO_2/propane, LO_2/RP, and UDMH/N_2O_4 propellants. The variation in required booster sizes for each of the three propellants is influenced by the drag for each of the three launch configurations. Presented in Figures 4-59 and 4-60 are curves for each of the three launch vehicles. Shown are forebody axial force coefficient versus Mach number and power-on base axial force versus altitude. Variation in drag is approximately 10 percent from maximum to minimum. The configurations

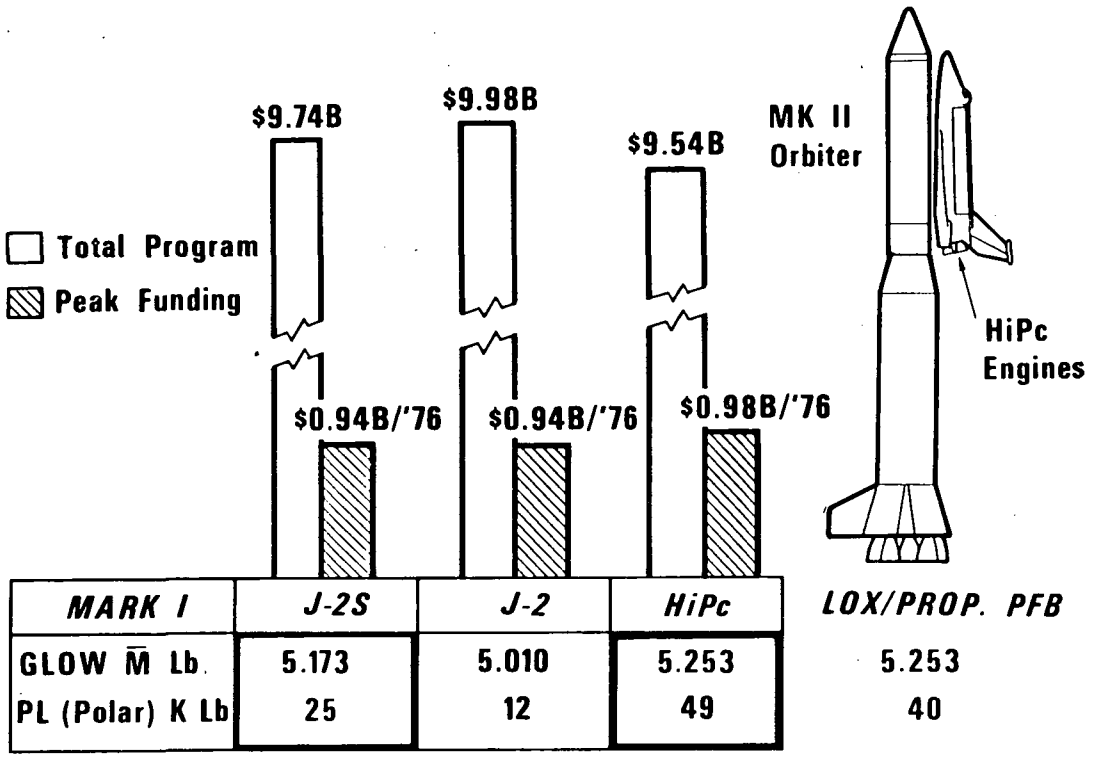

Figure 4-57. Mark I Options With Mark II HiPc for Recovering PFB

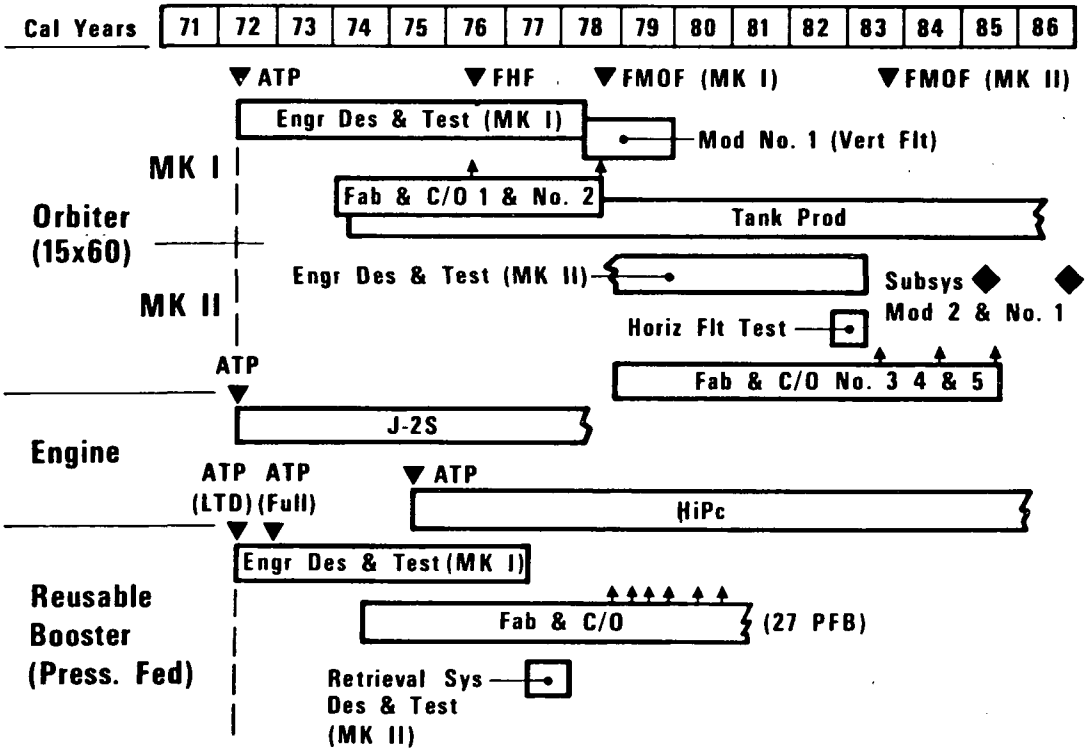

Figure 4-58. Program Schedule, PFB

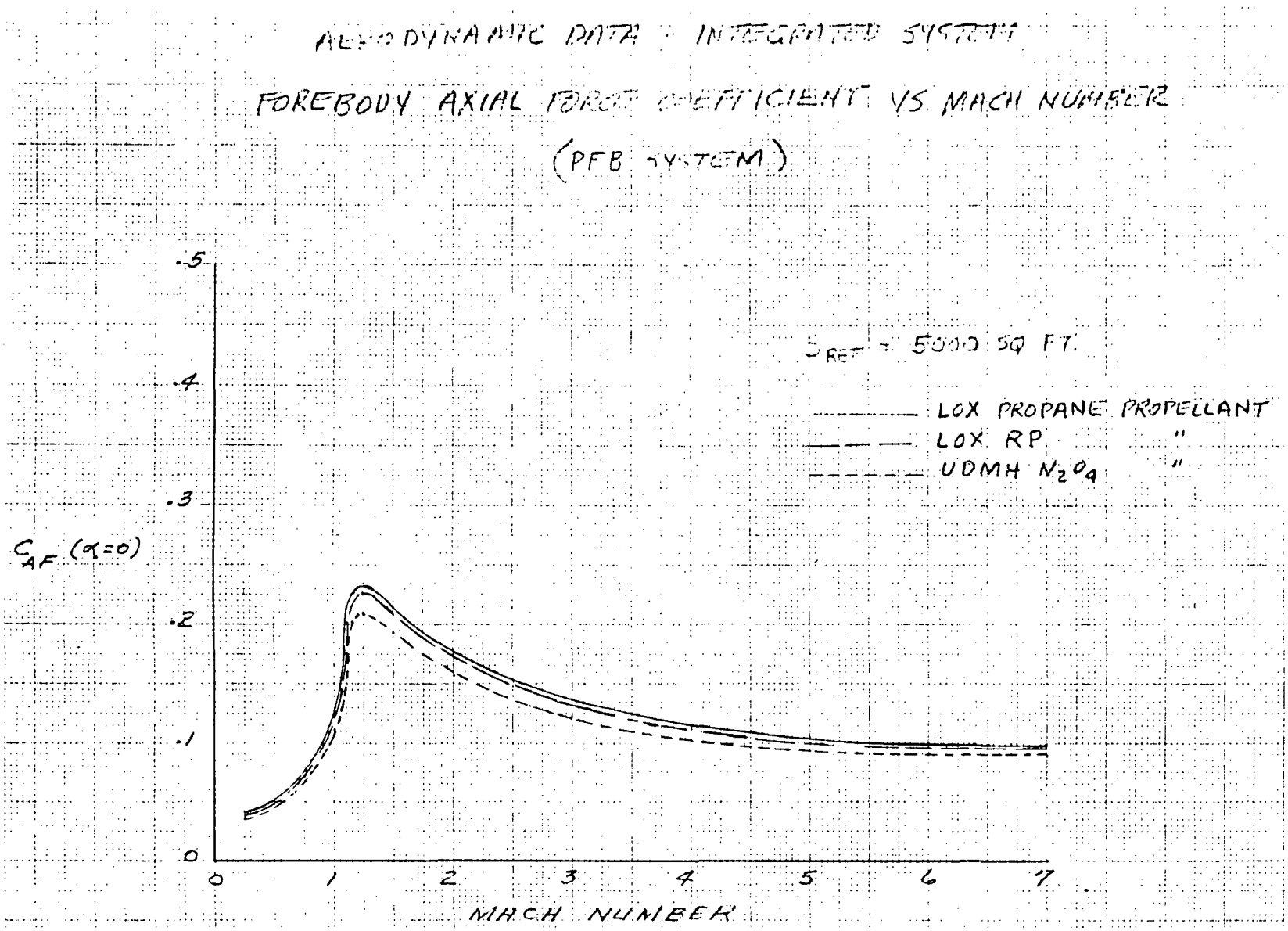

Figure 4-59. Axial Force Characteristics

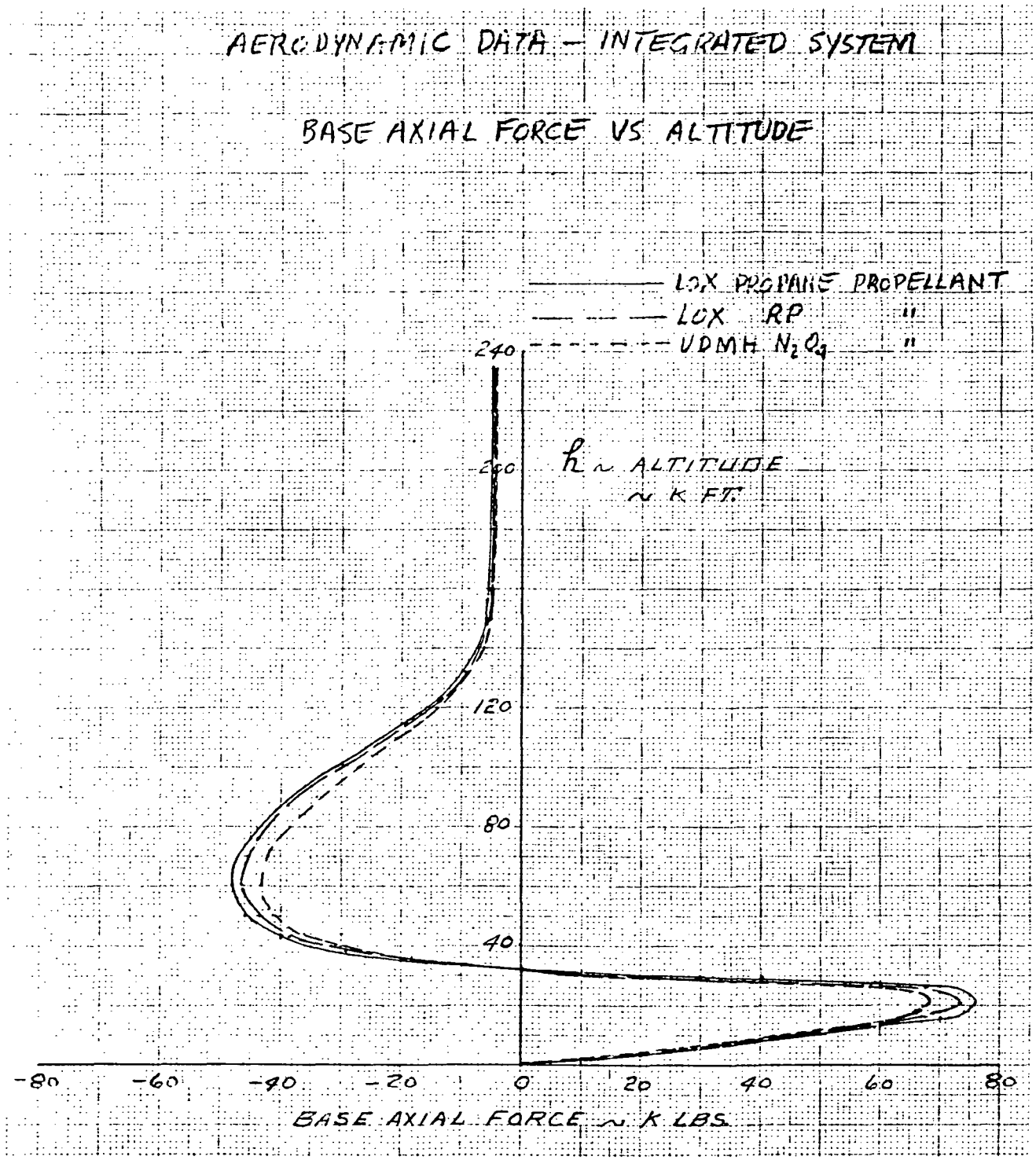

Figure 4-60. Power-On Base Force Characteristics

using LO_2/propane and LO_2/RP propellant have the higher drag. The configuration using UDMH/N_2O_4 propellant has the lower drag.

The flared skirt and fins on the booster provide static stability for the empty booster during entry, thus precluding tumbling.

The aerodynamic data for these configurations are based on correlation of predictions with available wind tunnel test data to account for differences between configuration. Predictions are based on NR and GDC in-house and DATCOM methods.

4.2.4.3 Ascent Control

The initial PFB design concept was characterized by four symmetrical fins mounted on a flared base to provide adequate vehicle stability during atmospheric flight. They are mounted 45 degrees from the Z axis, and result in a stability ratio (standard C_1/C_2 design criteria) of approximately 0.25, which is more than adequate. The design is such that the combined vehicle cg falls on or near the booster centerline during mated flight, therefore requiring little or no gimbal deflection for cg tracking. Liquid injection thrust vector control effective gimbal deflections required to trim an engine or TVC failure are less than 2 degrees. The maximum TVC deflection for the pressure-fed engine has been baselined at 5 degrees.

For preliminary analysis, it was assumed that the structural design criteria derived during Phase B shuttle activities would apply. These criteria indicated a maximum $\bar{q}\alpha$ and $\bar{q}\beta$ constraint of 2800 and 2400 psf-deg, respectively. Under these conditions, TVC angles of 2 degrees are required in pitch for maximum $\bar{q}\alpha$, and 2.7 degrees in roll and 1 degree in yaw are required for maximum $\bar{q}\beta$. It was further assumed that an allowance is required to control dynamic overshoots, bending, and slosh of 2 degrees (based on Phase B studies). When the effects of wind shears and gusts (maximum $\bar{q}\alpha$ and $\bar{q}\beta$) are combined with the dynamic allowance, there is a reasonable risk that the TVC requirement may exceed 5 degrees for roll control. One means for reducing the roll control TVC requirement would be to delete the upper two booster stabilizing fins and to enlarge the lower two. Alternately, the fin configuration discussed in Section 4.4.2.2 may suffice. The guideline is to provide a roll trim moment to offset the orbiter rolling moment, thus reducing the large roll gimbal deflection necessary to control in a crosswind. These approaches will be evaluated. Also, since the PFB/orbiter configuration differs significantly from the Phase B shuttle combined system, the $\bar{q}\alpha$ and $\bar{q}\beta$ constraints mentioned will be reappraised.

4.2.4.4 Abort Modes

Two features of the PFB concept suggest different planning for possible ascent phase abort from that for a reusable flyback booster: (1) the booster itself is unmanned and (2) the unit cost of an individual booster is a small fraction of that for a reusable flyback booster. Hence, if the rare requirement for an ascent-phase abort occurs, jettisoning the booster may be acceptable. In such an event, the booster engines would be cut off, and the orbiter engines started earlier than normal. The orbiter would separate from the booster in a manner that would give the orbiter and its crew the greatest chance for a safe landing. Since the pressure-fed booster is unmanned, competing requirements for booster crew safety obviously would be avoided. Only the cost of a lost booster need be considered in the overall program cost. To this end, costly equipment such as for guidance and control is located primarily in the orbiter, not the PFB.

Even in an ascent-phase abort, after booster engine cutoff and safe separation of the orbiter, booster recovery can be attempted. Operation of the PFB recovery equipment in some cases may lead to partial recovery of the booster vehicle and/or its equipment.

An abort decision that leads to cutting off all the PFB engines prior to propellant depletion should essentially eliminate any possibility of recontact of the booster with the orbiter after a safe separation. This is because the booster would be decelerating and the orbiter accelerating. Thus, the separation problems discussed in Section 4.2.3.4 would not be nearly as severe since the booster thrust would have been terminated. Significant problems can be anticipated if separation is required from a thrusting booster that retains an appreciable thrust-to-weight ratio.

Once safe separation has occurred, the orbiter abort modes should be identical with those discussed in Section 4.2.3.4.

4.2.4.5 Recovery Requirements

Recovery requirements for the pressure-fed booster are described in Section 4.2.2.

4.2.4.6 Pressure-Fed Booster Facility Requirements

Two trade studies were conducted during Phase B'. The first was directed toward evaluating the launch site facility requirements for a LO_2-propane PFB. The objective was to evaluate and select the most desirable vertical assembly building (VAB) floor plan for the storage, maintenance, and mating-erection of the PFB. The second objective was to determine the most desirable configuration of the launcher-vehicle arrangement. Concepts

developed for the VAB floor plan and mate-erection task are illustrated in Figures 4-61 through 4-65. Study of the VAB floor plan will be extended into Phase B''.

The second trade study was directed toward developing concepts for the retrieval of the PFB after launch. Figures 4-66 through 4-67 represent the retrieval concepts. Figure 4-68 compares the retrieval concepts, with Concept B (tow back) being the recommended method.

A new trade study will be conducted during Phase B'' to develop support equipment concepts. The objective is to develop and compare the ground support equipment approach that satisfies the space shuttle Level 1 and 2 requirements and airborne system requirements for the checkout, control, servicing, handling, and training throughout all phases of the Space Shuttle Program. This study will also evaluate and select a concept for both the PFB and LO_2-RP flyback booster and ultimately select the most desirable concept of the two boosters.

4.2.4.7 Test Requirements and Operations

The overall objectives of the PFB test program are (1) to assist in developing design concepts, (2) to certify by analysis and ground test and verify by flight test, as required, and (3) to provide data for space shuttle vehicles, support equipment, and software acceptance.

No major trade studies were performed in this contract phase involving test requirements or operations. Results of the analyses performed derived the baseline PFB test program as described under Section 4.4.6.

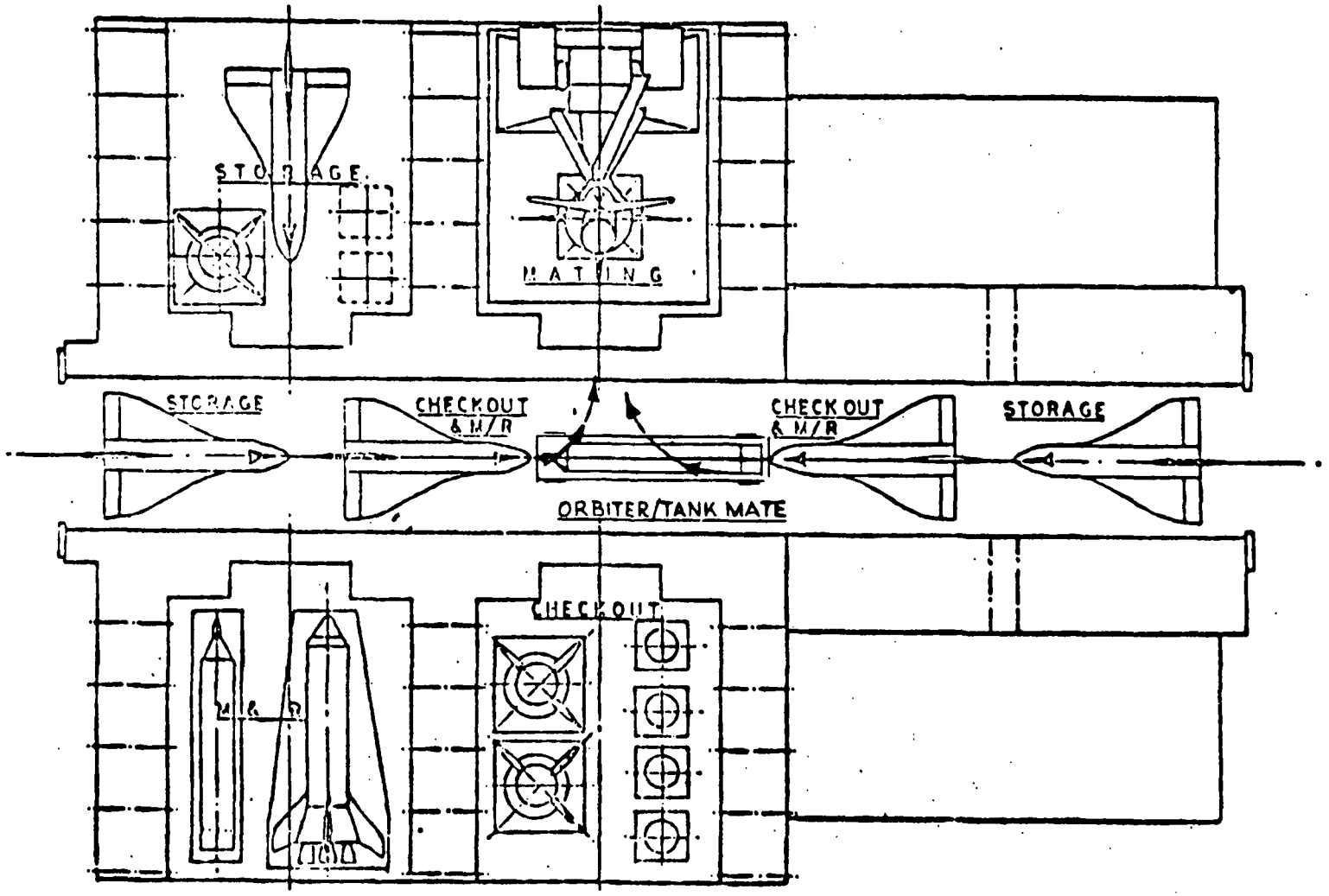

Figure 4-61. Pressure-Fed Booster VAB Floor Plan

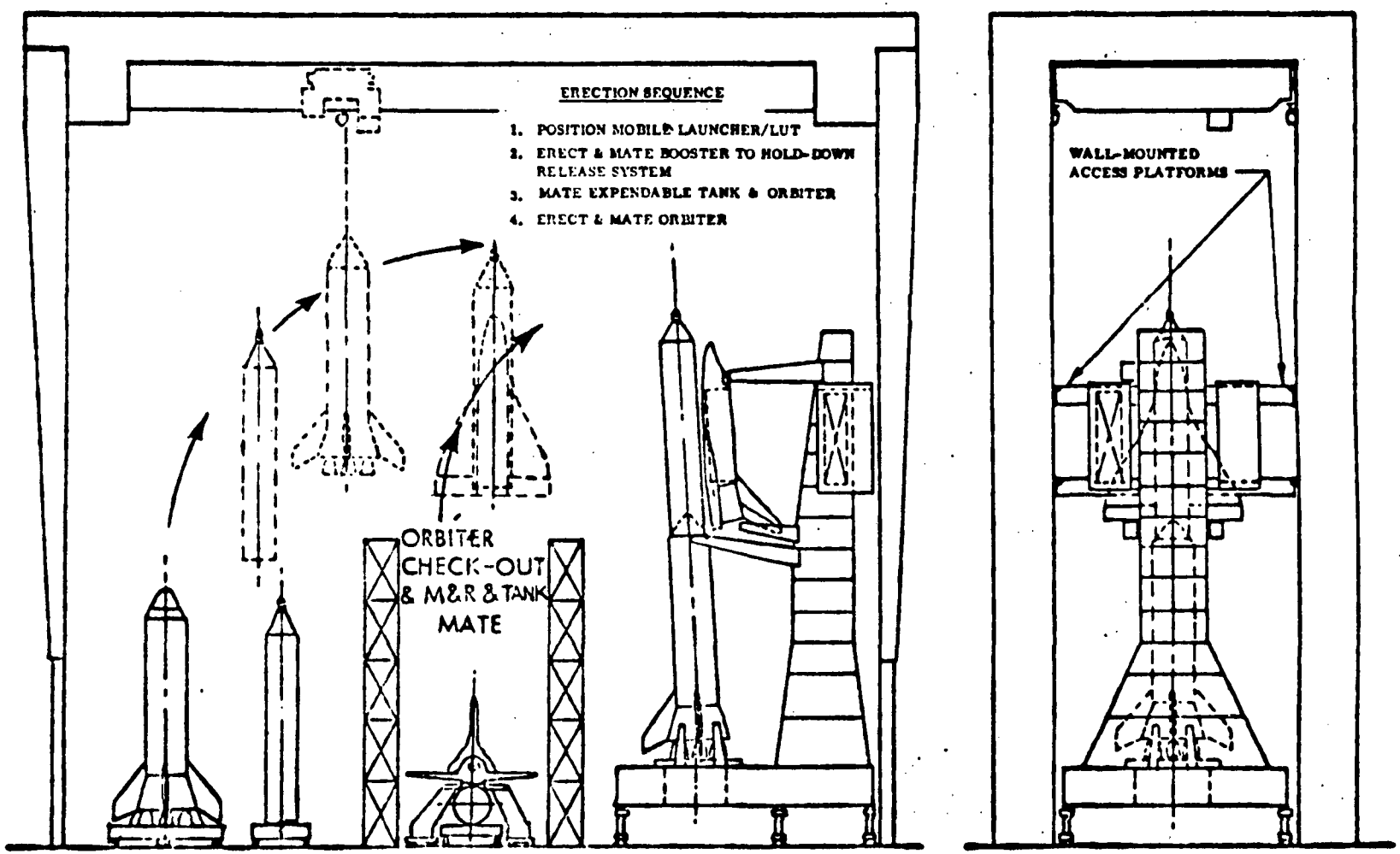

Figure 4-62. Pressure-Fed Booster VAB Vertical Erection and Mate

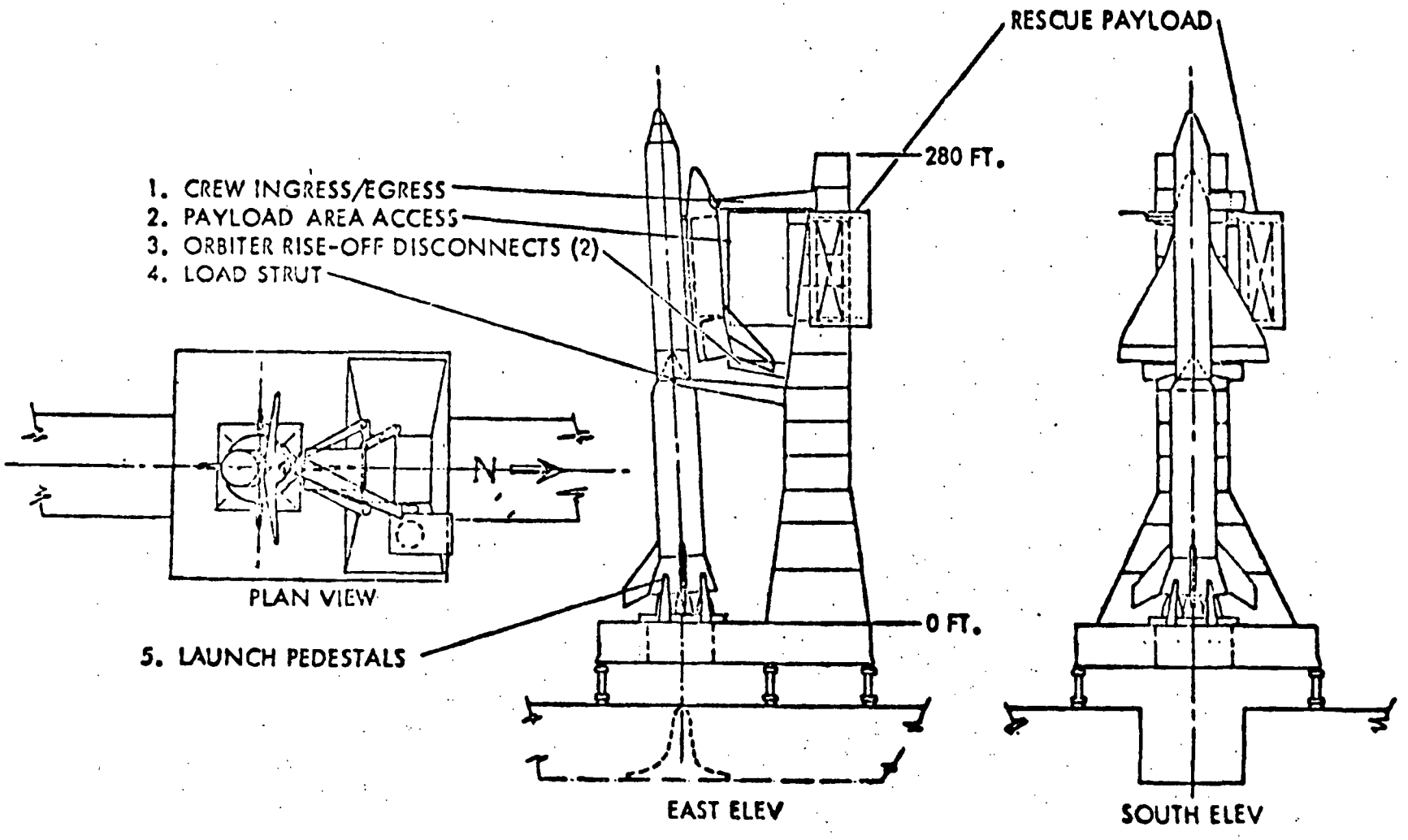

Figure 4-63. Pressure-Fed Booster Launch Pad Configuration

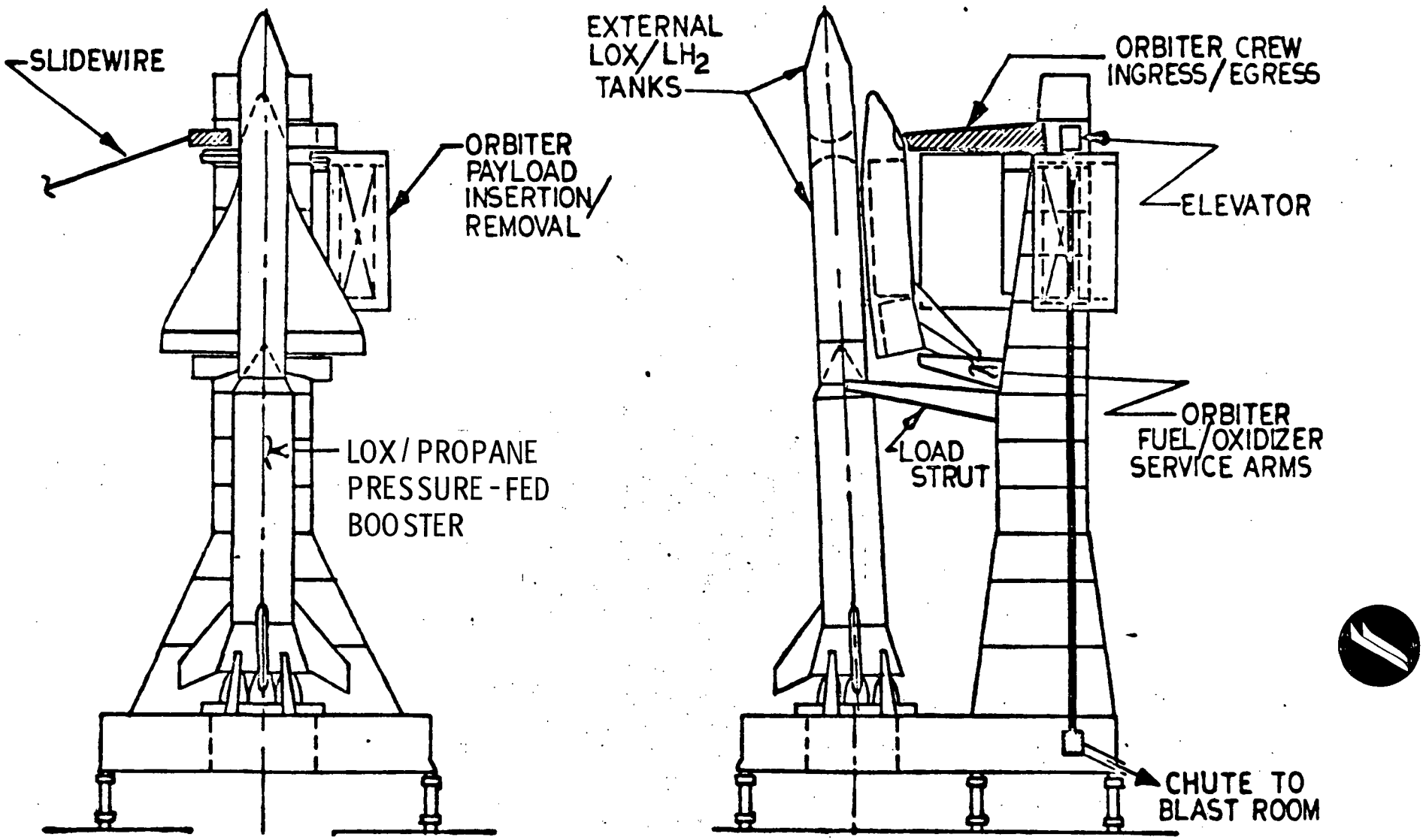

Figure 4-64. LO_2/Propane, Pressure Fed

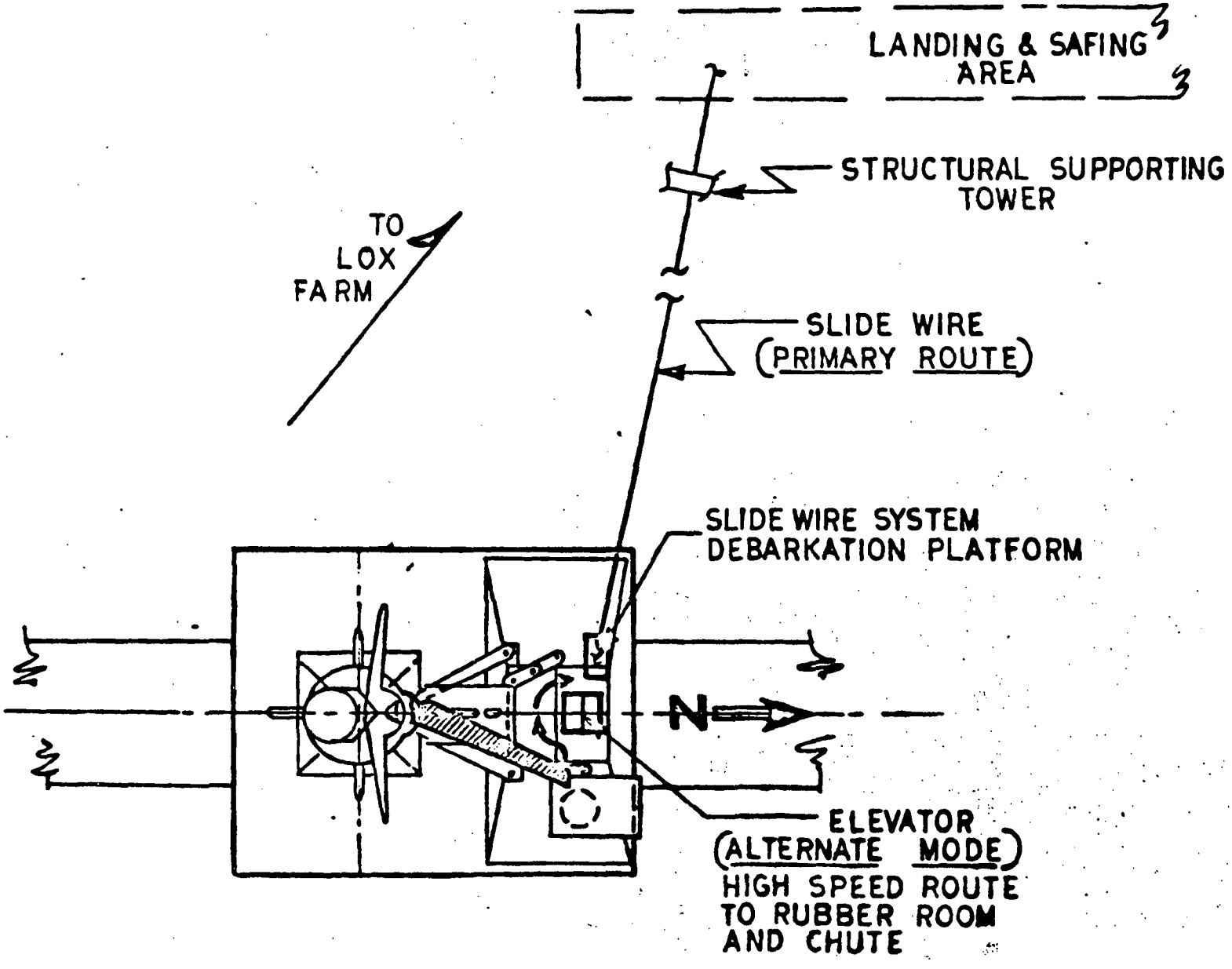

Figure 4-65. LO_2/Propane, Pressure Fed

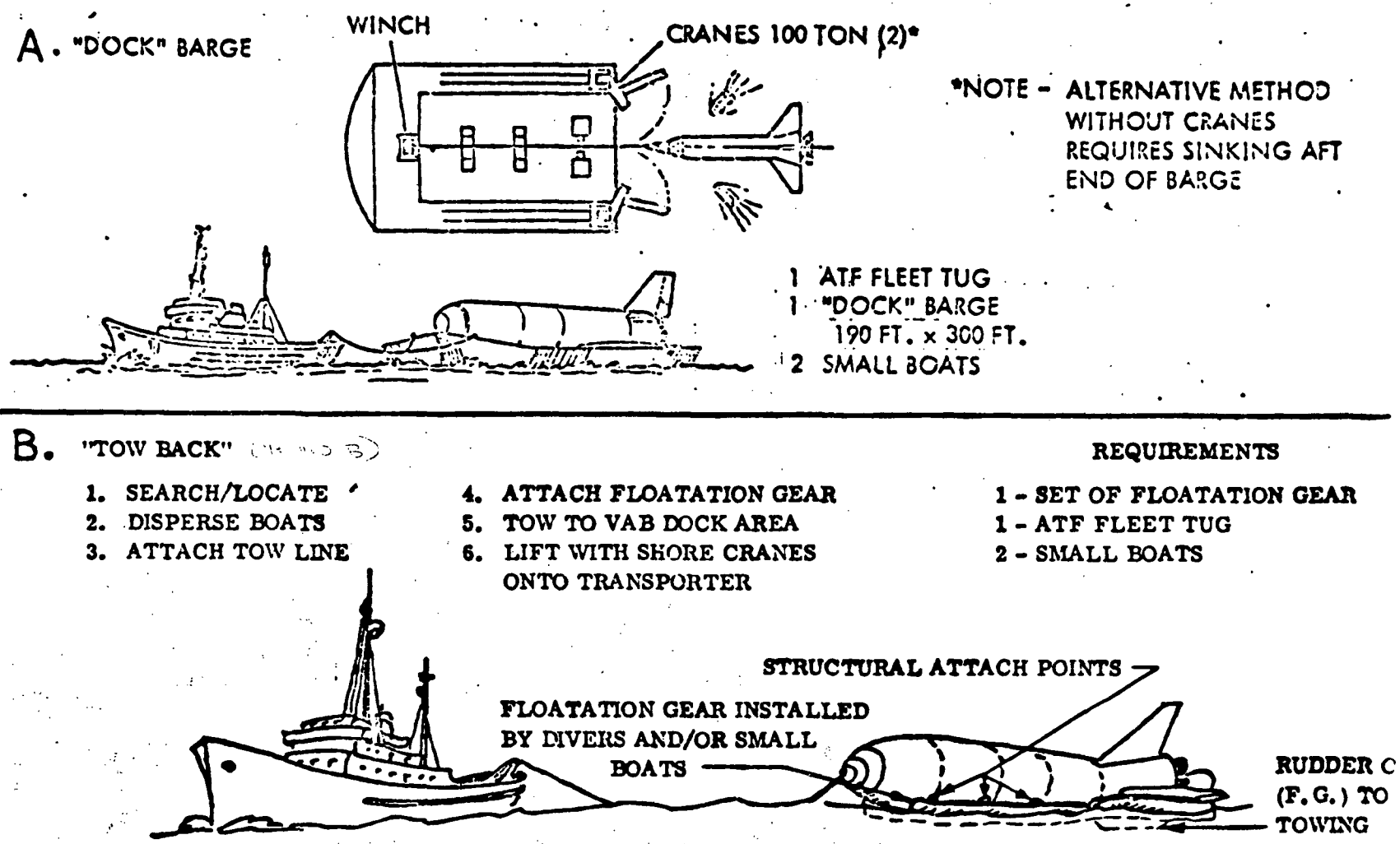

Figure 4-66. PFB Recovery Concepts, Dock Barge and Tow Back

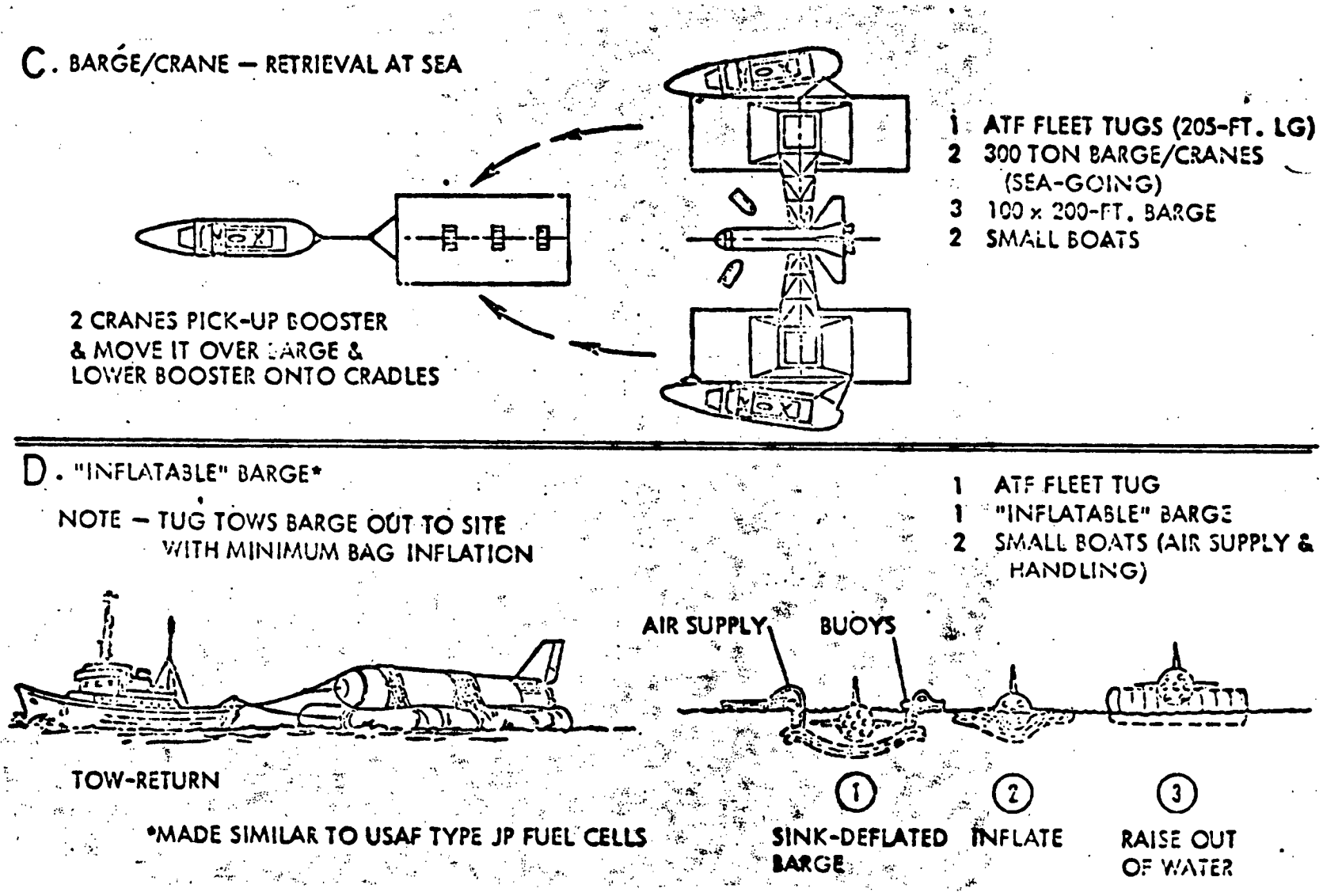

Figure 4-67. PFB Recovery Concepts, Barge/Crane (Retrieval at Sea) and Inflatable Barge

	ADVANTAGES	DISADVANTAGES
METHOD A DOCK BARGE	• STRETCHED STANDARD DESIGN BARGE • USES STANDARD EQUIPMENT	• HIGH-COST SPECIAL BARGE SIZE • DIFFICULT TO USE IN ROUGH SEA • MAY DAMAGE BOOSTER ENTERING DOCK IN ROUGH SEA
METHOD B "TOW BACK"	• MINIMUM CREW & NO SPECIAL EQUIPMENT • FASTEST RETURN	• BOOSTER IS IN "SEA" ENVIRONMENT 2 TO 3 DAYS
METHOD C BARGE/CRANE	• STANDARD TYPE EQUIPMENT	• HIGH RISK WITH LARGE CRANES AT SEA • HIGH-COST OPERATION (3 TUGS) • DIFFICULT TO SET BOOSTER DOWN "EASILY"
METHOD D INFLATABLE BARGE	• MINIMUM EQUIPMENT (NO ENGINES, CRANES, PUMPS, ETC.), JUST AIR BOTTLES • MINIMUM LIKELY DAMAGE TO BOOSTER	• NONSTANDARD APPROACH • HIGH FIRST COST BARGE

Figure 4-68. PFB Recovery Concepts Advantages and Disadvantages

4.3 TRADE STUDIES

4.3.1 Aluminum Versus Titanium Orbiter

A trade is being conducted to show the relative merit of aluminum and titanium orbiter structure. Results of a preliminary assessment to grossly assess the differences are reported here. The trade results are based on a configuration similar to the current baseline. The trade is continuing to provide a more in-depth definition of the differences and to update data to the latest baseline configuration.

4.3.1.1 TPS Requirements - Mark II and Mark I

The TPS candidates studied were an ablator (Martin SLA 561), a reusable surface insulation (RSI) (GE REI mullite), and a metallic radiative shingle system. The ablator system was sized for both a 200-nm (Mark I) and 1100-nm (Mark II) crossrange with an aluminum structure common to Mark I and Mark II. The RSI was sized for an 1100-nm crossrange vehicle with an aluminum structure and a titanium structure. For the aluminum structure the total wetted area was protected to 300 F with TPS, while the titanium was unprotected where maximum temperature was 850 F or less and covered to 650 F maximum bondline.

For the protected areas and design trajectories, the required thicknesses of ablator, reusable external insulation (REI), and internal insulation (under unprotected titanium) are shown on drawings VC70-0168 (ablator on aluminum, 200 nm cross range), VC70-0182 (ablator on aluminum, 1100 nm), VC70-0164 (RSI on aluminum, 1100 nm), and VC70-0174 (RSI on titanium, 1100 nm).

TPS weights are compared in Table 4-20. The first two columns show the different ablator weight requirements for a Mark I orbiter with 200-nm and 1100-nm cross-range capability if both systems have aluminum structures. Columns 2 and 3 show the weight advantage of an RSI system over an ablator system when a 1100-nm cross range is required and aluminum structure is used. Column 4 shows the TPS weight reduction possible by use of titanium structure over aluminum structure. The last column shows the radiative system to be substantially heavier than any of the other combinations. Therefore, that system was eliminated from consideration. The next section will discuss the structural weight trade.

Figures 4-69 and 4-70 show that for the range of axial loads (N_x) and heat loads (Q) covering Mark I and Mark II trajectories, 2024T86 aluminum was the most weight efficient alloy and 350 F was the design maximum temperature selected for the baseline resulting in minimum combined structure

Table 4-20. Thermal Protection System Weight Summary

Item	Ablator		RSI		Radiative Heat Shield
	Bond Temp 300 F 200-nm Crossrange Ablator Alum Struct	Bond Temp 300 F 1100-nm Crossrange Ablator Alum Struct	Bond Temp 300 F 1100-nm Crossrange RSI Alum Struct	650 F Bond 850 F Struct 1100-nm Crossrange RSI Ti Struct	300 F Struct 1100-nm Crossrange Metallic Alum Struct
Body weight (lb)	7,010	14,210	11,465	8,810	16,850
Wing weight (lb)	6,215	12,080	8,735	5,670	11,280
Tail weight (lb)	570	1,065	535	195	1,700
Total weight (lb)	13,795	27,355	20,735	14,675	29,830
Avg unit weight (lb/ft^2)	1.26	2.51	1.90	1.35	2.86
Covered avg unit weight (lb/ft^2)				2.67*	

*5,471 square feet
Reference total wetted area = 10,899 square feet. (Refer to Mark I orbiter 25,000-pound payload)
All weights for nominal trajectory.

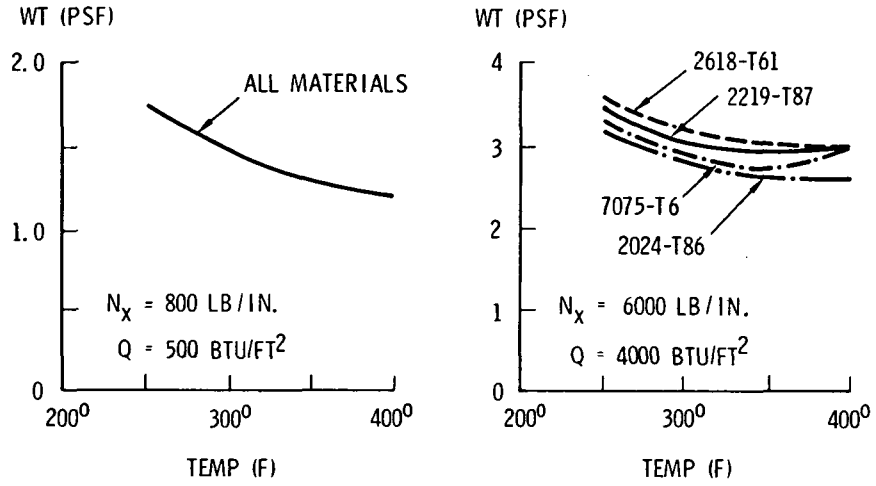

Figure 4-69. Mark I Low-Cross Range Ablator Optimization of Structure and Insulation Weight

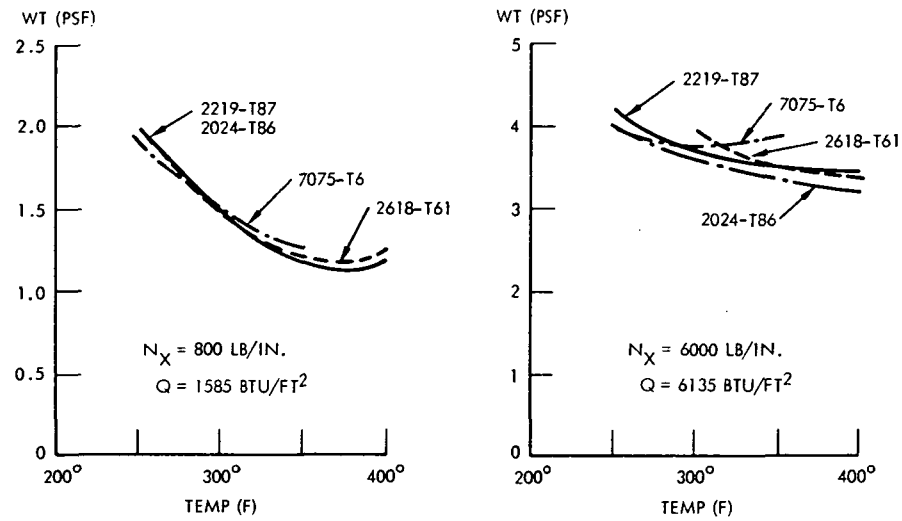

Figure 4-70. Mark II High-Cross Range RSI

and insulation weight. This backface temperature will be reflected in a weight statement addendum to the 300 F calculated weights in this report.

4.3.1.2 Structural Requirements

The objective here is to compare the optimum structural weights associated with an aluminum and a titanium orbiter for various load levels. Both curved and flat frames were considered in conjunction with skin-stringer construction. Material degradation effects from exposure to high temperatures and plasticity effects were considered. Figures 4-71 and 4-72 summarize study results. Also, these results are reflected in the configuration described in paragraph 4.3.1.1.

The optimum unit weight of the structure subjected to axial compressive loading was determined as outlined below:

$$\text{Weight/square foot} = K\,(\bar{t}_{total})\,\rho\,144$$

where

K = 1.3 (a constant factor to account for extra hardware such as splices, gussets, nonoptimum sections, etc.)

$\bar{t}_{total}$ = optimum equivalent thickness of skin-stringer plus frames

ρ = material density, lb/in.^{3}

The optimum equivalent thickness of skin-stringer and frames was calculated as follows. The equivalent thickness of the skin-stringer is given by

$$\bar{t}_{ss} = \left[\frac{N_x L}{\epsilon \eta E}\right]^{1/2} \qquad (1)$$

where

N_x = axial compressive loading, lb/in.

L = frame spacing, in.

ϵ = 0.93 (constant for hat sections)

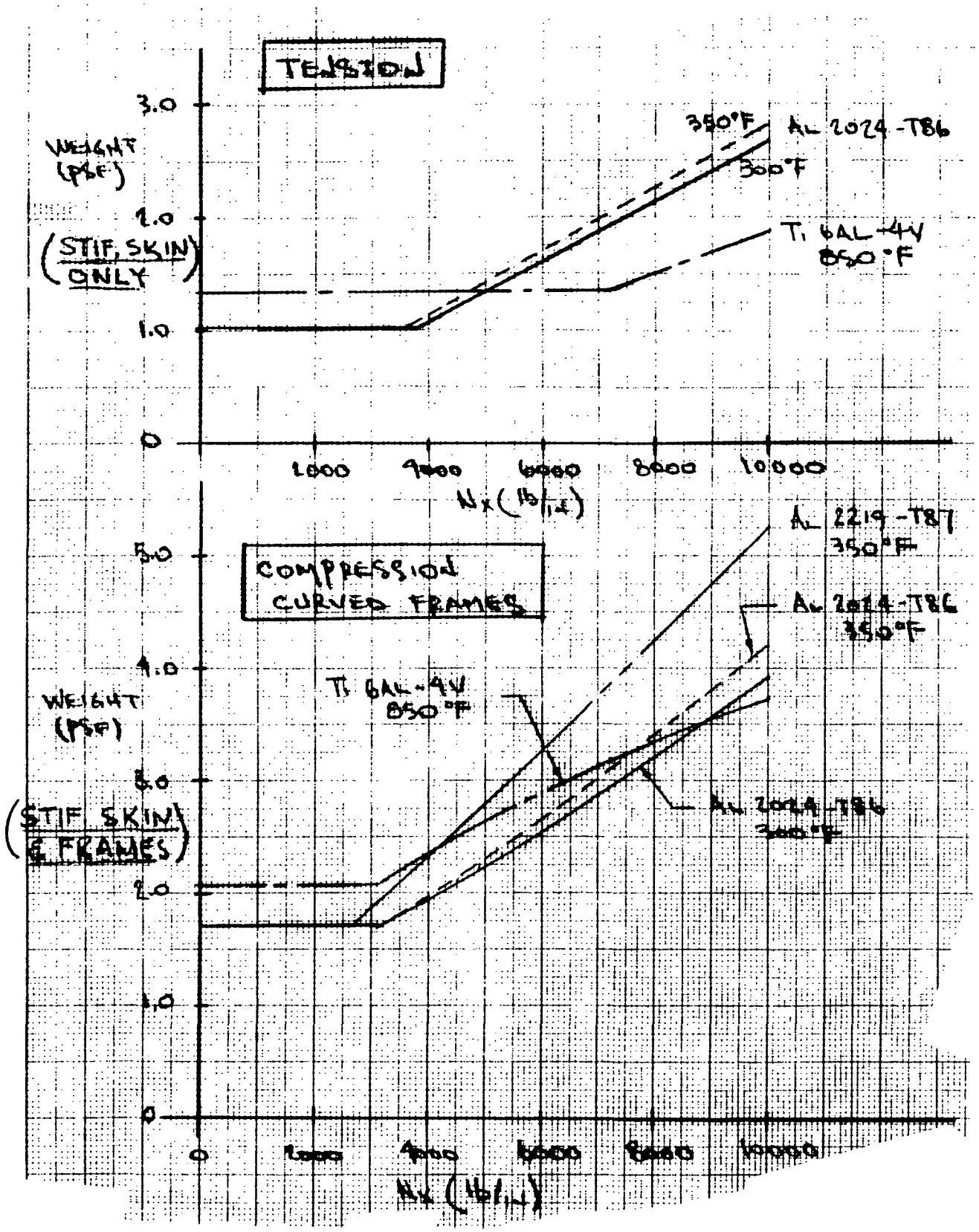

Figure 4-71. RT Weight Strength Variation of Al 2024-T86 and Ti 6Al-4V After 100 Hours Exposure to Indicated Temperature

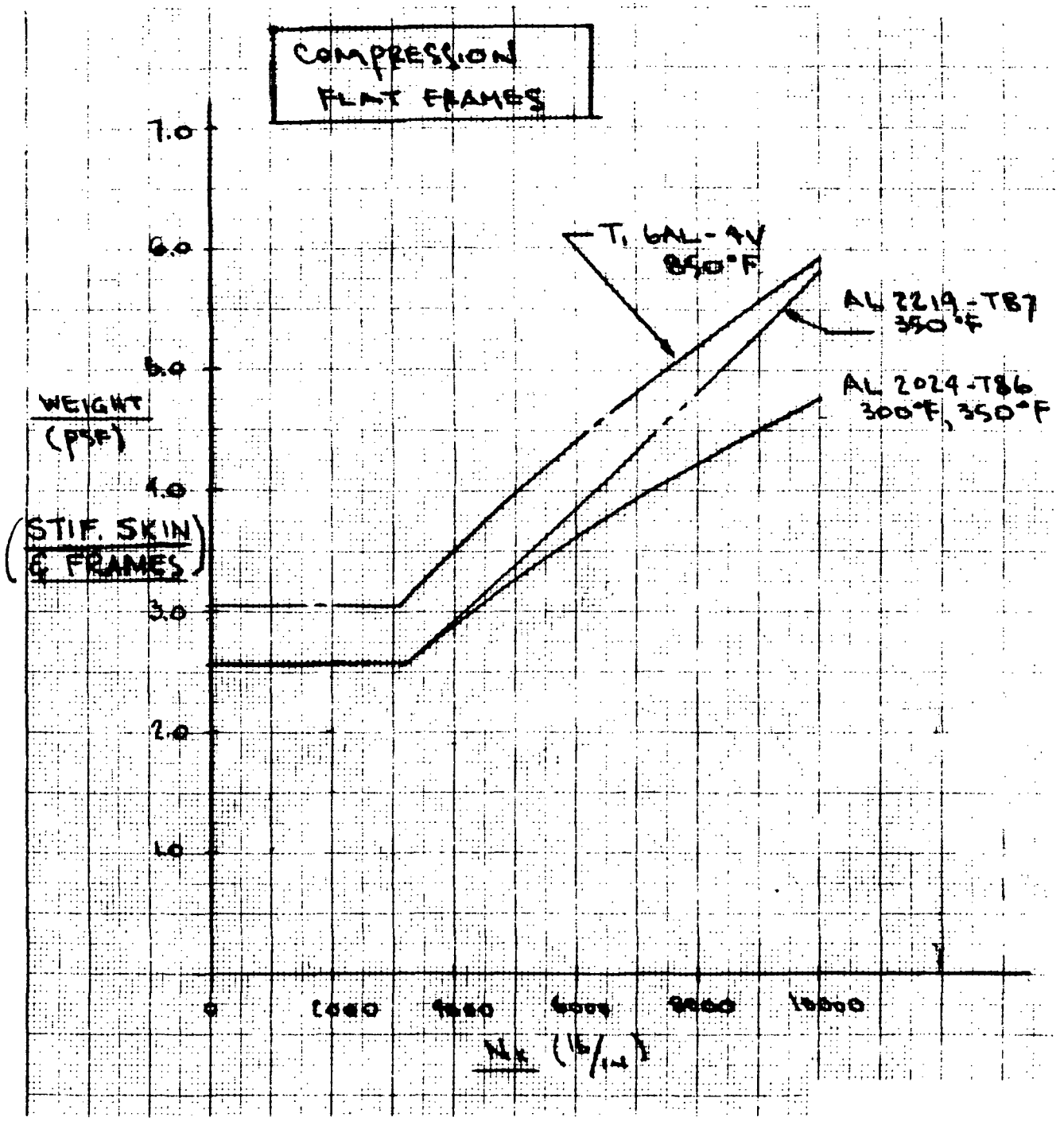

Figure 4-72. RT Weight Strength Variation of Al 2024-T86 and Ti 6Al-4V After 100 Hours Exposure to Indicated Temperature

ηE = reduced modulus, psi

$\eta = (E_T/E)^{3/4}$

E_T = tangent modulus, psi

Room-temperature stress-strain curves were generated for the aluminum alloys after 100 hours exposure to temperatures of 300 and 350 F. These curves were used to obtain the tangent moduli. The titanium material properties were not degraded from exposure of 100 hours at a temperature of 850 F, and are used as supplied.

The design equation for curved frames is given by

$$EI_{fr} = 0.000785\ R^4\ N_x/L \qquad (2)$$

where

R = 100 inches

N_x = axial compressive loading, lb/in.

L = frame spacing, in.

I_{fr} = frame moment of inertia, $in.^4$ (based on depth of frame = 7.5 in., web thickness = 0.020 in., titanium = 0.025 in., aluminum)

The design equation for flat frames is given by

$$EI_{fr} = 0.0407\ b^4\ N_x/L \qquad (3)$$

where

b = 100 inches

I_{fr} = frame moment of inertia, $in.^4$ (based on depth of frame = 15.0 in., web thickness = 0.020 in., titanium = 0.025 in., aluminum)

Then

$$\bar{t}_{fr} = \frac{A_{fr}}{L} \tag{4}$$

where

$\bar{t}_{fr}$ = equivalent thickness of frame, in.

A_{fr} = frame area, $in.^2$

Combining Equation 4 with 1 yields the total equivalent thickness of the structure

$$\bar{t}_{total} = \bar{t}_{ss} + \bar{t}_{fr} \tag{5}$$

where

$\bar{t}_{fr}$ = equivalent thickness of curved or flat frame.

Differentiating Equation 5 with respect to the frame spacing, L, yields

$$(L)^{5/2} = K_1 (N_x)^{1/2} + K_2 (N_x)^{1/2} L \tag{6}$$

where

L = optimum frame spacing, in.

K_1, K_2 = constants that include configuration, material, and plasticity effects

The optimum frame spacing and, hence, the optimum unit weight may then be determined for any load level.

In the case of tension loading, the equivalent thickness is given by

$$\bar{t} = \frac{N_x}{F_{tu}} \tag{7}$$

where

N_x = axial tension loading, lb/in.

F_{tu} = ultimate tensile strength after exposure to temperature, psi

Minimum gauge cutoffs are also shown in Figures 4-71 and 4-72 at the lower load levels. These cutoffs are based on minimum skin gauge plus a minimum hat section stringer for each material.

It should be noted that a comparison of the unit weights for skin-stringer construction with curved frames (Figure 4-71) to that with flat frames (Figure 4-72) reveals that the flat frame construction is substantially heavier than the curved frame construction.

For the orbiter load range, results in Figures 4-71 and 4-72 show that in tension design areas the aluminum structure will be about 22 percent lighter than the titanium structure. For compression design areas the aluminum orbiter should have about 17 percent less weight. In summary, the aluminum orbiter is estimated to weigh 2000 to 4000 pounds less than the titanium orbiter.

4.3.1.3 Cost Comparison

A preliminary cost comparison was made of aluminum structure versus titanium structure to identify gross differences. As shown, the RSI/aluminum system relative to the RSI/titanium system results in a $\Delta WT_{TPS} \approx +6000$ pounds and in a $\Delta WT_{STRUCT} \approx -3000$ pounds. The RSI/aluminum system is approximately 3000 pounds heavier and results in a somewhat larger orbiter tank and booster. However, when the LO_2/RP baseline booster is considered, the booster cost is not affected since the size increase is accommodated by on-loading additional propellant in available tank capacity. The preliminary cost estimate shows that the aluminum structure will result in a total program cost saving of approximately $80 million.

These trade results are currently being updated to the current baseline orbiter configuration and predicted entry thermal environment.

4.3.2 Passenger Location and Crew Compartment Size Trade Study

The phased funding, EOHT design and new mission model concepts for the Phase B extension study have raised questions as to whether a cargo bay personnel module is cost effective and necessary and what capacity it should have. A baseline concept for the integral cabin of two crewmen and two mission specialists (abbreviated: 2 + 2) was dictated by the program technical directive. However, mission studies indicate that providing sufficient volume and ECLSS capacity for a crew of two with four or six mission specialists (or space station passengers), depending on mission length, could have some cost advantages to the total Space Shuttle Program since the cargo bay personnel module design and development costs could thus be further deferred.

Results of this trade study indicate a potential advantage in a cabin concept providing for two crewmen plus four passengers adequate for seven days and convertible to a 2 + 6 capacity for three days. This could significantly defer the design and development costs of a cargo bay personnel module. Such a module might not need to be delivered until about 12 years after flight program initiation. The total program costs for the combination of module and integral crew compartment are not significantly greater than for a completely integral cabin for 14 persons. (A trade study early in the Phase B program had shown the cargo bay personnel module to be significantly more expensive, but still desirable for program cost delay and versatility). This difference is sensitive to the cost and features in a passenger/cargo module concept and could be significantly less.

The mission models used in the study are shown in Figures 4-73 and 4-74, in terms of flights per year at different personnel complements and percentage of different complements, respectively. Note that for Mark II vehicles total vehicle capacity of 2 + 4 is required as frequently as 2 + 2 (Figure 4-74). A crew compartment with volume sufficiently comfortable for six men for seven days (sortie missions) is considered adequate for eight men for one to three days (space station resupply mission or ascent/descent periods for a sortie mission). Thus, such a vehicle could be adequate until a further increase to a full 14-man complement is required, currently estimated as 12 years after start of test flight (Figure 4-73). At this time, a six-man module (or other size, as required) can be supplied if the need still exists. An economics and staffing procedures study may show, for example, that replacing fewer men more often is more desirable than rotating an entire 12-man crew at once.

Estimated costs for various combinations of capacity for cargo bay personnel modules and integral personnel compartments are indicated in Figure 4-75, as a function of the integral cabin capacity (seven-day mission). In all cases, an eventual total habitable volume capacity of 14 persons is

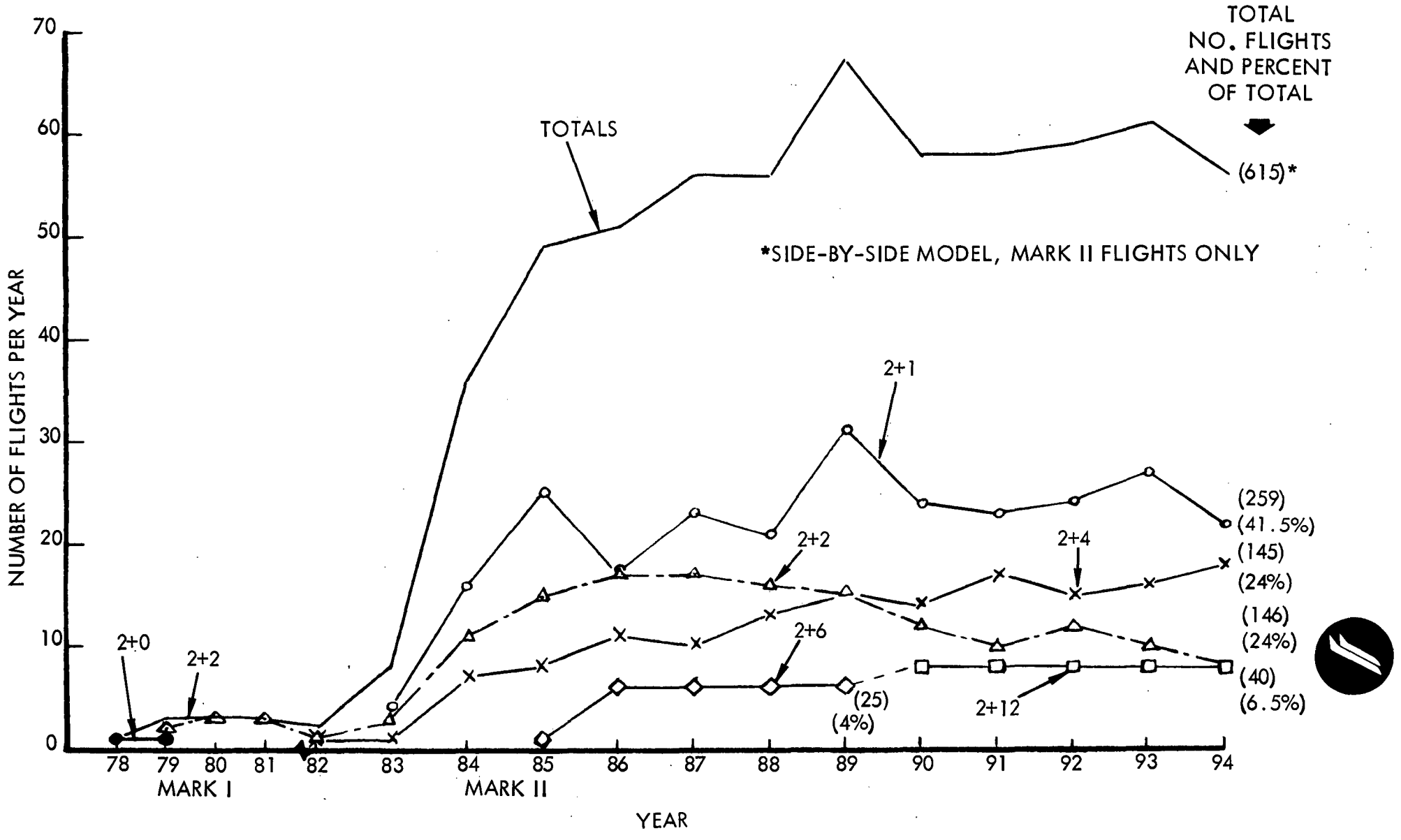

Figure 4-73. Earth Orbital Shuttle Manning Requirement, MSC Side-by-Side Loading Model

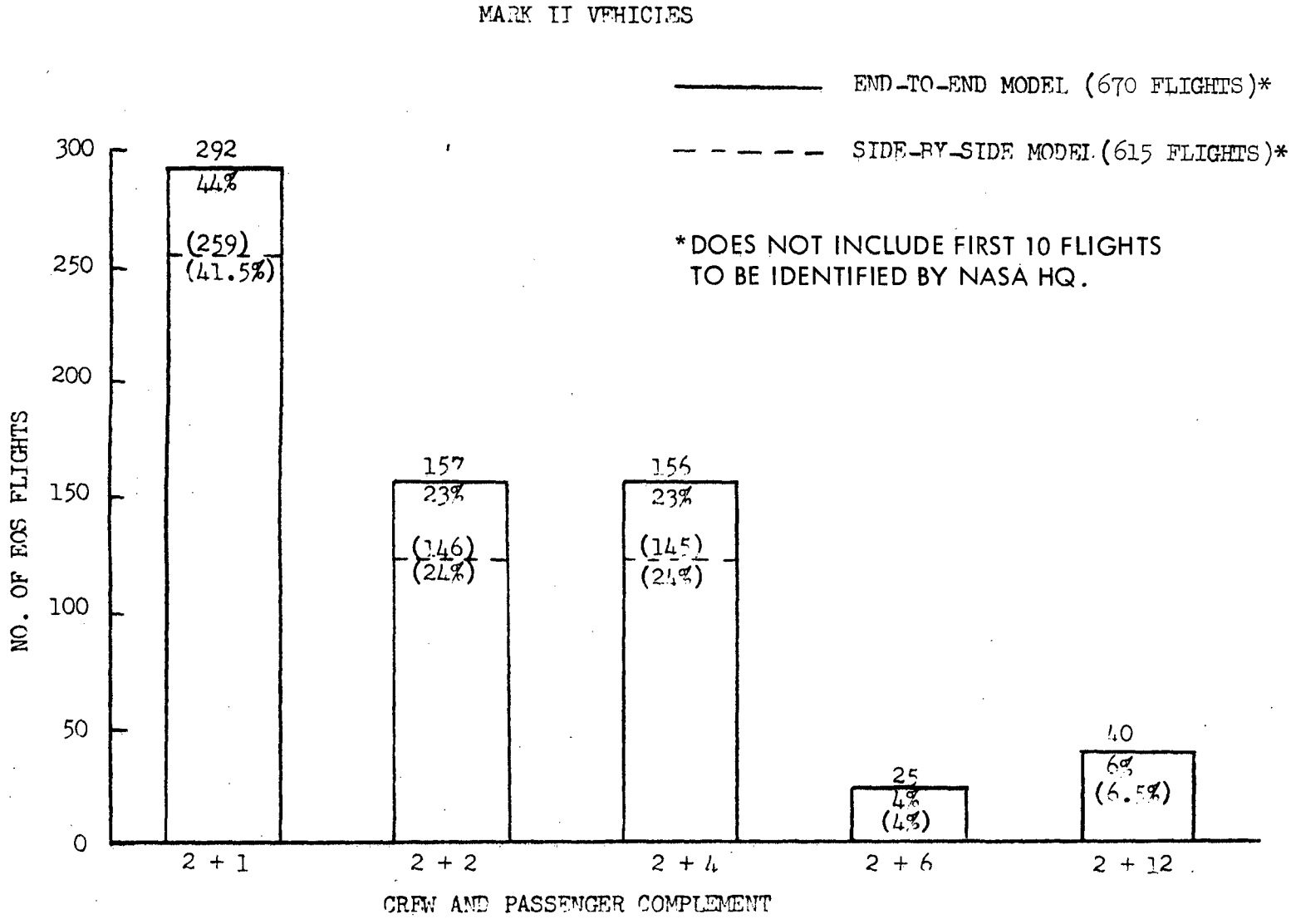

*Does not

Figure 4-74. Earth Orbital Shuttle Manning Requirement, MSC End-to-End and Side-by-Side Loading Models, Mark II Vehicles

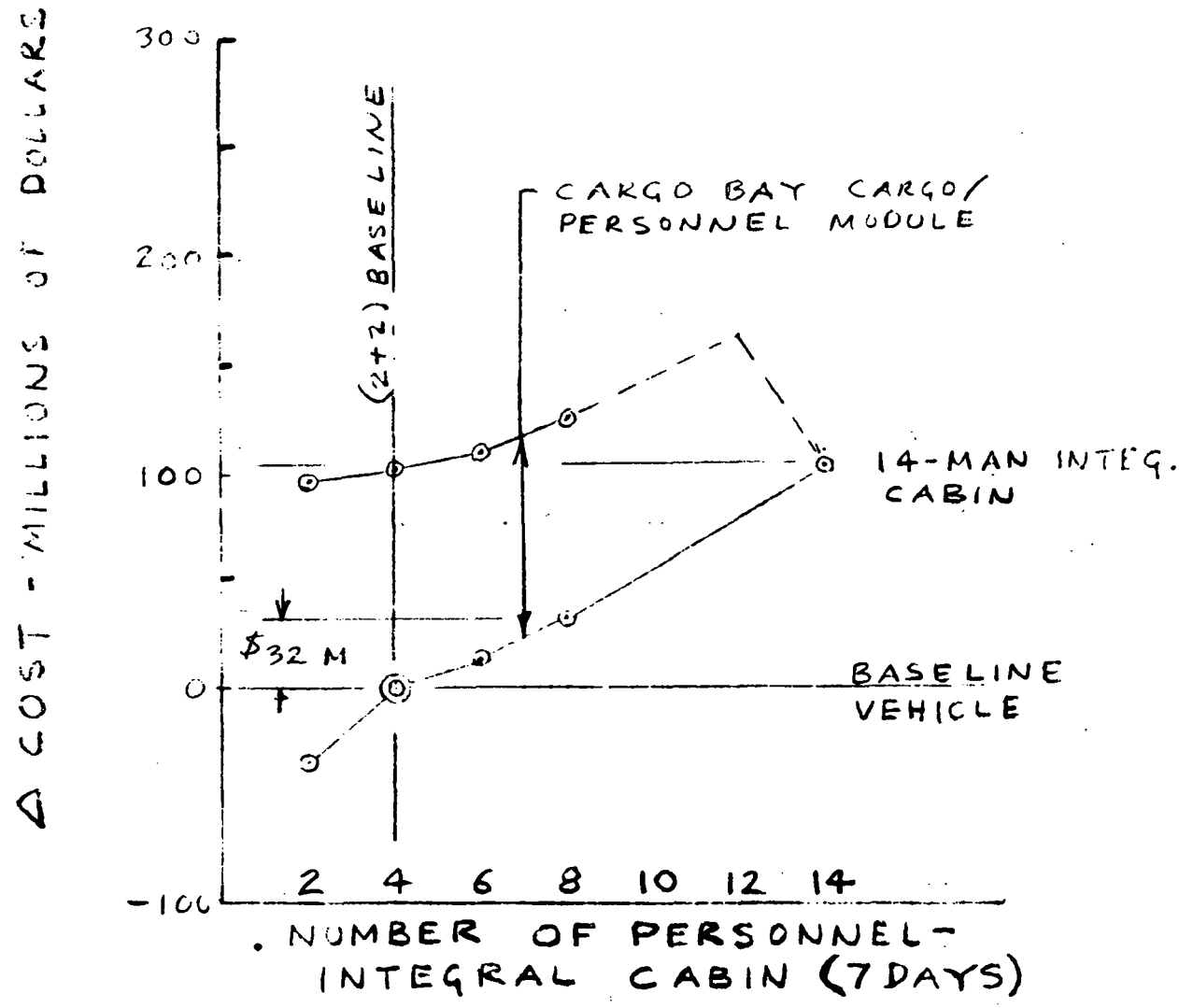

Figure 4-75. Total DDT&E Delta Costs, Orbiter Plus Module Habitable Volumes

presumed. Note that for some proposed RAM sortie missions and other missions a pressurized experiments operation module or monitor station module may be necessary in any case, but it need not provide seating for launch, reentry and landing if seating capacity is provided in the orbiter. The potential for cost deferment of the cargo bay personnel module is indicated in Figure 4-76. Years of deferment from first horizontal flight test until delivery of a module is required to support the mission model personnel complements are plotted as a function of integral cabin personnel capacity. The potential deferment for the six- to eight-man-cabin concept is beneficial in that the module development costs follow the peak engineering funding for the Mark II vehicle and all other design, development, test, and engineering major funding items.

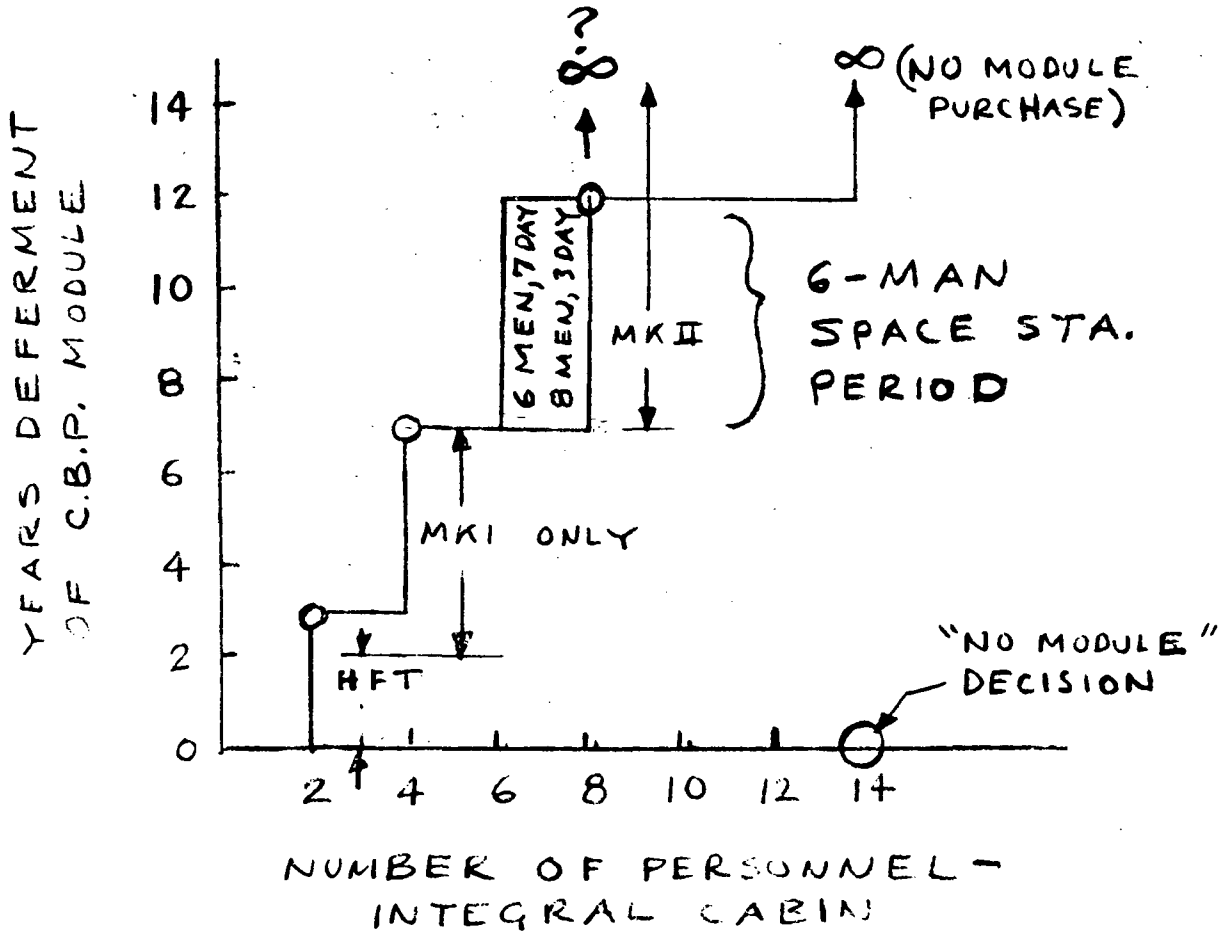

Figure 4-76. Cost Deferment

4.4 SHUTTLE SYSTEM DEFINITION

4.4.1 Integrated Vehicle Definition, LO_2-RP Flyback

The integrated vehicle baseline design and performance for an LO_2-RP flyback booster and external HO tank orbiter are defined in this section. A five F-1 engine booster and four J-2S (Mark I) and four HiPc (Mark II) orbiter have been selected, based on the trade studies described in Section 4.2.3. The integrated vehicle flight modes are illustrated in Figure 4-77. The baseline configuration and performance characteristics are shown in Figure 4-78. The mated ascent starts at lift-off with a thrust-to-weight ratio of 1.35. A maximum dynamic pressure of 650 is experienced by the combination during ascent. Staging occurs at 140 seconds from lift-off. At staging, the orbiter is separated from the booster by achieving orbiter thrust buildup and flying away from the booster during its thrust decay. The orbiter then continues the ascent trajectory to orbit; the booster returns to the launch site for landing.

4.4.1.1 Design and Mass Properties

The shuttle system configuration for the LO_2/RP reusable booster is shown in Figure 4-79. The orbiter is the NR baseline VC70-0176A mounted on a single external LO_2/LH_2 propellant tank. The booster is the General Dynamics baseline B18-E3 with tandem mounting provisions for the orbiter/tank combination. The orientation of the booster and orbiter results in the vertical surfaces of the vehicles being 180 degrees opposed to provide maximum clearance between the booster crew compartment and the orbiter main engine exhaust plume. This arrangement also minimizes the interferences with the launch facility orbiter umbilical arm. However, this orbiter/booster arrangement impacts the combined vehicle coordinate system by reversing the coordinate system of one vehicle. A common right-hand system with different points of origin, such as the previous belly-to-back arrangement, is not possible with this arrangement.

Mass properties for the orbiter/booster combination through the ascent phase of the booster are summarized in Table 4-21. These data are shown for two orbiter missions, the Mark I polar mission with 25,000 pounds cargo and the Mark I due-east mission with 65,000 pounds cargo at launch. The Mark II mission requirements establish the volumetric sizing of the tank, which is also used for the Mark I mission. The high-pressure engines of the Mark II orbiter are operated at a mixture ratio of 6 to 1; the J-2S engines at 5.5 to 1. Since the same tank is used for both Mark I and Mark II, for the Mark I missions, the orbiter fuel tank is loaded full and the oxidizer tank is off-loaded to the mixture ratio of 5.5.

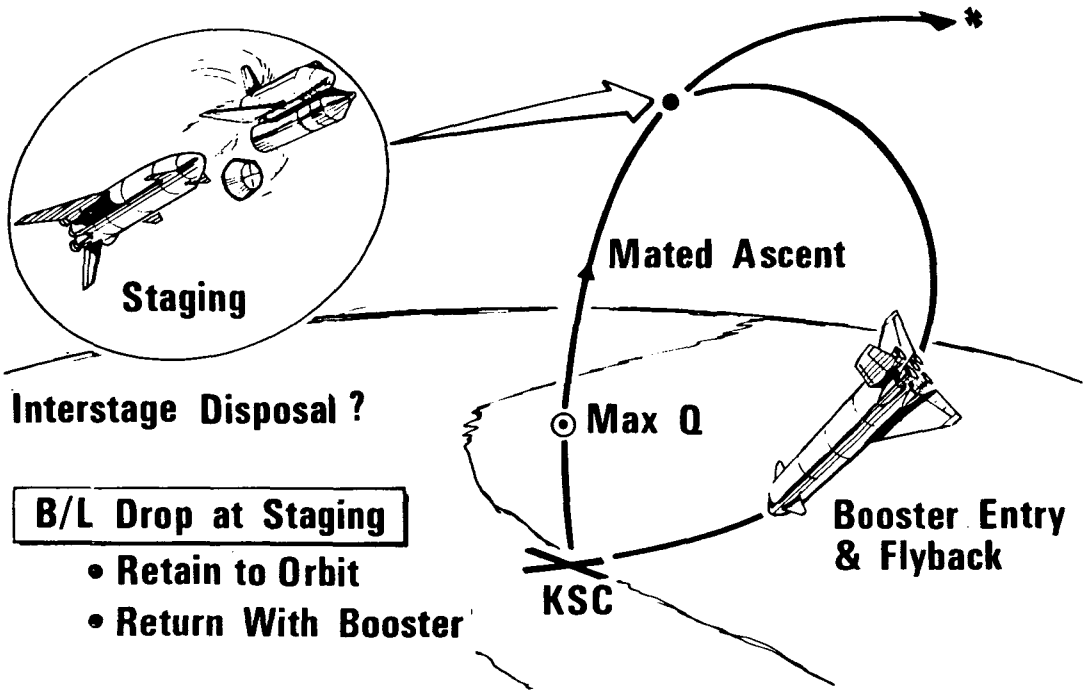

Figure 4-77. LO_2/RP F-1 Reusable Booster

SYSTEM PARAMETERS		MARK I		MARK II	
CARGO BAY		15 X 60		15 X 60	
PAYLOAD	(KLB)	25K POLAR		65K DUE EAST	
OMS V	(FPS)	650		900	
		BOOSTER	ORBITER	BOOSTER	ORBITER
SYSTEM GLOW	M(LB)	4.98		5.09	
T/W AT LO	M(LB)	1.35	1.06	1.35	0.95
STAGE GROSS WT	M(LB)	3.97	1.01	3.97	1.12
MAIN PROP. WT, USABLE	M(LB)	3.28	.776	3.28	0.836
OMS PROP. WT	K(LB)	–	9.8	–	18.1
FLYBACK FUEL	K(LB)	50.5	–	39.7	–
FLYBACK RANGE	(N MI)	183.5	–	152.4	–
*STAGE DRY WT (RV)	K(LB)	583.5	110	583.5	116.2
ORBITER EXT TANK WT	K(LB)	–	57.5	–	57.5
STAGE REENTRY WT	K(LB)	645.9	140.1	645.9	161.2
**STAGE LANDING WT	(LB)	606.1	138.7	606.1	159.7
MAX Q	PSF	650		650	
STAGING, Vr	(FPS)	6217		6000	
h	(FT)	166,900		147,400	
γ_r	(DEG)	17.8		16.9	
q	(PSF)	37		73	
MAIN ENG, F_{SL}	K(LB)	1.522	–	1.522	–
F_{VAC}	K(LB)	–	265	–	265
NO. OF MAIN ENG		5	4	5	4

*PAYLOAD & TANKS NOT INCLUDED
**INCLUDES PAYLOAD – 40K FOR MK II
25K FOR MK I

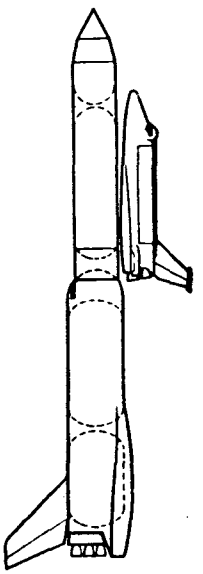

Figure 4-78. Integrated System Description, Selected Reusable LO_2/RP Booster

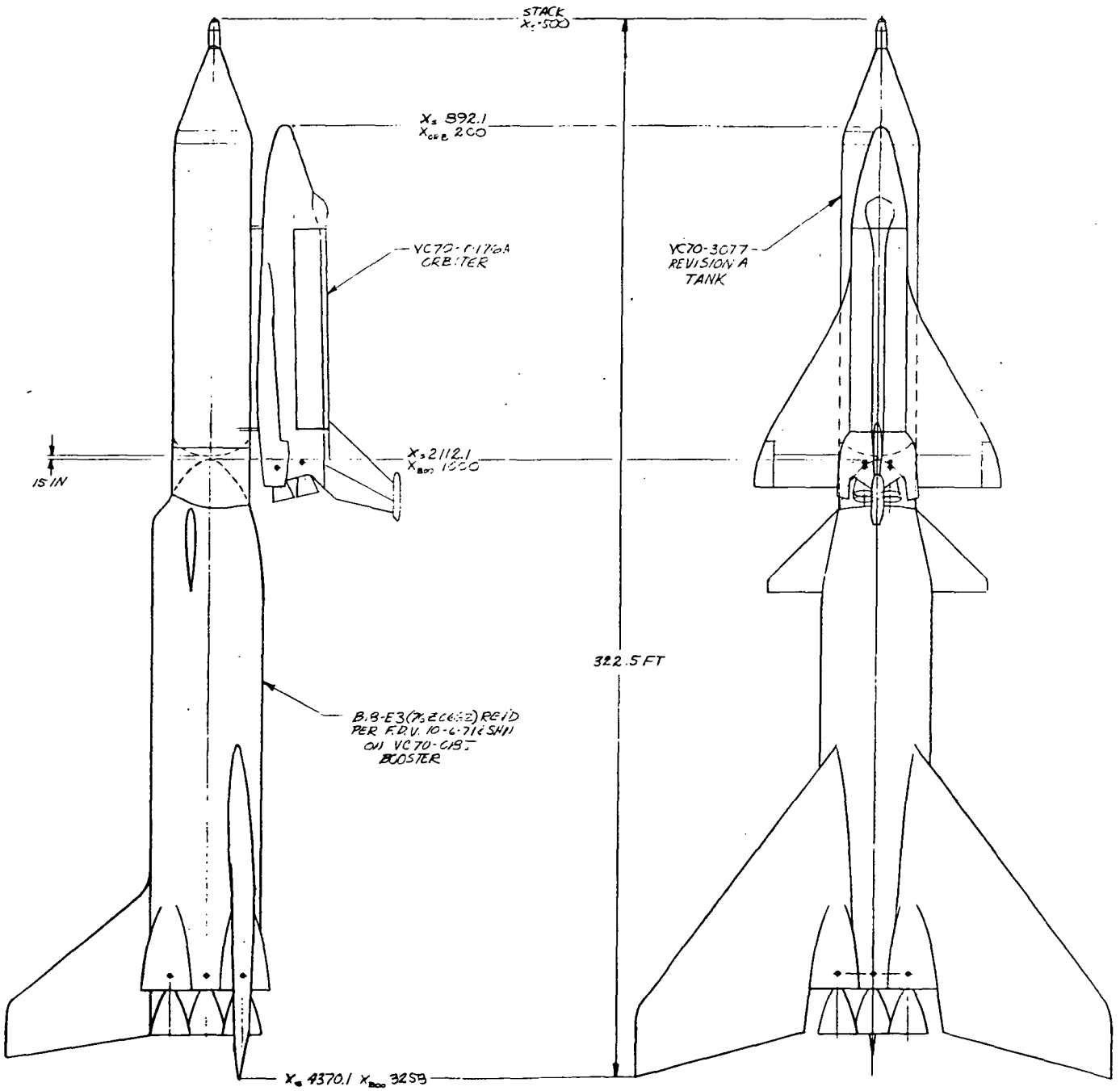

Figure 4-79. Orbiter, Tank, and Booster Stack

Table 4-21. Sequence Mass Properties Statement

CONFIGURATION: MK I & MK II ORBITER/B-18E-3 BOOSTER COMBINATION						BY		DATE		PAGE OF	
			CENTER OF GRAVITY			MOMENT OF INERTIA			PRODUCT OF INERTIA		
			INCHES			SLUG FT^2 X 10^{-6}			SLUG FT^2 X 10^{-6}		
NO.	MISSION EVENT	WEIGHT LB.	X	Y	Z	$I_{x\text{-}x}$	$I_{y\text{-}y}$	$I_{z\text{-}z}$	I_{xy}	I_{xz}	I_{yz}
MK	I POLAR 25K ORBITER/LO_2 - RP BOOSTER										
	LIFT-OFF	4973883	2819.0	0	406.4	13.291	914.303	913.984	0	-14.013	0
	BOOSTER ASCENT PROP	-1394689									
	MAX Q FLIGHT CONDITION	3579194	2725.8	0	408.3	12.096	847.631	847.308	0	-13.567	0
	BOOSTER ASCENT PROP	-1620372									
	3-G FLIGHT CONDITION	1958822	2303.9	0	415.0	10.700	641.676	641.448	0	-10.850	0
	BOOSTER ASCENT PROP	-264380									
	BOOSTER BURNOUT	1694442	2139.8	0	417.5	10.510	562.599	562.461	0	-9.806	0
MK	II DUE EAST 65K ORBITER/LO_2 - RP BOOSTER										
	LIFT-OFF	5088421	2787.5	0	409.0	14.104	966.433	965.369	0	-17.106	0
	BOOSTER ASCENT PROP	-1394689									
	MAX Q FLIGHT CONDITION	3693732	2685.3	0	411.9	12.895	893.274	892.219	0	-16.305	0
	BOOSTER ASCENT PROP	-1620372									
	3-G FLIGHT CONDITION	2073360	2254.8	0	421.0	11.457	664.516	663.601	0	-12.221	0
	BOOSTER ASCENT PROP	-264380									
	BOOSTER BURNOUT	1808980	2093.9	0	424.2	11.252	579.095	578.284	0	-10.703	0

NOTES:

NOSE OF TANK IN STACK = STA 500 (VC70-0186, Revision A)

CENTER LINE OF TANK = 400

Summary weights for the integrated vehicle with both Mark I and Mark II orbiters are shown in Table 4-22. The LO_2/RP booster was sized by the Mark II due east mission with 65K cargo using the orbiter and tank weights shown for Mark II.

4.4.1.2 Aerodynamics and Stability

The aerodynamic baseline launch configuration of the 040A (176A) orbiter/EOHT/B18-E3 Rev. booster shown in Figure 4-79 evolved from a series of trade studies of launch vehicles with manned flyback boosters using LO_2/RP propellant. The 176A orbiter with the belly-mounted EOHT is the second stage of the launch configuration. This stage is mounted atop the B18-E3 Rev. booster nose with the EOHT tandem to the booster body. In a side view, the orbiter is inverted relative to the booster. This arrangement was selected to minimize rolling moment due to yaw, thus minimizing the differential engine nozzle deflections required to counter the aerodynamic moment. It also improves yaw stability by eliminating the washout that would occur on the booster vertical fin if the orbiter were diametrically opposed.

The launch vehicle has a center of gravity location at liftoff 640 inches aft of the booster nose and moves forward during boost to a position 75 inches aft of the booster nose. Since the limits of travel of the pitch aerodynamic center fall between 923 to 1060 inches aft of the booster nose, the vehicle is statically stable in pitch across the boost Mach range.

In the yaw plane, the limits of travel for the yaw aerodynamic center fall between 332 to 540 inches aft of the booster nose. At liftoff, the launch vehicle has a margin of instability of 100 inches. As the vehicle accelerates, the unstable margin decreases and the vehicle becomes statically stable in yaw for Mach numbers above 4.0.

Stability and/or control is maintained during boost using thrust vector control by deflection of the gimbaled booster engine nozzles. Symmetrical deflections in the respective planes provide pitch and yaw control and differential deflections provide roll control.

The longitudinal aerodynamic characteristics for the baseline launch vehicle are presented in Figures 4-80 through 4-83. The forebody axial force coefficient shown in Figure 4-80 is used in conjunction with the power-on booster base axial force, which is shown as a function of altitude in Figure 4-81. The base axial force is based on flight test base pressure measurements from Saturn V flights. The assumption was made that altitude is the primary influence on base pressure and velocity a secondary factor.

Table 4-22. Integrated Vehicle Weight Statement, LO_2/RP Booster

	MK I - POLAR		MK II - DUE EAST	
ORBITER & TANK COMBINATION		1001093		1115631
Cargo	25000		65000	
Orbiter (Less Cargo & Tank)	129223		143429	
Ascent Propellant	776000		836332	
Tank Burnout	70870		70870	
BOOSTER (B-18E-3)		3972790		3972790
Ascent Propellant	3279441		3279441	
Burnout	693349		693349	
GLOW		4973883		5088421

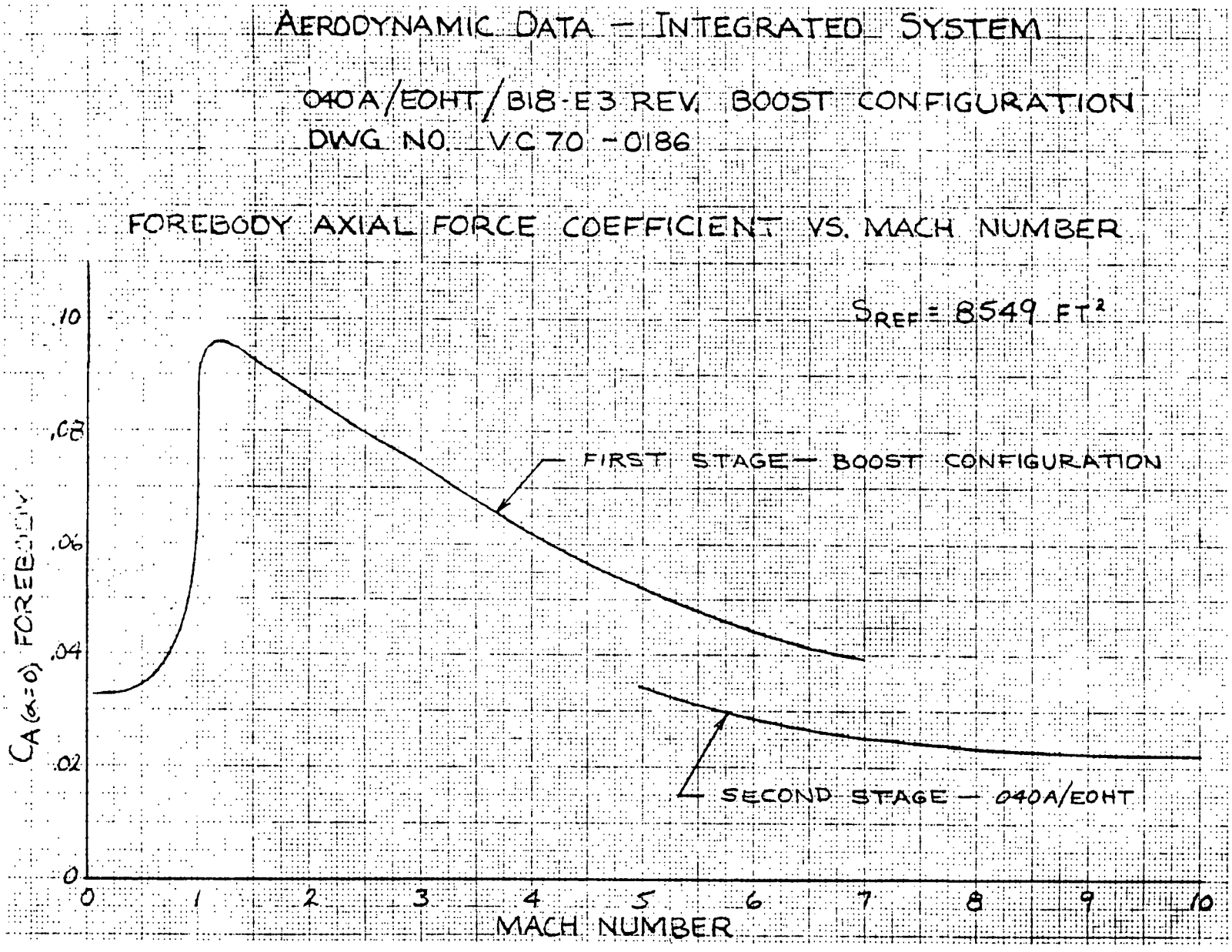

Figure 4-80. Axial Force Characteristics

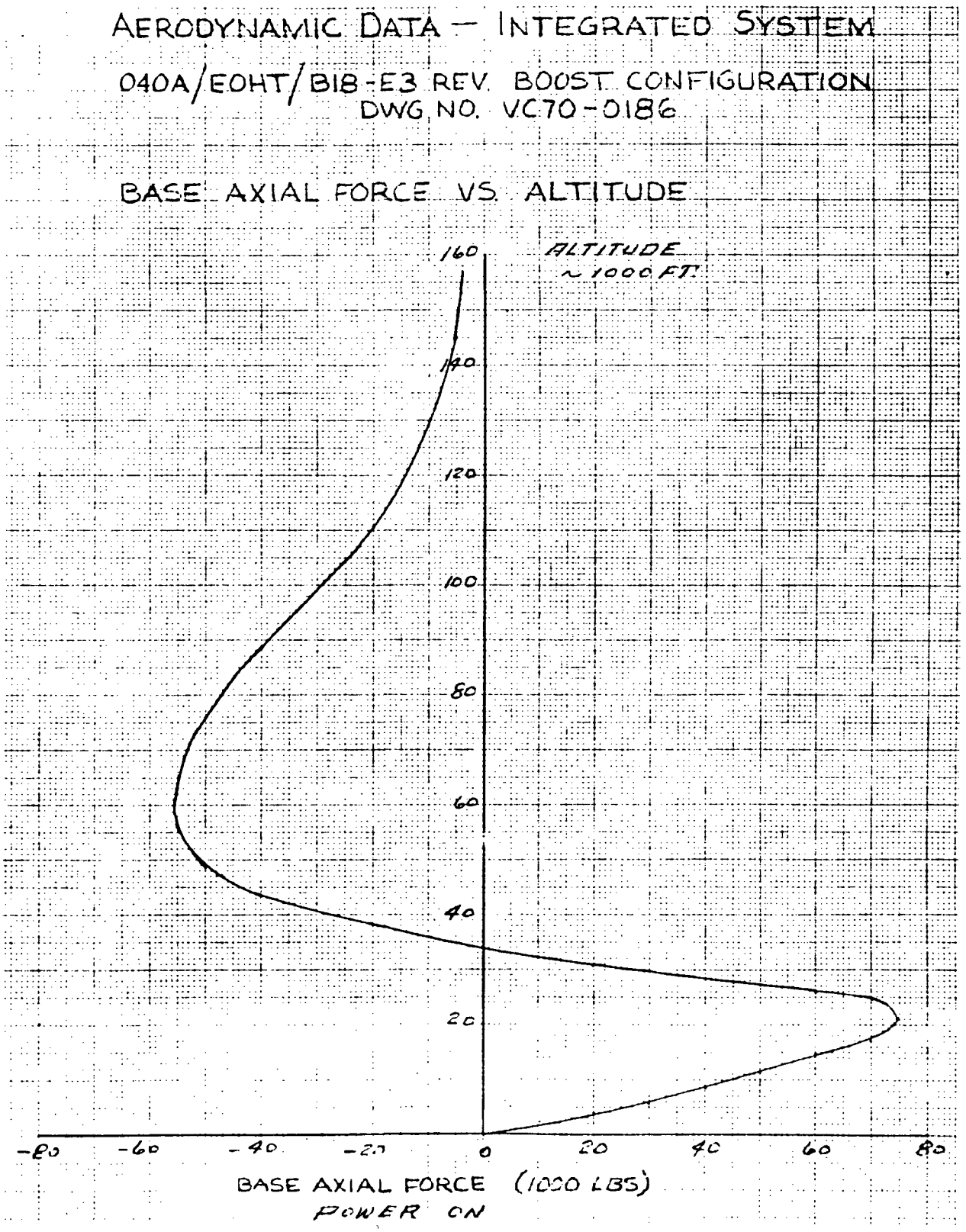

Figure 4-81. Base Force Characteristics

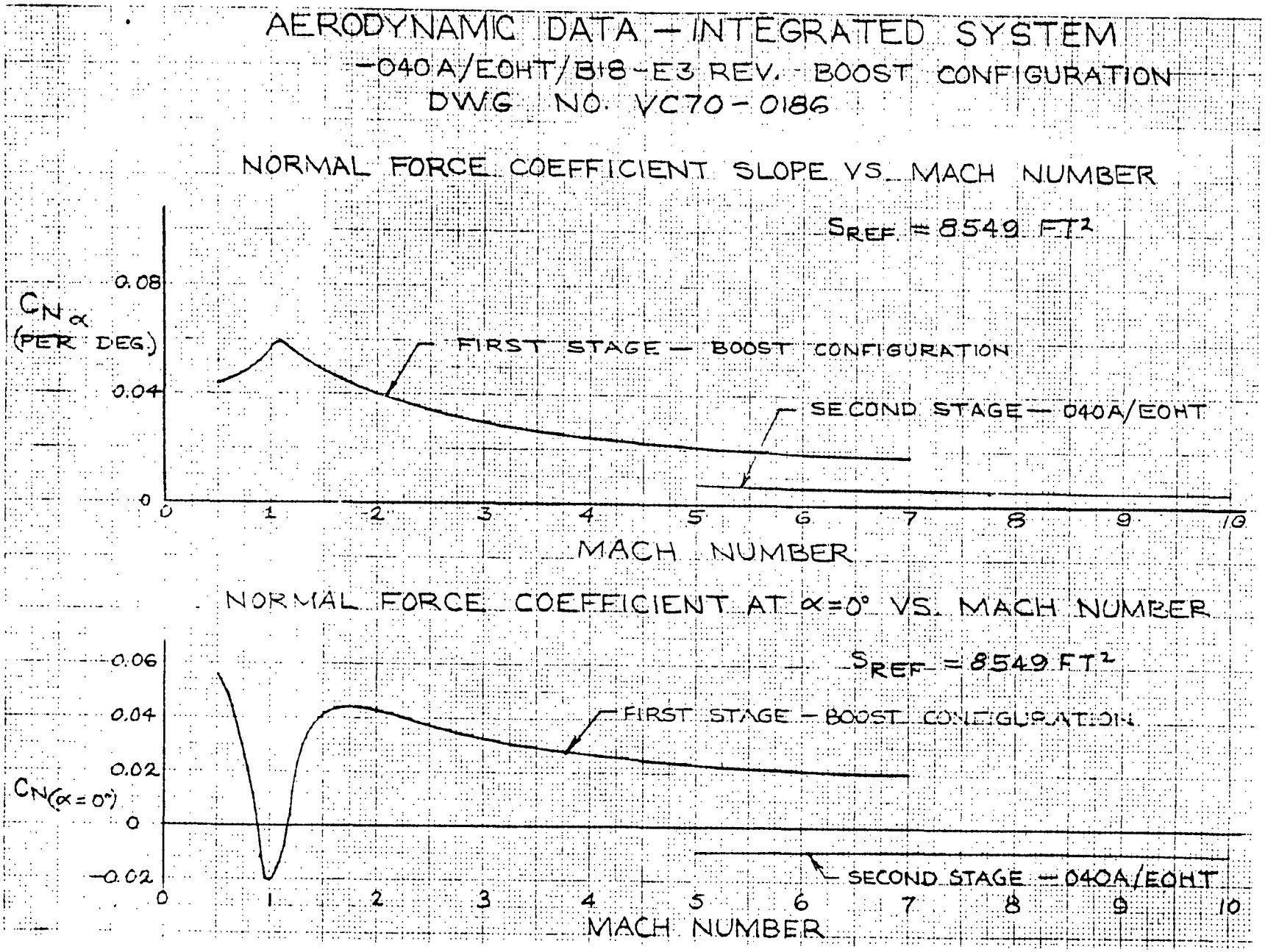

Figure 4-82. Normal Force Characteristics

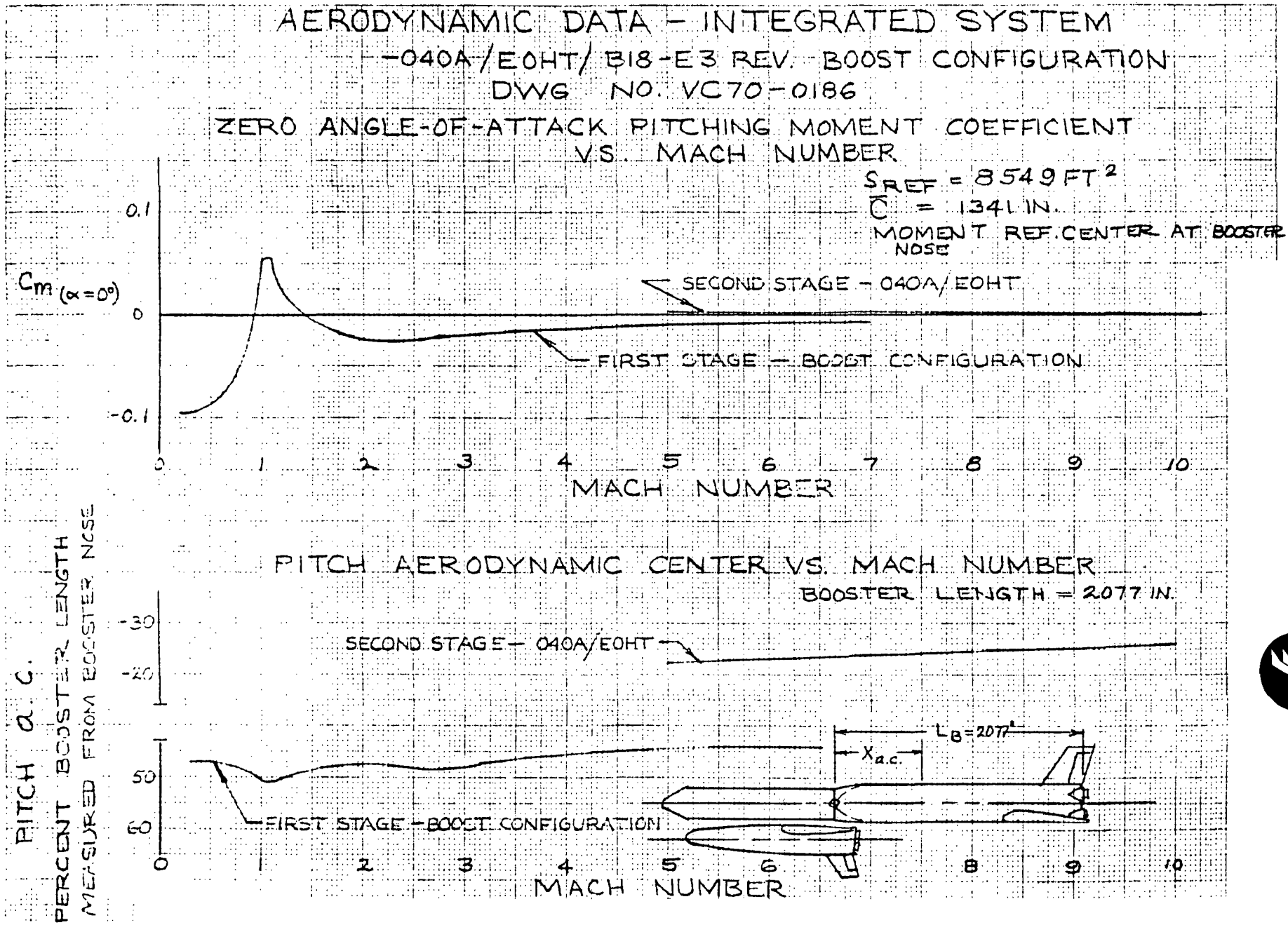

Figure 4-83. Pitching Characteristics

Under this assumption, base pressures were correlated to the space shuttle vehicle launch flight trajectory and base axial force derived.

Figure 4-82 presents the normal force coefficient at zero angle of attack and the slope of the normal force coefficient as functions of Mach number. Figure 4-83 shows the variation of the pitching moment coefficient at zero angle of attack and the aerodynamic center in pitch with Mach number.

Figures 4-84 and 4-85 present the lateral aerodynamic characteristics through the boost Mach range. The side force coefficient curve slope is shown as a function of Mach number in Figure 4-85. The center of gravity and pitch and yaw aerodynamic centers through the boost Mach range are shown, respectively, in Figures 4-86 and 4-87.

It is to be noted that the aerodynamic data presented are based on the velocity vector approaching the underside of the booster for positive angles of attack for the first stage vehicle (orbiter/EOHT/booster) and on the velocity vector approaching the underside of the orbiter for positive angles of attack for the second stage vehicle (orbiter/EOHT).

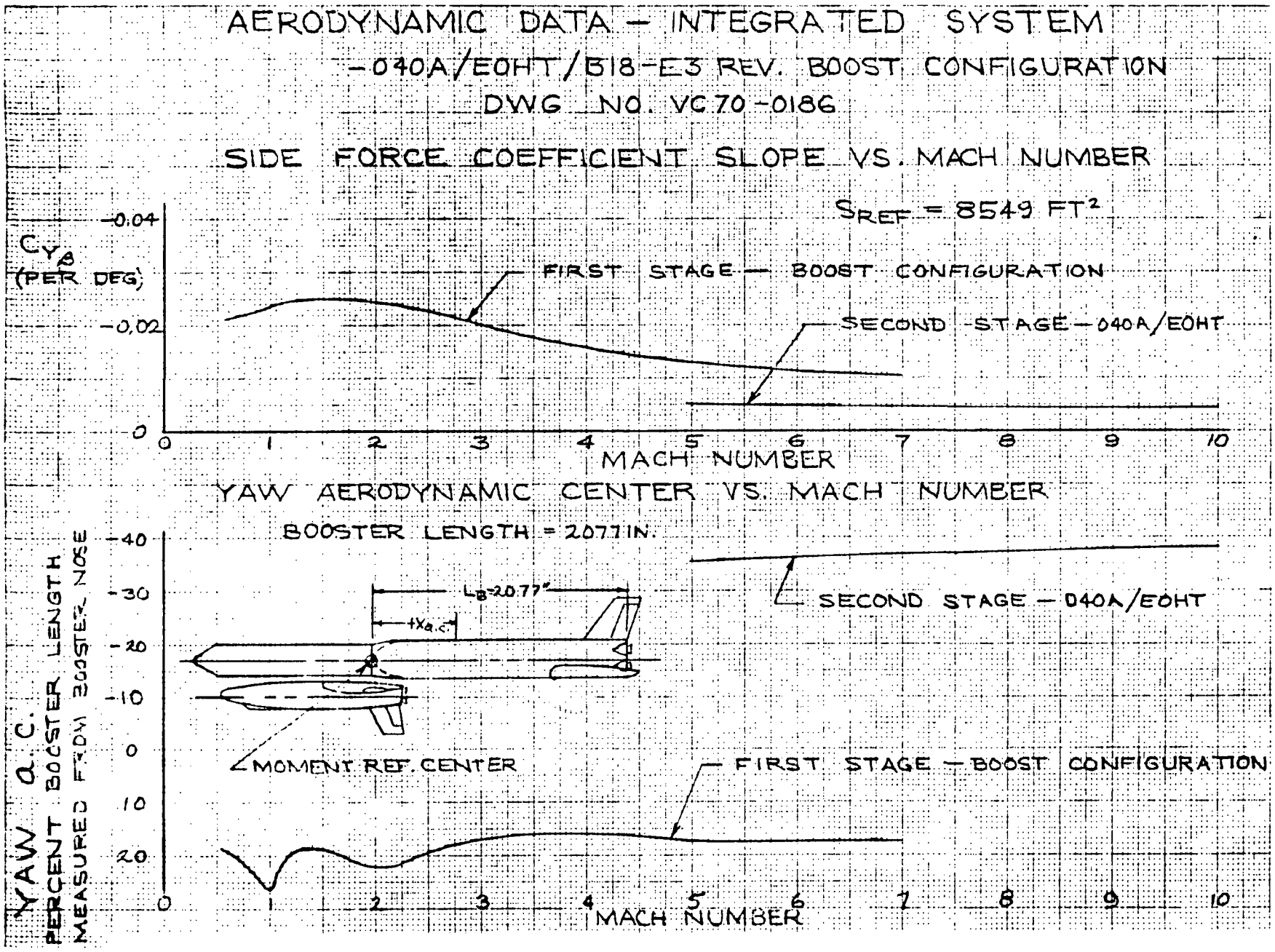

Figure 4-84. Side Force Characteristics

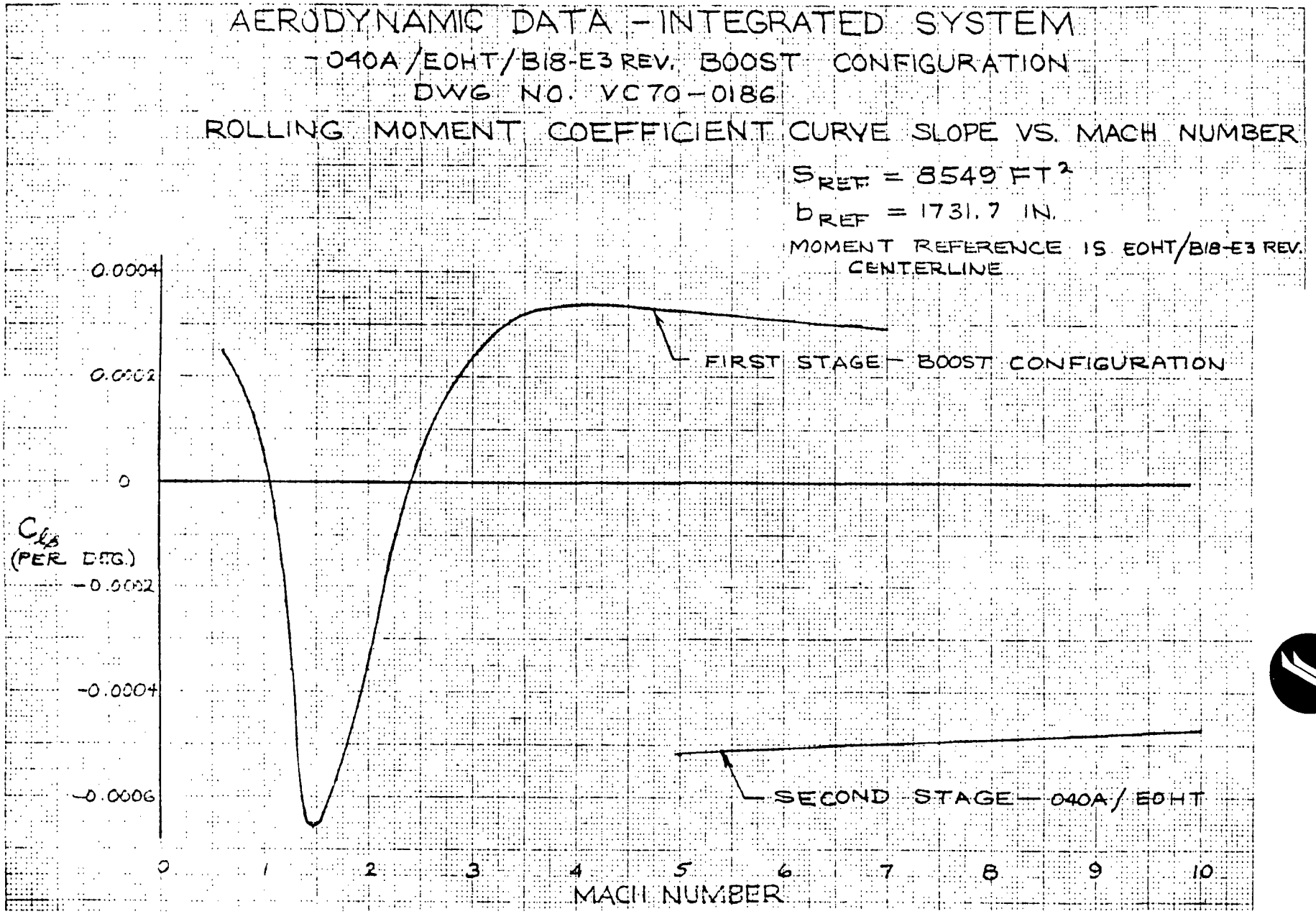

Figure 4-85. Rolling Characteristics

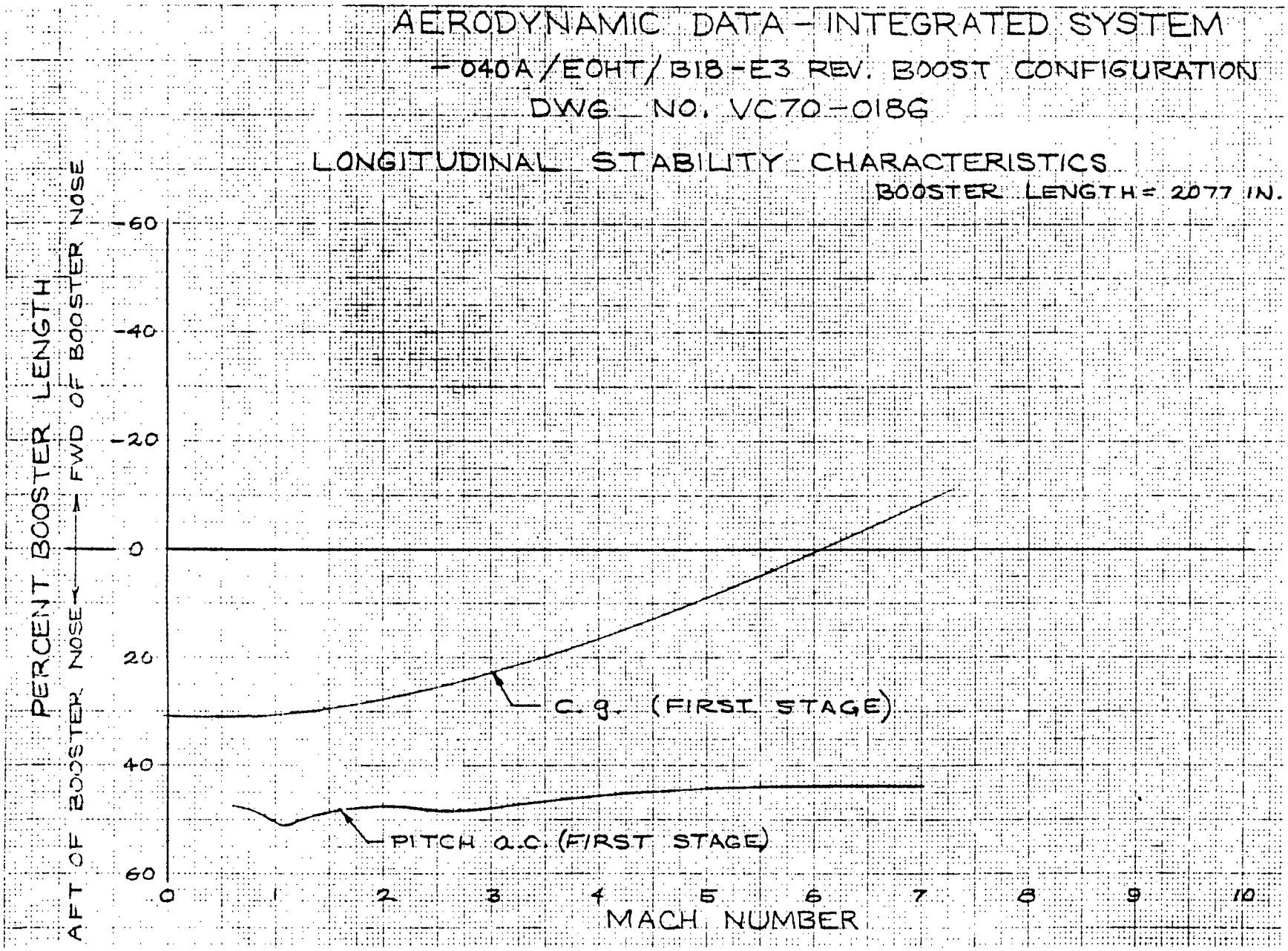

Figure 4-86. Pitch Stability Characteristics

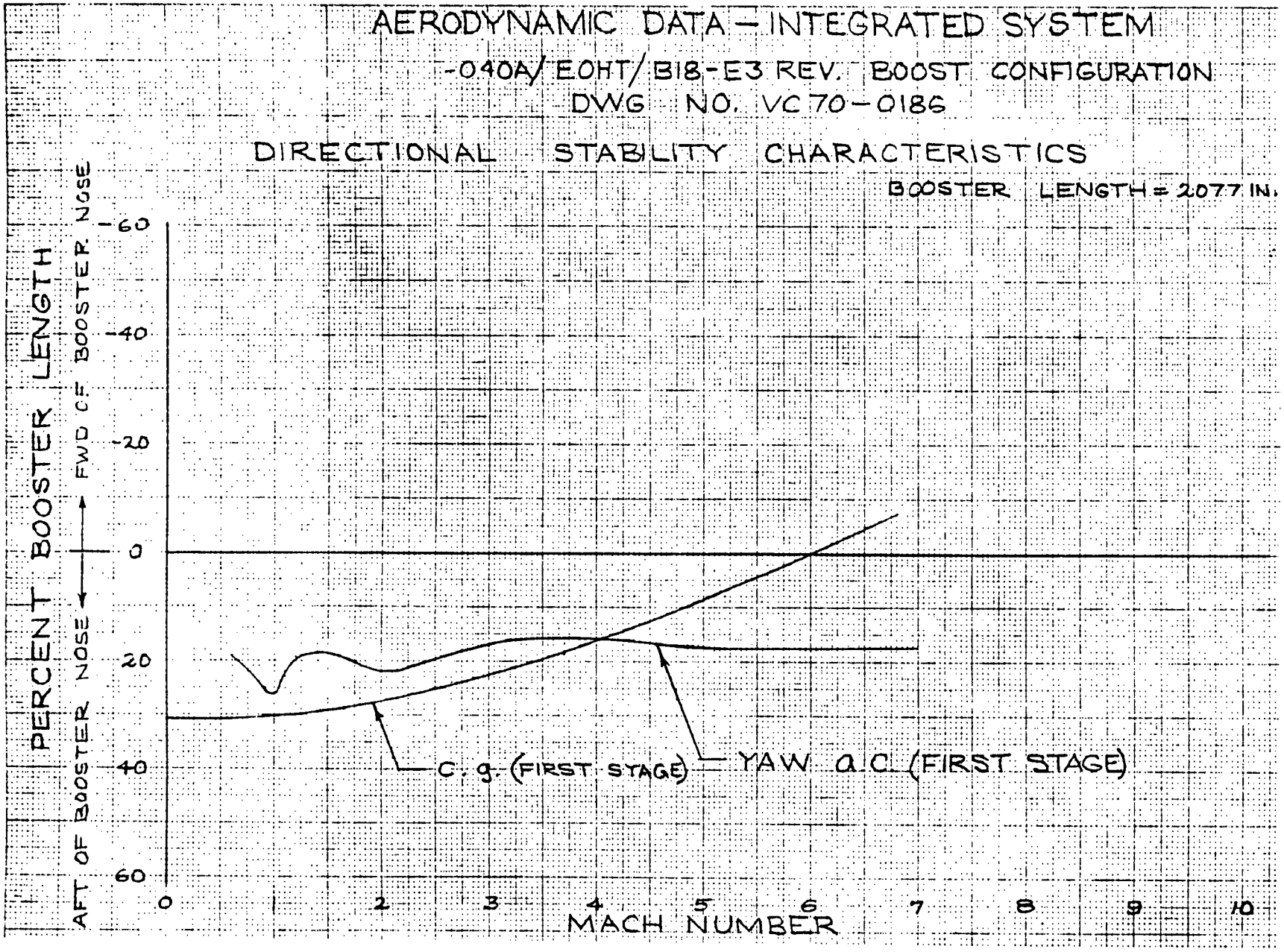

Figure 4-87. Yaw Stability Characteristics

4.4.1.3 Ascent Trajectory and Performance

A description of the baseline system resulting from the sizing analysis is given in Figure 4-78. The ascent performance data for the baseline vehicle were determined with the aid of a two-dimensional point mass computer program employing the following assumptions:

1. A 1963 Patric atmosphere
2. Instantaneous pitch maneuvers
3. No pre-ignition, thrust buildup, or thrust cutoff losses
4. Zero lift and thrusting colinear with the velocity vector during atmospheric flight (booster)
5. Optimum pitch-plane steering during exoatmospheric flight (orbiter)
6. Orbiter propellant weight is adjusted by a simple Ig $1n\mu$ calculation to account for orbiter drag losses.
7. A 2-1/2-second coast period is used to approximate staging losses.

The resulting nominal ascent trajectory profile and sequence of events are presented in Figure 4-88 and Table 4-23, respectively. The five F-1 engines are throttled to 90 percent of full thrust at liftoff and the center engine is cut off at 50 seconds to limit the maximum dynamic pressure to approximately 650 psf.

Payload performance capabilities of the Mark II and Mark I systems are given in Figures 4-89 and 4-90, respectively. Insertion occurs at the perigee of a 50 by 100 nm orbit, and the altitude is adjusted by performing a Hohmann transfer. Although the orbiter is designed to return a 25,000-pound Mark I payload and a 40,000-pound Mark II payload, the ascent payload was assumed to be returned. After determining the on-orbit delta-V allotment to perform the Hohmann transfer and direct entry maneuver, an additional 15 percent was allocated for contingencies.

The interstage, which mates the orbiter external tank to the booster, is assumed to be jettisoned at booster staging. The resulting impact points for the reference missions will vary from 120 to 150 nm, depending mostly on the orientation of the interstage during entry. If the interstage happens to impact a land mass for a particular mission, the interstage must be carried during the orbiter ascent until it can be jettisoned safely.

Table 4-23. Sequence of Events (LO_2/RP Baseline System)

Time (sec)	Event
0	Liftoff at 90-percent thrust, vertical boost
14.0	End vertical boost, pitch over, initiate gravity turn
50.0	Booster CECO
72.0	Max q = 646 psf
114.0	Begin 3-g throttling
138.0	Engines throttled 300,000 pounds, cut off two engines
140.6	Booster shut down and staged, begin coast (q = 73 psf, θ_λ = 38.5°)
143.1	End coast, orbiter ignited, initiate linear tangent steering
468.6	Begin 3-g throttling
503.5	Orbit insertion

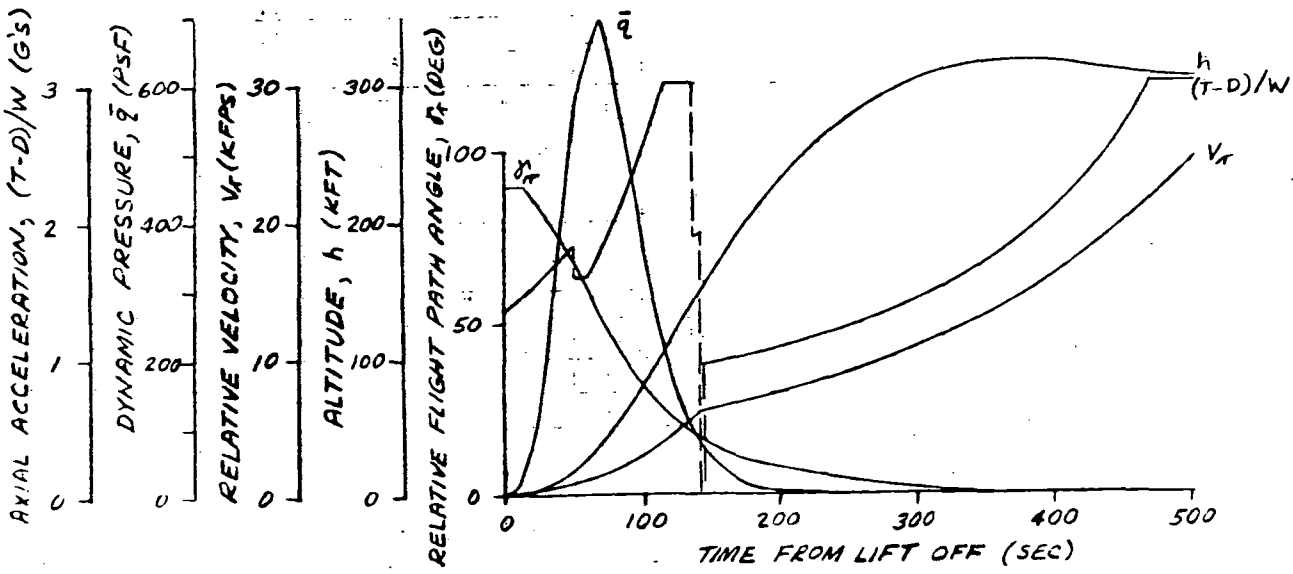

Figure 88. Ascent Trajectory Profile, Mark II LO_2/RP Baseline

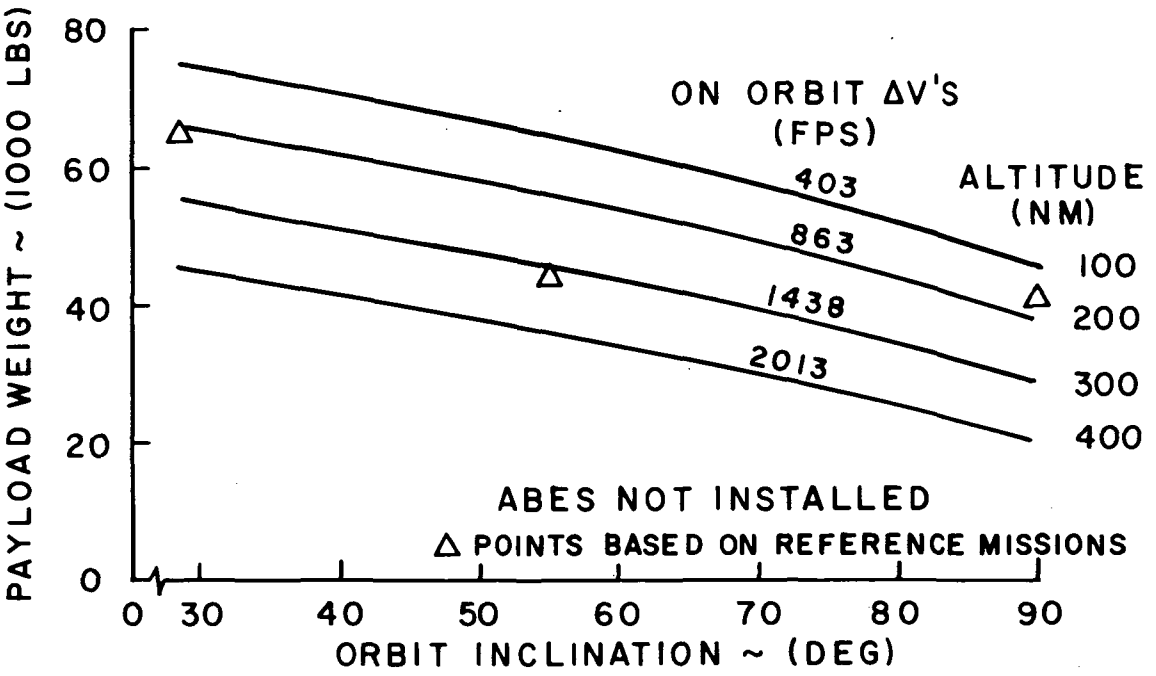

Figure 4-89. Mark II Orbiter

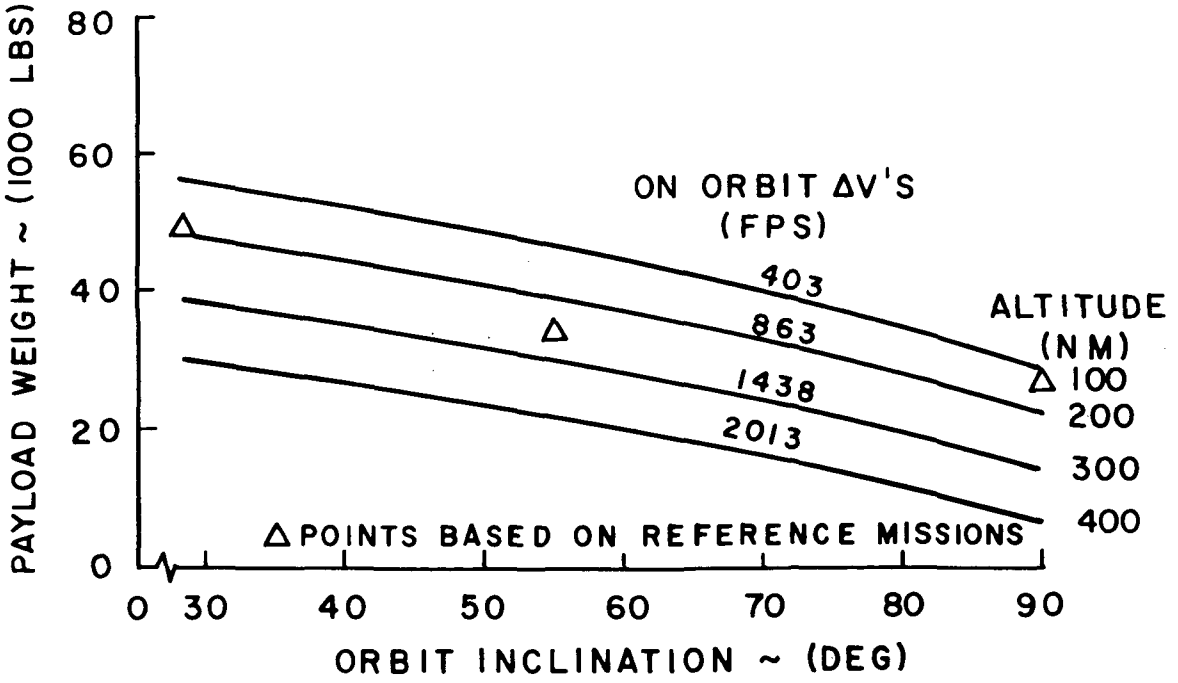

Figure 4-90. Mark I Orbiter

4.4.1.4 Ascent Control

Early in Phase 2, a LO_2-RP booster system was baselined incorporating four F-1 engines (configuration VC70-3058). Analyses to optimize the ascent trajectory and flight control system were initiated for this system. At a later date, the baseline configuration was updated to a five-engine propulsion system. Due to time constraints, however, the flight control system optimization continued on the four-engine version. It is believed that the trends and results will be applicable, primarily due to the ground rule constraint on the maximum dynamic pressure of 650 psf.

Preliminary trajectory optimization results are shown in Figure 4-91. Payload delivered to orbit in a due-east mission is shown as a function of the dynamic pressure limit. For the ground rule limit of 650 psf, a payload capability of approximately 60, 700 pounds is shown. These results do not consider booster flyback propellant or an OMS abort-to-orbit requirement. Also shown is the minimum throttle ratio necessary to limit the dynamic pressure to the abscissa value.

Payload capability as a function of the ascent angle-of-attack policy is shown in Figure 4-91. Whereas the Phase B baseline vehicle showed significant payload improvement for a lifting trajectory, this vehicle is essentially insensitive to angle-of-attack over the range of nominal interest. This characteristic will be exploited in planned follow-on studies as a tool to balance positive and negative aerodynamic loads induced by wind shears and gusts.

Flight control studies were initiated to establish booster control laws to minimize structural loads induced by wind shears and gusts, and the propellant penalties associated with flight path dispersions at staging. The control system performance was evaluated using the synthetic wind profiles found to be most critical during previous Phase B studies. Two wind profiles were used, one having a superimposed gust occurring at 12, 600 feet altitude and one having a gust at 32, 800 feet. Results were obtained using these profiles to simulate either a head wind, a tail wind, or a side wind. A pitch program for a zero angle-of-attack nominal trajectory was used in the boost simulation. The design objectives, based on Phase B study results, are:

1. Maintain aerodynamic loads within the following limits:

$$\bar{q}\alpha \leq 2800 \text{ psf - deg}$$

$$\bar{q}\beta \leq 2400 \text{ psf - deg}$$

2. Propellant weight penalty due to dispersions at burnout should be less than 2000 pounds (flight performance reserve)

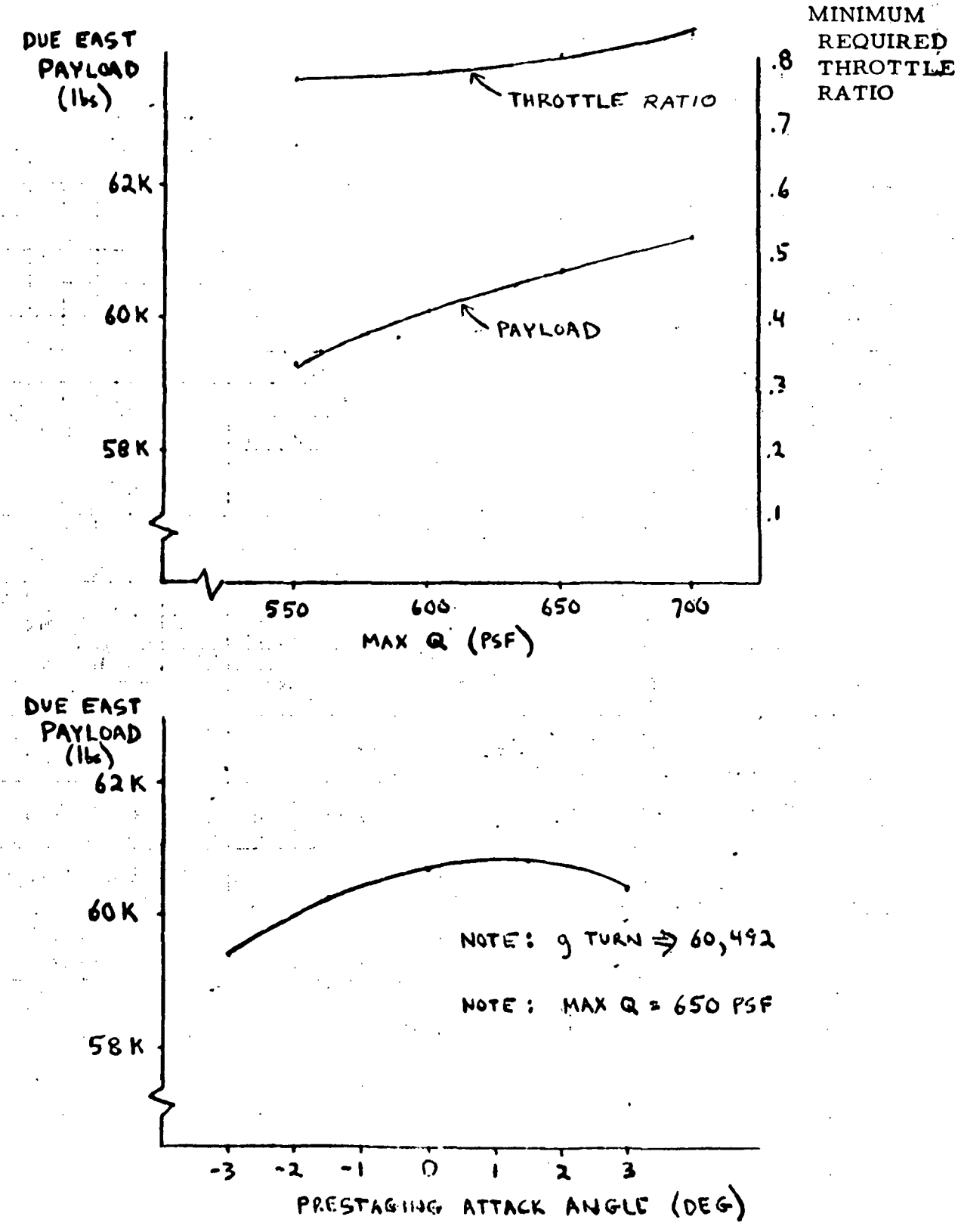

Figure 4-91. Trajectory Results for VC 70-3058

The study approach taken was to assume first a simple attitude-control system with fixed gains, compute dispersions and loads, and then modify the system to satisfy the design objectives. The initial performance results were obtained with a fixed gain attitude control system. The significant results obtained are shown in Table 4-24.

These results pointed out both a gimbal authority problem and a load relief problem in both the pitch and yaw axes. The gimbal deflection limit of the F-1 engine is ±6 degrees, and the gimbal rate limit is ±5 degrees per second. Clearly the ±6-degree deflection limit was exceeded; the allowed $\overline{q}\alpha$ limit was exceeded for a tail wind; and the allowed $\overline{q}\beta$ was exceeded for a side wind. The variation in propellant required (weight penalty) is not considered a serious variation. It was concluded from these results that a load relief-type control system is necessary during boost.

Design of a load relief control system was initiated to satisfy the $\overline{q}\alpha$ and $\overline{q}\beta$ design limits. The load relief system in both axes consisted of a blend of lagged acceleration and attitude feedbacks with a rate inner loop. The gains on acceleration and attitude were varied as a function of time. Although the control effectiveness does vary by a factor over the flight, the rate gain was held constant during these preliminary analyses. The value of rate gain selected was chosen on the basis of anticipated coupling with structural modes. Further analysis will be required to optimize the gains and filtering when the vehicle becomes better defined. A simple fixed-gain attitude control system was retained in the roll axis.

The results obtained with the load relief control system are summarized in Table 4-25.

The results shown in Table 4-25 show that acceptable load relief is obtained. The gimbal requirements are within the F-1 actuator capability. The $\overline{q}\alpha$ is within the groundrule design limit. The $\overline{q}\beta$ results indicate a potential reduction in this limit. Although the propellant weight penalty (2287 lb) exceeds the guideline limit of 2000 pounds, this result is considered satisfactory.

A significant point that should be mentioned is that a low gain roll attitude control was used to obtain these results. It was found in the study that the allowed $\overline{q}\alpha$ and $\overline{q}\beta$ constraints could not be satisfied with reasonable weight penalties unless the vehicle was allowed to roll. If the vehicle cannot be allowed to roll, then it is doubtful that the aerodynamic load constraints can be satisfied using load relief control. Of particular interest is the case of a tailwind. In this situation, the vehicle will roll (assuming a low-gain roll attitude control) automatically due to the fact that the aerodynamic center lies above the center of gravity in the body Z axis. Because of this natural weather cocking tendency, the aerodynamic load is automatically shared between the pitch and yaw axes, thereby keeping the loads within their allowed limits.

Table 4-24. Pure Attitude Control

Wind	Maximum Gimbal Rate (deg/sec)	Maximum Gimbal Deflection (deg)	Maximum $\bar{q}\alpha$ (psf-deg)	Maximum $\bar{q}\beta$ (psf-deg)	Propellant Weight Penalty (pounds)
None	0.3	4.82	962	84	347
Side	2.4	6.93	813	4126	210
Head	1.1	3.84	2607	74	2464
Tail	13.0	6.64	3672	99	-2370

Table 4-25. Load Relief Control

Wind	Maximum Gimbal Rate (deg/sec)	Maximum Gimbal Deflection (deg)	Maximum $\bar{q}\alpha$ (psf-deg)	Maximum $\bar{q}\beta$ (psf-deg)	Propellant Weight Penalty (pounds)
12,600 ft Side	1.9	2.74	1891	2073	1110
12,600 ft Head	1.7	3.71	2146	44	1613
12,600 ft Tail	1.4	5.53	2772	1396	752
32,800 ft Side	1.3	3.16	2745	595	1497
32,800 ft Head	1.2	4.7	2212	72	1709
32,800 ft Tail	2.4	5.77	2091	1991	2287

4.4.1.5 Ascent Thermal Environments

The ascent trajectory thermal environment inputs the design of each system element — the booster, orbiter, and orbiter HO tank. The discussion of the environmental effects is found under Thermal Environment in Sections 4.4.3, 4.4.4, and 4.4.5.

4.4.1.6 Abort Capability

Mark II Orbiter. Space shuttle intact abort capability during the mated ascent flight phase requires separation of the orbiter from the disabled booster, depletion of the booster propellant by burning, booster flyback with ABE's, orbiter rocket-powered flight to propellant depletion, orbiter tank separation, and orbiter normal glide to the landing site. The separation and booster flight modes are discussed in Section 4.2.3.4. This section presents a discussion of the orbiter abort flight modes after separation from the booster and after an engine failure during second-stage ascent.

Figure 4-92 is an illustration of the Mark II orbiter abort regimes and flight modes. Abort is not possible during approximately the first 20 seconds of ascent flight because the time delay to full orbiter main engine thrust and because the orbiter T/W is less than 1.0. The time at which abort capability is considered to be available depends on the selected ground rules. For example, the absolute earliest availability corresponds to the ground rule of no ground impact. In this case, the orbiter would decelerate during and after separation from the booster and its velocity would become negative (tail slide). Because of propellant usage, the T/W increases to 1.0 and the orbiter begins to accelerate. At the time it again attains a finite forward velocity, the altitude must be greater than zero. This flight mode is not practical because of the very low altitudes and negative velocities involved.

A more practical ground rule would be continuous orbiter forward (upward) velocity. This would specify that the orbiter T/W must exceed 1.0 before the velocity drops to zero. Figure 4-93 presents the flight profile for an abort initiated shortly after the minimum time defined by this ground rule. The minimum velocity is 75 fps and the velocity at abort separation is approximately 275 fps ($\approx$T + 20 seconds). It was assumed that the abort decision was made at approximately T + 15 seconds, allowing five seconds for the orbiter engines to reach full thrust and for three of the booster engines to be shut down. Figures 4-94 through 4-97 show the trajectory parameters for the flight. It should be noted that for the first 60 seconds of flight, the velocity decreases because the T/W is less than 1.0. The four orbiter engines are maintained at 109 percent emergency power level (EPL) until an altitude of 80,000 feet is reached at approximately 200 seconds after separation. The maximum dynamic pressure experienced during this time was 170 psf at two degrees angle of attack for a $\bar{q}\alpha$ of 340 psf-degrees. The

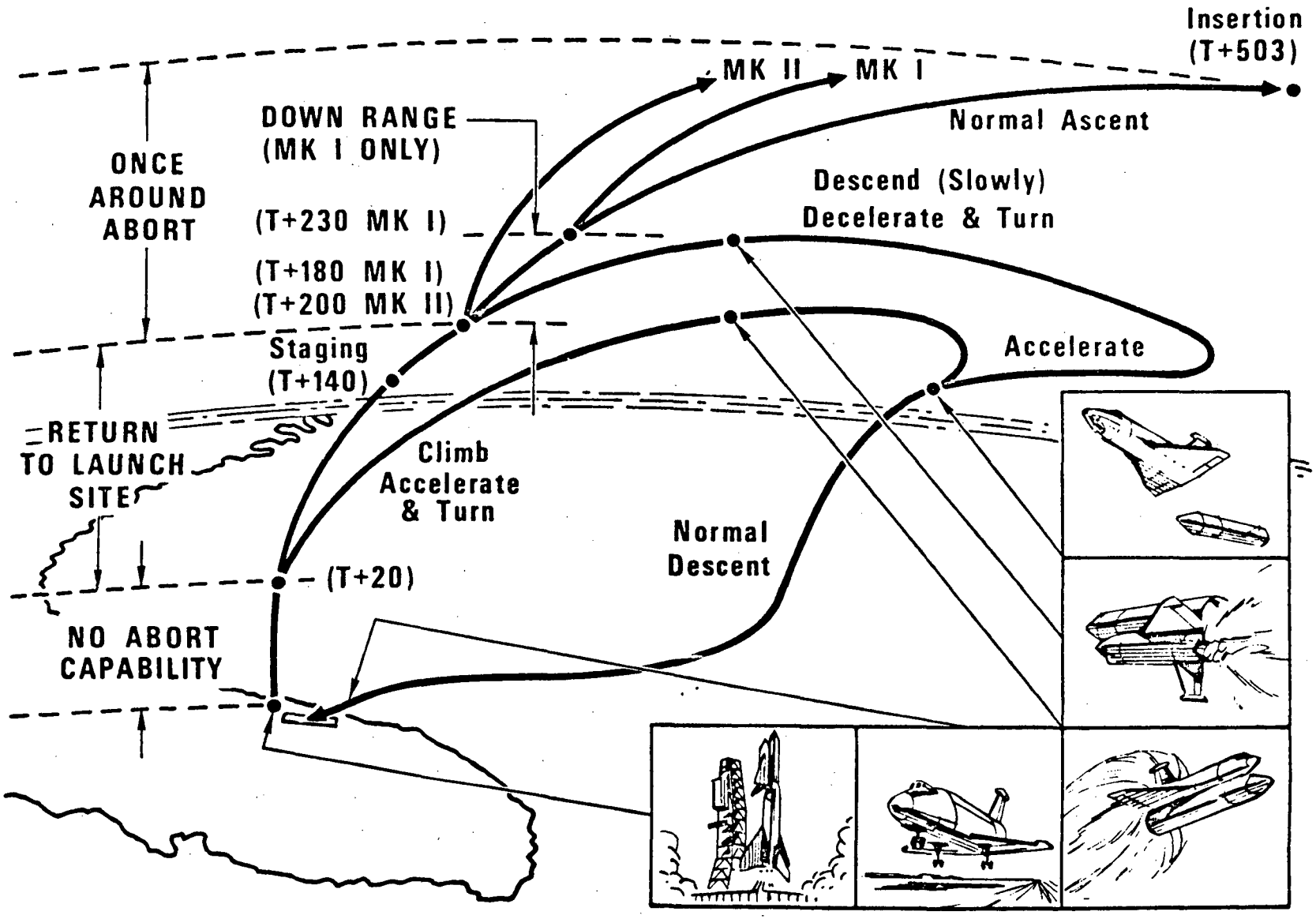

Figure 4-92. Orbiter Abort Regimes

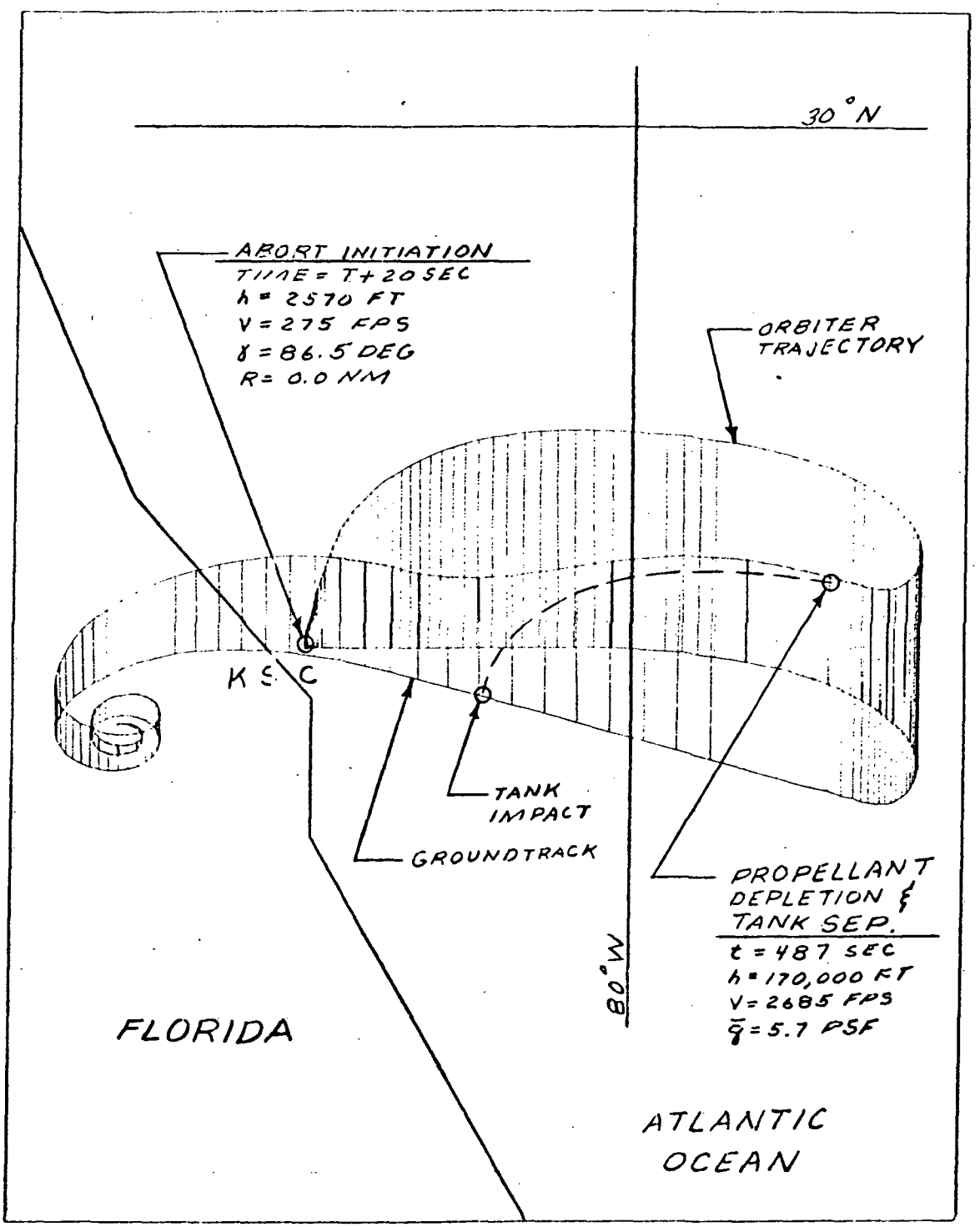

Figure 4-93. Abort Flight Profile, Abort at T + 20 Seconds

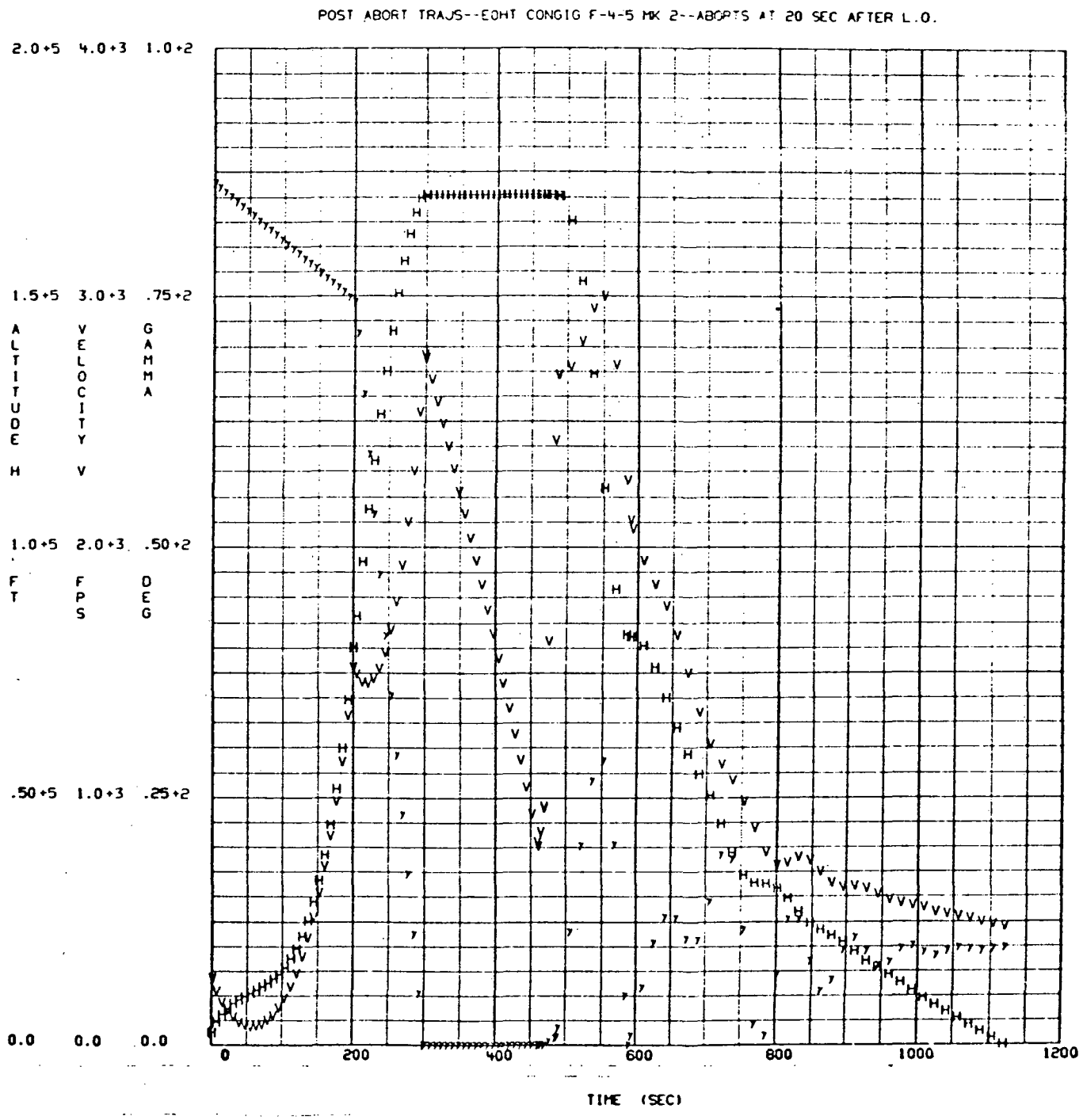

Figure 4-94. Abort Flight Trajectory Parameters, H, V, γ Abort at T + 20 Seconds

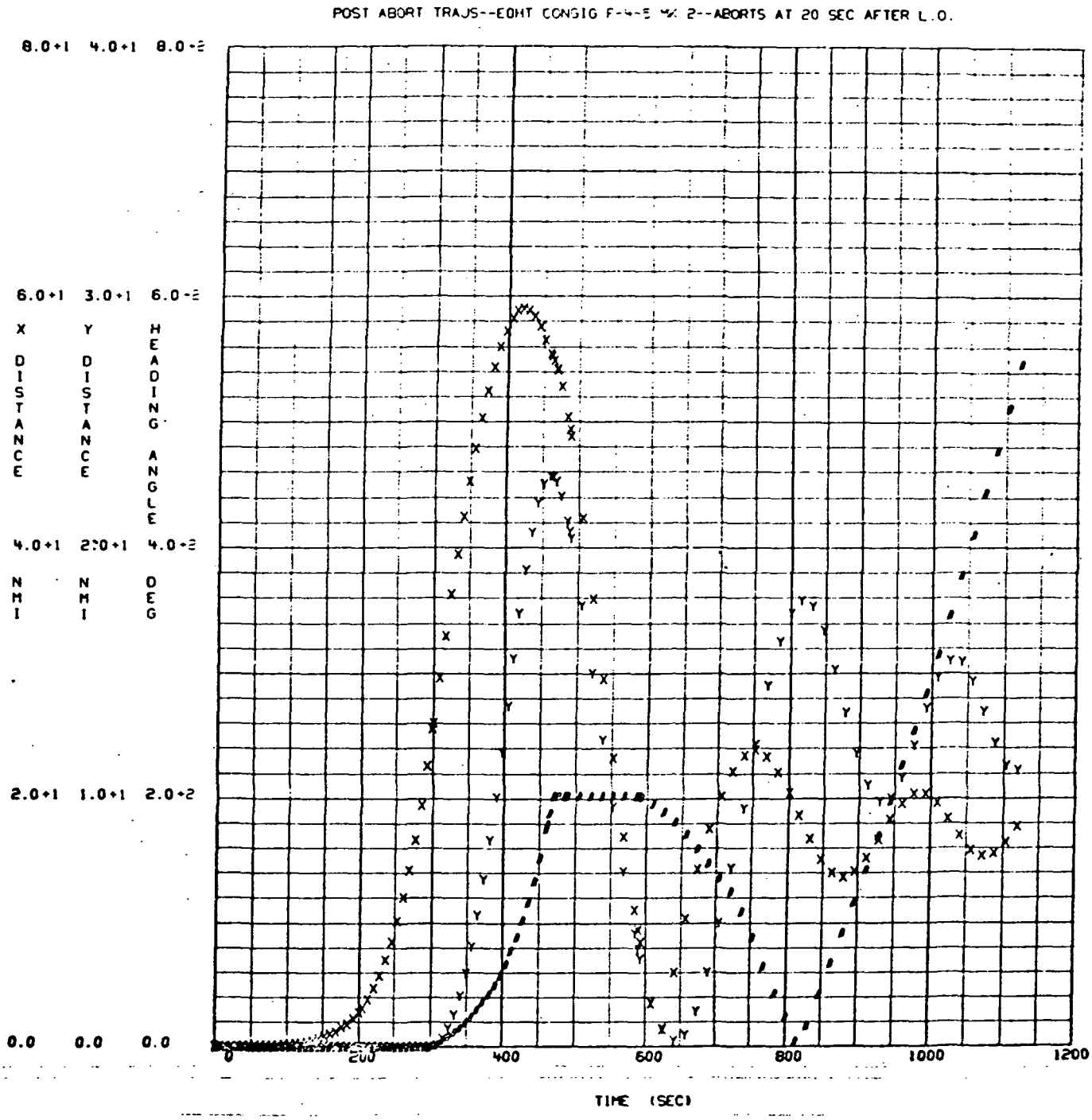

Figure 4-95. Abort Flight Trajectory Parameters, X, Y, B Abort at T + 20 Seconds

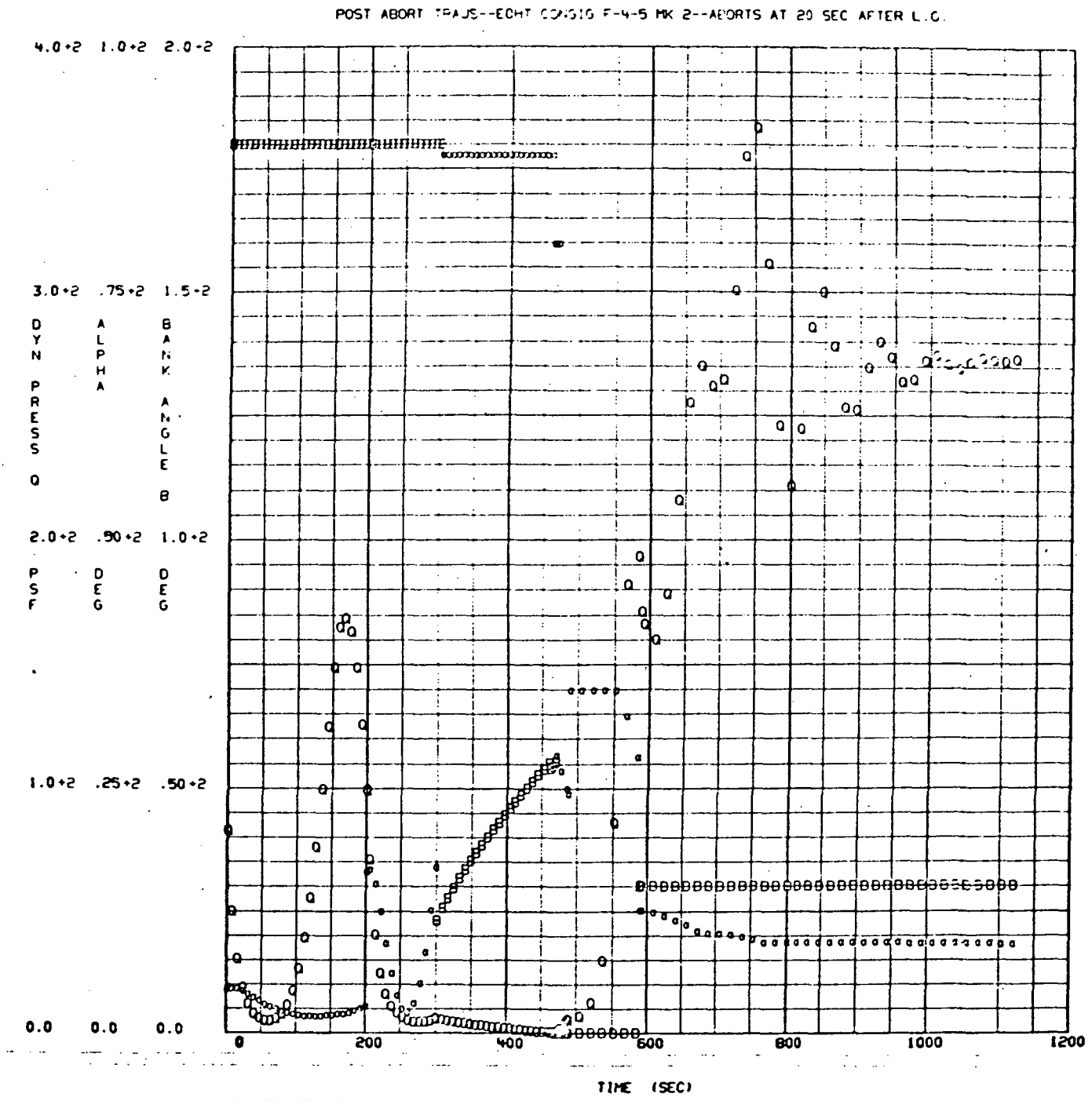

Figure 4-96. Abort Flight Trajectory Parameters, Q, α, B Abort at T + 20 Seconds

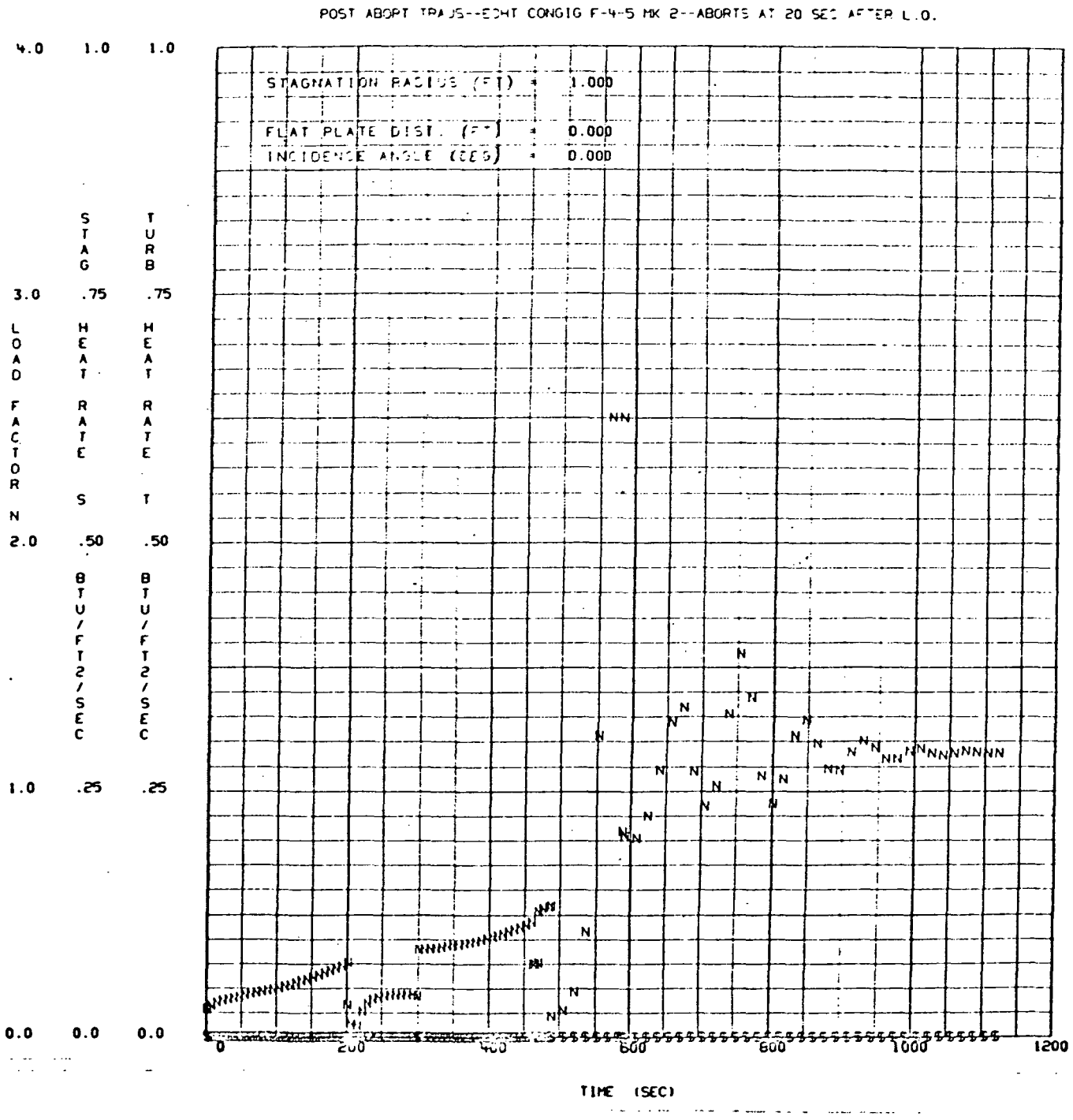

Figure 4-97. Abort Flight Trajectory Parameters, N, S, T Abort at T + 20 Seconds

vehicle is flown upside down to take advantage of the center of gravity offset and resulting thrust vector direction.

At 80,000 feet, the orbiter thrust is reduced to minimum (four engines at 50 percent) and a pitchover at -0.75 degrees per second ($\dot{\gamma}$) is commanded. An apogee of 170,000 feet is attained at a velocity of 2770 fps and at a range of 26 nm. Constant altitude, turning-flight is maintained from this point to propellant depletion. After separation of the empty propellant tank, the orbiter glides to a normal landing at the launch site. Figure 4-93 represents an open-loop (unguided) trajectory simulation and does not indicate the required spiral descent.

The abort flight mode (thrust, angle of attack, and bank angle time histories) described above is not a unique solution. Many variations are possible, some of which may be more desirable from the operations viewpoint. This is also true for the abort flight profiles discussed in subsequent paragraphs. The establishment of operational abort procedures, flight modes, etc., will require consideration of the emergency operations capabilities of the various orbiter systems, particularly the GN&C system.

The abort flight mode, after a successful abort separation (see Section 4.2.3.4) changes with increasing initial altitude, velocity, and downrange distance. The problem areas change from the low velocities and altitudes discussed above to high velocities, altitudes, and ranges, which make it difficult to fly the orbiter back to the launch site. Figures 4-98 through 4-101 show abort flight profiles for aborts initiated at approximately 5000, 6000 (staging), 7000, and 8000 fps during a due-east launch. Although right turns are shown, left turns may be desirable to avoid the Bahamas area. These flight simulations were made to determine near-optimum performance as defined by the amount of range available after flying over the launch site. During actual operations, the turn would be adjusted to provide propellant depletion at a near optimum position and velocity for the glide portion of the flight. Figure 4-98 shows that considerable excess performance is available at an ascent velocity of 5000 fps (T + 128 seconds). A more desirable flight profile would include delaying the initiation of the turn and perhaps making a wider turn. This would also move the tank impact point out to sea.

The excess performance decreases with increasing time from liftoff, increasing velocity, and increasing downrange position. Figure 4-99 shows considerable excess at staging and Figure 4-100 indicates a noticeable excess at 40 seconds after staging. Figure 4-101 shows a very marginal flight at 80 seconds after staging and because of tolerances on the various input data is considered unacceptable. The upper boundary of the return-to-launch-site abort regime is defined to be at 70 seconds after staging or 210 seconds after liftoff. Figures 4-102 through 4-105 present the trajectory parameters for an abort at staging due to ignition failure of one engine (flight profile shown in Figure 4-99).

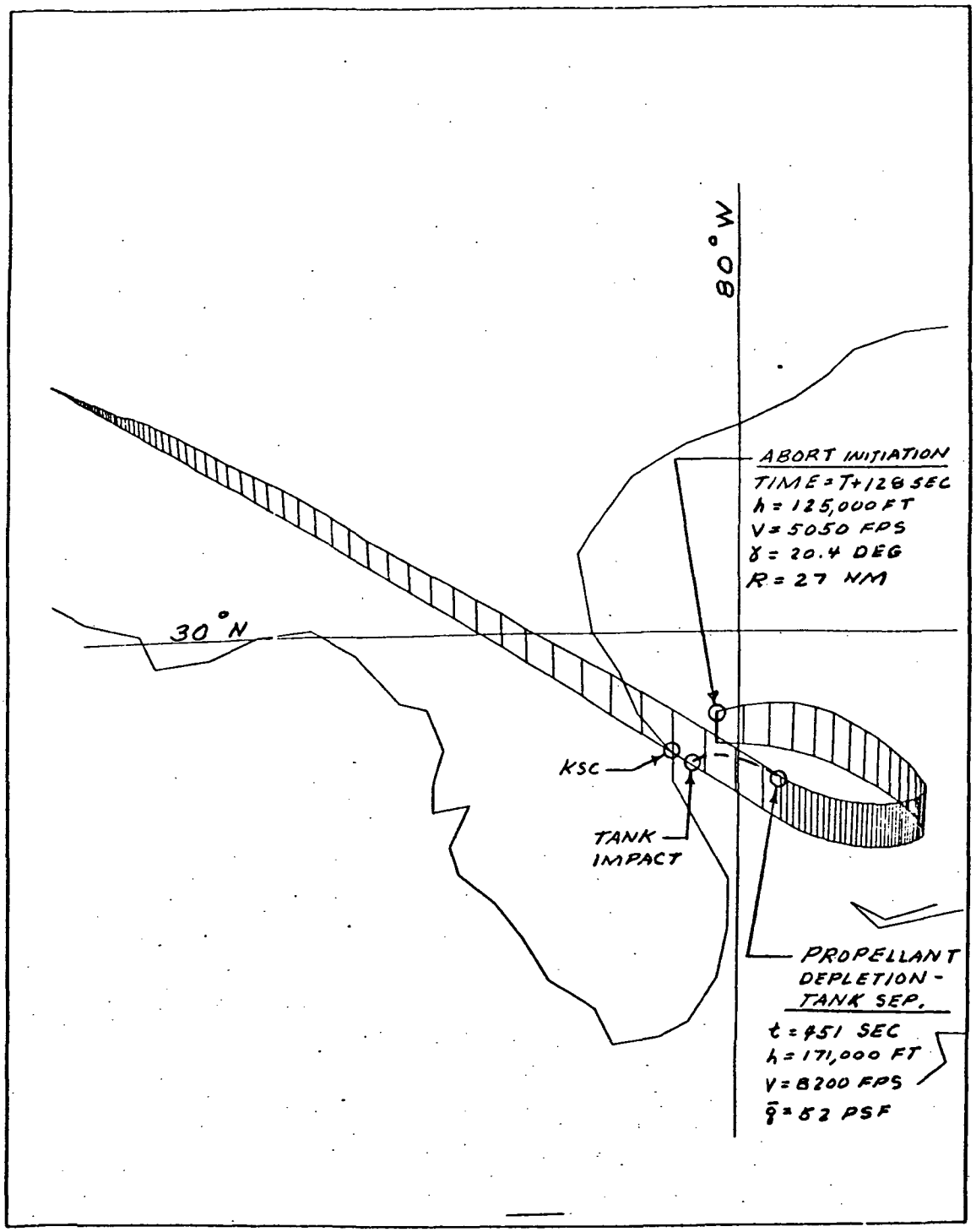

Figure 4-98. Abort Flight Profile, T + 28 Seconds

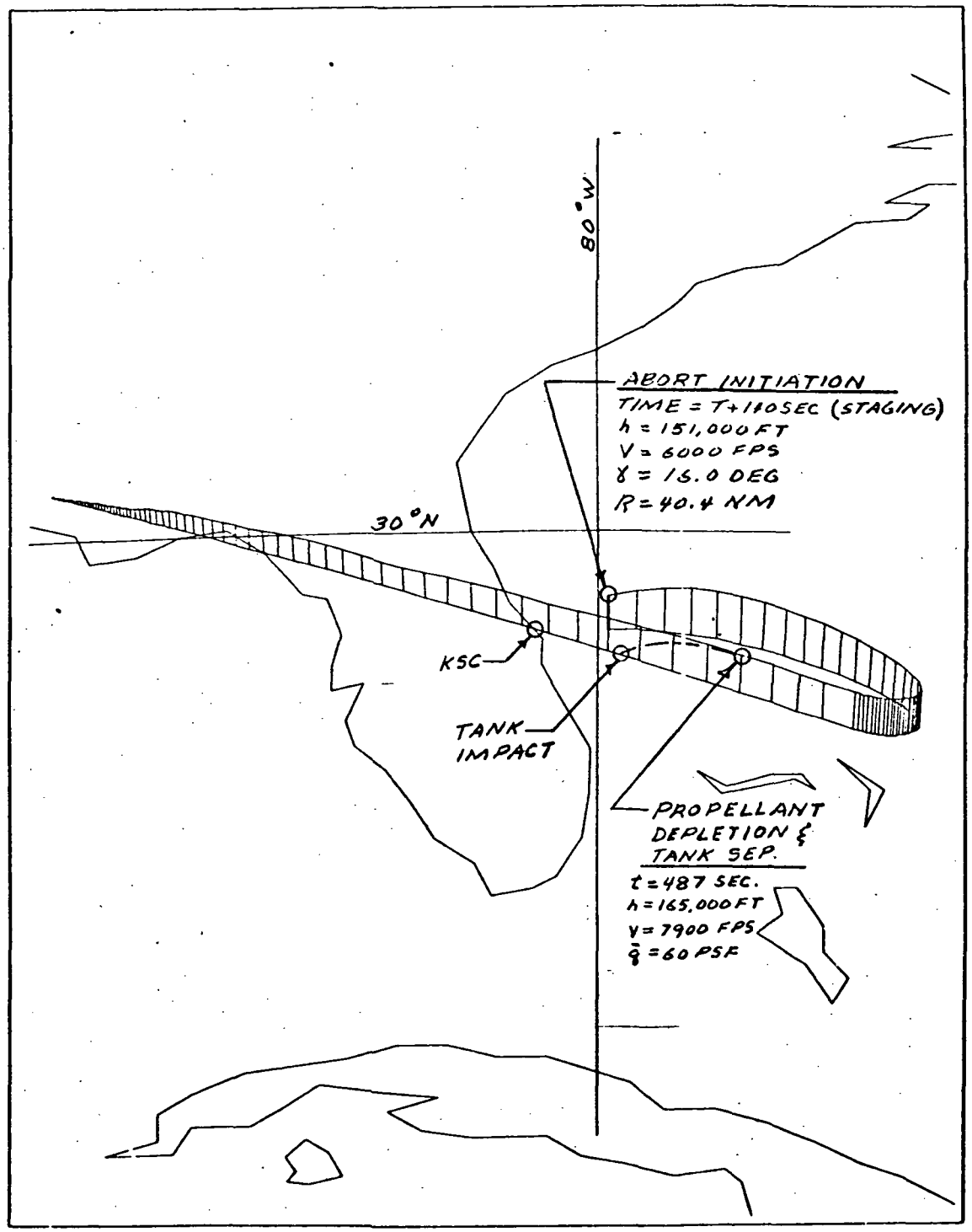

Figure 4-99. Abort Flight Profile, T + 140 Seconds (Staging)

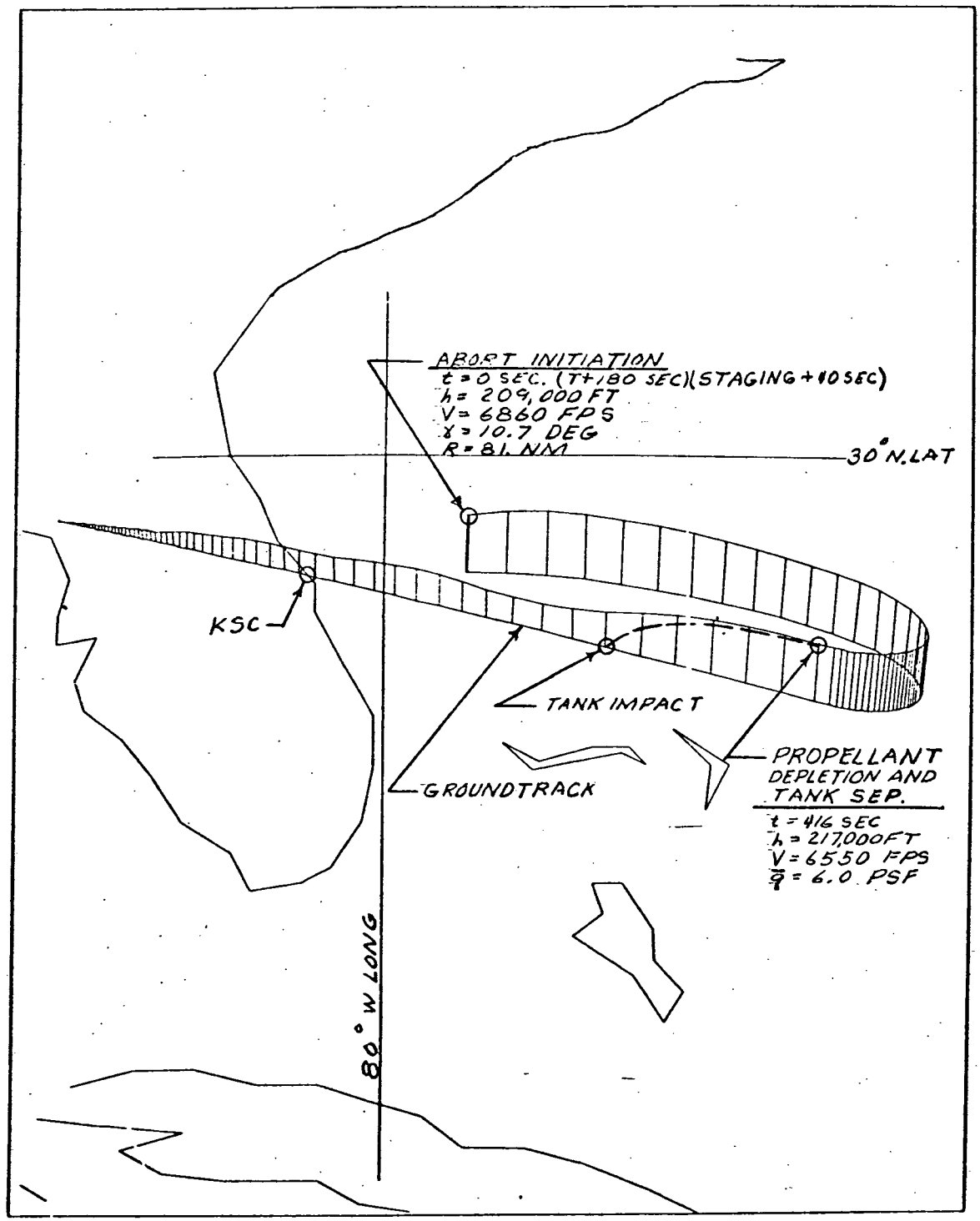

Figure 4-100. Abort Flight Profile, T + 180 Seconds (Staging + 40 Seconds)

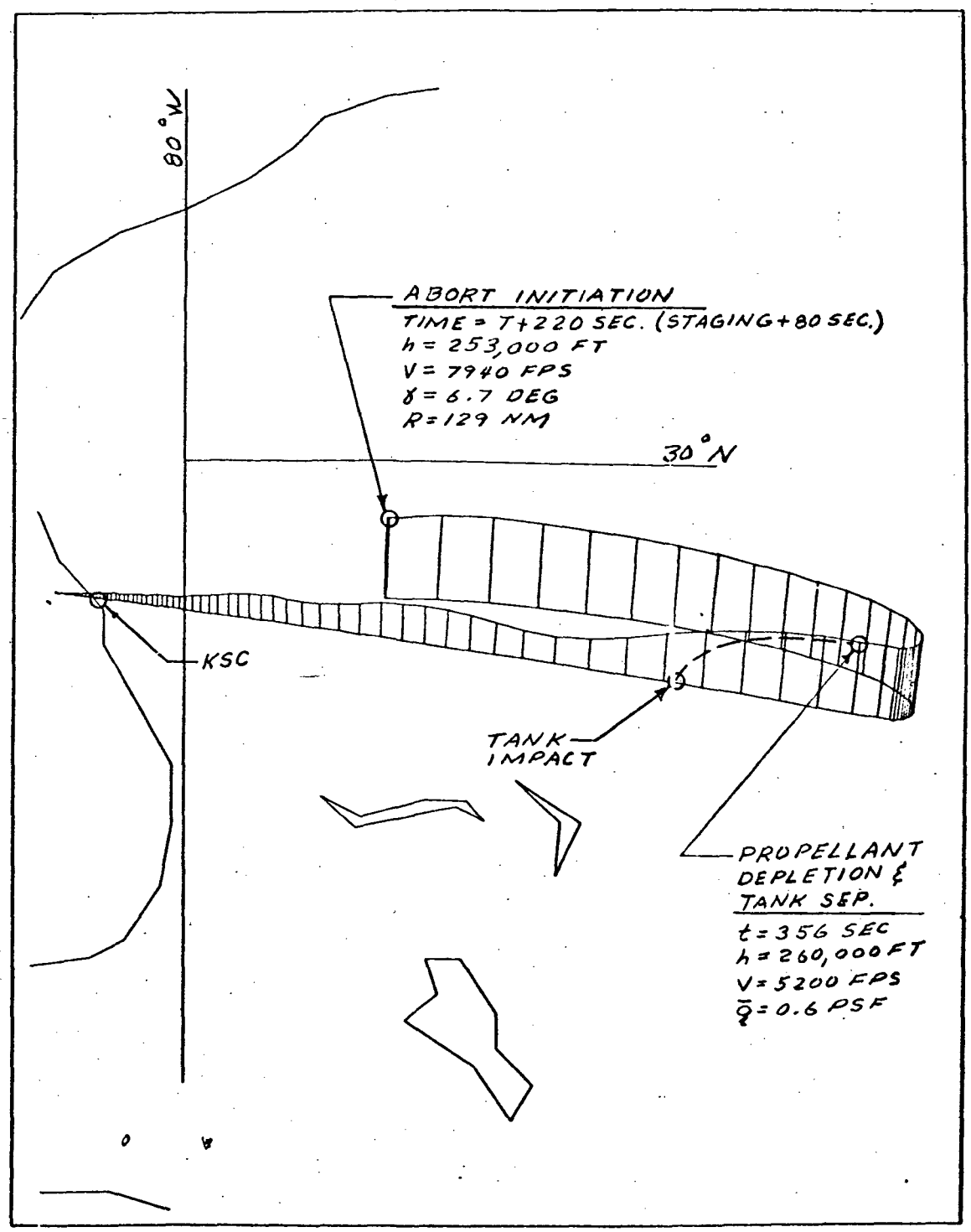

Figure 4-101. Abort Flight Profile, T + 220 Seconds (Staging + 80 Seconds)

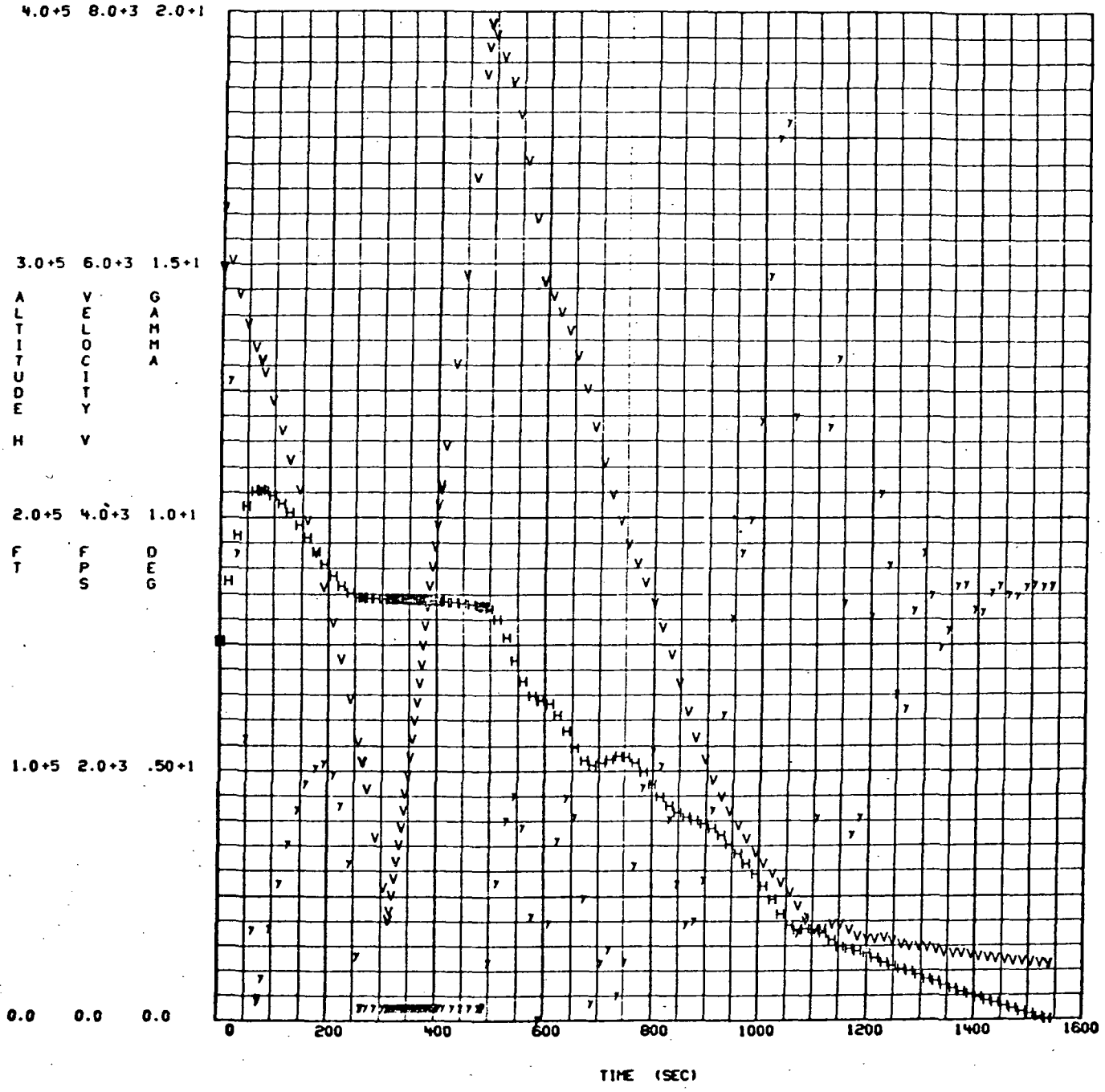

Figure 4-102. Abort Flight Trajectory Parameters, h, V, γ Abort at Staging

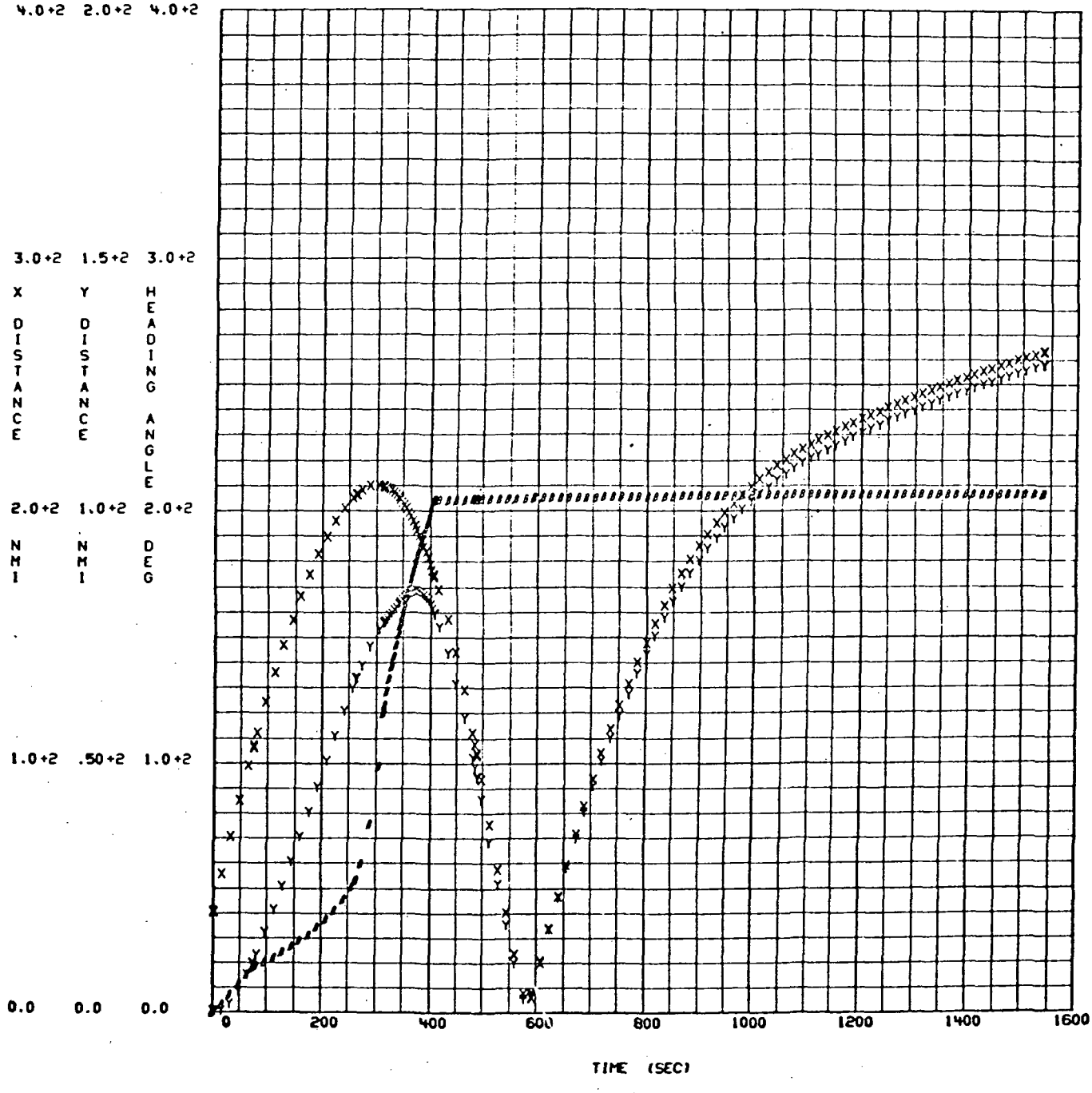

Figure 4-103. Abort Flight Trajectory Parameters, X, Y, B Abort at Staging

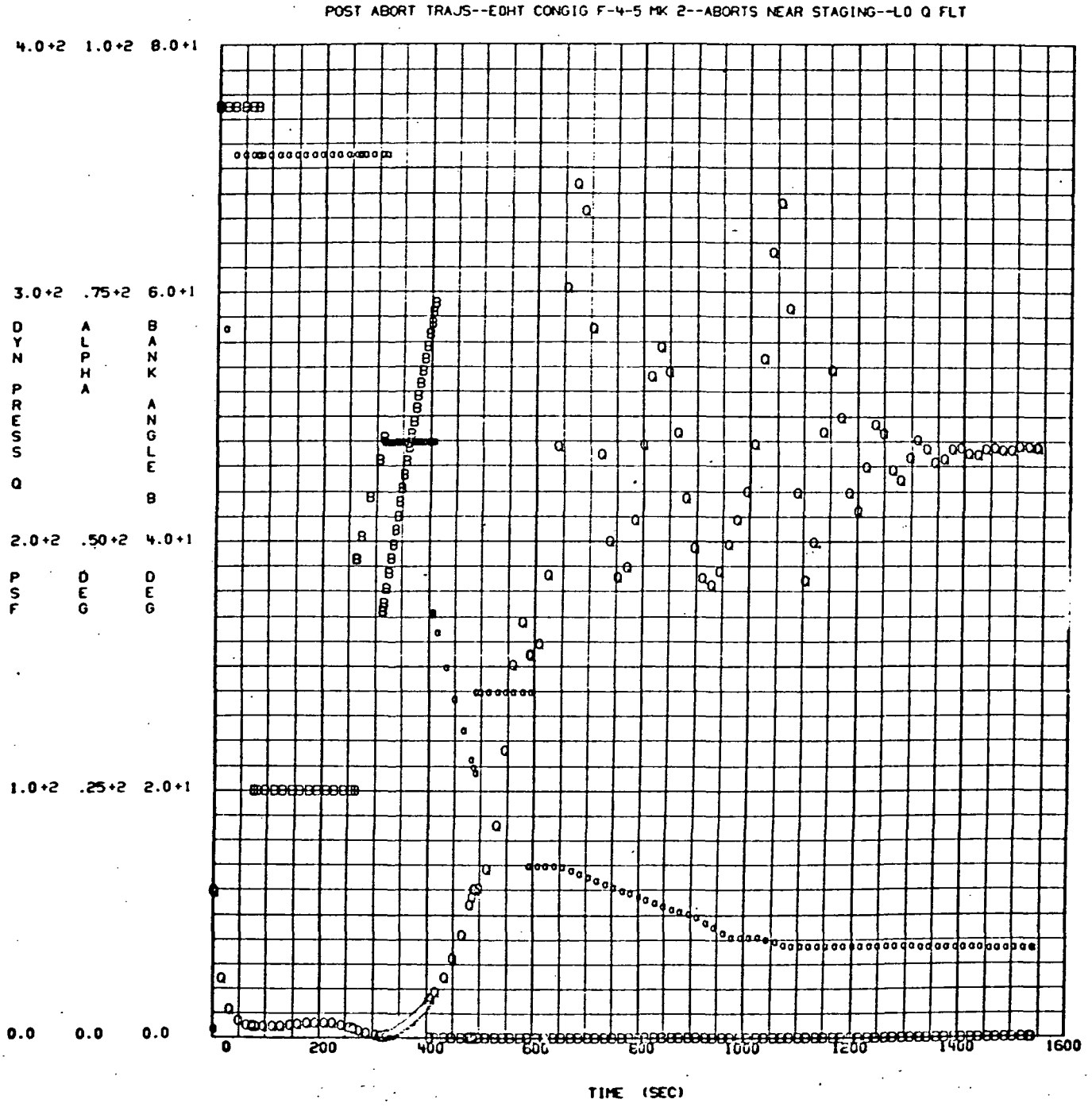

Figure 4-104. Abort Flight Trajectory Parameters, Q, α, B Abort at Staging

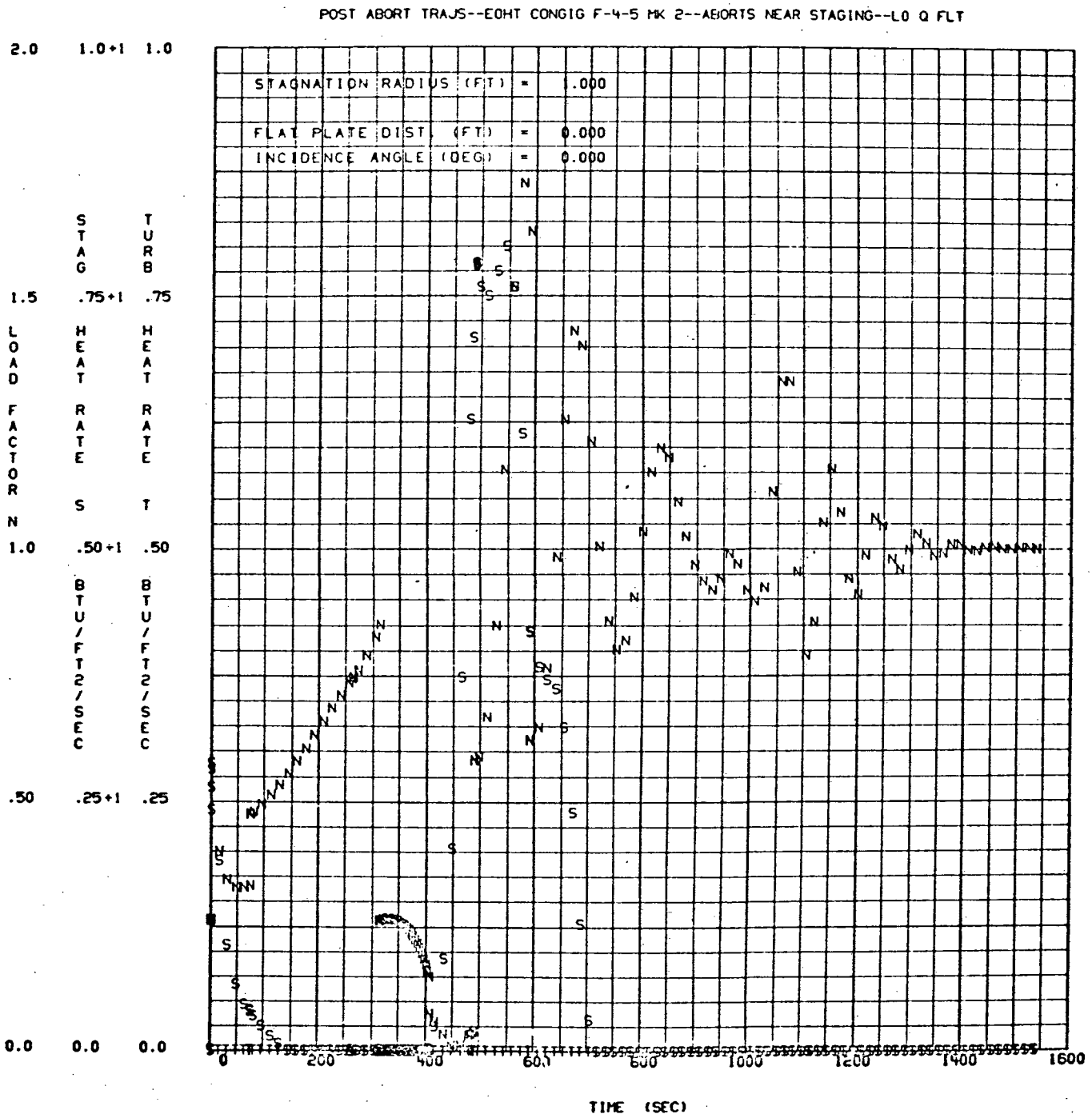

Figure 4-105. Abort Flight Trajectory Parameters, N, S, T Abort at Staging

The first maneuvers after verification of an engine failure are: (1) roll the orbiter about its velocity vector to a bank angle of 75 degrees; (2) raise the thrust of the remaining engines to 109 percent EPL; and (3) pitch to an angle of attack of approximately 120 degrees. These maneuvers are made simultaneously and at maximum rates within the control and structural capabilities of the vehicle. This attitude, which provides turning and deceleration, is maintained until a slowly descending flight path is established (approximately 70 seconds). Turning, decelerating, and descending flight is maintained for the next 240 seconds by angle of attack and bank modulation, terminating at a heading angle change of 120 degrees. The flight parameters at this time are:

Altitude = 168, 000 feet	Heading angle = 90° + 120° = 210°
Velocity = 810 fps	Dynamic pressure = 0.6 psf
Flight path angle = 0.25°	Time from abort = 314 seconds

At this point, the angle of attack is pitched down to 60 degrees to provide acceleration. The vehicle is still descending and turning.

At approximately 400 seconds after abort, the vehicle has turned to a heading toward the launch site. The remaining propellant is used to accelerate toward the launch site. As indicated on Figure 4-99, this preliminary flight profile overflew the launch site by many miles. It also indicates a dynamic pressure of 60 psf at tank separation. This is probably excessive; however, it can be reduced as required at the expense of some of the excess range.

If an abort is initiated later than 70 seconds after staging (T + 210 seconds), the orbiter cannot be turned around and flown back to the launch site. However, once-around abort capability is obtained at some time during second stage ascent. If this occurs before the return-to-launch-site abort capability is lost, the downrange abort mode is not required. Figure 4-106 indicates the once-around abort capability of the Mark II orbiter. The earliest acceptable once-around abort is shown to be at 60 seconds after staging, or ten seconds before the return-to-launch-site abort capability is lost.

Mark I Orbiter. The abort capabilities of the Mark I orbiter have not been defined in as much detail as those of the Mark II orbiter. However, a comparative evaluation has been made considering the differences between the two orbiter designs. The primary difference, from the abort standpoint, is the main propulsion system. Although the nominal vacuum thrust levels are equal (265, 000 per engine), the Mark II HiPc engines have improved I_{sp},

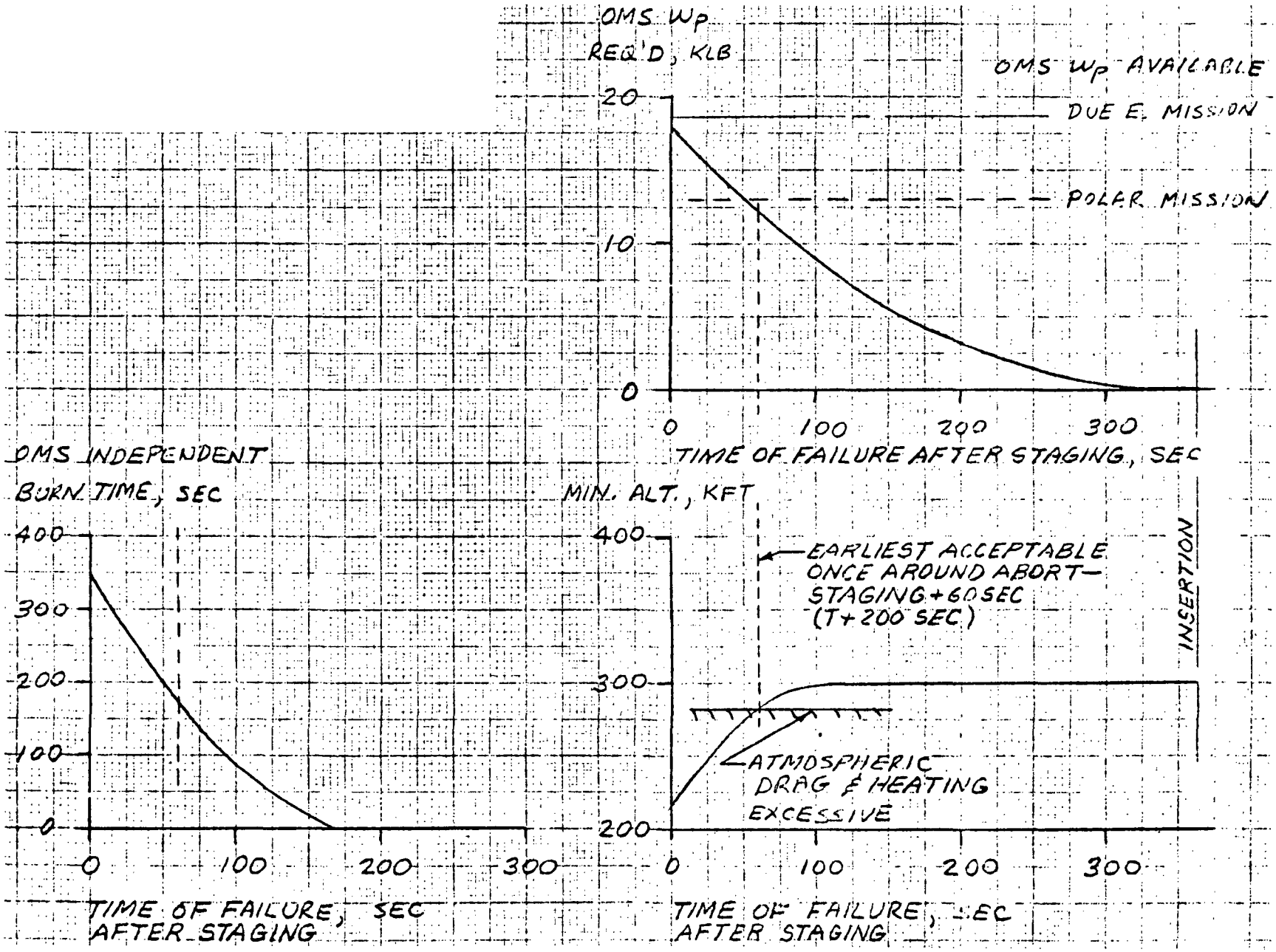

Figure 4-106. Mark II Orbiter Once-Around Abort Capabilities

higher thrust at sea level, emergency power level capabilities (109 percent of nominal), and an improved starting sequence. Weight and ascent trajectory differences between the two configurations have relatively minor influence on abort capabilities.

The no-abort-capability regime after liftoff is longer for the Mark I configuration. This is because the J-2S engines have lower sea level thrust and no emergency power level. The time at less than 1.0 T/W is therefore longer and the orbiter decelerates more. The minimum allowable separation velocity is therefore higher. It is estimated that Mark I return-to-launch-site abort capability is obtained at approximately 25 seconds after liftoff.

The Mark I return-to-launch-site abort flight modes are essentially identical to those for the Mark II, which were discussed in the preceding section. However, because of the lower I_{sp} and reduced propellant (MR adjustment), the Mark I delta-V capability is less. Also, because of the lack of EPL, the burning of the propellant is less efficient. Because of these conditions, the excess performance is less and the estimated upper end of the Mark I return-to-launch-site abort regime is at approximately T + 180 seconds, 30 seconds earlier than Mark II.

The Mark I once-around abort capability is significantly reduced by the lack of EPL capability on the J-2S engines. The loss of one engine results in a 25-percent thrust loss; a loss of one Mark II engine results in only an 18.25-percent thrust loss when the remaining three engines are increased to 109 percent power level. It is estimated that the Mark I once-around abort capability is obtained at approximately T + 230 seconds.

The Mark I orbiter abort mode to be used between the end of the return-to-launch-site abort regime (T + 180 seconds) and the beginning of the once-around abort regime (T + 230 seconds) is termed downrange abort. Figure 4-107 indicates the available downrange landing areas for aborts initiated between T + 180 seconds and T + 230 seconds. It should be noted that the areas overlap, allowing one site to be selected for all downrange aborts. This site must be between approximately 1000 and 7000 nm downrange from the launch site and within approximately 1200 nm of the nominal mission first-pass ground track.

4.4.1.7 Separation

Booster/orbiter separation data were generated with a three-degree-of-freedom, O/S 360 digital separation program. The program provides for basic aerodynamics of both stages individually and combined, booster aerodynamic effects due to impingement of the orbiter engine plume, and thrust tail-off and thrust buildup of the booster and orbiter engines, respectively.

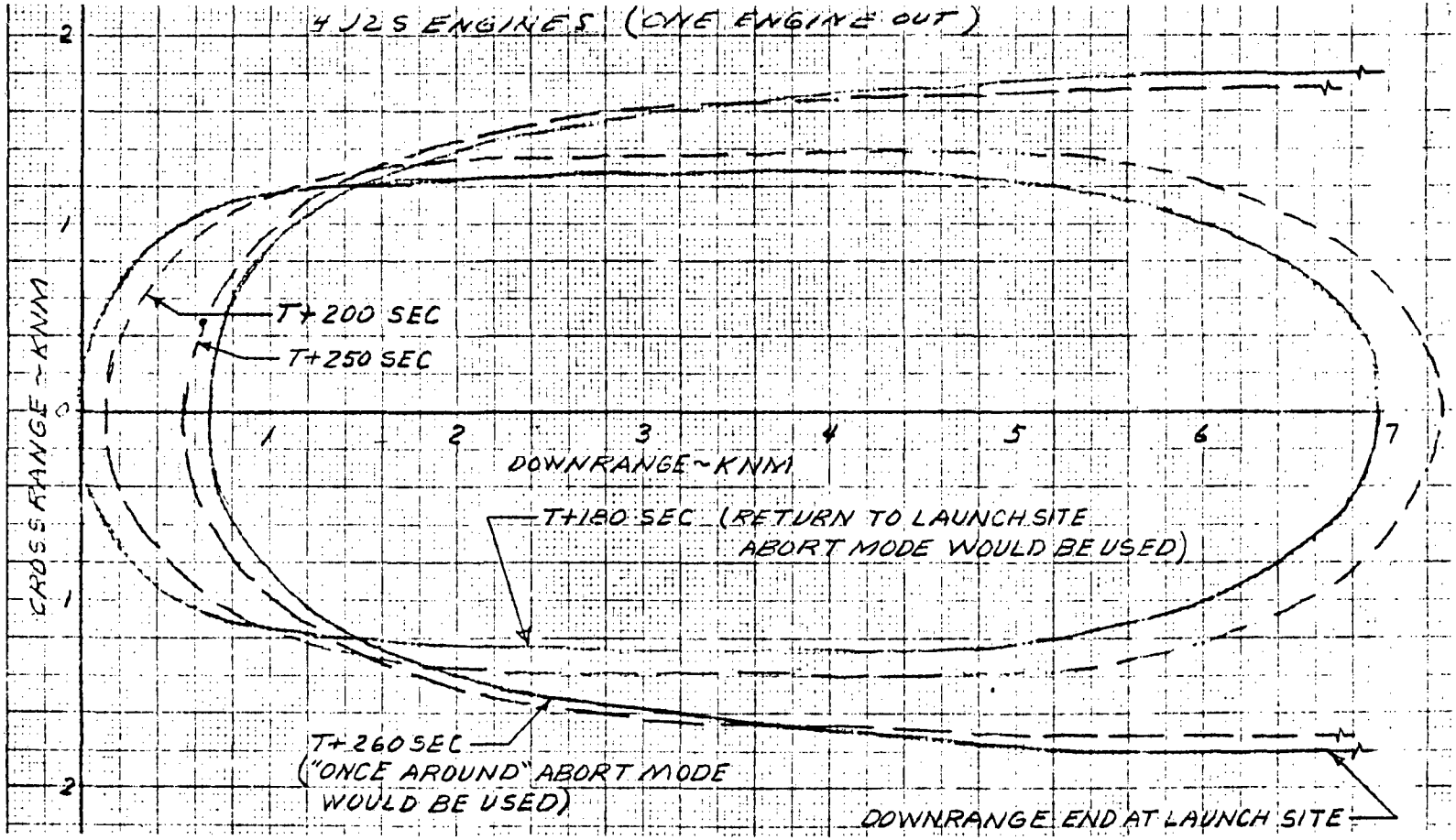

Figure 4-107. Available Landing Areas, Downrange Aborts, Mark I Orbiter

A control system based on pitch attitude and attitude rate is included for each stage. All of these provisions were utilized in generating data for the separation analysis.

The study was based on the mated vehicle configuration VC70-3058, consisting of the Mark II orbiter plus EOHT and reusable booster with four F-1 engines, only two of which were operating during separation. Separation characteristics were examined for an orbiter with four J-2S engines and for an orbiter with four HiPc engines. Thrust decay of the F-1 engines and thrust buildup of the orbiter engines are illustrated as a function of time in Figure 4-108. The orbiter engine thrust curves in the digital program can be translated horizontally to account for variations in the time increment between booster engine cutoff (BECO) and orbiter engine ignition (OEIG). The interstage between the EOHT and the booster was assumed to remain with the EOHT during separation.

Separation characteristics were examined for a basepoint separation technique and for several variations from this basepoint. The basepoint method involved initiation of orbiter main propulsion subsystem (MPS) thrust buildup when the axial load factor (AXLOF) of the combined stages reduced from its maximum value at BECO to a value of 1.0. Physical separation occurred when thrust buildup of the orbiter MPS engines was such that the axial load factors of the individual stages were equal. This is illustrated in Figure 4-109, which shows the AXLOF of the combined stages and of the individual stages as a function of time, using the four J-2S engine configuration. OEIG is seen to occur at an AXLOF of 1.0 on the combined stages curve, and separation occurs when AXLOF curves of the first and second stages cross. A final constraint imposed on the basepoint separation technique involved equal first and second stage vertical accelerations at the separation plane at the time of separation. This was accomplished by gimbaling the F-1 engines hard over at the maximum gimbal rate just prior to separation and then iterating on the required orbiter engine gimbal angle based on its maximum rate, which would yield the desired condition of equal vertical accelerations at the separation plane when physical separation occurred.

A CRT pictorial representation of the relative motion of the orbiter (J-2S engines) plus EOHT with respect to the booster during separation is shown in Figure 4-110. Successive images are at 0.2-second intervals. The orbiter plus EOHT is seen to pitch down while moving forward with respect to the booster. Inertially the booster is actually pitching up as the orbiter pitches down. The motion of critical points on the orbiter and EOHT with respect to the booster is shown in more detail in Figure 4-111. The circles identify relative motion using the J-2S orbiter engines and the square symbols identify relative motion using the HiPc engines. An expanded view of the motion of the upper portion of the interstage with respect to the booster

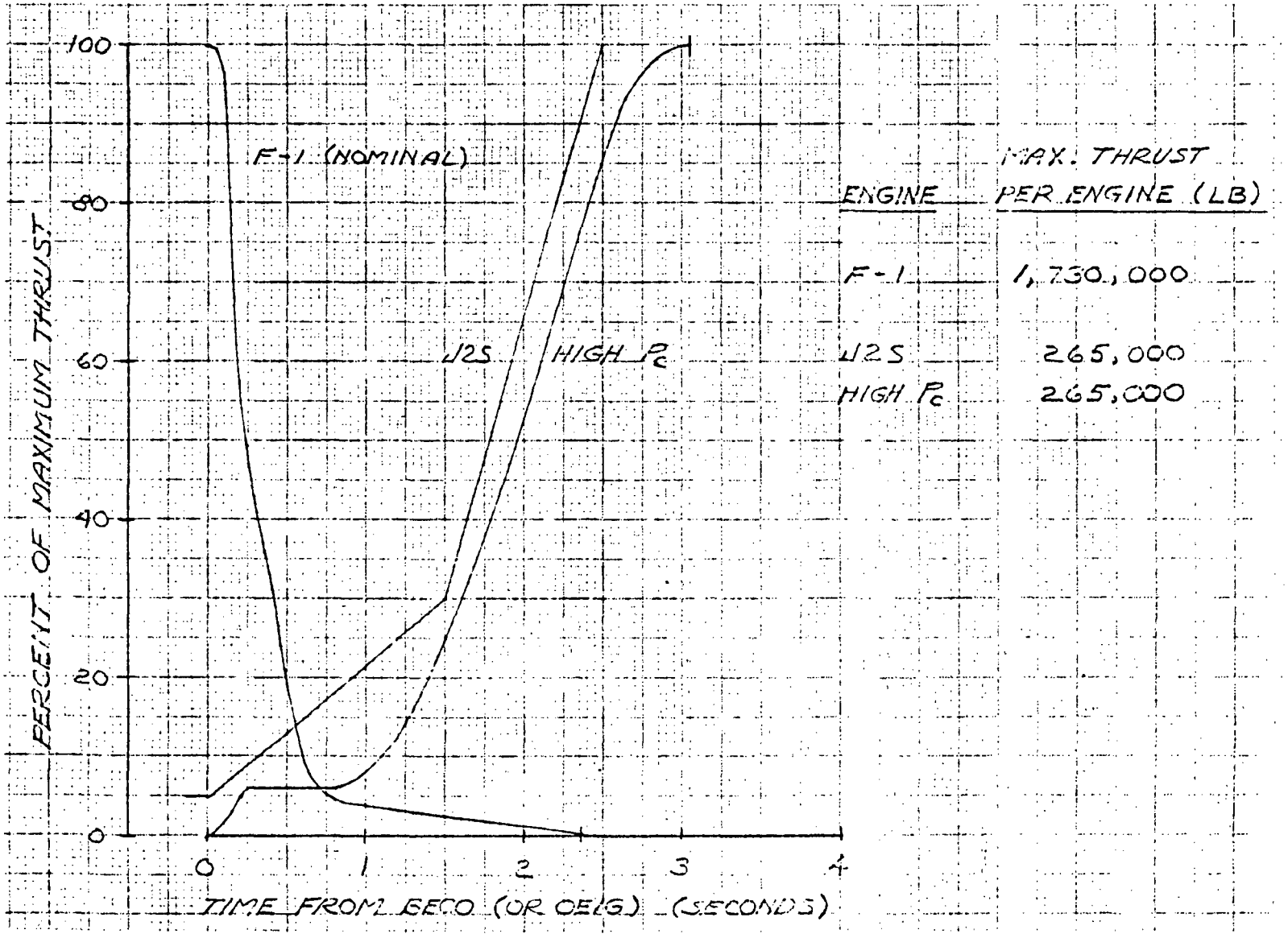

Figure 4-108. Booster Thrust Decay and Orbiter Thrust Buildup

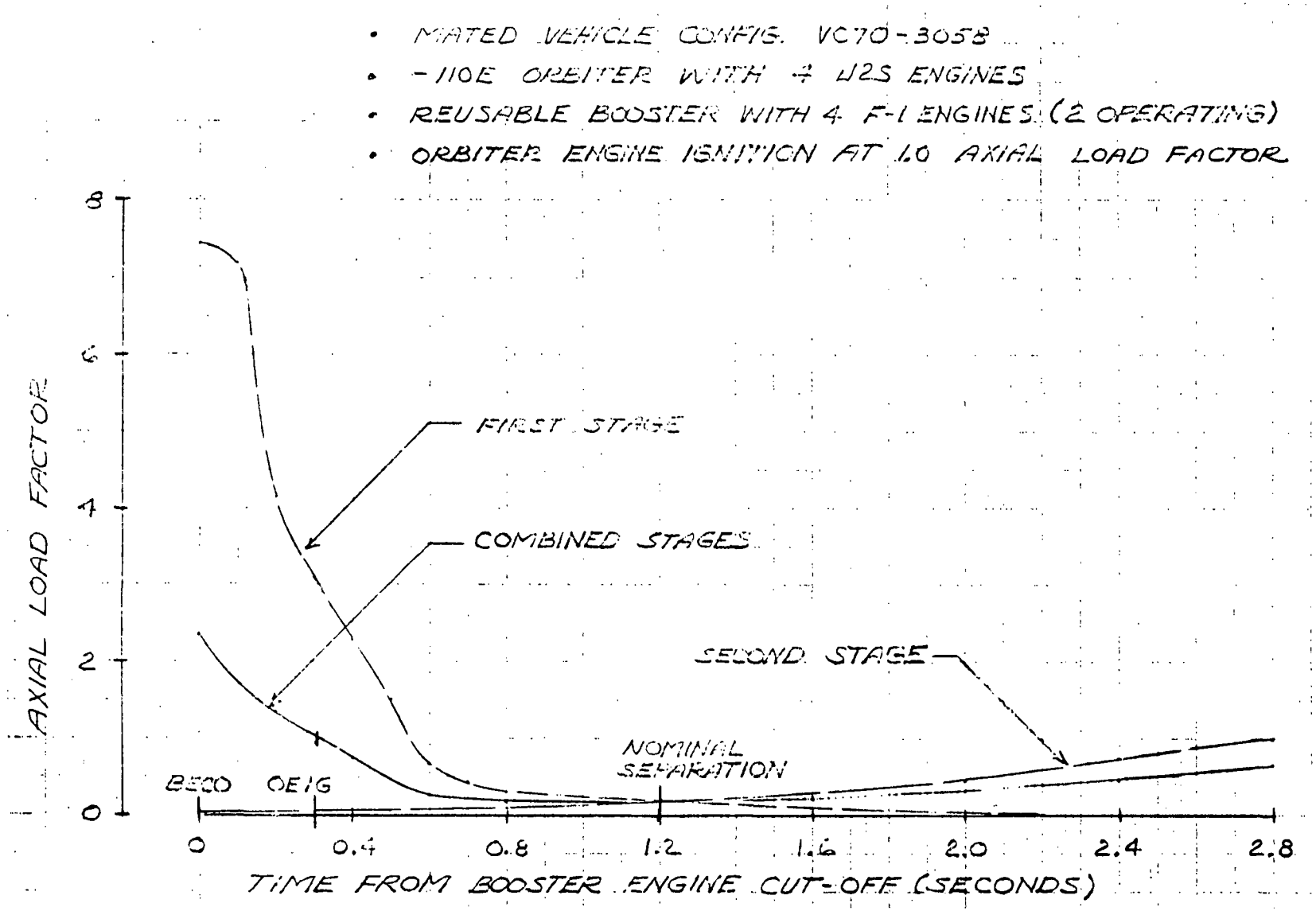

Figure 4-109. Axial Load Factor Time Histories

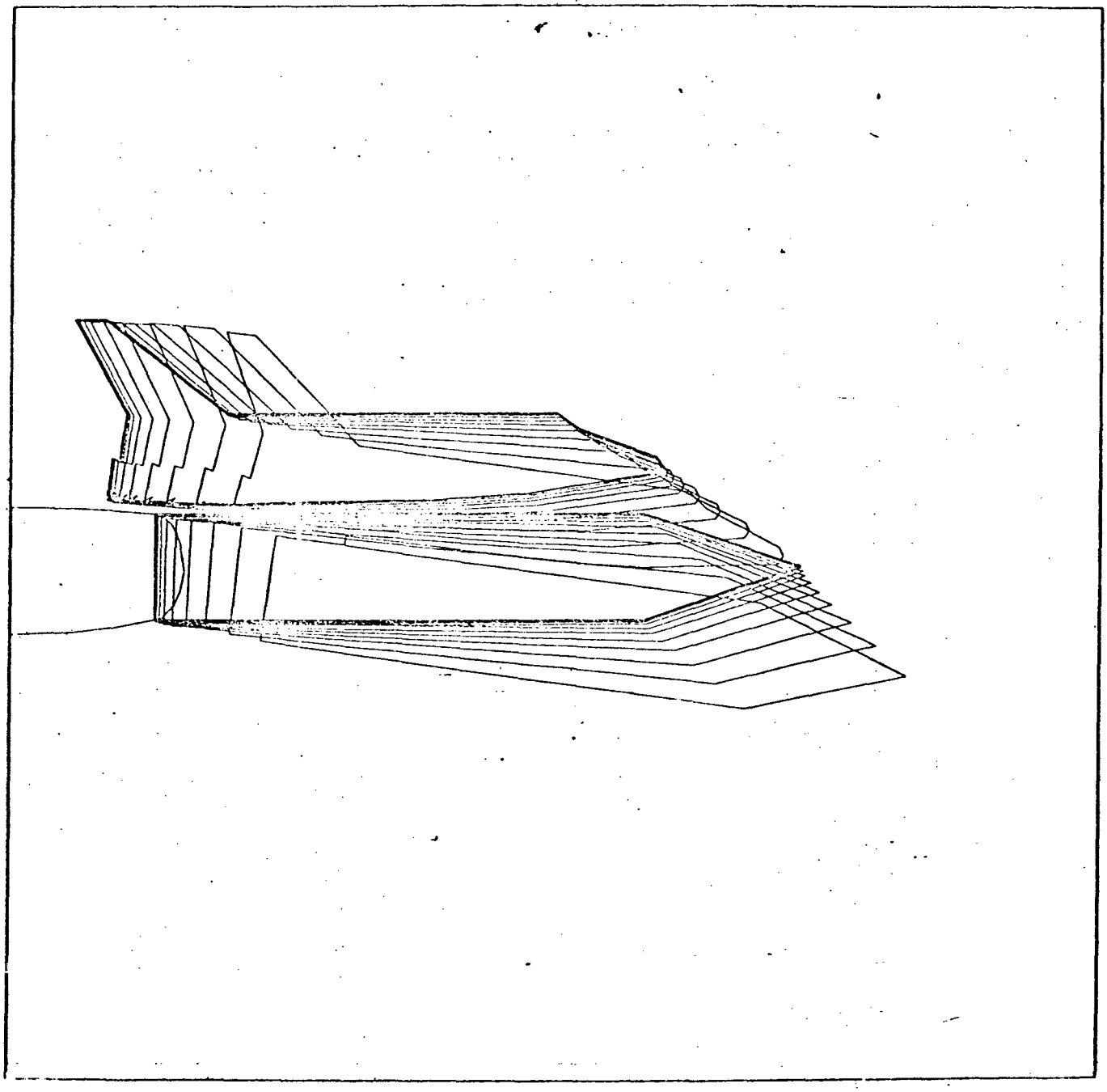

Figure 4-110. Booster/Orbiter Relative Position During Separation

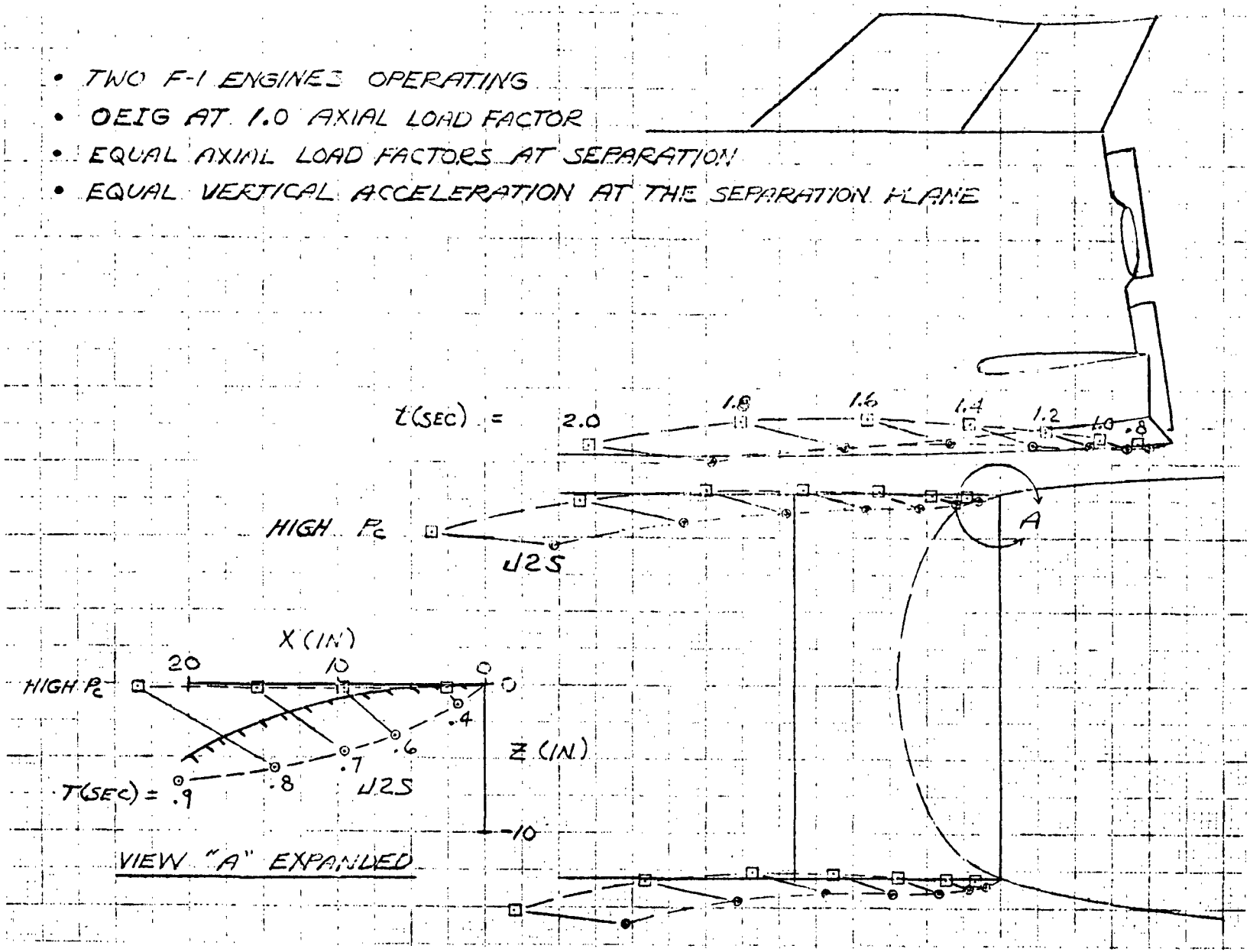

Figure 4-111. Separation Dynamics

nose is shown at the lower left of the figure. Contact between the interstage and the booster nose is seen to exist during nearly the entire first second of separation using the J-2S engines, a condition which is alleviated considerably with the HiPc engines. It is felt that this problem can be resolved through design modifications.

Some performance considerations associated with variation from the basepoint separation technique are illustrated in Figures 4-112 through 4-116. The velocity variation (measured with respect to the velocity at BECO) as a function of time from BECO to the attainment of full thrust from the orbiter engines is shown for J-2S and HiPc engine configurations in Figures 4-112 and 4-113, respectively. Curve B represents the basepoint separation technique in each case. The effect of holding constant the OEIG time and delaying separation until the orbiter engines attain full thrust is indicated by curve C in Figures 4-112 and 4-113 (the first and second stage axial load factors at separation are not equal for this case). A significant delta-V loss compared to the basepoint case B is evident. The effect of separation delay on the differential AXLOF and on the delta-V during separation is further illustrated in Figure 4-114 as a function of separation time for the J-2S engine configuration. The initial time of 1.2 seconds represents the basepoint separation time. A differential AXLOF of about 0.75 can be obtained by delaying separation from 1.2 seconds to 2.4 seconds after BECO with a corresponding velocity loss of only 4 fps.

Referring back to Figures 4-112 and 4-113, the effect of an earlier OEIG (equal AXLOF constraint at separation is maintained) is shown by curves A.

OEIG is coincident with BECO for this case and occurs at a combined stage AXLOF of about 2.3. This effect is also illustrated in more detail in Figure 4-115. The small increment between the two curves showing the AXLOF at OEIG occurs because the J-2S engines are operating in an idle mode at 5 percent of full thrust prior to OEIG. The increment between the curves showing the AXLOF at separation is due to the difference between the thrust buildup versus time curves for the J-2S and HiPc engines as shown in Figure 4-108. The delta-V during separation (not shown) over this same range of OEIG times is negligible.

The effect of delaying the J-2S OEIG from the basepoint (combined-stage AXLOF of 1.0 to an AXLOF of 0.1) while retaining the equal AXLOF constraint at separation is shown in Figure 4-108. Separation is shifted from 1.2 seconds to 1.52 seconds after BECO and a delta-V penalty of about 11 fps is incurred.

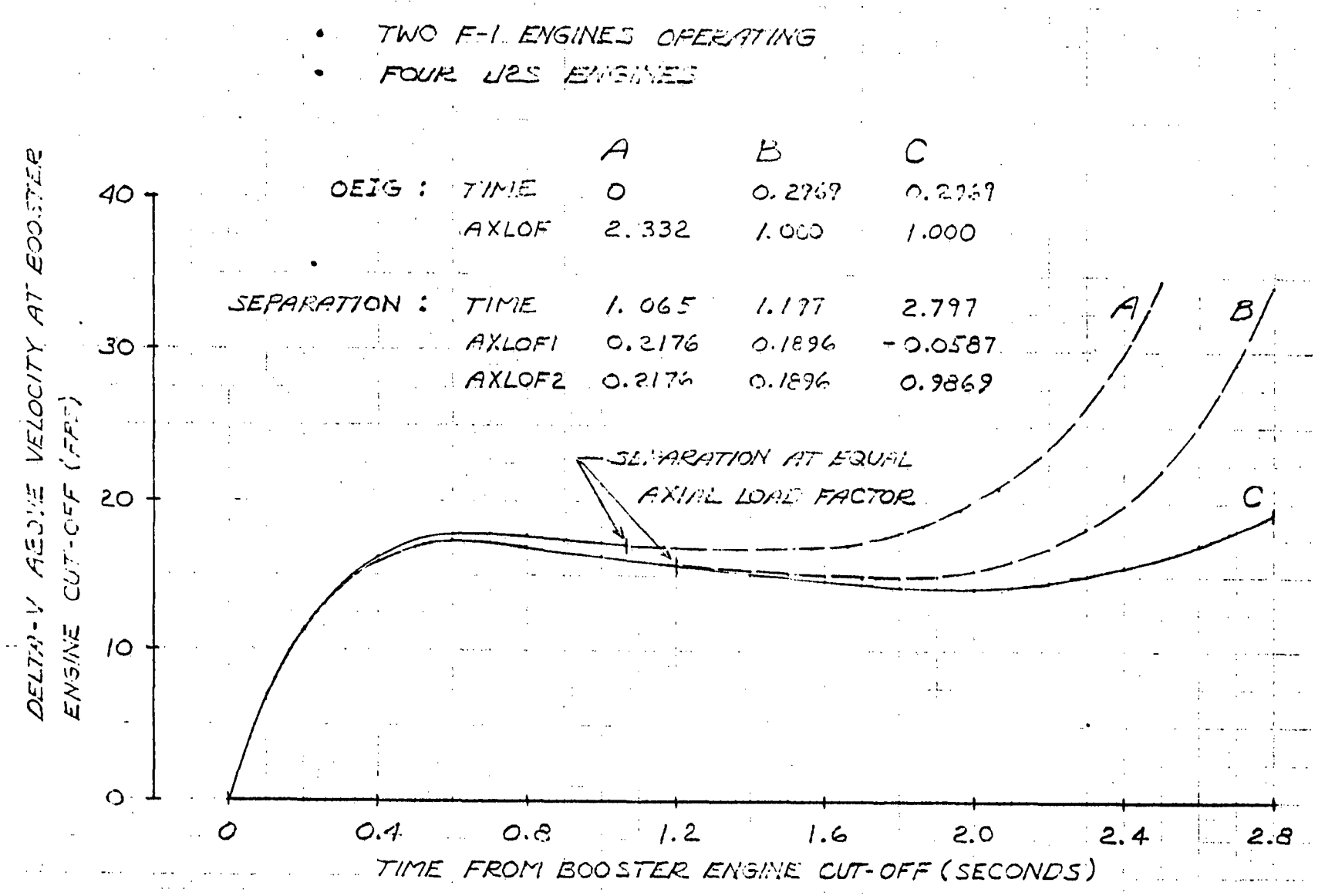

Figure 4-112. Velocity Variation During Booster/Orbiter Separation, 4 J2-S Engines

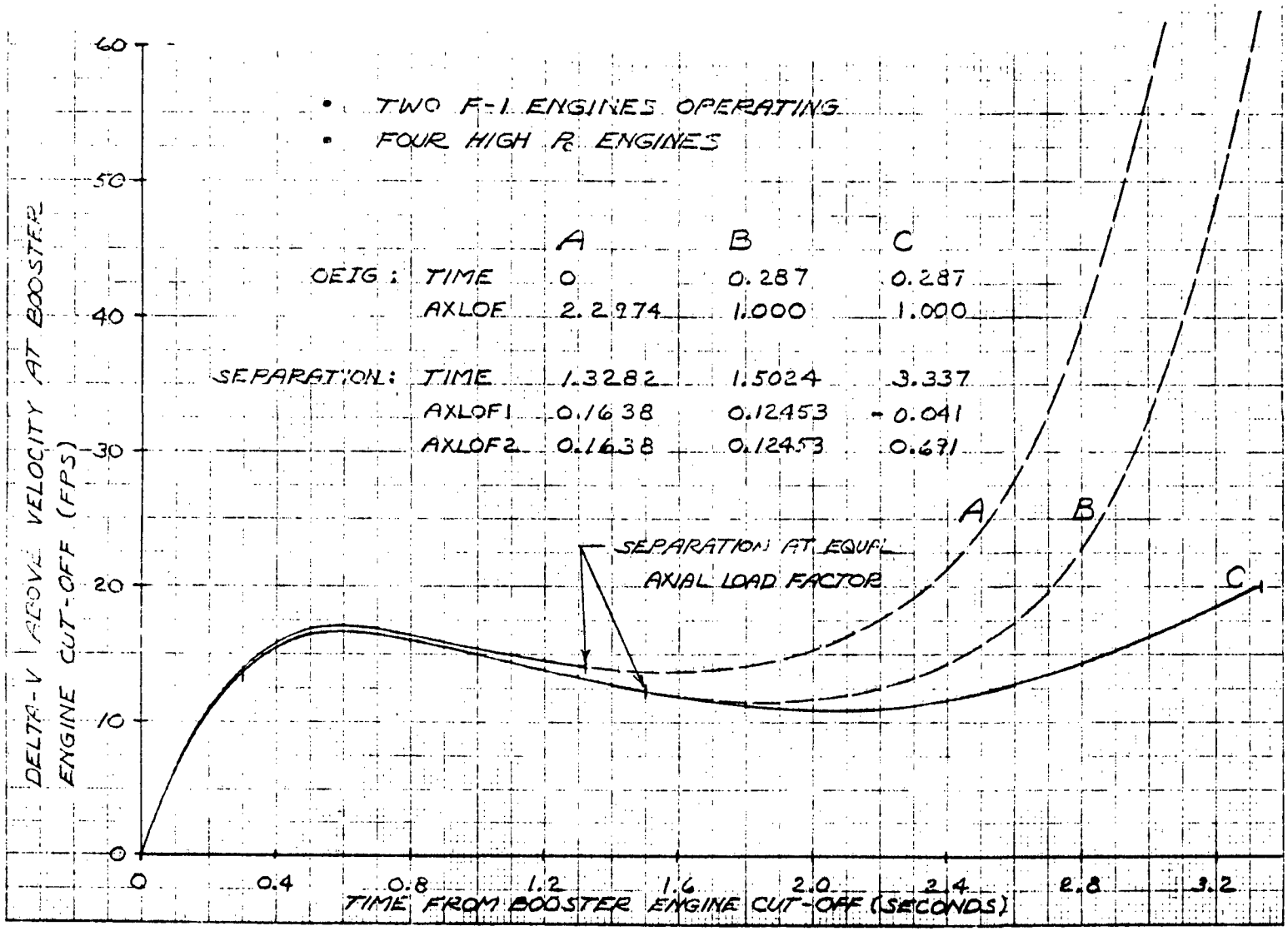

Figure 4-113. Velocity Variation During Booster/Orbiter Separation, Four HiPc Engines

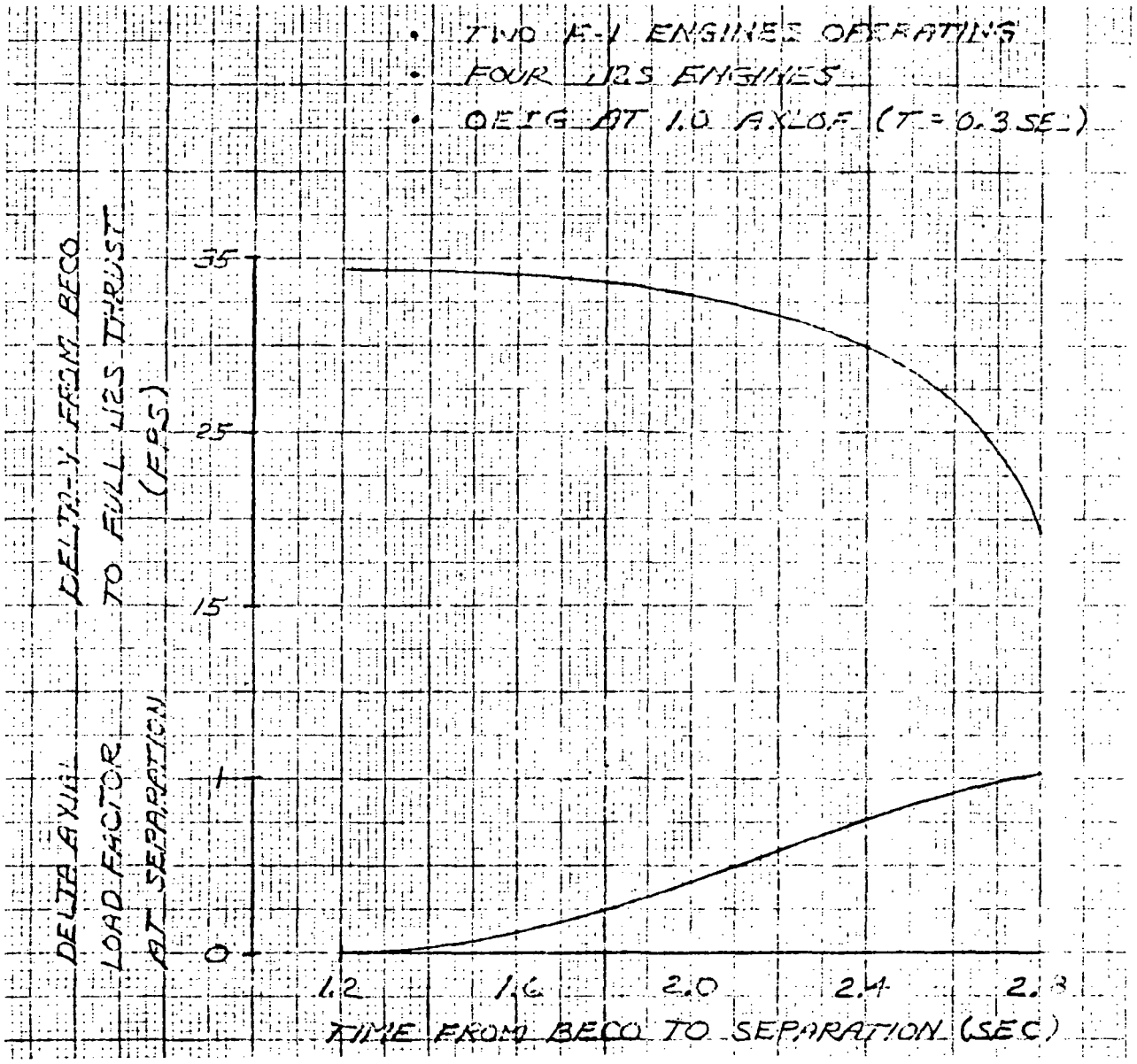

Figure 4-114. Effect of Separation Delay

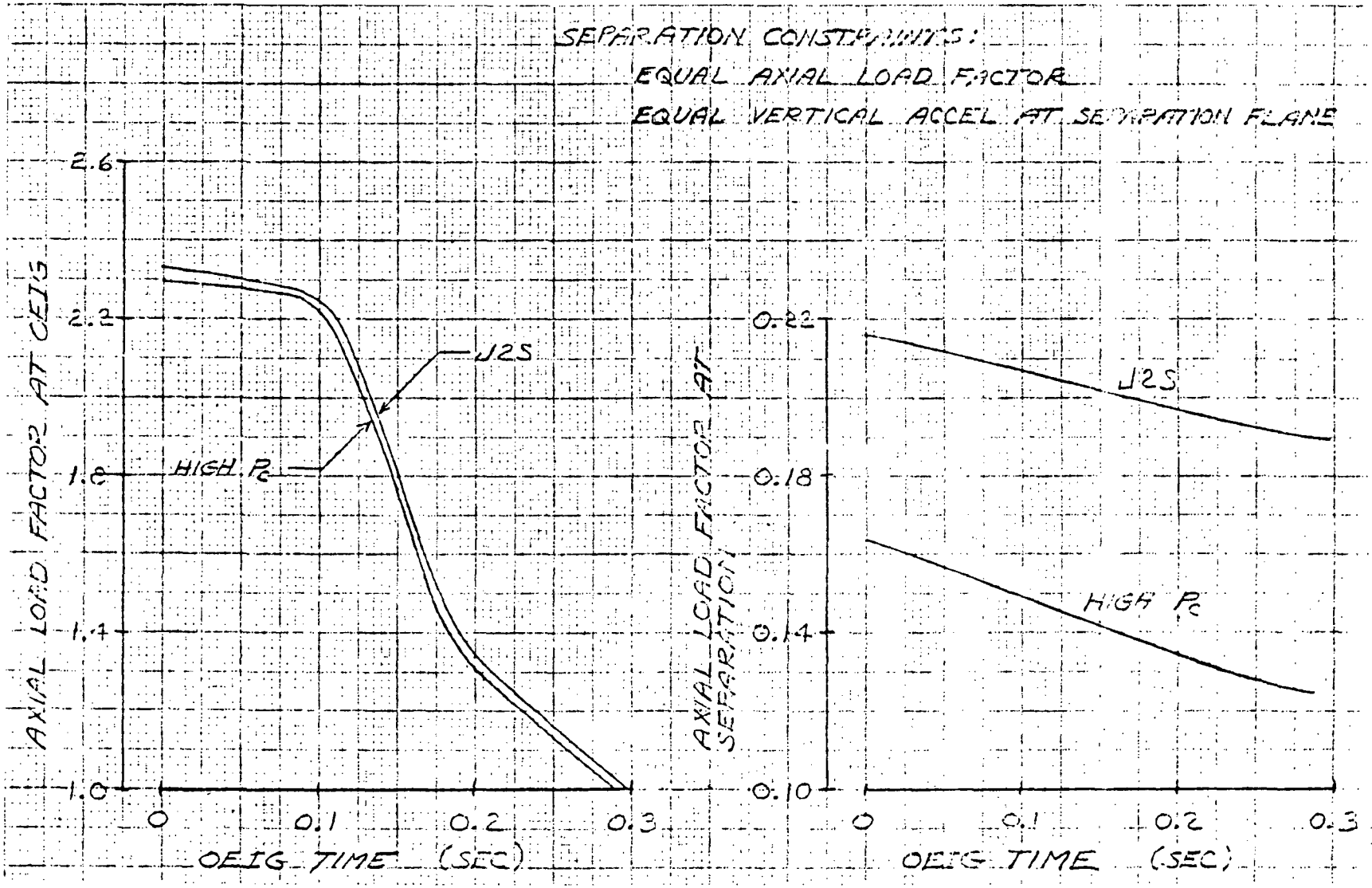

Figure 4-115. Axial Load Factors at Orbiter Engine Ignition and Separation

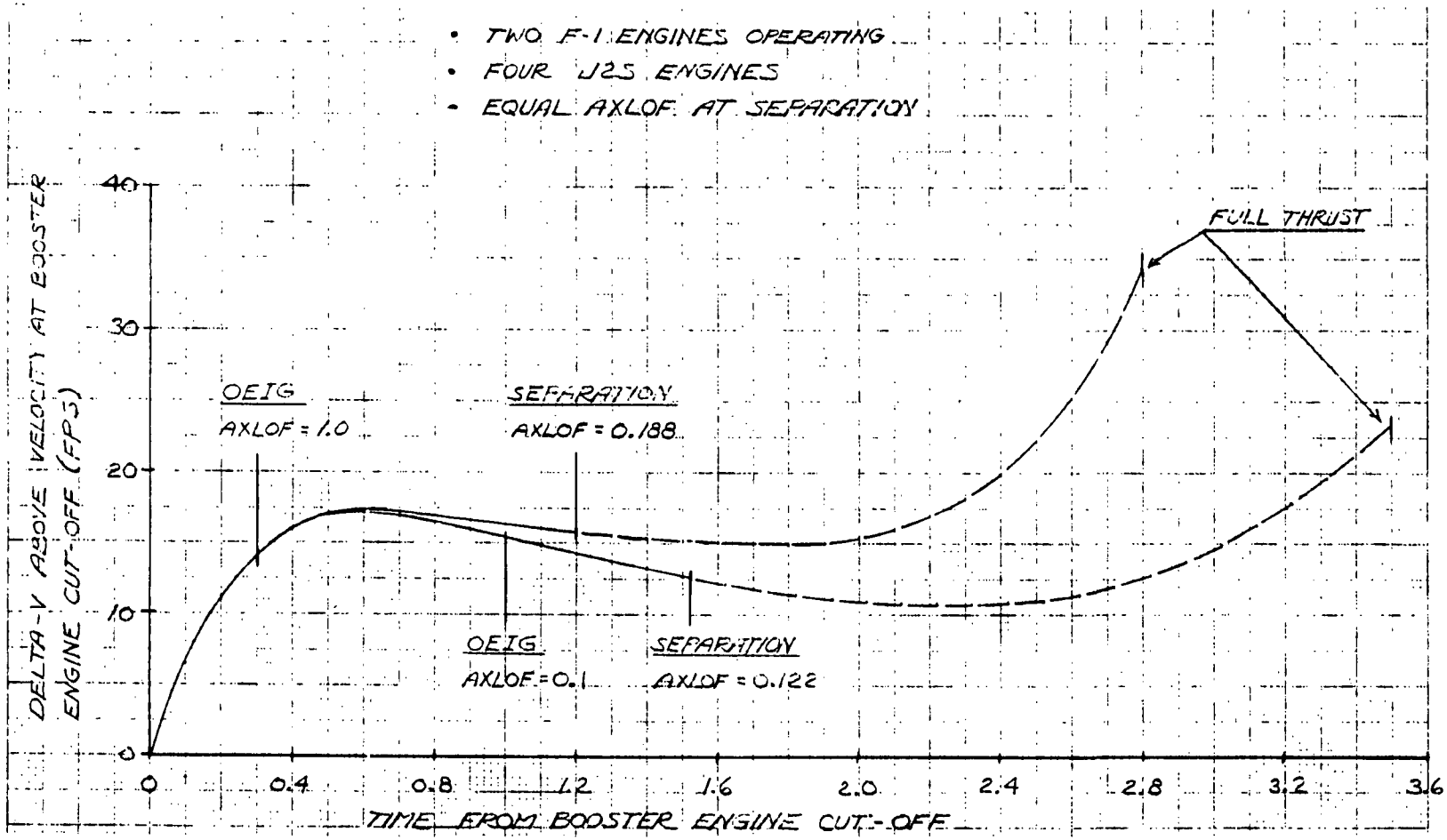

Figure 4-116. Effect of OEIG Delay to 0.1 AXLOF

In conclusion, several observations can be made from these cursory booster/orbiter separation study results. The basepoint separation technique appears to be satisfactory, although a design problem exists at the mating of the interstage with the booster nose — a problem which exists because of the shape of the booster nose and which can probably be resolved with design modifications. Also, the HiPc orbiter engine exhibits better performance during the separation phase than does the J-2S engine. In either case, significant variation from the basepoint separation conditions can be tolerated without a severe performance penalty, thus permitting the separation sequence to be dictated to some extent by other, nonrelated design criteria.

4.4.2 Integrated Vehicle Definition, PFB System

4.4.2.1 Design and Mass Properties

The baseline pressure-fed booster is described in Section 4.4.6. As indicated in Section 4.2.4.1, LO_2/propane propellants have been chosen for the baseline. The integrated vehicle is illustrated in Figure 4-117. The basic orbiter is identical with that described in Section 4.4.1.1. The EOHT, for the same staging velocity from the booster, is slightly lighter than for the reusable LO_2/RP flyback booster since an optimum performance ascent trajectory can be employed with the unmanned pressure-fed booster. Staging angle constraints do not appear to be needed to limit the booster entry deceleration. Hence, staging at a relative flight path angle, γ, of 21 to 23 degrees appears desirable for ascent performance for the PFB. Further evaluation will be made of the downrange impact effect of the selected staging conditions.

A summary of mass properties for the orbiter/booster combination through the ascent phase of the booster is presented in Table 4-26. These data are shown for two orbiter missions, the Mark I polar, with 25,000 pounds cargo, and the Mark II polar, with 40,000 pounds cargo at launch. The Mark II mission requirements establish the volumetric sizing of the tank, which is also used for the Mark I mission. The high-pressure engines of the Mark II orbiter are operated at a mixture ratio of 6 to 1, and the J2S engines, at 5.5 to 1. Since the same tank is used for both Mark I and Mark II, for the Mark I missions, the orbiter fuel tank is loaded full and the oxidizer tank is off-loaded to the mixture ratio of 5.5.

Summary weights for the integrated vehicle with both Mark I and Mark II orbiters are shown in Table 4-27. The LO_2/propane booster was sized by the Mark II polar mission with 40,000 cargo, using the orbiter and tank weights shown for Mark II.

Table 4-26. Sequence Mass Properties Statement

CONFIGURATION: MK I & MK II ORBITER/B-19-2 BOOSTER COMBINATION						BY		DATE		PAGE OF	
			CENTER OF GRAVITY			MOMENT OF INERTIA			PRODUCT OF INERTIA		
			INCHES			SLUG FT^2 X 10^{-6}			SLUG FT^2 X 10^{-6}		
NO.	MISSION EVENT	WEIGHT LB.	X	Y	Z	$I_{x\cdot x}$	$I_{y\cdot y}$	$I_{z\cdot z}$	I_{xy}	I_{xz}	I_{yz}
MK	I POLAR 25.6K ORB/LO_2 - PROPANE BOOSTER										
*	LIFT-OFF	5173086	2637.6	0.0	409.1	7.866	733.865	731.414	0	-8.595	0
	BOOSTER ASCENT PROP	-2127660									
*	MAX Q FLIGHT CONDITION	3045426	2542.7	0.0	415.4	6.613	664.280	661.898	0	-7.634	0
	BOOSTER ASCENT PROP	-735000									
*	3-G FLIGHT CONDITION	2310426	2348.1	0.0	420.2	6.153	572.733	570.395	0	-5.662	0
	BOOSTER ASCENT PROP	-749340									
	BOOSTER LOSSES	-62640									
*	BOOSTER BURNOUT	1498446	1909.5	0.0	431.1	5.443	368.458	366.230	0	-1.218	0
MK	II POLAR 40K ORB/LO_2 - PROPANE BOOSTER										
*	LIFT-OFF	5252744	2608.0	0.0	411.5	8.635	786.021	782.877	0	-11.045	
	BOOSTER ASCENT PROP	-2127660									
*	MAX Q FLIGHT CONDITION	3125084	2496.7	0.0	419.2	7.343	709.768	706.725	0	-9.584	
	BOOSTER ASCENT PROP	-735000									
*	3-G FLIGHT CONDITION	2390084	2297.1	0.0	425.0	6.857	606.934	603.967	0	-6.965	
	BOOSTER ASCENT PROP	-749340									
	BOOSTER LOSSES	-62640									
*	BOOSTER BURNOUT	1578104	1863.2	0.0	437.5	6.093	384.359	381.556	0	-1.270	

NOTES:

* NOSE OF TANK IN STACK = STA 500 (VC70-0188, Revision A)

CENTER LINE OF TANK: VERTICAL = 400

Table 4-27. Integrated Vehicle Weight Statement, LO_2/Propane Booster

	MK I - POLAR		MK II - POLAR	
ORBITER & TANK COMBINATION		974780		1054438
Cargo	25600		40000	
Orbiter (Less Cargo & Tank)	129272		136377	
Ascent Propellant	751300		809453	
Tank Burnout	68608		68608	
BOOSTER (B-19-2)		4198306		4198306
Ascent Propellant	3674640		3674640	
Burnout	523666		523666	
GLOW		5173086		5252744

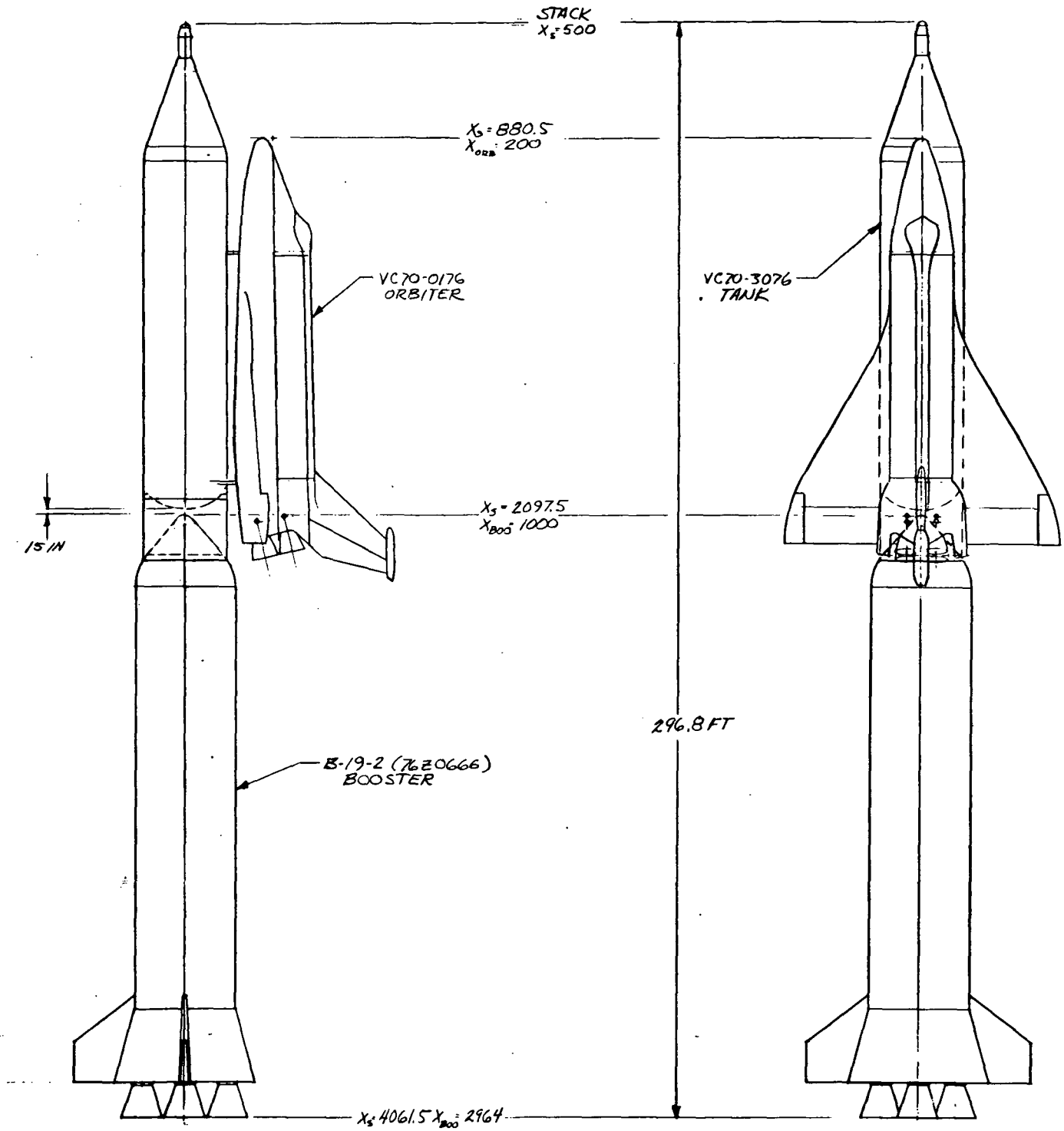

Figure 4-117. Baseline LO_2/Propane PFB With EOHT Orbiter

4.4.2.2 Aerodynamics and Stability

The 040A orbiter/EOHT/pressure-fed booster (PFB) baseline launch configuration is shown in Figure 4-117. The booster stage is unmanned and parachute-recoverable in a water landing. The booster employs fixed nozzles with thrust vector control. This control is achieved by injecting fluid along the nozzle walls in the vicinity of the nozzle throat, producing unsymmetrical flow regions. During boost, longitudinal and lateral/directional stability will be achieved using thrust vector control when necessary. Use of aerodynamic surface control is not anticipated.

The booster employs a three-fin, flared-skirt tail section. Two of the fins are attached parallel to the orbiter wing and protrude in a radial sense from the booster centerline. The third fin is aligned so that is is directed 180 degrees in relation to the orbiter vertical. The fin arrangement serves to aid in longitudinal and directional stability as well as to reduce the large rolling moments created by the orbiter at yawed angles. The flared skirt contributes significantly to longitudinal and directional stability at higher Mach numbers where the fins become less effective.

Preliminary center-of-gravity estimates and longitudinal aerodynamic data for the PFB configuration indicate static longitudinal instability below M = 3.5. Initial estimates also indicate static directional instability below M = 4.75. Preliminary control studies have considered these factors.

The axial and longitudinal data for the PFB launch configuration are presented in Figures 4-118 and 4-119. Lateral/directional data are shown in Figures 4-120 and 4-121.

The moment reference center is the booster nose and booster centerline. Angle of attack in the boost phase is defined as positive when the velocity vector is approaching the under side of the orbiter.

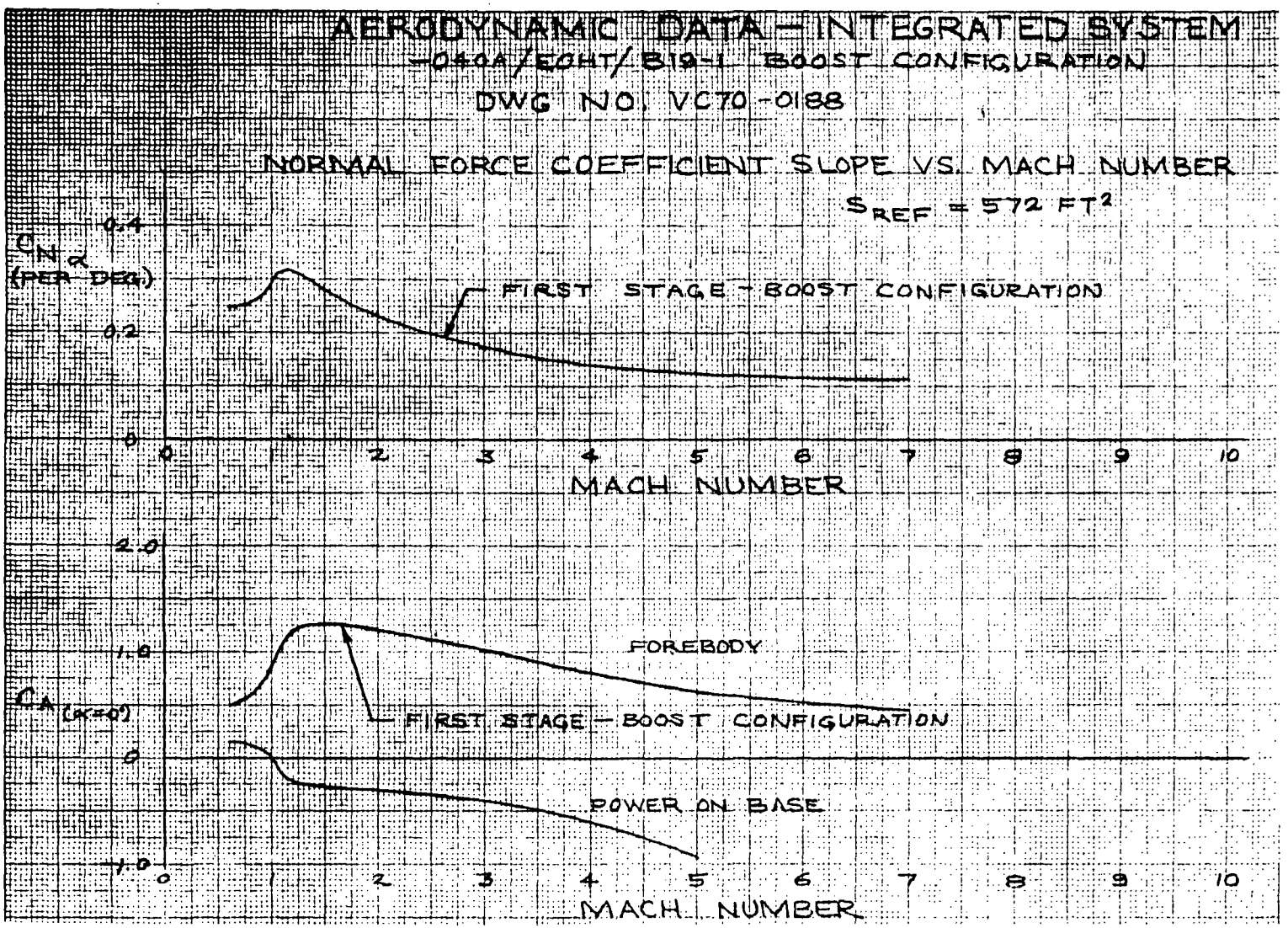

Figure 4-118. Longitudinal Aerodynamic Characteristics, Normal Force Coefficient Slope Versus Mach Number

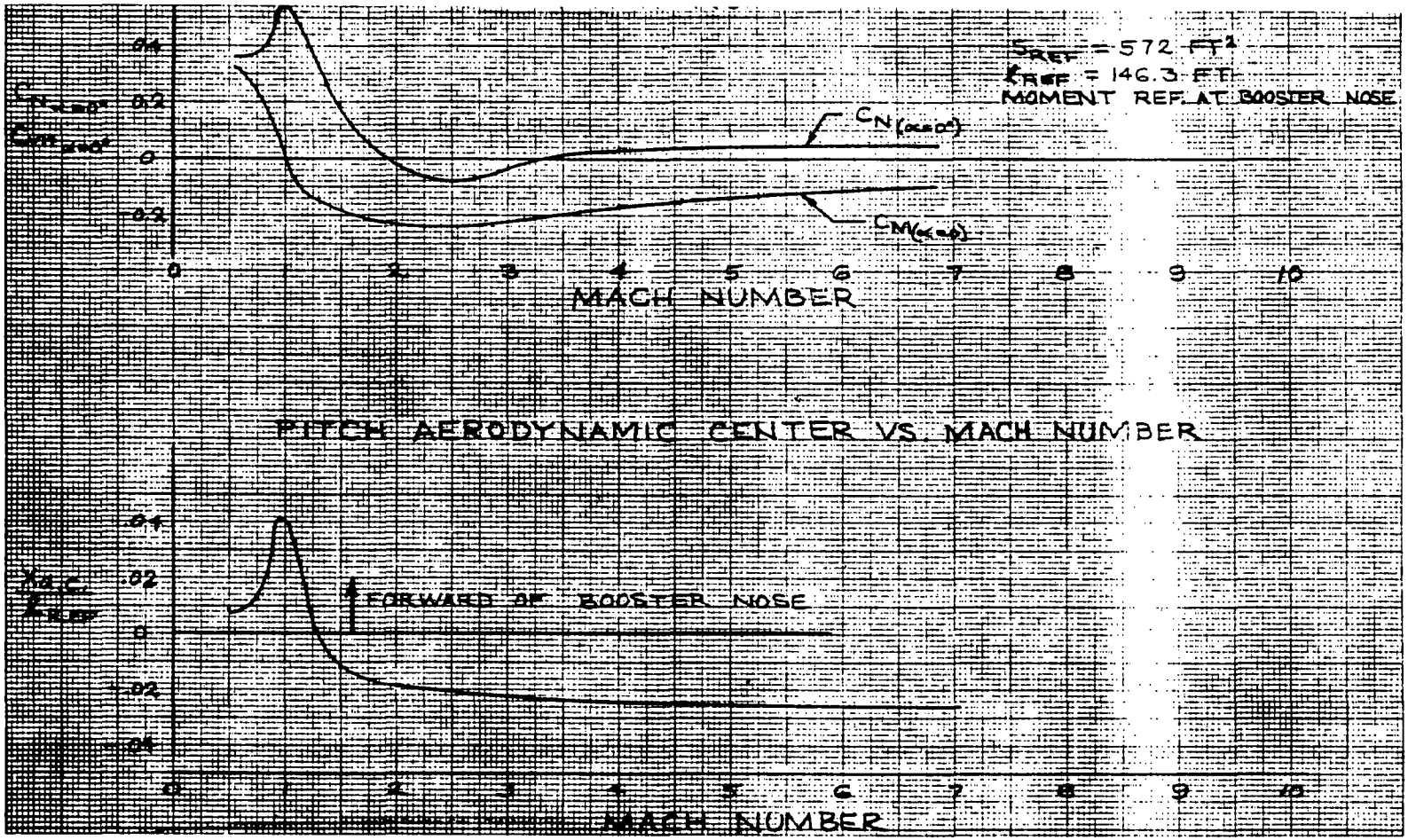

Figure 4-119. Longitudinal Aerodynamic Characteristics, Normal Force and Pitching Moment Coefficients at α = 0 Degrees Versus Mach Number

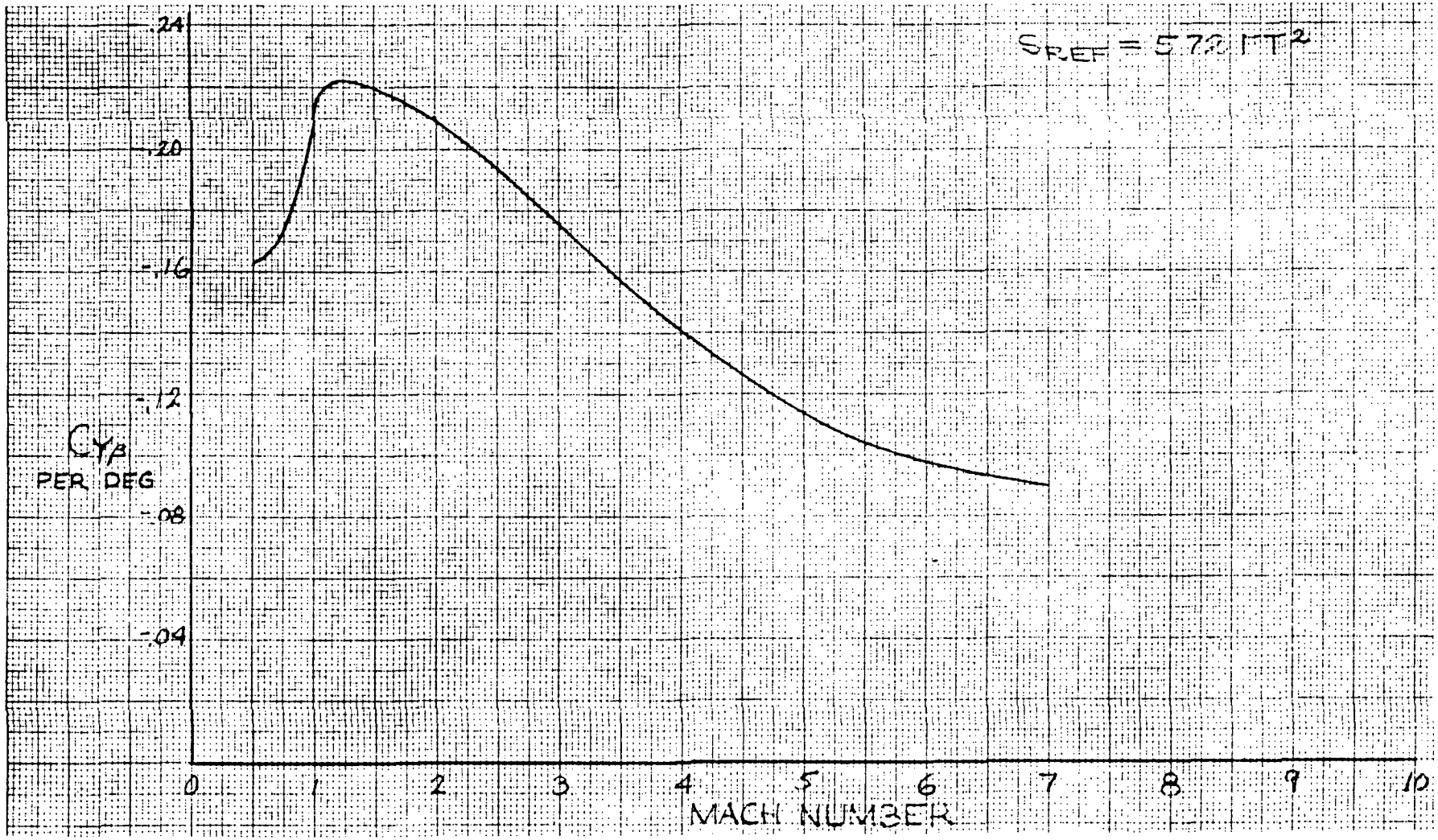

Figure 4-120. Lateral/Directional Aerodynamic Characteristics, Side Force Coefficient Versus Mach Number

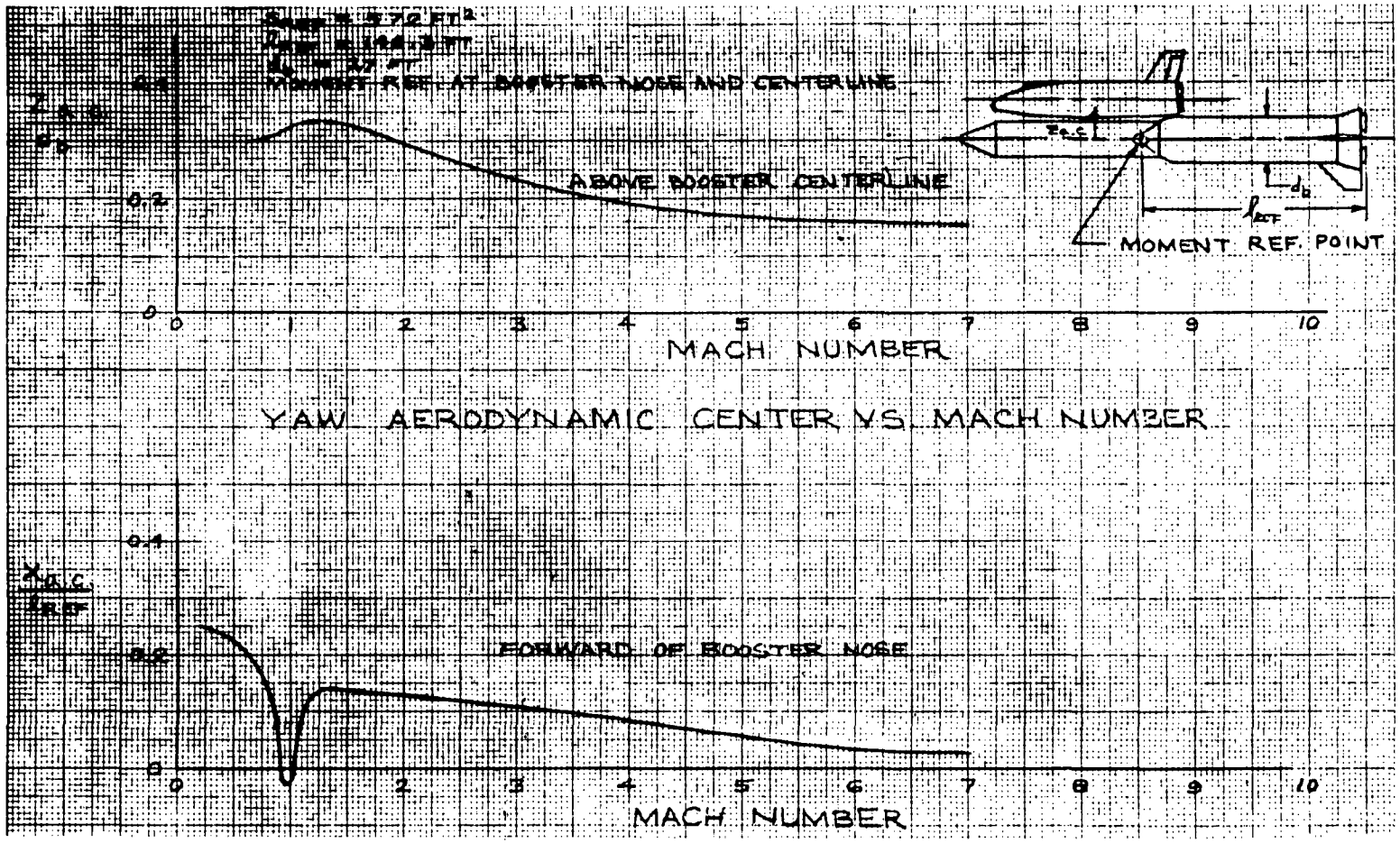

Figure 4-121. Lateral/Directional Aerodynamic Characteristics, Roll and Yaw Aerodynamic Center Versus Mach Number

4.4.2.3 Ascent Trajectory and Performance

Mark II System Performance. The Mark II selected baseline pressure-fed system which resulted from the trade studies discussed in Section 4.2.4 is described in Figure 4-122. This configuration consists of a pressure-fed LO_2/propane, seven-engine booster and a four HiPc engine external LO_2/hydrogen orbiter. The unmanned booster uses a parachute/water recovery system and a specific main engine shutdown sequence for limiting maximum dynamic pressure and axial acceleration. The sequence of events for the ascent phase is shown in Table 4-28.

Typical nominal ascent trajectory parameters are illustrated in Figure 4-123 for the selected Mark II system. The boost phase to orbit insertion is simulated by planar motion of a point mass over a spherical rotating earth. During booster operation the thrust and drag vectors are assumed to be aligned with the velocity vector. From orbiter ignition to insertion at an orbit of 50 by 100 nm, a linear tangent steering technique is used for optimum thrust vectoring. Approximately 31 percent throttling on the orbiter is required to limit axial acceleration to 3 g's prior to orbiter insertion.

The Mark II alternate mission capability is presented in Figure 4-124 for the selected baseline system. These data were determined assuming: (1) no yaw steering, (2) insertion into a 50 by 100 nm orbit for all inclinations, (3) payload up equals payload down, and (4) no structure penalty to extend OMS tank loading beyond 1000 feet per second. Consequently, mission capability is established by trading payload for OMS propellant. The on-orbit delta V's assumed for this analysis are based on impulsive maneuvers including a 15 percent contingency and are considerably smaller than the requirements specified for the design reference missions. Thus, the payload performance capability as shown is 5000 to 10,000 pounds greater than the design requirement as specified by the study ground rules. Utilizing the study ground rules for OMS delta V, performance of the PFB/orbiter system is given in Table 4-29.

Mark I System Performance. The Mark I system performance is shown in Figure 4-124 and Table 4-29 for the selected Mark II baseline system. The capability of the Mark I configuration was determined under the following assumptions:

1. Orbiter LO_2 tank is off-loaded to meet the J-2S engine mixture ratio requirement of 5.5:1

2. Corresponding vacuum I_{sp} and thrust per engine are 436 and 265,000 pounds, respectively.

MK-II ORBITER 4 X 265 KLB Hi Pc ENGINES

SYSTEM PARAMETERS			
CARGO BAY		15 X 60 Ft	
PAYLOAD (KLB)		40 POLAR	
OMS ΔV (FPS)		650 POLAR	
SYSTEM GLOW	(MLB)	5.253	
T/W @ LO		1.3	
STAGE GROSS WT	(MLB)	4.198	1.055
MAIN PROP WT	(MLB)*	3.674	0.818
OMS PROP WT	(KLB)		11.2
FLYBACK FUEL	(KLB)	--	
FLYBACK RANGE	(NMI)	--	
STAGE DRY WT	(KLB)	487	116
ORB EXT TANKS	(KLB)		56
STAGE LANDING WT	(KLB)	518	160
MAX Q	(PSF)	650	
STAGING V_R	(FPS)	5968	
γ_R		21	
MAIN ENGINE F_{SL}	(KLB)	976	
F_{VAC}	(KLB)	1185	265
NO. OF MAIN ENG.		7	4

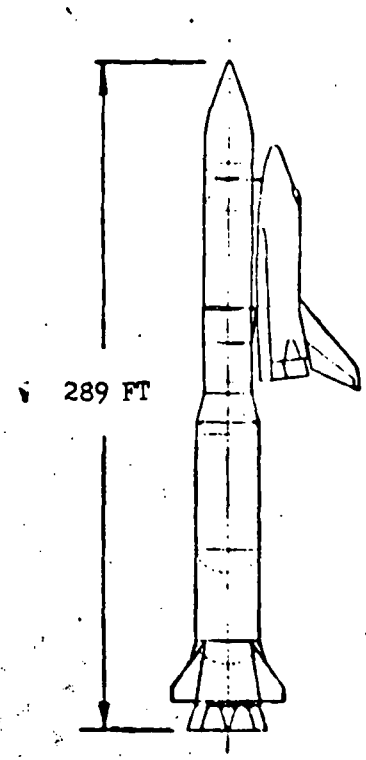

* INCLUDES TVC PROPELLANTS

Figure 4-122. Integrated System Description, Final Booster Weight Scaling

Table 4-28. Sequence of Ascent Events

Time (Sec)	Event
0	Liftoff vertical boost
14	End vertical boost, pitch over, initiate gravity turn
30	Booster CECO
76	Maximum q 654 psf
106	Shut down two main engines at 3-g limit
148	Shut down two main engines at 3-g limit
149.3	Booster cutoff and sequence (q = 23 psf V = 5968 fps h = 178,000 ft γ = 21 degrees)
151.8	End coast and ignite orbiter (q = 19 psf θ = 30 degrees)
451.7	Begin throttling for 3-g limit
506.9	Orbit insertion

3. Orbiter subsystem weight change from Mark II to Mark I = -6000 pounds.

4. Mark I booster is identical to the Mark II booster.

As a result of the off-loaded orbiter LO_2 propellant tank, the Mark I booster staging velocity is approximately 200 to 300 fps greater than that for the Mark II booster. Additionally, maximum dynamic pressure will be greater than 650 psf due to the greater liftoff thrust-to-weight ratio unless the trajectory is lofted higher or the main engine shut-down sequence is adjusted to limit dynamic pressure. This higher staging velocity presents a potential problem for north-launch polar missions in that the booster stage could impact on land. Preliminary results of ballistic entry trajectories without a drag device indicate that a Mark I due north launch would cause the booster to impact on the coast of South Carolina. However, a due south launch (if permissible) will result in a water impact approximately midway between Florida and Cuba. In the event coplanar launches are undesirable

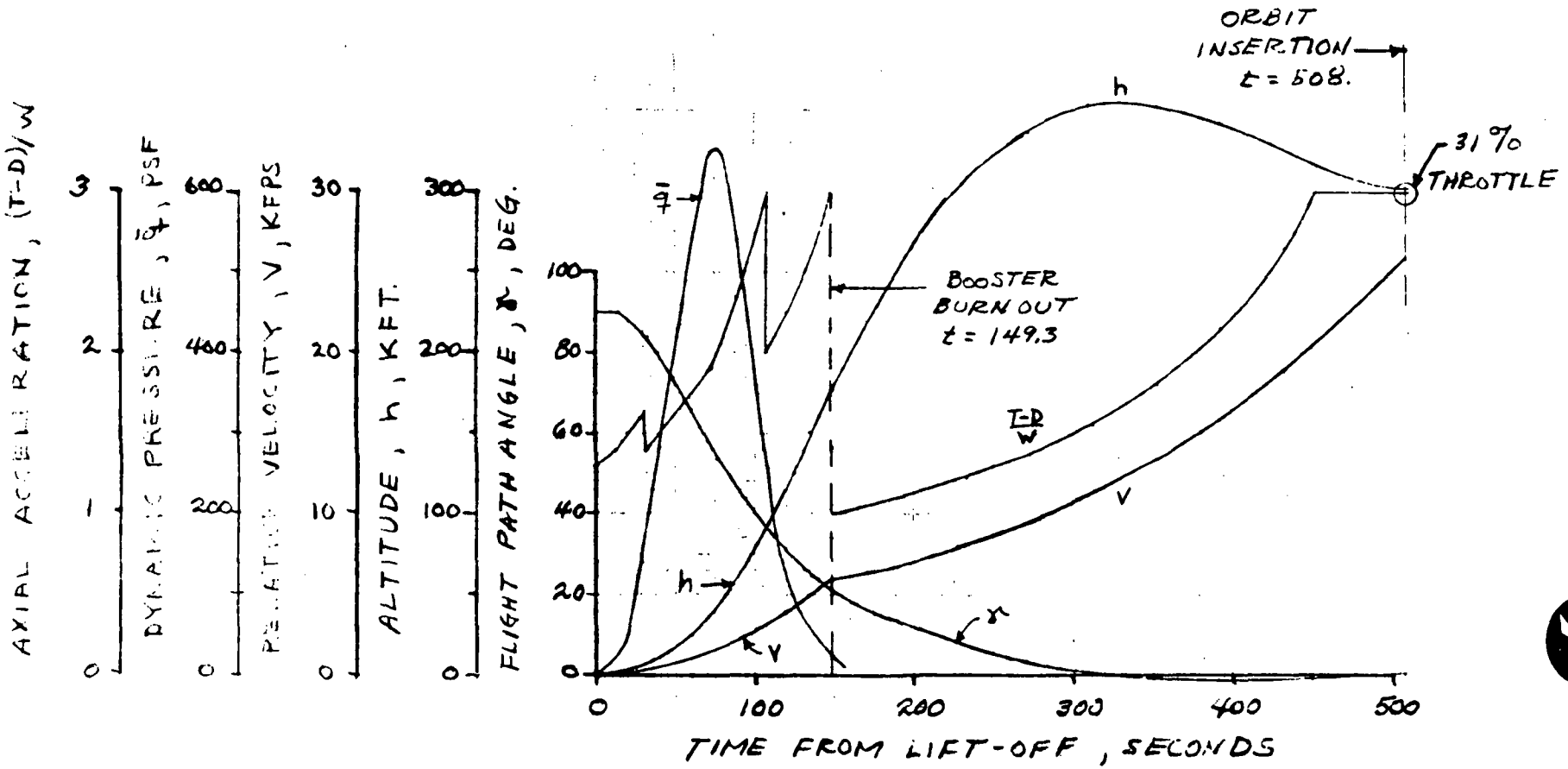

Figure 4-123. Baseline Ascent Trajectory, Mark II LO_2/Propane 4 HiPc System

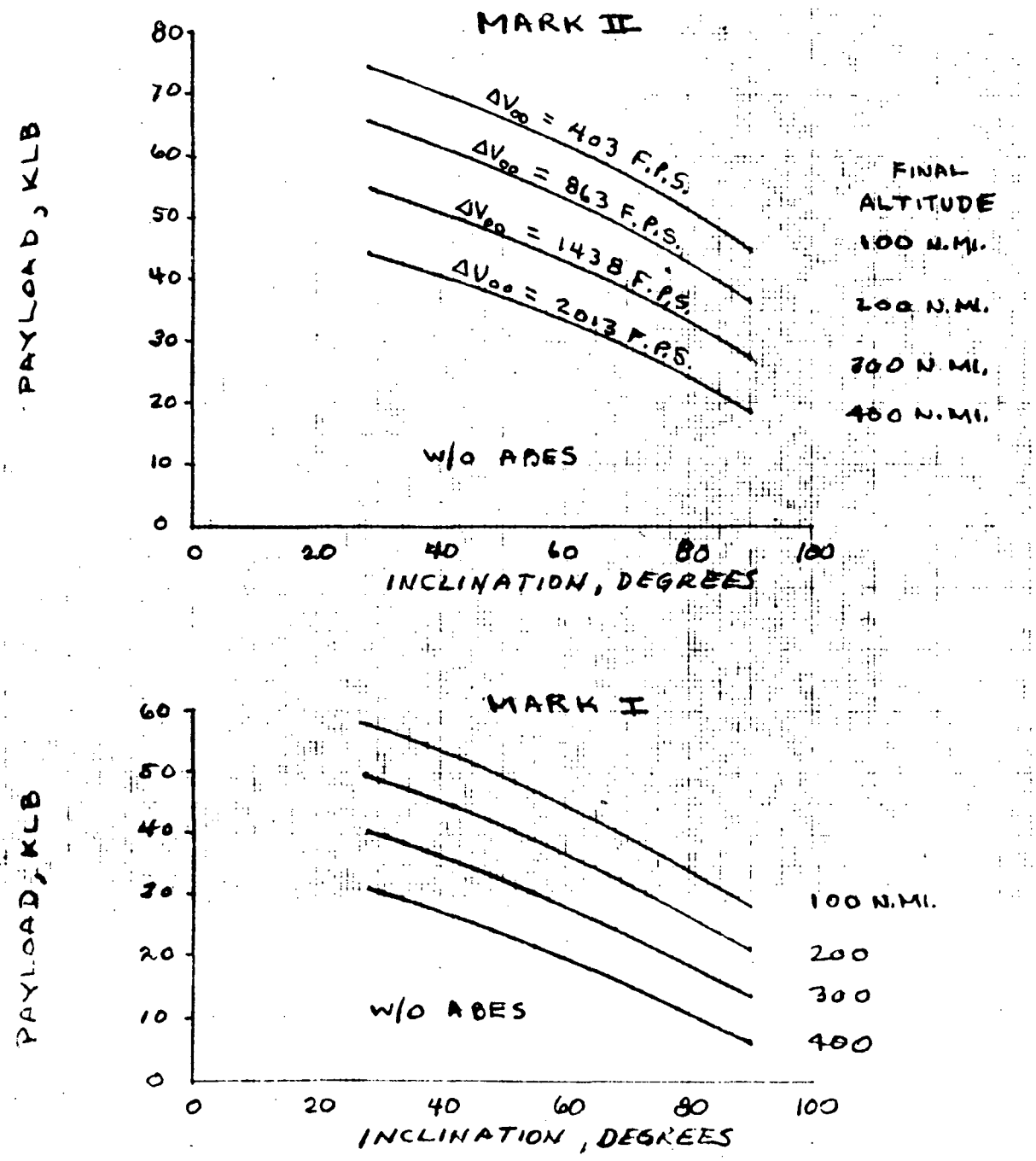

Figure 4-124. Mark II and Mark I Alternate Mission Capability, LO_2/Propane Baseline PFB

Table 4-29. Payload Capability of Mark I and Mark II Orbiter with Selected LO_2/Propane Pressure-Fed Booster

	Mark I			Mark II		
	Due East	Logistic 55 Deg	Polar	Due East	Logistic 55 Deg	Polar
Payload up (Klb)	49	30	25	65	44	40
OLOW (Klb)	1005	994	975	1086	1075	1055
Ascent Wp (Klb)	751	751	751	809	809	809
OMS Wp (Klb)	16	24	10	18	28	11
OMS ΔV (fps)	900	1500	650	900	1500	650

for polar missions, it will be necessary to investigate the effects of yaw steering on performance and booster impact location. These observations suggest that staging conditions for the pressure-fed booster need to be established with primary consideration of range safety factors for both Mark I and Mark II trajectory characteristics.

4.4.2.4 Ascent Control

Ascent control for the pressure-fed booster mated flight is discussed in Section 4.2.4.3.

4.4.2.5 Ascent Thermal Environment

Ascent thermal environment for the orbiter is discussed in Section 4.4.3.6, and for the booster in Section 4.4.6.8.

4.4.2.6 Abort Capability

Abort modes for the pressure-fed booster/orbiter system are discussed in Section 4.2.4.4. As indicated therein, since the PFB engines will be cut off in the event an ascent-phase abort is needed, abort capability will be governed largely by the ability of the orbiter to separate safely from the PFB and to fly to a safe landing. Abort intent would be to save the crew and the orbiter, as well as to assure that jettisoned hardware would fall into safe ocean areas.

4.4.2.7 Separation

Separation of the orbiter from the pressure-fed booster has not been analyzed as extensively as orbiter separation from the reusable, flyback booster (see Section 4.4.1.7) since it is felt that the problem is less critical for the PFB. Simplicity of separation for the PFB system is due to two basic factors. First, the unmanned booster imposes practically no constraints on the separation maneuver, which can thus be performed in a manner most advantageous to the orbiter without jeopardizing booster recovery. Secondly, the interstage adapter for the PFB system either remains with the booster after separation and is recovered with the booster, or if jettisoned separately, it will fall in the same general area as the booster. The design problem of separating the interstage adapter from a rounded booster nose, as exhibited for the flyback booster, would be eliminated with a recoverable adapter. Unless water impact requirements are determined to be too demanding on the PFB, recovery of the interstage adapter along with the booster will be pursued.

4.4.3 Orbiter Definition

The baseline orbiter selected for design definition is illustrated in Figure 4-125. The external mold line is the same as NASA MSC -040A configuration except for the manipulator arm stowage on top of the cargo bay doors. The Mark I and Mark II orbiters are the same except for:

1. Mark II TPS replaces the Mark I 200-nm ablator system with 1100-nm RSI system.

2. Mark II main propulsion system uses four 265,000 pounds vacuum thrust space shuttle main engines (SSME).

3. Mark II OMS engine uses a new regeneratively cooled engine in place of the Mark I L/M ascent engine to reduce refurbishment costs.

Definitions of the orbiter configuration and subsystem descriptions are provided in the following sections.

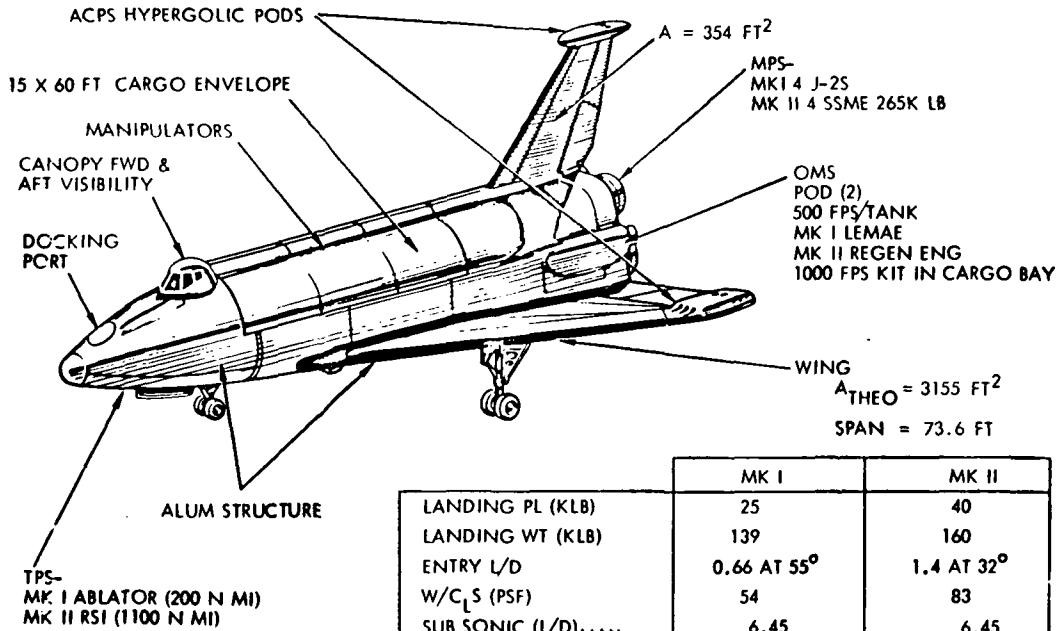

	MK I	MK II
LANDING PL (KLB)	25	40
LANDING WT (KLB)	139	160
ENTRY L/D	0.66 AT 55°	1.4 AT 32°
$W/C_L S$ (PSF)	54	83
SUB SONIC $(L/D)_{MAX}$	6.45	6.45
MIN TD SPEED (KTS)	150	161
BODY LENGTH (FT)	109.6	109.6

NOTE: PRELIMINARY ESTIMATES AT START OF DESIGN DEFINITION

Figure 4-125. Orbiter Configuration

4.4.3.1 Design

The baseline orbiter configuration established near the conclusion of this reporting period is a result of configuration trade studies and design coordination activities with NASA. Figure 4-126 shows the configuration that is based on the NASA 040A configuration with the following modifications: (1) dorsal fairing from crew compartment to vertical fin to house the manipulators, (2) forward retracting landing gear, (3) increased size of the OMS engine pod, and (4) revised flight deck lines.

The dorsal fairing is an integral part of the cargo bay doors and is designed to provide thermal protection and support for flight loads for the manipulator arms. The manipulator deployment and cargo door opening geometry is designed to provide for a full door travel in the event of a failure to release the manipulators from their stowed position.

The landing gear, both the nose wheel and main gear, are forward retracting in order to provide free fall capability for landing gear extension in the event of hydraulic system failure. The main gear is mounted in the wing panel and retracts forward into a wheel well in the forward section of the wing. The wing is of sufficient depth to house the dual 44-by-13 Type VII wheels and tires without refairing the wheel well area. The nose gear is moved forward and is pivoted at the forward end of the crew compartment structure. This location requires a slightly longer nose gear strut. There is no significant landing load increase in the nose strut because of the longer distance from the main gear since the main gear is located as with conventional aircraft with respect to c.g. in order to achieve proper rotation control during takeoff and landing.

The OMS engine pod is modified in size and shape in order to accomodate propellant tankage for 1000 fps delta-V as compared to approximately 650 fps delta V capability of NASA 040A. The OMS pod is designed as a complete unit that can be removed for service and maintenance. The propellant tankage has been so arranged to provide a compact installation with minimum protrusion beyond the basic body mold line.

The contours of the cockpit or flight station area have been revised to accommodate an exposed windshield design to eliminate retractable heat shields. The NR baseline configuration considers that all aerodynamic and space flight will be controlled by forward-looking flight stations for the commander and pilot. The manipulator operator station is aft of the flight station and has minimal spacecraft control in addition to full manipulator controls. The flight deck windows are flat panels of high-temperature glass and are designed to provide visibility over the nose and to the side as well as overhead to monitor the manipulator operations in that area. The manipulator operator station has glass panels that are covered by the cargo doors

during launch and entry and thus are not subjected to high temperatures. The panels provide visibility into the cargo bay and overhead to the extent of overlapping the flight deck overhead visibility. This arrangement results in a cockpit fairing similar to that of standard transport aircraft.

The general internal arrangement of the orbiter vehicle, shown in Figure 4-127 (inboard), consists of a reentry vehicle (orbiter) and the main propellant tankage. The orbiter subsystems are located primarily in the body with the nose section containing the crew compartment; the mid body has the cargo bay and wing carry-through; and the aft section contains the main propulsion engines, OMS pods, and vertical tail support structure.

The nose section contains the crew compartment, docking port and airlock, and the nose landing gear. The crew compartment pressure shell is designed for cabin pressure only, with the external shell designed for flight and landing loads. The external shell is configured to the required aerodynamic shape. The docking loads are taken into the airlock structure that is mounted to the crew compartment pressure shell. The internal arrangement of the crew compartment consists of an upper deck or flight deck, a lower deck, and an ECS bay. The upper deck has the flight stations and the manipulator operator station. The flight station is designed as a combined aircraft and spacecraft controls and displays arrangement with both flight crew members facing forward. The controls and displays are arranged with aircraft-type controls and displays in designated locations. The spacecraft controls and displays are similarly located. The dual-usage displays are situated to satisfy both operational modes. Forward and overhead visibility is provided for the aircraft mode of operation and for spacecraft maneuvering and docking operations. There is an overlap of overhead visibility with that of the manipulator operator in order to monitor the manipulator operations that perform a transition from aft to forward sectors. The manipulator operator has windows for viewing the payload or payload bay as well as overhead windows to provide full visibility for the aft sector of operations. The manipulator station has the necessary controls and displays for the manipulator operations plus minimal spacecraft controls and displays for final positioning and stabilizing of the spacecraft during manipulator operations. Although there are three stations on the flight, only two are used at any one time. Access to the lower deck is through a door in the upper deck floor. The lower deck has provisions for the avionics equipment, galley, waste management/hygiene, payload monitor station, two passengers for launch, and a sleep area for four crew members. The avionics bays are located at the aft bulkhead and along each side of the habitable area. The bays are sealed with doors designed for 10 inches of water pressure differential to prevent noxious or toxic gases from entering the living area. The avionics bays are located to essentially isolate the redundant systems for additional protection from fire. The passenger seats are foldable in order to provide access to the galley or the waste management

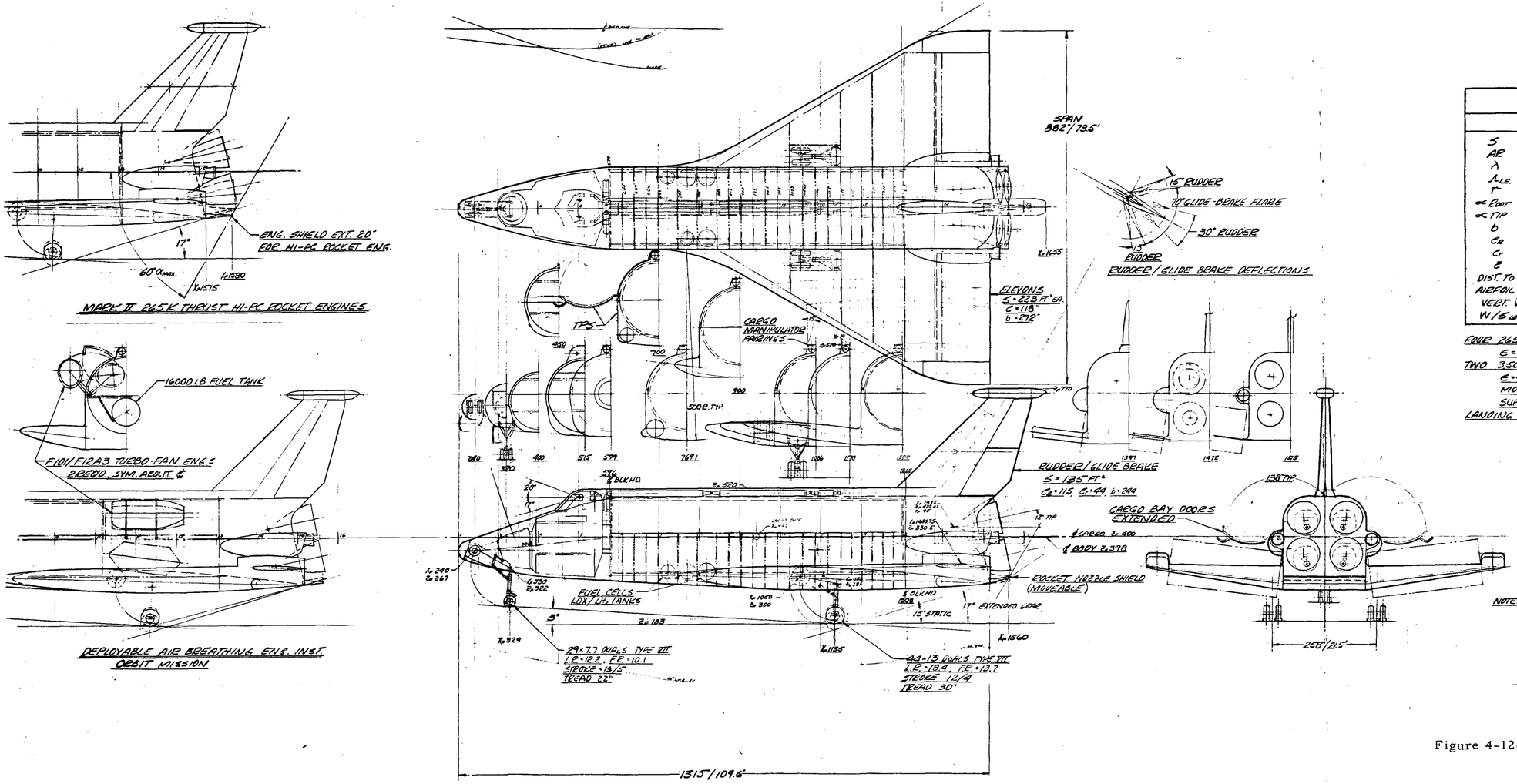

GEOMETRY			
		WING	VERT.
S	FT²	3155.299	359.375
AR		1.712	1.428
λ		0.148	0.313
Λ LE.		60°	45°
Γ		7°	———
∝ ROOT		1.5°	———
∝ TIP		1.5°	———
b	IN	882	270
C_R	IN	897	288
C_T	IN	133.3	90
C̄	IN	609.5	206.3
DIST. TO C̄	IN	166	111.4
AIRFOIL		0008-64	0012-64
VERT. ▽		———	
W/S LDG		95 PSF	———

FOUR 265000 LB THRUST J2S ROCKET ENGINES.
ε=90:1, I_SP=436, NOZ. DIA.=81"
TWO 3500 LB THRUST (LM ASCENT) ROCKET ENG.
ε=90:1, I_SP=309.7 NOZ. DIA.=31"
MODULAR ENG. & TANK W/C FOR 1000 FPS ΔV
SUPPLEMENTAL TANKS FOR 1000 FPS ΔV IN CARGO BAY
LANDING WT. EST. = 190,000 LBS

NOTES: THE FOLLOWING IS A LIST OF CHANGES MADE TO THE 040A DWG.
1. CARGO MANIPULATOR FAIRINGS — FUS. CHNGS. ℄.
2. FWD. RETRACTING MAIN & NOSE LDG. GEAR.
3. REFAIRED CREW STA. CANOPY.
4. RESIZED & REFAIRED MODULAR OMS PKGS.
5. MOVEABLE SHIELD FOR MAIN ROCKET ENG. NOZ. STA'S. 1515 TO 1634
6. RUDDER SPLIT 70° FOR SPEED BRAKES.

Figure 4-126. Orbiter Configuration Schematic

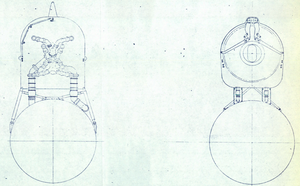

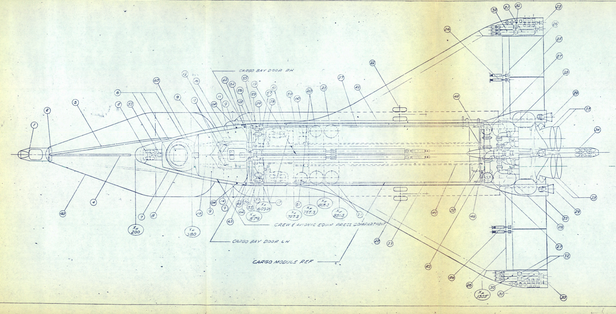

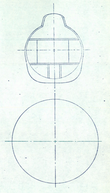

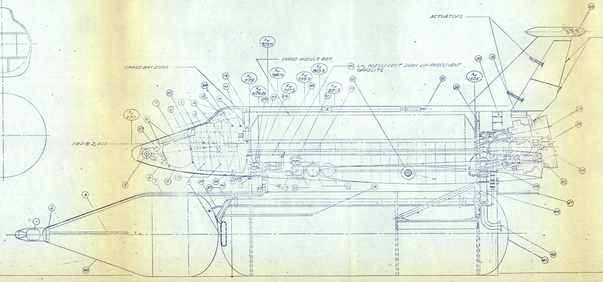

(A) ALSE MOUNTED OPTIONAL ENGINE INSTL IN VERTICAL STABILIZER TO FUS
(B) MAIN PROPULSION SYSTEM ENGINE (2)
(C) AUXILIARY POWER UNITS
(D) FLIGHT CREW COMPARTMENT
(E) UNDER CHINE STA WITH ATTACHED DOOR
(F) AVIONIC AFT PRESSURIZED EQUIPMENT
(G) MAIN PROPULSION SYSTEM LOX TANK
(H) MAIN PROPULSION SYSTEM LH2 TANK
(I) MAIN PROPULSION SYSTEM LOX FEED LINE
(J) ELECTRICAL HARNESS (ROUTED TO MID TUNN)
(K) MAIN PROPULSION SYSTEM LH2 FEED LINE
(L) MAIN PROPULSION SYS LOX PRESS LINE
(M) MAIN PROPULSION SYS LH2 PRESS LINE
(N) ELECT HARNESS (ROUTED TO BOOSTER)
(O) ELECT OUTLET
(P) LH2 PRESSURIZATION LINE
(Q) LOX TANK PRESSURIZATION LINE
(R) MAIN PROPULSION SYS LOX PRESS LINE
(S) LH2 GROUN SERVICING VENT
(T) ELEC ECS HEAT EXCHANGER
(U) ELEC FUEL CELL HEAT EXCHANGER
(V) ELEC POTABLE WATER TANK (2)
(W) ELEC WASTE WATER TANK (2)
(X) ELEC WATER HEAT EXCHANGER (2)
(Y) ELEC FREON PUMP ASSY (2)
(Z) ELEC HYDROGEN HEAT EXCHANGER
(AA) ELEC SUBLIMATOR (2)
(AB) ELEC HIGH PRESSURE HYDROGEN TANK (2)
(AC) UHF/VHF ANTENNA (2)
(AD) S-BAND ANTENNA (4)
(AE) C-BAND ANTENNA (2)
(AF) STRETCH (2)

(1) EXTERNAL LOX & LH2 TANK RECOVERY MOTOR
(2) MAIN PROPULSION SYSTEM PROPELLANT PRESS GAS DISTRIBUTION
(3) LOX RECIRCULATION/VENT LINE
(4) PROPELLANT LOADING & QUICK DISCONNECTS
(5) ORBITER NOSE LANDING GEAR
(6) AVIONIC BAY UNPRESSURIZED COMPARTMENT
(7) ORBITER DOCKING PORT
(8) AVIONIC COMPARTMENT
(9) AVIONIC EQUIPMENT PRESSURIZED BAY
(10) SLEEP AREA
(11) GALLEY AREA
(12) FLIGHT CREW COMPARTMENT (CREW & GALLEY)
(13) MAIN PROPULSION SYS LH2 RECIRC LINE
(14) WASTE MANAGEMENT COMPARTMENT
(15) CREW-PASSENGER COMPARTMENT HATCHES-SIDEWISE HATCH
(16) CARGO MONITOR STATION
(17) APCU FUEL CELL POWERPLANTS (3)
(18) FUELS EQUIPMENT AREA
(19) RADIATOR (4 TOTAL)
(20) PAYLOAD ELECTRICAL DISTRIBUTION
(21) PAYLOAD/CARGO (4)
(22) MAIN LANDING GEAR
(23) LOX FEED LINE (MAIN PROPULSION SYSTEM
(24) ELEVON ACTUATOR
(25) ELEVON
(26) ELEVON SEAL PANEL
(27) FORE RCS/OMS TANK
(28) OMS FUEL TANKS
(29) OMS ENGINE
(30) RCS FUEL THRUST INSTL (4 AFT & 4 FWD
(31) RCS OXIDIZER THRUST INSTL (4 AFT & 4 FWD
(32) RCS HELIUM TANKS INSTL (4 AFT & 4 FWD
(33) MAIN PROPULSION SYSTEM FUEL TANKS INSTL IN EACH WING FOR BOTH

Figure 4-127. Inboard Profile

area. The aft bulkhead avionics is accessible through the walls of the galley and the waste management areas. Storable couches are provided for four crew members to permit the entire crew to sleep at the same time. The ECS is located beneath the lower deck floor and is accessible through removable floor panels. Hatches are provided for (1) pad ingress/egress in the upper deck and (2) payload bay access and airlock access. The airlock has a hatch in the docking port and one into the nose gear wheel well for on-ground horizontal access.

The midbody section is designed around the payload requirements of a clear volume about a 15-foot-diameter by 60-foot-long volume. A clearance of three inches is maintained all about this volume. The cargo bay doors are hinged near the horizontal reference plane of the payload and are designed to open to clear that reference plane. The forward end of the doors extends beyond the payload bay to cover the aft windows in the crew compartment and the manipulator deployment arms. The mating edges of the doors have slotted fairings to provide stowage for the manipulator arms and thermal protection through the launch and entry portions of flight.

The manipulator arms are attached to deployment struts that are capable of positioning the shoulder of the manipulator above the body contours to maximum clearance for all manipulator operations. The geometry of the deployment system will permit door opening in the event of deployment system failure. The lower section of the midbody is the primary structural element carrying body bending, torque, and wing carry-through loads. The fuel cell tankage is located near the forward end of the midbody by installing spherical tanks between the body frames. The tanks are accessible from the payload bay with the payload removed. The fuel cells are located ahead of the forward midbody bulkhead and are accessible through the space between the crew compartment pressure bulkhead and the cargo bay bulkhead.

The aft body features an integrated structure that combines the requirements for main engine thrust loads and the vertical fin loads. The structure is designed to transfer these loads into the midbody longerons, thus reducing the load-carrying requirements of the outer shell. This concept permits the use of large doors for access to the APU installation and the aft compartment avionics bay. The OMS engine installation is designed as an independent pod that is simply attached to the aft structure. This design feature permits pod removal for servicing and maintenance of the OMS engines, valves, and tanks. The APU installation is designed to discharge the exhaust products upward through a duct in the vertical fin and out the trailing edge just below the ACPS tip pod.

The vertical surface is a symmetrical airfoil shape with the rudder hinge line at 60 percent chord. The rudder is in two spanwise sections to reduce hinge loads due to spanwise deflections. The rudder is split along

the chord plane to act as a speed brake for velocity modulation during atmospheric flight. The pitch ACPS pod is located at the tip of the fin. This pod is a complete unit consisting of thrusters, tankage, pressurant, and control valves within an aerodynamically shaped fairing.

The wing is an 8-percent-thick symmetrical airfoil with a delta planform using a 60-degree sweep leading edge. The elevons are of constant chord, and they span the exposed trailing edge from the elevon trim line to the tip-mounted ACPS pod. The ACPS pod contains thrusters for axial, roll, and yaw control. The pod is designed to be mounted on the upper surface for thermal protection during entry. The main landing gear is installed completely in the wing. The wing is attached to the body with a four-spar carry-through system and two shear connections, one at the rear spar and one near the leading edge.

The orbiter shown in Figures 4-125 and 4-126 represents the Mark I orbiter. The Mark II orbiter utilizes the Mark I configuration with the J-2S engines being replaced with space shuttle main engines with 265,000 pounds vacuum thrust and a nozzle expansion ratio of 90:1. The Mark I thrust structure and propulsion system are utilized in Mark II. The other major design change is the use of RS1 insulation on the Mark II orbiter in place of the ablator insulation used on the Mark I orbiter.

4.4.3.2 Aerodynamics and Flight Characteristics

The aerodynamic characteristics of the orbiter as summarized in this section are based on analysis supplemented by wind tunnel results correlated to account for differences between the configurations tested and the 040A baseline design. NR in-house testing of a configuration similar to the 040A baseline is summarized in Table 4-30. To develop the estimated baseline aerodynamic characteristics, correlations were made between experimental data from these tests, NASA-sponsored test S-065, and from Phase B tests and predictions using NR in-house and DATCOM methods.

Aerodynamic Configuration. The orbiter aerodynamic configuration is illustrated in Figure 4-126, and predominant geometric characteristics are summarized in Table 4-31. The fuselage bottom is slightly cambered, both the forward and after portions having a ramp angle of approximately 3 degrees and the maximum depth of the fuselage occurring at about 71 percent of its length. The nose is ogival in plan form, with cross-sections tending to be cupcake-shaped in appearance, with a flat bottom segment, rounded corners, outward canted sides and a semi-circular top surface. This cross-sectional shape is maintained for about 35 percent of the body length, after which the cross-section becomes flat on the bottom with vertical sides and sharp corners between them. The canopy is of the blister type and protrudes above the upper fuselage surface.

The wing is a 60-degree leading-edge sweep, blended delta with faired tips, having a dihedral angle of 7 degrees at the trailing edge, and a total area of 3155 square feet. The airfoil section is a NACA 0008-64 and does not vary with the span. The wing has a 1.5-degree incidence angle but has no spanwise twist.

The orbiter entry and recovery trajectory is characterized by two distinct flight phases: entry and post-entry. The flight environment encompasses a wide range of dynamic pressure and velocity; consequently the trim and damping technique for the three rotation modes (pitch, roll, and yaw) will change depending on the flight phase. At entry (Mach No. ∞ to $\approx$ 3.0), the vehicle is operating like a spacecraft; and for this phase, the pitch trim is supplied by the aerodynamic surfaces (elevons) while damping is supplied by the attitude control propulsion system (ACPS) mounted in pods on the wing tips and vertical tail. Roll and yaw trim and damping are supplied by the ACPS. For the post-entry phase (Mach No. 3.0 to landing), the vehicle is operating in a conventional aircraft mode. Aerodynamic pitch and roll control is provided by elevons which extend from spanwise station Y110 to station Y386. Directional stability is provided by a single vertical tail located on the fuselage centerline. The vertical tail is sized to provide a minimum subsonic $C_{n\beta}$ of 0.001 per degree. Yaw control is supplied by a rudder located in the vertical tail and

Table 4-30. NR Wind Tunnel Test Summary

Facility (Test No.)	Mach No.	Test Hours	Model	Objective	Results
NAAL (660)	0.26	20	0.0181 scale 110E (EOHT orbiter)	Stability and control	Vehicle exhibits static longitudinal and lateral-directional stability to an angle of attack of 27 degrees. Adequate pitch, yaw, and roll control over flight angle of attack range.
NR TWT (245)	0.6 to 1.5	15	0.0128 scale 0500 (EHT orbiter)	Stability	Stable over test Mach and angle of attack range. Rearward transonic shift in center of pressure of 0.07L at α = 10 degrees.
	0.6 and 0.9	10	0.0148 scale 0056 (EHT orbiter)		Stable for test angle of attack range. Wing tip stall at α = 16 degrees, wing stall at α = 23 degrees.
	0.6 to 3.3	145	0.0181 scale 110E (EOHT orbiter)	Stability and control Effect of ACPS pods and alternate canopy	Stable in pitch over test α and Mach ranges. Laterally-directionally stable except directionally unstable for M = 1.5 and α > 14 degrees. Trimmable in pitch through desired α range. ACPS pods promoted wing tip stall. Bubble canopy caused 50 percent reduction in $C_{n\beta}$.
MSFC TWT (509)	0.6 to 5.0	29	0.0044 scale 110D (EOHT orbiter)	Stability and control Orbiter alone, effect of alternate nose and canopy Orbiter plus tanks	Analysis in process.

Table 4-31. Orbiter Aerodynamic Configuration Summary

Fuselage	Wing	Vertical
Ogival plan-form nose with cupcake-shaped cross-sections	Delta with faired tips and leading edge blended into fuselage	Fuselage centerline
Cambered bottom	Total area = 3155 ft^2	Area = 355 ft^2
No boattail	AR = 1.71	AR = 1.425
Fineness ratio = 5.5	λ = 0.15	λ = 0.31
Maximum width = 205 inches	Λ = 60 degrees	Λ = 45 degrees
Maximum depth = 238 inches	Γ = 7 degrees at TE	b = 270 inches
Length = 1315 inches	i_w = 1.5 degrees at root	C_R = 289 inches
	b_{ref} = 882 inches	C_T = 90 inches
	C_R = 896 inches	$\bar{c}$ = 206 inches
	C_T = 135 inches	Airfoil: 0012-64
	$\bar{c}$ = 611 inches	
	Airfoil: 0008-64	

extending from vertical station Z500 to station Z745. The rudder is split, in the plan-form view, so that it may be deflected as a conventional rudder or trailing edge outboard in order to function as a subsonic glide brake and to improve directional stability at supersonic speeds. The flared rudder also provides additional longitudinal trim capability during transition from the spacecraft to the aircraft flight mode.

The air-breathing engines (ABE's) are stowed in the fuselage during entry and deployed out of the top of the body for use during approach and landing.

Stability boundaries and control power limits are illustrated in Figure 4-128 for an elevon deflection range of -50 to +20 degrees. At the forward center-of-gravity position, the vehicle exhibits static and dynamic stability over the entire flight range except for static directional instability $C_{n_\beta} < 0$ at Mach number 0.9 and at Mach numbers greater than approximately 4.0.

In this section, the following areas are discussed:

1. Aerodynamic characteristics of the baseline orbiter during entry and post-entry flight phases.

2. Flying qualities of the basic airframe without stability augmentation.

3. Aerodynamic design studies in progress to improve flight characteristics of the baseline orbiter.

4. Approach and landing and ferry performance characteristics of the baseline 040A orbiter.

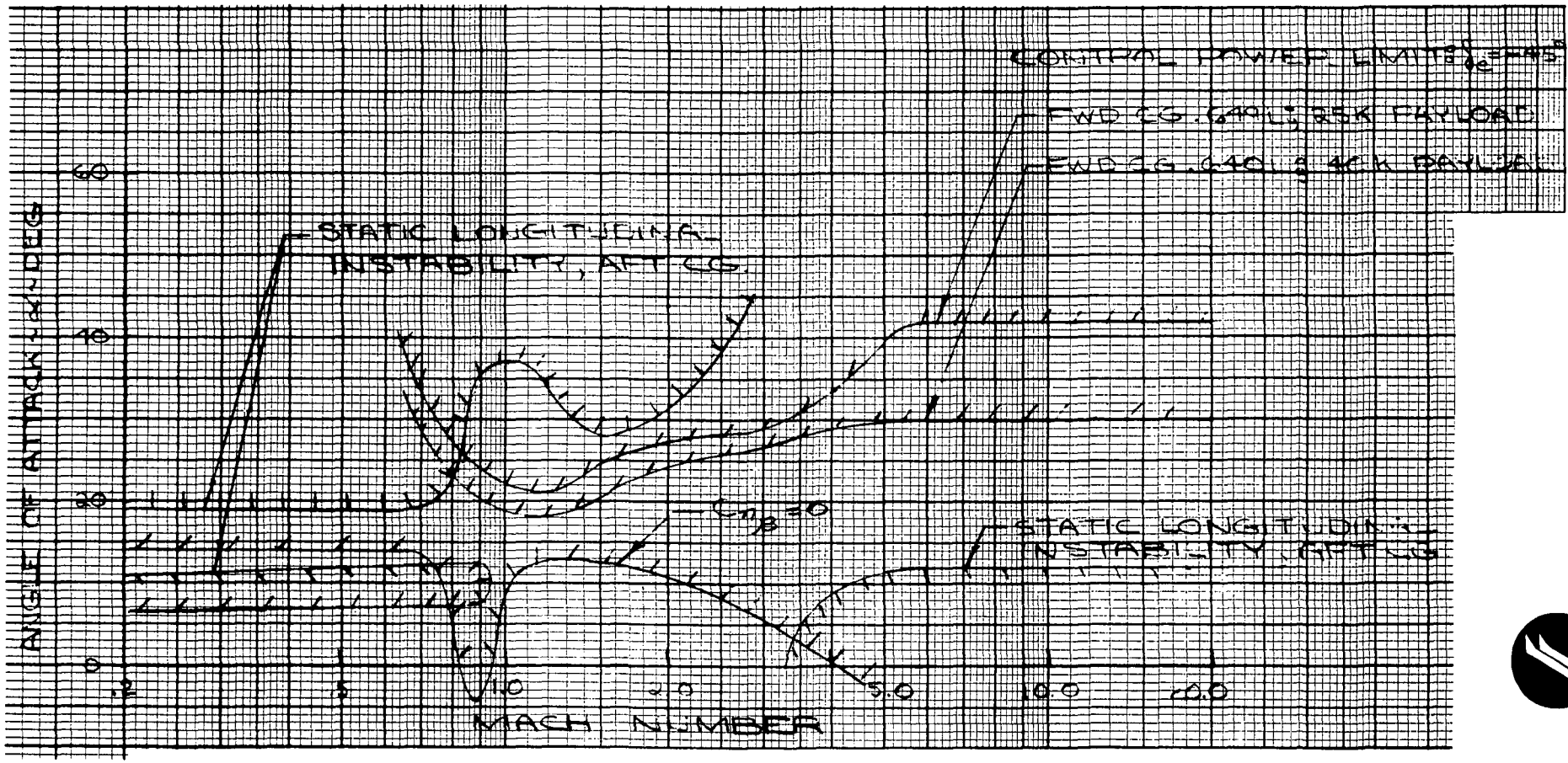

Figure 4-128. Stability Boundaries; Rudder Flared 40 Degrees, 040A

Entry Aerodynamics. The entry flight phase begins at the entry interface at an altitude of 400,000 feet and ends at Mach 3.0 where transition to low angle-of-attack flight is initiated. During entry, the orbiter is flown in the spacecraft flight mode, which is characterized by flight at essentially a constant angle of attack with the bank angle modulated to achieve the desired crossrange. Definition of the entry flight modes for the Mark I and Mark II orbiters is presented in Section 4.4.3.3. The modes differ in angle of attack, Mark II is flown at approximately 35 degrees to achieve the required crossrange, while Mark I is flown at a higher pitch attitude to minimize thermal design environment.

Estimated untrimmed hypersonic lift and drag (L/D) variation with Mach number and angle of attack is presented in Figures 4-129 and 4-130 and compared with Newtonian estimates. The Newtonian values are adjusted for friction ($C_{D_f} = 0.0090$) and correlated with experimental data to yield the estimates for Mach 20 and Mach 10. Viscous interaction effects reduce the maximum L/D to 2.02 at an altitude of 200,000 feet and Mach number of 20.0.

Hypersonic pitching moment characteristics are shown in Figure 4-131 for a range of elevon travel from -50 to +20 degrees and a center of gravity travel from 64.0 to 66.8-percent body length. These values correspond to preliminary estimates of the vehicle forward center of gravity with 40,000 pounds of payload centered in the cargo bay, and the aft location without payload. The vehicle exhibits static longitudinal stability at both the forward and aft center-of-gravity limits over the angle-of-attack range from 60 to 10 degrees. Trim angle-of-attack limits as a function of center-of-gravity location are shown in Figure 4-132. For the forward center of gravity location, the maximum trim angle of attack is 30 degrees. Positive (downward) elevon deflections are not required over the predicted center-of-gravity range for either Mark I or Mark II entry trajectories.

Lateral-directional data are displayed in Figure 4-133 at a nominal center-of-gravity position of 66-percent body length. The vehicle exhibits an unstable static directional stability derivative (C_{n_β}) of -0.0015 per degree at zero-degree angle of attack and -0.0022 at 60-degree angle of attack (body axis). The variation with angle of attack is essentially linear. The lateral stability derivative, C_{ℓ_β}, has a magnitude of -0.0002 per degree at zero-degree angle of attack and -0.0012 at 60-degree angle of attack. Like the directional stability derivative, the variation of C_{ℓ_β} with angle of attack is essentially linear. The dynamic derivative

$$C_{n_{\beta\,dyn}} = (C_{n_\beta}) \cos\alpha - \frac{Iz}{Ix} C_{\ell_\beta} \sin\alpha$$

has a magnitude of +0.00785 at 60-degree angle of attack. At 30-degree angle of attack, C_{n_β} dynamic has a magnitude of +0.00119, indicating marginal dutch roll characteristics at this angle of attack.

An improvement in hypersonic directional stability may be realized by decreasing the destabilizing input from the fuselage forebody. This can be accomplished by changing the 040A outward sloping sides to inward sloping sides. It is estimated that C_{n_β} dynamic can be increased to +0.00204 at 30-degree angle of attack and +0.00855 at 60-degree angle of attack by this method.

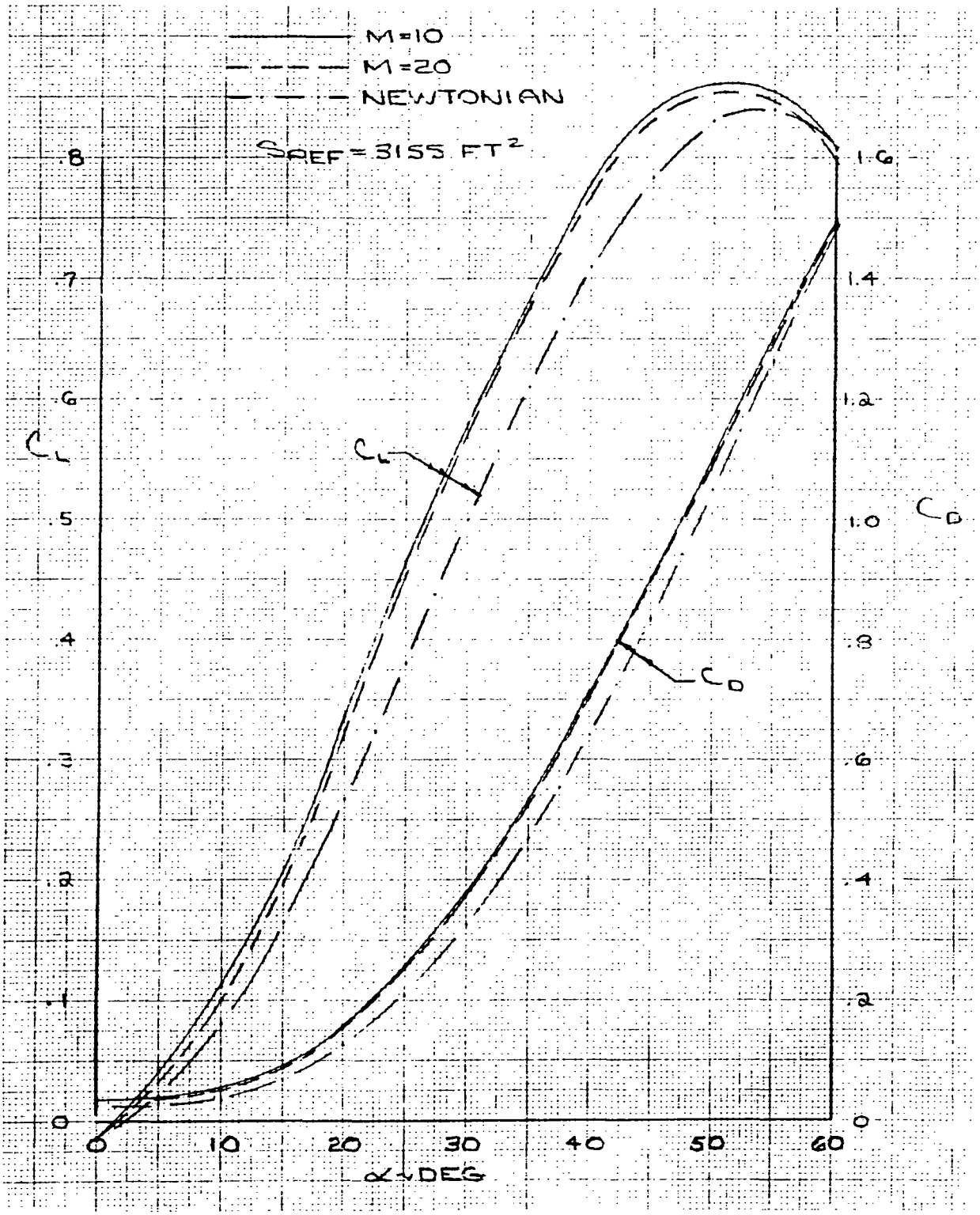

Figure 4-129. Hypersonic Lift and Drag Characteristics, 040A

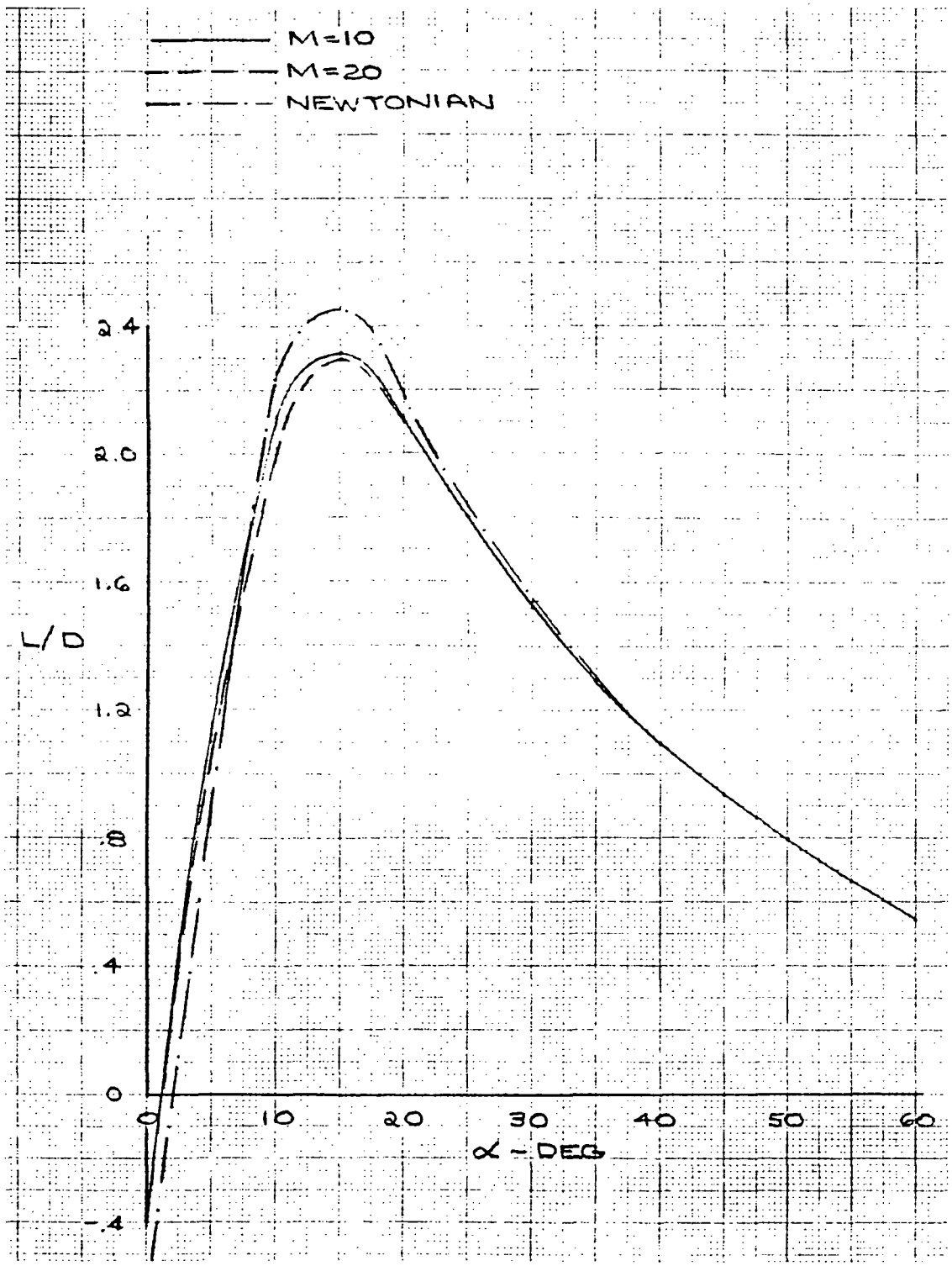

Figure 4-130. Hypersonic Lift-to-Drag Ratio, 040A

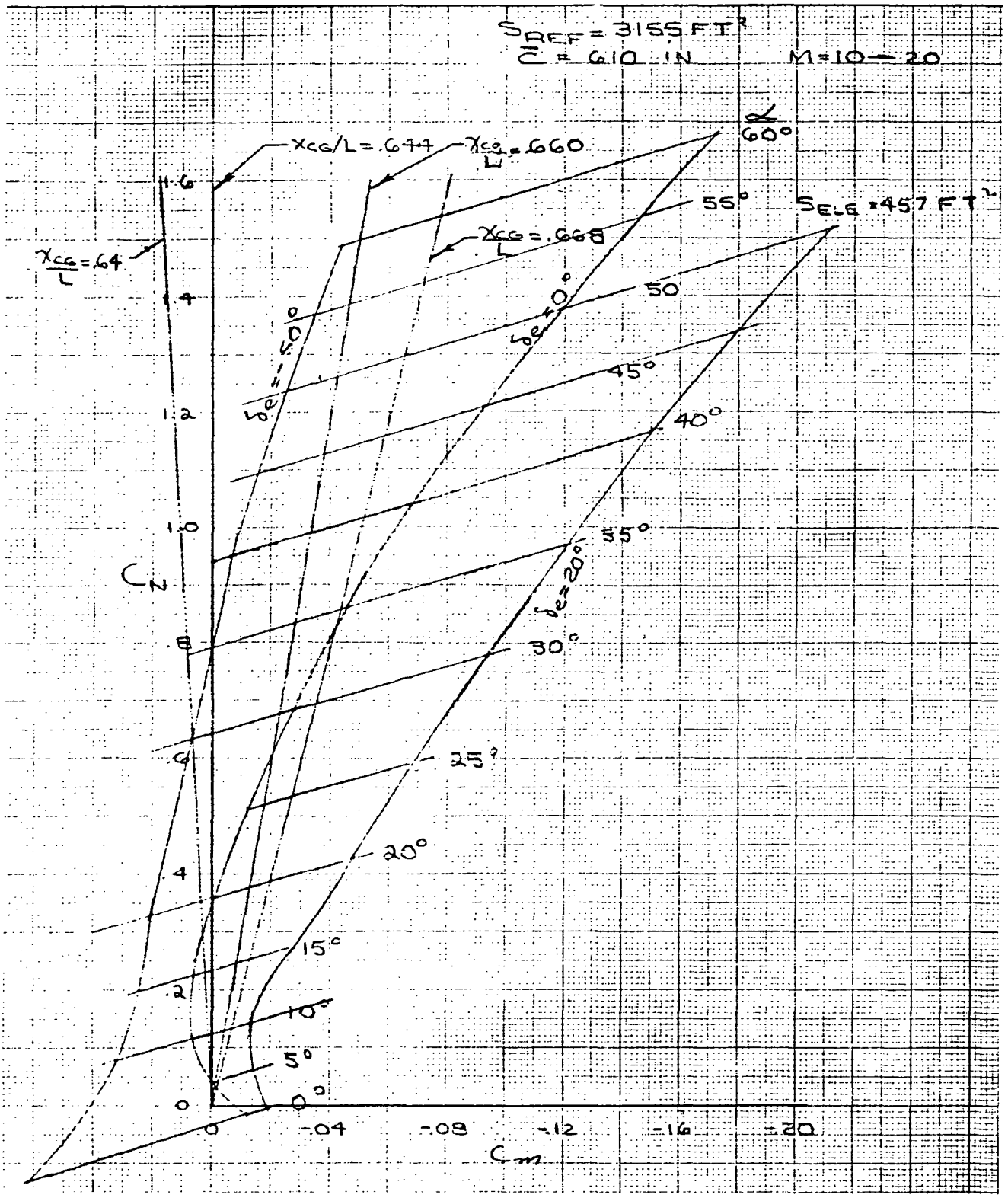

Figure 4-131. Hypersonic Pitching Moment Characteristics, 040A

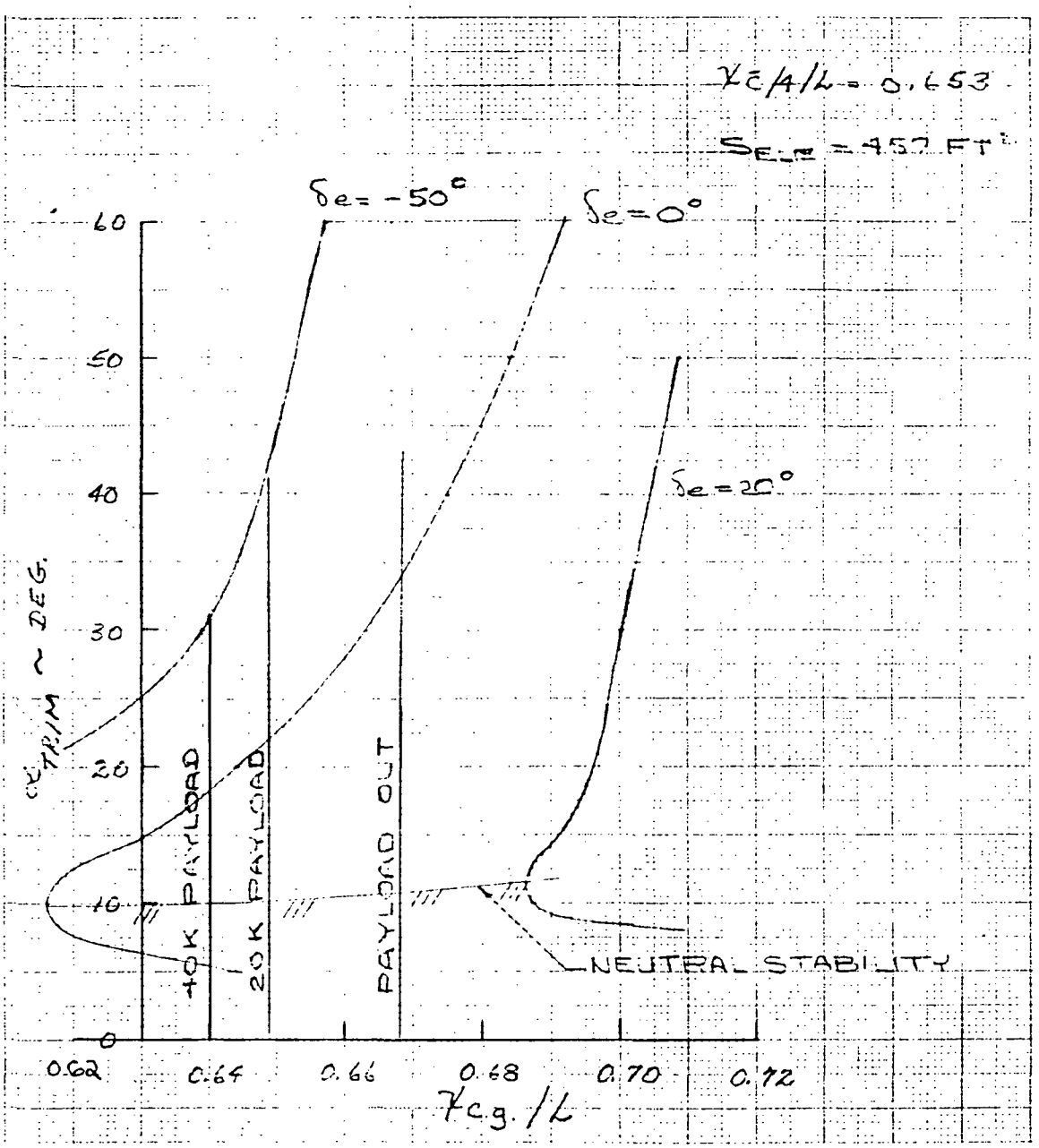

Figure 4-132. Hypersonic Trim Diagram, 040A

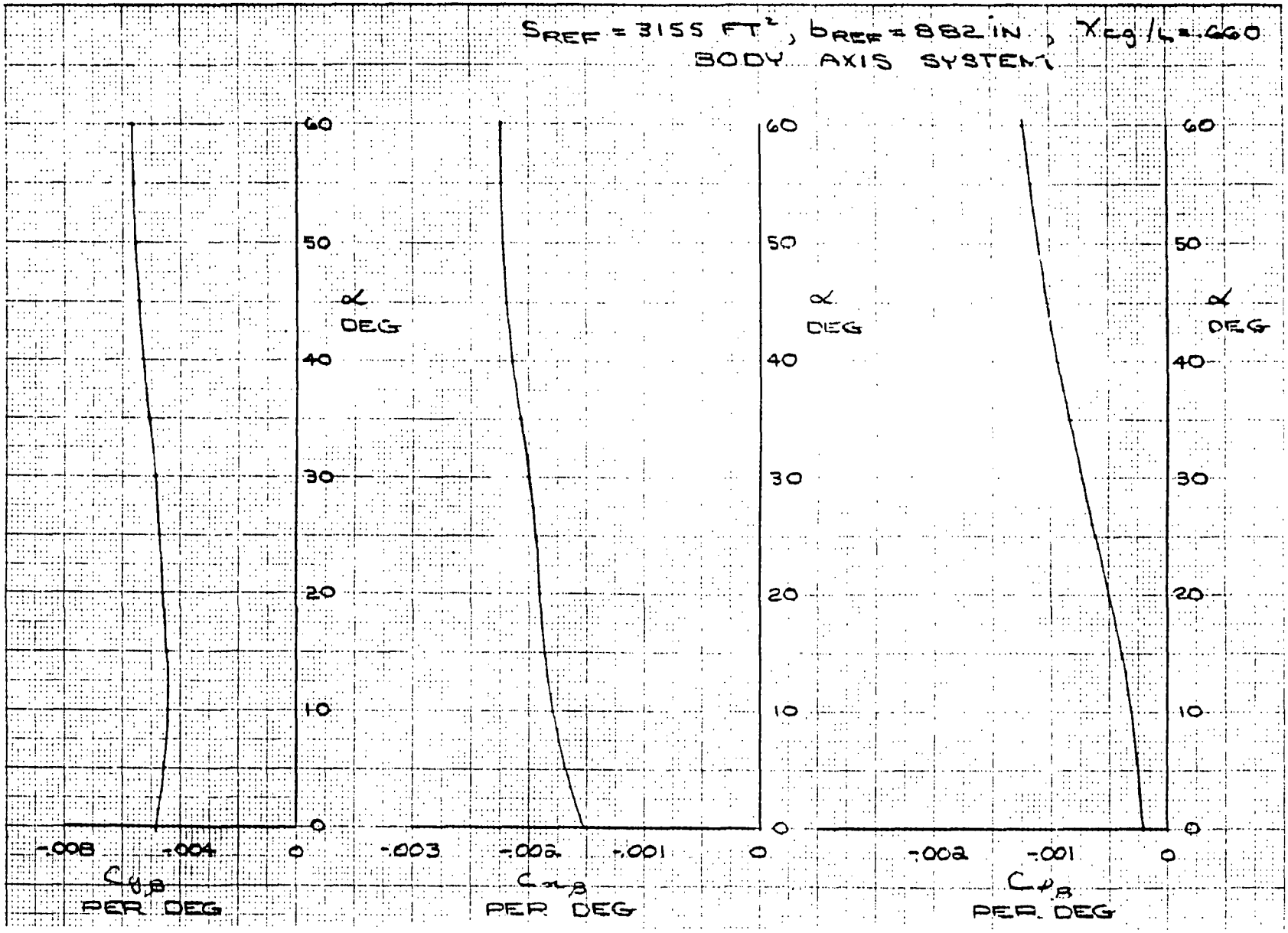

Figure 4-133. Newtonian Lateral-Directional Characteristics, 040A

Post-Entry Aerodynamics. The aircraft flight mode begins at Mach 3.0 with initiation of transition from the entry angle of attack to glide near maximum lift-to-drag ratio. Estimated aerodynamic characteristics for this flight phase were based on NR and MSFC S-065 test results over the speed range from Mach 4.96 to Mach 0.26.

Low-Speed Aerodynamics. Low-speed results are presented for a Mach number of 0.26 and are based on the MSFC and NAAL 660 wind tunnel data. Figure 4-134 presents the lift and pitching moment characteristics for a nominal center-of-gravity position (25,000-pound payload) of 64.9 percent body length (L = 1315 inches). For this center-of-gravity location, the vehicle is essentially neutrally stable in pitch for angles of attack between 6 and 9 degrees. Elevon effectiveness is presented in Figure 4-135. The elevon required to trim to the nominal center of gravity is approximately 4 degrees, trailing edge up. The trimmed C_L at 17-degree angle of attack is 0.60 for the nominal center of gravity. It should be noted that the vehicle is statically unstable for angles of attack between 6 to 9 degrees for elevon deflections between +5 and -20 degrees. The instability occurs in the operating region for approach and landing, and for cruise at maximum lift to drag ratio. The decrease in stability at these conditions is not serious; however the change in trim associated with the change in stability will increase the pilots work load during the critical approach and landing maneuver, and should be eliminated. The instability is associated with early wing tip stall due to the influence of the ACPS pods. Redesign or relocation of the pods will be investigated.

The untrimmed drag polar is presented in Figure 4-136, and the lift-to-drag ratio is shown in Figure 4-137. Also presented in Figure 4-137 is the longitudinal center of pressure expressed in terms of the body length. Landing gear drag coefficient as a function of angle of attack is shown in Figure 4-138. The effect of the split rudder glide brakes on drag lift and moment is displayed in Figure 4-139 for various glide brake deflections and angles of attack.

Low-speed lateral-directional stability characteristics are displayed in Figure 4-140. The vehicle displays positive dihedral effect up to 27-degree angle of attack. The vehicle is directionally unstable at angles of attack above 17 degrees. Increased vertical tail size (485 square feet) would extend the stable region to above 17 degrees, thus allowing a stable margin for landing at the maximum tail-down angle of 17 degrees. Rudder effectiveness and roll/yaw coupling are shown in Figure 4-141. The rudder yawing and rolling moment derivatives are adequate for coordinated turns. The data show proverse yaw due to roll, which is in a direction for favorable handling qualities. Elevon effectiveness in roll is shown in Figure 4-142. The roll control available should be adequate to meet Level I Category C flying qualities

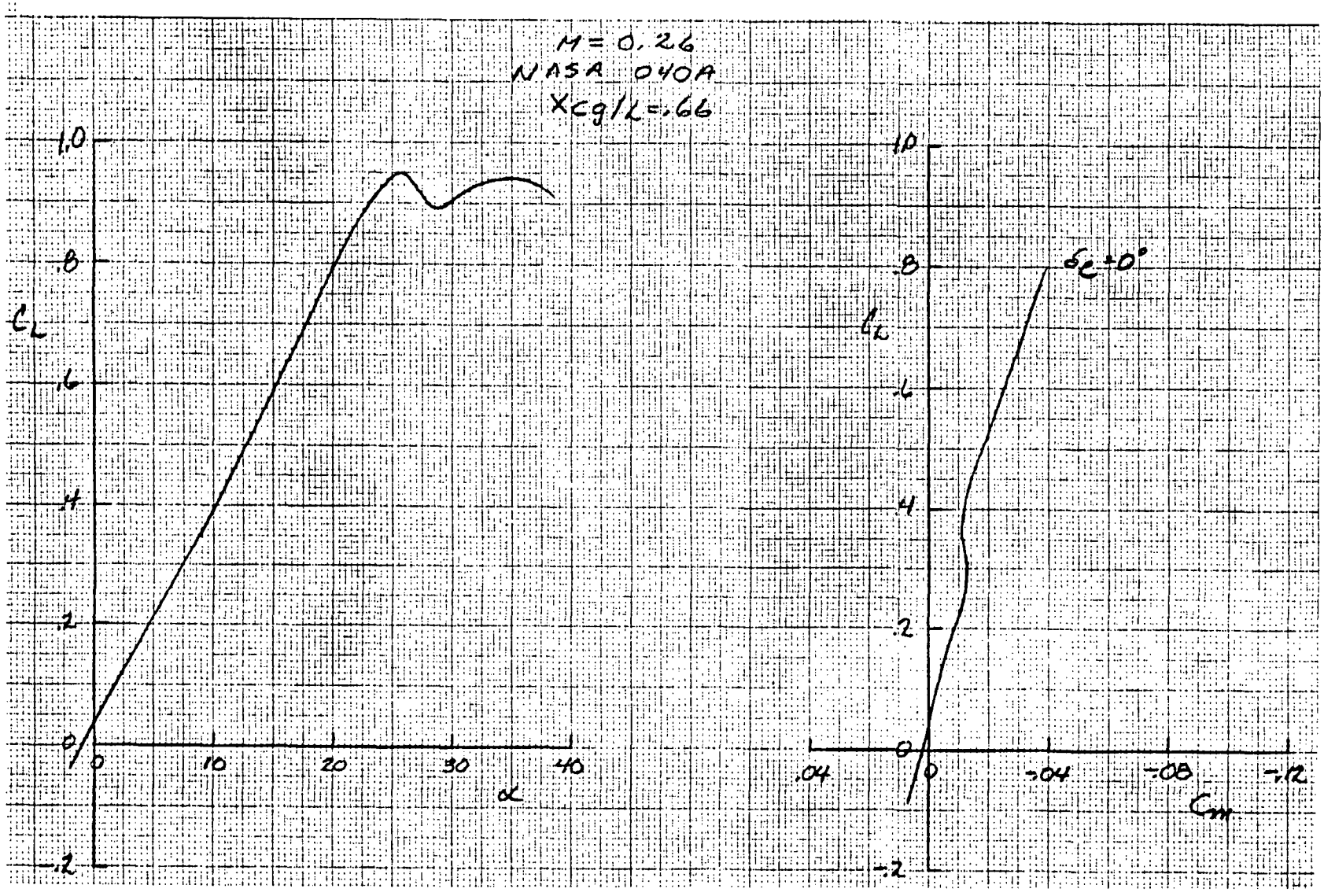

Figure 4-134. Low-Speed Lift and Pitching Moment Characteristics

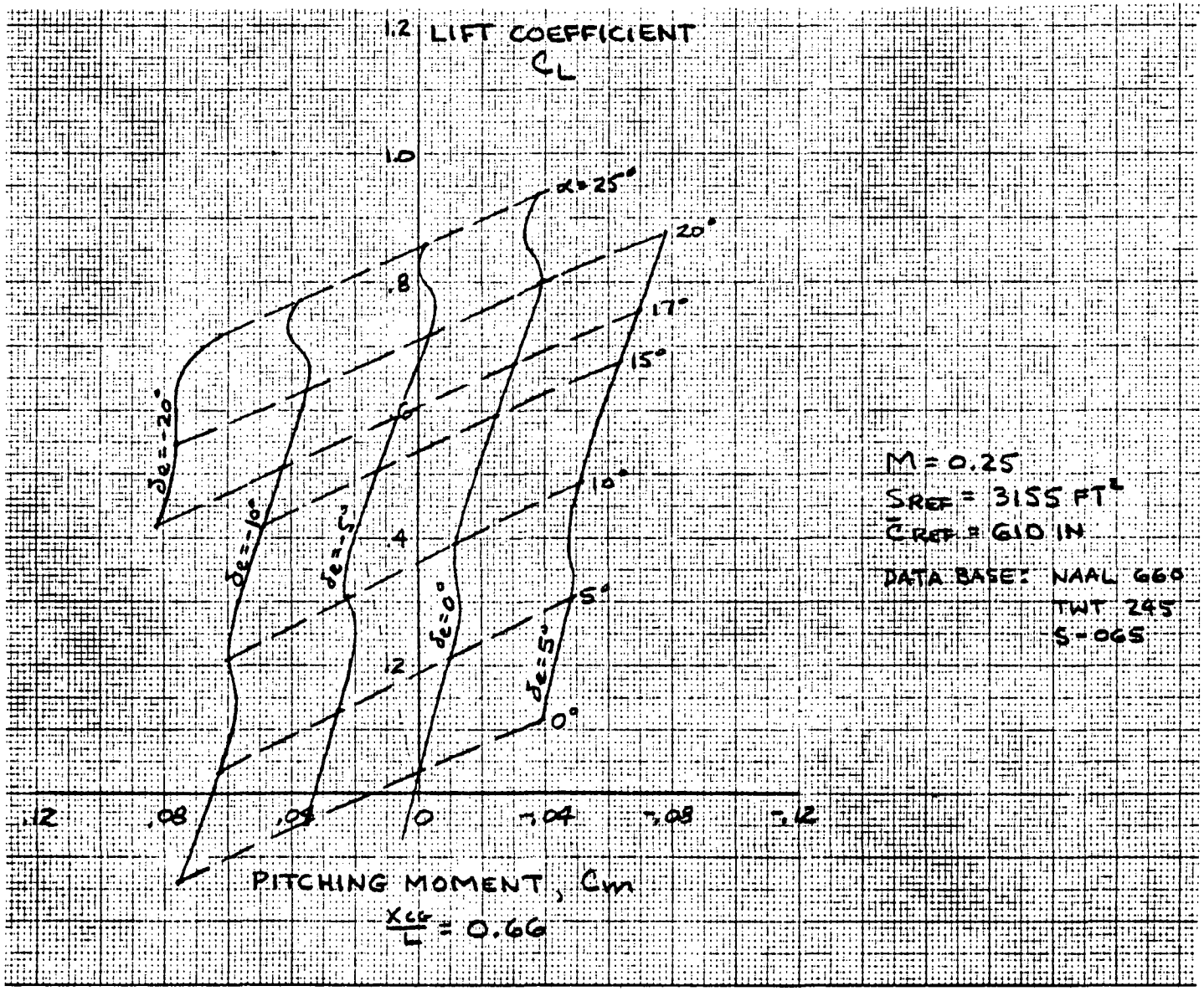

Figure 4-135. Low-Speed Elevon Effectiveness in Pitch, 040A

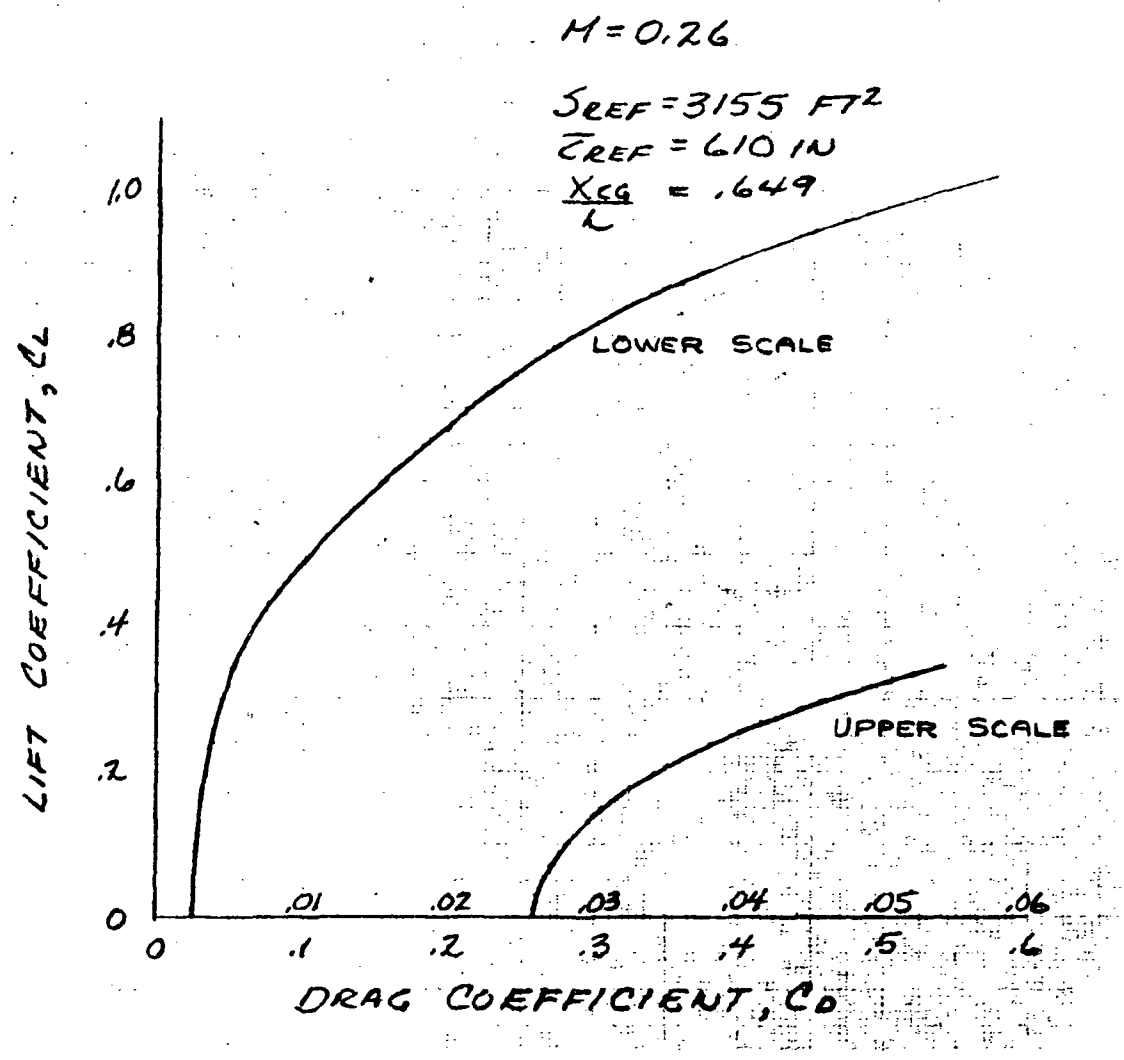

Figure 4-136. 040A Untrimmed Drag Polar

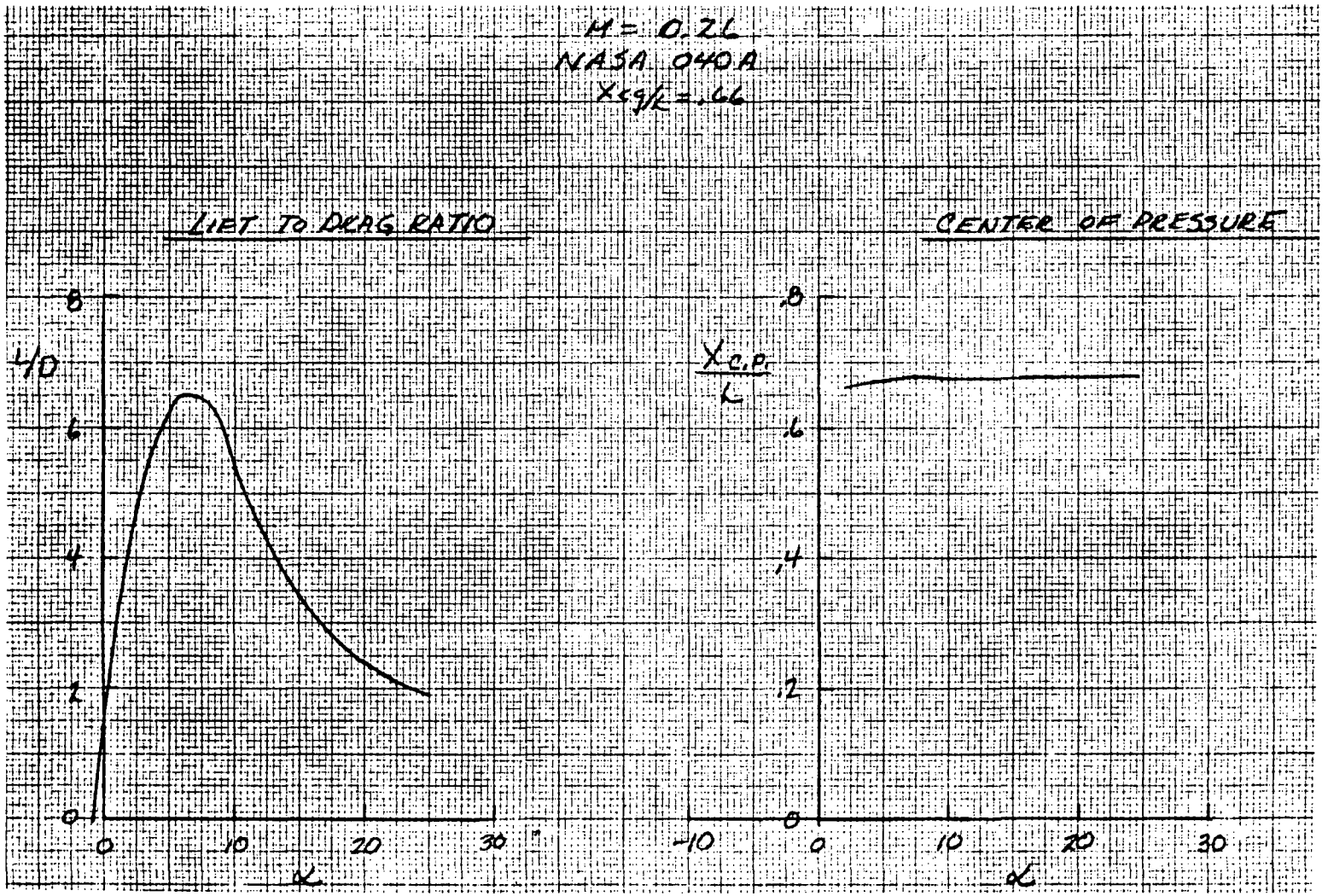

Figure 4-137. Low-Speed Lift-to-Drag Ratio and Center of Pressure

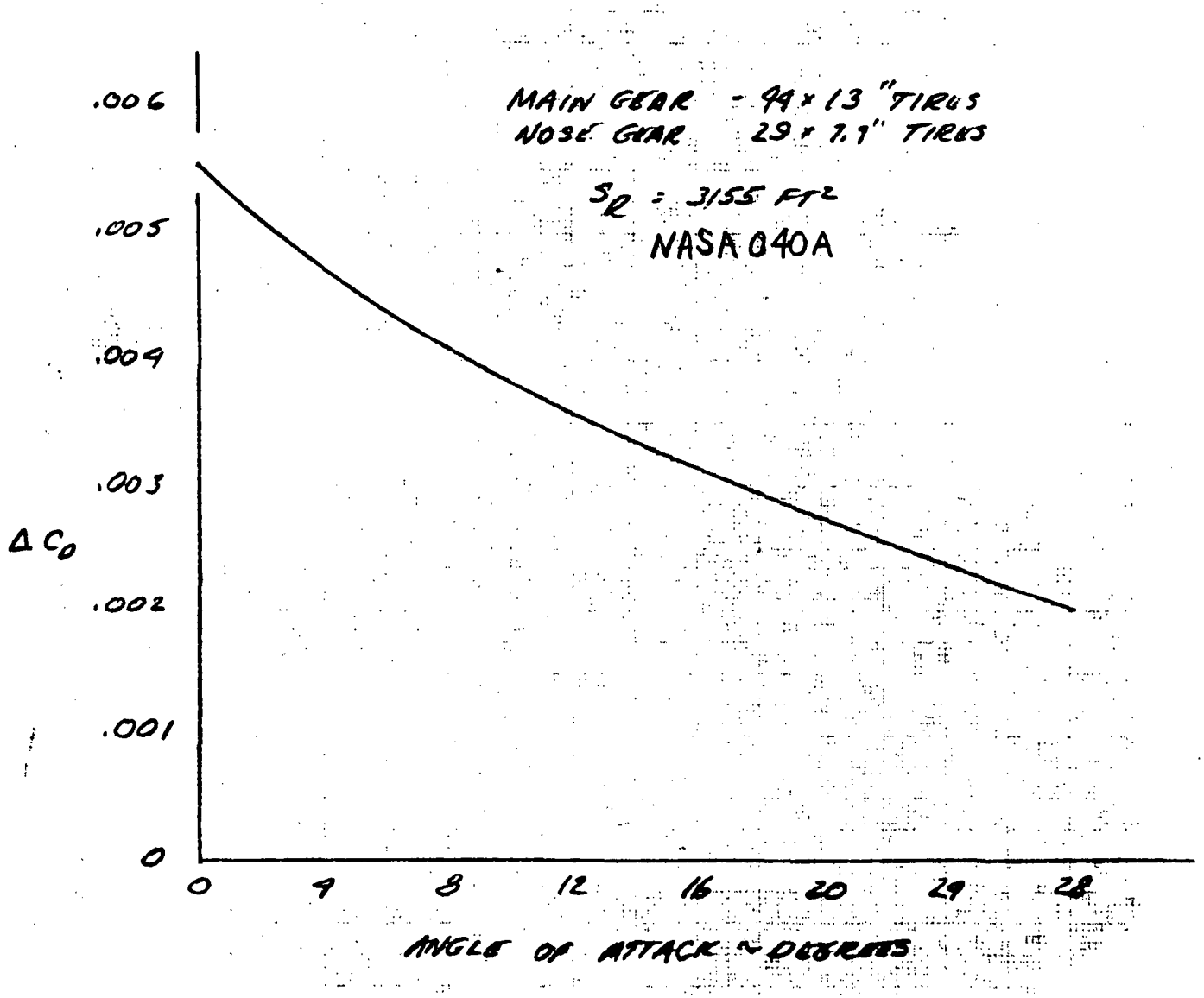

Figure 4-138. Landing Gear Drag Coefficient

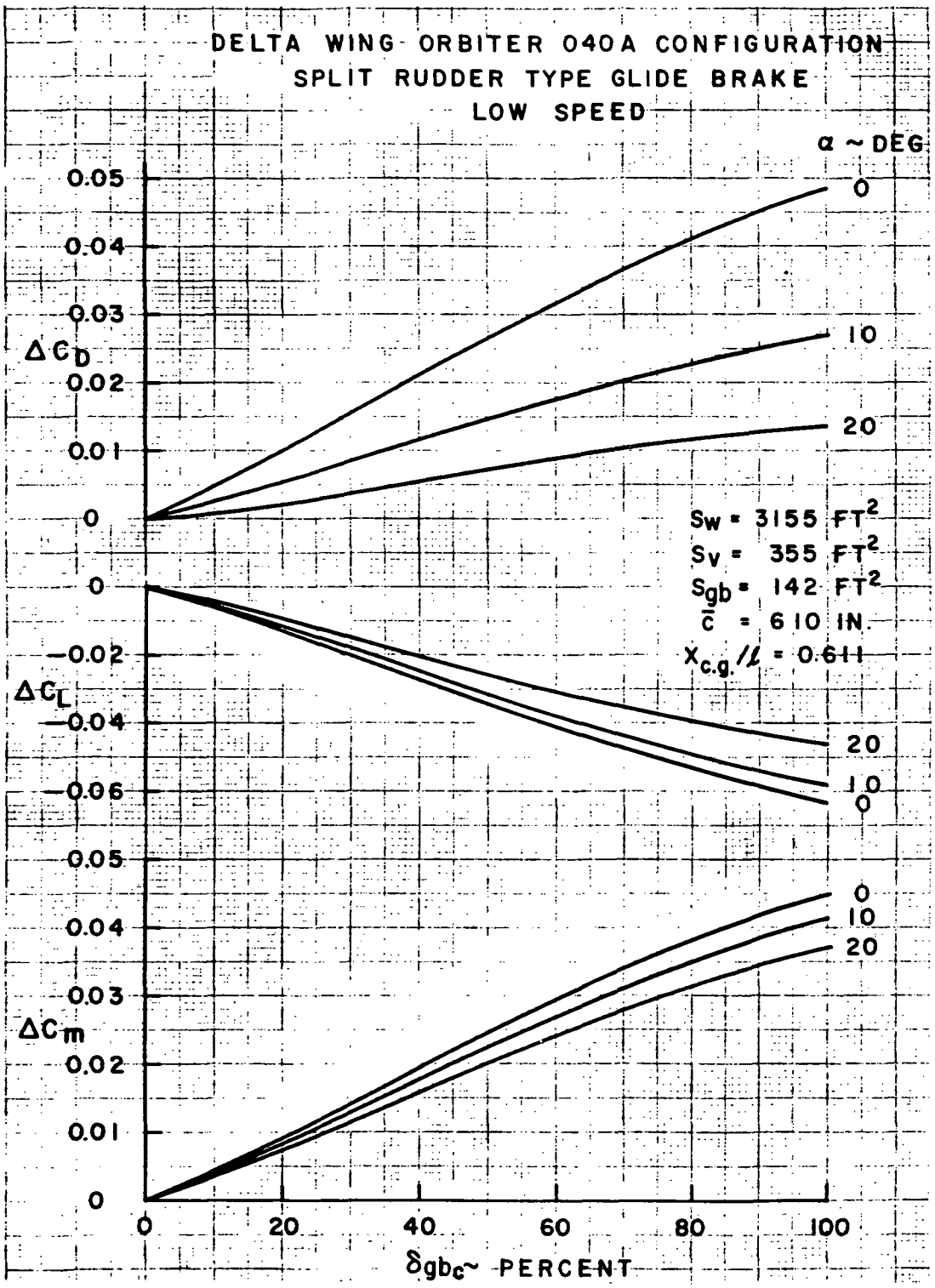

Figure 4-139. Low-Speed Glide Brake Effect on Drag, Lift, and Pitching Moment

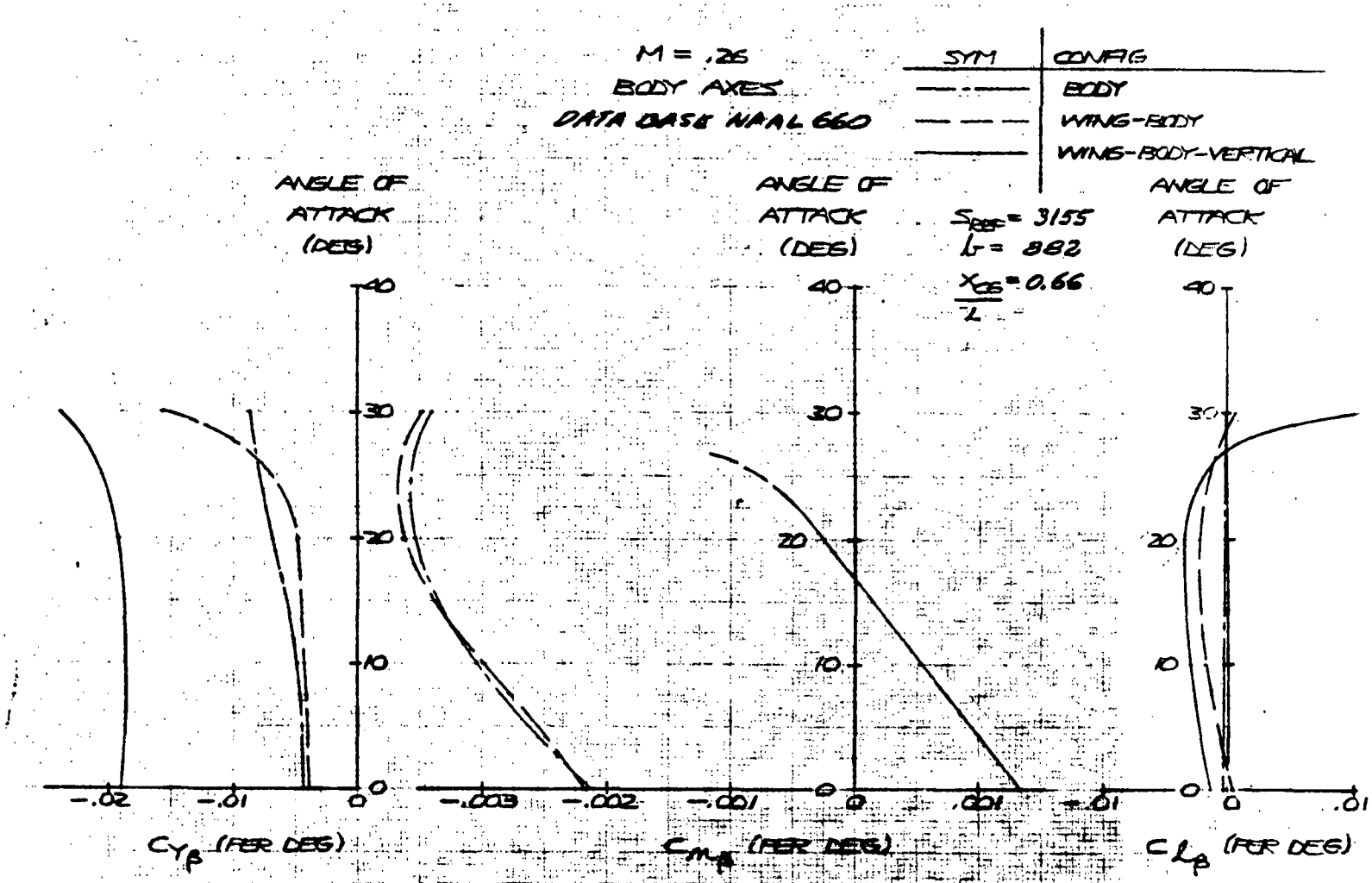

Figure 4-140. Low-Speed Lateral-Directional Stability, 040A

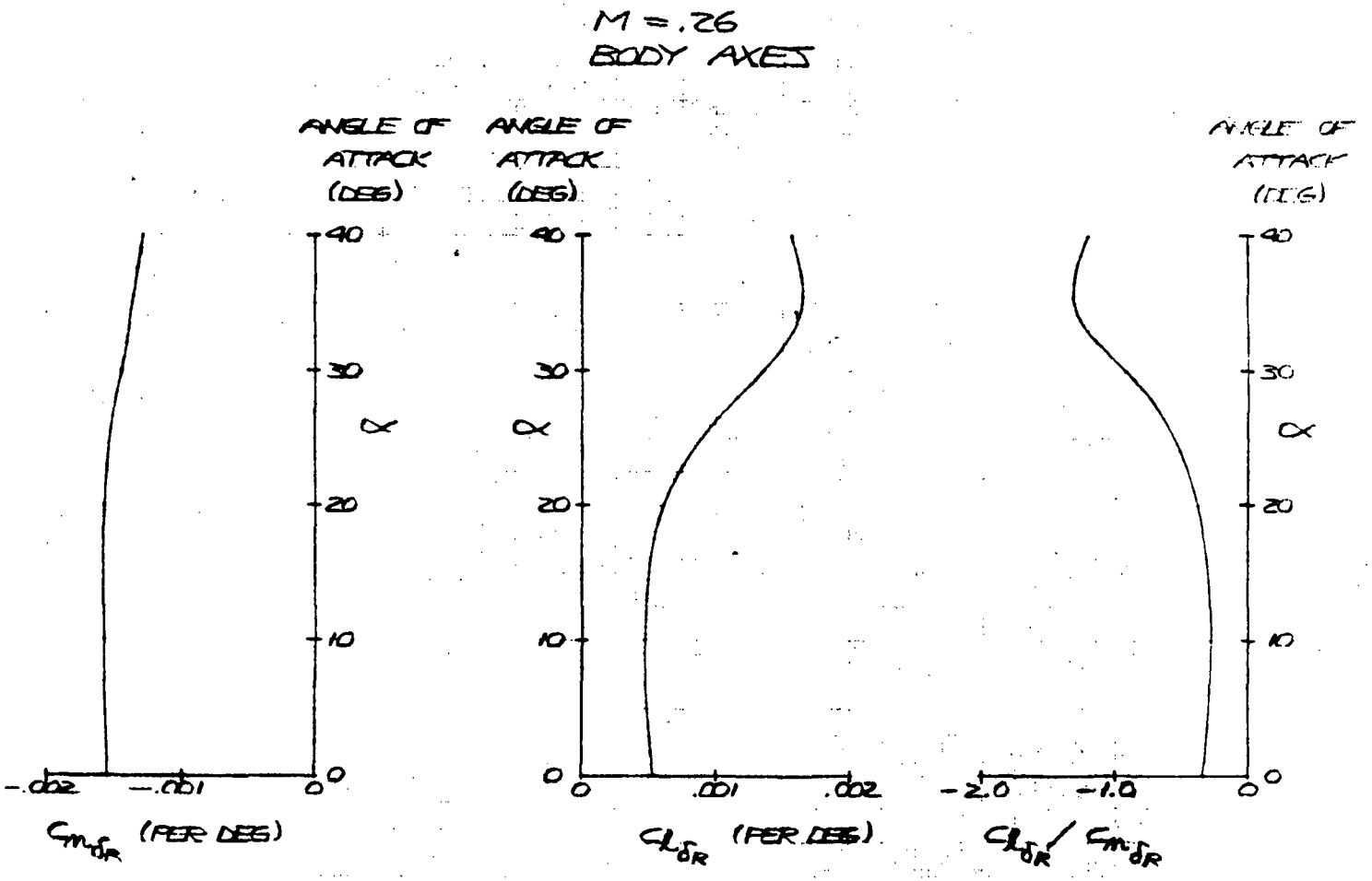

Figure 4-141. Rudder Effectiveness and Coupling, 040A

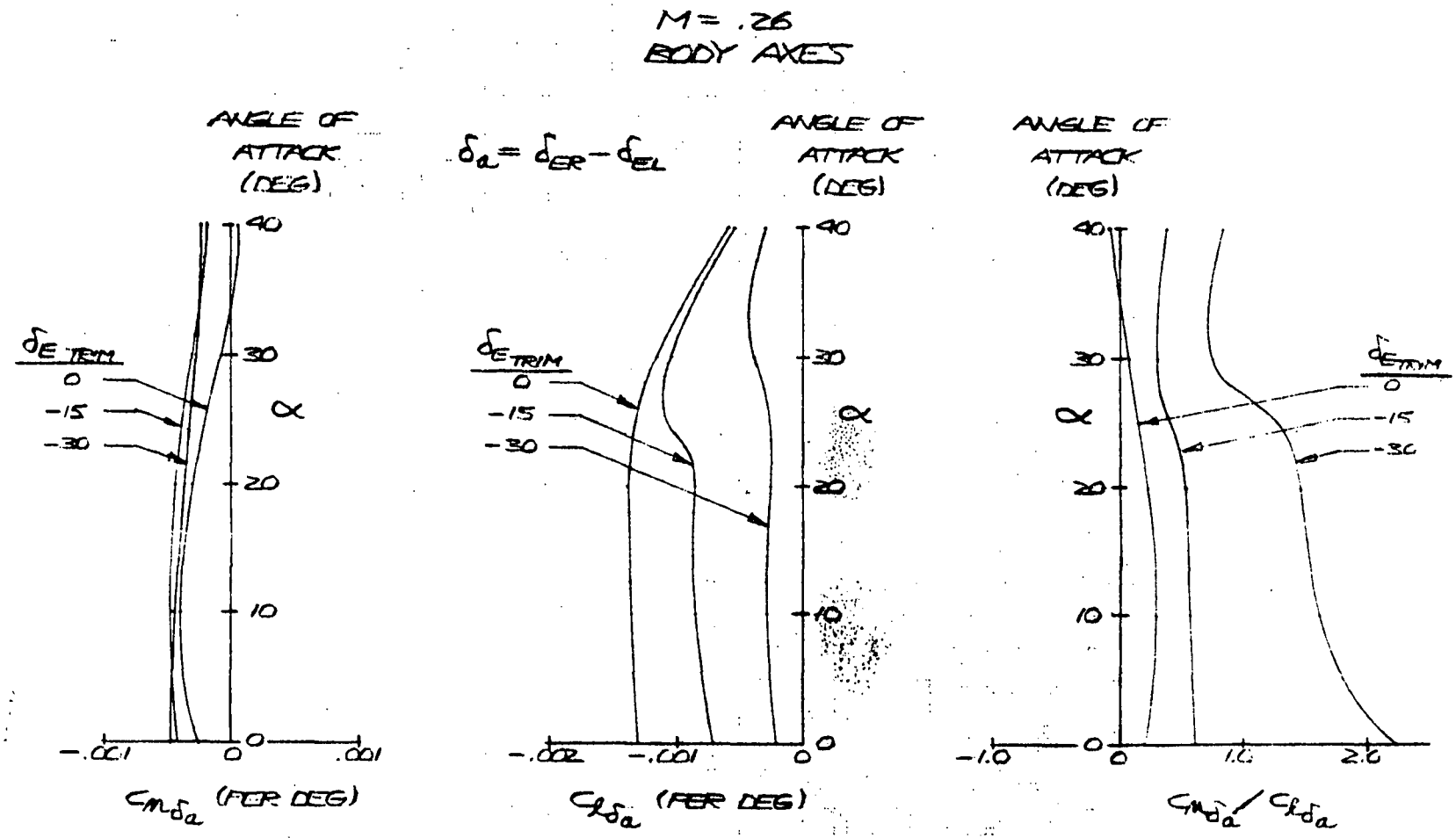

Figure 4-142. Aileron Effectiveness and Coupling, 040A

requirements. The vehicle is seen to have stable proverse roll-yaw characteristics in that a positive rolling moment is accompanied by a positive yawing moment.

Transonic and Supersonic Aerodynamics. Aerodynamic characteristics are presented for Mach numbers of 0.6, 0.9, 1.2, 1.5, 2.5, and 3.3 based on test data from the NR TWT 245 and S-065 wind tunnel tests. Figure 4-143 presents lift and pitch stability characteristics for Mach numbers from 0.6 to 3.5. The pitching moment data show a region of essentially neutral stability for an angle of attack range of 7 to 14 degrees for Mach 0.6 and Mach 0.9. The change in stability is attributed to flow separation at the wing tip due to the ACPS pods. It is noted from the lift curves that the decrease in stability is not accompanied by a corresponding decrease in lift. Thus, the change in stability is due to a forward shift in the center of pressure followed by an aft shift of similar magnitude while the magnitude of the total lift remains unchanged. Redesign or relocation of the ACPS pods would eliminate the change in stability. Longitudinal center of pressure is presented in Figure 4-144 (at 10- and 20-degree angles of attack) as a function of Mach number and angle of attack for the complete body-wing vertical configuration. These data show that center-of-gravity positions aft of 68-percent body length may result in longitudinal instability at subsonic speeds. At hypersonic speeds, neutral stability will occur in the vicinity of the angle of attack for maximum lift/drag ratio (approximately 15 degrees). Figure 4-145 presents the longitudinal pitching moment characteristics for Mach numbers of 0.6 and 1.2 for various elevon deflections. The elevons are seen to afford adequate longitudinal control at subsonic and transonic Mach numbers. The data show that the change in stability due to the ACPS pods is not present at Mach 1.2, which supports the contention that the observed instability is due to the ACPS pods interfering with the subsonic wing vortex.

The lateral-directional stability characteristics for the 040A configuration are presented in Figure 4-146. The vehicle has positive dihedral effect throughout most of angle-of-attack and Mach range presented. The vehicle is directionally unstable at Mach 3.3 and is unstable for angles of attack greater than 10 degrees at M = 1.5 and 14 degrees at M = 0.6. A significant portion of this instability is due to the bubble-type canopy as shown on Figure 4-147. The 040A configuration with the canopy bubble removed is directionally stable at α = 10 degrees throughout the Mach range presented, except at Mach 0.90.

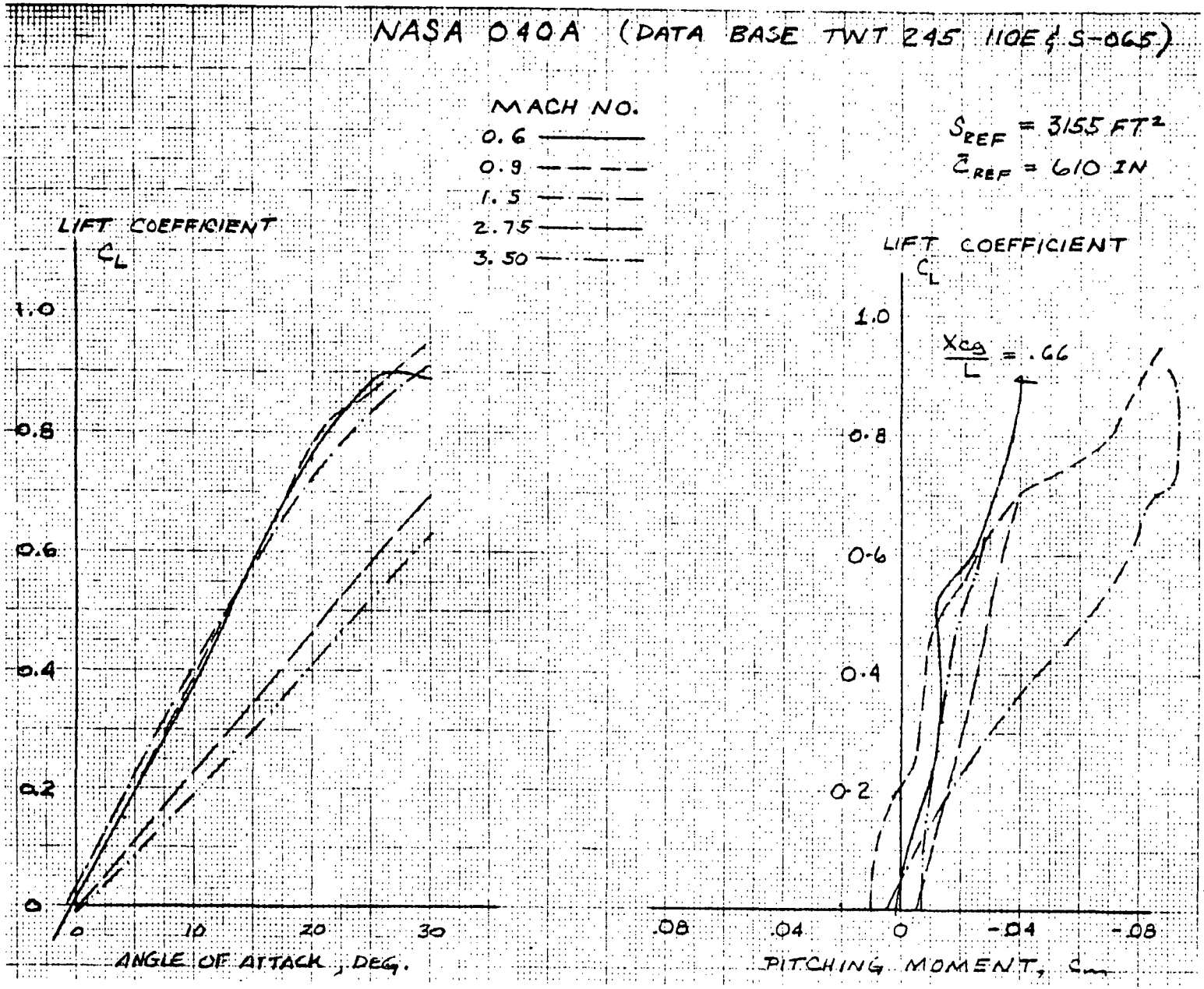

Figure 4-143. Lift and Pitch Stability Characteristics

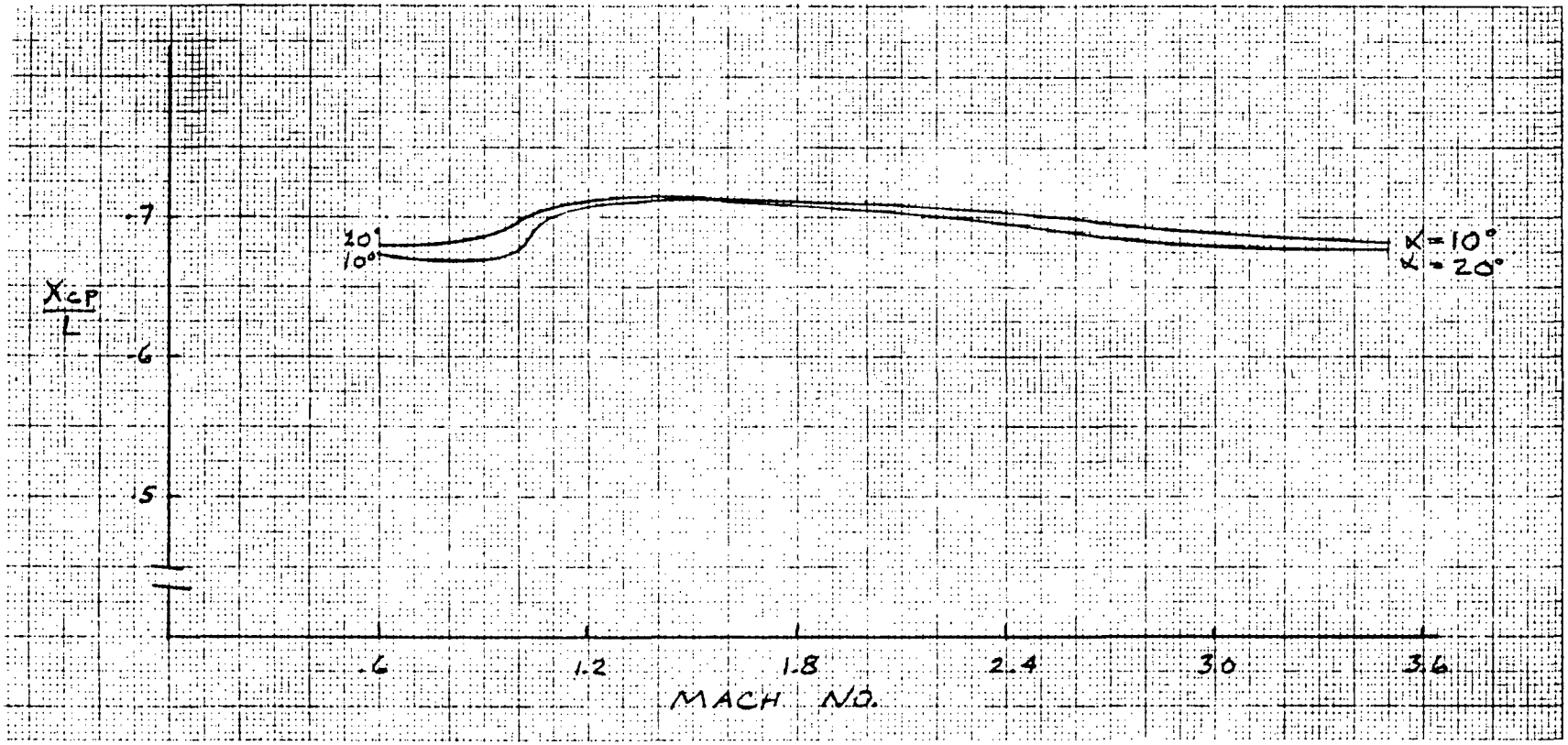

Figure 4-144. X_{cp} (Percent Body Length) as a Function of Mach Number, 040A

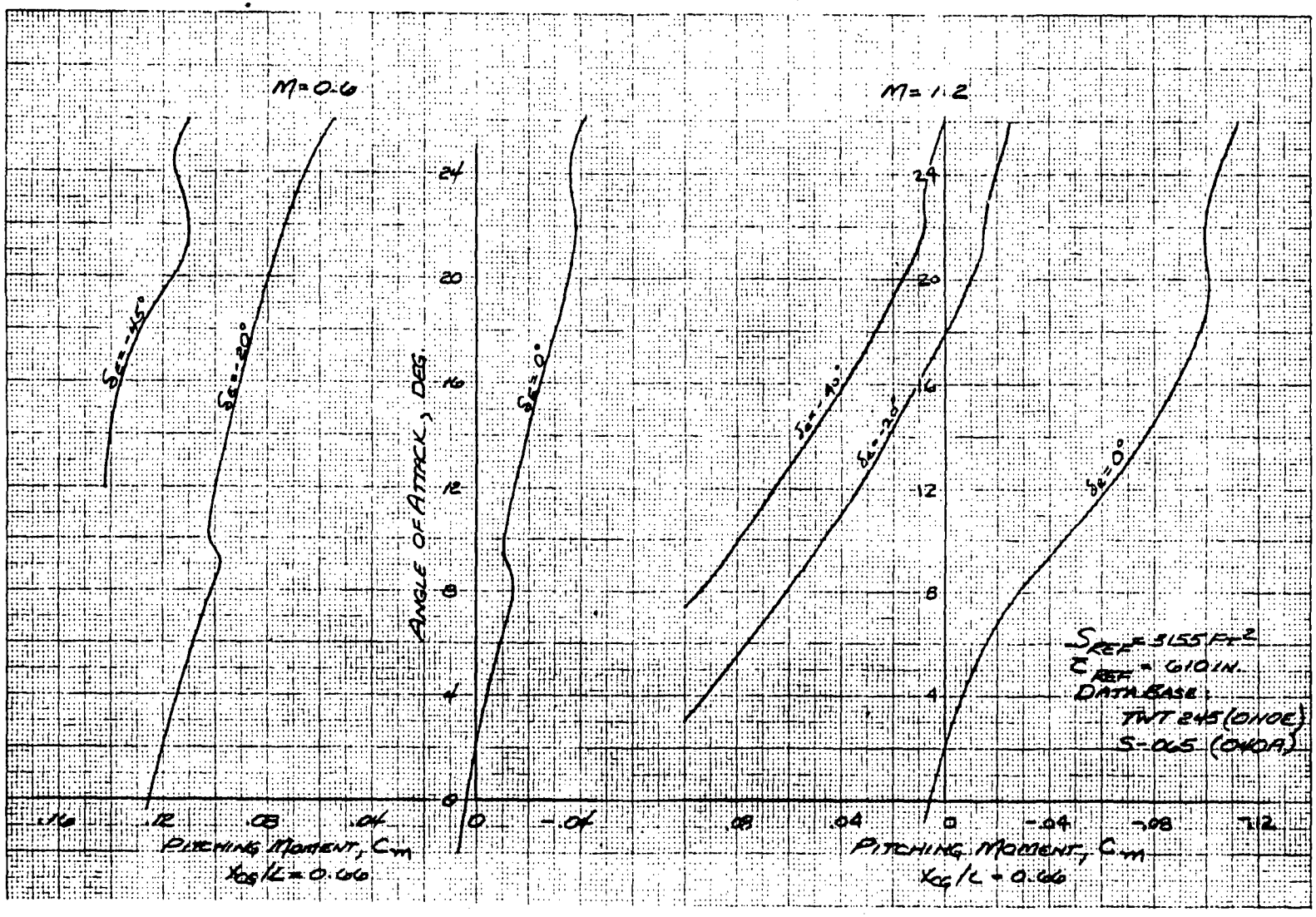

Figure 4-145. Longitudinal Pitching Moment Characteristics, 040A

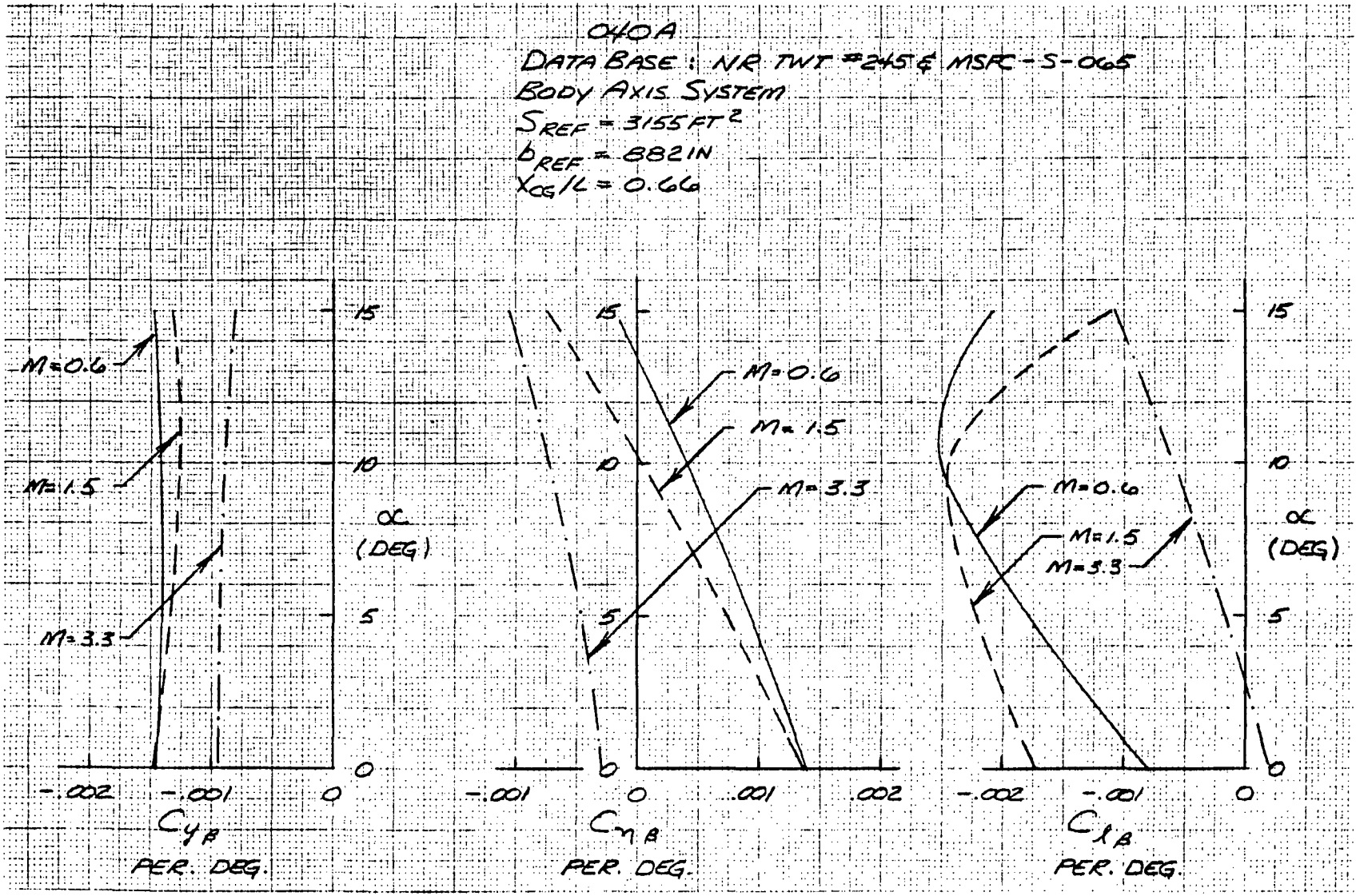

Figure 4-146. Lateral-Directional Stability Characteristics

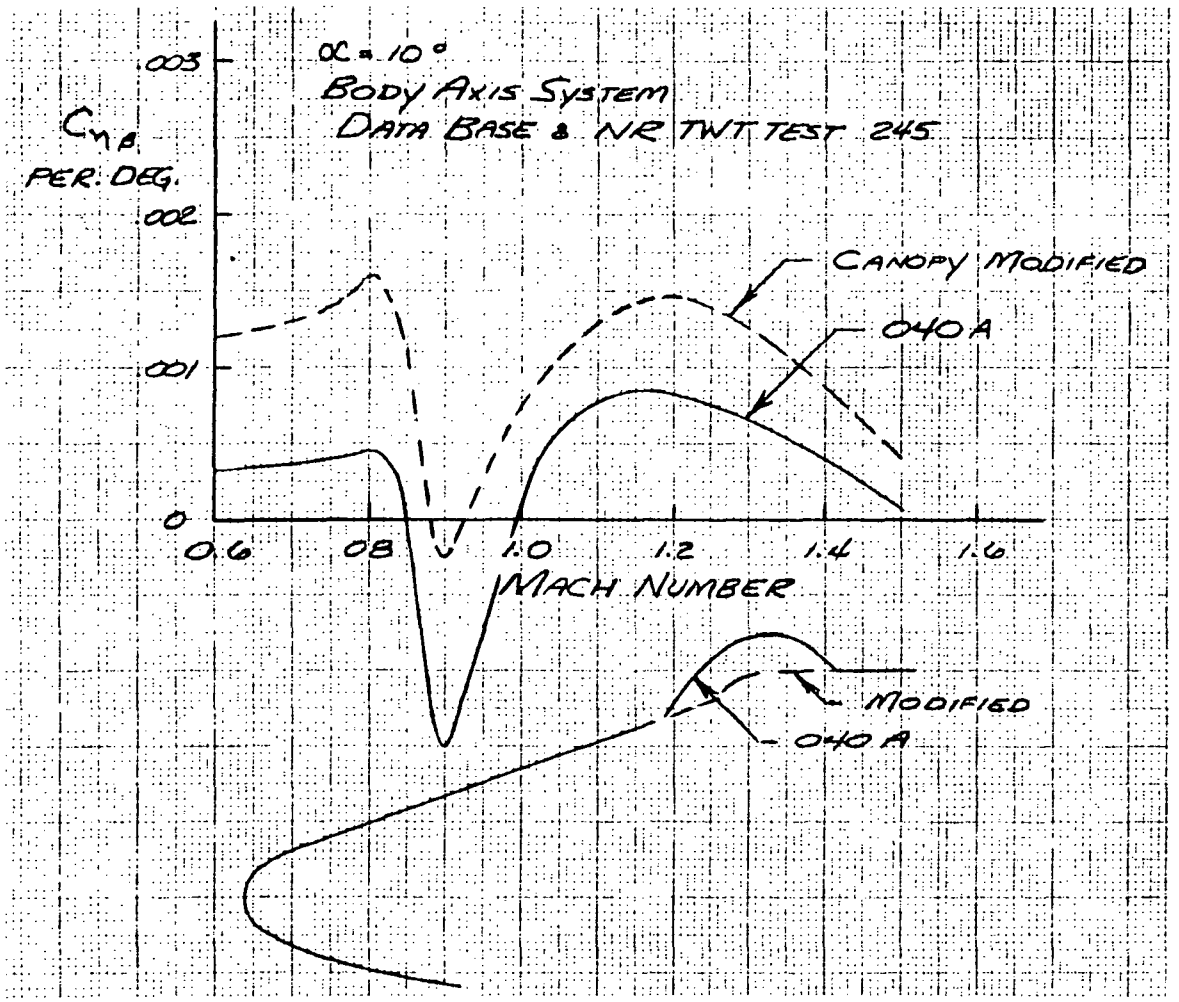

Figure 4-147. Effect of Canopy Shape on Static Directional Stability

The effect of rudder flare on the directional characteristics is presented on Figure 4-148. The flared rudder can be used as a glide brake or as a directional stability augmentor at higher Mach numbers. At Mach = 1.5, the rudder flare increases the directional stability; at lower Mach numbers (M = 0.6 and 1.2) it decreases the directional stability. The decrease in stability at lower Mach numbers is due to separation on the vertical tail. At low supersonic Mach numbers, the flared rudder will propagate disturbances forward through the locally subsonic flow and separate the flow on the vertical tail. At those Mach numbers where the flow is locally supersonic, the flow will not separate and the increased effectiveness of the flared rudder will be realized. The loss in vertical tail effectiveness can be minimized by selecting tail thickness ratios on the order of 8 percent.

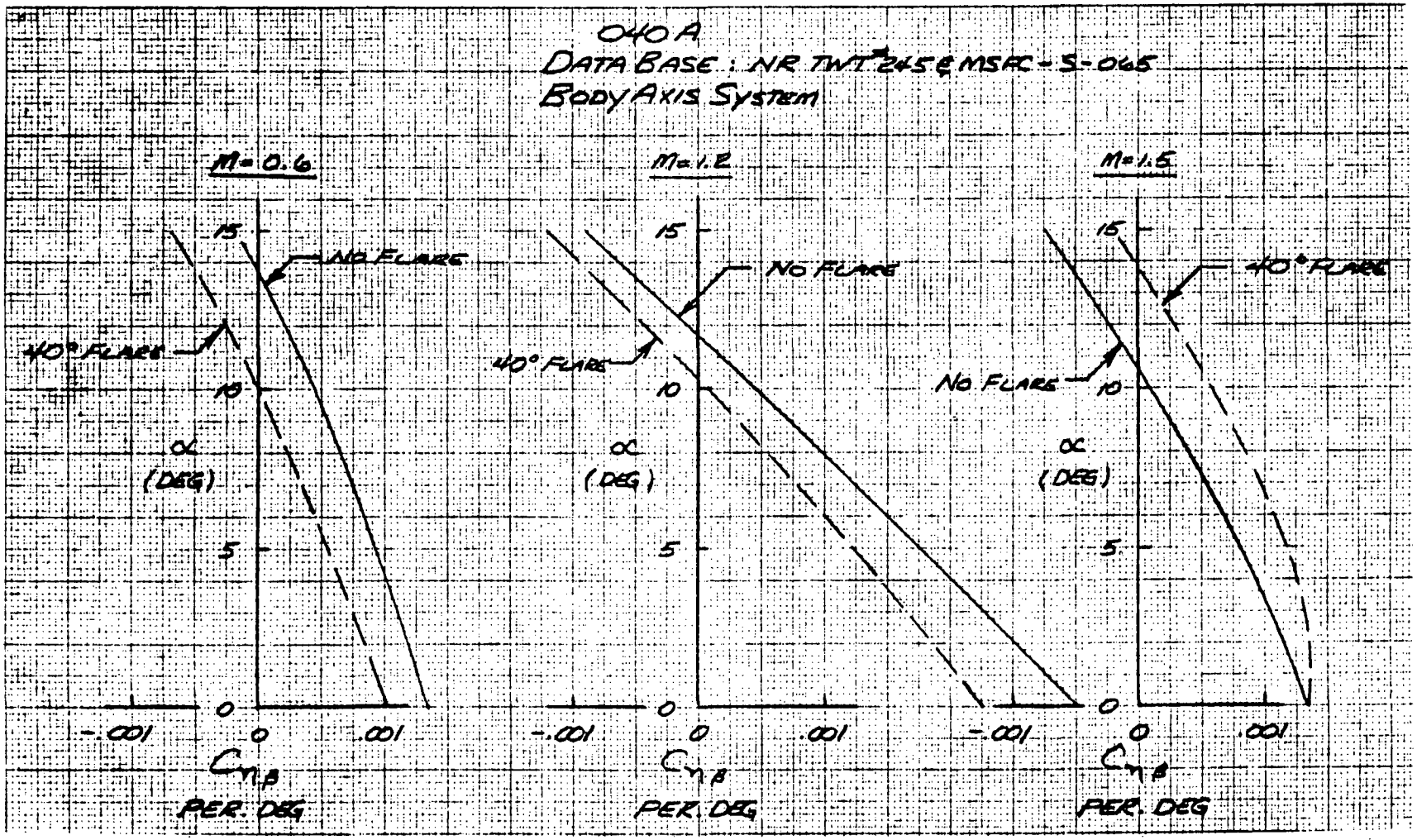

Figure 4-148. Effect of Rudder Flare on Directional Characteristics, 040A

Flying Qualities. Previous analyses of delta wing orbiters indicated marginal-to-poor longitudinal handling qualities during approach and landing without stability augmentation. This characteristic is a consequence of low subsonic static margins resulting from optimizations centered around other conditions (hypersonic control power, thermal considerations, etc.). During the period that these optimizations were performed, the formal guideline (TD 2518) concerning unaugmented handling qualities specified only that short-period longitudinal and lateral modes should not exhibit an unstable divergence.

In an effort to minimize dependency on the autopilot during critical flight phases, a study was initiated to explore means of improving unaugmented flying qualities. The goal of the study is to provide Cooper-Harper (C-H) ratings of about 5 or better. Meeting this goal will require a significant improvement in longitudinal characteristics during approach and landing. The obvious approach is to increase the static margin. Some preliminary results from the study are presented in the following paragraphs. These results are based on 161C rotary derivatives and unverified mass properties data. They are therefore only qualitative.

Figure 4-149 shows the effect of static margin on the longitudinal short-period frequency and acceleration sensitivity at sea level. To provide Level 2 handling qualities (C-H rating of 6.5 or better) during approach and landing, a minimum static margin of about 5-percent MAC is seen to be required. For a C-H rating of 5, it is estimated that the margin would have to be increased to about 6 percent.

These desired increases in margin may have an adverse effect on available C_L for landing as well as ability to trim to high angles of attack at hypersonic speeds. There is an additional consideration which is directly related to handling qualities—the requirement for a reasonable damping ratio, ζ, of the short period mode. The damping constant, $\zeta\omega_n$, is essentially independent of static margin. Hence, as the static margin is increased, causing ω_n to increase, ζ will be steadily reduced. This effect is illustrated in Figure 4-150 where the resultant ratios are compared with MIL specification boundaries. The limiting static margins for fixed levels of performance in Figures 4-149 and 4-150 have been combined in Figure 4-151 to show the range over which static margins may be permitted to vary at each angle of attack. At higher altitudes, these ranges are reduced. Each boundary moves toward the other, those on the right moving to the left and vice versa. Obviously, it becomes increasingly difficult to accommodate large center-of-gravity ranges as angle of attack decreases (i.e., as aerodynamic pressure, $\bar{q}$, increases). Currently, the design center-of-gravity range is 3-percent body length.

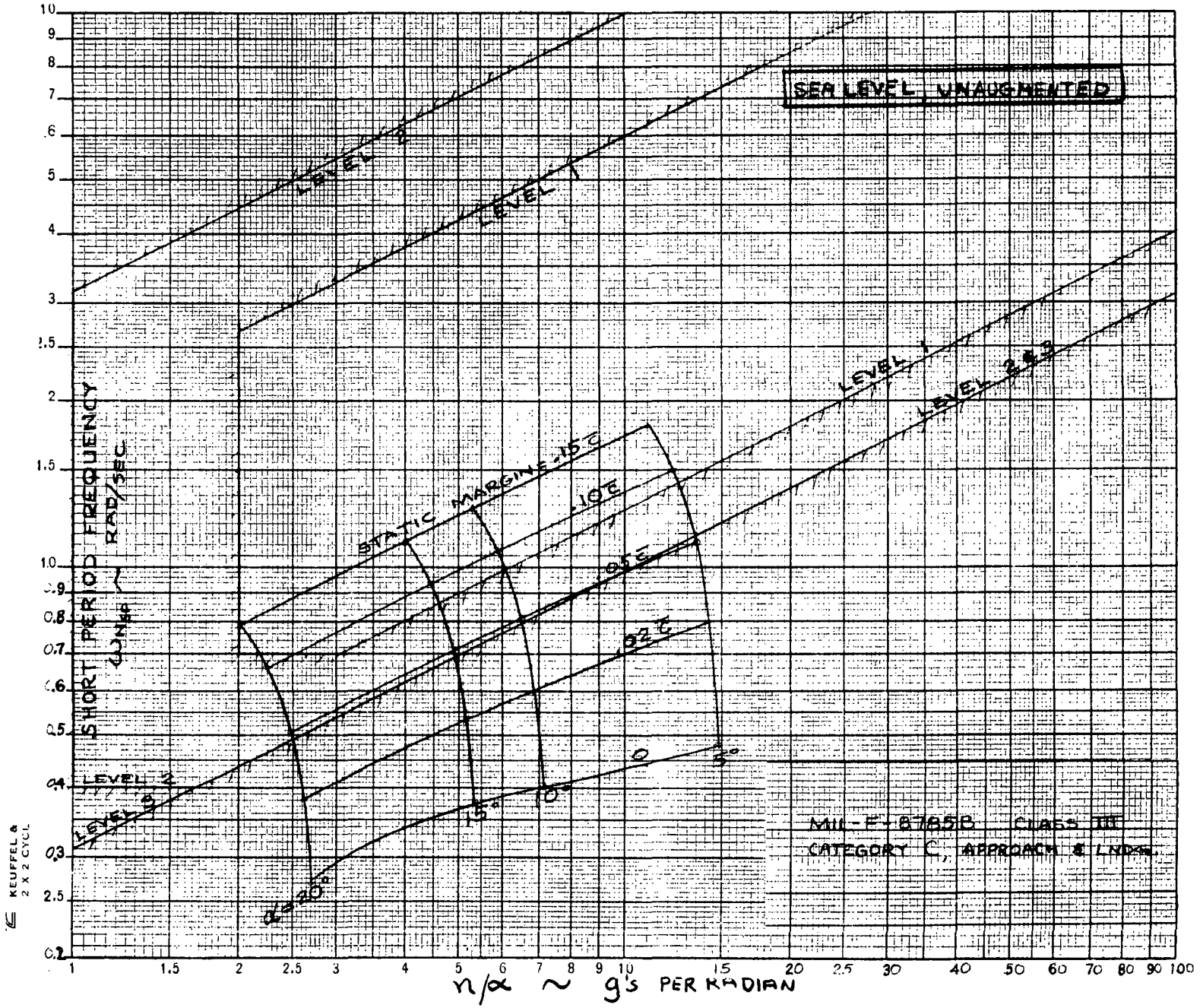

Figure 4-149. Effect of Static Margin on Longitudinal Characteristics, 040A Orbiter

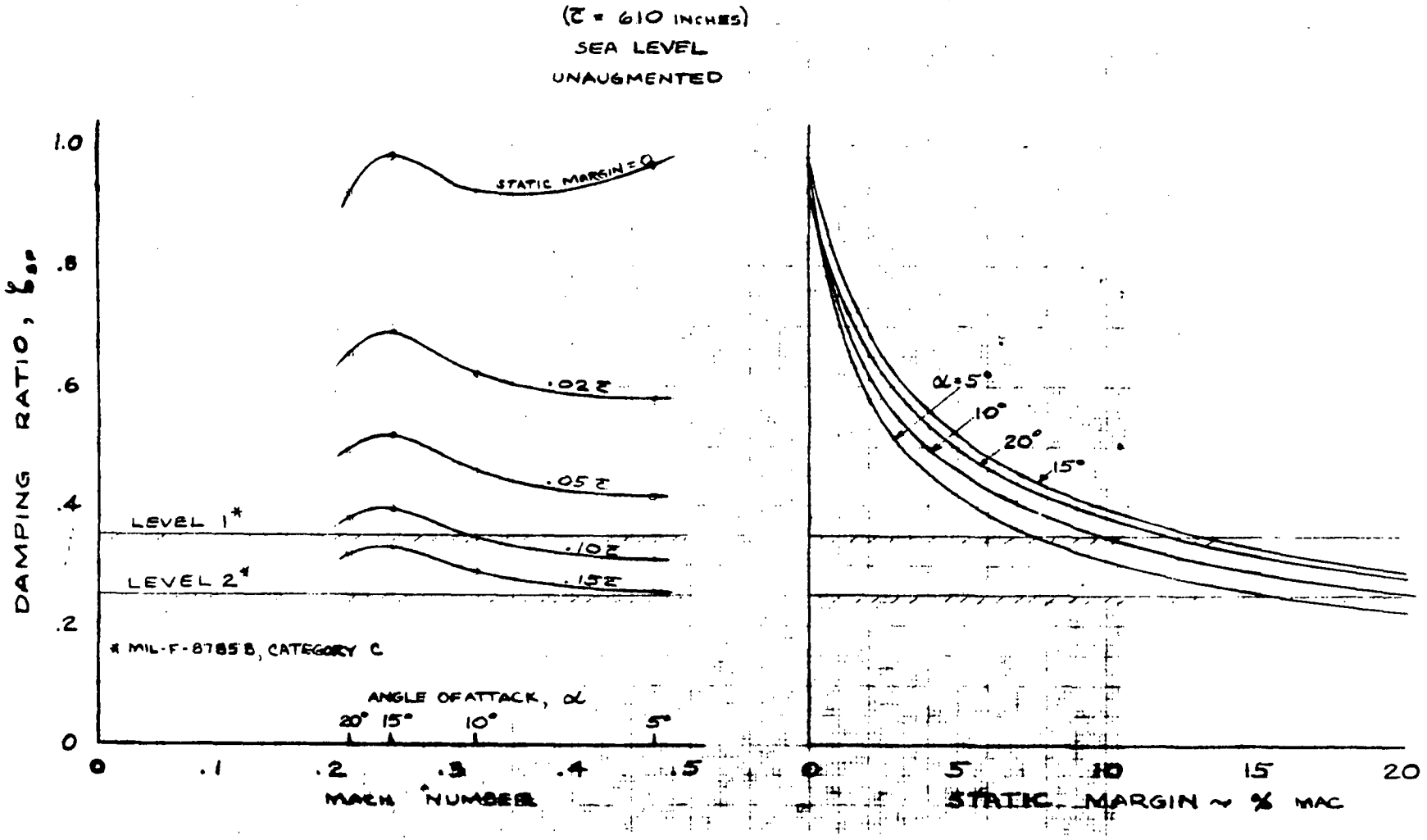

Figure 4-150. Effect of Static Margin on Short-Period Damping Ratio, 040A Orbiter

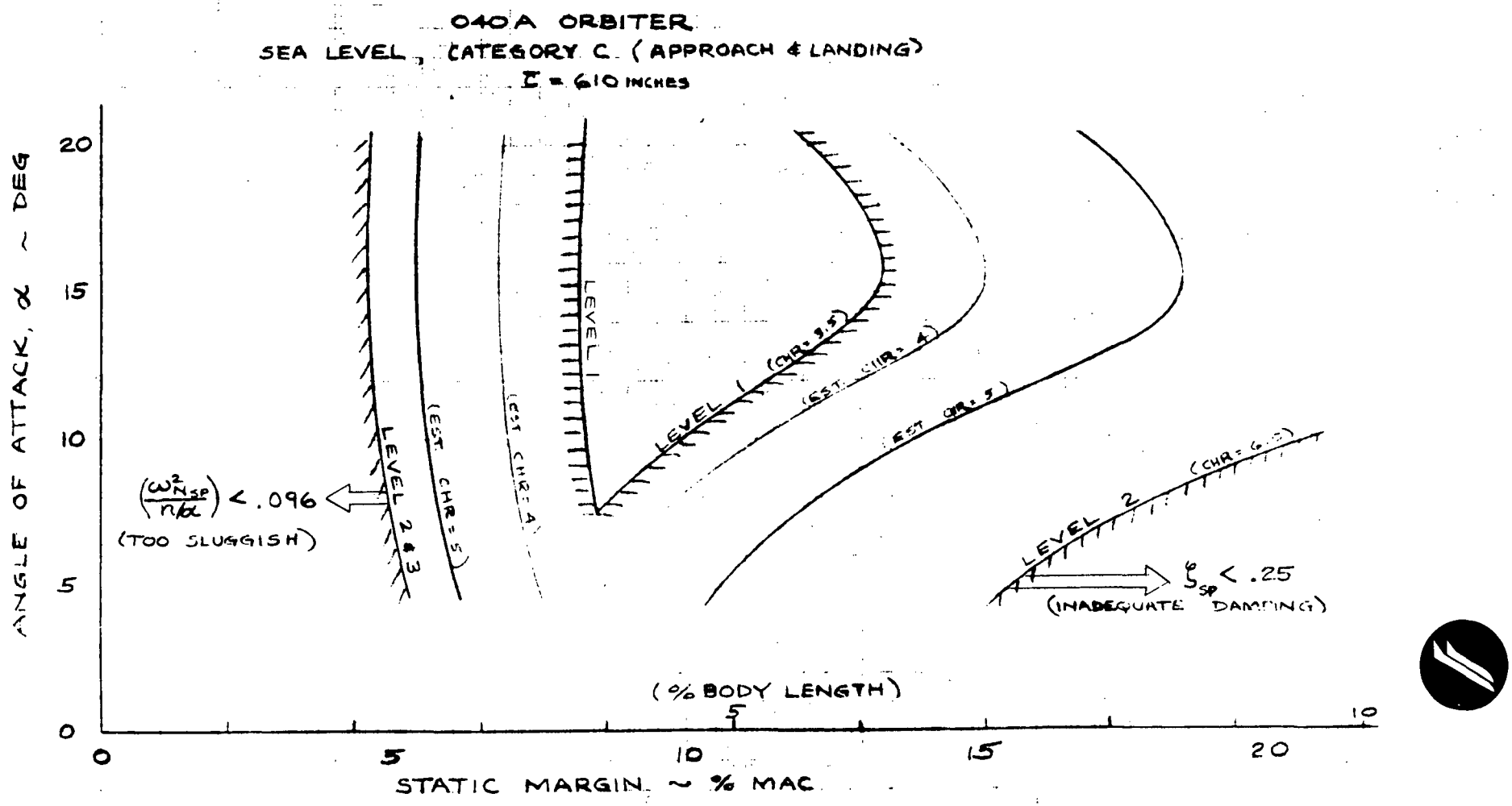

Figure 4-151. Static Margin Requirements for Acceptable Flying Qualities Without Augmentation

Studies of the effect of wing sweep and location are being conducted to define the desirable wing design for improved flying qualities. Preliminary results indicate an improvement in static margin of 6-percent MAC can be obtained by shifting the existing wing aft so that the trailing edge is aligned with the main propulsion system nozzle exit plane. Another is to reduce the wing sweep from 60 to 50 degrees, adjusting the wing area to provide essentially the same low-speed lift. It appears that at least Level 2 requirements can be met at the extremes of center-of-gravity location and that hypersonic trim capability will be satisfactory with this approach.

As noted earlier, these results are preliminary. They will be updated as more reliable data become available. In addition, the effect on longitudinal characteristics during entry, lateral-directional handling qualities, thermal protection and structural weight, etc., remain to be evaluated.

Figures 4-152 and 4-153 deleted.

Aerodynamic Configuration Studies. Aerodynamic configuration studies have been initiated at NR to improve the flight characteristics of the 040A orbiter. Body shape, wing and tail geometry, canopy shape, and OMS and ACPS pod locations are being investigated. Design guidelines for these studies are presented in Table 4-32. Configuration modifications associated with center-of-gravity locations as far aft as 70-percent body length are being evaluated. A status of these studies is summarized in Figure 4-154.

Body Shaping. Forebody camber and cross-section shaping can be used to adjust the hypersonic trim and stability characteristics without major impact on performance, as illustrated in Figure 4-155. As shown, reduced forebody camber increases the available center-of-gravity trim range from 66.2 percent L_B (forward center-of-gravity, $\alpha = 60°$, $\delta_e = 50°$) and 67.6 percent L_B (aft c.g., $\alpha = 20°$, $\delta_e = 20°$) to 67.0 percent L_B (forward center-of-gravity) and 71.1 percent (aft center-of-gravity) for a total incremental increase of 2.7 percent for a constant elevon size. The significant factor is that an increase in center-of-gravity travel capability accompanies a decrease in forebody camber without an increase in elevon size. This increase occurs because, when the bottom surface is made flat, there is less sensitivity to the hypersonic center-of-pressure location due to angle of attack. In other words, the vehicle becomes less stable at hypersonic speeds.

Wing Twist and Incidence. Wing twist and incidence were investigated to determine the effect on subsonic trim losses and hypersonic performance and trim capability. These effects are presented in Figures 4-156, 4-157, and 4-158 and show that twist and incidence do not have a significant influence on the entry aerodynamic performance characteristics. The significance is that twist and incidence will be determined by subsonic or hypersonic stability and control considerations. Figure 4-157 presents the effect of wing twist and incidence on the hypersonic trim range, for both the 040A forebody unmodified and the 040A configurations with the forebody camber reduced. Reducing wing incidence and introducing wing twist shifts the available center-of-gravity range forward due to a down load on the washed out wing tips. The 040A configuration with reduced forebody camber with wing washout comes very close in meeting Mark I and Mark II goals. The trim range for angles of attack from 20 to 60 degrees occurs for center-of-gravity locations 65.8 to 69.5-percent body length. Another effect of wing twist and incidence is on the subsonic characteristics, Figure 4-158. The effect of eliminating the -5 degree twist (washout) and introducing 1.5-degree wing incidence resulted in an increase of the untrimmed lift coefficient from 0.62 to 0.70 at α = 17-degrees. However, because of the effect on $(C_m)\ C_L = 0$ and the resultant higher trim losses, the effect on the trimmed C_L becomes rather negligible, C_L = 0.53 to 0.55 at α = 17 degrees.

Thus, from the aforementioned results, reducing forebody camber and introducing -5 degree twist allow for improved hypersonic trim capabilities for Mark I and Mark II goals, and are recommended for incorporation into the MSC wind tunnel program.

Table 4-32. Aerodynamic Design Guidelines

	MARK I	MARK II
1. DESIGN ANGLE OF ATTACK RANGE		
HYPERSONIC	40 TO 60	20 TO 40
SUBSONIC	-5 TO 20	-5 TO 20
2. c.g. RANGE		
MAX FWD c.g. DURING ENTRY & LANDING (% L)	63.9	63.9
MAX AFT c.g. DURING ENTRY & LANDING (% L)	70.0	70.0
MAX EXCURSION OF 40K PAYLOAD FROM CENTROID OF CARGO BAY		
LONGITUDINAL	±24 IN.	±24 IN.
VERTICALLY	± 6 IN.	± 6 IN.
LATERALLY	± 6 IN.	± 6 IN.
3. PAYLOAD DOWN	25K LB	40K LB
4. LANDING WEIGHT (WITH DOWN PAYLOAD)	140K LB	160K LB
5. LANDING SPEED, NO GROUND EFFECTS	150 KNOTS	161 KNOTS
6. STABILITY CONSIDERATIONS		
LONGITUDINAL (STATIC MARGIN)	2% $\bar{c}$	2% $\bar{c}$
DIRECTIONAL (C_{N_β} M = .6)	+.001	+.001

Mach Matching with a 60 Degree Swept Wing. The effect of wing position and center-of-gravity location on subsonic static stability and hypersonic trim capability is displayed in Figure 4-159. The baseline wing position is at 65.3-percent body length. In the figure, it can be seen that the subsonic aerodynamic center is at 64.8 percent of the body length. The vehicle will be statically unstable for all center-of-gravity locations aft of this location. The trim angle of attack corresponding to the forward center-of-gravity location (64.9-percent body length, 25,000-pound payload) is 42 degrees. The vehicle can be trimmed to an aft center of gravity of 69.7-percent body length at 20-degree angle of attack with 20-degree trailing edge down elevon. It can be seen that the hypersonic trim capability is not matched with the subsonic static stability. The wing should be moved aft in order to provide some positive static margin at the aft center-of-gravity location. The effect of moving the wing aft so that the wing trailing edge is aligned with the main propulsion system nozzles is also shown on Figure 4-159. A positive static margin of 2.6-percent MAC now exists at the aft center-of-gravity location. However, the maximum trim angle of attack at the forward center-of-gravity location for 50-degree elevon deflection has been reduced to 25 degrees. The maximum trim angle of attack at the most aft center of gravity is 42 degrees. Moving the wing aft has resulted in a better matching of the subsonic static stability characteristics and the hypersonic trim capabilities provided the limitations on the maximum trim angle of attack at the forward center of gravity is acceptable. Design trade studies are in progress to develop configuration changes to provide optimum matching of the subsonic static stability characteristics and the hypersonic trim capabilities.

ELEMENT	ALTERNATIVES	MAJOR CONSIDERATIONS	STATUS
BODY SHAPE	 CAMBER MSC 0.075 ALT 0.030	• HYPERSONIC TRIM RANGE • ALLOWABLE c.g. RANGE • HEATING • LATERAL STABILITY	• REDUCE CAMBER TO 0.03 • INCORPORATE IN MSC W.T. PROGRAM
	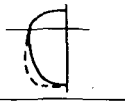 CORNER RADIUS		• TO BE DETERMINED • INCORPORATE IN MSC W.T. PROGRAM
WING GEOMETRY	INCIDENCE: 0°, 1°, 2° TWIST: 0° TWIST -5° TWIST THICKNESS: 0.04 TO 0.10 SWEEP: 60° TO 45°	• MAXIMIZE LOW SPEED C_L • MACH MATCHING • STRUCTURAL WEIGHT	• REDUCE INCIDENCE TO ZERO • INCORPORATE -5° TWIST • RETAIN 8% t/c • INCORPORATE IN MSC W.T. PROGRAM
VERTICAL TAIL	WEDGE AIR FOIL SYMMETRIC AIRFOIL	• DIRECTIONAL STABILITY AT SUPERSONIC & SUBSONIC SPEEDS	• TRADE REQUIRED • INCORPORATE IN MSC W.T. PROGRAM
WING-BODY MATCHING	LONGITUDINAL WING POSITION WING SWEEP	• HYPERSONIC TRIM • SUBSONIC STABILITY	• IN PROGRESS • INCORPORATE IN MSC W.T. PROGRAM

ELEMENT	ALTERNATIVES	MAJOR CONSIDERATIONS	STATUS
OMS LOCATION	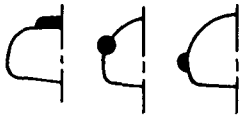	• PITCHING MOMENT (LOW SPEED, TRANSONIC) • DRAG	• INCORPORATE IN MSC W.T. PROGRAM
ACPS PODS LOCATION	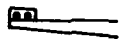 WING UPPER SURFACE 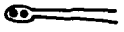 WING TIP	• WING TIP STALL • LATERAL-DIRECTIONAL STABILITY • ELEVON EFFECTIVENESS	• M = 0.6 TO 1.5 TUNNEL DATA HAS BEEN OBTAINED ON WING UPPER SURFACE LOCATION • INCORPORATE IN MSC W.T. PROGRAM
CANOPY SHAPE	 BUBBLE  FAIRED	• LATERAL DIRECTIONAL STABILITY • VERTICAL TAIL EFFECTIVENESS • HEATING	• M = 0.6 TO 1.5 TUNNEL DATA OBTAINED

Figure 4-154. Summary of Aerodynamic Configuration Studies

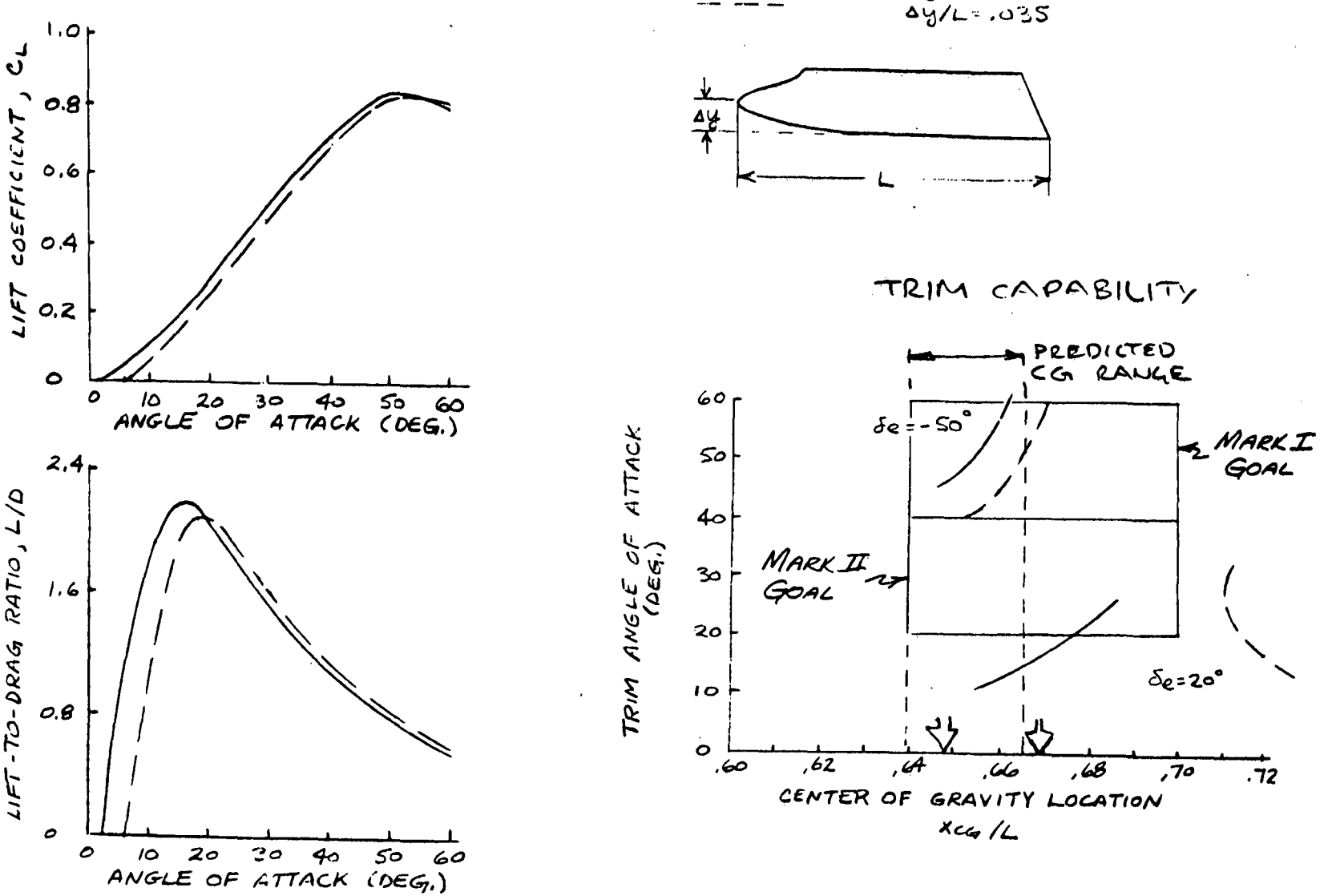

Figure 4-155. Hypersonic Aerodynamics Effect of Reduced Forebody Camber

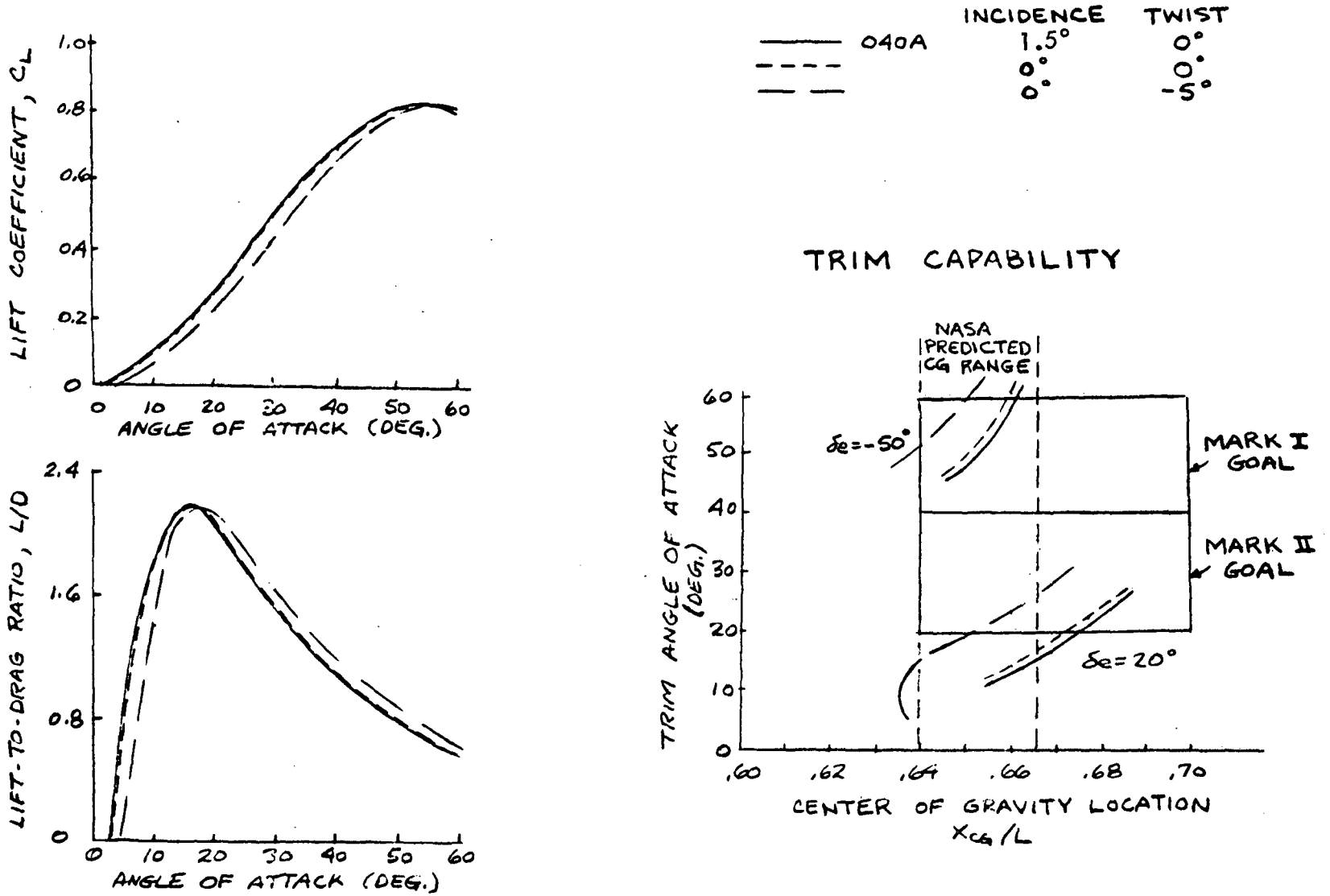

Figure 4-156. Hypersonic Aerodynamics Effect of Wing Twist and Incidence

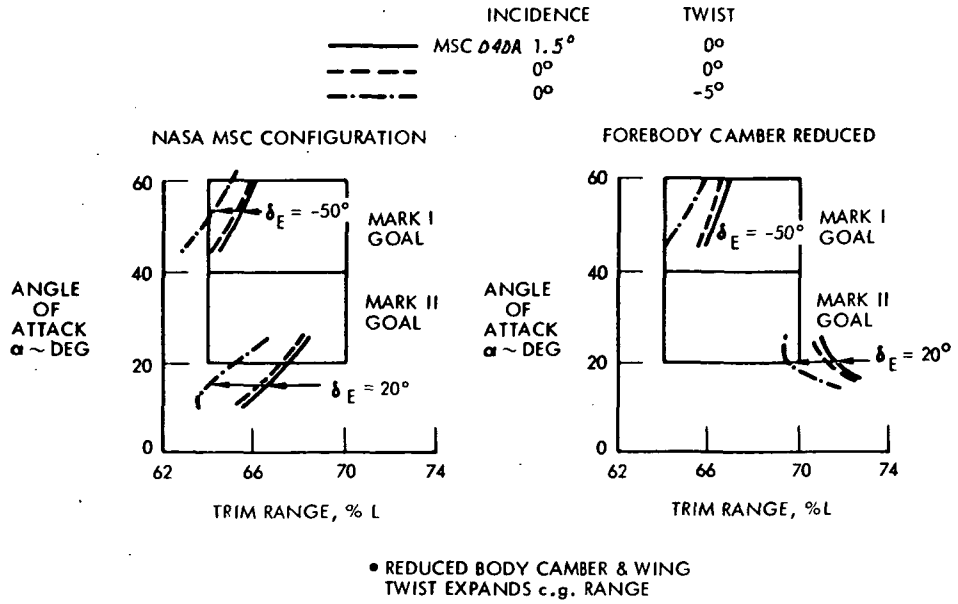

Figure 4-157. Effect of Wing Twist and Incidence on Hypersonic Trim Range

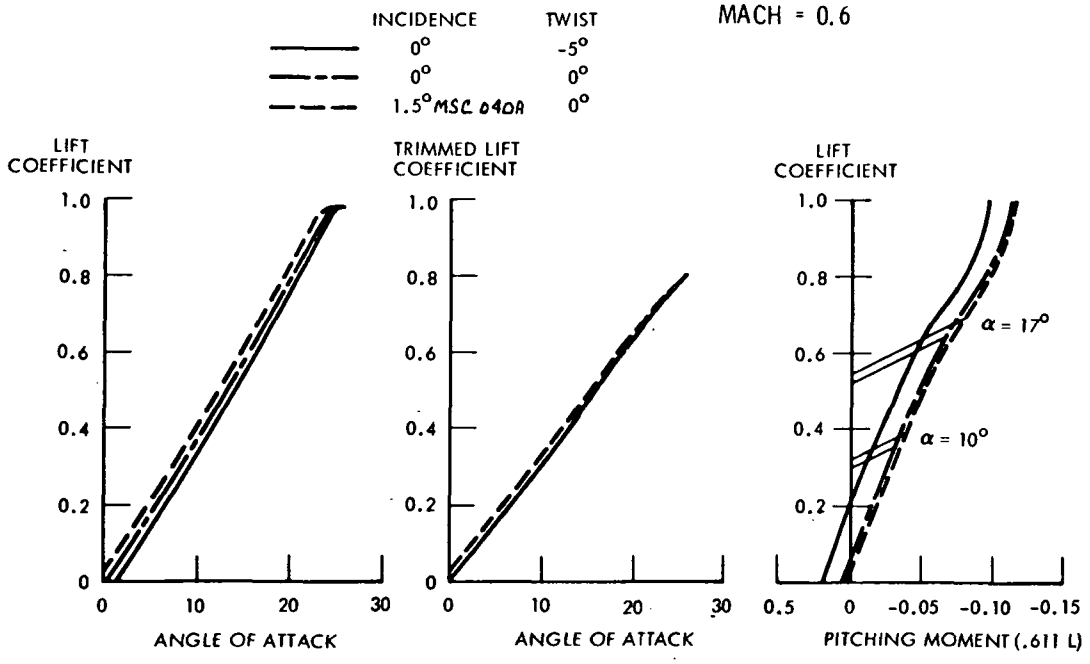

Figure 4-158. Effect of Wing Incidence and Twist on Subsonic Aerodynamics

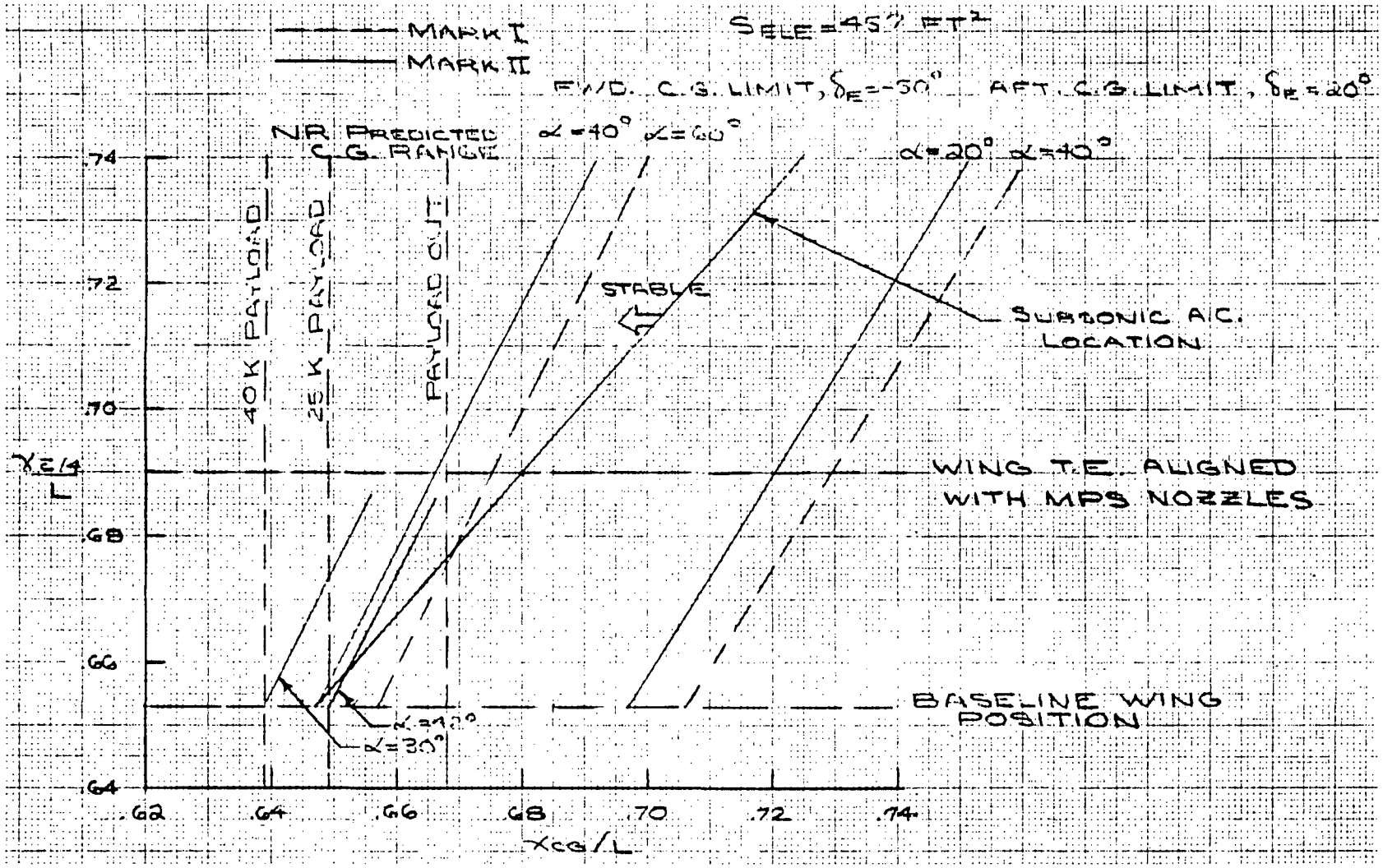

Figure 4-159. 040A Aerodynamic Balance

Approach and Landing.

Approach Performance. Orbiter approach is initiated at an altitude of 40,000 feet and at an indicated velocity of 220 knots. This velocity provides near maximum lift-to-drag ratio (L/D_{max}) and maximum glide range, with the landing gear retracted and the glide brakes closed. At approach initiation, the glide brakes are extended 45 percent (22.5 degrees included angle) which provides a steeper nominal glide path with approximately equal increments of slope modulation available either to extend or to reduce the design glide range. If the ABES is employed, the engines are deployed and started at 40,000 feet, which is the maximum altitude for air starts. The engines are throttled and maintained at idle power throughout the remainder of the approach and to the termination of the landing roll. The approach, flare, and landing are assumed to be pilot controlled. Coarse and fine position data will be available to the pilot. Orbiter attitude and velocity will be maintained by the aerodynamic control surfaces. Approaches and landings with the deployed ABES will be conducted as if the ABES were not present. For all operations, except ferry flights, the ABES is a stand-by to be used for one go-around in the case of a missed approach or for emergency approach range extension, without subsequent go-around capability, in the case of a missed entry target. The landing gear will be lowered at 10,000 feet, after it has been determined that a satisfactory approach has been established and that utilization of the ABES for range extension will not be required. Figure 4-160 illustrates orbiter performance capabilities based on a nominal straight-in approach path at a constant indicated airspeed of 220 knots. The straight-in approach is consistent with previous recovery patterns for manned spacecraft, but the superior L/D performance of the orbiter permits other high key approach patterns to be flown, e.g., 180, 270, or 360 degree overheads, to initiate final approach closer to the recovery site. Figure 4-160 shows that glide approach range can be modulated between 23.3 and 40.2 nautical miles by aerodynamic means alone for a straight-in approach at 220 knots indicated airspeed. When the ABES are employed during an approach terminating a space mission, the orbiter configuration has two GE F101/F12A3 turbofan engines deployed from the payload bay and positioned shoulder high near the fuselage. For performance calculations, the idle thrust was assumed to exactly cancel the added drag. The engines were selected for their ability to provide go-around capability at 5000 feet on a hot day as well as for their compatibility with ferry mission performance requirements.

Figure 4-161 presents ABES engine air start performance capabilities. The engines should be started and checked out as soon as possible to permit concentration on approach and landing procedures. Total elapsed time from 40,000-feet altitude to touchdown is short, varying from five to eight minutes, depending upon the approach glide configuration.

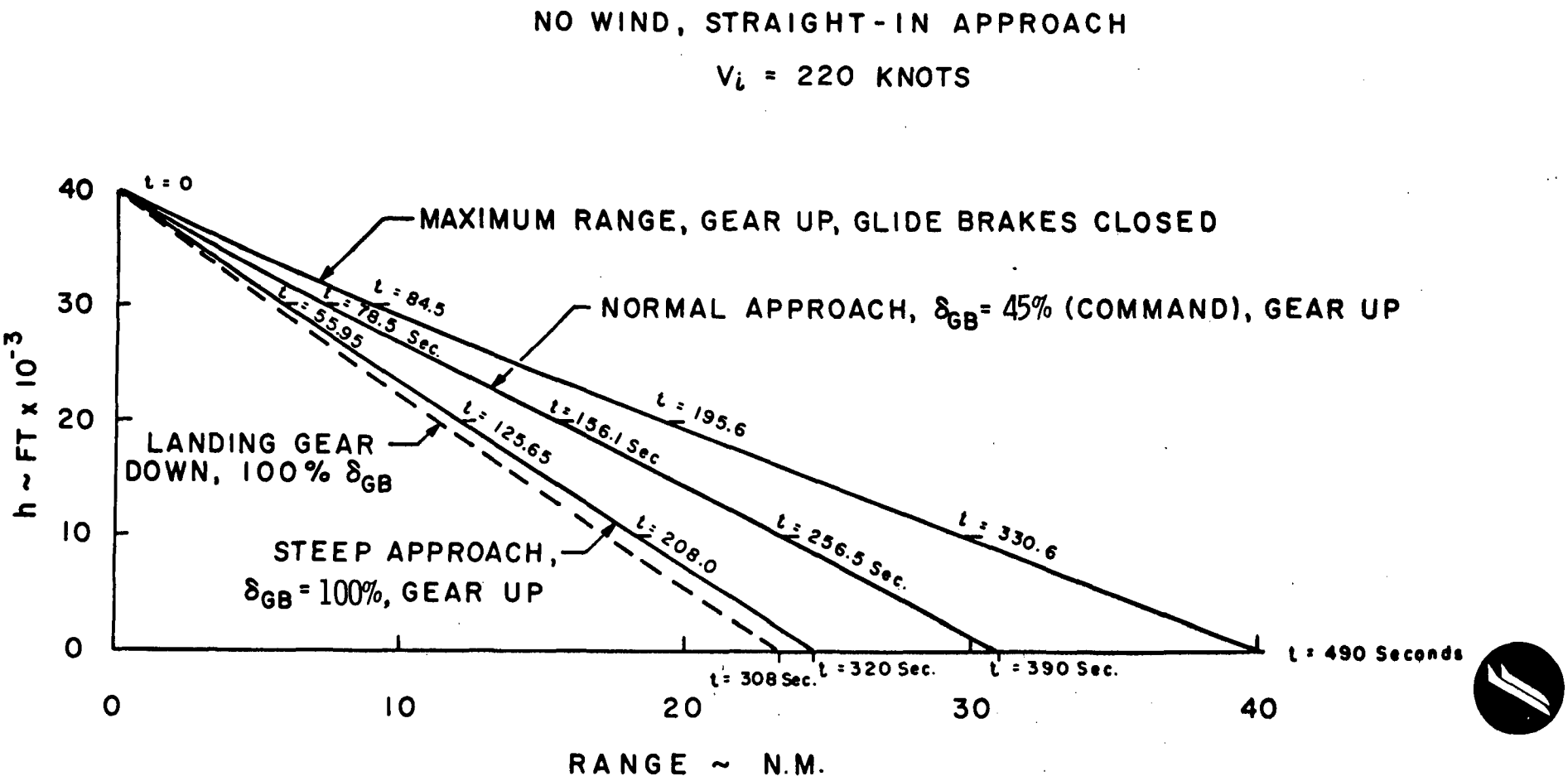

Figure 4-160. Orbiter Approach Performance

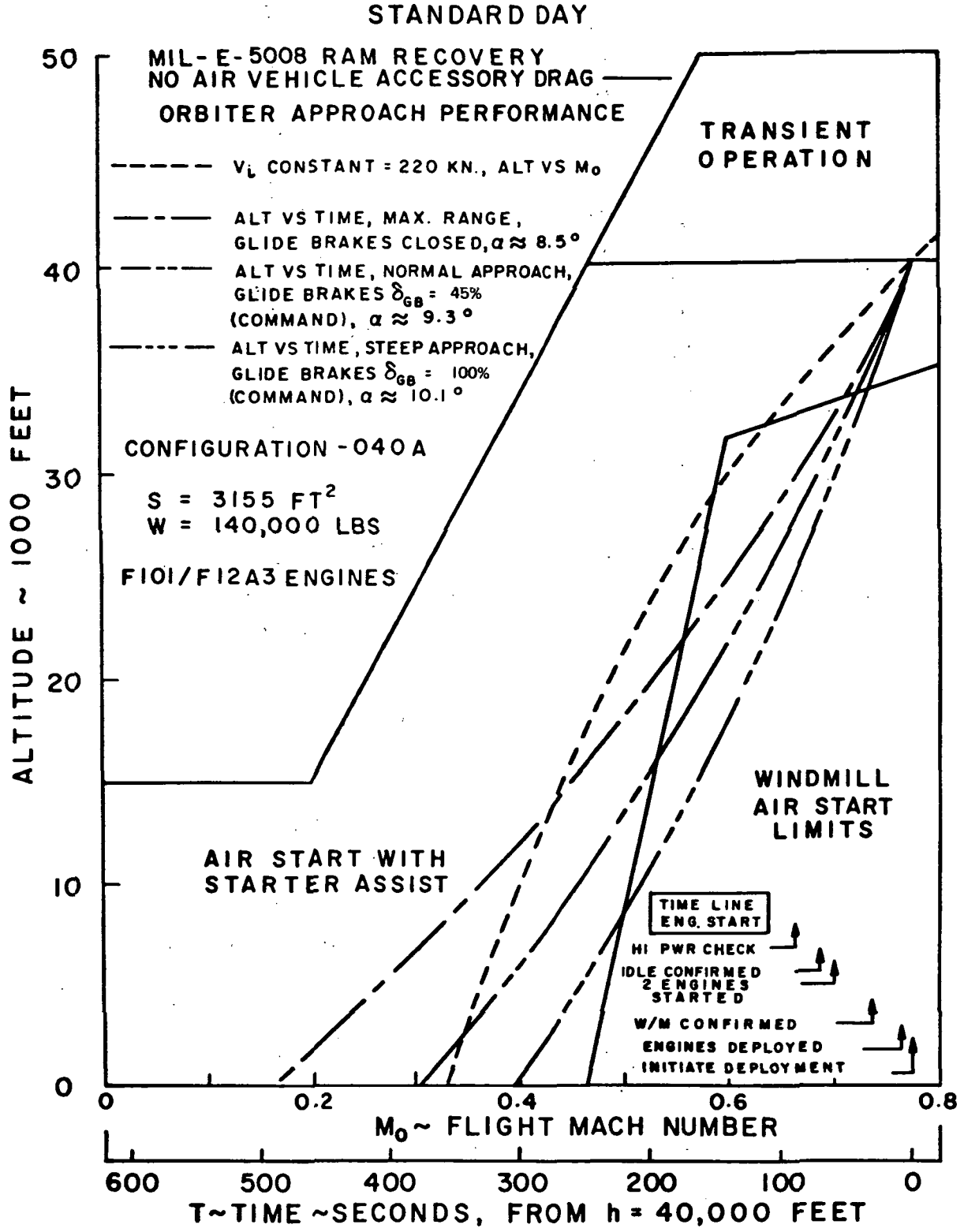

Figure 4-161. Airstart Envelope

Flare. Flare is initiated at an altitude of 700 feet and 220 knots indicated air speed. The objective of the flare maneuver is to decrease the approach velocity to the design touchdown velocity (170 knots) and to decrease the approach rate of sink (75 fps) to a low value (2 to 3 fps) for firm contact but below the design value (10 fps) for the landing gear structure. The initial flare maneuver is a 1.2- to 1.3-g pull-up. A deceleration phase follows in which both horizontal and vertical velocity components are reduced as the flight path approaches the touchdown point asymptotically. Time in the flare is nominally 25 seconds; longer times produced erratic touchdown behavior, such as ballooning, while shorter flare times generally resulted in hard impacts. The design touchdown velocity of 170 knots at 10-degree angle of attack is consistent with the 220-knot approach velocity and the flare procedure. At the limiting touchdown attitude, tail scrape at an angle of 17 degrees, the touchdown velocities for both Mark I and Mark II weights are below 150 knots, without ground effect.

Landing Performance. The effect of landing weight on approach and landing speeds is summarized in Figure 4-162. The stall speed (V_S) shown occurs at an angle of attack of 25 degrees and is defined by degradation of lateral control. Touchdown speed is 50 percent above the lateral control defined stall speed at an attitude of 10 degrees. Approach speed is 30 percent above touchdown speed at 1.95 V_S and an attitude of 6 degrees. The approach and touchdown speeds shown, corrected to true airspeed, were used in calculating landing runway length requirements presented in Figure 4-163. Requirements are shown for sea level and 4000 feet elevation sites on standard and hot days. It should be noted that available runways are considered to be 10,000 feet for sea level and 13,000 feet for 4000 feet elevation. Consequently, even though longer runway lengths are required for landings at 4000 feet sites, the landing performance is less critical than at sea level because of the longer runways that are available. The Mark I landing weight of 140,000 pounds is indicated on the plot, and landing performance requirements are met or exceeded for all landing conditions. For the Mark II landing weight of 160,000 pounds, the required runway length is indicated to be slightly in excess of the desired 10,000 feet for hot day conditions. As previously noted, in all cases the 4000 feet elevation site landing performance betters requirements because of the longer runway length that is available. Required landing distance lengths have been calculated to meet the over-a-50-feet obstacle clearance distance divided by 0.6, in accordance with FAR 25 regulations. Landing distances have been calculated for dry runways and without a drag chute. NR considers a drag chute to be a weight and cost effective system and has included it as a design element.

Go-Around Performance. Climb capabilities available for hot day go-around performance with two GE F101/F12A3 engines are shown in Figures 4-164 and 4-165. Approach configuration (gear up) go-arounds are

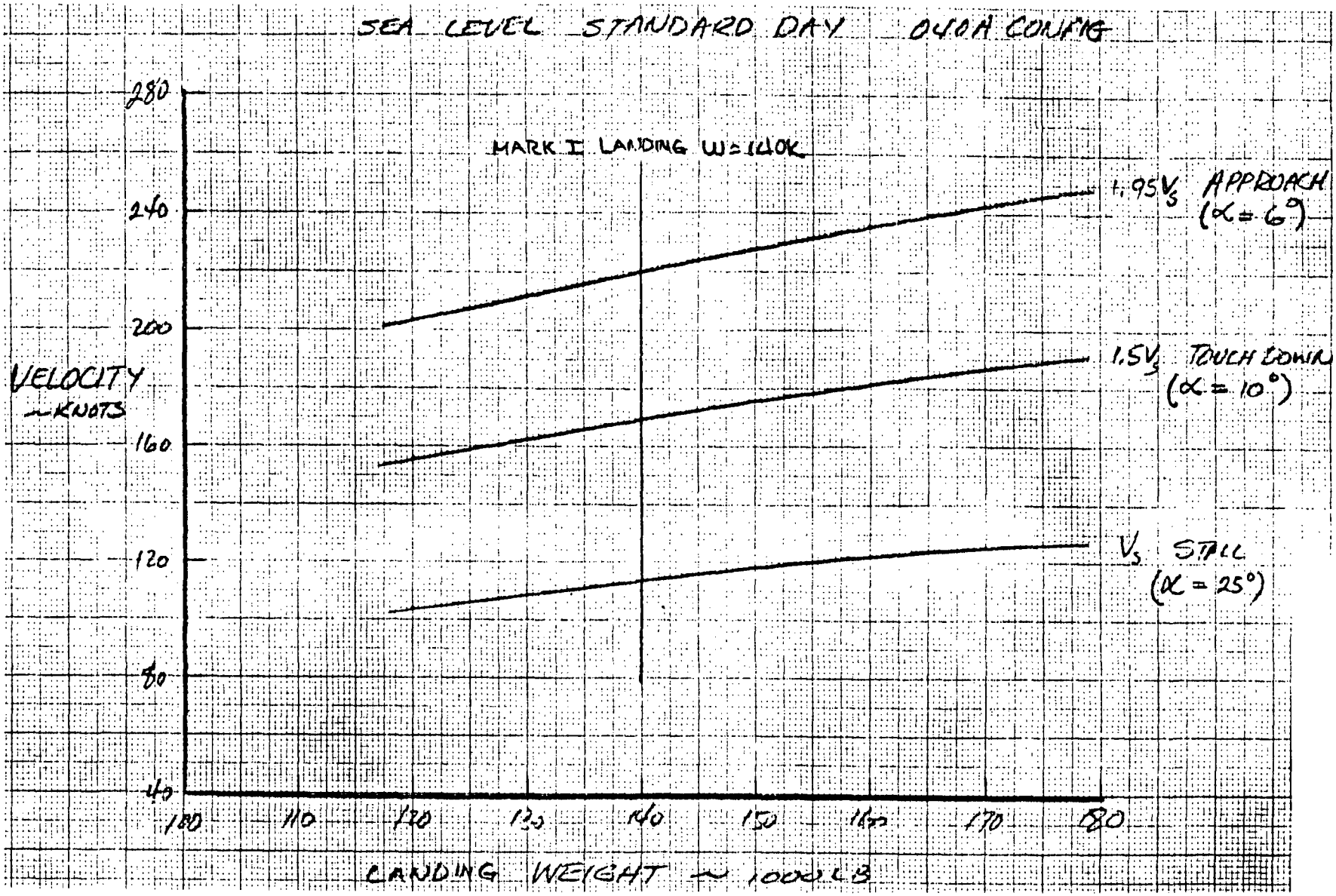

Figure 4-162. Effect of Weight on Approach and Landing Speeds

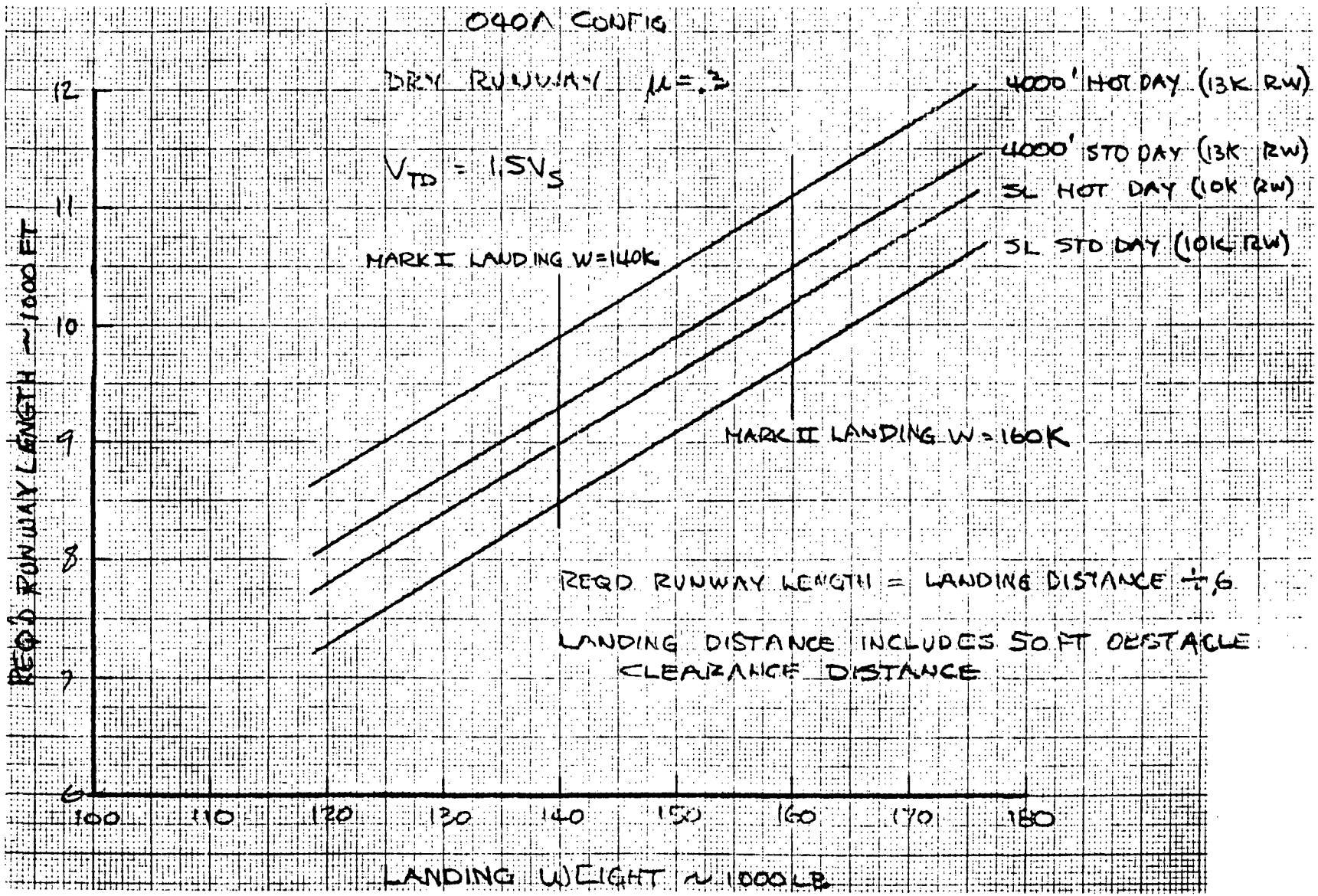

Figure 4-163. Landing Performance

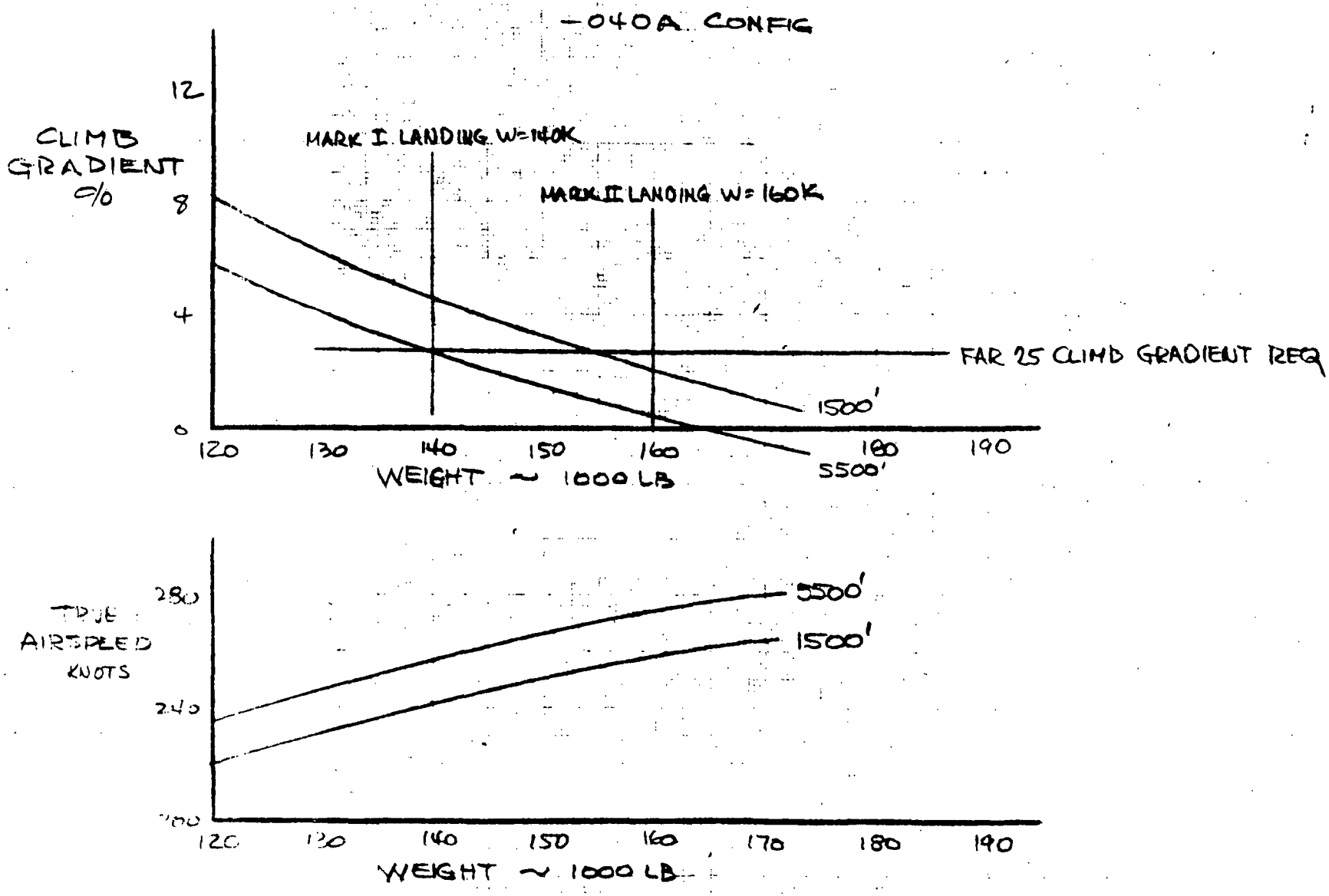

Figure 4-164. Two-Engine Gear-Up Climb Capability, Hot Day

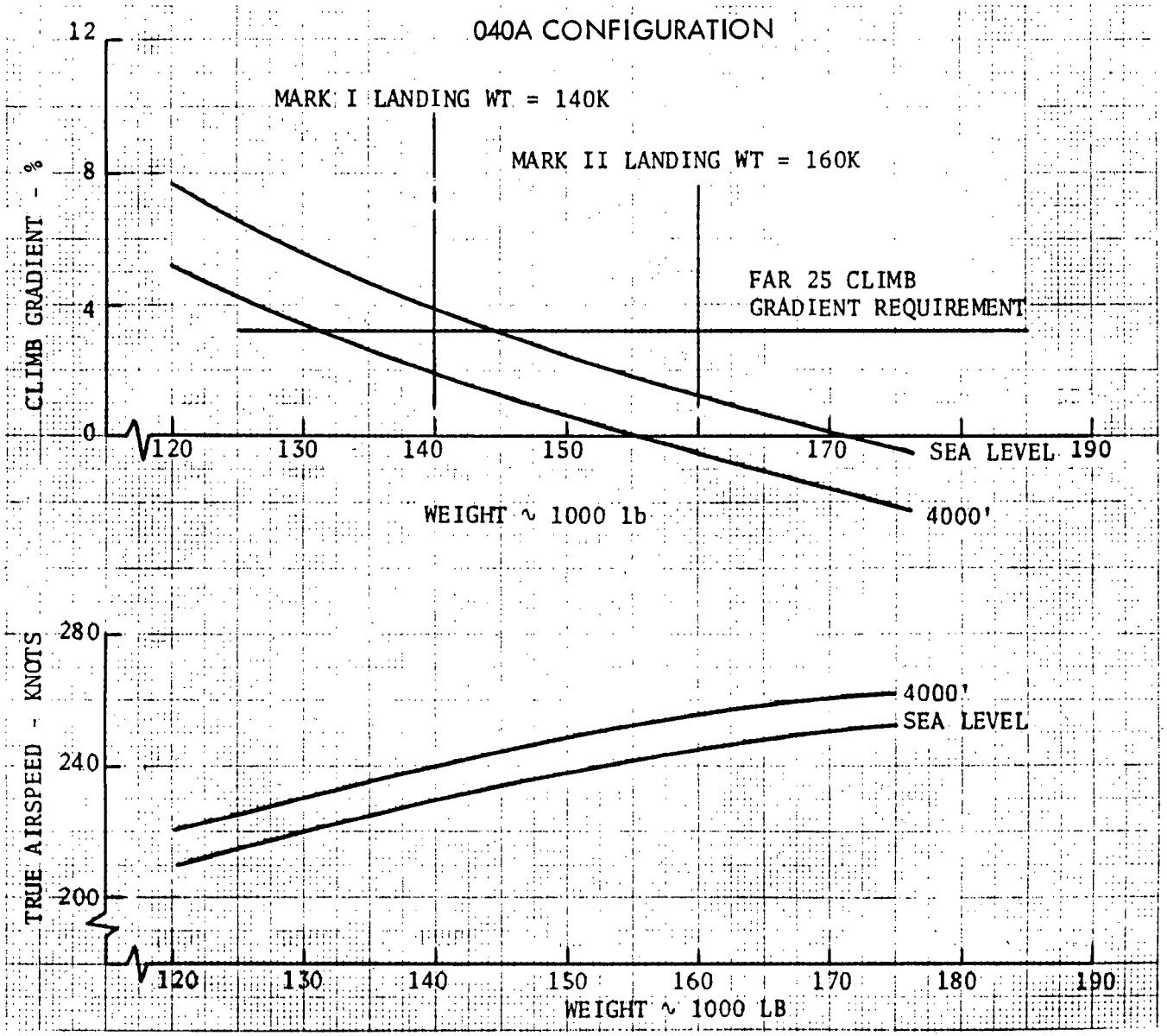

Figure 4-165. Two-Engine Gear-Down Climb Capability, Hot Day

to be made at 1500 feet above the ground so climb capability is shown at 1500 and 5500 feet for landing elevations at sea level and 4000 feet, respectively. The FAR 25 climb gradient requirement for the go-around condition is 2.7 percent (normally considered with an engine out, but not in the present case) as indicated on the plots. For standard day conditions the required climb gradients are met up to the Mark II landing weight except at 5500-foot altitude where a lower positive climb gradient (1.8 percent) is available. For hot-day conditions however, only the 1500-foot altitude condition at Mark I landing weight meets the FAR 25 climb gradient and a very slightly positive climb gradient can be achieved at 5500 feet with Mark II landing weight. Though the hot-day climb gradients are generally low, an approach configuration go-around can be made utilizing energy transfer with some reduction of the go-around altitude. Energy transfer would involve increasing the 220 knot indicated approach speed to operate in a higher performance region of the flight envelope.

Landing configuration (gear down) go-arounds are to be initiated at 200 feet above the ground so hot day climb capability is shown for sea level and 4000 feet. The FAR 25 climb gradient requirement is 3.2 percent as indicated on the plots. FAR 25 climb gradients are not met at either standard or hot day conditions for Mark II landing weight, but they become negative only for hot-day conditions for the Mark II at 4000 feet. The gear-down go-around maneuver is initiated at such a low altitude that the energy transfer technique cannot be used. However, rapid pilot action in retracting the gear and applying power may make a go-around practical even for these adverse conditions. Continued study of the maneuver is planned with emphasis upon the go-around initiation altitude, piloting techniques, and the possible use of more powerful GE F101/F12B3 engines.

Descent Range Extension. In addition to providing go-around capability the ABES can be used to extend range in descent. The range extension available is a function of the fuel available. If it is desired to use go-around fuel for range extension, approximately 20 nautical miles can be achieved in place of a go-around. Maximum practical range extensions are illustrated in Figure 4-166 for Mark I and Mark II configurations. The Mark I fuel of 15,637 pounds is based on zero payload return. From the normal payload of 25,000 pounds, weight increments are subtracted for ABES, tankage, and fuel for startup, checkout, idle descent, and landing. A range extension of 283 nautical miles is provided by the 15,637 pounds of fuel. Mark II fuel availability is calculated on the basis of a 25,000 pound payload return. When the 25,000-pound payload and the above weights are subtracted from the 40,000-pound nominal payload, 5,765 pounds of fuel are available. In this case a range extension of 92 nm is provided.

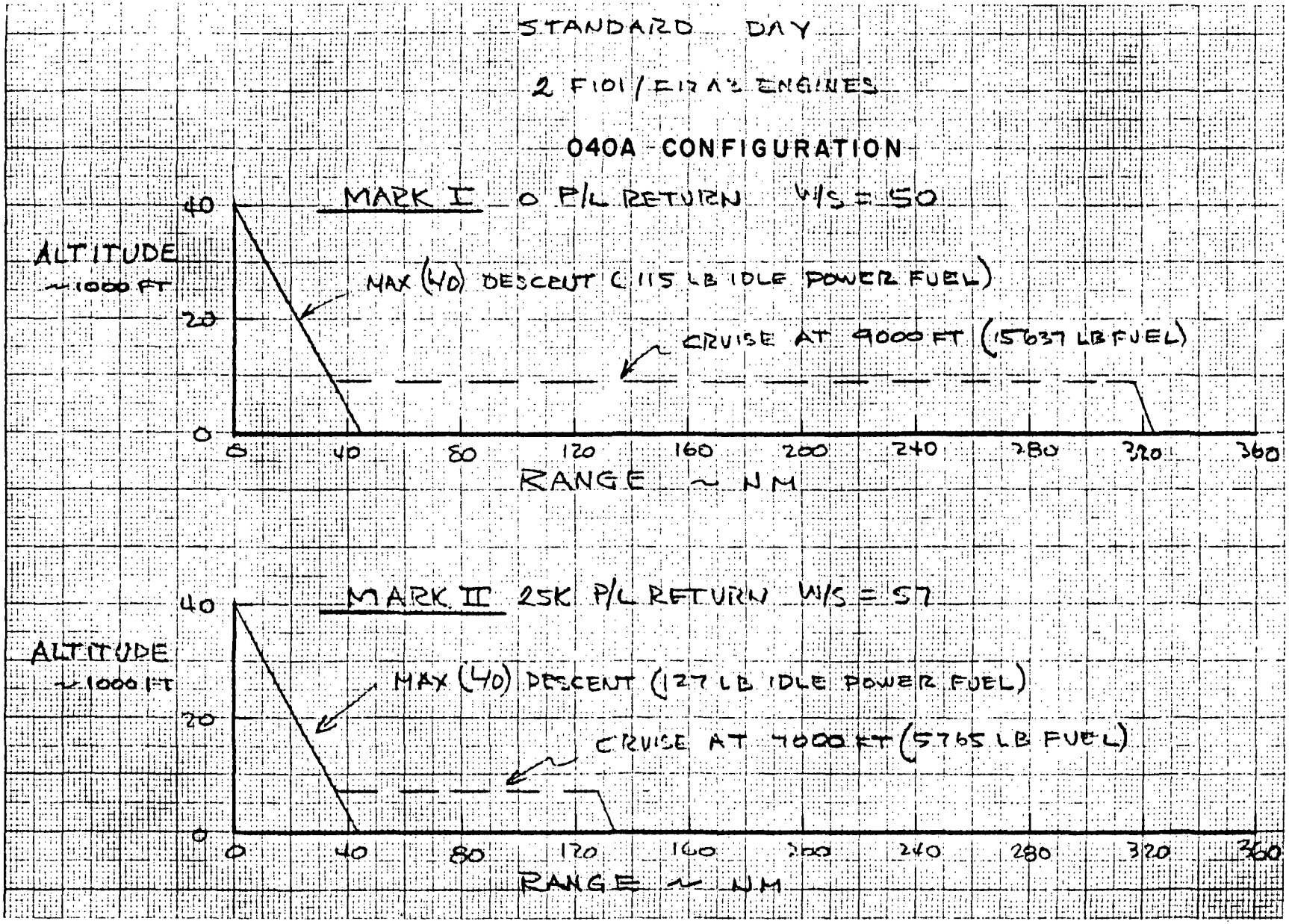

Figure 4-166. ABES Descent Range Extension

Ferry Performance.

Ferry Configuration. The ferry configuration of the orbiter utilizes four F101/F12A3 engines deployed near the center of gravity, shoulder high on the fuselage. Two of the engines are from the basic space-rated on-board ABES installation, the other two are strap-ons. All air-breathing engines, tanks, plumbing, the air-start systems, controls (other than remote cockpit mounted controls and displays) and supporting structure are mounted from the payload bay and may be removed with minimum scar weight. Four GE F101/F12A3 engines were selected for a ferry range of 440 nautical miles, the maximum distance needed to ferry anywhere within the continental United States. Weight, size, cost, and FAA performance requirements were considered in making the engine selection. The hot day rate of climb requirement with an engine failure at takeoff from a runway at 4000-feet elevation established the number of engines required.

Takeoff and Climb. Four F101/F12A3 engines are required to take-off with an adequate fuel load to provide both a design ferry range of 440 nautical miles and to assure an adequate climb performance margin for a single engine failure at takeoff. Figure 4-167 shows take-off weight considerations for operations on a standard day from sea level and from 4000-feet elevation runways. Figure 4-168 presents the same data for hot day conditions. (Statistical data on the lengths of runways considered for shuttle element recoveries show that the minimum length is 13,000 feet for landing fields situated at elevations around 4000 feet). Both FAR takeoff distance considerations are shown in the figures: the 115-percent takeoff distance over a 35-feet high obstacle and the critical field length for an engine failure at takeoff. In every case the critical field length is the more severe and establishes the takeoff field length requirement. Maximum takeoff weights, considering only the critical field length and ignoring reduced landing gear structural design load factors, are designated at the termini of the curves and are, for a standard day, 210,000 pounds at sea level and 195,000 pounds at 4000 feet. The corresponding weights for hot-day conditions are 190,000 and 178,000 pounds. All these weights include fuel loads which exceed requirements for the design 440-nautical-mile ferry range.

Engine-out hot-day climb capability is presented in Figure 4-169 for the ferry configuration (four engines deployed and three operating). Maximum cruise weight for a 440-nautical-mile ferry flight corresponds to a wing loading of 57 pounds per square foot; the resulting climb gradient is 5 percent. Three-engine climb performance at 10,000 feet is very good, and a positive climb gradient could be maintained with two engines operating in cruise flight. However, a three-engine ferry configuration will not meet all of the takeoff performance requirements.

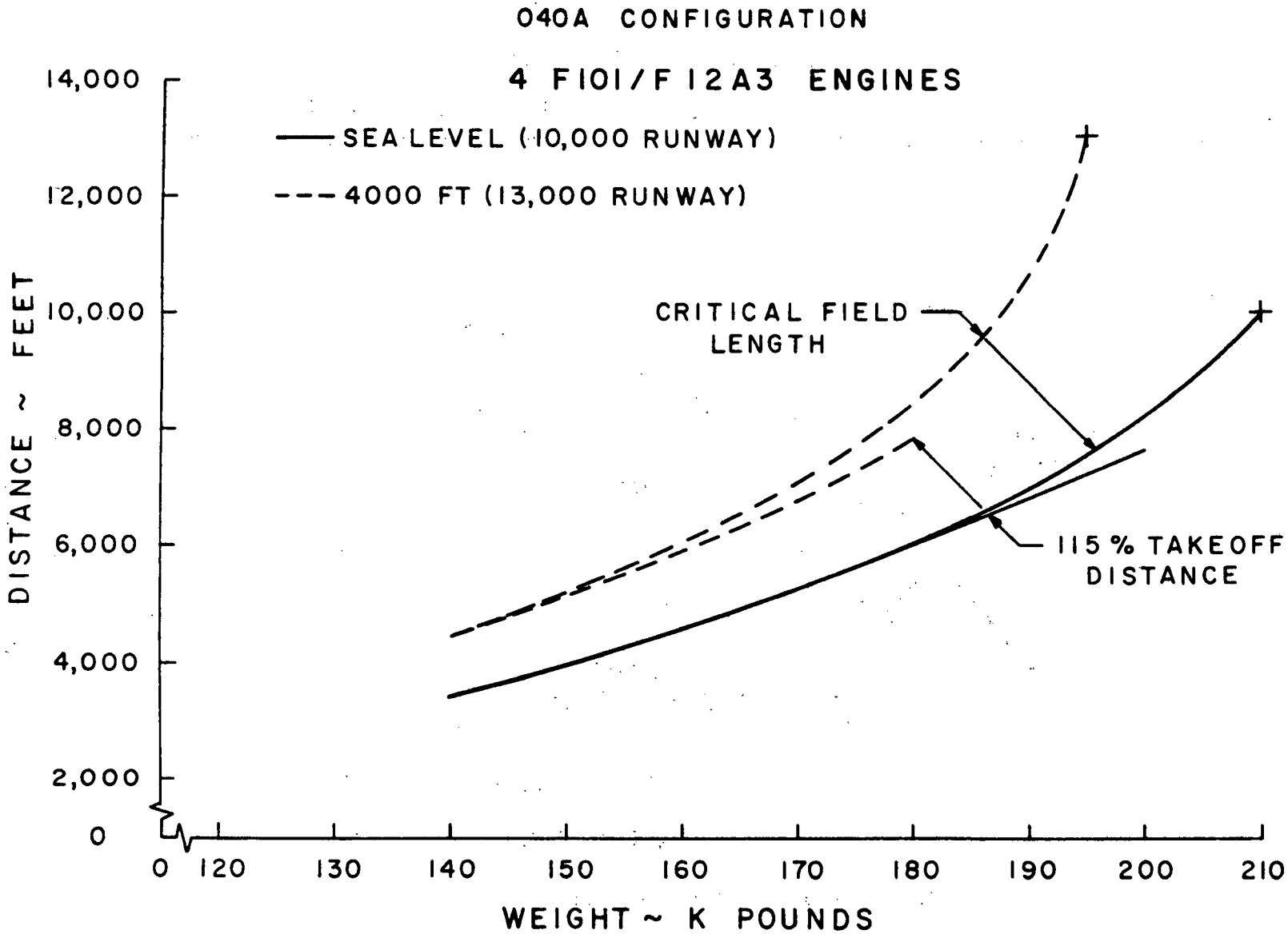

Figure 4-167. Takeoff Weight Limitation, Standard Day

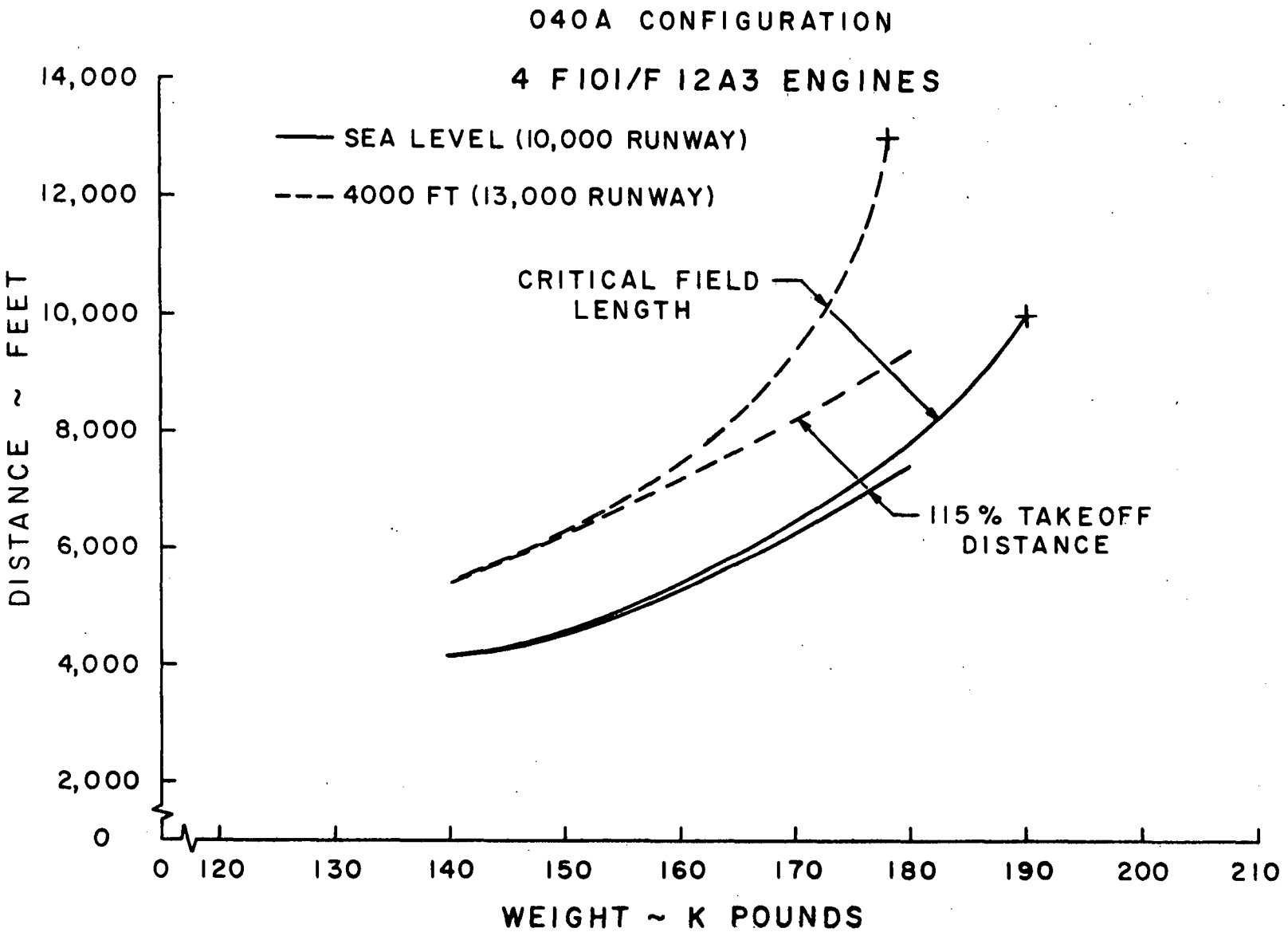

Figure 4-168. Takeoff Weight Limitation, Hot Day

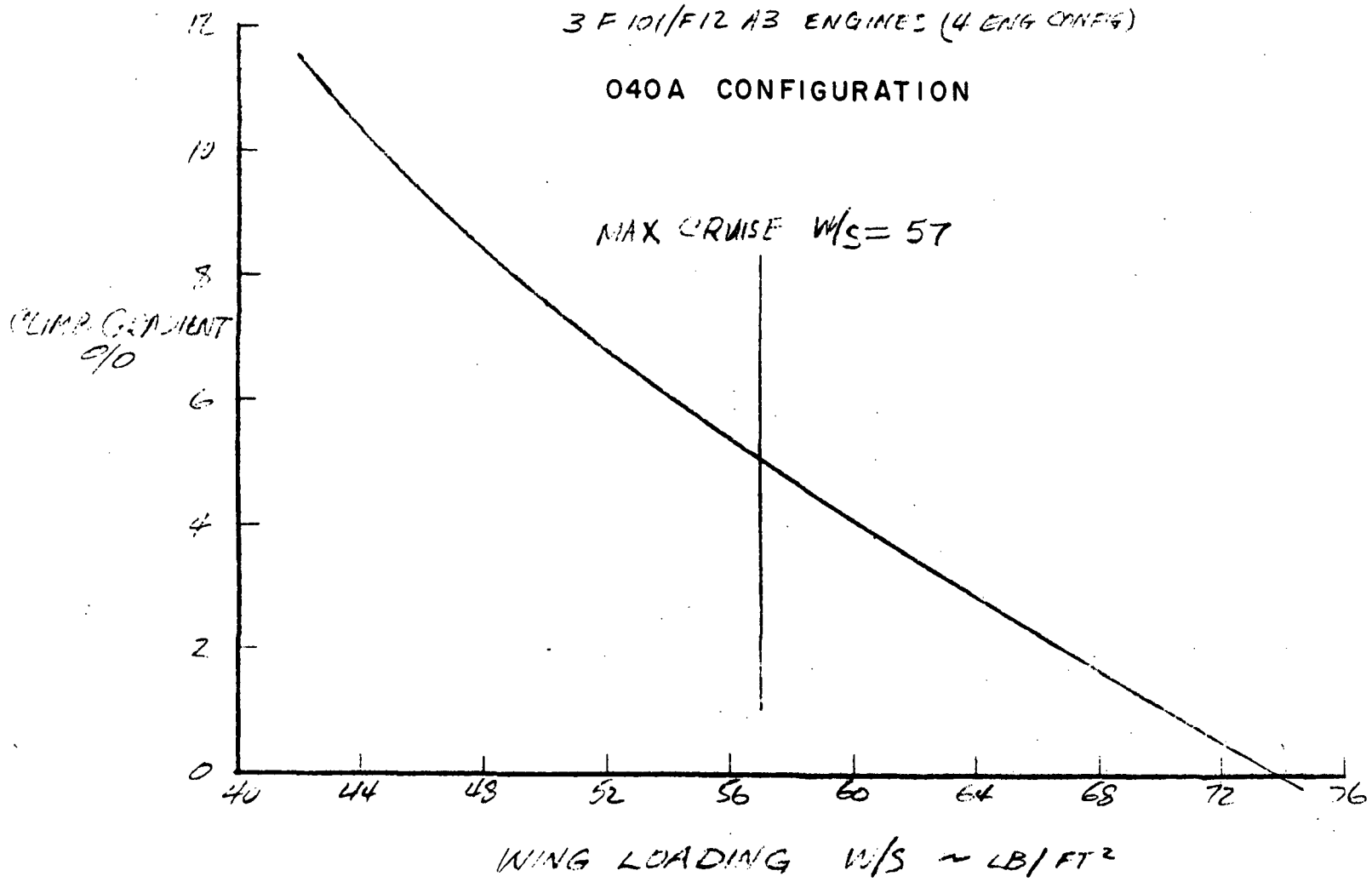

Figure 4-169. Engine-Out Climb Gradient at 10,000 Feet, Hot Day

Ferry Cruise Flight and Range. Takeoff fuel allotment assumes 20 minutes at idle power followed by one minute at takeoff power. Climb is performed at maximum continuous power at best climb speed to the cruise ceiling for the end-climb weight. Flight is continued at the cruise ceiling at best cruise speed against an assumed 50-knot head wind. The loss of an engine during cruise is considered. For this condition, it is assumed that no loiter fuel will be required, and the three-engine cruise range is the same as the design ferry range. The descent is conducted at idle power and near maximum lift-to-drag ratio. A landing reserve fuel allowance is assigned to provide 20 minutes of loiter. Landing reserve and go-around fuel requirements are shown in Figure 4-170. For the ferry flight landing weight, about 140,000 pounds, the 20-minute loiter fuel required is 4800 pounds. For a nominal 15.3-nautical-mile visual flight rule (VFR) go-around flight path, 1000 pounds of fuel are required.

Figure 4-171 presents ferry cruise times. These data were used to calculate the effect of head wind during cruise and are of interest with respect to flight test planning. Figure 4-172 shows cruise fuel required with and without head winds. A 31,000-pound fuel load is required for the 440-nautical-mile design ferry range.

Mach Number-Altitude Boundaries. Figure 4-173 summarizes Mach number-altitude orbiter performance capabilities under ABES power in level flight, for both the space mission configuration (two-engines) and the ferry configuration (four-engines). Entry and landing weights correspond to wing loadings of about 45 pounds per square foot.

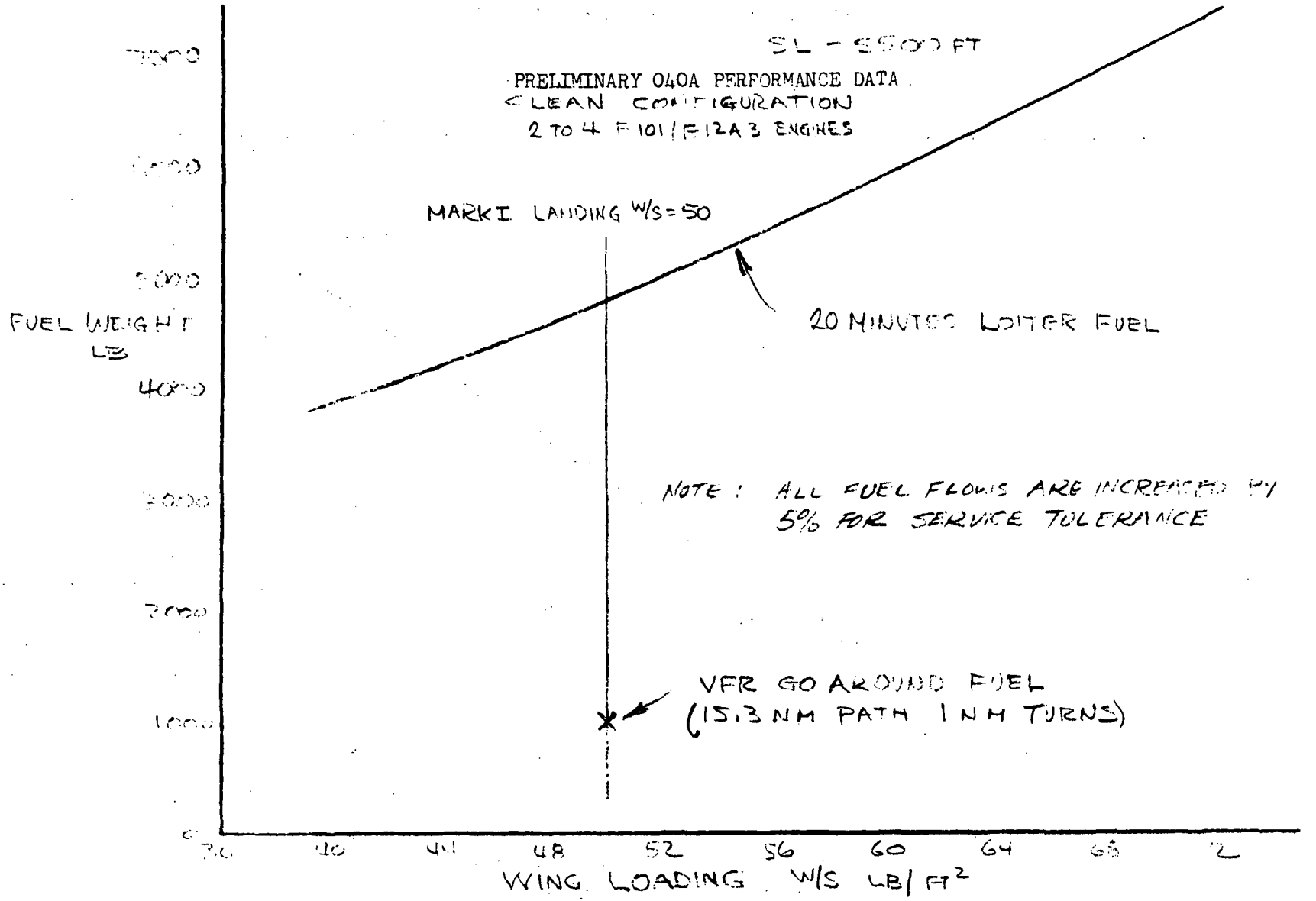

Figure 4-170. Landing Reserve and Go-Around Fuel Requirements, Standard or Hot Day

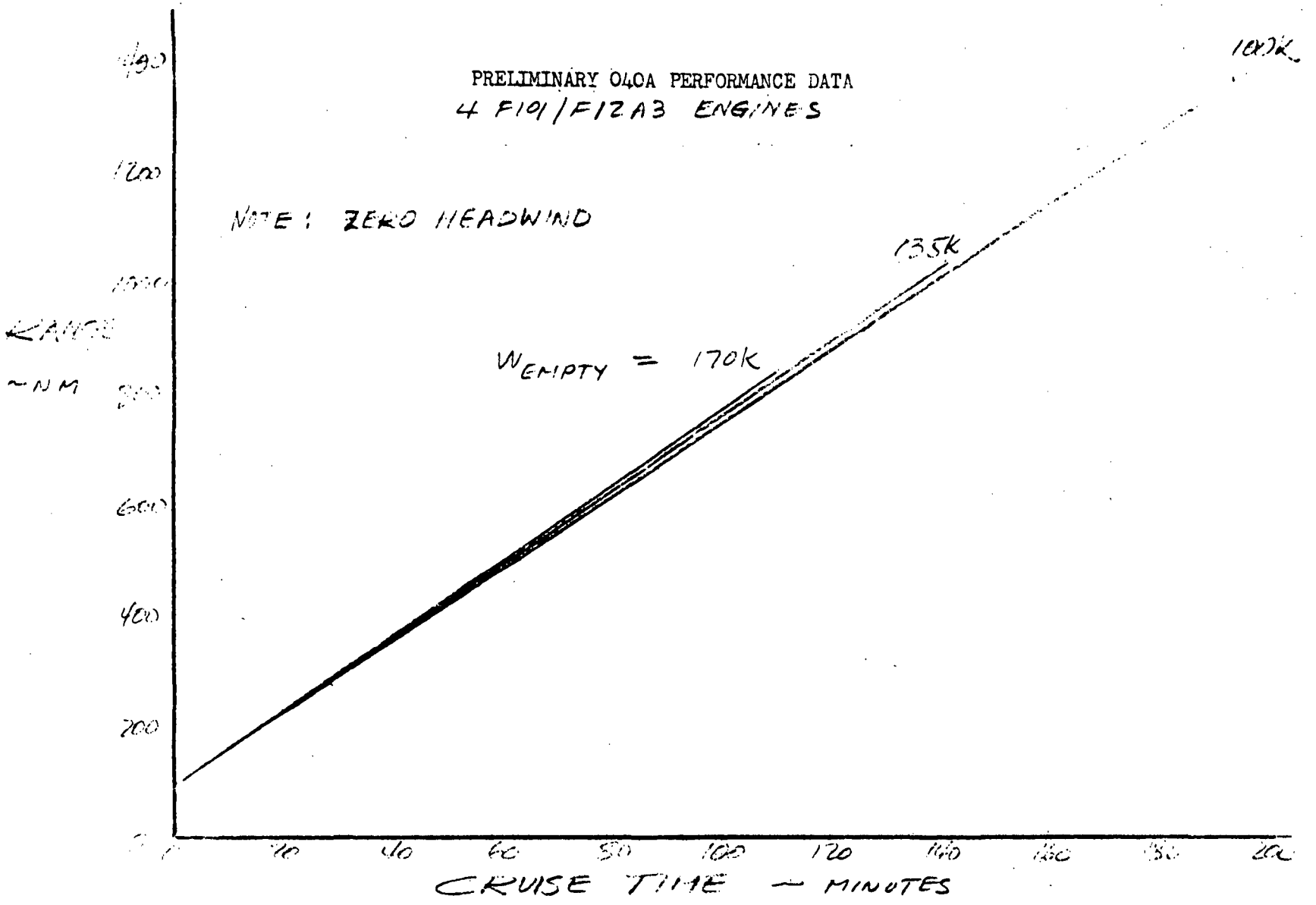

Figure 4-171. Ferry Performance, Cruise Time

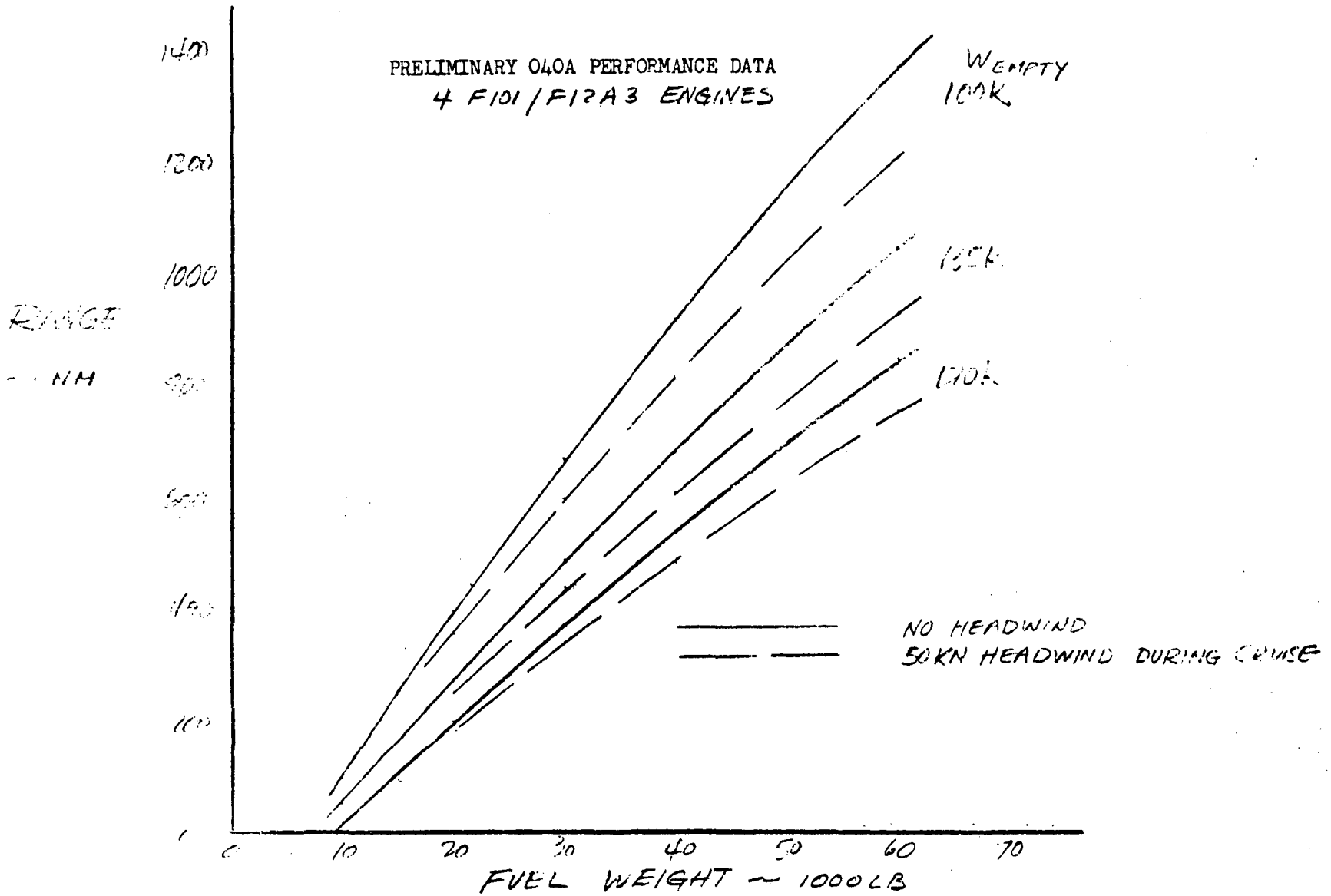

Figure 4-172. Ferry Performance, Fuel Required

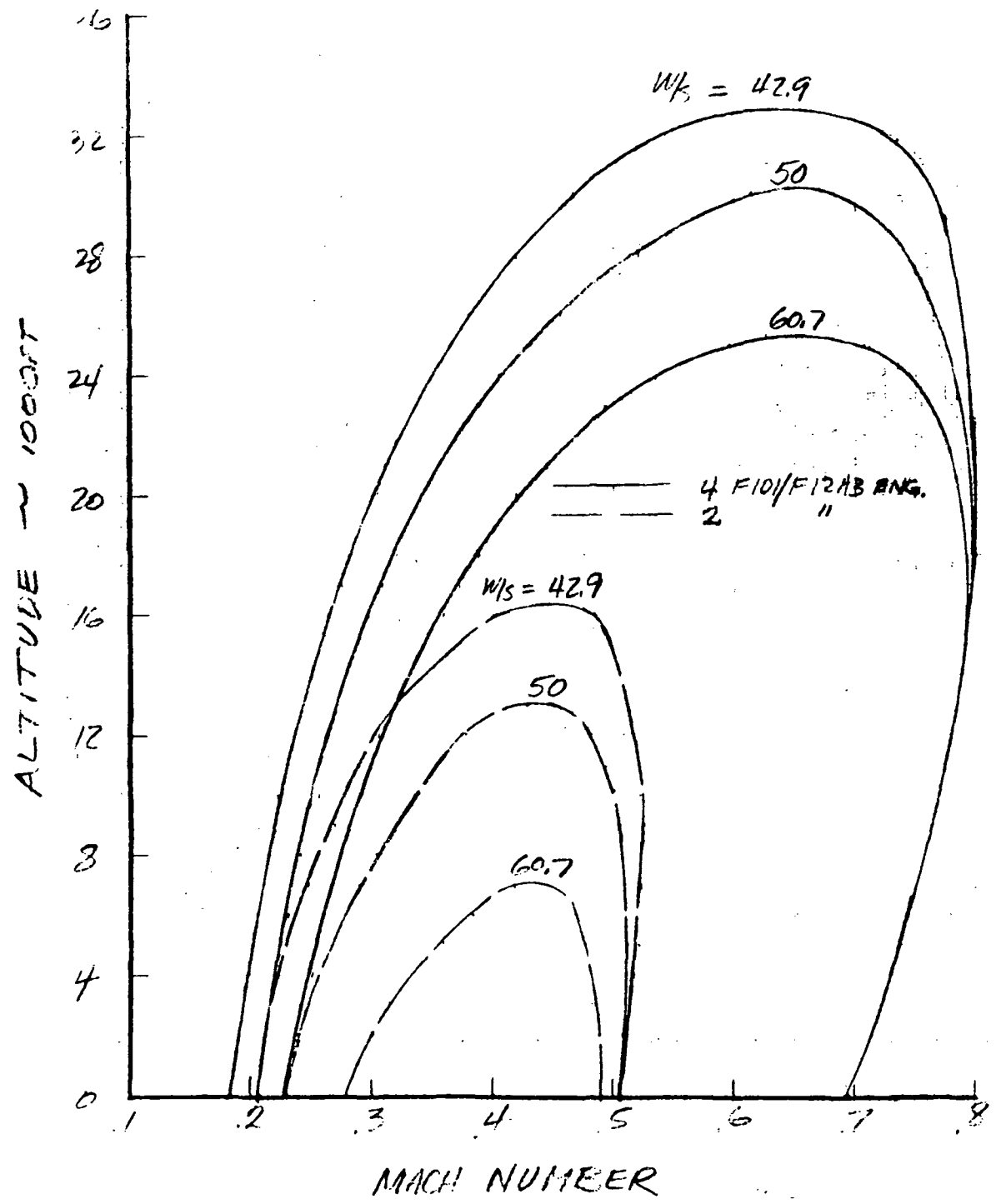

Figure 4-173. Mach Number, Altitude Profile, Standard Day

Figures 4-174 through 4-182 deleted.

4.4.3.3 Entry Trajectories

A necessary prerequisite to evaluating TPS requirements is the computation of a series of entry trajectories which equally meet required mission objectives. By doing so, a variation of the TPS environment can be obtained as an evaluation parameter. This computational step and its presentation can be illustrated by a single format of a spectrum of entry trajectories relating entry interface state (or deorbit delta V) and control mode variables with performance parameters such as lateral range and heating indicators. An example format is presented in Figure 4-183 for an orbiter configuration which was assumed to deorbit with horizontal retrothrusting from a 100-nm circular polar orbit. The entry interface state was uniquely implied with the scalar magnitude of deorbit delta V. The many-faceted control mode, described in a later section, was implied by the trim angle of attack of the vehicle through the major part of the entry flight. Thus, by use of a preliminary crossplot of lateral range, it is possible to include the four performance parameters of deorbit delta V, lateral range, stagnation heating rate, and stagnation heating load in a co-related presentation as a function of control mode.

Selection of TPS Evaluation Trajectories. The lateral range contours in Figures 4-183 and 4-189 for Mark I and Mark II orbiters, respectively, are an expression of the total ranging capability. Due to a near-symmetry of the inertial characteristics of the entry trajectories from polar orbits, the footprint width is essentially equal to twice the inertial lateral range traversed by the vehicle in either a left or right bank mode. Therefore, all trajectories selected for detailed thermal and TPS evaluations were computed with bank angle turns arbitrarily to the right.

For the short-range orbiter, Mark I, four trajectories were selected in the vicinity of a 400-nm lateral range contour (200-nm traverse) as noted by circles No. 1, No. 2, No. 3, and No. 4 on Figure 4-183. Ground tracks are illustrated in Figure 4-184. The time history of trajectory No. 4 is presented in Figures 4-185 through 4-188.

Three trajectories were selected from Figure 4-189 for the long-range orbiter, Mark II, along the 2400-nm lateral range contour (1200-nm traverse), similarily noted by circles. Ground tracks are illustrated in Figure 4-190. The time history of trajectory No. 2 is presented in Figures 4-191 through 4-194. This time history and the preceding one augment the description of the flight mode to follow.

Flight Mode. The entry flight mode consisted of a series of open-loop guidance computation legs chosen and constrained in the various state vector

regimes. These controls were an accumulation of best-results experience of several analysts and can be summarized as follows:

Leg 1: Flight at constant angle of attack (usually at zero bank angle) from the entry interface state to the pull-out state.

Leg 2: Flight at constant stagnation heating rate (pull-out value) by bank angle modulation at constant angle of attack (when possible) until a descent limit flight path angle of -0.2 degree was reached. This stage cutoff was conditional to an altitude in excess of 230,000 feet.

Leg 3: Flight at a constant rate of change of flight path angle of -0.00025 deg/sec by bank angle modulation at a constant angle of attack until a bank angle limit of 15 degrees from the vertical plane was attained.

Leg 4: Flight at a constant angle of attack at the fixed bank angle of cutoff of Leg 3 to a velocity cutoff of 3000 fps.

Leg 5: This terminal leg was defined by a constant pitch rate from the constant value of flight angle of attack to a value of 15 degrees in the leg time of 200 seconds. Termination of the entry phase was subsequently defined at an altitude cutoff of 50,000 feet.

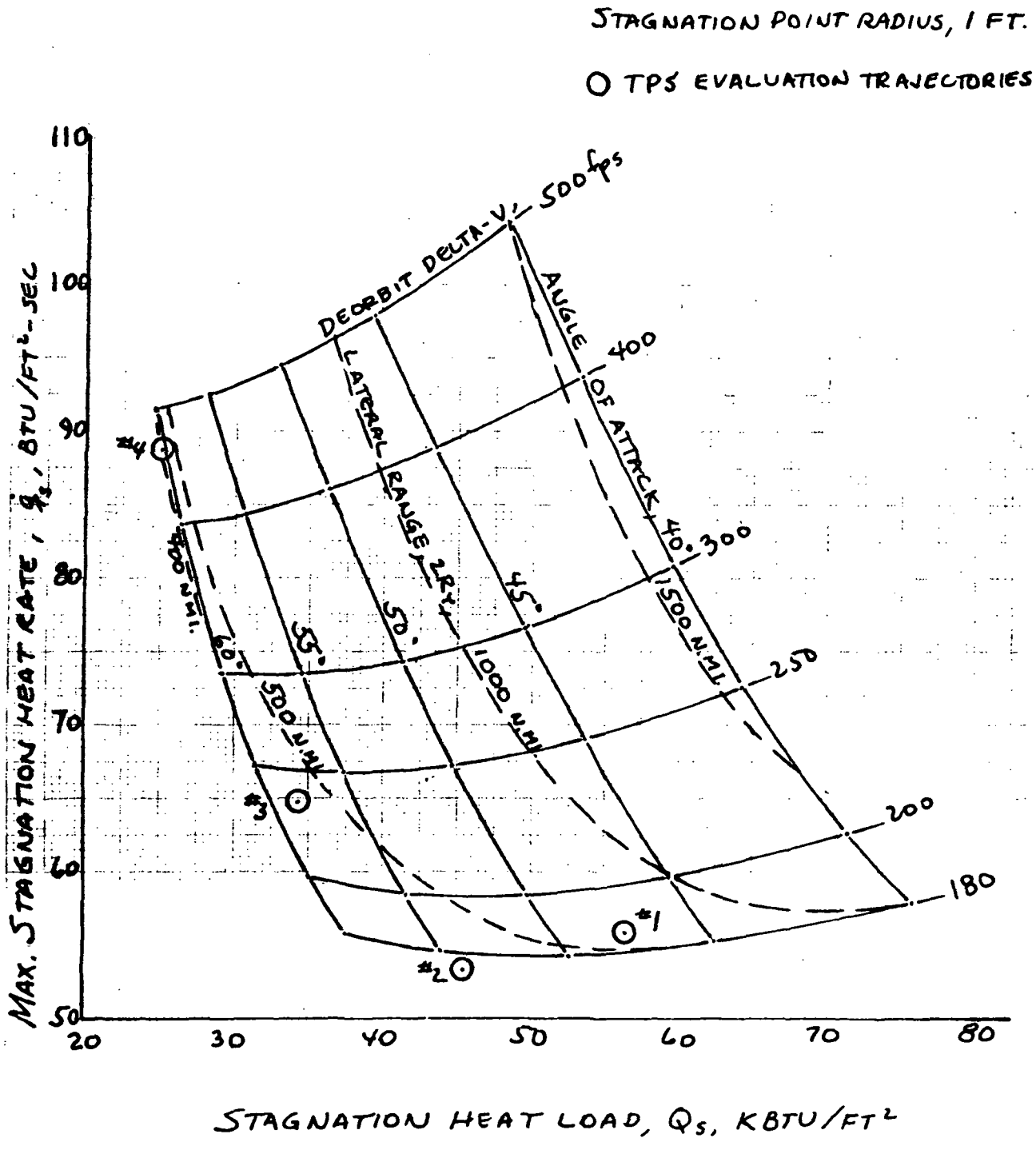

Figure 4-183. Entry Heating Indicator Performance Format, Short Cross-Range Orbiter, Mark I

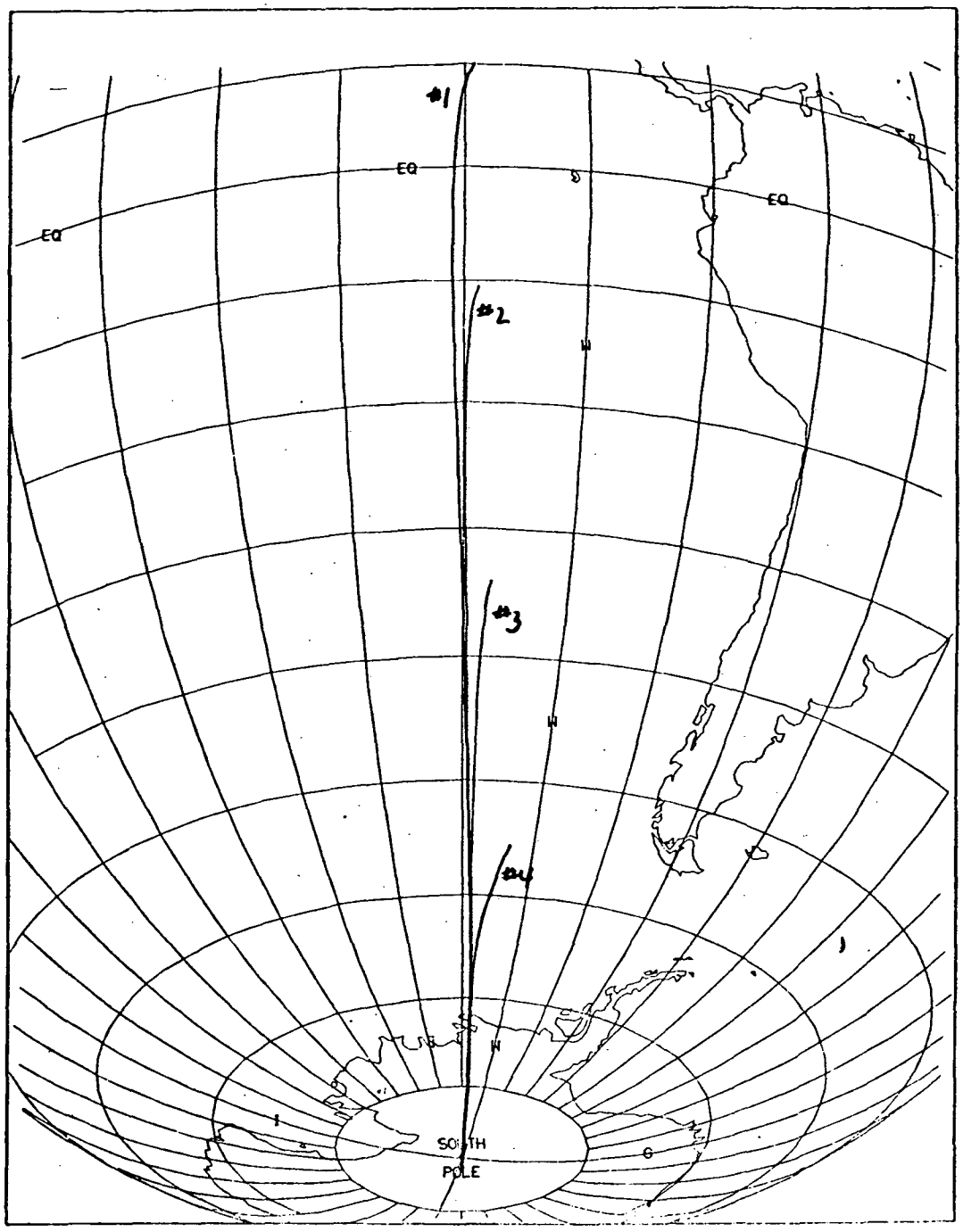

Figure 4-184. Ground Track of TPS Evaluation Trajectories, Short Cross-Range Orbiter, Mark I

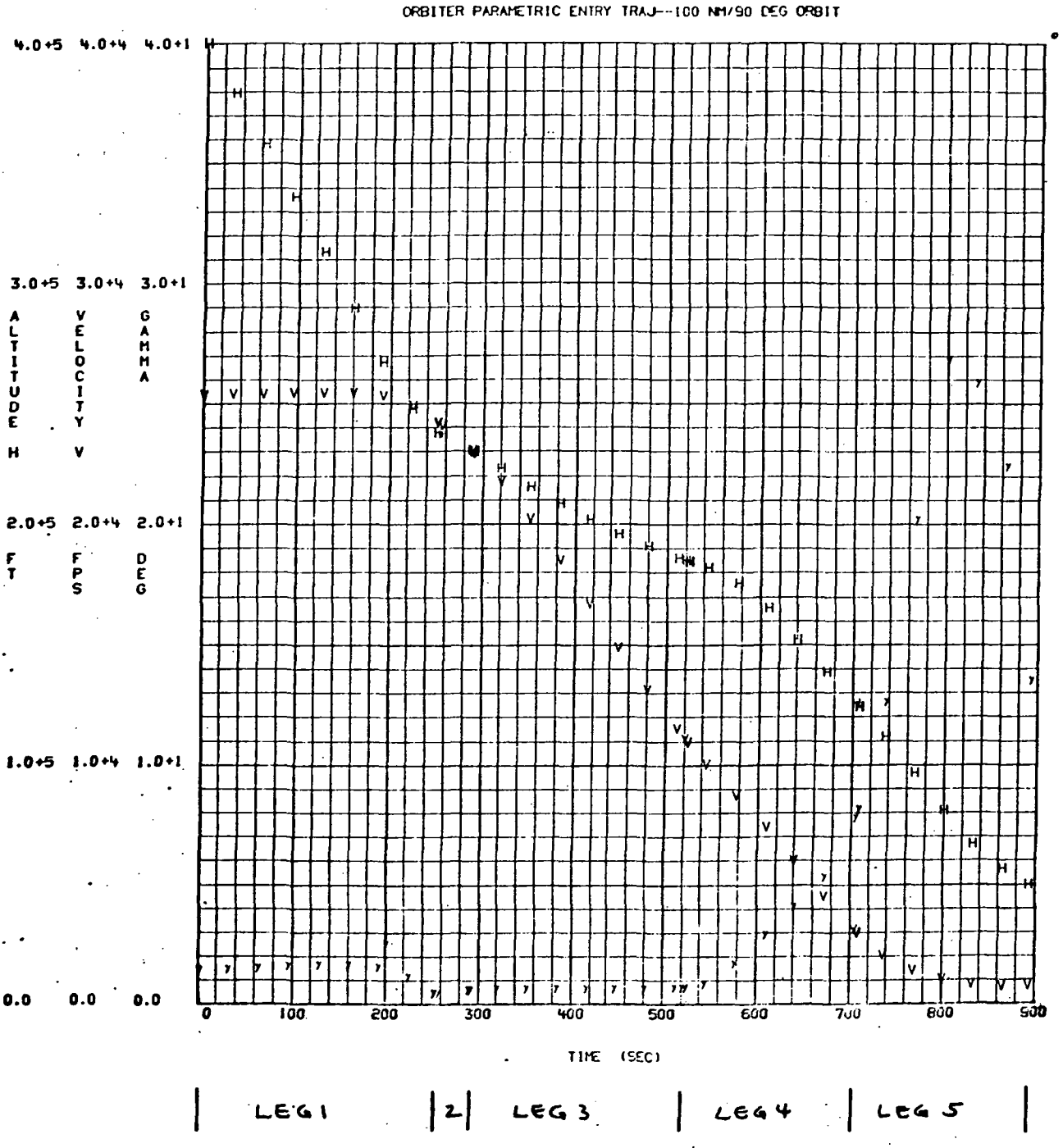

Figure 4-185. Entry Time History, Altitude, Velocity, and Flight Path Angle; Short Cross-Range Orbiter, Mark I

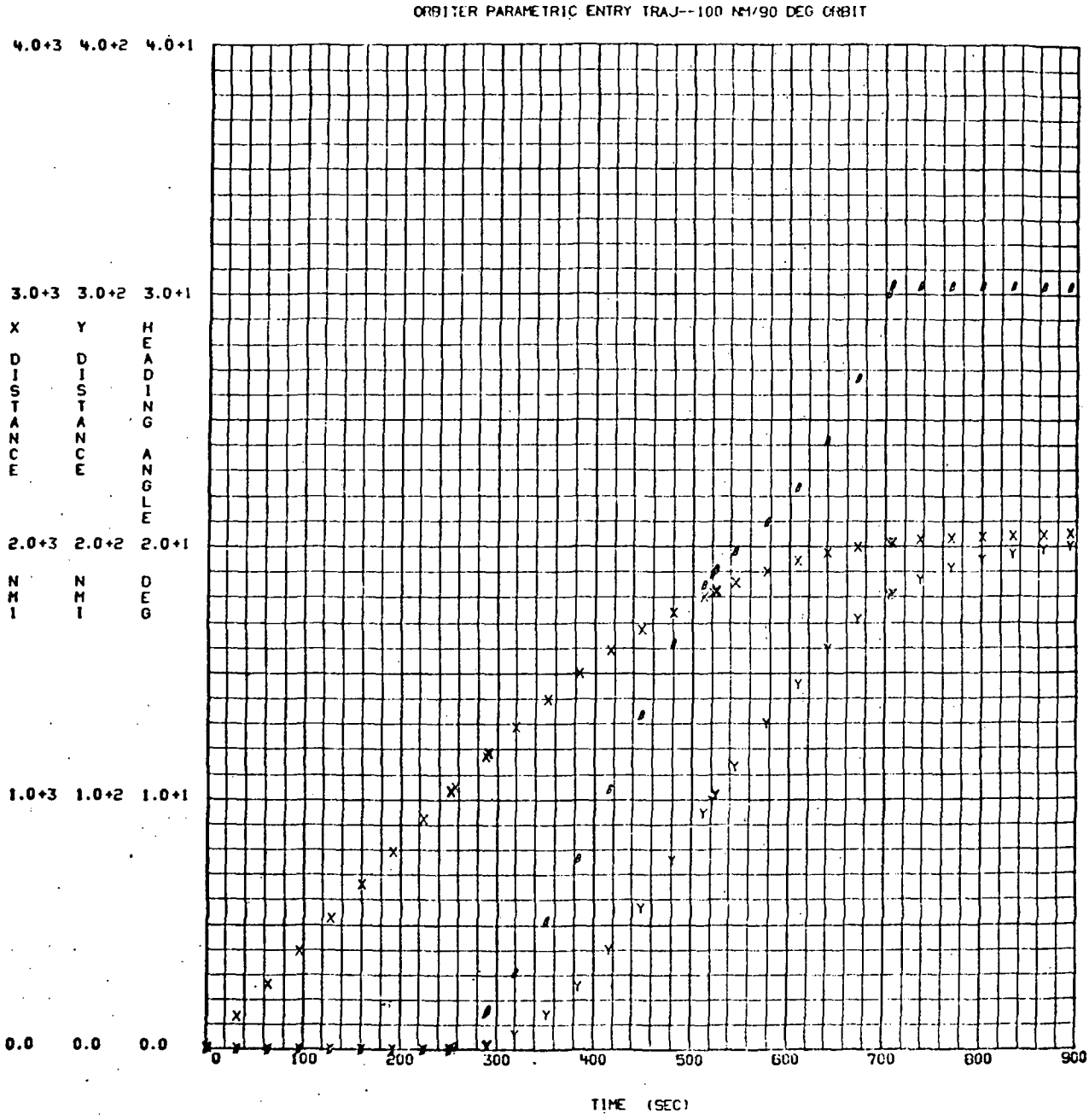

Figure 4-186. Entry Time History, X-Range, Y-Range, and Heading Angle; Short Cross-Range Orbiter, Mark I

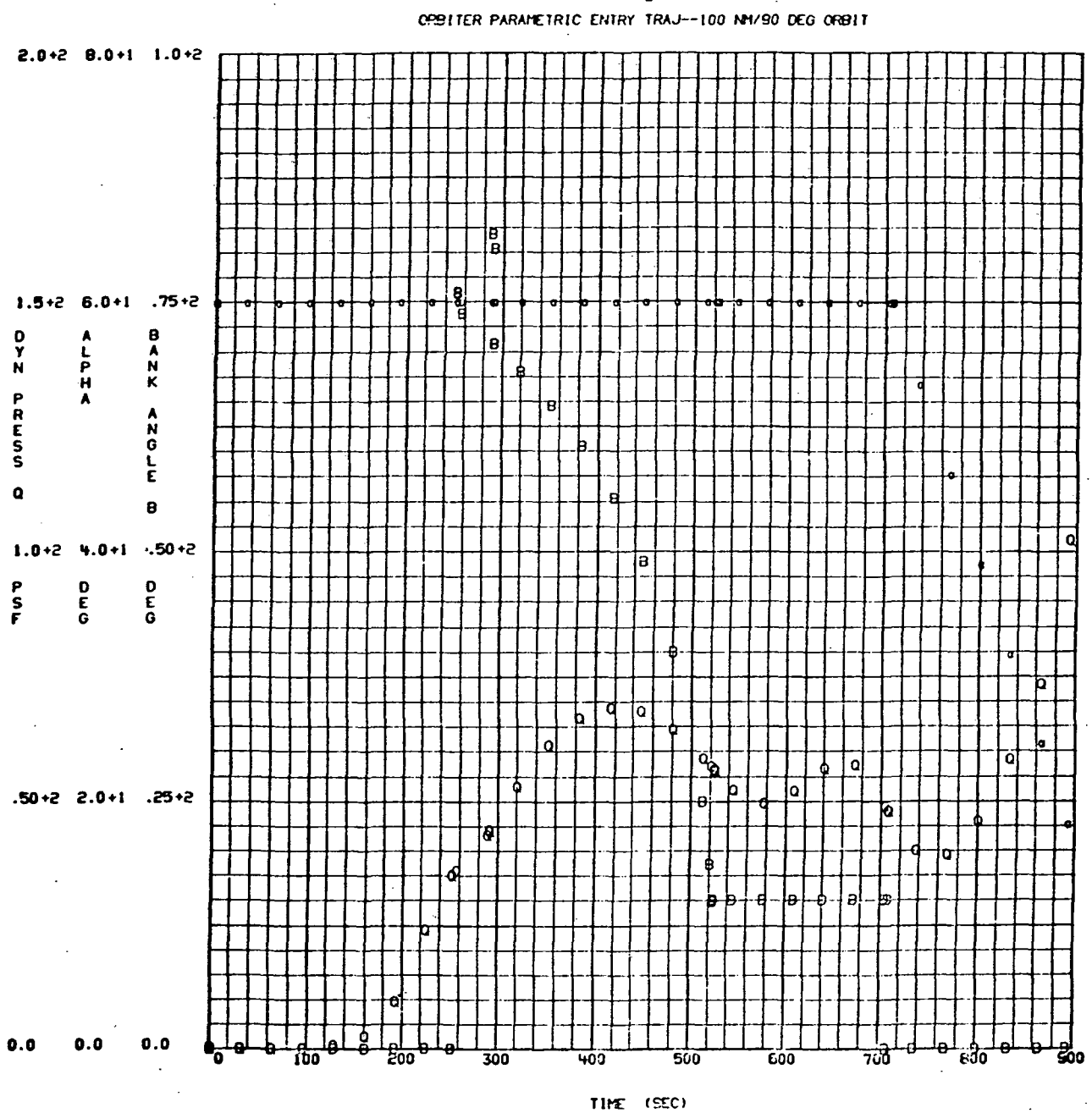

Figure 4-187. Entry Time History, Dynamic Pressure, Angle of Attack, and Angle of Bank; Short Cross-Range Orbiter, Mark I

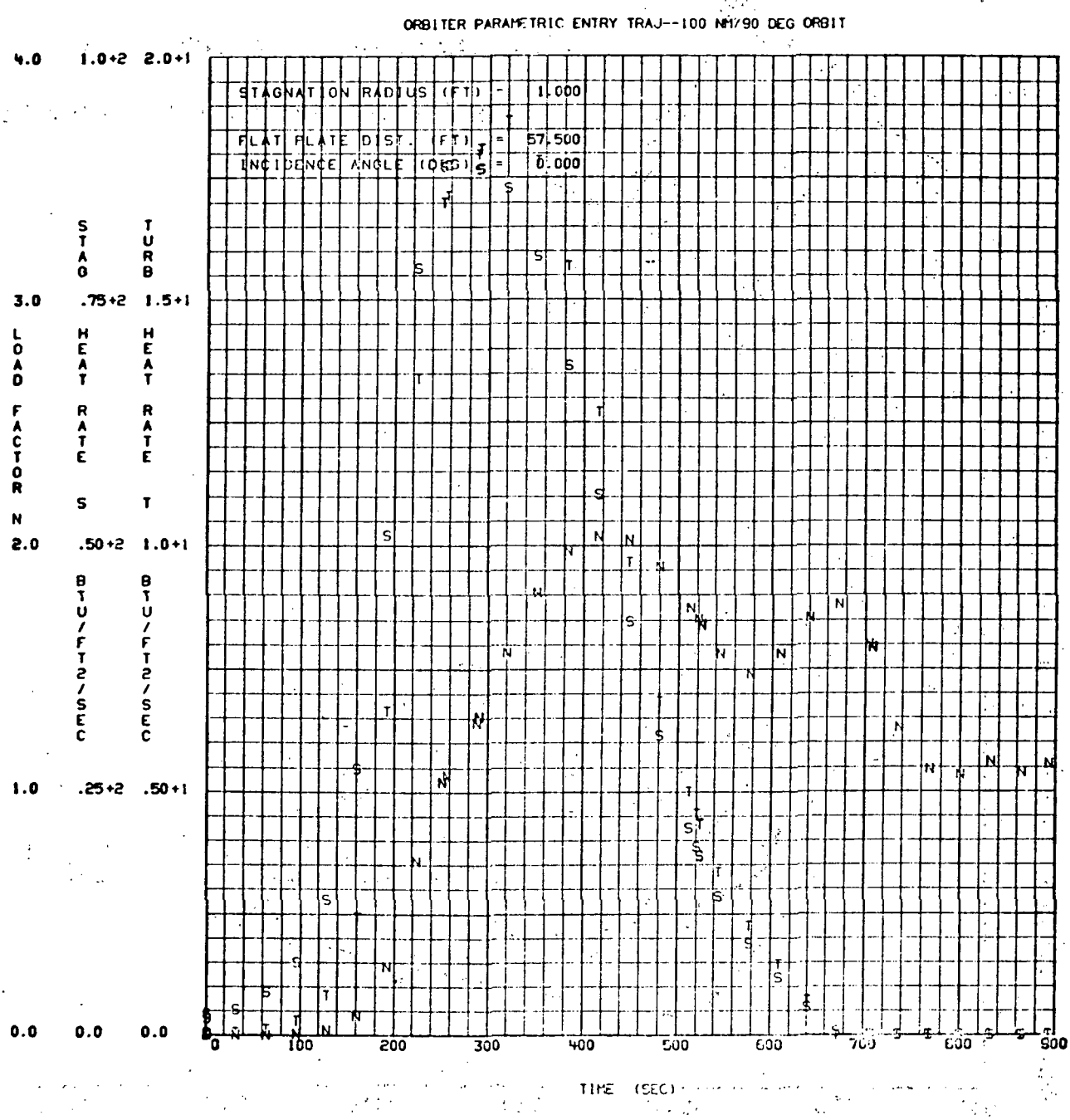

Figure 4-188. Entry Time History, Load Factor, Stagnation Heating Rate, and Turbulent Heating Rate; Short Cross-Range Orbiter, Mark I

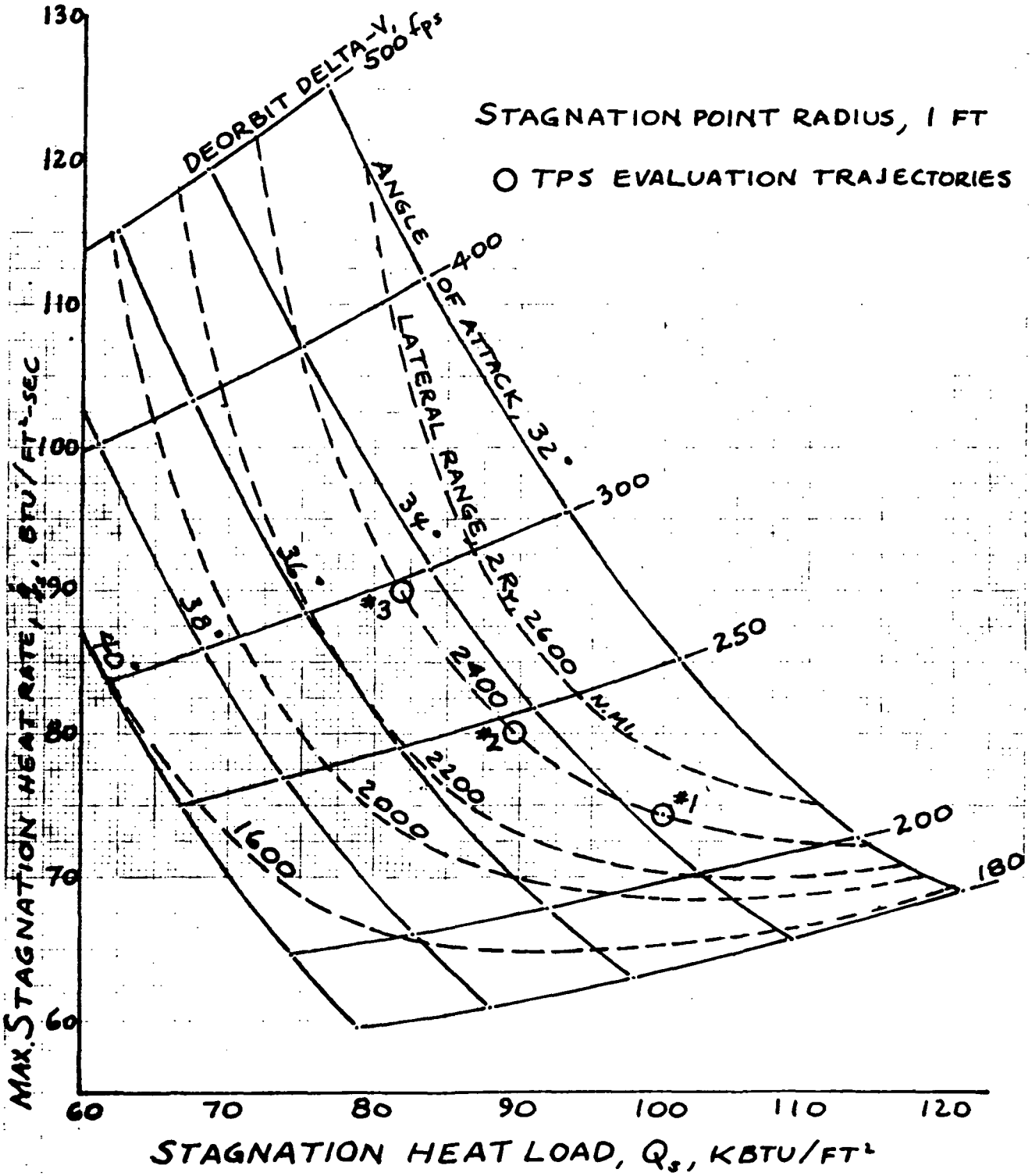

Figure 4-189. Entry Heating Indicator Performance Format; High Cross-Range Orbiter, Mark II

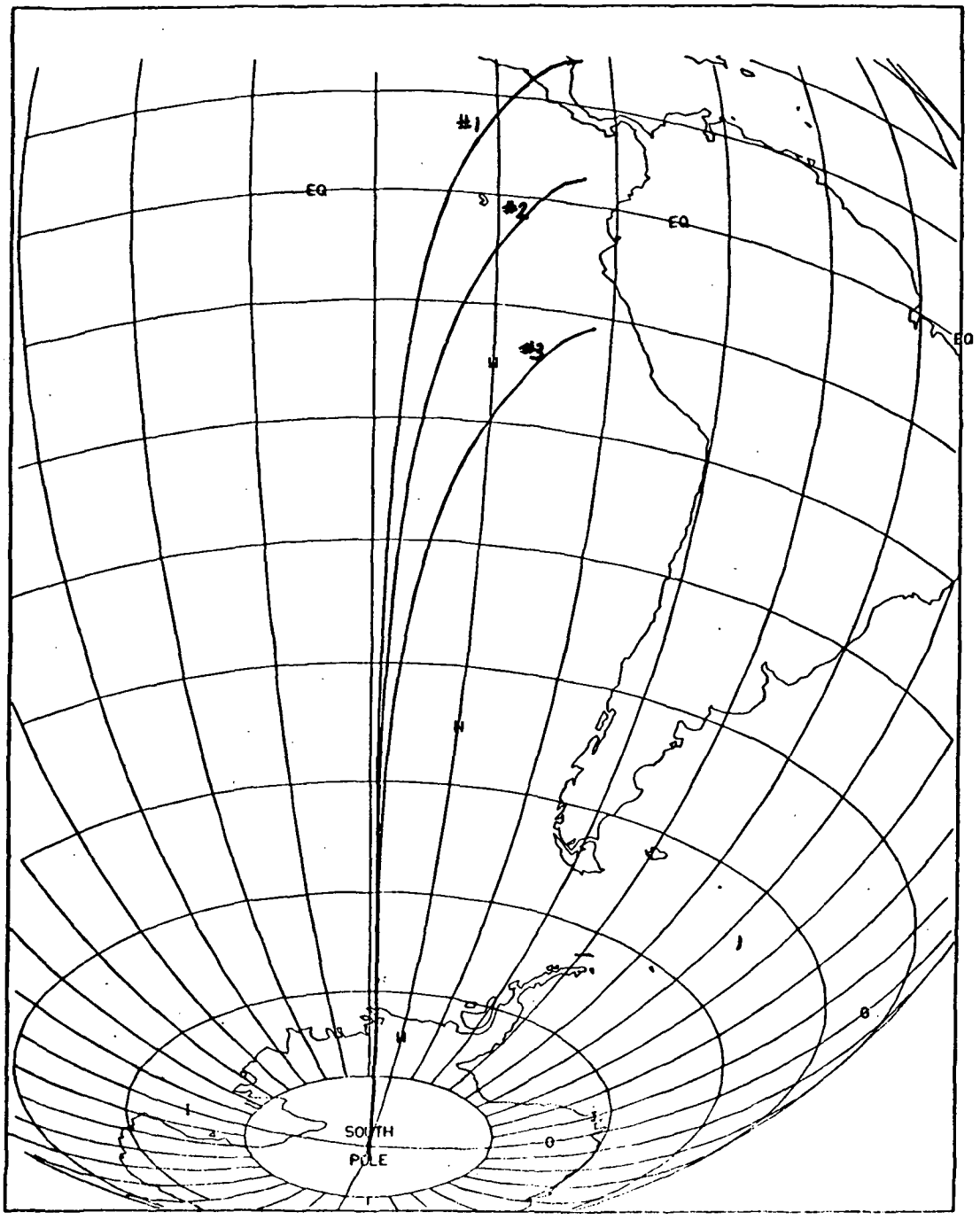

Figure 4-190. Ground Track of TPS Evaluation Trajectories; High Cross-Range Orbiter, Mark II

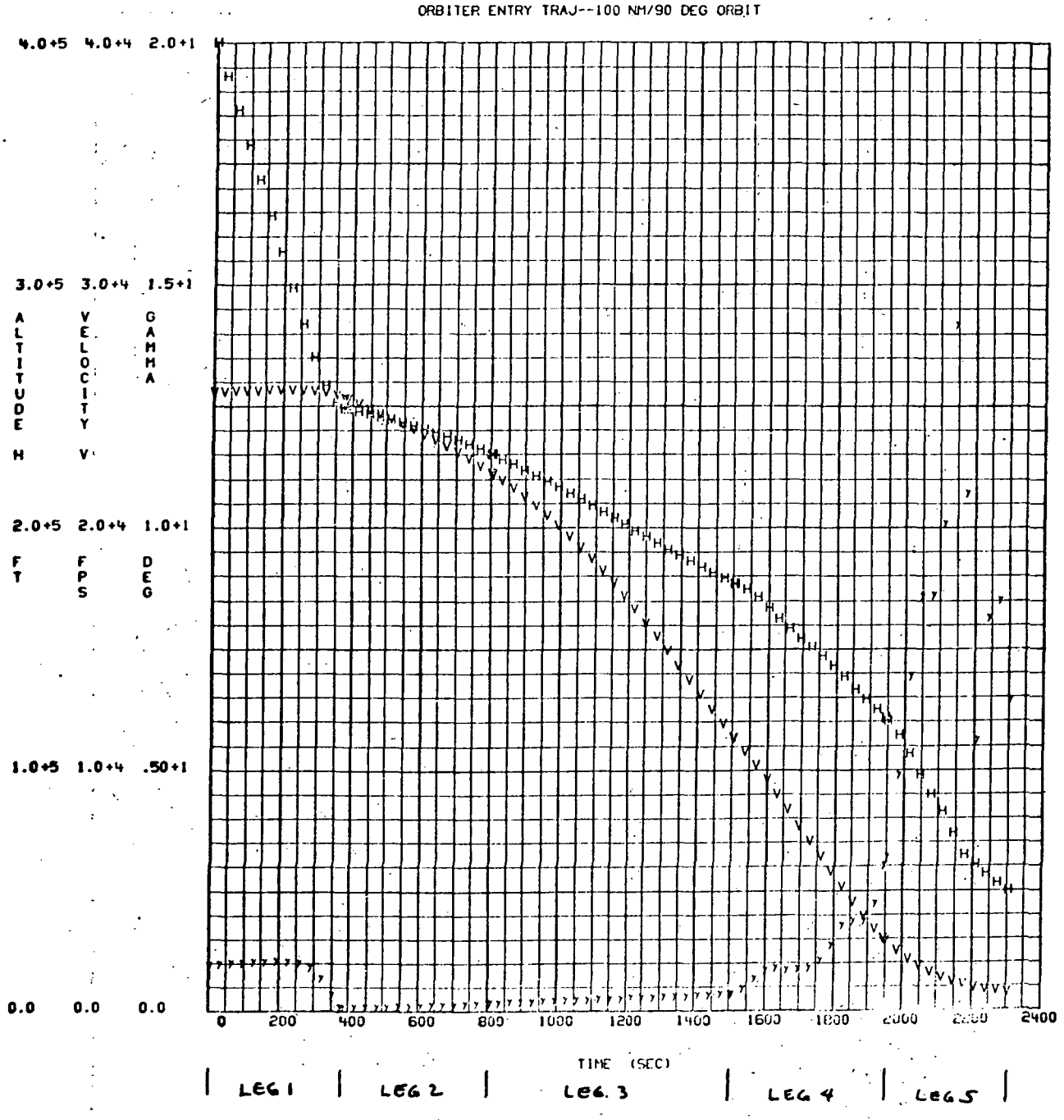

Figure 4-191. Entry Time History, Altitude, Velocity, and Flight Path Angle; High Cross-Range Orbiter, Mark II

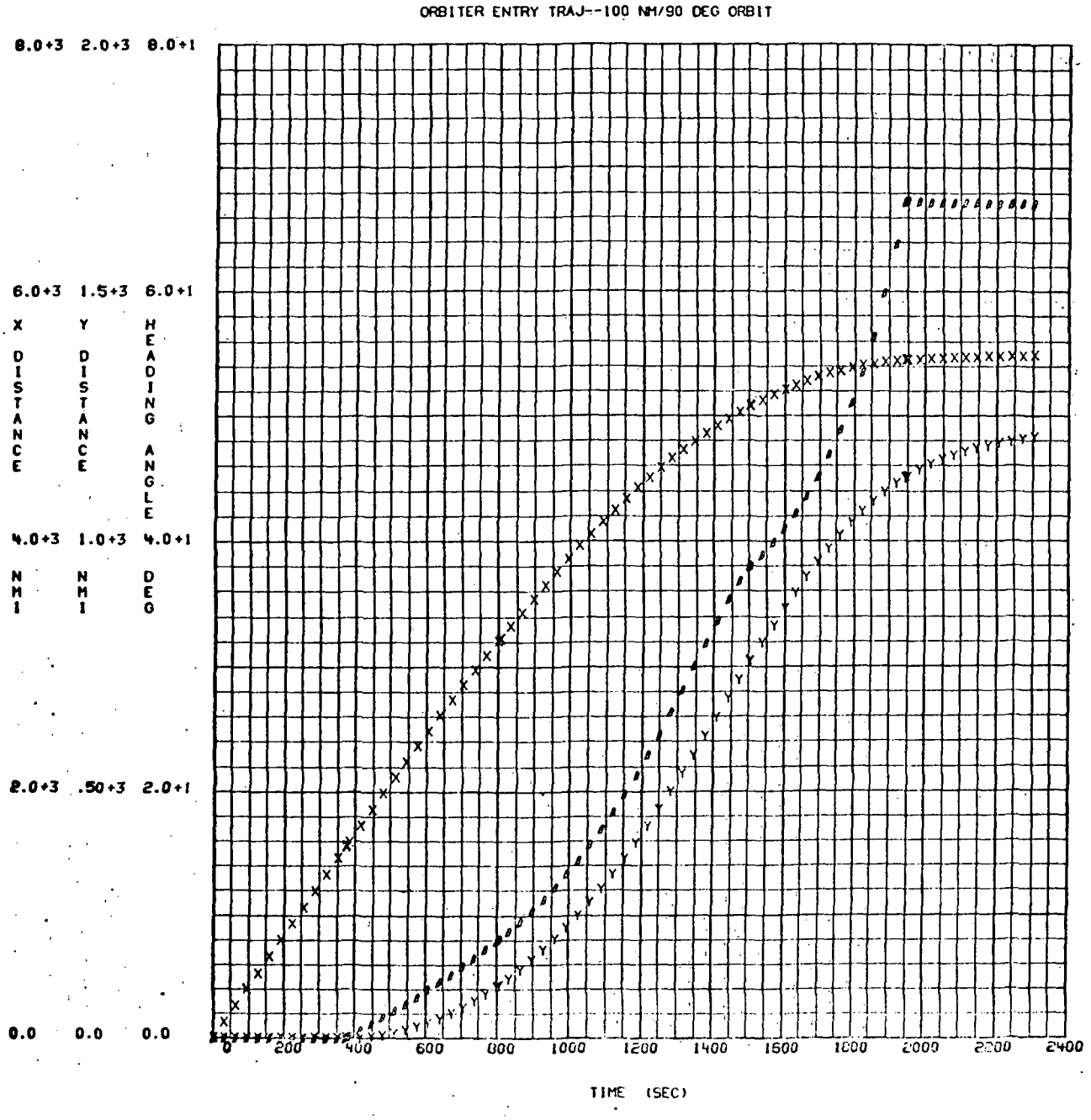

Figure 4-192. Entry Time History, X-Range, Y-Range, and Heading Angle; High Cross-Range Orbiter, Mark II

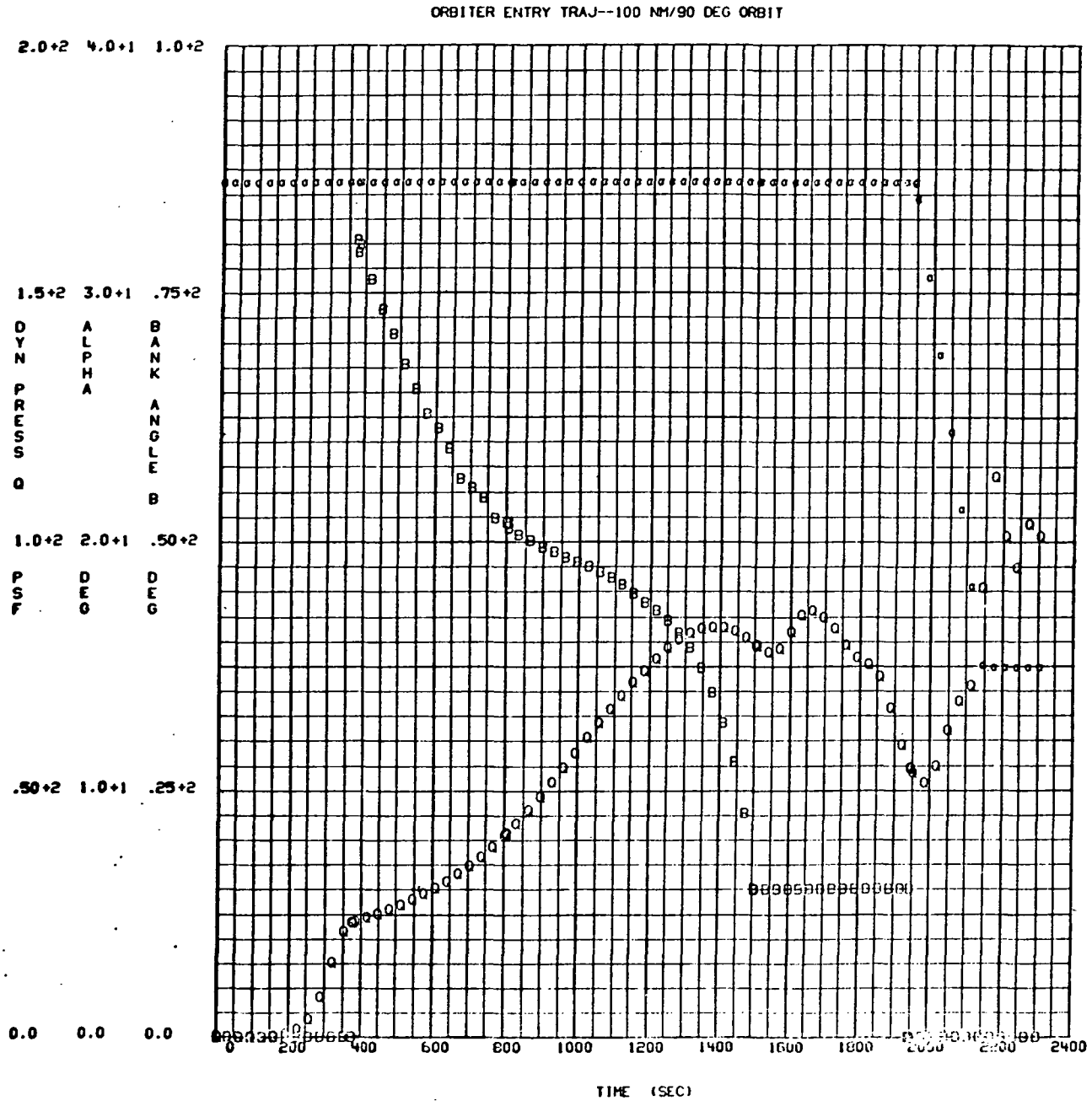

Figure 4-193. Entry Time History, Dynamic Pressure, Angle of Attack, and Angle of Bank; High Cross-Range Orbiter, Mark II

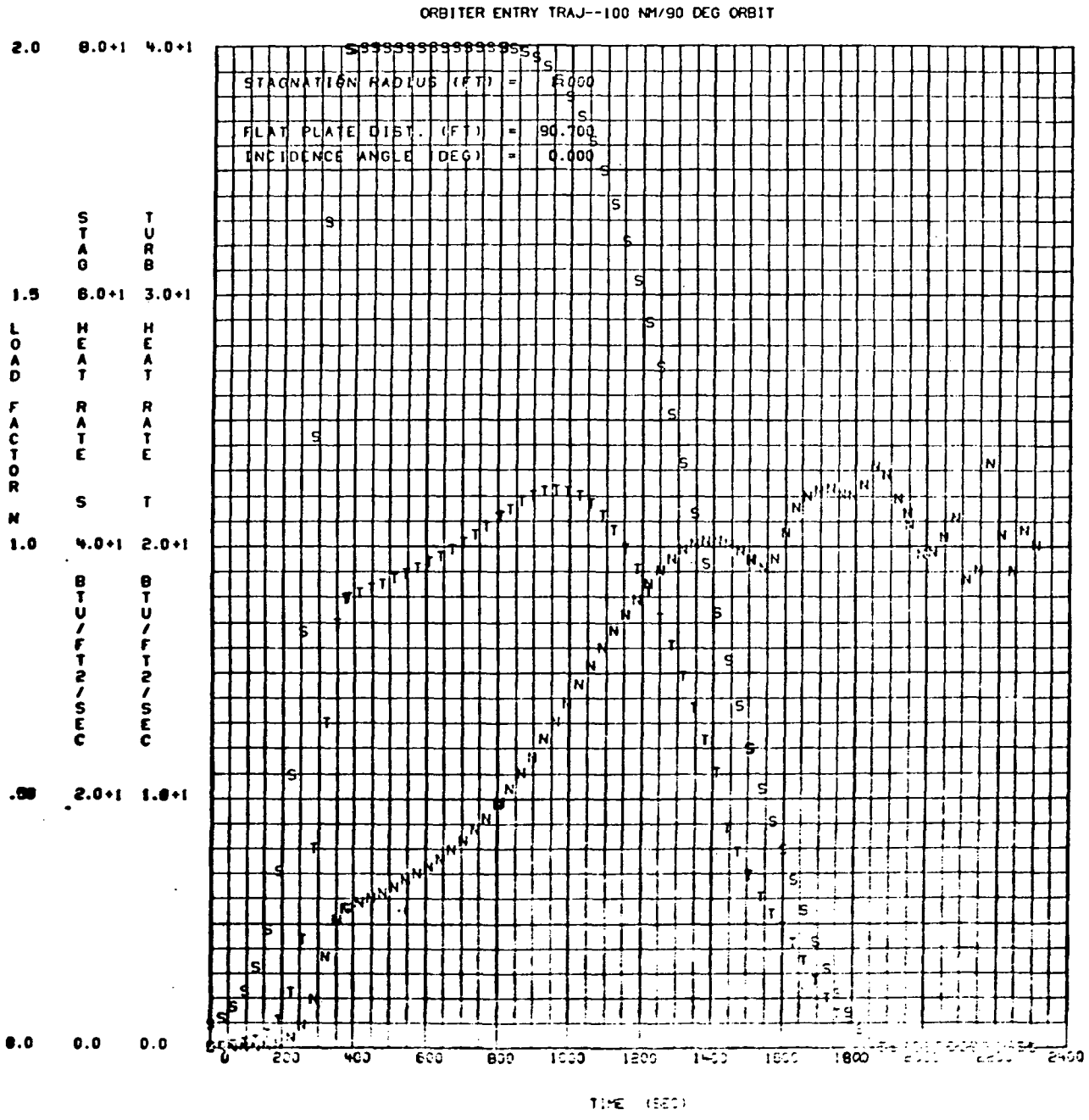

Figure 4-194. Entry Time History, Load Factor, Stagnation Heating Range, and Turbulent Heating Rate; High Cross-Range Orbiter, Mark II

4.4.3.4 Orbiter Control Requirements

The orbiter MPS consists of four J-2S engines and utilizes off-the-shelf J-2 actuators. The total gimbal throw available is 14.6 degrees peak-to-peak. The gimbal requirement is defined by the center-of-gravity travel during boost, the capability to trim engine or actuator failures, and an allowance to account for dynamic transients and bending and slosh suppression. The nominal center-of-gravity travel requires thrust vector angles in pitch ranging from -6.3 degrees to -13 degrees relative to the fuselage centerline. To additionally handle one engine out, this range increases to -4.25 degrees to -14.25 degrees. An actuator failure hard-over exceeds the J-2 actuator capability. An actuator failed to null requires -5 degrees to -14.75 degrees. If a dynamic allowance of 1.5 degrees (estimated from Phase B studies) is superimposed, the total range becomes -2.25 degrees to -16.75 degrees, a total range of 14.5 degrees. The J-2 actuator can thus control the orbiter, but requires a fail-to-null actuator design.

The orbiter is equipped with 32 ACPS thrusters contained in two pods located at the wing tips and a third pod mounted on the vertical tail (see Figure 4-195). The thrusters develop 1050 pounds of thrust and have an I_{SP} of 290 seconds. Maneuver propellants, shown in Table 4-33, represent requirements for 1 deg/sec rotational maneuvers, 1 ft/sec translation, and ±1 deg limit cycles.

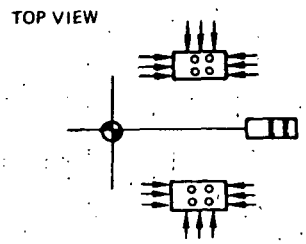

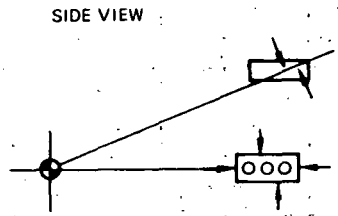

MANEUVER ROTATIONS	SECOND ORDER EFFECTS	THIRD ORDER EFFECTS	REMARKS
PITCH	X COUPLE INTO X & Z	X & Z TRANSLATION REDUCE PITCH ACCELERATION	TRUE FOR ALL CASES
ROLL	X COUPLE INTO Z TRANSLATION (FOR SINGLE ENGINE FIRE)	———	CORRECTIVE Z FIRING WILL NEGATE ROLL
	NO X COUPLE WHEN 2 THRUSTERS ARE FIRED	———	———
YAW	FIRE ± X TRANSLATION THRUSTERS NO X COUPLING	———	———
TRANSLATIONS			
±X	NO X COUPLING	———	MUST FIRE THRUSTER IN PAIRS
±Y	X COUPLING IN YAW	FIRE ± X TRANSLATION	———
±Z	X COUPLING IN PITCH	FIRE PITCH THRUSTERS WHICH IN TURN REQUIRES X & Z THRUSTER FIRING	REQUIRES ADDITIONAL PROPELLANT

Figure 4-195. Pod Installation Cross Coupling

Table 4-33. On-Orbit Maneuver Propellant Consumption

On-Orbit		*Docking	
Rotation	Limit Cycle	Rotation	Translation
ϕ 2.7	0.00244	2.7	X 42
θ 12.1	0.00543	54.4	Y 84
ψ 22.2	0.00294	22.2	X 147
*Includes propellant required for cross-coupling compensation.			

The roll and yaw rotation ACPS control are pure couples, but pitch rotation results in both X and Z translation. For translation control, plus X translation is accomplished without cross-coupling, plus Y translation produces 0.325 deg/sec^2 yaw angular acceleration, and Z translation results in 0.675 deg/sec^2 in pitch. The latter results in large propellant penalties during rendezvous and docking.

The control of the orbiter during entry was evaluated using an all-ACPS control mechanization with aero surface trim assist. The analyses were performed using the 110E aerodynamics and mass inertia properties, and the high cross-range entry profile.

The baseline entry control mechanization consists of an angle-of-attack command with pitch rate feedback in pitch, roll attitude and roll rate in roll, and lateral acceleration and yaw rate in yaw. The ACPS acceleration requirements during entry are summarized in Figure 4-196. The most stringent requirement is that of yaw with 1.30 deg/sec^2 of yaw acceleration being required. This requirement was derived based on the entry profile of Figure 4-197 and a side slip budget consisting of 0.86 degree of side slip occurring with 2.0 deg/sec roll reversals, and 0.3 degree associated with a lateral acceleration bias induced by antisymmetric structural mode displacement of 0.2 degree. A wind gust of 30 feet/sec at an altitude of 70,000 feet was also included in the budget to raise the side slip angle safety margin to 1.75 degrees. The yaw acceleration requirements sized the ACPS jet thrust level at 1050 pounds.

The entry ACPS propellant consumption requirement is 750 pounds. Trim control of the orbiter is achieved by use of the elevons. The elevon hinge moment requirement of 1.92 (10^6) inch-pound for entry is no longer the determining factor in sizing the hydraulic subsystem because of the low

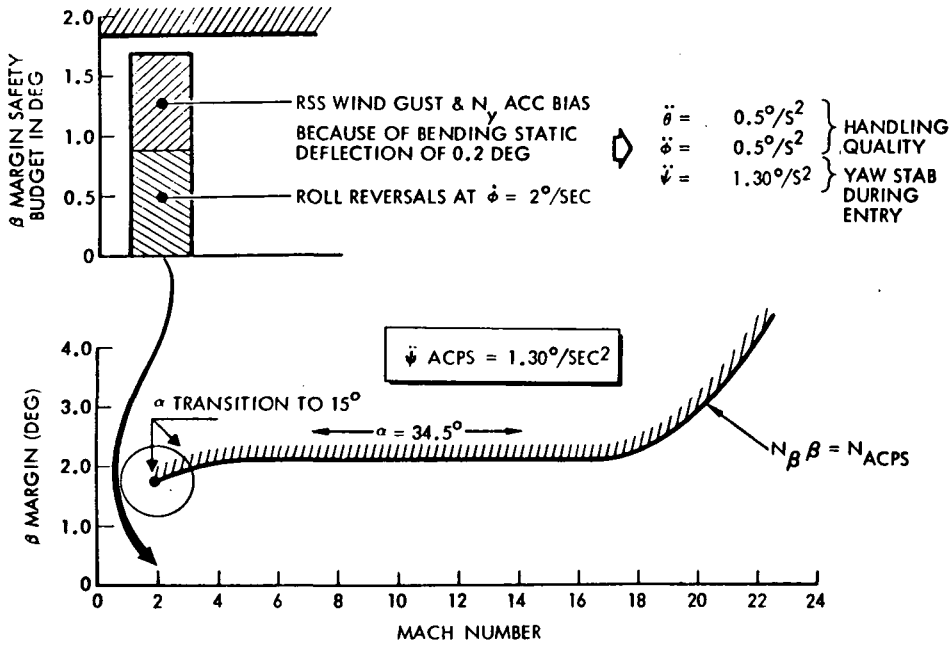

Figure 4-196. Mark II ACPS Acceleration Requirement

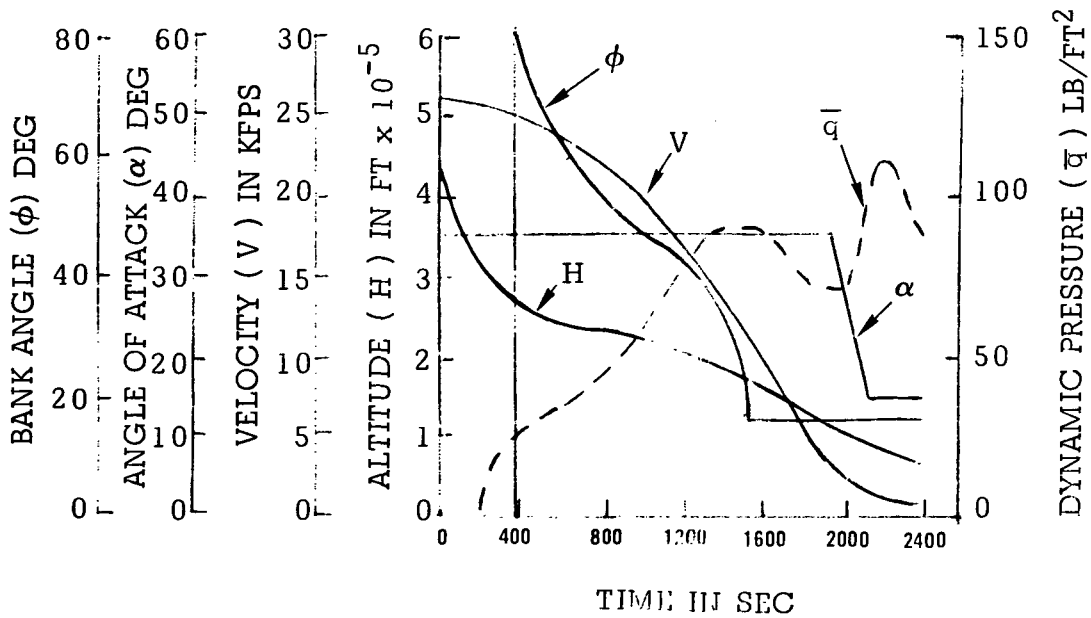

Figure 4-197. 110E (Mark II) Entry Profile

dynamic pressure (120 psf) associated with the 110E orbiter during entry. The elevon hinge moment required during approach to meet the 30 degrees of bank angle in 2.5 seconds requirement equals that required during entry.

An alternate control mechanization was evaluated, consisting of full elevon pitch control with ACPS control in roll and yaw. This concept does not increase the elevon hinge moment requirement and results in an ACPS propellant consumption saving of 300 pounds or a 40-percent reduction. This concept has not been incorporated in the baseline control because the increase in system complexity incurred with blended aero surface and ACPS control has not been fully evaluated.

The switch over from ACPS to aero surface control is scheduled to take place subsequent to the termination of the angle-of-attack transition from 34.5 degrees to 15 degrees. The switchover is to occur on all three axes simultaneously at the end of the angle-of-attack transition because the rudder does not become effective until the angle of attack has been reduced below 20 degrees. The aero surface control switchover will occur without severe transients since the aero surfaces have been utilized for trim control during the earlier phase of entry.

4.4.3.5 Orbiter Loads

Structural loads were computed for selected conditions found to be critical in Phase B studies. The loads for the maximum $q\alpha$ boost condition were based on a 95-percentile wind speed envelope plus gust at 10-km altitude. Flight control studies conducted during Phase B yielded the following design criteria: maximum $q\alpha = \pm$ 2800 psf-degrees for headwind and tailwind cases, and maximum $q\beta = \pm$ 2400 psf-degrees for cross-wind cases. Subsequent studies have shown those criteria to be adequate for the configurations studied during the Phase B extension, although control system optimization studies are continuing. Loads were also computed for the maximum acceleration condition at booster end burn and for the orbiter start burn, maximum thrust, and end burn conditions. Other load conditions included in the study were orbiter entry, subsonic maneuver, landing and taxi. Orbiter limit loads are shown in Tables 4-34 and 4-35.

Table 4-34. Orbiter Limit Loads, Body Loads

Load Condition	Body at Station 534 Forward			Body at Station 1250 Forward		
	Axial (10^3 lb)	Shear (10^3 lb)	Moment (10^6 in-lb)	Axial (10^3 lb)	Shear (10^3 lb)	Moment (10^6 in-lb)
High q boost headwind	-93.8	-24.4	2.3	-377.0	123.6	-71.3
Tail wind	-80.8	24.4	-4.1	-336.7	9.2	-77.2
Booster end burn	-81.7	5.0	-2.1	-410.5	96.8	-69.2
Orbiter start burn	-31.0	-6.9	0.2	-156.0	-82.4	4.3
2.5-g maneuver	-	7.8	3.3	-	-176.5	-12.2
Landing	-31.0	48.3	-4.5	62.5	-62.3	-18.6
Positive loads when integrating nose to tail: forward axial down shear up moment						

Table 4-35. Orbiter Limit Loads, Wing Loads

Load Condition	Wing Loads at Root BP 125	
	Shear (10^3 lb)	Moment 10^6 (in-lb)
High-q boost head wind	-87.3	9.1
High-q tail wind	215.2	-31.8
2.5-g maneuver	-147.8	21.1
Positive loads: down shear up moment		

4.4.3.6 Thermal Environment

Aerodynamic Heating. An evaluation was made of the ascent and entry environments of the VC70-0176 orbiter configurations. Because of the geometric similarity between the VC70-0176 configuration and previous configurations, use was made of the aeroheating analysis results for these similar configurations in predicting the ascent heating environment of the -0176 configuration. Phase B methods were used in analyzing the aerodynamic heating.[1] Tank-orbiter interference flow field phenomena, during ascent, were analyzed using semiemperical methods, Titan III, and Phase B ascent configuration experimental data to obtain ratios of interference to the undisturbed heat transfer rates.

Ascent Aerodynamic Heating. The maximum undisturbed convective heat transfer rate and integrated heat load distributions on the orbiter with the LO_2/RP flyback boost ascent trajectory are presented in Figures 4-198, 4-199, and 4-200. Data are presented for the fuselage lower and upper centerline and the wing lower surface at 50 percent of the exposed span.

The undisturbed aeroheating analysis results for the pressure-fed booster system ascent flight mode are presented in Figures 4-201 through 4-206. The data are based on analysis of a geometrically similar orbiter configuration. The maximum convective heat transfer rate and integrated heat load distributions are presented for the fuselage lower and upper surface centerlines, the leading edge of the vertical tail, the vertical tail sides at 50 percent exposed span, and the lower and upper surface of the wing at 50 percent exposed semispan.

Figure 4-207 presents the interference heating factors as a function of ascent flight time and selected locations on the lower surface centerline of the orbiter. In the transition flow regime (continuum to free molecular), the interference heating was assumed to vary expotentially with Knudsen number.

[1] Space Shuttle Phase B Final Report, Vol. II, Technical Summary, Book 2, Orbiter Definition, Space Division, North American Rockwell Corporation, SD 71-114-2 (26 Mar 1971).

Entry Aerodynamic Heating. The maximum heating rate and total heat load distributions on the lower and upper surface centerline and on the wing upper and lower surface at 50 percent of the exposed semispan are presented in Figures 4-208 through 4-211, respectively, for the Mark I entry flight mode. Corresponding data are presented in Figures 4-212 through 4-215 for the Mark II entry flight mode. Laminar to turbulent boundary layer transition is based on the criteria of $Re_\theta/M_L = 225$. The entry trajectories are defined in Section 4.4.3.3. Trajectory 4 (Figures 4-185 through 4-188) was used to predict the environment for Mark I, while Trajectory 2 (Figures 4-191 through 4-194) was used for Mark II.

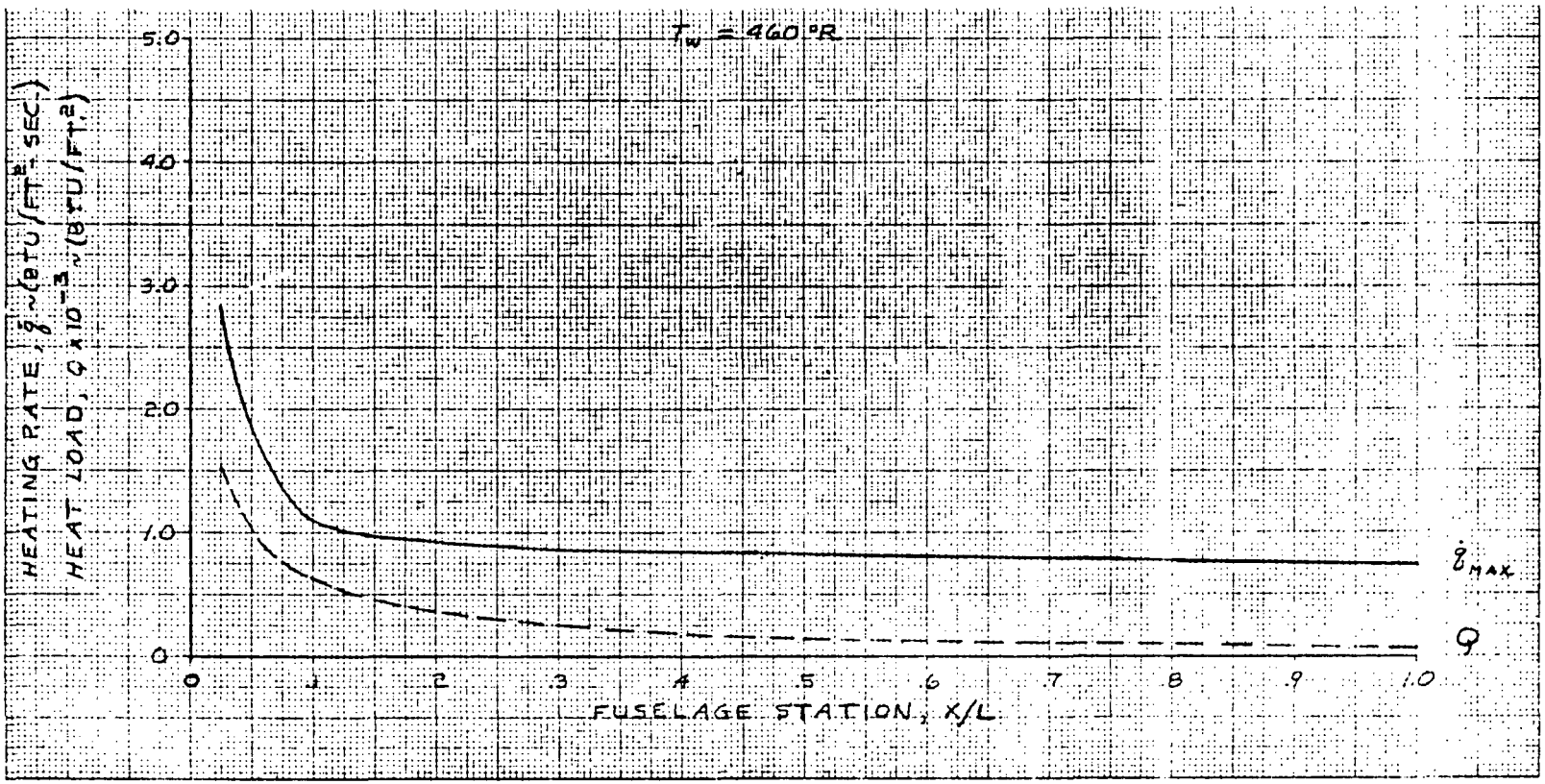

Figure 4-198. Maximum Heating Rate and Load Distribution on Orbiter Fuselage Lower Centerline, Ascent, LO_2/RP Flyback System

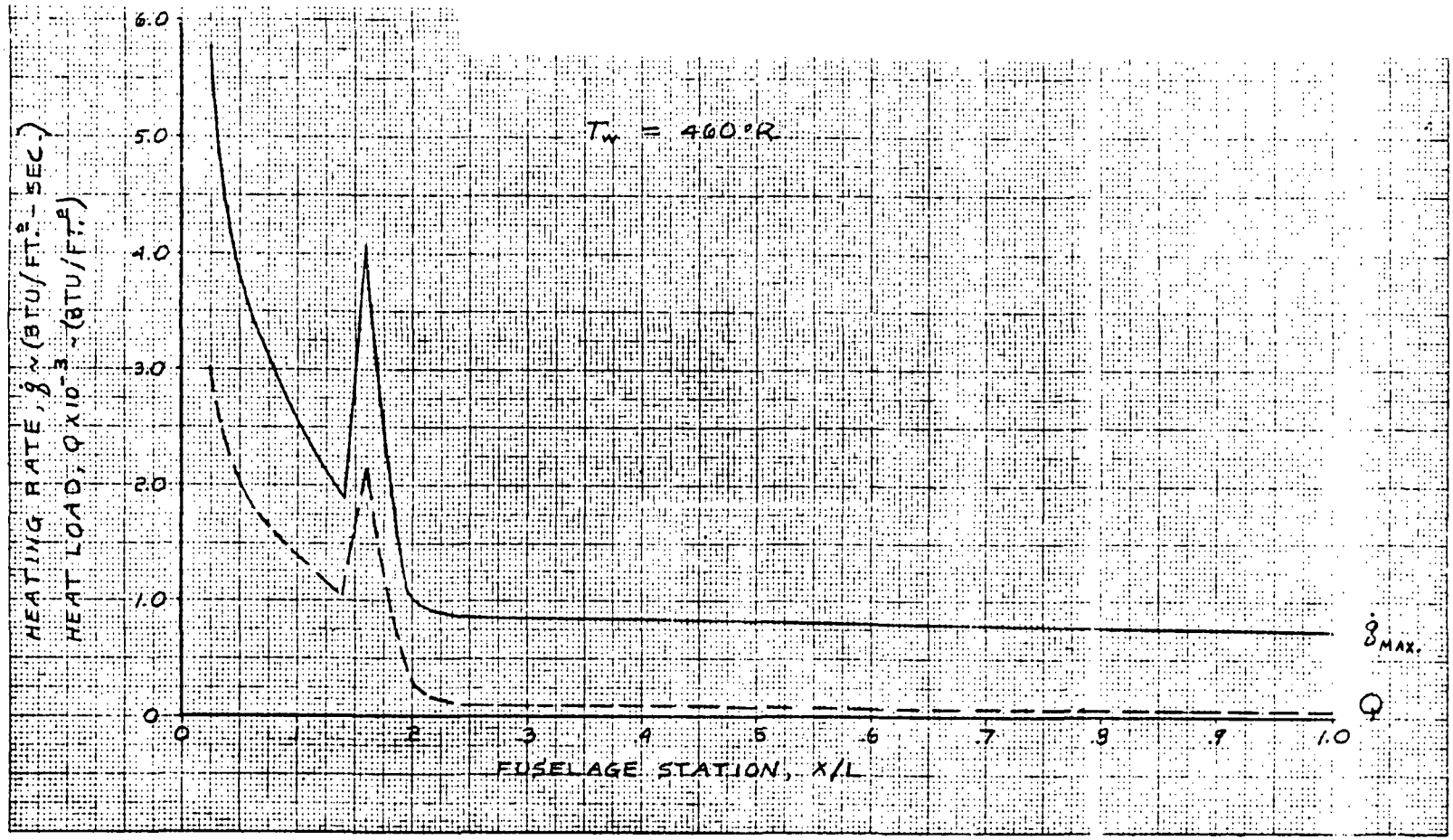

Figure 4-199. Maximum Heating Rate and Load Distribution on Orbiter Fuselage Upper Surface Centerline, Ascent, LO_2/RP Flyback System

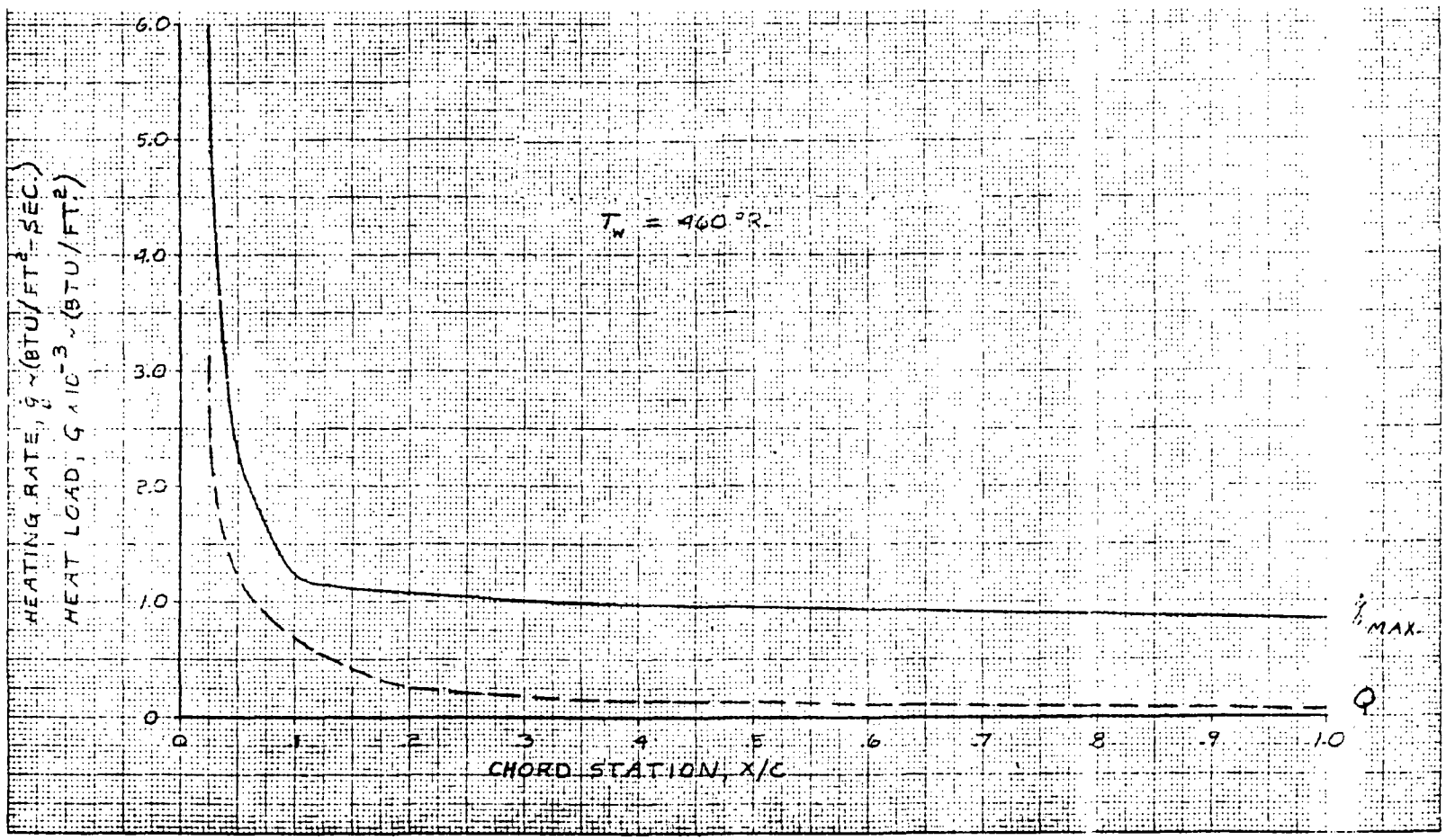

Figure 4-200. Maximum Heating Rate and Load Distribution on Wing Lower Surface, 50-Percent Exposed Span, Ascent

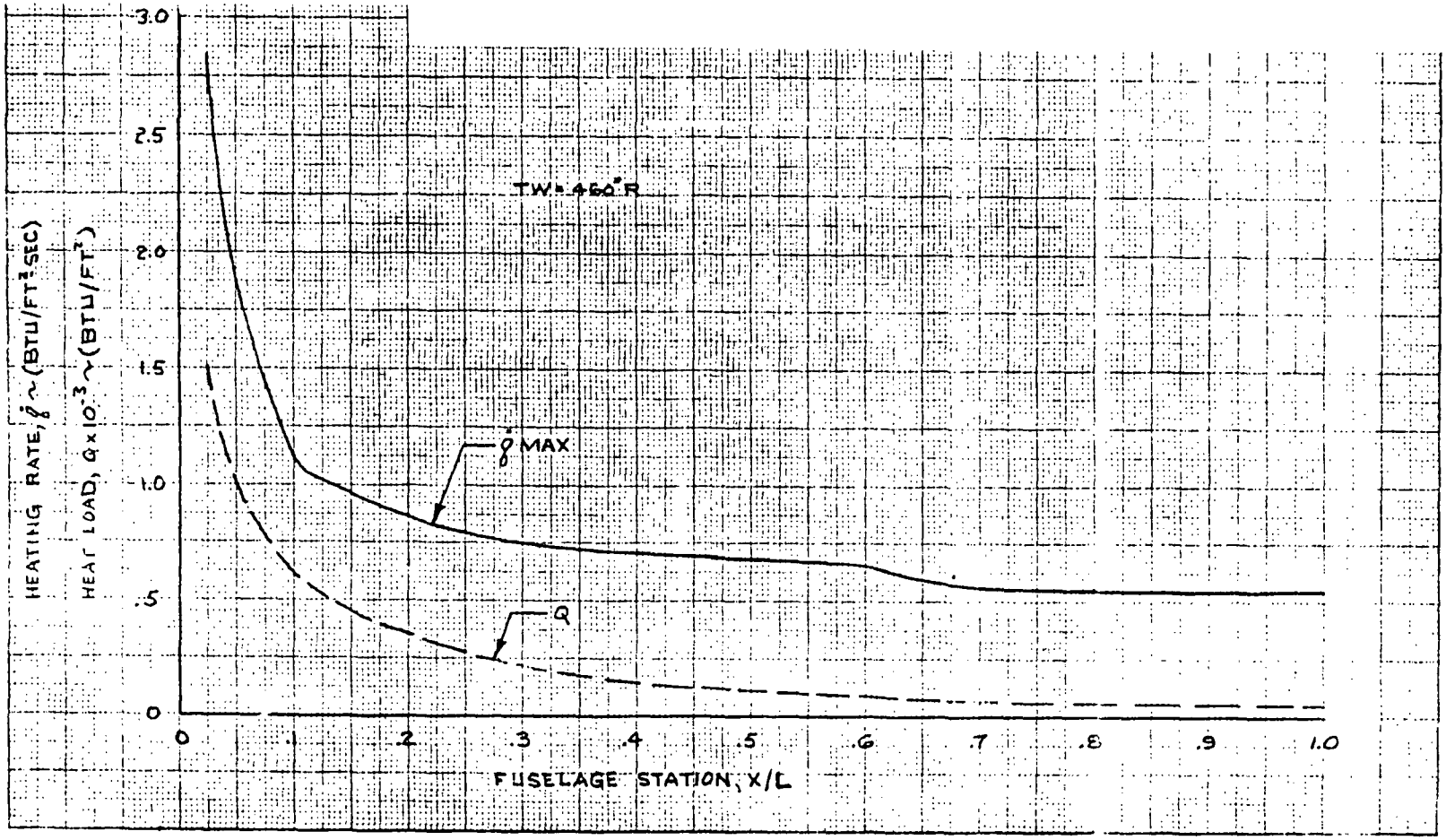

Figure 4-201. Maximum Heating Rate and Load Distribution on Orbiter Fuselage Lower Surface Centerline, Ascent, Pressure-Fed System

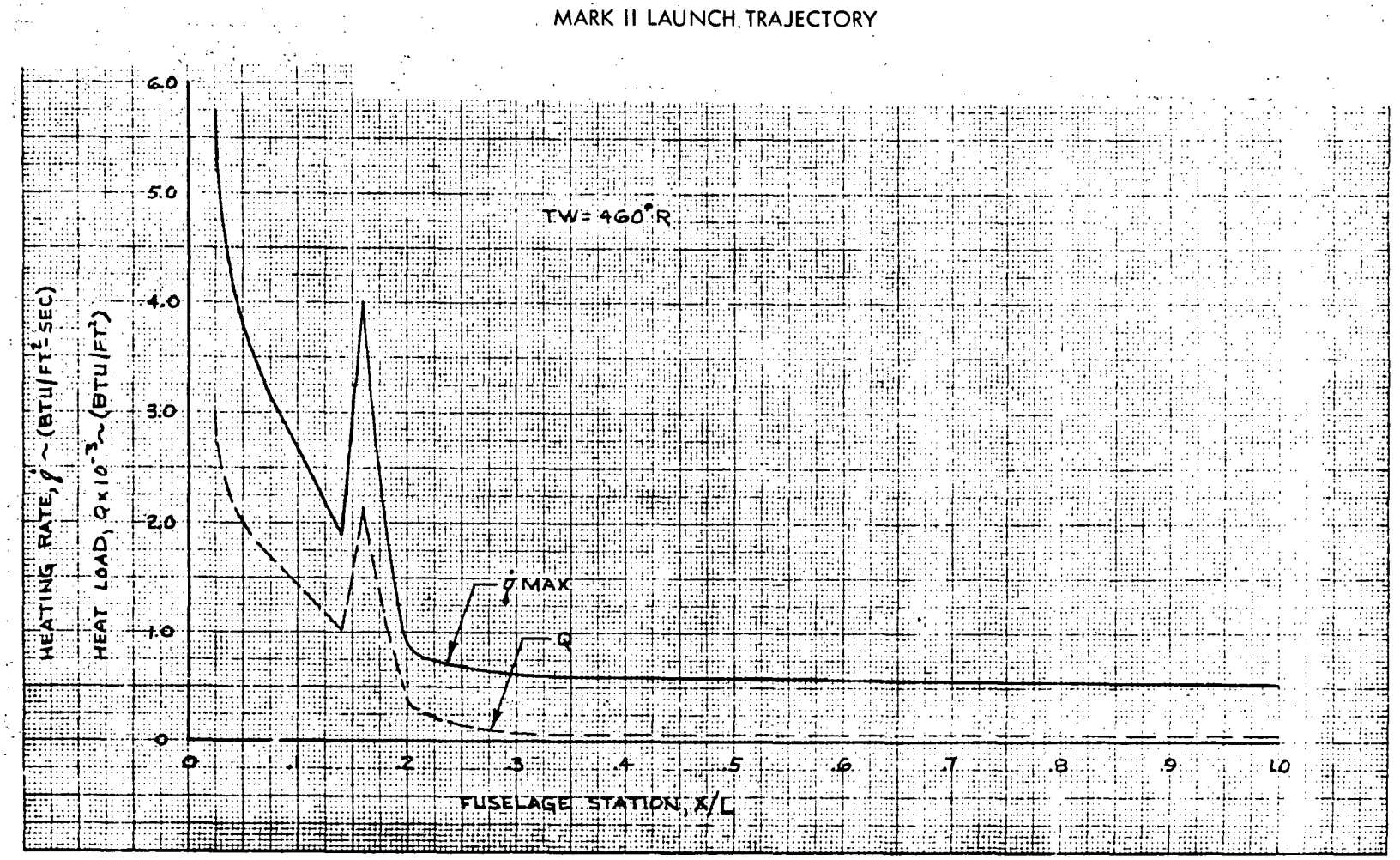

Figure 4-202. Maximum Heating Rate and Load Distribution on Orbiter Fuselage Upper Surface Centerline, Ascent, Pressure-Fed System

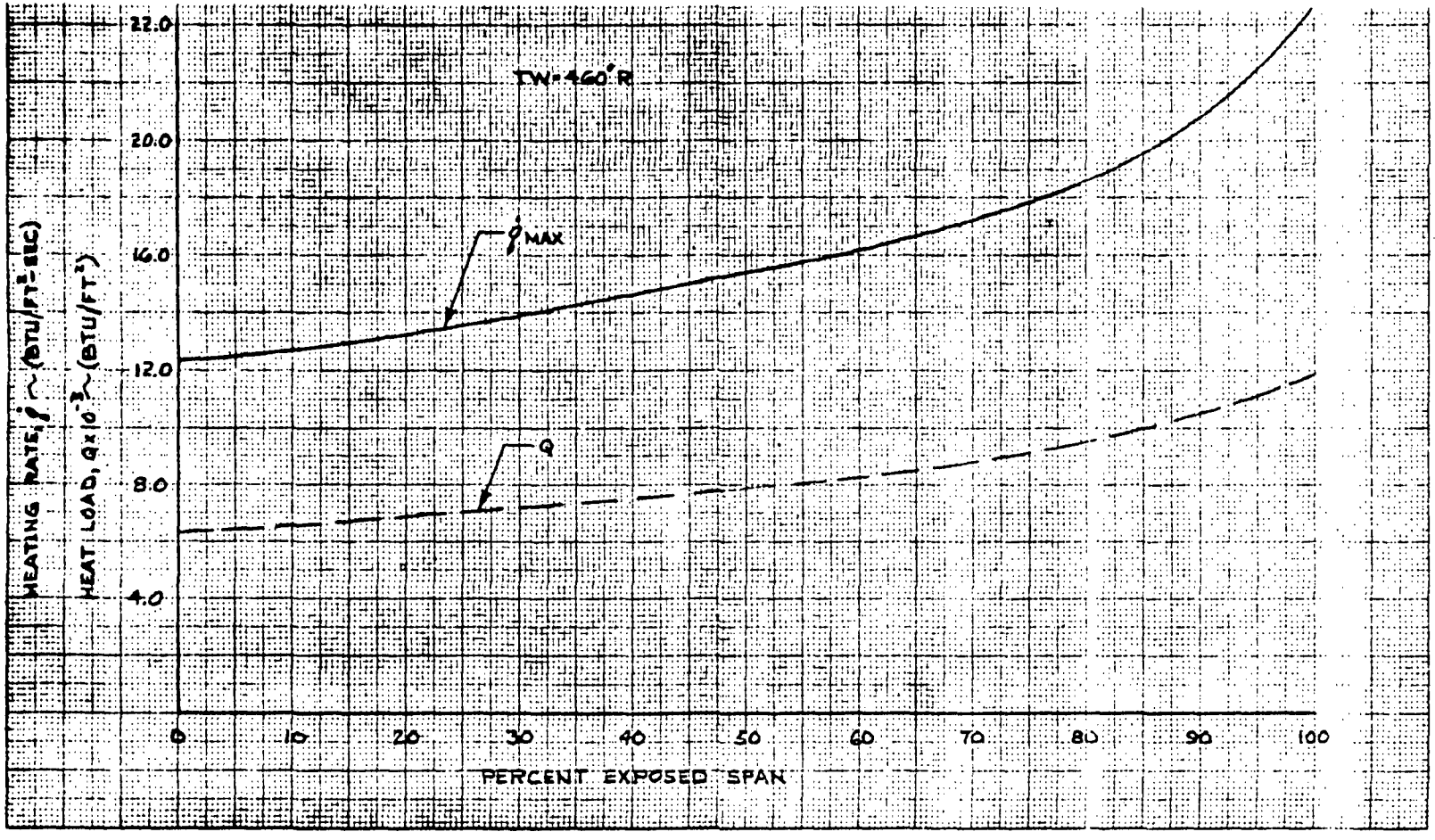

Figure 4-203. Maximum Heating Rate and Heat Load Distribution on Orbiter Vertical Tail Leading Edge, Ascent, Pressure-Fed System

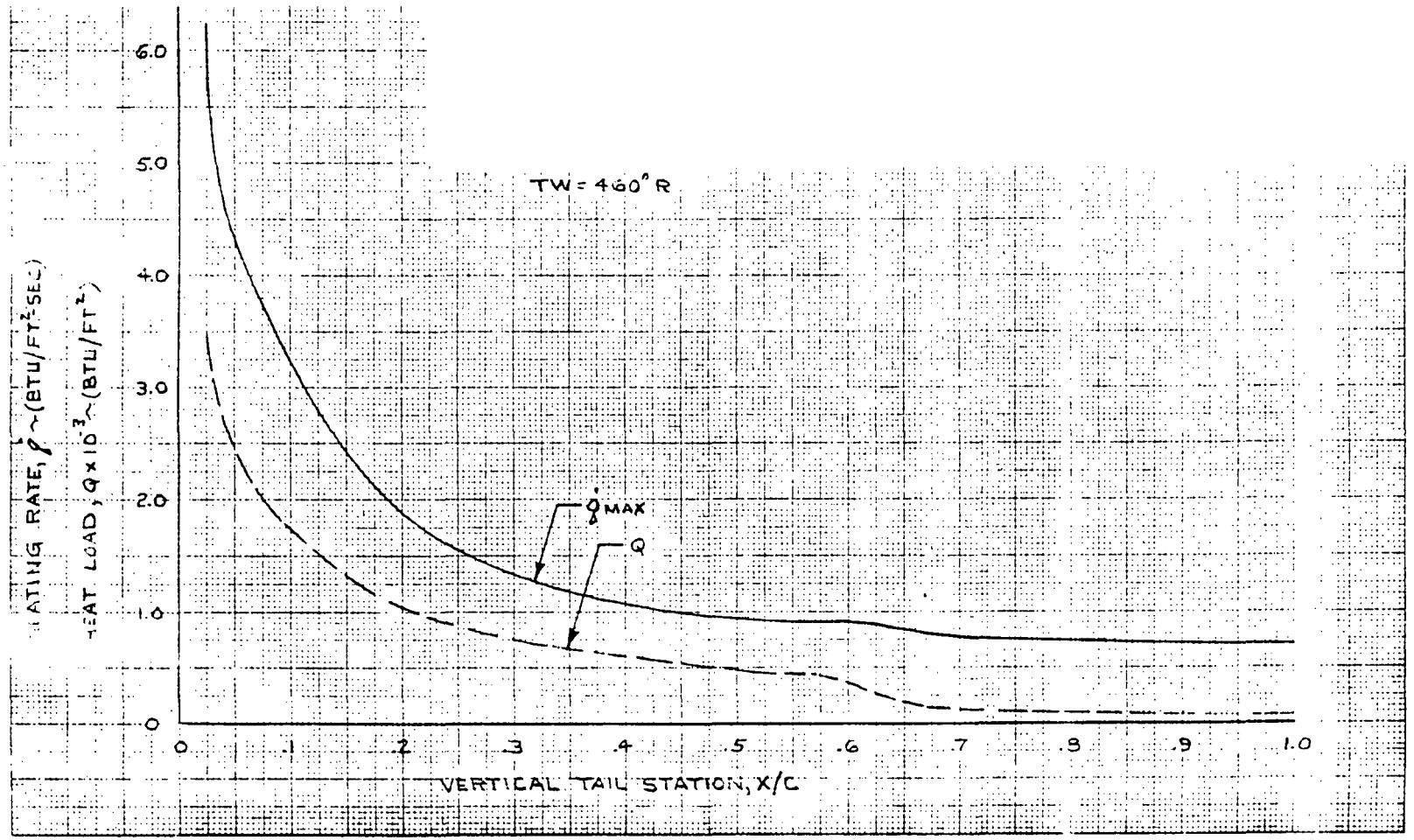

Figure 4-204. Maximum Heating Rate and Heat Load Distribution on Orbiter Vertical Tail, 50-Percent Exposed Span, Ascent, Pressure-Fed System

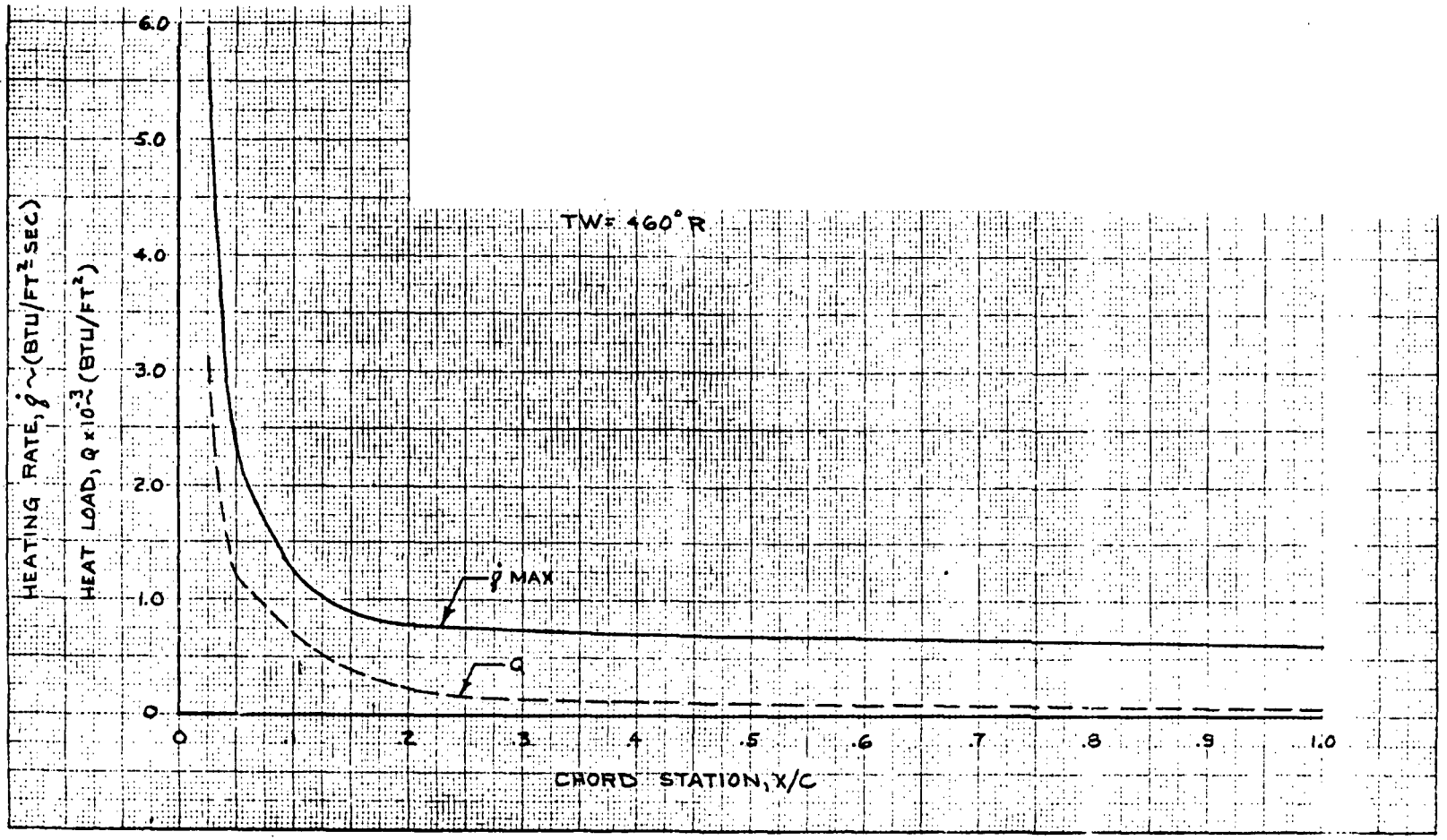

Figure 4-205. Maximum Heating Rate and Load Distribution on Orbiter Wing Lower Surface, 50-Percent Exposed Span, Ascent, Pressure-Fed System

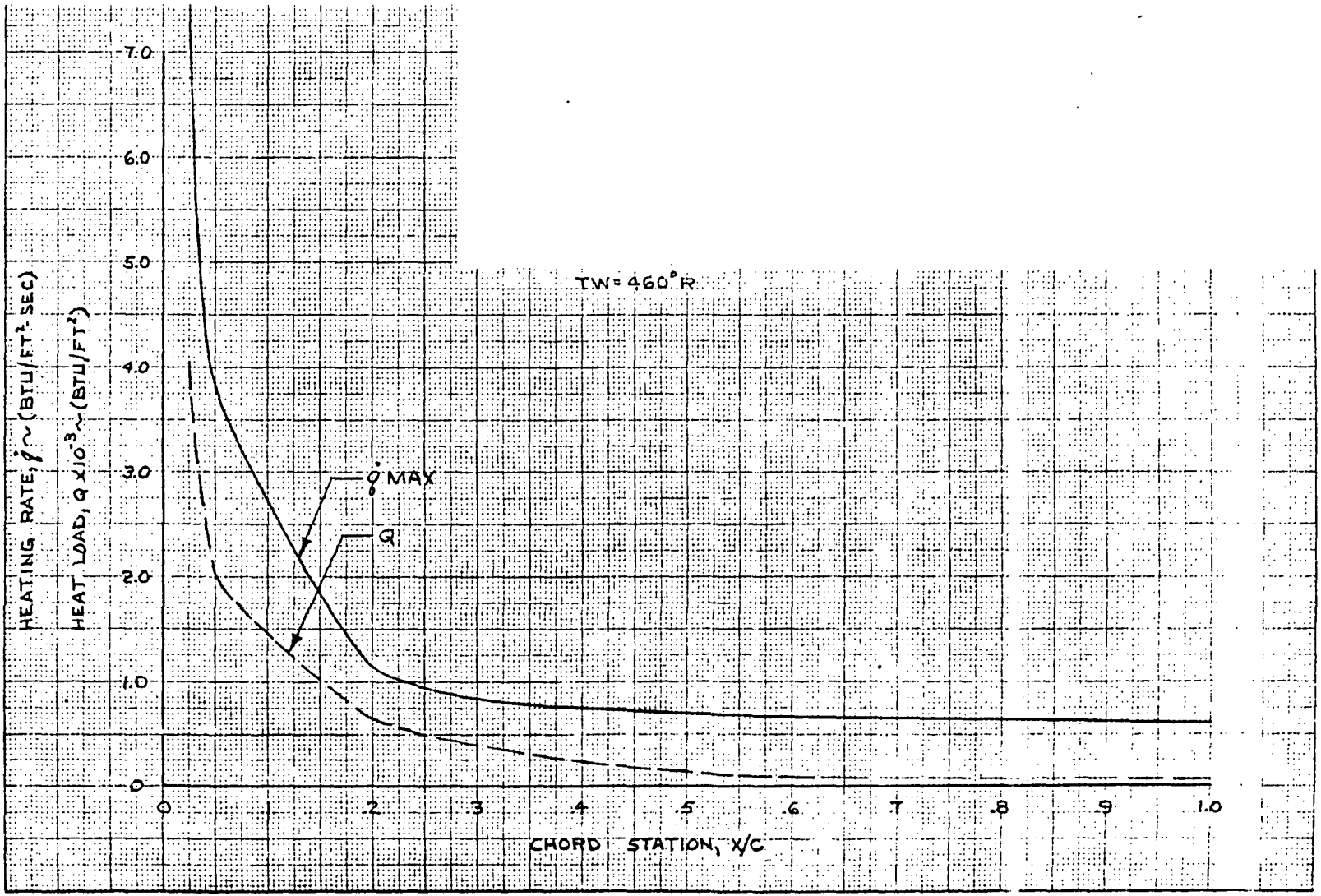

Figure 4-206. Maximum Heating Rate and Heat Load Distribution on Orbiter Wing Upper Surface, 50-Percent Exposed Span, Ascent, Pressure-Fed System

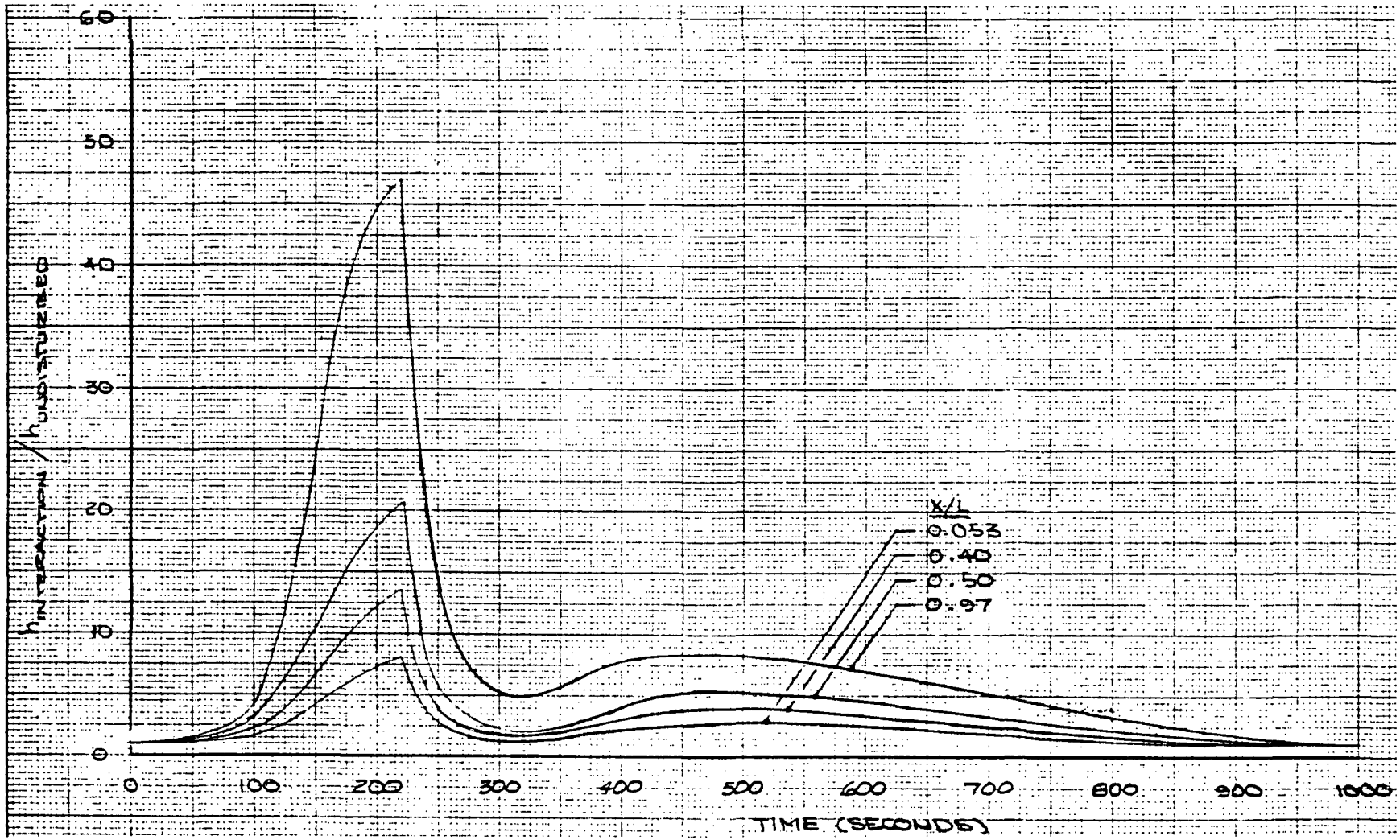

Figure 4-207. Variation of Interference Heating on Orbiter During Ascent

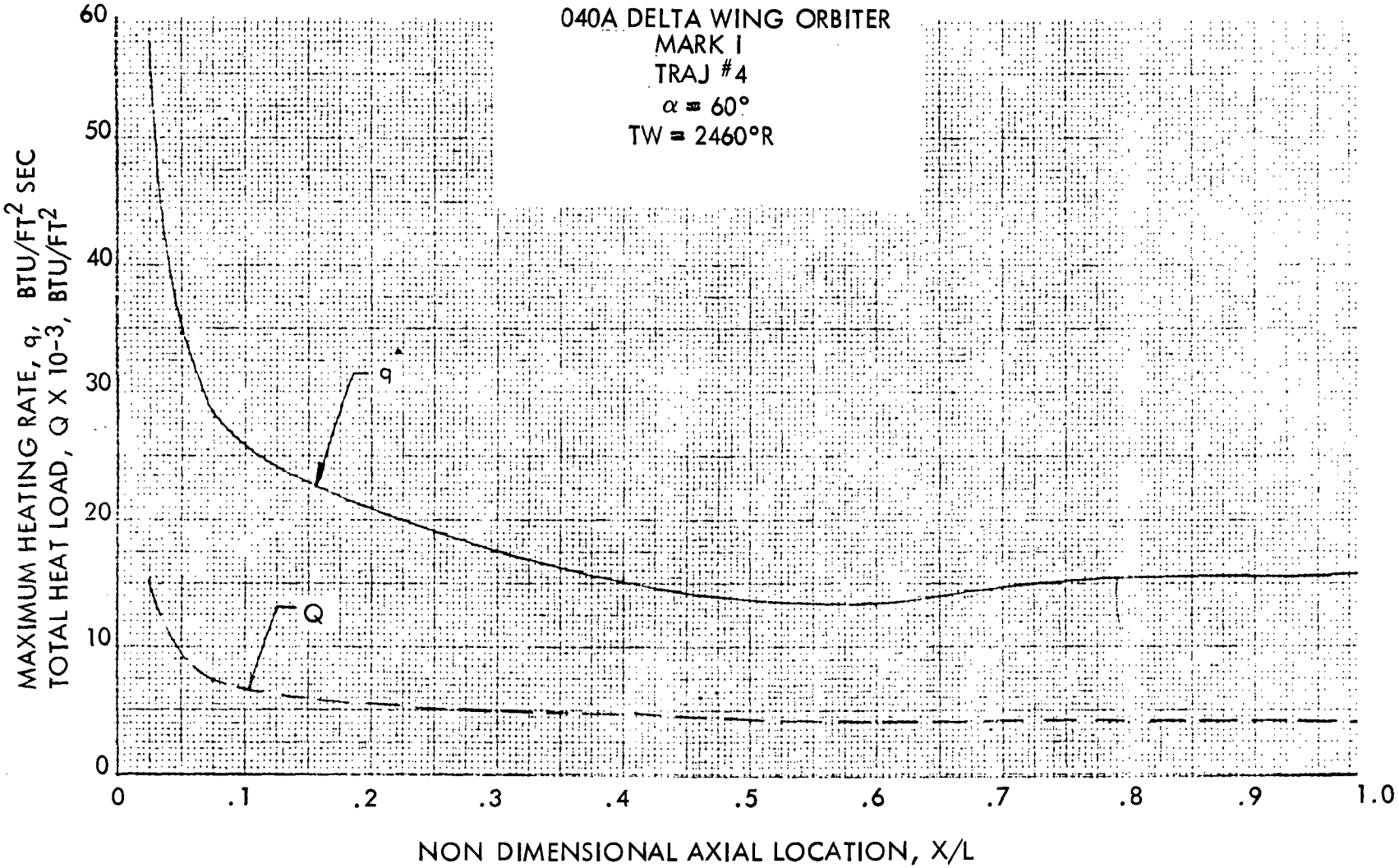

Figure 4-208. Maximum Heating Rate and Total Load Distribution on Orbiter Fuselage Lower Surface Centerline

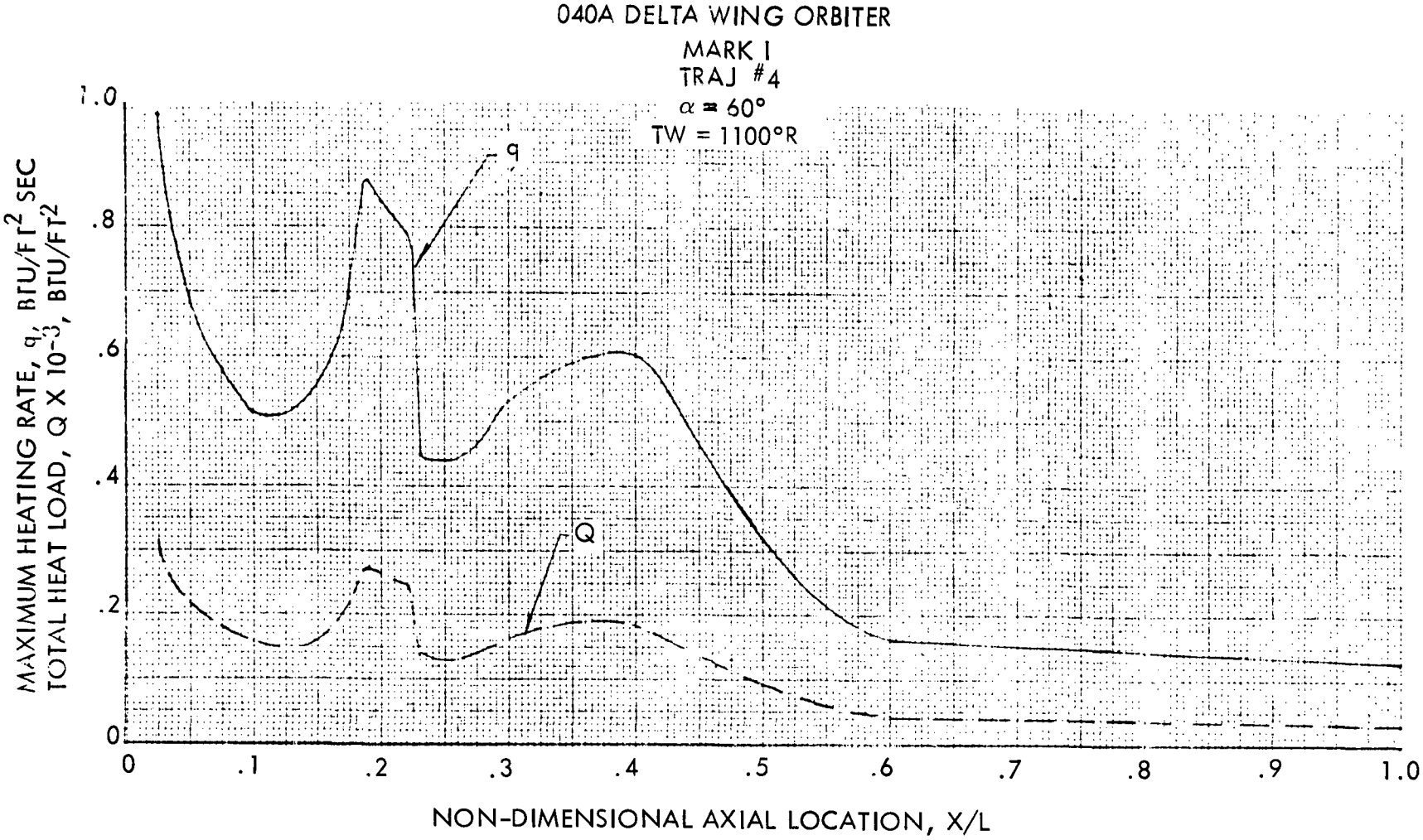

Figure 4-209. Maximum Heating Rate and Total Heat Load Distribution on Orbiter Fuselage Upper Surface Centerline

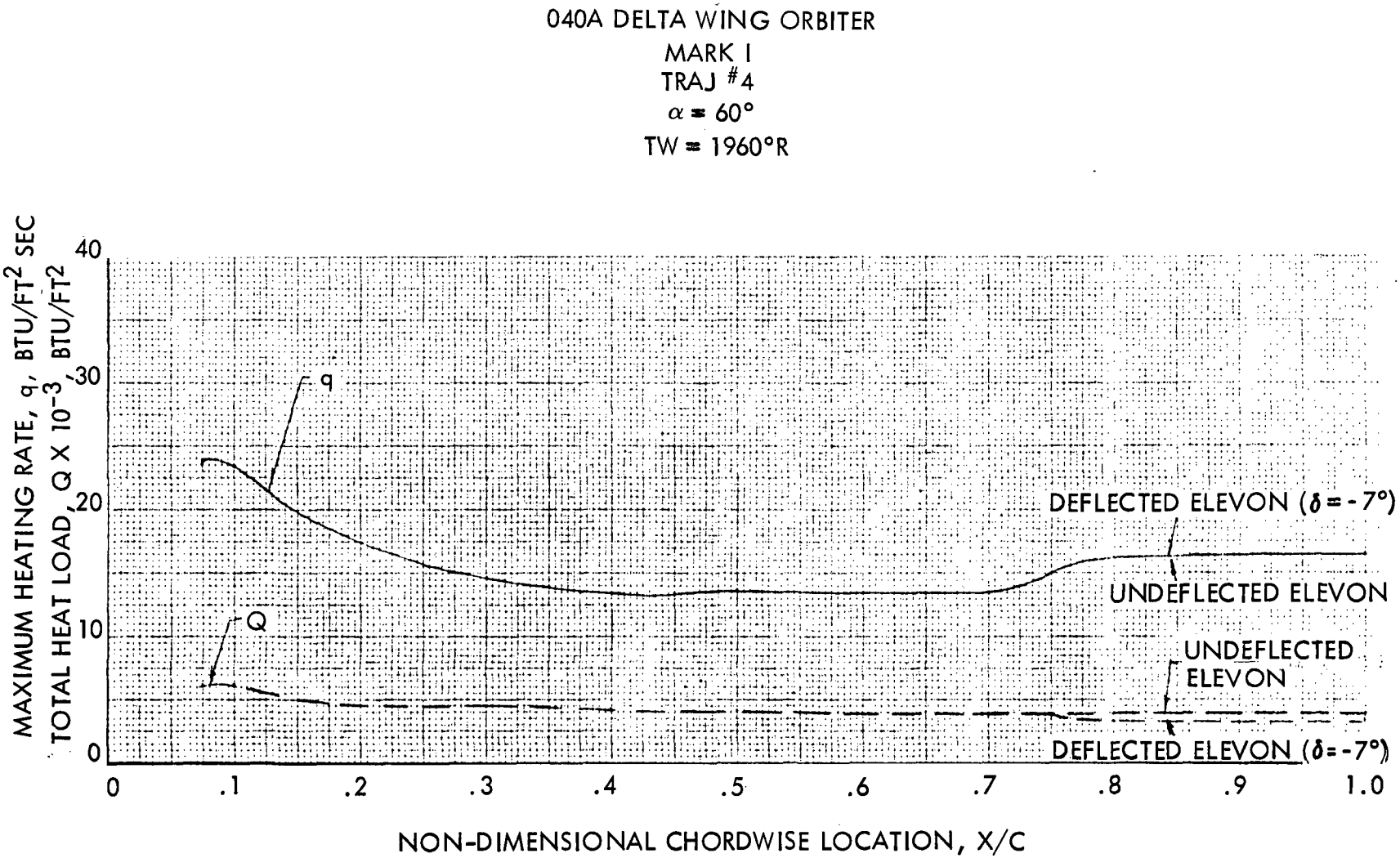

Figure 4-210. Maximum Heating Rate and Total Heat Load Distribution on Orbiter Wing Lower Surface at 50-Percent Exposed Semispan

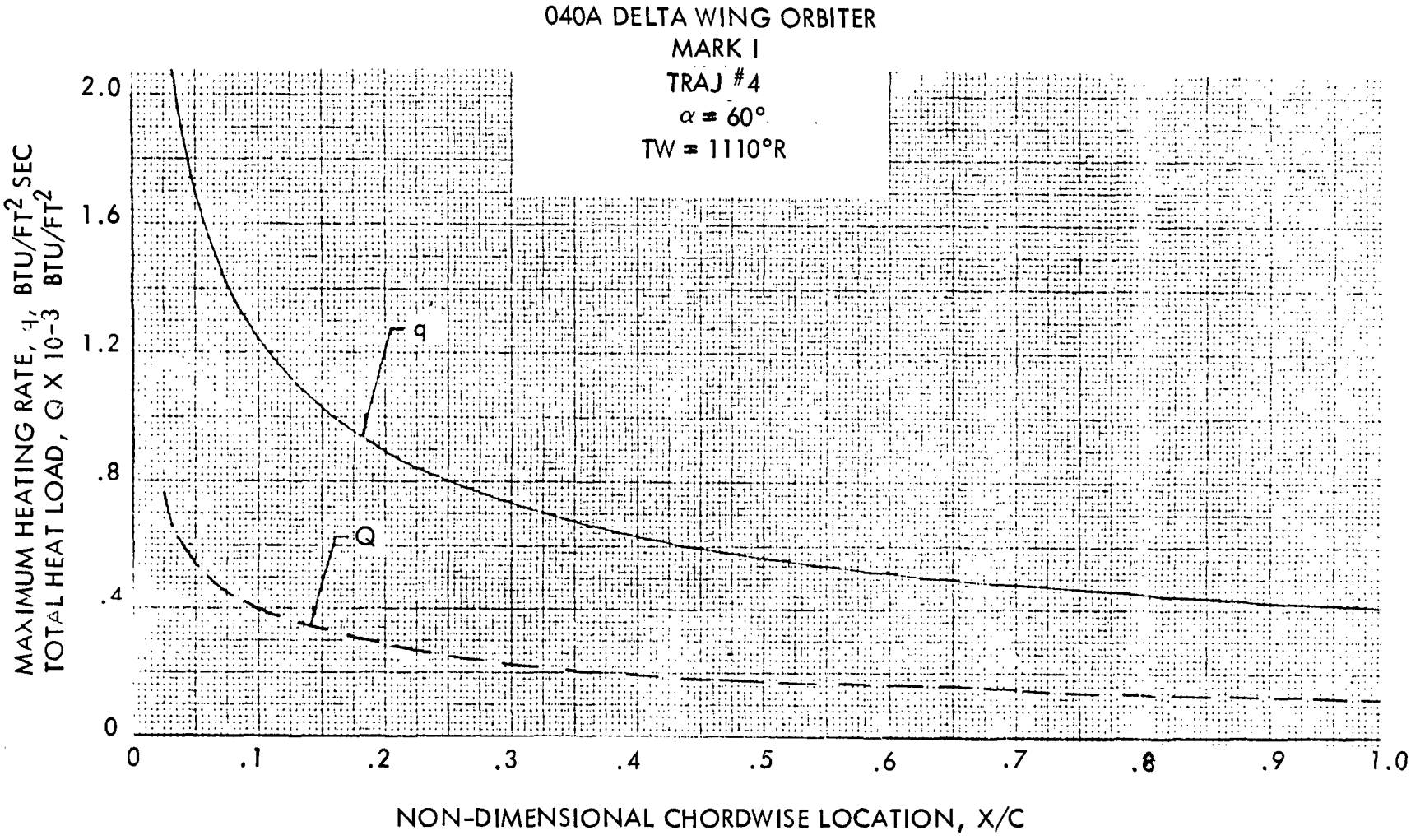

Figure 4-211. Maximum Heating Rate and Total Load Distribution on Orbiter Wing Upper Surface at 50-Percent Exposed Semispan

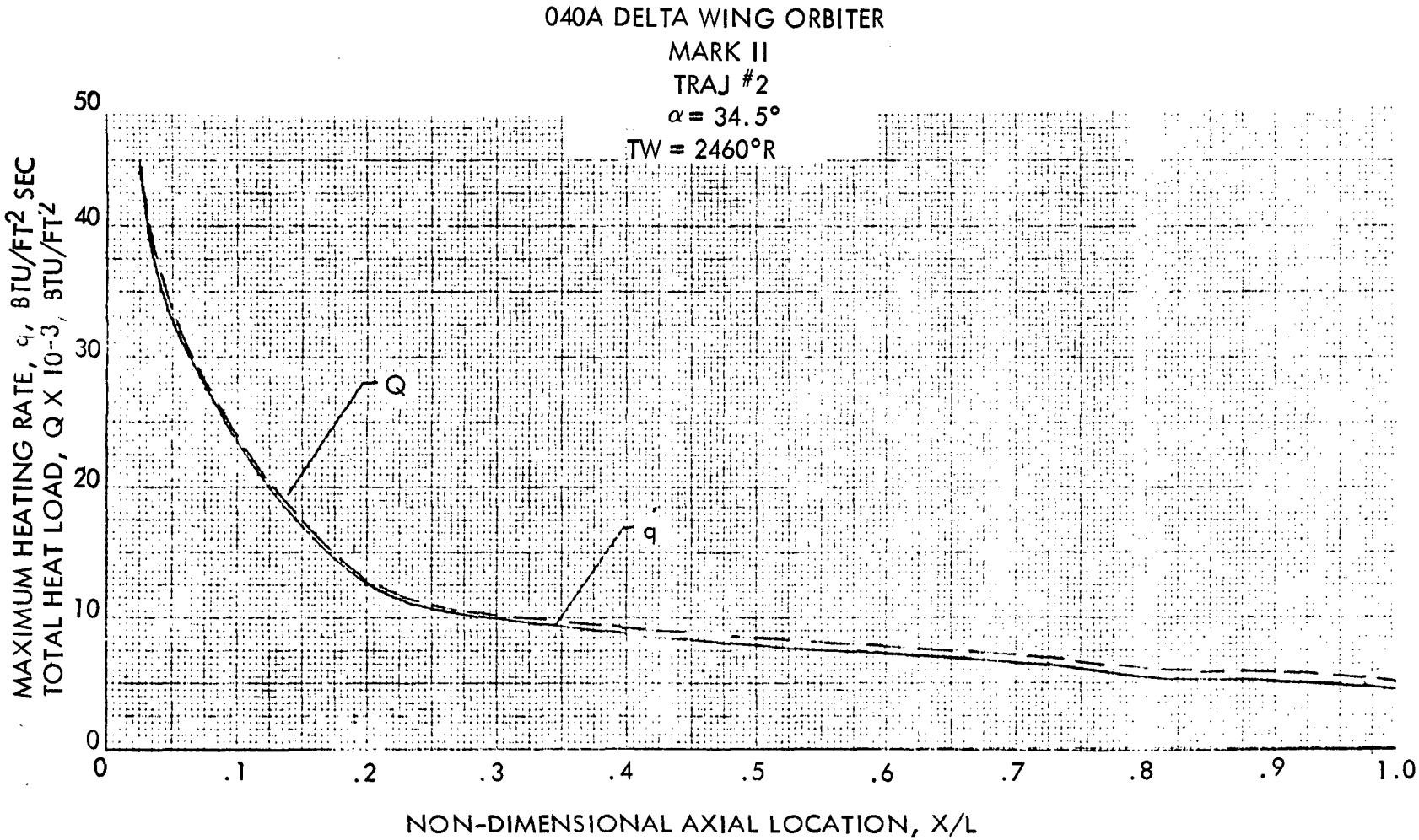

Figure 4-212. Maximum Heating Rate and Total Load Distribution on Orbiter Fuselage Lower Surface Centerline

SD 71-542

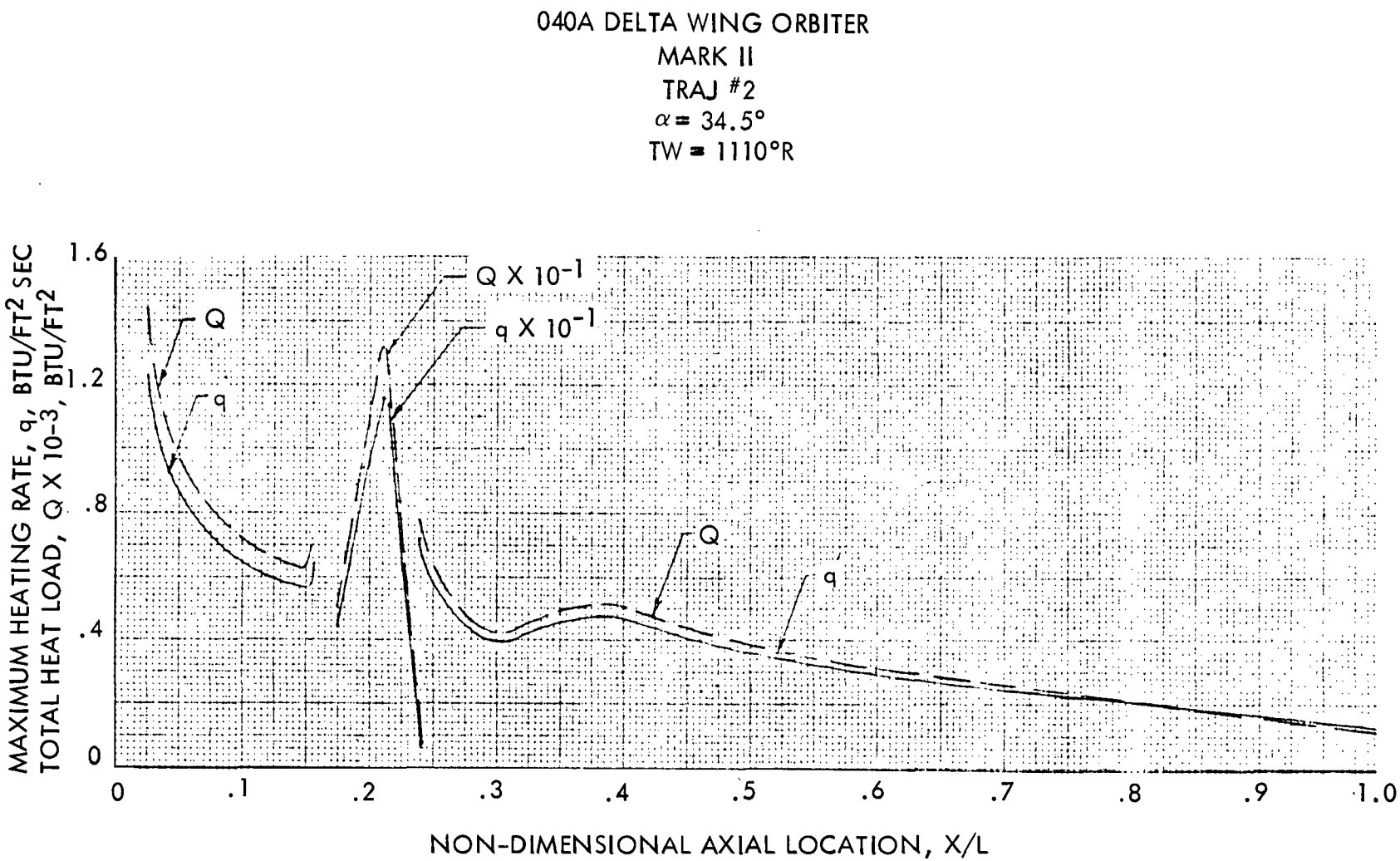

Figure 4-213. Maximum Heating Rate and Total Load Distribution on Orbiter Fuselage Upper Surface Centerline

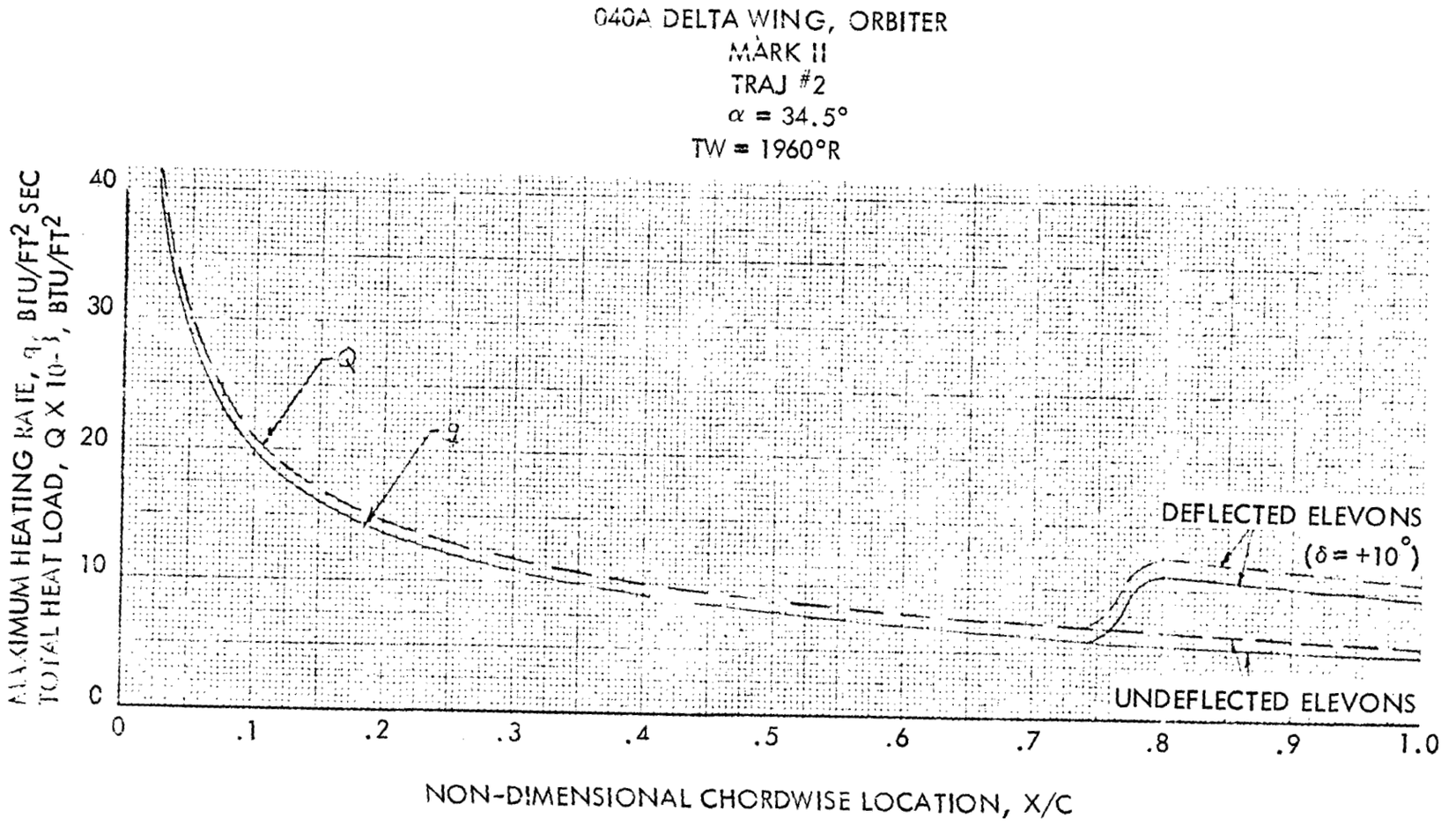

Figure 4-214. Maximum Heating Rate and Total Load Distribution on Orbiter Wing Lower Surface at 50-Percent Exposed Semispan

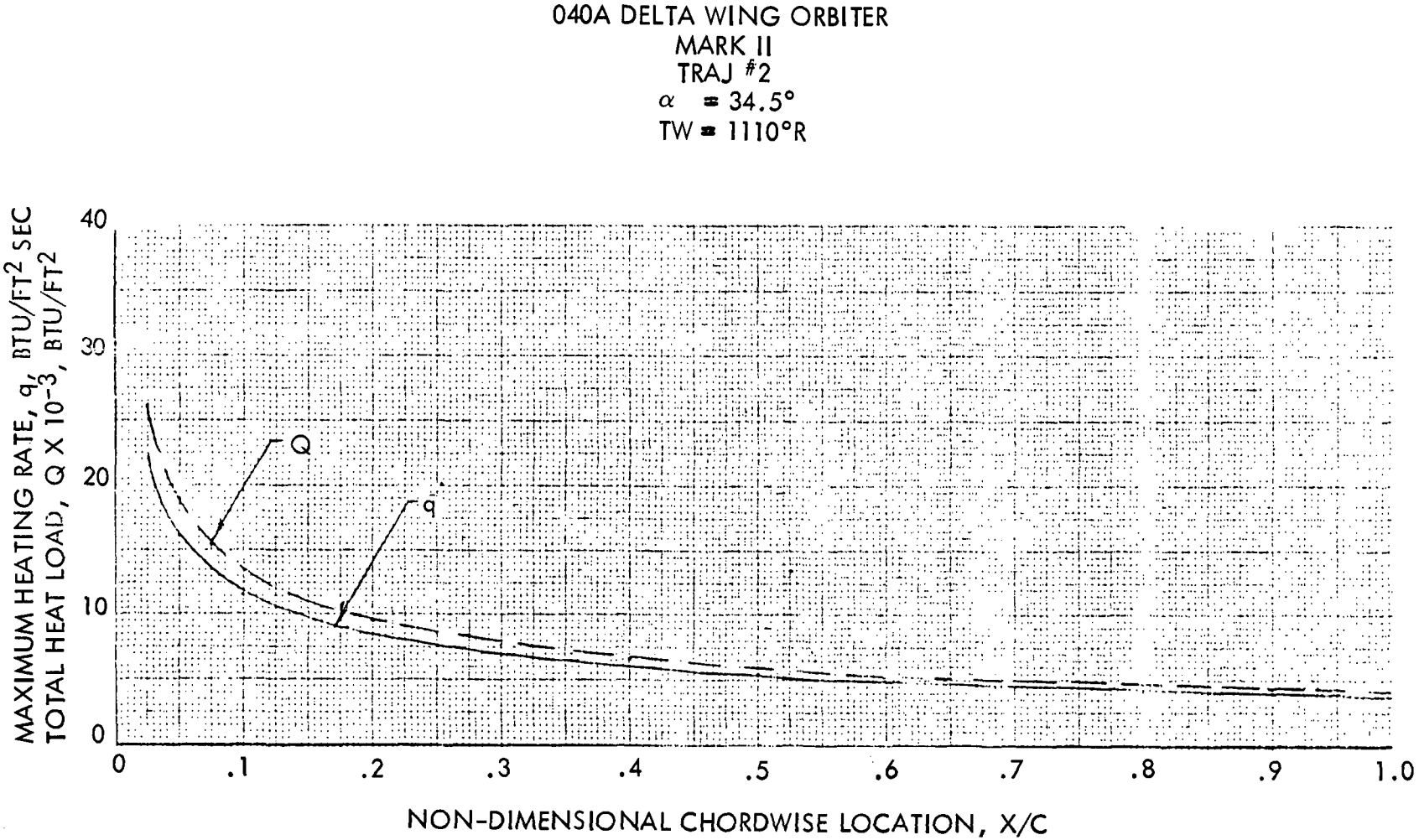

Figure 4-215. Maximum Heating Rate and Total Heat Load Distribution on Orbiter Wing Upper Surface at 50-Percent Exposed Semispan

TPS Thermal Design Analysis. Ablator and RSI TPS's on aluminum primary structure vehicles are currently being emphasized in the thermal design analysis. Thermal design sensitivity analyses on the aluminum and titanium (alternate for evaluation) structure vehicle include those delineated in Table 4-36. These sensitivity results, coupled with structural analysis and design results, have been used to define the TPS requirements for the baseline aluminum structure vehicles - Mark I and Mark II. The thermal criteria used for the TPS definitions are presented in Table 4-37. The TPS requirements for these vehicles are illustrated in Figures 4-216 and 4-217.

Examples of thermal design data developed from the sensitivity studies are shown in Figures 4-218 through 4-221. Figures 4-218 and 4-219 illustrate the variations of TPS plus structure weight as a function of primary structure thickness. For all cases examined, these sensitivities indicate that the structure should be designed for minimum weight, based on structural loadings. Adding primary structure as a heat sink to reduce the required thickness of RSI or ablator results in a heavier combined structure/TPS system. Figure 4-220 shows the decrease in TPS weight with increase in maximum structure temperature; these data were employed in determining the optimum maximum operating temperature of the primary structure. Figure 4-221 illustrates the importance of the initial preentry temperatures on TPS requirements; these results show the weight advantage realized by the use of thermal control coatings and/or on-orbit attitude orientation constraints prior to vehicle entry. In terms of the RSI TPS design for the Mark II, the total TPS weight penalty for not having a thermal control coating or preentry attitude constraints was calculated (for a nominal entry) to be 7400 pounds. This significant weight impact is being further evaluated and trades will be made to determine the best balance between coating property requirements, coating reuse capability, mission capabilities, and TPS weight.

Other studies under way include aluminum versus titanium structure trades with both ablator and RSI TPS's, continued TPS/structure maximum temperature optimization (titanium and aluminum), and RSI and ablator property (ablator candidates) optimization. Special analyses are being performed to determine the extent of ablator degradation during boost and to define a realistic approach to specifying the additional ablator requirements.

Table 4-36. TPS Sensitivity Parameters

Trajectory	TPS/Structure	Sensitivity Variables	Fixed Parameters
200-NM crossrange (nominal)	SLA-561/aluminum	$\bar{t}_{Al}$, $T_{Max_{Al}}$, Q	$T_{initial}$ = 100 F
	RSI/aluminum	$\bar{t}_{Al}$, $T_{Max_{Al}}$, Q	$T_{initial}$ = 100 F
	SLA-561/titanium	Q	T_{Ti} = 650 F, t_{Ti} = 0.03", T_o = 100 F
1100-NM crossrange (nominal)	SLA 561/aluminum	$\bar{t}_{Al}$, $T_{Max_{Al}}$, Q	$T_{initial}$ = 100 F
	REI/aluminum	$\bar{t}$, $T_{Max_{Al}}$, Q, $T_{initial}$	
	REI/aluminum	α/ϵ = 0.4 and 1.0	$\bar{t}_{Al}$ = 0.12", T_{Max} = 300 F
	RSI/titanium	Q	T_{Ti} = 650 F, t_{Ti} = 0.03 in., T = 100 F

Table 4-37. TPS Criteria

Initial preentry temperature		100 F
Maximum aluminum temperature		350 F
Heating		Nominal trajectories
Surface emissivity (boost and entry)		0.8
Postlanding Cooling		None
Ablator acreage Leading edges	Mark I	14.5 pcf SLA-561 32 pcf Avcoat 5026-39
Acreage TPS Leading edges	Mark II	12 pcf RSI Reinforced carbon-carbon

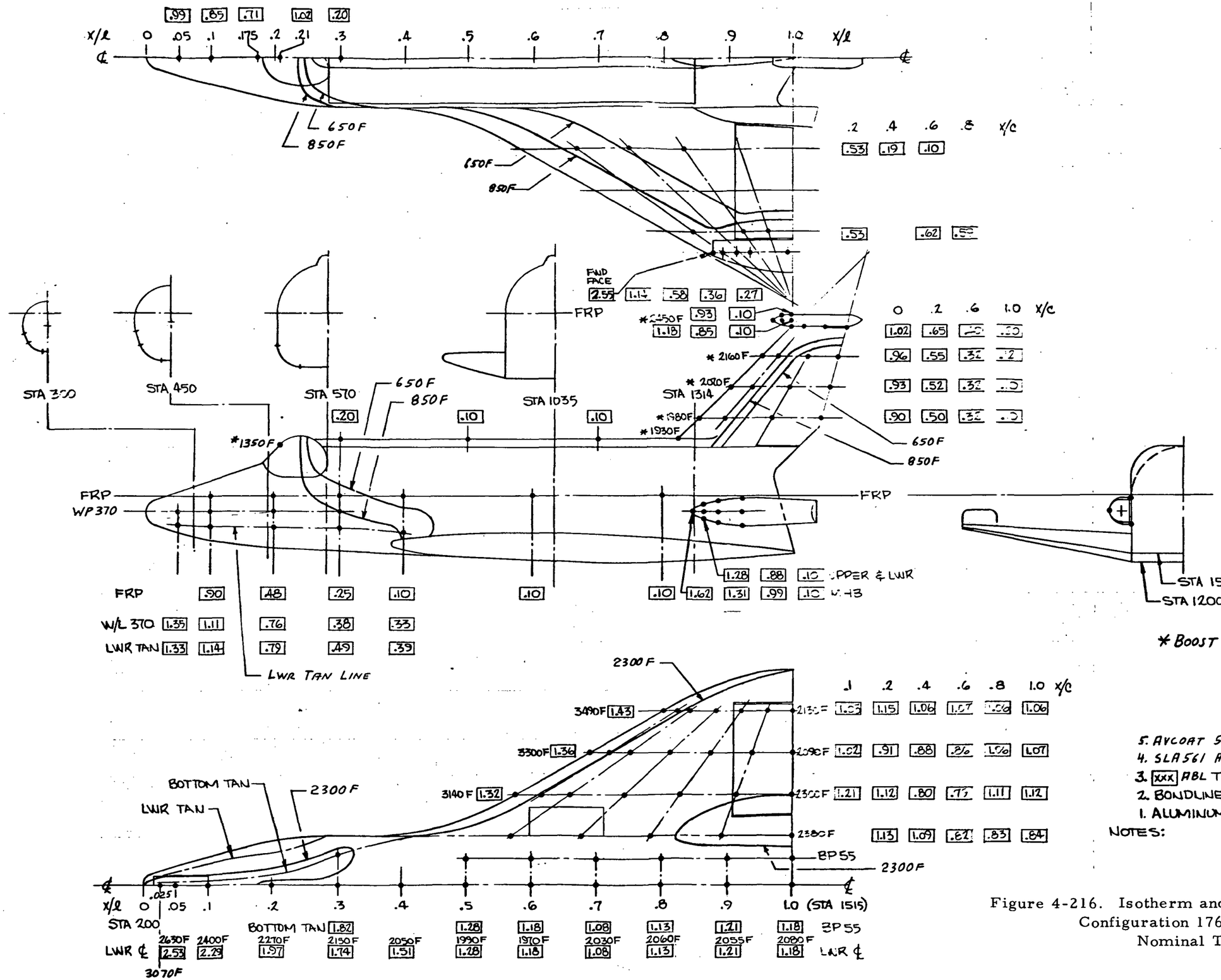

5. AVCOAT 5026-39M ABLATOR (L.E.), ρ = 32 PCF
4. SLA 561 ABLATOR (ACREAGE), ρ = 14.5 PCF
3. [XXX] ABL THICKNESS (INCHES)
2. BONDLINE TEMP 350 F MAX
1. ALUMINUM PRIMARY STRUCTURE

NOTES:

Figure 4-216. Isotherm and Material Requirements Map, Configuration 176, Ablator TPS, LCR, Nominal Trajectory 4

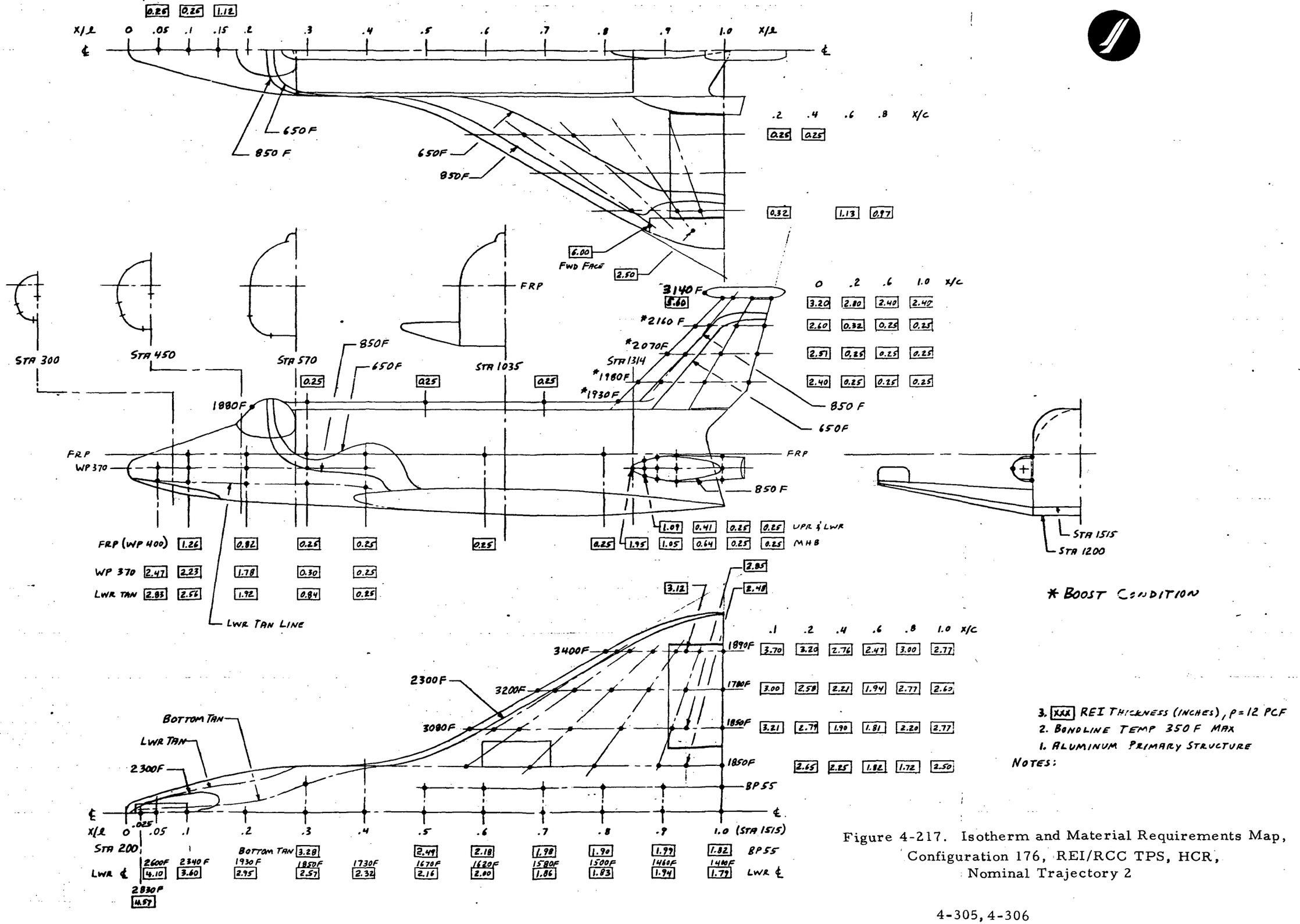

Figure 4-217. Isotherm and Material Requirements Map, Configuration 176, REI/RCC TPS, HCR, Nominal Trajectory 2

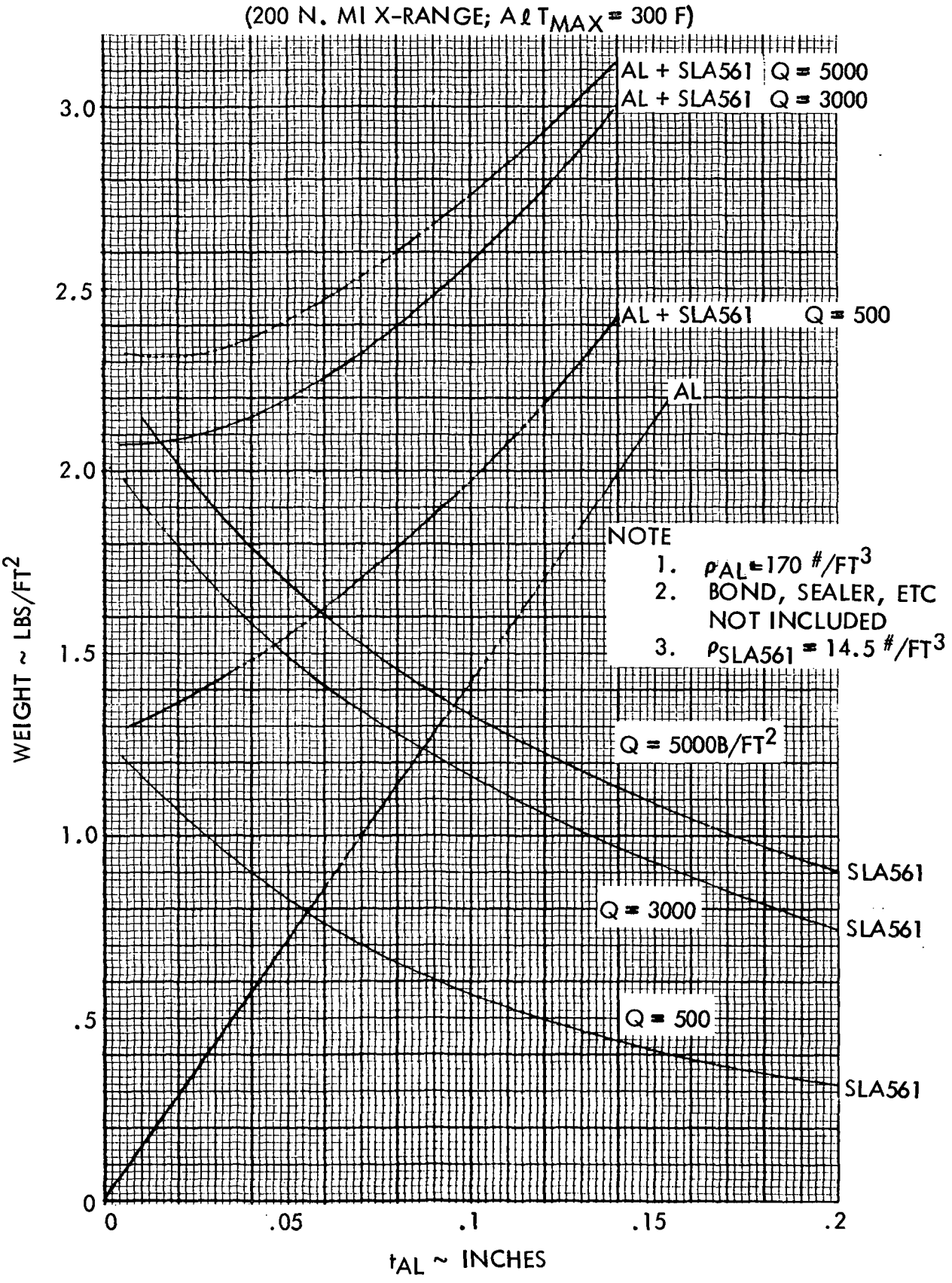

Figure 4-218. Substructure Heat Sink Ablator TPS, Structure Weight Sensitivity

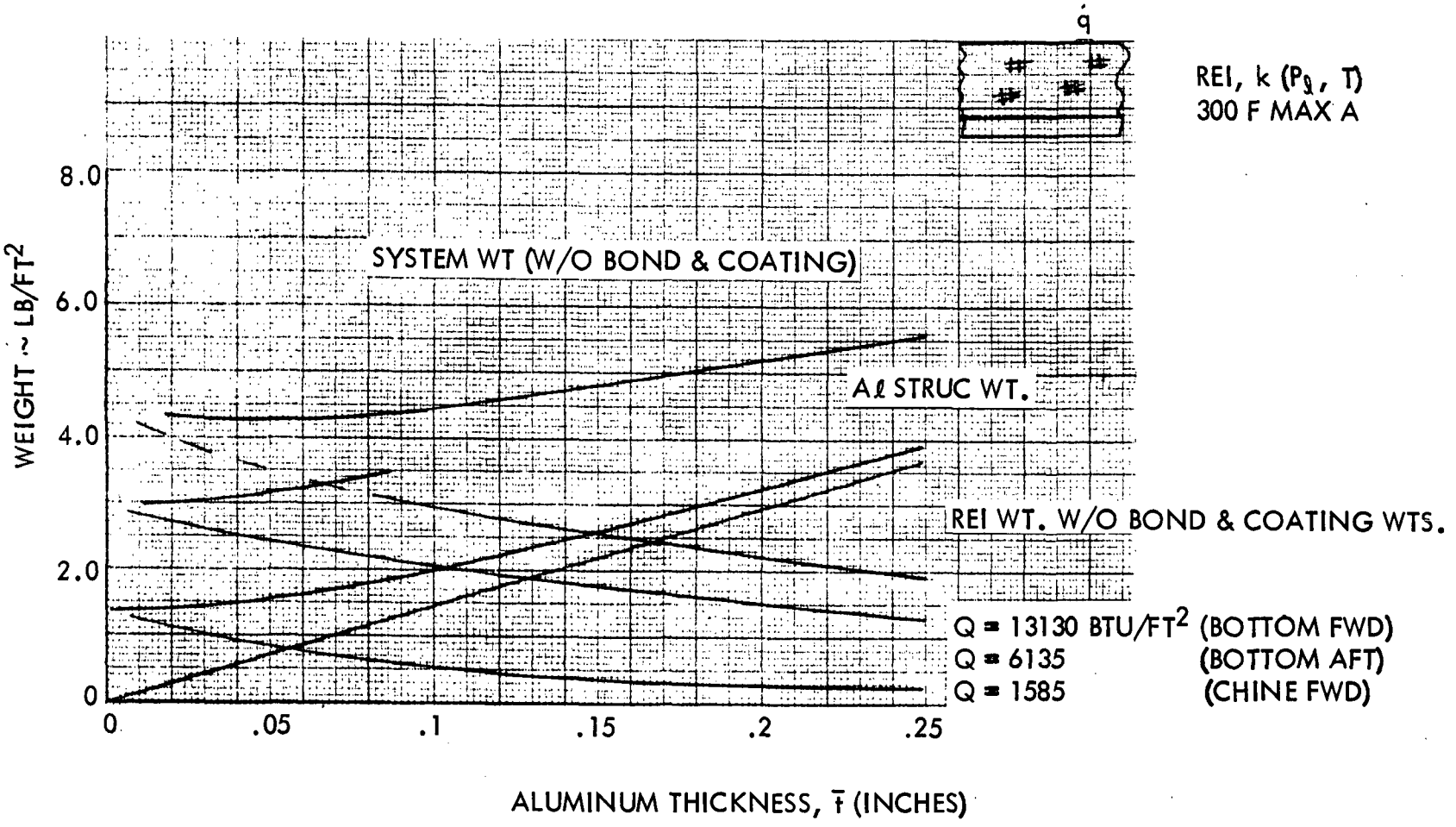

Figure 4-219. Substructure Heat Sink REI TPS, Structure Weight Sensitivity

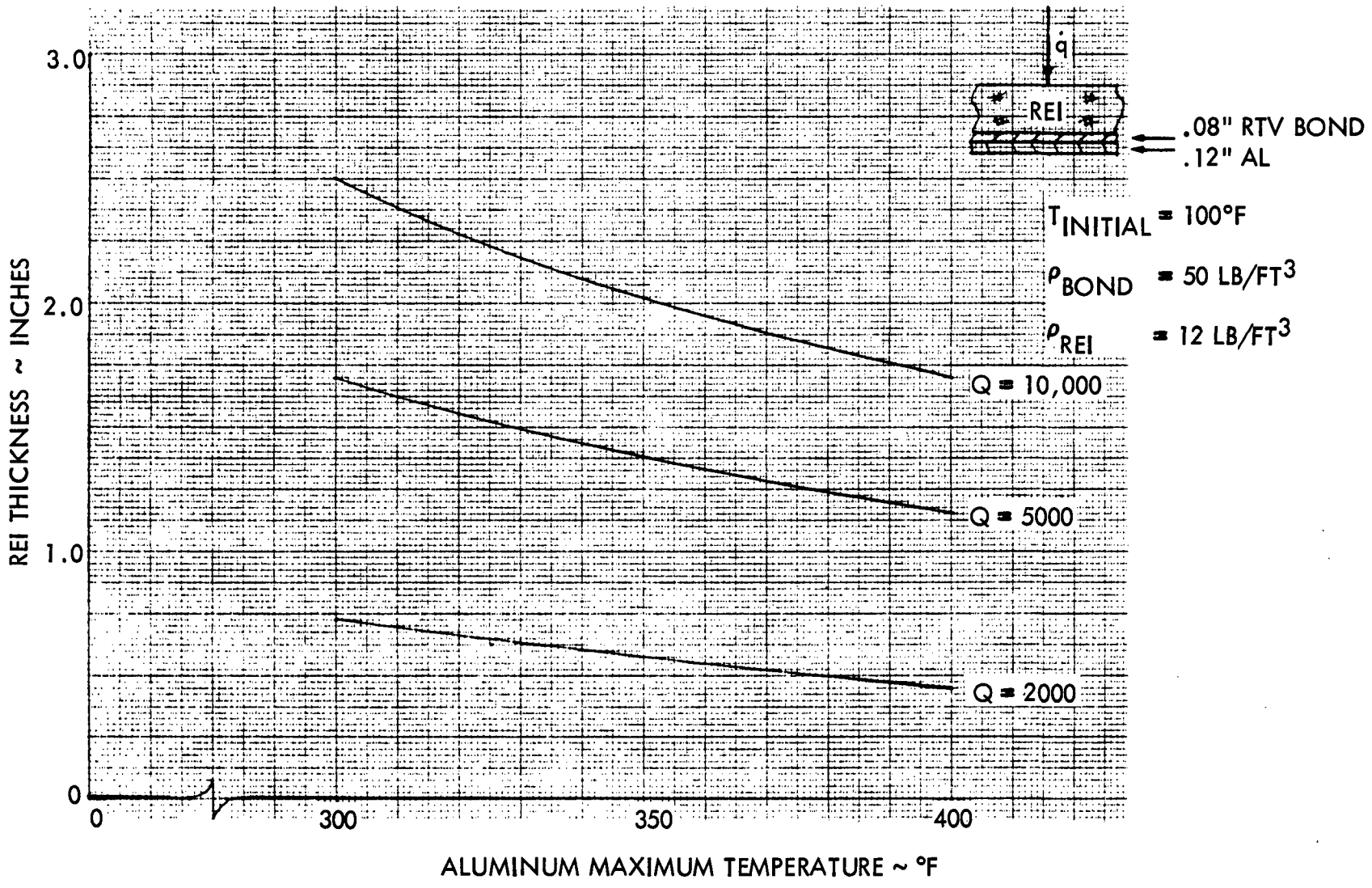

Figure 4-220. Effect of Maximum Aluminum Temperature on TPS Requirements (1100 NM Cross-Range Entry)

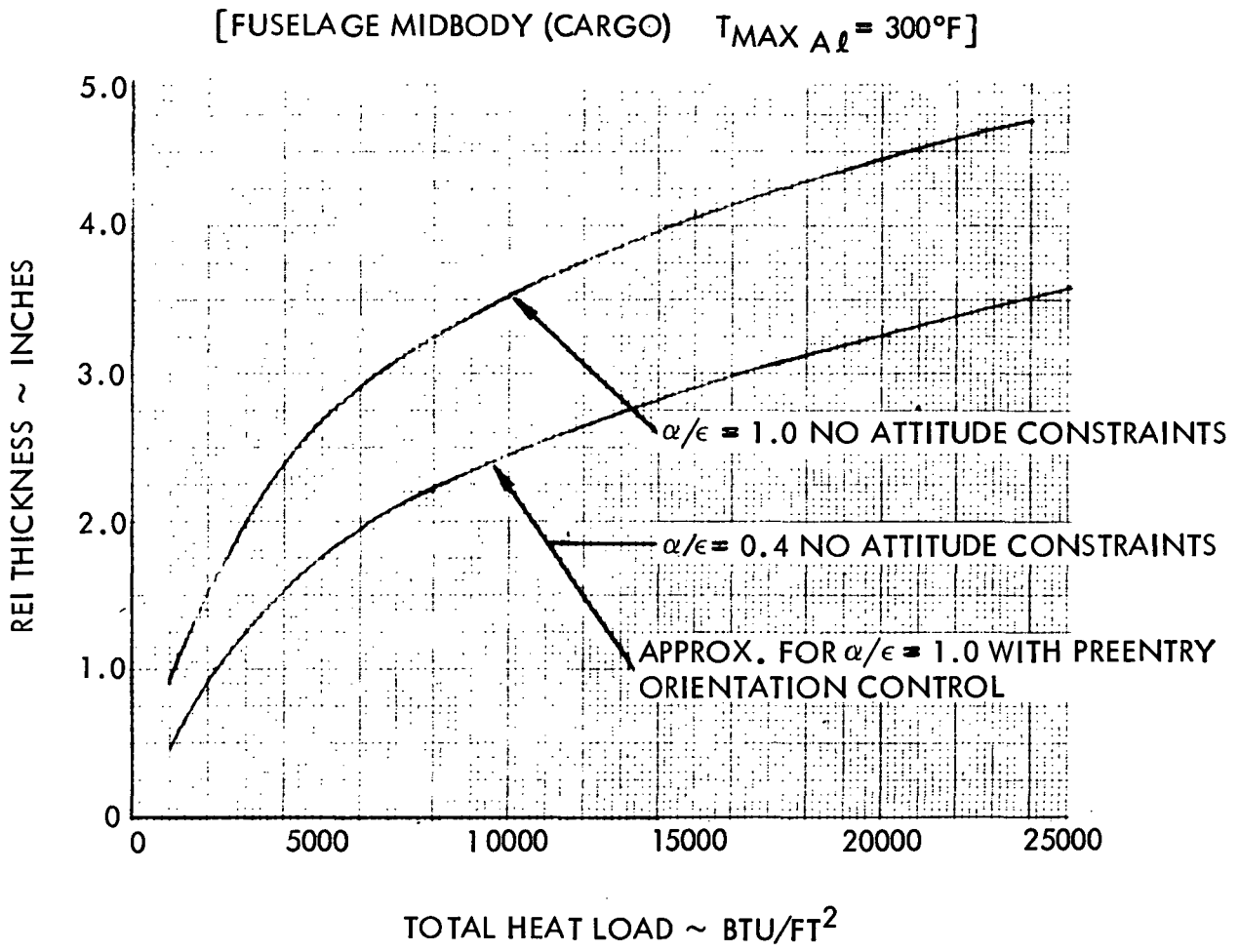

Figure 4-221. REI Thickness Sensitivity to Surface Optical Properties

TCS Thermal Analysis. Tentative component temperature limits for the baseline vehicle are listed in Table 4-38. Temperature control of the various subsystems/components outside of the pressurized cabin will be accomplished by employing insulation, coatings, and electrical heaters. The cabin and fuel cell temperatures will be controlled mainly by the ECLSS — the hydraulic fluid is circulated through the system to obtain temperature control.

The temperature limits of the OMS, ACPS, and APU's were determined by the earth storable propellants used. Somewhat higher short-term maximum temperatures may be permissible, depending on the precise design chosen.

The maximum MPS subsystem temperature of 140 F is the current value supplied by the engine manufacturer; however, this limit requires clarification and/or redefinition. Since the main engines were designed for booster use only, some requalification for space storage and reentry survival will be required.

Table 4-39 shows the preliminary heater power budget requirements for the various subsystem areas. The values listed under the heading WORST CASE (which corresponds to the no TCS vehicle attitude constraint requirement) represent the baseline heater requirements. If extreme-type vehicle attitude requirements were eliminated (e. g. , flying with the vehicle tail toward the sun with the orbit plane perpendicular to the sun earth line), the heater power requirements could be substantially decreased (e. g. , last column of Table 4-39). Heater power requirements could be further reduced by activating a barbecue mode-type operation.

Figure 4-222 shows representative maximum TPS preentry temperatures for the Mark I vehicles. The maximum structure temperature is much more sensitive to surface optical properties than to ablator thickness. Similar results have been calculated for the Mark II TPS.

Figure 4-223 shows the time required to cool the TPS to 100 F from the hot-soak values shown in Figure 4-222 for the ablator TPS. For an ablator TPS with an exterior coating with an α/ϵ ratio of one, between 7 and 30 hours are required to cool the TPS to 100 F from the hot-soak values near 250 F. The corresponding results for the RSI case indicate that between 18 and 55 hours are required to cool the TPS from the hot-soak maximums to 100 F (for an α/ϵ ratio of one).

Table 4-38. Tentative Allowable Temperature Limits for Orbiter Components

Subsystem	Minimum Temperature (F)	Maximum Temperature	
		Long Term* (F)	Short Term** (F)
Propulsion			
ABES	-65	200	275
OMS	40	125	150
ACPS	40	125	150
MPS	-150	140	140
Power			
APU	40	125	150
Hydraulics	-40	275	275
Landing gears	-65	250	300
Avionics (unpressurized)	0	160	190
Cabin wall	60	105	120

*Several hours to several days per flight.
**Up to about two hours per flight.

Table 4-39. Preliminary TCS Heater Power Requirements

Subsystem*	Minimum Allowable Temperature (F)	Heater Power Worst Case; No Attitude Constraints (W)	Heater Power With Selected Attitude Constraints (W)
Propulsion			
ABES	-65	300	70
OMS	40	310	200
ACPS	40	270	180
Power			
APU	40	180	120
Hydraulics	-40	1050	230
Landing gears	-65	140	40
Avionics (unpressurized)	0	180	100
Total		2430	940

*Cargo and ECLSS requirements not included.

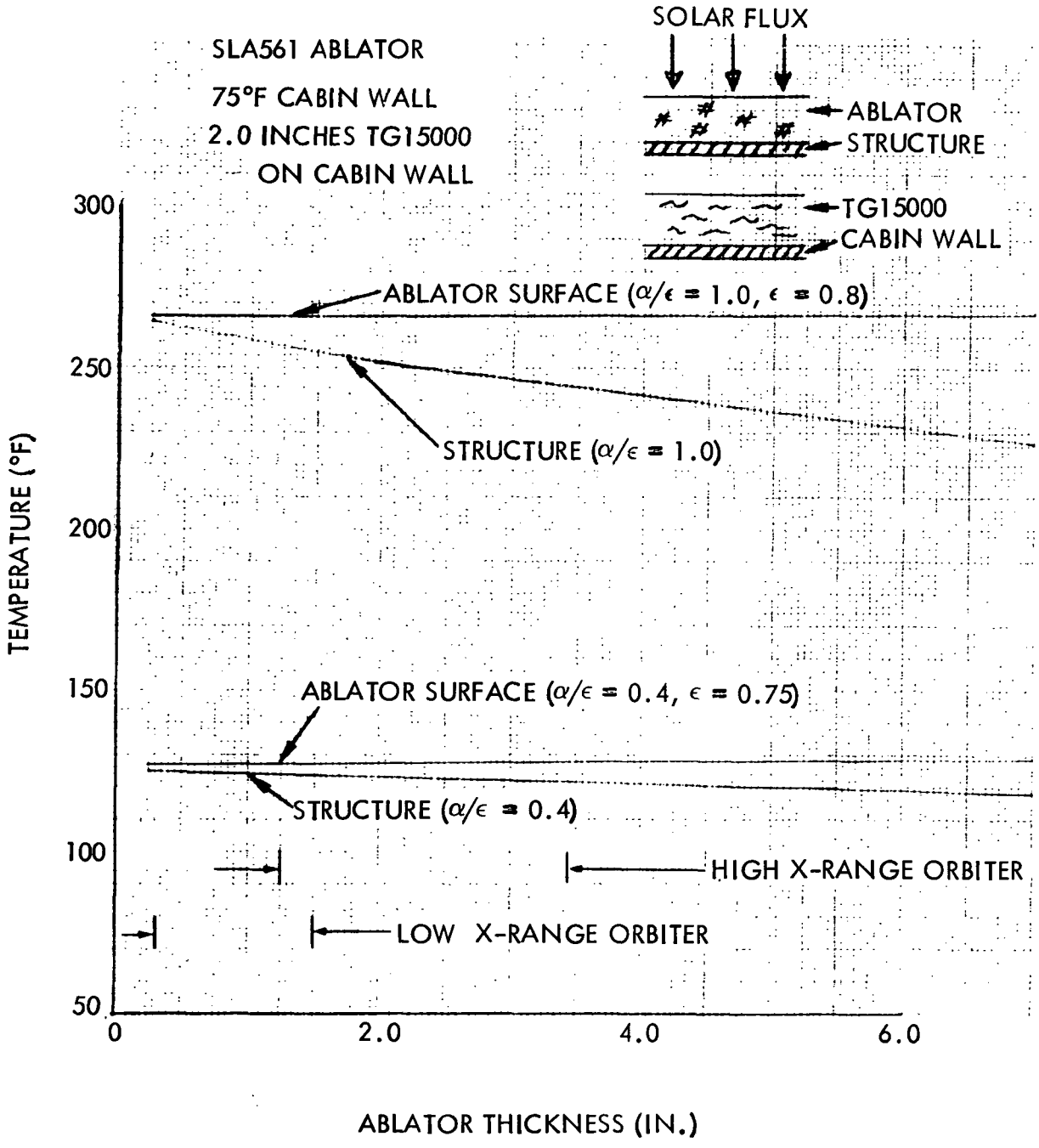

Figure 4-222. Ablator TPS Maximum Orbital Temperatures

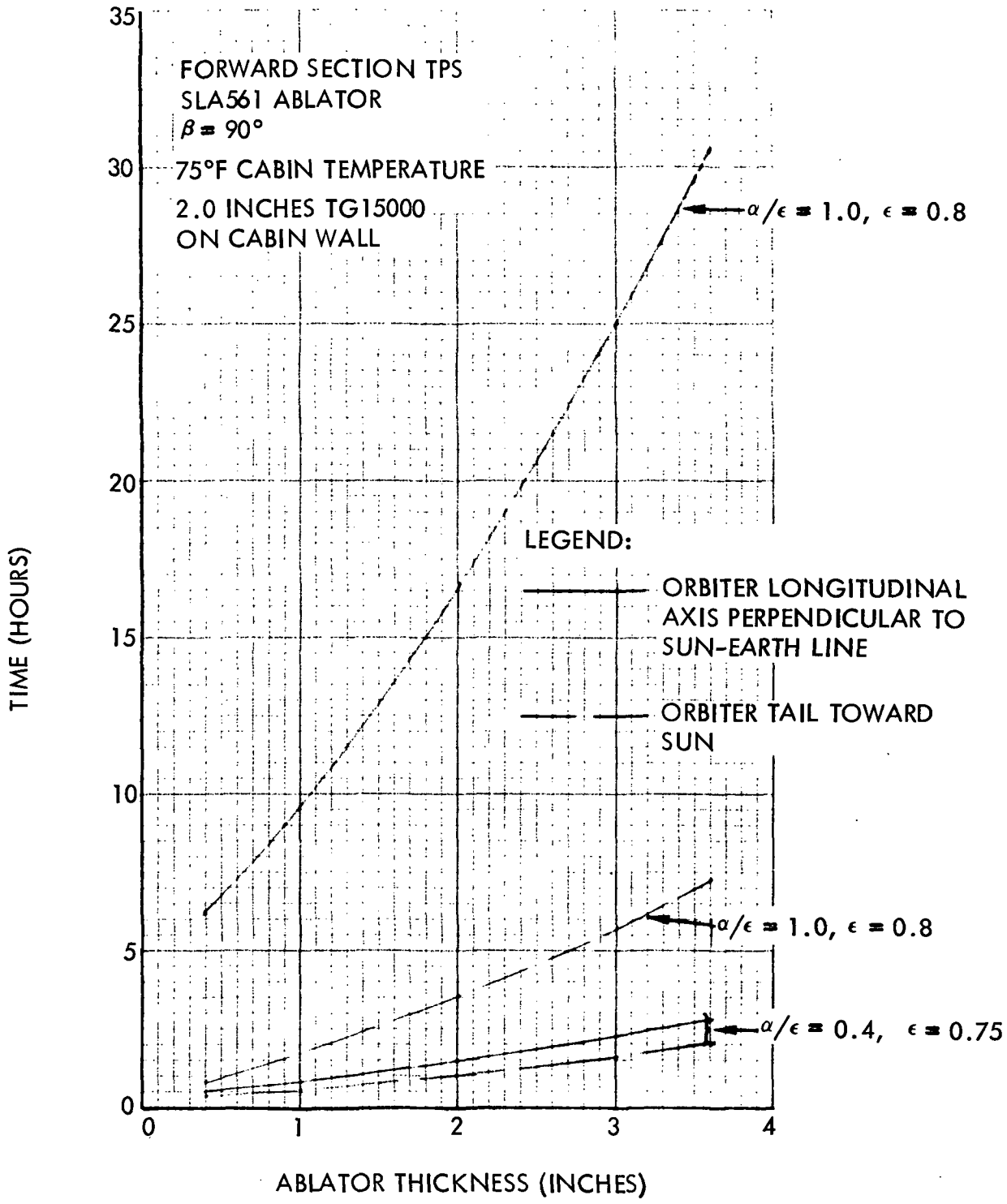

Figure 4-223. Time Required to Cool Ablator Bondline From Maximum Orbit Temperature to 100 F

4.4.3.7 TPS Structure

TPS. The Mark I TPS is a planned refurbishment system which incorporates ablative material for protection of the entire wetted area of the aluminum (2024T86) structure. Two different ablators are used. The vehicle "acreage" is covered with 14.5 pcf Martin Marietta SLA 561 in a honeycomb core. The wing and vertical stabilizer and other selected areas are protected by Avco 5026-39M moldings at 32 pcf for improved performance under high heating rate, high aerodynamic shear environments. The ablator is sized to limit the maximum temperature at the interface between the primary structure and the RTV 560 silicone adhesive (.040 thick) to 350 F. Thicknesses and areas covered by the two ablators are shown in Drawing VC70-0179.

The Mark II fully reusable TPS is applied over an aluminum primary structure, which is essentially the same structure as used for the Mark I vehicle. The TPS for the leading edges of the wing and vertical stabilizer are fabricated from reinforced carbon-carbon (RCC) with an oxidation-inhibitor coating for multimission reuse. Since the RCC operates with a high backface temperature, zirconia bulk fiber insulation is used to lower the temperature at the wing spar to 350 F. The insulation is packaged on the five hot sides using platinum foil, while the fiberglass packaged "cool" side is attached to the structure with metallic hook and pile. The mechanical attachments for the leading edges are located internally, and the fasteners are protected to 1800 F, maximum. The vehicle "acreage" is protected by reusable surface insulation (RSI) fabricated by General Electric's Reentry and Environmental Systems Division. The mullite fiber, mullite binder RSI tiles, coated with a waterproof ceramic on five sides, are received from GE as finish machined tiles that are bonded with an adhesive sandwich consisting of two layers of PD200 full-density silicone 0.005 inches thick bonding 0.070 thick PD200-28 foam (28 pcf) to the structure and RSI tile uncoated face. Gaps between RSI tiles are filled with a silica omniweave fabric compressed 50 percent from its woven thickness on installation. This material is used at the RSI/RCC interface as well to prevent plasma ingestion. Thicknesses of RSI and RCC locations are shown in Figure 4-217. Interface and special problem area designs are shown in Figure 4-224.

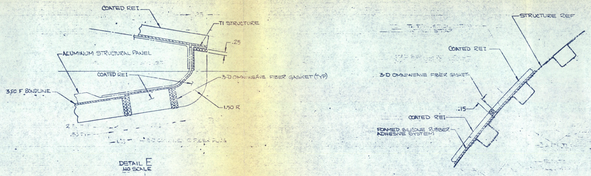

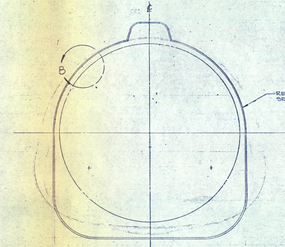

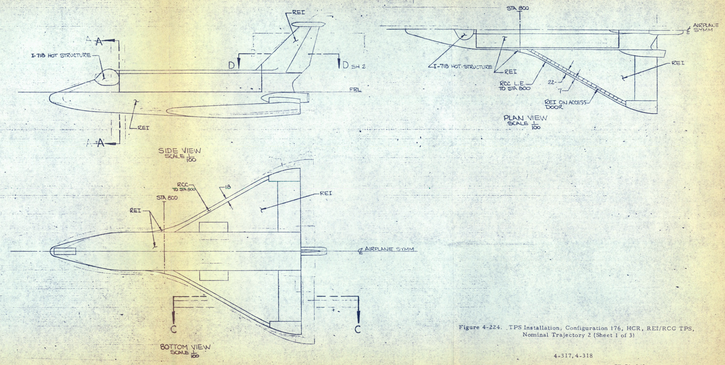

Figure 4-224. TPS Installation, Configuration 176, HCR, RET/RCC TPS, Nominal Trajectory 2 (Sheet 1 of 3)

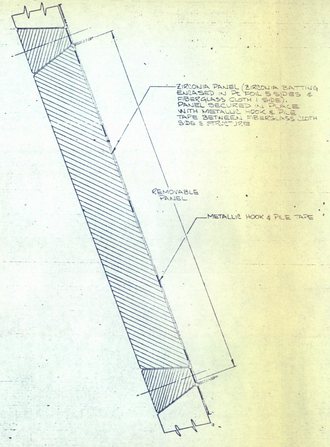

SECTION N-N
SCALE ½

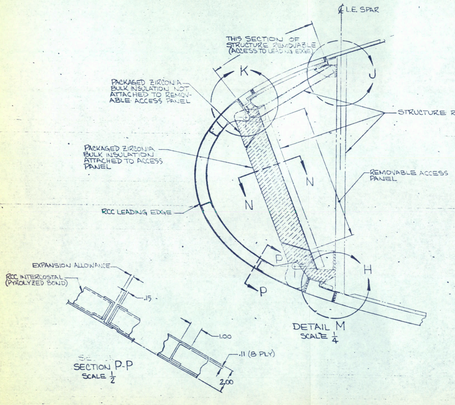

DETAIL M
SCALE ¼

SECTION P.P
SCALE ½

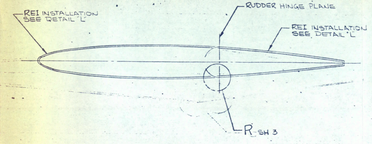

SECTION D-D SH 1
SCALES ½, 10

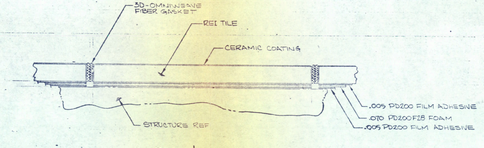

DETAIL L
SCALE ½

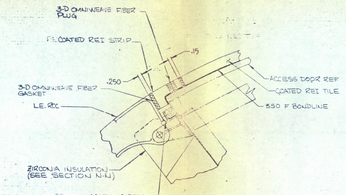

DETAIL K
NO SCALE

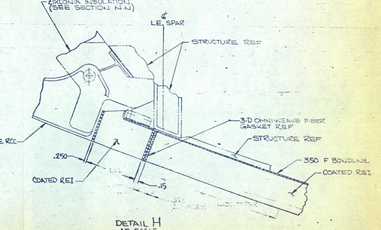

DETAIL H
NO SCALE

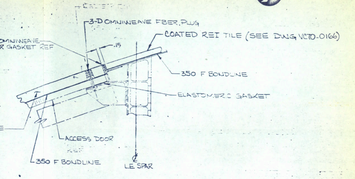

DETAIL J
NO SCALE

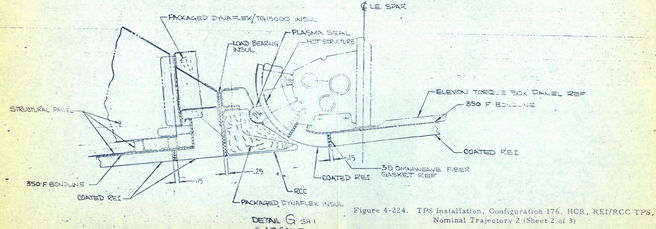

DETAIL G SH 1
NO SCALE

Figure 4-224. TPS Installation, Configuration 176, HCR, REI/RCC TPS, Nominal Trajectory 2 (Sheet 2 of 3)

4-319, 4-320

SD 71-342

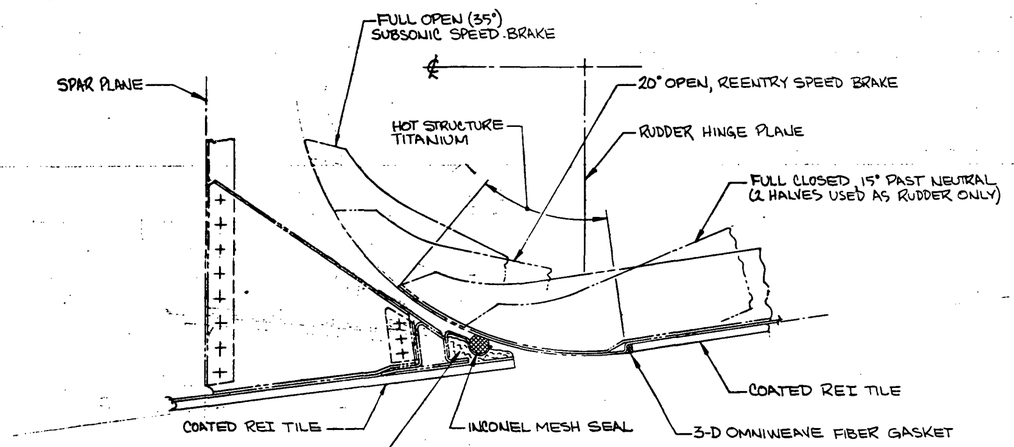

DETAIL R SCALE 1/2 SH 2

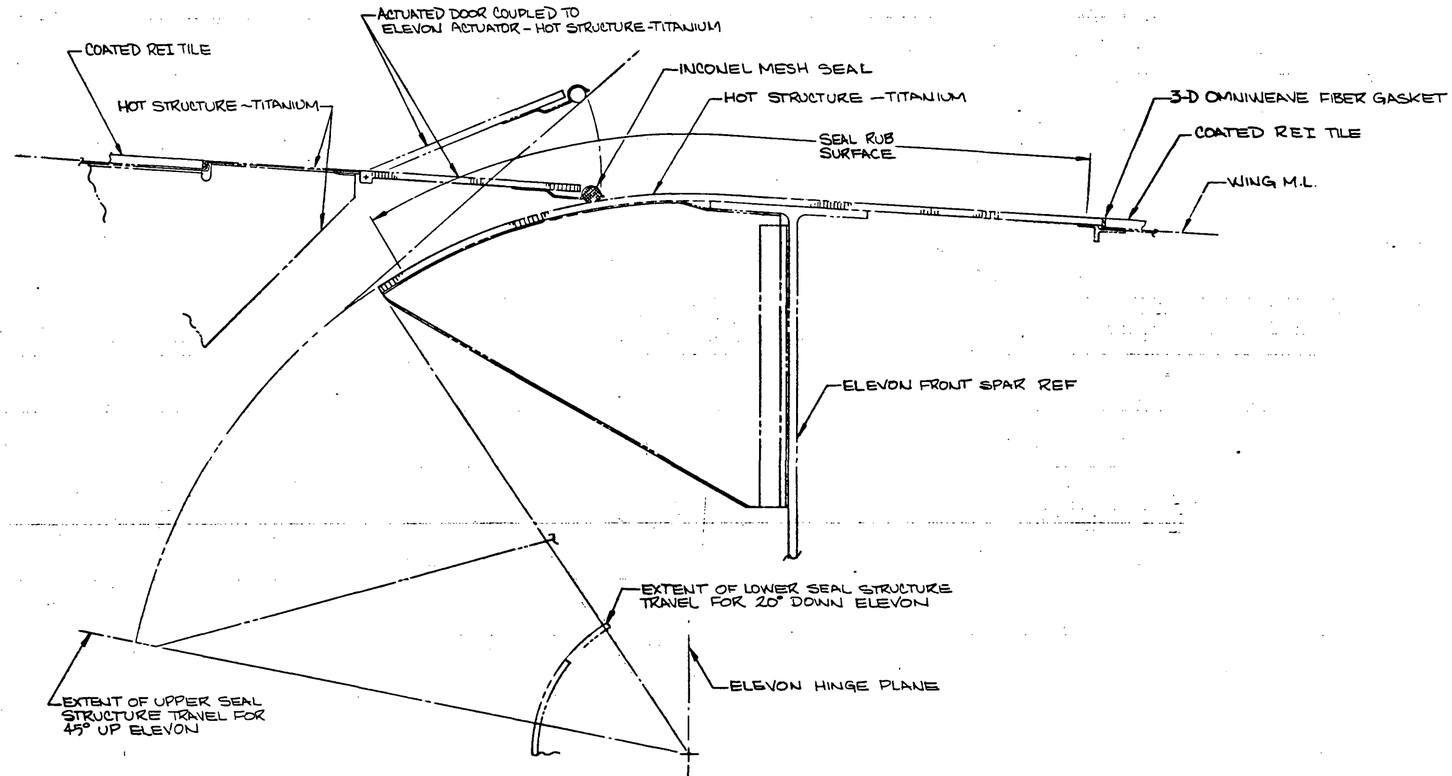

DETAIL F SCALE 1/2 SH 1

Figure 4-224. TPS Installation, Configuration 176, HCR, REI/RCC TPS, Nominal Trajectory 2 (Sheet 3 of 3)

Structure. The structural arrangement of the orbiter is shown in Figures 4-225 and 4-226. All major structural components are basically aluminum, with ablator TPS provided to limit the maximum temperature to 350 F.

The external expendable propellant tanks are attached at Stations 576 and 1305. The first-stage booster thrust to the orbiter and orbiter thrust to the orbiter MPS tanks occur at the aft attachment (Station 1305).

In the midbody section, provisions are made for installing and attaching a 15-foot-diameter and 60-foot-long cargo pod. Alternate attachment locations are provided to accommodate variations in payload size. Large deployable doors cover the payload bay. On-orbit radiators are attached to the inner surface of the doors.

The major components are described separately.

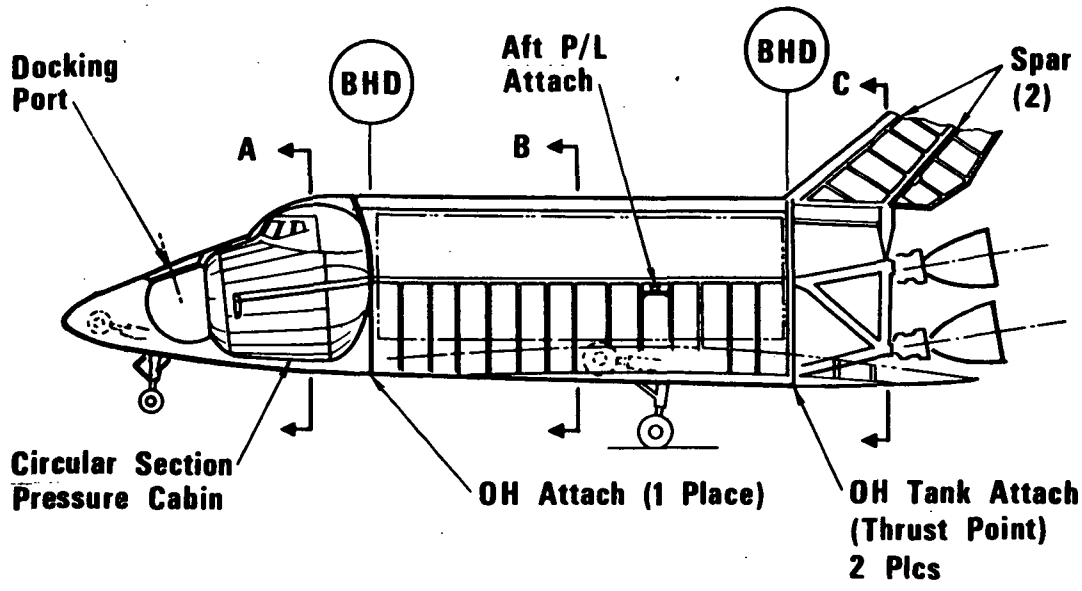

Figure 4-225. Orbiter Structure

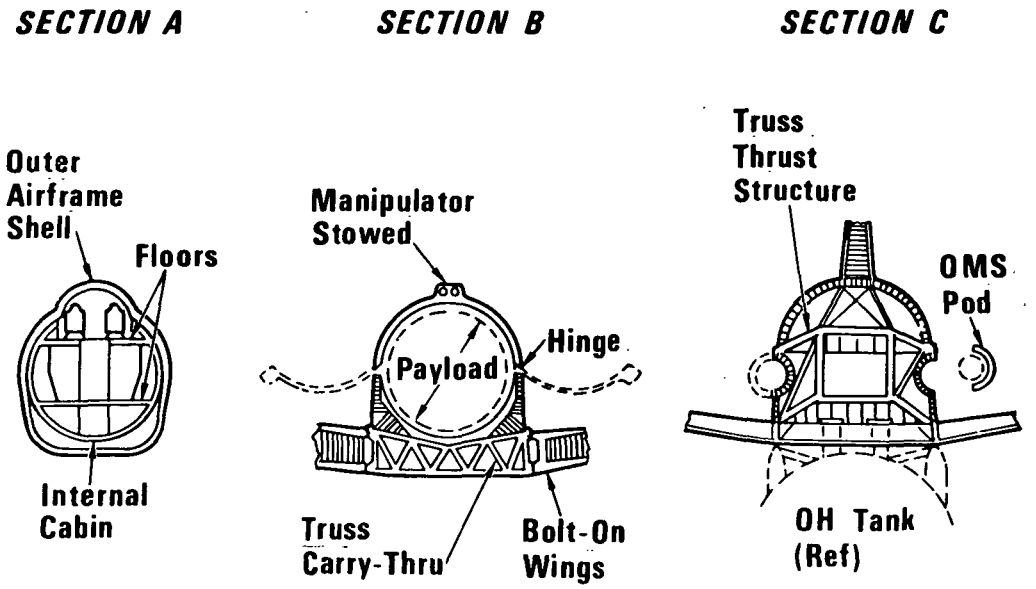

Figure 4-226. Structural Features

Forward Body, Including Crew Compartment. The forward body structure reacts air loads and nose gear landing loads, and consists of two major components: the outer structure accepting the air loads and landing loads; and the pressurized crew compartment. The outer structure is a semimonocoque aluminum structure except in the windshield area, where high-temperature nickel alloy steel is required. The body frames are numerical-control machined rings, and the stretch-formed skins are stiffened by riveted-on hat section stringers.

Midbody. The midbody, made of aluminum skin-stringer and frames, contains the payload compartment. The body bending, shear, and torsion from wing, nose, and aft body section are reacted by the side and bottom panels. (The payload bay doors do not react any of the body loadings, but do carry pressure loadings.) The numerical machined frames are made in three pieces, with identical side portions from Stations 700 to 1273.

The skin and hat stringers are riveted to the body frames and carry-through spars. Four main wing bending carry-through spars are machined trusses, which also act as body lower frames.

Aft Compartment. The aft compartment shell structure is of aluminum sheet-stringer frame construction. A machined aluminum "shelf" is used to transfer in-plane thrust loads from the upper two main engines to the midbody upper longerons, and a similar lower "shelf" transfers in-plane thrust loads from the lower two main engines to the midbody central longerons. The aluminum fin support structure attaches to the forward bulkhead, the upper thrust beam, and the aft compartment outer shell to react all fin loading conditions. Engine actuation loads are reacted by fittings attached to the thrust "shelves."

The heat shield structure consists of movable spherical segments attached to the engine skirts in combination with fixed bulkhead-type segments attached to the orbiter. The movable and fixed segments are made of Inconel 718 sandwich construction. The stabilizing cruciform beam is also of Inconel 718 construction.

Wing and Elevon. The wing is a 60-degree delta, composed of detachable outer wings and a multispar carry-through built integrally into the fuselage. The outer wings comprise the entire exposed wing area of the orbiter and are detachable at the fuselage to allow the orbiter to be moved by surface transportation, thus enhancing producibility. The outer wings provide mounting for the main landing gear members, the wing tip reaction control system pods, and the elevons and their subsystems. The wings are constructed primarily of 2024 aluminum alloy.

The elevon is of two-spar conventional aluminum wing construction. It is split into two panels which are pinned together at midspan. This arrangement prevents hinge binding when the wing deflects under load. The elevon-to-wing sealing surfaces are "hot structure" – the upper surface being skinned with titanium panels, and the lower skin is of Haynes 188, in the area of the seals only. These panels are insulated from the rest of the structure.

4.4.3.8 Propulsion and Fluid Systems

Main Propulsion System.

Mark I. The orbiter main propulsion system provides the velocity increment for insertion of the space shuttle into a 50 by 100 nm orbit following booster separation. In the event of premature booster separation or orbiter engine failure, the main propulsion system provides the velocity increment for an intact abort. The normal staging mode of separation between booster and orbiter provides a positive acceleration for main engine starts. The main engines provide the vehicle steering in pitch, yaw, and roll during the orbiter burn phase.

The system concept differs from the system described in the Phase B final report, SD 71-114-2, in that external LO_2 and hydrogen tanks (LO_2 forward, hydrogen aft) are utilized in place of vehicle integrated tankage (hydrogen forward, LO_2 aft), and J2-S engines are used in place of high Pc engines for the Mark I orbiter.

The main propulsion system employs a cluster of four J-2S rocket engines located in the orbiter aft fuselage. Each engine provides a vacuum thrust of 265K lb using LO_2/LH_2 propellants at a mixture ratio of 5.5 to 1 (see Table 4-40). The engines are capable of being throttled from 100 to 50 percent thrust to limit vehicle acceleration to 3 g. Propellants are supplied to the engines from external tankage, consisting of a single liquid oxygen tank located forward of the single liquid hydrogen tank. Propellant gaging is provided for control of propellant loading and for engine cutoff phasing. The main propulsion system is illustrated in the system schematic diagram of Figure 4-227.

Prestart engine conditioning is provided by propellant recirculation of both oxidizer and fuel from the external propellant tankage. Oxidizer recirculation flow is induced by natural convection from the tank through the feedlines and engines and returned to the tank through the recirculation line. The LH_2 is pumped through the engines via the recirculation lines and returned to the tank through the feedlines. Ground prepressurization using cold helium provides the tank pressures necessary for engine start conditions. An engine-mounted starter cartridge (solid-propellant gas generator) supplies the gases for spinning up the engine turbopumps. During operation, the turbopumps are driven by combustion gas bled from the engine thrust chamber. An open-loop mixture ratio control is used. Tank pressurization is obtained autogeneously by oxygen and hydrogen gas bleed from the engine. In addition, a pneumatic subsystem using helium is employed to supply inflight purge gas and valve actuation pressure.

Table 4-40. J-2S Engine Characteristics Summary

Item	Sea Level	Vacuum
Thrust (lb)	196,400	265,000
Specific impulse (sec)		
Nominal	323	436
Minimum	320	432
	Characteristics	
Mixture ratio (O/F)	5.5	
Controllable mixture ratio	4.5 to 6.0	
Chamber pressure (psia)	1,200	
Nozzle area ratio	40 to 1	
Throttling ratio	2 to 1	
Gimbaling capability (deg)	±7-1/2	
Length (in.) (from gimbal block flange)	119.5	
Exit diameter (in.)	80	
Inlet line diameter (in.)	8	
Weight, dry (lb) (w/access., 1 start, and sea level capability)	3,800	
Propellant flow rate, (lb/sec, 100% nominal, MR=5.5)	607.79	
Design Life		
Starts	30	
Duration (sec)	3,750	
Propellant Inlet Requirements		
Mainstage NPSP (100% Thrust)		
LO_2 (psi)	19.2	
LH_2 (psi)	4.4	

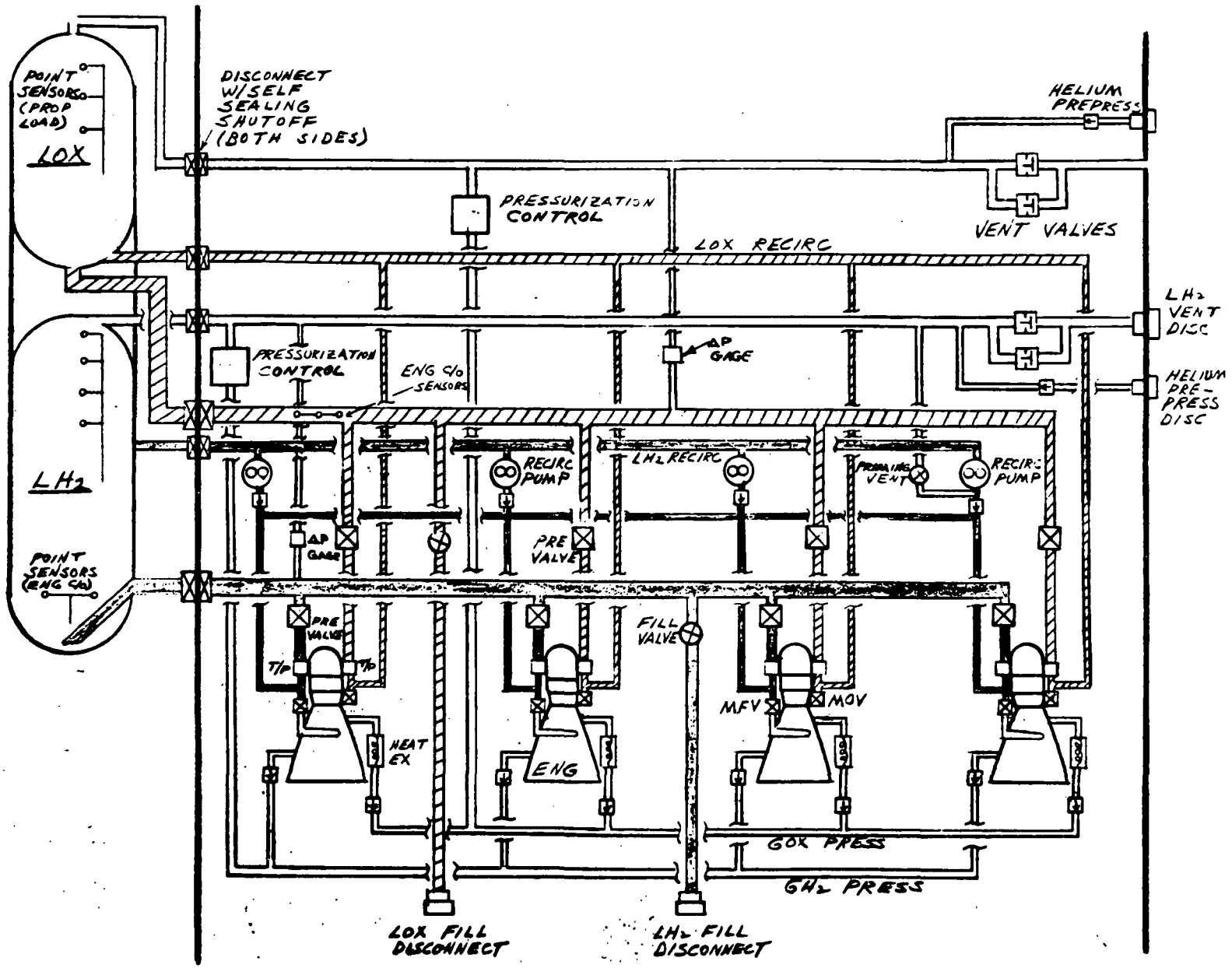

Figure 4-227. Main Propulsion System, 4 J2-S/SSME Engines

The LH_2 is fed from the external tank to the engines through a single manifold which divides into individual engine feedlines in the aft engine compartment. Prevalves in the feedlines provide for propellant isolation during nonoperating periods. The LO_2 tank is connected by a similar manifold-feedline arrangement to the engine inlets. Feedlines located inside the orbiter are vacuum-jacketed for insulation. External feedlines and the external tankage use a fixed insulation material applied to their external surfaces. See Paragraph 4.4.4.7 for external tank details.

Self-sealing disconnects are located in all the propellant and pressurization lines to the external tanks. The external tankage is separated from the orbiter vehicle after the main ascent burn.

Other system components include vent valves and recirculation and pressurization controls. Connections are provided for ground servicing of propellants and prepressurization gases.

The main propulsion system interfaces with other systems are as follows:

1. Nitrogen-ground supply - engine and areas purge
2. Helium-ground supply - tank prepressurization and engine purge
3. Helium-stage supply - system pneumatic requirements
4. Electrical power supply - redundant ac and dc to engines and components
5. Hydraulic power supply - redundant to gimbal actuation system and engines
6. Body structure - system and engine installation
7. TPS - spherical brush seal closeout
8. GN&C - system command signals
9. Displays and controls - system monitoring and commands
10. Data control and management - system instrumentation
11. Checkout and fault isolation - system monitoring and redundancy

Mark II. The functions, requirements, and operation of the main propulsion system are similar to that described for the Mark I. The primary difference is that the four J-2S engines (Mark I) are replaced on a one-for-one basis with four high-P_c (3000 psi) space shuttle main engines. Each SSME provides the same vacuum thrust (265K Lb) as the J-2S, but with greatly improved performance and design life (Table 4-41). The SSME operate at a nominal mixture ratio of 6 to 1 (O/F), whereas the J-2S is 5.5 to 1.

The propellant feed and external tankage is identical to Mark I. The feedlines are identical except for adapters for interface differences. The Mark I tankage was sized for Mark II requirements and are loaded full, whereas the same tankage with J-2S engines for Mark I had an offloaded oxidizer tank to account for differences in the engine mixture ratio, specific impulse, and bleed gas temperatures for autogenous pressurization of the tanks. Mark I and Mark II propellant inventories are presented in Section 4.4.4.7.

Other changes for Mark II are provided in the pressurization subsystem and the stage-mounted pneumatic helium system. In the pressurization subsystem, one of the control component operating pressure bands is revised to be compatible with the SSME requirements and operating characteristics. The operating bands have been selected to permit use of the same components for Mark I and Mark II. The operating bands are the same, except for the flight pressurization of the LO_2 tank at 20-22 psia versus 34-36 psia in Mark I. The inflight pressurant flow control solenoid valve flow area will be smaller for Mark II to be compatible with the higher pressurant delivery pressure and temperature of the SSME.

The stage-mounted pneumatic helium system will be modified to include the additional helium supply for pneumatic requirements for the SSME, whereas the J-2S engine in Mark I has an engine-mounted helium tank for engine pneumatic requirements.

Orbit Maneuvering Subsystems. The orbit maneuvering subsystem provides the velocity increment necessary for orbit circularization, orbit transfer, rendezvous, and deorbit. The mission functions served by the OMS are the same as those served by the system as described in the Phase B report, SD 71-114-2. The system, however, has been revised from a LH_2-LO_2 system to a system utilizing storable propellants. The system consists of two complete and independent pod assemblies mounted on the aft fuselage. Each pod consists of one hypergolic bipropellant rocket engine, a propellant pressurization system, a propellant storage and feed system, and a quantity gaging system. The system is shown schematically in Figure 4-228.

Table 4-41. SSME Engine Characteristics Summary

Item	Sea Level	Vacuum
Thrust (lb)	200,057	265,000
Specific impulse (sec)		
Nominal	342.14	453.2
Minimum	339.14	450.2
Mixture ratio (O/F)	6.0	
Controllable mixture ratio	5.5 to 6.5	
Chamber pressure (psia)	3,000	
Nozzle area ratio	90 to 1 (fixed)	
Throttling ratio	2 to 1	
Gimbaling capability (deg)	±8	
Length (in.) (From Gimbal Block Flange)	147.5	
Exit diameter (in.)	75	
Propellant inlet diameter (in.)	9	
Weight, dry (lb) (with access., multistart, and sea level capability)	3,125	
Propellant flow rate, (lb/sec) 100% nominal MR = 6.0	584.73	
Design life:		
Starts	100	
Duration (sec)	27,000 (7.5 hr)	
Propellant Inlet Requirements		
NPSP (50 - 100% Thrust)		
LO_2 (psi)	8	
LH_2 (psi)	2	

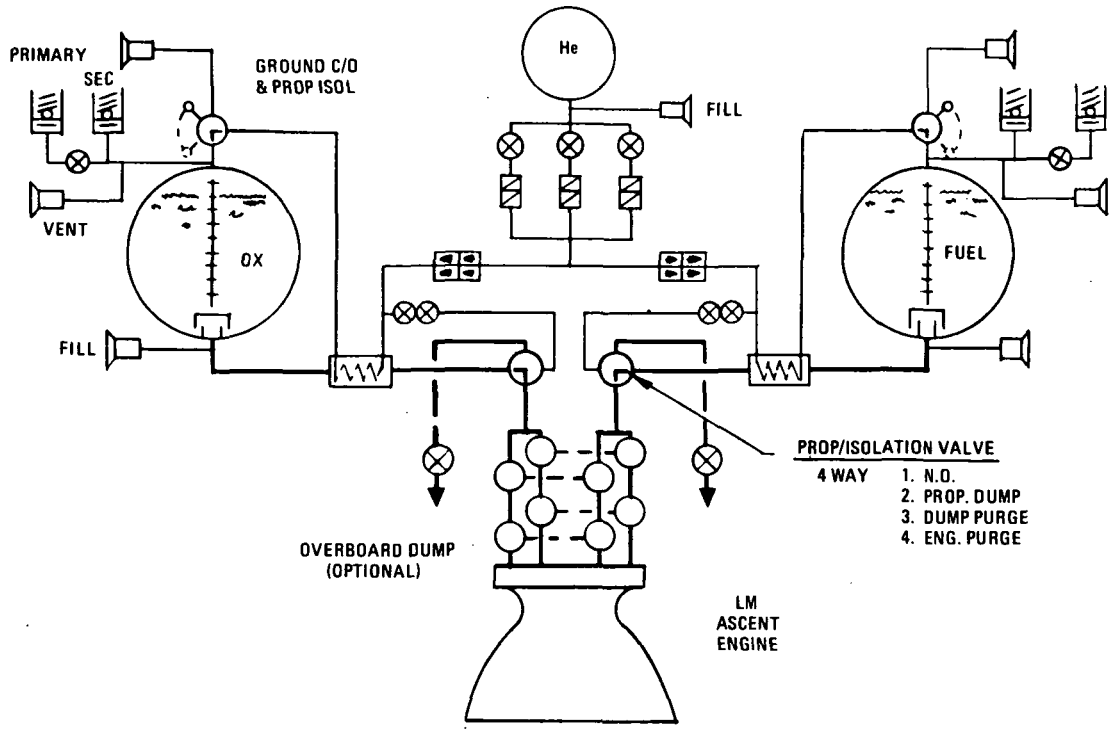

Figure 4-228. Orbital Maneuvering System, Earth Storable Propellants, Two Pods

The propellant pressurization system uses helium gas stored at high pressure. A normally closed solenoid valve isolates the high-pressure gas when the system is inoperative. During system operation the pressure is reduced by one of three regulators installed in parallel. Each regulator assembly contains a primary and secondary regulator in series. Helium flows equally to the fuel and oxidizer tanks through series parallel check valves and then through heat exchangers to the propellant tanks. An alternative system that utilizes a separate helium storage and pressure-reducing system for each propellant tank is under consideration. Further study may indicate that the heat exchangers are not required to stabilize the helium temperatures. Heat exchangers have been included for space and cost considerations.

Pressure relief valves are provided in each tank pressurization system. The primary valve, consisting of a burst disk and a poppet/spring device, is set at slightly above maximum system operating pressures. If the primary pressure relief valve actuates and subsequently fails to reseat, a solenoid valve will isolate the primary valve. The secondary relief valve is set at tank proof pressure. The relief valve system will be sized to relieve a failed-open regulator.

Each pod assembly, shown in Figure 4-229, contains one fuel and one oxidizer tank. The system uses a 50-50 blend of hydrazine (N_2H_4) and unsymmetrical dimethylhydrazine (UDMH) as the fuel, and nitrogen tetroxide (N_2O_4) as the oxidizer. The propellant ratio of oxidizer to fuel of 1.6:1 by weight results in equal volume tankage.

The tank internal configuration includes a retention reservoir at the tank outlet, containing sufficient propellant to provide restart capability in a zero-g environment. Propellant retention screens will be provided as capillary barriers and baffles, in conjunction with the reservoir, to position the propellant and minimize the possibility of gas ingestion to the engine.

The propellant tanks will be derivatives of tanks used on the Apollo program (LM descent system) with revised mounting provisions.

Provisions for propellant jettison are provided as shown schematically on Figure 4-228. Studies will continue to determine the effects of dumping propellants during the abort mode as well as for dumping mission residual propellants.

A propellant quantity gaging system is provided to enable the crew to monitor the quantity of propellants remaining in each OMS pod. Quantity sensing probes are installed in each propellant tank. A low-level warning lamp will indicate incipient propellant depletion.

The engines are non-throttleable, fixed position, pressure-fed rocket type consisting of an ablative cooled combustion chamber, a radiation-cooled nozzle extension, and series-parallel bipropellant control valves with

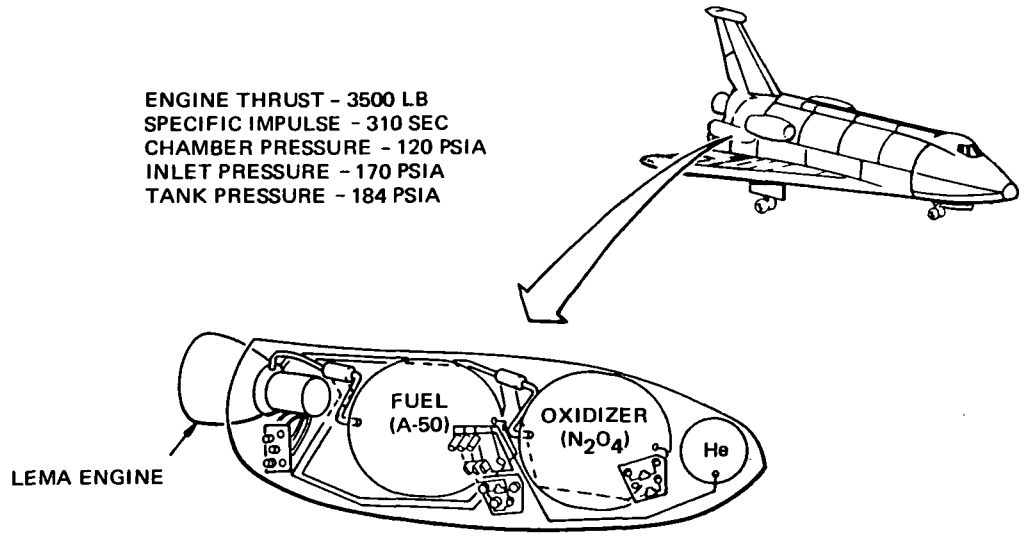

Figure 4-229. OMS Fuel and Oxidizer Summary

mechanical interlinks. The LM ascent engine RS1801C (Rocketdyne) or a derivative is being considered for this application in the Mark I orbiter. A study will be made to determine the cost impact to modify the valve actuation system to improve decontamination procedures. Consideration also will be given to possible modifications of the engine to meet Mark II reusable requirements. Engine characteristics are given in Figure 4-229.

Reaction Control Systems. Orbiter attitude control functions are provided by the RCS during all exoatmospheric flight conditions and for entry up to aerodynamic control transition. This system consists of three pods, containing a total of 32 thrusters, arranged as shown on Figure 4-230. All pitch maneuvers are accomplished by six thrusters located in the tail pod. All other maneuver functions are accomplished by 26 thrusters located 13 to a pod on both wing tips.

Based upon Phase B and B' study effort, the critical thrust level design condition was determined to be the entry yaw acceleration, $\approx 1.3^{o}/sec^{2}$. Individual thruster thrust level of 1050 pounds was determined from data summarized in Table 4-42. An earth-storable propellant combination of nitrogen tetroxide and Aerozine-50 was used for this study phase based on commonality with the orbit maneuvering system. Propellant loading requirements are based on the SD due east mission which previous study determined to be the critical mission from the standpoint of RCS propellant usage.

The mission total impulse equals 1.32×10^{6} lb-sec, which results in an impulse propellant requirement of 4550 pounds (Isp = 290 sec). This includes a contingency of 7-percent impulse propellant. Accounting for residuals and bellow tank expulsion efficiencies, the total loaded propellant quantity is 4790 pounds. Propellant apportionment between the three pods is essentially equal, predicated on mission timeline propellant usage. Based on a design mixture ratio of 1.6, each pod will contain four equal-volume bellows tanks (D = 17.6 in; L = 53 in). Figure 4-231 shows the typical physical arrangement of a wing tip pod.

A typical wing pod schematic is shown on Figure 4-232. This schematic was used for component arrangement and FO/FS analysis. As a safety measure, a purge valve is utilized to provide for thruster purge capability before landing.

Additional study effort is planned to include system maintainability optimization, alternative propellant combinations, and potential integration with the orbit maneuvering system.

Table 4-42. Vehicle Design Data and Thruster Sizing

Item	Characteristics			
Physical Characteristics				
Flight condition	Vehicle Mass (lb)	Roll (SLUG -	Pitch FT^2 X	Yaw 10^6)
Entry - 40K lb payload	179,000	0.673	5.685	5.923
On orbit - 65K lb payload to docking	204,000	0.678	5.982	6.228
Moment Arms				
Roll	392 in. = 32.75 ft 8 eng. firing up and down			
Pitch	690 in. = 57.5 ft 6 eng. firing up and down X degrees from FRL			
Yaw	392 in. = 32.65 ft 12 eng. fore and aft firing			
	430 in. = 35.8 ft 6 eng. side firing			
Thrust Level				
Critical design condition	Torque = Fn NL = Fn (35.8 + 3 (32.65)) = Fn (133.75)			
Yaw at entry $\ddot{\psi} = 1.3^o/sec^2$	$Fn = \frac{I\ddot{\psi}}{57.3\ NL} = \frac{5.923 \times 10^6\ (1.3)}{57.3\ (133.75)} \approx 1050$ $Fn = \underline{\underline{1050\ lb}}$			

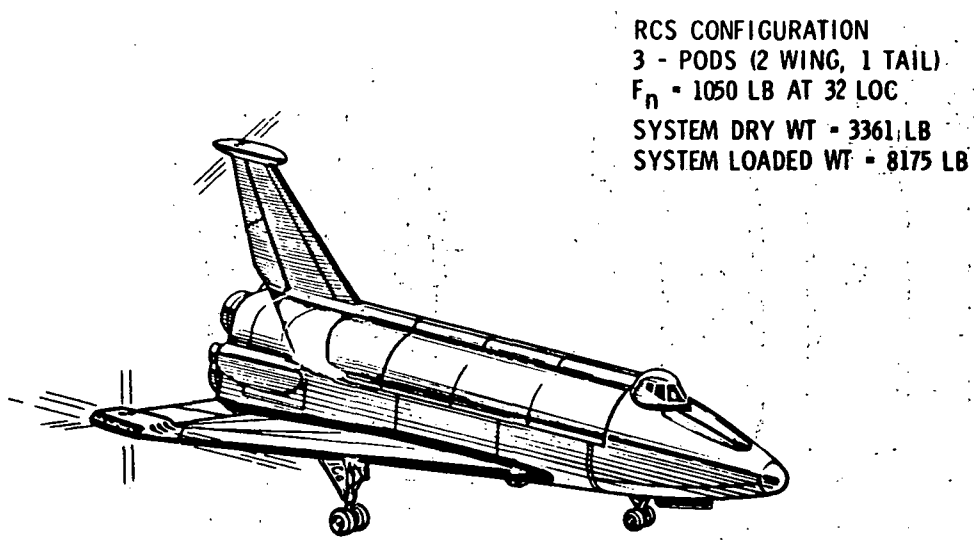

Figure 4-230. NR/SD Baseline RCS Configuration

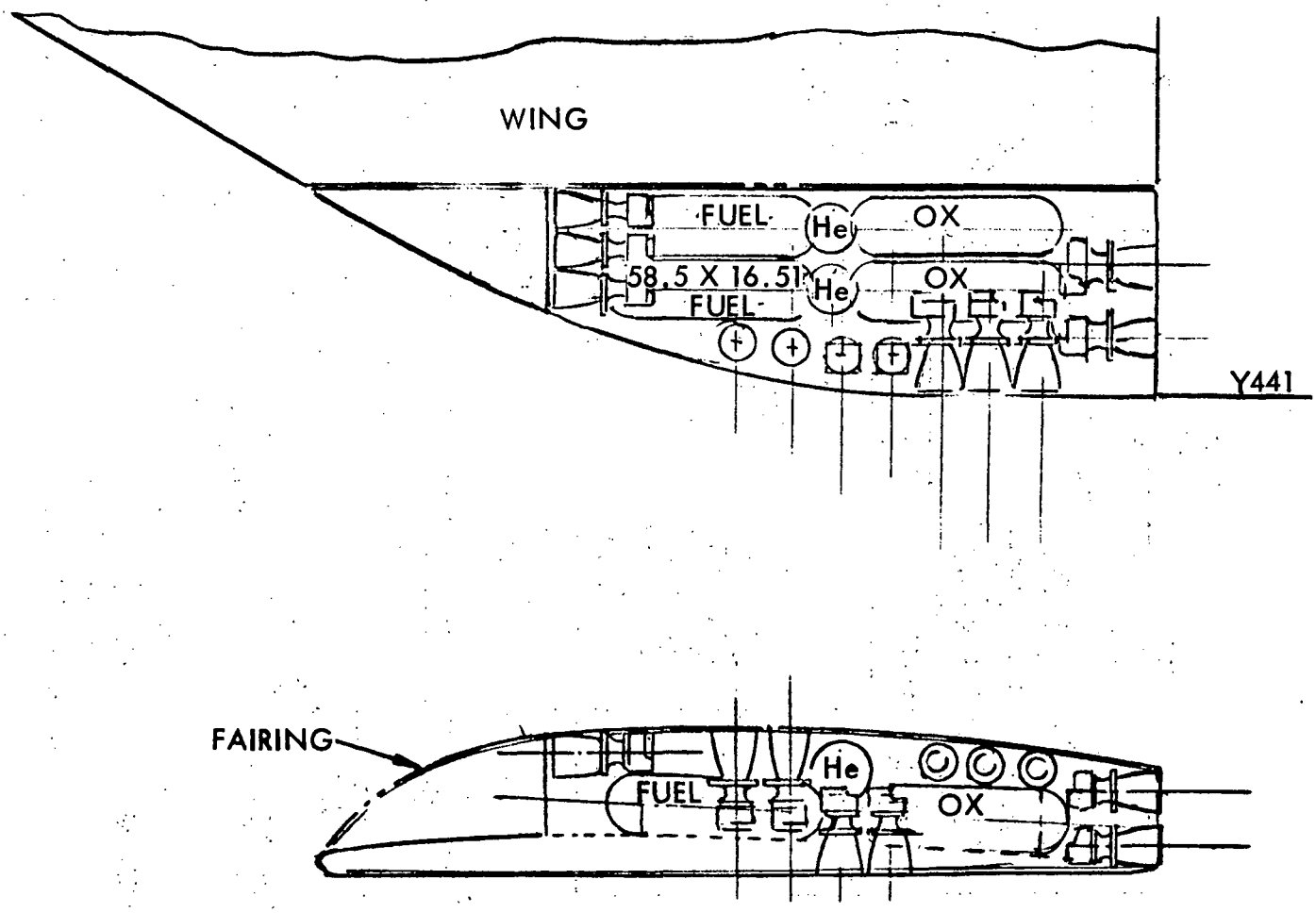

Figure 4-231. RCS Wing Tip Pod Installation

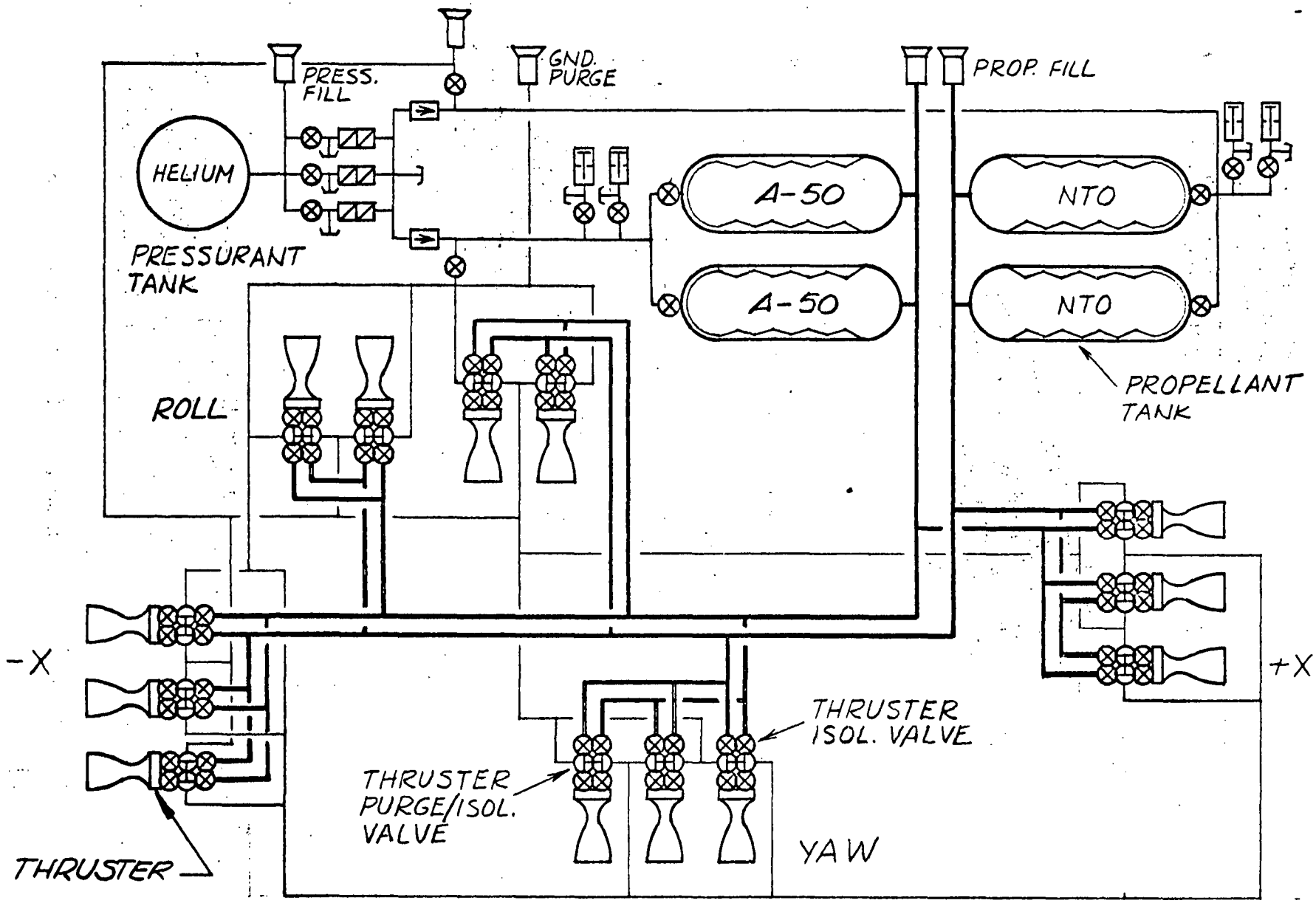

Figure 4-232. Orbiter Reaction Control System, Earth Storable Propellants, Typical Wing Pod

Air-Breathing Propulsion System. Air-breathing engines are required on the orbiter for landing go-around on return from an orbital mission, atmospheric flight range extension on return from orbital mission, and self-ferry between horizontal flight test ranges and from alternative landing sites to the launch site. The orbital air-breathing propulsion system (ABPS) will be installed in the payload bay and considered part of the payload weight capability. The ferry ABPS includes installation of necessary additional engines, supporting subsystems, and fuel tankage to provide for 440 nm ferry range (maximum for continental U. S. ferry flight) under FAR landing and takeoff requirements. Reference fields for ferry are: sea level - 10,000 feet long/ 4000 feet altitude - 13,000 feet long. Hot day atmosphere and engine performance will be used for orbit and ferry go-around and for ferry takeoff performance capability evaluation. Ferry cruise and orbit range extension capability will be based on standard day atmospheric engine performance. Selection of an engine to meet the design objectives will be weighed in favor of meeting ferry mission requirements, minimum cost, and commonality with booster ABPS requirements.

ABPS Description. The ABPS is packaged as a module installed in the aft section of the cargo bay at the approximate c. g. of the vehicle (Figure 4-233). Two GE F-101/F-12A3 engines are installed in individual nacelle pylon assemblies. Nacelles are deployed by rotary motion about a pylon longitudinal axis. Deployment actuation power is provided by linear hydraulic actuators. The cargo bay doors are of segmented configuration. When the ABPS is installed, a special mission door assembly segment is installed incorporating hydraulically actuated engine nacelle deployment doors. The ABPS cargo door remains closed during orbit operation for environmental control considerations. An active environmental control system is provided (insulation and electric heaters) to maintain the engine system and bulk fuel within design limits (engine -65F min/275F max, fuel -65F min/200F max). The installation module also incorporates lateral beams for support of orbit fuel tank and as thrust/load carry through structure when the ferry engines are installed. The fuel tank has been sized to contain a quantity of fuel equivalent to the difference between the dry installed weight of the entire ABPS and the payload capability (25K lb) of the Mark I configuration orbiter. This fuel quantity, approximately 1599K lb, is contained in a single tank attached to the lateral support beams. Of this, approximately 360 lb are allocated for air start, high-power checkout, idle descent to range extension altitude, and ground idle, landing/taxi. The remainder, approximately 1563K lb, is available for range extension or go-around.

The fuel system design stresses simplicity and maximum use of off-the-shelf components to achieve reliability and minimum cost. Two "747" plug-in type booster pumps are used in the engine feed system (individual uninsulated line to each engine). An atmospheric air venting system is

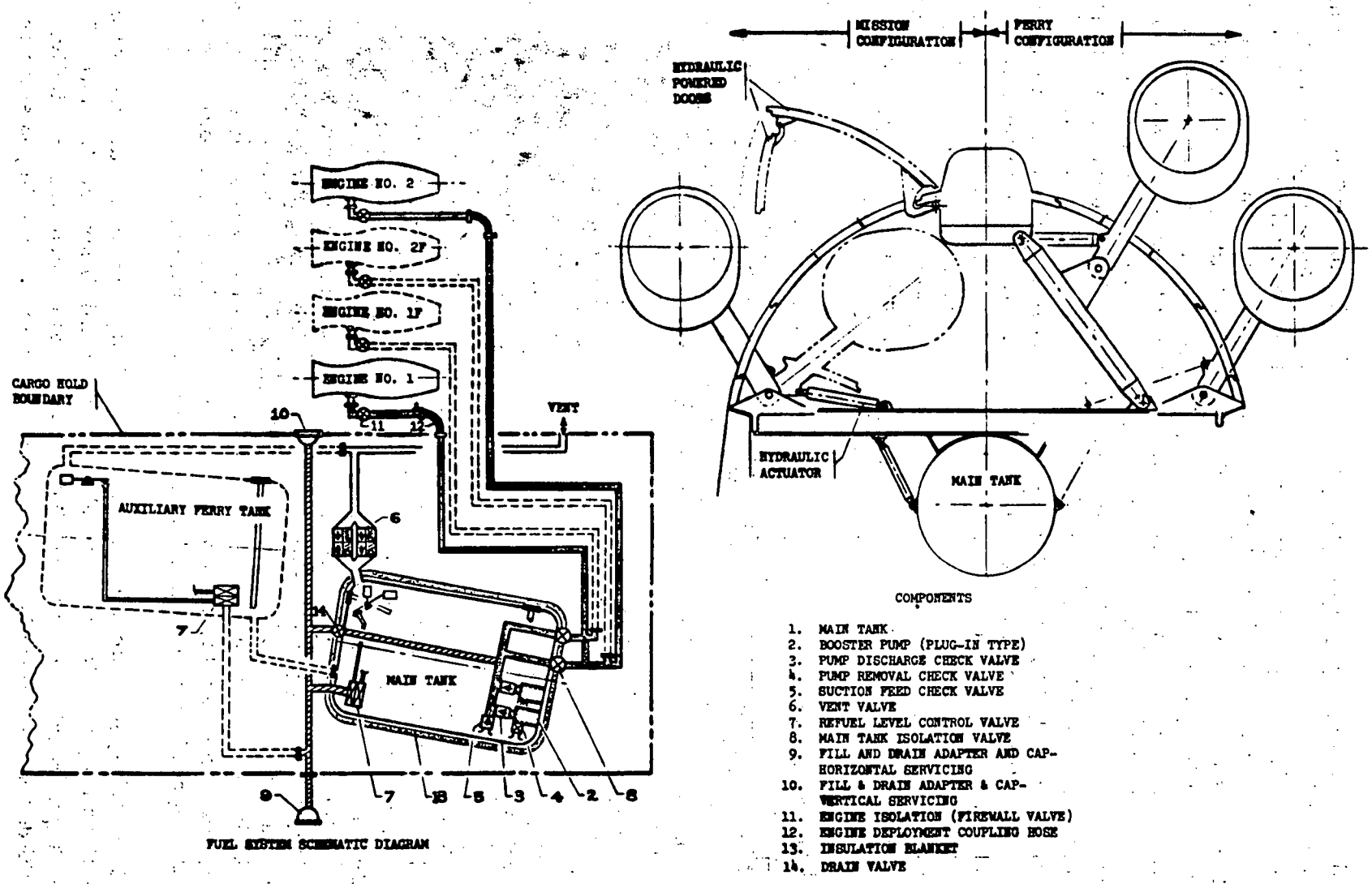

Figure 4-233. Air-Breathing Engine System

provided and series/parallel vent valves maintain on-orbit tank pressurization and fuel isolation. Refueling and defueling capability is provided for both the vertical and horizontal vehicle attitude using aircraft level control valves for capacity control. Tank insulation and electric heaters maintain bulk fuel temperature within operational requirements. Capacitance gaging systems are provided in both vertical and horizontal orientation. Tank design and orientation will provide operational liquid location control.

ABPS supporting subsystems will be comparable to those incorporated in the Phase B baseline vehicle. These include nacelle fire detection system, nacelle fire extinguishing system (dual bottle/dual shot per nacelle), electric thrust control system (closed-loop main mode/open-loop alternate mode), and an air start assist system. Cartridge/pneumatic air start system is baselined for the present configuration.

To provide for the ferry range capability two additional F-101/F-12A3 engine/nacelle assemblies are installed (fixed) on the vehicle upper shoulder in the approximate plane of the orbit engine locations. These engine/nacelle configurations will be identical, as far as possible, to the orbit nacelle assemblies to provide minimum cost. Supporting subsystems (i.e., fire extinguishing, ETCS, starter system, etc.), will be identical to the orbit configuration with the following exception. For the ferry mode and the horizontal flight test mode the vehicle APU system will not be used for vehicle power generation. ABPS engine-driven remote gearbox, hydraulic, and electrical power generation systems will be provided on three of the AB engines. These APU systems will provide vehicle power requirements. Vehicle power generation components or shelf-type components will be used in this configuration to minimize cost.

The Mark II vehicle ABPS will be identical to the Mark I vehicle system (both orbit and ferry configurations).

ABPS Performance. Performance capability of the Mark I orbiter with ABPS installed is summarized in the following paragraphs. Gross weight of the Mark I orbiter at initiation of ABPS operation for following performance evaluation is 138,652 pounds. For the orbit configuration:

1. Tanked fuel quantity, 15,99K lb, provides for 34 nm idle descent range (40,000 feet to 9,000 feet); Range extension 283 nm (55 minutes) – 9,000 feet altitude – standard day; 1.5-minute descent (15° γ nom) 9000 to sea level; and 3.5-minute idle-land, taxi, and shutdown. (Note: No go-around included).

2. Two engine thrust provides following go-around capability.

Geardown Configuration

2.0% climb gradient—hot day, 4000-foot field—max fuel load

3.7% climb gradient—hot day, 4000-foot field—min fuel load

4.1% climb gradient—hot day, sea level—max fuel load

6.5% climb gradient—hot day, sea level—min fuel load

For the ferry configuration:

1. Four engine thrust provides hot day takeoff, standard day cruise against 50 Kn headwind ferry range of 440 nm with a 31K lb takeoff fuel load.

2. Thrust-limiting takeoff gross weight capability is as follows:

Sea Level	Standard day	10,000-foot runway : 77K lb fuel range =	1100 nm
	Hot day	10,000-foot runway : 57K lb fuel range =	800 nm
4000 Feet	Standard day	13,000-foot runway : 62K lb fuel range =	950 nm
	Hot day	13,000-foot runway : 45K lb fuel range =	700 nm

The limiting takeoff gross weight for the above conditions will be a function of landing gear design limits.

Performance capability of the Mark II orbiter with ABPS installed is summarized in the following paragraphs. Gross weight of the Mark II orbiter at initiation of ABPS operation for following performance evaluation is 159,700 pounds. For the orbit configuration:

1. Tanked fuel quantity; 6128 lb (limited because of requirement of providing a 25K lb payload capability in addition to ABPS weight charged to payload capability) provides for 36 nm idle descent range (40,000 feet to 7,000 feet), range extension 92 nm—7,000 feet altitude—Std Day, 1.5-minute descent ($15^{\circ}\gamma_{NOM}$) 7,000 feet to sea level, and 3.5-minute idle-landing, taxi and shutdown. (Note: No go-around included)

2. Two-engine thrust provides following go-around capability.

Geardown Configuration

-.5% climb gradient—hot day, 4,000-foot field—max fuel load

+.1% climb gradient—hot day, 4,000-foot field—min fuel load

+1.3% climb gradient—hot day, sea level field—max fuel load

+2.0% climb gradient—hot day, sea level field—min fuel load

Because of the limited geardown go-around capability of the Mark II vehicle with the F-101/F-12A3 engines installed, an evaluation with the F-101/F-12B3 engine was made. The use of this engine would increase the go-around climb gradient to the following respective values: +1, +1.5, +2.7, and +3.3%. The above performance evaluations were based on an interim configuration and gross weight Mark I and Mark II orbiter. Further analysis of the finalized Mark I and II configurations will be required to ascertain vehicle orbit reentry and ferry flight capability, and approach and go-around procedures for selection of optimum ABPS installation.

Electrical Power Generation. The electrical power generation subsystem provides power for operation of the space shuttle orbiter integrated avionics and electrical usage subsystems from activation prior to launch through orbiter landing. Electrical loads such as main engine and landing aids required to be powered only during periods of APU mechanical power demand, are supplied electrical power from the APU-driven ac generators. The air-breathing engines drive electric generators to satisfy all electrical demands during ferry flights. The subsystem contains H_2/O_2 fuel cell powerplants, batteries, heat transfer equipment, product water elements, controls, and reactant storage, pressurization, and feed equipment.

The predicted average electrical power profile for a seven-day mission is depicted in Figure 4-234. Figure 4-235 presents the results of the peak load analysis for the normal mission and the 24-hour emergency powerdown cases. An integration of the power profile results in an energy requirement of 1224 kwh for the normal mission case and 182 kwh for a 24-hour emergency powerup case. These values are used to size the reactant storage tanks. The power profile and peak load analysis is summarized as follows:

Load	Power (kw)
Phase average load	6.4 to 10.5
Continuous load (2 min.)	3 to 13
Peak load (normal)	17
Peak load (emergency)	9

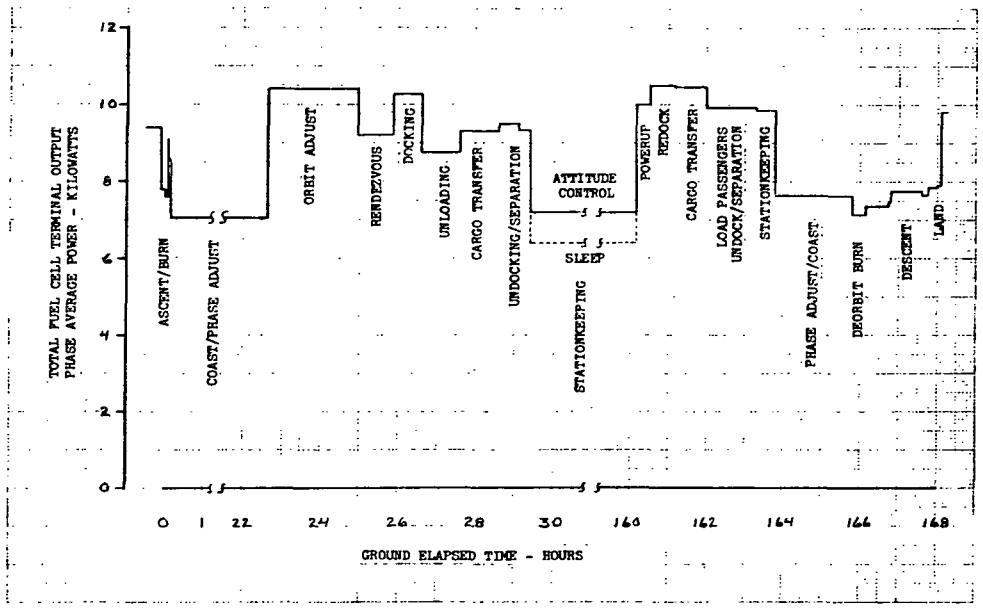

Figure 4-234. Orbiter Electrical Load Profile (Phase Averages)

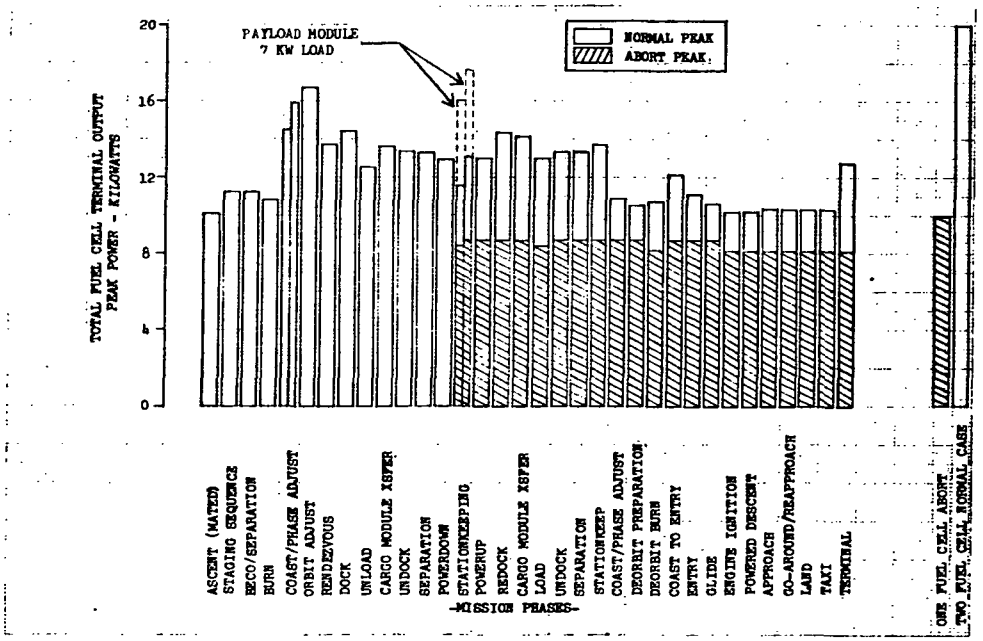

Figure 4-235. Orbiter Electrical Load Profile (Phase Peaks)

Based on these power requirements and a redundancy criteria of fail operational/fail safe; three fuel cell powerplants rated at 7 kw continuous and 10 kw peak are selected. This selection provides 20 kw of peak power and 14 kw of continuous power under normal or loss of one source conditions and 10 kw of peak power under emergency loss of two power sources condition. The electrical load analysis is based on the current baselined integrated avionics and propulsion systems, no attitude constraints, a sleep cycle during long-duration mission phases, and a 75-percent dc to ac conversion efficiency with 4 percent line losses for dc loads and 1-percent line losses for ac loads.

The reactant storage vessel selected is a spherical dewar for supercritical state storage. The oxygen vessel sizing is based on common storage for the fuel cell powerplants and all ECLSS oxygen demands. These requirements are satisfied by two 0_2 vessels. Each is 36 inches in diameter and weighs 181 pounds. Both 0_2 vessels provide a total storage capacity of 1512 pounds. The hydrogen vessel sizing is based on common storage for the fuel cell powerplants and the ECLSS demand for entry and landing cooling. These requirements are satisfied by two H_2 vessels. Each vessel is 56 inches in diameter and weighs 212 pounds. Both H_2 vessels provide a total storage capacity of 265 pounds.

The subsystem schematic is depicted in Figure 4-236. The major change in the subsystem when comparing it to the Phase B configuration is in the reactant storage fluid expulsion network. The H_2 vessel internal heaters and fans have been replaced with an external loop. This external loop utilizes redundant pumps and electrical heaters for normal mission tank pressurization. This loop interfaces, through valving, with a network to supply H_2 to the ECLSS H_2/Freon heat exchanger for entry and landing cooling. During this phase of the mission, some of the heated H_2 exiting the heat exchanger is returned to the H_2 vessel for pressurization; the remaining heated hydrogen is vented overboard. This approach matches the vessel pressurization sources with the wide variation in H_2 flow rate demands ranging from 0.3 to 100 pph of H_2. The 0_2 vessel internal heaters also have been replaced with an external loop. This external loop utilizes redundant pumps and electrical heaters for all mission tank pressurization requirements.

The advantages of external heaters and pumps are considered to be safety, accessibility of active components, and flexibility to adapt to electrical or fluid heat exchanger energy input and external energy sources for ground fill pressurization. The disadvantages of external heaters and pumps are considered to be weight and initial hardware cost. The safety advantage is the prime consideration for the 0_2 vessel baseline choice and design flexibility is the prime consideration for the H_2 vessel baseline choice. The initial hardware cost disadvantage is considered to be offset by the field repair and replacement cost advantage.

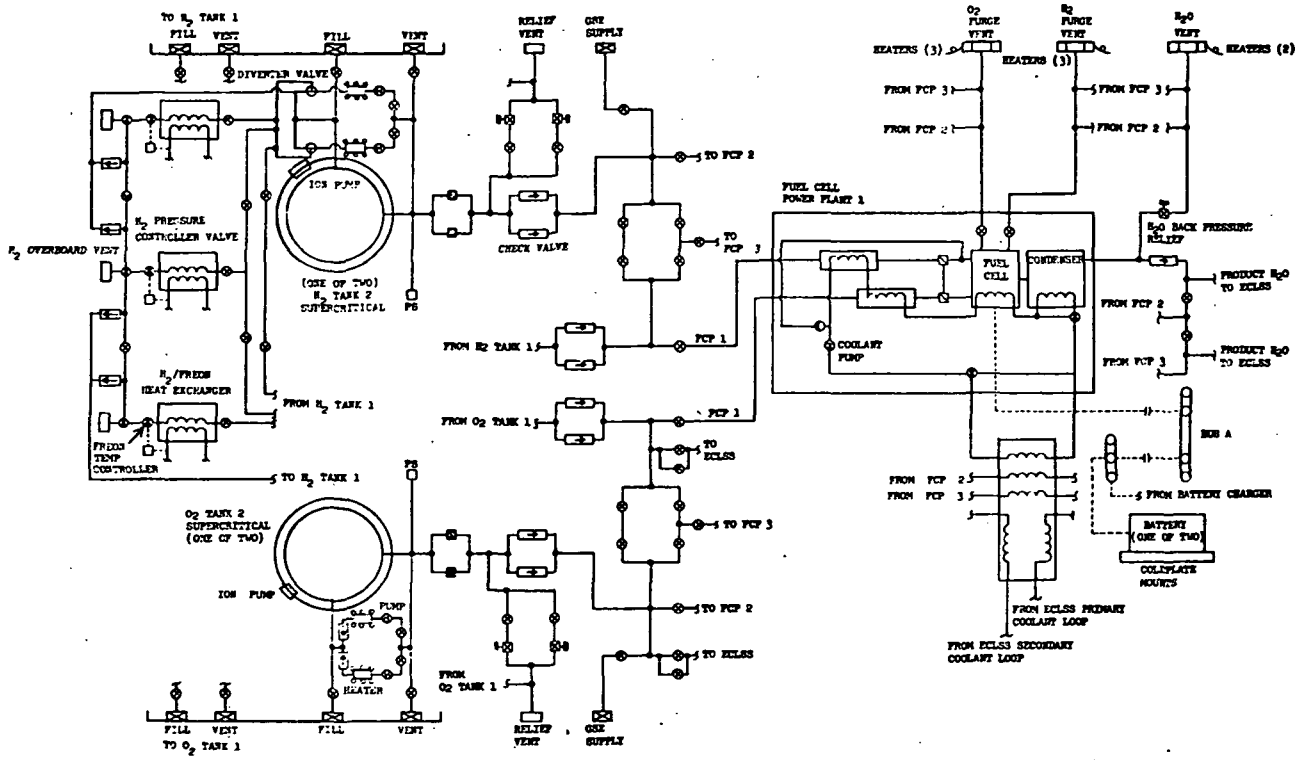

Figure 4-236. Electrical Power Generation Subsystem Schematic

The use of Apollo hardware in the subsystem design has been studied. The cost, weight, and installation volume penalties of Apollo fuel cell powerplants negate further consideration of this option. The cost penalty and structural integrity of Apollo supercritical dewars under repeated space shuttle vibration criteria rule out this option. A number of Apollo components such as check valves and solenoid-operated shutoff valves, are identified for usage in the subsystem.

Mechanical Power Generation. Each auxiliary power unit (Figure 4-237) provides shaft power for a 100-gpm hydraulic pump and a 20/30kva spray-oil cooled generator, resulting in a total shaft power load of 235 hp. Three APU's are used to provide FO/FS capability. Operation is required during launch phases and during entry and landing. Capability is provided for a checkout run prior to deorbit burn.

A centrifugal pump-fed boostrap APU concept using hydrazine monopropellant has been selected as the baseline. The metal bellows tank pressure is set at 100 psia to provide bootstrap capability and pump suction head requirements. Two tanks per module are needed to avoid exceeding design and fabrication capabilities in diameter or L/D ratio.

Each of the three APU systems contains a fuel tank/pressurization module attached to access doors in the aft body and an APU module located below the tank modules. Provisions are included for purging and isolating lines and equipment remaining in the vehicle as well as checkout of the module interface connections. The module separation points were selected to permit proper checkout after re-installation and to avoid separating hot gas lines and hydraulic system lines.

APU turbine speed control is maintained in accordance with MIL-STD-704A by using a throttling valve. The gas generator must provide stable operation over a wide flow range (10:1) and must exhibit a decomposition temperature compatible with long turbine life (1550 to 1600 F). The gas generator also must be capable of startup and shutdown under both vacuum and sea level conditions and must be capable of long life or easy replacement. The approach which appears to meet these requirements best is an electrically-heated, low-activity HA-3 catalytic bed. Other approaches use noble metal catalysts, thermal bed, or start chambers.

Lube oil cooling to a maximum temperature of 250 F is provided by a water boiler and air cooler which is common with the hydraulic system. Hydrazine pump and control system heat is rejected to the inlet hydrazine. Pump shaft seal purge is anticipated; however, this could be eliminated by employing a magnetic drive similar to that used on the Apollo ECS water-glycol pumps.

Pump- and pressure-fed concepts using both neat hydrazine and bipropellant storable propellants were studied and compared against a supercritical H_2/O_2 concept during the Phase B extension program. Bipropellant storable concepts were discarded because they offered no significant advantages other than propellant commonality and hypergolic ignition while exhibiting questionable ability to survive one mission because of carbon formation, severe maintainability problems to remove carbon

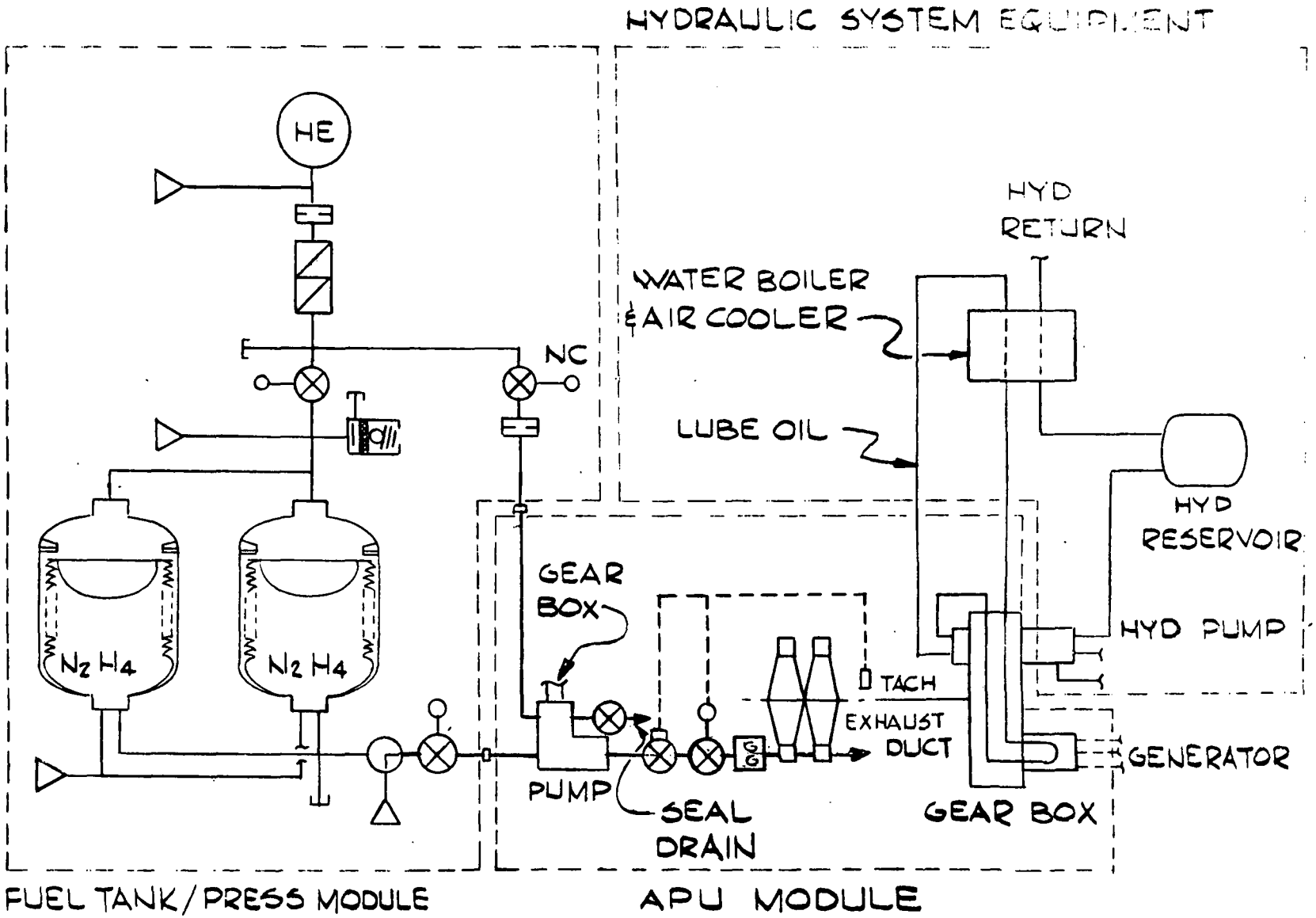

Figure 4-237. APU System

deposits, and more complexity, higher cost, and less safety when compared to neat hydrazine monopropellant. The pump-fed concept was selected over the pressure-fed since a system weight savings of approximately 500 pounds could be realized and since much lower fuel tank pressures and helium sphere sizes resulted.

Neat hydrazine was selected over supercritical H_2/O_2 for the following reasons:

1. Lower program cost (-$26M)
2. Minimum risk
3. Lower vulnerability to failure
4. Smaller volume (≈80 cubic feet less)
5. Less weight
6. Shorter lead time (≈8 months less)
7. Improved exhaust duct safety aspects
8. Technology applicable to booster selection

Principal areas of investigation for follow-on studies include comparison of metal bellows, screen retention, and rubber diaphragm tanks; tank pressurization method, gas generator design concept comparison; and pump-type and drive comparison.

Hydraulic System. The hydraulic system provides power to actuate the aerodynamic flight control surfaces, main engine gimbals, main and nose landing gear, wheel brakes, and air-breathing engine deployment. The hydraulic power is provided by three independent 3000-psi subsystems. Each system is powered by a 100-gpm variable displacement pump driven by a separate APU (Figure 4-238), a feature that contributes to the redundancy of power sources. The systems provide full mission capability after a single failure and safe flight and landing in the event of a second failure, regardless of the maneuver at the time of the second occurrence. Subsystems are described in the following paragraphs.

Aerodynamic Flight Controls. The aerodynamic surfaces are powered by single, balanced piston-type hydraulic actuators. Two actuators drive each of the movable surfaces (two elevon and two rudder/glide brake surfaces). The actuators are positioned by spool valves operated by a mechanical cable/lever system in conjunction with full authority

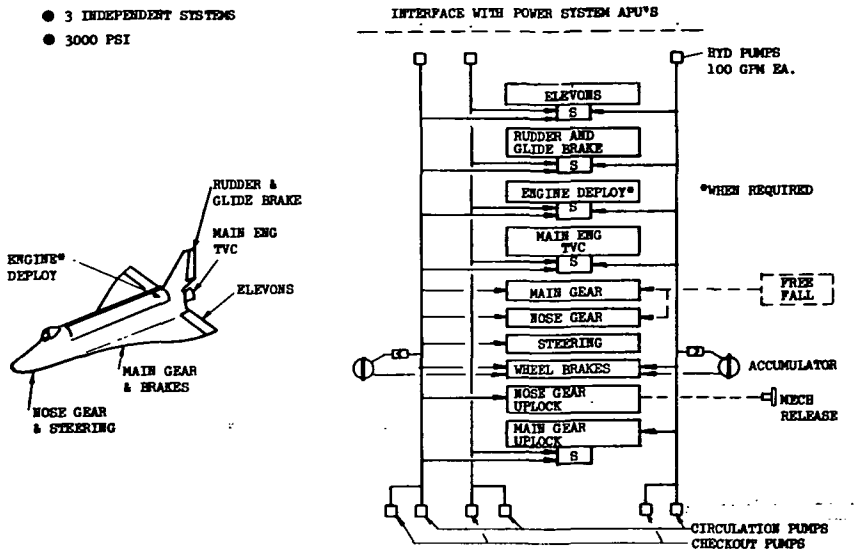

Figure 4-238. Orbiter Hydraulic System

"fly-by-wire" control servos. One control servo provides inputs to each pair of actuators.

Hydraulic power to the actuators is provided by one system at a time. In the event of loss of a system, pressure-actuated switching valves located in the actuators shuttle to one of the two standby systems. In like manner, the remaining third system would be ported to the actuator if a second system failure occurred.

The control servos are electro-hydraulic secondary actuators capable of providing full performance after a double failure. Each unit consists of three channels, one active and the other two on standby. Each channel is hydraulically powered by one of the independent systems. Two electrical inputs are required per channel to drive dual servo valves; one to power the secondary actuator and the other to monitor the performance of the former valve. In the event of a failure, the primary channel is bypassed and the first standby channel is switched in. A dual channel failure would activate the second standby channel.

In comparing the Phase B' extension concept with the Phase B concept, the former is a fly-by-cable/fly-by-wire system using active/standby control servos and single, balanced piston actuators with system switching valves. The Phase B system is pure fly-by-wire using majority voting, force summed servos, and both single balanced (rudder/glide brake) and dual tandem (elevons) actuators with no system switching valves.

Main Engine Gimbaling. Each of the four main engines is gimbaled by two (one per axis) single, balanced piston-type servoactuators. Three hydraulic systems provide power to the eight actuators through pressure-actuated system selector valves. The actuator utilizes an integrally mounted, control servo identical in concept to the 3-channel, majority voting unit developed for the Saturn S-IVB. Performance is unaffected after a single channel failure. A dual failure can result in a potential hardover engine, requiring engine cutoff.

In the Phase B concept, in which two engines were specified, an active/standby servoactuator was used and contained a device for centering the engine in the event of a dual failure.

Landing Gear Actuation. The main landing gear, nose landing gear, and steering are supplied normal actuation power by hydraulic system No. 1. A manual release for the nose landing gear uplock is provided in the cockpit in the event of system No. 1 loss. Emergency power for the main landing gear uplock is supplied by system No. 2 in the event of loss of system No. 1; system No. 3 supplies power upon a second failure. Release of the uplocks provide for free fall extension of the gear.

The hydraulic wheel brake actuators obtain simultaneous power from two systems. An accumulator provides power in the event of two-system failure and for the parking brake. The brakes are used to augment the steering if required.

Two sets of transmission lines to the nose landing gear were eliminated, as shown in the Phase B configuration, by the addition of the manual uplock release. Elimination of the accumulator for the main landing gear was accomplished by providing three sets of small-diameter uplock hydraulic lines in the wheel well, thus saving weight, cost, and maintenance.

Air-Breathing Engine Deployment. Hydraulic subsystem No. 3 supplies normal power to operate the engine deployment and door linear actuators. In the event of loss of system No. 3, pressure-actuated switching valves in the actuators shuttle to one of the two standby systems. The remaining third system would be ported to the actuators upon a second loss.

The rationale for the change from 4000 to 3000 psi is noted in Paragraph 3.11.2. The selection of a three-system configuration over four systems was based on less weight, cost, maintenance, and servicing. Further detailed studies are required to optimize final system configuration.

The reduction in structural environmental temperatures permitted the selection of MIL-H-83282, a synthetic hydrocarbon hydraulic fluid instead of the Chevron M2-V fluid chosen for the Phase B vehicle. The MIL-H-83282 fluid was developed to replace MIL-H-5606 fluid in hydraulic systems using a drain and fill procedure, within a minus 40 F to plus 275 F

operational temperature and with a reduction in fire hazard. This interchangeability of fluids provides the capability of purchasing off-the-shelf hydraulic components designed for MIL-H-5606 fluid, resulting in a lower hydraulic system cost. The higher minimum operation temperature of minus 40 F, rather than minus 65 F, requires additional heating of the hydraulic fluid systems during the cold orientation orbital mode.

Environmental Control and Life Support Subsystems. The major system configuration changes to the ECLSS are the deletion of the cabin heat exchanger, combining the urinal and waste collector, deletion of active cooling of the remote electronic bays, and cooling a larger percentage of the avionics with forced air in compartments isolated from the crew compartment. The functions and selected concepts of the current ECLSS are basically the same as shown in Table 6.5.1-1 of SD 71-114-2(2), Phase B Final Summary Report.

The basic requirements are essentially the same as shown in the Phase B final report. One major difference is that the system is to provide shirtsleeve environment, life support, and waste management for four crew members for seven days instead of two crew and two passengers for seven days and 12 passengers during boost and entry.

Waste Management System. The selected system differs from Figure 6.5.1-1 of the Phase B final report in that one urinal collector is deleted and the other is combined in the collector package to facilitate female use and to simulate earth facilities. The concept is similar to that selected by NASA MSC for development under a technology contract.

Atmospheric Revitalization. The major change to the ECLSS resulted from isolation of the avionics equipment and a change from conduction cooling to convection cooling in many areas. With isolation of the avionics a large part of the heat is no longer dissipated to the cabin air system, permitting the cabin heat exchanger and fan to be deleted. The humidity control heat exchanger and fans have been enlarged slightly to satisfy the new total cabin cooling requirements. The environmental heat gain to the cabin is reduced to 1700 Btu/hr and the heat loss is reduced to 1000 Btu/hr. These changes result from the new warm walls of the avionics bay together with the revised cold wall panels.

The CO_2 control and atmospheric supply is changed from the Phase B report because of changes to the OMS. The Phase B system included a primary and secondary O_2 control system with 7.5 lb/hr O_2 flow supplied from the fuel cell cryogenic storage and a third emergency high-O_2 flow system with 55 lb/hr for 10 minutes supplied from the OMS cryogenic storage. Elimination of the cryogenic propellants for the OMS deletes

the third emergency O_2 system. The emergency O_2 function was added to the primary and secondary O_2 systems to provide both functions of normal and emergency flow rates.

Heat Transport System. The heat transport system is essentially as defined in the Phase B report. The revision may be determined by comparing the simplified schematic shown in Figure 4-239 with that shown in Figure 6.5.1-4. The forced-air cooled electronics and the coldplate cooled electronics are located in the Freon loop, thereby reducing the interface heat exchanger size. This is possible since the avionics bays are isolated from the crew compartment and a Freon line rupture would not contaminate the crew cabin.

The bladders of the waste water tanks are pressurized by the cabin atmosphere instead of regulated N_2. This reduces system complexity and allows the isolation of potable water tank bladders from the waste tank bladders.

The hydrogen used for atmospheric heat sink is now provided from the fuel cell supply since the OMS no longer utilizes hydrogen.

Interfaces. The basic interfaces are the same except as noted in the descriptions above. Figure 4-240 summarizes the major interfaces, stressing those that are different than shown in Figure 6.5.1-9 of the Phase B report.

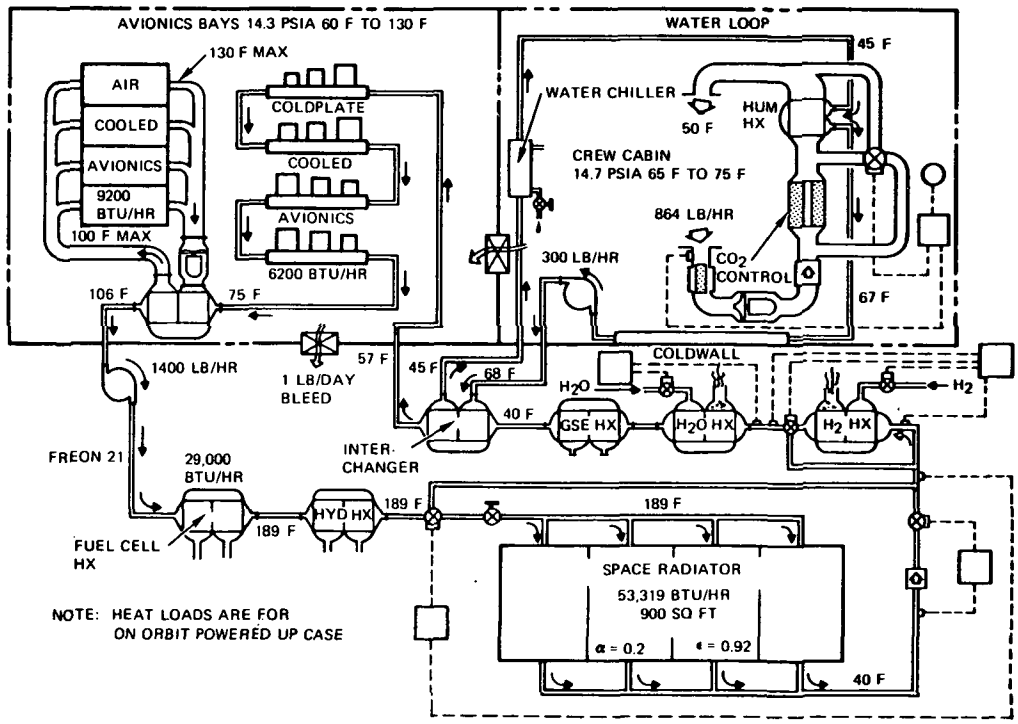

Figure 4-239. ECLSS Coolant Circuit

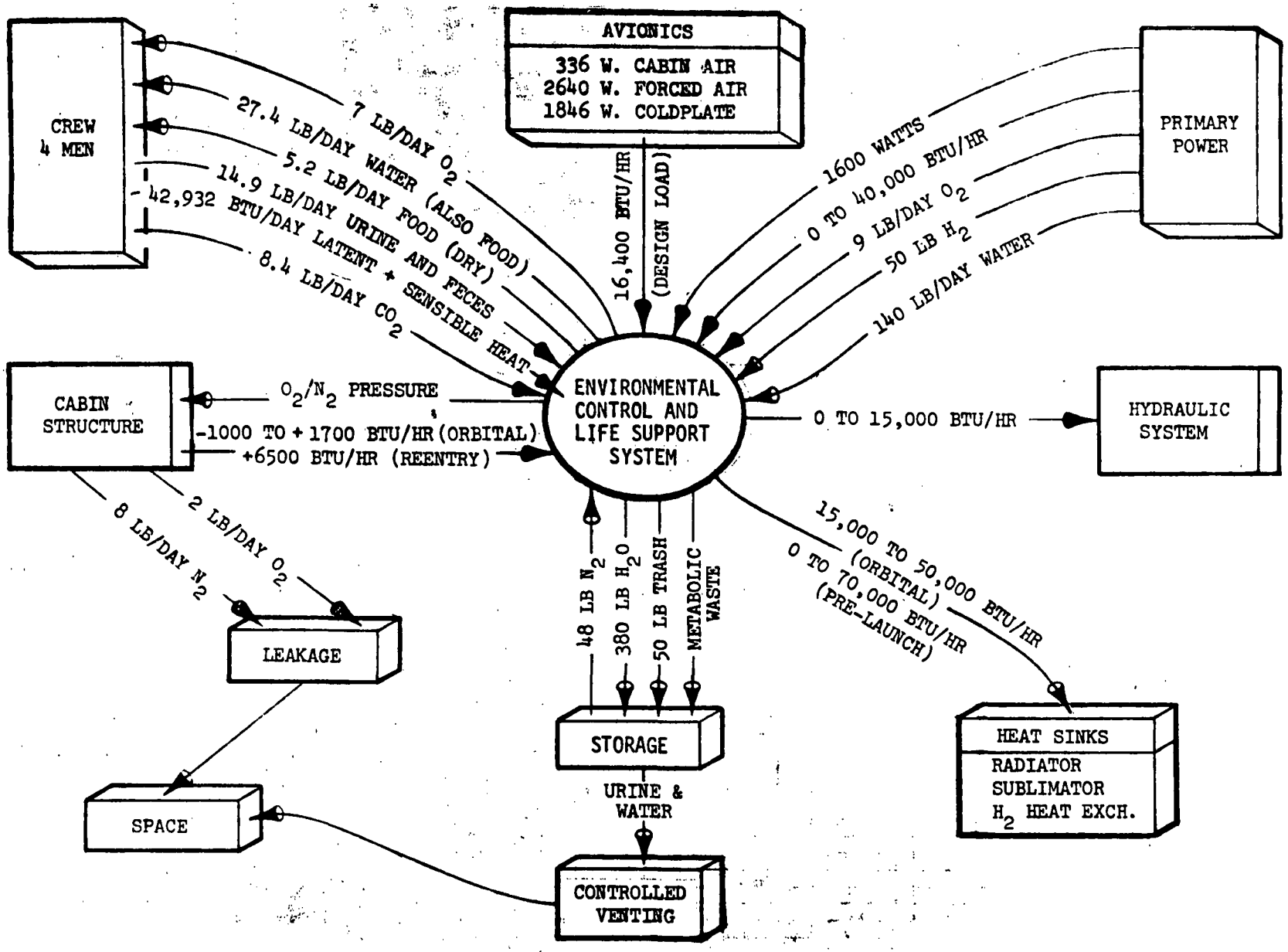

Figure 4-240. ECLSS Interface Logic

4.4.3.9 Avionics

Alternative avionic configurations were studied to select the candidate system that would best satisfy the prime study objective of minimizing design, development, production, and operations costs. A key objective was to select a configuration that required minimum development and would be compatible with the phased development approach. The study emphasized the cost benefits of phased development and of utilizing off-the-shelf components. The use of simple conventional minimum-risk concepts was considered essential to accomplishing the minimum development objective. The cost of management and integration of an avionic system is a function of system complexity and the studies emphasized approaches in which accountability could be maintained at the subsystem level.

The level of redundancy for the candidate systems studied was determined by analyses of the various components and functional paths, considering criticality, experience, and cost factors, rather than attempting to apply a single criterion to the total system. Manual backup flight control system studies are an example of this approach.

Low-cost avionics systems must emphasize reduced use of automated displays and controls, with the related reduction in software, thus increasing the utilization of the crew. This reduction of automation also includes utilizing a single-string redundancy management concept rather than the previously planned approach of individual LRU fault isolation and switching.

The following study ground rules were developed, in addition to those developed for the earlier low-cost study described in Section 3.11.2, to assure the maximum benefit from the avionic system studies:

1. The Phase B study (Level 1, Level 2, and Level 3) requirements would be re-evaluated.

2. Mark I, horizontal flight, avionic configurations will be minimum-complexity aircraft-type systems and components. Mark I vertical flight hardware would be added as a kit.

3. Less vehicle autonomy would be traded for increased ground support and GSE.

4. An increase in "dedicated" systems concepts would be considered.

5. Protecting systems from the environment rather than developing more rugged components would be encouraged.

6. A one-month turnaround for Mark I was assured and two weeks for Mark II.

Figure 4-241 shows the study sequence. This process led to the definition of alternative configurations that were evaluated to define the phased development for 11 candidate systems, identified in Tables 4-43 and 4-44. Significant characteristics are included in the tables. The phased development cycle consisted of: Mark I, horizontal flight test configuration; Kit 1, upgrading the vehicle for Mark I vertical flight test; and Kit 2, upgrading the avionics from Mark I to Mark II, the operational configuration.

Configuration Selection. The 11 candidate avionics configurations were evaluated considering the characteristics shown on Table 4-44. Figure 4-242 shows the selected system configuration. Significant characteristics are:

1. A dedicated GN&C computer is used rather than a centralized DCM computer.

2. Hardwire control and measurement techniques are used rather than data bus techniques.

3. Major D&C changes were made, such as deleting multiformat CRT's and adding more conventional aircraft displays, adding a center stick, adding a subsystem management station.

4. Tacan is used rather than the precision ranging system.

5. An independent flight control system is included.

The sequence in which the system would be developed and installed in the orbiter is shown by the coding on Figure 4-242. For Mark I horizontal flight test, only the basic aircraft avionics would be installed. Equipment added as Kit 1, to support the Mark I vertical flight program, would include the GN&C computer, IMU, and star tracker; controls and displays associated with the main propulsion system, TVC, OMS, and ACPS systems; controls and displays for fuel cell and APU systems; and other equipment such as maintenance recorders, telemetry, and tracking transponders. Kit 2, added to convert to the operational configuration, would include the horizon sensors that provide autonomous navigation capability. The space station docking umbilical would also be a part of Kit 2. Development flight instrumentation would be removed from vehicle number 4.

Subsystem Considerations. A key configuration decision in the avionics system study was the selection of the GN&C computer interface technique. Figure 4-243 shows the three basic alternatives studied and the comparative evaluation in the areas of development cost, change impact, management interface complexity, and functional interface considerations.

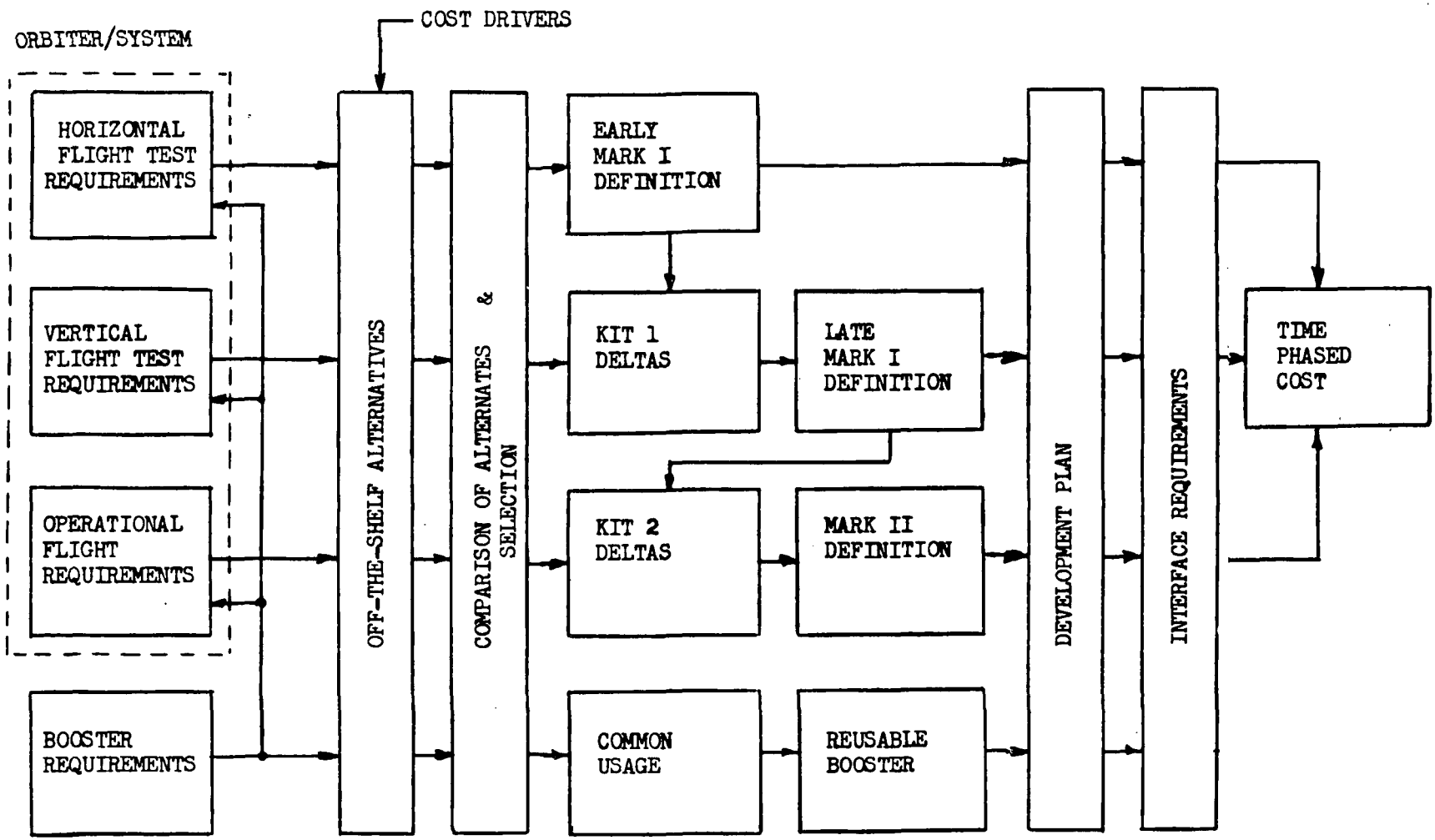

Figure 4-241. Avionics Definition Logic

Table 4-43. Alternate Concept Descriptions

SYSTEM	REMARKS
1	ϕB BASELINE CONCEPT WITH HARDWIRED, DIGITAL GN&C BACKUP
1a	FEDERATED COMPUTER VERSION OF 1
2	2 DIGITAL GN&C STRINGS + ANALOG F/C BACKUP, CRT DISPLAYS, NO DATA MGMT COMPUTER
2a	3 DIGITAL GN&C STRINGS; DEDICATED DISPLAYS; NO DATA MANAGEMENT COMPUTER
3	2 DIGITAL GN&C STRINGS; ANALOG F/C BACKUP; DATA MANAGEMENT COMPUTER
3a	SIMILAR TO 3 BUT HAS 3 DIGITAL GN&C STRINGS
3b	3 DIGITAL G&N COMPUTERS; 3 ANALOG FLIGHT CONTROLS; DATA MANAGEMENT COMPUTER
3c	3 GN/DM COMPUTERS; 3 ANALOG FLIGHT CONTROLS
4	2 G&N COMPUTERS; 3 ANALOG FLIGHT CONTROLS; NO DATA MANAGEMENT COMPUTER
4a	3 GN&C COMPUTERS; DATA MANAGEMENT COMPUTER; ALPHA-NUMERIC DISPLAYS
5	3 ANALOG AERO STAB AUG SYSTEM; 3 SPACE GN&C STRINGS; ALPHA-NUMERIC DISPLAYS

Table 4-44. Comparison of Alternate Configurations

CHARACTERISTIC	CONFIGURATION										
	1	1A	2	2A	3	3A	3B	3C	4	4A	5
ADAPTABLE TO PHASED DEVELOPMENT	~~NO~~	~~NO~~	~~NO~~	~~NO~~	~~NO~~	YES*	YES	YES	YES	YES*	YES
OFF-THE-SHELF EQUIPMENT - NO MODS	~~NO~~	~~NO~~	YES	YES	YES	YES	YES	YES	YES	YES	YES
REDUCED AUTOMATED FUNCTIONS	~~NO~~	~~NO~~	YES	YES	YES	YES	YES	YES	YES	YES	YES
MINIMUM RISK/SIMPLE/ CONVENTIONAL	~~NO~~	~~NO~~	~~NO~~	~~NO~~	~~NO~~	~~NO~~	YES	YES	YES	~~NO~~	YES
MANUAL FLIGHT CONTROL BYPASS	~~NO~~	~~NO~~	YES	~~NO~~	~~NO~~	~~NO~~	YES	YES	YES	~~NO~~	YES
SIMPLIFIED REDUNDANCY MANAGEMENT	~~NO~~	~~NO~~	YES	YES	YES	YES	YES	YES	YES	YES	YES
SUBSYSTEM ACCOUNTABILITY	~~NO~~	YES	YES	YES	YES	YES	YES	~~NO~~	YES	YES	YES
PARALLEL DEVELOPMENT OF BACKUP	~~YES~~	~~YES~~	~~YES~~	NO	~~YES~~	NO	NO	NO	~~YES~~	NO	NO
DEDICATED AIRPLANE & SPACECRAFT CONTROLS	~~NO~~	~~NO~~	~~NO~~	~~NO~~	~~NO~~	~~NO~~	~~NO~~	~~NO~~	~~NO~~	~~NO~~	YES

*THROUGH SOFTWARE

SELECTED CONFIGURATION IS 5

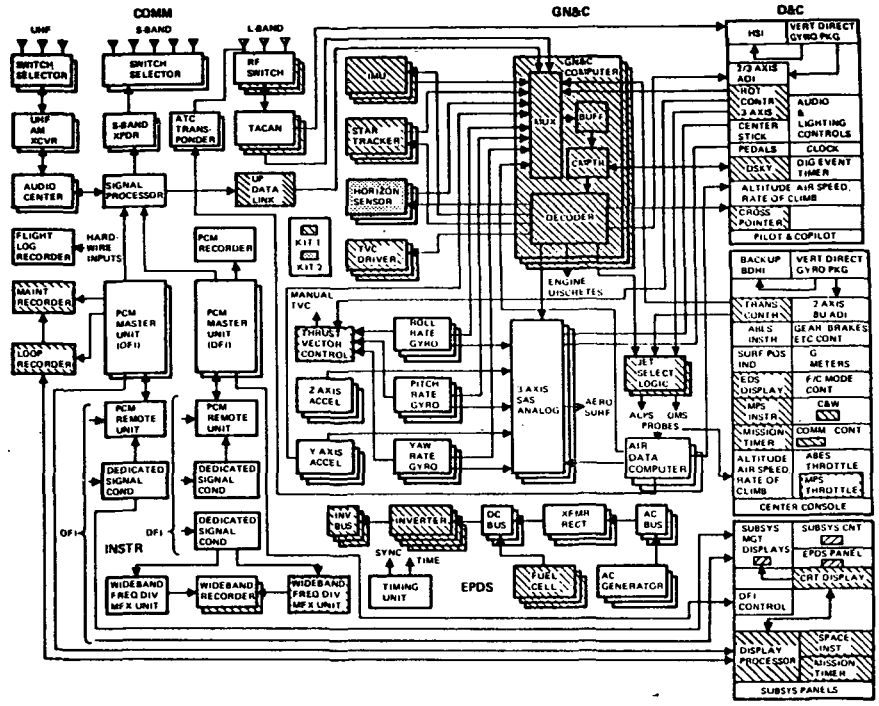

Figure 4-242. Space Shuttle Avionics Interim Configuration, Orbiter

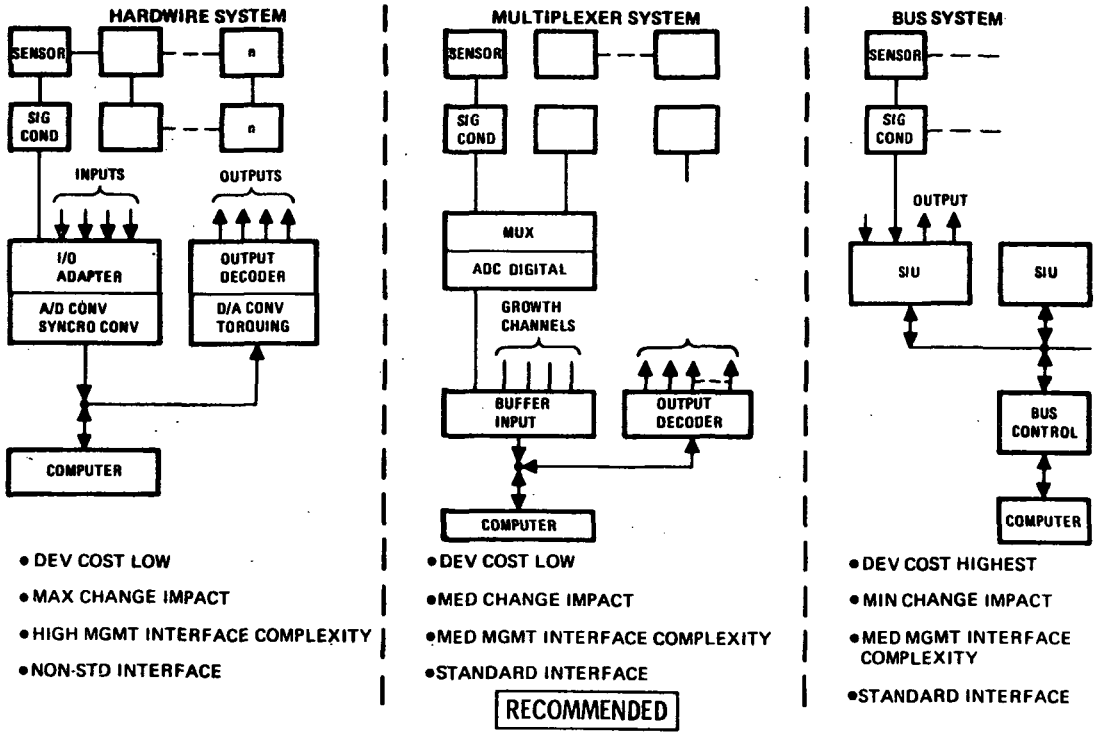

Figure 4-243. GN&C Computer Interface Technique Comparison

The main features of the display and control system concept are shown in Figure 4-244. Key points are the use of conventional instruments, the addition of the center stick, and the identification of subsystem management controls and displays at the aft console.

Antenna locations (Figure 4-245) depict the latest configuration, including an S-band antenna located on the external HO tank to prevent shadowing effects of the tank.

The installation concept for the avionics is shown in Figures 4-246 and 4-247. The forward bays below the crew compartment house the majority of the avionic equipment and are provided with their own environmental control system. Aft bays, with no cooling, will house those equipment items associated with engine and power systems which cannot be installed in the forward bays.

Weight and Power Impact. The estimated weight and power requirements for the interim avionics configuration are compared to those of the 360-day baseline configuration in Table 4-45. Weight requirements increase for the interim configuration because of the hardware concepts selected and power requirements drop because of decreased numbers of components.

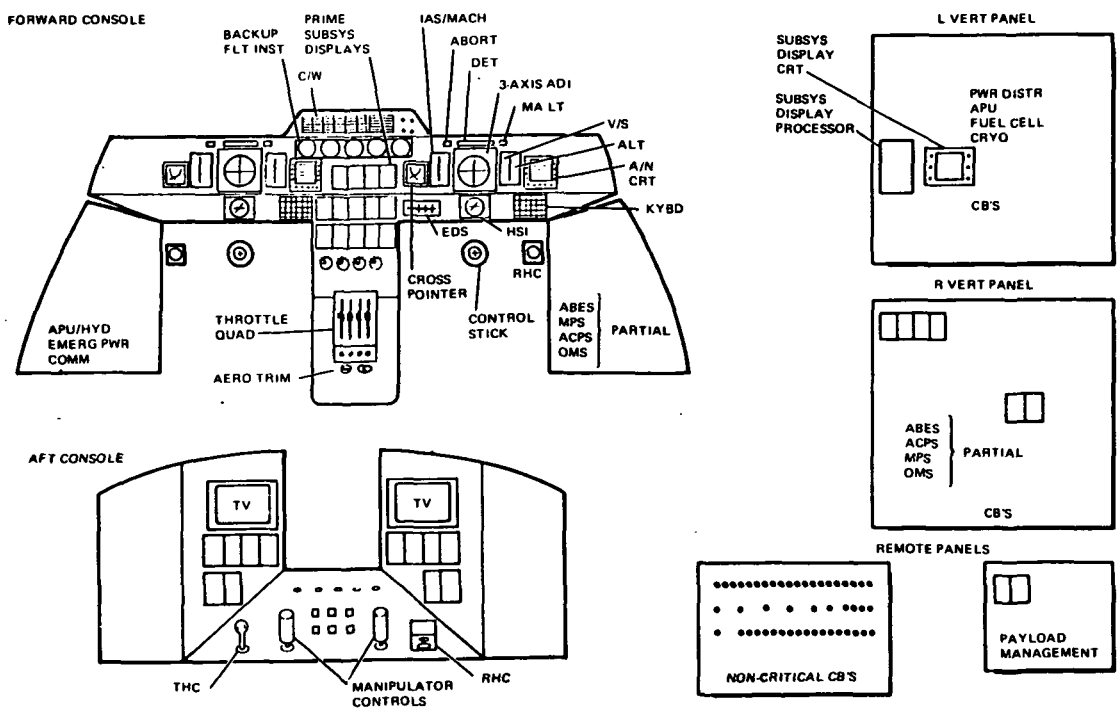

Figure 4-244. Preliminary Panel Arrangement, Orbiter

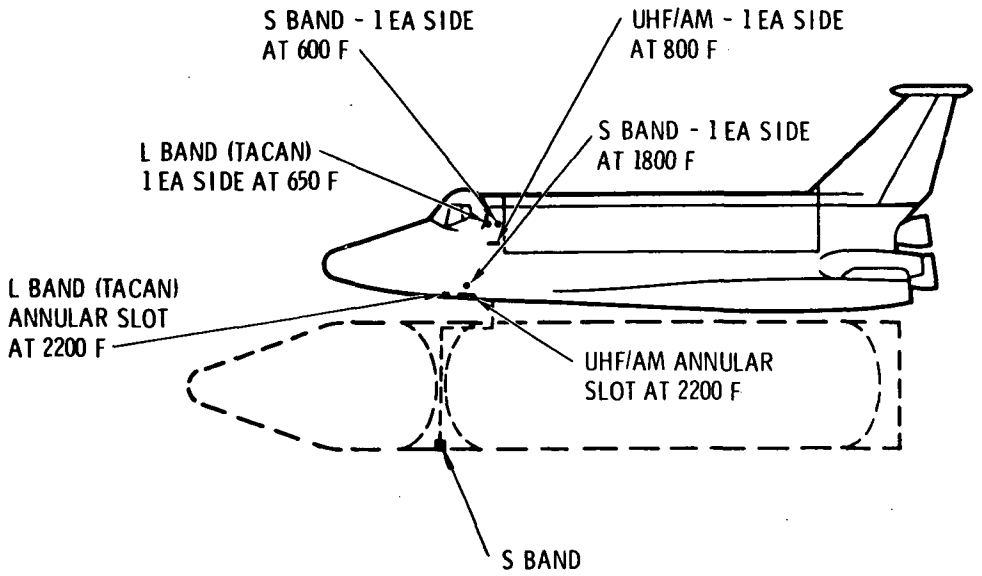

Figure 4-245. Orbiter Antenna Locations

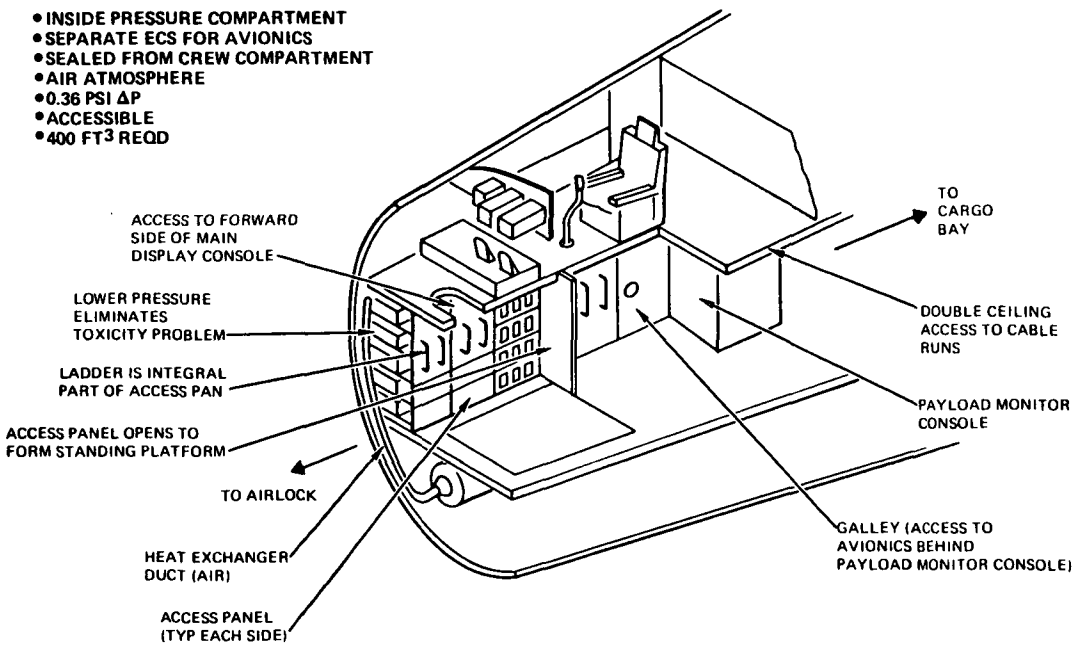

Figure 4-246. Orbiter Forward Avionics Bay

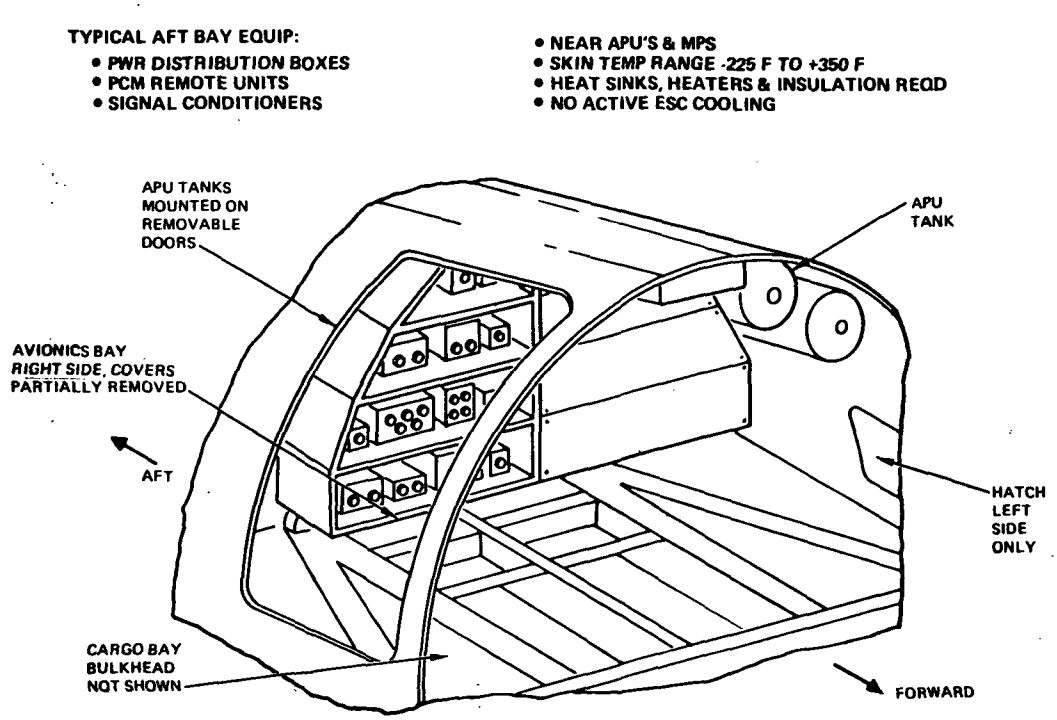

Figure 4-247. Aft Avionics Bays, Left and Right Sides

Table 4-45. Orbiter Avionics Weight and Power

Item	Baseline	Interim
Avionics system weight, (lb.)		
Operational	7,038	6,915
DFI	4,006	5,084
TOTAL	11,044	11,999
Avionics system power, (watts) (max. continuous)		
Operational	10,280	9,820
DFI	2,000	2,175
Orbital AC Power, All Subsystems	1,277	2,661
Inverter system operational capacity (VA)	1,500	3,750

Avionics Development Test Plan Analysis. The successful implementation of a low-cost avionics program for the space shuttle system will depend to a great degree on the manner in which the development test program is defined and performed. Maximum cost savings to the development program result from employing all levels of test for certification and qualification of components and systems, with the higher levels (subsystem and system-level tests) preferred over component-level testing.

The departure from the fully integrated avionic system to the concept of dedicated systems permits more flexibility in the integrated avionics system test program. More reliance can be placed on subcontractors for early major subsystem development, reducing duplication of test hardware and providing earlier design confidence.

Figure 4-248 shows the interim development test program logic utilizing individual dedicated subsystem test for the majority of the systems and limiting the integrated system test programs to those systems such as GN&C and D&C which must be tested in an integrated mode, with software verification included. The integrated avionics system tests would be conducted in a manner to permit integration of the test facility with simulators, iron bird test facilities, mission evaluators, and other hardware evaluation test facilities.

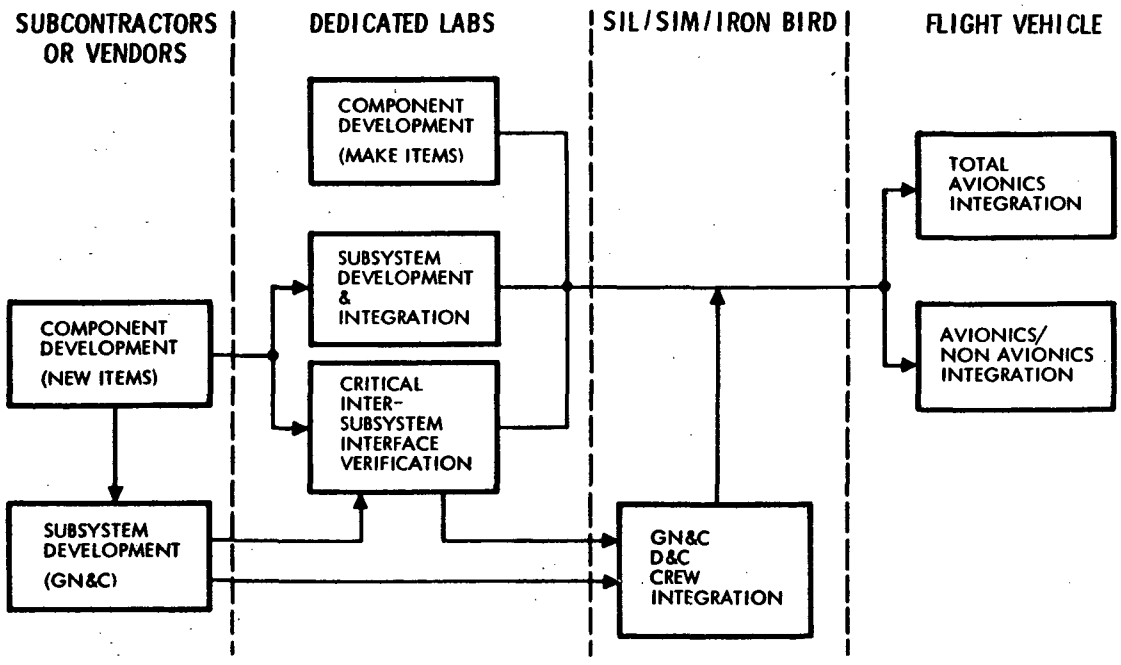

Figure 4-248. Development Test Logic

Reliability Assessment. Several special studies were performed, including an expansion to the component level of the avionics redundancy level optimization trade performed during Phase B. The results of this trade indicate that three success paths (FO/FS) are most cost-effective when aborts are considered and that the decision is relatively insensitive to actual failure rates. Recommendations from the study include the use of an alternate method of performing a function as one of the paths, the cross-strapping of low reliability components only, and the incorporation of capability to detect the loss of any path.

An analysis was performed of identified support equipment. A gross FMEA identified approximately 26 percent as potentially critical requiring a detailed FMEA.

Off-the-shelf hardware was evaluated utilizing a potential supplier questionnaire and checklist form. The initial data review indicated that Apollo hardware will generally meet the shuttle documentation and control requirements, but commercial and military hardware will require further evaluation. Limited protection or testing to assure compliance with shuttle requirements may be required.

Conclusions and Summary. The key features of the avionic system defined in the study are the use of dedicated subsystems, employing a digital computer for GN&C only, and the use of hardwire control rather than a multiplexed data bus system. The system includes triple redundancy in flight-critical systems and employs single-string redundancy management.

The only significant functional capability that was included in the 360-day baseline but which is not provided by the avionics configuration defined in this study is the autoland capability. VFR conditions are assumed for all landings with the configuration described. A total orbital vehicle weight increase of less than 200 pounds was estimated in the study, with the major increase resulting from the addition of control linkage for the manual flight control system. The weight of the avionics, ECLS, and power generation subsystems were all estimated to decrease. There was no significant change in peak electrical power or energy requirements. Ground checkout studies indicate a decrease in GSE development costs and a corresponding slight increase in operational costs, with a potential net cost reduction and no impact on ground turnaround requirements.

In summary, the avionic subsystem defined in the study could be developed at a cost significantly lower than the avionics configuration described in the 360-day report. The only decrease in functional capability would be the autoland capability, and there would be no significant vehicle weight impact.

4.4.3.10 Mechanical Systems

Landing System. The orbiter landing system is comprised of the nose and main landing gear and deceleration parachute. Ground maneuvering and control are provided by nose wheel steering, main wheel brakes, and the deceleration parachute.

The nose gear subsystem contains a shock strut, dual wheels and tires, drag brace, trunnion fittings, gear actuation and indication systems, uplock, downlock, steer and shimmy damper, fairing door, and door actuation and locking mechanism. The main gear subsystem consists of right- and left-hand gear assemblies, each of which contain a shock strut, dual wheels, tires and brakes, drag brace, trunnion fittings, gear actuation and indication systems, uplock, downlock, antiskid brake control system, fairing door, and door actuation and locking mechanism. Figure 4-249 and 4-250 illustrate the main and nose landing gears. The landing gear, brakes, and steering are hydraulically powered and electrically controlled. The gears retract forward, resulting in free-fall capability for emergency gear extension.

The deceleration parachute subsystem contains a main drag chute, drogue chute and deployment mortar, attach fittings, jettison mechanism, and actuators.

Aero Surface Flight Control System. The aero surface (elevons, rudder-glide brake) flight control system is a stability and control avionic-electronic augmentation system (SAS) with manual flight control (MFC) backup (Figure 4-251). The MFC includes the conventional control stick and rudder pedals mechanically linked through a system of push-pull rods, cables, and bellcranks to hydromechanical master cylinders (elevon and rudder modes). Artificial feel is provided by the use of bungees between the pilot and master cylinders. A manually operated electromechanical trim actuator is included in series with the master cylinders. The SAS parallels the MFC and has the ability to augment the pilot commands.

The aero surface actuators are hydraulically powered, mechanically controlled, servo-valve linear actuators. The servo valve is mechanically linked by a system of push-pull rods, cables, and override bungees to the master cylinders of SAS and MFC. A mechanical linkage, surface-to-surface actuator servo valve is included which matches the aero surface position with the master cylinder command of SAS and MFC. This linkage is made up of push-pull rods, bellcranks, and connects through a summing bellcrank to the surface actuator servo valve to close the loop controlling aerosurface positioning.

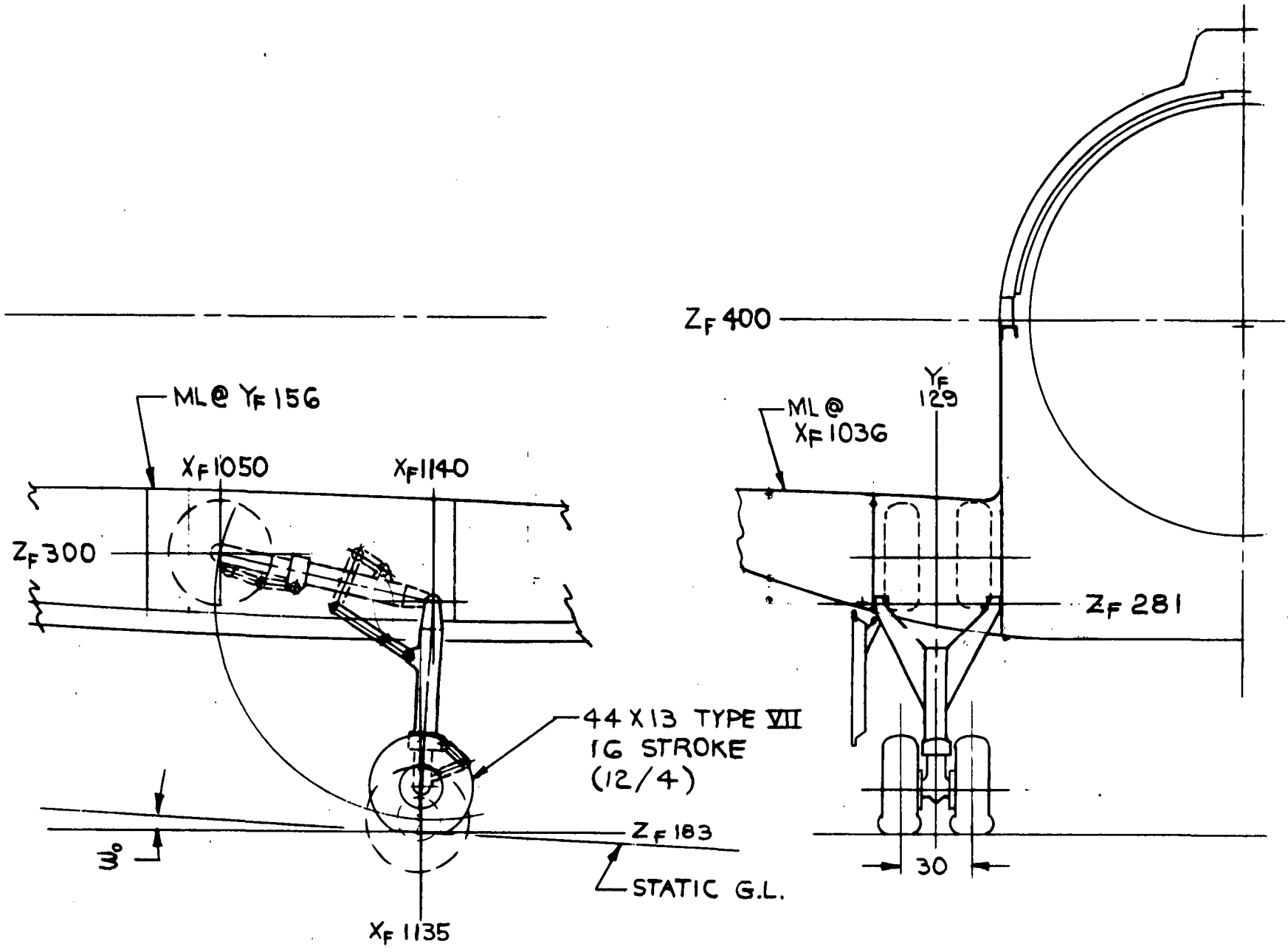

Figure 4-249. Main Landing Gear

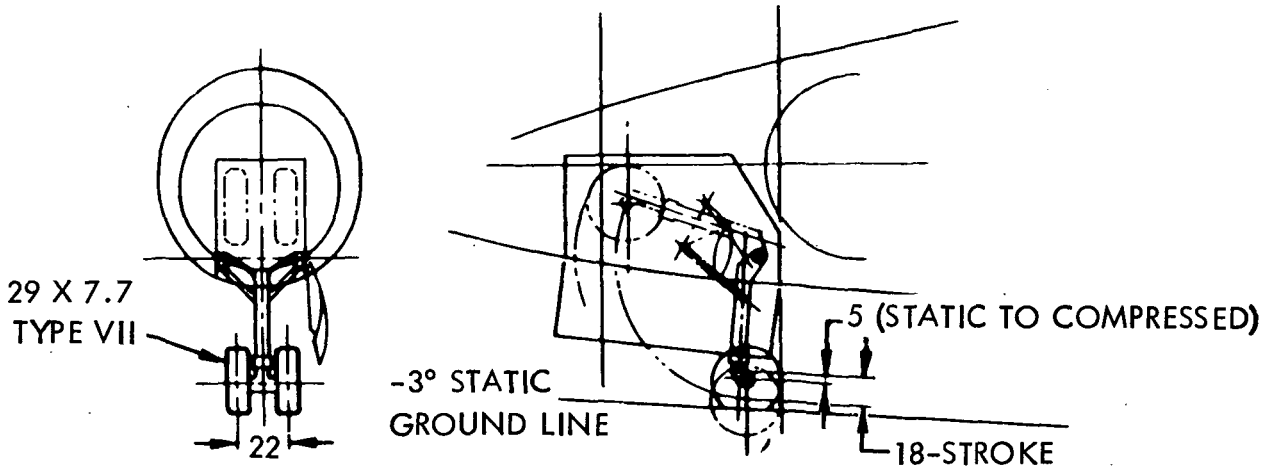

Figure 4-250. Nose Landing Gear

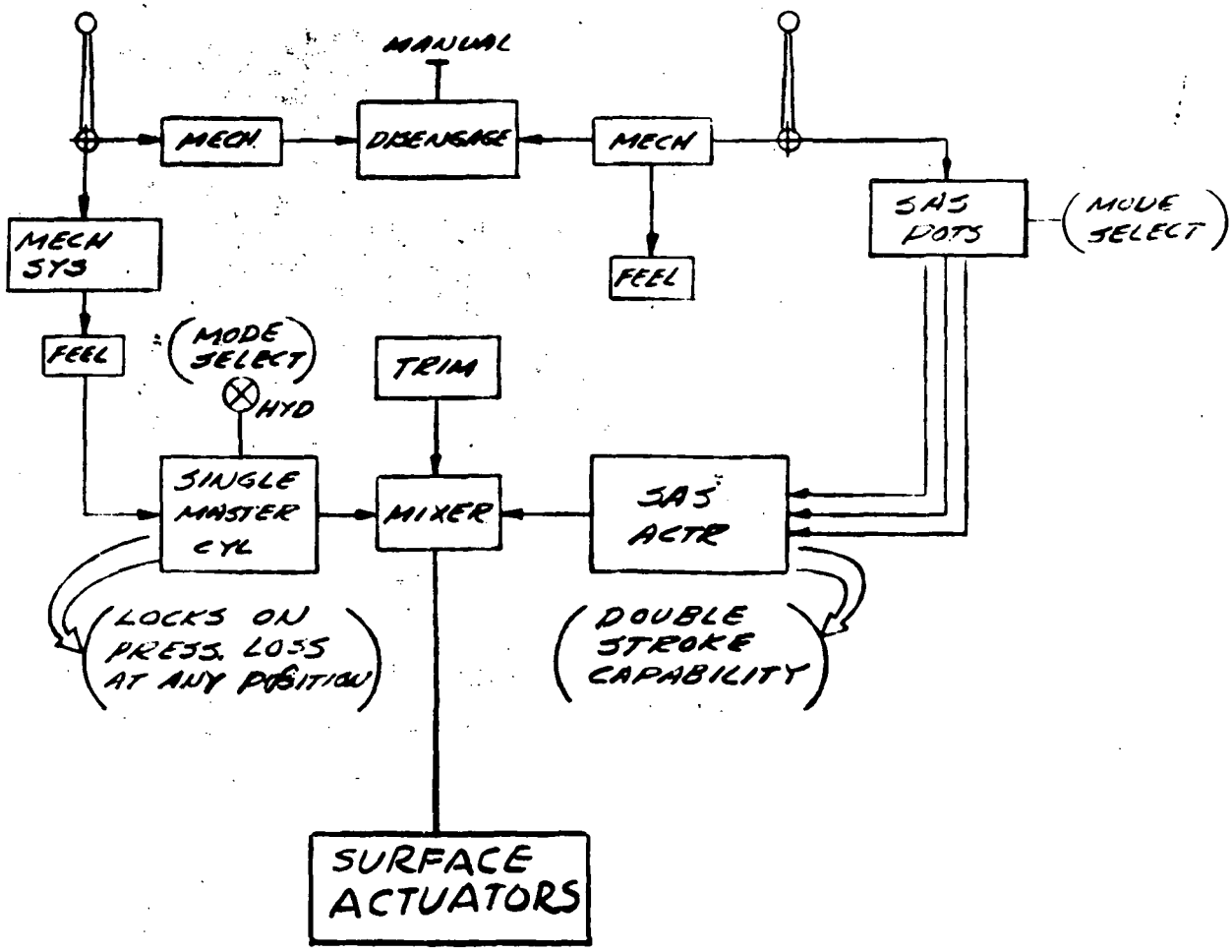

Figure 4-251. Flight Control System Block Diagram

Orbiter-Tank Separation System. The orbiter-tank separation sequence can begin any time after the tank and feedlines have been vented from nominal operating pressure to approximately 5 psi. These vent valves are located in the orbiter. Figure 4-252 indicates the location of these and other orbiter-tank separation interfaces. The actual separation occurs in two distinct stages. The first stage of separation disconnects all lines associated with the propellant transfer system. Also separated at this time will be the tank and booster umbilicals. These are combined into one at the orbiter. The interfaces that are in proximity to one another are combined into a single separation device.

The orbiter and tank are then oriented as shown in Figure 4-253. Simultaneously, the three structural attachments are released and the pre-programmed ACPS is activated to translate the orbiter laterally from the tank as shown in Figure 4-253. The initial translation triggers a timer within the tank's retro system that will either automatically fire the tank's retrorocket after sufficient clearance has been attained between the orbiter and tank or will arm the retro-motor igniter circuit for subsequent activation via orbiter ratio command link (Figure 4-253).

Payload Retention Assembly. Figure 4-254 shows the three-point trunnion retention assembly. The payload retention assembly accommodates payloads 15 feet in diameter by a length that can vary from payload to payload. Retention lugs on the payload extend beyond the 15-foot diameter.

Both side fittings take vertical and longitudinal loads, only one side fitting takes lateral loads, and the bottom centerline fitting takes only vertical loads. The bottom centerline fitting also accounts for up to three inches of thermal or structural deflection in the lateral direction.

The retention fittings are designed to permit angular and dimensional misalignments within the constraints of the payload clearance envelope. The latches are self-aligning and are provided with remotely controlled latching mechanisms. Lock and unlock indicators are provided at the DCHS operator station. Normal maintenance of the latch and locking mechanism is accomplished with the payload removed. All fittings are completely accessible from inside the cargo bay.

Cargo Bay Door Actuation and Latching System. The door is basically a clam-shell type with each half hinged along the longeron having a latching system at each end and along the mating centerline. The hinge is a theoretical center dual-link type allowing 138 degrees of door rotation. Each of the doors is made up of four panels and has 16 hinges, 4 per panel. One hinge per panel will be powered by a hydro-mechanical linear actuation system. Each of the door halves has two end latches at the forward and aft end. The end latches are an over-center toggle type with a roller on the locking pawl. The roller rides on the striker plate, allowing fore and

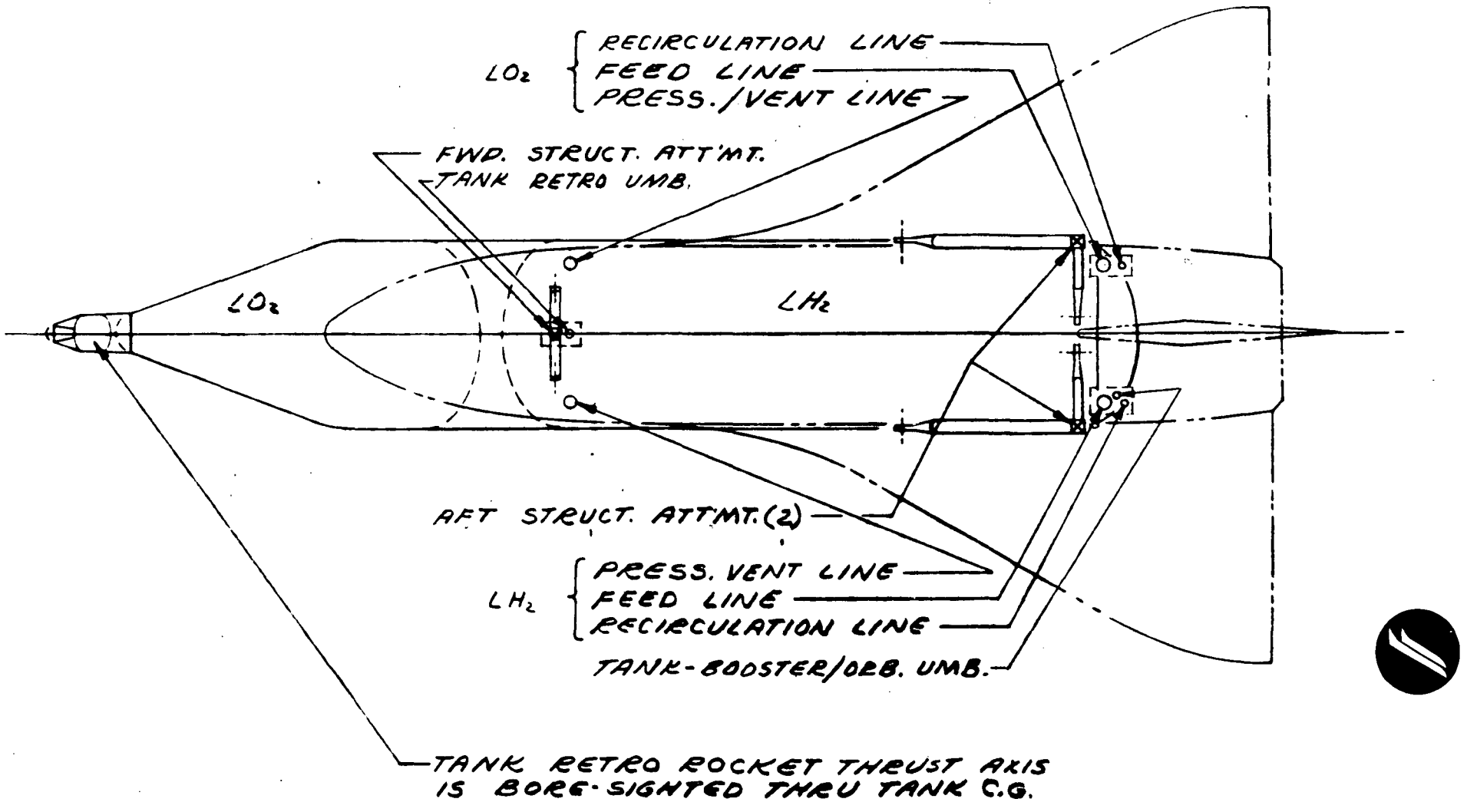

Figure 4-252. Orbiter/Tank Separation Interfaces

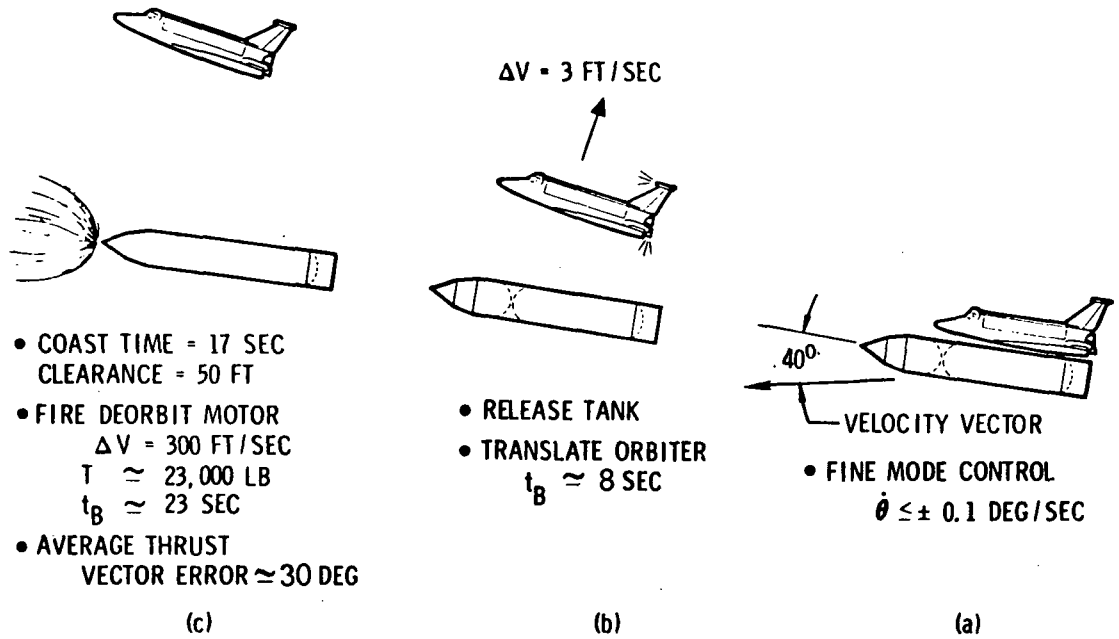

Figure 4-253. Nominal Tank Separation Concept

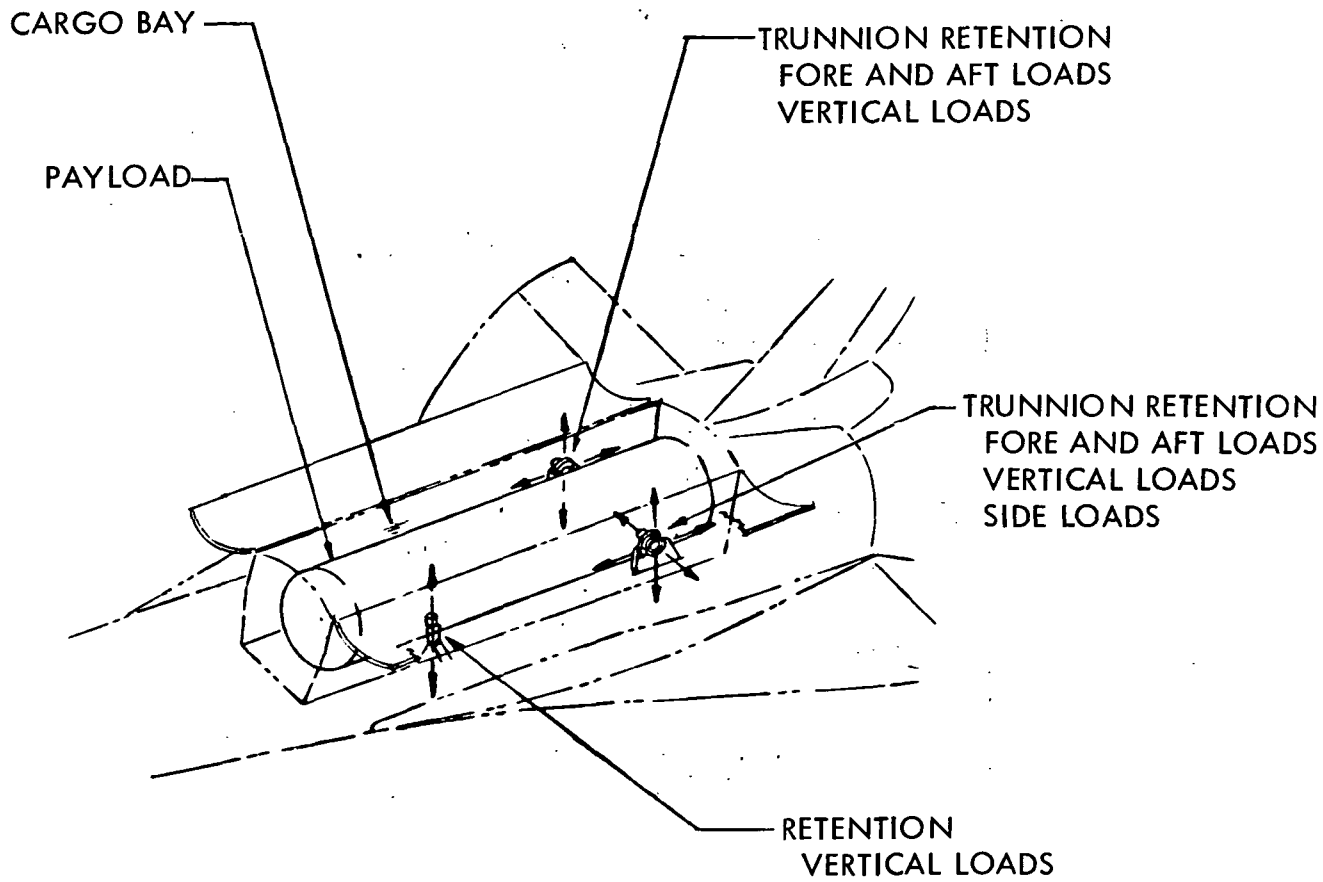

Figure 4-254. Payload Retention

aft movement during body deflections. Along the mating centerline each of the four mated door panels has four over-center toggle claw latches. Each latch is powered open or closed by pneumatic linear actuators. Sequencing and proximity electric switches are employed for synchronizing latching.

Docking and Cargo-Handling System. Docking, payload deployment, and payload retrieval are accomplished through the use of a pair of manipulator arms. A manipulator operator station is integrated into one of the cargo specialist stations, with direct viewing and closed-circuit television capability. Figure 4-255 shows the significant features of the docking and cargo-handling system (DCHS).

The total DCHS consists of two manipulator arms, a payload retention assembly, a docking port integrated with the airlock and personnel transfer port, illumination, and closed-circuit TV. The DCHS is responsive to the principal functions shown in Figure 4-255 and to the resulting criteria and requirements listed in Figure 4-255 and Table 4-46.

Two DCHS manipulator arms are installed and stowed in the cargo bay area (Figure 4-255). In their stowed position, they are above the payload. Each arm is 577 inches long (from shoulder joint to the tip of end effector) with a maximum diameter of 15 inches.

Each arm has a shoulder, elbow, and wrist joint with two degrees of rotational freedom at the shoulder and wrist and one degree of rotational freedom at the elbow. In event of a malfunction, the entire manipulator is capable of being jettisoned to allow closure of the cargo bay doors. Each arm joint consists of a gear reduction system driven by redundant 28-vdc motors. Each joint is torque-limited to prevent damage to the manipulator arm. Torque limits resulting from a 10-pound normal force limit (end of arm) are listed in Table 4-46.

The end effector is capable of continuous rotation in either direction, thereby creating a third degree of rotational freedom at the wrist. Tools may also be changed to accommodate specialized tasks. One TV camera and one floodlight are mounted near the end effector to illuminate and televise the work area.

A tube shape has been selected for the main arm members because of the space limitations in the cargo bay and the multidirectional loading. A tube provides maximum bending and torsion capability with minimum weight and fabrication complexity. A graphite/epoxy composite has been recommended for the tube.

Each arm is sized to deploy a 65K lb payload (15 feet in diameter by 60 feet) a distance of 600 inches vertically out of the cargo bay and to rotate

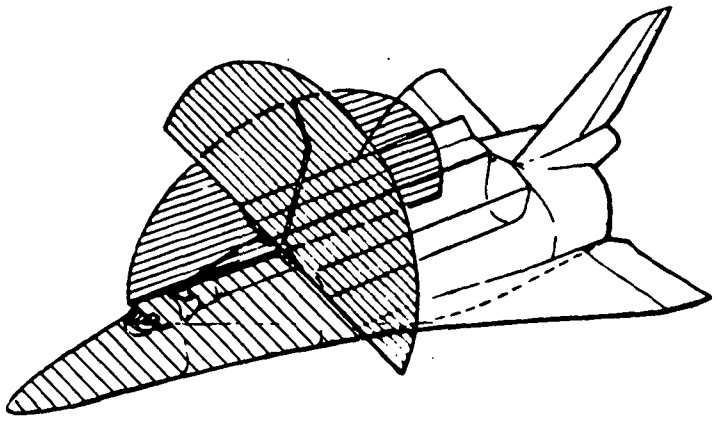

REACH ENVELOPE

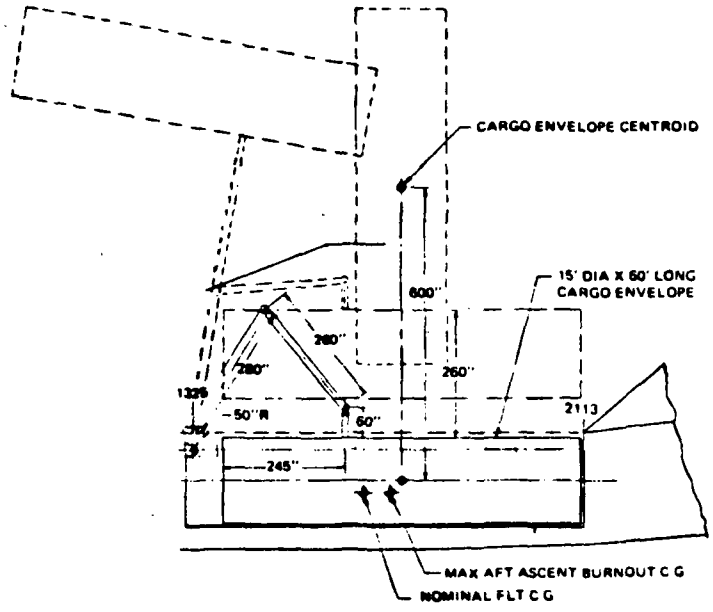

ARM GEOMETRY FACTORS

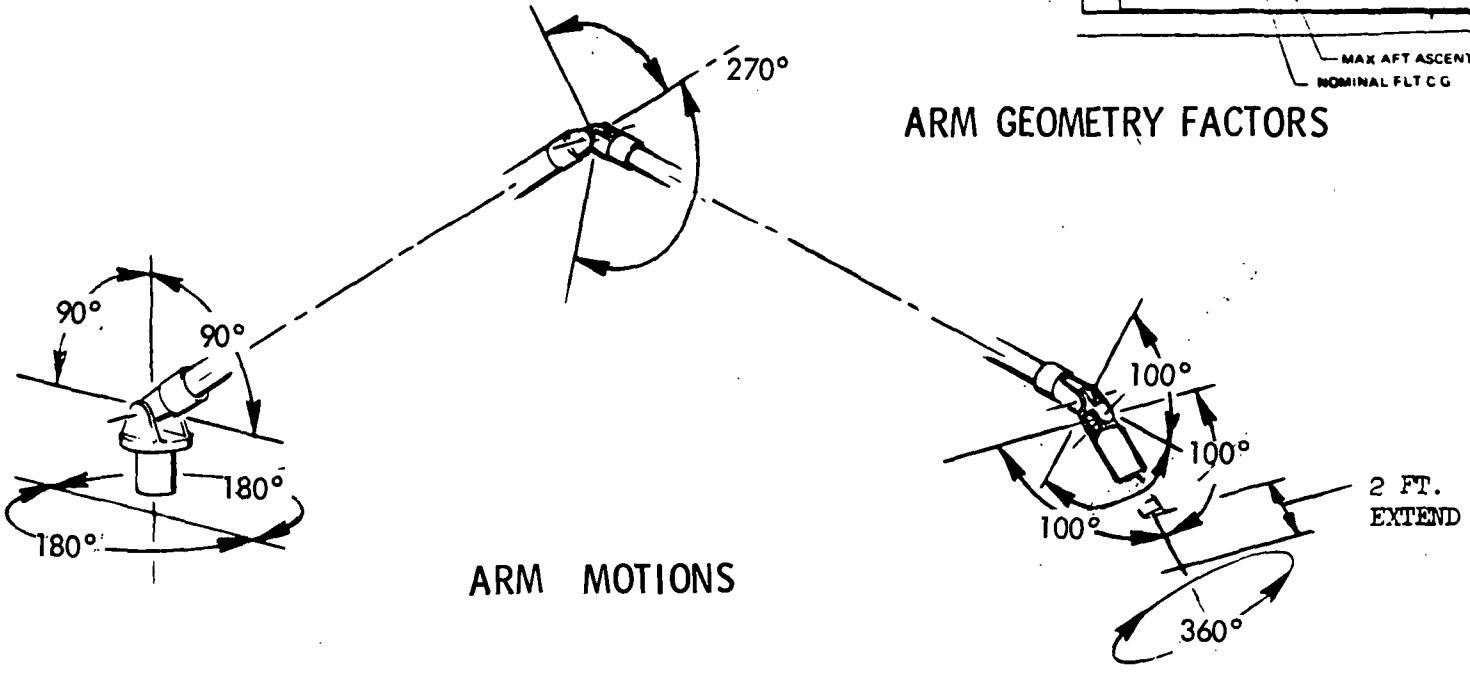

ARM MOTIONS

Figure 4-255. ARM Geometry

Table 4-46. Manipulator Joint Torque Limits

Joint Movement	Torque Limit (in-lb)
Shoulder	
Pitch	6000
Yaw	6000
Elbow	
Pitch	3600
Wrist	
Pitch	2400
Yaw	2400
Roll	750

it 90 degrees (Figure 4-255). This operation is completed in a maximum of 5 minutes. Docking to another shuttle requires approximately 15 minutes from initial contact of end effector to positioning of the shuttles within 6 inches of one another prior to actual mating.

Manipulator arm drive motors, switches, and solenoids all operate off 28 vdc. Each arm requires 450 watts maximum. Each TV camera operates off 28 vdc and requires 10 watts maximum. Each floodlight operates off 110 vac and requires 500 watts maximum.

The DCHS includes a docking port integrated with the shuttle's airlock. The docking port contains four drogue petals which are equally spaced and occupy approximately 45 degrees each of the port's circumference. Docking latches also are equally spaced around the port. A passive seal is provided. Because of use of manipulator arms in docking, no attenuation capability is provided at the docking port.

When docking, the meshing sets of drogue petals cause the cargo module to align radially and axially. The latches are then actuated during the final docking movement. This docking port will provide the orbiter with the ability to dock directly to both cargo modules and the space station.

Figure 4-256 shows the baseline docking geometry which is anticipated to apply to 95 percent of docking operations. An estimated five percent of the space docking missions would require use of a docking adapter as illustrated in Figure 4-257. With the docking adapter, the orbiter would have the capability of docking with a USSR spacecraft.

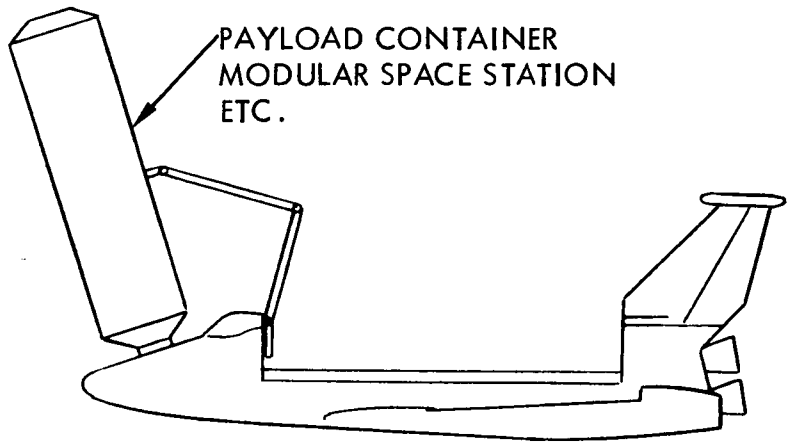

Figure 4-256. Baseline Docking Geometry

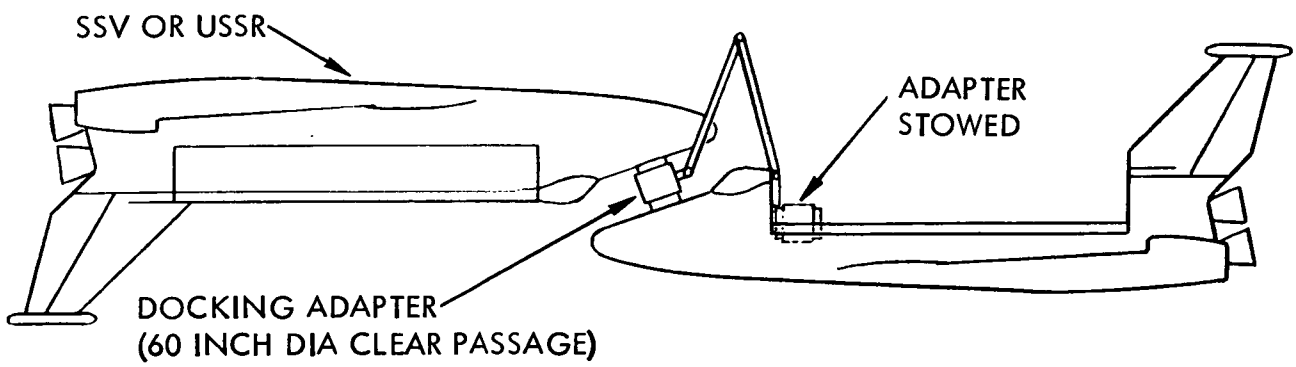

Figure 4-257. Docking Adapter

Transfer Tunnel System. Provision for personnel access between the crew compartment and a manned module or a cargo module is provided by the transfer tunnel located at the aft side of the crew compartment.

As shown in Figure 4-258, the transfer tunnel has an extendable section to provide the necessary clearance for module deployment and retrieval. The tunnel is extended to engage the manned module docking ring after stowage of the module. The reverse procedure is required before deployment of the module. The standard orbiter docking latches and seal are used for the tunnel manned module interface.

ABES Deployment System. The deployment system is shown in Figure 4-259. The ABES compartment door is powered open and closed by a pair of linear hydraulic two-position actuators located at the forward and aft ends of the door. The door folding panel is powered by an electric motor-driven gearbox driving a torque shaft to a series of planetary gear hinge actuators. The door folding panel actuation system is initiated by sequencing switches tripped when the ABES has been fully deployed. The door is latched in either the extended or folded modes by a series of toggle-roller latch mechanisms. The door latches are opened and closed through a push-pull rod and bellcrank linkage powered by a linear hydraulic actuator. The engine pylon is deployed with two linear hydraulic actuators and locked in the deployed position through an internal mechanical lock within the hydraulic actuator. The lock is unlocked when hydraulic power is applied to retract.

In the stowed position the nacelle is held and locked to structure with an over-center toggle mechanism hydraulically actuated to unlock. The entire system functional operations are sequenced using plunger-type electrical position switches.

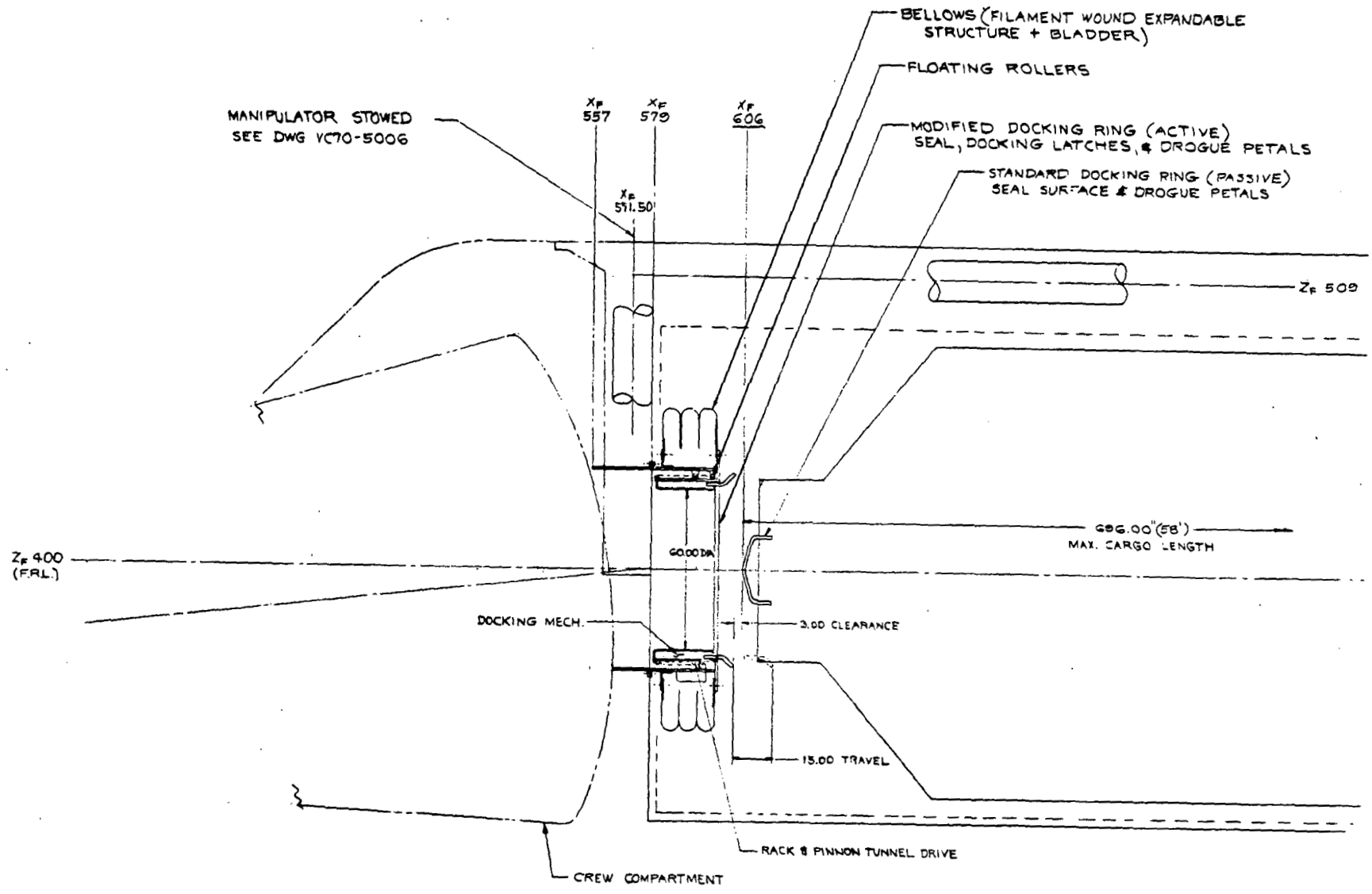

Figure 4-258. Transfer Tunnel

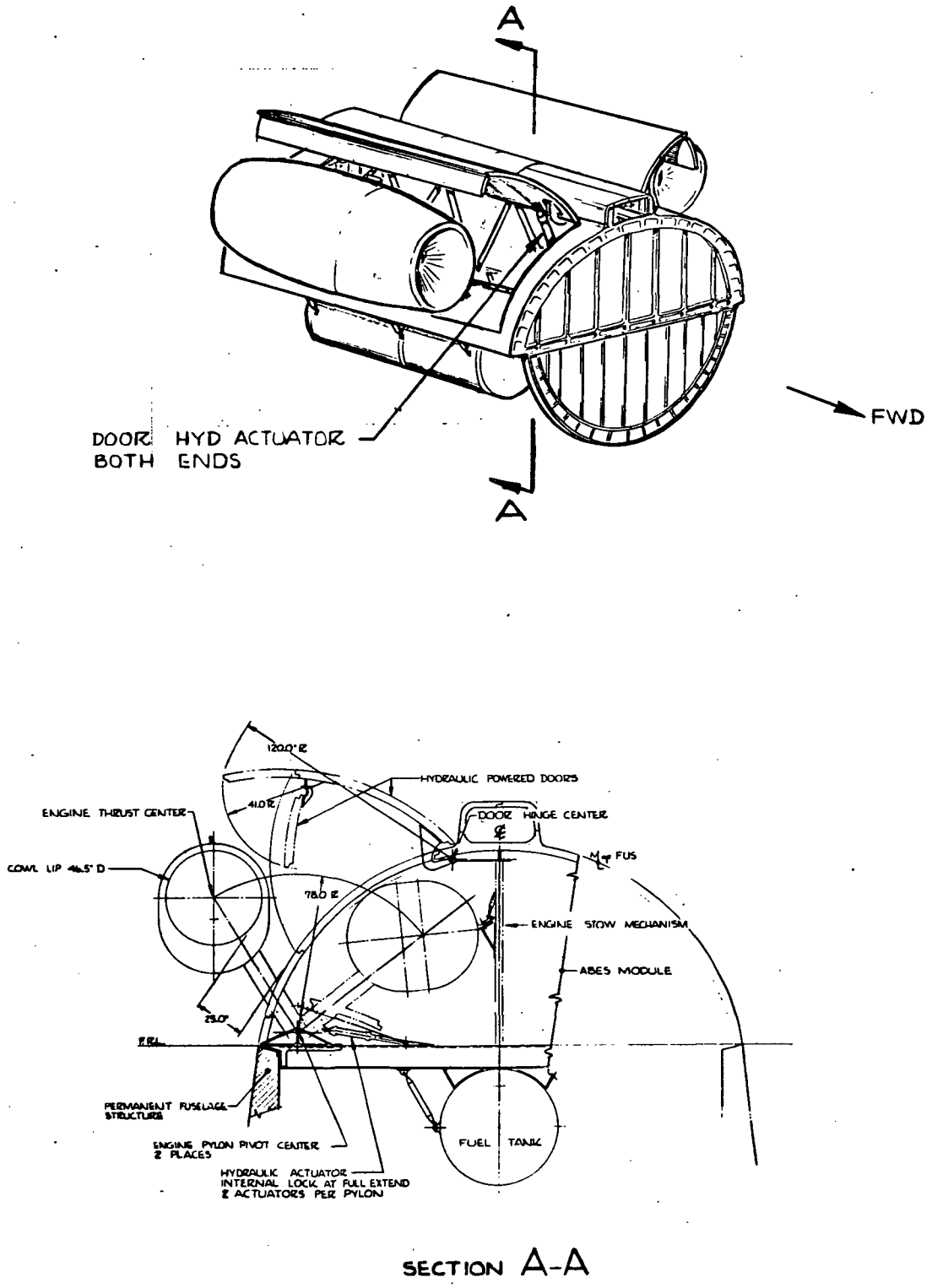

Figure 4-259. Air-Breathing Engine System Deployment Mechanism

4.4.3.11 Crew Compartment

Primary activities in the crew compartment design studies included a trade study of crew size and passenger location and configuration design studies. The trade study is described in Section 4.3.2. Configuration studies described here were based on a NASA baseline of two flight crew members and two mission specialists.

A number of crew compartment configurations were investigated during the total configuration development. Dual and single compartment concepts were investigated. Introduction of the NASA 040A configuration initiated a series of crew compartment layouts depicting differing relationships of flight crew, mission specialists, and other personnel. These configuration studies will be continued as part of further studies, concomitant with other mission payload manipulator system studies, low-cost avionics approaches, manipulator operator control station locations, and airlock placement options.

The design concept evolved during this period is shown in Figures 4-260 through 4-265. Two flight crewmen are located in an upper flight deck which includes controls and displays for the aerodynamic flight, launch, ΔV burns, and deorbit with the crew in a side-by-side forward-facing position. A separate, aft-facing station for manipulator payload and docking operations, including minimal translation and attitude controls, is provided on the vehicle centerline. The crewman occupies this station in a semi-standing position to permit a wide range of vision aft, downward into the cargo bay and upward (-Z direction), including some forward vision.

The lower crew compartment is configured to install the avionics in sealed compartments designed for a pressure differential of 10 inches of water to prevent equipment outgassing, smoke, or fire-suppressant vapors from entering the living volume atmosphere. The avionics equipment of the flight stations and payload monitoring station will require modifications to reduce outgassing of contaminants to an acceptable level. The galley, waste management/hygiene station, and seating for the two mission specialists also are located in this area.

Pressure hatches, designed to the full cabin pressure of 14.7 psi, are provided for pad ingress and egress and access to the airlock, docking port, and payload bay.

In-Flight Escape System Study. The Phase B study efforts defined an ejection seat adaption to the orbiter horizontal and vertical test flight vehicles. This study resulted in the identification of an existing, high-performance, open ejection seat suitably modified for orbiter inclusion. The modifications considered include interface fittings for an installation carriage to permit seat pitch articulation, fore-aft adjustment, rails for vertical adjustment,

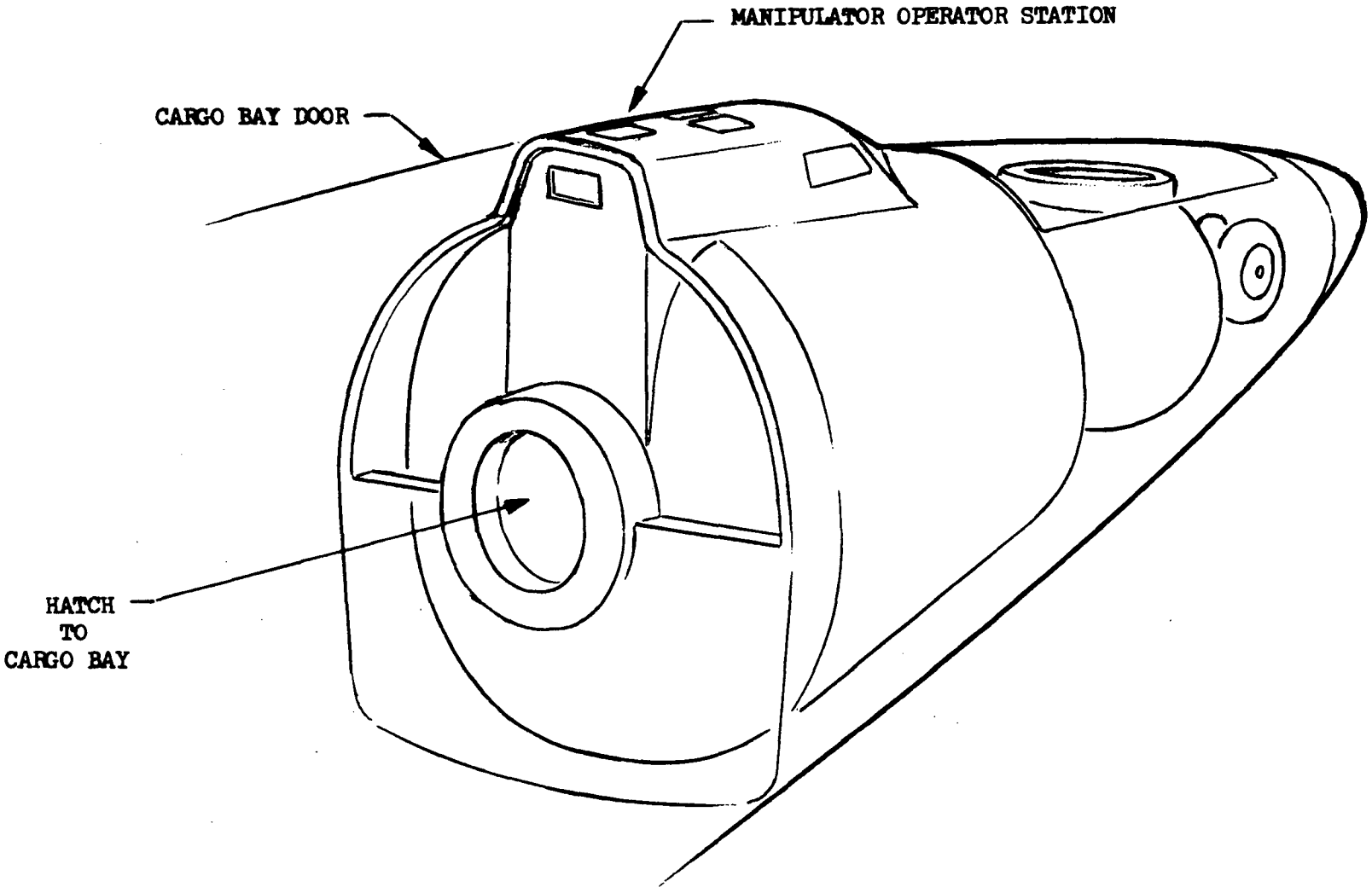

Figure 4-260. Manipulator Operator Station Crew Compartment

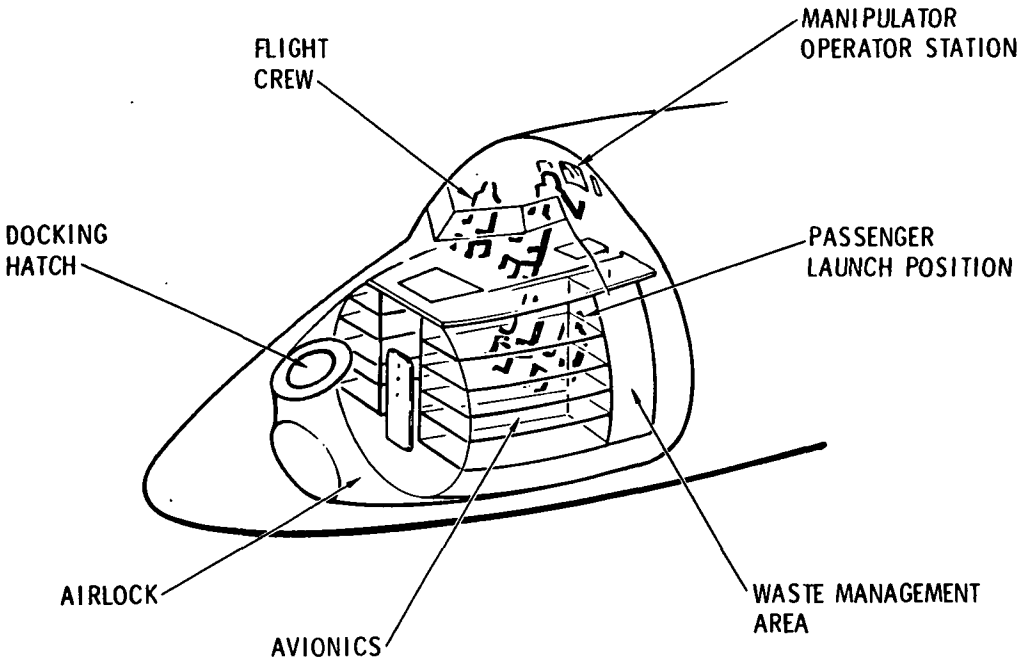

Figure 4-261. External View Crew Compartment

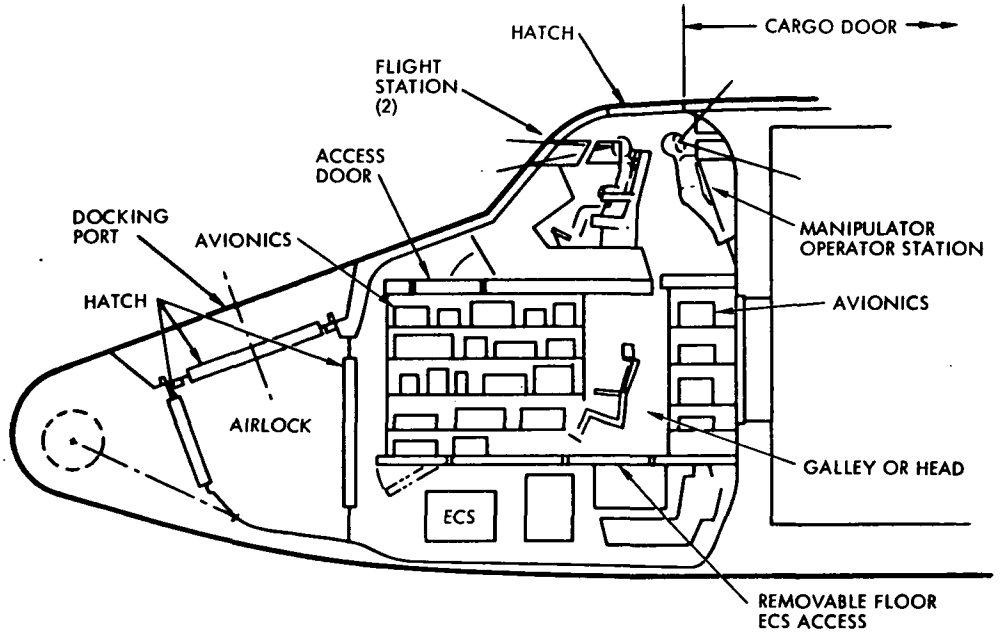

Figure 4-262. Crew Compartment

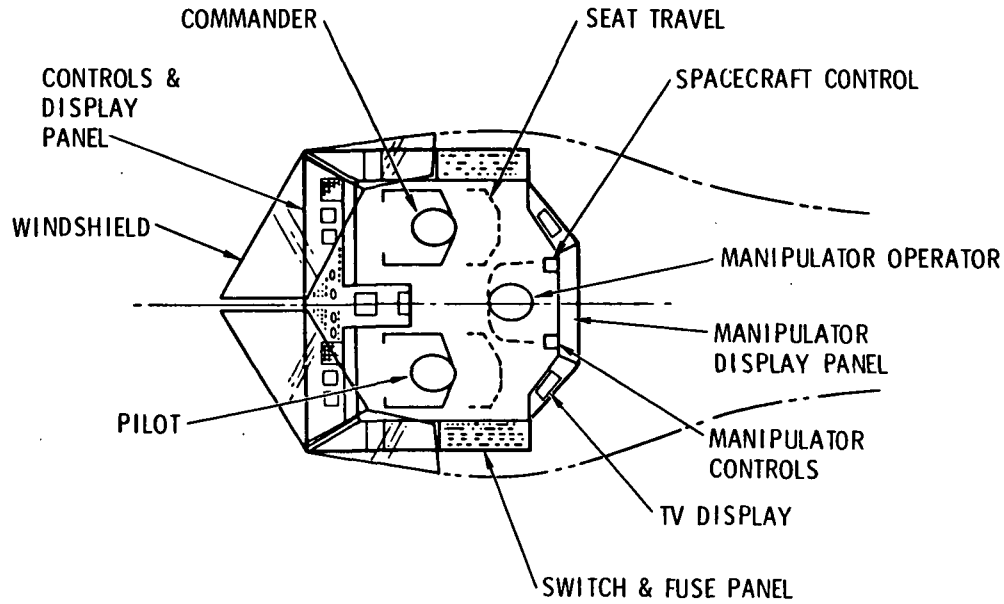

Figure 4-263. Flight Deck

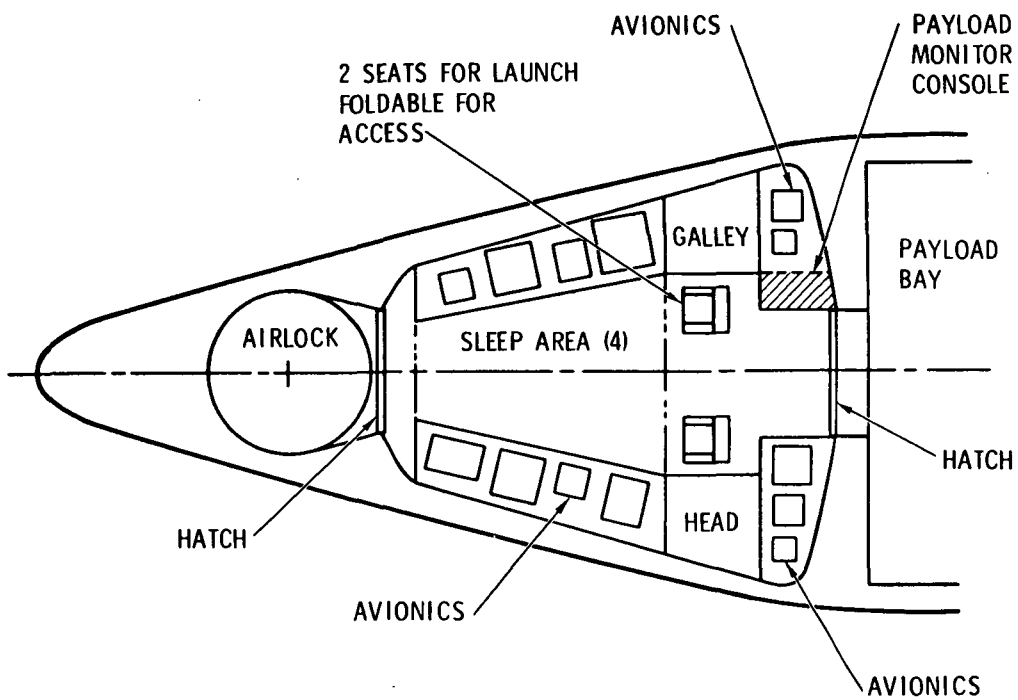

Figure 4-264. Lower Deck

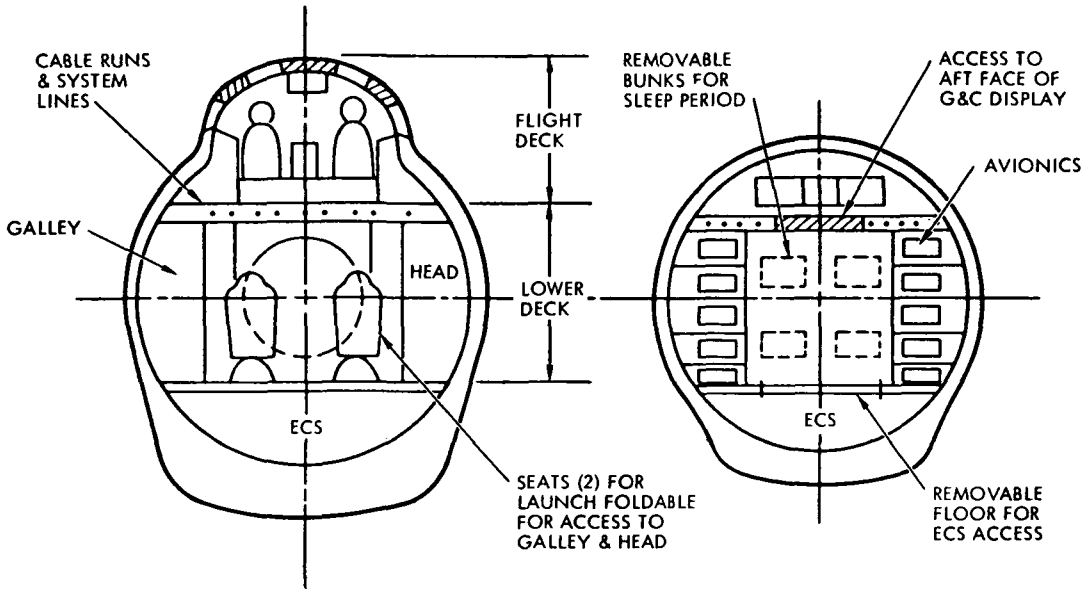

Figure 4-265. Crew Compartment Cross Sections

and the provisions for the addition of a sustainer rocket during vertical flight test operations.

Studies further substantiated the validity of the concept of adapting an existing, qualified ejection seat to reduce flight test development and operational cost by identification of ejection seat performance envelopes and development issues, and the preparation of a preliminary procurement specification draft to a cost a system.

The baseline crew compartment is designed for operational requirements with modifications required to the canopy and seat supports to accommodate ejection seat installation for the flight test phase.

4.4.3.12 Orbiter Weights

A summary dry weight breakdown for the Mark I and Mark II orbiters is presented in Table 4-47. The Mark I and Mark II orbiter basic airframe design and subsystems are the same except for TPS, main propulsion, and avionics. The structure is designed to the requirements of the Mark II orbiter, 65K lb up-payload plus 900 fps OMS ΔV propellant loaded and 40K lb down-payload. The OMS tankage is sized to provide 1000 fps ΔV when loaded full. The Mark I orbiter design uses an ablator TPS sized for 200-nm cross-range capability. The additional Mark I ablator TPS weight to provide 1100-nm cross-range capability is approximately 11K lb The Mark II orbiter design uses RSI TPS sized for 1100-nm cross-range capability. The Mark I main propulsion system uses four J-2S engines which are replaced with four 265K lb vacuum thrust high-P_c engines in the Mark II orbiter design. The Mark II orbiter avionics system adds a horizon sensor subsystem.

Table 4-47. Orbiter Weight Statement

Item	Mark I	Mark II
Wing group	13,805	13,805
Tail group	2,767	2,767
Body group	26,372	26,372
Induced environment protection	15,378	23,135
Landing, docking	11,659	11,659
Propulsion, ascent	21,453	19,100
Propulsion, cruise	64	64
Propulsion, auxiliary	5,244	5,244
Prime power	3,411	3,411
Electrical conversion and distribution	3,447	3,447
Hydraulic conversion and distribution	1,454	1,454
Surface controls	1,936	1,936
Avionics	3,376	3,472
Environmental control	2,817	2,817
Personnel provision	1,101	1,101
Growth	9,780	10,600
Dry weight	124,064	130,384

The sequenced mass properties for the Mark I and Mark II orbiter are presented in Table 4-48 for the LO_2/RP booster and in Table 4-49 for the LO_2/propane booster.

Table 4-48. Orbiter Sequence Mass Properties Statement, LO_2/RP Booster

ORBITER SEQUENCE MASS PROPERTIES STATEMENT

CONFIGURATION: ORBITER/TANK COMBINATIONS & ORBITERS ALONE | BY | DATE | PAGE OF

NO.	MISSION EVENT	WEIGHT LB.	CENTER OF GRAVITY INCHES			MOMENT OF INERTIA SLUG FT^2 X 10^{-6}			PRODUCT OF INERTIA SLUG FT^2 X 10^{-6}		
			X	Y	Z	I_{x-x}	I_{y-y}	I_{z-z}	I_{xy}	I_{xz}	I_{yz}
MK	I ORBITER - POLAR - LO_2/RP BOOSTER										
*	ORB/EOHT COMBINATION BEGIN ASCENT	1014733	1205.7	0.0	447.2	3.235	36.359	34.196	0	6.148	0
*	ORB/EOHT COMBINATION END ASCENT	238139	1685.6	0.0	600.9	1.648	10.227	9.651	0	1.177	0
(1)	ORB. FLT. VEHICLE - FULL	171210	1099.1	0.0	379.5	0.659	5.362	5.599	0	0.113	0
(1)	ORB. FLT. VEHICLE - ENTRY	156522	1075.9	0.0	381.4	0.613	4.884	5.168	0	0.144	0
(1)	ORB. FLT. VEHICLE-LANDING	153300	1069.9	0.0	381.2	0.613	4.780	5.062	0	0.132	0
MK	II ORBITER - DUE EAST - LO_2/RP BOOSTER										
*	ORB/EOHT COMBINATION BEGIN ASCENT	1128296	1225.5	0.0	455.0	3.845	41.097	38.393	0	7.403	0
*	ORB/EOHT COMBINATION END ASCENT	291964	1688.9	0.0	612.4	1.740	10.820	10.232	0	1.187	0
(1)	ORB. FLT. VEHICLE - FULL	225830	1077.7	0.0	374.6	0.730	6.042	6.287	0	0.140	0
(1)	ORB. FLT. VEHICLE - ENTRY	178518	1060.2	0.0	374.0	0.699	5.037	5.291	0	0.193	0
(1)	ORB. FLT. VEHICLE-LANDING	174620	1053.2	0.0	373.8	0.667	4.900	5.157	0	0.189	0

NOTES:
* Nose of Tank = Sta 500 (VC70-3077, Revision A)
(1) Nose of Orbiter = Sta 200
Center Line of Tankage: Vertical = 400 for Combination
Center Line of Cargo Bay: Vertical = 400 for Orbiter Alone

MK I Orbiter Payload 25K Up & Down
MK II Orbiter Payload 65K Up & 40K Down

Table 4-49. Orbiter Sequence Mass Properties Statement, LO_2/Propane Booster

ORBITER SEQUENCE MASS PROPERTIES STATEMENT

CONFIGURATION: ORBITER/TANK COMBINATIONS & ORBITERS ALONE | BY | DATE | PAGE OF

NO.	MISSION EVENT	WEIGHT LB.	CENTER OF GRAVITY INCHES			MOMENT OF INERTIA SLUG FT^2 X 10^{-6}			PRODUCT OF INERTIA SLUG FT^2 X 10^{-6}		
			X	Y	Z	I_{x-x}	I_{y-y}	I_{z-z}	I_{xy}	I_{xz}	I_{yz}
MK	I ORBITER - POLAR - LO_2/PROPANE BOOSTER										
*	ORB/EOHT COMBINATION	988529	1219.4	0.0	447.5	3.136	34.948	32.886	0	5.776	0
	BEGIN ASCENT										
*	ORB/EOHT COMBINATION	236802	1674.3	0.0	598.5	1.606	10.109	9.577	0	1.144	0
	END ASCENT										
(1)	ORB. FLT. VEHICLE - FULL	171210	1099.1	0.0	379.5	0.659	5.362	5.599	0	0.113	0
(1)	ORB. FLT. VEHICLE - ENTRY	156522	1075.9	0.0	381.4	0.613	4.884	5.168	0	0.144	0
(1)	ORB. FLT. VEHICLE-LANDING	153300	1069.9	0.0	381.2	0.613	4.780	5.062	0	0.132	0
MK	II ORBITER - DUE EAST - LO_2/PROPANE BOOSTER										
*	ORB/EOHT COMBINATION	1100113	1221.0	0.0	455.3	3.719	40.598	38.030	0	7.157	0
	BEGIN ASCENT										
*	ORB/EOHT COMBINATION	290560	1676.7	0.0	609.4	1.695	10.721	10.175	0	1.156	0
	END ASCENT										
(1)	ORB. FLT. VEHICLE - FULL	225730	1077.7	0.0	374.6	0.730	6.042	6.287	0	0.140	0
(1)	ORB. FLT. VEHICLE - ENTRY	178518	1060.2	0.0	374.0	0.699	5.037	5.291	0	0.193	0
(1)	ORB. FLT. VEHICLE-LANDING	174620	1053.2	0.0	373.8	0.667	4.900	5.157	0	0.189	0

NOTES:
* Nose of Tank = Sta 500 (VC70-3076, Revision A)
(1) Nose of Orbiter = Sta 200
Center Line of Tankage: Vertical = 400 for combination
Center Line of Cargo Bay: Vertical 400 for orbiter alone

MK I Orbiter Payload 25K Up & Down
MK II Orbiter Payload 65K Up & 40K Down

4. 4. 3. 13 Manufacturing

Manufacturability trade studies were conducted and requirements for design, development, and manufacturing were evaluated during Phase B' to establish appropriate perspective of the total orbiter manufacturing task. The task analyses performed revealed that the manufacturing technology required to fabricate the vehicle is understood. Certain items identified as problems and concerns represent but a small percentage of the total task and involve primarily the approaches to planned manufacturing techniques. The product task complexity associated with each orbiter assembly, Model 176, is summarized in Table 4-50. The assemblies noted may be identified in the manufacturing breakdown (Figure 4-266).

The following sections contain discussions of manufacturing producibility analysis, major manufacturing concerns, and items causing substantial program impact. Items identified as major manufacturing problems are

Table 4-50. Manufacturing Task Analysis - Orbiter Vehicle

	Forward Fuselage	Crew Module	Mid Fuselage	Aft Fuselage	OMS/ACPS Pods	Wing Assembly	Stabilizer	Payload Bay Doors	Air Breathing Engine Module	Thermal Protection System	Manipulators	Ferry Tank
Fabrication	S	C	S	S	S	S	S	S	S	S	S	S
Processing	S	S	S	S	S	S	S	S	S	S	S	S
Assembly	S	C	S	S	S	S	S	S	S	S	S	S
Installations	S	C	S	C	S	S	S	S	S	C	S	S
Checkout	S	C	S	C	S	S	S	C	S	NA	C	S
Handling	S	S	S	S	S	S	S	S	S	S	S	S
Transportation	S	S	S	S	S	S	S	S	S	S	S	S
Inspection	S	S	S	S	S	S	S	S	S	S	S	S
Tooling	S	C	S	S	S	S	S	S	S	S	S	S

Key: S - State of the art C - Concern NA - Not applicable

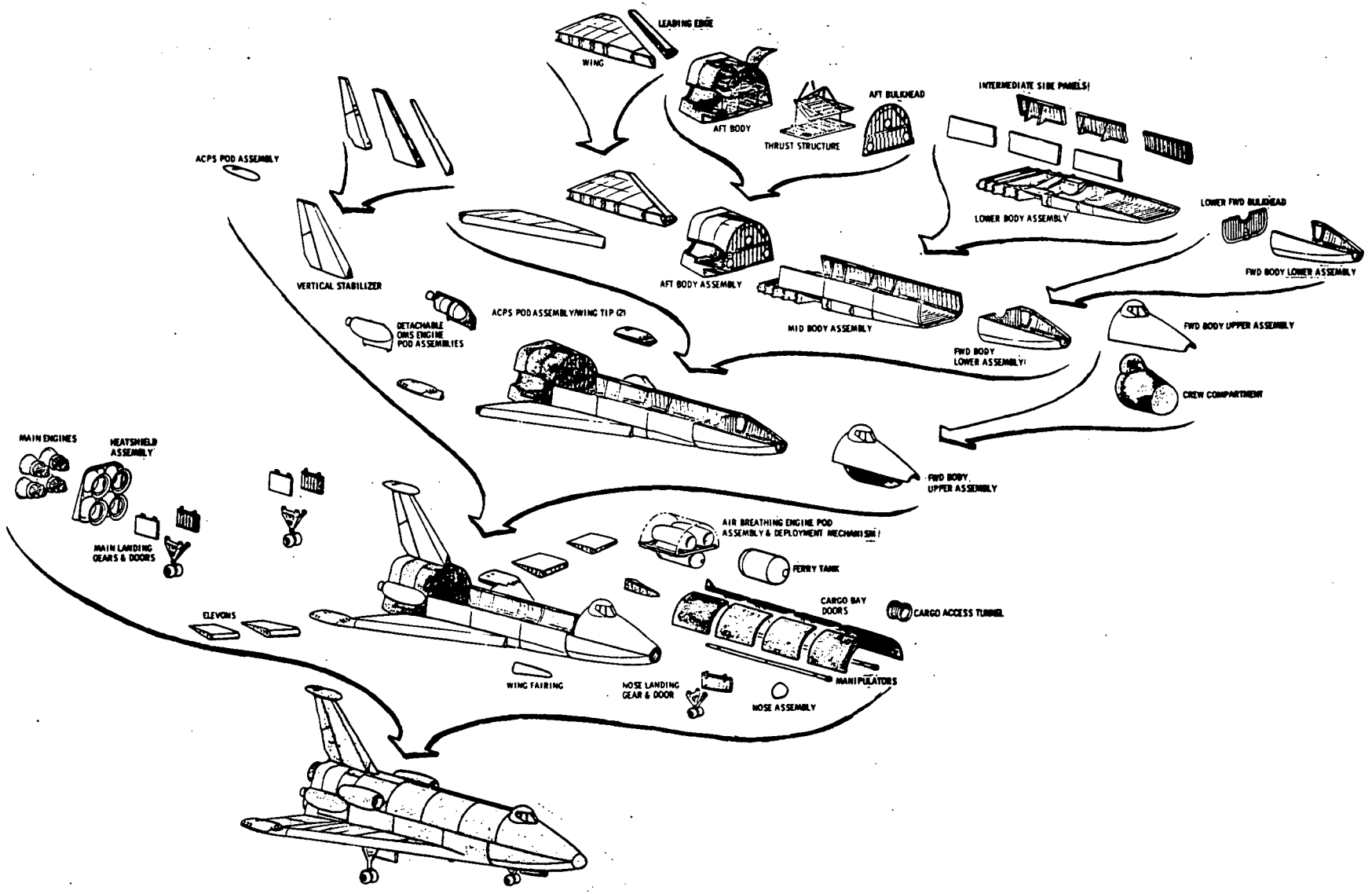

Figure 4-266. Manufacturing Breakdown

those capable of substantial program impact. Manufacturing concerns are limited to areas involving significant manufacturing complexity, but not threatening general impact.

Manufacturing Producibility Analysis. The orbiter configuration studied during Phase B' was considerably smaller than the Phase B orbiter. This reduction in size, the removal of the integral tank LH_2 and LO_2 tank from the orbiter interior, the changes in orbiter structural material from titanium to aluminum, thermal protection material from reusable external insulation, carbon/carbon and ablator to all ablator were identified as major items reducing orbiter vehicle manufacturing complexity. The change from an integrated avionics system to a conventional system and to an external main propulsion tank from an internal integral LH_2 tank and internal LO_2 tank increased the complexity of systems installations, checkout, and added tank transportation requirements, respectively. In addition, the phased approach, Mark I and Mark II and subsystem cost reduction studies introduced several subsystem changes such as interim ablative thermal protection, B-1 air breathing engines, interim J-2S main propulsion engines and hypergolic fueled orbital maneuvering engines, reaction control engines, and auxiliary power units. All of these changes have been evaluated as to their effect on manufacturing operations. A summary of manufacturing orbiter vehicle complexity factors, Model 161C compared to Model 176, is identified in Table 4-51. These factors, in conjunction with the producibility analysis, were applied by manufacturing to develop a detailed plan containing sequential flows for tooling, fabrication, assembly, system installation, checkout, and inspection. Items of manufacturing problems and concerns have been identified from the plan and are discussed in the following section.

Major Manufacturing Problems. Based on the analyses performed, there were no items identified as major manufacturing problems.

Table 4-51. Manufacturing Complexity Factors - Orbiter

	Fabrication	Processing	Assembly	Installations	Checkout	Handling	Transportation	Inspection	Tooling	Material	Cost	Schedule
161C	M	M	M	L	L	M	M	M	M	M	M	M
176	L	L	L	M	M	L	L	L	L	L	L	L
Key: M - More complex L - Less complex N/C - No change												

Manufacturing Concerns

Crew Compartment Module. Detail study of the crew module design, fabrication, and assembly sequences exposed a requirement for extremely complex tooling. The compound contours involved in the shape of the module and the limited production requires unique initial tool configuration for fabrication and assembly. An approach to the tooling required to support fabrication and assembly fitup for weld is being developed concurrently with mockup development.

Crew Compartment Module. Deletion of the onboard checkout capability requires the addition of support equipment to perform checkout operations. Accessibility and maintainability are major considerations for both installation and checkout operations. The crew compartment is considered a high density area for both personnel and equipment. Sequencing of installations and checkout operations is a mandatory requirement to support manpower and schedule requirements.

Aft Fuselage. The reduced size of the overall orbiter vehicle has increased the density of subsystems in the aft fuselage. Subsystems installation and checkout will be limited to serial-type operations. Sequencing of installations and checkout operations is a mandatory requirement to support manpower and schedule requirements.

Payload Bay Doors and Manipulators. Assuming a requirement will exist to perform a functional check of both the payload bay doors and manipulators, a manufacturing concern exists in direct support of engineering requirements. The solution to this item is to provide the necessary environment and equipment required when the checkout is defined.

Thermal Protection System. Mold line control is a manufacturing concern. Both the outer and inner mold lines are variables requiring special consideration. The approach to this concern is the determination of the nominal tolerance allowables and development of installation techniques to obtain these tolerances.

Items Causing Substantial Program Impact. Items that could cause substantial program impact were assessed by manufacturing task teams assigned to conduct in-depth evaluations of manufacturing and engineering design issues. Trade studies and design analysis were performed by Manufacturing in conjunction with Design Engineering during the Phase B' study to assure manufacturability of the orbiter. These studies included factors concerning technology, tooling, material, handling, fabrication, assembly, installations support equipment, manufacturing checkout, personnel, cost, schedule, facilities, quality assurance, safety, and transportability. The

conclusions reached by these teams were presented to the Production Operations Review Board to establish the optimum manufacturing methods and processes, based on current design vehicle configuration.

Results of these assessments and studies indicate that there are no areas in the present manufacturing plan that would present a substantial program impact.

4.4.3.14 Facilities

The orbiter configuration studied during Phase B' was considerably smaller than the original Phase B configuration. In addition, the phased approach, Mark I and Mark II and subsystem cost-reduction studies introduced several subsystem changes, such as interim ablative thermal protection, B-1 air-breathing engines, interim J-2S main propulsion engines, and hypergolic fueled orbital maneuvering engines, reaction control engines, and auxiliary power units. These changes have been evaluated as to their effect on the facilities baseline defined in the "Facility Utilization and Manufacturing Plan for Phase C/D," Volume I, Orbiter, SD 71-104-1. There is no significant change to the baseline facilities required for the Phase B' orbiter configuration except as described below.

Development Test Facilities. The primary effect is a reduction in the physical size of the required facilities, such as structural test buildings, which should reduce the cost of modifications to use existing facilities. The OMS and RCS hypergolic fueled engines can be tested at existing WSTF installations and the airbreathing engine tests can be performed at a test site being developed for the B-1 engine test program. Additionally, the Mark I main propulsion static firing program, with J-2S engines, simplifies the early facility requirements (no altitude simulation required) and use of existing Saturn S-II support systems will be economically feasible.

The ablative thermal protection system will require additional work in structural test labs and plasma arc facilities but does not add new facility requirements.

Manufacturing Facilities. The final assembly building requirements were changed because of the orbiter being reduced in size, eliminating the need for a new final assembly building. This operation can now be accomplished in existing facilities at Seal Beach Building S-14 with minor modifications. After completion of final assembly and checkout, the wings and vertical stabilizer are removed for overland shipment to Edwards Air Force Base for final mating and horizontal flight test.

Flight Test Facilities. Orbiter horizontal flight test operations will be at Edwards Air Force Base as proposed in the Facilities Baseline Plan,

with an additional minor task of final mate of wings and vertical stabilizer. This has eliminated the need for the barge trip to Point Mugu and preflight test facilities at Point Mugu.

Modular, or pad, configuration for the hypergolic fueled OMS, RCS, and APU will add a requirement for a remote facility for service and maintenance of these subsystems at the vertical flight test site, KSC.

4.4.3.15 Test

Communication and Instrumentation. The VHF, short range precision ranging, recovery beacon, radar altimeter, and ATC transponder have been deleted, reducing the communications system test program by approximately 50 percent.

ECLSS. The development test program is phased to reflect deferral of radiators, water system, and hydrogen heat exchanger to the first MOF, and the sublimators, and waste and food management to Mark II.

Power Generation. Because the APU now uses hydrazine propellant, it is no longer tested at a combined subsystem level with the APS. Instead, the APU and its exhaust and hydrazine storage and feed assemblies are integrated at a separate test article. APU development has been deferred to reflect first usage on Orbiter 2.

For Phase B, integration of the fuel cells and PRSD took place during the horizontal flight test program. Since fuel cells have been deleted from the Orbiter 1 horizontal flight test program, a fuel cell-PRSD integration test article has been added for B'.

Hydraulic Power. There are no significant differences in the hydraulic power test program.

Integrated Thermal Control. The vehicle purge system was reduced in scope because of changeover to external tanks. As a result, the vehicle purge test article has been deleted. A 3/8 scale model thermal vacuum test program has been added to augment the existing on-orbit thermal vacuum tests.

DCM. Elimination of the central computer/data bus has resulted in deletion of the DCM and its test program for Phase B'.

ABPS. No change.

MPS. As a result of the change in engine configuration from high P_c engines to J-2S, it is expected that the Mark I MPS development program will

be reduced significantly. Many of the component requirements can be satisfied by existing S-II hardware or minor adaptations of current designs. A further evaluation of the cluster firing test article revealed that the cost of that article could be substantially reduced by utilizing a boilerplate structure for all but the AFT body without compromising the overall objectives of the test program.

Consequently the configuration of the main propulsion test article (MPTA) has been redefined to consist of a flight-weight external tank (less de-orbit and separation systems), a production AFT body structure, four prototype J-2S engines, and a complete MPS installation consisting of a mixture of production and prototype components. As a result, the structural/dynamics-oriented test objectives have been deleted from the MPTA program and are accomplished instead during the vertical ground vibration test.

It is also planned to utilize the external tank from the MPTA to accomplish the flight readiness firings of Orbiter 1 and 2. The Mark II MPS high P_c development program will be approximately the same as identified in Phase B.

Structures Subsystem. The structural test program remains essentially the same. Because the crew compartment is no longer a floating structure and is now integral with the forward fuselage, the cabin structure tests will be conducted in conjunction with the structural test article. The MPS tank structural tests are now covered under the new EOHT subsystem since the current design has removed the LO_2 and LH_2 tanks from the body structure. In general, the overall reduction in vehicle size and utilization of an all-aluminum airframe has considerably reduced facility and test fixture requirements.

External LO_2/LH_2 Tank Subsystem (New for Phase B'). The external tank will be tested in a vertical attitude in a manner similar to the previous Phase B LH_2 tank design. However, the new tank concept with an interstage adapter to the booster has additional requirements for structural tests, pyrotechnic separation tests, de-orbit rocket engine tests, and a more sophisticated approach to functionally demonstrate the orbiter/tank separation system.

Payload Handling and Retrieval Subsystem. Test requirements for this subsystem remain essentially unchanged except that current system definition has revealed additional requirements for full and subscale simulation tests of the manipulator control system and the need for more sophisticated approach to adequate demonstration of the control system electrical, electronic, and mechanical components.

Docking Adapter Subsystem. The Phase B' cabin redesign and attendant redesign of the airlock and cabin docking hatch has had minimal impact on the docking system test requirements, and as such the test program is essentially unchanged.

Landing System. The landing subsystem test requirements for Phase B' remain the same as defined for Phase B.

Thermal Protection Subsystem. The Mark I TPS has been redefined as an ablative-type thermal protection system. Generally, the same type of test program defined for the Phase B TPS will be followed with some exceptions: considerable plasma arc testing will be required to adequately evaluate material properties of candidate material, fastening techniques, and joint designs. The Mark II TPS consisting of RSI/RCC material will be phased to provide for obtaining development test data from the Mark I orbiter flights. Acceptance, development, and qualification tests will be conducted as cited in the Phase B test plan.

OMS-ACPS. The OMS/RCS test program is simplified by separating the two systems and by modularizing each of them. Separate development test programs will be conducted on each of the subsystems, probably at the same facility.

Acceptance checkout and prelaunch checkout requirements also will be more readily accommodated at the modular level than as installed systems.

D&C. Deletion of multifunctional displays and controls and their massive DCM interface essentially eliminates all D&C testing at the subsystem level and greatly reduces the integration task required.

EPD&C. The deletion of DCM/data bus/ACT control of the EPD&C subsystem eliminates a large integration effort.

GN&C. With advent of control cables for flight control, the "Iron Bird" will serve as the cable flight control system test article. The iron bird also will require a cockpit mockup which was previously unnecessary.

Flight Test. The major change to the Horizontal Flight Test Program from Phase B was to increase the total flight test hours from 180 to 200. Major changes occurred in the following:

	Phase B	Phase B'
Preliminary evaluation	0 hr	20 hr
Stability and control	60	75

There is no significant change to the vertical flight test program.

Manufacturing Checkout. In-process acceptance checkout has been revised to reflect the buildup scenario of the B' vehicle. Combined and integrated subsystem checkout remains essentially unchanged.

4.4.4 Orbiter Hydrogen/Oxygen Tank Definition

A key issue in assessing the relative merit of the external LO_2/LH_2 tank concept is the cost of the expendable tank. Therefore, the tank design trade was continued during Phase 2 to select the best tank design concept and conduct a detail tank cost analysis. To support this analysis, a detail tank design was prepared so manufacturing analysis and cost analysis could be conducted to provide a high degree of confidence in the results. The results of this continuing trade are reported. Final tank sizes defined in the integrated vehicle sections are provided. For the baseline tank concept, the results of the requirements analysis, tank design and manufacturing, facilities, and test requirements are reported.

4.4.4.1 Design Options and Selected Tank Design

Design Options. The Phase 2 effort for the design of the external hydrogen/oxygen (HO) tank was initiated by the definition of four HO tank options selected from the various conceptual designs developed during Phase 1. The designs that were continued are shown in Figure 4-267, and are identified by option, type, and the reasons for their respective selection. The tank study continuation arrived at the final selection of a tank design that results in the least initial or least total program costs and minimizes risk. It was estimated that the baseline tank design would yield the least initial costs, whereas the alternate 1 tank design would yield the lowest total program cost. The semimonocoque alternate 2 tank was continued because

CONTINUE STUDY OF THE FOLLOWING TANK DESIGNS:

OPTION	CONFIGURATION	TYPE	REASON
BASELINE	3032 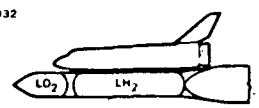	HEAVY WALL MONOCOQUE LH_2 TANK	LOWEST INITIAL PROGRAM COST
ALTERNATE NO. 1	3031 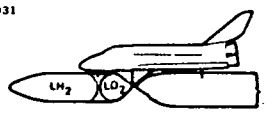	THIN WALL MONOCOQUE LH_2 TANK	LOWEST TOTAL PROGRAM COSTS
ALTERNATE NO. 2	3033 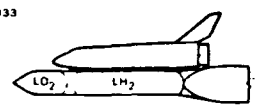	SEMI-MONOCOQUE LH_2 TANK	FALL BACK DESIGN FOR BASELINE
ALTERNATE NO. 3	3034 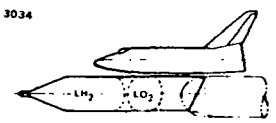	THIN WALL MONOCOQUE LH_2 TANK	POSSIBILITY OF UTILIZING BEST DESIGN/COST FEATURES

Figure 4-267. Initial Selected Tank Designs

of its lower weight and as a fall back design for the baseline tank. The alternate 3 tank design appeared to incorporate all of the best design and cost features of the baseline and alternate 1, —without the penalties of either.

The baseline tank design utilizes the LH_2 tank as the primary structure. Both the LO_2 tank and the LH_2 tank are monocoque, but the LH_2 tank has been simplified in its design in that the tank walls are thick and react the prelaunch stack loads by plate buckling. The LO_2 tank walls are thin. The tank assembly is installed in tandem by an interstage to the booster. The orbiter is mounted in parallel with the tank and supported by the orbiter bulkheads at each end of the payload. The alternate 2 tank is similar to the baseline design except that the thick wall monocoque LH_2 tank has been replaced by a more efficient, but more costly, semimonocoque skin/stringer/frame construction.

The alternate 1 tank design utilizes relatively thin wall monocoque LH_2 and LO_2 tanks mounted in parallel to the orbiter. Behind the tank, and also in parallel to the orbiter, is the booster. The booster thrust load is directed into the aft conical end of the LO_2 tank via a ball/socket thrust fitting and along the LO_2 tank sidewalls via an interstage into the LH_2 tank. Both the tank assembly and the booster are supported via trusses by the orbiter. The thrust load path from the booster to the heavy propellant masses is direct; the lateral loads (in both planes) between the tank, orbiter, and booster are reacted by the orbiter as a structural bridge between the tank and the booster.

The final alternate 3 option utilizes thin wall monocoque LO_2 and LH_2 tanks—with the LO_2 tank located aft of the LH_2 tank (similar to option 1) to allow the direct boost load into the heavy LO_2 propellant. A semimonocoque interstage structurally connects the tank assembly to the forward end of the booster (similar to baseline). The tank assembly is supported below (parallel) the orbiter by local attachments (similar to baseline).

The approach utilized in the design, cost, and for the selection of the final tank design is shown in Figure 4-268. As noted, a constant propellant volume was retained for the original tank configuration options during the Phase 1 effort; in contrast, during Phase 2 the propellant volumes for the four selected tank designs were defined from individually synthesizing the four shuttle programs i.e., total vehicle propellant distribution optimization. From the four tank designs, a final tank design was selected for a complete preliminary design. The basic goals attempted to be attained throughout the entire study are also listed on the figure.

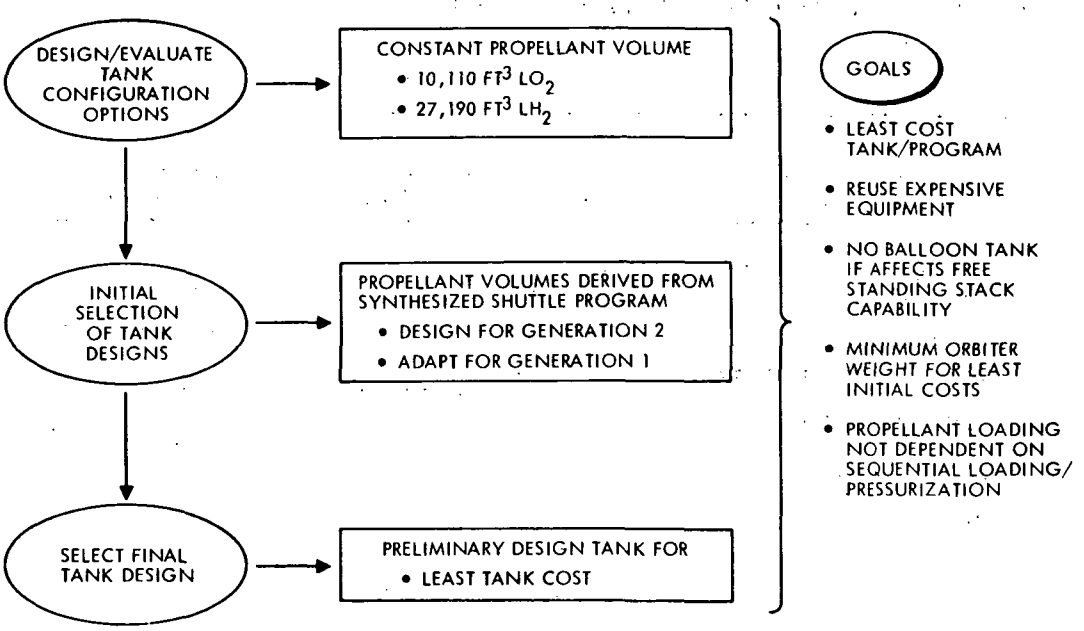

Figure 4-268. Design/Cost Study Approach

The continuation of the Phase 2 study utilized the previous data developed during the study for the external LH_2 tank system, as well as during the Phase 1 EOHT configuration study. The data are listed as basic design and system requirements in Figure 4-269. In addition, the basic structural and TPS materials and fabrication methods also are listed. The 2219-T87 aluminum was selected for the tank structure because of its good strength-to-weight ratio, easy fabrication, good weldability, toughness, and its resistance to stress, corrosion, and cracking. The material is well characterized in that complete design data are available and NR, as well as the total industry, have years of experience with this material. These reasons resulted in selecting this material for the expendable tank hardware. In addition, automatic butt fusion welding has been selected for the tank assembly because it is the most efficient structural connection, yielding a complete pressure seal. Fusion welding is a single operation (setup, trim, then weld) and is compatible for fitup for both longitudinal and circumferential welds. Again, NR has years of experience and miles of successful welds in the accomplishment of its past programs including Apollo and S-II.

The hydrogen tank requires a cryo insulation and the successful spray-on foam insulation (SOFI) developed during the S-II program has been selected for the material. Both the material and method of application yield the least cost application, especially when applied to the outer rather than the inner surface of the LH_2 tank. Where additional protection is

- UTILIZE APPLICABLE DATA PREVIOUSLY DEFINED FOR THE EXTERNAL LH_2 TANK SYSTEM WHICH ARE

DESIGN REQUIREMENTS

- TANK BREAKUP AFTER DEORBIT ACCEPTABLE
- PROVIDE ASCENT TPS ONLY
- CRYO INSULATION REQUIRED
- DEORBIT INITIATED BY G&N SYSTEM
- DEORBIT ΔV = 300 FPS
- SPIN STABILIZE TANK

SYSTEM REQUIREMENTS

- REDUCE COST OF EXPENDABLE HARDWARE
- REUSE EXPENSIVE HARDWARE
- UTILIZE OFF THE SHELF TECHNOLOGY/EXPERIENCE

MATERIAL/ FABRICATION

- 2219-T87 ALUMINUM
- AUTOMATIC BUTT FUSION WELDING
- S-II SOFI
- CORK TPS BONDED ON SOFI

Figure 4-269. Previous Data

required locally in areas of shock interaction, bonded cork will be utilized—whether it is bonded directly to the intertank aluminum structure, the LO_2 aluminum tank, or to the outer surface of the SOFI on the LH_2 tank—again, for least cost. Where possible, bonding of cork to SOFI will be avoided to circumvent difficulties experienced on the S-II program.

A contributing factor to the tank configuration is shown in Figure 4-270 for single tanks located below the orbiter. The forward end of the tank, if shaped less than a 30-degree half angle, will satisfy the aero/drag requirements and, therefore, can be designed primarily by either manufacturing or material limitations for least cost assembly. The forward fairing will house the retro motor. The design can, therefore, be simplified in that the machined and welded dollar ring, utilized for bolt sealing the manhold cover, also can be utilized for the attachment of the forward fairing.

Conceptual design studies with reasonable depth to define the basic tank structure, load paths, assembly sequence, system definition, and installation for each of the four tank designs listed in Figure 4-267 were completed to allow a basic weight and cost definition for each of the tank designs. In addition, various trade studies were also completed in attempts to either reduce the weight and/or the cost of the individual designs. In conjunction with the four tank designs, the tank design influences on the orbiter, the booster, and the booster interstage also were determined. The influences included the structural, thermal, and system equipment penalties as applicable.

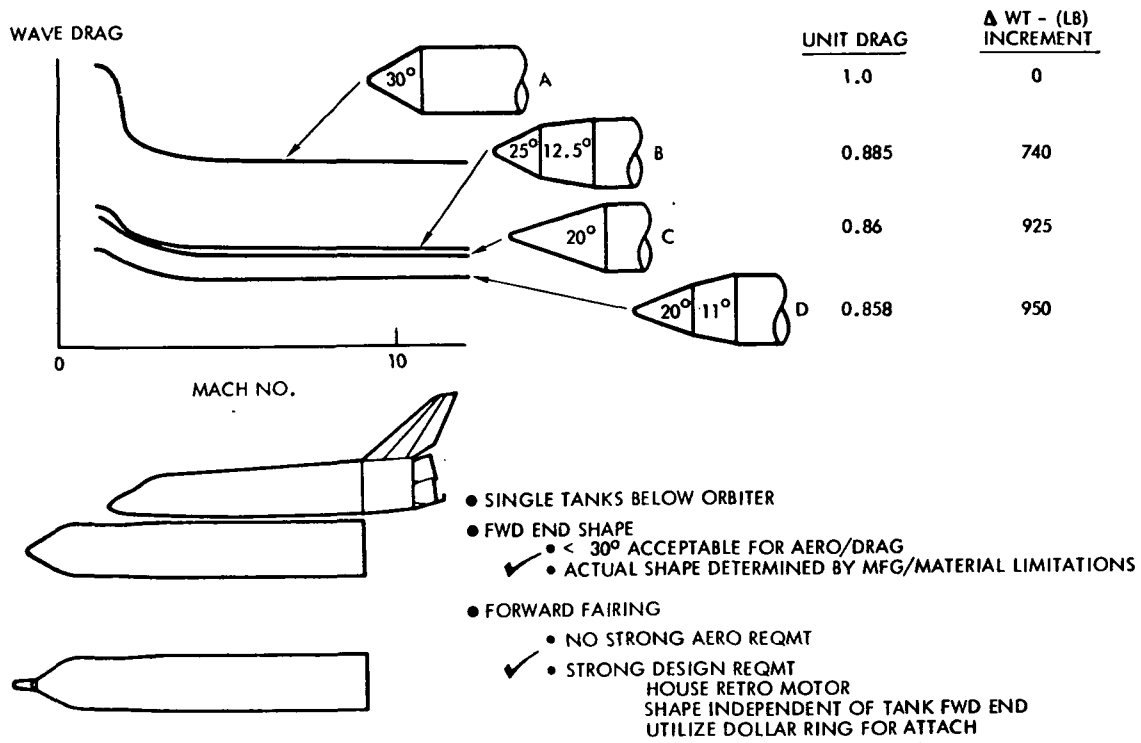

Figure 4-270. Tank Forward End Requirements

A weight comparison for the four tank design options is given in Figure 4-271. The weights are listed for the tank assembly and the booster interstage as total weights. For the orbiter and booster, the weights for the three alternates are given as delta's to the baseline option. Individual tradeoff weight savings are also listed for the task assemblies for each of the applicable options. The tank weights include a two percent weight contingency. As noted, the baseline tank weight is still the heaviest of the tank options. The use of bolted cork substructure reduces the weight slightly—but the increased cost nullifies the weight reduction. The weight reduction for the increased stock width is more important for the decreased cost that also results. The weight for the expendable booster interstage is also given.

The alternate 2 option tank weight is appreciably less than the baseline tank weight. A substantial weight reduction is also possible with the use of a common honeycomb sandwich bulkhead instead of the separate bulkheads with an intertank structure. A weight saving is available for both the orbiter and the booster because of the reduced tank weight which has been synthesized in the orbiter and booster weights.

The alternate 1 option has the least tank assembly weight. Weight reductions are available if a common bulkhead is utilized and/or a boost cover with the cork bonded directly to the cover is used instead of the cork

TANK			WEIGHTS (LB)				
OPTION	CONFIGURATION	DESIGN	Δ TANK	TANK ASSEMBLY	BOOSTER INTERSTAGE	Δ ORBITER	Δ BOOSTER
BASELINE	3032 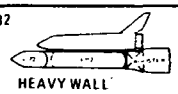 HEAVY WALL MONOCOQUE LH_2 TANK	FOR LEAST INITIAL PROGRAM COSTS	—	53,550	8,600 (EXPENDABLE)	0	0
		INCREASED STOCK WIDTH	+160				
		BOLTED CORK/SUBSTRUCTURE	+145				
		FOR LEAST TOTAL PROGRAM COSTS	—	53,245			
ALTERNATE NO. 2	3033  SEMI-MONOCOQUE LH_2 TANK	FOR LEAST INITIAL PROGRAM COSTS	—	41,350	8,600 (EXPENDABLE)	+2,465	+26,800
		BOLTED CORK/SUBSTRUCTURE	+175				
		COMMON BULKHEAD	+2,035				
		FOR LEAST TOTAL PROGRAM COSTS	—	39,140			
ALTERNATE NO. 1	3031 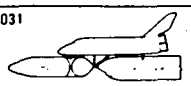 THIN WALL MONO-COQUE LH_2 TANK	FOR LEAST INITIAL PROGRAM COSTS	—	28,420	300 (REUSABLE)	+5,090	+30,700
		INCREASED STOCK WIDTH	+220				
		BONDED CORK ON BOOST COVER	+1,580				
		COMMON BULKHEAD	+1,180				
		FOR LEAST TOTAL PROGRAM COSTS	—	25,440			
ALTERNATE NO. 3	3034  THIN WALL MONO-COQUE LH_2 TANK	FOR LEAST INITIAL PROGRAM COSTS	—	37,840	0	+3,170	+28,600
		INCREASED STOCK WIDTH	+220				
		BONDED CORK ON BOOST COVER	+1,580				
		COMMON BULKHEAD	+1,180				
		FOR LEAST TOTAL PROGRAM COSTS	—	34,860			

Figure 4-271. Weight Comparison, Initial Selected Tank Designs

bonded to the exterior surface of the SOFI. The weight of the booster interstage is drastically reduced to 300 pounds and represents the upper/aft link attachment between the booster and the orbiter—which is recoverable with the booster and reusable for subsequent flights. The orbiter weight is increased because of the structural penalty imposed upon the orbiter—two loads paths in the orbiter which is the structural tie between the task and booster for all lateral loads. The weight of the booster is reduced because of the reduced tank weight.

Alternate 3 has a heavier tank weight than alternate 1 because of the large semimonocoque structure between the tank and the booster. Similar weight reduction for the tank assembly also are available at increases in cost. There is no expendable booster interstage as the booster is attached directly to the aft end of the semimonocoque structure—(i.e., the interstage structure between the booster and the tank is carried with the tank and is utilized to attach the tank assembly to the orbiter). Both the orbiter and booster are reduced in weight because of the reduced tank weight.

The final determination of the tank option to be selected for preliminary design was based on program costs and technical reasons. Figure 4-272 lists the individual tank costs (for a ship set) and the total program costs for the major vehicles as deltas to the baseline. Figure 4-273 defines the reasons for the selected tank design.

Figure 4-272 indicates the alternate 2 tank option is the most expensive total program—which results primarily from the high individual tank cost (semimonocoque LH_2 tank construction) for 457 tanks. Alternate 1

$ MILLIONS

TANK CONFIGURATION		AVERAGE COST/ SHIP SET	TANK Δ	ORBITER Δ	BOOSTER Δ	BOOSTER INTERSTAGE Δ	TOTAL Δ
BASELINE	3032 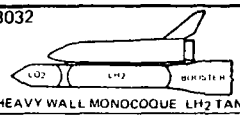 HEAVY WALL MONOCOQUE LH_2 TANK	1.40	0	0	0	0	0
ALTERNATE NO. 2	3033 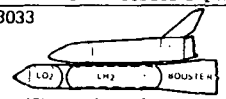 SEMI-MONOCOQUE LH_2 TANK	1.95	+277	-11	-71	0	+195
ALTERNATE NO. 1	3031 THIN WALL MONOCOQUE LH_2 TANK 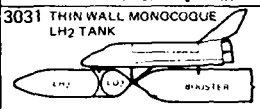	1.31	-48	+22	-82	-45	-153
ALTERNATE NO. 3	3034 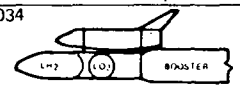 THIN WALL MONOCOQUE LH_2 TANK	1.57	+86	-14	-76	-53	-57
PEAK TIME PERIOD		COSTS SPREAD OVER OPERATIONS PERIOD		76 - 77	80 - 81		

Figure 4-272. Total Program Cost Comparison, Initial Selected Tank Configuration Options

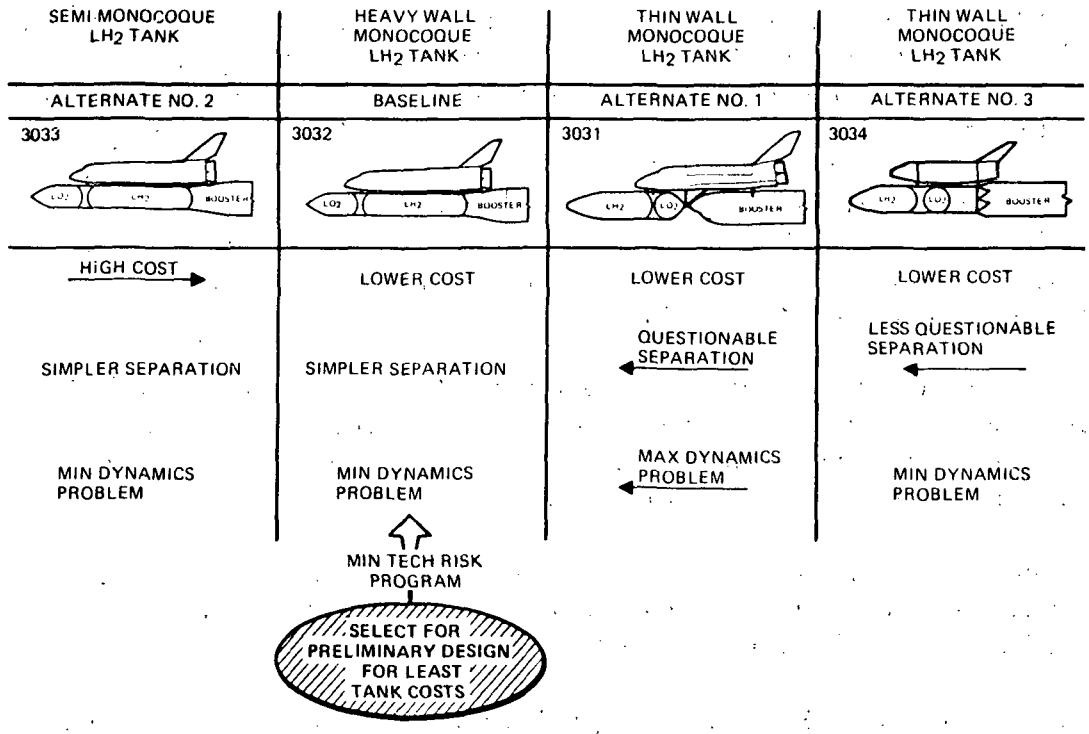

Figure 4-273. Tank Selection

has the lowest total program cost—which is a direct result of the low weight thin-wall monocoque tank construction yielding the lowest (per ship set) tank cost. The peak funding for the increased orbiter cost is during the early 1976-1977 period. Alternate 3 has a moderate total program cost reduction relative to the baseline tank with the cost reductions primarily available in the orbiter, booster, and booster interstage hardware.

The baseline option with the heavy wall monocoque LH_2 tank has been selected for continued study and preliminary design for the reasons depicted in Figure 4-273. The major reason for the tank selection is for a shuttle program with the least technical risk even if it is not projected as the least cost program.

Alternate 2 is the most expensive program—and was ruled out for that reason. Alternate 1 is the least cost program, but the questionable separation of the booster from the orbiter/tank assembly and the extreme dynamics problem between the tank, orbiter, and booster caused by the lateral loads ruled out this option.

The major structural dynamics decision in the selection of orbiter-EOHT-booster configuration arrangement involved vehicle bending mode considerations and separation dynamics. The baseline configuration (Figure 4-273) permits a relatively stiff booster to tank interface while alternate 1 is expected to be more flexible. Thus, for the latter arrangement to have a first vehicle bending frequency equal to that of the baseline vehicle would require an increase in orbiter body bending stiffness. Even if this were done, the first lateral bending mode of alternate 1 would probably still be lower than desired. It was concluded that the potential for adverse structural feedback and possible divergent oscillations was high for this concept and less risk was evident for the baseline configuration. Also, the separation of booster from the tank-orbiter combination is simplified for the baseline vehicle because of the lower probability of recontact with the orbiter aft fuselage.

Alternate 3 is a cost saving program (relative to baseline)—but the resulting orbiter main rocket engine high angle installation and large gimbal angle requirements are questionable and will be further studied in an attempt to minimize the booster separation problem.

The resultant choice for final selection for tank design, therefore, is the baseline concept which was continued for preliminary design and which will now be discussed in further detail.

Selected Tank Design. The preliminary design for the baseline concept was initially designed for the least initial cost shuttle program, which meant utilizing the present capabilities available from technology,

machinery, or facilities (Figure 4-274). Various tradeoffs and studies were investigated in an attempt to design the tanks for the least total program costs by extending some of the limiting capabilities, which usually meant an outlay of monies during the initial part of the program. In all cases, attempts were made to reduce the cost of the expendable tank and to reuse the expensive hardware by relocating this hardware, if possible, in the orbiter.

The preliminary design for the baseline tank utilized separate domes between the tanks, with all domes being fabricated by utilizing stretch-forming machinery. Stretch-forming machinery capable of handling stock 10 feet wide, 30 feet long, and approximately 0.3 inch thick is available at Boeing, McDonnell Douglas, and North American. As noted previously, fusion butt welding was selected for joining the tank skins.

Aluminum sheet or plate of large overall size is available in sufficient quantity from the ALCOA mill in Davenport, Iowa. The sheet stock (0.15 inch in thickness, minimum) is available in a maximum width of 154 inches and a maximum length of 68 feet. Plate stock (0.5 inch in thickness and up) is also available in lengths of 68 feet, but the width is wider—220 inches (Figure 4-275).

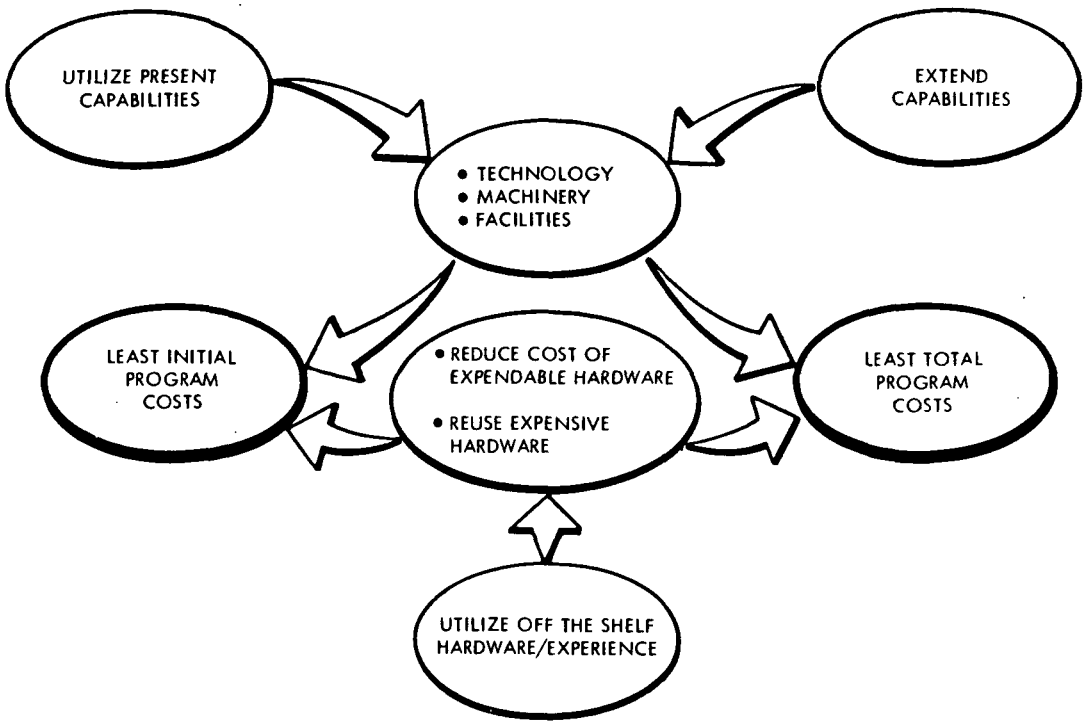

Figure 4-274. Design/Cost Approach

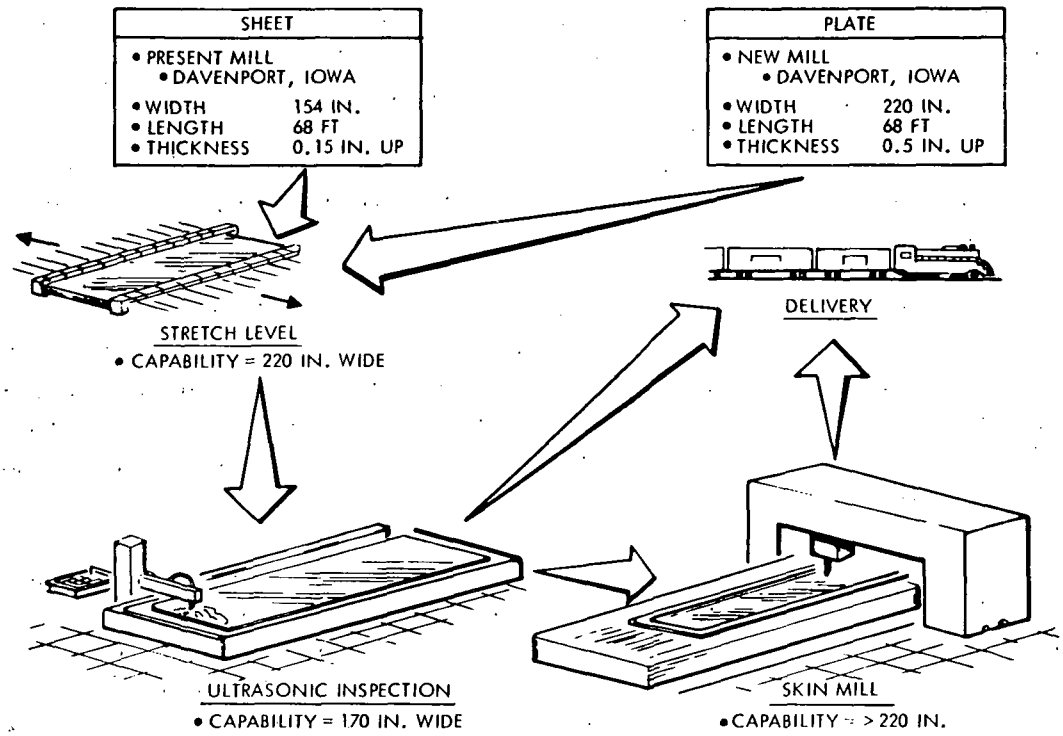

Figure 4-275. Aluminum Material Size Availability

The resultant usable stock width for design is less than the rolled width. The edge losses due to rolling, stretch leveling—and in the case of the wider plate stock—the ultrasonic inspection limitation is shown in Figure 4-276. It is advantageous to use the widest stock width available as it reduces the number of pieces (skins or gores) and the amount of welding required. Therefore, a trade study was conducted to have ALCOA machine-mill the wider plate stock as required or down to sheet stock thinner than 0.5 inch. The machine milling would incorporate any skin thickness reductions, and weld lands as required. The machine milling would also eliminate the requirement for chem-milling. The ALCOA skin mill is not tape-controlled and is basically only applicable for machine milling of simple monocoque skins—not complex semimonocoque skin-stringer panels, etc. It was resolved that it was advantageous (cost reduction) for ALCOA to machine-mill the skins as required and thus provide the widest possible stock.

The baseline tank was designed about the capabilities of the stretch-forming machine and the maximum size of premachined plate stock (Figure 4-277). The diameter was selected to provide a tank configuration containing the correct propellant volume, a reasonable L/O fineness ratio, and the correct structural load path and attachment to the orbiter. The diameter also was selected to allow the use of the fewest number of skins

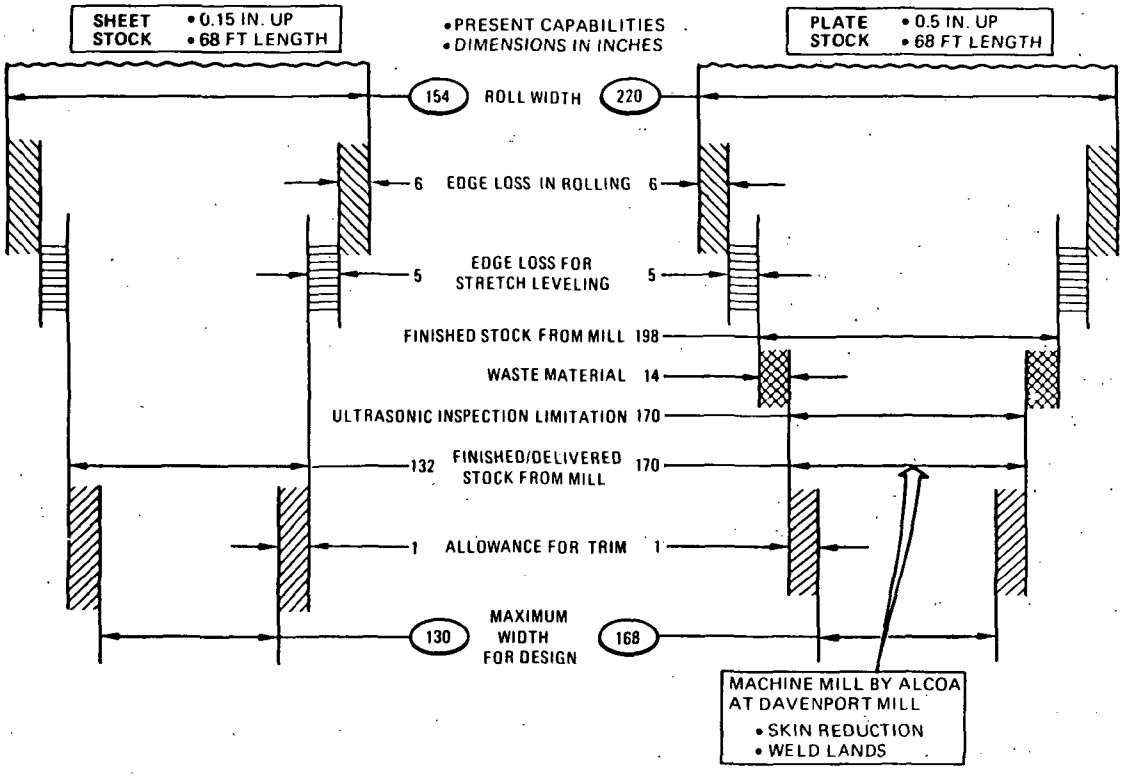

Figure 4-276. Aluminum Material Stock Size

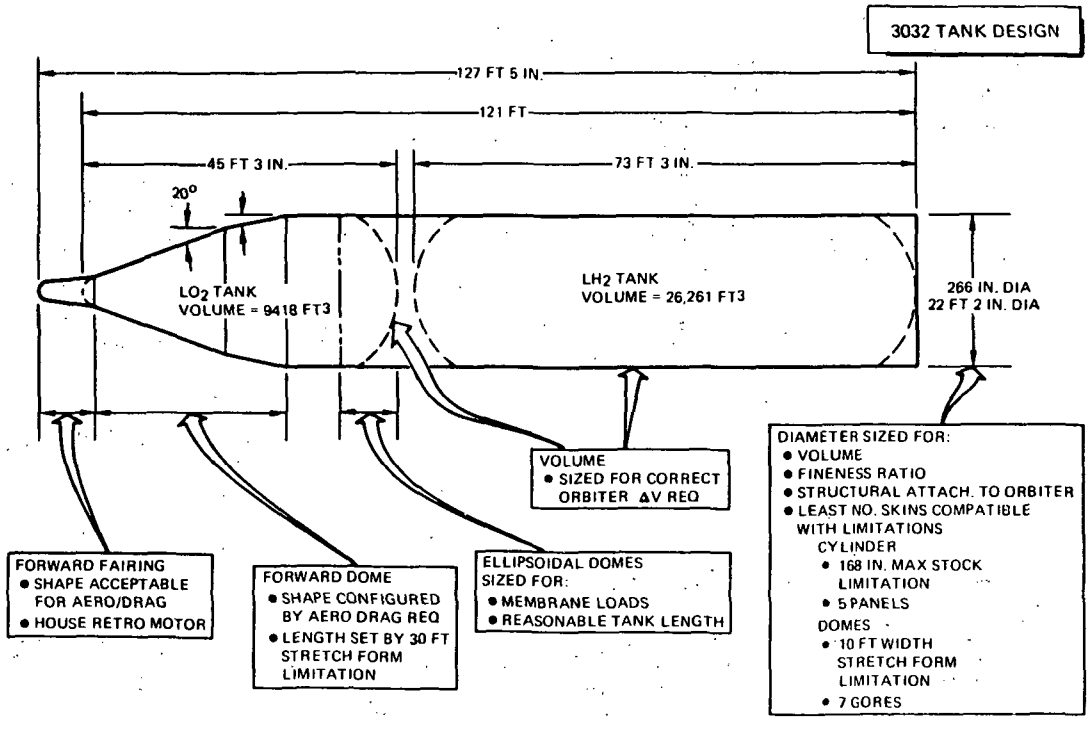

Figure 4-277. Baseline Tank Configuration for Detail Cost Studies

compatible with the 168 maximum stock limitation and the ten-foot width stretch form machine limitation. The forward end of the tank was shaped within the aero/drag requirements, but the length of the conical end was determined by the 30-foot stretch form machine limitation.

The baseline tank structure is shown in Figure 4-278. The tank assembly consists of the fusion butt welded LO_2 tank assembled from a conical forward dome made from seven preforward (stretched) gores, a short cylindrical shell (draped from two panels), and the aft elliptical dome (prewelded from seven stretched gores). The mid interstage between the tanks is semimonocoque construction (skin, stringers, frames) assembled from six premachined skin stringer panels riveted together with internal frames rivited to the inner caps of the stringers. The width of the semi-monocoque panels is limited to 12 feet, which is the maximum available capability of tape-controlled machine mills. A heavy reaction frame (forward tank attachment to the orbiter forward bulkhead) is also riveted to the mid interstage.

The LH_2 tank is assembled with the two end ellipsoidal domes (welded from seven prestretched gores) and two cylindrical shell sections, each cylindrical shell section consisting of five rolled panels. The aft reaction frame is located directly forward of the aft elliptical dome; another reaction frame is located between the shell sections to react the kick load of the

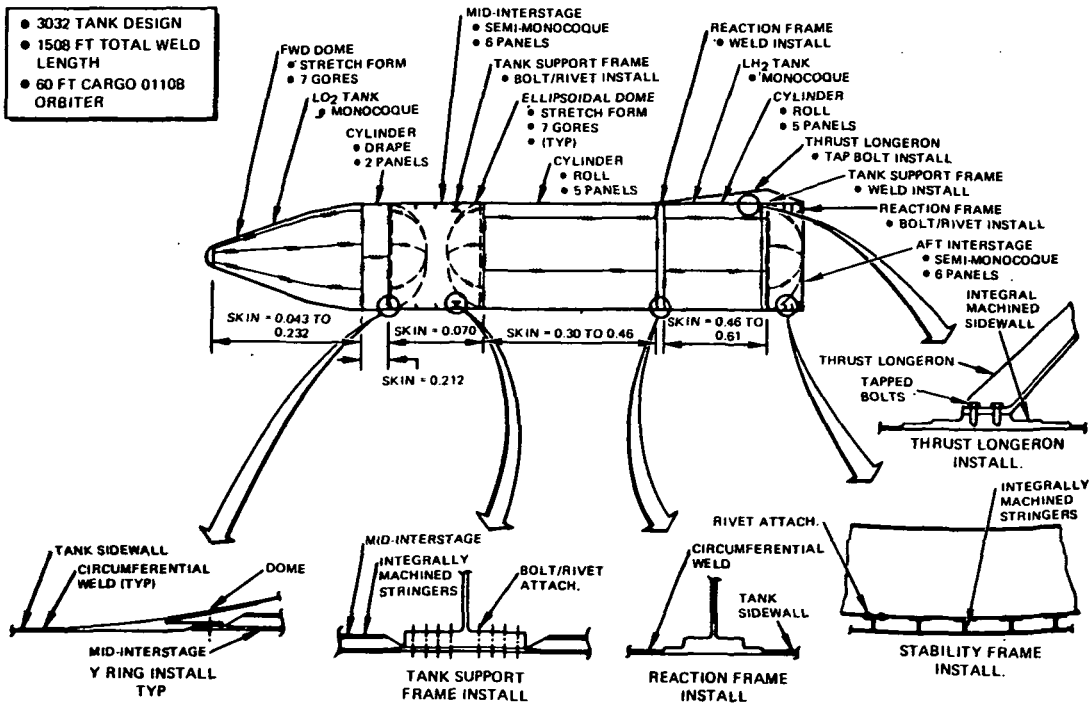

Figure 4-278. Baseline Tank Structure for Detail Cost Studies

single thrust longeron bolted to the upper surface of the tank. The two frames are welded to the tank assembly. The figure also shows the basic welded and rivet sections that comprise the tank assembly.

The thermal protection system (TPS) design for the baseline tank is composed of an exterior SOFI which covers the entire surface of the LH_2 tank. Cork is bonded to the LO2 tank over the entire conical area as well as in the local interference heating areas between the tank and orbiter (LO_2 tank and tank interstage).

The resulting systems installed on the tank assembly are few and have been simplified. Only the propellant system lines are utilized; the expensive vent components for the LO_2 and LH_2 tanks have been installed on the orbiter (Figure 4-279). There are disconnect interfaces between the tank lines and the orbiter lines. No PU system is utilized; only point sensors for propellant fill. A retro motor activated by a battery and a timing device is utilized. The roll motors have been deleted from the tank as orbiter separation from the tank is accomplished by translating the orbiter away from the tank, resulting in minimum disturbing impulses to the tank. The tank is attached to the orbiter at three points; the separation mechanism for tank disconnect is located in the orbiter for reuse for the next mission.

A weight breakdown for the baseline tank design used for detail cost analysis is given in Table 4-52.

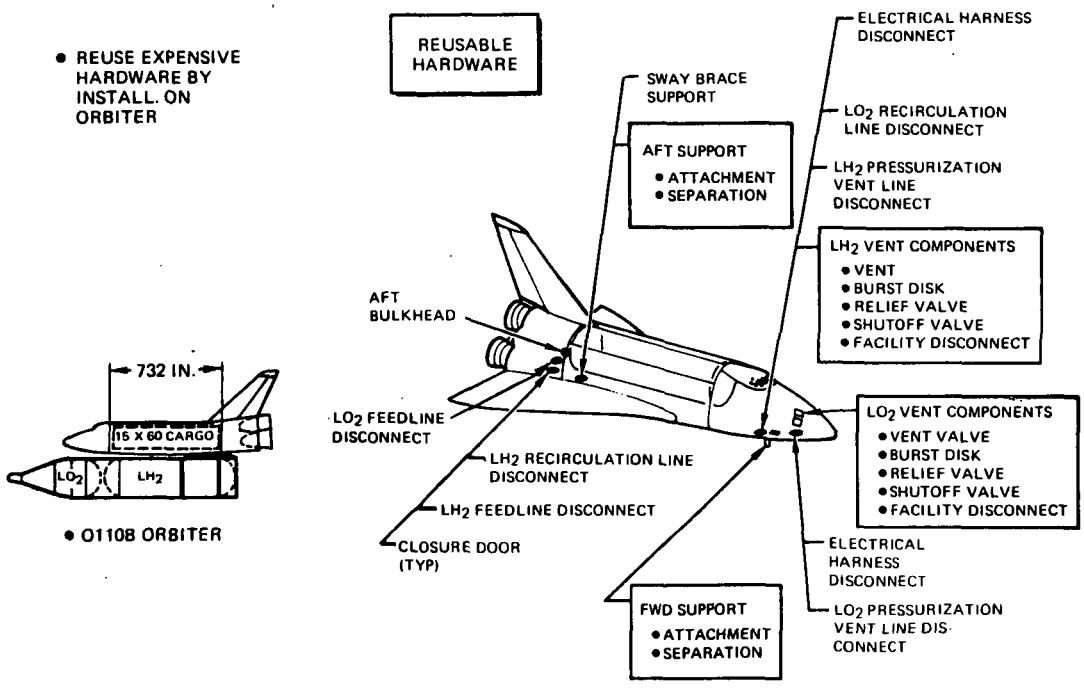

Figure 4-279. Baseline Tank Installation on Orbiter for Detail Cost Studies

Table 4-52. Weight Statement, 3032 Tank Design

System	Weight (lb)	
Structure		45,140
Forward fairing	195	
LO_2 tank	6,890	
Intertank structure	4,096	
LH_2 tank	29,625	
Aft skirt	2,534	
Tank supports	1,800	
Insulation		4,423
SOFI	1,108	
TPS	3,315	
Separation		140
Propellant		785
Deorbit		2,010
Growth (2%)		1,052
Dry weight		53,550

The preliminary design for the baseline tank continued with improvements to the design as available from various increased capabilities and improved design ideas. The improvements to the design were done to decrease the costs of the tank. The increased capabilities were obtained by utilizing explosive or bulge-forming of the dome end gores rather than stretch-forming. Explosive or bulge-forming is a present state-of-the-art forming technique but requires a new facility and new tooling. The size of sheets by explosive or bulge forming is only limited to stock size limitations. The costs for these items are nominal—the facility is a hole-in-the-ground—and the tooling is approximately $100,000. The original facility for the explosive/bulge forming of the S-II dome end gores has been filled in.

Another increased capability is the future increase in ultrasonic inspection capability to at least 220 inches that ALCOA will provide with its own funds. The increase in ultrasonic inspection capability increased the stock width availability to 195 inches.

Engineering and manufacturing design improvements also required that the available 195-inch width stock be limited to approximately 164 inches for design purposes to allow 12 to 16 inches per side of sheet for lead-in to the rollers—if the sheets are rolled to shape—and/or edge wrinkles caused by forming of the gore panels whether explosive/bulge or stretch-forming.

Final Tank Sizes. The previous discussion and tank design data were part of a major trade study to select the best tank design concept and define the tank design in sufficient depth for detail manufacturing and cost analyses. Based on the selected integrated vehicle requirements reported in Sections 4.4.1 and 4.4.2, the required tank sizes were established and are shown in Figures 4-280 and 4-281 for the shuttle vehicle with LO_2/RP booster and LO_2/propane booster, respectively. The detail tank design studies, although conducted on slightly different sizes, are applicable. The external tank systems assembly is shown in Figure 4-282.

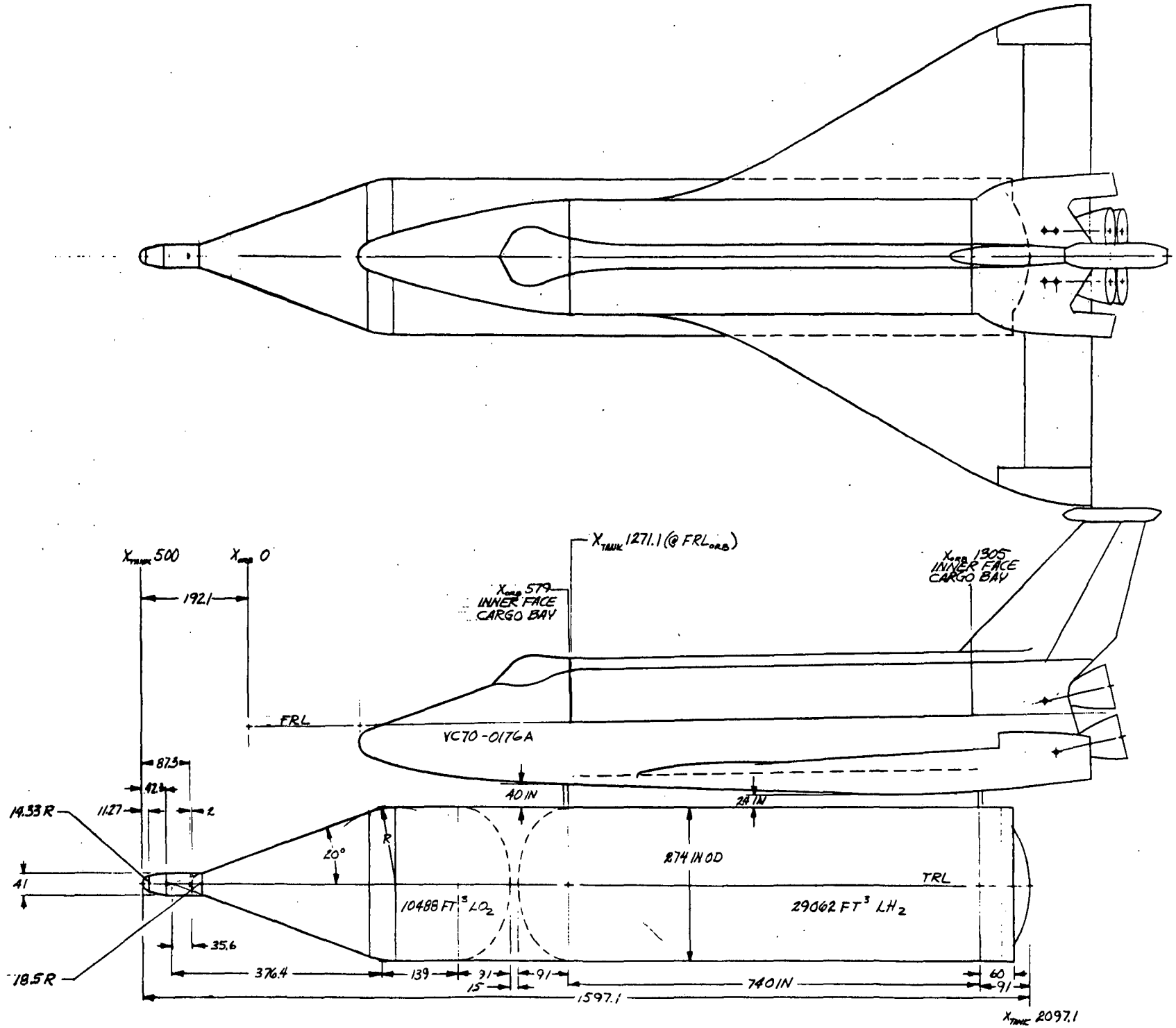

Figure 4-280. Orbiter General Arrangement, LO_2/RP Flyback Booster System

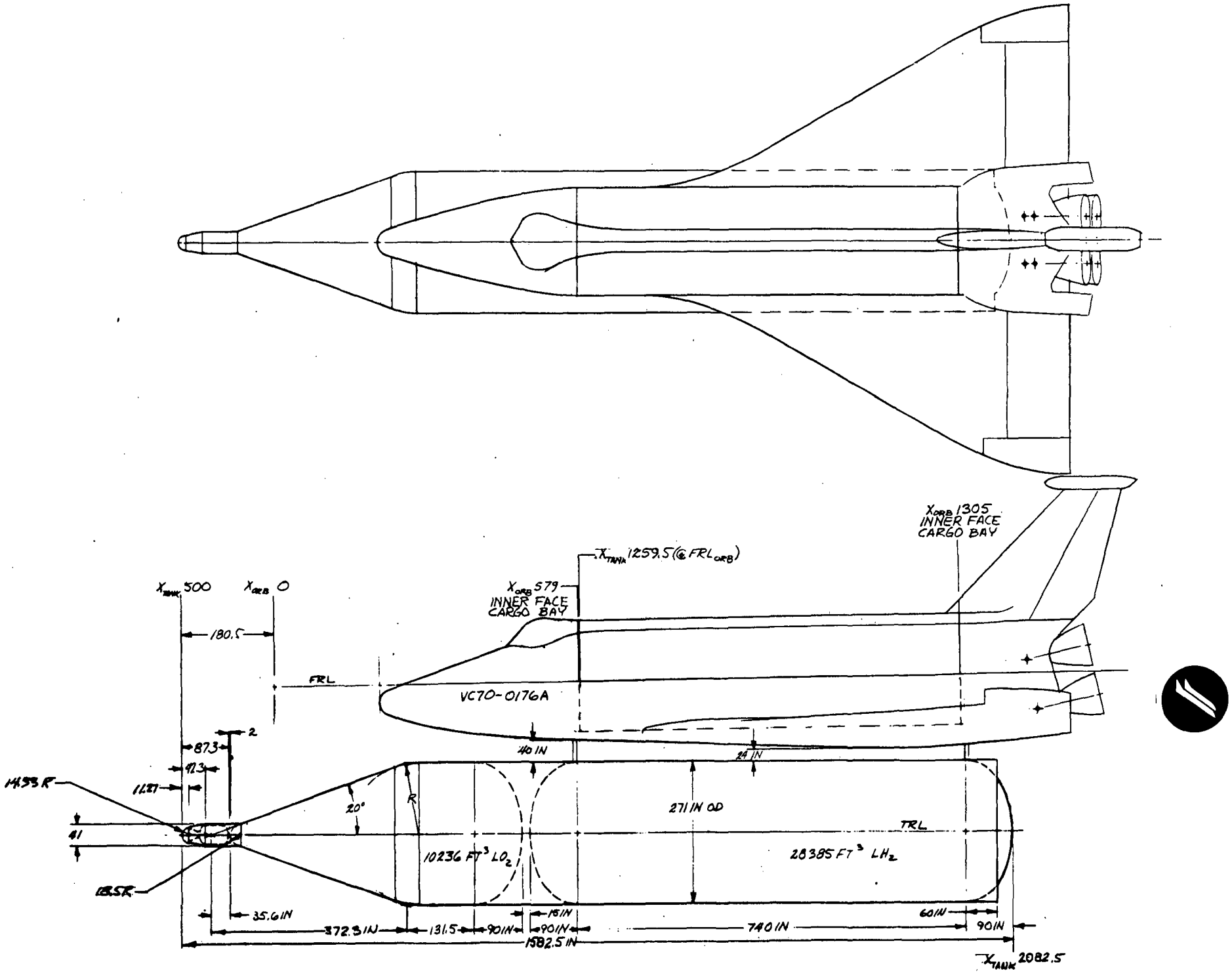

Figure 4-281. Orbiter General Arrangement, LO_2/Propane PFB Booster System

Page Intentionally Left Blank

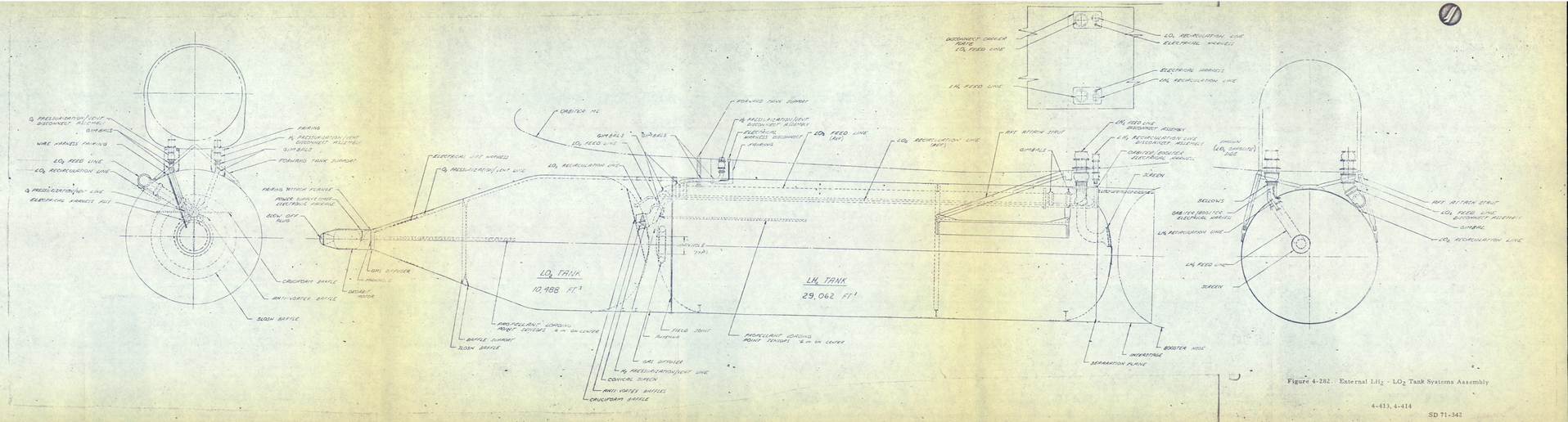

Figure 4-282. External LiH_2 - LO_2 Tank Systems Assembly

4.4.4.2 Tank Separation

Nominal Tank Separation. During the ascent coast, the external tank is separated from the orbiter and given a retro impulse so that the tank will enter and impact at the all-azimuth nodal point (-28.6° latitude) in the Indian Ocean. A study of the projected shipping densities in this area resulted in the following requirements for tank deorbit:

1. 300 fps retro velocity
2. Thrusting attitude in plane with 40° above velocity vector
3. Allowable attitude error during the retro burn = 30° about the desired thrusting attitude
4. No orientation or stabilization requirement during entry

These requirements account for additional uncertainties such as injection errors, timing errors, retro impulse errors, and aerodynamic variations due to a tumbling or nontumbling entry.

Four separation and deorbit concepts were identified; (1) eject the tank from the orbiter and fire the deorbit motor on a time delay signal; (2) release the tank and translate the orbiter (flyaway), and fire the deorbit motor on a time delay; (3) install an active attitude control system on the tank; and (4) install the tank on rails and thrust it off the orbiter. The first two concepts were proven feasible; therefore, an active control system concept was discarded. The rail concept in comparison imposes too high a weight penalty. It, too, was discarded.

The tank ejection concept is sensitive primarily to uncertainties in the delivered impulse of the ejection devices (best estimate is a ±10 percent uncertainty in each), the tank c.g. (estimated at 1 foot), and thrust vector misalignment of the deorbit motor (estimated as 1/4 degree). These sensitivities are displayed in Figure 4-283, which shows their effect on attitude rate at separation, and the attitude error as a function of the tank clearance distance from the orbiter. Since the latter is independent of separation velocity, a nominal value of 5 fps was selected. A clearance distance of 50 feet before deorbit motor ignition was selected to minimize plume impingement on the orbiter. For the estimated impulse and c.g. uncertainties, the attitude rate at separation is approximately 0.75 deg/sec. At a clearance distance of 50 feet, the attitude error is 7.5 degrees. The thrust vector misalignment will cause further attitude error during the retro burn, the magnitude of which is shown in Figure 4-283 as a function of the thrust level. To achieve an average error less than the allowable 30 degrees will require a thrust level of at least 33 Klb. The associated burn time is 17 seconds to achieve a 300 fps ΔV.

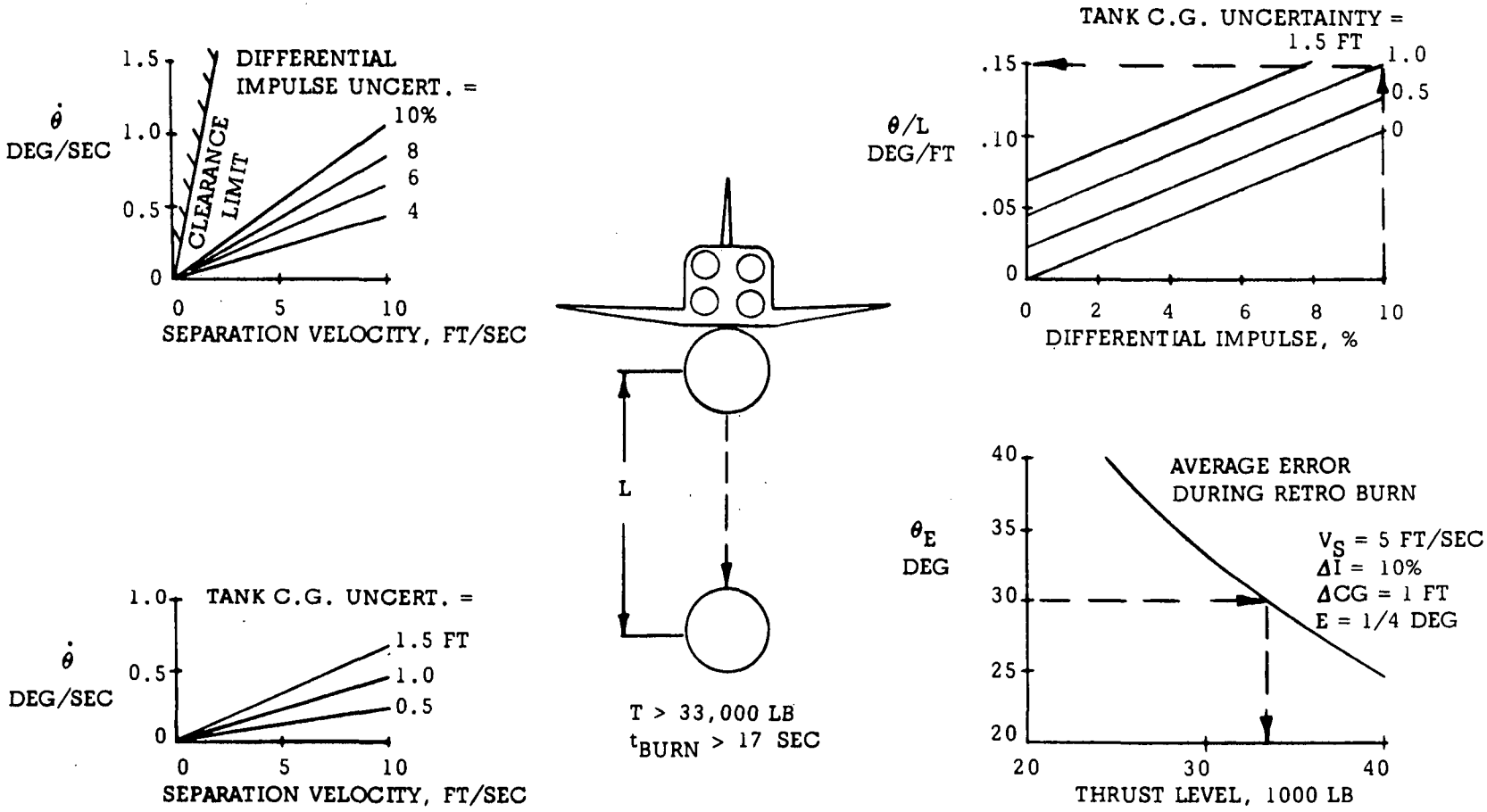

Figure 4-283. Tank Ejection and Deorbit Sensitivity Parameters

An alternative to this concept is to spin-stabilize the tank prior to deorbit motor ignition. For the current tank configuration and mass properties, however, it did not offer sufficient benefit to warrant the addition of a spin system.

The flyaway concept, shown in Figure 4-284, is less sensitive to uncertainties than the ejection concept. Attitude rate errors at separation are established by the capability of the orbiter flight control system. The only other significant error source is the thrust misalignment. Since the attitude rate errors are smaller than for ejection devices, a larger attitude error due to thrust misalignment is permissible. To maintain an average error no greater than 30 degrees dictates a retro thrust level of 23 Klb or greater. The corresponding burn time for 300 fps is 23 seconds. The flyaway concept, which does not require ejection devices and requires a smaller thrust deorbit motor, was selected as the baseline concept.

During ascent coast the mission sequence will first position the orbiter so that the retro thrust vector will be oriented to the 40-degree thrusting attitude. Tank release will be timed so the tank is targeted to the impact point. After release, the orbiter will translate away from the tank in the Z-axis direction. A nominal velocity of 3 fps has been selected. After a 17-second delay to achieve the 50-foot clearance, the deorbit motor is ignited.

The Z-axis translation at 3 fps requires an 8-second burn of the ACPS thrusters, expending 180 pounds of propellant. Further effort is planned to trade this weight penalty against a lower velocity, a longer coast delay time, and the resultant higher deorbit motor thrust level to maintain the allowable 30-degree attitude error.

Jettisoning of EOHT Tank After Abort. Following the powered-flight segment of a return-to-launch-site abort, the EOHT must be jettisoned before the orbiter can initiate unpowered gliding flight. A study of the dynamics of the orbiter and the EOHT during the time of separation showed the critical factor to be the angle of attack at the moment of jettison.

A three-degree-of-freedom, pitch-plane, two-body separation, digital computer program was used to evaluate the dynamic motion of the orbiter and the EOHT caused by a jettisoning of the EOHT at the flight conditions given in the following list:

Velocity (fps)	8, 586. 9
Altitude (ft)	184, 240
Flight path angle (deg)	-0. 588
Dynamic pressure (psf)	34. 94

The effect of the proximity of the orbiter and the EOHT to each other was included in the computation of the aerodynamic forces. Because of the static instability of the EOHT, successful separations were realized only when the angle of attack at jettison was on the order of a negative ten degrees. The pitch rates occurring at this angle are of opposite sign and of reasonable magnitude, which causes the orbiter and EOHT to separate smoothly as depicted in Figure 4-285. In the figure all motion is shown relative to the orbiter, whereas in actuality the orbiter is pitching up while the EOHT is pitching down. At the end of three seconds the closest point on the EOHT is 17.5 feet below the orbiter belly and the EOHT pitch attitude is 19.4 degrees less than the orbiter. The flight conditions existing after three seconds of separation time are given in the following list:

	EOHT	Orbiter
Velocity (fps)	9,050	8,472
Flight path angle (deg)	-1.40	-1.25
Angle of attack (deg)	-20.9	-1.6
Pitch attitude (deg)	-22.3	-2.9
Pitch rate (deg/sec)	-6.5	3.4
Pitch acceleration (deg/sec^2)	3.0	-1.0
Pitch attitude change (deg)	-11.7	7.7

4.4.4.3 Entry Trajectories and Impact Dispersions

Acceptable disposal of the expended external orbiter propellant tank requires consideration of impact areas, impact dispersions, and deorbit systems and procedures. Of the several possible disposal modes, three were selected for serious evaluation:

1. Jettison before insertion
2. Retro after insertion to provide impact at the all azimuth nodal point (-28.6 latitude for KSC launches)
3. Jettison after orbiter deorbit.

Mode 2 was selected primarily because it provides for a single, secluded (sparse shipping) impact area for all launch azimuths and mission variations, including once-around aborts.

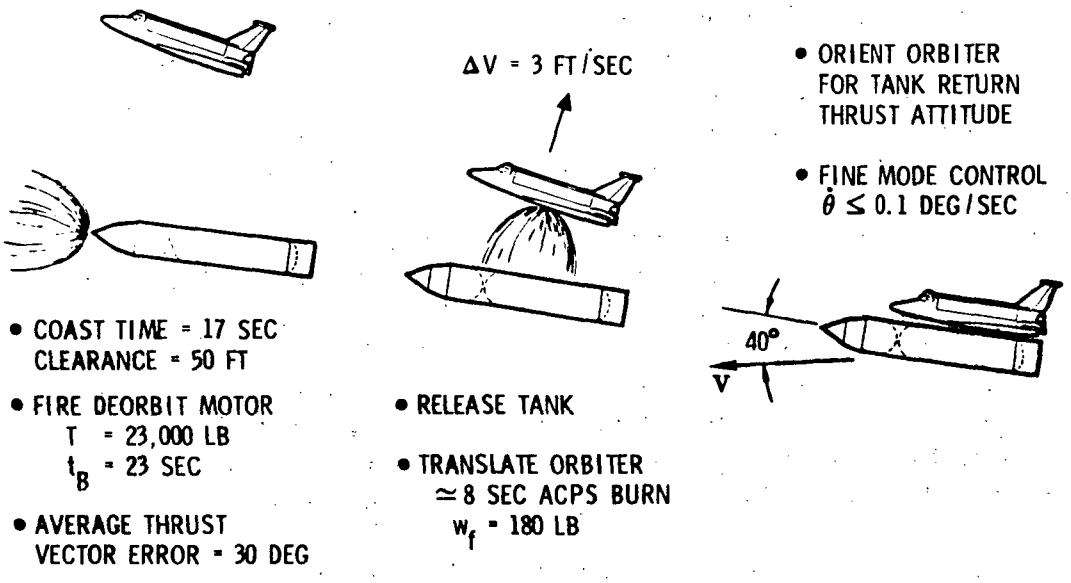

Figure 4-284. Flyaway Separation Concept

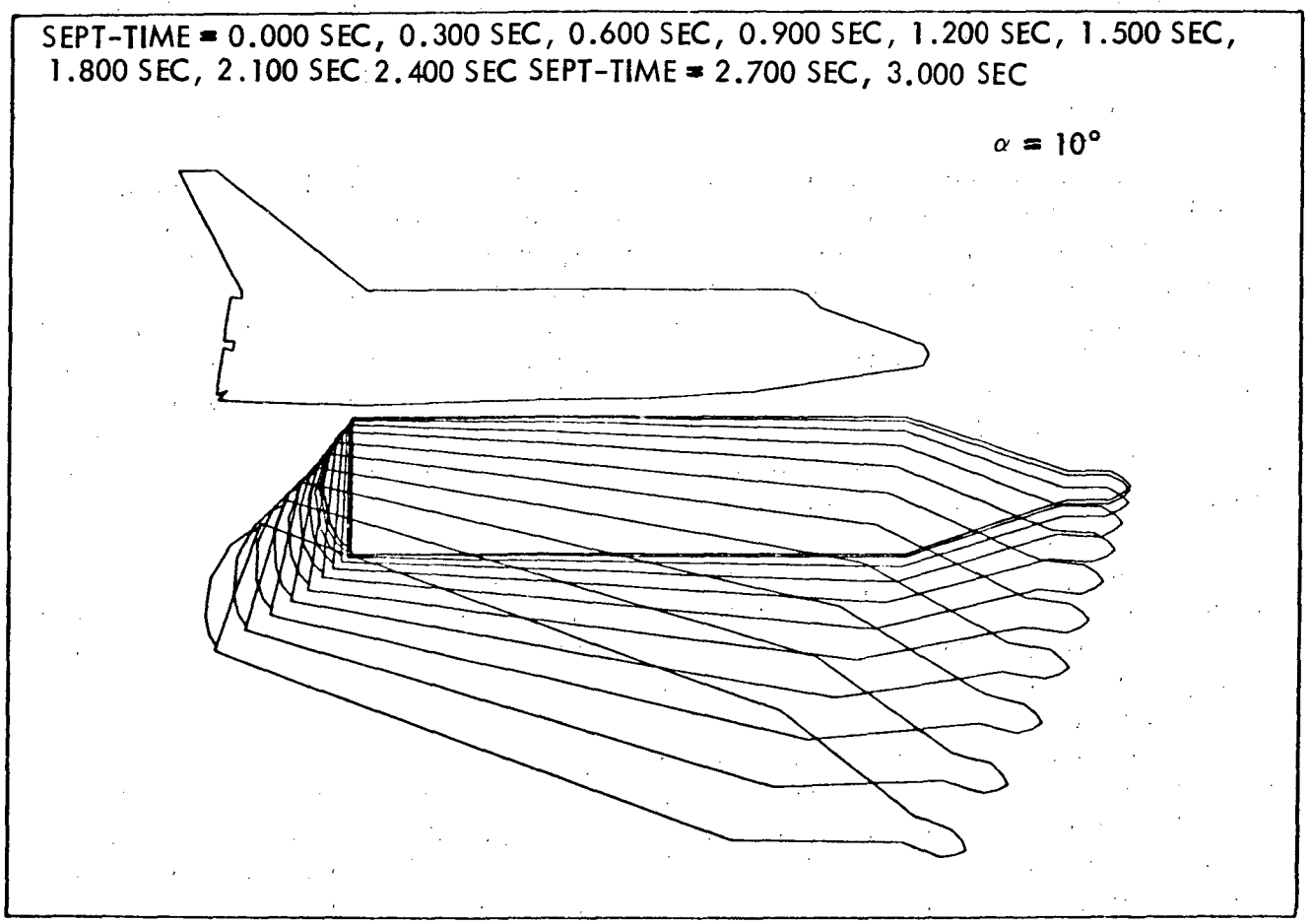

Figure 4-285. Pictorial Presentation of the Jettisoning of the EOHT Subsequent to an Abort

This disposal mode requires a tank retro impulse. The selection of the retro ΔV is indicated in Figure 4-286. As shown, the impact dispersions decrease and the time from insertion increases with increasing ΔV. The 300 fps value was selected to limit dispersions and to provide a reasonable time between insertion and tank separation for systems checkout.

Figure 4-287 shows the effect of deorbit thrust attitude on tank impact range and also indicates the impact dispersions due to attitude errors. Minimum range from deorbit to impact is provided at a thrust attitude of approximately 40 degrees. For a 3-phase attitude dispersion of ±30 degrees, the total impact dispersion is only 490 nm. This compares favorably with the 1170 nm. total dispersion resulting from a 3 phase error of ±20 degrees about a nominal of zero degrees. (A tank spin system would probably be required to restrict the 3-phase dispersions to ±20 degrees.)

Impact dispersion also will be caused by aerodynamic variations and, in the event of tank breakup, by the W/C_DA differences of the fragments. Figure 4-288 presents the results of the impact dispersion analyses. Figure 4-289 presents nominal tank entry profiles for a normal mission and for a once-around abort.

4.4.4.4 Loads

Structural loads were computed for selected prelaunch and ascent flight conditions. The prelaunch loads were based on the following wind criteria at KSC: 99 percentile wind speed, one-day exposure period for the fueled and unpressurized condition, and 99-percentile wind speed, two-week exposure period for the unfueled and unpressurized condition. The effects of gust and vortex-shedding were estimated and included in the analysis. Loads for the maximum $q\alpha$ boost condition were based on the design criteria described in paragraph 4.4.3.5. Loads were also computed for the maximum acceleration condition at booster end burn, and for the orbiter start burn, maximum thrust, and end burn conditions.

Tank Dynamic Considerations. The major structural dynamics decision in the selection of orbiter-EOHT booster configuration arrangement involved vehicle bending mode considerations and separation dynamics. The baseline configuration (Figure 4-273) permits a relatively stiff booster to tank interface while alternate 1 is expected to be more flexible. Thus, for the latter arrangement to have a first vehicle bending frequency equal to that of the baseline vehicle would require an increase in orbiter body bending stiffness. Even if this were done, the first lateral bending mode of alternate 1 would probably still be lower than desired. It was concluded that the potential for adverse structural feedback and possible divergent oscillations was high for this concept and less risk was evident for the baseline configuration.

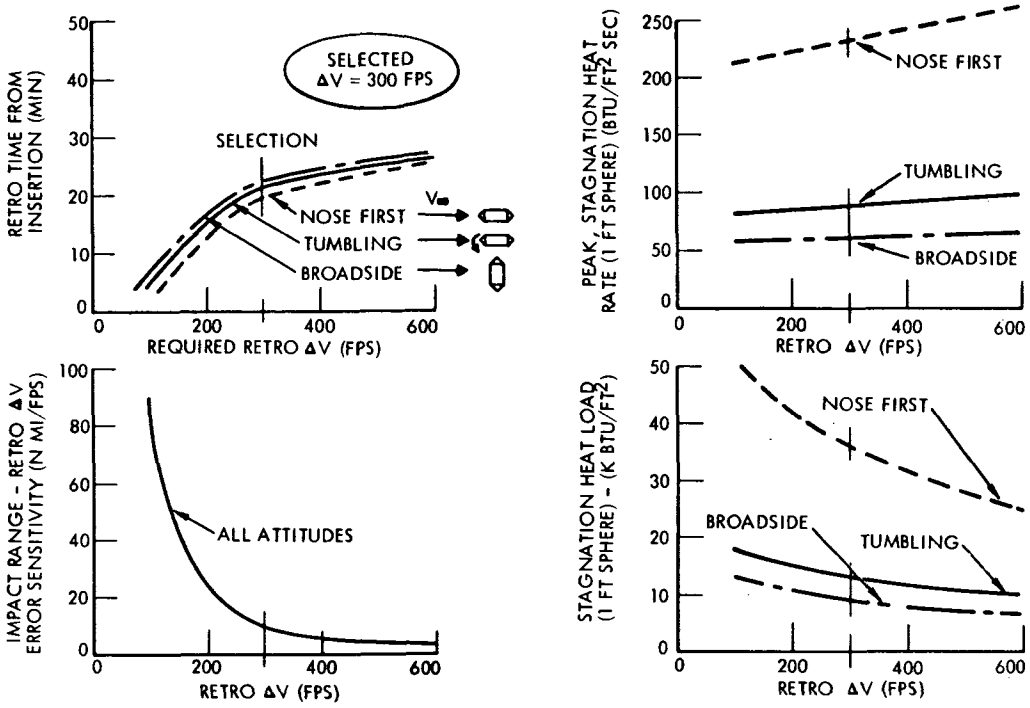

Figure 4-286. Tank Retro ΔV Selection

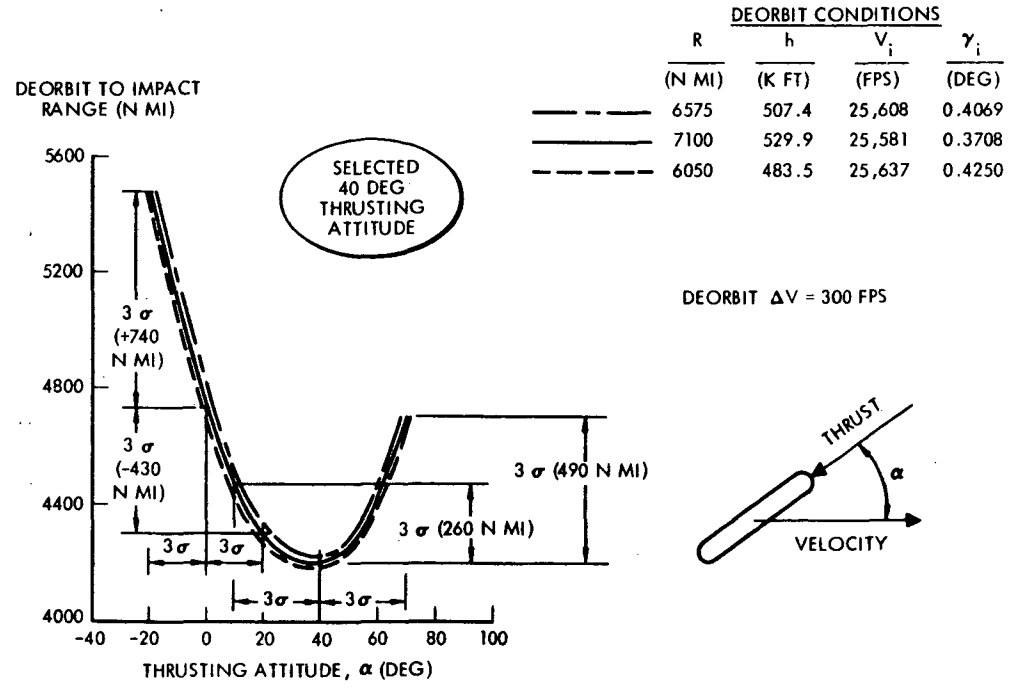

Figure 4-287. Effect of Thrust Attitude on Tank Impact Range

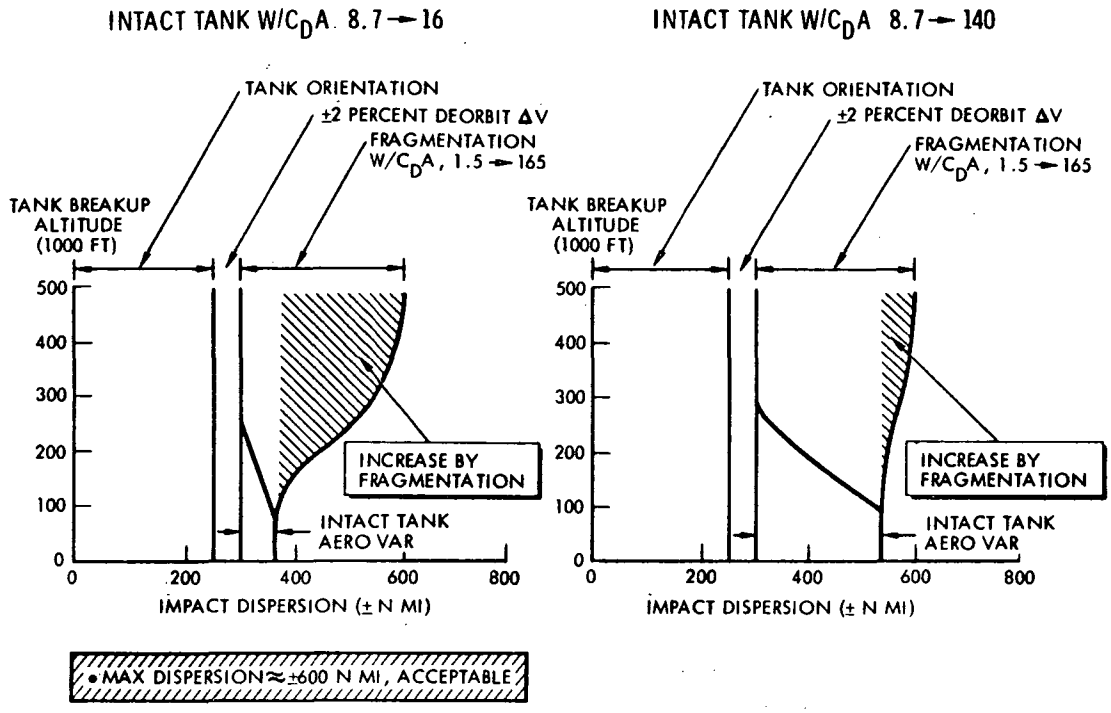

Figure 4-288. Tank Impact Dispersion

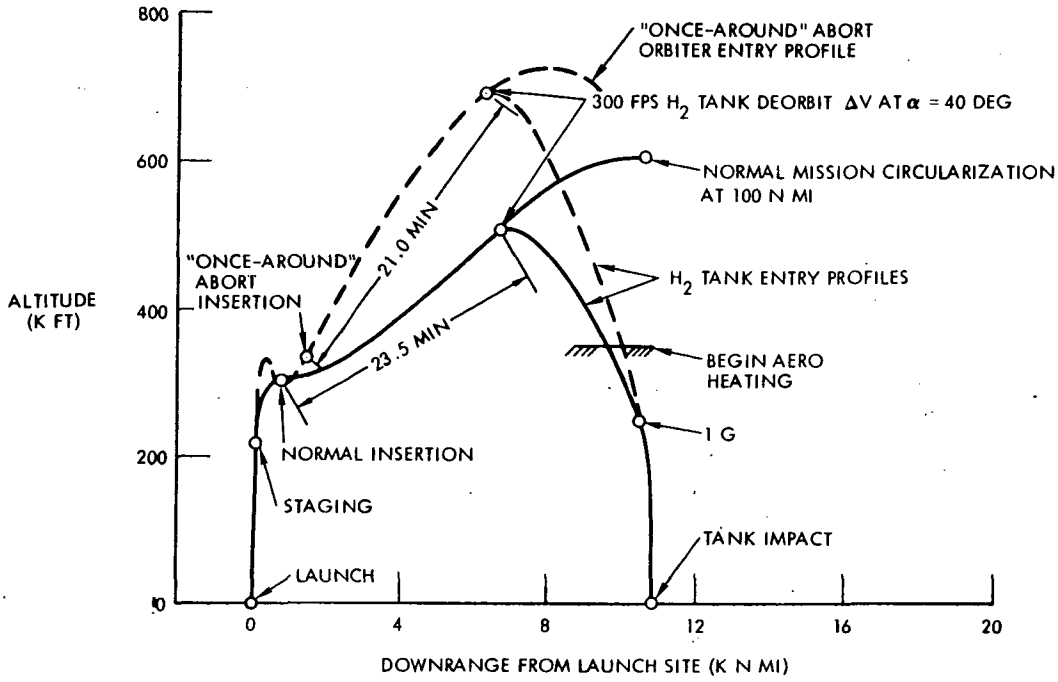

Figure 4-289. Tank Entry Profiles

Miscellaneous Structural Dynamics. Detailed structural dynamic studies have not been conducted at this point in the study. However a comparison of the fully reusable shuttle configuration with the current concept shows only a few instances where dynamics considerations will be different. The external tank approach requires two separations (e.g., booster from orbiter/tank and tank from orbiter) instead of one, but the fully reusable booster-orbiter single separation appears much more complex from a dynamics standpoint. Acoustic excitation and the resulting vibration response will be approximately the same for either shuttle concept. The current configuration will experience slightly less aerodynamic interference effects around the orbiter nose because of the cleaner profile of the tank-orbiter configuration. The external tank nose projects forward enough to place the orbiter nose behind the bow shock in the high dynamic pressure flight regime. However, current trajectories achieve slightly higher max q than that for the fully reusable shuttle concept; consequently, the overall vibration response will be about the same.

No new problems are seen in the areas of flutter/aeroelasticity and pogo. A nonlifting booster (i.e., P.F.B) obviously eliminates any wing flutter problems associated with the booster alone or with the mated configurations. In the case of pogo, the orbiter analysis will be more complex because of the coupled modes of the tank and orbiter. However, this does not necessarily mean that the potential for pogo occurrence is any greater than it was in the earlier shuttle configurations. The probable use of existing engines (F-1 and J-2 or J2S) for Mark I should result in good engine analytical data being available earlier than it would be if a new high-pressure engine is selected.

4.4.4.5 Thermal Environment

Aerodynamic Heating. Heat transfer rates and integrated heat loads were evaluated on the LO_2-RP and the PFB systems for both Mark I and Mark II ascent flight modes. Tank-orbiter interference flow effects were incorporated into the heat transfer rates as flow field dependent corrections to the undisturbed (tank alone) heat transfer rates.

Undisturbed Heating. Figures 4-290 and 4-291 present the maximum heat transfer rate and integrated heat load distributions for the Mark I launch trajectories for the LO_2-RP and the pressure feed booster systems, respectively. Corresponding data are presented in Figures 4-292 and 4-293 for the Mark II launch trajectories.

Interference Heating. Interference heating factors for selected locations on the tank are presented in Figure 4-294 as a function of time. The interference heating factors are similar to those experienced by the orbiter during ascent.

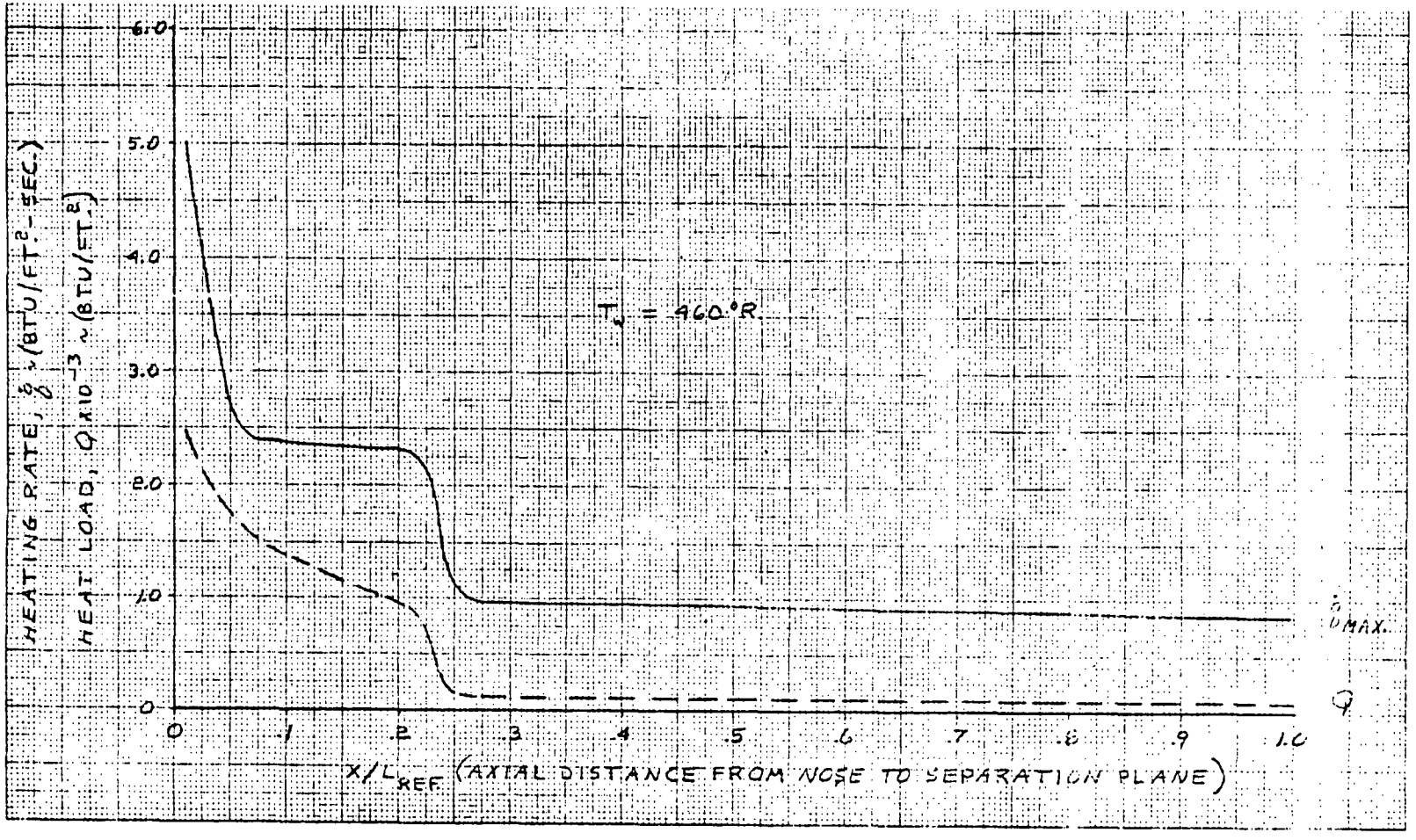

Figure 4-290. Maximum Heating Rate and Heat Load Distribution on External LH_2/LO_2 Tank, Undisturbed Flow (LO_2/RP Flyback System, Mark I)

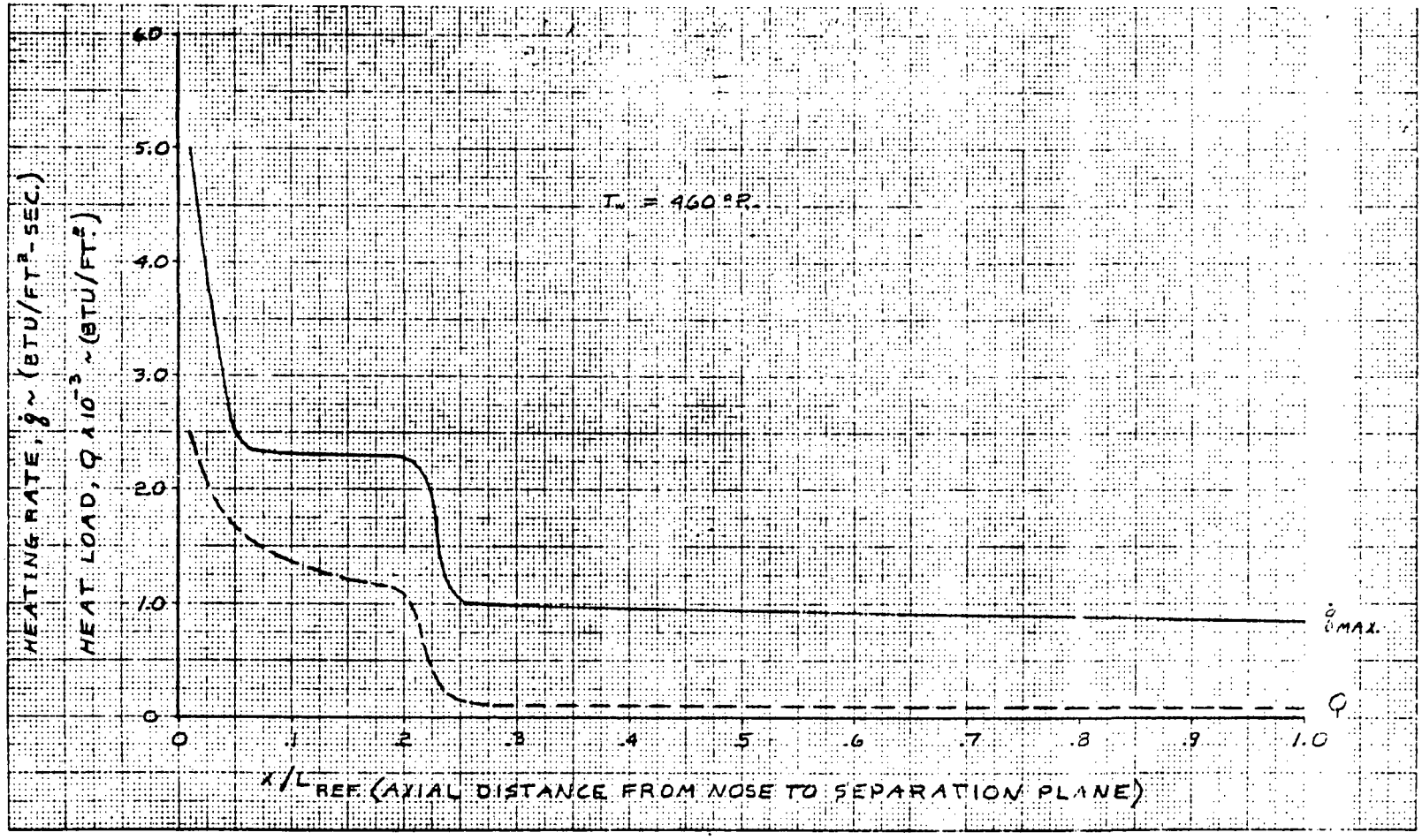

Figure 4-291. Maximum Heating Rate and Heat Load Distribution on External LH_2/LO_2 Tank, Undisturbed Flow (Pressure-Fed System, Mark I)

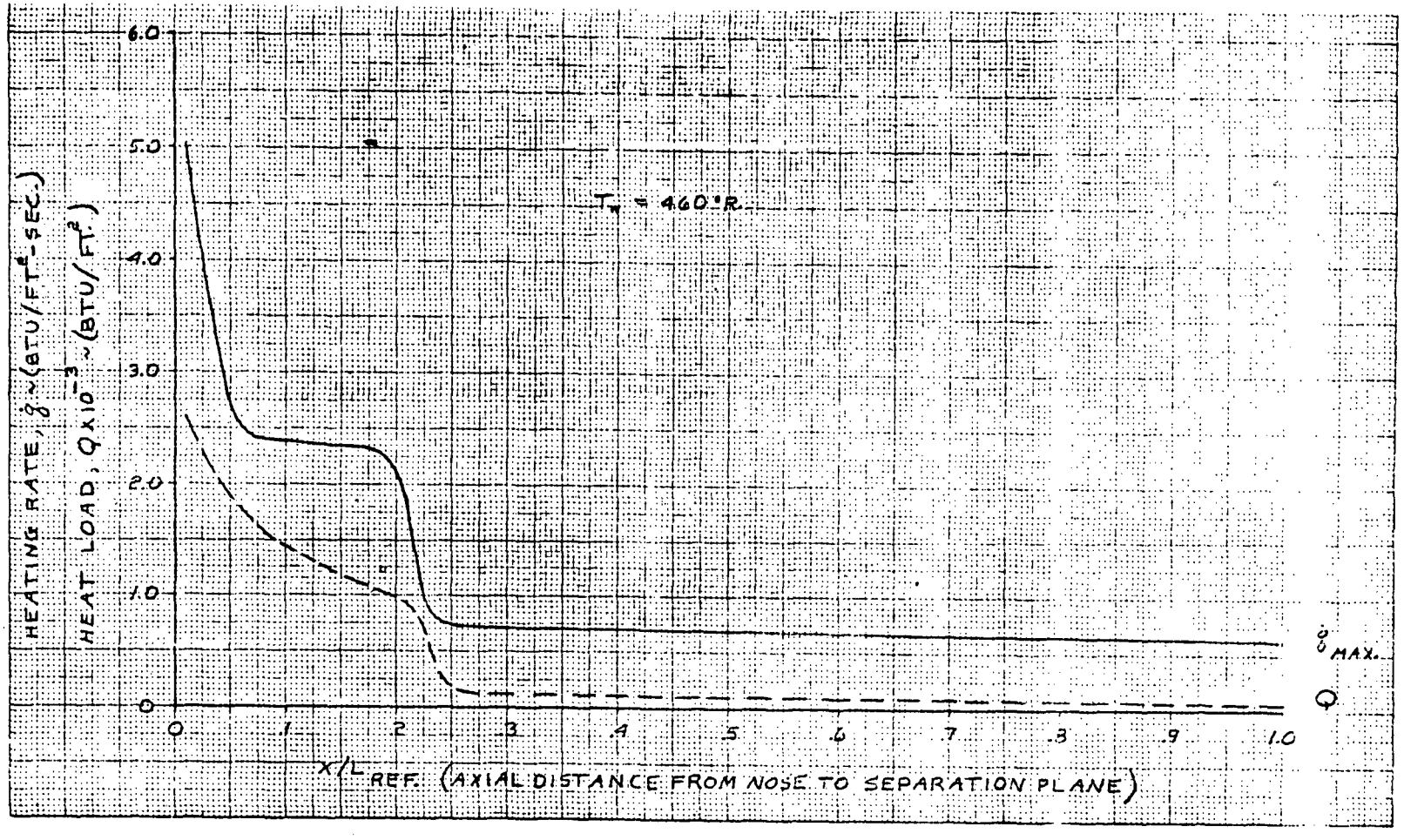

Figure 4-292. Maximum Heating Rate and Heat Load Distribution on External LH_2/LO_2 Tank, Undisturbed Flow (LO_2/RP Flyback System, Mark II)

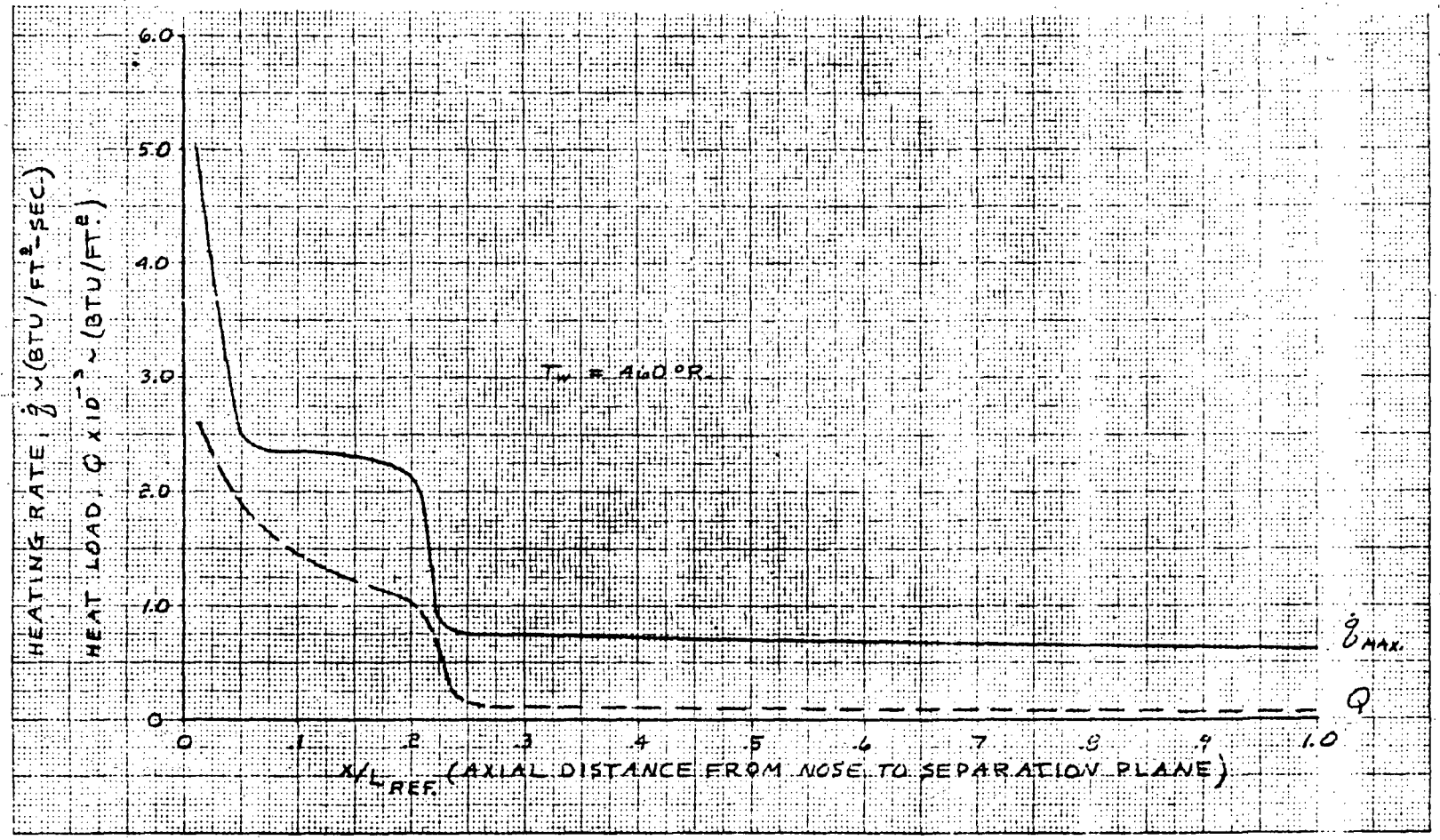

Figure 4-293. Maximum Heating Rate and Heat Load Distribution on External LH_2/LO_2 Tank, Undisturbed Flow (Pressure-Fed System, Mark II)

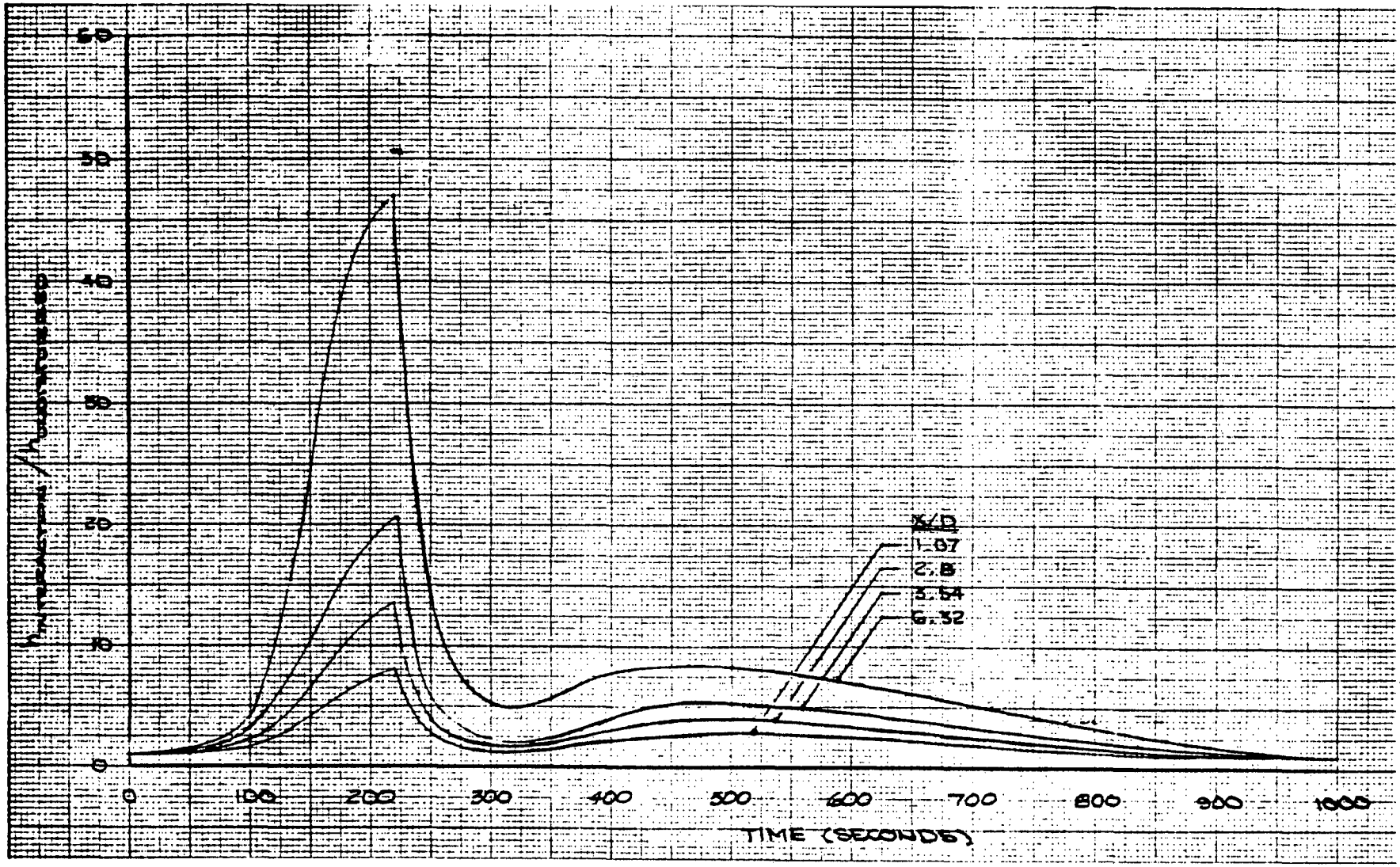

Figure 4-294. Interference Heating Factor on Tank During Ascent

TPS Thermal Design. TPS requirements were determined for the single belly tank configuration with either the LO_2 or LH_2 tank forward. The TPS concept employed SOFI on the LH_2 tank, cork ablator on the conical portion of the LO_2 tank, and on uncooled interference heating regions and Avcoat 5026-39 on the nose cap where heating rates exceeded 10 Btu/ft^2 sec. Study results for the LO_2 forward configuration (baseline) are shown in Figure 4-295. The TPS thicknesses, materials, and areas to be protected are (1) 0.75-inch SOFI on the LH_2 tank, (2) 0.4-inch (average) cork ablator on the LO_2 tank conic section, (3) 0.55-inch (average) cork ablator on the intertank fairing in the orbiter/tank interference heating region, and (4) 0.55-inch Avcoat 5026-39 on the tank nose cap. Areas requiring ablator on and adjacent to protuberances were identified but thicknesses or materials have not been defined.

4.4.4.6 EOHT Structural Analysis

The primary structural characteristics of the EOHT structures described in Figure 4-296 pertain to the configuration shown on Drawing VC70-3048. The structure is designed to sustain the total spectrum of applied limit loads and peak combined hydrostatic and ullage pressures (the most significant are shown) for an ultimate safety factor of 1.4 and to the appropriate structural temperatures/material allowables listed in NR's SD Material Properties Manual (Vol. I, October 1969). The most critical condition of either Mark I or Mark II orbiters was used to effect one design that is structurally suitable for both orbiter generations. Tank proof-test requirements are accounted for in the LO_2 and LH_2 tank designs as shown in Figure 4-296. The LO_2 tank is designed by the hydrostatic proof test shown, with the proof pressure at "A" equal to 1.05 x p_A (max g) x the ratio of the material tensile yield strength at room temperature to that at max g. The intertank, aft skirt, and interstage unpressurized structures designed by the high q and max g loads are of integrally machined skin-stringer frame construction and were selected over riveted hat section stringers from a cost savings viewpoint. The LH_2 tank pressure/construction/weight tradeoffs conducted also are shown in the figure.

The baseline LH_2 tank cylinder wall monocoque design (the gauges are presented in the upper left hand corner of Figure 4-296) is based on the basic pressure stabilization provided by the Mark II space shuttle main engines (SSME) minimum regulator pressures. For the baseline design, prelaunch/max g and high q loadings are critical at respectively the forward and aft end of the tank. The potential LH_2 tank weight reduction due to increased flight pressures and the associated required on-pad pressure during prelaunch (LO_2 can be fueled prior to LH_2 tank pressurization) is shown for monocoque and longeron stiffened designs. The additional bulkhead and pressurant weights are included in the weights shown (the kick frames and A frame attach longeron are not included). Of primary significance is the requirement of on-pad pressure during prelaunch to effect a significant weight savings over the baseline design. In view of this, the baseline design to the basic SSME required pressure schedule was selected.

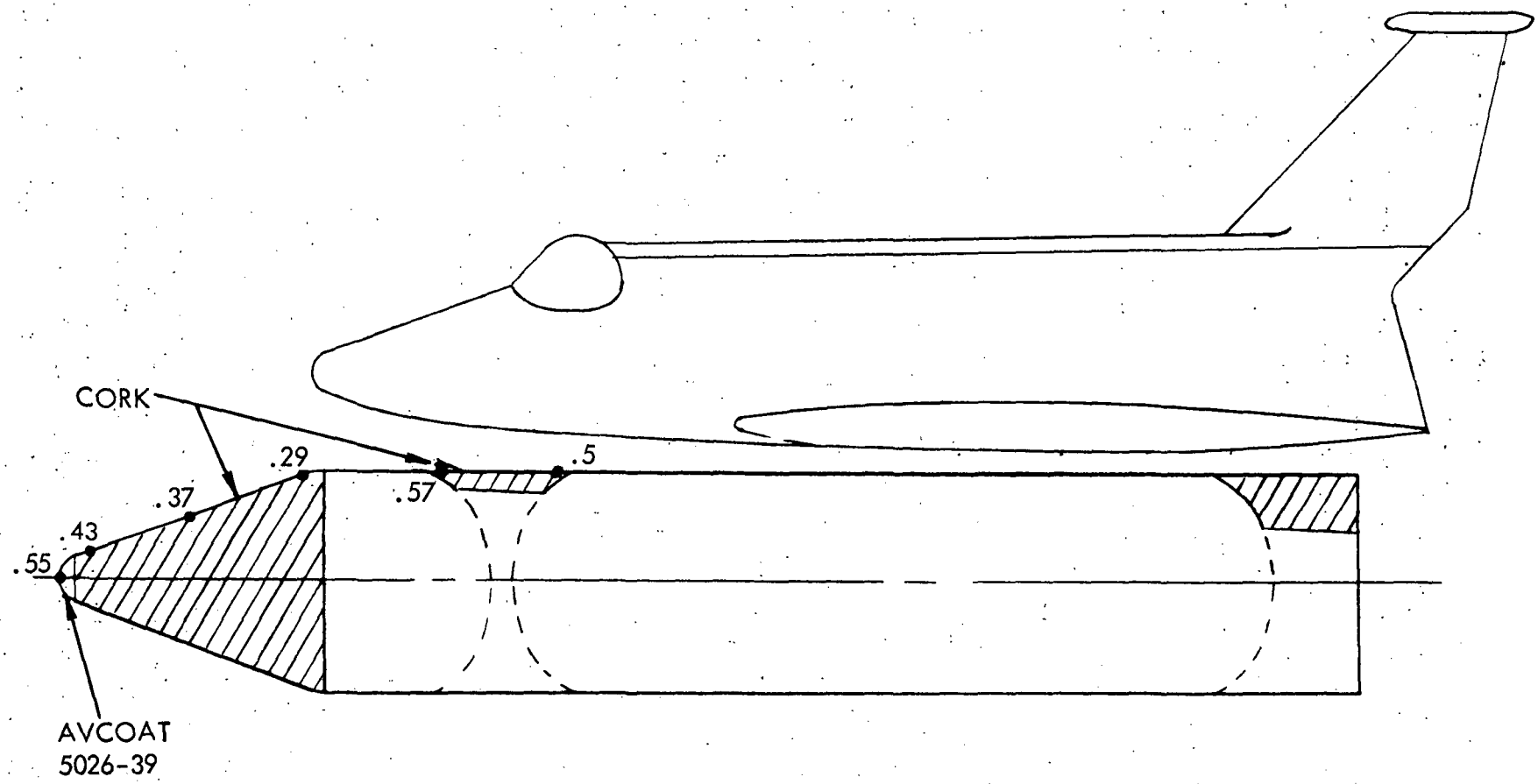

Figure 4-295. EOHT TPS Requirements

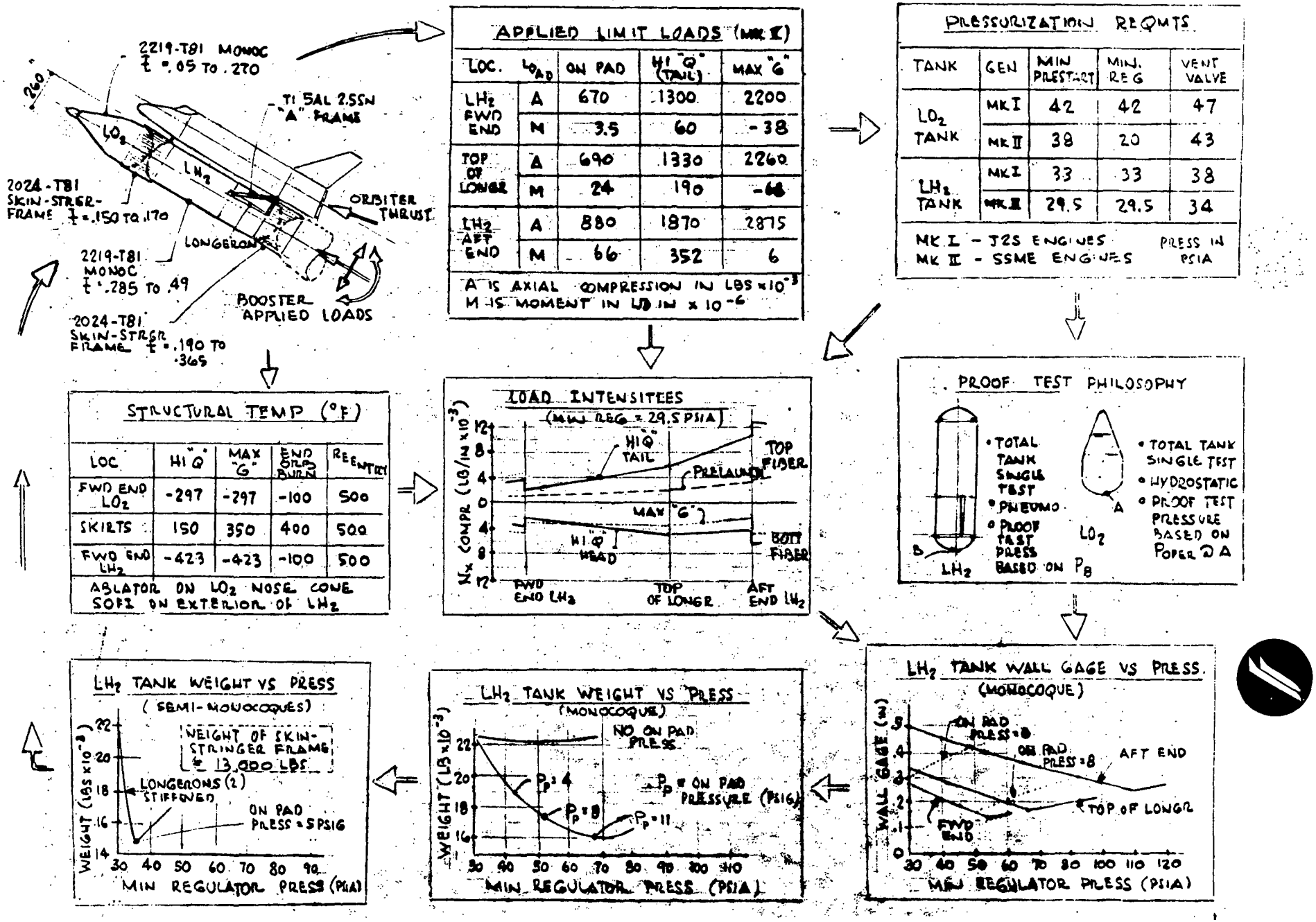

Figure 4-296. Primary EOHT Structural Characteristics

4.4.4.7 Propulsion and Fluid Systems

Main Propulsion System (External Propellant Tankage Requirements). Refer to Figure 4-227 (Paragraph 4.4.3.8) for external tanks and system. The external propellant tank module, consisting of a forward LO_2 and aft LH_2 tank, will supply the required propellants for main engine operation (ascent burn). The tanks also will contain additional volumetric capacity for minimum engine performance, flight performance reserve propellant, propellant for pressurization, residual propellants, and ullage space. Tables 4-53 and 4-54 represent a propellant inventory for the baseline Mark I and Mark II orbiters, respectively. Note the same tank is used for both Mark I and Mark II. The Mark I LO_2 tank is off-loaded so that the tanked mixture ratio is 5.5:1 for the J-2S engines.

The external tank module is capable of separation from the orbiter, after orbit injection or abort, with fluid line isolation provided at the tank/orbiter interface. The fluid lines will be disengaged prior to separation of the tank module from the orbiter.

External Tank System Description and Operation. The propellant loading control signals to the ground facility system will be provided by the point sensors. A backup monitoring gauging system (ΔP transducer) will be provided in the orbiter.

Propellant utilization will be achieved by an open-loop system. Propellants will be tanked to the preflight predicted performance of the J-2S engines. Nominal engine mixture ratio is 5.5 (LO_2/LH_2); however, the engine mixture ratio control band is 4.5 to 6.0. The engine flight mixture ratio will be programmed in compliance with mission requirements. A LH_2 propellant loading bias will be provided to minimize average total residual propellants and LO_2 depletion prior to LH_2 depletion.

Engine cutoff will normally occur on a velocity signal from the guidance and control system when orbit injection velocity is reached. In the cases where all usable propellant (either LO_2 or LH_2) is depleted before a vehicle velocity cutoff is achieved, the engines will be shut down by the engine cutoff system (ECO). The ECO consists of a cluster of 5-point sensors near the LH_2 tank outlet plus a cluster of 5 point sensors in the LO_2 manifold (inside the orbiter).

Dumping of residual propellants and depressurization of the tanks to 5 psia before tank jettison in orbit is accomplished through the engine and the drain line which exits at the aft end of the orbiter. At the completion of tank depressurization, the tank/orbiter fluid disconnects are separated, followed by tank jettison.

Table 4-53. Mark I Propellant Inventory

(4 - 265K J-2S - Orbiter)
(5 - F-1 Engines - Booster)

	Fuel	Oxidizer
Impulse (nominal)	119,476	657,118
performance reserves (includes 1200 lb LH_2 bias)	2,073	4,802
Total usable (lb)	121,549	661,920
Residual propellants		
Pressurant	1,216	2,790
Tanks	410	400
Lines	321	285
Engines	26	426
Total Residuals (lb)	1,973	3,901
Total propellants loaded (lb)	123,522	665,821
Tank propellant requirements		
Line and engine residuals	-347	-711
Line usable propellant	0	-12,304
Total propellants loaded in tanks (lb)	123,175	652,806
Tank volume requirements		
Propellant in tanks	27,994	9,195
Minimum I_{sp} allowance	407	139
Ullage	661	1,154
Total tank volume (Ft^3)	29,062	10,488
Maximum prestart pressure (psia)	33	40
Maximum regulated pressure (psia)	33	36
Propellant densities (Lb/ft^3)	4.4	71

Table 4-54. Mark II Propellant Inventory

(4-265K SSME Engines - Orbiter)
(5 LO_2/RP Engines - Booster)

	Fuel	Oxidizer
Impulse (nominal)	119,476	716,856
performance reserves-	811	4,864
bias (1200 lb LH_2)	1,200	0
Total usable (lb)	121,487	721,720
Residual propellants		
Pressurant	512	1,651
Tanks	410	400
Lines	321	285
Engines	75	1,425
Total residuals (lb)	1,318	3,761
Total propellants loaded (lb)	122,805	725,481
Tank propellant requirements		
Line and engine residuals	-396	-1,710
Line usable propellant	0	-11,305
Total propellants loaded in tanks (lb)	122,409	712,466
Tank volume requirements		
Propellant in tanks	27,820	10,035
Minimum I_{SP} allowance	407	152
Ullage (3%)	835	301
Total tank volume (ft^3)	29,062	10,488
Maximum regulated prepress level (psia)	31.5	40
Maximum regulated run level (psia)	31.5	22
Propellant densities (lb/ft^3)	4.4	71

The external tank LH_2 and LO_2 lines are insulated with spray-on foam insulation (SOFI) to minimize throwaway hardware costs. This insulation method is in contrast to the vacuum jacketed lines inside the orbiter where maximum reusability is desired.

External Tank Pressurization. The pressurization subsystem is included in Figure 4-227. Vent/relief valves are provided in the orbiter to vent propellant boiloff during tanking and to limit maximum tank pressure in flight. Vent flow is ducted from the external tanks to the orbiter through self-sealing disconnects. On the ground, the LO_2 boiloff is vented directly to atmosphere; the LH_2 boiloff is ducted to a burnoff area for safe disposal. Pneumatic actuators, integral with the vent valves, close the vent valves in flight. Two vent valves are provided for each tank. The primary vent valve operates at a lower pressure setting than the secondary valve in order to assure a preferred operating sequence. The vent systems are designed to limit the back pressure during the propellant topping operation to 15 psia for LO_2 and 16 psia for LH_2, thereby limiting the propellant bulk temperature at liftoff.

Pressure for engine start is obtained by prepressurizing the ullages with helium before liftoff. To minimize pressure decay due to ullage chilling during first-stage boost, chilled helium is used as the pressurant. Helium flow is controlled by airborne pressure switches which operate SE shutoff valves. This prepressurization system also is used for maintaining ullage pressure for detanking in event of mission abort. The pressurant during detanking may be helium (ambient temperature or cold), ambient temperature nitrogen (LO_2 tank), or ambient temperature hydrogen (LH_2 tank).

Pressurization for run is accomplished by evaporated propellants extracted from the engines. Pressurant flow control for each tank is accomplished by solenoid valve assemblies acting in response to ullage pressure. These solenoid valve assemblies act as manifolds for the pressurant lines from the four engines, and, in addition to housing the solenoid valve, also contain check valves and parallel primary orifices to assure that at least the minimum permissible pressurant flow rate is extracted from each engine.

The pressurization subsystem component operating bands are shown in the following list:

	LO_2 (psia)	LH_2 (psia)
Ground prepressurization	30-40	31-33
Flight pressurization	34-36	31-33
Vent valve (primary)	41-43	34-36
Vent Valve (secondary)	43-45	36-38

4.4.4.8 Tank Avionics System

The design of the external tank avionics system was driven by a number of key ground rules: (1) minimum cost; (2) minimum external tank hardware; (3) hardwire interface with orbiter; and (4) orbiter provides command and control prior to orbiter/external tank separation. Based on these ground rules, analysis of the external tank mission requirements resulted in the minimum avionics system illustrated in Figure 4-297. The following avionics systems are required: propellant gaging, instrumentation, and separation and de-orbit.

The propellant gaging system, which is used for control of propellant loading and determination of propellant depletion, consists of only point sensors hardwired to the orbiter. During the development flight program, 22 level monitoring point sensors and 5 engine cutoff point sensors are located in the LH_2 tank, and 22 level monitoring point sensors are located in the LO_2 tank. The five LO_2 engine cutoff point sensors will be installed in the propellant feedline of the orbiter. The orbiter will provide signal conditioning, timing, loading logic, and engine cutoff logic.

The propellant gaging system will require a 98-wire (20 gage) interface with the orbiter. At the beginning of the operational flight program, the number of level monitoring point sensors can be reduced to six or less per tank, which will reduce the amount of interface wiring accordingly. All point sensors will be similar to those presently used on the Saturn S-II.

As a minimum, the instrumentation system will consist of 36 transducers hardwired to the orbiter during the development flight program. These measurements are tabulated in Figure 4-297. The orbiter will provide excitation voltages, reference voltages, signal conditioning, multiplexing, recording, and transmission (RF link) to ground stations for all external tank measurements. Based on early program testing, the number of measurements will be reduced so that the indicated interface (see Figure 4-297, approximately half of the wiring is twisted-shielded pairs) will be less for operational flights. No new hardware requirements have been identified since the proposed orbiter-type transducers can be used in the external tank.

The separation and deorbit system will control the following ordnance systems: (1) booster/interstage assembly separation; (2) interstage assembly/external tank separation; and (3) deorbit motor ignition. The system will consist of a sequencer for timing, inhibit logic, and permit logic; two batteries; and six single bridge-wire initiator/detonators which are similar to the electrically initiated, hotwire, igniter cartridges used on Apollo. During ground operations, the orbiter will provide electrical power to the external tank. During flight, electrical power will be furnished to the separation and deorbit system by the two onboard batteries.

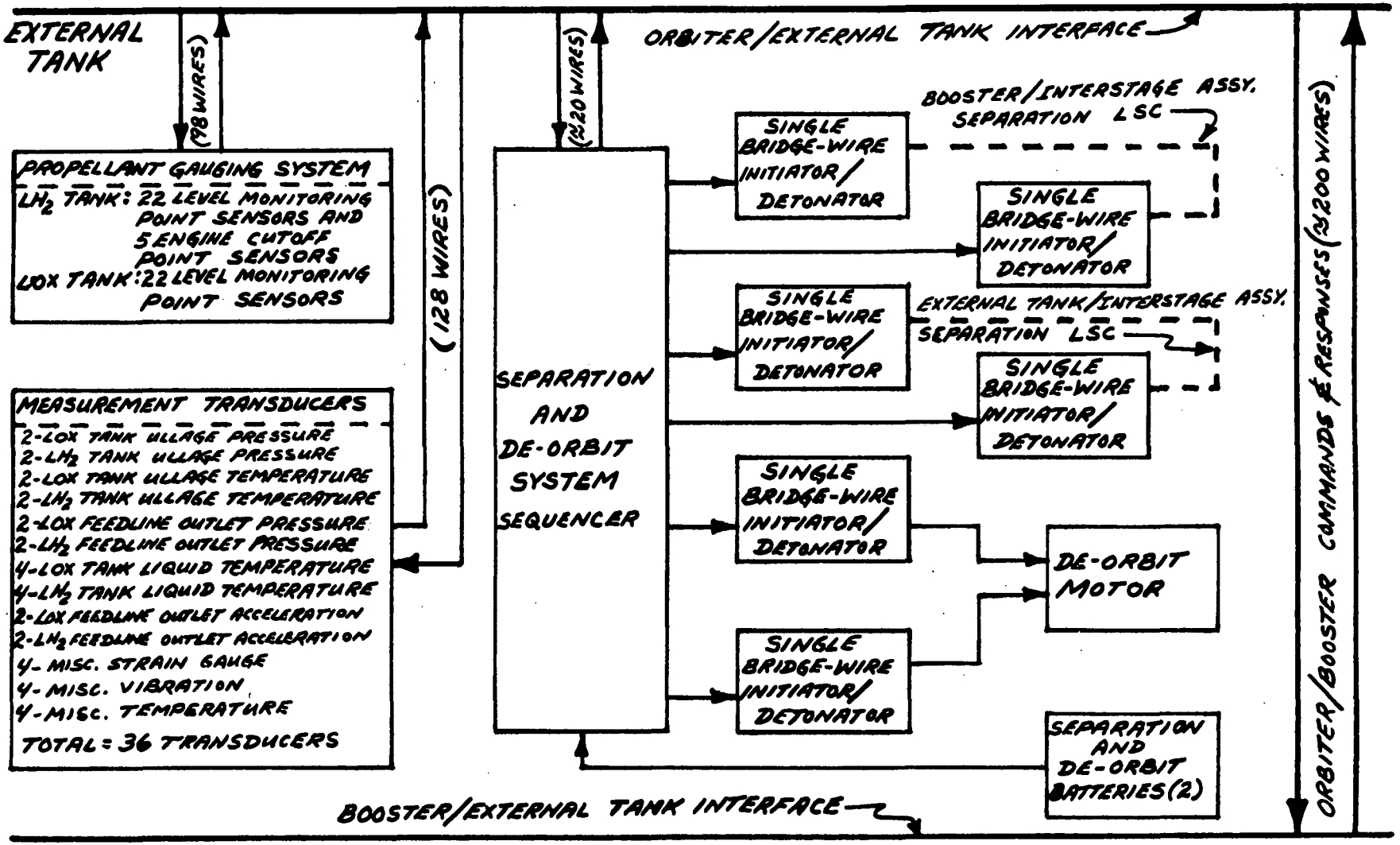

Figure 4-297. External Tank Avionics Block Diagram

The external tank and interstage assembly also must provide for a large wiring interface between the orbiter and booster. This interface is estimated to be approximately 200 wires. This wiring will pass from the booster, through the interstage assembly and external tank, and into the orbiter. The design of the connector disengagement mechanism used during separation will be similar to the connector carrier plate pull away system used on the Saturn S-II.

This system meets the established requirements and ground rules for a low-cost avionics system using proven off-the-shelf hardware. Only the minimum number of avionic components necessary to meet operational requirements were included on the external tank in order to reduce the amount of throwaway hardware.

4.4.4.9 EOHT Weights

The EOHT dry weight is broken down in Table 4-55 for two shuttle systems: LO_2/propane reusable booster (ballistic) system and LO_2/RP reusable booster (flyback) system. Both tanks are sized to the requirements of the Mark II orbiter for the due-east mission. The tank is the heavy-wall monocoque, the concept described in Section 4.4.4.1. The induced environment protection weight includes cork on the LO_2 tank nose section and unpressurized structure in the tank/orbiter interference region to protect the tank during ascent heating, as defined in Section 4.4.4.5. The cryogenic insulation (SOFI) is applied to the external surface of the LH_2 tank. The SOFI (spray-on foam insulation) is unprotected in the tank/orbiter interference region.

Complete EOHT weight statements, with propellant loadings for the various missions, are shown in Sections 4.4.1.1 and 4.4.2.1.

Table 4-55. EOHT Weight Statement

Item	Weight (lb)	
	Mark II Orbiter LO_2/Propane Booster	Mark II Orbiter LO_2/RP Booster
Body	(43,471)	(44,181)
Nose	195	195
LO_2 tank	7,816	7,955
Intertank	3,126	3,162
LH_2 tank	29,248	29,770
Skirt	1,136	1,149
Supports to orbiter	1,810	1,810
Separation system	140	140
Induced Environment Protection	(3,182)	(3,227)
SOFI (LH_2 tank)	1,254	1,277
Cork (LO_2 tank cone and intertank)	1,928	1,950
Propulsion System	3,700	3,700
Deorbit System	2,010	2,010
Growth	1,047	1,062
Dry Weight	53,410	54,180

4.4.4.10 Manufacturing

The perspective of the external tank manufacturing task was established during Phase B through manufacturability trade studies and evaluation of requirements for design, development, and manufacturing. Results were applied to develop a detailed plan containing sequential flows for tooling, fabrication, assembly, system installation, checkout, and inspection. The task analyses have revealed that most of the items identified as problems and concerns represent only a small percentage of the total task. They involve primarily the approaches to planned manufacturing techniques. The product task complexity associated with the tank major assemblies and thermal protection system is summarized in Table 4-56. The assemblies noted may be identified in the manufacturing breakdown (Figure 4-298).

The sections that follow discuss manufacturing producibility, major manufacturing problems, manufacturing concerns, and items causing substantial program impact. Items identified as major manufacturing problems are those capable of substantial program impact. Manufacturing concerns are limited to areas involving significant manufacturing complexity, but not threatening general program impact.

Manufacturing Producibility Analysis. An external LH_2/LO_2 tank instead of an internal tank is a major configuration change from the Phase B orbiter concept and resulted in manufacturing producibility studies to determine the best approach to manufacturing such a tank. Prime drivers in the selection were the use of maximum sizes, which minimize welding footage, and incorporation of fabrication techniques requiring little or no development. Manufacturing tank complexity factors, an internal tank compared to an external tank are summarized in Table 4-57.

Table 4-56. Manufacturing Task Analysis for External Tank

	Fabrication	Processing	Assembly	Installations	Checkout	Handling	Transportation	Inspection	Tooling
LO_2 tank	S	S	S	S	S	S	S	S	S
LH_2 tank	S	S	S	S	S	S	S	S	S
TPS	S	S	N/A	C	S	S	S	S	S
Key: S - state of the art C - concern N/A - not applicable									

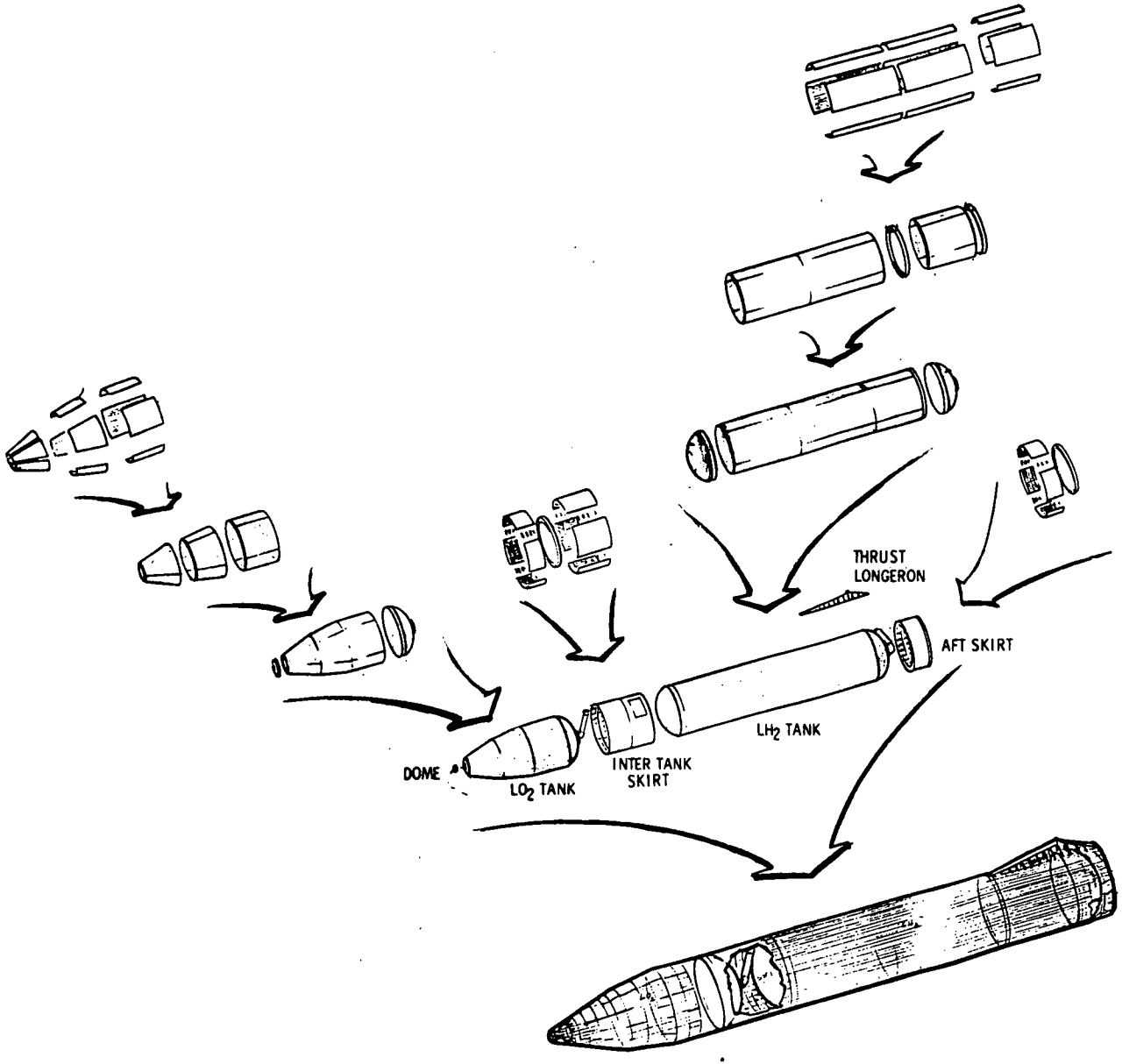

Figure 4-298. Manufacturing Breakdown

Table 4-57. Manufacturing Complexity Factors, Internal Versus External Tanks

	Fabrication	Processing	Assembly	Installation	Checkout	Handling	Transportation	Inspection	Tooling	Material	Cost	Schedule
Internal	M	N/C	M	N/C	M	M	L	M	M	N/C	M	M
External	L	N/C	L	N/C	L	L	M	L	L	N/C	L	L
Key: M - more complex; L - less complex; N/C - no change												

Major Manufacturing Problems. Based on the analysis performed, there were no items identified as major manufacturing problems.

Manufacturing Concerns. Application of spray-on foam insulation with minimum closeouts is a manufacturing concern. This technique is desirable to reduce cryo pumping of insulation during tanking and detanking. The proposed method of resolving this concern is a single application of SOFI to the total tank with a definite limiation of areas requiring separate application. Development is required to provide equipment and sequencing to perform this operation.

Items Causing Substantial Program Impact. Items that could cause substantial program impact were assessed by Manufacturing task teams. They conducted in-depth evaluations of manufacturing and engineering designs issues. Trade studies and design analyses were performed by Manufacturing in conjunction with Design Engineering during the Phase B' study to assure manufacturability of the external tank. These studies included factors concerning technology, tooling, material, handling, fabrication, assembly, installations support equipment, manufacturing checkout, personnel, cost, schedule, facilities, quality assurance, safety, and transportability. The conclusions reached by these teams were presented to the Production Operations Review Board to establish the optimum manufacturing methods and processes based on current design vehicle configuration.

Results of these assessments and studies indicate that there are no areas in the present manufacturing plan that would substantially impact the program.

4.4.4.11 Facilities

The external LH_2/LO_2 tank is a large tank assembly (approximately 22 feet in diameter and 127 feet long), and the dual plane separation interstage (tank to booster) adapter and the new orbiter/tank separation system result in significant changes to facility requirements identified in the Phase B baseline document Facility and Manufacturing Plan for Phase C/D, Volume I, Orbiter, SD 71-104-1.

Development Test Facilities. An air-bearing level floor approximately 100 feet by 125 feet may be required for development and functional tests of the EOHT/orbiter separation system. Dummy mass-balanced test articles simulating the EOHT and the orbiter would be equipped with separation links and release mechanism hardware and would be used for a three-degree-of-freedom separation simulation test program. Each vehicle would be suitably instrumented and carry its own on-board air supply system in K-bottle racks. This facility would have design requirements similar to those for the cargo handling and docking adapter subsystem development tests. The possibility of one test facility to support all three test programs may prove feasible.

Demonstration of the full-scale dual plane ordnance system will require a remote test facility. The facility will require a minimum rating of 0.50 pound of TNT or equivalent.

The major tank structural tests will require a large test tower approximately 150 feet high by 40 feet wide by 40 feet deep with a strongback capability of a 5 million-pound column loading and provisions for application of aerodynamic and inertial side shear loads. A base bearing pad capable of 5 million-pound compression load will also be required. Adjacent LN_2 dewar and pumping capacity for approximately 150,000 gallons and a 4000 kva power source will be required to simulate associated thermal environments. Two overhead cranes rated at 25 tons and 5 tons will be required for hoisting the test article and test fixtures.

Manufacturing Facilities. The major manufacturing operations to support tank fabrication are identified as the LO_2 assembly and the final assembly. The building requirements are estimated to be:

	Height (ft)	Square Feet
LO_2 tank assembly	60	100,000
LH_2 tank assembly	90	160,000
Final assembly	140	40,000
		300,000

Additional areas to perform tank proof testing will be needed as follows:

1. Hydrostat in-process manufacturing acceptance tests will be required on the LO_2 tank aft bulkhead and the forward and aft LH_2 tank bulkheads. A complete hydrostat test of the 44-foot by 22-foot-diameter LO_2 tank in a vertical attitude will be necessary to proof-test the assembled tank.

2. The LH_2 complete tank assembly will require a hazardous pneumostat proof test similar to that conducted on the Saturn S-II LH_2 tank. This test may be conducted with the tank in a horizontal test area such as the field revetment, with a remote control blockhouse to protect equipment and personnel.

A site evaluation study of existing production facilities was performed on a number of candidate sites such as Tulsa, Forth Worth, MSFC, Michoud, KSC, Seal Beach, Huntington Beach, and San Diego.

As a result of the study, it has been determined that many contractors have the capability and that existing facilities are adequate and available, with minor modification, to support fabrication of orbiter external tanks. Tank fabrication and final assembly can be separated. This affords maximum use of existing facilities, and work can be placed where skills are available.

Flight Test Facilities. The large external tank imposes new storage and checkout facility requirements at the flight test and operations site, Kennedy Space Center. The details of tank operations are still evolving along with specified facility requirements and recommendations.

4.4.4.12 Test

Structural Tests. Since the EOHT tanks are disposable, they experience a limited number of pressure and load applications. The tank and its separation linkage will, therefore, be subjected to static structural tests only. Current design and fabrication approaches will be used to minimize development tests except on components involved with highly concentrated loads or complex load distributions such as the separation linkage and its immediate backup structure on the tank.

Structural acceptance testing will be limited primarily to the pressurized portions of the tank structure. Proof-pressure tests will be conducted in conjunction with subsequent nondestructive evaluation and inspection techniques to provide the required confidence in the structure to withstand its life spectrum of loading without compromising mission requirements. Testing methods were selected to permit use of low-cost

test procedures while attempting to minimize potential weight penalties. Based on this concept, the following acceptance tests will be performed:

1. The LO_2 tank aft bulkhead will be proof-pressure-tested hydrostatically.

2. The complete LO_2 tank assembly will be proof-pressure-tested in a vertical attitude hydrostatically.

3. The LH_2 tank forward and aft bulkheads will be proof-pressure-tested hydrostatically.

4. The complete LH_2 tank assembly will be proof-pressure-tested in a horizontal attitude pneumostatically.

A structural qualification test program will be performed on the complete tank and separation linkage structural assemblies to verify their structural integrity for their critical design limit and ultimate loads. The basic tank structural test article will consist of all of the flight article structure from a point approximately four feet above the LO_2 tank equator extending aft to the bottom of the booster interstage structure, with a short simulated section of the booster-interstage backup structure. This test article will be tested in a vertical attitude with LN_2 and high density spheres (for simulation of LO_2 inertia loads) in the LO_2 tank and a partial fill of LN_2 in the LH_2 tank.

The partial fill of the LH_2 tank, utilized with GN_2 ullage pressure, presents a stored energy hazard but it is considered a reasonable approach to simulation of critical thermal environments and internal inertia loads. The use of cryogenic fluid is required to assess the thermal stresses and their interaction with load-induced stresses at the critical bulkhead-to-sidewall attachment areas. Also important are the cryogenically induced radial deflections at both ends of the intertank (mid-skirt) structure and the resultant effects on its column compression capability. A second qualification test article consisting of the LO_2 tank structure above the aft bulkhead equator will be used to verify the upper portion of the LO_2 tank structure. The tank will be hydrostatically tested at ambient temperature to ultimate design pressure appropriately corrected for material property variations between operational and test temperatures.

Qualification tests on the two test articles described will verify the EOHT structural integrity for:

1. The LH_2 prelaunch free-standing capability with a fully loaded LO_2 tank

2. The intertank and interstage structure under booster high q, end burn, and tank bending loads

3. The forward and aft orbiter separation linkage and tank backup structure

4. The LH_2 tank structure for critical bending loads

5. The LO_2 tank aft bulkhead, forward cone structure, and the entire LH_2 tank for design burst pressure

6. The tank internal load distribution at critical tank and nonpressurized sidewall discontinuity areas for their critical design limit and ultimate loads

7. The deorbit rocket engine backup structure for its critical design limit and ultimate loads

8. The fluid system and vent lines for their critical flight and disconnect limit and ultimate loadings

Separation System Tests. The current EOHT tank configuration includes two separation systems: the orbiter/tank separation system and the pyrotechnic dual-plane interstage adapter separation system.

The orbiter/tank separation system linkage and tank backup structure will be verified for its structural integrity during the EOHT structural test program. The orbiter electromechanical release mechanisms, fluid and electrical disconnects, and the linkage attachment fittings and their backup structure will be verified for structural integrity in conjunction with the orbiter structural test article test program. Functional development, evaluation, and system operation may be demonstrated on full-scale hardware with an air-bearing three-degree-of-freedom facility and mass simulated dummies of the orbiter and external tank.

The dual-plane interstage adapter separation system will require development tests to verify the adequacy of the linear shape charge, its retention system, initiators, and separation mode. After the development program, a full-scale interstage adapter, with short sections of the EOHT LH_2 aft skirt structure and the booster attachment backup structure, will be used for a functional demonstration of the dual-plane separation under critical design loads and environments. The test will also demonstrate functional operation of the disconnect for the 300-wire umbilical running from the booster to the orbiter through the interstage adapter.

Thermal Protection System Tests. The external tank thermal protection system will consist of SOFI on the LH_2 tank and ablator TPS material on the LO_2 tank nose cone and unpressurized structure in interference regions. Since the proposed design is similar to that qualified and used on the Saturn S-II stage, only a minimal test program is anticipated. Development tests will be conducted as required on selected panels for combined structural, thermal, and acoustic environments and for critical or unique areas of application. The structural test article will include the thermal protective cover installation during static structural loading tests at cryogenic temperatures to verify the insulation for induced strain.

Manufacturing in-process acceptance tests of the EOHT will be conducted in a manner similar to that used on the Saturn S-II program with appropriate nondestructive evaluation and inspection methods used.

Electrical Power System Tests. The electrical power system consists of two batteries and eight Apollo-type single bridge-wire initiator/detonators, a wiring harness and a sequencer for timing, and inhibit logic and permit logic. This system controls the booster/interstage assembly separation, the interstage/external tank separation, and the deorbit motor ignition.

Since the system hardware is similar to that developed for the Apollo program, only a minimal development test effort will be required.

Existing qualified hardware will be used to the extent possible. Hardware not previously qualified for the anticipated shuttle environments will be fully qualified for functional operation after exposure to their critical design environments.

Manufacturing in-process acceptance tests will be conducted on all hardware items to verify adequate performance. Conventional nondestructive evaluation and inspection methods will be used.

Fluids System Test. The fluids system consists of the propellant feed/fill and recirculation and pressurization/vent line assemblies and disconnects associated with each tank as well as the H_2 and O_2 pressurization diffusers and the anti-vortex and slosh baffles inside the LO_2 tank.

Since most of the technology required for the design of the fluid lines, gas distributors, and propellant baffles has been developed, only minimal material and process development testing is anticipated. The major development items are the tank-to-orbiter disconnects, which will be developed and qualified as part of the orbiter design. The tank half of the disconnect will probably represent less of a development problem than that of the orbiter. It is expendable and has a short service life.

Qualification testing will be accomplished at the component level to verify functional performance in accordance with the design requirements. Of primary concern will be verification of the design to accommodate the relative motions between the orbiter and tank resulting from cryogenic, pressure, and boost loads. Ultimate subsystem certification will be achieved upon the successful completion of all subsystem-related test objectives of the cluster firing test program.

Deorbit Propulsion System Test. The deorbit propulsion system consists of a single solid-propellant motor sized to provide the ΔV required for deorbit of the complete tank assembly.

Development/qualification testing will consist primarily of a series of hot firings accomplished by the solid rocket motor supplier to evaluate repeatability of motor ballistics, case and propellant grain integrity, nozzle ablative characteristics, and ordnance control and ignition performance.

Supplier acceptance testing will be limited to batch tests of the propellant grain and nondestructive evaluation (NDE) of the assembly motor.

Manufacturing in-process and acceptance tests will consist of motor alignment checks to assure the motor thrust vector is accurately aligned to the tank assembly c.g., electrical ignition circuit checks, and NDT of the propellant grain/case integrity.

Propellant Gaging System Tests. The propellant gaging system consists of liquid level monitoring point sensors, engine cutoff sensors, and wire harnesses connecting to the orbiter/tank electrical disconnect.

The point sensors are expected to be similar to the design developed for the S-II program. Therefore, no significant development testing is anticipated. The main propulsion test article will provide the primary means of subsystem certification.

Manufacturing acceptance testing will consist only of continuity and insulation resistance checks.

Measurement System Tests. The measurement subsystem consists of approximately 36 pressure, temperature, acceleration, vibration, and strain-gage transducers along with the wire harness connecting the sensors to the orbiter/tank electrical disconnect.

The design requirements of the required transducers are within current technology and are available as qualified off-the-shelf components.

Consequently, no special development testing is required beyond that provided by the main propulsion test article.

Manufacturing in-process and acceptance testing will include pre-installation calibration, proof, and leak test of all fluid system transducers and a functional check to the degree that each sensor can be practically stimulated.

4.4.5 LO_2/RP Flyback Booster Definition

4.4.5.1 Design

The current B-18E-3 heat sink booster configuration was derived from a series of B-18E booster design and tradeoff studies discussed in Section 4.2.2. The differences between the trade study and the final configuration presented in this section are the removal of ballast from the nose, sweeping of the wing for balance purposes, and a synthesis resizing accounting for these changes. Figure 4-299 shows the configuration. The main feature of the configuration is its commonality with the Saturn S-IC propellant tanks and propulsion systems as adapted to a fully reusable booster design. The booster consists of eight basic elements: the nose section, oxidizer tank, intertank adapter, fuel tank, propulsion bay, wings, canard, and vertical tail.

To adapt the S-1C elements to a fully reusable booster, a nose section is attached to the LO_2 tank providing support for the forward canard control surfaces, the crew compartment, nose landing gear, orbiter interstage adapter/separation mechanism, subsystems, and equipment installations. The intertank section between the RP and LO_2 tank domes is 120 inches long to allow for installation of four airbreathing cruise back engines in the body. Each of the four airbreathing engines in the body is deployable from the lower surface for operation. These four body located engines tend to improve vehicle balance, a critical configuration requirement. Also, there is insufficient span available to locate all engines in the wings without excessive wing thickness at the outboard engines. Five F-1 engines are attached to the thrust structure in a manner similar to the S-1C installation. The thrust structure distributes loads into the booster body and provides attachment for the wing and vertical stabilizer structure.

A delta wing with a leading edge sweep of 53° attaches to a carry-through structure that is integrated with the intertank, fuel tank and thrust structure. Wing area is chiefly a function of landing speed limitations. Wing sweep requirements are determined by aerodynamic balance. Each wing provides for the installation of three airbreathing cruise engines deployable through the lower surface. The main landing gear is stowed in the wing inboard of the airbreathing engines. The gear has a conventional mechanism and rotates down and aft for landing. The gear length gives a touchdown clearance of 10 inches during a 15-degree attitude landing. Retracting part of the lower main engine fairings reduces the gear length requirements. (During launch this fairing is extended to allow engine gimballing.)

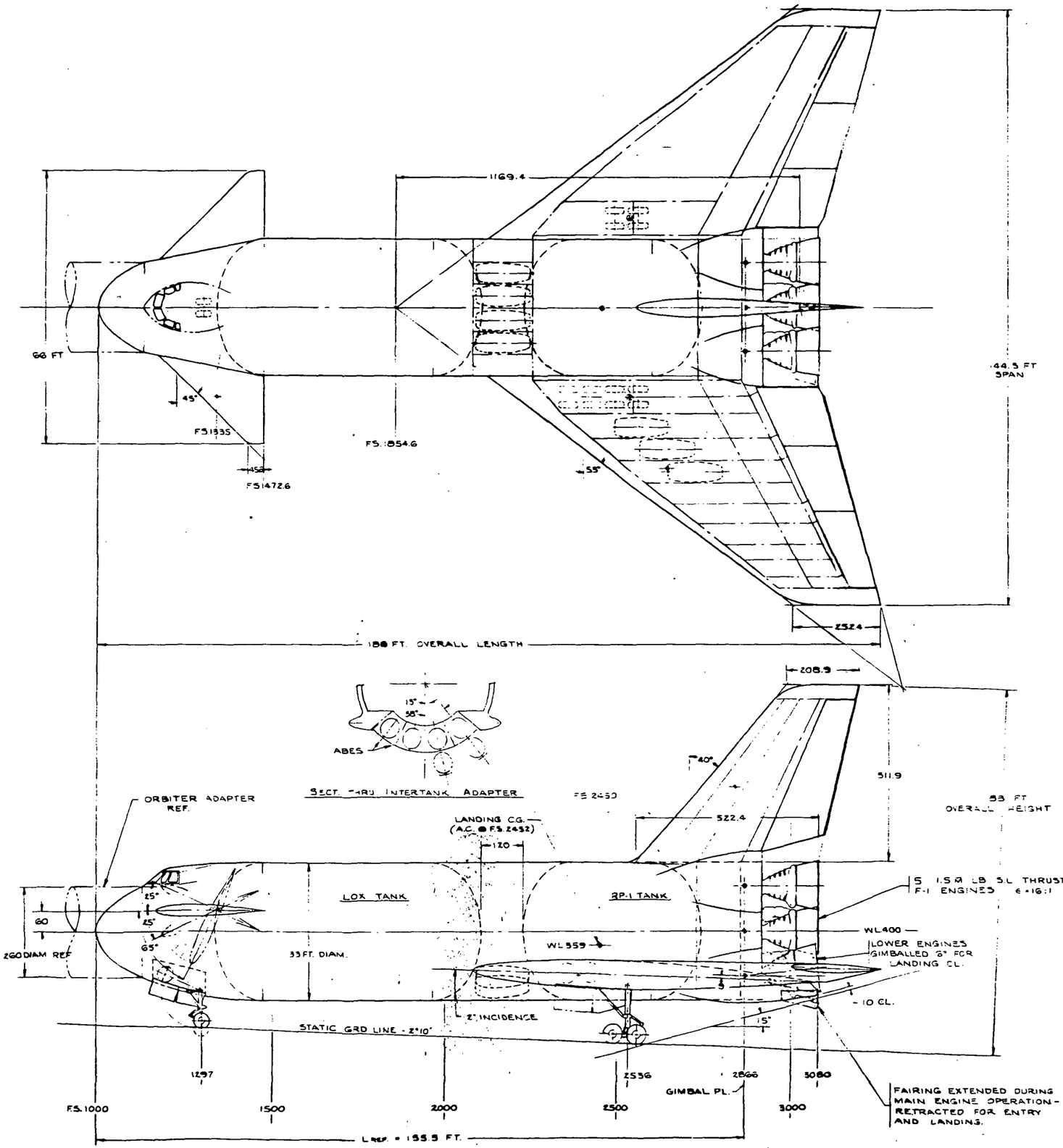

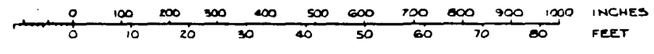

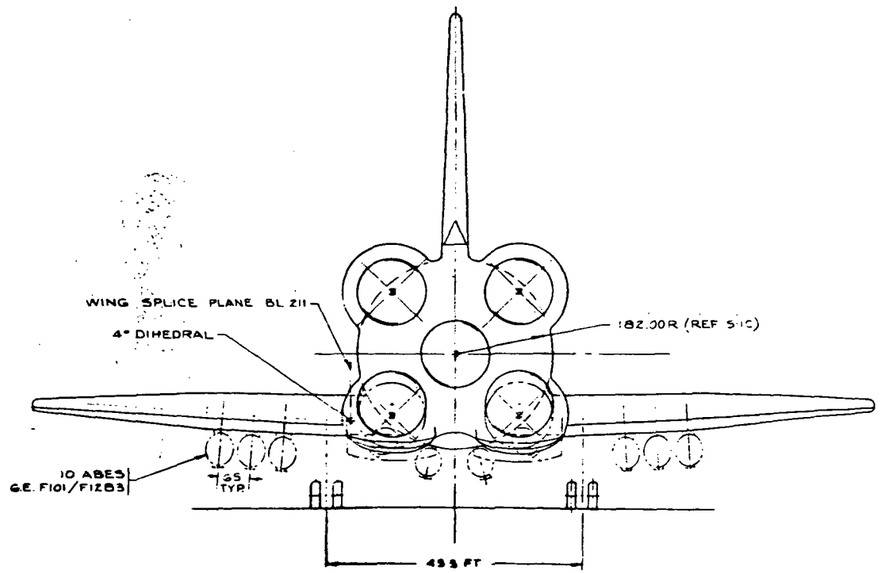

Figure 4-299. Basic Configuration, B-18E-3 Booster

A single vertical stabilizer is located on the upper body centerline with main spar attachments at the wing and at the thrust structure. The stabilizer has a 40° leading edge sweep angle. The lower portion of the rudder is trimmed to provide launch holddown fitting clearance.

A forward canard is used for control and is located in the nose section. It is pivoted at approximately 50% of the root chord and moves 25° leading edge up and 65° down for subsonic and hypersonic flight requirements respectively. To minimize entry heating effects in the canard/body intersect region, the body is faired to provide a sealing face forward of the pivot for all canard positions required during high heating flight conditions.

Performance and dimensional data for the B-18E-3 booster are given in Table 4-58. The orbiter is mounted in tandem and attached to the nose of the booster on a 260-inch diameter ring.

S-1C tankage capacity is more than adequate to perform the design reference mission of 65k payload due east launch out of ETR. For the design reference mission the S-1C tankage is loaded to approximately 75% of its capacity. This is because the orbiter design and performance essentially fixes the staging velocity of the system, and consequently the booster propellant load. Loading the booster tanks to full capacity is a critical design condition which with the same orbiter design and performance would cause an increase in staging velocity (increase in booster inert weight) and increased payload capability.

Table 4-58. Details of B-18E-3 Booster System

Overall Weight					
GLOW	MLB	5.09			
BLOW	MLB	3.97			
OLOW	MLB	1.12			
Boost. Ascent Propel.	MLB	3.28			
Orb. Ascent Propel	KLB	836			
Boost. Dry Struc.	KLB	583.5			
Boost. Landing	KLB	606.1			
Propulsion					
Boost. No. Main Eng.		5			
Type Main Eng.		F-1			
Boost. Eng. SL Thrust	MLB	1.522			
Boost. SL I_{sp}	SEC	265.4			
Boost. Vac I_{sp}	SEC	304.1			
Orb. No. Main Eng.		4			
Type		SSME Hi-Pc			
Orb. Eng. Vac. Thrust	KLB	265			
Orb. Vac I_{sp}	SEC	453.2			
No. Boost. A/B Eng.		10			
Type Boost. A/B Eng.		GE F101/F12BE			
A/B Eng. Max. Thrust 10KFT	KLB	12.8			
Performance					
V_{stage} Relative	FPS	6000	L/D Cruise		5.58
Q_{max}	PSF	650	V_{cruise}	KTS	245
Q_{stage}	PSF	73	SFC		.729
T/W_{LO}		1.35			
h Stage	KFT	147.4			
γ Stage	DEG	16.9			
Payload	KLB	65			
Mission		East			
Launch Site		ETR			
Geometry					
Length Nose to Gimbal	FT	155.5	RP Tank Vol.	FT^3	30220
Body Dia.	FT	33	LO_2 Tank Vol.	FT^3	48220
S_{wing} Theo.	FT^2	8549	Body Vol.	FT^3	125130
S_{canard} Exp.	FT^2	485			
S_{vert}	FT^2	1300			

4.4.5.2 Ascent and Entry Performance

The booster operational mission flight profile is presented in Figure 4-300, significant events from lift off through landing of the booster are presented.

The open-loop performance trajectory for the baseline LO_2/RP booster was generated with the Mark II orbiter for the due east mission (65k payload) from KSC; ascent trajectory parameters are given in Figure 4-301. The main engines are throttled to 90% of full thrust at liftoff for engine-out capability yielding a thrust/weight at liftoff of 1.35 g. At 50 seconds after liftoff, one main engine is shutdown to limit the maximum dynamic pressure to 650 psf for vehicle design load considerations. The four operable main engines are then increased to full thrust. As propellant is depleted, along with increased thrust at altitude, the vehicle acceleration reaches 3 g. At this point, approximately 116 seconds after liftoff, the main engines are throttled to maintain the 3-g limit in axial acceleration until the maximum engine throttling limit of 300k pounds is reached. At this time (138 seconds) two F-1 engines are cut off and the booster ascent is completed under 2 F-1 engines at full thrust. The ascent phase is terminated on indication of propellant depletion at approximately 140.6 seconds after launch.

The booster entry phase begins at staging and terminates, by definition, when the booster descends to 20,000 feet. Initial angle-of-attack for entry is 60°; the vehicle subsequently uses a supersonic transition whereby angle of attack is reduced with decreasing Mach number. Pitch and bank angle scheduling is used to minimize flyback distance to the launch site.

Time histories of the pertinent performance parameters during entry flight are presented in Figure 4-302. During the first 40 seconds following staging, the booster pitches to 60 angle of attack and banks to 75°. The resultant normal load factor reaches 3.2 at 110,000 feet altitude and Mach 2.7; maximum supersonic dynamic pressure of 240 psf is experienced at Mach 1.3 and 54,000 feet altitude. Transonic flight is accomplished at 5° angle of attack to alleviate Mach buffet. The angle of attack is increased subsonically to maximize gliding lift-to-drag ratio. Entry flight terminates at Mach 0.5 and 20,000 feet altitude with a required flyback range of 124 nautical miles.

4.4.5.3 Flyback Performance

Subsonic cruise performance for the booster returning to the launch site is presented in Figure 4-303. The data represent two conditions: (1) cruise in still air with all engines operating and (2) cruise against the NASA directional winds for the due east launch mission with one engine inoperative. The mission profiles include idle descent from 20,000 feet to start of cruise altitude, followed by a climb cruise at maximum specific

Page intentionally left blank

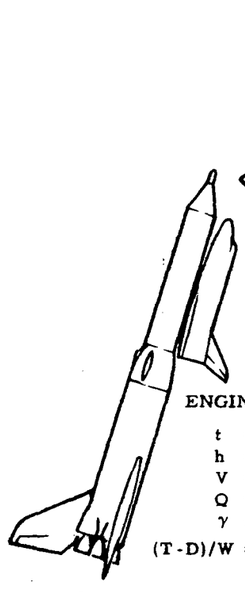

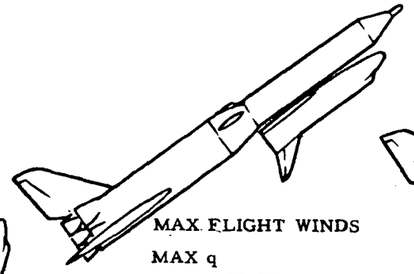

MAX FLIGHT WINDS

MAX q
- t = 72 SEC
- h = 41,500
- V = 1470 FPS M = 1.53
- Q = 646 PSF
- γ = 51 DEG

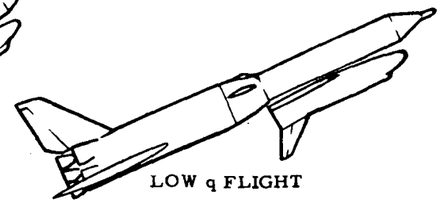

LOW q FLIGHT

THROTTLE TO 3G
- t = 116 SEC
- h = 104 K FT
- V = 4028 FPS
- Q = 219 PSF
- γ = 25 DEG

(T-D)/W = 3

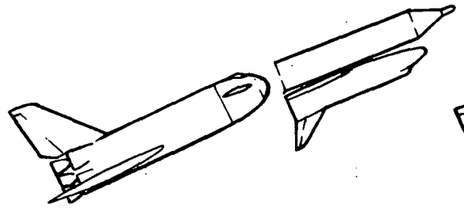

SEPARATION
PROPELLANT DEPLETION
START ORBITER ENGINES
REDUCE BOOSTER THRUST
RELEASE ORBIT
SHUTDOWN BOOSTER

- t = 140.6
- h = 147.4 K FT
- V = 6000 FPS
- Q = 73 PSF
- γ = 16.9 DEG

(T-D)/W = G

M = 5.58

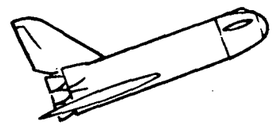

ORIENTATION FOR ENTRY
TO APOGEE
ACPS CONTROL
ROLL TO 75 DEG
PITCH TO 60 DEG

APOGEE
- t = 206
- h = 205.3 K FT
- V = 5129 FPS
- q = 6.12 PSF
- M = 5.04
- α = 60 DEG
- γ = 0.0 DEG

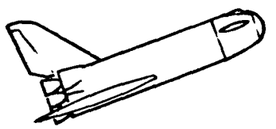

ENTRY - BEGIN PITCH
MODULATION
- t = 296
- h = 111.7 K FT
- V = 2707 FPS
- q = 70.1 PSF
- M = 2.66
- α = 60 DEG
- γ = -19.7 DEG

MAX DYN PRESSURE
- t = 351
- h = 54.1 K FT
- V = 1200 PSF
- q = 241.5 PSF
- M = 1.28
- α = 14.04 DEG
- γ = -36 DEG

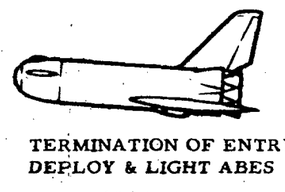

TERMINATION OF ENTRY
DEPLOY & LIGHT ABES
- t = 655 SEC
- h = 20 K FT
- V = 543 FPS
- q = 184 PSF
- M = 0.51
- α = 6 DEG
- γ = -5.6 DEG

CRUISE 95% HEADWIND
ONE ENGINE OUT
8000 FT CRUISE ALTITUDE

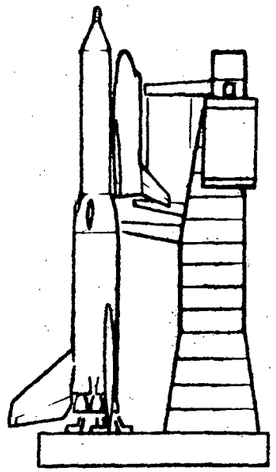

IGNITION & LIFTOFF
- t = 0 SEC
- W_B = 3.97 M LB
- W_O = 1.12 M LB
- W_{TOT} = 5.09 M LB
- T/W = 1.35 (5 ENGS @ 90% C_T)

LANDING
DEPLOY LANDING GEAR
INITIATE FLARE AT 50 FEET
178 KT
163 KT LANDING SPEED

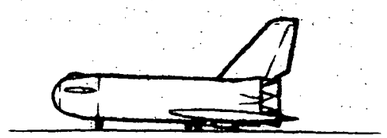

Figure 4-300. Operational Mission Flight Profile

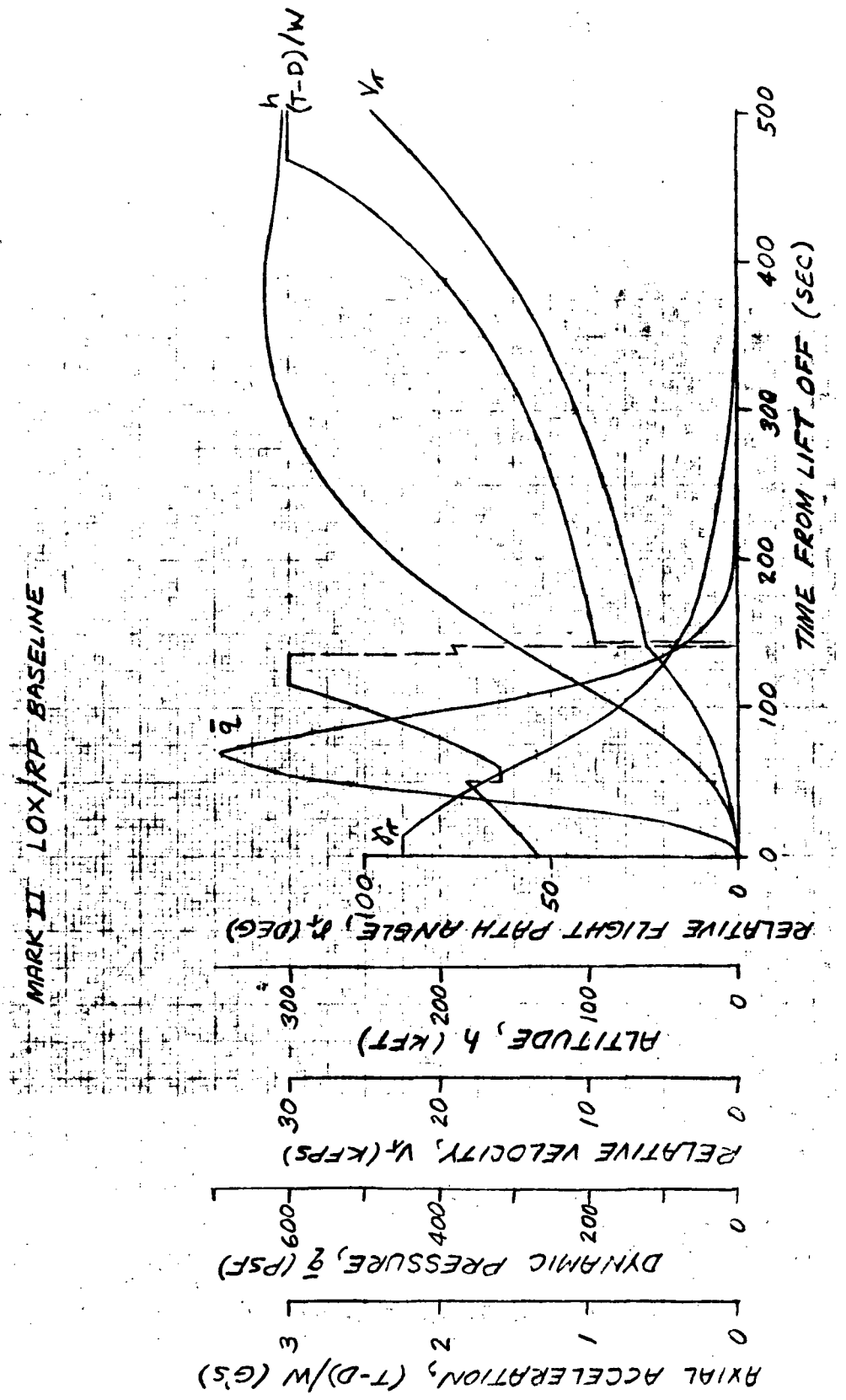

Figure 4-301. Ascent Trajectory Parameters

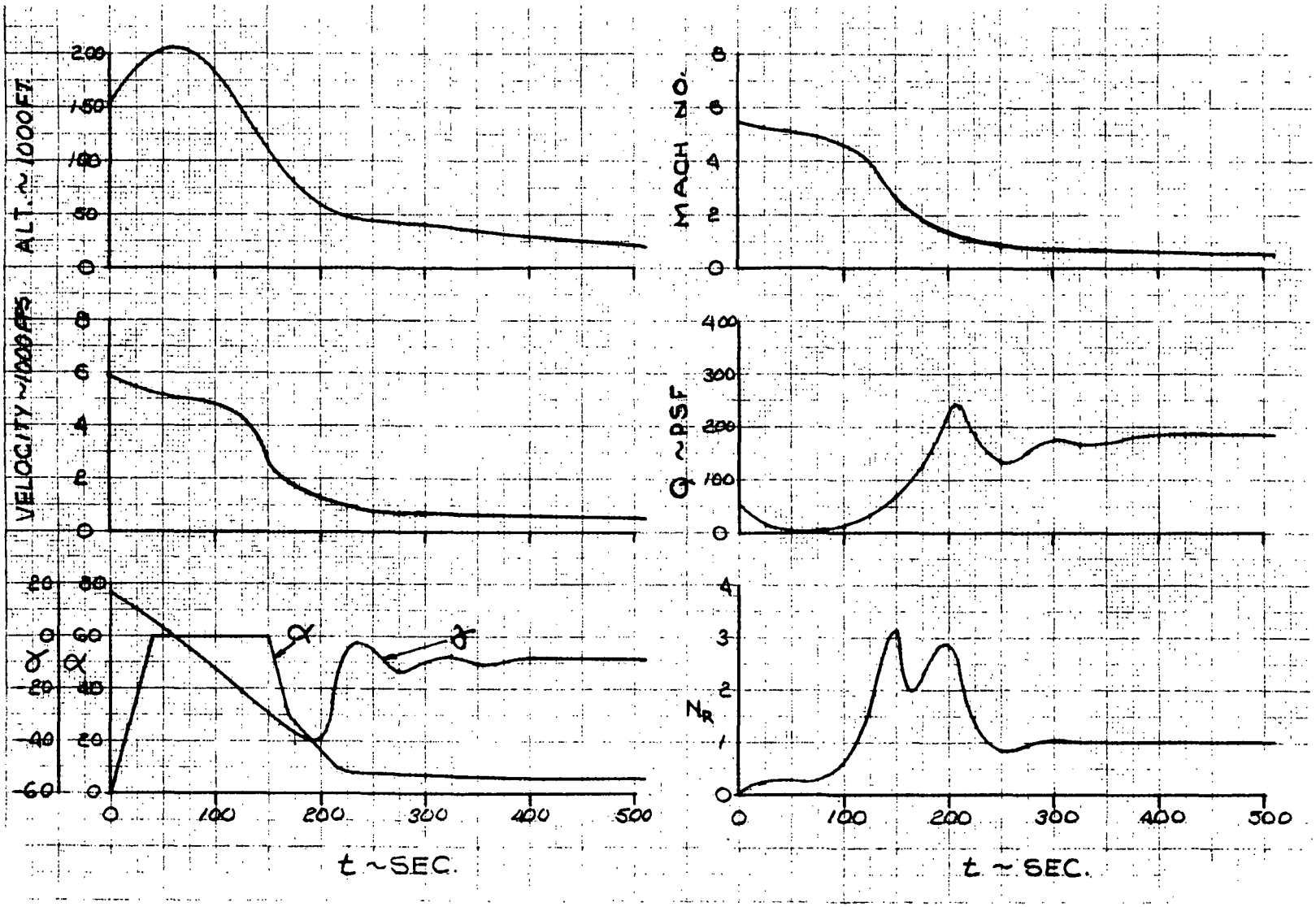

Figure 4-302. Booster Entry Trajectory

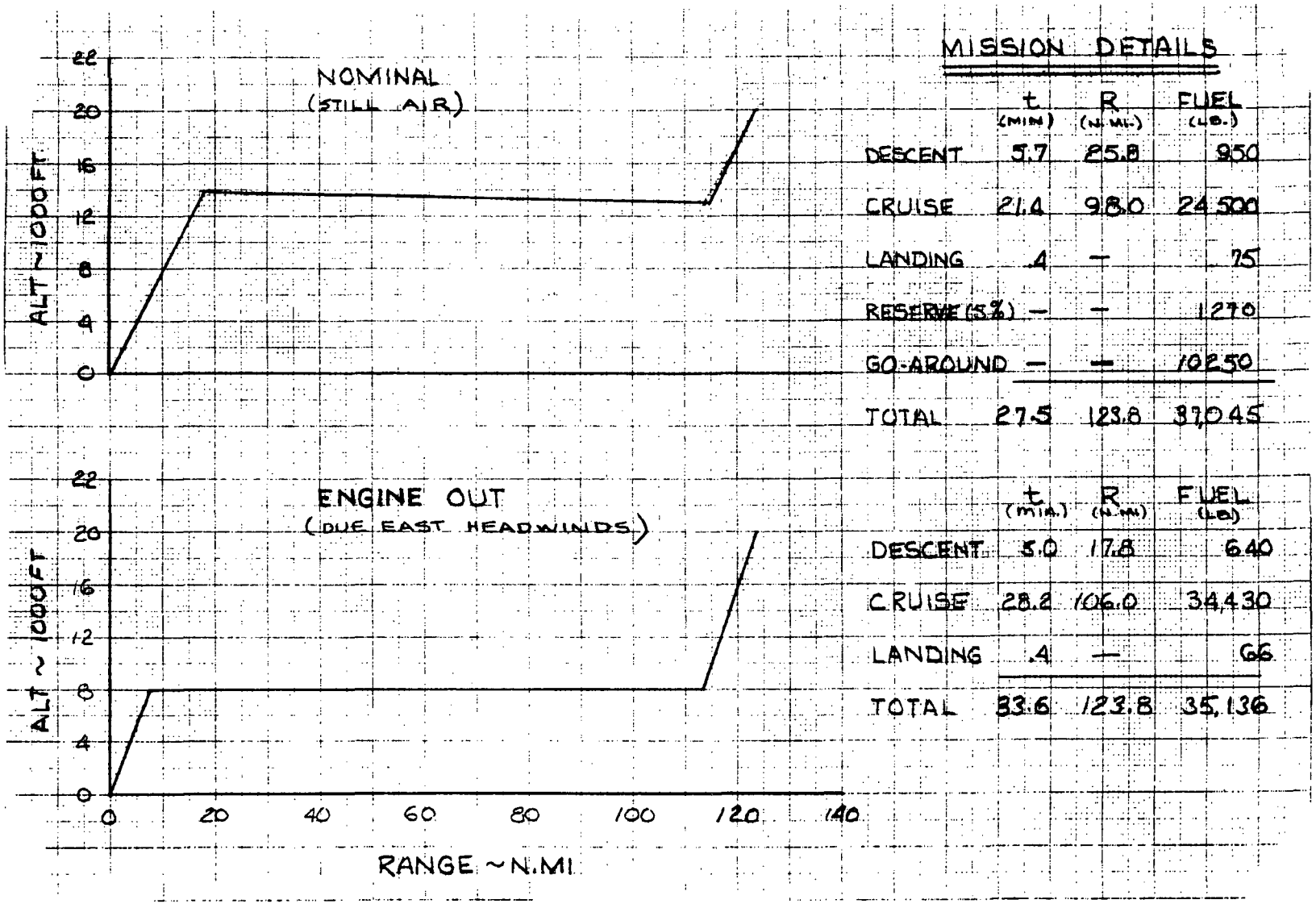

Figure 4-303. Cruise Performance

range to the start of an idle power descent to sea level, to complete the required flyback range of 124 nautical miles. The cruise performance is based on the trimmed aerodynamic data in the following pages and engine characteristics of the GD F-101 turbofan burning kerosene.

Landing performance of the booster is presented in Figure 4-304. Approach and landing speeds are based on the landing configuration aerodynamics presented in the following pages with approach speed (at the 50-foot obstacle) defined as 120% of free air minimum velocity. Landing distance includes distance over the 50-foot obstacle plus stopping distance from touchdown; required field length, defined by Federal Airworthiness Regulations, is established by dividing the landing distance by the 0.6 factor. The data are presented for sea level, standard-day conditions and braking coefficient of 0.34 (dry concrete runway).

4.4.5.4 Ferry Performance

The booster ferry performance capability is presented in Figure 4-305. Balanced field takeoff length as a function of gross weight is shown at sea level for standard and hot day conditions. The aerodynamic takeoff configuration includes comparison of the effect of a tail-cone added to eliminate base drag. From the data it is indicated that for a cruise range requirement of 300 nautical miles, the fuel requirement is equivalent to a takeoff gross weight of 757,000 pounds for the basic configuration, but is reduced to 721,000 pounds if a tail cone is added. This gross weight, derived from performance requirements, has not as yet been investigated from the structural design standpoint. The 757,000-pound takeoff weight requires a balanced field length of approximately 13,000 feet on a standard day; hot day field requirements exceed 15,000 feet. With a tail cone used, takeoff can be achieved in 12,000 feet on a hot day with the gross weight required for 300-nautical-mile ferry range.

4.4.5.5 Aerodynamics

This section contains data summarizing the aerodynamic characteristics of the B-18E-3 booster throughout the operational flight regime, including launch, entry, transition, cruise and landing. The booster aerodynamics are based primarily on experimental data obtained on configurations geometrically similar to the B-18E-3, primarily the B-9U Phase B baseline configuration. Geometric differences between wind tunnel configurations and the B-18E-3 configuration have been adjusted using component build-up data.

Aerodynamic characteristics of the baseline launch configuration are presented in Figures 4-306 and 4-307. These data, including longitudinal and lateral-directional data, are based on data from NASA MSFC 14-inch TWT Test No. 506, modified to account for geometrical differences between the tested and baseline configuration.

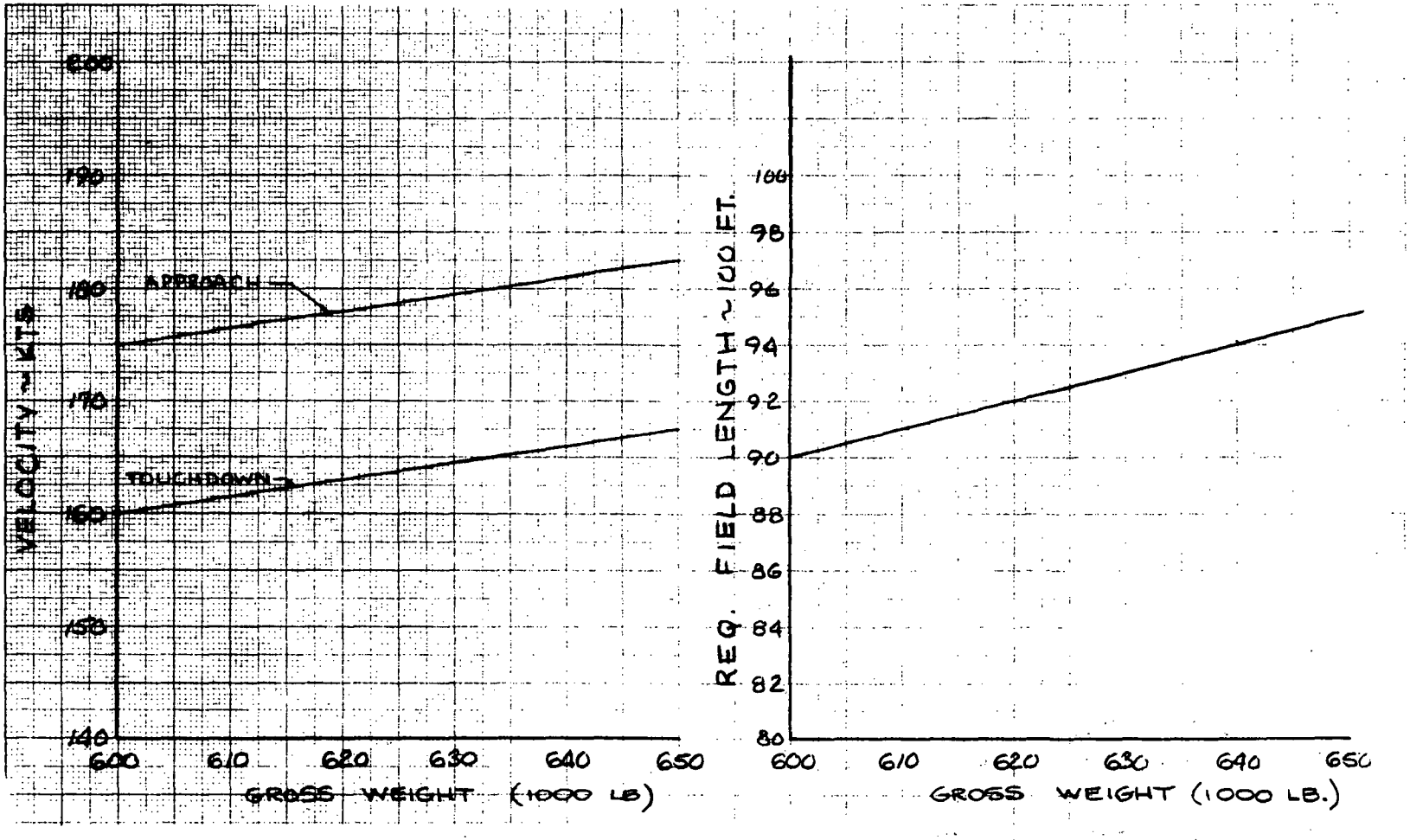

Figure 4-304. Landing Performance Summary

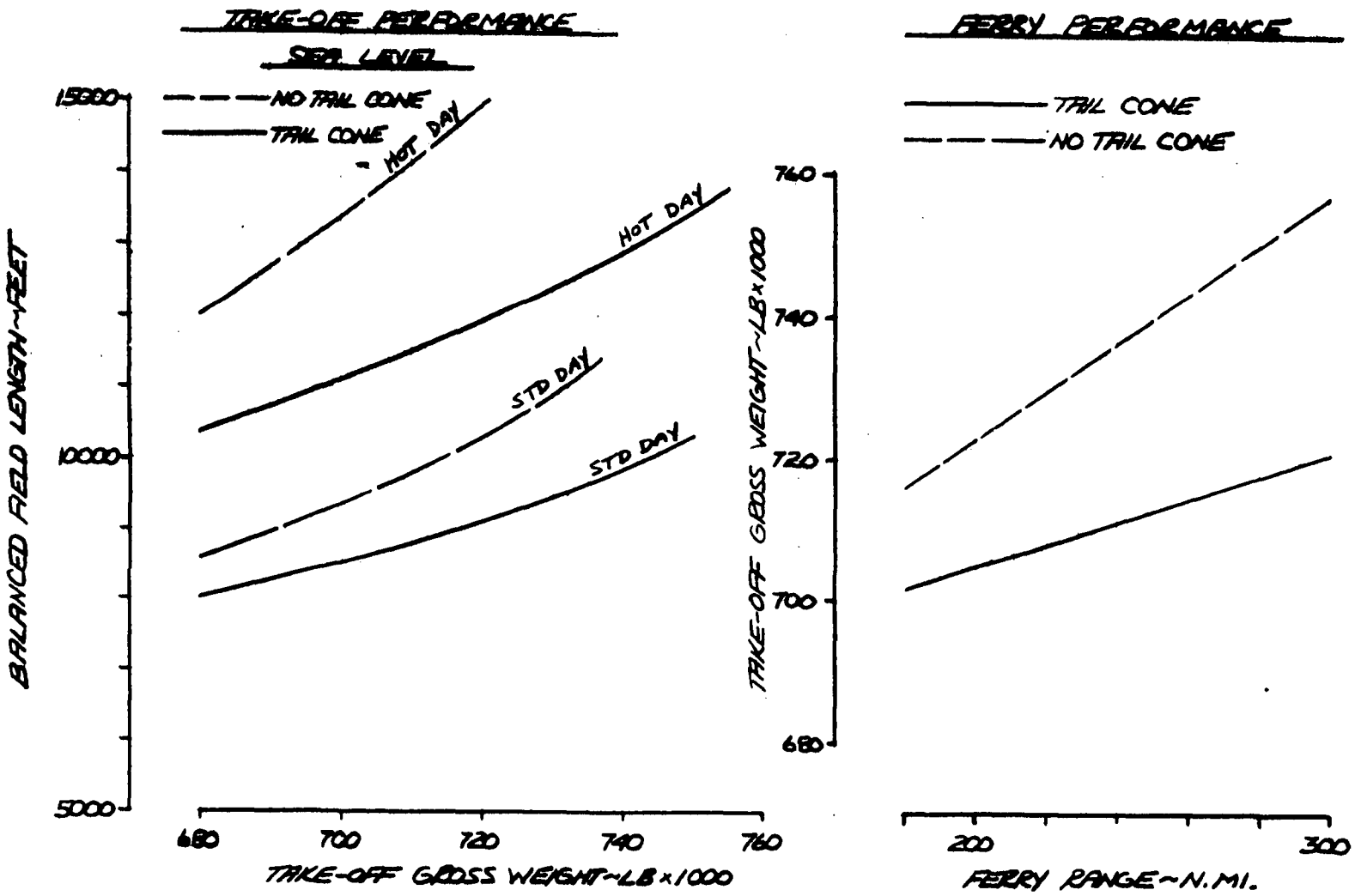

Figure 4-305. Ferry Performance Summary

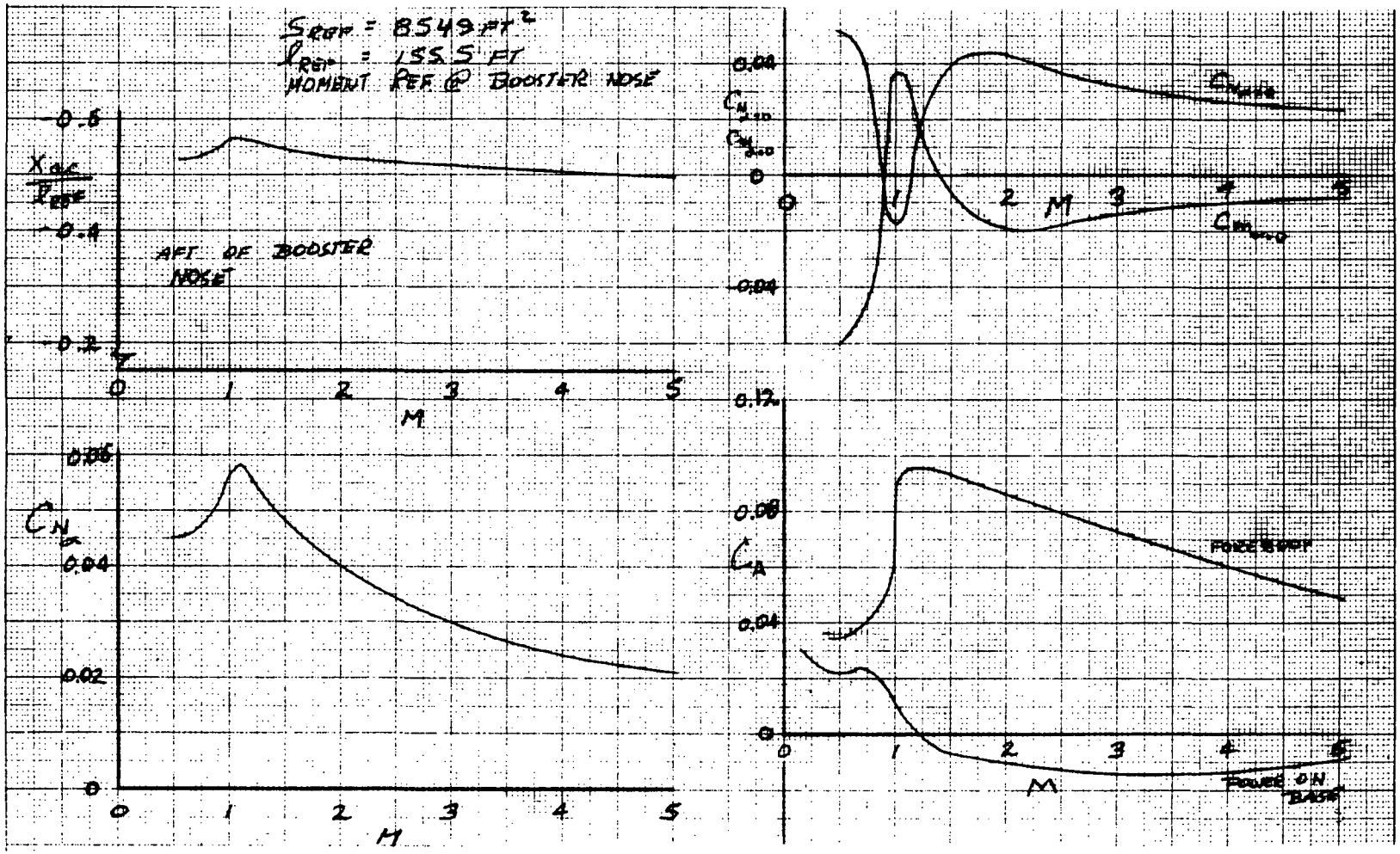

Figure 4-306. Booster Longitudinal Characteristics in Pressure of Orbiter

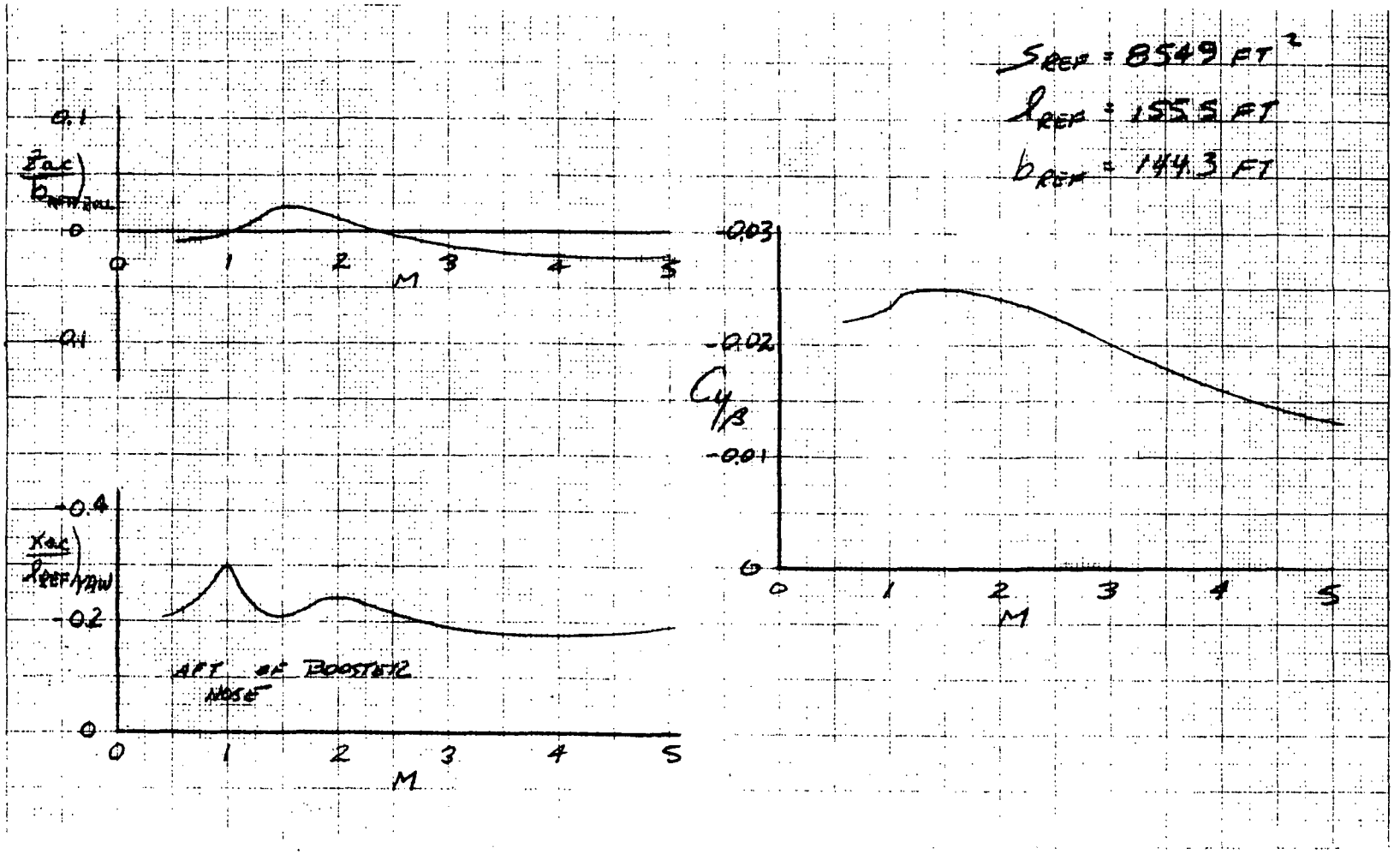

Figure 4-307. Booster Lateral Directional Characteristics in Pressure of Booster

The hypersonic aerodynamic characteristics of the booster are presented in Figure 4-308. The characteristics were predicted using the Hypersonic Aerodynamic Prediction Program, using modified Newtonian theory, adjusted by empirical correlation data. Basic longitudinal characteristics at Mach 6 are shown for discrete elevon deflections with the canard aligned at δ_c = -60 deg. The configuration is seen to be stable over the range of angles of attack from 20 deg to over 60 deg. With the center of gravity at Fuselage Station 2424 and the canard aligned at δ_c = -60 deg, the vehicle cannot be trimmed with the elevon at 60 deg angle of attack. By providing aft movement of the c.g., the vehicle can be brought into trim at the 60 deg angle of attack design point; at the aft limit set by the cruise configuration neutral point (FS 2478), the vehicle trims with elevon at δ_e = -20 deg. The canard, however, can be used to trim; with the canard held at δ_c = 0 deg, the c.g. can be ahead of the landing configuration neutral point (FS 2424) to effect trim at 60 deg angle of attack.

Transition stability characteristics of the booster are presented in Figure 4-309; Mach 2 is considered the most stringent condition for longitudinal stability as angle of attack is reduced with decreasing Mach number. Existing component data (body, wing, canard, tail) were used, with the body data adjusted using supersonic tangent-cone analysis to represent the lower fineness ratio body of B-18E-3. As in the entry case, with the c.g. at FS 2424, the vehicle cannot be trimmed to the design angle of attack at M = 2 of 30 deg with the canard aligned at $\delta_c = -\alpha = -30$ deg. By moving the c.g. to FS 2478, trim can be achieved with δ_c = -30 deg and δ_e = -10 deg. As at M = 6, the canard can be used to trim; with the canard at δ_c = 0 deg, a c.g. location of FS 2450 provides trim with the elevon at less than -20 deg.

The B-18E-3 booster cruise and landing characteristics are presented in Figures 4-310 and 4-311. Included are lift and pitching moment data for variations of canard and elevon deflections and trimmed lift and lift-drag ratio for fixed canard deflections. The data, based primarily on subsonic tests conducted in the NASA LRC/Low Turbulence Pressure Tunnel of the B-9U configuration, have been adjusted to represent B-18E-3 using component buildup data. Scale corrections have been applied to adjust from model to full scale Reynolds number.

Estimated aerodynamic loads for the booster are presented in Figures 4-312 and 4-313 for conditions corresponding to ascent maximum headwind and tailwind conditions. Body load distributions are shown, plus the contributions of the wing, canard, vertical tail and orbiter and tank, represented as point-loads.

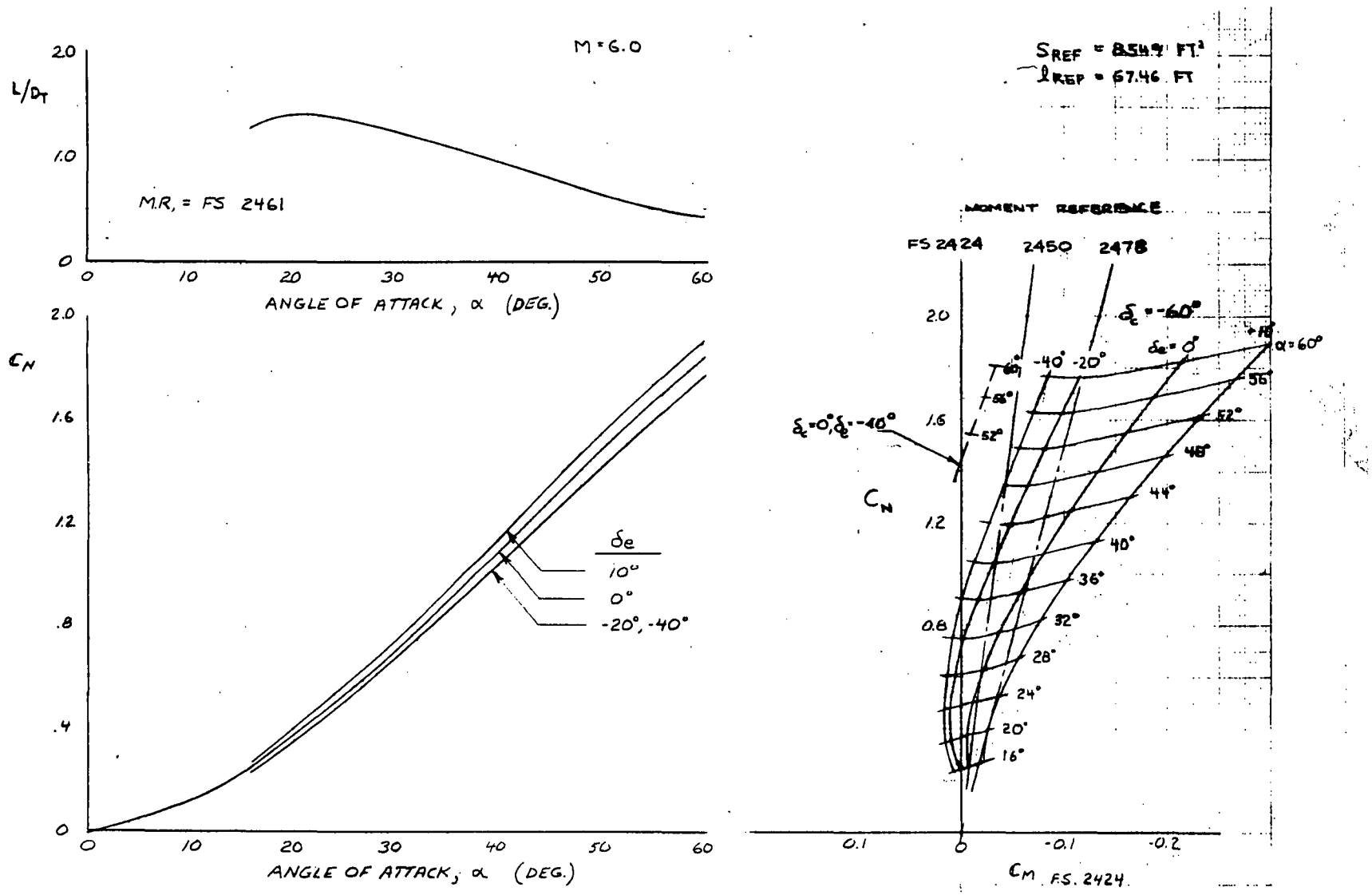

Figure 4-308. Booster Entry Longitudinal Characteristics

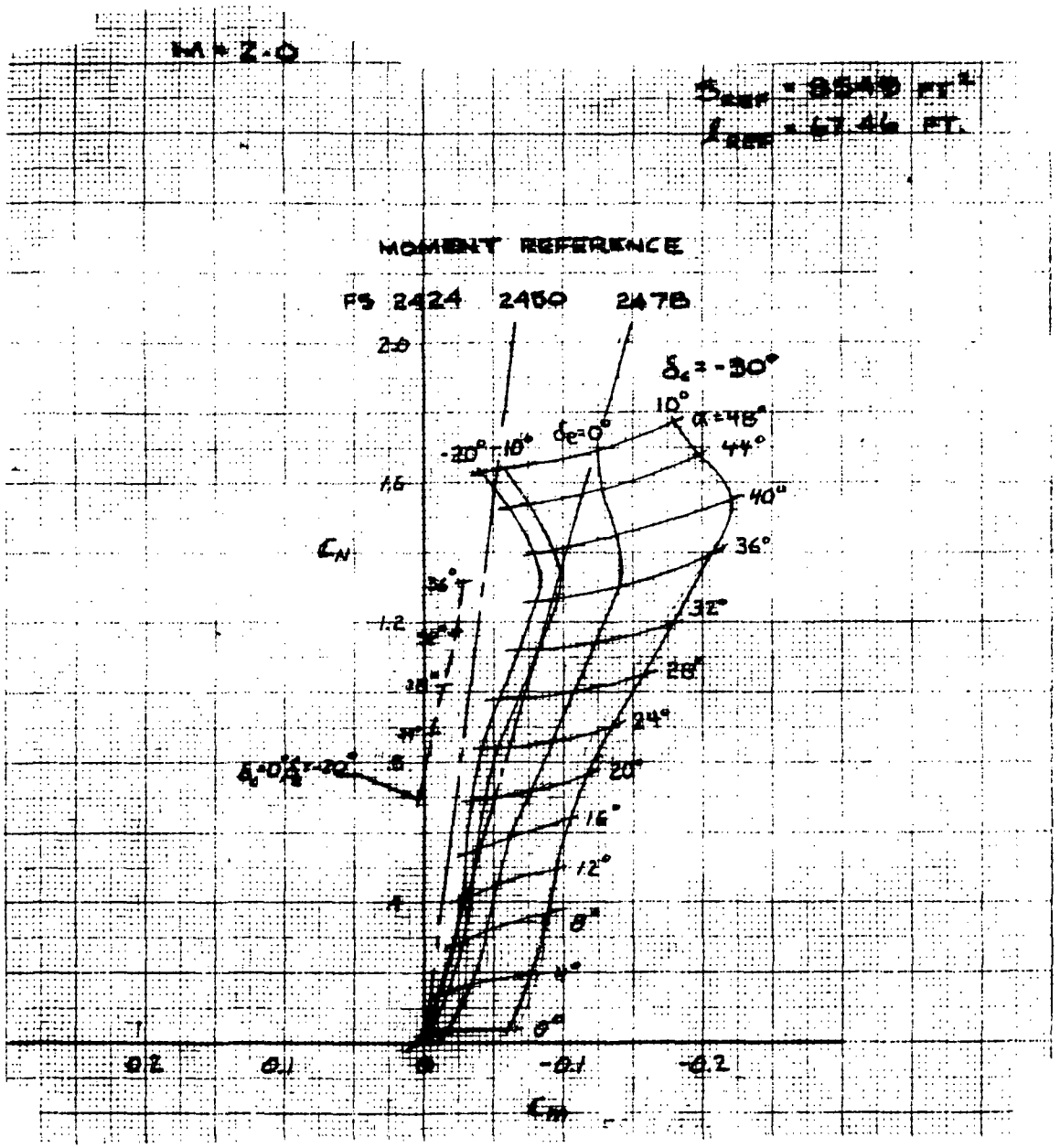

Figure 4-309. Booster Transition Stability Characteristics

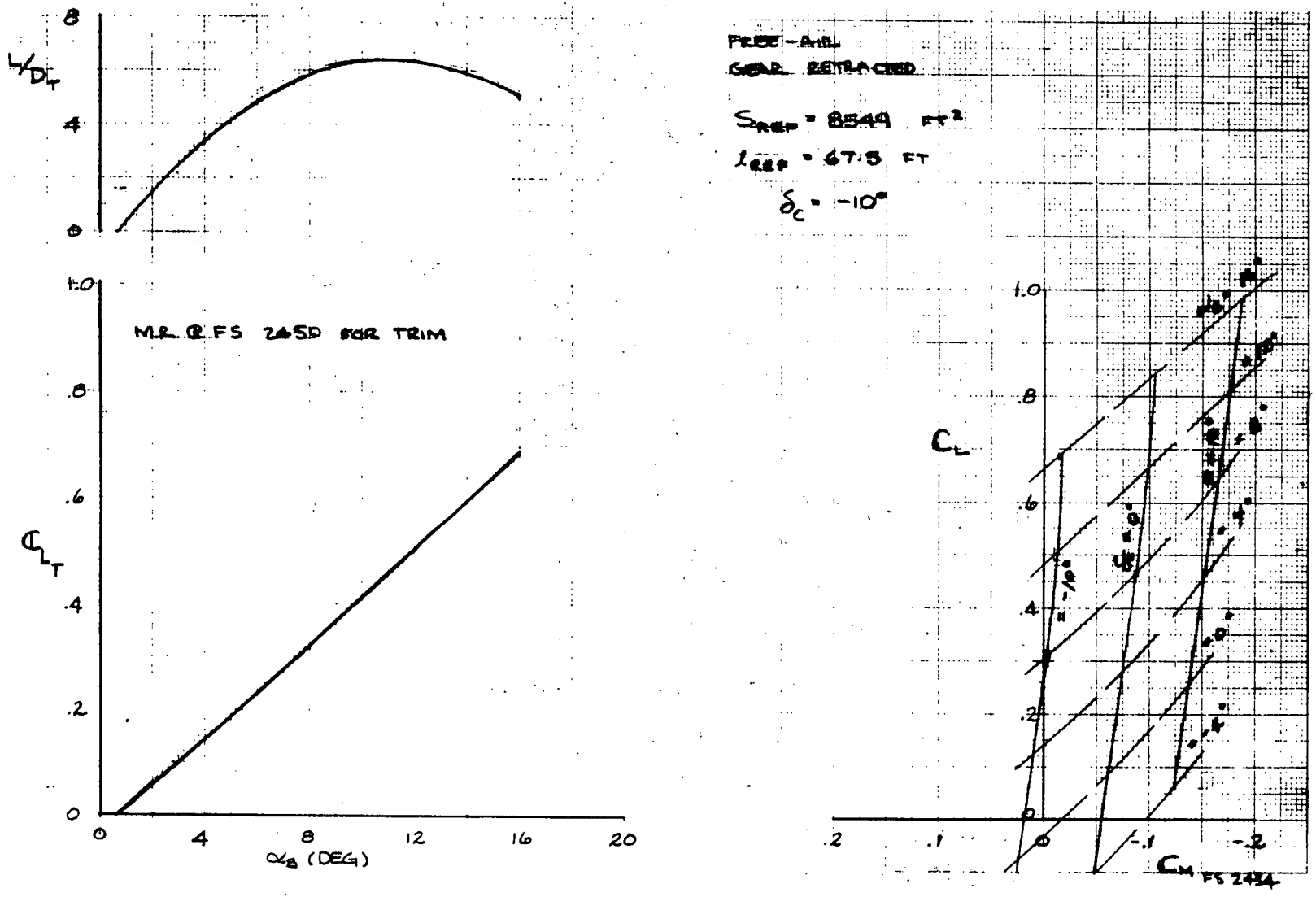

Figure 4-310. Booster Cruise Longitudinal Characteristics

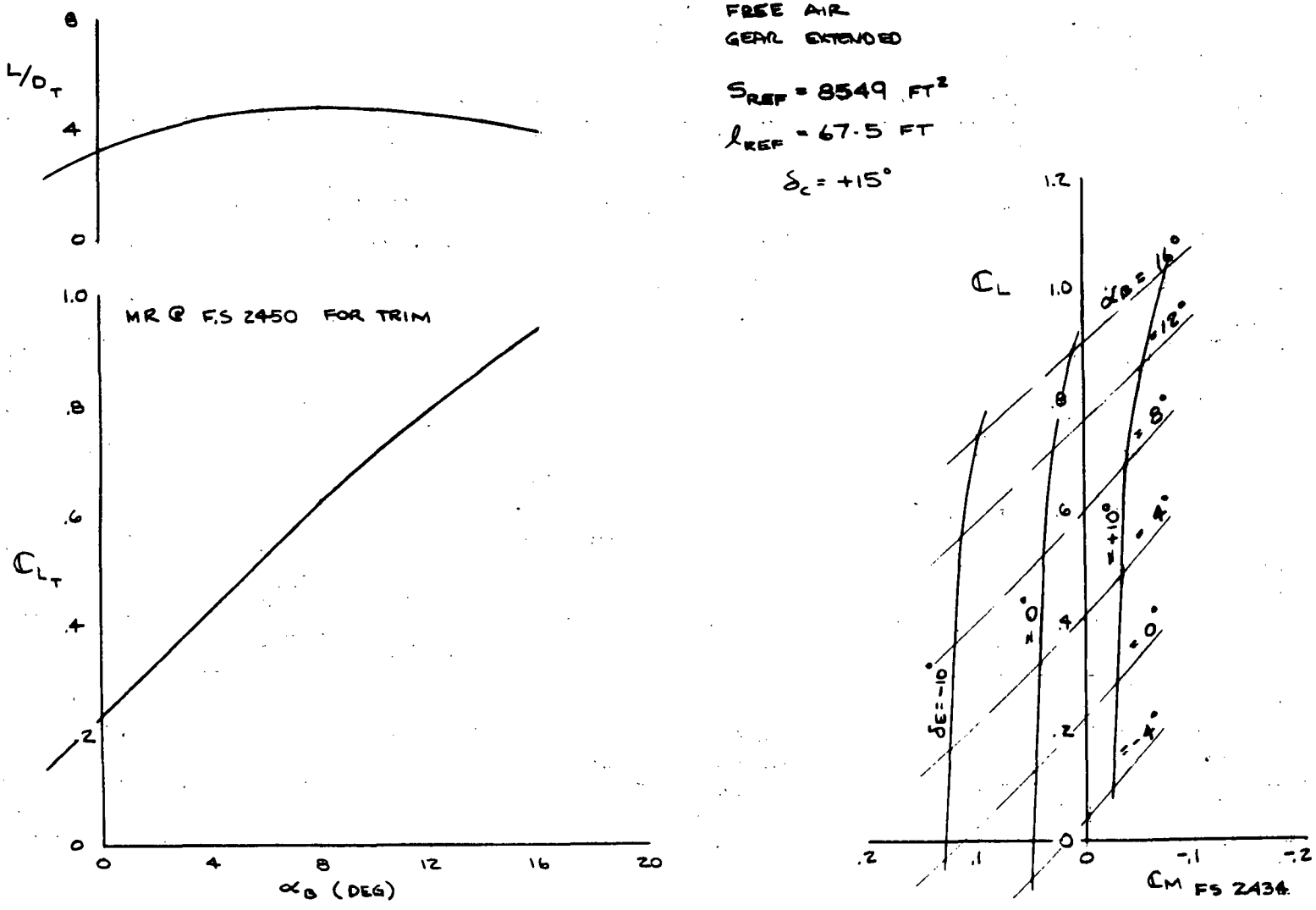

Figure 4-311. Booster Landing Longitudinal Characteristics

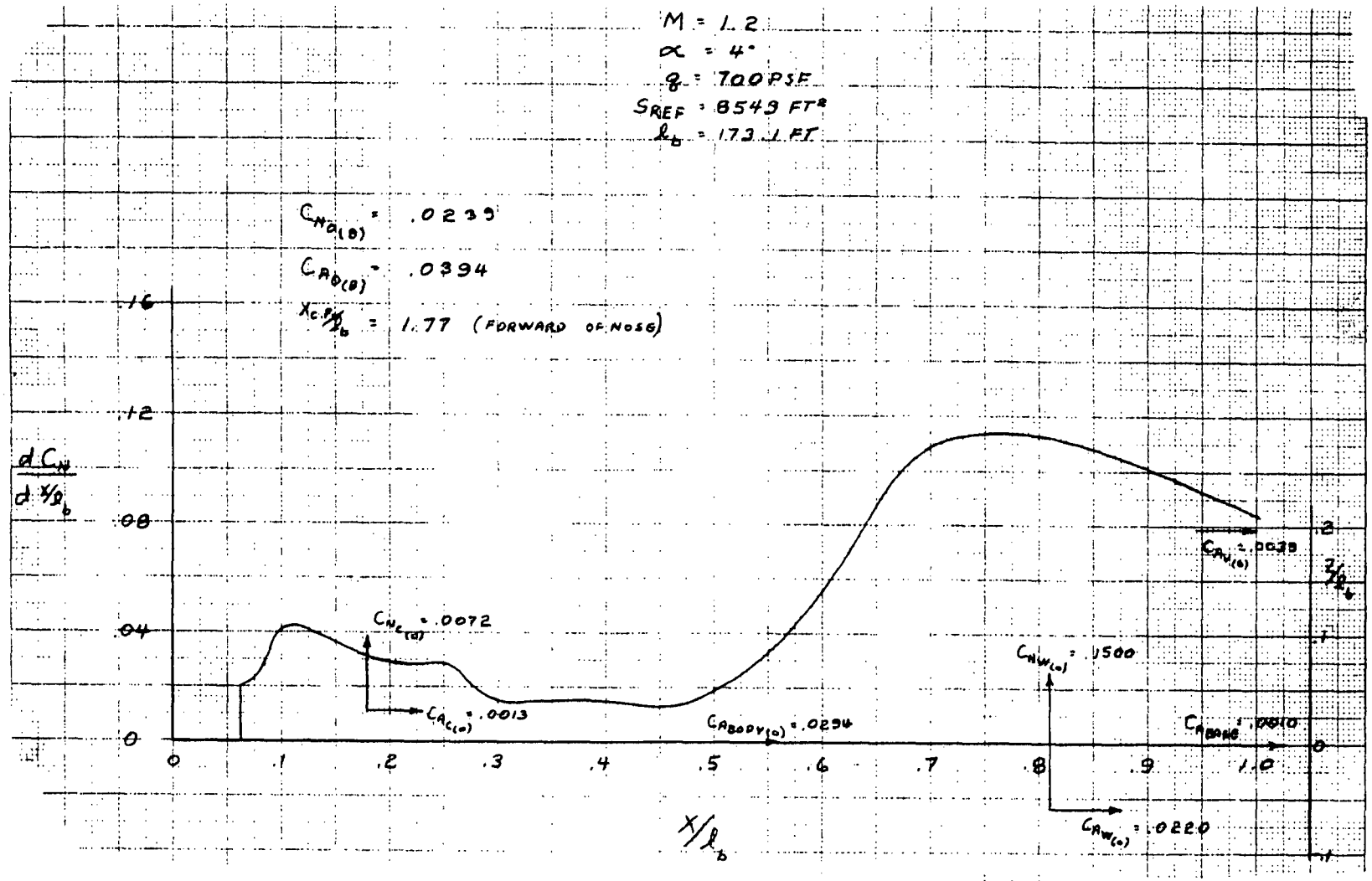

Figure 4-312. Booster Airload Distribution for Max αq Headwind Condition

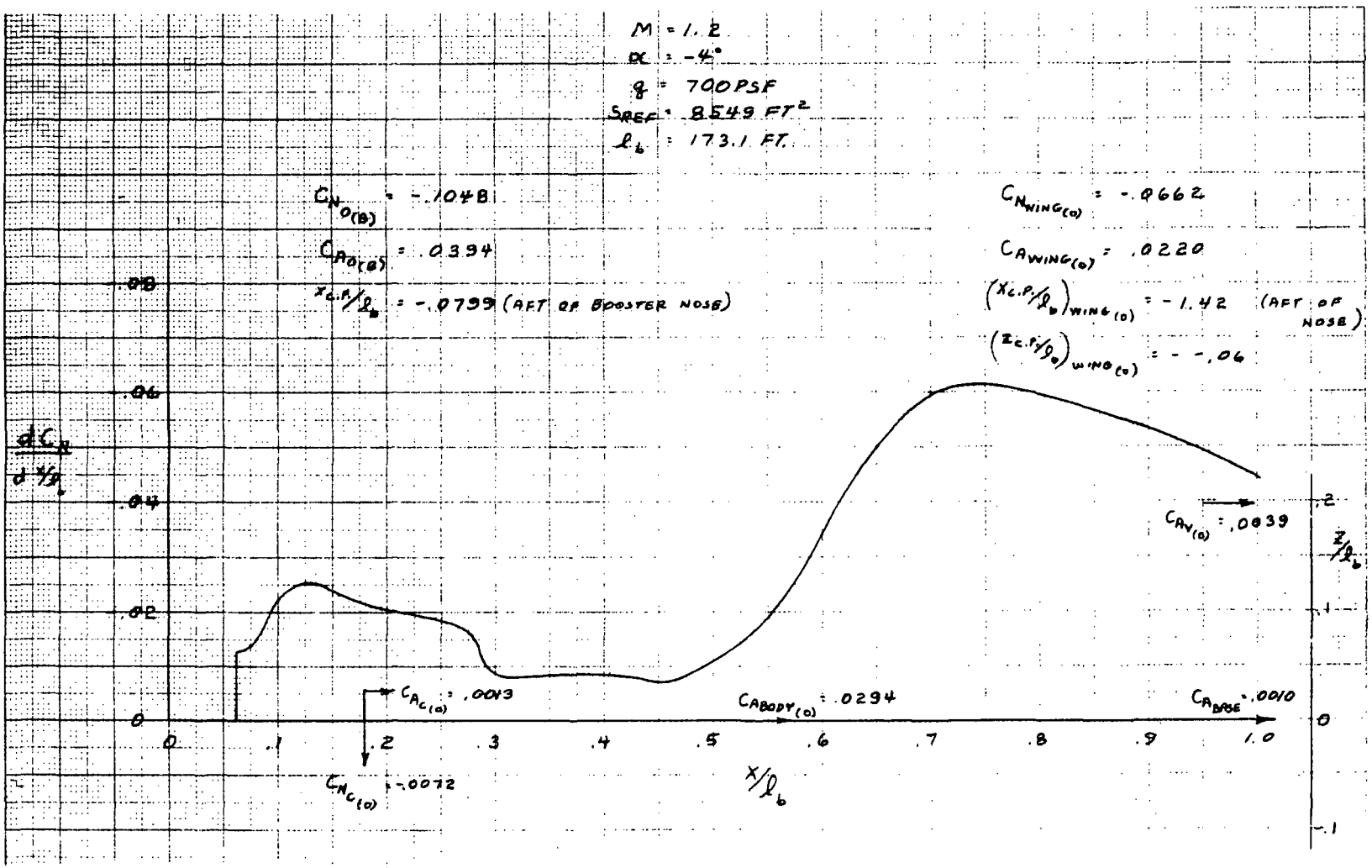

Figure 4-313. Booster Airload Distribution for Max αq Tailwind Condition

Additional primary stability and control characteristics of the B-18E-3 include directional stability during cruise and landing (vertical tail sizing) and nose gear unstick capability. Figure 4-314 presents the variation of directional stability over the angle of attack range up through landing attitude; the vehicle is seen to be statically stable for both cruise and landing. The effectiveness of the booster control system to unstick the nose gear during take-off is presented in Figure 4-315. Variations in nose unstick speeds as a function of gross weight and canard and elevon deflection are shown. Nose gear unstick speed is based on the take-off requirements of being able to rotate at or before a speed corresponding to 0.9 V_{min} (minimum usable speed). The data indicates that for a canard setting of +10°, an elevon deflection of -5° is required for all take off gross weights.

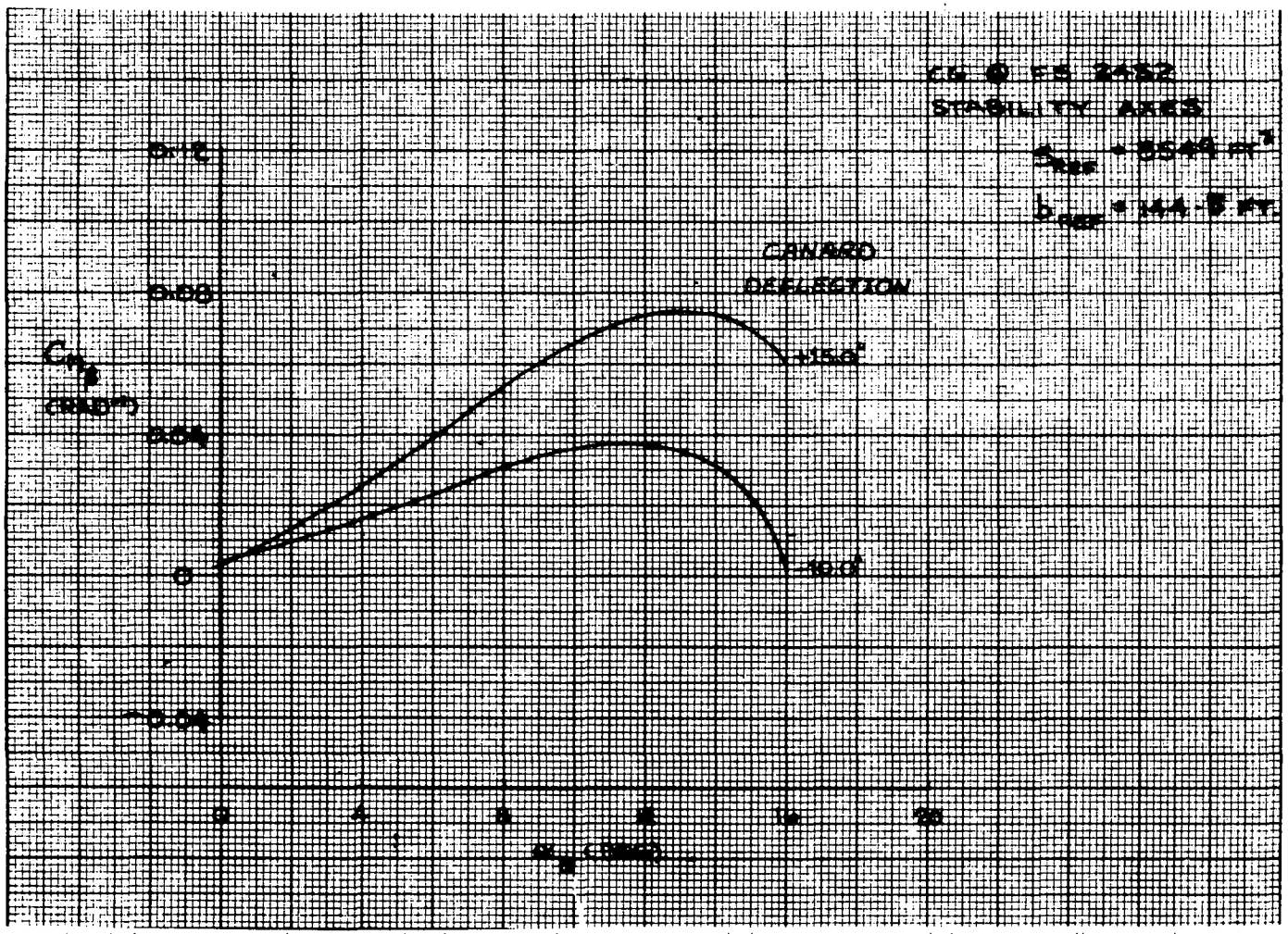

Figure 4-314. Booster Cruise and Landing Directional Stability

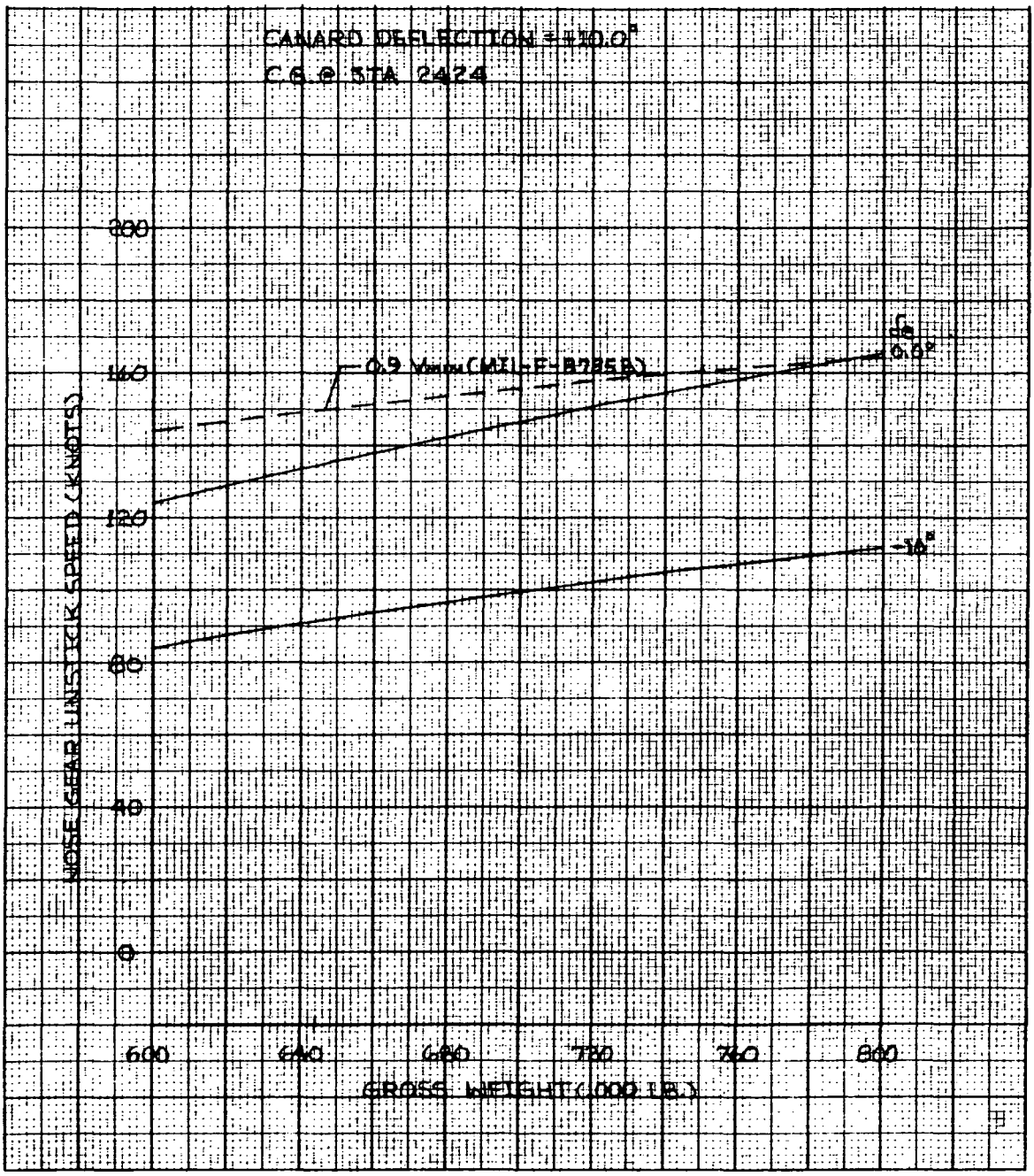

Figure 4-315. Booster Nose Gear Unstick Capability

4.4.5.6 Flight Control System and ACPS Requirements

The B-18E continues to use the flight control approach described in the Phase B final report. Following separation, control is provided primarily by ACPS, although the higher staging dynamic pressure permits use of elevons for pitch and roll control for about 30 seconds. After apogee the pitch and roll ACPS are replaced by elevon control as dynamic pressure builds up. Yaw ACPS is retained until Mach 2 and low angle of attack.

Pilot commands throughout the flight are into a pitch rate and bank rate command system with automatic turn coordination. Both channels include attitude hold functions when the pilot centers his controls. The pitch channel contains a g-limiter to control entry load factor and eliminate the danger of over stressing the vehicle.

ACPS requirements were determined from B-9U simulation experience. The following fail-safe angular acceleration requirements were set:

Pitch	0.35 deg/sec^2
Roll	0.35 deg/sec^2
Yaw	1.20 deg/sec^2

Total impulse requirements were set by scaling B-9U expenditure.

Pitch Up	76,000 lb-sec in 150 sec
Pitch Down	27,800 lb-sec in 150 sec
Roll	42,600 lb-sec in 150 sec
Yaw	399,900 lb-sec in 250 sec

The roll expenditure is divided equally between plus and minus roll. The yaw expenditure is divided 55:45 depending on the direction of turn.

The selected system uses twenty-eight 2360-16 thrusters: four on top at the nose for pitch down, four on each wing for pitch up and roll, and eight on each side at the nose for yaw.

Fail-safe acceleration capability is as follows:

Pitch	0.44 deg/sec^2, -0.42 deg/sec^2
Roll	1.09 deg/sec^2
Yaw	1.20 deg/sec^2

4.4.5.7 Loads

Ullage pressure schedules and resulting limit pressures (including head pressures) are given in Figures 4-316 and 4-317 for the LO_2 tank and in Figures 4-318 and 4-319 for the RP-1 tank.

These pressures were combined with external and inertial loads for various conditions to obtain internal design loads. Figure 4-320 shows the resulting envelope of ultimate interval loads and the conditions which are critical along the length of the body structure. Design load factors are summarized in Table 4-59.

Orbiter/booster interface loads are shown in Table 4-60.

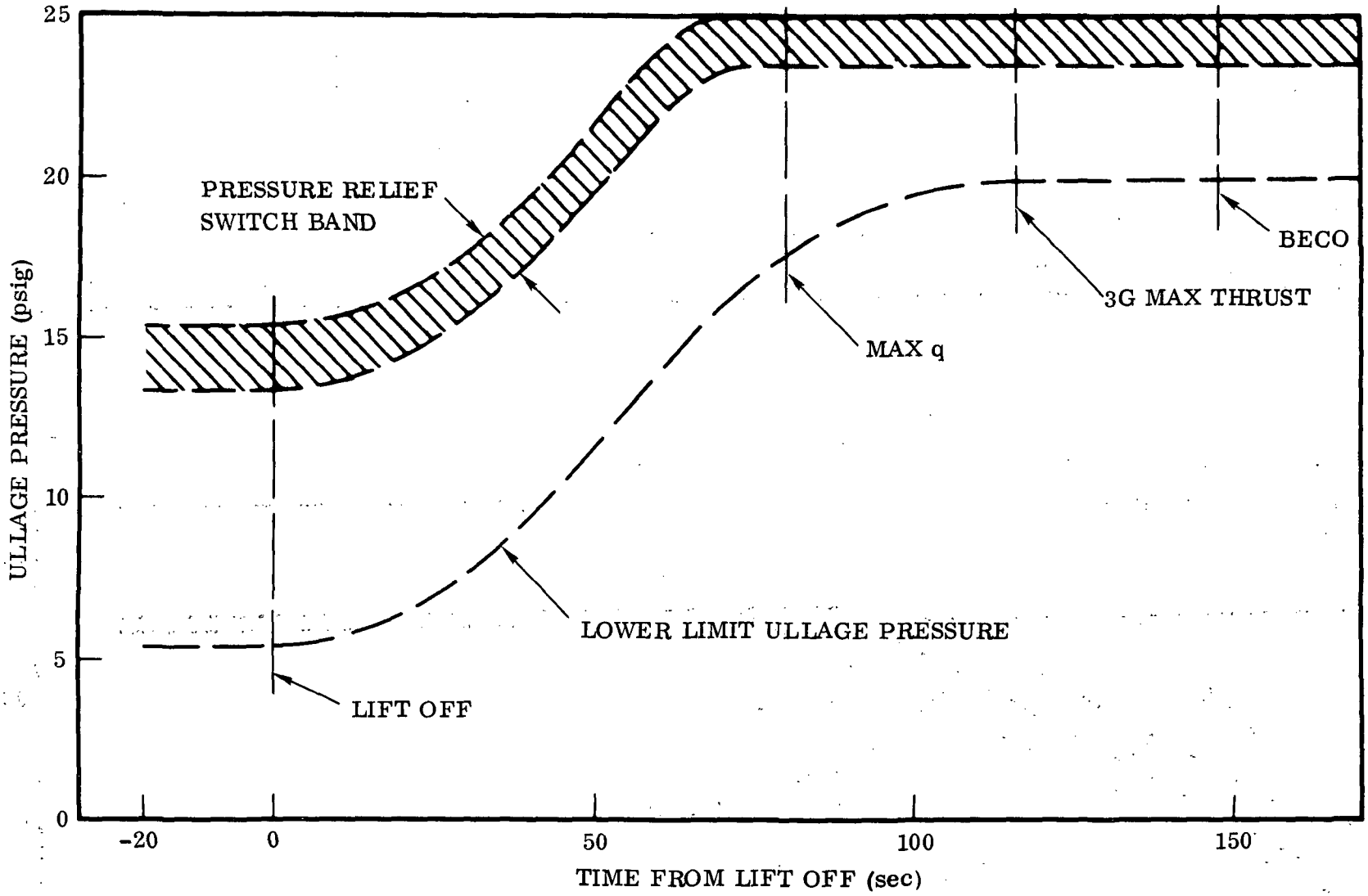

Figure 4-316. B-18E3 LO_2 Tank Pressure Schedule

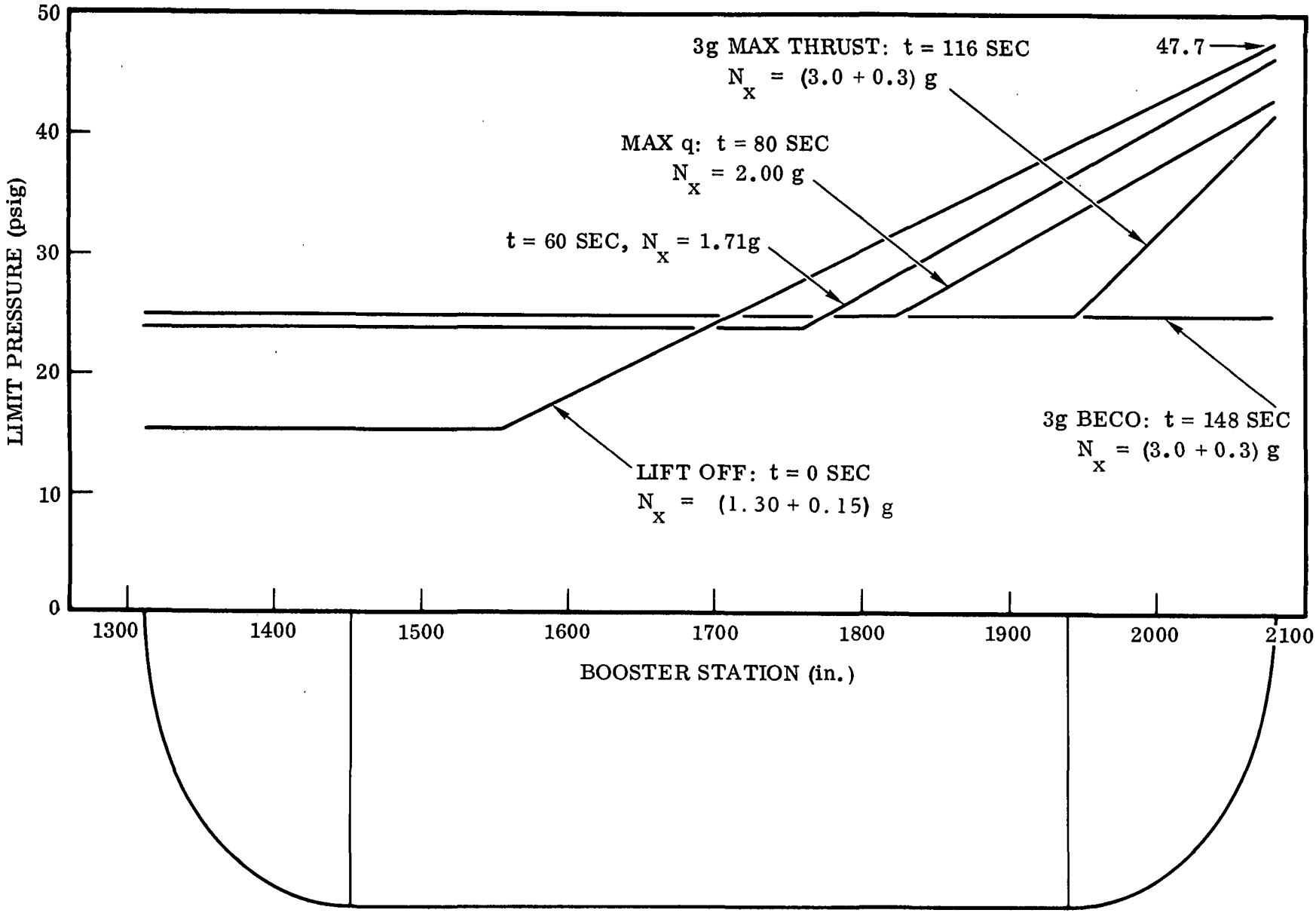

Figure 4-317. B-18E3 LO_2 Tank Limit Pressures

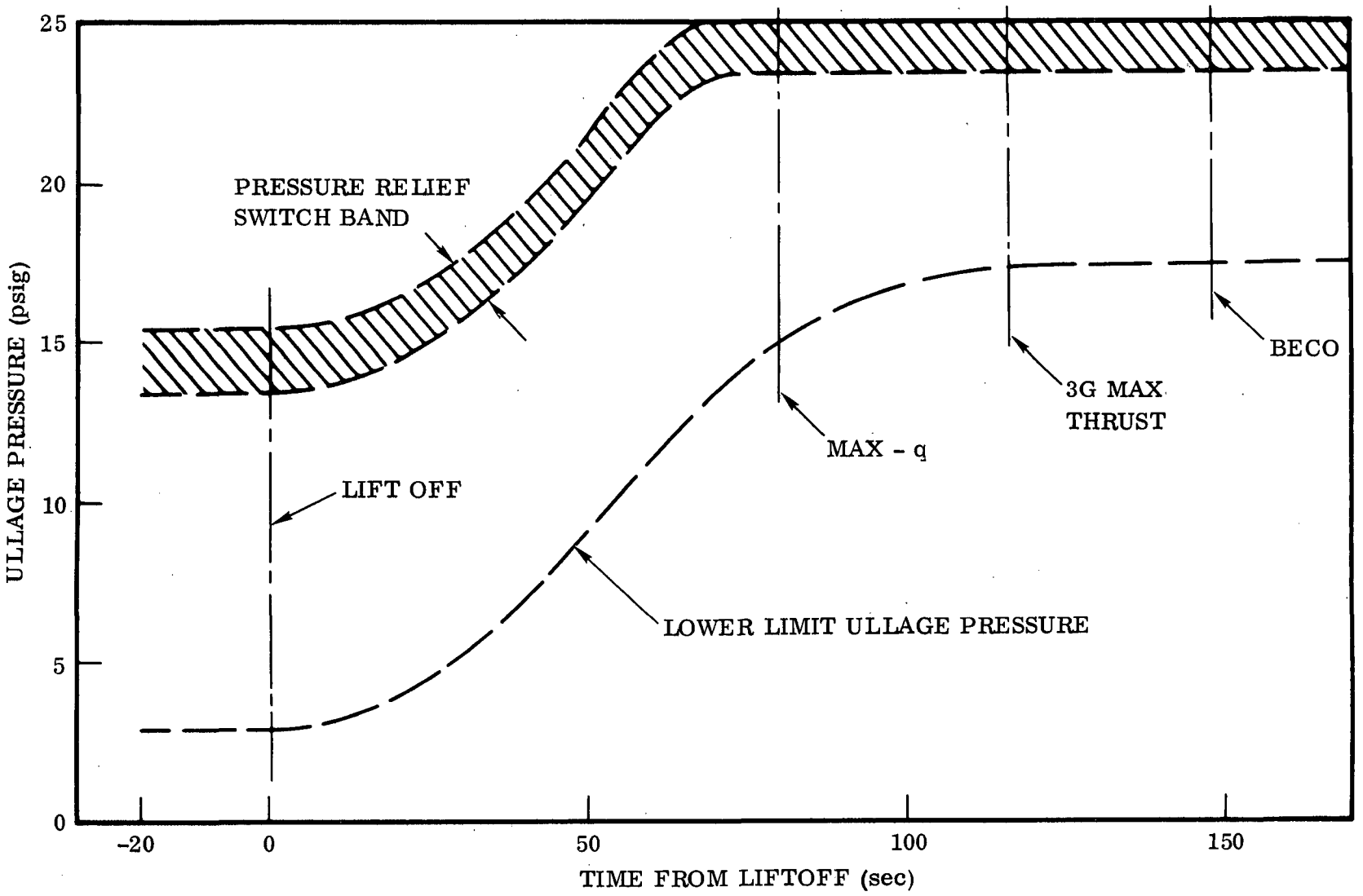

Figure 4-318. B-18E3 RP-1 Tank Pressure Schedule

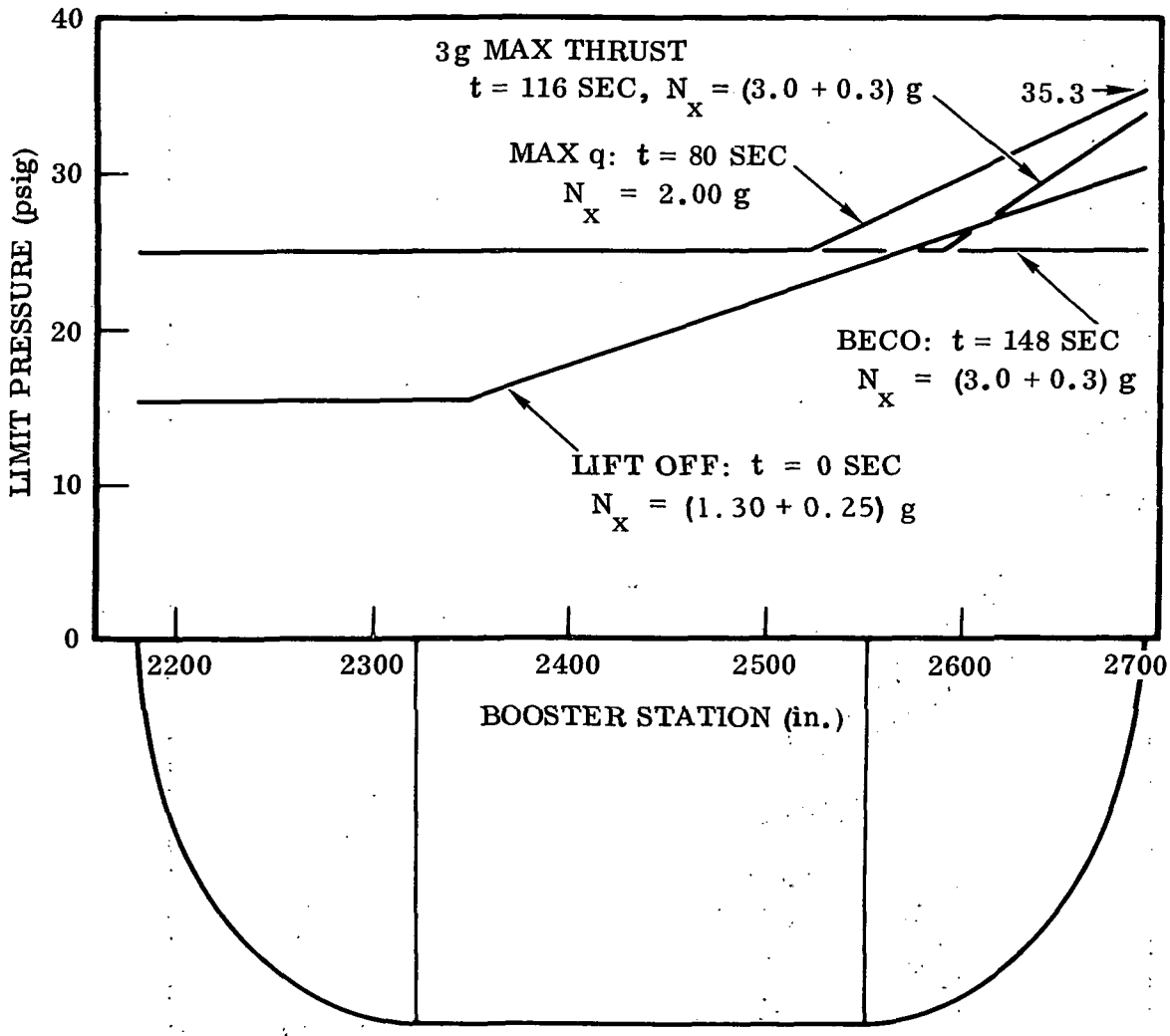

Figure 4-319. B-18E-3 RP-1 Tank Limit Pressures

1 1 Hour Groundwinds Headwinds
2 1 Hour Groundwinds Tailwinds
3 1 Hour Groundwinds Sidewinds
4 Liftoff With Headwinds
5 Liftoff With Tailwinds
6 Liftoff With Sidewinds
7 Max Q Headwinds
8 Max Q Tailwinds
9 3 G Maximum Thrust
10 3 G Booster Burnout
11 Maximum Tank Pressure

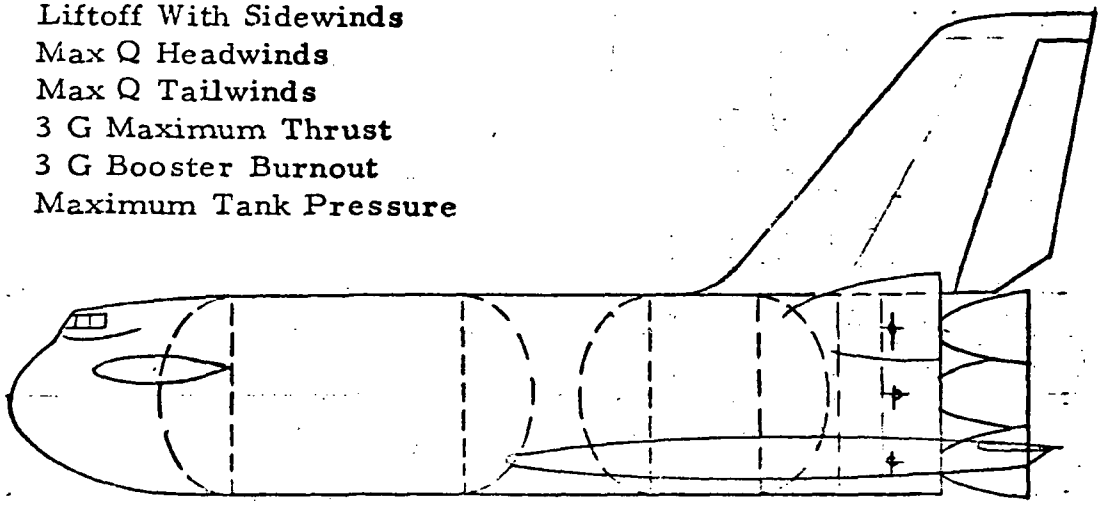

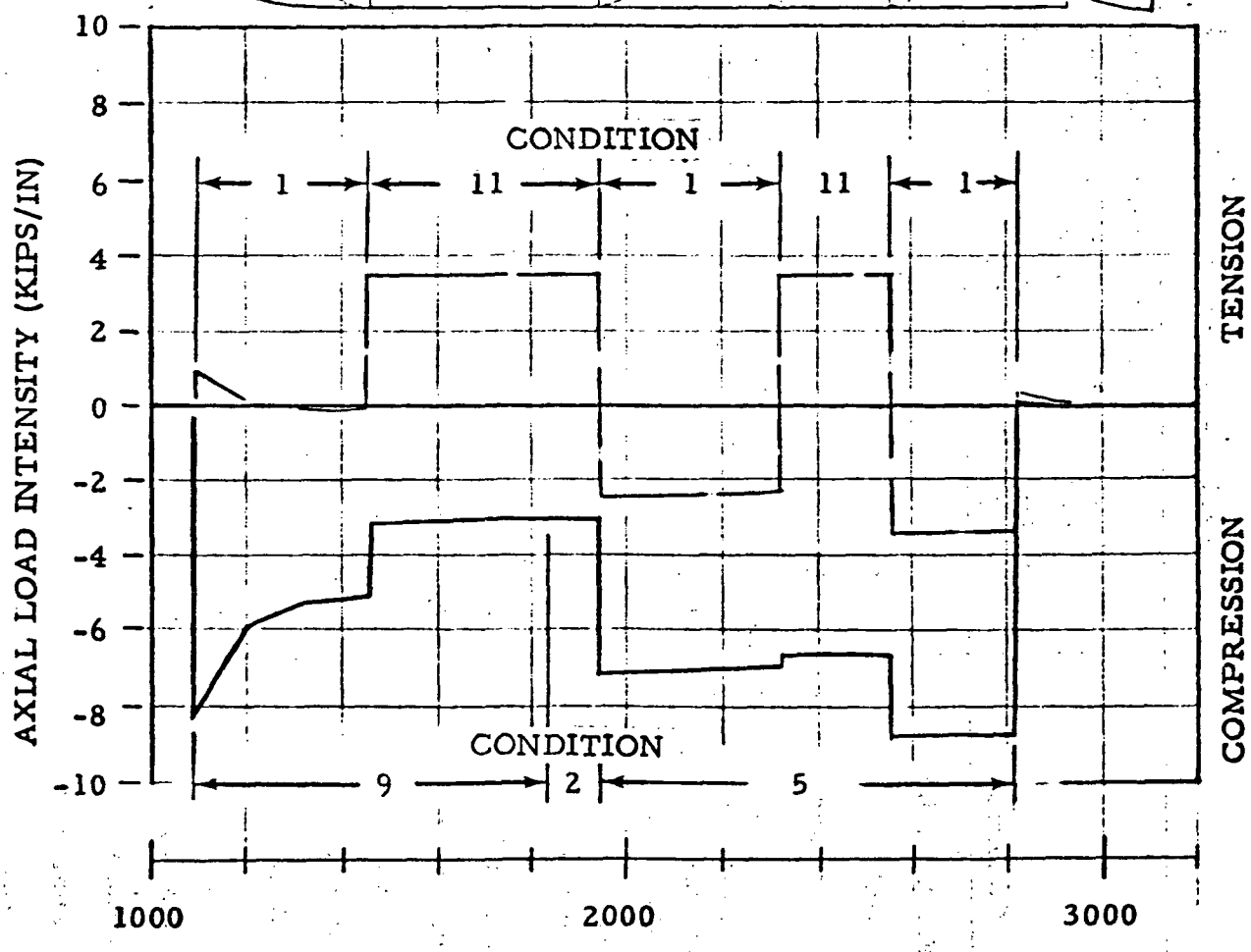

Figure 4-320. B-18E3 Ultimate Internal Loads

Table 4-59. Summary of Design Conditions

Condition	Axial Load Factor (g)	Lateral Load Factor (Yaw) (g)	Normal Load Factor (Pitch) (g)	Wind Speed at 18.3 Meters, or αq (βq)	Remarks
Two-week Standby	1.0	-	-	37.1 meters/sec	Unfueled, unpress.
One-day Hold	1.0	-	-	25.2 meters/sec	Fueled, pressurized
One-hour Launch	1.0	-	-	17.7 meters/sec	Fueled, unpress.
Liftoff				17.7 meters/sec	
LO_2 Mass	1.30 ± 0.15	0.022	-0.055		
LH_2 Mass	1.30 ± 0.25	0.022	-0.055		
Orbiter & Other	1.30 ± 0.20	0.022	-0.055		
Max Dynamic Pressure					
Headwind	1.74	-	+0.60	+2800 deg-psf	Use 1.2 factor for gust response and aeroelasticity
Tailwind	1.74	-	-0.25	-2800 deg-psf	
Crosswind	1.74	±0.18	+0.20	±2400 deg-psf	
Maximum Thrust	3.0 ± 0.30	±0.10	-0.07	±480 deg-psf	
Booster Burnout	3.0 ± 0.30	±0.10	-0.08	±100 deg-psf	
Booster Recovery	-0.46	-	4.0		
Subsonic Gust	0.23	-	2.2		
2.5g Maneuver	0.22	-	2.5		
-1.0g Maneuver	-0.04	-	-1.0		
2-Point Landing	-0.22	-	2.1		
3-Point Landing	-0.64	-	1.0		
2g Taxi	-	-	2.0		

Table 4-60. Orbiter/Booster Interface Loads

ULTIMATE APPLIED LOADS AT STATION 1084.00

COND --	PZ (LBS)	MY (IN-LB)	PX (LBS)	PY (LBS)	MZ (IN-LB)	MX (IN-LB)
1	117642	-13660991	-1452112	0	0	0
2	-78281	121718696	-1452112	0	0	0
3	19681	54028852	-1452112	100786	79981853	20113520
4	76014	77406673	-2181680	0	0	0
5	-17515	85731313	-2181637	0	0	0
6	29247	81563041	-2181500	46634	12787286	17187957
7	421228	243229727	-2854236	0	0	0
8	65275	-69584572	-2863771	0	0	0
9	104224	130014219	-4791280	0	0	0
10	118612	112866100	-4790972	0	0	0

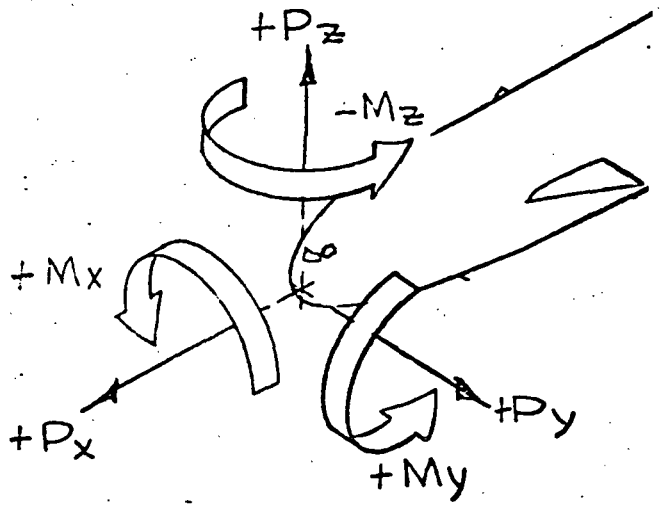

4.4.5.8 Thermal Environment

The thermal environments for the B-18E-3 space shuttle booster were predicted using the flight trajectory shown in Figure 4-321 and the 1963 Patrick Atmosphere (Ref. Terrestrial Environment (Climatic) Criteria Guidelines for Use in Space Vehicle Development, TMX-53872, George C. Marshall Space Flight Center, Alabama, 15 March 1970.) The aerodynamic heat heating methods selected conform to the Phase B methods (Ref. Phase B Final Report, Volume II Technical Summary, Book 3 Booster Vehicle Definition, Report No. SD 71-114-2 (MSC-03307), 25 June 1971.) and were verified by test program experimental data (Ref. Roberge, A.M. and Otwell, R. L., Heat Transfer Verification Test, Convair Report 76-549-4-195, 6 August 1971).

The reported heat transfer rates are for nominal trajectory, prediction methods and atmospheric conditions. These rates were calculated using heat sink thermostructural models to determine skin thicknesses required to maintain the maximum predicted temperature at a pre-determined level.

Maximum temperatures, material types and thickness requirements are for the heat transfer rates and are shown in the Structure and TPS section.

Subsequent to development of the environmental data presented in this section the flight trajectory shown on Figure 4-321 was changed. The staging velocity was decreased to 6000 fps from the 6450 fps of Figure 4-321. Figures 4-300 and 4-301 show the final trajectory. A check point on the oxygen tank indicated that the peak recovery heating was reduced to 1.12 Btu/ft^2 sec. However, the energy input and hence wall temperature was less on the revised trajectory because of the reduced flight time associated with the lower staging velocity. A complete analysis of the reduced staging velocity trajectory will be accomplished at a later date.

Fuselage. The recovery stagnation point during ascent was analyzed as a 30° cone and during descent as an 8 foot diameter sphere to account for the relative high angle of attack entry. Points on the body lower surface were analyzed as a flat plate during ascent and as a turbulent swept cylinder at angles of attack above 20°. Boundary layer transition onset was taken at a Reynolds number of one million and completion at two million for flat plate and conical flow. Figures 4-322, 4-323, and 4-324 show heating rate histories.

Wing. The wing lower surface was analyzed as a flat plate during ascent when the angle of attack is nearly zero and as a flat faced turbulent swept cylinder during the high angle of attack entry phase. The flat plate boundary layer transition criterion used was the same as the fuselage lower surface points. Figure 4-325 shows a typical heating rate history.

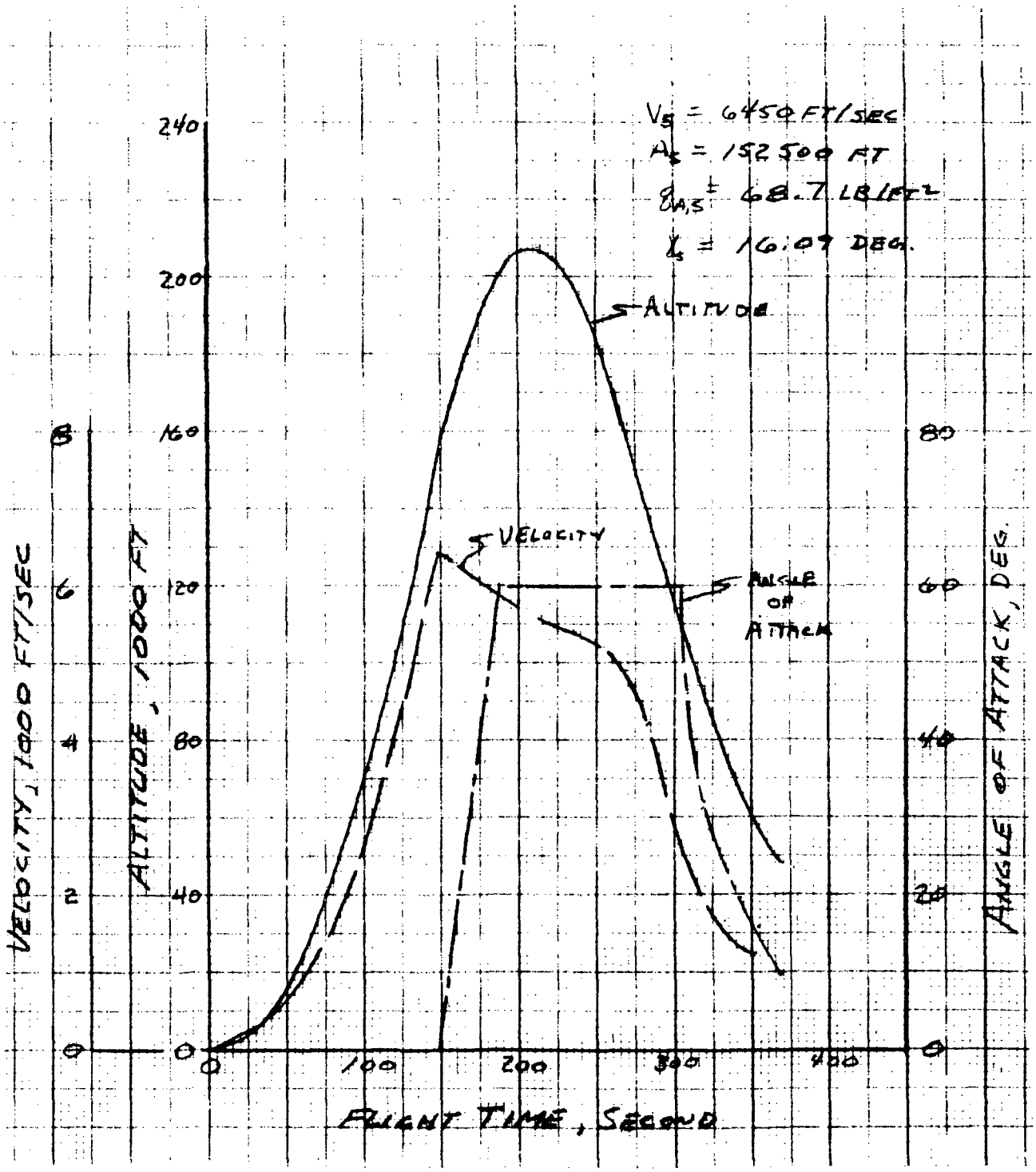

Figure 4-321. Space Shuttle Booster Flight Trajectory Number T-B18-E03

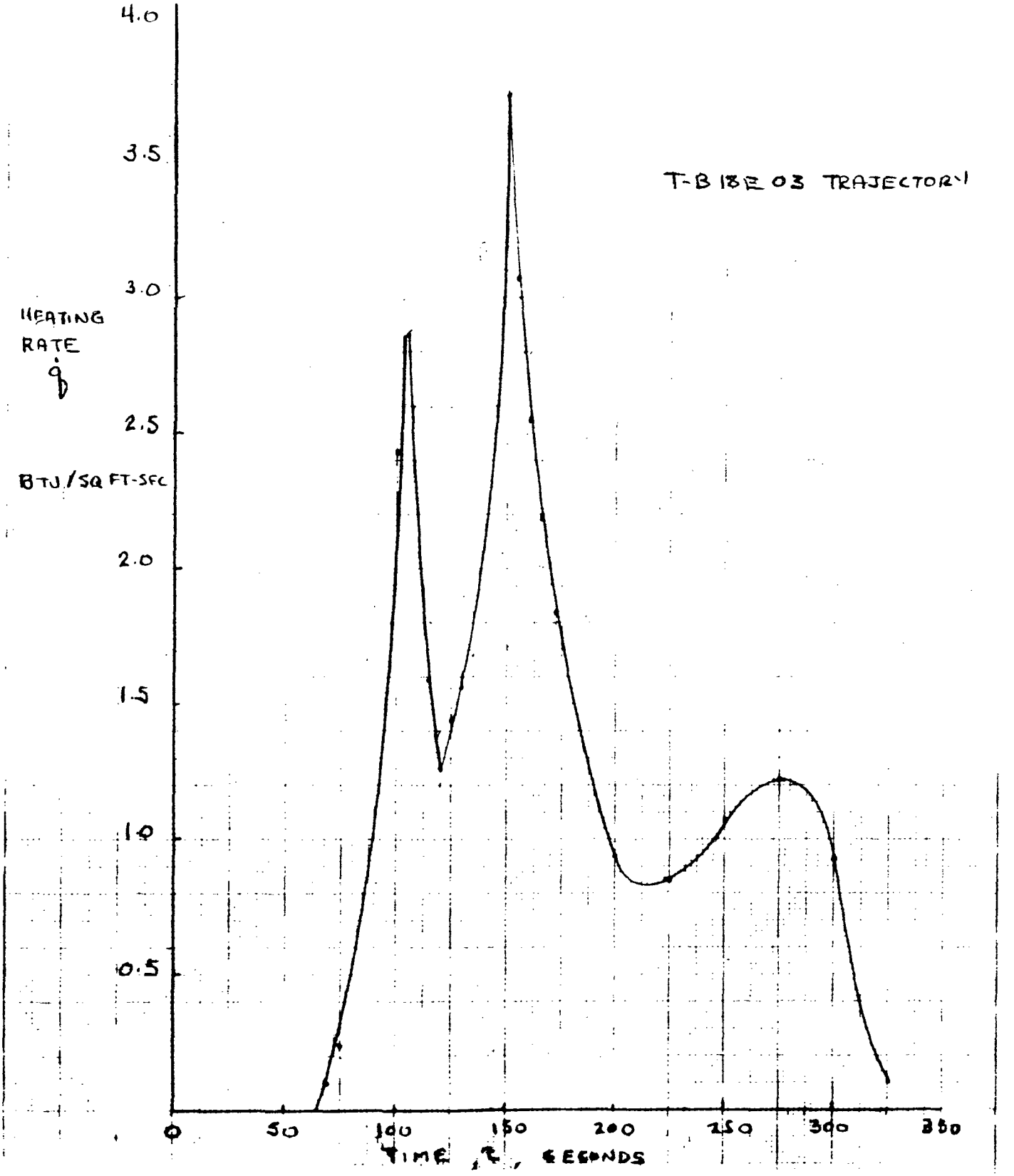

Figure 4-322. Recovery Stagnation Heating Rate History

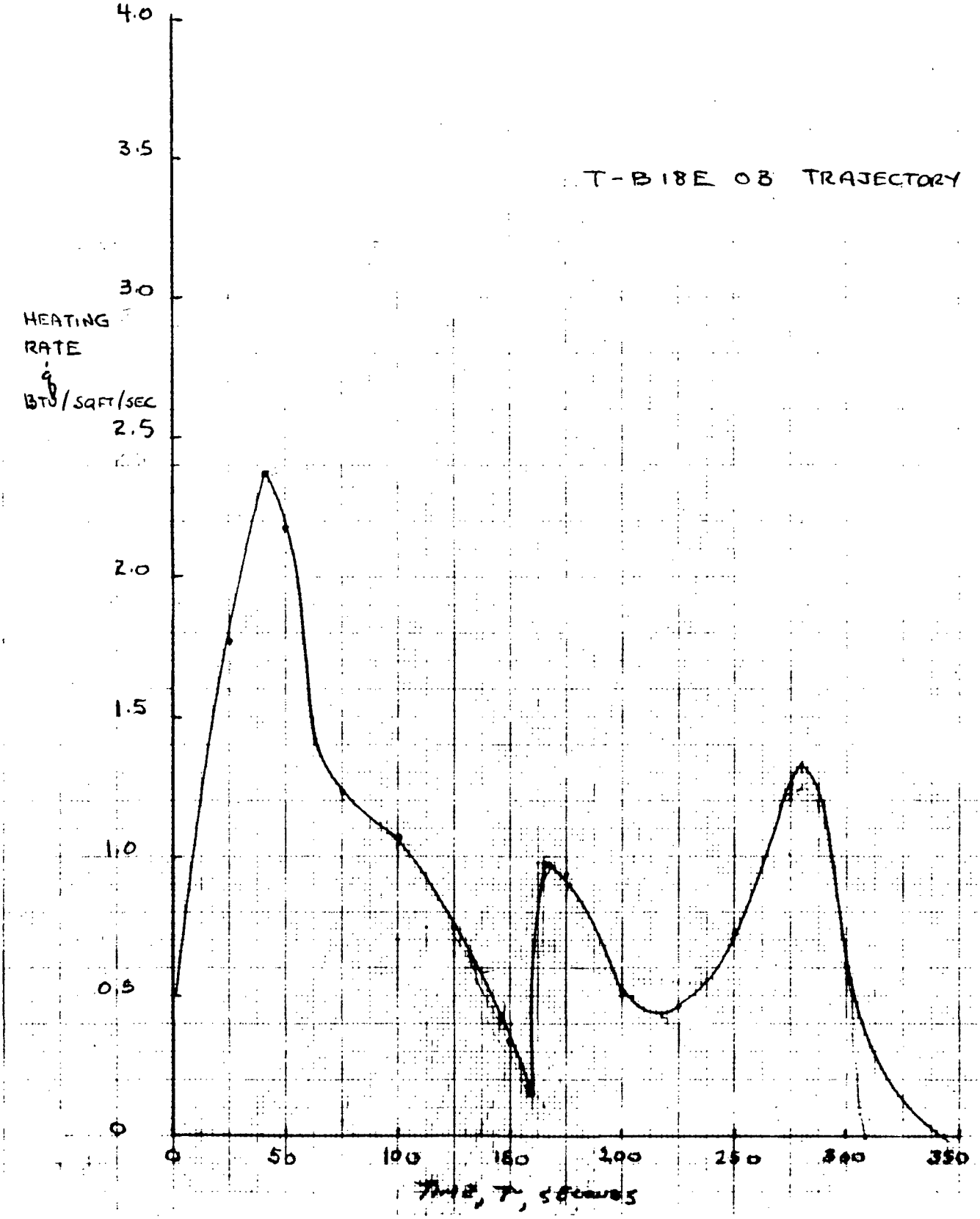

Figure 4-323. LO_2 Tank Bottom Centerline Heating Rate History

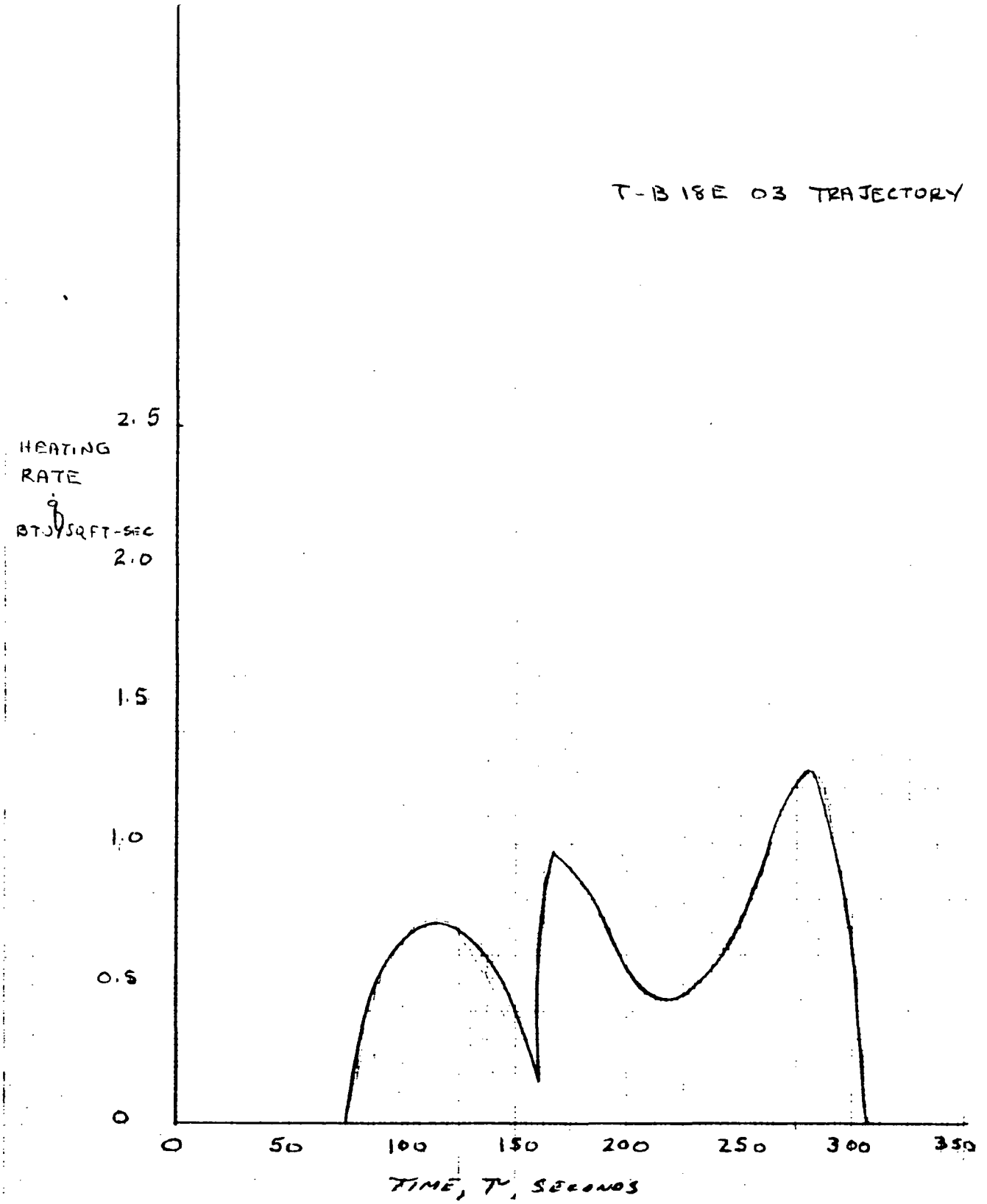

Figure 4-324. Intertank Adapter Centerline Heating Rate History

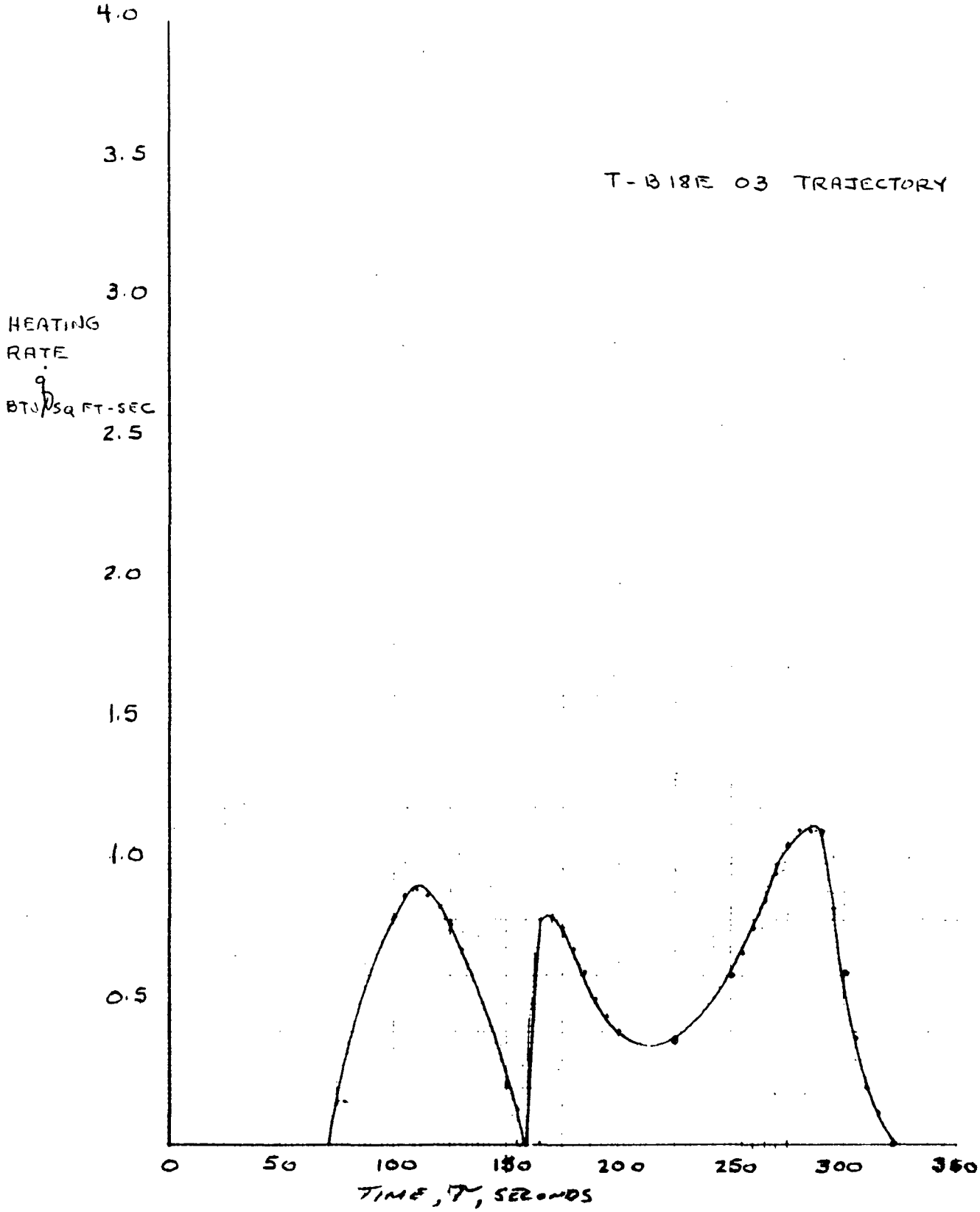

Figure 4-325. Wing Lower Surface Heating Rate History

The wing will be subjected to heating from the F-1 engine exhaust plumes. This potential problem will require further investigation.

Base. The base heating environment is shown in Figure 4-326. These values were measured during S-1C flight AS-502 (Ref: Mullen, C. R. and Bender, R.L., Saturn V/S-1C Stage Base Thermal Environment, J. Spacecraft, Vol. 6, No. 10, October 1969.

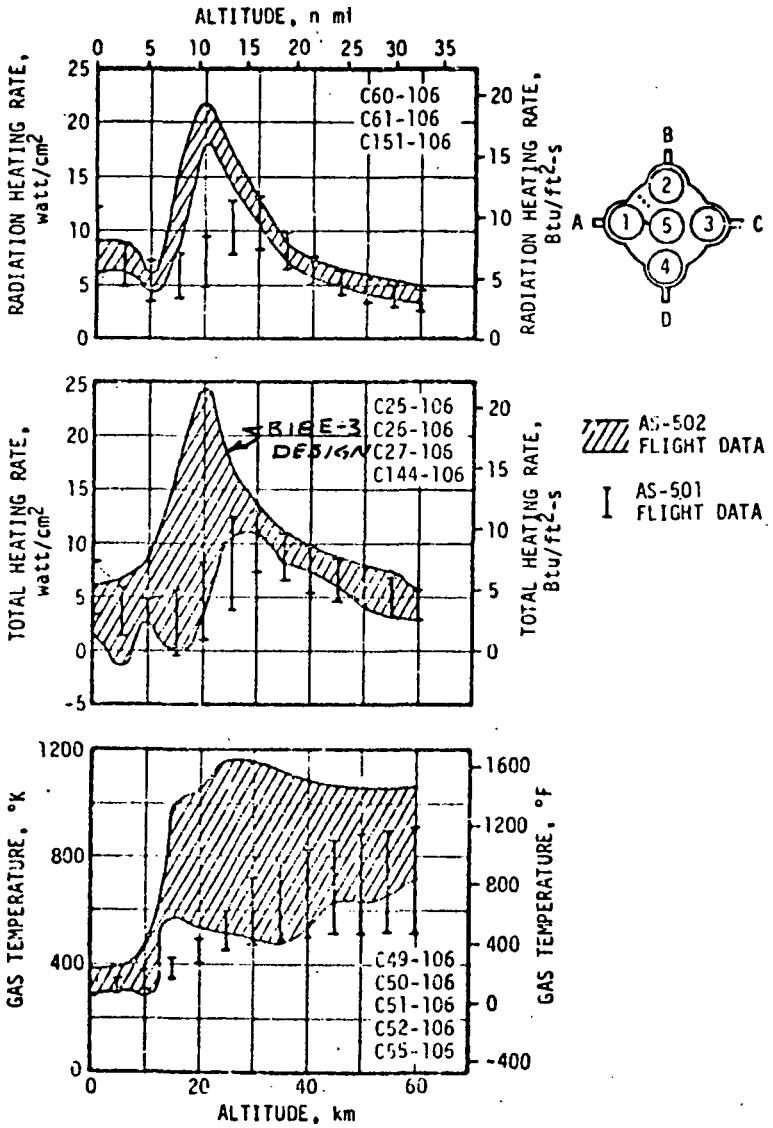

Figure 4-326. B-18E-3 Base Heat Shield Environemnt (SIC Environment)

4.4.5.9 Structure

Design Criteria. The criteria used in the booster structural design conform to those listed in Section 6.1.1 of SD 71-114-2, "Space Shuttle Phase B Final Report, Volume II, Technical Summary."

Current structural design has been accomplished on the basis of thermal data derived for the 6450 fps staging velocity trajectory presented previously. The final systems synthesis in the study reduced the staging velocity to 5904 fps. Figures 4-332 and 4-334 give an indication of the difference in heat sink requirements due to the reduced velocity.

Materials. Materials used on the B-18E booster are shown in Figure 4-327 and listed in Table 4-61. A discussion of these materials and a summary of the temperature dependent properties is given in Section 6.1.1 of SD 71-114-2.

Table 4-61. Materials Used in B-18E Booster

Material	Max. Permissible Temperature (F)	Rationale
Aluminum 2219-T87	300	Above 300 F material strength decreases rapidly.
Aluminum 2024-T851	400	Reasonable creep allowable; avoids severe degradation at higher temperatures.
Titanium 6AL-2 Sn-4 Zr-2Mo Duplex Annealed	900 (Leading Edges)	Good creep allowable; severe reduction in creep strength at higher temperatures.
Titanium 6AL-4V Annealed	650 (Structure)	Stress corrosion cracking limits use above 650 F to very short time and low stress.
Rene' 41 HT and Aged	1650	Above 1600 F intergranular oxidation occurs. Exposure time at 1650 F on the booster is short enough to be acceptable.

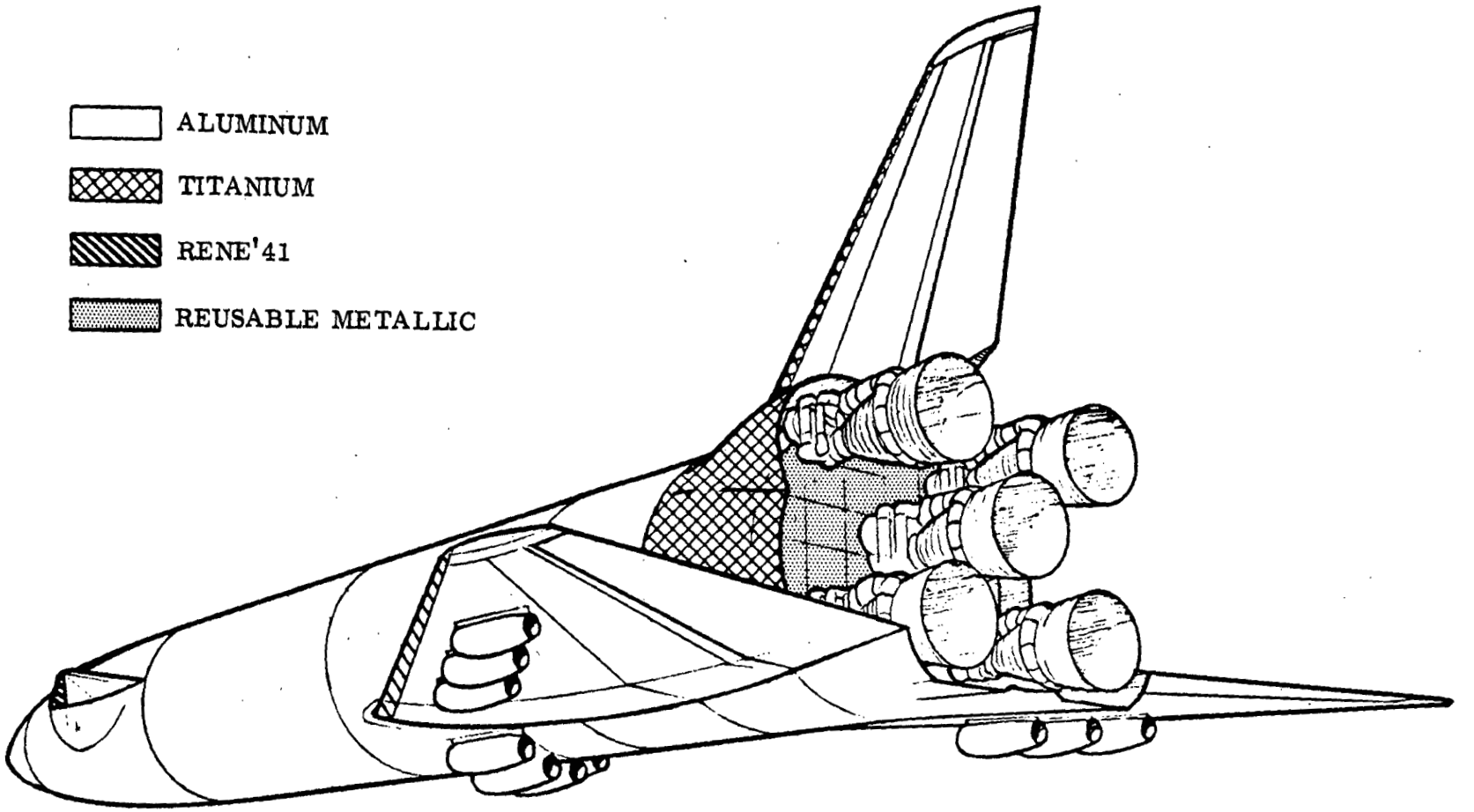

Figure 4-327. B-18E Materials

Structural Analysis. A study has been made to determine the suitability of the S-1C LO_2 and RP-1 tanks with the B-18E booster structural requirements. Tank pressures and design loads were presented previously.

LO_2 Tank. The S-1C LO_2 tank structure is over strength for B-18E loads. A comparison of S-1C and B-18E structural requirements is presented in Figure 4-328.

RP-1 Tank. The S-1C RP-1 tank structure is over strength for B-18E loads. A comparison of S-1C and B-18E structural requirements is presented in Figure 4-329.

Intertank. A new intertank structure is required (Figure 4-330). The length is increased 120 inches from the S-1C intertank to accommodate flyback engines. Loads have been given previously in Section 4.4.5. The shell sizes for the top and sides are presented in Table 4-62. Longerons provide structural continuity through the engine bays. The intertank shell on the lower surface requires a heat sink skin thickness of 0.33 in.

Table 4-62. Intertank Shell Sizes
(Material 2024 - T851)

	b_s	t_s	b_w	t_w	b_f	t_{BAR}	$N_{X\,ult}$
TOP	4.0	.10	2.0	.130	.80	.187	6800
SIDES	4.0	.10	2.0	.130	.80	.187	6800
LWR QUARTER	4.0	.11	2.0	.120	.80	.190	7300

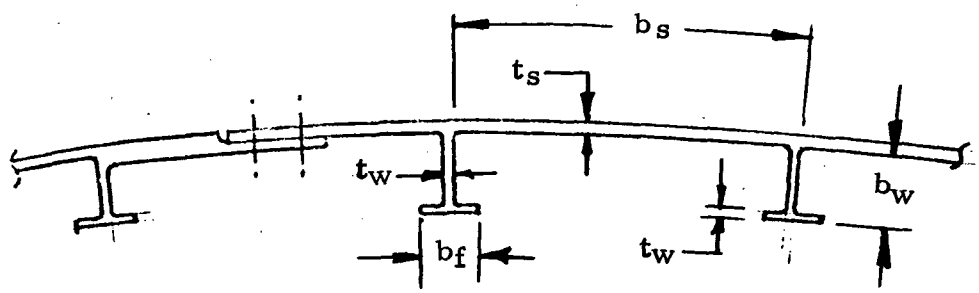

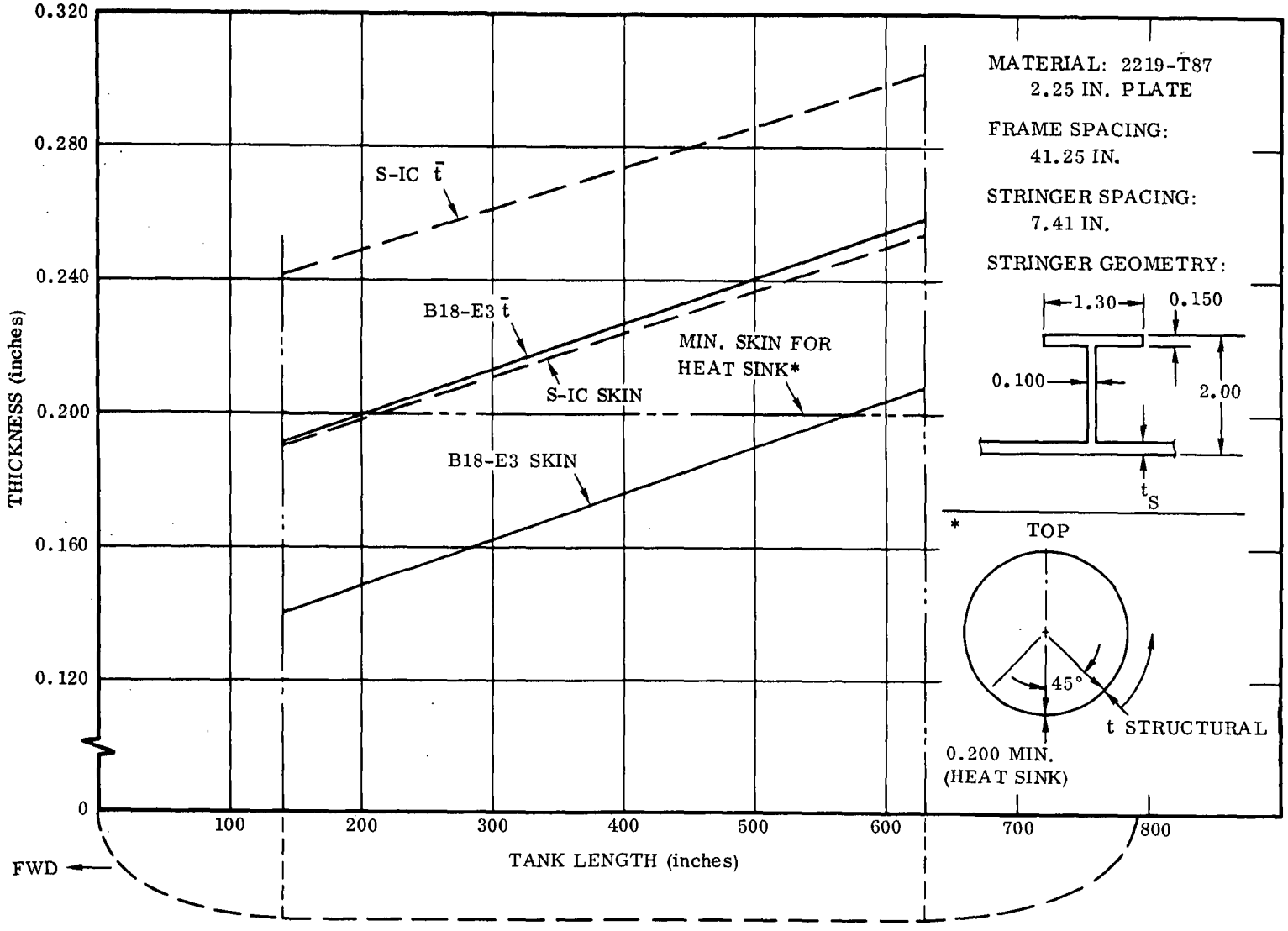

Figure 4-328. Comparison S-1C and B-18E LO_2 Tank Structural Requirements

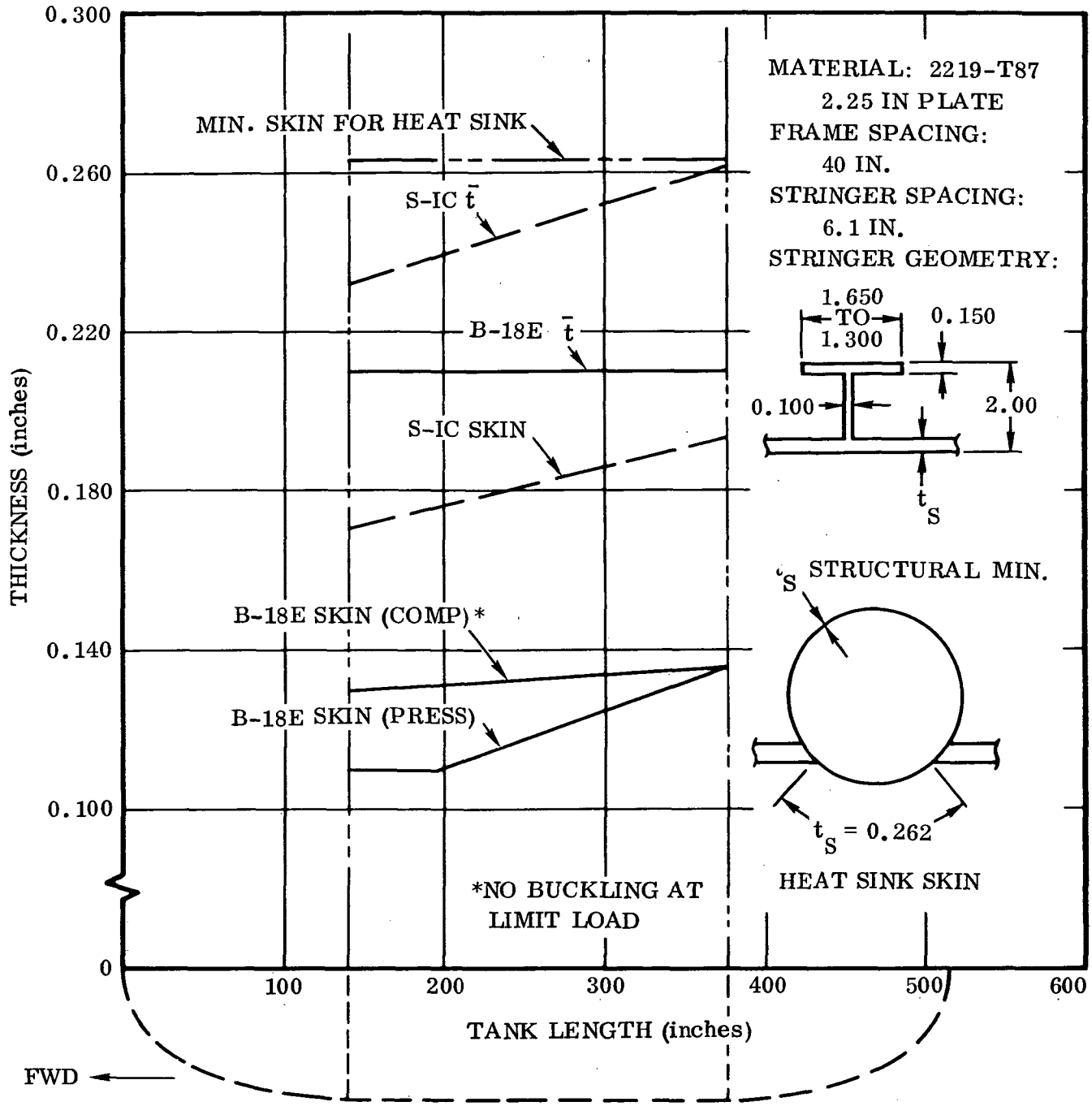

Figure 4-329. Comparison S-IC and B-18E RP-1 Tank Structural Requirements

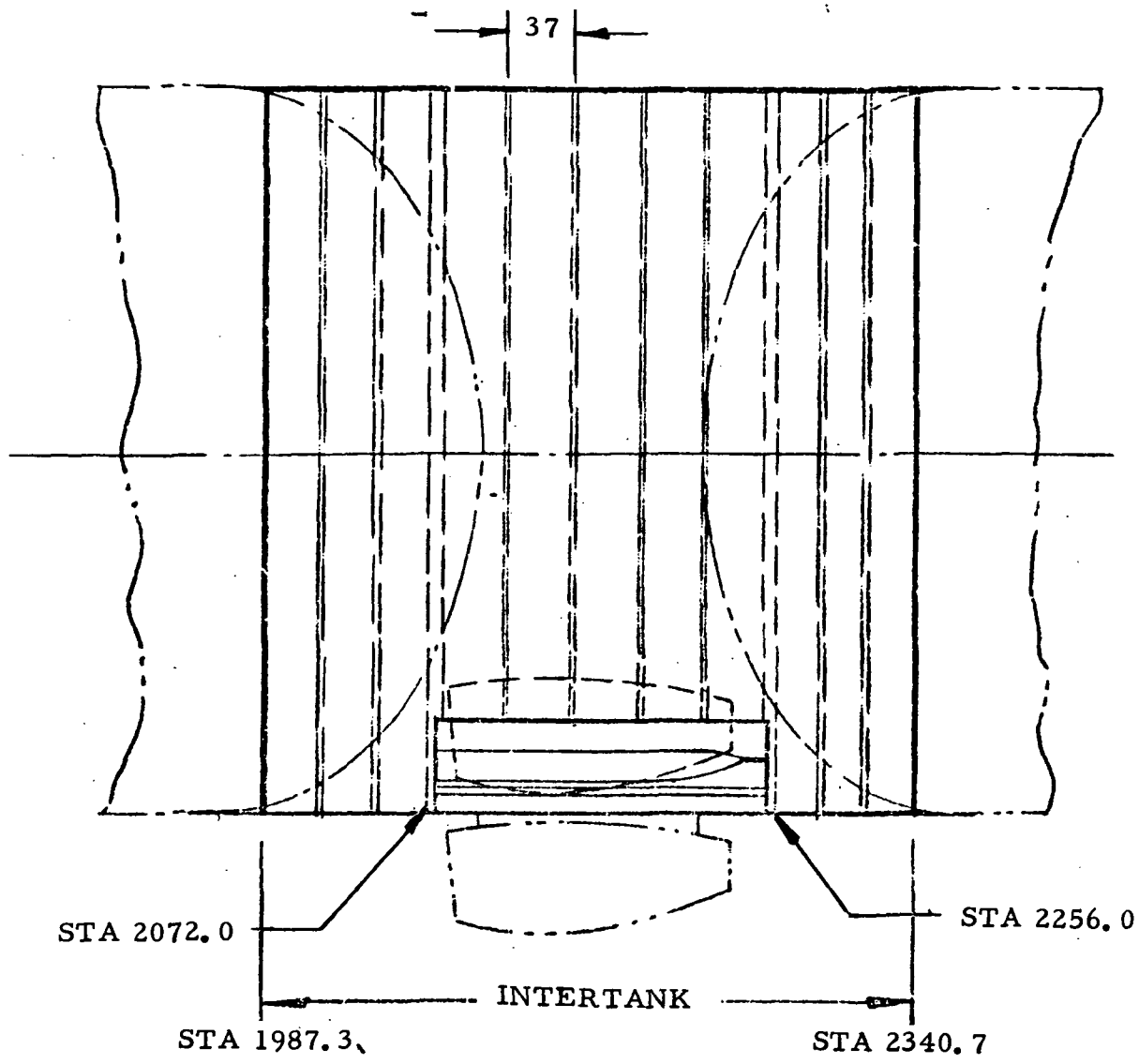

Figure 4-330. Intertank

General Description

Nose Structure. Figure 4-331 depicts the aluminum heat sink nose structure arrangement. It is a semimonocoque structural shell utilizing heat sink aluminum skins supported by ring frames and longerons. The structure has been primarily designed to accommodate the high load intensity produced by the orbiter and local loads introduced by the canard and the nose landing gear. The orbiter compressive axial loads are distributed uniformly through the nose structure skins. Longerons are provided to react the tension loads introduced by the discrete bolt attachments of the

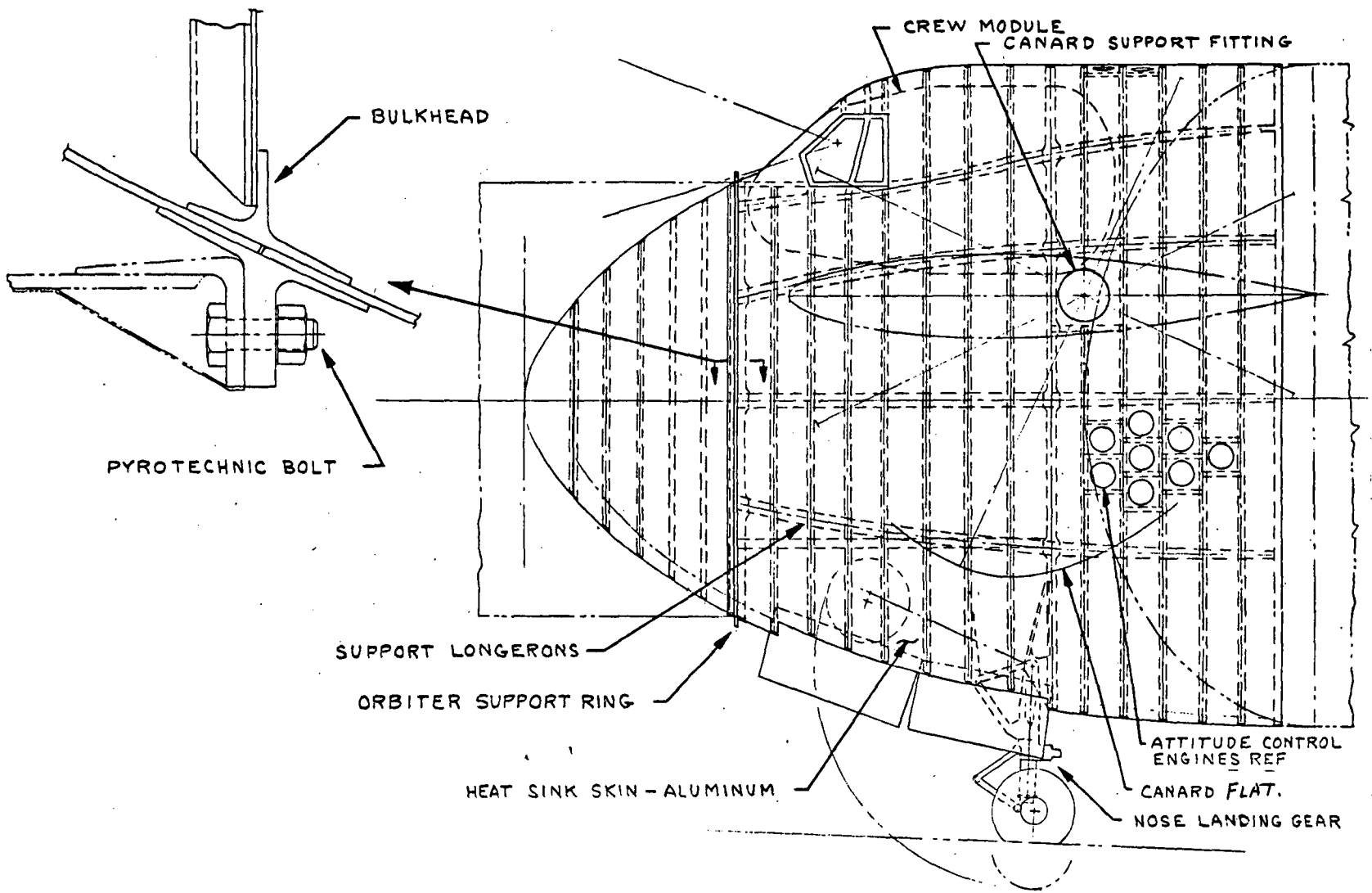

Figure 4-331. Nose Structure

orbiter adapter. These longerons also contribute to the stability of the shell structure. Major frames with local fittings are provided to react the loads introduced by the canard and nose landing gear.

The crew compartment is installed inside the nose structure enclosure as a separate unit. It is supported at four points in the upper portion of the nose structure and maintains a common interface at the wind shield. The compartment is a semi-monocoque aluminum structure incorporating ring frames and longitudinal stiffeners. Ingress/egress to the compartment is through a door in the lower surface of the compartment. Side hatches are provided for escape.

Oxidizer Tank. The B-18E oxidizer tank shown in Figure 4-332 is identical to the Saturn S-1C oxidizer tank except for the addition of 0.010 inch of thickness to the forward 5 feet of tank skin in the Position II quadrant. This change affects 3% of the tank surface area and is required for heat sink during reentry.

The oxidizer tank is a container of 345,000 gallons capacity and is the airframe structure between the nose section and the intertank. It is 396 inches in diameter and 769 inches long with a cylindrical section 495 inches long capped with ellipsoidal end domes. The cylindrical shell is integrally stiffened with tees two inches deep on 7.4 inch spacing. Thirteen ring frame/slosh baffles that are 30 inches deep stabilize the stiffeners. LO_2 is removed from the tank and supplied to the engines through five 25.2-inch-diameter lines that are installed at the base of the tank aft bulkhead.

Intertank Section. The intertank section illustrated in Figure 4-333 is a shell structure with a circumferential attachment bolt pattern at each end for attachment to the Saturn S-1C oxidizer tank and the RP-1 fuel tank. It is of aluminum alloy construction consisting of integrally stiffened skin, sized adjacent to the bottom centerline for heat sink, and ten frames. All structure is mechanically fastened since liquid retainment is not required.

The intertank structure houses and supports four airbreathing engines in the lower quadrant. Five longitudinal beams support the engines and carry body bending loads in their lower caps. These loads are redistributed by fittings and skin while still in the intertank area to provide uniformly distributed loading at attachment to tanks. An inner skin covers the entire engine compartment acting as a firewall and closing the torque box to maintain the torsional rigidity of the intertank. The engine compartment is further supported by machined frames at the forward and aft end.

	FWD			AFT		
	Top	Side	Bottom	Top	Side	Bottom
S-IC	0.190	0.190	0.190	0.254	0.254	0.254
6450 fps	0.190	0.190	0.200 ①	0.254	0.254	0.254
5904 fps	0.190	0.190	0.190	0.254	0.254	0.254

① Heat sink critical

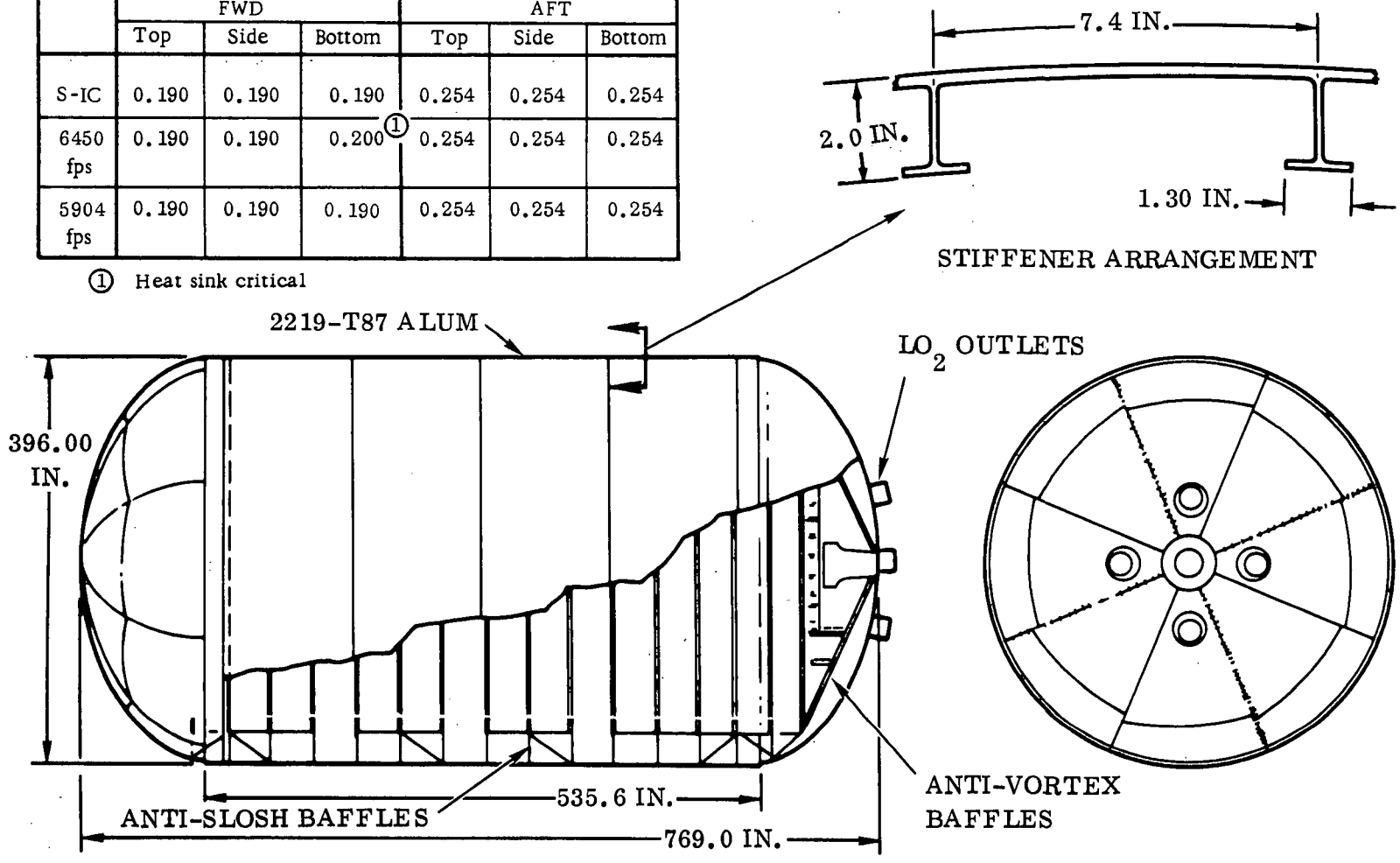

Figure 4-332. Oxidizer Tank

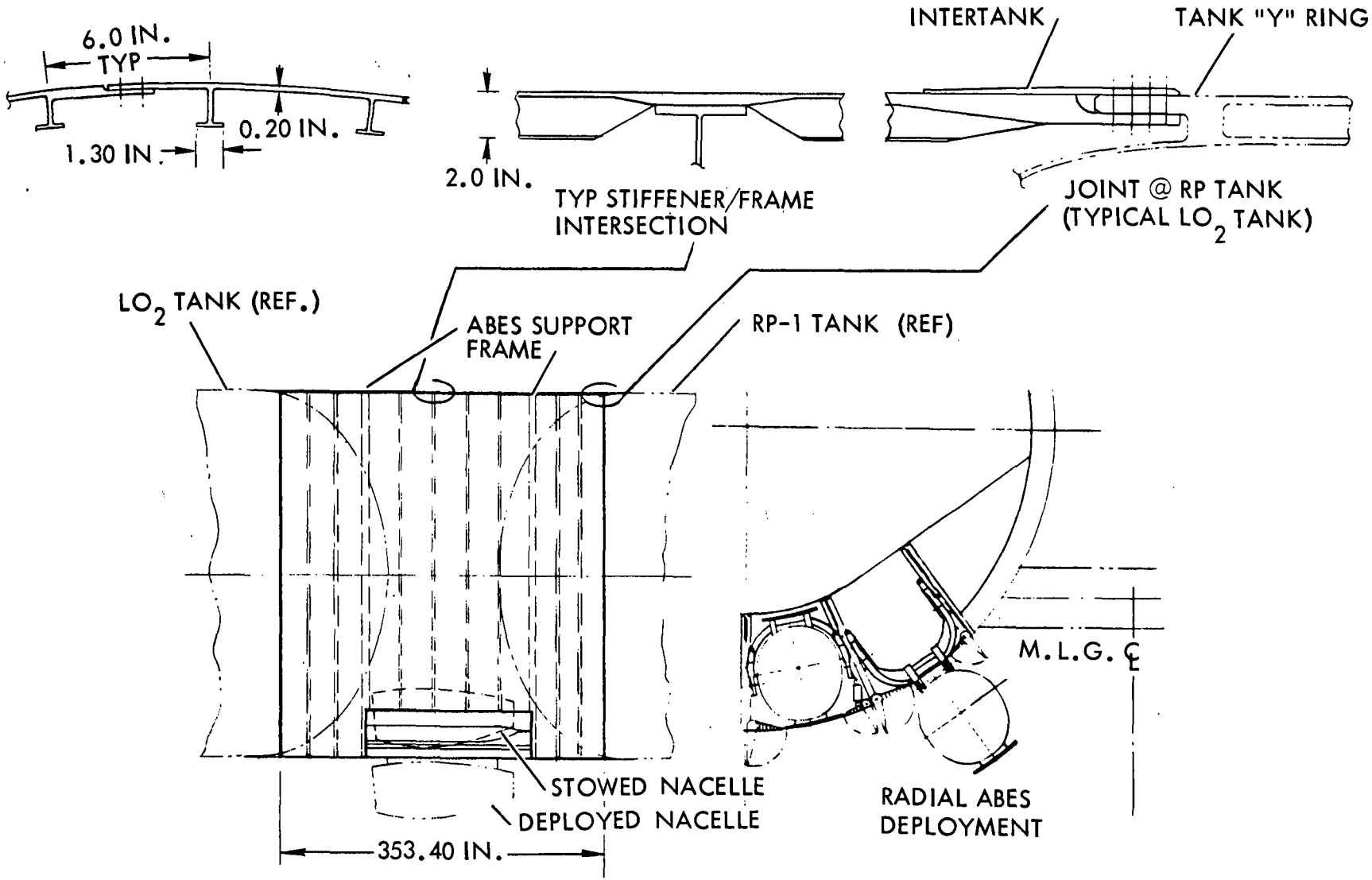

Figure 4-333. Intertank Section

Fuel Tank. The B-18E fuel tank is shown in Figure 4-334 and is identical to the Saturn S-1C fuel tank except for the addition of heat sink skin and a bulkhead to support the wing and provide spar carry-through. For heat sink, the Position II quadrant skin requires an additional thickness of 0.092 at the front end tapering to 0.069 at the aft end. This change affects 25% of the tank surface area. Wing support and spar carry-through requires the addition of a bulkhead similar in geometry to the S-1C frame/baffles with the spar running across the bulkhead below the Fin A and Fin B LO_2 lines.

The fuel tank is the load carrying structure between the intertank and thrust structure with a capacity for 216,000 gallons of RP-1. It consists of a cylindrical section 237 inches long by 396 inches in diameter capped with ellipsoidal end domes that make the total tank length 517 inches. The tank is made of 2219-T87 aluminum with the cylindrical shell an integrally stiffened structure. The stiffeners are 2-inch deep tee sections spaced 6.1 inches apart. Seven ring frame baffles 30 inches deep stabilize the stiffeners.

Thrust Structure. The thrust structure, illustrated in Figure 4-335, is geometrically similar to the S-1C thrust structure. The structural configuration for transmitting the thrust loads to the outer shell is also similar. This is also the case in the location and configuration of the hold-downs and the method of support for the base heat shield. The four peripheral engines are supported by thrust fittings mounted directly to the outer skin. The center engine is supported by cross beams that also backup the hold down fittings. A major difference from the S-1C thrust structure is introduced by the need to support the wing aft torque box and to provide carry-through structure across the fuselage. Loads from this torque box are transmitted to the cylindrical shell structure by the two major bulkheads. The vertical fin is also supported from the thrust structure. The baseline B-18E thrust structure uses titanium stiffened skins to minimize weight and to contribute to vehicle balance. The major geometrical features of the thrust structure, however, are common to the S-1C to enable the use of major tooling.

Base Heat Shield. The base heat shield is located in the station plane at the aft face of the thrust beams. The thrust beams and an intermediate matrix of subsidiary beams provide support for the shield. This method of support is similar to the S-1C arrangement. The baseline heat shield features corrugated metallic cover panels overlaying fibrous dynaflex insulation. Thermal expansion of the cover panels is accommodated laterally by flexure of the corrugations and longitudinally by slip joints at the panel edges and slip attachments to the support beams. The panels will be designed for adequate life under the base pressures through the relevant temperature range while subject to the acoustical environment.

	FWD			AFT		
	Top	Side	Bottom	Top	Side	Bottom
S-IC	0.170	0.170	0.170	0.193	0.193	0.193
6450 fps	0.171	0.171	0.262 ①	0.193	0.193	0.262 ①
5904 fps	0.171	0.171	0.225 ①	0.193	0.193	0.225 ①

① Heat sink critical

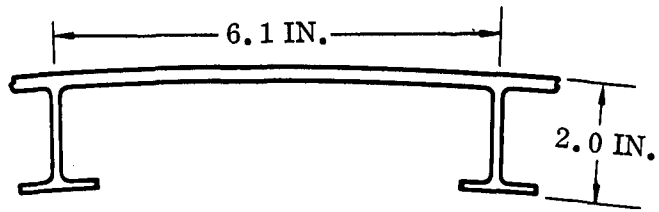

STIFFENER ARRANGEMENT

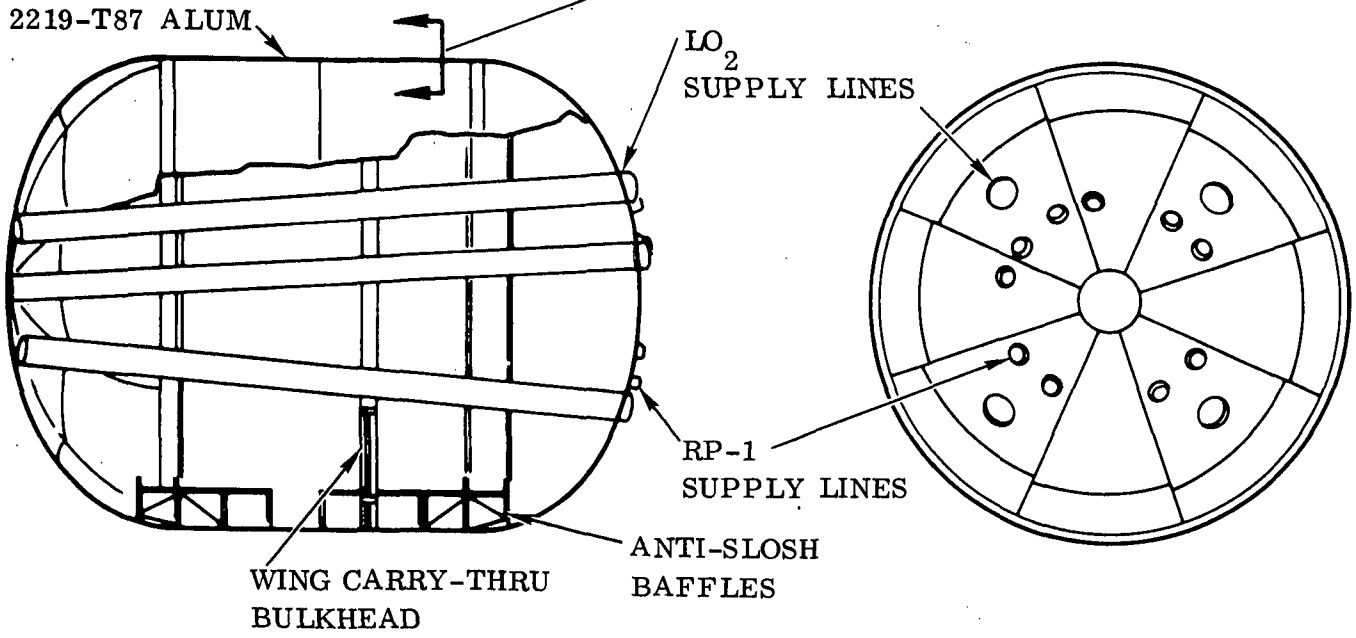

Figure 4-334. RP-1 Tank

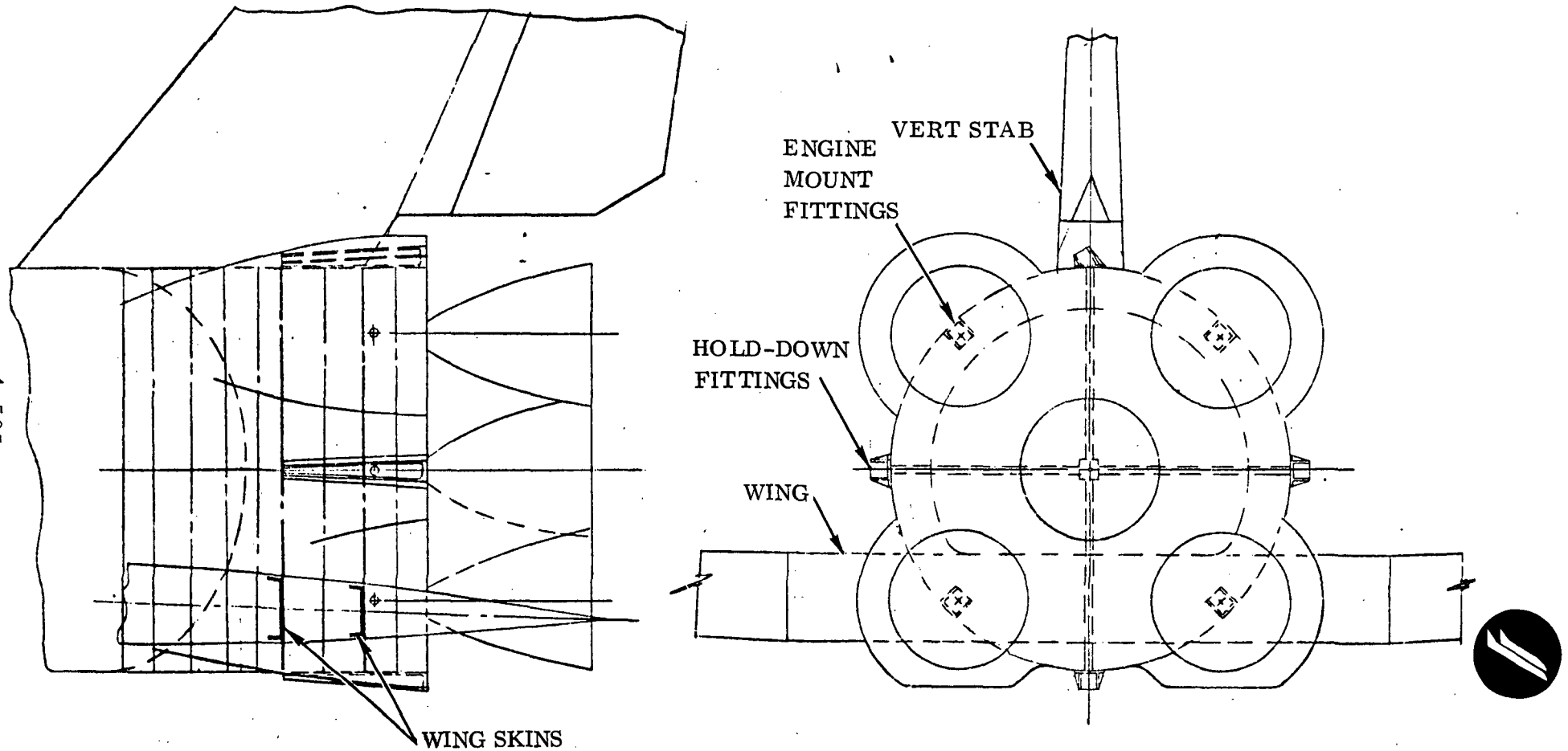

Figure 4-335. Thrust Structure

Alternate heat shield concepts are also under investigation. The reusability of the S-1C heat shield is being considered although this is doubtful in view of previous cracking problems with the titanate/asbestos/colloidal silicone material. Ablative concepts will be evaluated on the basis of cost effectiveness.

Wing. The wing structural arrangement is shown in Figure 4-336. It is a fail-safe multi-spar, multi-rib configuration utilizing smooth aluminum skin/stringer upper surface panels and aluminum heat sink integrally stiffened lower surface panels. The lower surface has adequate thickness to "heat sink" the structural temperature to 400 F or less. The aluminum heat sink concept was selected as a result of the wing concepts trade study.

The wing leading edge is heat sink designed with titanium. The trailing edge elevons are of similar construction to the wing structural box. Six flyback, airbreathing engines are submerged in the wing structure during boost and recovery and are deployed for cruise and landing. The main landing gear is housed in the inboard forward wing box area. Wing loads are reacted through spar-to-body attach fittings. The forward two spar-to-body attach fittings or "spar gates" are designed to transmit bending moments and vertical shear but are free to move in a fore-and-aft direction. This accommodates relative thermal expansion between the wing and the RP tank. The aft attach fittings provide a rigid support between the wing and the thrust structure. Bending moments, vertical shear, and drag loads are reacted at the thrust structure.

A trade study was performed to select a baseline wing construction concept for use on a "heat sink" type booster.

The following candidate concepts were investigated and evaluated. Concepts are identified in Table 4-63.

1. Titanium heat sink with corrugated upper surface and plate/stringer lower surface.

2. Titanium heat sink with smooth plate/stringer upper and lower surfaces.

3. Aluminum heat sink with smooth plate/stringer upper surface and integrally stiffened lower surface.

4. Aluminum heat sink with corrugated upper surface and integrally stiffened lower surface.

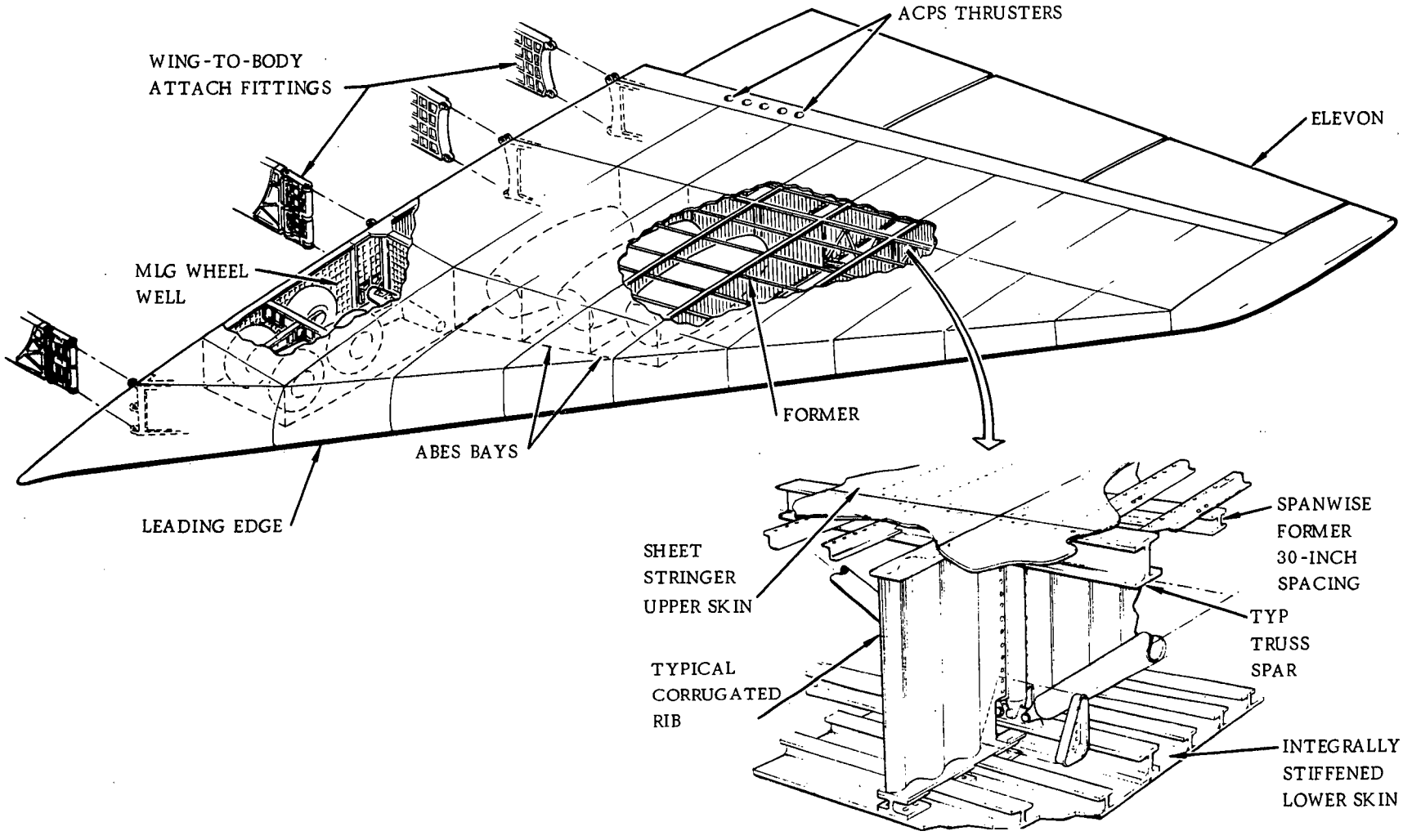

Figure 4-336. B-18E Wing

Table 4-63. Wing Concepts Trade Study Configurations

CONFIGURATION IDENTIFICATION	UPPER SURFACE CONSTRUCTION & DESIGN TEMP.	LOWER SURFACE CONSTRUCTION & DESIGN TEMP.	COMMENTS Δ WEIGHT
"A" B17E TI HEAT SINK	 650°F OPEN CORRUGATIONS	 650°F RIVETED HEAT SINK SKIN & STRINGERS	STUDY BASELINE
"B-1" TI PLATE-STRINGER	 650°F SMOOTH SKIN, RIVETED AIRLOAD STIFFENERS	650°F SAME AS "A"	-445 LBS
"C-1" AL HEAT SINK SMOOTH UPR SKIN	400°F SAME AS "B-1" EXCEPT MATERIAL IS ALUMINUM	 400°F INTEGRAL MACHINED HEAT SINK SKIN-STRINGER PANEL	+2543 LBS
"C-2" AL HEAT SINK CORR. UPR SKIN	400°F SAME AS "A" EXCEPT MATERIAL IS ALUMINUM	400°F SAME AS C-1	+2552 LBS
"D-1" AL-BERYLLIUM HEAT SINK	400°F SAME AS "C-1"	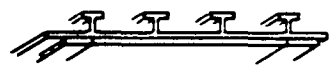 300°F / 600°F AL PLATE-STRINGER SKIN BERYLLIUM HEAT SINK TILES	-54 LBS
"E" TI-INCONEL HOT STRUCTURE	650°F SAME AS "A"	 1250°F OPEN INCONEL CORRUGATIONS	+1535 LBS

5. Aluminum smooth plate/stringer upper and lower surfaces with beryllium heat sink tiles on lower surface.

6. Hot structure design with corrugated titanium upper surface and corrugated Inconel 718 lower surface.

The wing concepts were investigated in sufficient depth to allow a quantitative comparison of weight and cost. Other evaluation criteria included development risk, growth capability, and reliability.

The aluminum heat sink wing with smooth plate/stringer upper surface and integrally stiffened lower surface is currently selected as a baseline for the B-18E booster. This configuration was cost effective with minimum development risk.

Canard. The canard structure is shown in Figure 4-337. The canard is a fully movable surface with a total exposed area of 485 ft^2. The lower temperatures associated with a lower staging velocity and with a heat sink design make possible the use of aluminum in all areas except for the leading edge and the pivot tube. The leading edge is heat sink designed with Rene' 41. The skin panels are integrally stiffened aluminum. The spars and ribs consist of corrugated webs welded to a cap strip which is mechanically attached to a machined cap member. The structural box is fixed to a titanium pivot tube at the inboard rib. The outboard pivot tube/rib attachment is a sliding joint to accommodate differential thermal expansion between the pivot tube and outer surfaces. Bending loads are carried through the pivot tube and reacted through two bearings supported in the nose structure. Spherical self-aligning bearings are used to allow for structural deflections.

Vertical Stabilizer. The vertical stabilizer structure is shown in Figure 4-338. The structural arrangement is a three spar, multi-rib configuration with skin/stringer cover panels. Spar and rib webs are of corrugated or trussed construction to allow for differential thermal expansion. The rudder is of similar construction. Aluminum is used throughout except for the leading edge and spar-to-thrust structure attach fittings, which are titanium. The leading edge is a heat sink design of titanium. Vertical stabilizer bending loads are reacted through spar-to-thrust structure attach fittings at the center and rear spars. Torsional loads are reacted at the front spar-to-tank pin joint and the rear spar attach fittings. The APU exhaust line is vented at the vertical stabilizer tip.

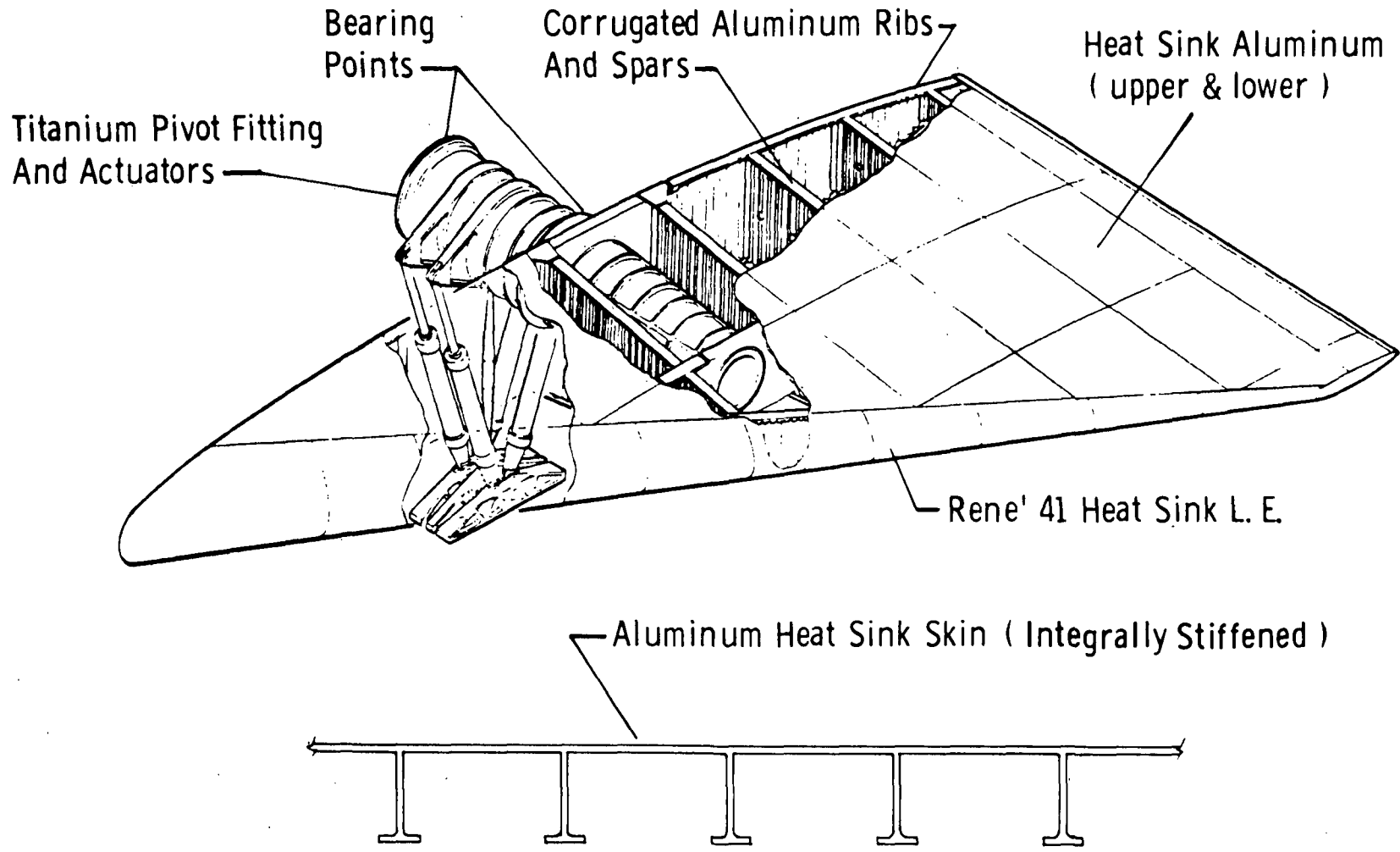

Figure 4-337. B-18E Canard

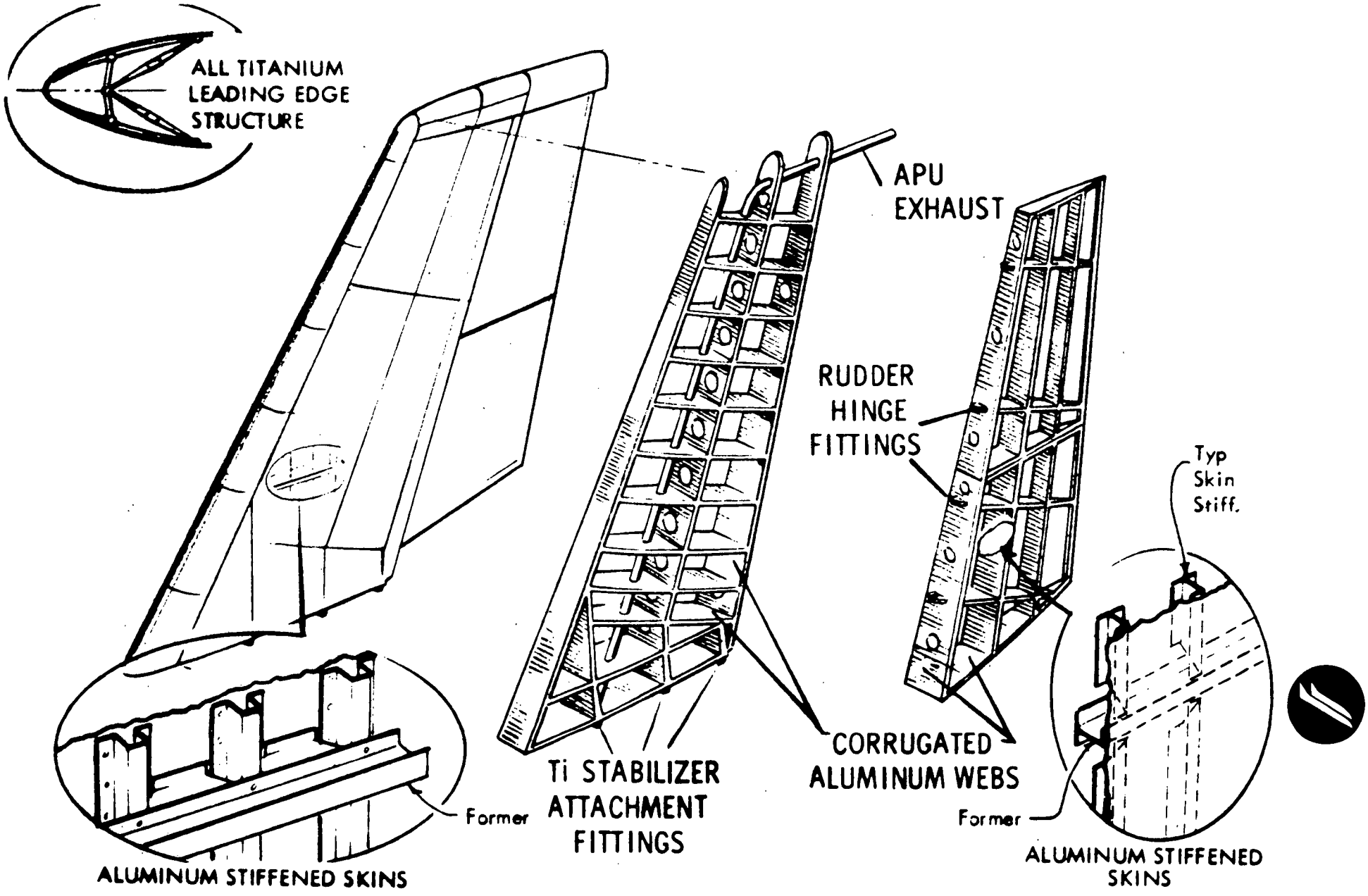

Figure 4-338. B-18E Vertical Stabilizer

4.4.5.10 Propulsion and Fluid Systems

Main Propulsion System. The main propulsion system is designed for maximum commonality with the Saturn S-1C. The basic system configuration is identical to the S-1C except for an increase in intertank adapter and LO_2 feed line length required to provide space for flyback engines. Other differences are modifications for gimballed center engine, riseoff fill and drain disconnects, and system reusability.

Engines. The baseline engine is the same as the F-1 engine used on the Saturn S-1C except the thermal insulation system (TIS) is redesigned to reduce cost and capability for throttling over a 300,000-pound thrust band has been added. The engine overall characteristics are summarized in Figure 4-339.

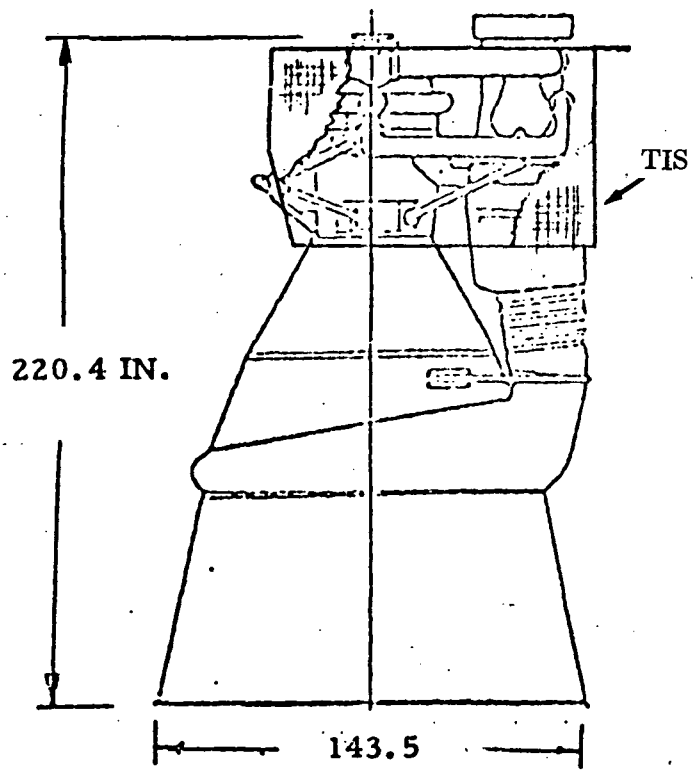

NORMAL OPERATION

F_{NOM}	1522 K LB
F_{MIN}	1222 K LB
ISP_{SL}	265.4 SEC
ISP_{VAC}	304.1 SEC
WT	18,567 LB
ϵ	16

EFFECTIVE GIMBAL ANGLE ±6°

ENGINE OUT OPERATION

F_{MAX}	1,522 K LB
ISP_{SL}	265.4 SEC

Figure 4-339. Baseline F-1 Engine

With one engine out, a thrust-to-weight ratio of 1.19 is obtained at liftoff if the remaining four engines are operated at the 1.522-million-pound

maximum thrust level. Vehicle altitude versus time from launch for both the normal operation and the engine-out condition is shown in Figure 4-340.

Feed System. The propellant feed system uses Saturn S-1C components and is identical in configuration to the S-1C except as follows:

1. The recirculation ports for the O_2 ducts have been relocated to a point above the prevalves to prevent geysering in the event of an on-the-pad prevalve closure.

2. The LO_2 fill and drain valves and disconnects have been relocated from the intertank area to the thrust structure area to enable use of a rise-off disconnect system and therefore eliminate the need for a gantry swing arm in the intertank area. Connection to the feed system is made through the recirculation ducts as shown in Figure 4-341.

3. Additional sections have been inserted in the O_2 ducts in the interstage area (Figure 4-342) due to 7.5 ft lengthening of the interstage to provide for room for the flyback engine installation. The sections are flanged at each end and no modifications to existing hardware are required.

The pressurization and vent subsystems for the booster utilize S-1C hardware and concepts. The O_2 system is the same as the S-1C and tank pressure schedules are identical, just satisfying engine requirements. The fuel tank pressurization and vent schedule is shown in Figure 4-343. The lower liquid level in the RP tank in comparison with the S-1C results in a requirement for 4 psi higher fuel tank initial pressure to meet start-up requirements. The maximum tank design pressure requirement has been lowered by (1) narrowing the pressure control band by use of closed loop pressure switch control of the tank pressure, replacing the preprogrammed scheduled pressurant flow of the S-1C, and (2) use of a vent valve control system like that used on the O_2 system lowering the relief valve setting at high altitudes. Regulation band is 21 ± 1 psia and the relief band at BECO is 24 ± 1 psia, down 10 psi from the S-1C. The reduced pressure minimizes the requirements for design of the tank for reusability.

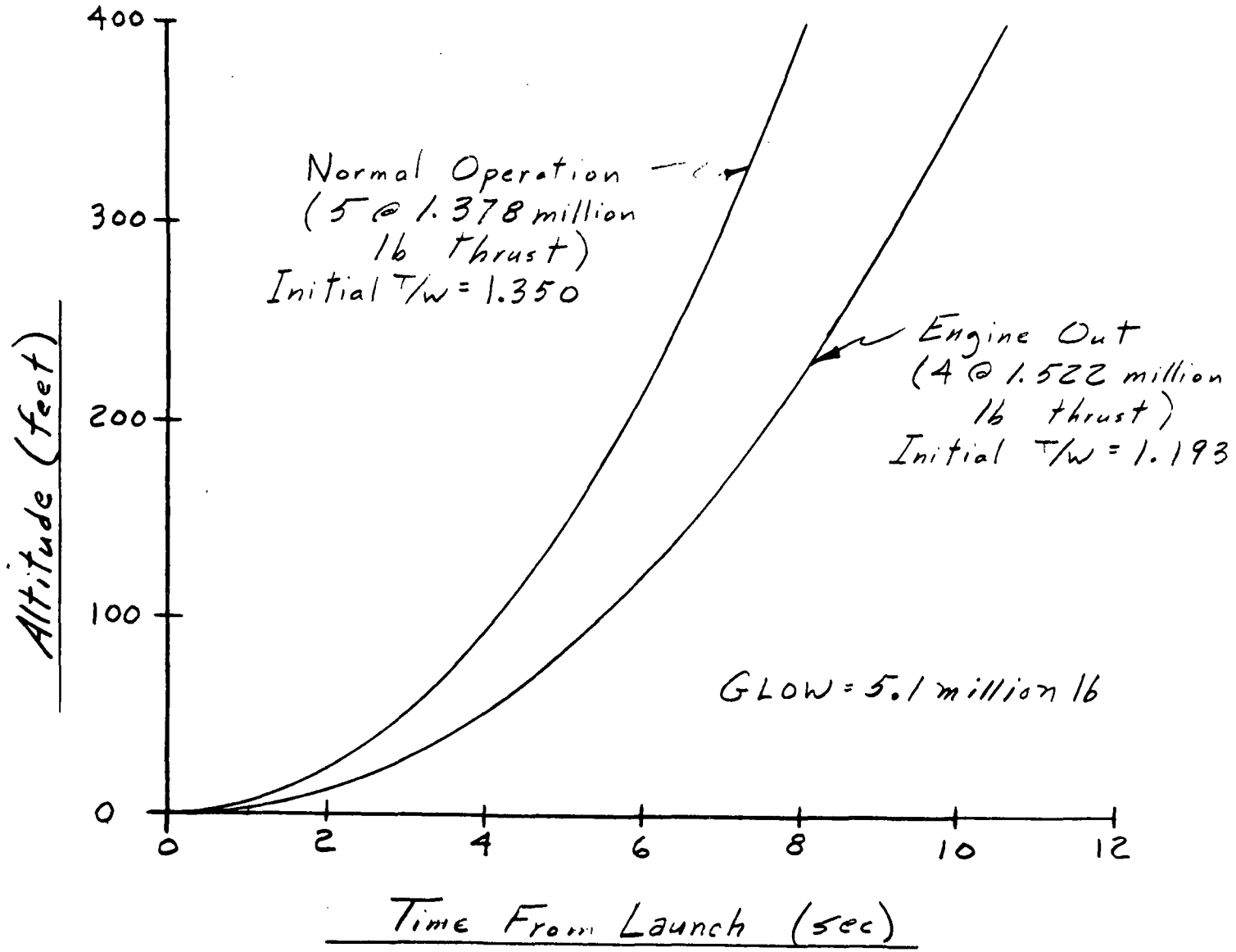

Figure 4-340. Engine Out Capability

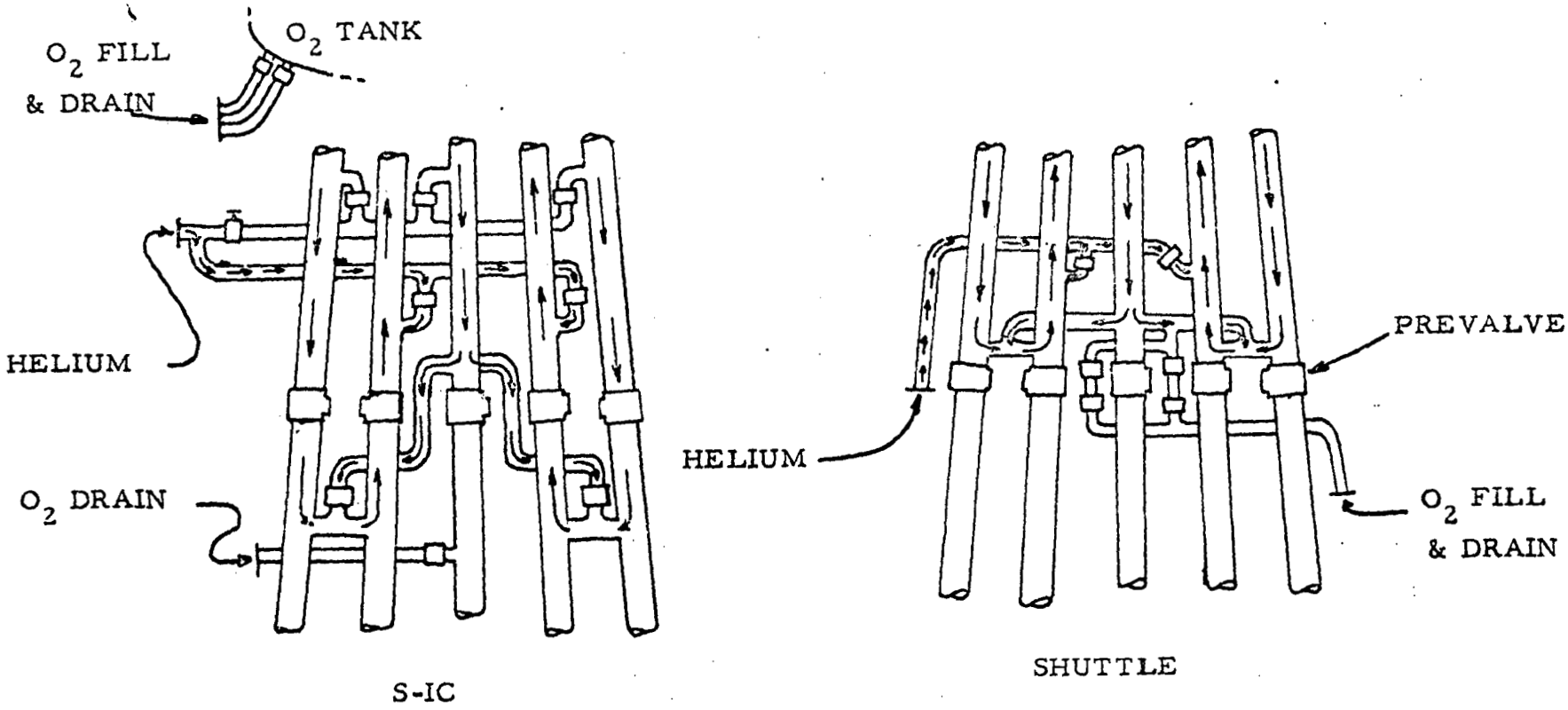

Figure 4-341. Recommended S-IC Feed System Changes

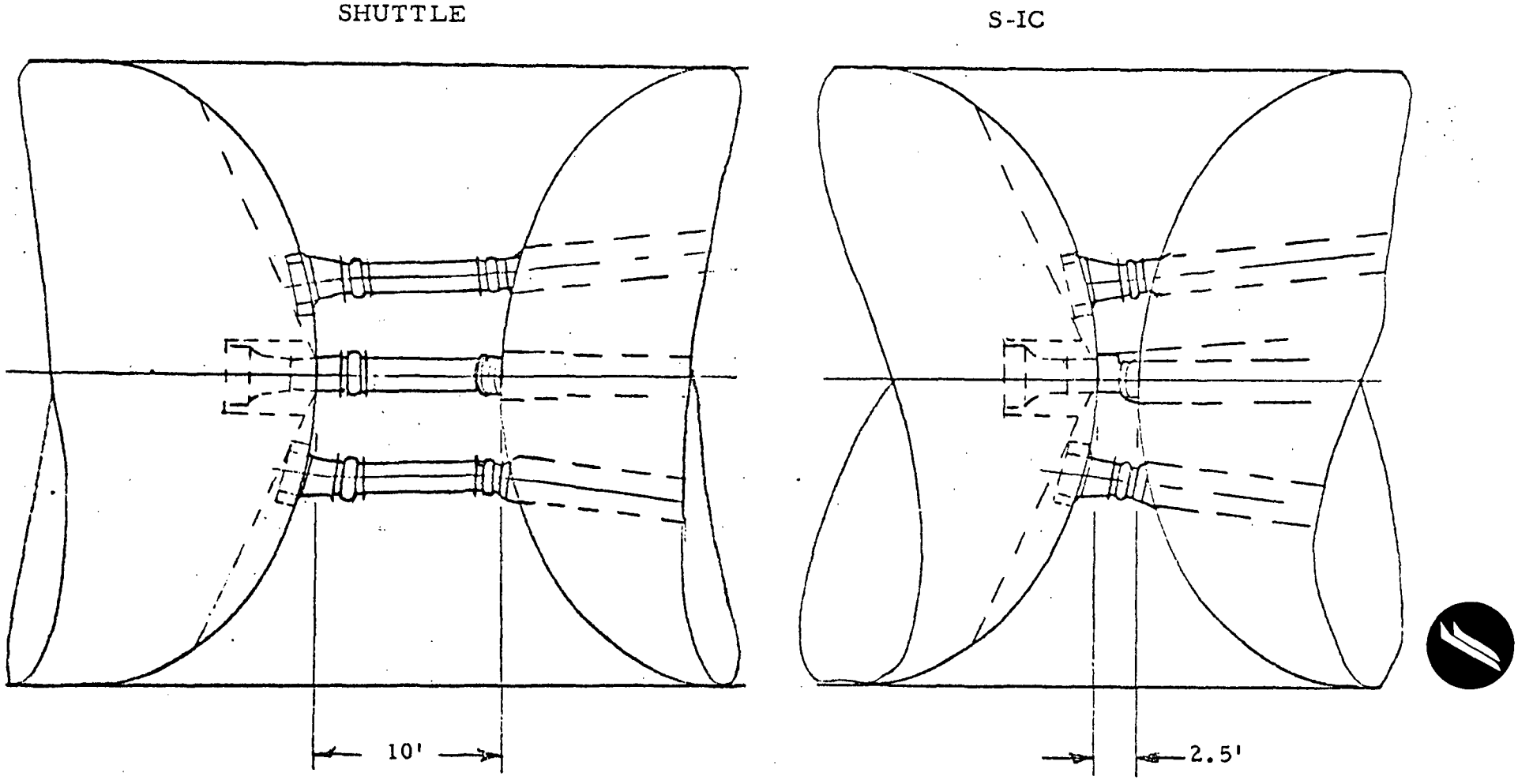

Figure 4-342. Feed System Changes for Increased Intertank Length

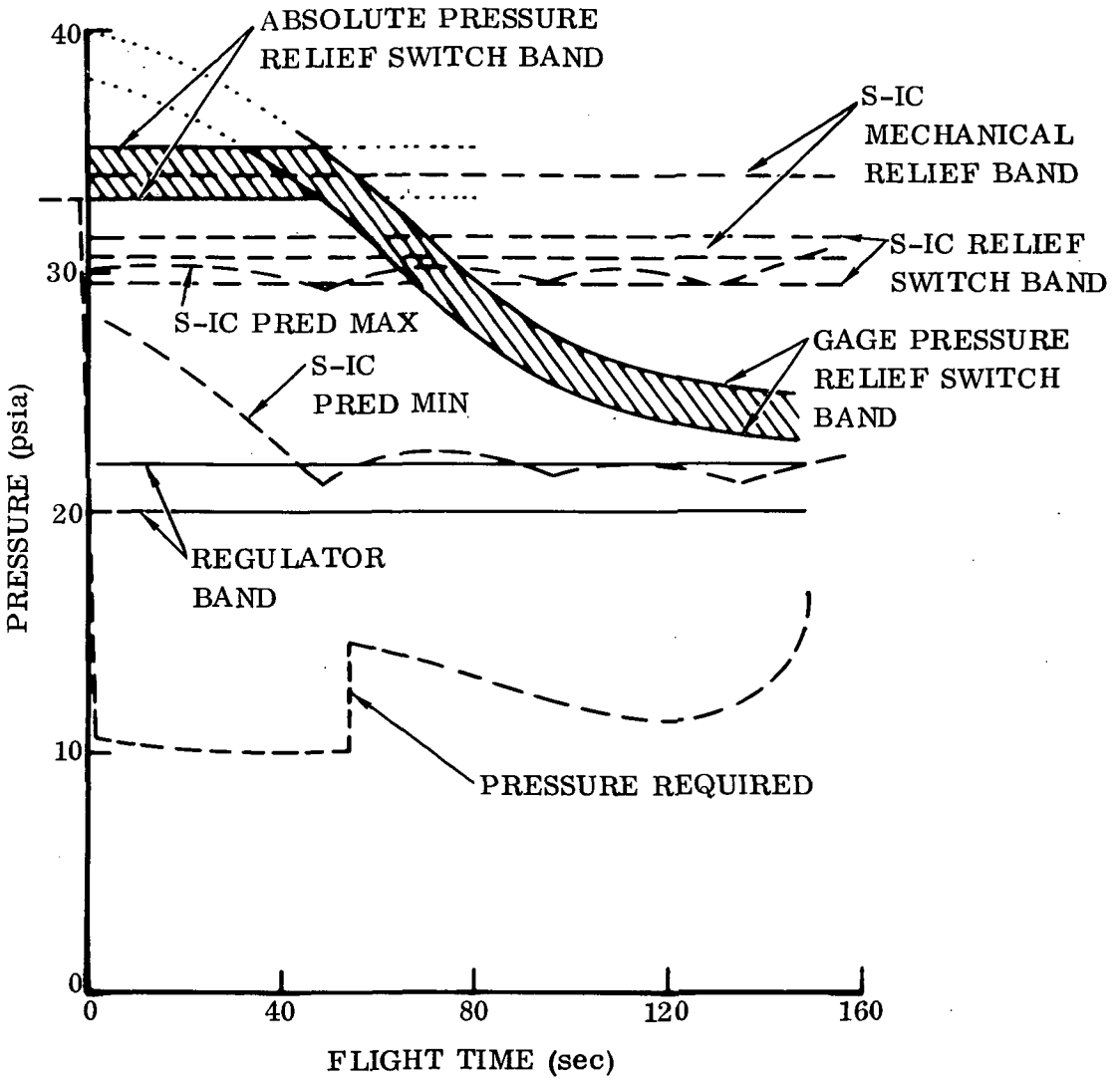

Figure 4-343. Fuel Tank Pressure Schedule

Auxiliary Propulsion System

The APS must provide propulsive thrust to perform maneuvers and maintain three-axis control of the booster attitude during reentry. This requirement exists from booster/orbiter staging until transition to aerodynamic control flight mode. The propulsive thrust is generated by attitude control engines fed with hydrazine (N_2H_4) monopropellant. The system is required to produce a total of 546,000 lb-sec of impulse and provide minimum vehicle angular accelerations, as specified previously in Section 4.4.5, in pitch, yaw, and roll from separation to +150 seconds and in yaw from +150 to +250 seconds. These required rates shall be provided after the failure of any two system components (excluding pressure vessels and feed lines). Minimum impulse bit in any axis shall be 236 lb-sec and shall be provided by operation of any one engine in that axis.

The APS shall provide N_2H_4 at a pressure of 330 psi minimum to the APU's continuously from 10 minutes prior to launch until deployment of the airbreathing engines at 663 seconds after orbiter separation. Maximum APU flow rate is 1.19 lb/sec of N_2H_4 for each of four APU's.

The APS (Figure 4-344) includes N_2H_4 monopropellant storage tanks, high pressure helium storage tanks, propellant distribution lines, attitude control engines, and appropriate flow and pressure control valving and regulators. N_2H_4 monopropellant was selected versus storable bipropellants based on competitive weight, lower costs, and minimum maintainability and reusability problems.

N_2H_4 storage tank, pressurization, and feed subsystems (per Figure 4-344) are located both forward and aft on the booster. The forward storage and supply system feeds 16 yaw engines and 4 negative pitch engines located forward of the LO_2 tank. The aft system feeds eight engines located in the wings for roll and positive pitch control and four APU's mounted in the wings behind the wheel wells.

The N_2H_4 storage tanks are identical (4.2 ft dia) titanium tanks with a capillary screen device for propellant acquisition and outflow control during low g periods. The tanks are pressurized to 360 psi and have a capacity of 2140 lb of N_2H_4 each. The aft tank will be loaded to partial capacity, approximately 1610 lb, to satisfy the lower total consumption requirements of the aft engines and APU's.

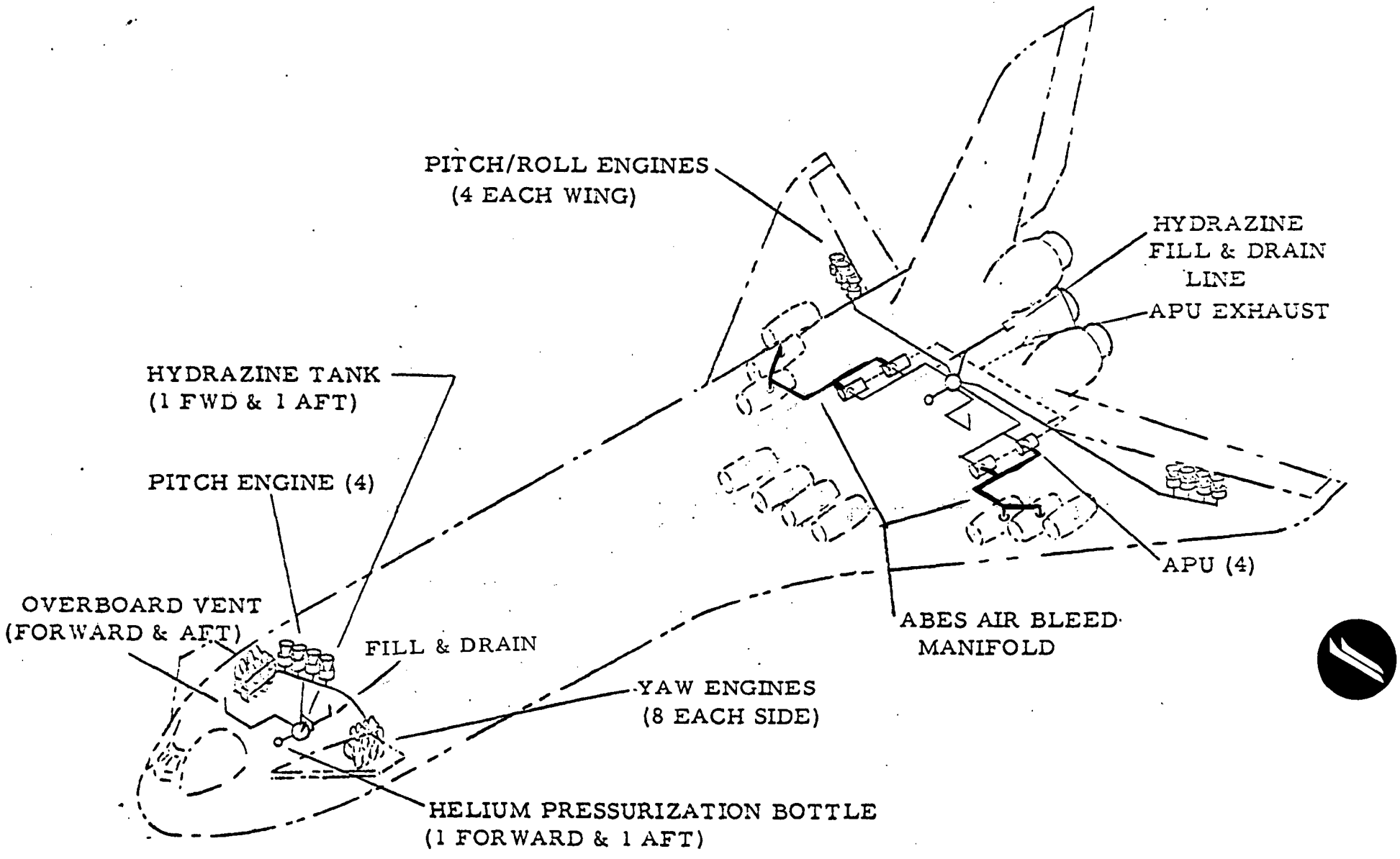

Figure 4-344. Booster Auxiliary Propulsion System

The pressurization gas (helium) is stored in identical bottles forward and aft at a pressure of 3000 psia. The gas is supplied to the propellant tanks through regulators at a pressure of 360 psia.

Twenty-eight engines at 2360 lb thrust each, satisfy vehicle attitude control requirements. The engine has a single propellant feed valve supplying N_2H_4 to a catalyst bed where decomposition of the propellant occurs. The engine operates with a feed pressure of 330 psia and a chamber pressure of 200 psia. The chamber pressure was selected to minimize engine development problems at a system weight penalty of approximately 200 lb. An expansion ratio of 20 was selected to reduce engine installation penalties while retaining an I_{sp} of 226 sec steady-state.

Operation. The N_2H_4 for the forward tank is loaded prior to prelaunch operations of the vehicle. The aft tank is loaded during prelaunch operations since a N_2H_4 ground supply for APU operation prior to launch is required.

The APU's are individually started and checked out during the prelaunch phase and remain on throughout the mission. N_2H_4 for ground operation is supplied through a riseoff disconnect which also provides propellant fill, drain, and topping capability for the aft tank. APU operation from the airborne supply begins at T-10 minutes and continues through the boost and entry phases of flight.

Attitude control engine operation begins at orbiter separation and continues until aerodynamic controls become effective in pitch and roll at separation +150 sec and +250 sec in yaw.

APU operation on N_2H_4 supply continues until deployment and startup of the airbreathing engines at 663 sec after launch. The APU's are driven by ABES bleed air throughout the remainder of the mission.

After landing, the engines and APU decomposition chamber are purged with 150°F GN_2 to remove N_2H_4 residuals. Residual N_2H_4 in the storage and feed system is left aboard and the system pressure is vented to a low level, 5-10 psig, to maintain an inert atmosphere until the subsequent prelaunch cycle begins.

Airbreathing Engine System. The airbreathing engine system (ABES) for booster B-18E differs significantly from that of the Phase B baseline B-9U in only three aspects:

1. Ten F101/F12B3 engines are installed instead of 12 JTF22A-4 engines.

2. A vertical deployment concept is used for deploying the engines after reentry.

3. Flyback fuel is reduced from 144,000 pounds to 36,000 pounds due to range reduction and better cruise SFC.

The ABES provides cruise thrust and fuel for booster flyback to the launch site where landing is accomplished in the manner of a conventional aircraft. The system also provides thrust and fuel for booster ferry flights. The ABES is designed to fulfill the following requirements:

1. Engines qualified for 500-hour life.

2. High altitude environment (75,000 to 210,000 feet) for less than 4 minutes per mission.

3. High temperature environment during reentry.

4. Fuel temperatures between -40 F and +140 F.

5. Operation during subsonic flight below 30,000 feet; cruise below 20,000 feet.

6. Provide engine bleed air for ECS and APU drive during flyback and ferry missions.

7. Two-week maintenance and refurbishment time between launches.

8. Two failures (except fuel tanks) shall not cause the loss of more than two engines or 75% of the reserve fuel.

9. Provisions for aerial refueling capability.

The ABES consists of several major subsystems including the engines, the nacelles (pod, pylon, inlet and exhaust fairings), the deployment system, engine control and starting, engine lubrication, bleed air system, and fuel system. A general arrangement isometric layout of the major elements of

the ABES is shown in Figure 4-345. The engines are installed in identical interchangeable nacelles: three are stowed in each wing outboard of the main landing gear and four are stowed in the fuselage intertank volume.

The engines are deployed vertically: deployment system reliability with this concept is enhanced by the inclusion of free fall capability. This added capability serves as a backup to the primary and reserve hydraulic systems. (The earlier Phase B baseline B-9U used a 180-degree rotation concept for deploying the engines: this concept did not have free fall capability.)

The engines use JP fuel. The fuel system includes engine feed, fuel transfer, refuel/defuel, vent, pressurization, jettison, and quantity gaging subsystems. Fuel is stored in two tanks: a main tank located in the intertank volume above the four center engines and a forward tank located ahead of the LO2 tank above the nose landing gear. The forward tank is filled only for boost missions to help maintain c.g. control during the reentry phase. A simplified schematic of the fuel system is shown in Figure 4-346.

REQUIREMENTS:

10 G.E. F101/F12B3 LOW BPR TURBOFANS
36,000 LBS OF JP-5
ENGINE DEPLOYMENT
AT 30K FEET

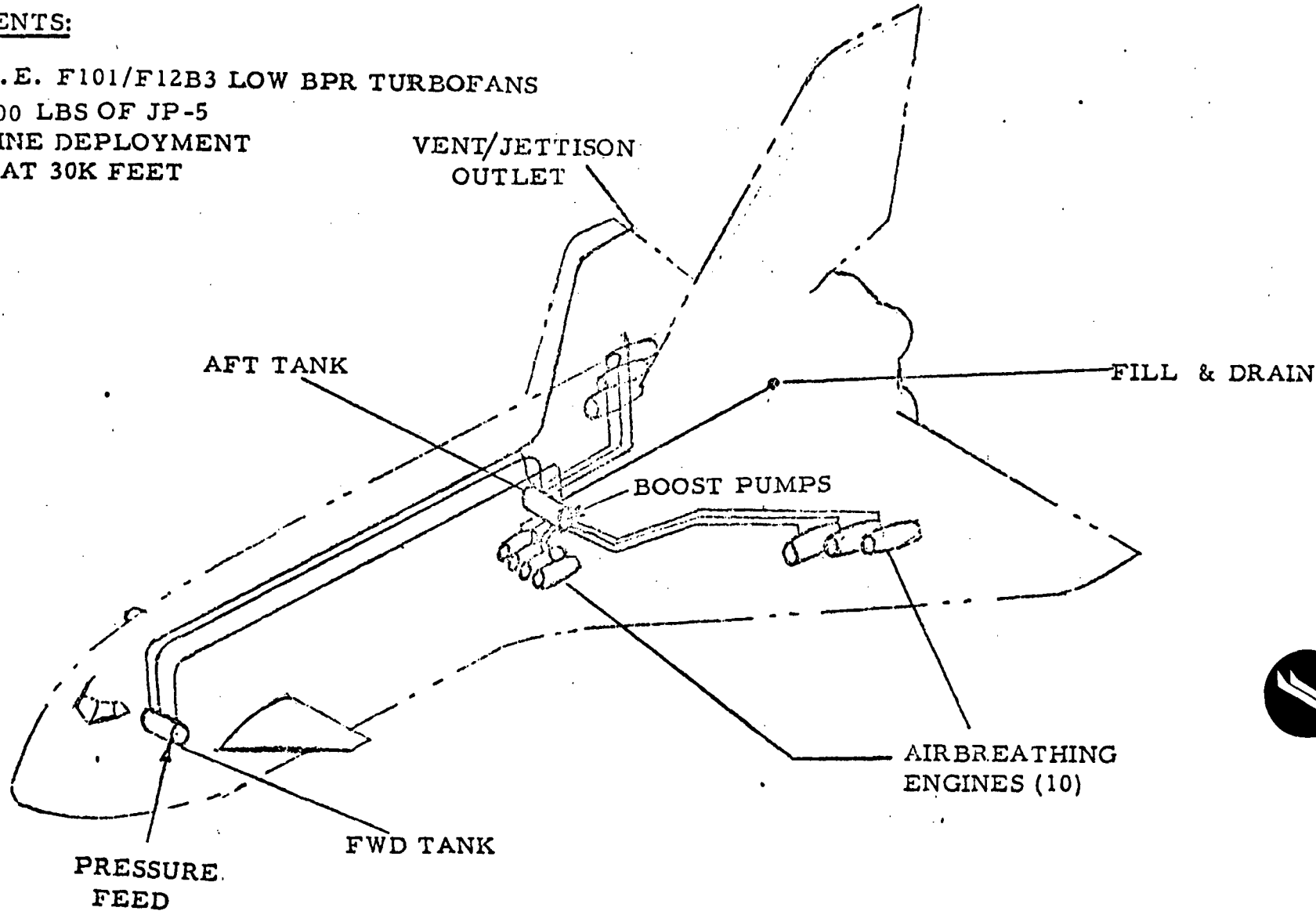

Figure 4-345. Airbreathing Engine System

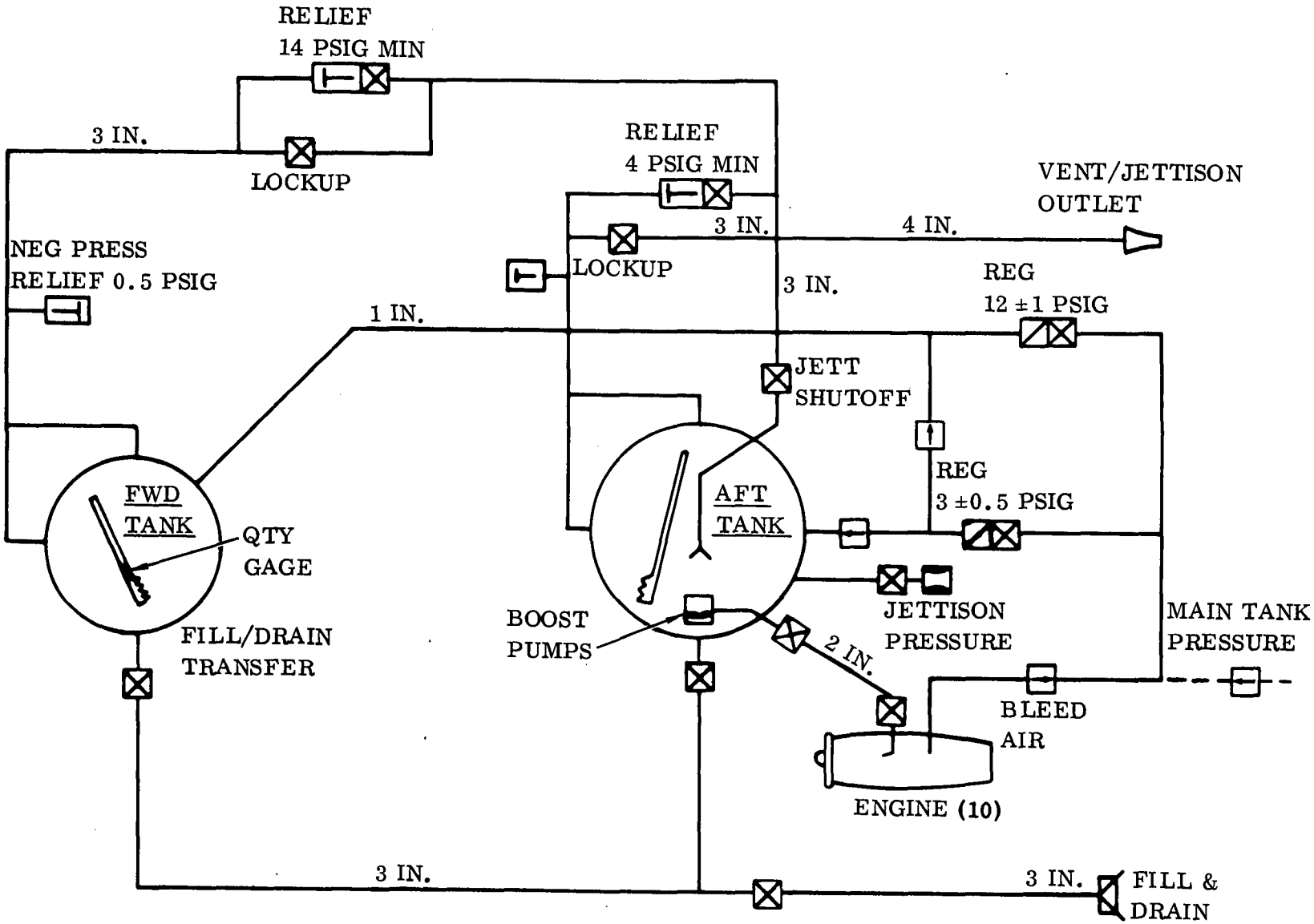

Figure 4-346. Airbreathing Engine Fuel System Simplified Schematic

Auxiliary Power Units (APU)

Design Requirements. Four identical 778 horsepower APU's provide for continuous generation of electric and hydraulic power from preflight through post-landing for both vertical launch and horizontal takeoff modes of operation. Each APU provides for a simultaneous maximum demand of 50 electrical horsepower and 728 hydraulic horsepower at 12,000 and 4,000 rpm, respectively. Total vehicle required energy from four APU's during the vertical launch mission is 138 hp-hr during boost and entry and 467 hp-hr during flyback and landing.

General Description. Each APU (Figure 4-347) consists of a gearbox with one generator and three hydraulic pump mounting pads, a hydrazine turbine and catalyst bed, a bleed air turbine, a lube oil pump and appropriate lines, valves and controls. Two APU's are mounted in each wing as shown in Figure 4-345. The hydrazine turbine exhaust is routed to a riseoff disconnect for controlled disposal of the products of decomposition prior to launch.

Hydrazine is supplied to the APU's from the aft auxiliary propulsion system (APS) storage tank from 10 minutes prior to launch through boost and entry phases. After start up of the airbreathing engines at launch +663 seconds, bleed air is ducted to the air turbine on the APU to drive the APU throughout the cruise, landing, and postflight phases.

The IDG lube oil and the APU gearbox lube oil are pumped through separate coils of a heat exchanger located in the hydraulic pump fluid feed line. The cooled oils are then circulated back to the IDG and gearbox for lubrication and cooling

The APU integration with the ABES allows minimum system weight, simplified hydraulic and electrical ground checkout, simplifies ferry and horizontal flight test operations, and is cost effective compared to operation on N_2H_4 throughout the mission.

System Operation for Baseline Mission. Two hours prior to launch the aft APS hydrazine storage tank is pressurized and the APU's are powered by the hydrazine turbines. The APS tank is replenished with hydrazine from the ground until 10 minutes prior to launch. The APU's continue to operate on hydrazine until the airbreathing engines are started following reentry. Bleed air from the compressor section of the airbreathing engines is then used to power the air turbine on the APU. Overrunning clutches allow either turbine to operate the unit without windmilling the idle turbine. The APU's are operated on bleed air until vehicle shutdown following landing and taxi.

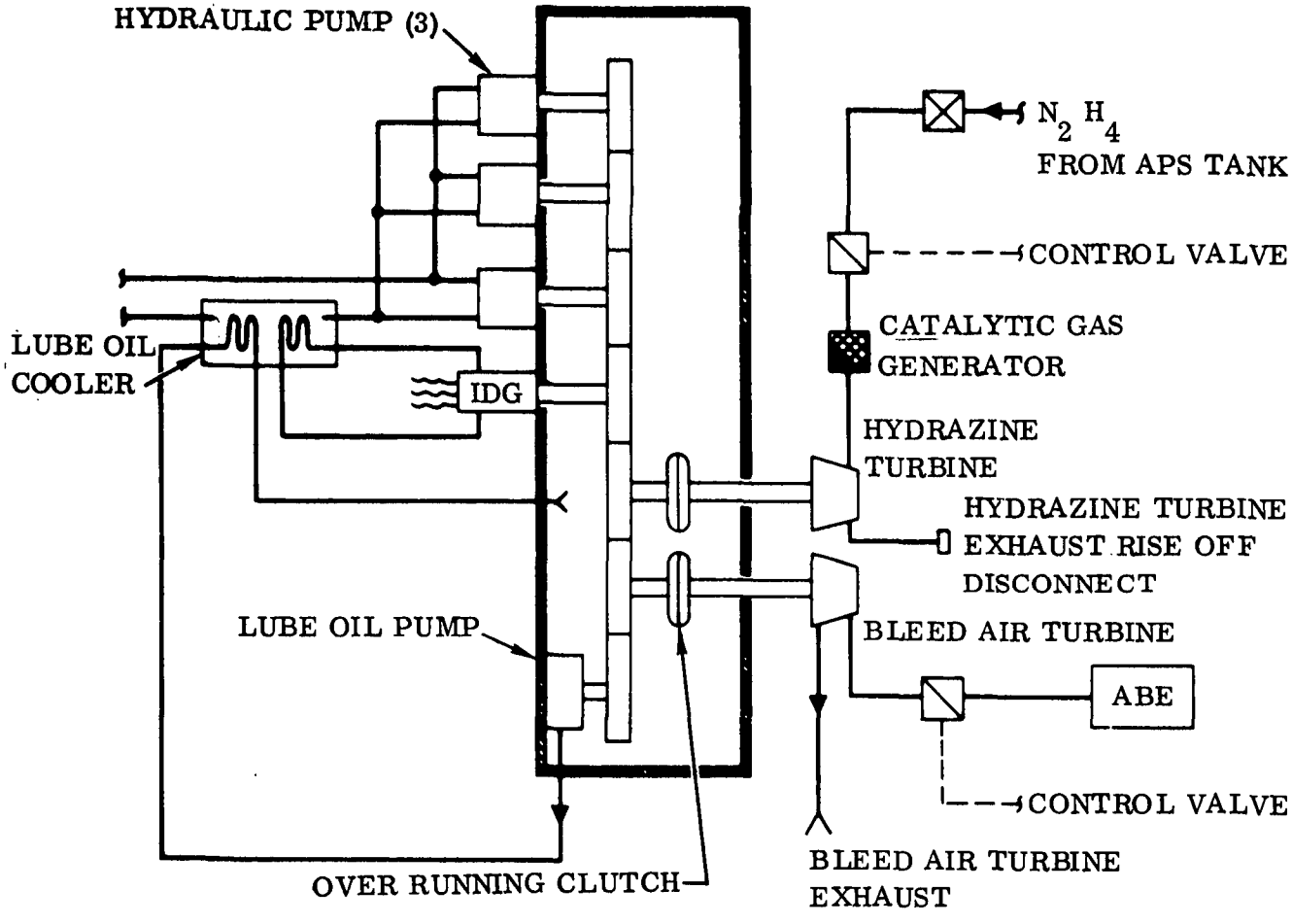

Figure 4-347. APU Schematic, B-18E-3

There is no scheduled postflight maintenance other than a hot GN_2 purge downstream of the feed valve to remove any residual N_2H_2 and dry the area exposed to atmosphere. Analysis of flight data will provide indications of system degradation and requirement for component or unit replacement. Ground checkout of the APU's will be performed by connecting an external pneumatic supply to the bleed air manifold to operate the air turbine. Residual propellants upstream of the N_2H_4 feed valve will remain in the system between flights and a helium blanket will maintain an inert atmosphere.

Hydraulics

Requirements. See Table 4-64.

Power Generation. The hydraulic system consists of four independent circuits physically separated and isolated from each other. Each circuit is a type II per MIL-H-5440 using MIL-H-83282 fluid and is powered by three APU-mounted variable displacement, 3000 psig constant-pressure pumps. The pumps are equipped with electrical depressurization to allow shut down during low power demand flight regimes. The total flow of each circuit is 366 gpm (122 gpm per pump). See Figure 4-348 for the APU and hydraulic power generation equipment location.

For ground operation the hydraulic systems are powered by an air-turbine motor mounted on the APU, which is supplied by ground cart air for ground operation.

The hydraulic fluid is cooled by a ram air heat exchanger during ground operations and horizontal flight. During ascent and until airbreathing engines are deployed and started, the fluid is cooled by fuel-to-oil coolers located in the JP fuel tank.

Subsystems. See Figure 4-349. The elevon and canard surfaces are powered by all four hydraulic circuits (all active). Each power actuator piston, one per circuit per surface, contributes 50 percent of required hinge moment. An electro-hydraulic control servo for each surface accepts four command inputs to provide two fail-operate capability. The outputs of the four channels are force summed to provide a single synchronized input to the power stage spools. This arrangement provides full surface capability after two failures. The rudder is mechanized in the same way except that each power actuator piston contributes 33% of the required hinge moment. After two failures the rudder hinge moment is degraded to 67%.

The landing gears (nose and main) are powered normally by one hydraulic circuit. Solenoid valves control pressure to the door actuators and locks and gear actuator and uplocks in sequence. An alternate power circuit and accumulator provide two backups to release locks allowing free fall downlock of the gear.

Dual anti-skid braking is provided on the main gear with each wheel being braked independently. The brake system is supplied by 2 hydraulic circuits (both active); however, one circuit is capable of providing full braking capability. Accumulators provide additional power backup should both active circuits fail.

Table 4-64. B-18E-3 Booster Hydraulic System Requirements

Function	No.	Travel (deg)	Hinge-Moment (ft-lb)	Rate (deg/sec)	Operating Time (Sec)	Redundancy
TVC/Axis/Eng (F-1)	5	±5	380,000	5	148	F/S
Elevons/Side	2	±30	0 960,000	20 0		F/O, F/S 100% HM for F/S
Canard/Side	2	+25 -65	0 208,000	20 0		F/O, F/S 100% HM for F/S
Rudder	1	±25	0 107,000	30 0		F/O, F/S 67% HM for F/S
Main Gear (EA)						
Retract Extend	2	102 102	300,000		15 15	F/S (Free Fall)
Nose Gear						
Retract Extend	1	105 105	75,000		15 15	F/S (Free Fall)
ABES/Eng						
Deploy Start	10		32,000 300			F/S (Free Fall) F/O, F/S (8 Eng Start)

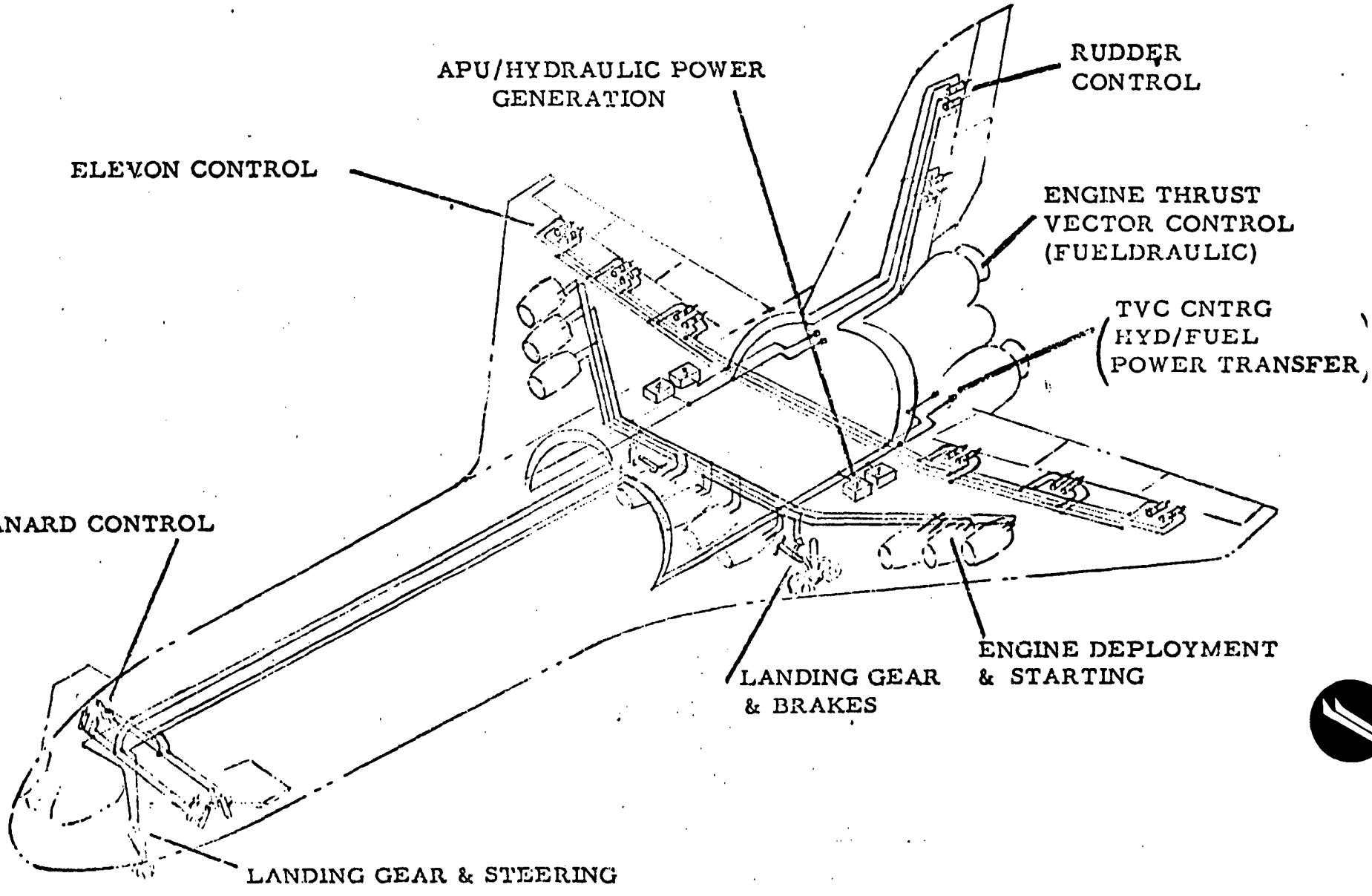

Figure 4-348. Hydraulic System Arrangement, B-183 Booster

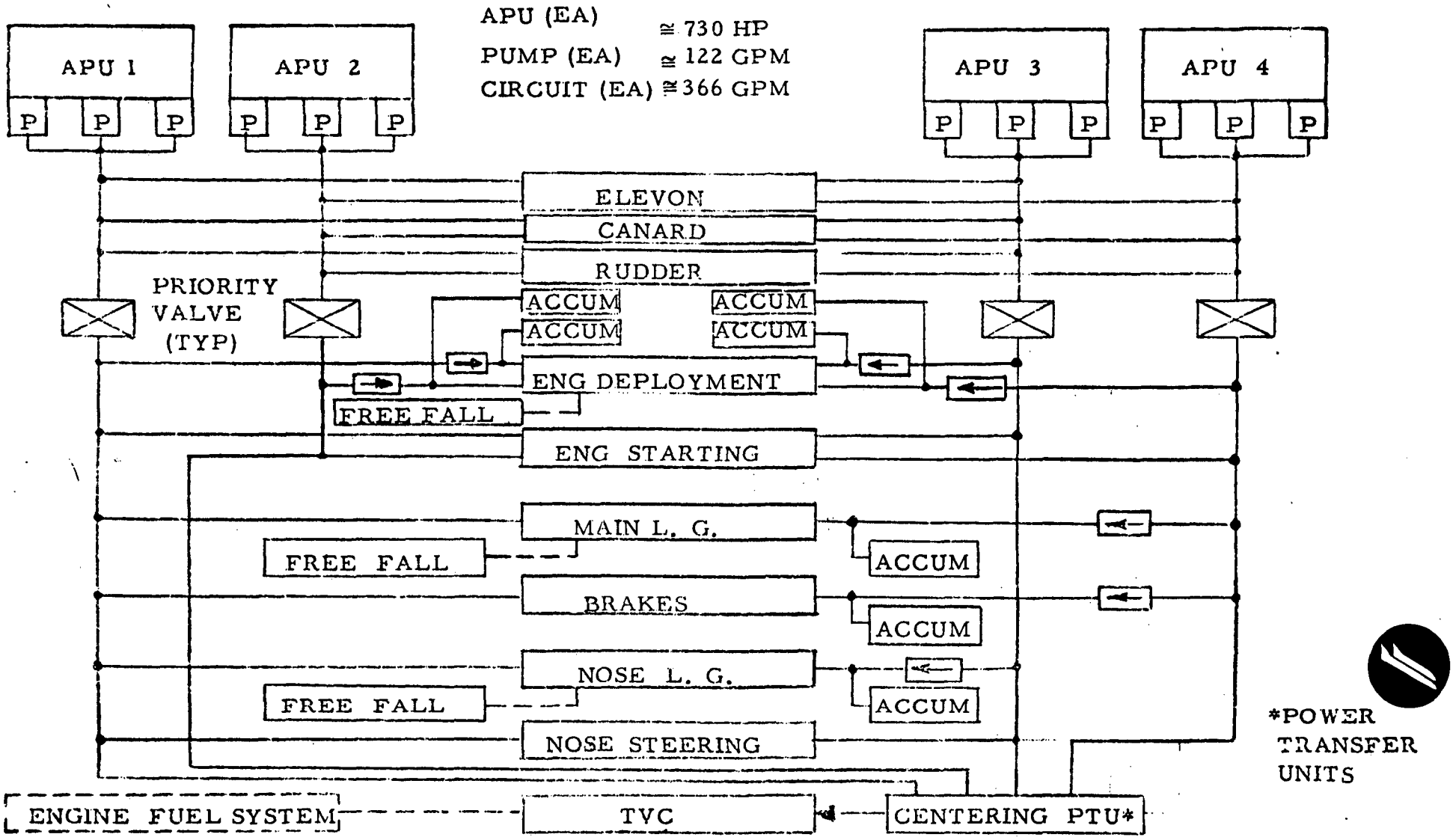

Figure 4-349. B-18E3 Booster Hydraulic Subsystems

Nose wheel steering is powered by two hydraulic circuits on an active/standby basis. If both circuits fail, the nose wheels castor and directional control is maintained by the rudder and differential braking at high speeds and differential braking at low speeds. Circuits 1 and 4 supply braking and circuits 1 and 3 supply steering to endure that either full braking or full steering capability is available after two failures.

All four circuits are used to deploy and start the airbreathing engines. Solenoid operated selector valves control pressure to the door actuators and deployment actuators in sequence. Emergency uplock release and door opening is provided by alternate circuits and accumulators allowing free fall deployment of the engines. The circuits and backup accumulators are arranged such that all ten engines can be deployed with three hydraulic power failures. After one hydraulic failure all ten engines can be started hydraulically. After two hydraulic failures, eight engines can be started hydraulically and two by RAM air starting. After three hydraulic failures, five engines can be started hydraulically and five by RAM air starting. This shows that there is a good probability (dependent on air start capability) that ABES deploy and start for safe return can be accomplished with up to three hydraulic circuit failures. Even though hydraulic powered flight controls are designed to sustain two failures and still be safe, once the vehicle is through reentry and is in the cruiseback segment, the burden on flight controls is reduced (i.e., hinge moments are lower) and control may be possible with only one hydraulic system remaining intact. Therefore, it is desirable to provide adequate propulsion at the minimum level of hydraulic operation that will provide controlled flight.

The thrust vector control system is essentially the same fueldraulic arrangement used on the Saturn S-1C stage. Additional hydraulic motor/pumps are installed (one per hydraulic circuit) to keep the engines centered after cutoff (see Figure 4-350). Hydraulic motor power drives a pump that pressurizes residual fuel to keep the TVC actuators centered. An electrical command is required prior to landing on the two lower engines to hold an "up" position to prevent ground interference at touchdown. This approach reflects minimum change and cost, and is applicable so long as the requirements remain basically unchanged from the S-1C. Should requirements change sufficiently to cause major redesign of the present system, then hydraulic servoactuators should be re-evaluated for use in the TVC system.

Figure 4-351 shows the hydraulic power profile throughout the flight. The constant losses are pump and system leakage losses. Average power includes the constant losses, steady state cycling, and peak power transients. The peak power is shown for the various flight segments with the predicted percentages of time at this peak level listed.

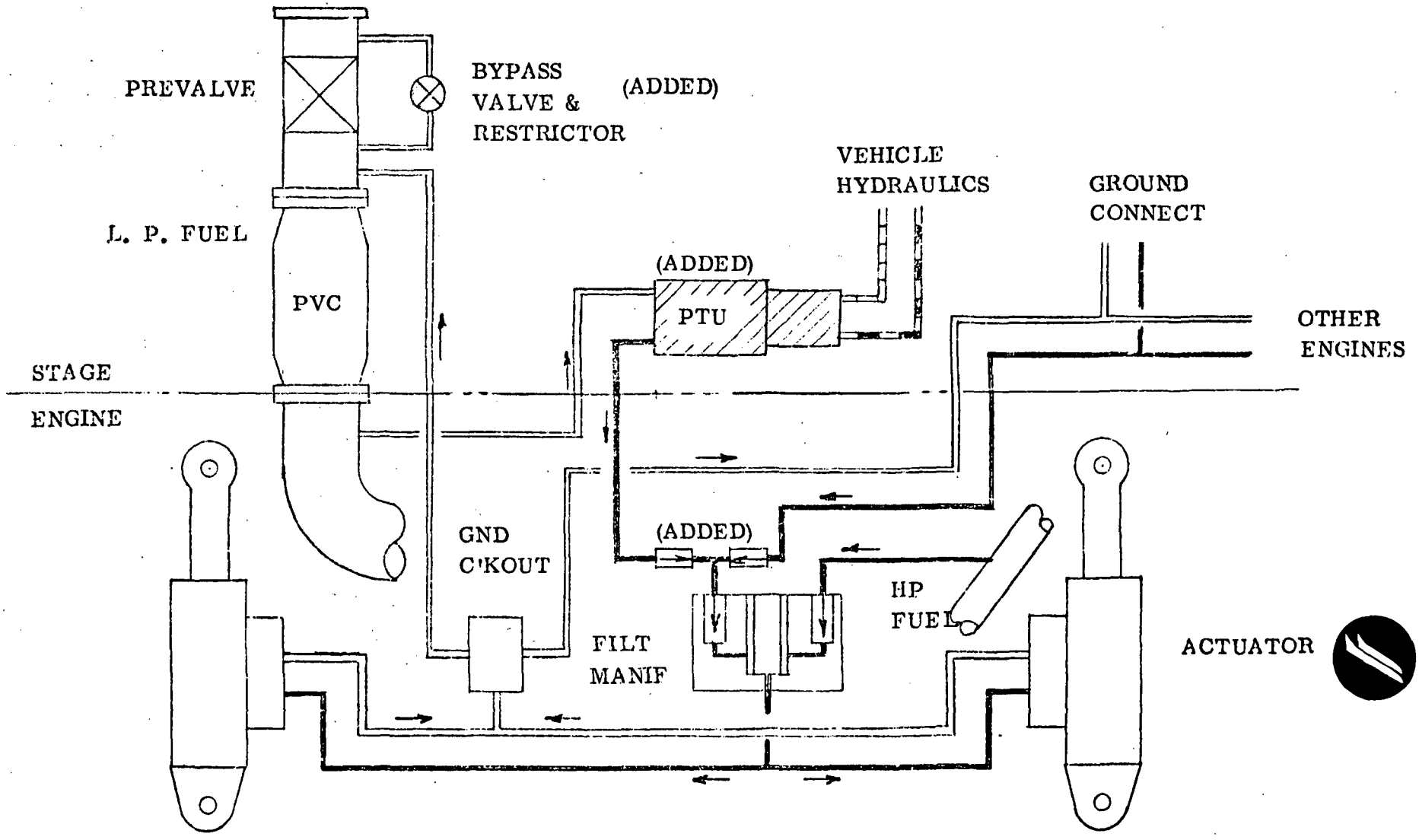

Figure 4-350. Fueldraulic TVC System

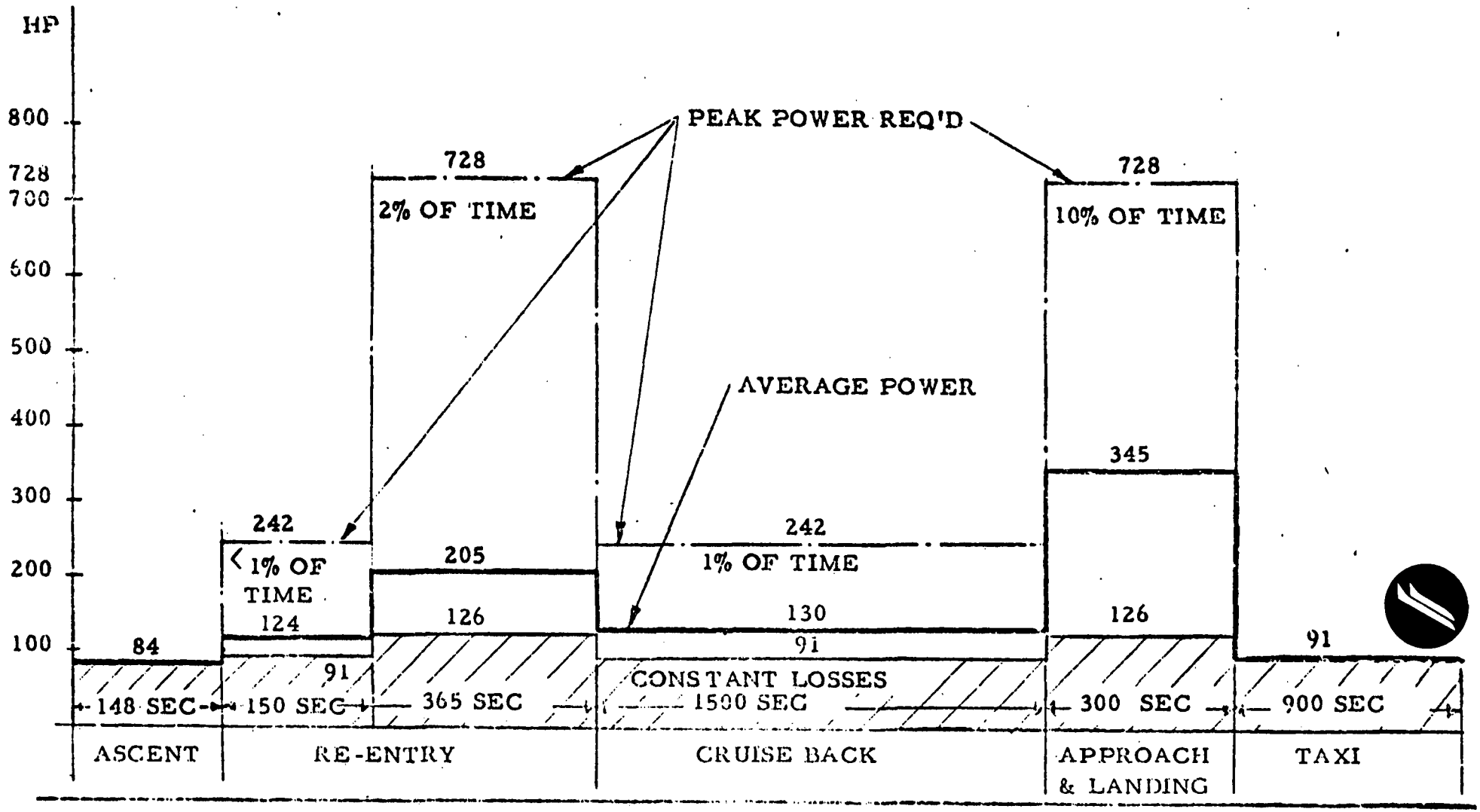

Figure 4-351. Hydraulic Power vs Time Each of Four Circuits

Environmental Control and Life Support System (ECLSS)

Requirements. The ECLSS is required to provide equipment and personnel thermal and pressure control.

The cabin and avionics equipment pressure shall be maintained so the minimum pressure is greater than 11.2 psia (7000 feet altitude). The crew compartment shall be shirt sleeve environment.

Cabin temperature shall be maintained at 65 to 80F. Cooling shall be provided to the avionics to maintain MIL-E-5400, Class II equipment.

System Description. The thermal control and pressurization schematic is presented in Figure 4-352.

Bleed air extracted from the main air engines is ducted through a precooler to reduce the bleed air temperatures to a maximum of 400F. The air then passes to the primary heat exchanger and to the turbine-driven compressor where the pressure is increased. Air is then passed through the secondary heat exchanger and across the expansion turbine to remove heat of compression plus additional heat. Temperature control of the air is accomplished by bypassing bleed air around the refrigeration units and mixing it with the cold air from the refrigeration unit. Moisture in the bleed air is removed by the water separator. Air from the refrigeration units is ducted to the cabin and forward avionics racks and is discharged to the ambient through the cabin pressure regulators.

During prelaunch operations, conditioned air is supplied from the GSE ECU through a rise-off disconnect.

In the boost phase the cabin pressure regulator is closed to maintain the cabin at approximately 14 psia at staging. Cooling is maintained by recirculating fans.

During reentry the cabin pressure regulator remains closed until the air engines have been started and the refrigeration units are providing cooling flow.

Purge and Vent.

Design Requirements. The purge and vent system is required to perform the following functions:

1. F-1 Engine Turbopump LO_2 Seal Purge
   Flow rate = 0.034 lb/sec/engine of GN_2 at 85 ±10 psig.

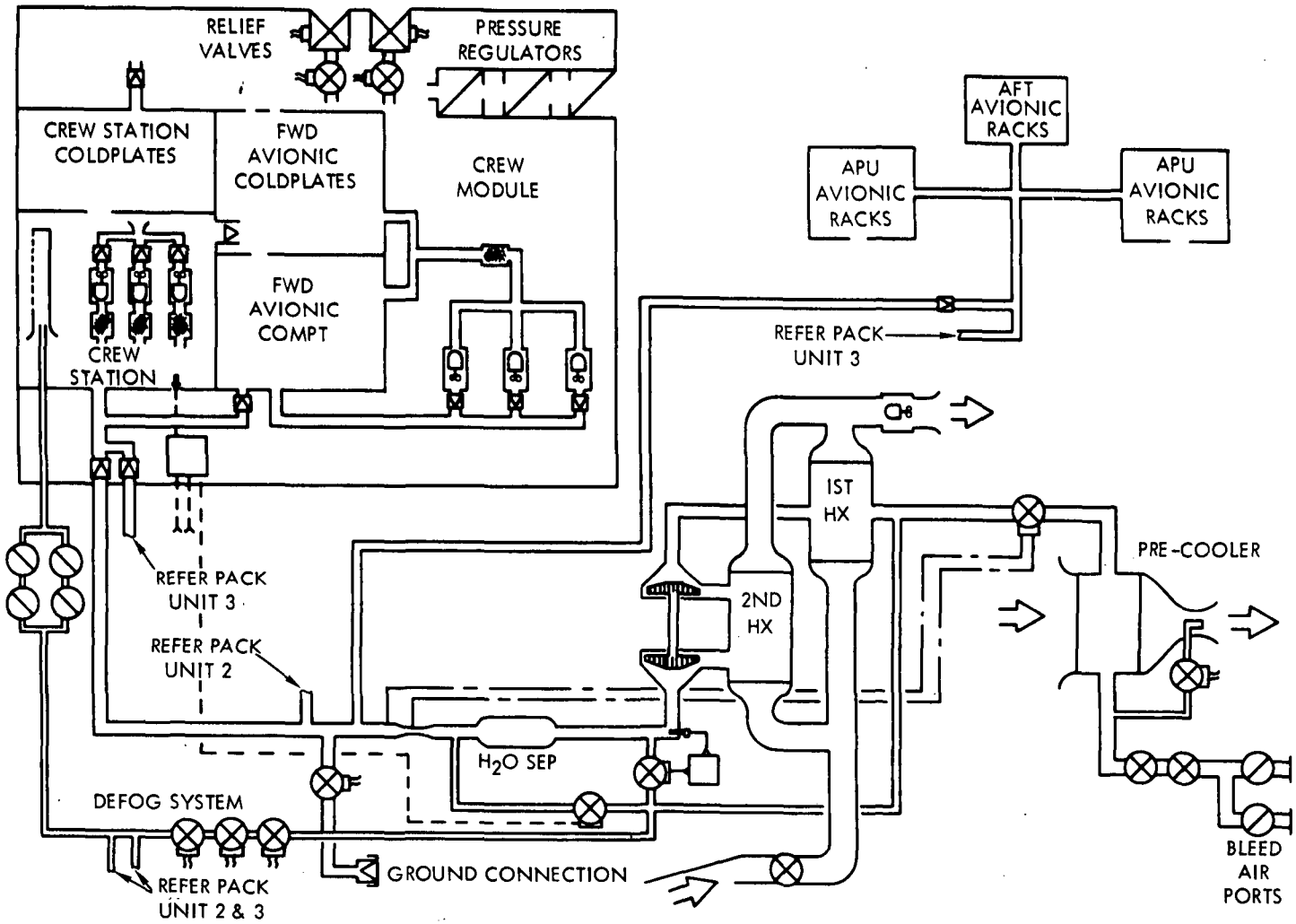

Figure 4-352. Booster Personnal Pressurization and Equipment Cooling System

The purge is required from time propellants are loaded and is continuous throughout launch preparation and through flight until propellants are depleted.

2. LO_2 Dome and Gas Generator LO_2 Injector Purge

   Max flow rate = 1.8 lb/sec/engine of GN_2 at 600 to 1000 psig.

   The purge is required prior to fuel loading and also when the F-1 engines' thrust chamber jackets are filled with prefill fluid and when engine gimbaling checks are made after prefill fuel loading. Purge is discontinued after lift-off.

3. Engine Cocoon Thermal Conditioning and Purge

   Flow rate ≈ 21 to 22.8 lb/minute total flow of GN_2 at ≈200 psig. Purge is manually controlled by operations to control temperature of critical engine parts plus purge explosive gas mixtures. Purge is also turned on 5 minutes prior to engine ignition and continues until umbilical disconnect.

4. Thrust Structure Compartment Thermal Conditioning and Purge

   Compartment temperature prior to lift-off shall be maintained at 80 (±20)F. Maximum oxygen concentration should be less than 5% prior to engine ignition. Compartment pressure shall be controlled to maintain a maximum ΔP of internal pressure to external pressure of ±2 psi as measured across the upper structure at the top centerline. Temperature control and purge continues until umbilical disconnect at lift-off.

   Structural leakage shall be less then 5 pounds per minute with an internal pressure of zero psia and an external pressure of 2.0 psia on the lower surface varying to 0.1 psia on the upper surface, and external air temperatures of 2500F.

5. Inner Tank Compartment Pressure Control

   Compartment shall be vented to ambient to maintain a maximum ΔP of internal pressure to external pressure of ±2 psi as measured across the upper structure at the top centerline.

   Structure leakage allowable is same as thrust structure.

6. Forward Structure Compartment Thermal Conditioning and Purge

Compartment temperature prior to lift-off shall be maintained at 80 (±20)F. Compartment pressure shall be controlled to maintain a maximum ΔP of internal pressure to external pressure of ±2 psi across the upper structure at the top centerline.

Temperature and purge control continue until umbilical disconnect at lift-off.

Structure leakage allowable is same as thrust structure.

System Description

Engine Purge System. The engine purge system performs the function of LO_2 seal purge, LO_2 dome and GG LO_2 injection purge, and engine cocoon thermal conditioning and purge.

GN_2 is supplied to this system through the umbilical disconnect for ground operation and charging of the three 2200 cubic inch spherical airborne storage bottles to 3250 psig. (Bottle pressure reduces to 400 psig minimum in a flight period of 156 seconds).

The three airborne bottles provide the GN_2 for inflight purge of the engine turbopump LO_2 seal. The supply GN_2 flows through a filter and pressure regulator with integral relief valve to each of the five engines.

GN_2 for the LO_2 dome and GG injection purge is applied at the umbilical couplings by a GSE source and is distributed to each of the five engines by distribution lines with flow control orifices. Supply pressure is 120 to 220 psig for the low level flow and 600 to 1000 psig for the high level purge flow required just prior to lift-off or for one hour following a pad abort.

GN_2 for the engine cocoon is supplied by GSE at the umbilical coupling. The heated GN_2 (250 to 327F) is distributed to each of the F-1 engine cocoons with flow controlled by an orifice in each of the distribution lines. Pressure at the engine interface is 165 to 200 psig.

Structure Compartments. The structure compartment purge and vent system performs the functions of purging and controlling the internal compartment temperatures on the ground, plus controlling the inflight compartment pressures.

The thrust structure and the forward compartments are conditioned on the ground to 80 (±20)F by temperature controlled air supplied by the GSE ECU at the umbilical couplings and is maintained during launch preparations up to LO_2 loading when the flow medium in the thrust structure compartment is switched to GN_2 to provide the additional purge function.

Compartment pressures are controlled on the ground by venting the compartment volume through the vent doors in the top surface of the forward and aft compartments. The inner tank structure volume is connected to the aft thrust structure volume by the LO_2 line sleeves through the RP-1 tank. The forward compartment has one 2.5 sq ft door and the thrust structure compartment has two 2.5 sq ft doors.

At lift-off the internal flow is discontinued and the vent doors remain open to allow the compartment internal pressure to bleed down and follow the ambient pressure. When the internal pressure reduces to 2.0 psia, the vent doors are closed by the GN_2 actuated cylinders.

During entry from apogee to approximately 60,000 feet, the vent doors remain closed to minimize the entry of hot air. The GN_2 regulated gas to the vent door actuators allows the doors to compress the actuating cylinders and open when the external pressure at the top centerline of the structure is 1.0 (±0.50) psi above internal pressure. This would give a maximum altitude opening of 80,000 feet where the repressuring air temperature is less then 300F and a minimum altitude opening of 53,000 feet where the repressurizing air is ≈ ambient.

4.4.5.11 Avionics

Integrated Avionics System. In conjunction with crew activities this system provides functional management and control, display, and management of the vehicle operational subsystems. The baseline configuration minimizes development cost and risk, simplifies integration complexity, provides manual backup for all flight control functions, and sufficient dedicated controls and displays for the single string redundancy management. The results of the alternate avionics approach trade study has shown this system to be less costly than the original phase B avionics system.

In general the avionics elements are dedicated to either the aerodynamic flight phase or the space craft phase. Figure 4-353 depicts an avionics block diagram with the equipment added for the first manned orbital flight kit(1) accented with shading. Most of the avionic equipment will be installed in the forward avionics equipment bay shown in Figures 4-354 and 4-355.

The equipment will be installed in physically separated compartments to minimize single point failure modes. The equipment will be connected in three independent strings with a minimum amount of cross-connections between strings and switching of elements within a string.

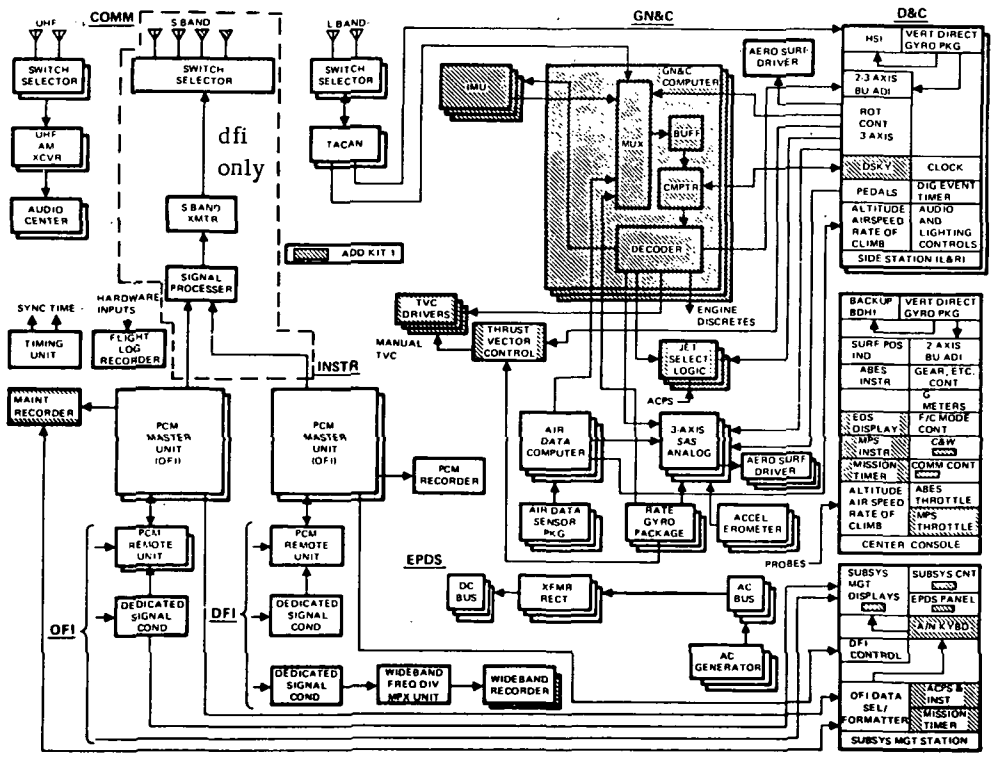

Figure 4-353. LO_2/RP Flyback Booster Avionics Configuration

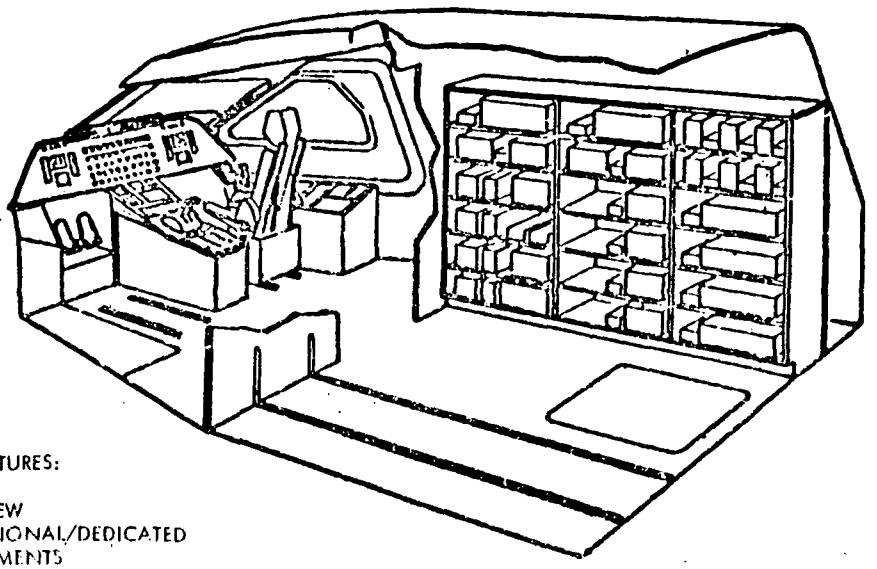

PRIMARY FEATURES:

- 2 MAN CREW
- CONVENTIONAL/DEDICATED INSTRUMENTS
- ACCESS TO AVIONIC EQUIPMENT VEHICLE VERTICAL & HORIZONTAL

Figure 4-354. Avionics Compartment

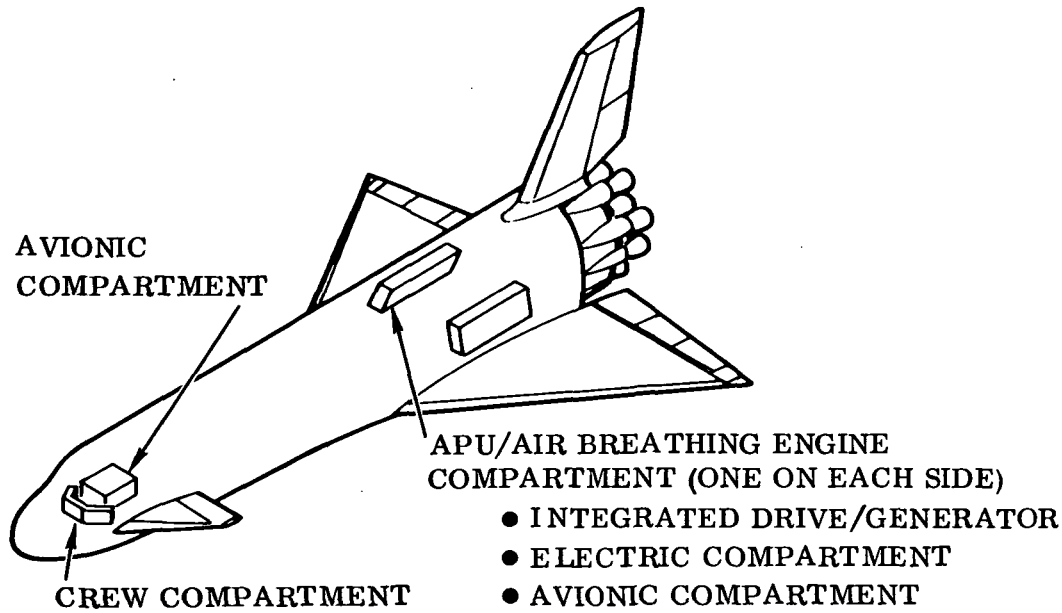

Figure 4-355. Booster (LO_2-RP) Avionic Equipment Location

Adopting this baseline has resulted in a minimal increase in both subsystem weight and electrical power requirements. Table 4-65 shows the weight of the subsystems compared to the original phase B baseline. Table 4-66 shows the avionics power requirements.

The guidance, navigation, and control equipment necessary for the aerodynamic mode, consists of a three-axis rate gyro, an air data system, a three-axis stability augmentation, and the servo drivers for the aero surfaces. Included for space mode operation are a computer, four-gimbal IMU, jet select logic for the ACPS system, and the servos and drivers for thrust vector control of the main engines. Provisions for manual control of aero surfaces, ACPS, and TVC are included.

The instrumentation subsystem provides for both development flight (DFI) and operational flight (OFI) instrumentation. During development flight testing the OFI PCM, DFI PCM and the wided band data are recorded onboard and the PCM data streams are telemetered. During the operational

Table 4-65. Booster Avionics Weights

SUBSYSTEM	B9U B PHASE BASELINE	B18E B' AVIONICS STUDY
DCM	3,301	
PgD&C (WIRE FOR POWER ONLY)	1,448	1,899
GN&C	723	1,244
COMMUNICATIONS	553	371
DISPLAYS & CONTROLS	755	1,185
OPERATIONAL INSTRUMENTATION	250	586
OFI WIRING		4,137
SUB TOTAL	7,030	9,422
DFI	5,332	1,147
DFI WIRING		3,515
TOTAL WEIGHT	12,362	14,084

Table 4-66. Booster Avionics Power

SUBSYSTEM	B9U B PHASE BASELINE	B18E B'AVIONICS STUDY
DCM	1,824	
PGD&C	1,105	578
GN&C	685	2,678
COMM	676	602
D&C	1,570	5,980*
OPERATIONAL INSTRUMENTATION		760
TOTAL OPERATIONAL	5,860	10,598

*INCLUDES 3000 W LANDING LIGHTS

flights the DFI equipment is removed and the OFI data are recorded onboard. This subsystem also provides the central timing and flight log recording equipment.

Power Generation, Distribution and Control. The primary electric power source consists of three 20/30 kva, 120/208 volts, three phase, 400 Hz ac generators, together with their associated generator control units, current transformers, and line and bus tie contactors. The generators are spray oil cooled and are integrated with a constant speed drive. The integrated drive-generator (DG) unit is driven by the APU. This arrangement relieves the APU of precise speed control requirements and provides a high degree of isolation from the severe frequency transients caused by the hydraulic pump loads. The generators operate unparalleled and are synchronized to eliminate heat frequencies. Each generator is connected to a main three phase ac bus through a generator line contactor. See Figure 4-356.

A three phase transfer bus provides a central point for interconnecting the main buses through three bus tie contactors in the event of failure of one or two generating channels. The transfer bus also serves as the tie point for ground power. Three ac distribution feeders are routed from the main ac buses in the APU compartment to the avionics compartment forward.

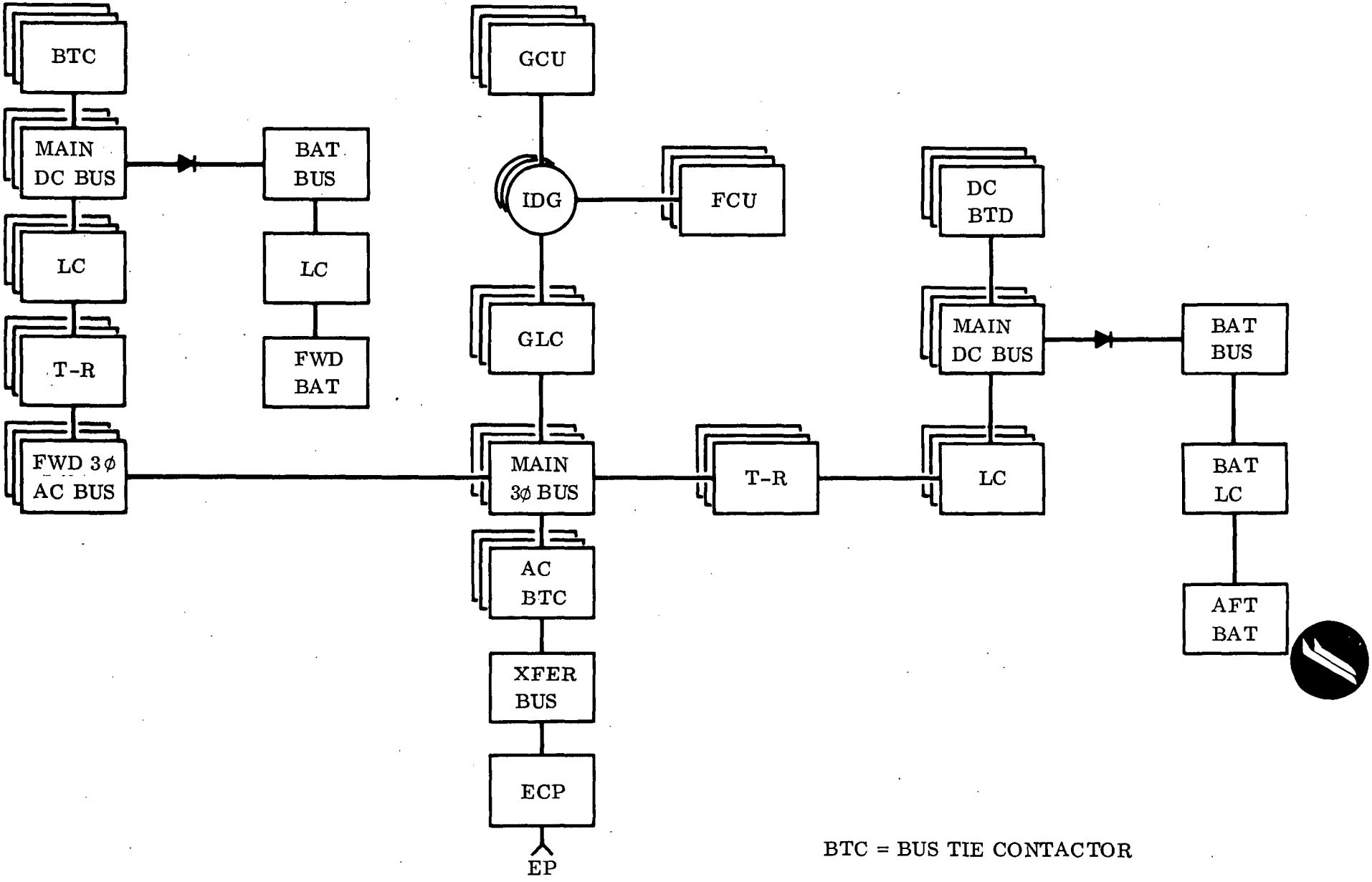

Figure 4-356. Electric Power Generation, Distribution and Control

Ac and dc loads in the forward and aft area are served through remoted controlled circuit breakers (RCCB). These are thermal circuit breakers using an electromagnetic actuating mechanism energized by switch action from the crew compartment as shown in Figure 4-357. Trip status is indicated by a lamp.

At each forward and aft area, the ac power is converted to 28 volts dc with transformer rectifiers (T-R). Three T-R's are provided to each location together with dc buses, T-R output contactors, and RCBB's. The main dc buses may be interconnected through bus tie contactors arranged in a ring configuration.

A 10-ampere-hour nickel cadmium batter supplies 28 volts dc power for system initialization and management functions under emergency conditions. One battery is provided in each forward and aft location. Power is distributed through a battery line contactor and battery bus. The battery bus is unilaterally isolated from the main dc bus with a power diode.

Crew Systems. Booster vehicle geometry, avionics configuration, crew workload and environmental considerations were driving factors leading to the baseline flight deck arrangement.

Crew Station. The baseline design provides a functional and efficient crew station geometry for a two man crew (5th through 95th percentile - 1980 baseline) seated side by side in a pressurized compartment. Reference Figure 4-358.

Most of the avionics equipment is located in an adjacent compartment within the same pressure vessel. When the booster is on the launch pad in the vertical position, ingress/egress is via the gantry swingarm through a hatch. Access to the avionics equipment bay is through a door between compartments using a ladder. With the vehicle in the horizontal position, ingress/egress from the ground is by a ladder through the wheel well and a hatch in the floor of the avionics bay. Emergency egress in the vertical configuration is via a fast elevator and in the horizontal by the use of controlled descent devices. An ejection capability is provided for during the development phase.

Displays and Controls Mechanization. The commander (RH seat) and pilot (LH seat) operate in a fairly conventional aircraft configuration based on overall booster mission requirements. Figure 4-354 illustrates the general physical arrangement and functional organization of the D&C configuration. The primary manual flight controls include two three-axis sidestick type rotation controllers for attitude and maneuver commands; two pedal assemblies for control of rudder, nosewheel steering, and wheel brakes; and a centrally mounted throttle quadrant for ABES engines.

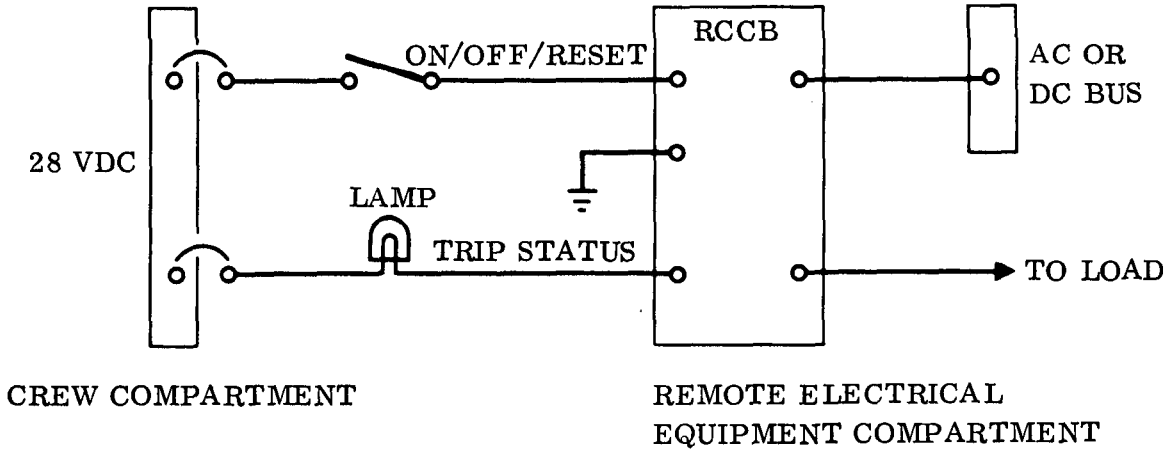

Figure 4-357. Remotely Controlled Circuit Breaker

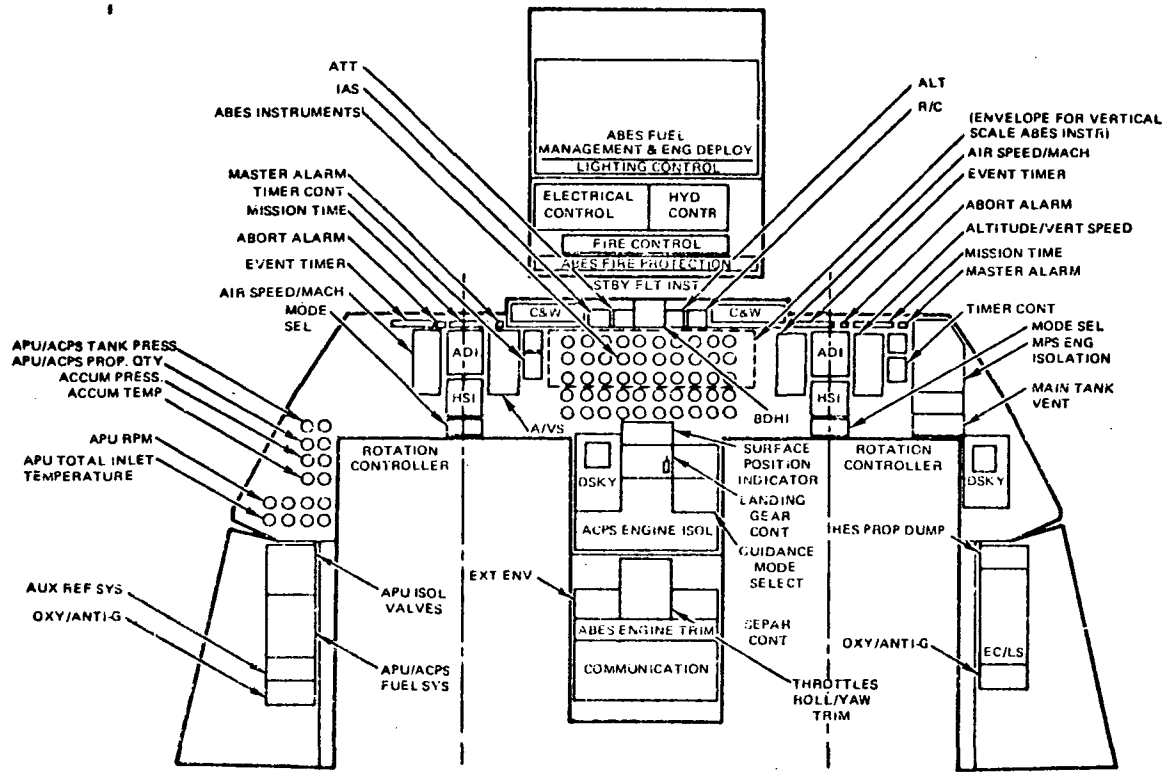

Figure 4-358. Space Shuttle Booster Crew Station

Secondary controls located on the flight deck include landing gear, parking brakes, ABES engine deployment, main rocket engine shutoff, etc. Command access is provided in the vehicle for all functions essential to flight and personnel safety. The flight crew have provisions to intervene and command the vehicle to a safe state if malfunctions or contingency situations occur. Control tasks will normally be performed automatically only to the extent necessary to satisfy high precision, short reaction time and fuel economy requirements. Separate, guarded controls are provided for critical functions where the effect of inadvertent initiation would be hazardous or irreversible. Sufficient redundancy is incorporated in displays, crew control, command, and sequencing functions to ensure safe return following failure. Operation of the primary manual flight controls is selectable as a function of flight mode. For ACPS attitude modes, command is effected via the side-stick rotation controllers, providing discrete rate commands in the vehicle roll, pitch and yaw axes. Manual steering takeover capability is provided for mated-ascent thrust vector control. Aerodynamic flight modes employ the side stick rotation controllers in a proportional rate command mode for pitch and roll control, and pedals for yaw. During landing at nosewheel touchdown the pedals are enabled for nosewheel steering. Toe motion of the pedals applies wheel brakes during taxi and

disengages the parking brake, if applied. Only manual control modes are available for aerodynamic flight and landing. The principal flight displays consist of a basic set of conventional aircraft instruments for each crewman except that a space type three-axis ADI is used in place of the usual two-axis ADI.

A full set of flight displays including a two-axis g-meter is also provided as a dedicated backup and mounted between the crewman. Each crewman also has access to a small alpha-numeric format CRT and keyboard. This display/keyboard (DSKY) provides crew interface with the GN&C computer and allows presentation of navigation data and certain selectable subsystem data as required to aid in redundancy management.

Conventional dedicated displays and switches are used for power up, power down, operational reconfiguration, normal monitoring, redundancy management and emergency override capability by the crew.

Discrete controls for system configuration and operation are organized by related system and function. The crew has direct, single operation access to major and critical system functions.

Major parameters for monitoring ABES conditions are located on the center main panel. During the low cost avionics study it was determined that either round dial or tape type instruments could be used. Tape type instruments provide the advantages of requiring less panel space and somewhat less crew scan time.

Caution and Warning. The caution and warning system employs a flexible logic capability to identify failures by related system and function. Caution and warning indicators are located in the center glare shield area within the preferred vision zone.

Communications Subsystem

The communications subsystem provides for voice contact with the ground, interphone, and bearing and distance information for the navigation function. Two UHF/AM transceivers provide radio contact with the ground. The flight profile of the booster is such that line-of-sight communications with the launch site is possible throughout the mission. The interphone permits duplex communications between the crew stations, selected maintenance stations, and the orbiter crew. Three TACAN sets provide bearing and distance data for display to the crew and for the navigation calculations.

Redundancy Management

Redundancy management is basically a crew function. During boost phase and entry, the timing requirements are such that it is necessary to provide automatic switching, with manual override, of certain flight critical functions. Operation of the avionic and nonavionic subsystems is accomplished through dedicated control and display panels. Wherever possible, the subsystems are organized into functional loops which have a minimum of cross strapp and switching of elements within the loop.

4.4.5.12 Mechanical Systems

Separation. The relationship of the orbiter to the booster and location of the interstage interface is shown in Figure 4-359. The axial load is reacted in the booster through a continuous ring located at the separation interface. This provides for a distributed load path in both the booster nose and interstage adapter.

Ten dual pyrotechnic bolts equally spaced around the ring secures the orbiter to the booster. Tension, shear, and torque loads are reacted through these bolts. The dual pyrotechnic bolt is illustrated in Figure 4-360. Pressure developed by gas generated from the main charge drives the piston against the captured rubber core. The rubber pressure resulting from this force acts on the internal diameter of the bolt producing a force that fails the bolt in tension. Redundancy is achieved by providing dual pistons, four main charges and four initiators.

Landing Gear. The landing system, Figure 4-361, consists of a nose and main gear in a conventional tricycle arrangement. The gear is located to provide tip back and turnover stability and ground clearance for takeoff and landing. The gear is designed for a normal landing speed of 178 knots on a 10,000-foot runway in accordance with FAR part 25 at a limited sink speed of 10 fps. Both the nose and main gear retract forward providing free fall capability.

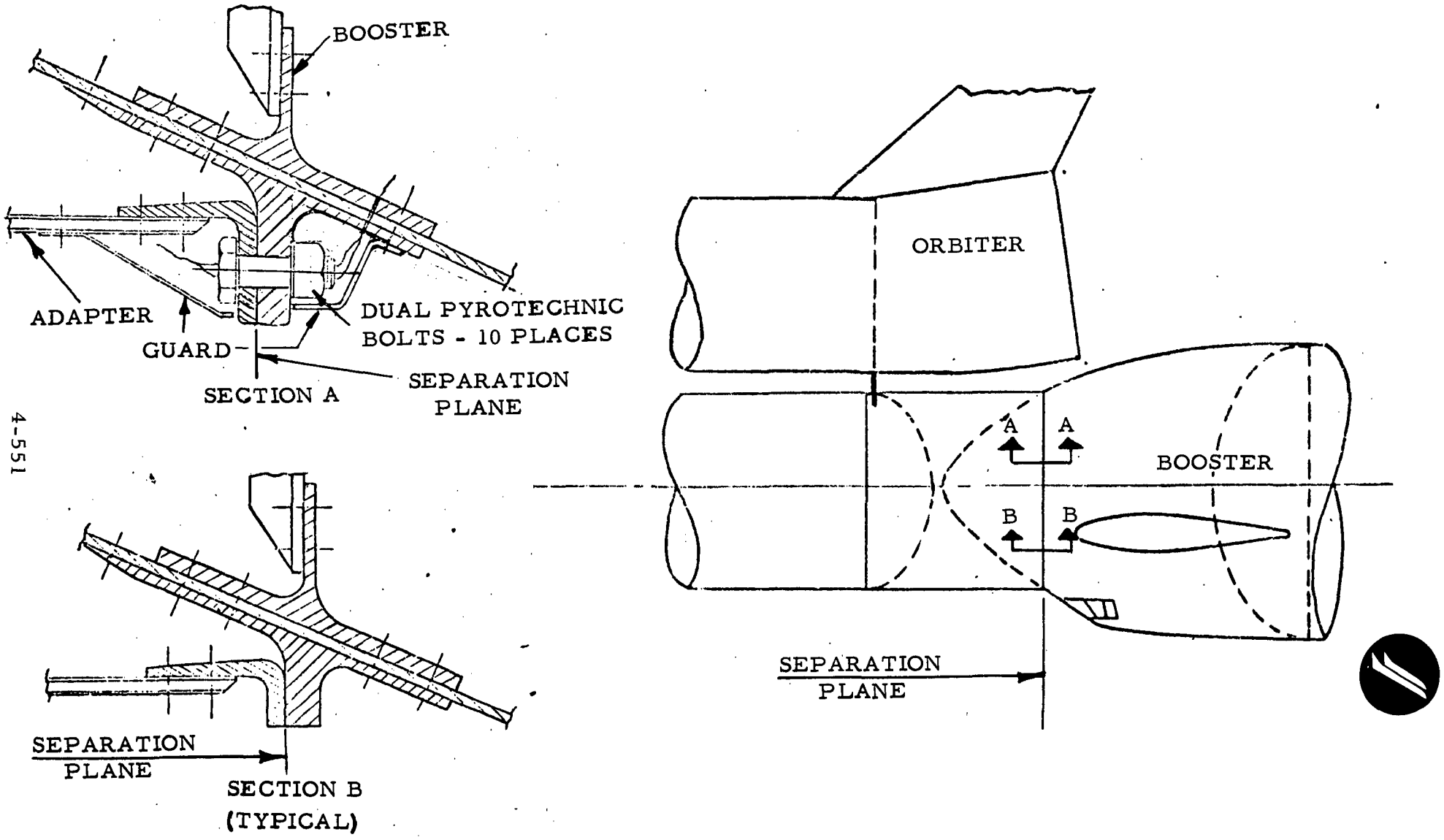

Figure 4-359. Interstage Adpater Attachment

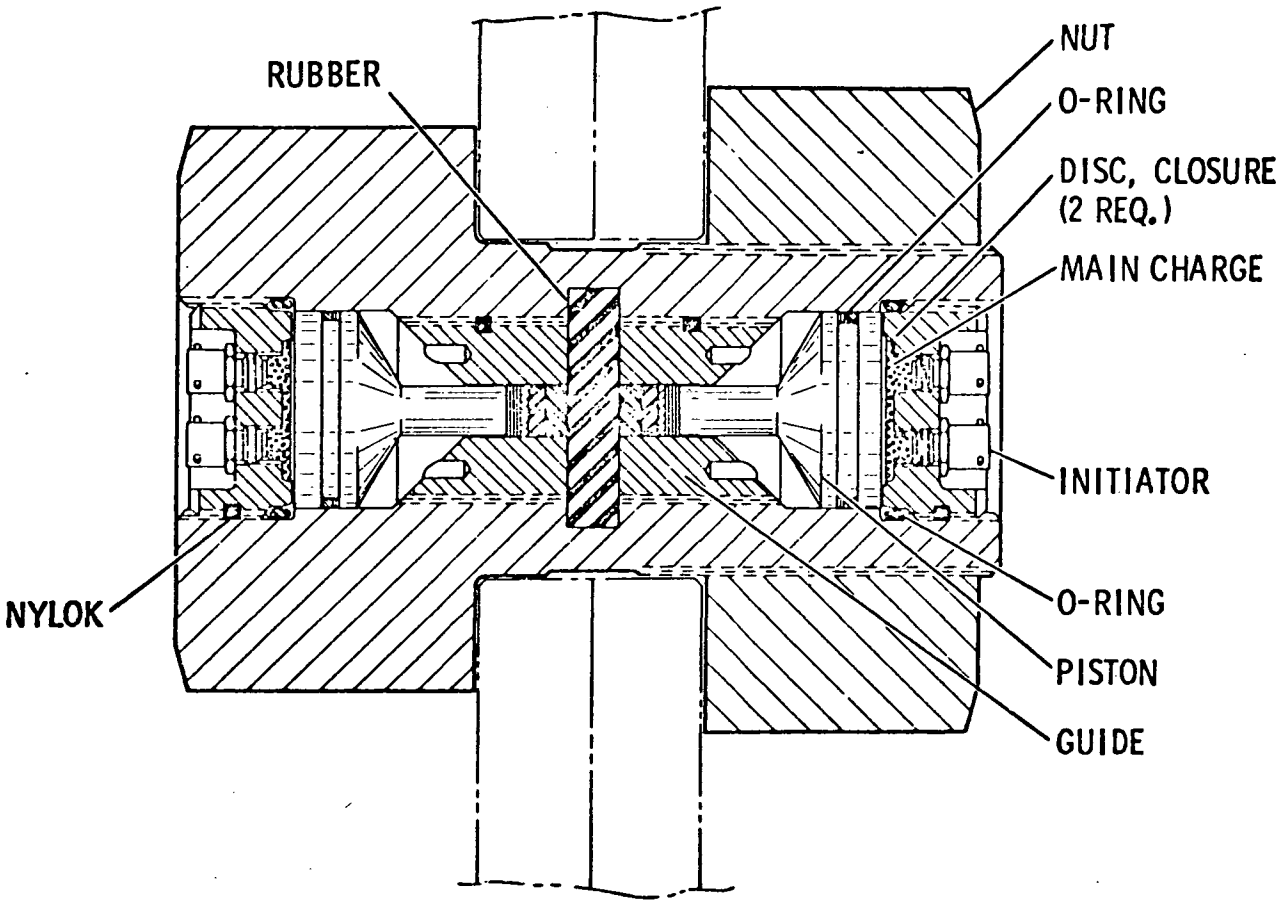

Figure 4-360. Typical Pyrotechnic Bolt Arrangement

Each main gear consists of a conventional air-oil shock strut, a folding drag brace, 56 x 18.5 - 28 twin tandem tires, four steel heat sink brake, and an antiskid system with independent wheel control. The static load on each tire is 73,000 pounds.

The nose gear consists of a conventional air-oil shock strut, folding drag brace, 46 x 16 twin tires and steering system which consists of actuators, control valve and mechnical feedback. These are existing gear, tire, wheel and steering presently used on a large commercial aircraft. The static load on each tire is 24,000 pounds.

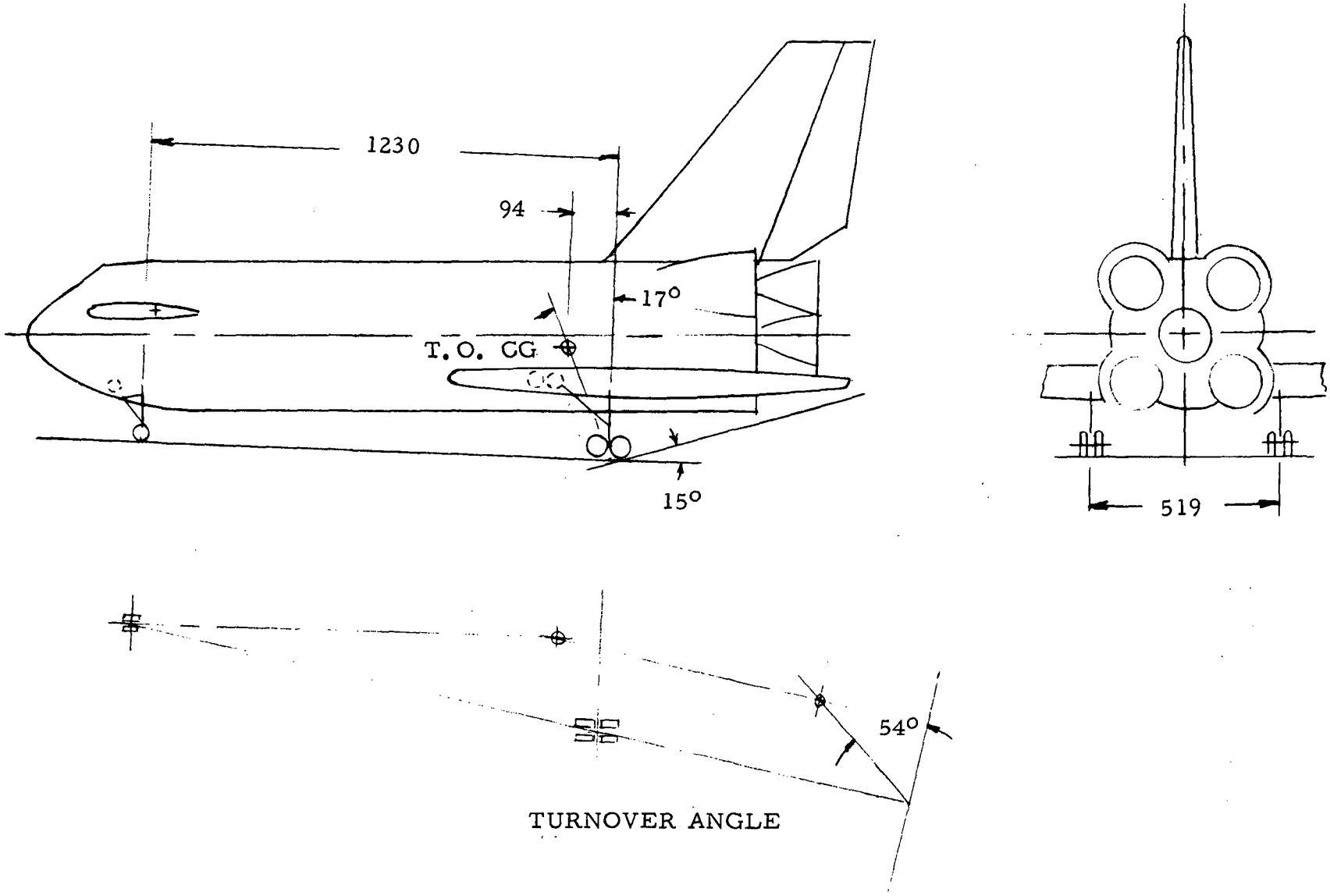

Figure 4-361. Landing Gear General Arrangement

4.4.5.13 Weight Statement

Table 4-67 is a weight breakdown for the B-18E-3 booster, with propellants sufficient to provide 6000 fps relative staging velocity. A growth allowance of 10% on dry weight items, excluding ascent engines and cruise engines, is included. Table 4-68 shows sequence mass properties.

Table 4-67. B-18E-3 Weight Statement

		WEIGHT (LB)
AERODYNAMIC SURFACES		98,422
WING (8549 FT^2)	79,402	
CANARD (485 FT^2)	7,372	
VERTICAL (1300 FT^2)	11,648	
BODY		199,348
FUEL TANK	28,782	
OXIDIZER TANK	38,823	
NOSE, INCL. ORBITER PENALTIES	37,030	
INTERTANK	19,277	
THRUST STRUCTURE	40,000	
WING & LG BULKHEADS	9,646	
FAIRINGS (ENGINE, WING, ETC.)	18,890	
BASE HEAT PROTECTION	5,000	
CREW & AVIONICS COMPARTMENTS	1,900	
LANDING GEAR		26,395
PROPULSION, ASCENT		138,833
MAIN ENGINES	93,075	
TVC	3,543	
ENGINE INSTALLATION	5,215	
PROPELLANT SYSTEMS	37,000	
PROPULSION, AIRBREATHING		44,050
ENGINES (10)	26,750	
NACELLES, DEPLOYMENT, SYSTEMS	14,500	
FUEL TANKS	2,800	
PROPULSION, AUXILIARY (ACPS)		3,000
POWER SOURCES (APU)		2,000
ELECTRICAL		2,000
HYDRAULICS		2,900
SURFACE CONTROLS		11,300
AVIONICS		5,600
ENVIRONMENTAL CONTROL, PURGE		5,800
PERSONNEL PROV., FIRE DET. & EXT.		1,700
GROWTH ALLOWANCE (10%, EXCL. ENGINES)		42,152
DRY WEIGHT		583,500
CREW		476
RESIDUALS AT LANDING		33,850
INFLIGHT LOSSES		35,595
ACS PROPELLANTS		3,728
CRUISE PROPELLANTS		35,851
ASCENT PROPELLANTS		3,280,000
GROSS LIFT-OFF WEIGHT		3,973,000

Table 4-68. B-18E-3 Sequence Mass Properties

EVENT	WEIGHT (LB)	X CG(1)	Z CG(2)	SLUG $FT^2 \times 10^{-6}$			
				I_{XX}	I_{YY}	I_{ZZ}	P_{XZ}
LIFT-OFF	3,973,000	2119	396	9.6	162.4	164.7	-2.1
MAX Q	2,578,311	2212	393	8.4	106.1	108,4	-1.7
MAX G	957,939	2355	381	7.0	61.4	63.8	-1.1
BURN-OUT	692,250	2397	374	6.8	54.9	57.4	-1.0
CRUISE	653,677	2374	367	6.9	53.4	55.7	-1.1
LANDING	617,826	2442	360	7.2	43.1	45.3	-0.8

(1) NOSE = 1000 + AFT

(2) TANK C_L = 400 + UP

4.4.5.14 Manufacturing

The principal components of the LO_2/RP booster and their sequence of assembly is shown in Figure 4-362. The plan reflects an analysis of design requirements, material availability, fabrication procedures, tooling and facility requirements. Use of conventional fabrication procedures and existing (Saturn S-1C) tooling and facilities has been emphasized. The plan assumes use of the NASA Michoud facility for assembly and checkout of the booster vehicle.

The LO_2 and RP tanks are 33 feet in diameter by approximately 64 and 43 feet respectively in length. They are made from 2219 aluminum alloy and are of all-welded construction. Each tank consists of two end closure bulkheads and a series of cylindrical skin sections. A structural wing attach frame will be incorporated into the RP tank.

Tank bulkheads and cylinder sections will be fabricated from plate stock. Detail parts will be milled to produce weld lands, formed and aged, trimmed to net size and welded together to form the bulkhead and cylindrical section subassemblies. Mating "Y" rings made from forged aluminum billet will be rolled, welded, machined and aged prior to being welded to their respective bulkheads. Existing S-1C tooling and facilities will be used for most of the detail fabrication and subassembly tasks. Very little new tooling or facilities will be required.

Bulkheads and cylindrical sections will be progressively joined together to form the propellant tanks. Tanks will be assembled vertically, proof and leak tested, and cleaned in vertical assembly building using existing tooling and facilities. The LO_2 duct tunnels passing through the RP tank will be fitted and joined to the tank during the tank buildup.

The intertank adapter is a mechanically joined aluminum alloy structure 33 feet in diameter and approximately 30 feet long. It consists of machined fittings, frames, longerons, rolled rings, and milled skin panels. Main frames and skins will be machined from plate stock. Skin panels will be age formed to contour after machining. The structure will be assembled in a vertical assembly fixture which locates and holds the fittings, frames, longerons, rings and skin panels in proper relation for mechanically joining. The S-1C intertank adapter assembly fixture will be modified for this purpose.

The thrust structure is a 33-foot diameter aluminum structure, not including fairings, approximately 20 feet long. It is fabricated from plate, extrusions, rolled shapes, and forgings that are mechanically joined. Major subassemblies include thrust and wing attach frames, longerons, engine support beams, and thrust posts. Frame and skin panel details will be milled from plate. Skin panels will be age formed to contour.

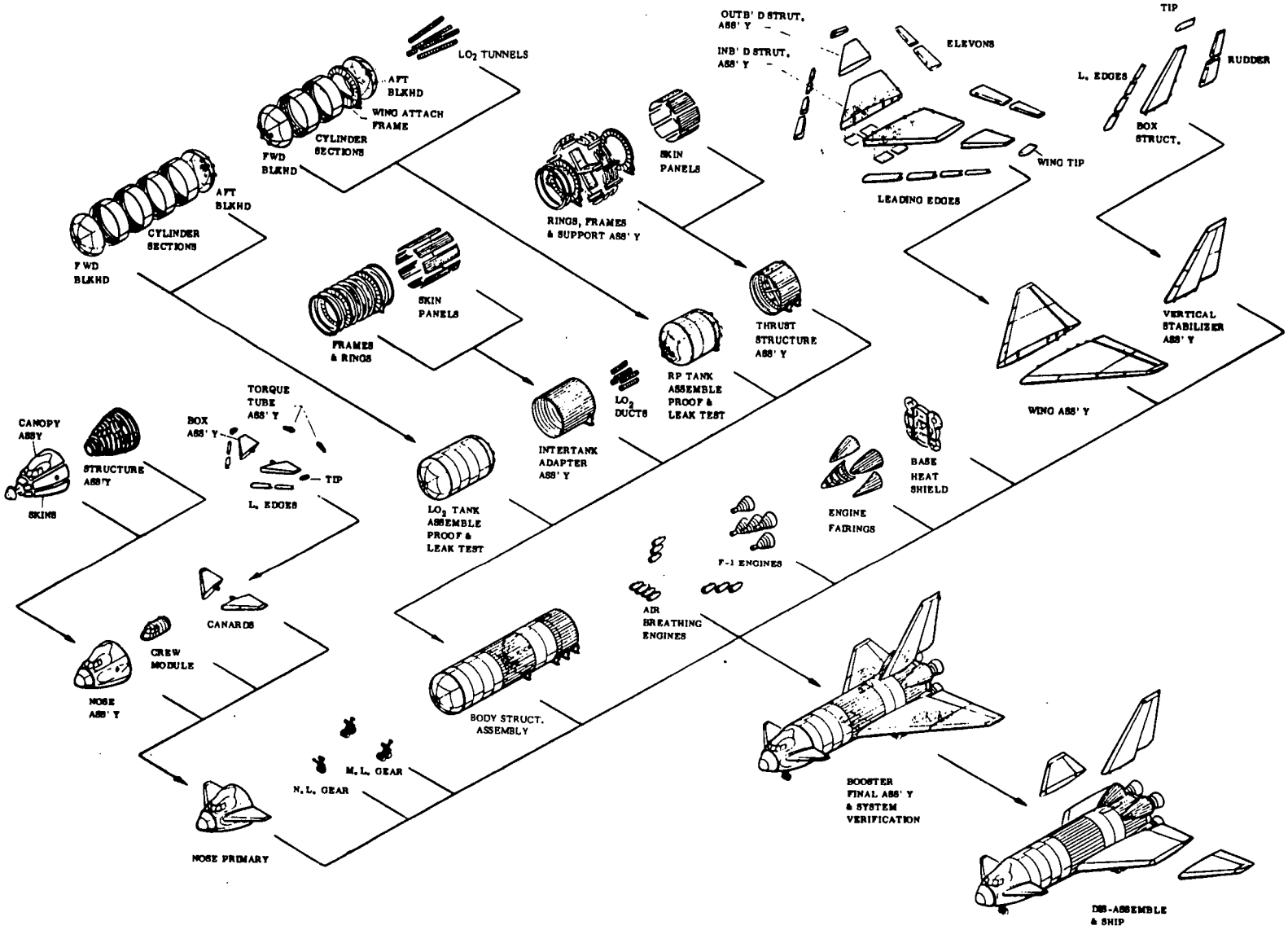

Figure 4-362. Manufacturing Assembly Sequence

Frames, longerons, beams and posts will be subassembled prior to final assembly. The thrust structure will be assembled in the vertical attitude to simplify tooling and improve work access. The existing S-1C thrust structure assembly fixture will be modified for this purpose.

The propellant tanks, intertank adapter and thrust structure will be mechanically mated in the Michoud vertical assembly building. Laser optics, supplemented by hard interface control tools, for critical interfaces such as wing attachment, will be used for alignment. LO_2 propellant ducts will be lowered through the intertank adapter and into the duct tunnels in the RP tank prior to mating the LO_2 tank to the adapter. Ducts will be attached to the LO_2 tank after mating.

The booster nose is of conventional commercial aircraft construction except for heavier skin panels and high temperature high strength windshield requirements. Most of the structure, including the outer skin, is made from aluminum alloy.

Skin panels will be stretch formed and chem-milled in selected areas where pocketing is required. Frames will be stretch or hydro-press formed. Window frames will be N/C milled. Certain portions of the structure, including the nose wheel well, nose landing gear doors and the canopy, will be subassembled. Structure assembly will be performed with the structure vertical. A special fixture will be provided for this purpose.

The crew module, canards, ballast tank, and related equipment will be fitted and installed in the nose structure prior to mating with the tank body structure. The nose structure will be supported horizontal in a special handling dolly during these installations.

The wings are designed as separate right and left hand sections that are mechanically attached to carry through fittings in the body structure. The basic structure, skins, and most of the component parts of the wing are made from aluminum.

The structural wing boxes are broken down into inboard and outboard assemblies to provide transportation breakpoints. This will permit shipment of the assembled booster (less outboard wing sections) to the launch site using available barge equipment. Ribs and spars will be subassembled then joined together to form an egg crate structure. Upper and lower skin panels will then be joined to the structure. Integrally stiffened skin panels will be milled from plate, formed to contour and aged. The wing boxes will be assembled in vertical assembly fixtures. Laser line of sight will be used as the basic alignment reference.

Mating of the inboard and outboard wing boxes and final assembly of the wings will be performed with the wing horizontal in cradle type support fixtures. Dummy engines and main landing gear assemblies and their related equipment will be installed at this point along with the leading and trailing edges, wing tips, elevons and associated equipment. Following fit and function test, the dummy engines and landing gear will be removed.

Fabrication and assembly procedures for the vertical stabilizer and canards will be similar to those used for the wing. Vertical assembly fixtures will be provided for final assembly operations.

Final assembly of the booster vehicle will be accomplished with the booster horizontal. Wings, vertical stabilizer, and the nose will be structurally mated to the body structure using special handling tools. Interconnecting wiring and tubing runs will then be completed. Installation of the landing gear, the main propulsion system, including fairings and heat shield, the airbreathing engines and their related systems, and the attitude control and auxiliary power systems will follow.

When all component installations have been completed, the systems will be checked out and verified. The vertical stabilizer and outer panel sections of the wings will then be removed to facilitate shipping and the booster, after suitable shipping preparation, will be barged to the launch site.

4.4.5.15 GSE and Facilities

Facilities. Maximum use will be made of the basic facilities now in existence at KSC. The runway, taxiway, safing area, and towway are the same as those described for the Phase B baseline concept. The VAB will require modifications. The existing crawlerways can be used with no alterations.

Vehicle Assembly Building. In using the existing VAB to support the LO_2-RP booster, the structural alterations required are:

1. Widening the doors at each end of the transfer aisle.
2. Addition of a stationary 200 ton winch in HB-1.
3. Widening of HB-1, HB-2, and HB-3.
4. Addition of 350-ton crane (in place of the 250 ton in HB-1).
5. Addition of floor area to accommodate booster checkout and vehicle stage.

Studies are continuing to determine the most efficient building utilization and to minimize new construction.

Launch Site. The concept for using the launch complex 39A requires no changes to the existing facility. All structural hard points for the mobile launcher will be used without alterations. The flame deflector, deluge system, etc., will be used "as is." The launch pad configuration for the LO_2-RP booster is shown in Figure 4-363.

Mechanical GSE

Mobile Launcher/LUT. Major changes are required to the existing mobile launcher/LUT. The launch pedestals and its main structural support will be added to the existing launcher. The required swing-arms and payload handling equipment will be added as shown in Figure 4-363.

Holddown and Release System. A new holddown and release system will be required for the LO_2-RP booster as shown in Figure 4-364.

Booster/Orbiter Access Service Arms. Access service arms will be used for ingress and egress of the booster and orbiter crew compartments. A separate arm will be provided for each vehicle as shown in Figure 4-365. The access arms also form an integral part of the emergency egress system which is shown in Figure 4-366.

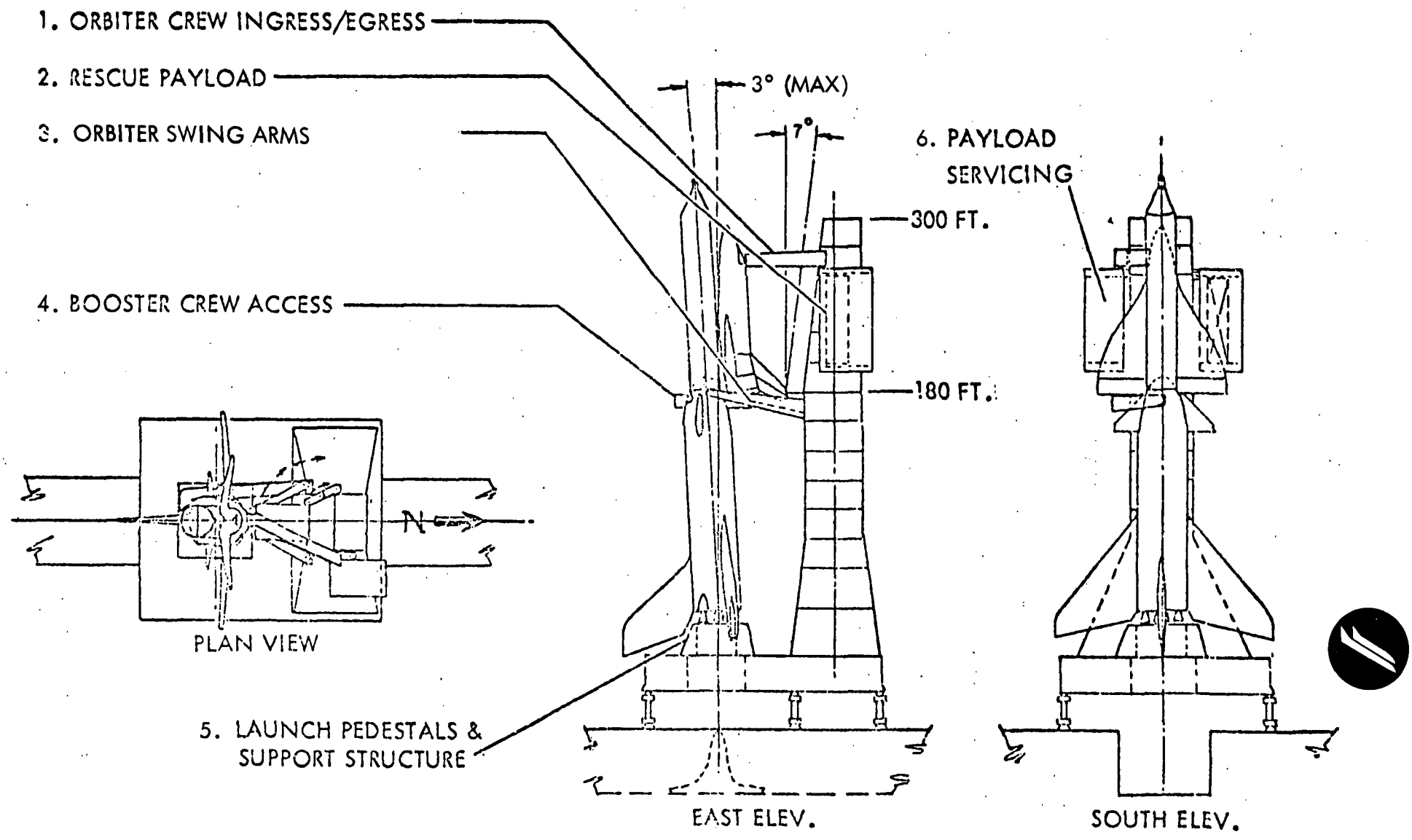

Figure 4-363. LO_2/RP Flyback Launch Pad Configuration

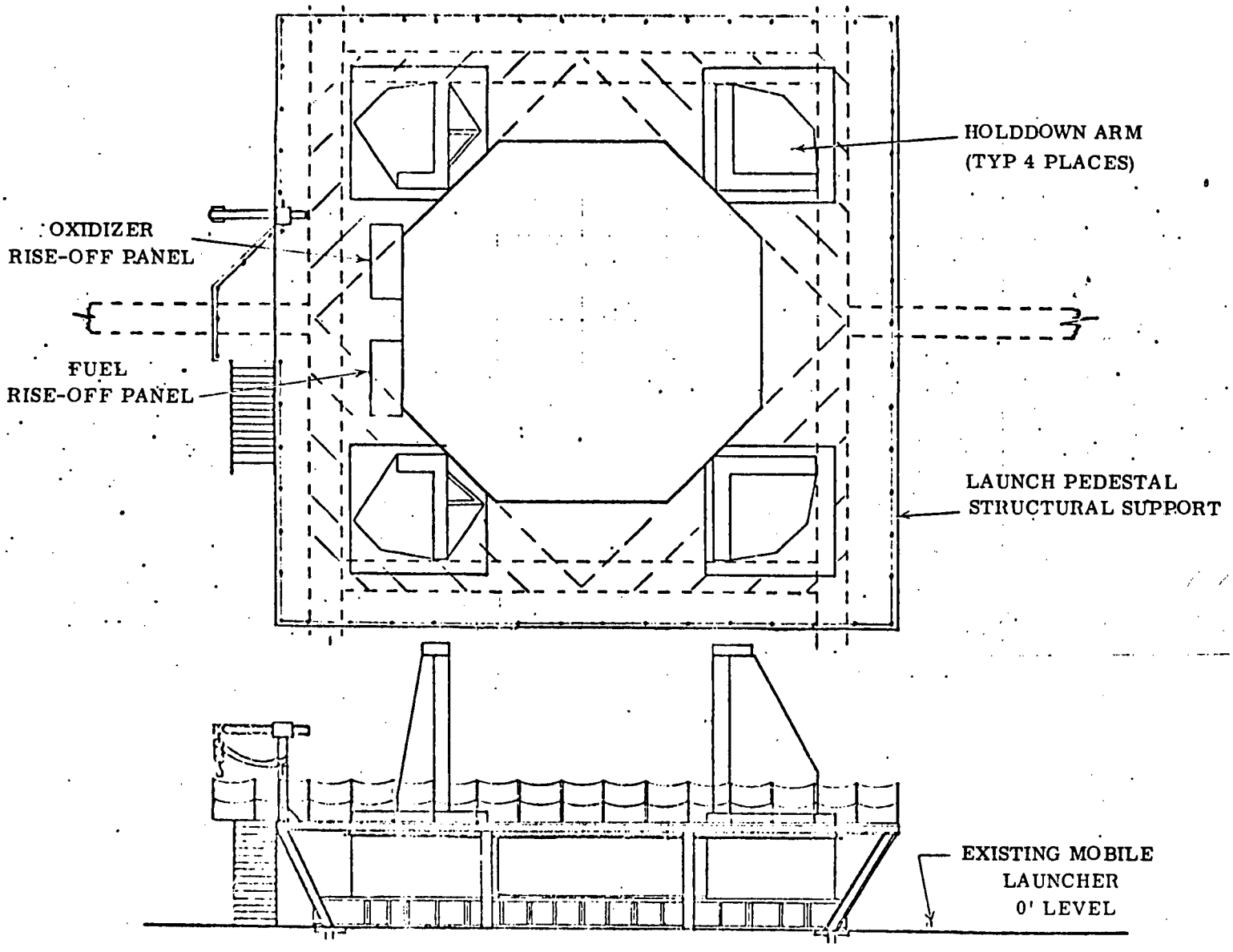

Figure 4-364. Holddown and Release System

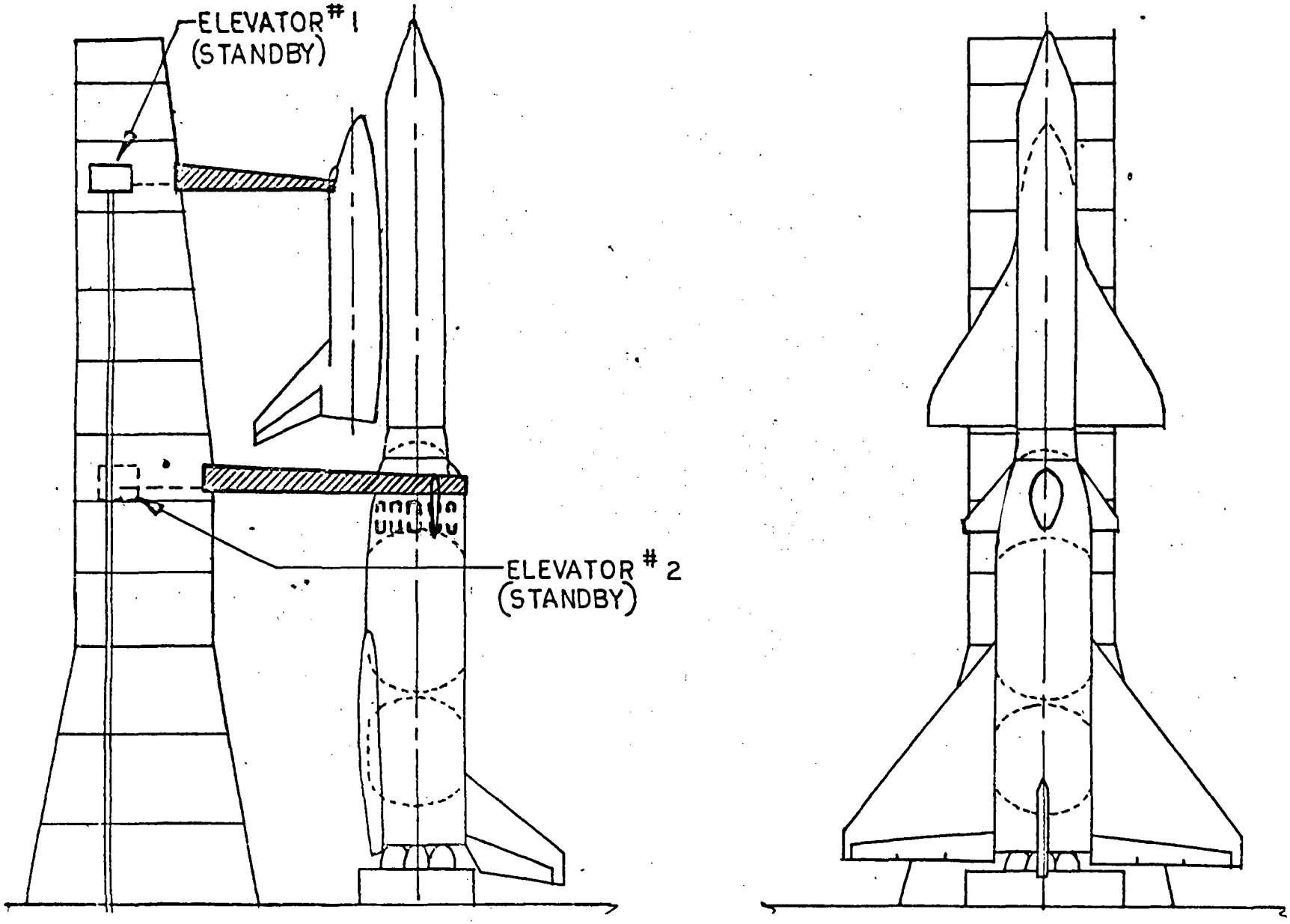

Figure 4-365. LO_2/RP-1, F-1 Engine - Flyback

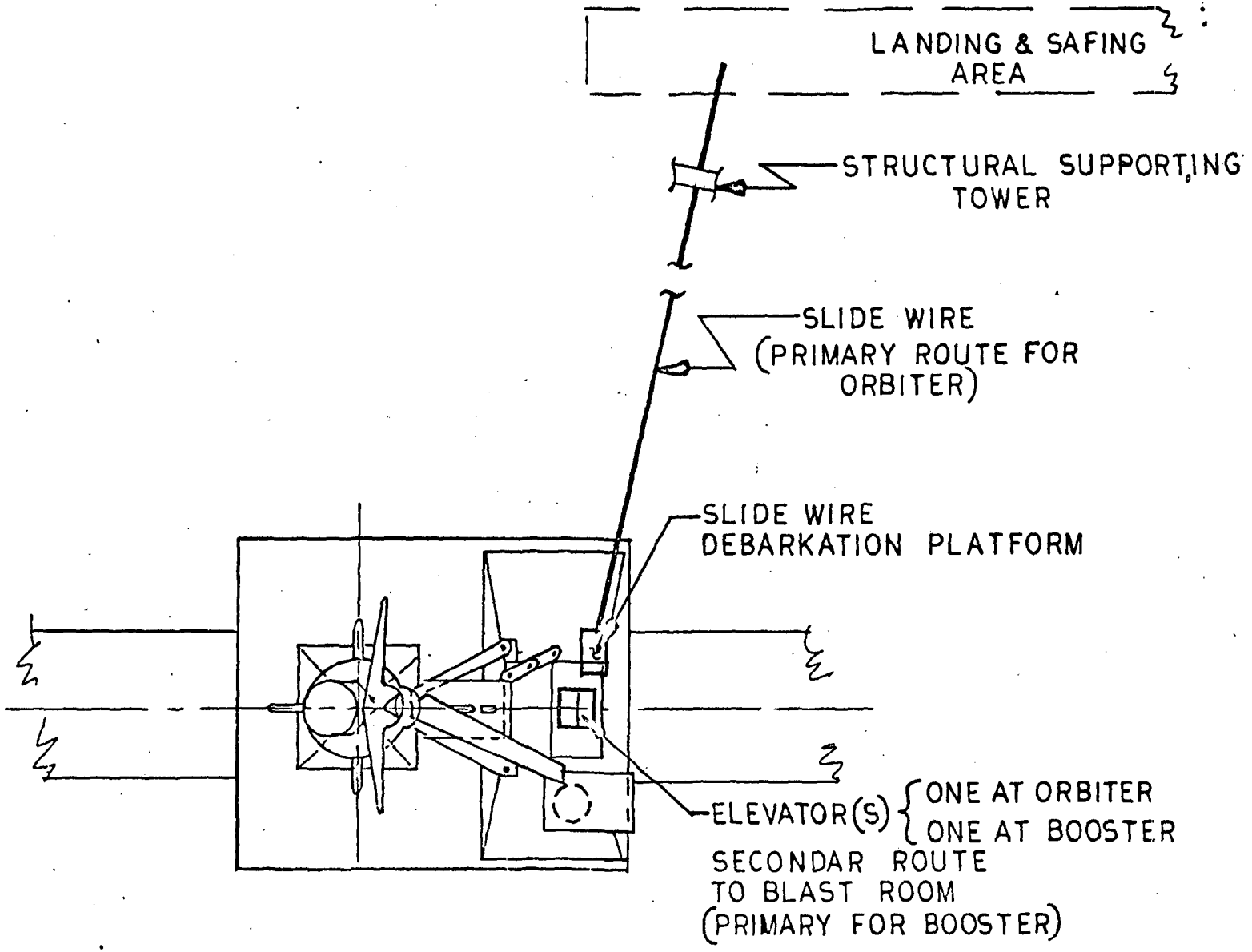

Figure 4-366. LO_2/RP-1, F-1 Engine - Flyback

Riseoff Disconnect Panels. Riseoff disconnect umbilical panels will permit the ground half of the umbilical disconnects to separate axially as a result of first vehicle motion. Booster panels will be located in the launcher/vehicle support structure and the orbiter panels will be located at the end of the in-flight service arms which are retracted at the beginning of vehicle motion.

Stabilization System. A stabilization system is required to stabilize the launch vehicle during movement from the VAB to the launch pad and during periods of high wind conditions while the vehicle is located at the launch pad. The system will basically consist of a sway strut located at the forward structural ring of the booster.

Servicing GSE.

Propellant Transfer System. The propellant servicing system for the LO_2/RP booster and the orbiter is shown in Figure 4-367. The system provides for the transfer of LO_2, RP, and LH_2 between the facility storage tanks and the vehicles. Also, it provides for JP fuel which is used for the booster and orbiter ABES.

Hypergolic. A remote facility will be utilized for hypergolic servicing of the orbiter OMS and RCS pads. Booster and orbiter APU hypergolic tankage will also be serviced there.

Pneumatic Servicing System. The pneumatic servicing system for the booster and its associated GSE is shown in Figure 4-368.

Safing Area. Safing support equipment will include pneumatic panels for vehicle purge control, propellant drain system, and portable environmental condition system.

Electrical/Electronic GSE

Launch Operations. The ground checkout system is comprised of control and display consoles, a ground computer, and ground support equipment which interfaces with the servicing equipment, propellant loading system, and the vehicle subsystems.

The propellant loading system is the existing KSC system used for the Apollo program that includes an electronic/electrical control and a data transmission system (Figure 4-369).

Many of the avionics subsystems have an inherent-built test/self-test capability. The self-test must be manually controlled from controls in the crew compartment. The results will be reviewed on displays in the crew compartment, analyzed, and corrective action instituted.

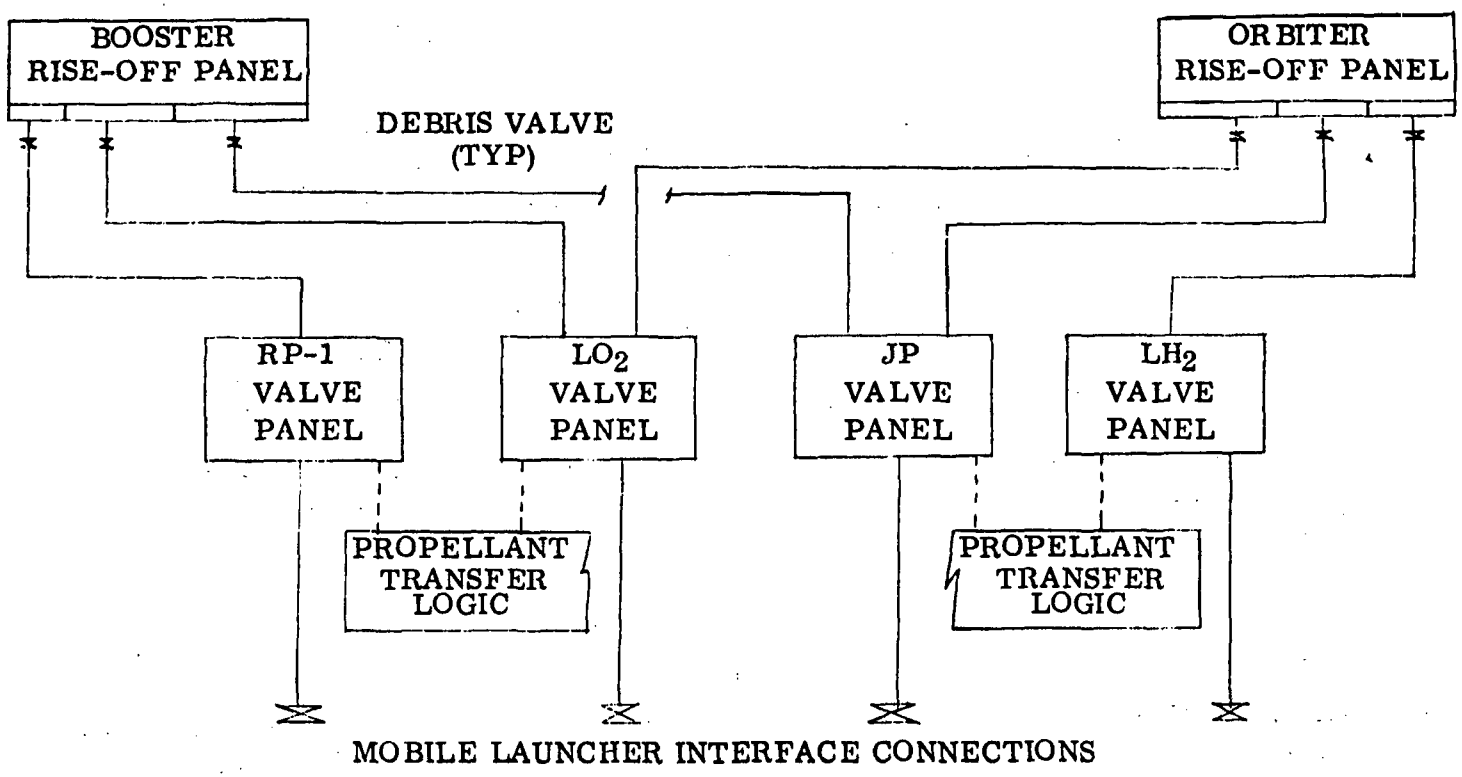

Figure 4-367. Propellant Servicing Equipment Interconnect Diagram

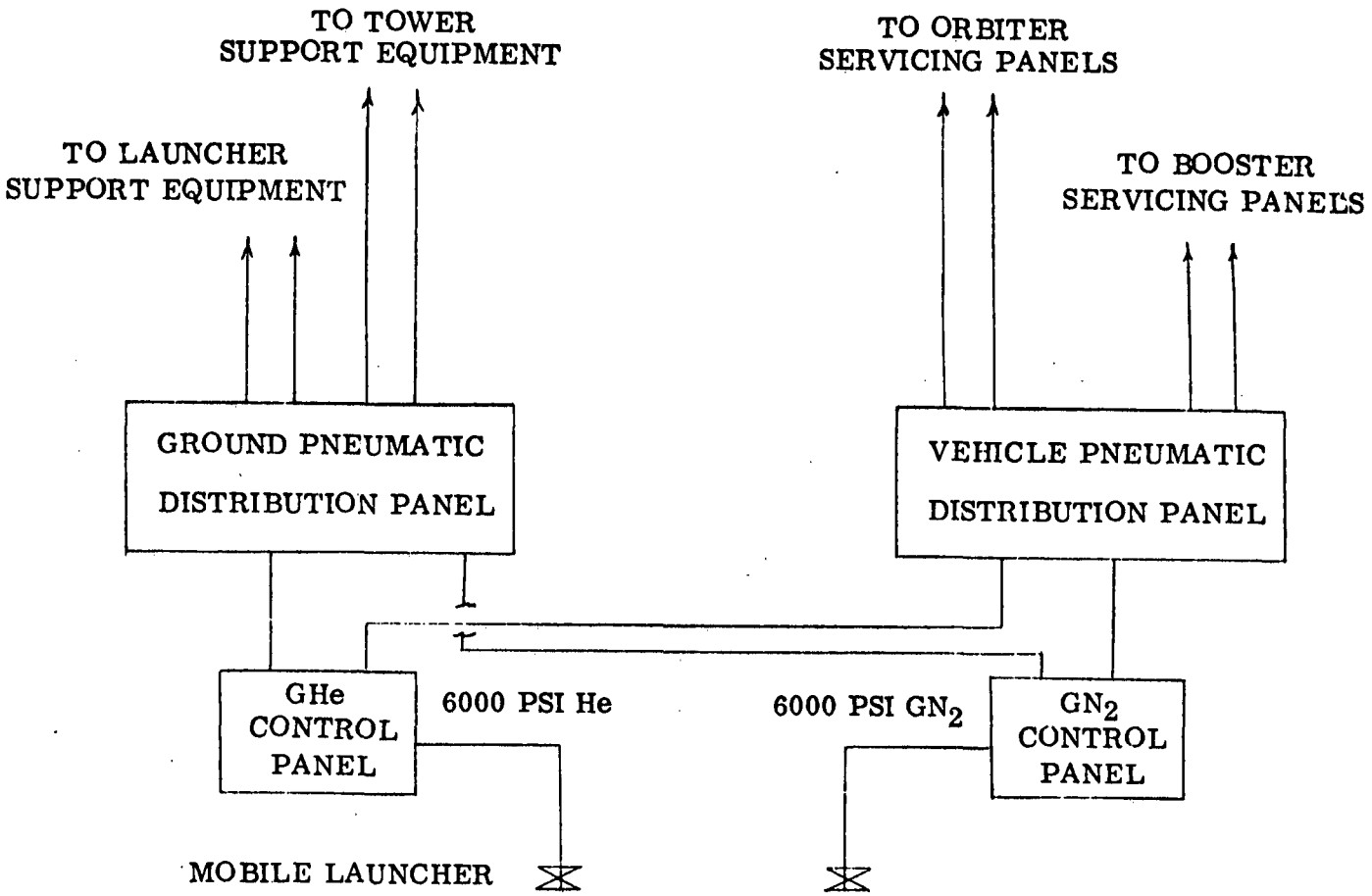

Figure 4-368. Pneumatic Servicing Equipment Interconnect Diagram

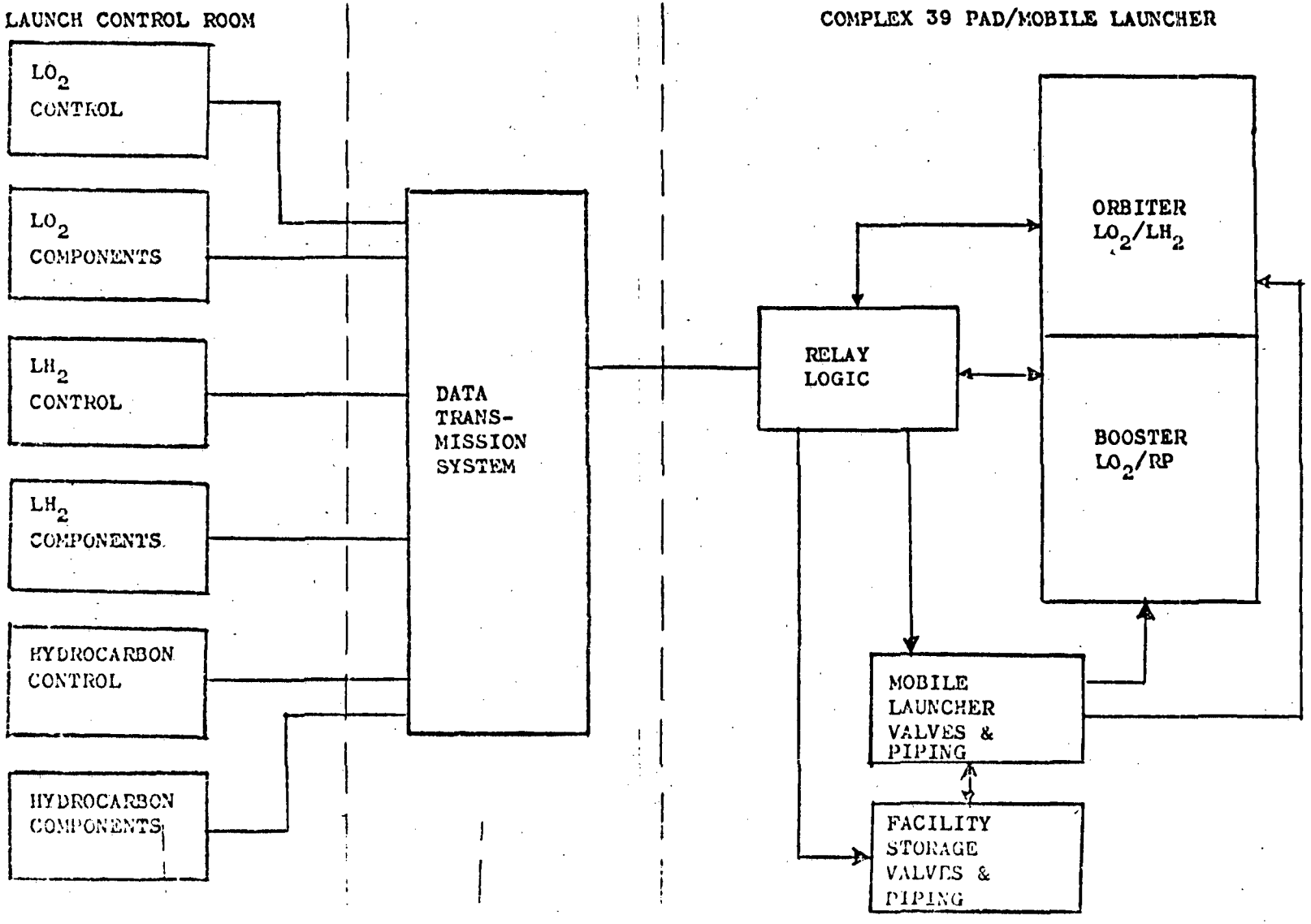

Figure 4-369. Propellant Loading System (LO_2/RP Flyback or Pressure Fed Booster)

Voice communications are accomplished via the hardware umbilical between launch control and the vehicle.

Navigational Aids. TACAN ground stations will be installed for enroute distance and bearing information to the landing site during flyback and ferry missions.

A voice communication air link with the air traffic control will be accomplished utilizing the UHF-AM radio station at the KSC airport tower.

Level I Maintenance. A ground checkout system essentially the same for prelaunch checkout operations will be utilized together with on-board tests commanded from the crew compartment. The results of the on-board tests will be viewed on instruments and displays in the crew compartment, and faults will be isolated to the LRU level wherever possible. To further isolate problems to the LRU level, the ground checkout system will be connected to vehicle test points and additional tests conducted with the results displayed or ground equipment. After a maintenance action has been completed, either the on-board checkout capability or the ground checkout system will be used as appropriate to verify the corrective action.

RF antenna hats will be used to minimize RF radiation in the maintenance and repair area.

Level II Maintenance. A level II avionics maintenance shop consisting primarily of conventional airplane and standard laboratory test equipment will provide LRU and module test support for the booster and orbiter subsystems (Ref. Figure 4-370).

The shops major elements consists of the following: Digital test equipment, analog test equipment, RF test equipment, electrical test equipment, rate table, navigation displacement table, pneumatic pressure source and a calibrated light source (orbiter only).

Manufacturing. Vehicle final assembly checkout and acceptance testing is accomplished by a ground checkout system (same type used at launch operations and Level I maintenance), a TACAN beacon simulator and a UHF-AM radio test set.

Major subassembly wiring is checked out and tested using an automatic circuit analyzer. Vehicle simulators provide loads and stimuli for closed loop testing the crew compartment and the main fuselage section.

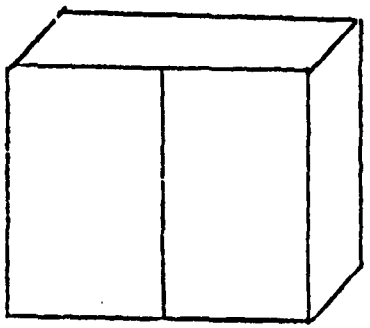

RF TEST EQUIPMENT

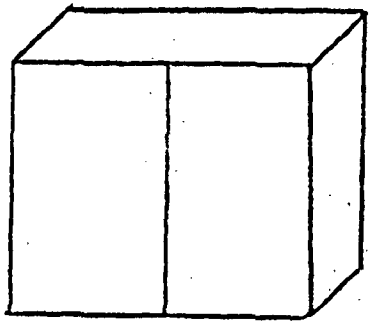

ANALOG TEST EQUIPMENT

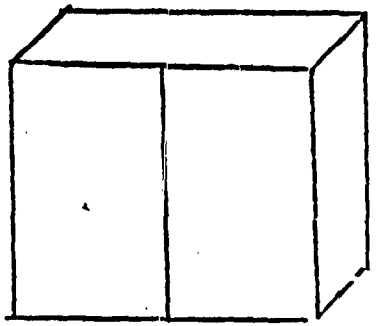

DIGITAL TEST EQUIPMENT

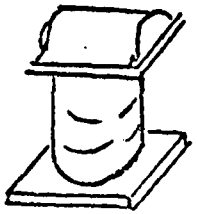

NAVIGATION
DISPLACEMENT TABLE

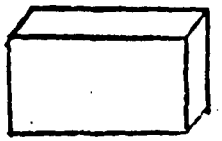

PNEUMATIC SOURCE

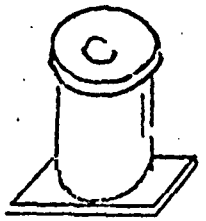

RATE TABLE

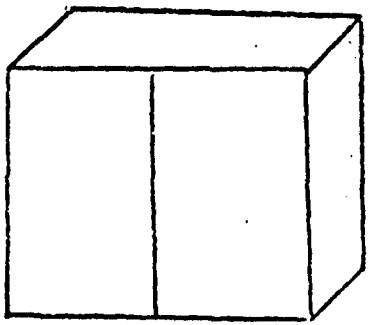

ELECTRICAL TEST EQUIPMENT

CALIBRATED LIGHT SOURCE
(ORBITER)

Figure 4-370. Shuttle Maintenance Shop

4.4.5.16 Test

The test philosophy for the LO_2/RP F-1 booster is the same as for the booster baseline presented in Report 71-105-3 (Preliminary Test Plan for Phase C/D, Volume III Booster). A summary of the major test articles is shown in Figure 4-371.

Ground Test. The use of a smaller heat sink booster introduces several changes in the booster test program as follows.

The structural qualification test program will be conducted on a single set of flight hardware for a combined static-fatigue test. Body structure will be tested at room temperature and aerodynamic surfaces at elevated temperature. The TPS structure is greatly reduced resulting in a major reduction of TPS test requirements. Use of RP fuel eliminates the test requirements associated with LH_2 insulation.

The tandem staging configuration results in a simplified static and dynamic separation test program. Dynamic tests to verify the math model will include scale model testing and full scale tests on the booster in the horizontal condition. A vertical vibration test will be conducted.

The baseline ASIL concept for avionics/non-avionics test will be changed from a totally integrated avionics laboratory to a system integration laboratory which will contain the G&C system plus a portion of the D&C. The SIL laboratory will interface with the iron grid.

Horizontal Takeoff Flight Testing. The horizontal flight test program remains the same as the baseline test plan. Boosters 1 and 2 will be flown approximately 190 hours to demonstrate the subsonic flight envelope performance.

Vertical Flight Testing. Upon completion of the ground test certification program, scale model testing, and the horizontal demonstration flights, a series of mated and manned booster/orbiter flights will be accomplished to demonstrate the capability of the vehicle to perform design reference and alternative missions. These flights will be programmed with progressive variations of conservative trajectories until operational capability is attained.

LOX TANK
NOSE
PARTIAL INTERSTAGE ADAPT.
PARTIAL INTERTANK ADAPT.

CANARD

CREW CABIN

LANDING GEAR

RP TANK
INTERTANK ADAPTER
THRUST STRUCTURE
STUB WING

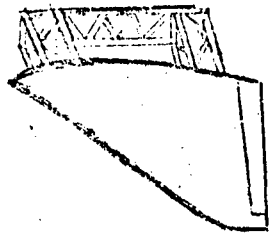

WING & CARRY-THRU

VERTICAL FIN

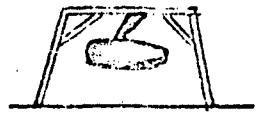

ABES

CLUSTER ENGINE
FIRING
(2) 20 SEC FRFS'

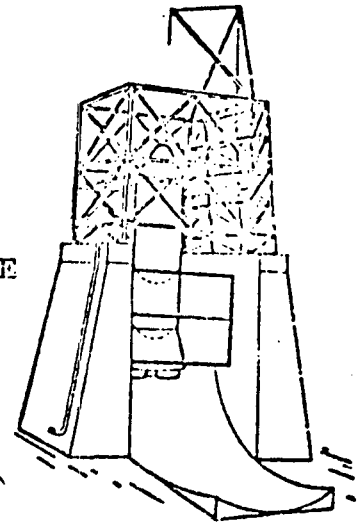

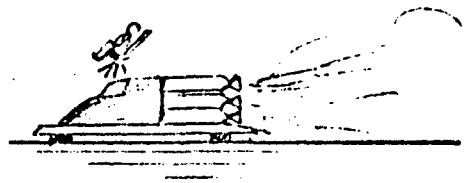

CREW ESCAPE

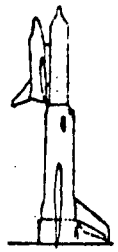

DYNAMIC
MODEL

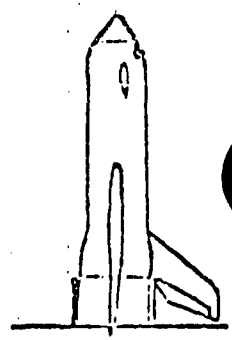

FULL SCALE
VIBRATION

COMBINED STATIC - FATIGUE
STRUCTURAL TEST ARTICLES

Figure 4-371. Ground Test Summary LO_2/RP Reusable Booster

4.4.6 Pressure-Fed Booster Definition

Design

The current B19-2A pressure fed booster (PFB) configuration was derived from a series of design and trade-off studies, summarized in Section 4.2.2, using vehicles defined in previous NASA and USAF studies as a point of departure (Figure 4-372). The main features of the configuration are ruggedness and simplicity, which permits recovery by ocean landing, retrieval, refurbishment, and re-use at low cost.

The mission and configuration for the pressure fed booster are summarized in Figures 4-373 and 4-374. Lift-off is at a thrust/weight ratio of 1.3 (1.3g's), obtained by using seven fixed thrust engines. Constraints of 650 psf on maximum dynamic pressure and 3 g on acceleration are met by discrete engine shutdown, one at 30 seconds and two at 105 seconds after launch. After staging, fins stabilize the vehicle for entry and drag flaps located in the aft skirt are deployed, increasing the drag area to slow the booster for drogue chute deployment at 28,800 feet. Main chutes are deployed at 18,000 feet, reducing booster terminal descent velocity to 150 ft/sec for impact in the ocean. The stage is retrieved by an LSD, and returned to the launch site for refurbishment and re-use.

The main elements of the booster configuration (Figure 4-374) are the propellant tanks, thrust structure/aft skirt, engine installation, fins, and parachute/recovery installation. The propellant tanks are Inconel 718 averaging 0.49-inch wall in the cylindrical sections and 0.35 inches in the conical nose section. The forward portion of the tank is conical (80 degrees) to minimize shock at water impact. A common 2 bulkhead divides the forward O_2 and aft C_3H_8 tanks. The bulkhead and internal O_2 line are designed for full pressure in the forward O_2 tank, with zero gage pressure in the aft C_3H_8 tank to obviate the need for critically scheduled tank pressurization, i.e., concurrent pressurization of both tanks. The O_2 is always pressurized first, and the C_3H_8 tank is depressurized first.

The heat sink type Inconel 718 thrust structure reacts the engine, fin, and recovery parachute loads. It consists of a truss structure connecting forward and aft thrust bulkheads and a conical skin-stringer structure to carry loads to the equator of the $\sqrt{2}$ aft tank bulkhead. The thrust bulkheads consist of cross beams, with ends attached to circular frames to which the outer stringer-stiffened skin is attached. The engines are rigidly attached to the aft thrust bulkhead near the top of the combustion chamber.

The base heat shield extends from the aft thrust bulkhead aft approximately eight feet. Included in this structure are eight retractable drag skirts, the supports for their actuation mechanisms, and provisions for mounting

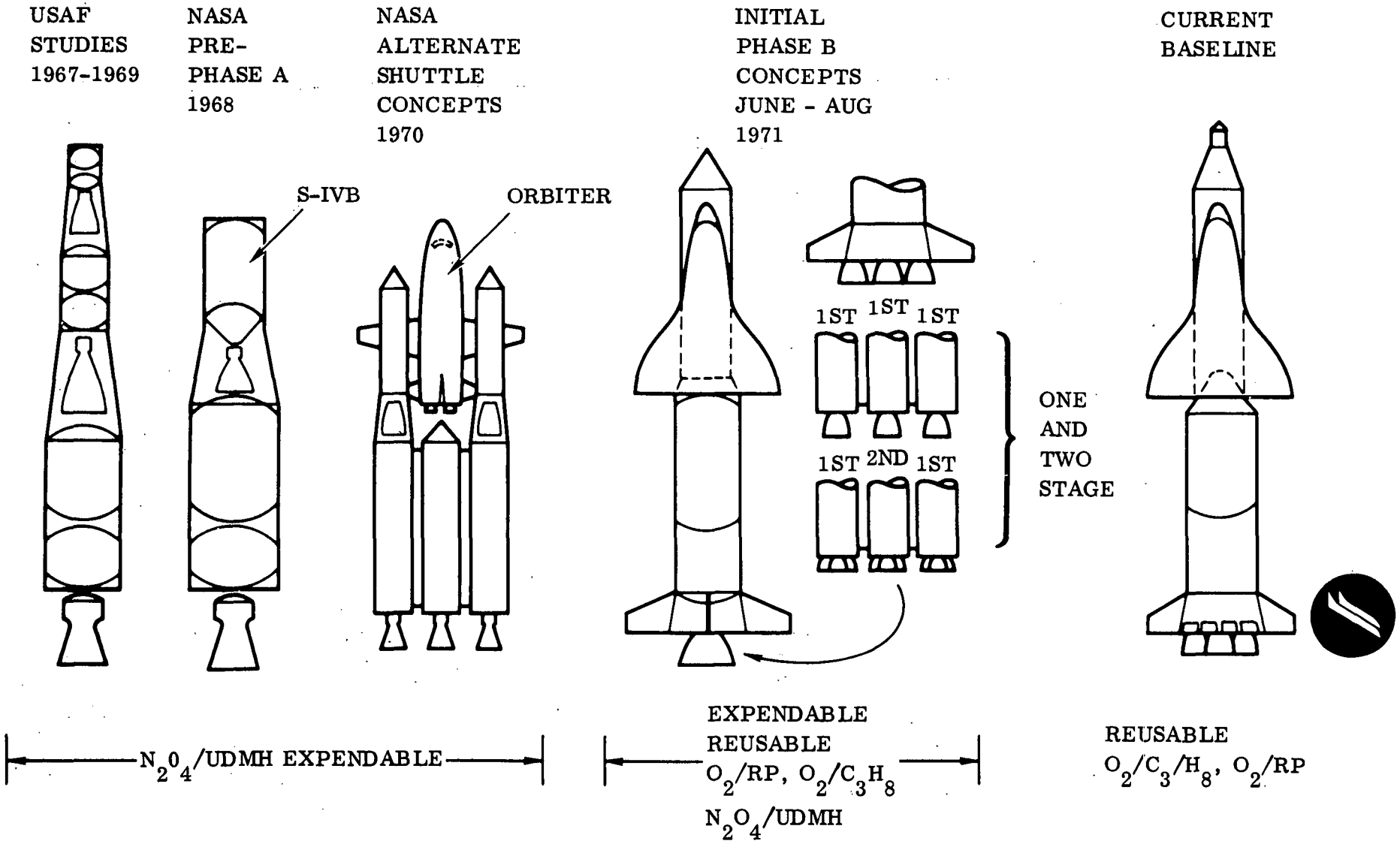

Figure 4-372. Configuration Evolution

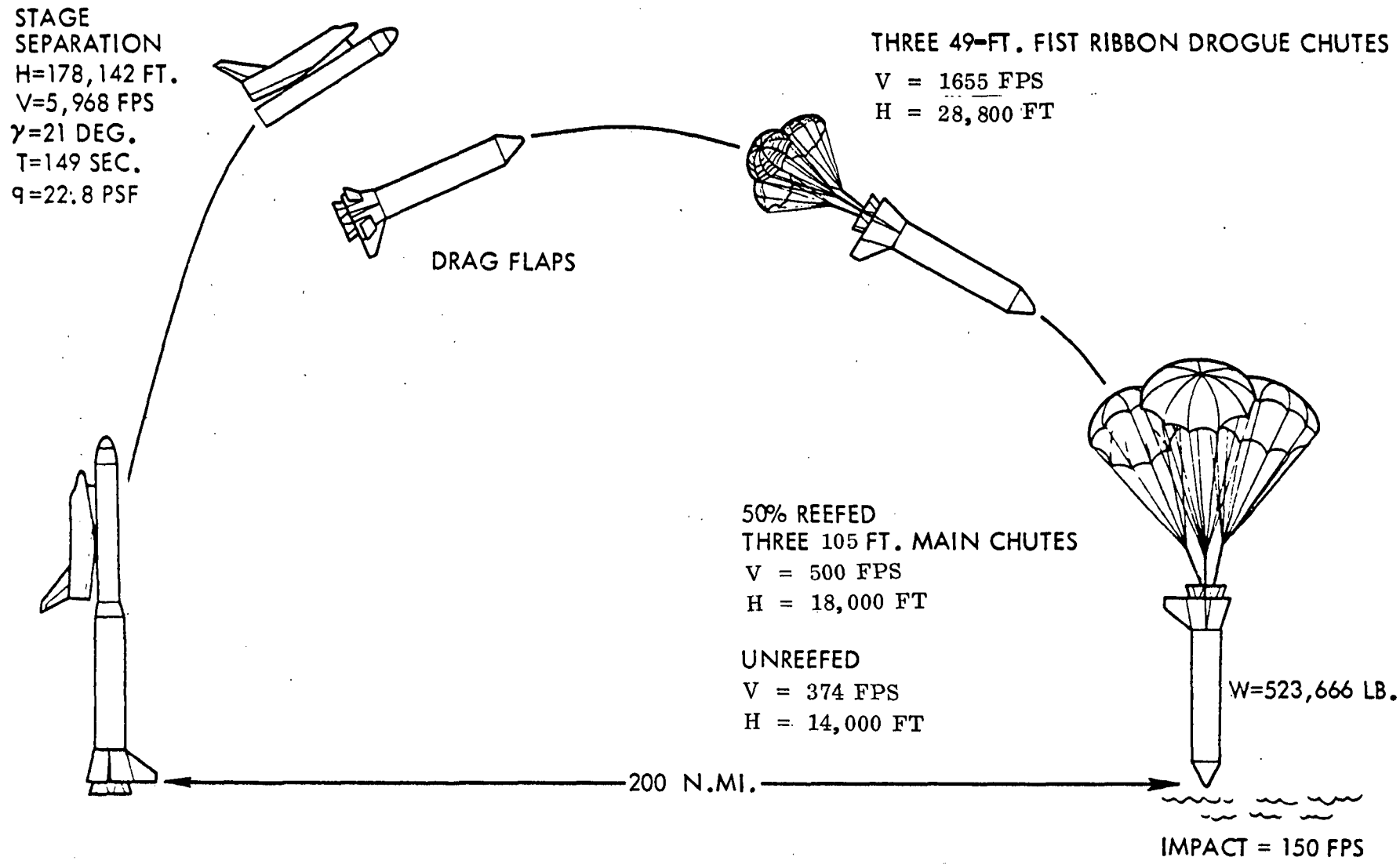

Figure 4-373. Flight Profile

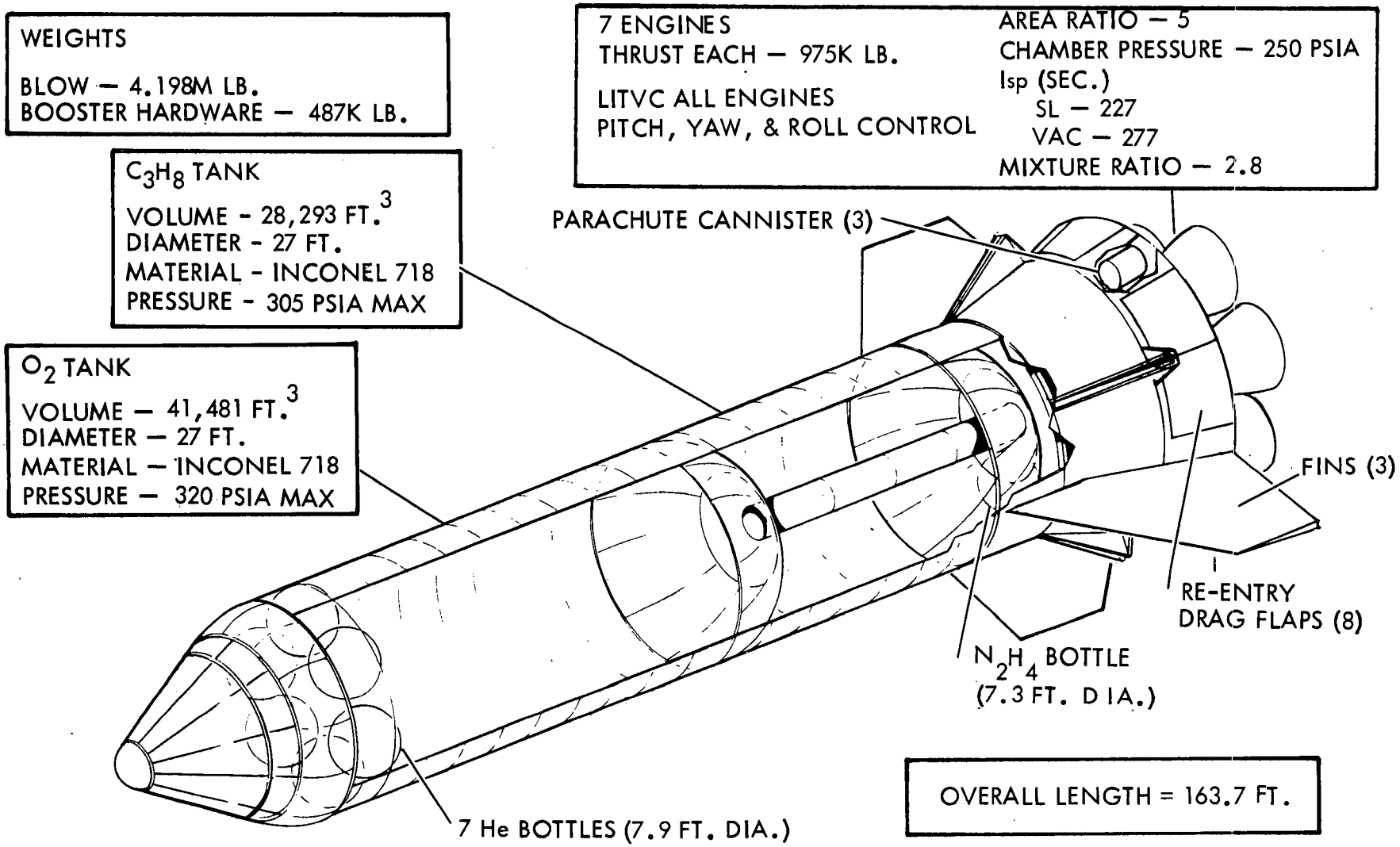

Figure 4-374. Baseline Booster Configuration

the parachute containers. The thrust/heat shield structure form a closed compartment which, with post-landing purge, excludes water from the entire vehicle aft compartment.

The seven engines operate at a chamber pressure of 250 psia and a mixture ratio of 2.8. Pressurization for the O_2 tank (305 psia nominal) is provided by 900 R helium, heated to this temperature after storage at 3000 psia in the O_2 tank in seven Inconel 718 spheres. A hydrazine (N_2H_4) monopropellant gas generator/heat exchanger warms the helium, and the heat exchanger exhaust is used to pressurize the C_3H_8 tank (290 psia nominal). Ascent control of the vehicle is provided by liquid injection thrust vector control (LITVC) using O_2 drawn from the engine inlet supply as the injectant. Maximum side force provided is equivalent to 5 degrees engine deflection.

Performance and dimensional data for the B19-2A booster are given in Table 4-69. The orbiter is mounted in tandem and attached to the forward bulkhead of the booster on a 260-inch diameter ring.

Table 4-69. Details of B-19-2A Booster System

Weight Summary		
GLOW	MLB	5.25
BLOW	MLB	4.198
Booster Ascent Propellant	MLB	3.67
Booster Dry Struc.	KLB	487
Booster Landing	KLB	524
Propulsion		
Booster No. Main Engines		7
Type Main Engines		Fixed Thrust
Booster Eng. SL Thrust	KLB	975
Booster SL I_{sp}	SEC	227
Booster Vac I_{sp}	SEC	277
Orbiter No. Main Eng.		4
Type		SSME Hi-Pc
Orbiter Eng. Vac. Thrust	KLB	265
Orbiter Vac I_{sp}	SEC	453.2
Performance		
V_{stage} Relative	FPS	6000
Q_{max}	PSF	650
Q_{stage}	PSF	23
T/W_{LO}		1.3
h Stage	KFT	178.1
γ Stage	DEG	21
Payload	KLB	40
Mission		Polar
Geometry		
Length	FT	163.7
Body Diameter	FT	27
S_{fins}	FT^2	700
C_3H_8 Tank Vol	FT^3	28293
O_2 Tank Vol	FT^3	41481

Ascent and Entry Performance

The operational mission flight profile is presented in Figure 4-375. Significant events from liftoff through recovery of the booster are presented.

The open-loop performance trajectory for the baseline pressure-fed booster was generated with the Mark II orbiter for the south polar mission (40k payload); ascent trajectory parameters are given in Figure 4-376. The thrust/weight at liftoff is 1.30 g. At 30 seconds after liftoff, one of the seven main engines is shut down to limit the maximum dynamic pressure to 650 psf for vehicle design load considerations. As propellant is depleted, along with increased thrust at altitude, the vehicle acceleration reaches 3 g. At this point, approximately 105 seconds after liftoff, two more engines are shut down. The remaining four engines continue to burn until near staging, when two are shut down to reduce acceleration during orbiter engine start. BECO occurs at 149.3 seconds after liftoff.

The booster entry trajectory begins at staging and terminates at drogue deployment, which initiates the recovery phase. Drag flaps are deflected to increase drag and decrease ballistic coefficient (W/C_DS) in order to decrease terminal velocity and permit deployment of a supersonic drogue chute. Fins are sized to maintain static stability throughout the entry trajectory. Fin and drag flap sizing relationships are shown in Figure 4-377. To meet a drogue chute requirement of M = 1.7 at 30,000 ft altitude, the drag flap must be deflected to 45°; a fin area of 885 ft^2 is required to move the vehicle center of pressure behind the center of gravity, using a fin wedge angle of 8°.

The entry trajectory of the booster is presented in Figure 4-378 along with the reference heating trajectory. Peak axial load factor of 6.9 g occurs at 52,000 feet altitude at a velocity of 4060 fps. Termination of entry, with drogue chute deployment, occurs at 28,800 feet altitude, with a velocity of 1655 fps and a dynamic pressure of 1290 psf.

The drogue and main parachutes are sized to decelerate the booster from initial conditions of 1655 fps velocity at 28,800 feet altitude to terminal conditions of 150 fps at sea level. Chute sizing analyses are summarized in Figure 4-379; three main chutes of 105-foot diameter are established to meet the terminal requirements.

Aerodynamics

Aerodynamic characteristics of the launch vehicle are presented in Figures 4-380 and 4-381. These data, longitudinal and lateral directional characteristics over the Mach number, are based on data obtained in buildup runs of MSFC 14" Trisonic tunnel test No. 506 where the booster was tested without wing and tail. Adjustments for geometrical differences were made analytically, including predicted fin contributions to the booster.

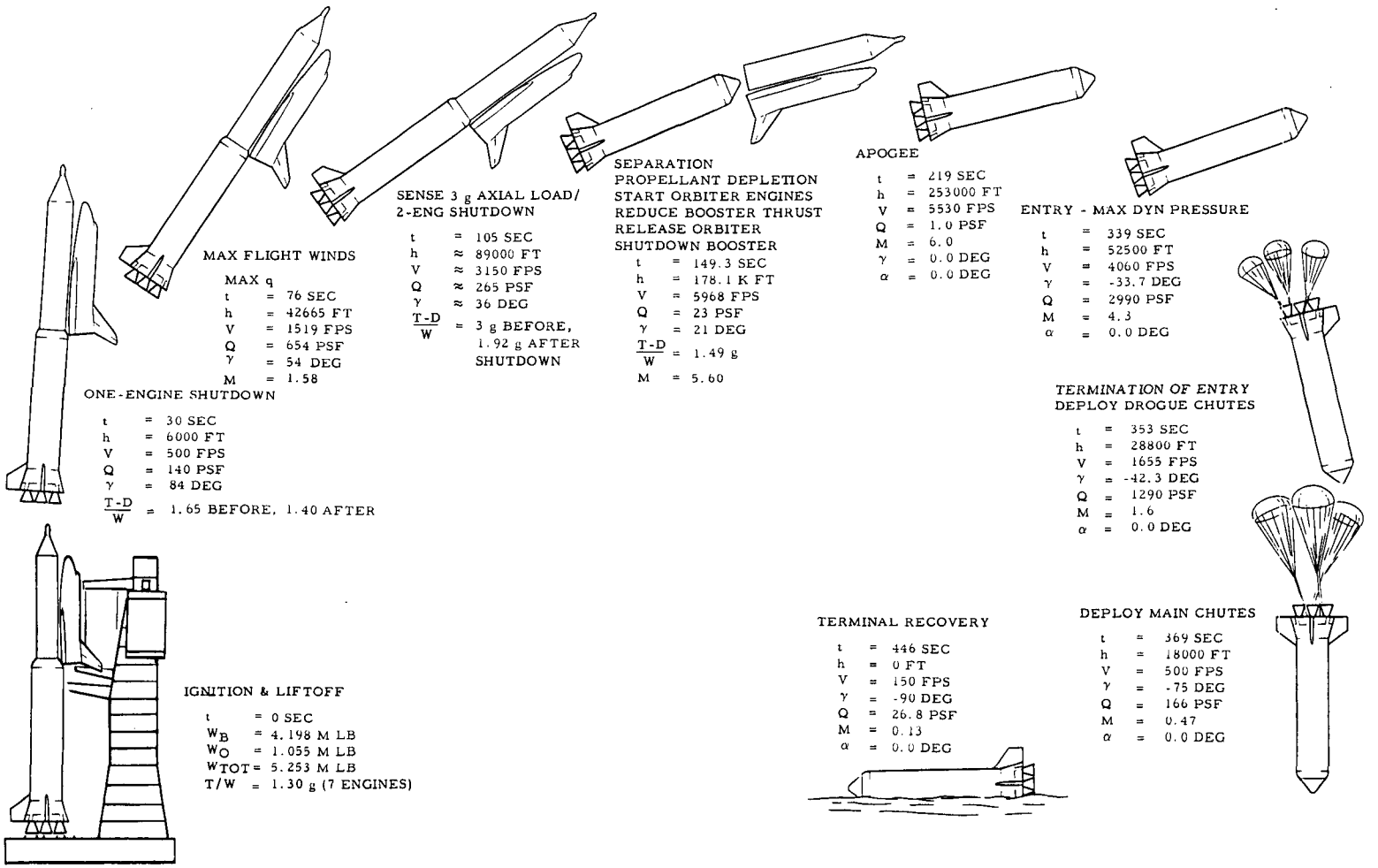

Figure 4-375. Operational Mission Flight Profile

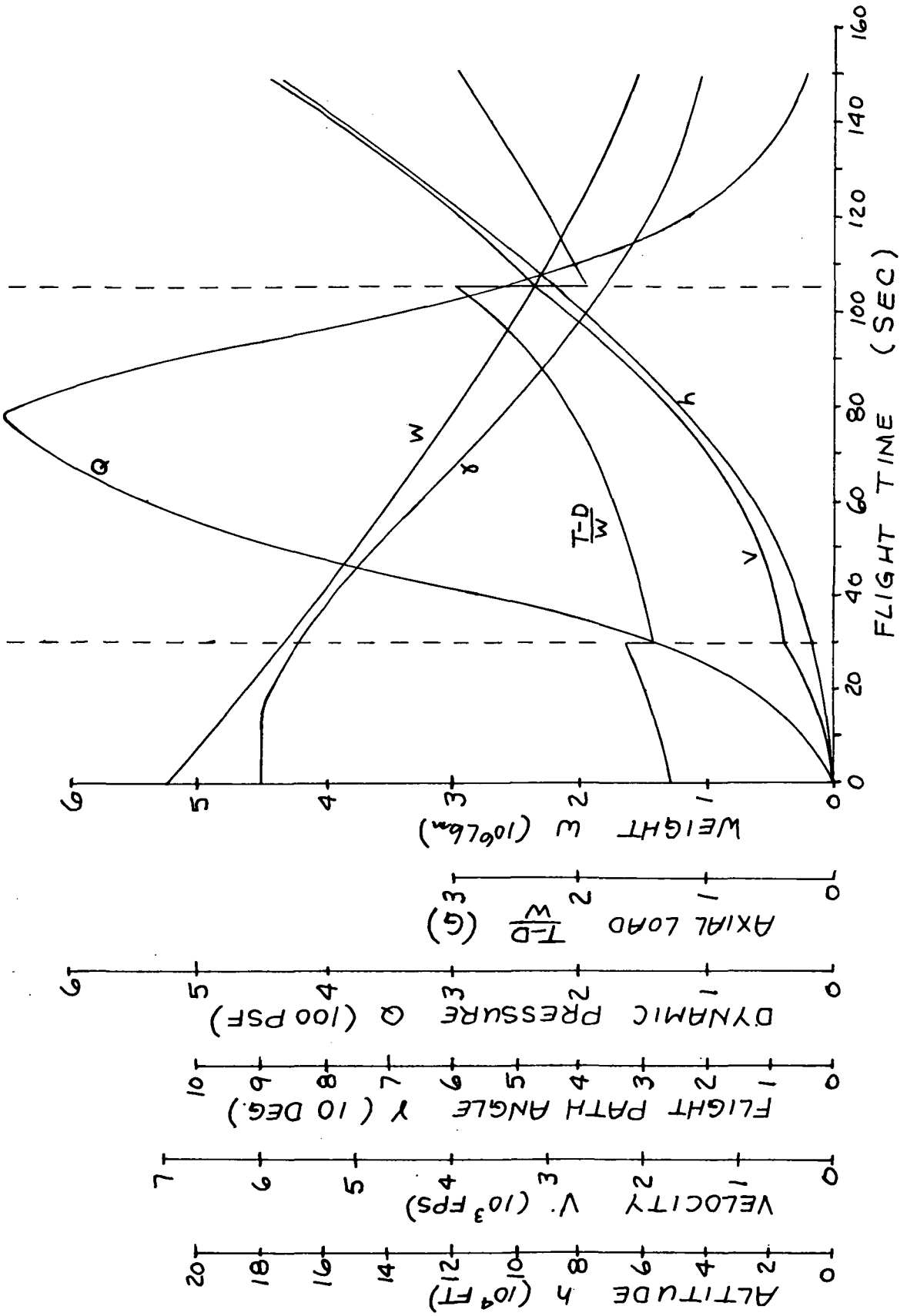

Figure 4-376. Ascent Trajectory Parameters

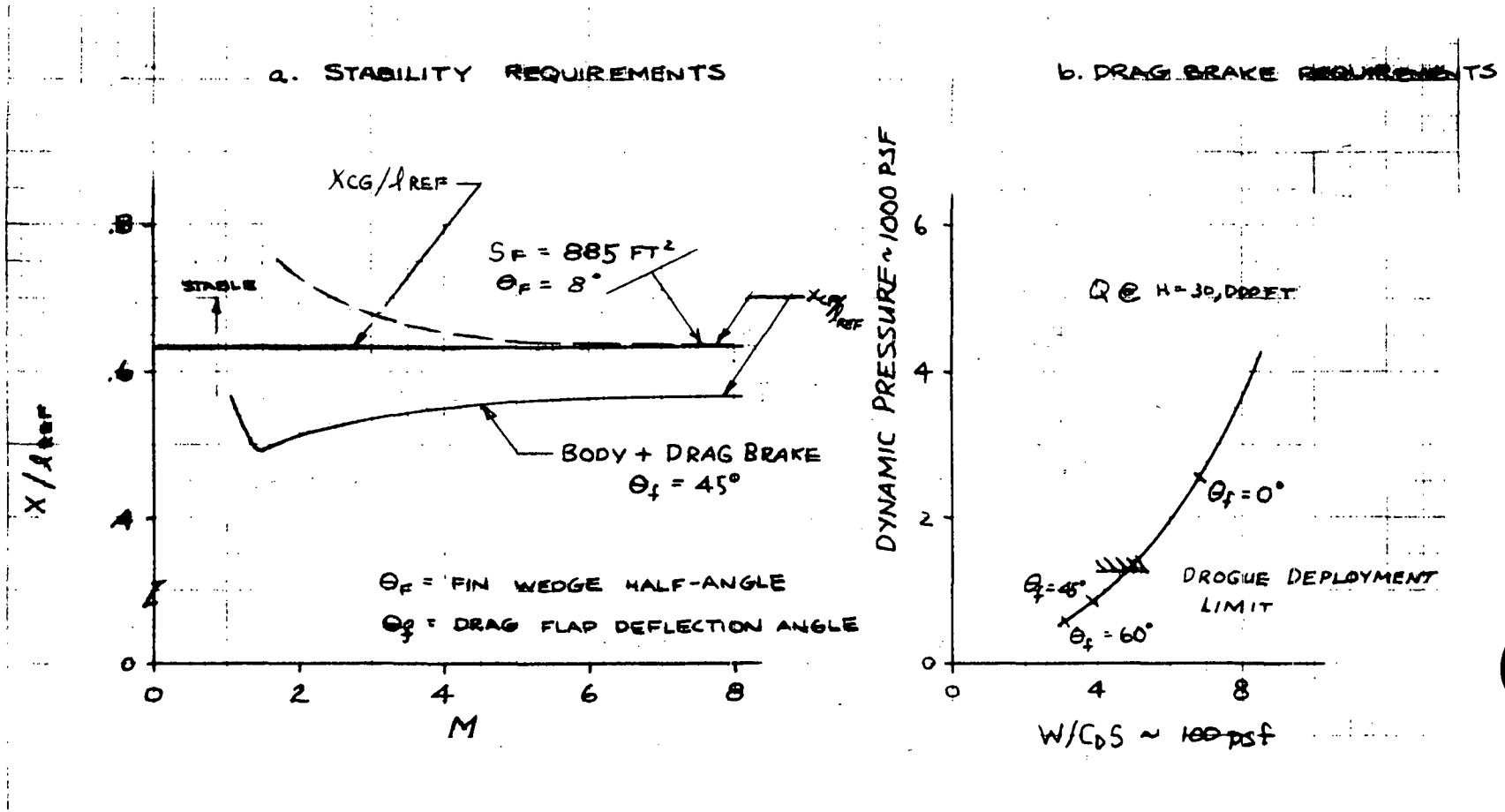

Figure 4-377. Fin and Flap Design Consideration for Entry (Sheet 1 of 2)

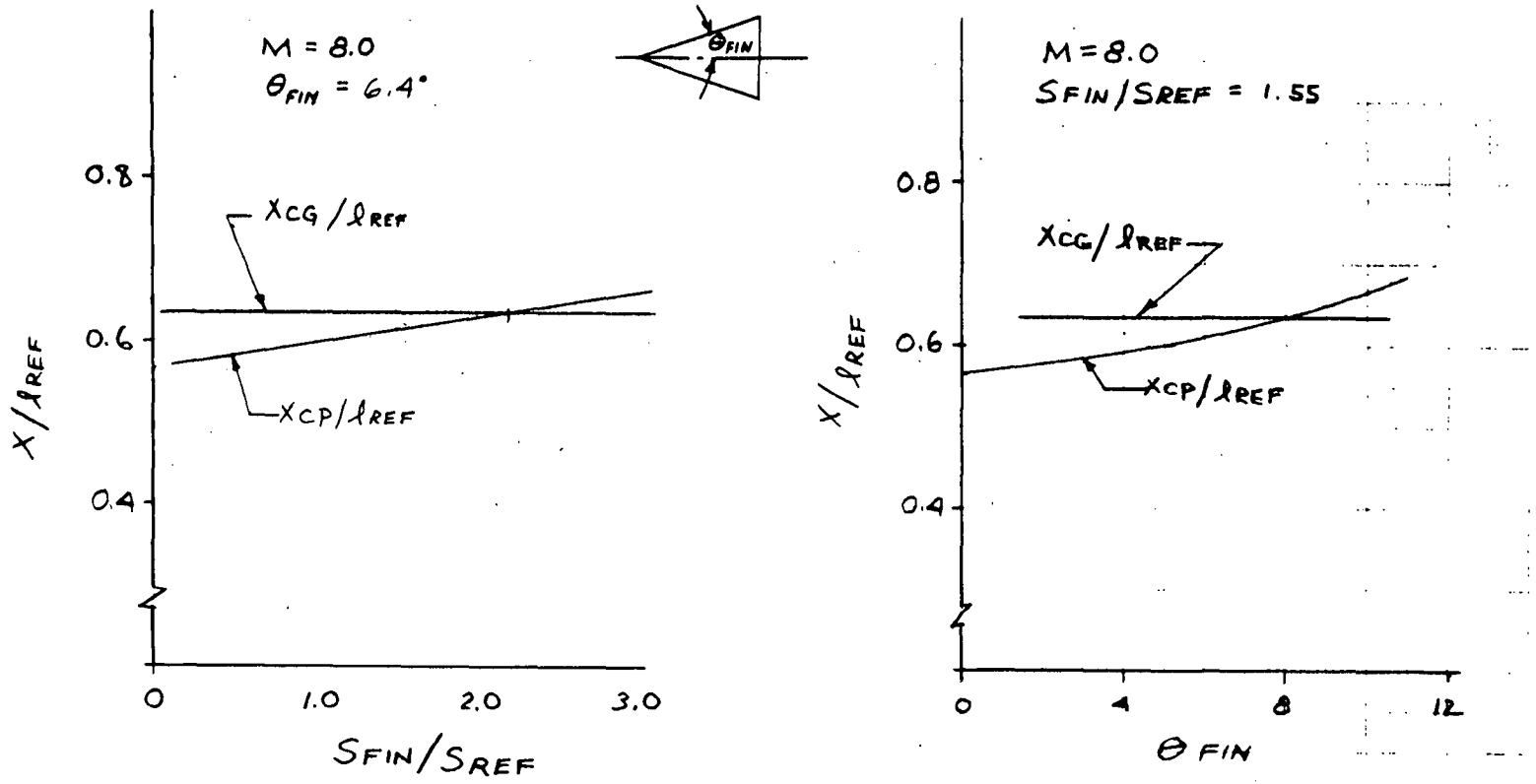

Figure 4-377. Fin and Flap Design Consideration for Entry (Sheet 2 of 2)

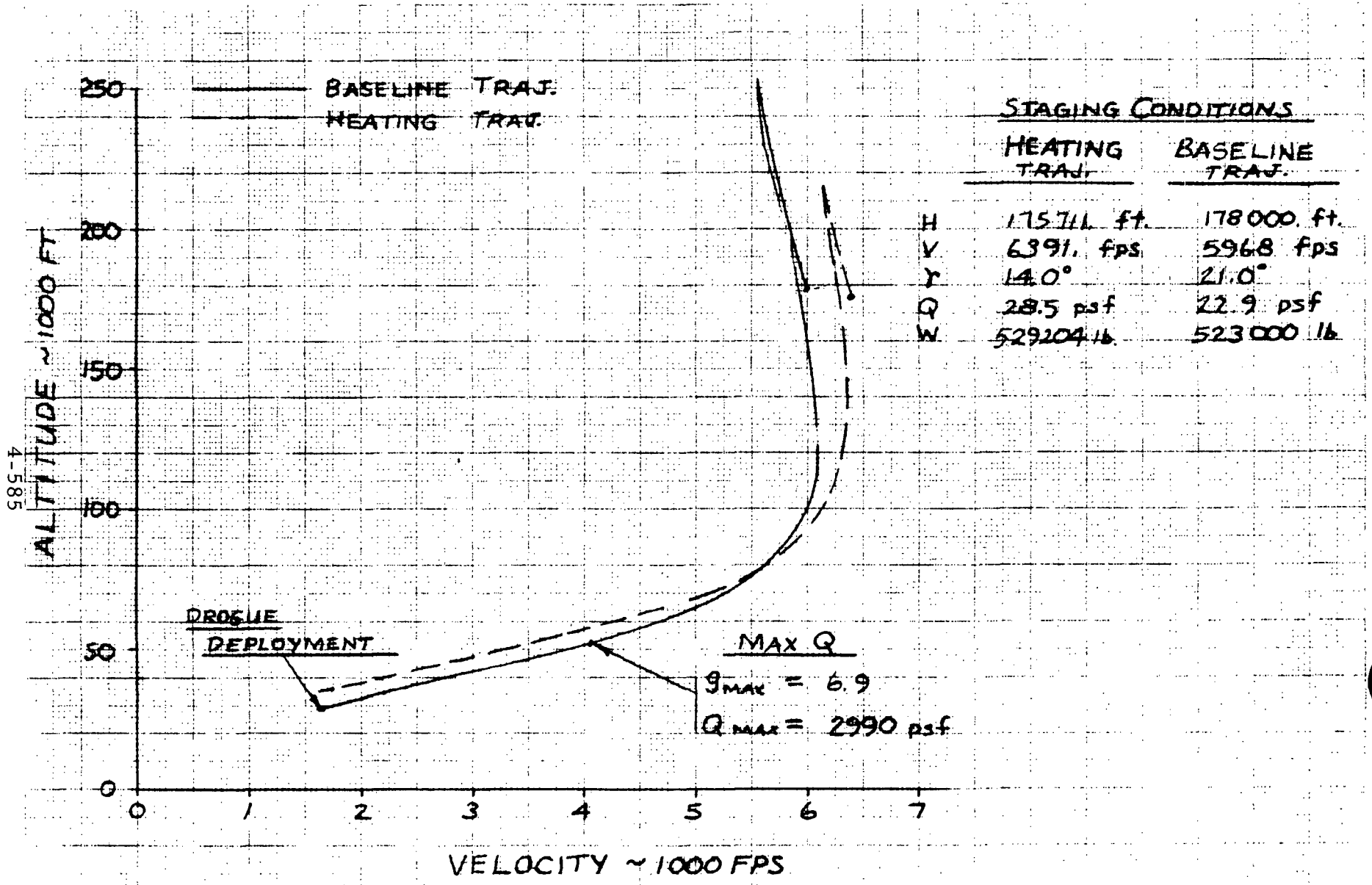

Figure 4-378. Booster Entry Trajectory

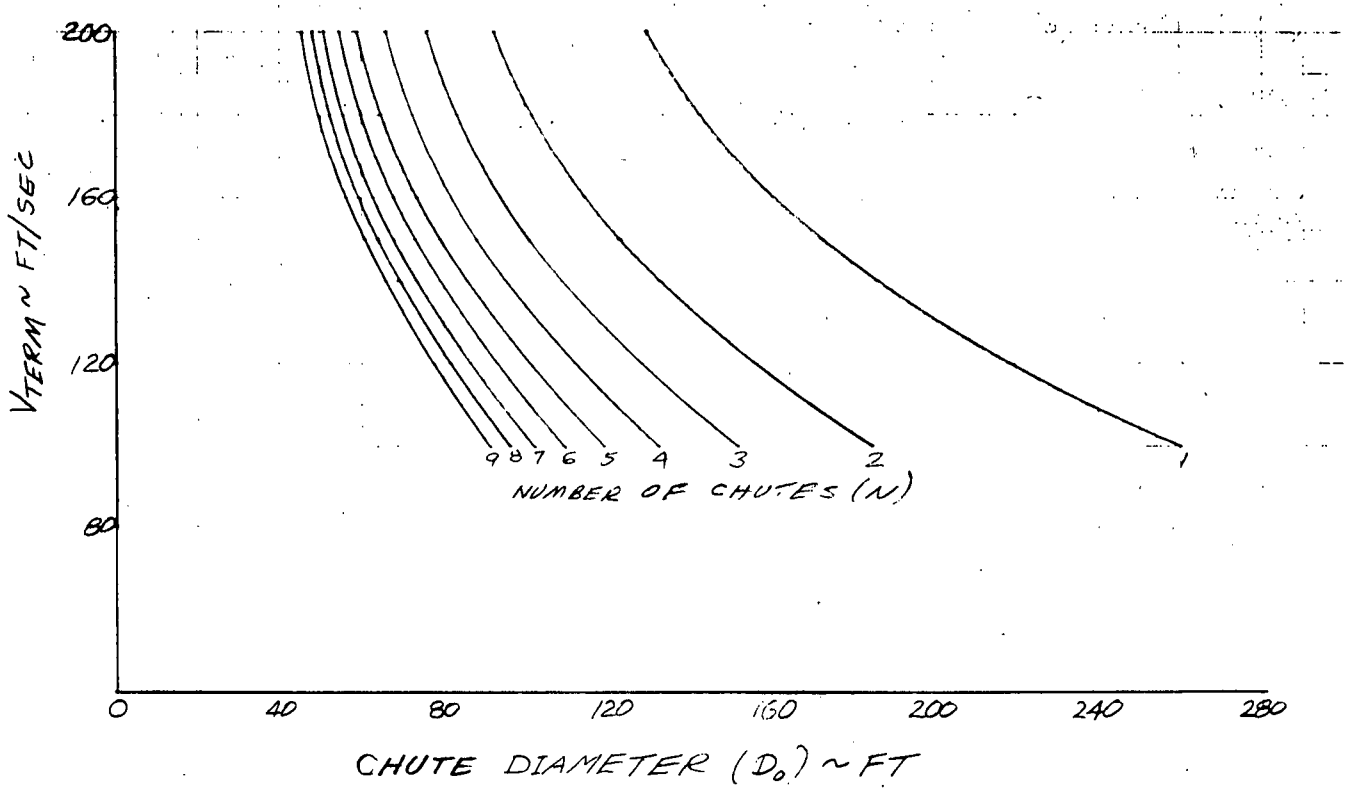

Figure 4-379. Parachute Sizing Considerations for Recovery

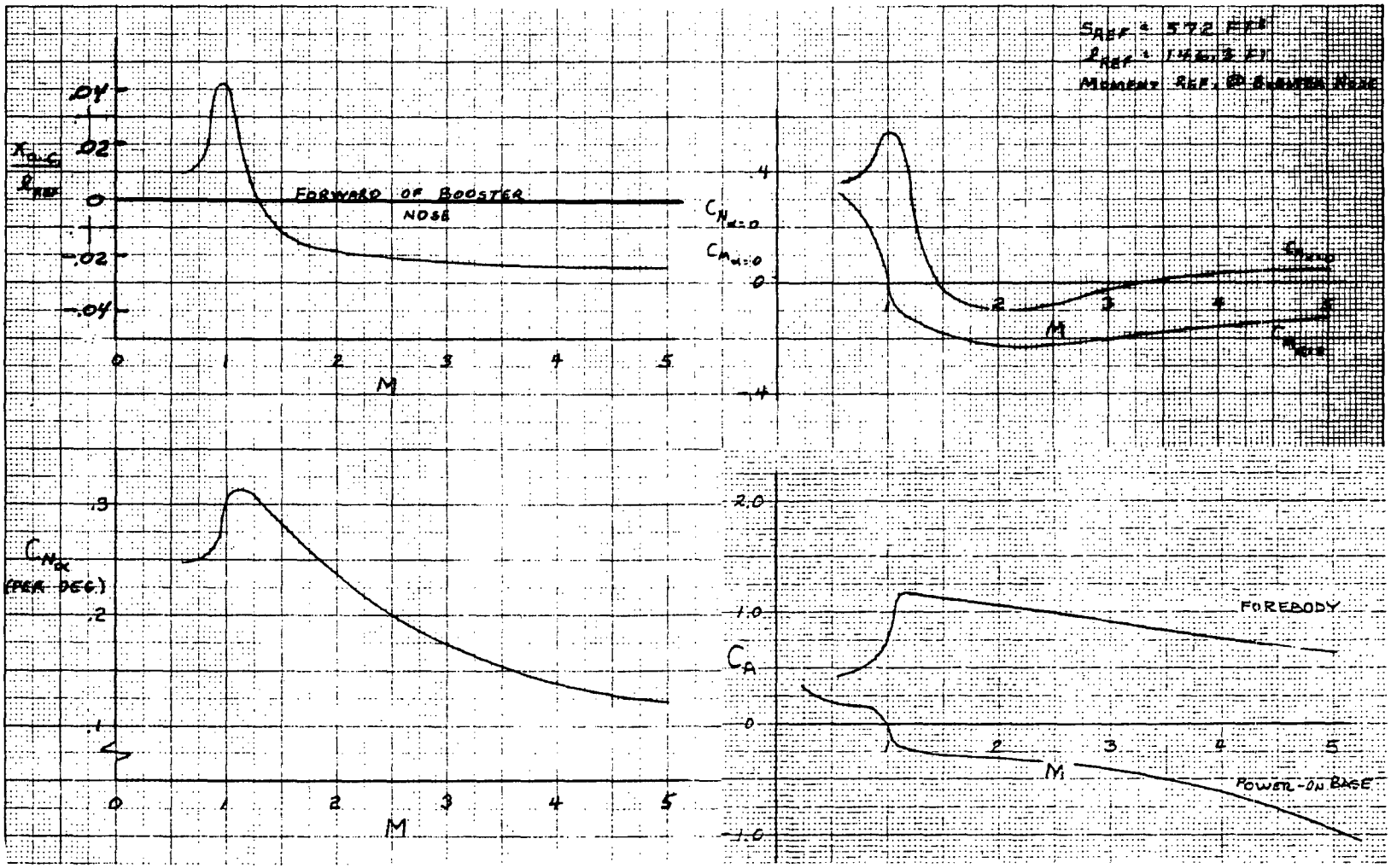

Figure 4-380. Launch Configuration Longitudinal Aerodynamics

Figure 4-381. Launch Configuration Lateral/Directional Aerodynamics

Basic Loads

Ullage pressure schedules and resulting limit pressures (including head pressures) are presented in Figures 4-382 and 4-383 for the main propellant tanks. Internal loads due to external and inertial loads fall well within the load capability of the booster as designed by internal pressure alone. Design load factors are summarized in Table 4-70.

Impact Loads. Dynamic analyses were conducted to determine loads and accelerations during water recovery. Assistance was provided by the Pomona operation of Electrodynamics Division of General Dynamics. Their extensive impact analysis background includes Redeye missile development studies of warhead impact and a $3.2 M Air Force contract to analytically and experimentally determine effects of advanced reentry vehicles impacting water, earth, and concrete.

Two basic recovery modes were investigated: vertical impact and oblique impact. Vertical impact (vehicle body axis normal to water surface) occurs when parachutes are used to slow the vehicle. Oblique impact can occur when the vehicle sways under the parachute in pendulum fashion due to wind disturbances. Oblique impact also occurs in the concept wherein the vehicle performs an aerodynamic pitch-over prior to water entry.

Figure 4-384 shows water immersion trajectories for 0, 30, 45 and 60-degrees obliquity and 150 fps impact velocity. Rebound, the condition that occurs when the tail of the vehicle impacts the water after the nose has resurfaced, is seen to occur only for obliquities of 30 degrees or less. Maximum accelerations during water impact and immersion are summarized in Table 4-71. These accelerations are dependent upon nose shape. For this analysis, a cone was assumed with height equal to diameter. High stresses in the immediate area of the cone apex during initial impact can be alleviated by use of energy absorbing material such as crushable honeycomb.

In the analysis to date, the velocity vector at impact has been assumed to be aligned with the vehicle body axis. Effects of skewed velocity vectors such as would be caused by wind drift have not been analyzed. Lateral loads due to rebound also remain to be examined in detail.

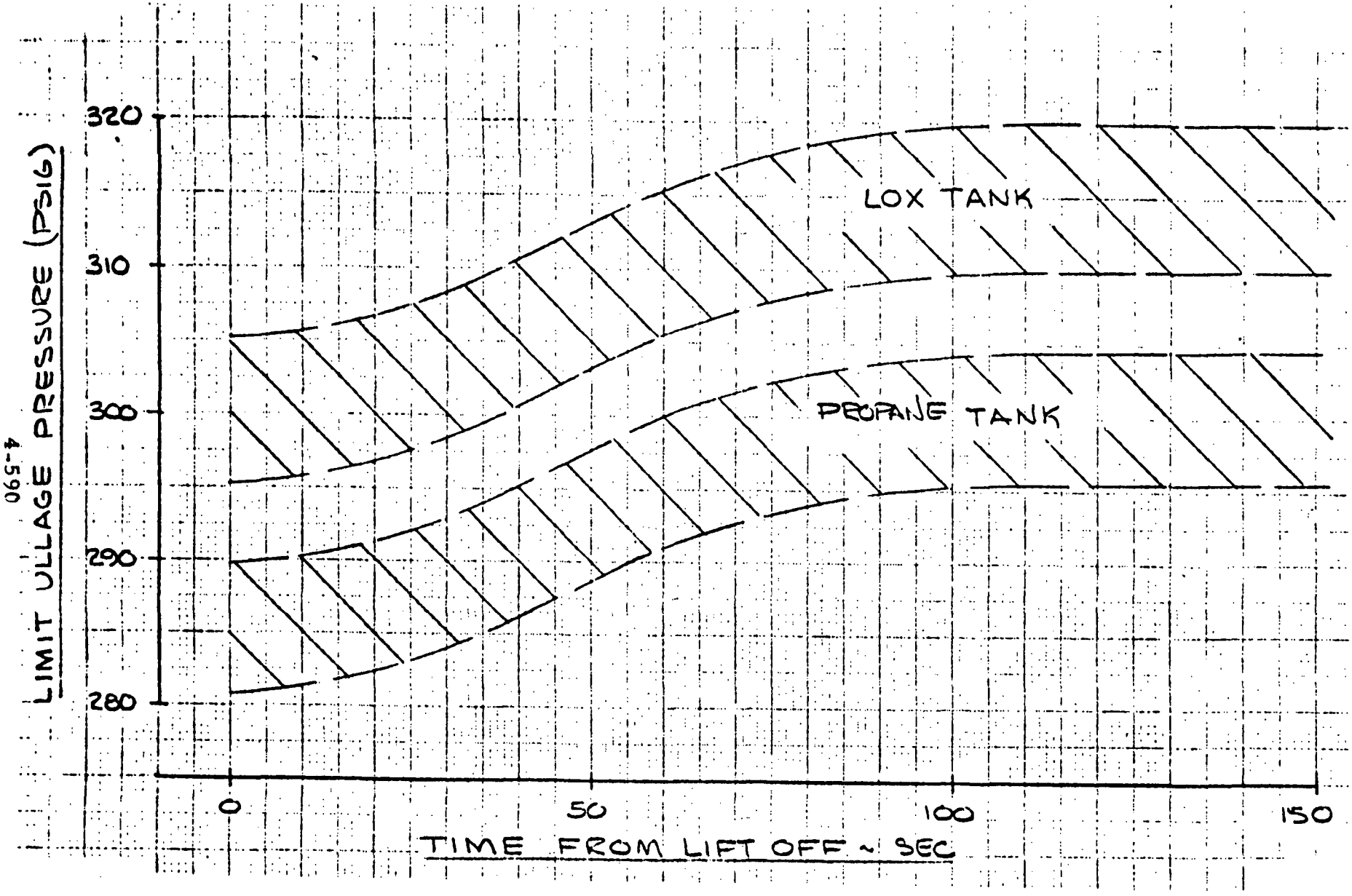

Figure 4-382. Pressure Fed Booster Propellant Pressure Schedules

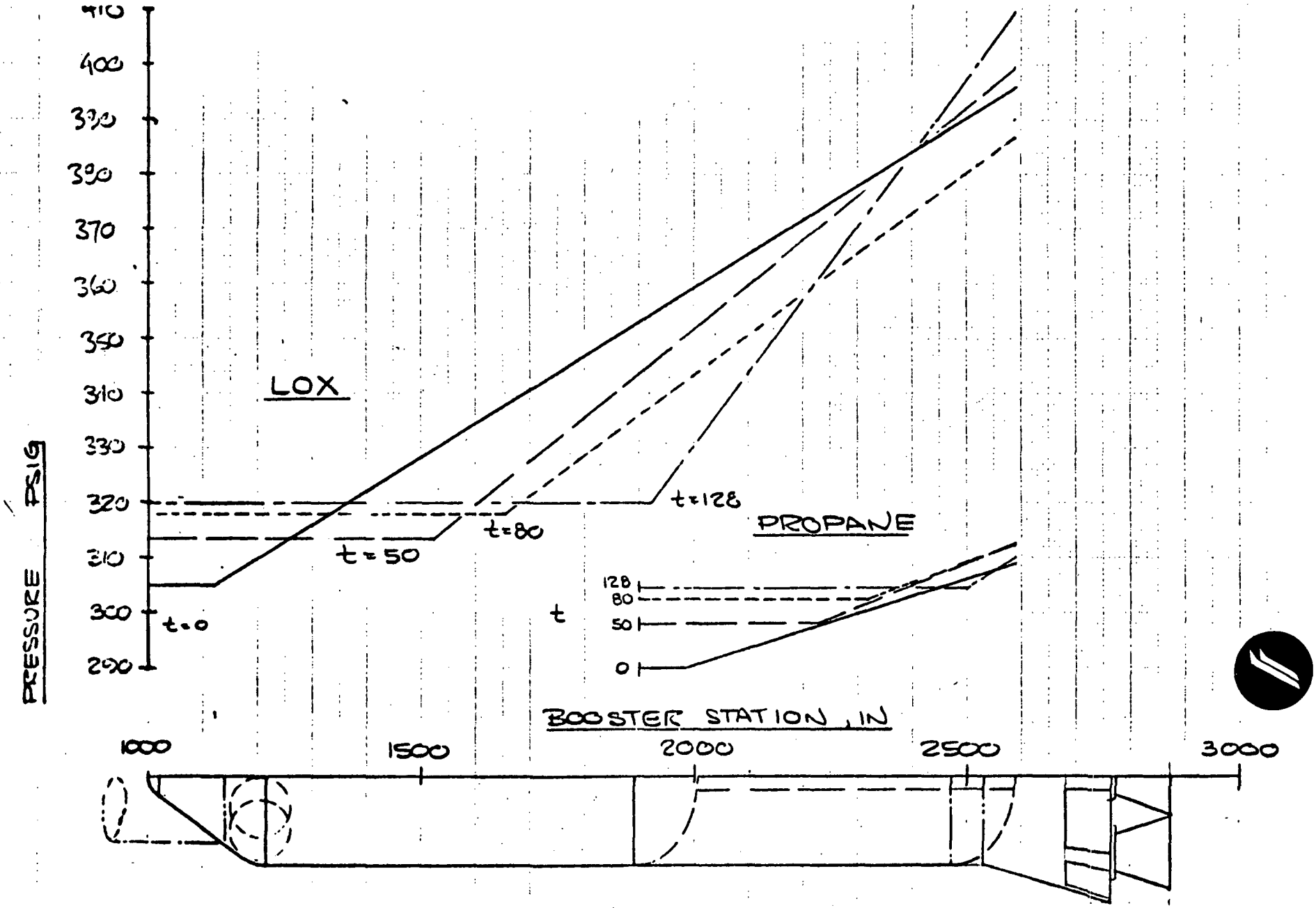

Figure 4-383. Pressure Fed Booster Limit Pressure

Table 4-70. Summary of Design Conditions

Condition	Axial Load Factor (g)	Lateral Load Factor (Yaw) (g)	Normal Load Factor (Pitch) (g)	Wind Speed at 18.3 Meters, or αq (βq)	Remarks
Two-week Standby	1.0	—	—	37.1 meters/sec	Unfueled, unpress.
One-day Hold	1.0	—	—	25.2 meters/sec	Fueled, pressurized
Liftoff				17.7 meters/sec	
LO_2 Mass	1.30 ± 0.15	-.022	-.055		
LH_2 Mass	1.30 ± 0.25	-.022	-.055		
Orbiter & Other	1.30 ± 0.20	-.022	-.055		
Max Dynamic Pressure					
Headwind	1.74	—	.60	+2800 deg-psf	Use 1.2 factor for gust response and aeroelasticity
Tailwind	1.74	—	-0.25	-2800 deg-psf	
Crosswind	1.74	±0.18	+0.20	±2400 deg-psf	
Maximum Thrust	3.0 ± 0.30	±0.10	+0.20	±480 deg-psf	
Booster Burnout	2.2 ± 0.3	±0.10	+0.35	±100 deg-psf	
Booster Water Impact	-6.2	—	—		

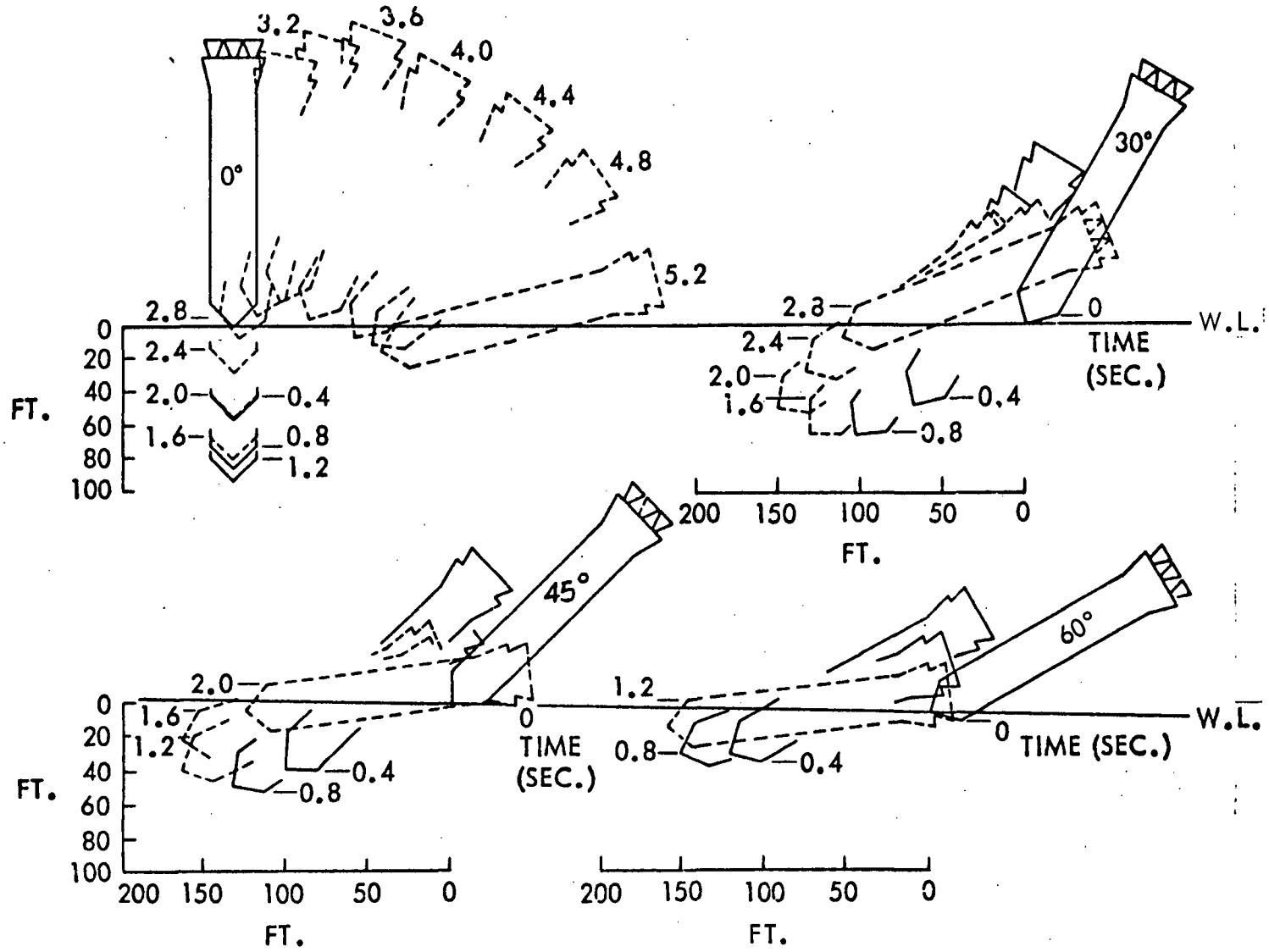

Figure 4-384. Water Immersion Trajectories for 0, 30, 45, and 60-Degree Obliquities

Table 4-71. Water Impact Acceleration Summary

Impact Angle (deg)	$\ddot{X}_{MAX}$ (g)	$\ddot{Y}_{MAX}$ (g)	
		Nose	Tail
0	6.2	0	0
30	6.2	+2.9 -1.2	+0.8 -1.0
45	6.2	+3.8 -1.6	+0.9 -1.4
60	6.2	+4.5 -2.6	+0.5 -1.7

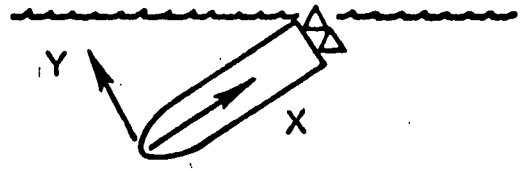

Thermal Environment

The thermal environments for the B-19 space shuttle booster were predicted using the ballistic flight trajectory shown in Figure 4-385, and the 1963 Patrick Atmosphere (Ref: Terrestrial Environment (Climatic) Criteria Guidelines for Use in Space Vehicle Development, TMX-53872, George C. Marshall Space Flight Center, Alabama, 15 March 1970.) The aerodynamic heating methods selected conform to the Phase B methods (Ref: Phase B Final Report, Volume II Technical Summary, Book 3 Booster Vehicle Definition, Report No. SD 71-114-2 (MSC-03307), 25 June 1971).

The reported heat transfer rates are for the nominal trajectory, prediction methods, and atmospheric conditions. Using heat sink thermostructural models, these rates were calculated using the skin thicknesses required to constrain the maximum predicted temperature to a predetermined limit.

Maximum temperatures, material types, and thickness requirements for the heat transfer rates given here are shown in the next section (Structure and TPS).

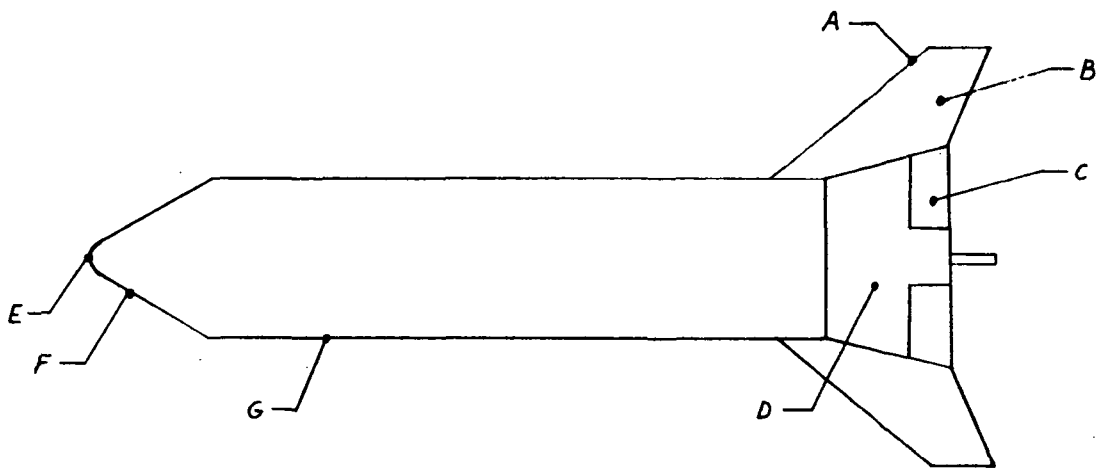

Figure 4-385. Pressure-Fed Booster - Thermal Environment Areas

Body. The areas examined are illustrated in Figure 4-385. The nose (Point E) was modeled as a 2.5-foot radius sphere. The conical nose (Point F) was modeled as a 40° cone with a 17.1-foot run length. The tank wall (Point G) was modeled as a 15-foot flat plate. The skirt (Point D) was modeled as a 15° wedge with a 9.0-foot run length. In the fin shock impingement areas of the shirt, a heat transfer multiplier of 4.0 was applied to the heating of Point D. The drag flap (Point C) was modeled as a 6.75-foot diameter sphere with a flat face correction and shock interference factor of 10.0. The heating rates at those points are shown in Figure 4-386.

Fin. The fin leading edge (Point A) was modeled as a laminar swept cylinder with 41° sweep. The fin surface (Point B) was modeled as a 16.0-foot flat plate. The heating rates at these points are shown in Figure 4-387.

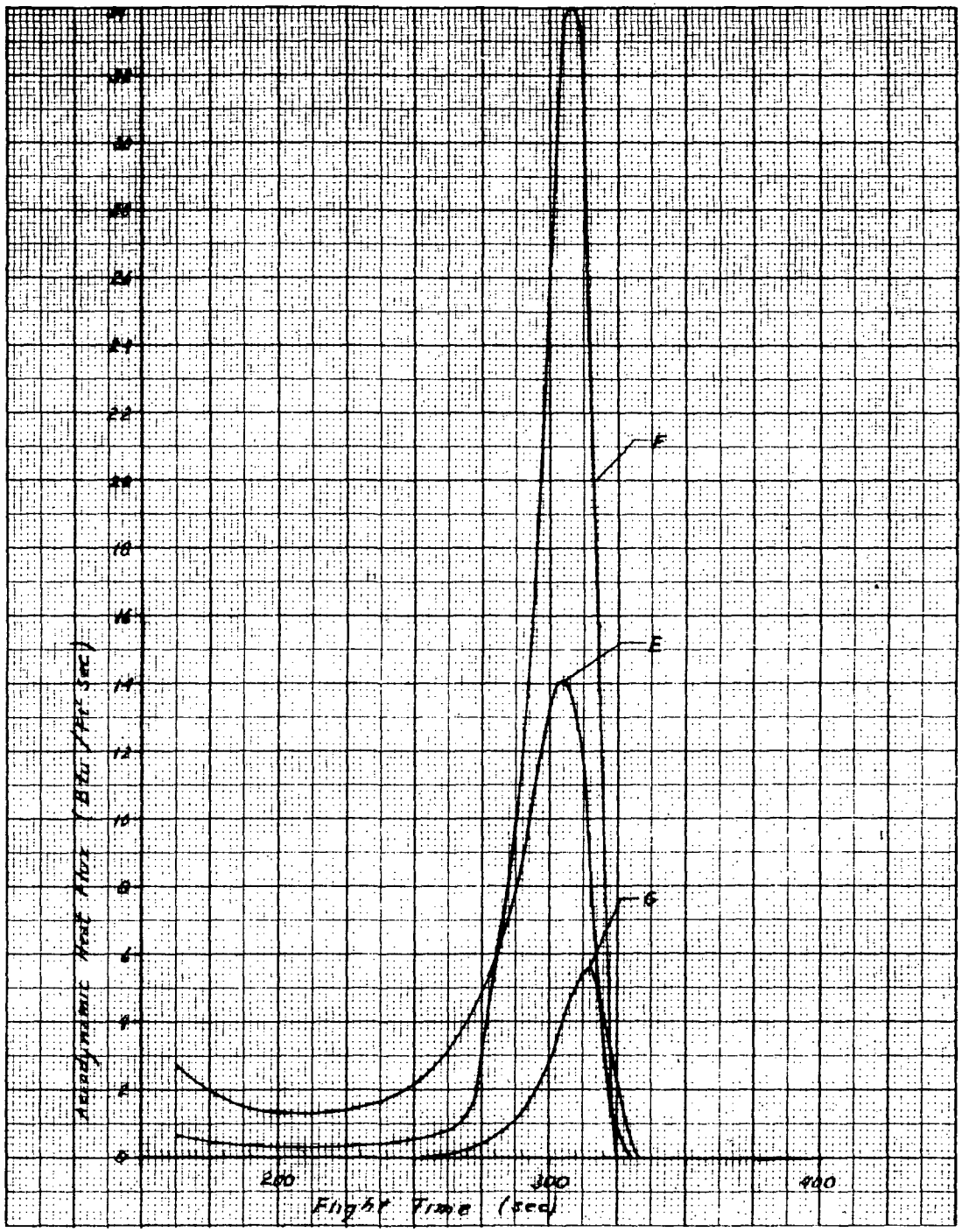

Figure 4-386. Pressure-Fed Booster Thermal Environment - Body
(Sheet 1 of 2)

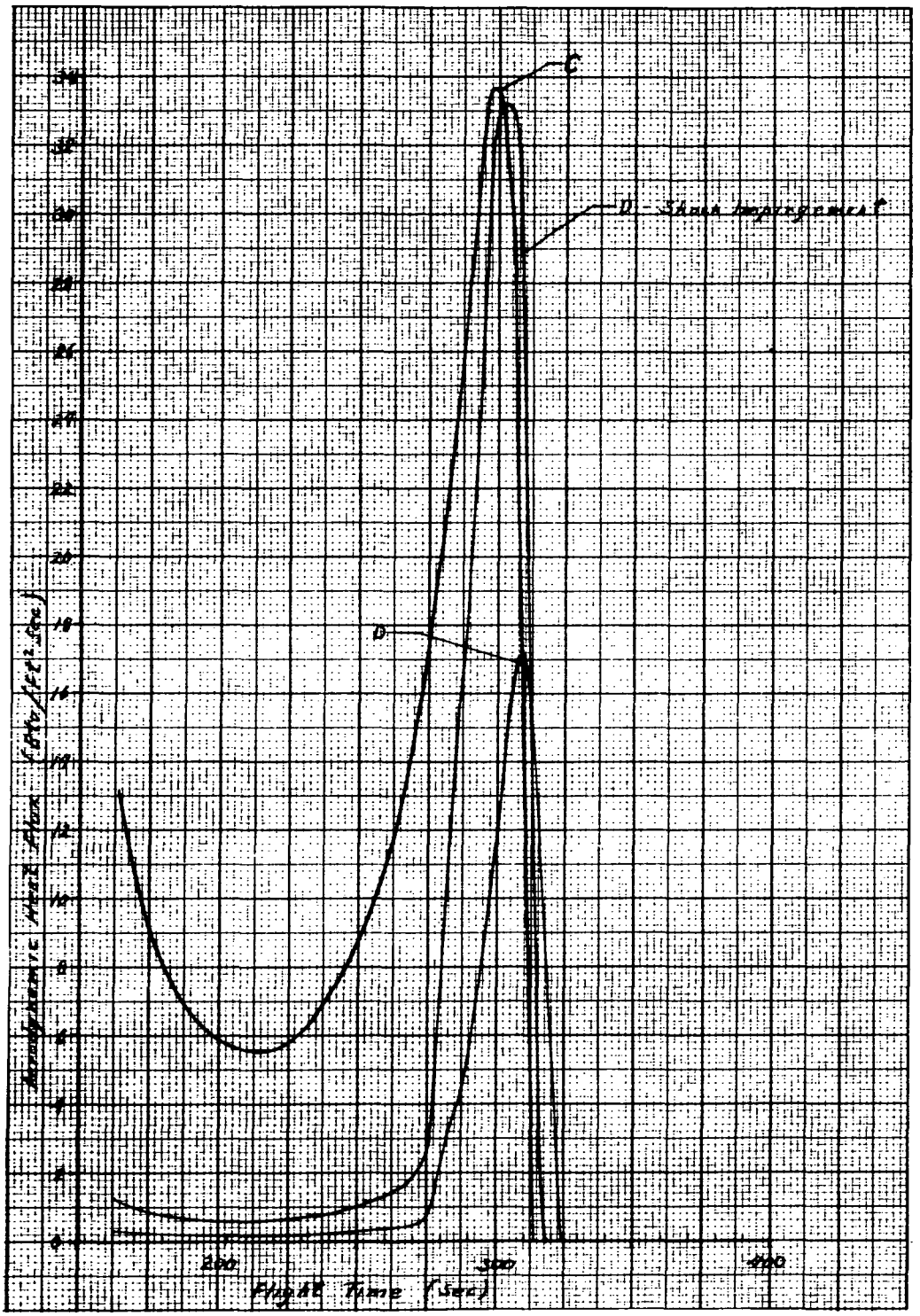

Figure 4-386. Pressure-Fed Booster Thermal Environment - Body
(Sheet 2 of 2)

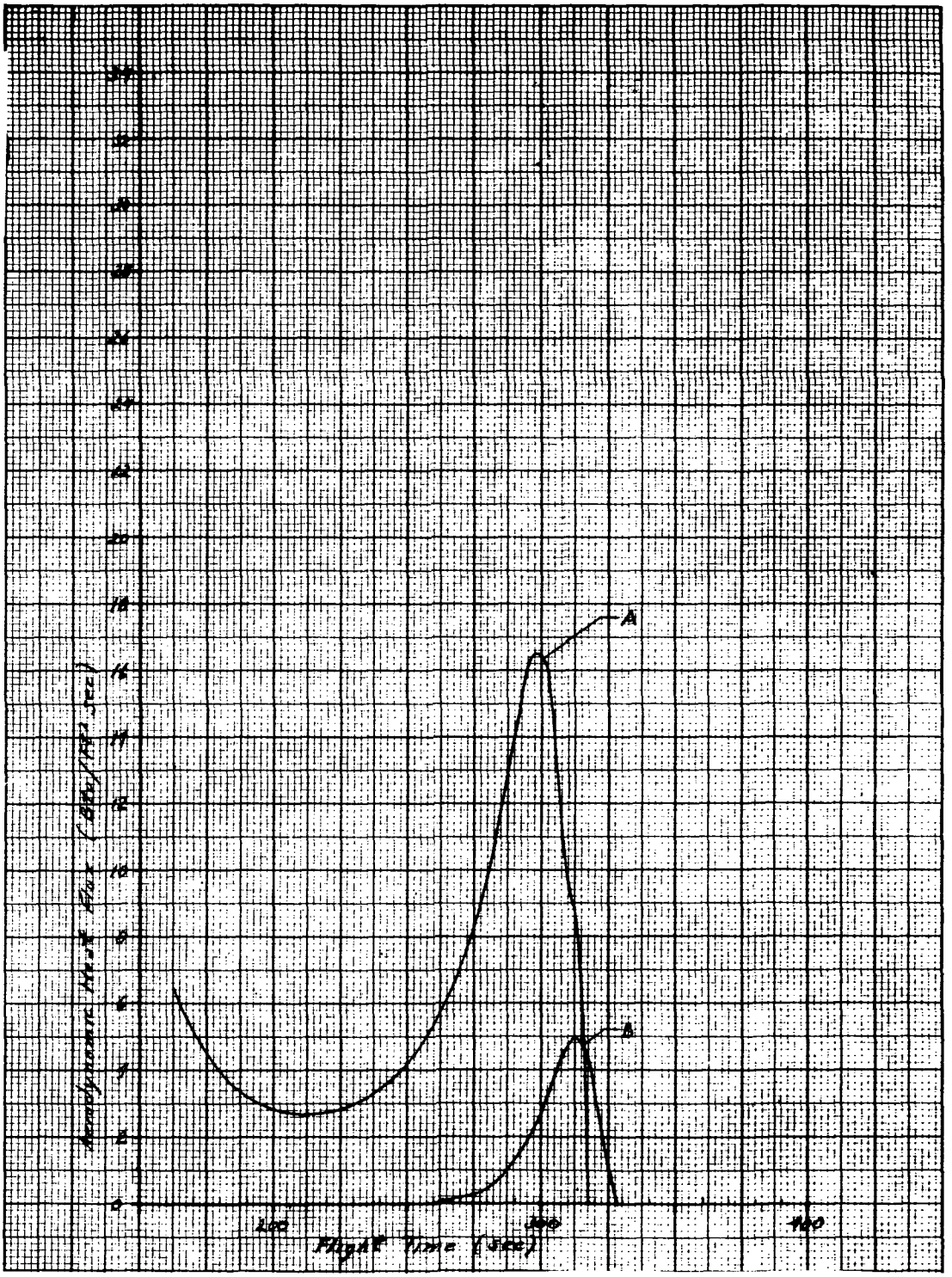

Figure 4-387. Pressure-Fed Booster Thermal Environment - Fin

Structure

Design Criteria. The LO_2 and propane tanks, made from Inconel 718, were sized using the pressure curves of Section 4.4.6 and the following criteria:

Pressures

$P_{ullage} = 315 \pm 1.5\%$ psia, max $P_{ullage} = 319.7$ psig (for LO_2 tank)
$P_{ullage} = 300 \pm 1.5\%$ psia, max $P_{ullage} = 304.5$ psig (for propane tank)
$P_{limit} = P_{ullage} + \Delta P^*_{head}$
$P_{yield} = 1.10\ P_{limit}$
$P_{ult} = 1.40\ P_{limit}$
$P_{proof} = 1.25\ P_{limit}$

$*\Delta P_{head} = 1.304 \times 1.5$ rho H (@ lift off)
$\Delta P_{head} = 1.00$ rho H (proof test with H_2O at room temperature)
1.304 = axial load factor at lift off
1.15 = dynamic amplification factor at lift off

The LO_2 - propane common bulkhead and the LO_2 feed line were sized for the full LO_2 tank ullage and 1 g head pressure with the propane tank unpressurized, a condition possible during LO_2 loading.

Materials. Inconel 718 is the basic material used throughout the pressure-fed booster structure except for the nose cone energy absorption system and the base heat shield. The maximum permissible temperature for the Inconel 718 is 1350 F, which is the aging temperature. Use at temperatures above this point severly degrades the material. The fin leading edges, the skirt and the drag flaps are "heat sinked" to limit the temperatures to 1350 F or less.

The material properties for Inconel 718 are:

	At Room Temp	At -300 F (LO_2)
F_{tu}	180,000 psi	209,000 psi
Welded & Aged	135,000 psi	158,000 psi
F_{ty}	150,000 psi	175,500 psi
Welded & Aged	108,000 psi	126,500 psi
E	29.6×10^6 psi	30.1×10^6 psi

Structural Analysis. The tank wall gages required for the pressures and loads given in above are shown in Table 4-72.

Table 4-72. LO_2 and Propane Tank Pressures and Wall Thicknesses

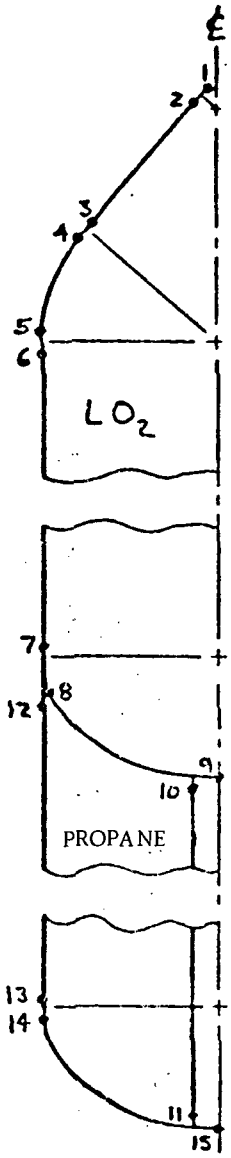

LOCATION	PRESSURES				THICKNESS	
	LIMIT	YIELD	ULT.	PROOF		
1	319.7[3]	351.7	447.6	411.3	.400	6
2	319.7[3]	351.7	447.6	411.8	.400	
3	319.7[3]	351.7	447.6	415.7	.400	
4	319.7[3]	351.7	447.6	415.7	.238	
5	319.7[3]	351.7	447.6	419.4	.238	
6	319.7[3]	351.7	447.6	419.4	.477	
7	355.0[1]	390.5	497.0	443.8[5]	.505	
8	338.4[4]	372.2	473.8	434.8	.353	7
9	343.2[4]	377.5	480.5	439.0	.353	
10	343.2[4]	377.5	480.5	439.0	.080	
11	368.1[4]	404.9	515.3	460.1[5]	.084	
12	304.5[3]	335.0	426.3	380.6[5]	.432	
13	308.0[2]	338.8	431.2	385.9	.439	
14	308.0[2]	338.8	431.2	385.9	.219	
15	312.0[2]	343.2	436.8	390.0[5]	.314	

NOTES:

1. Pressure at t = 0 seconds
2. Pressure at t = 80 seconds
3. Pressure at t = 128 seconds
4. LO_2 tank pressure during loading (propane tank empty)
5. 1.25 x limit pressure
6. Required for water impact
7. Common bulkhead with a reverse pressure capability of 8.5 psi limit

General Description.

Nose Cone - Energy Absorption System. The conical nose section of the booster is subjected to high impact loads during the water entry phase of recovery. To limit this shock load, an energy absorption system has been installed. This system is depicted in Figure 4-388. The system is basically a designed crushable structure assembled from an aluminum honeycomb core with face sheets protected by an outer cork ablator. The conical assembly is designed to be mechanically installed to the tank nose structure. Upon impact, the crushing action of the honeycomb will absorb the initial impact shock, thereby minimizing shock loads in the tank structure. The crushed assembly can be removed and replaced prior to the next mission.

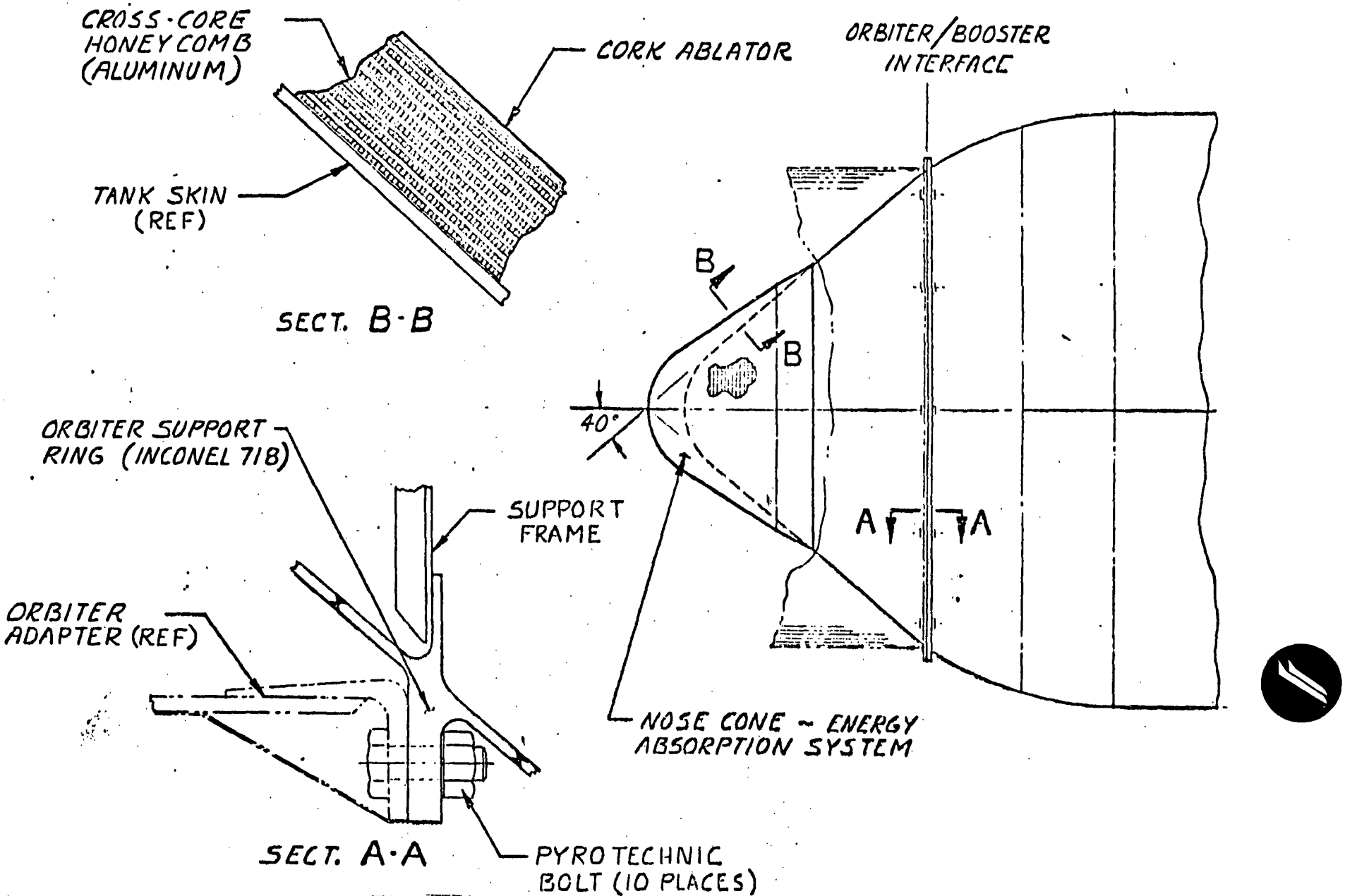

Figure 4-388. Energy Absorption System

Propellant Tanks. The oxidizer and fuel tanks shown in Figure 4-389. are monocoque shells that form a structure 131 feet long and 27 feet in diameter. The tanks are made from 718 nickel plate rolled and fusion welded into a cylinder with a conical dome on the forward end and an ellipsoidal dome on the aft end. An ellipsoidal internal bulkhead divides the 69, 774 cu ft structure into a 41, 481 cu ft oxidizer tank and a 28, 293 cu ft fuel tank. The cylinder is fabricated in 15 sections with each section made from 6 skins machined to provide edge weld lands. Size of the skins is limited in width (less than 90 inches) by width of rolls at the rolling mill and in length (less than 72 inches) by the size of skin mills that have the capacity for machining 718 nickel plate. The ellipsoidal bulkheads are made in 16 gores. Gore width is established by the width of material that can be rolled with adequate tooling allowance for the forming process.

Support for subsystems and other structures is provided at two stations in the LO_2 tank. An internal frame is located in the forward dome to support lateral loads from the orbiter. A second bulkhead located at the base of the forward dome and with the orbiter bulkhead provide support for seven helium bottles. A 53-inch-diameter line runs through the propane tank to supply LO_2 to the rocket engines.

Thrust Structure. The baseline thrust structure is shown in Figure 4-390. The outer shell structure is an Inconel 718, heat sink structure. It is attached to the propane tank by means of a Y-ring, bolted flange concept. The skins are machined to provide the thicknesses required to support high local loads. Formed stringers are then attached to them with mechanical fasteners.

Seven engines are mounted to the aft thrust bulkhead. This bulkhead distributes the lateral loads to the skin. A matrix of trusses and thrust posts, combined with the forward and aft bulkheads and their cross members, supports the engines at the engine thrust flanges. This arrangement forms beams with a depth equal to the distance between the bulkheads (eight feet), and carries the thrust loads to the shell structure.

The forward and aft bulkheads also support the spars of the three fins and resist the moment reactions from the four hold-down fittings.

Three formed intermediate frames are used to reduce the column length of the skin stringers and the aspect ratio of the skin panels.

Base Heat Shield. The base heat shield consists of a flared skirt and a station plane radiative cover panel system. The flared skirt extends from the aft thrust bulkhead approximately eight feet. Included in this structure are eight retractable drag flaps, the supports for their actuation mechanisms,

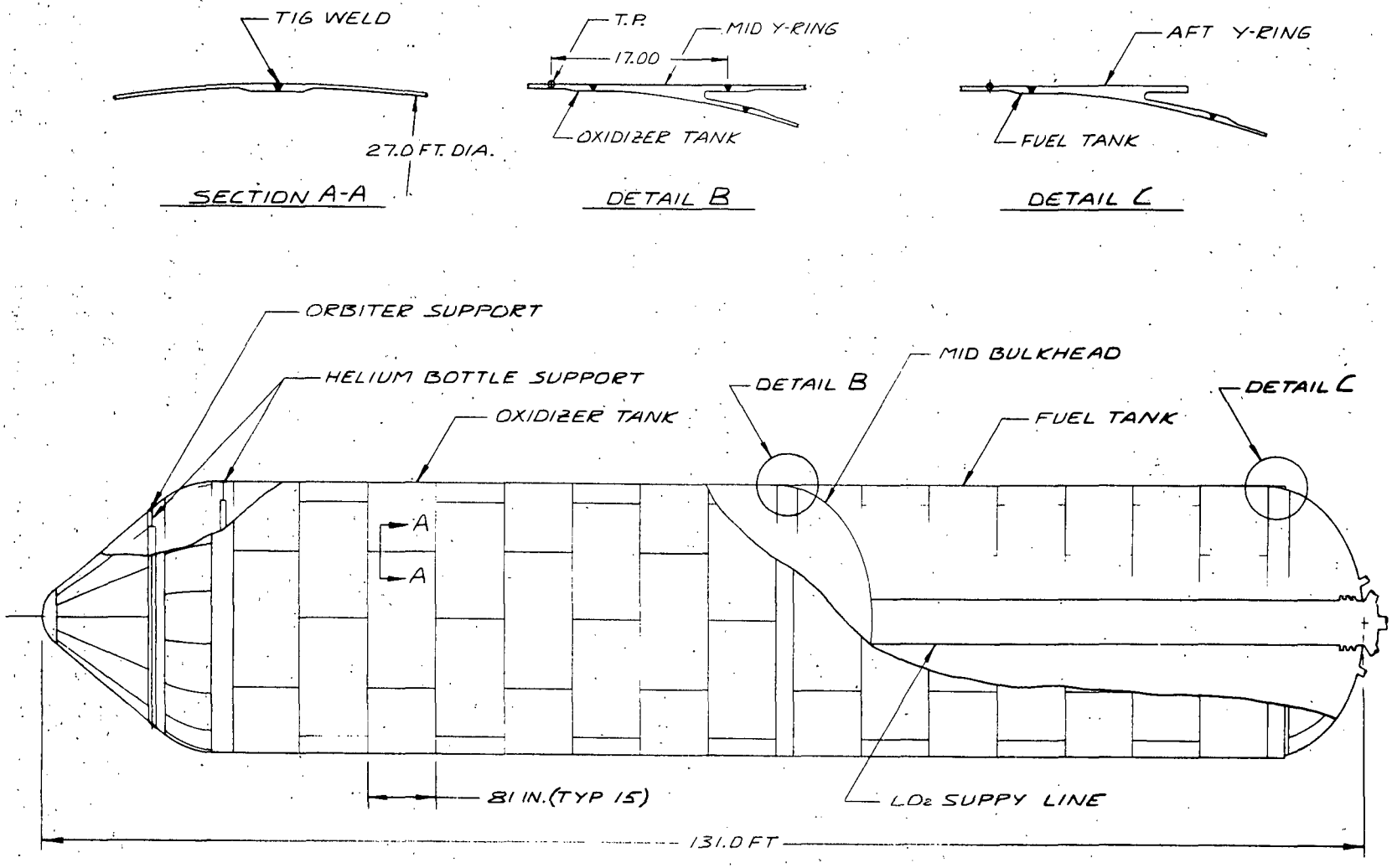

Figure 4-389. Propellant Tanks

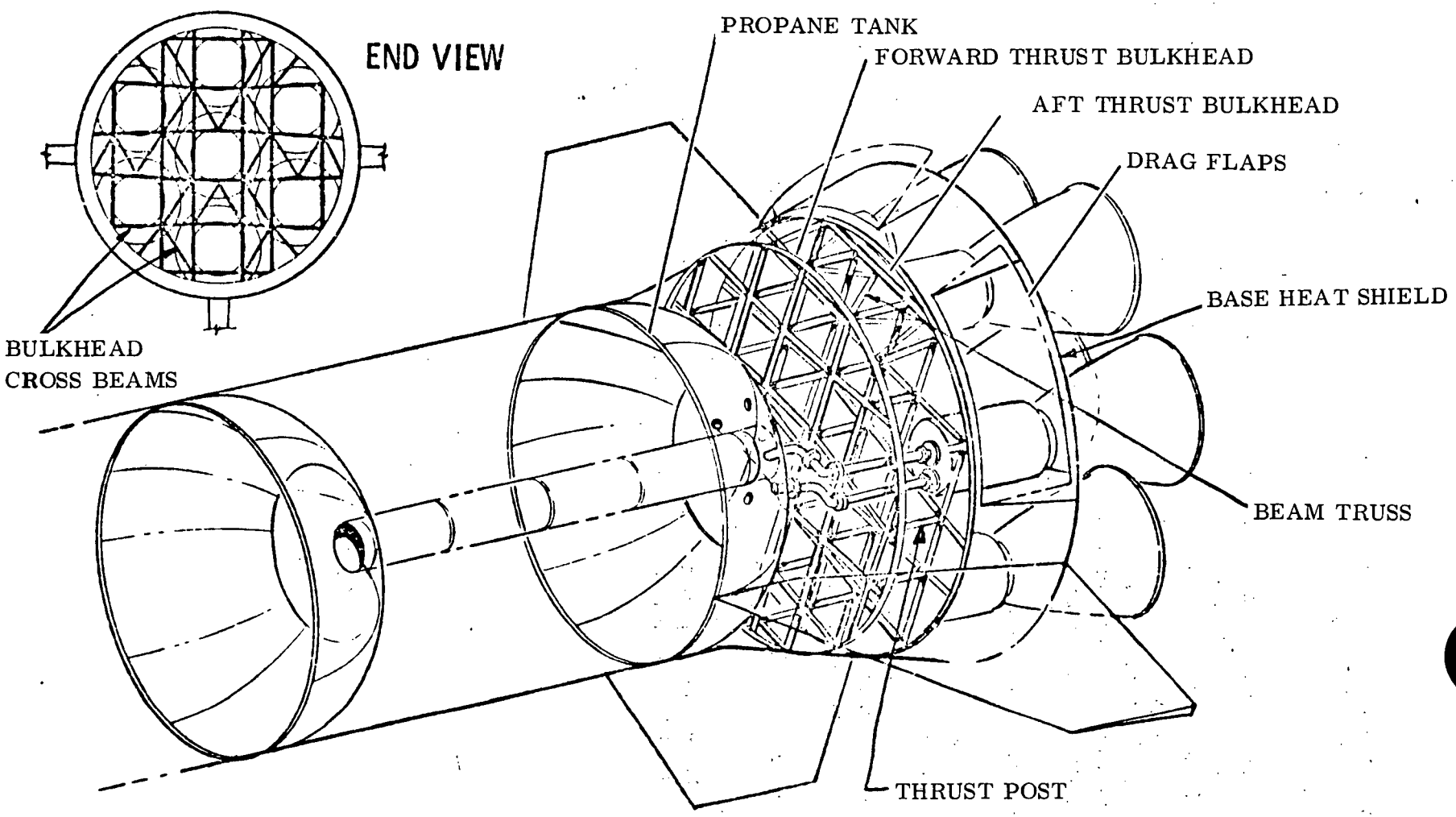

Figure 4-390. Thrust Structure of Pressure-Fed Booster

and provisions for mounting three parachute containers. The flaps reduce the vehicle velocity during reentry; the parachutes regulate the landing descent speed.

The station plane radiative system is a series of removable, metallic, corrugated panels with a layer of Dynaflex insulation on the forward side. The panels will be designed to be capable of carrying the base pressure load through the relevant temperature range and to withstand the acoustical environment. Thermal expansion of the cover panels relative to the supporting beam structure is accommodated laterally by flexing of the corrugations and longitudinally by slip joints and slip attachments.

Aerodynamic Surfaces.

Fin. The fin will be a three-spar, multi-rib structure with Inconel 718 plate/stringer skin panels and corrugated or trussed spars and ribs. The leading edge will be a heat sink design of Inconel 718 to withstand the reentry thermal environment. Fin bending and shear loads will be reacted through fin-to-skirt attach fittings.

Drag Flap. The drag flap will be a two-spar, multi-rib structure with heat sink Inconel 718 plate/stringer skin panels. Panel thickness will be sufficient to limit temperature to 1350 F or less. Each drag flap segment (eight total) will be supported by two hinges fixed to the skirt structure and be actuated with a pneumatic actuator at each actuator/hinge rib.

PFB Structure Trade Studies

Materials Selection Study. Five materials were considered for the fabrication of the propellant tanks. They were 2219-T87 aluminum, 200 maraging steel, 140 Hy steel, 718 nickel (solution treated and aged), and filament wound fiberglass. The study considered aspects of producibility with the different materials (Table 4-73), weight comparison for a particular tank configuration (Figure 4-391) based on the fracture toughness and mechanical property data presented in Table 4-74 and other structural characteristics summarized in Table 4-75.

A refinement of the study covering 718 nickel, 2219 aluminum, and fiberglass was made and the results of this study are reported in Tables 4-76 and 4-77. As shown in Table 4-77, 718 nickel was selected for the baseline vehicle.

Table 4-73. Tank Producibility Concepts

Aluminum 2219 -T87	Steel Maraging 200	Steel Hy 140	Nickel 718 150	Fiberglass Filament Wound
Rolled Ring Forgings	Rolled Ring Forgings	Rolled Ring Forgings	Plate	Continuous filament wound composite of S-glass over mandrel with liners.
• Eliminates longitudinal welds	Same	Same	• Ingot size not practical	
• Reduces thickness 40%	• Reduces thickness 10%	Same	• Heat treatable welds	
• As welded final cond.	• Heat treat welds	Same	• Form and weld in annealed condition	
• Constraints diameter to 27 ft.	Same	Same	• No diameter constraint • Thicknesses too great for cold working	

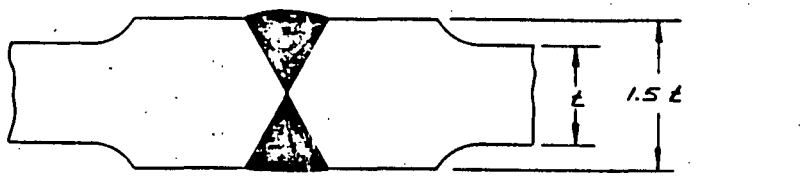

ALUMINUM WELD JOINT

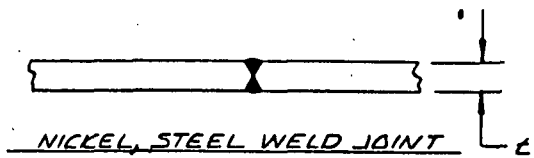

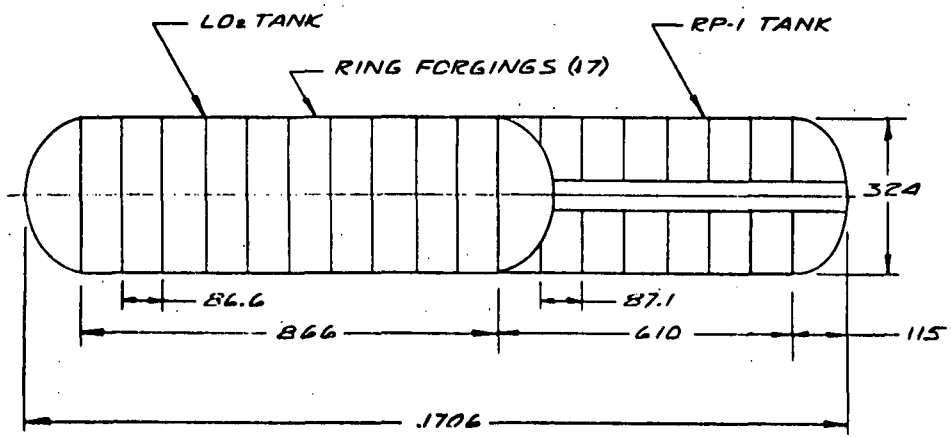

MATERIAL THICKNESSES

	ALUM 2219 -T87	STEEL MARAG. 200	STEEL HY 140	NICKEL 718 150	FIBER-GLASS FILMT WOUND
LO2 TANK					
FWD DOME, TOP	.967	.437	.583	.329	
FWD DOME, BASE	.684	.309	.413	.233	
CYLINDER, TOP	1.368	.618	.824	.465	
CYLINDER, BASE	1.596	.721	.962	.543	
AFT DOME, TOP	.243	.108	.145	.082	
AFT DOME, APEX	.243	.108	.145	.082	
TUNNEL, TOP	.063	.028	.037	.021	
TUNNEL, BASE	.091	.041	.056	.032	
RP-1 TANK					
CYLINDER TOP	1.452	.656	.875	.494	
CYLINDER BASE	1.565	.707	.943	.532	
AFT DOME TOP	.781	.354	.437	.267	
AFT DOME APEX	1.11	.499	.667	.376	
WEIGHT	264K	341K	455K	257K	

Figure 4-391. Weight Comparison

Table 4-74. Material Selection - Fabricability

		718 INCONEL	2219 AL.	FIBERGLASS
TOUGHNESS		GOOD	GOOD	—
WELDABILITY		VERY GOOD (AGED WELDS)	GOOD (EXCEPT THICKEST SECTIONS?)	—
MACHINEABILITY		FAIR (CHEM. MILL GOOD)	EXCELLENT	—
DIFFUSION BONDING		OK	NO	—
DAMAGE TOLERANCE		EXCELLENT	SUSCEPTIBLE TO COATING DAMAGE	SUSCEPTIBLE TO HANDLING DAMAGE
LOX COMPATIBILITY		EXCELLENT	EXCELLENT	NEEDS LINER
FORMING	CYLINDRICAL	ROLL RING FORGING OR PLATE	ROLL RING FORGING ONLY	—
	$\sqrt{2}$ DOME GORES	OK	DIFFICULT (TOO THICK)	—
	SPHERICAL GORES	OK	OK	—
FABRICABILITY RANKING		1	1	2

Table 4-75. Material Selection

		718 INCONEL	2219 AL.	FIBERGLASS
σ_{ALLOW}/ρ	@ 70°F	458,000	451,000	—
	@ -320°F	643,000	461,000	—
MAX. OPERATING TEMPERATURE (°F)		1,300	350	600
CRITICAL FLAW SIZE (IN.)		0.075	0.110	?
NOMINAL WALL THICKNESS (IN.)				
	MAXIMUM	.42	1.25	1.0
	MINIMUM	.24	0.65	0.55
MAX. CYL. WELD THICKNESS (IN.)		.42	1.88	N.A.
MAX. DOME WELD THICKNESS (IN.)		.42	2.25	N.A.
CORROSION RESISTANCE		EXCELLENT	FAIR (NEEDS COATING)	EXCELLENT
MANUFACTURING RANK		1	1	2
WEIGHT		192,200	194,200	?
SELECTED FOR BASELINE		✓		

Table 4-76. Fracture Toughness and Mechanical Properties

		Aluminum 2219-T-87	Steel Maraging 200	Steel Hy 140	Nickel 718 150	Fiberglass Filament Wound
K_{1C} @ R. T. (ksi $\sqrt{in}$)		35 - 40	110	≈ 250	85	–
K_{1C} @ -30 F (ksi $\sqrt{in}$)		35 - 43	≈ 40	≈ 30	100	–
Critical crack length for "leak before break"		Thick gages make "leak before break" impractical	→	→	→	–
Assumed crack length (in.)		2.00	0.50	0.50	1.25	–
Allowable working stress, σ allow (ksi)	@ R. T.	38	200	140	12.2	
	@ -30 F	38	92	69	143	
Tension yield stress (ksi)	F_{ty} @ R. T.	51	200	140	152	
	F_{ty} @ -320 F	61	TBD	TBD	190	
$\frac{\sigma_{allow}}{\rho} \times 10^5$	@ R. T.	3.72	6.90	5.00	4.11	
	@ -320 F	3.72	3.17	2.46	4.72	

Table 4-77. Structural Design Summary

		Aluminum 2219-T-87	Steel Maraging 200	Steel Hy 140	Nickel 718 150	Fiberglass Filament Wound
Weight (lb)		264,000	341,000	455,000	257,000	
Cost ($)						
Fabricability (Ranking)		3	2	1	3	4
LO_2 compatibility		Not critical	Not critical	Not critical	Not critical	Critical; needs liner
Corrosion resistance		Requires protective coating	Requires protective coating	Requires protective coating	Good; no coating required	Good; no coating required
Fracture Toughness specific strength $\frac{\sigma_{allow}}{\rho} \times 10^5$	@ R. T.	3.72	6.90	5.00	4.11	
	@ -320 F	3.72	3.17	2.46	4.72	
Handling toughness (damage tolerance)		Susceptible to coating damage	Susceptible to coating damage	Susceptible to coating damage	Excellent; no coating to damage	Susceptible to handling damage

Table 4-77. Structural Design Summary (Cont)

	Aluminum 2219-T-87	Steel Maraging 200	Steel Hy 140	Nickel 718 150	Fiberglass Filament Wound
Surface heating	Heat sink	Heat sink	Heat sink	Heat sink	Requires reentry nose heat shield
Peak reentry temp (°F)					
Max operating temp (°F)	350	700	600	1250	600
Water impact capability (500 psi - 1000 psi)					

Thrust Structure Trades. Several configurations of thrust structure are subject to trade studies. A promising alternate to the baseline is described below and shown in Figure 4-392.

This configuration employs two concentric stiffened shell structures to transmit the engine thrust loads to the propellant tanks. The six peripheral engines are mounted to the aft thrust bulkhead and the pattern of radial beams which react the lateral loads and distributes the thrust loads to the stringer stiffened, inner and outer skins. The skins take the thrust loads, through the Y-ring attachment, directly into the propane tank. The center engine is also supported by the aft thrust bulkhead and radial beams, the thrust loads being reacted through two load paths; beam bending and four diagonal trusses that extend from the engine-bulkhead interfaces to the intersection of the cylindrical skin and the propane tank.

The Inconel 718 skins are machined to provide the thicknesses required to support high local loads. Formed stringers are then attached to them by mechanical fasteners.

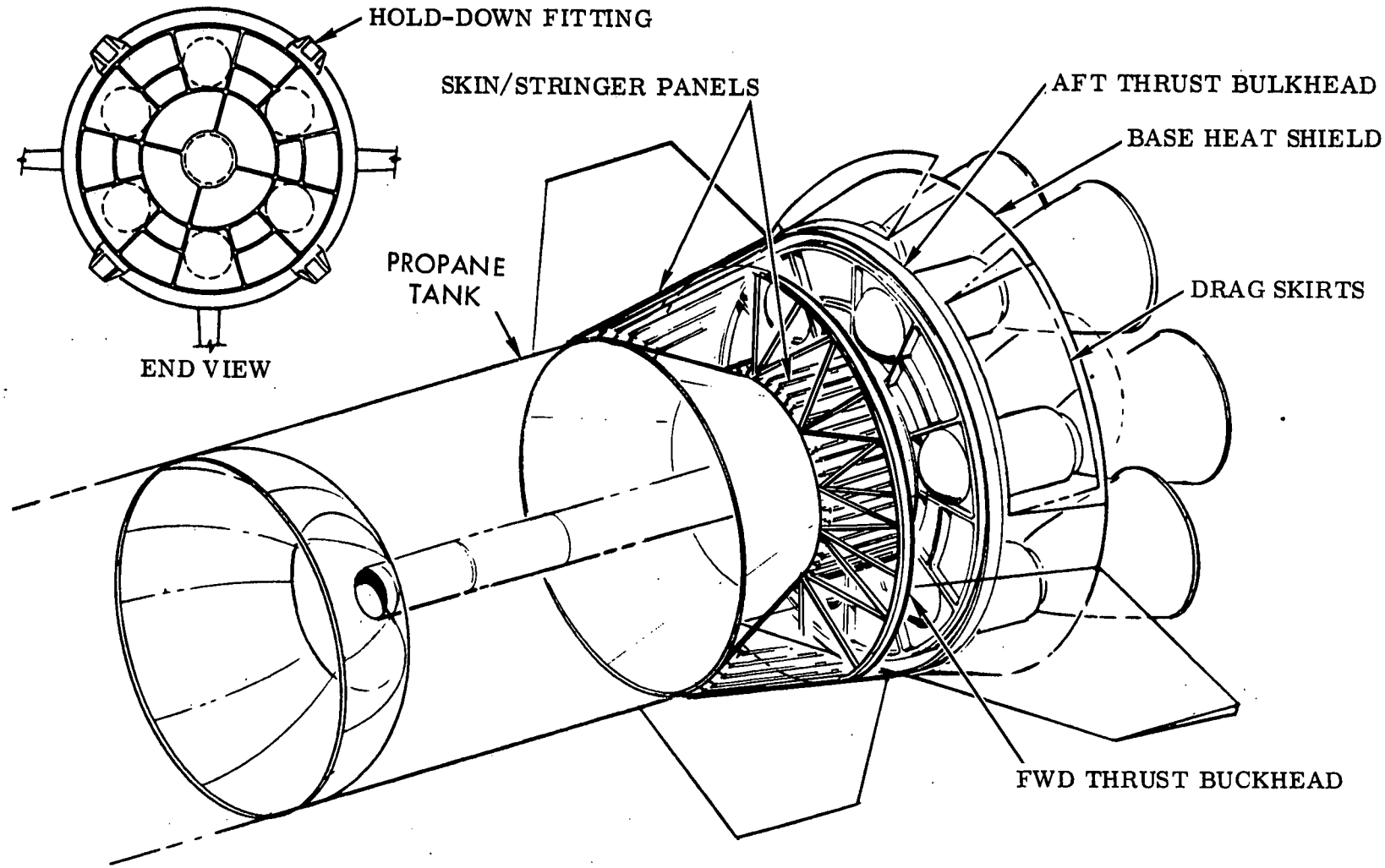

Figure 4-392. Thrust Structure

Main Propulsion System

The main propulsion system provides propulsive thrust to the two-stage space system from launch through orbiter vehicle separation. Seven fixed thrust engines (975 k lb thrust nominal) clustered in the vehicle base provide ascent thrust and vehicle pitch, yaw, and roll control using liquid injection for thrust vector control (LITVC). Vehicle maximum q and g constraints are met by shutting down engines as required during the ascent trajectory.

Engines. Characteristics of the baseline engine are summarized in Figure 4-393. It is a fixed thrust engine (no throttling) fixed to the vehicle thrust structure (no gimballing). Chamber pressure (250 psia) and area ratio (5) are optimized for the stage application. The combustion chamber is cooled by a single downpass cooling jacket, which takes 13 percent of the fuel flow and returns it to the nozzle just upstream of the throat. The remainder of the nozzle is film cooled. Pressure loss through the coolant path to point of injection in the chamber is no more than through the injector so no additional engine inlet pressure is required. Main propellant valves are located at the engine inlets. The O_2 inlet valve is controllable to smooth out variations in the stage supplied pressure (head suppression) and to provide mixture ratio variations of ±5 percent for propellant utilization (PU) control. The C_3H_8 inlet valve controls during start and shutdown only.

To meet the 650 psf maximum dynamic pressure constraint, one engine is cut off approximately 30 seconds after launch. A pair of engines is cut off when the maximum allowable acceleration of 3 g's is reached. The resulting dynamic pressure and acceleration histories during powered booster ascent are shown in Figure 4-394.

The baseline vehicle has a gross lift-off weight of 5.25 million pounds and seven main engines of 975 thousand pounds thrust each, for a lift-off thrust-to-weight ratio of 1.30. With one engine out, the thrust-to-weight ratio at lift-off drops to 1.11.

Liquid Injection Thrust Vector Control System. The engine includes a liquid injection thrust vector control (LITVC) system, using O_2 as the injectant. The O_2 injectant is extracted from the engine inlet duct. The injectant then flows through a 10.5-inch diameter duct to any of 12 6-inch control valves, and on to the point of injection into the nozzle at area ratio 1.8, dia. 80 inches.

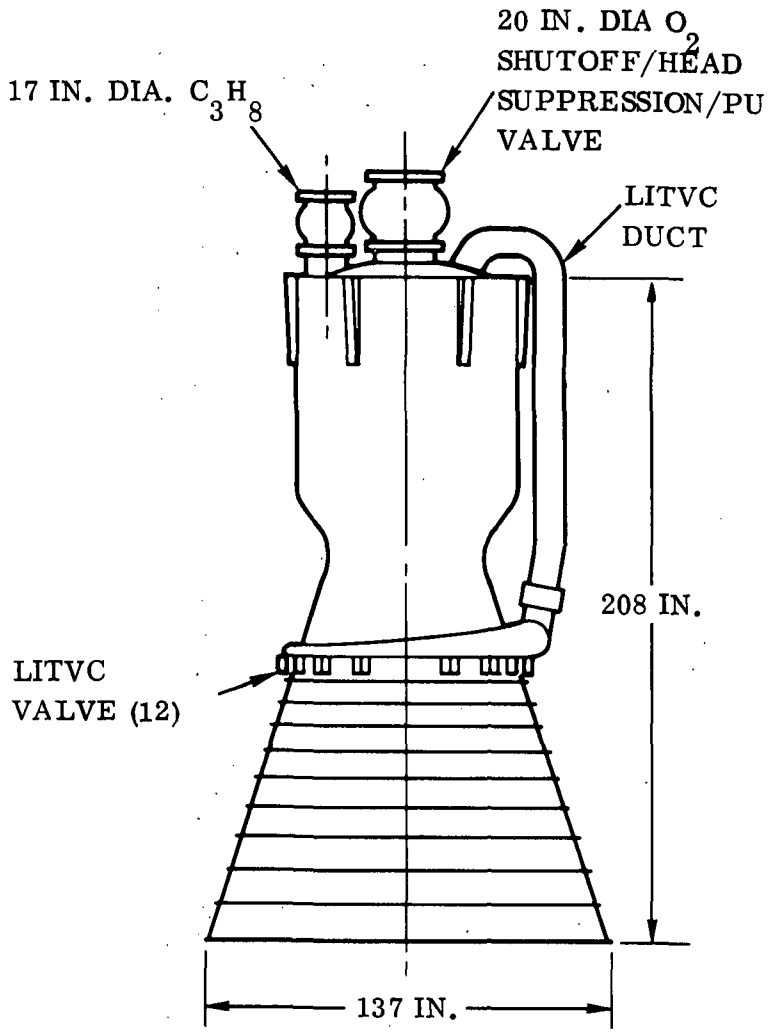

NUMBER	7
PROPELLANTS	O_2/C_3H_8
THRUST (SL)	975K
NOMINAL MIXTURE RATIO	2.8
CONTROLLABLE MIXTURE RATIO	2.66 TO 2.94
AREA RATIO	5
I_{sp} (SL)	227
I_{sp} (VAC)	277
CHAMBER PRESSURE	250 PSIA
INLET PRESSURE, NOMINAL	365/320 PSIA
WEIGHT	9,025 LB.
THRUST VECTOR CONTROL	
LIQUID OXYGEN INJECTANT	
5° EFFECTIVE ANGLE	
12 SEGMENTS	
w_o = 710 LB./SEC. AT 5°	
75 REUSES WITH NO REFURBISHMENT	

Figure 4-393. Pressure Fed Engine

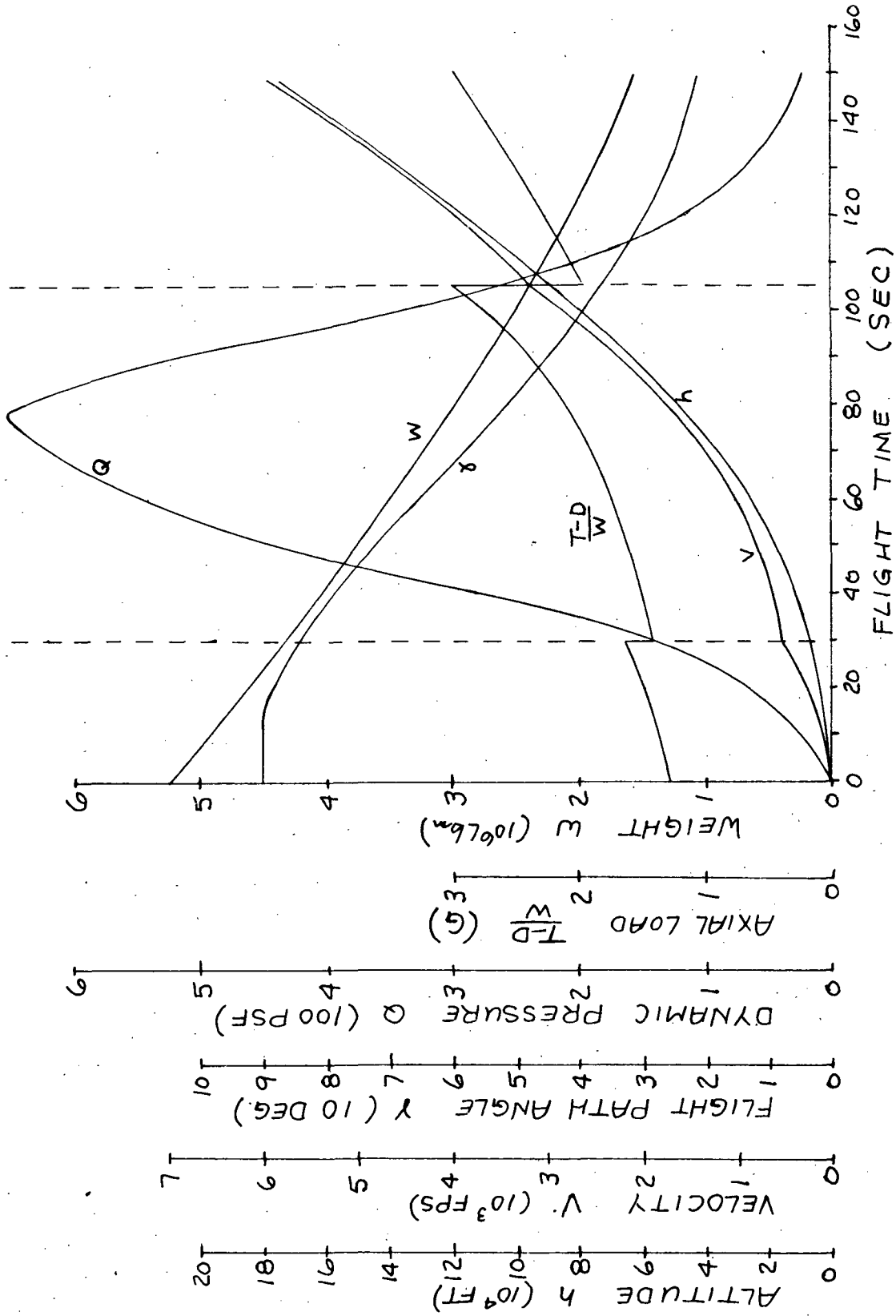

Figure 4-394. Dynamic Pressure and Acceleration Limiting

The maximum side force developed is 85.3 k lb per engine, equivalent to 5 degrees deflection. LITVC performance (I_{sp} versus effective angle) dury cycle requirements, and system weight are summarized in Figure 4-395.

Pressurization System. Tank pressure schedules for the baseline vehicle are shown in Figure 4-396. Pressures in both tanks are constant with time, 305± 5 and 290± 5 psia for O_2 and C_3H_8 respectively. Pressures supplied at the engine inlet valves vary with propellant level and vehicle acceleration, with step discontinuties when engines shutdown, as shown. The O_2 engine inlet valves throttle (i.e., introduce a variable pressure drop) to eliminate these variations and to provide mixture ratio (MR) variation for PU control. O_2 engine inlet pressure band is 350 to 380 psia, depending on MR command. C_3H_8 inlet pressure variations are small, so the C_3H_8 engine inlet valve is fixed open (no throttling) during engine operation.

The pressurization system selected for the baseline uses helium pressurization for the O_2 tank and hydrazine decomposition products for pressurant in the propane tank. Both tanks are pressurized immediately prior to launch with 700 R helium, the LO_2 tank first to prevent bulkhead reversal. The overall system schematic is shown in Figure 4-397. The helium is stored just below the initial liquid surface in the LO_2 tank in seven Inconel spheres. Helium/helium heat exchangers are used in the bottles to minimize bottle residuals. The hydrazine is stored in the thrust section as a liquid in a titanium bottle which is pressurized with helium. The hydrazine catalyst bed gas generator supplies the energy source to heat the helium. The system uses seven catalyst beds, helium heat exchangers, and pressurant storage bottles to provide smooth flow control as engines shut down and to allow development of a single engine with 1/7 of the pressurization system.

Flow control regulators are placed near the tank forward bulkhead to minimize required line sizes. These regulators maintain constant ullage pressures within 5 psi.

The vent system for each tank consists of a vent valve actuated by a gage pressure switch with backup by a mechanical relief actuation; this type of valve is currently used on the S-1C for vent control. Settings for these vent valves are 310 to 320 psig for the oxidizer and 295 to 305 psig for the fuel tank.

Propellant Feed. The propellant feed ducting consists of an individual fuel and LO_2 duct to each engine, as shown in Figures 4-398 and 4-399. Three gimbal joints provide for thermal expansion, manufacturing tolerances and structural deflections of each duct. The ducts are flange mounted to the engine propellant valves and to the fuel tank outlets and LO_2 sump. Only two duct designs are required since ducts for the six outboard engines are identical, while the center engine ducts are shorter.

DUTY CYCLE REQUIREMENTS

CG TRACKING

1/8° FOR 149 SEC.

DISTURBANCE CORRECTION

1/8° FOR 149 SEC.

MAXIMUM CORRECTION (MAX. q)

4° FOR 20 SEC.

MAXIMUM CAPABILITY

5° DURING TOTAL FLIGHT

INJECTANT	62,468

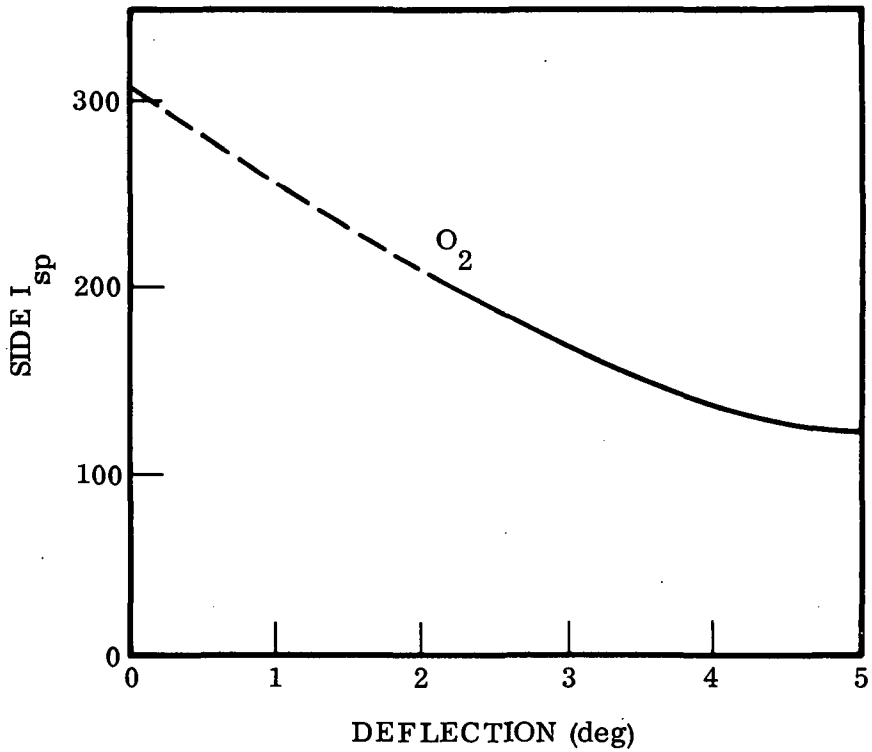

Figure 4-395. Liquid Injection Thrust Vector Control

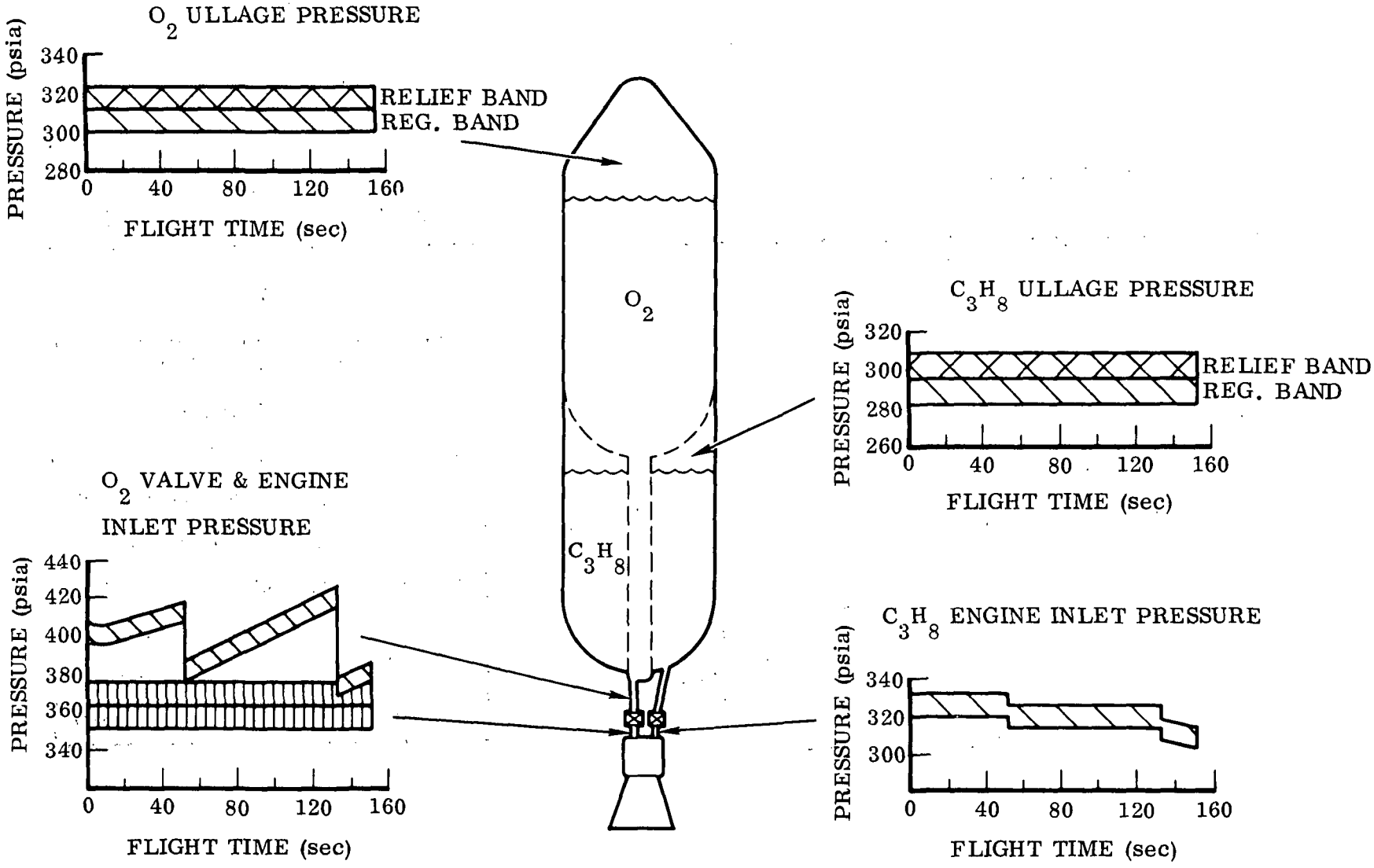

Figure 4-396. Propellant Tank and Engine Pressure Schedules

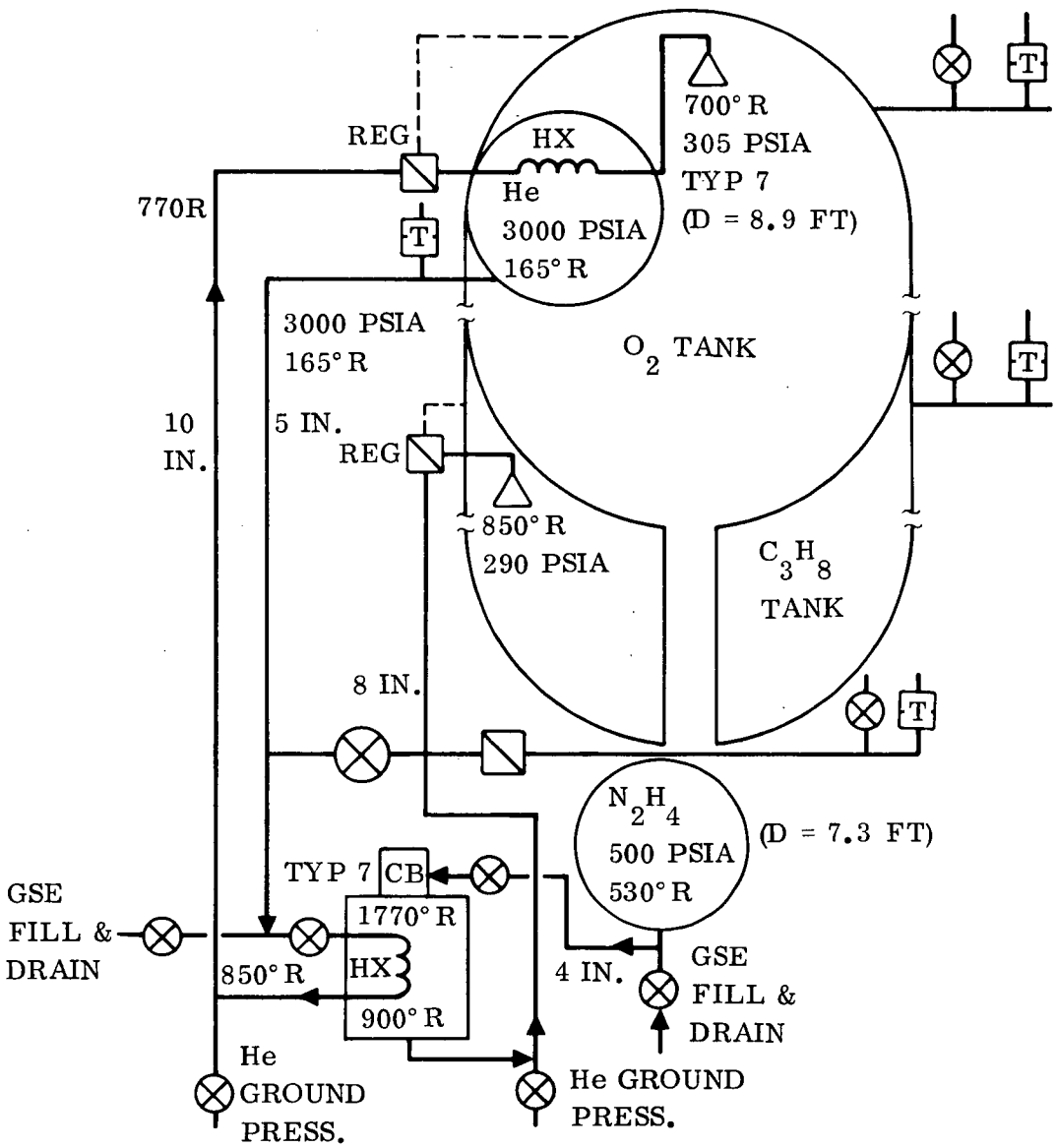

Figure 4-397. Pressurized System Schematic

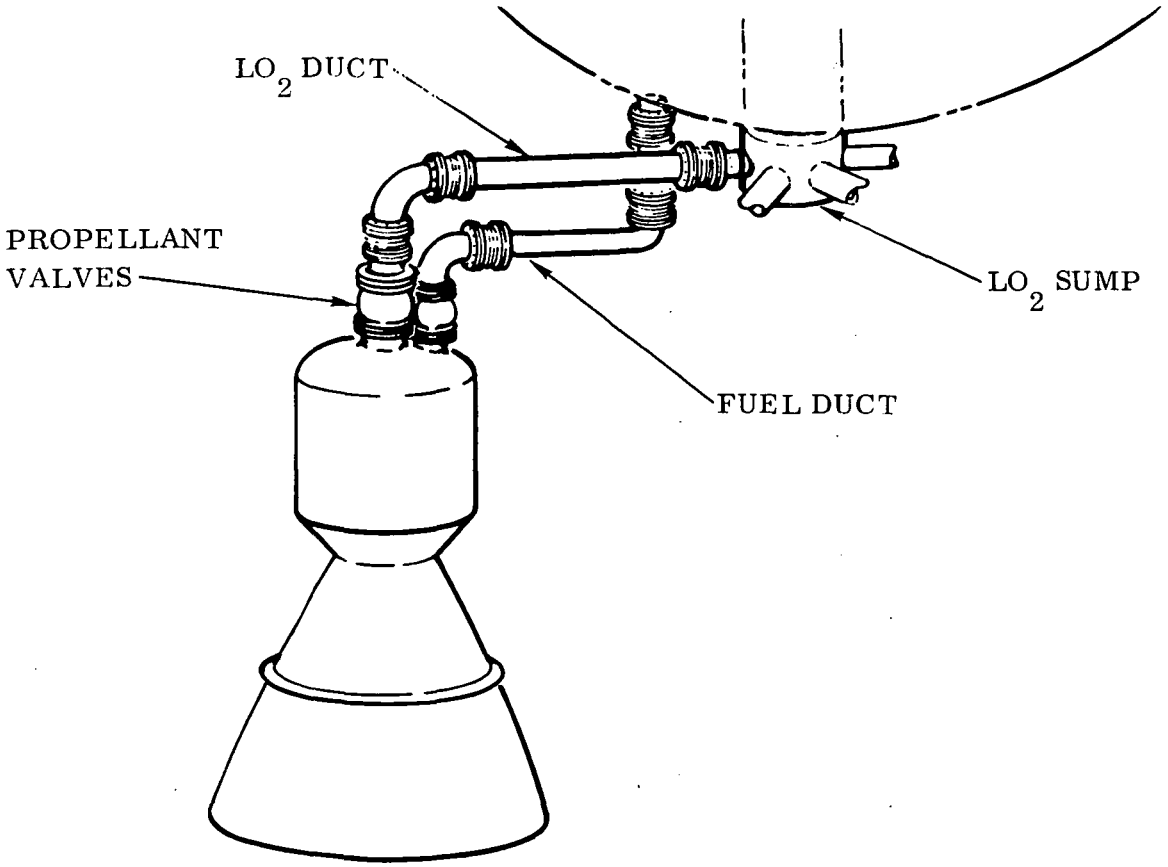

Figure 4-398. Propellant Feed Systems

Propellant Utilization. The baseline vehicle uses a propellant utilization system to reduce residual errors, primarily those due to the tolerances on propellant tank ullage pressures. The 3σ residual propellant weight versus the tolerance on ullage or engine inlet pressure is shown in Figure 4-400 for a system without PU control. The mixture ratio (MR) correction capability required increases from 2.4 percent for zero ullage pressure tolerance (required to eliminate propellant tanking error, including level, volume, and density uncertainties, and engine mixture ratio dispersion) to 7.75 percent with 3 percent ullage pressure tolerance. A 1.5 percent tolerance assumed for the baseline load suppression system requires ±5 percent MR capability.

The propellant utilization system selected for the baseline booster vehicle utilizes differential pressure sensing for quantity gaging and throttling the engine LO_2 inlet valve for engine mixture ratio variations, as shown in Figures 4-399 and 4-400. A propellant residual weight of 0.5 percent of the ascent propellant quantity is obtained.

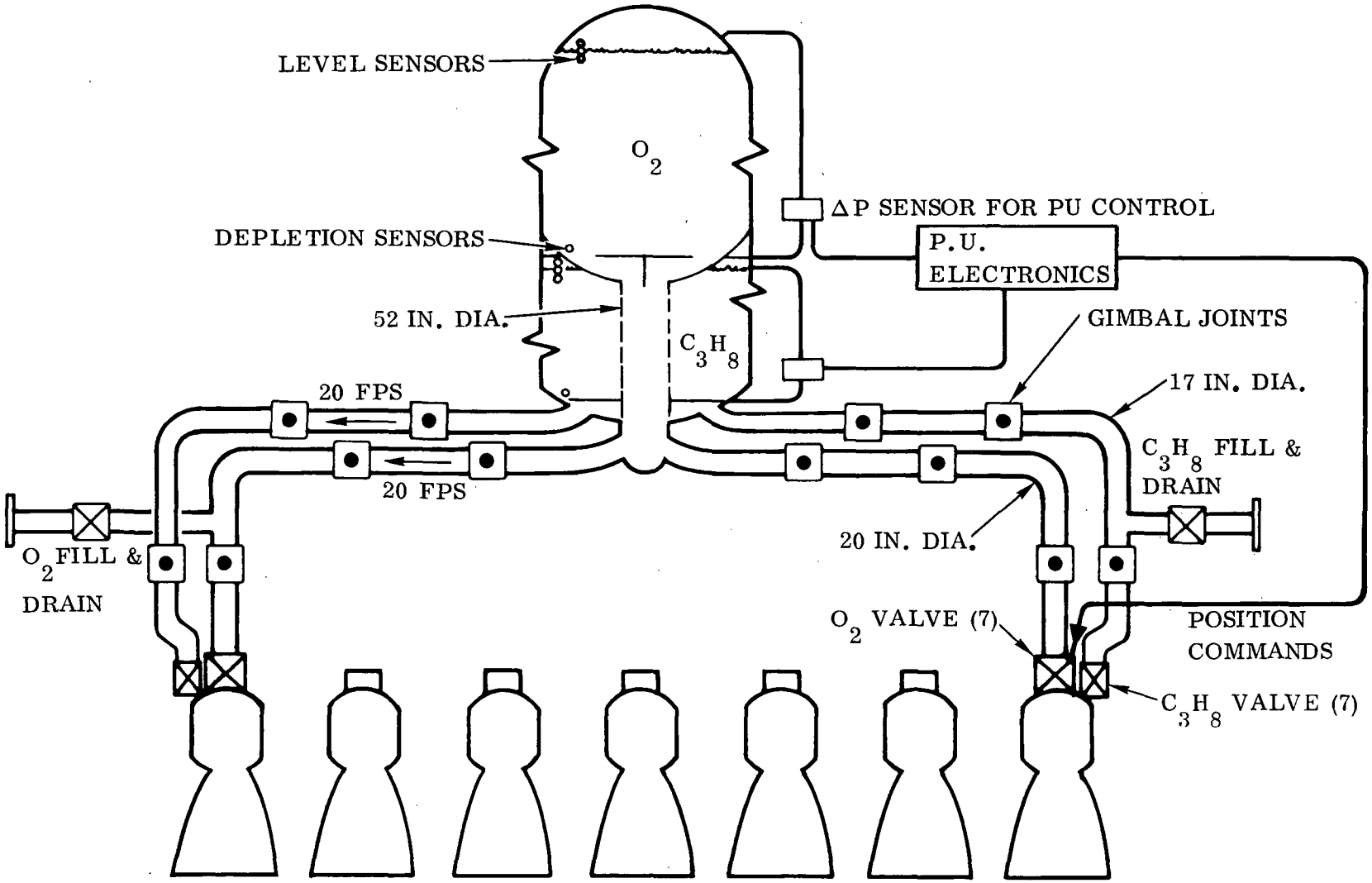

Figure 4-399. Propellant Supply

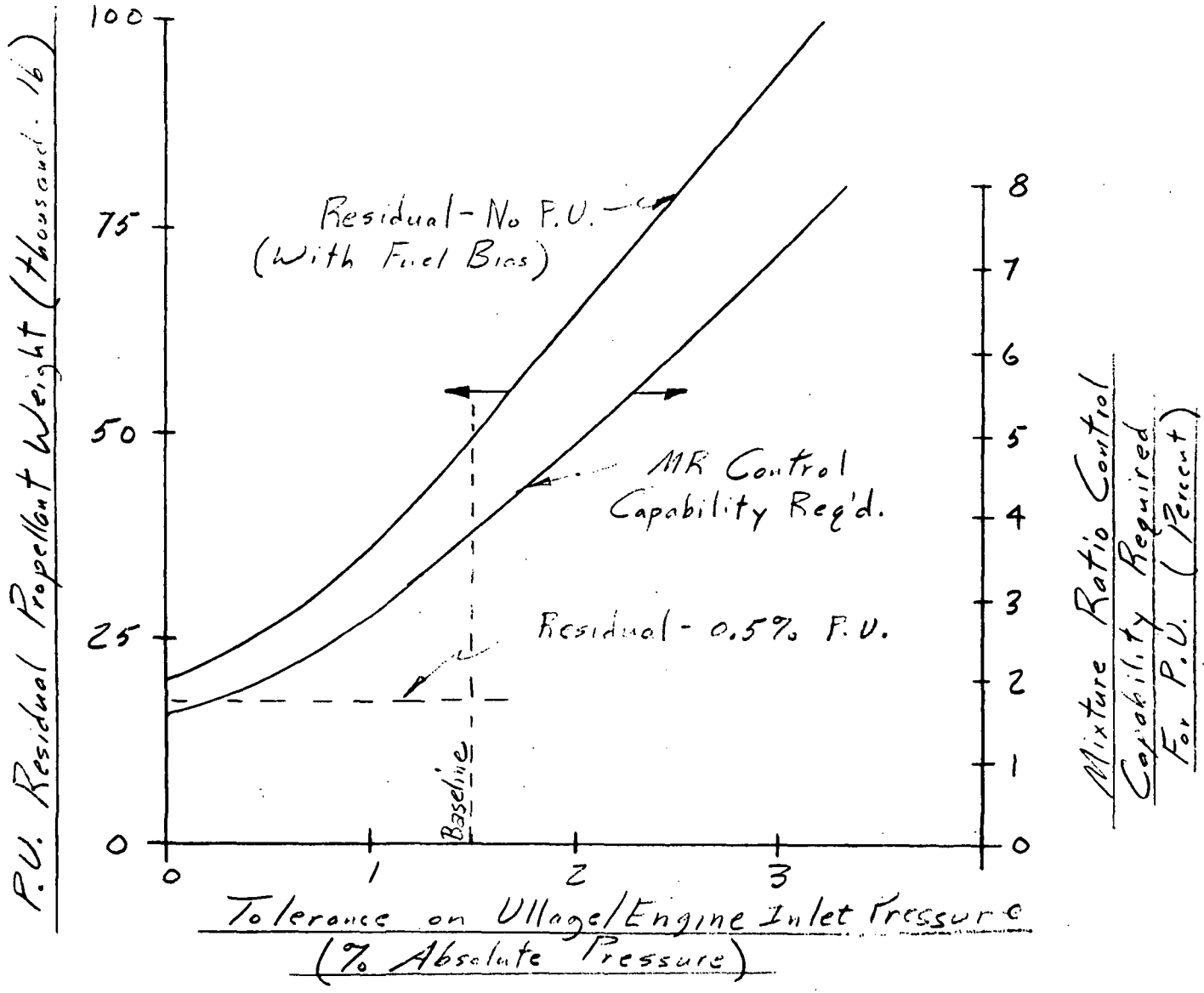

Figure 4-400. Propellant Utilization Requirements

Pneumatics

Drag Flap Deployment. The drag flap actuation system is required to deploy the eight flaps after booster/orbiter separation and to stow the flaps piror to splashdown.

Figure 4-401 shows a schematic diagram of the system, which achieves redundancy through two parallel circuits, either of which is capable of deploying and stowing the drag flaps. Residual helium from the LO_2 tank pressurization system, at approximately 500 psia, is used to power linear actuators. Two actuators per flap operate toggle linkages located at each of the two hinge points on the panel. Figure 4-401 shows the physical location of the drag flaps on the vehicle.

Gas from the pressurization system passes through the solenoid control valves to the distribution plumbing. Restrictors in the inlet ports of the actuators control the drag flap rates. First motion of either actuator per flap unlocks the surface -- allowing it to deploy. As the toggles go over center, a spring actuated lock is activated to retain the flap in the extended position. To stow before splashdown, the solenoid valves admit pressure to operate two extend lock release actuators per flap, either of which can unlock the toggle linkage. Pressure is also admitted to the retract side of the deployment actuator through restrictors. Restrictors on the extend side of the actuator maintain snubbing pressure throughout the stroke to oppose flap loads aiding to drive the flaps stowed. As the drag flaps reach the stowed position, the stow locks are reset by retract motion of the deployment actuators.

The deployment actuators are sized to deploy the flaps when dynamic pressure is low (approximately 30 lb/ft^2). The stow actuation load tends to drive the flaps to stow position. Therefore, the actuators are never required to oppose large externally applied loads to actuate the flaps and are relatively small (approximately 80 in^3 displacement volume each). However, the downlock is designed to hold against external loads induced during the maximum dynamic pressure.

The redundancy shown is subject to further study. The method of redundancy (if any is required at all) needs further refinement to ensure that maximum protection is provided against the most common occurring failure modes.

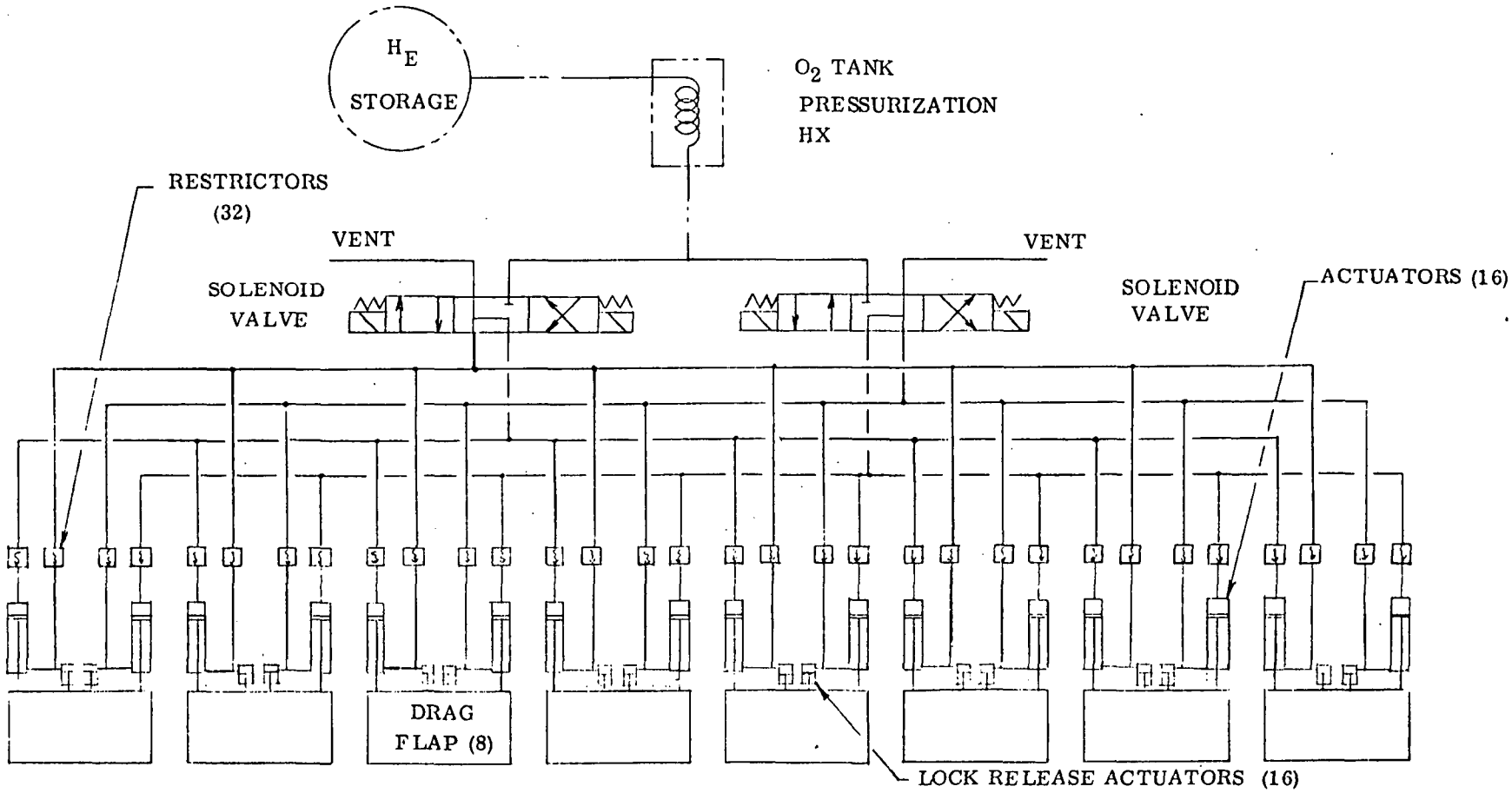

Figure 4-401. Drag Flap Actuation System Schematic

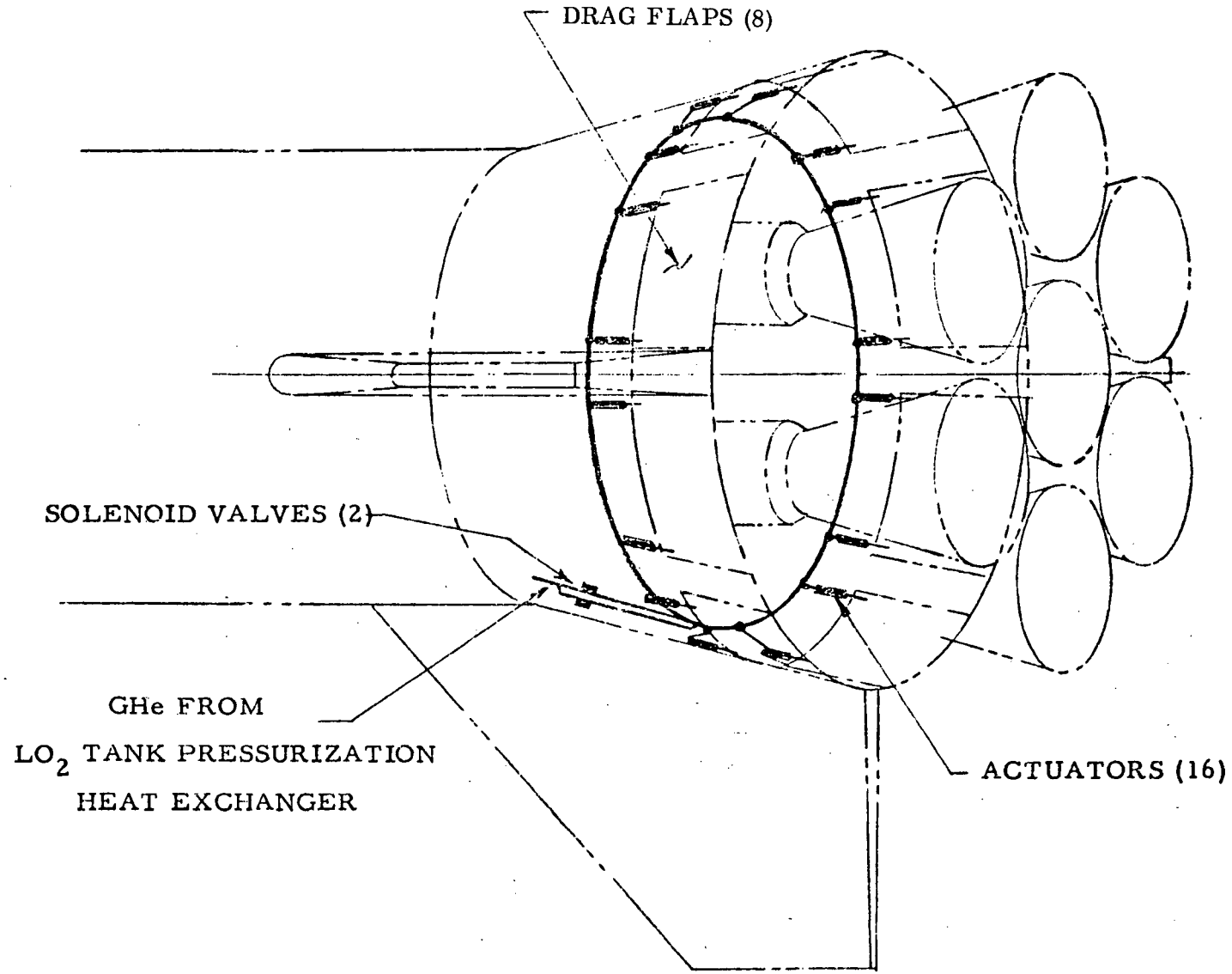

Figure 4-402. Drag Flap Location

Purge and Vent System. The purge and vent system shall perform the following functions:

1. Thrust structure compartment thermal conditioning and purge. Compartment temperature prior to lift-off shall be maintained at 80 (±20) F for batteries and electrical components. Maximum oxygen concentration shall be less than 5%.

2. Compartment pressure control. Compartment shall be vented to ambient to maintain a maximum ΔP of internal to external pressure of ±2 psi.

The thrust structure compartment is conditioned on the ground by conditioned air supplied by the GSE ECU at the umbilical couplings and is maintained during launch preparations up to propellant loading when the flow medium is switched to GN_2.

Compartment pressures are controlled on the ground by opening the thrust structure compartment vent door when purging. At lift-off the door remains open to allow the compartment internal pressure to bleed down and follow the external ambient pressure. When the internal pressure reaches 2.0 psia, the vent doors are closed by the electro-mechanical actuators and remain closed during entry.

Following engine shut down and during descent, when the external pressure is 1.0 psi above the internal pressure, the compartment air is repressurized by using the residual helium in the main propellant tank pressurization system storage bottles.

A line is tapped off of the main tank pressurization system downstream of the heat exchanger and the thermal mass of the heat exchanger is used to heat the helium required for compartment presurization. The helium is ducted through the ΔP pressure regulator which controls the thrust structure compartment pressure to 1 psi above ambient static pressure.

Avionics

One of the primary objectives in the design of the pressure-fed booster was simplification. To achieve this objective, a simple design with a minimum of avionics is essential. In addition, utilizing hardware common with the orbiter and/or off the shelf will help to reduce development costs early in the program. The reduced number of vehicle subsystems and a reduction in the level of avionics support contribute to the simplification of the avionics subsystem.

The overall block diagram, Figure 4-403, shows the booster avionics and its relationship to the orbiter avionics. It should be noted that the elements, which provided the man-machine interface, have been replaced with subsystems providing booster to orbiter and booster to ground interfaces.

All major elements of the avionics system will be mounted in an environmental chamber within the thrust section as shown in Figure 4-404. In addition to providing isolation to acoustic energy and vibrational energy, it will be sealed to provide protection from immersion in sea water. Details of the cooling remain to be determined, but will probably involve a fuel cooled heat exchanger. All harnesses and other equipment located outside this compartment will be water proof.

The changes in the communications subsystem are a result of going to an unmanned vehicle, which permitted the removal of intercommunications, UHF radio, and the TACAN. The orbiter/booster data link has been expanded to approximately 200 circuits.

The command destruct and tracking beacon were added to meet the range safety requirements for unmanned vehicles. The receiver decoders, logic unit, tracking beacon, and batteries are very similar to the respective elements used on the Centaur D-1 vehicle. The power for the range safety equipment is supplied by redundant batteries which are isolated from the main vehicle supply. The destruct system requires omnidirectional antenna coverage. Four antennas were provided to supply this coverage. During the design phase it may be possible to reduce the number of antennas based on actual pattern tests.

The guidance, navigation, and flight control (GN&C) computations are to be accomplished in the orbiter GN&C computer. Basic inertial data will be derived from the orbiter IMU and rate data from the three-axis rate gyros located on the booster. Thrust vector commands will be transferred from the orbiter to the liquid injection thrust vector control (LITVC) logic and control box on the booster. This box also contains the drivers for the injection valves.

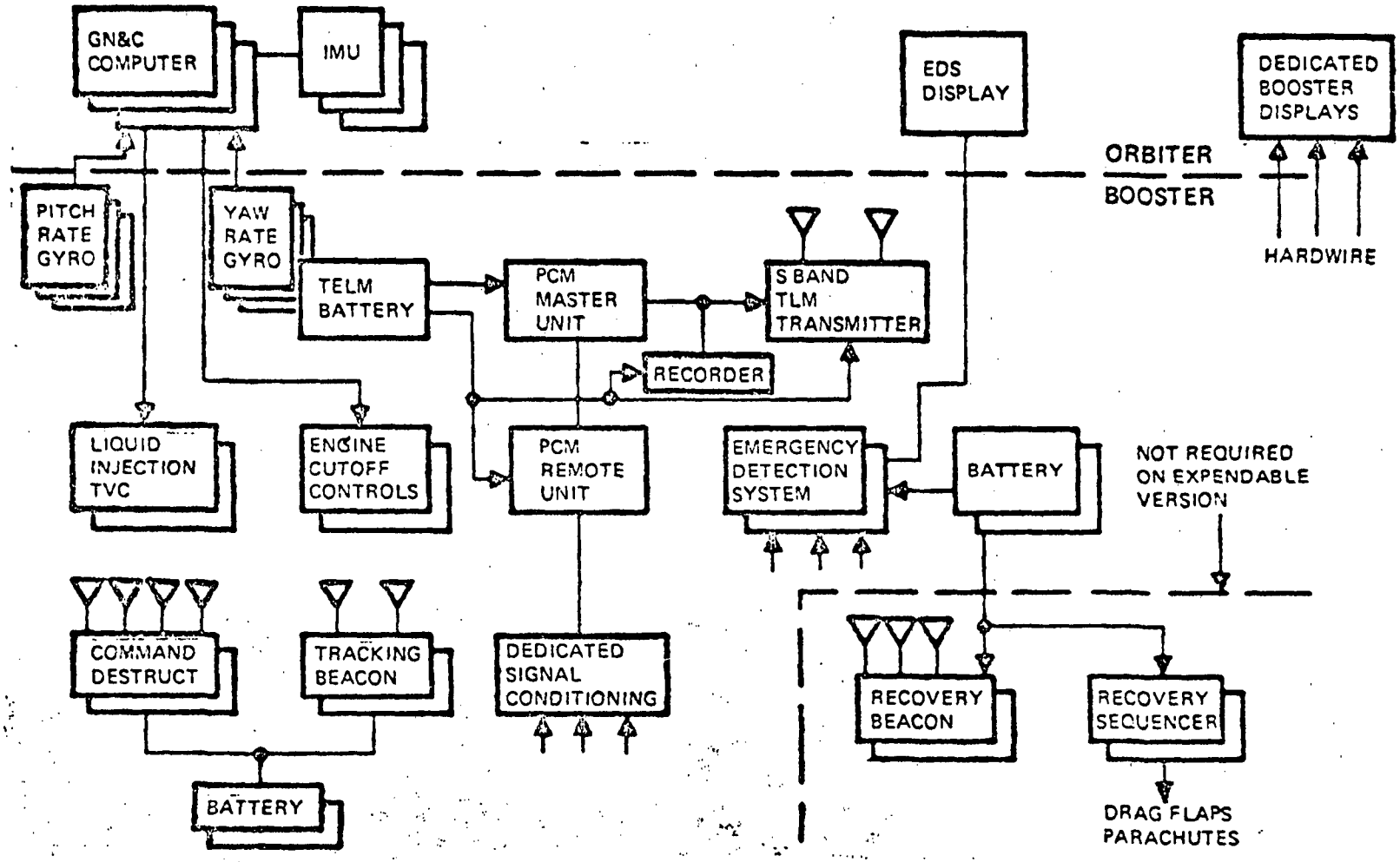

Figure 4-403. Pressure-Fed Booster Avionics

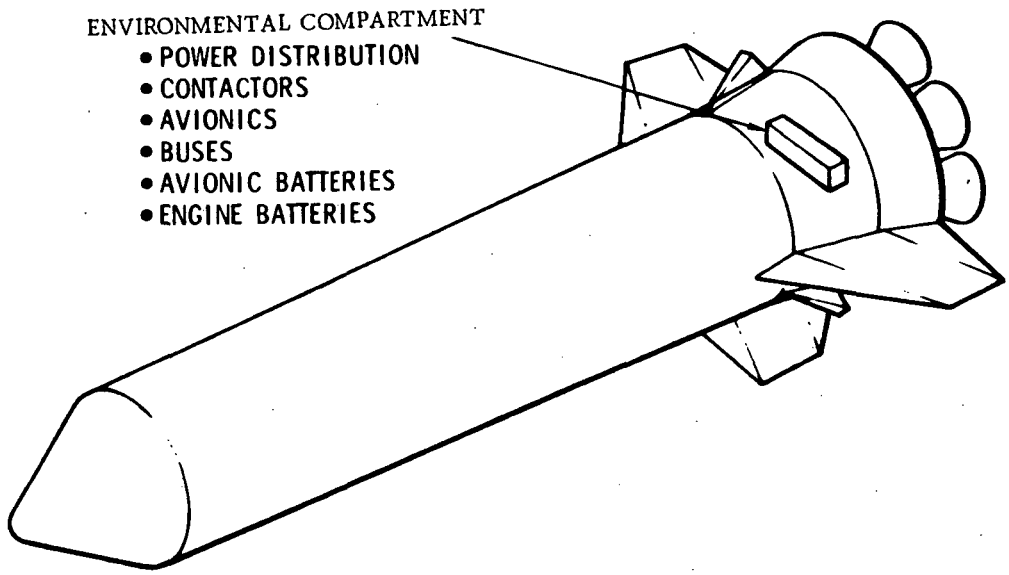

Figure 4-404. Booster (Pressure-Fed) Avionic Equipment Location

The instrumentation subsystem performs the function of gathering data for subsequent analysis. Certain selected data are to be displayed and the balance is recorded and/or telemetered. Maintaining the same basic instrumentation concepts developed for the reusable booster and the orbiter, it uses the same building blocks where similar functions are performed. Separate batteries are provided for the instrumentation system to provide isolation from operational hardware which is being monitored.

The recovery sequencer will provide the necessary sensors, logic, and drivers to control the fins, drag flaps, and parachute release. The emergency detection system gathers certain critical parameters and transfers them to the orbiter for display and action.

The basic redundancy level concept is fail-safe for critical items. The hardware assembly level at which redundancy is applied is generally the functional loop. The details of applying the redundant elements -- whether, for example, switching after self-test or after comparison, are undetermined.

A Phase B prime redundancy study has determined that fail-safe is more cost effective than fail-operational/fail safe. Fail-safe is defined as that condition in which the most critical failure will leave the vehicle in a safe condition, meaning that the vehicle can return to a water landing and land without major damage.

Electric Power

The primary electric power source consists of two electrically independent, redundant battery groups to eliminate voltage transient interaction between avionic/vehicle loads and the main propulsion subsystem loads. Two batteries operating in parallel are supplied for each application to provide fail-safe operation. Under normal conditions the batteries share load equally. In the event of failure, usually cell short circuiting, a reverse current sensing element in each battery line contactor will operate to remove the failed battery, thereby protecting the redundant battery. The reverse current contactor, located within the main dc bus enclosure also provides protection against battery feeder faults endangering the single main bus. See Figure 4-405.

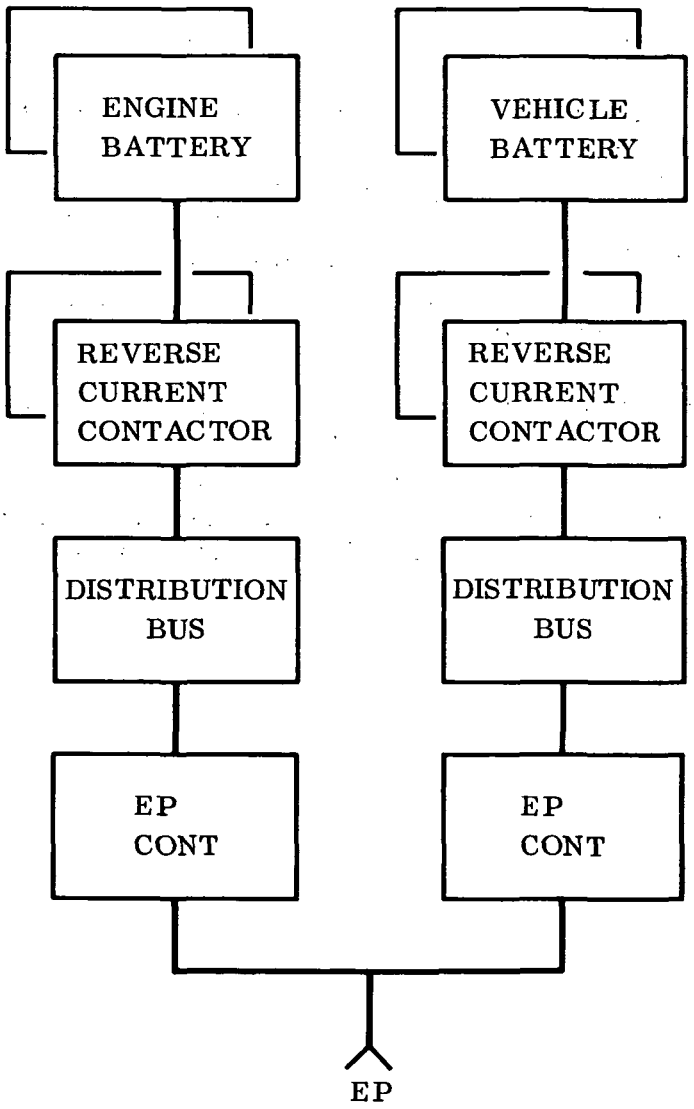

Figure 4-405. Electric Power

Developed, qualified battery systems will be employed that have had previous application in space programs. Requirements for additional capacity may be readily accommodated by adding modular battery units.

Distribution circuits to the utilization equipment are located primarily in the aft area. Circuit protection for wiring is not required for the majority of the loads. Since redundant loads are operated at all times, switching is not required for load management or reconfiguration. All utilization equipment identified operates from direct current power, making converters unnecessary and thereby increasing the utilization efficiency of battery energy and increasing system reliability.

A dc external power receptacle and contactor provides the facility for servicing and checkout.

Mechanical Systems

Separation. The relationship of the orbiter to the booster and location of the interstage interface is shown in Figure 4-406. The axial load in reacted in the booster through a continuous ring located at the separation interface. This provides for a distributed load path in both the booster nose and interstage adapter. Ten dual pyrotechnic bolts equally spaced around the ring secure the orbiter to the booster. Tension, shear, and torque loads are reacted through these bolts.

Although separation performance was not evaluated for this configuration, it is expected that the characteristics and pertinent parameters to be investigated will be similar to that discussed in Section 4.4.5. Emphasis will be placed on defining a system which requires only one separation plane, and in which the necessary interstage adapter is recovered as part of the pressure fed booster.

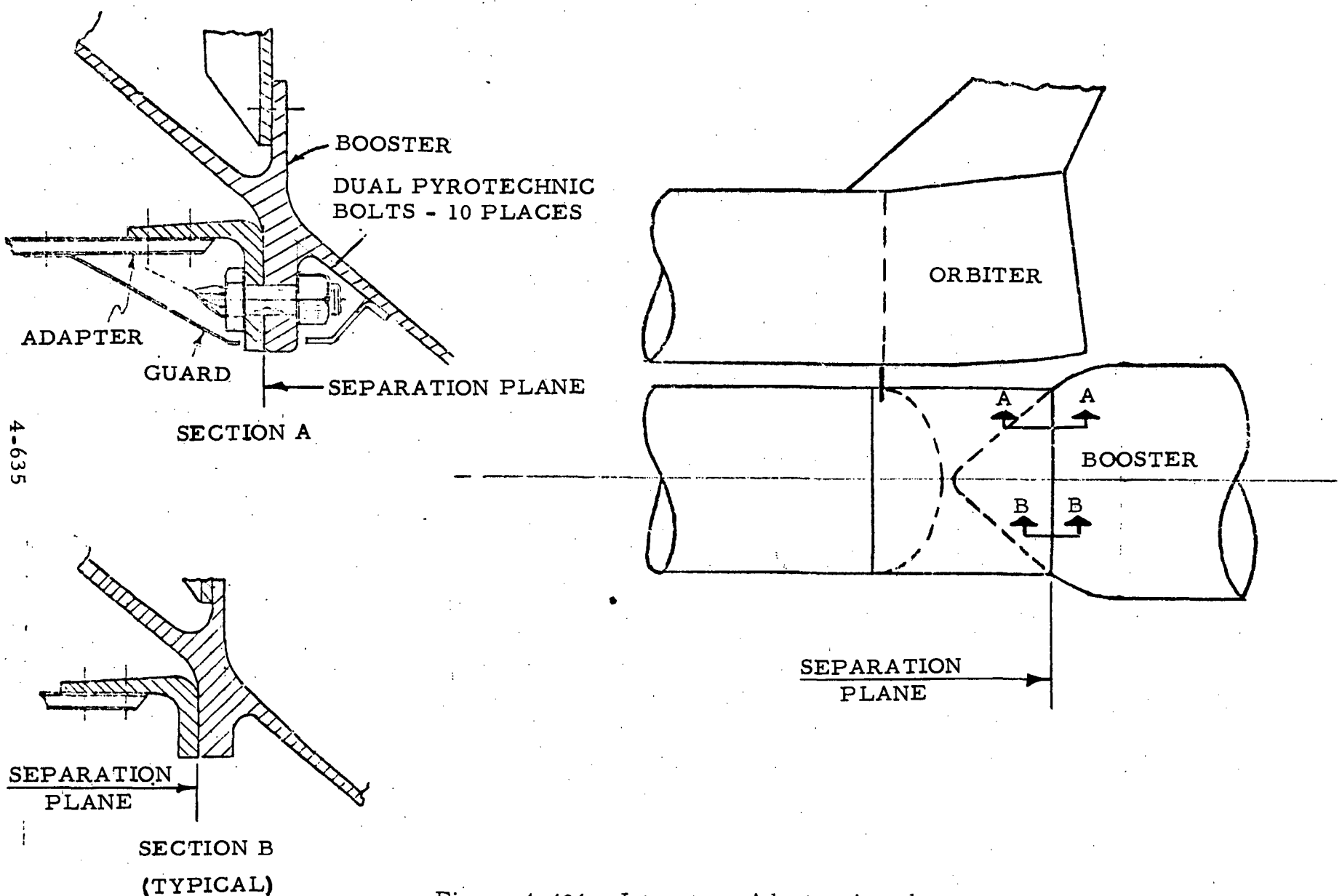

Figure 4-406. Interstage Adapter Attachment

Recovery System

The recovery system consists of four major design elements: (1) deployable high speed drag skirts integrated with the booster skirt/thrust ring and hold-down structure, (2) deceleration parachute system in sealed canisters on periphery of booster base bulkhead, (3) shock absorbing nose cone for water impact; and (4) recovery system attachment hooks for booster retrieval.

1. Drag Skirts. The drag skirts are deployed after stage separation at trajectory apogee. The skirts are extended by pneumatic cylinders and mechanical toggle linkages and remain deployed throughout the recovery sequence. The base drag area is increased from 1132 ft^2 to 1399 ft^2 with deployment.

2. Deceleration Parachutes. The parachute system is comprised of three identical clustered elements consisting of (1) canister with integral cover ejector, (2) pilot chute, (3) FIST ribbon drogue chute, (4) flat circular main chute with reefing provisions, and (5) structural attachments including drogue and main latching mechanisms and reefing cutters. Figures 4-407 and 4-408 depict the installation elements and deployment sequence.

   a. Canister. The canister is a sealed sheet metal cylinder with equally spaced ballistic ejectors for its cover assembly. A suspension line tray and fairing provide controlled routing from the canister to the structural attachment area.

   b. Pilot chute. The pilot chute and sleeve is pulled from the canister by the ballistic ejection sequence of the canister cover. The sequence is initiated by altitude q sensors adjacent to the canisters.

   c. FIST ribbon drogue. The drogue chute is a conventional 48 ft diameter FIST ribbon design which is sleeve deployed from the canister by the pilot chute. Structural attachment to the booster is via its suspension lines and "D" ring latch mechanism.

   d. Flat circular main. The main parachute is a conventional 105 ft diameter flat circular design with 50% reefing provisions for load and deceleration programming. The main chute is deployed in its bag upon drogue suspension release with initial filling in its reefed position. After an eight-second delay, actuation of the reefing cutters permit controlled, full diameter filling of the three chute cluster. Structural

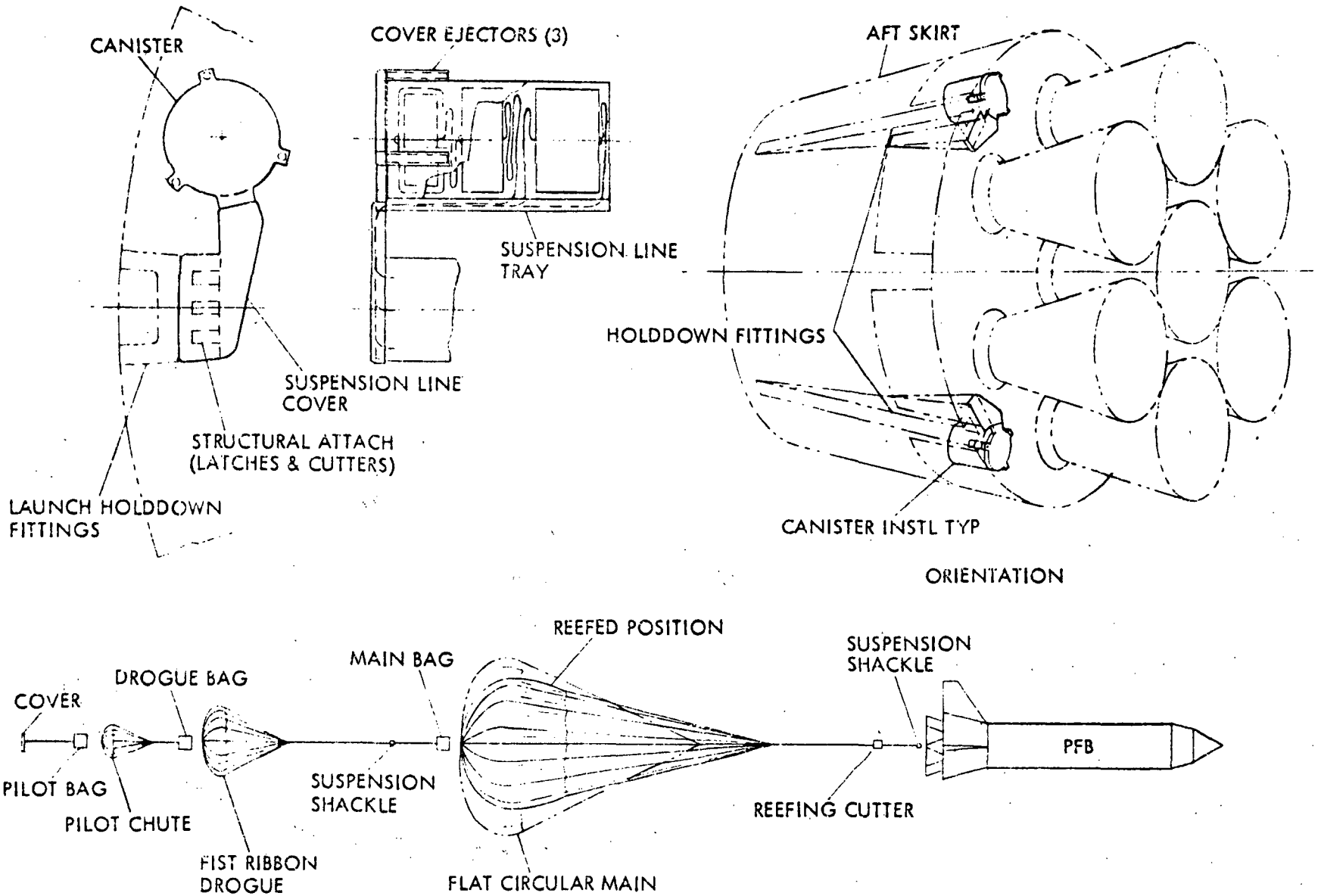

Figure 4-407. Recovery System

"Page missing from available version"

attachment to the booster is via its suspension and reefing lines, the reefing cutter, and the D ring latching mechanism. Chute release is scheduled for missile splashdown.

e. Structural attachments. The main and drogue chutes are structurally attached to the booster via a ballistically actuated latch mechanism integrated into the launch pad hold-down structure. Standard reefing cutters are located adjacent to the latch mechanisms.

3. Nosecone. The shock absorbing nosecone that cushions the initial water impact is shown above, where the trajectories, accelerations, loads and stresses induced during water impact and immersion are discussed.

4. Recovery System. The water retrieval/recovery systems and booster attachment devices also are discussed above.

Mass Properties

Table 4-78 is a weight breakdown for the pressure-fed booster. Propellants are O_2 and C_3H_8. The weights were scaled to the proper vehicle size by using a synthesis computer program. A growth allowance of 10% on dry weight items, excluding ascent engines, is included. Table 4-79 shows c.g. and moments of inertia for lift-off and burnout conditions.

Table 4-78. Pressure-Fed Booster Weight Statement

		WEIGHT (LB)
AERODYNAMIC SURFACES (FINS)		15,320
BODY		300,980
FUEL TANK	98,200	
OXIDIZER TANK	155,100	
AFT SKIRT	11,060	
THRUST STRUCTURE	33,220	
BASE HEAT PROTECTION	3,400	
RECOVERY PARACHUTES		2,990
PROPULSION, ASCENT		126,590
ENGINES	63,170	
PU SYSTEM	750	
PRESSURANT SYSTEM (DRY)	53,200	
PROPELLANT SYSTEMS	9,470	
POWER SOURCES		700
ELECTRICAL CONTROL & DISTR.		426
AVIONICS		1,114
ENVIRONMENTAL CONTROL		300
GROWTH ALLOWANCE (10%, EXCL. ENG.)		38,561
DRY WEIGHT		486,981
RESIDUALS		36,185
PRESSURANT	19,400	
PROPELLANT	16,785	
ICE AND FROST		500
TVC OXIDIZER REQUIREMENT		62,468
ASCENT PROPELLANTS		3,612,000
GROSS LIFT-OFF WEIGHT		4,198,134

Table 4-79. Mass Properties Data

	WEIGHT (LB)	X C.G. (1)	Z C.G. (2)	SLUG $FT^2 \times 10^{-6}$		
				I_{XX}	I_{YY}	I_{ZZ}
LIFTOFF	4198134	1878	400	12.37	177.2	177.2
BURNOUT	523166	2116	400	2.135	39.96	39.95

(1) NOSE = 1000, + AFT

(2) TANK $\mathbb{C}_L$ = 400, + UP

Manufacturing

The principal booster components and their sequence of assembly are shown in Figure 4-409. The plan reflects an analysis of design requirements, material availability, fabrication procedures, tooling, and facility requirements. Use of conventional fabrication procedures, standard tooling, and available facilities has been emphasized.

Tank bulkheads, cylindrical sections, and propellant ducts will be fabricated from annealed alloy 718 plate. Detail parts will be milled to produce weld lands, where required, formed, trimmed, fitted and welded together to form subassemblies which will then be heat treated. Special tooling will be provided to form, trim, and assemble the parts. A special aging furnace will be required to heat treat the welded subassemblies. Bulkheads and cylindrical sections will be progressively joined together to form the propellant tanks. Tanks will be assembled in the horizontal attitude. Special tooling rings on the tank together with standard weld positioning equipment will provide means for rotating the tank during welding operations. A postweld heat treatment of the circumferential weld joints will be accomplished at this point using portable strip type heater, age oven or combination of both. Tank assembly is planned for existing factory area at the NASA Michoud facility. Following weld assembly the tanks will be hydrostatically proof tested, cleaned, and leak tested using existing facilities at Michoud.

Thrust structure skin panels, frames, rings, and special fittings will also be fabricated from annealed alloy 718 plate. Detail parts will be heat treated (aged) after the thrust structure and base heat shield have been assembled and match mated to each other and to the tank assembly. This will require an added disassembly and reassembly operation for the thrust structure but will permit the major portion of the final fitup and drilling of attach hole to be performed with material in the annealed condition, which will simplify these tasks. Structural assembly operations will be accomplished with the thrust structure in the vertical attitude to simplify tooling.

The base heat shield will consist of skin panels, frame rings, stiffeners and heat shield panels. Type of material has not been determined. The heat shield will be assembled and mated to the thrust structure prior to mating the thrust structure to the tank. This will reduce the task at the final assembly level. The heat shield will be assembled in the vertical attitude to simplify tooling and handling.

The thrust structure will be mated to the tank assembly with the tank horizontal. Final assembly operations including installation of engines and related systems, drag skirts and actuators, fins, recovery chutes, etc., will also be accomplished with the tank horizontal to minimize handling. The nose cone will be installed concurrent with final assembly operations.

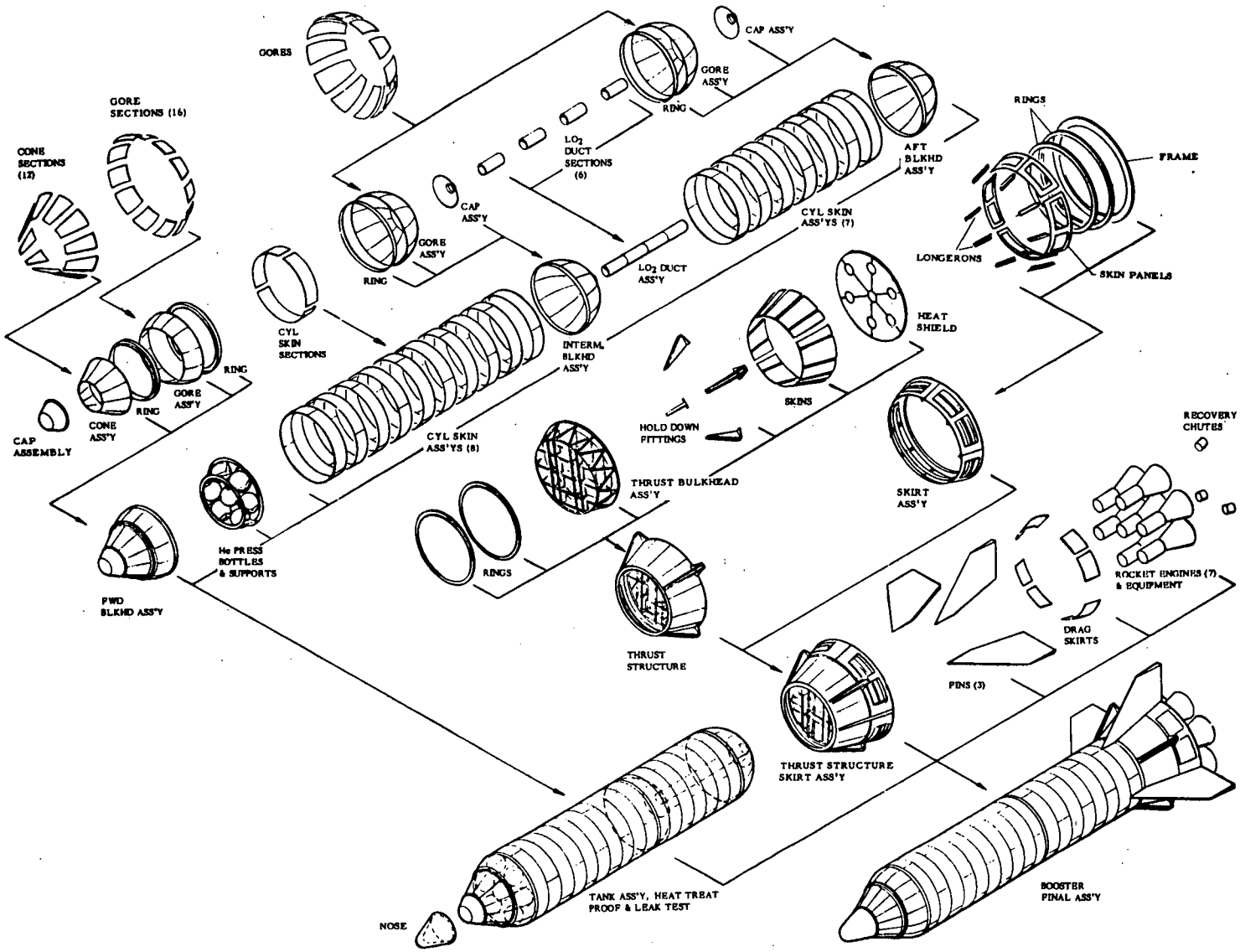

Figure 4-409. Manufacturing Breakdown and Assembly Sequence for Pressure-Fed Booster Vehicle B-19

Following final assembly, checkout, and acceptance of the booster, the fins will be removed and the booster will be barge shipped to the launch site where the fins will be reinstalled prior to prelaunch checkout.

GSE and Facilities

Facilities

Vehicle Assembly Building. A concept for using the existing VAB to support the pressure-fed booster is shown in Figures 4-410 and 4-411. The only structural alterations required will be the widening of the doors at each end of the transfer aisle, widening the vertical doors in the high bay, and the addition of a 350 ton crane (instead of the existing 250 ton crane). The transfer aisle crane is used in conjunction with the HB-1 and HB-2 350-ton crane to make the horizontal to vertical transition of the mated orbiter/tank. Vertical high bay doors will be modified to allow passage of the payload change out modules on the service tower of the mobile launcher.

Launch Site. The concept for using launch complex 39A for the pressure-fed booster requires no changes to the existing facility. All structural hard points for the mobile launcher will be used without alterations. The flame deflector, deluge system, etc., will be used as is. The launch pad configuration for the pressure-fed booster is shown in Figure 4-412.

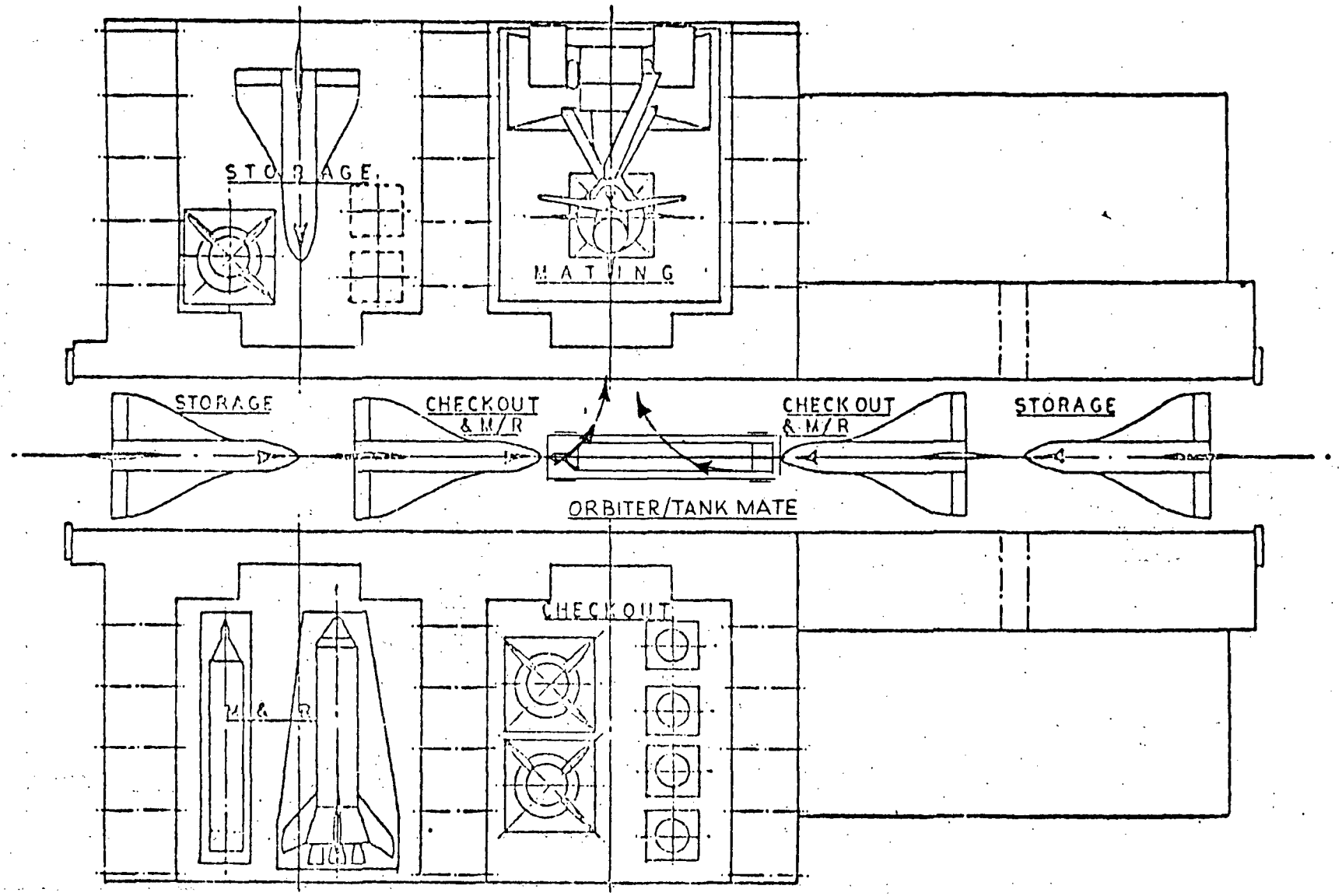

Figure 4-410. Pressure Fed Booster VAB Floor Plan

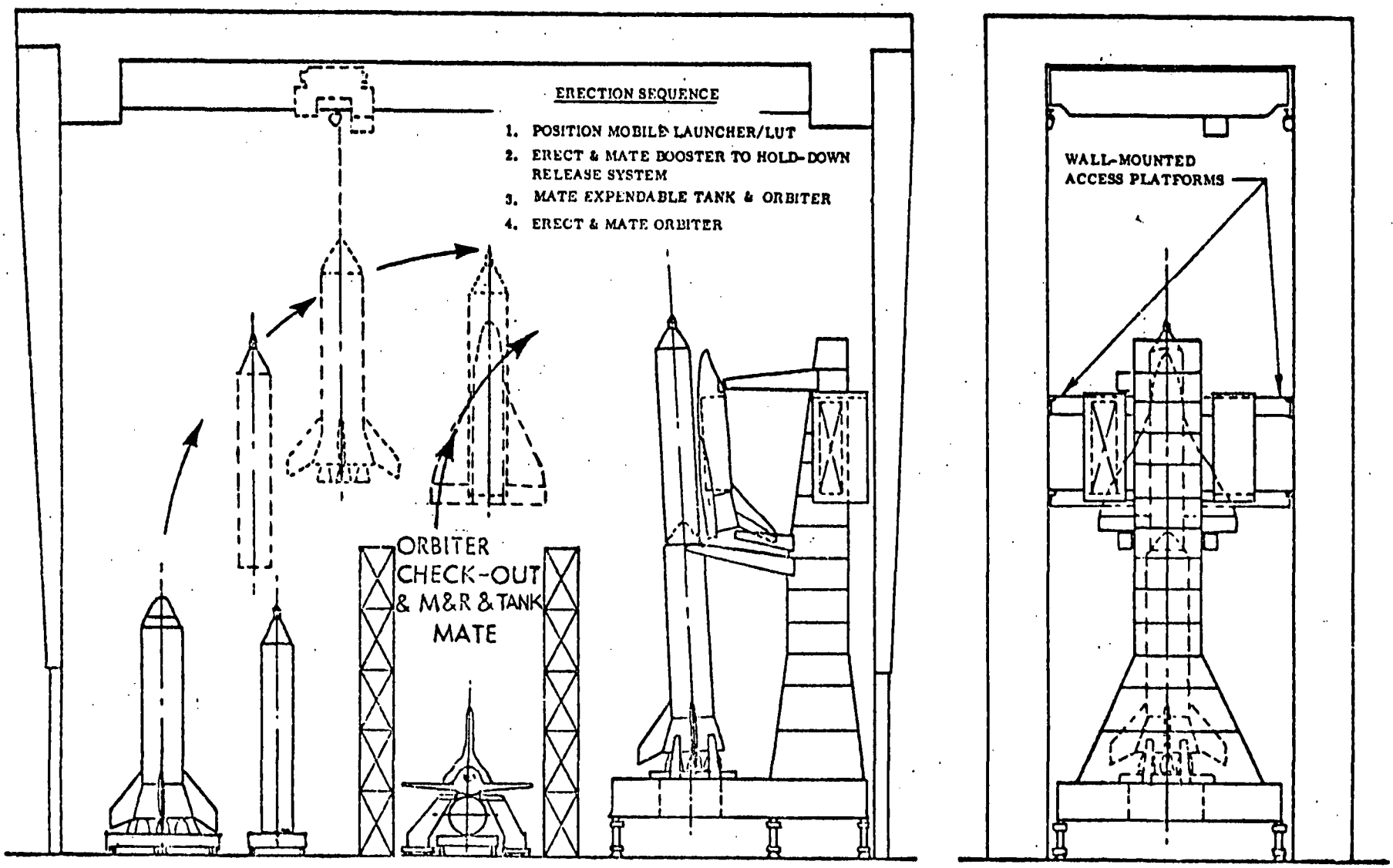

Figure 4-411. Pressure Fed Booster VAB Vertical Erection and Mate

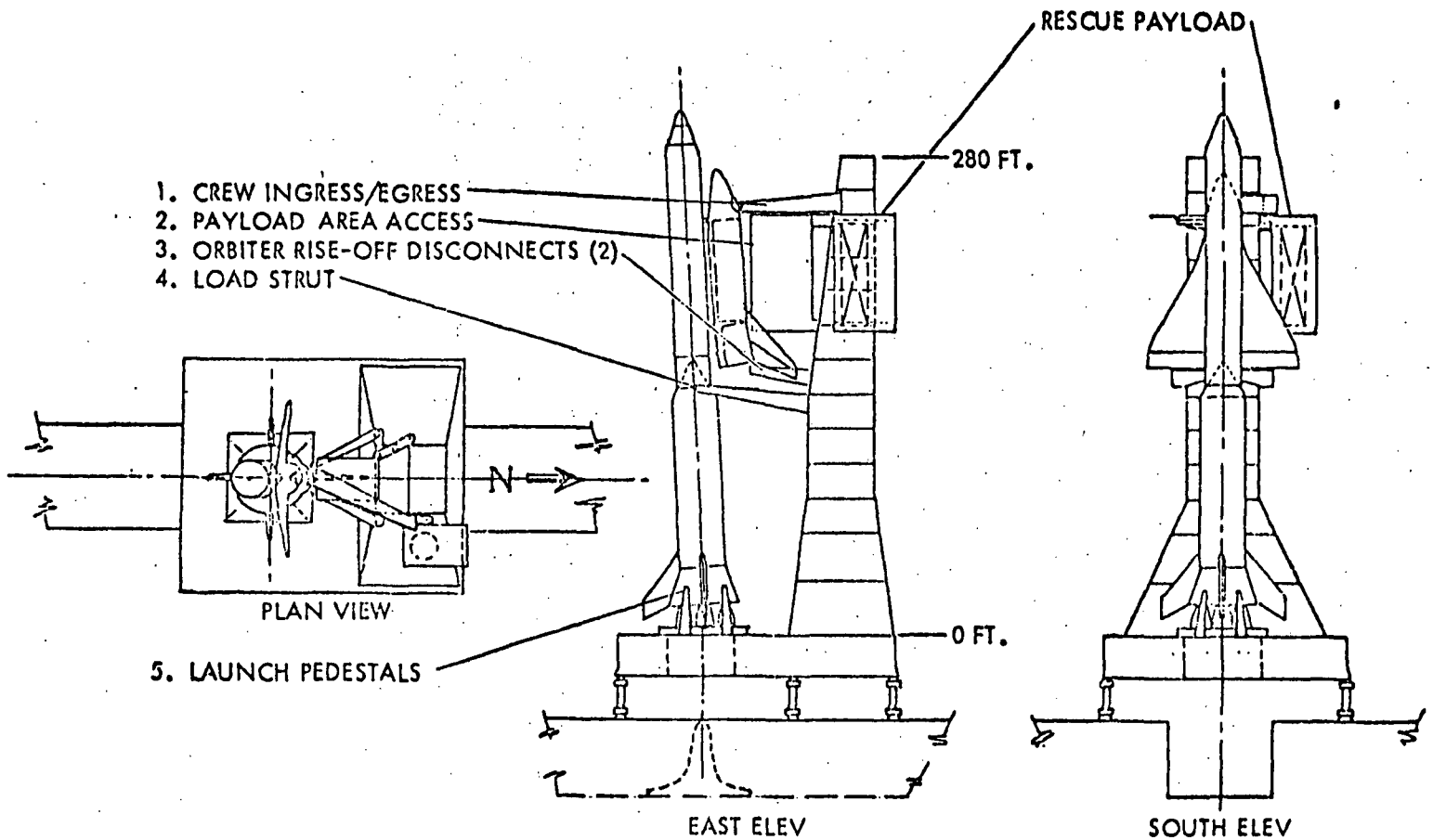

Figure 4-412. Pressure-Fed Booster Launch Pad Configuration

Mechanical GSE

Mobile Launcher/LUT. Minor changes are required to the existing mobile launcher/LUT. The launch pedestals and its main structural support will be added to the existing launcher. The required swing-arms and payload handling equipment will be added as shown in Figures 4-412 and 4-413. Lift-off drift clearance will be provided by scarfing back the upper inside face of the service tower.

Holddown and Release System. A new holddown and release system will be required for the pressure-fed booster. This system is essentially the same as that required for the LO_2-RP booster (F-1 Flyback).

Recovery. The recovery at sea method recommended for the pressure-fed booster is Method B(shown in Figures 4-414 and 4-415 and Table 4-80). This system requires a minimum size "fleet" for recovery and provides the fastest return to base. The barge unloading area at the VAB will require the addition of two 175 ton shore based cranes to lift the booster from the water onto a transporter (not illustrated).

Booster/Orbiter Access Service Arms. As access service arm will be used for ingress and egress of the orbiter crew compartment. This arm will also form an integral part of the emergency egress system which is shown in Figure 4-416.

Riseoff Disconnect Panels. Riseoff disconnect umbilical panels will permit the ground half of the umbilical disconnects to separate axially as a result of vehicle first motion. Booster panels will be located in the launcher/vehicle support structure and the orbiter panels will be located at the end of in-flight service arms which are retracted at vehicle first motion.

Stabilization System. A stabilization system is required to stabilize the launch vehicle during movement from the VAB to the launch pad and during periods of high wind conditions while the vehicle is located at the launch pad. The system will consist of forward attachment of a Saturn V type damper strut mechanism to the forward end of the orbiter external propellant tank.

Servicing GSE. The servicing ground support systems for the pressure-fed booster will be essentially the same as that for the LO_2-RP booster shown in Figure 4-363.

Electrical/Electronic GSE

Launch Operations. The ground checkout system and propellant loading system are the same as described for LO_2-RP booster.

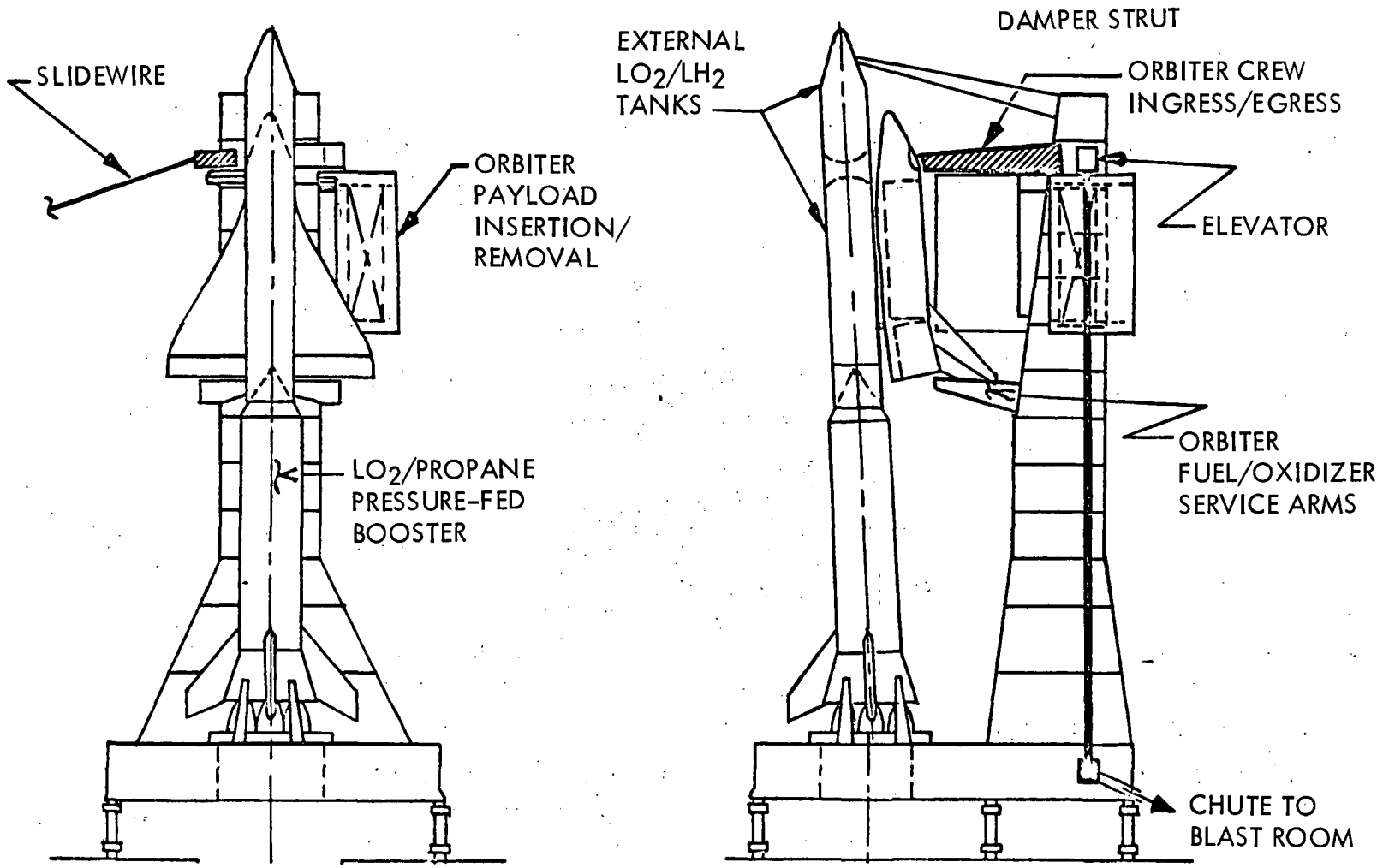

Figure 4-413. LO_2/Propane Pressure-Fed Launch Configuration

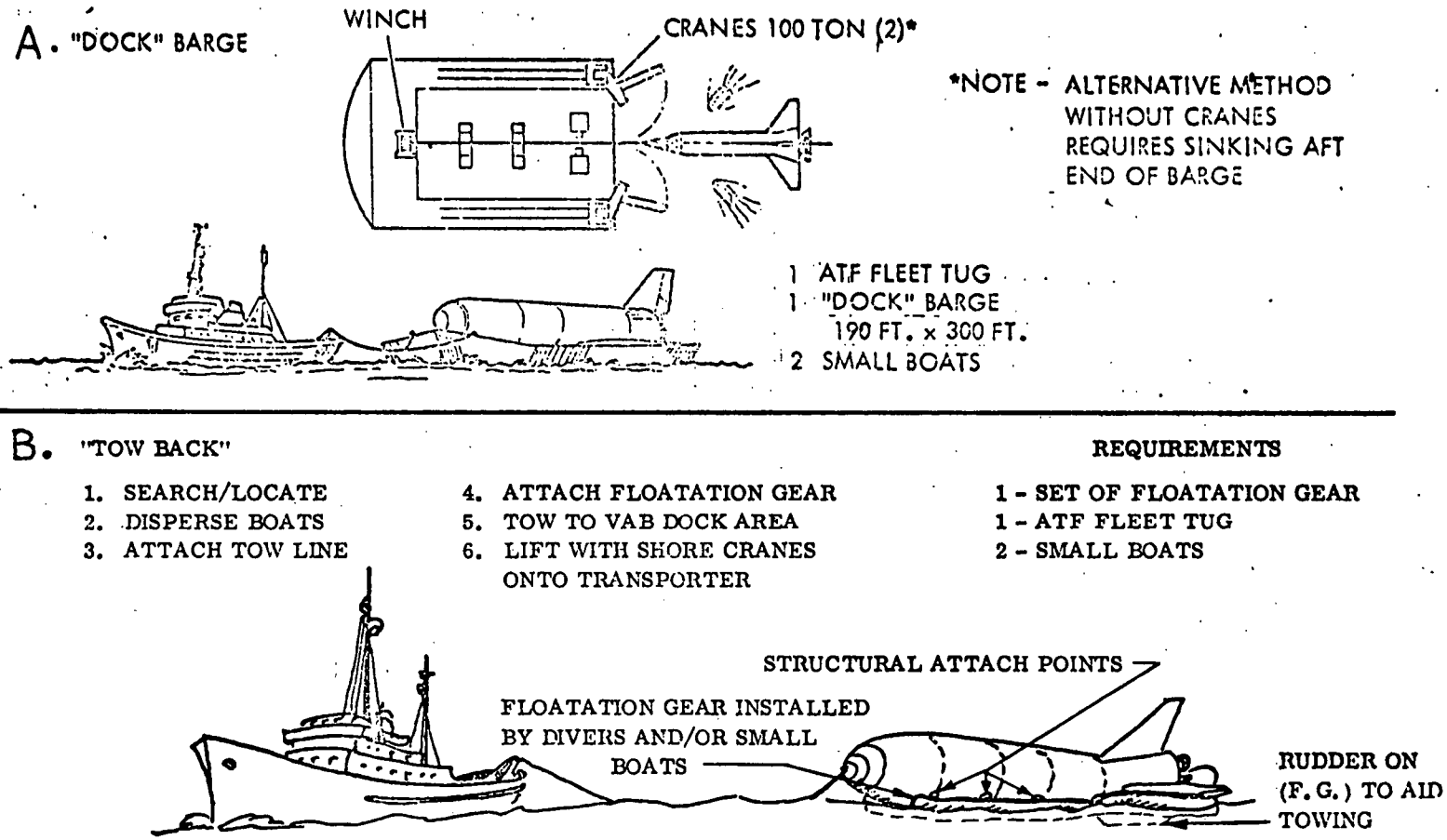

Figure 4-414. Pressure-Fed Booster - Recovery Concepts

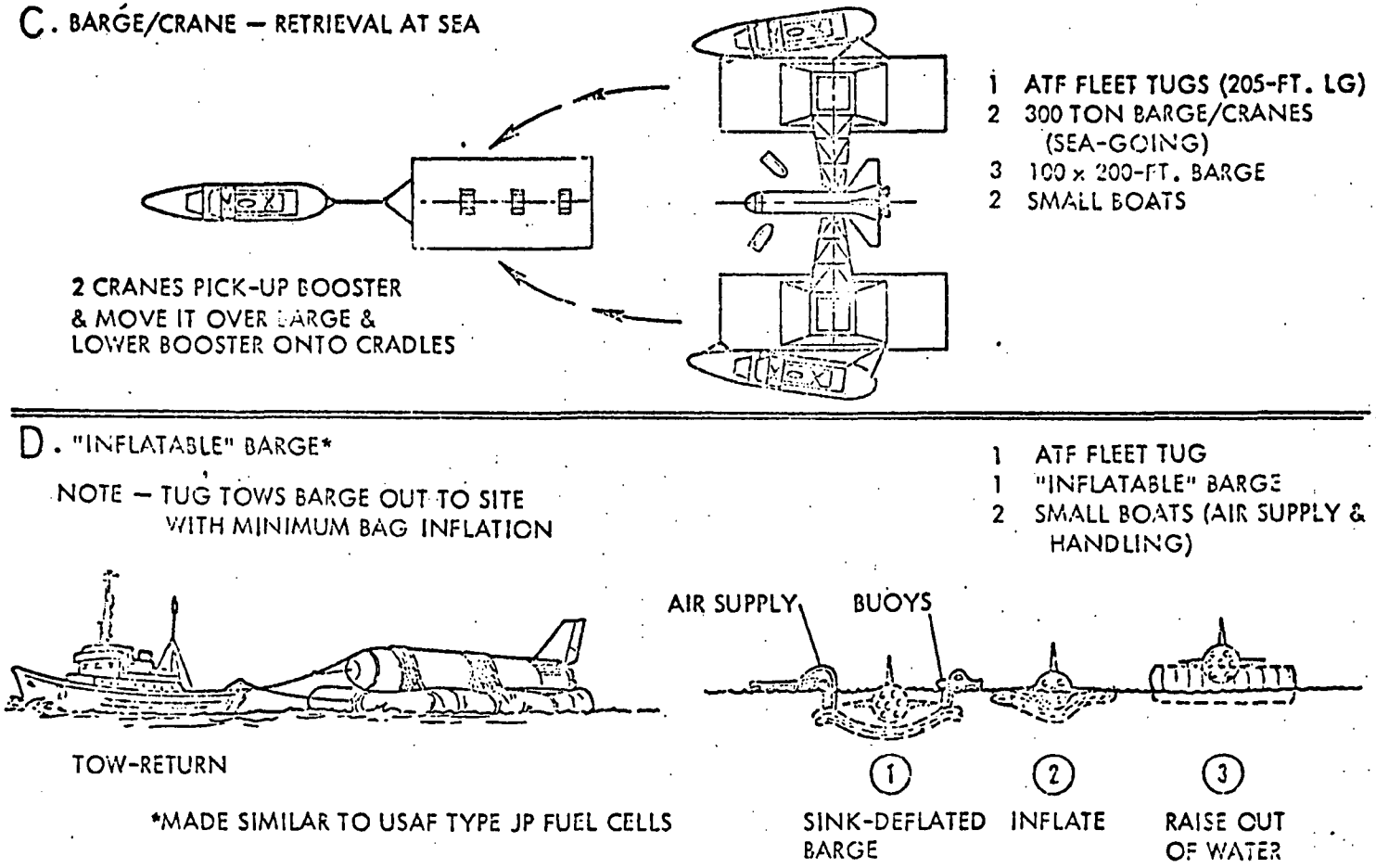

Figure 4-415. Pressure-Fed Booster Recovery Concepts

Table 4-80. Pressure-Fed Booster - Recovery Concepts

	ADVANTAGES	DISADVANTAGES
METHOD A DOCK BARGE	• STRETCHED STANDARD DESIGN BARGE • USES STANDARD EQUIPMENT	• HIGH-COST SPECIAL BARGE SIZE • DIFFICULT TO USE IN ROUGH SEA • MAY DAMAGE BOOSTER ENTERING DOCK IN ROUGH SEA
METHOD B "TOW BACK"	• MINIMUM CREW & NO SPECIAL EQUIPMENT • FASTEST RETURN	• BOOSTER IS IN "SEA" ENVIRONMENT 2 TO 3 DAYS
METHOD C BARGE/CRANE	• STANDARD TYPE EQUIPMENT	• HIGH RISK WITH LARGE CRANES AT SEA • HIGH-COST OPERATION (3 TUGS) • DIFFICULT TO SET BOOSTER DOWN "EASILY"
METHOD D INFLATABLE BARGE	• MINIMUM EQUIPMENT (NO ENGINES, CRANES, PUMPS, ETC.), JUST AIR BOTTLES • MINIMUM LIKELY DAMAGE TO BOOSTER	• NONSTANDARD APPROACH • HIGH FIRST COST BARGE

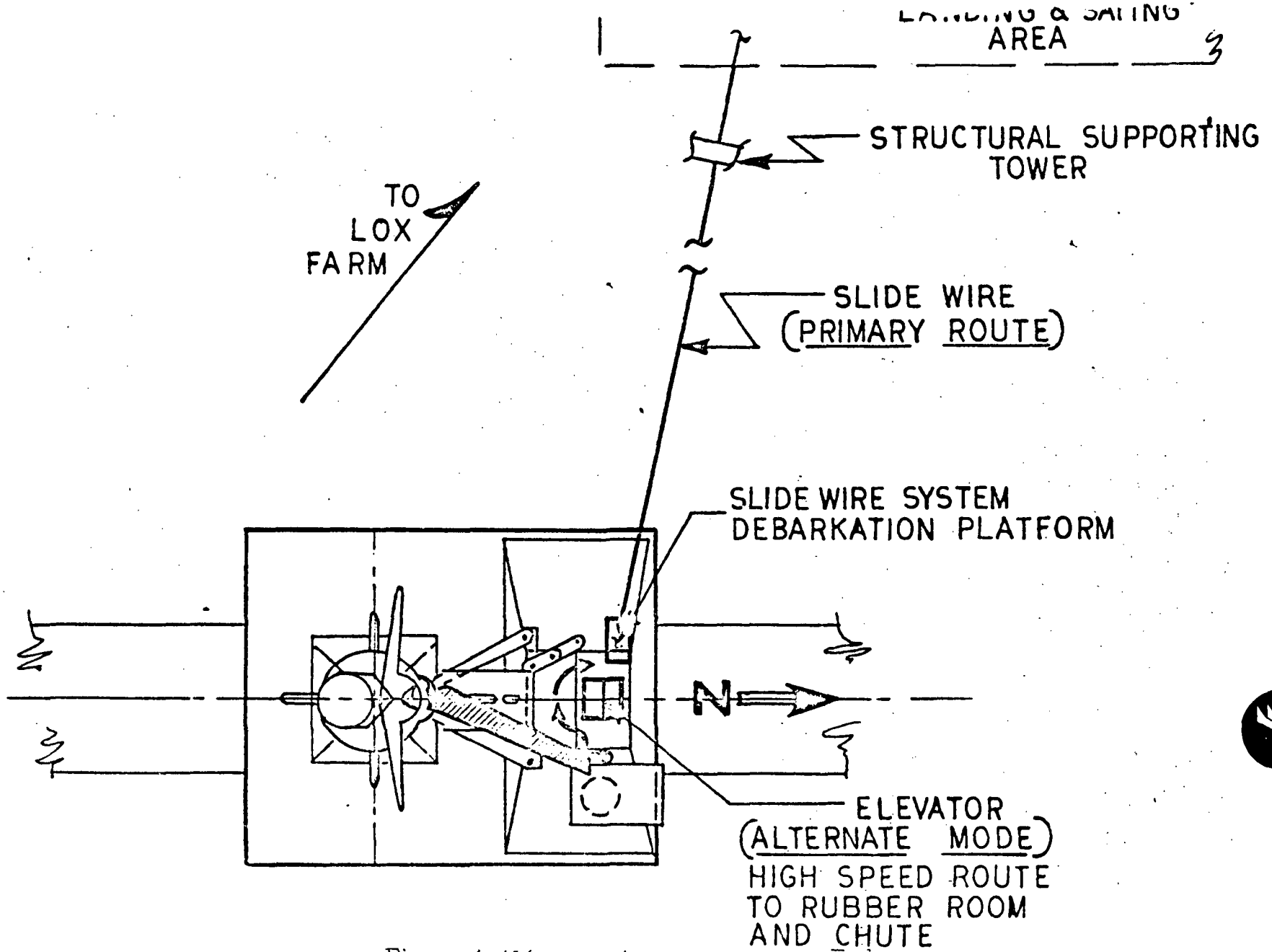

Figure 4-416. LO_2/Propane, Pressure Fed

A voice communications link is not required with the booster, but a hardwire data link back to the LCC will be provided.

The vehicle tracking beacon is activated by C-band ground interrogators located on the Florida main land and tracking ships.

The vehicle recovery beacon signal is located and monitored by UHF-ADF receivers on the recovery aircraft and ships.

Level I Maintenance. Ground checkout system (same type as used for launch operations).

Level II Maintenance. Same as described for the LO_2-RP (F-1 Flyback) booster.

Manufacturing. Vehicle simulator not required. Automatic circuit analyzer required for wire harness checkout.

Test

The overall objectives of the pressure-fed booster test program are (1) to assist in developing design concepts, (2) to certify by analysis and ground test and verify by flight test as required, and (3) to provide data for space shuttle vehicles, support equipment, and software acceptance.

The major development test programs for the reusable pressure-fed booster will be the certification of the body structure, the propellant pressurization and propulsion systems, and the recovery operations. Certification of the tankage structure will be accomplished by proof test, pressure cycling to four times, plus ultimate pressure test with mechanical loads being applied. Combined static/fatigue tests will be run on the thrust structure, fins, drag flaps, and interstage adapter. The pressurization system tests will be performed on a set of stub tanks using flight type heat exchangers, reaction beds, storage bottles, and propellant utilization system. A propulsion test vehicle will be used to qualify the main propulsion system in a series of propellant tankings and engine cluster firing tests. Development and certification of the booster recovery system will be accomplished on five of the expendable vehicles during actual flights. Water recovery techniques and procedures will also be verified. The test plan summary, Figure 4-417, shows the major test programs planned for the pressure-fed booster. Multi-use of test articles and existing facilities will be considered for cost reduction.

The flight test development vehicles will be instrumented to provide flight data on structural loads, thermodynamic and dynamic data, propulsion performance, and separation. One booster, dynamically ballasted to the mated lift-off weights, will be launched to verify the total system. If flight data indicate a successful launch and separation, the system will be considered man-rated.

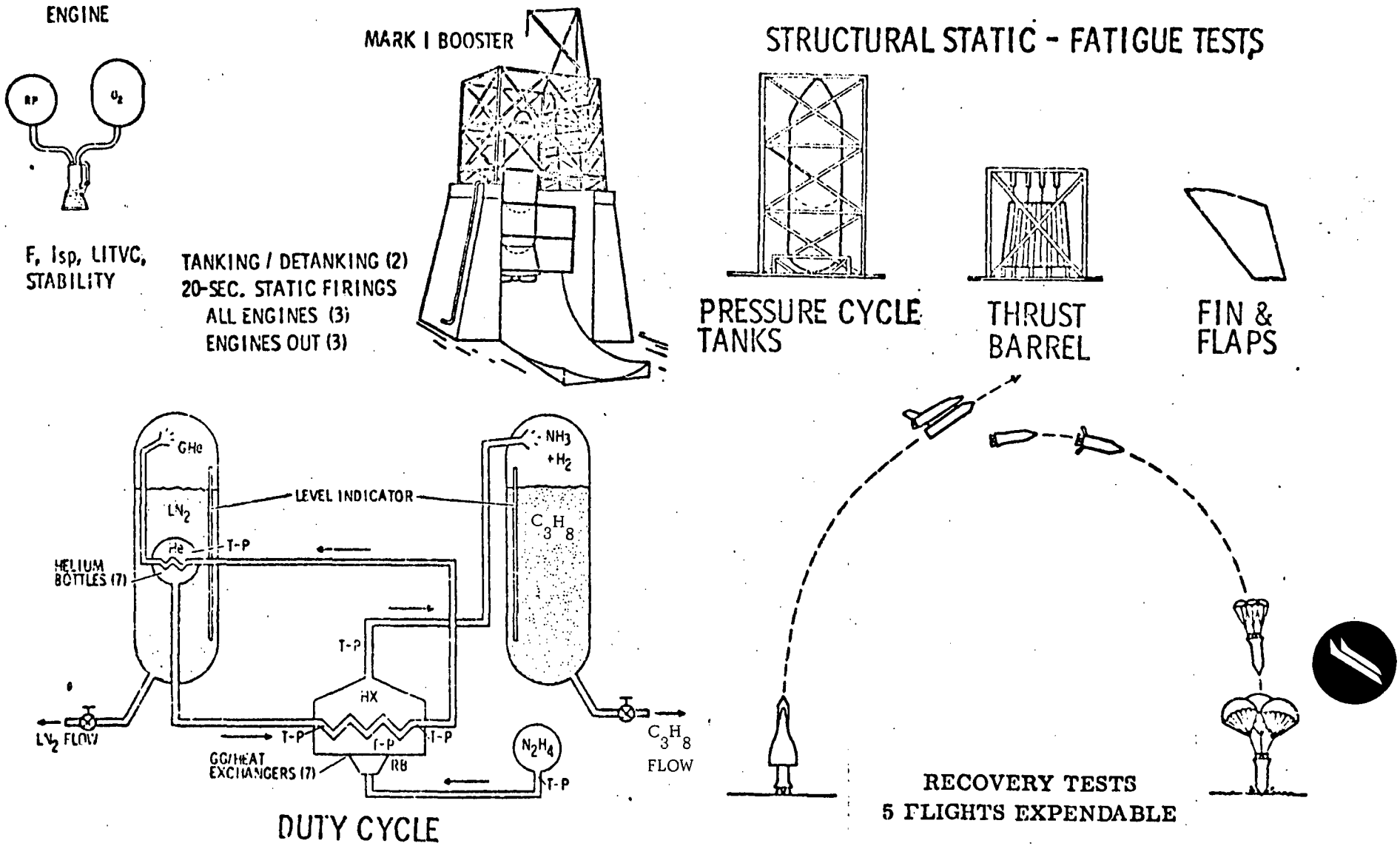

Figure 4-417. Pressure-Fed Booster Test Summary

4.4.7 Flight Test Operations

4.4.7.1 Orbiter

Horizontal-Flight-Test Program. A reassessment of the Phase B horizontal-flight-test program was initiated as a part of the Phase B' study plan. Several factors contributed to this assessment:

1. Evaluation of reduced subsystems in the orbiter to reduce peak funding

2. Configuration changes created to the vehicle as a result of Phase B' redirection.

3. Additional analysis of the flight hours required to accomplish testing identified during Phase B

The approach used for the assessment is presented as Figure 4-418 and is:

1. Review and update the flight test requirements and establish the flight time needed to attain those requirements.

2. Study aspects of the program that dictate flight rate and establish a realistic prediction concerning test flight rate.

3. Through an in-depth analysis of the tests to be performed and applying the effective use of the capability for air-to-air refueling (AAR), establish the total number of flights required.

4. By applying flight rate and total flights, determine the calendar time required to complete the horizontal-flight-test program.

The configuration of the Mark I orbiter is presented as Figure 4-419. The configuration for horizontal flight test is presented as Figure 4-420.

Flight test hours for Phase B and B' are summarized in Table 4-81. Deltas to the Phase B baseline flight hours beyond those created by configuration changes were established as a result of a better appreciation of the testing required to verify the test points that establish the parameters which define the airworthiness of the orbiter. It must be emphasized that the planned testing continues to be a success-oriented program that does not provide for multiple incremental test points to reach the extreme required flight condition. Rationale for the individual differences in flight time is presented in Table 4-82.

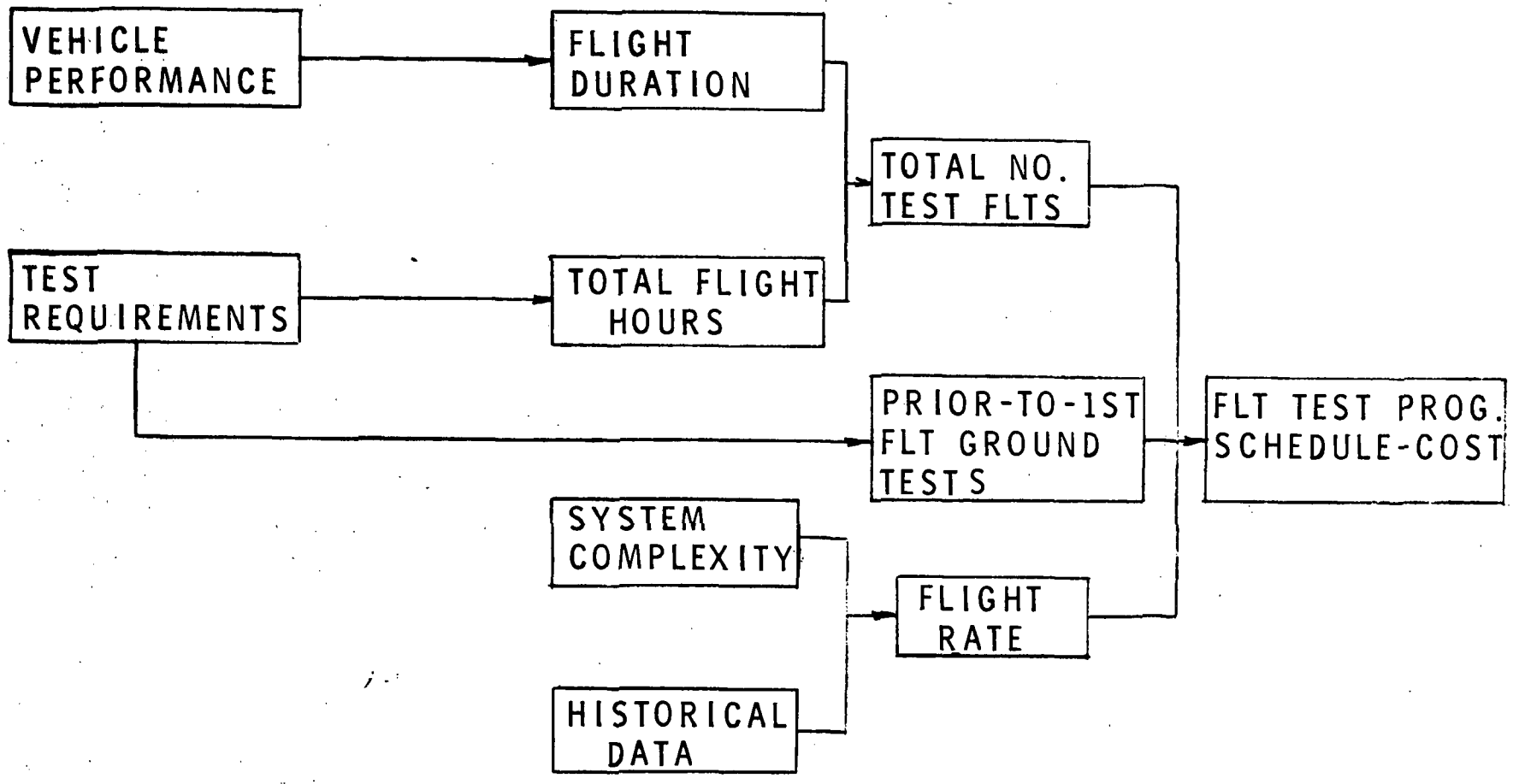

Figure 4-418. Horizontal Flight Test Program Elements

DELTA WING VEHICLE
EXTERNAL H_2O_2 TANKS
4 J2S MPS ENGINES
15 x 60 CARGO BAY
LEM ASCENT ENG'S - OMS
TPS
650 PSF DESIGN q

200K MI X RANGE
25K PAYLOAD DOWN
LOW COST AVIONICS
- UHF RADIO - S-BAND
- XPONDER - TACAN

ABES - 2 - CARGO BAY
ALUMINUM STRUCTURE
HYPERGOLIC ACPS
BODY SHAPE - MSC 040A

MONOPROPELLANT APU'S
H_2O_2 FUEL CELLS
3000 PSI HYDRO SYSTEM
AERO FLT. CONTROL SYS.
- CENTER STICK-MECHANIC TO POWER ACTUATOR
- PARALLEL STAB. AUG.
- FAIL SAFE TO MECHANICAL OR FLY BY WIRE

FERRY KIT
- 2 ADDITIONAL ABES
- FERRY FUEL TANK
- CARGO BAY DOORS
- ABES GEAR BOX
  - HYDRO
  - ELECT
- ECLS - VAPOR CYCLE HEAT SINK

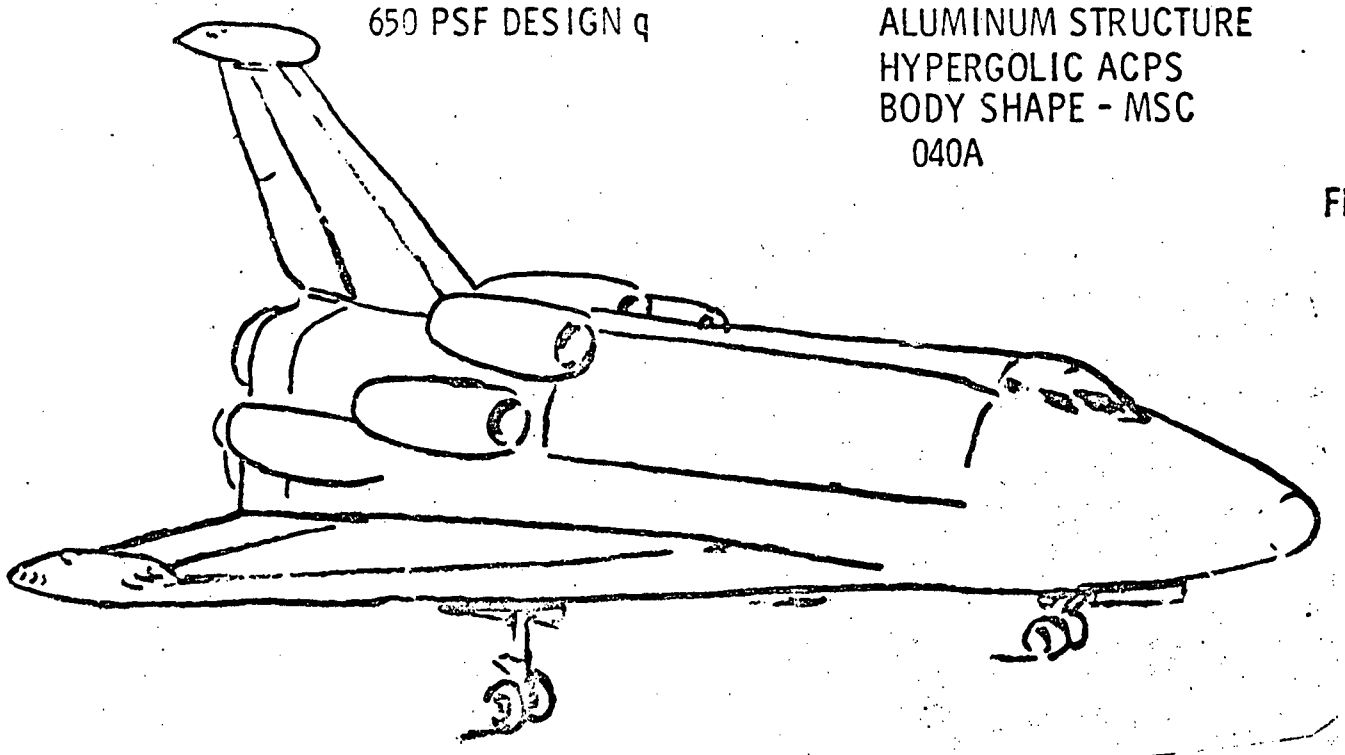

Figure 4-419. Mark I Orbiter Configuration

DELTA FROM BASELINE VEHICLE

ADDED	DELETED
DEV. FLT TEST INSTRUM.	TPS
TM	MPS ENGINES
GRND TRACK	ACPS
FERRY KIT	OMS
DUMMY MPS ENGINES	APU'S - FUEL CELLS
AIR-TO-AIR REFUELING	FOOD, H_2O & WASTE MGMT
EJECTION SEATS	MANIPULATOR ARMS
BALLAST	

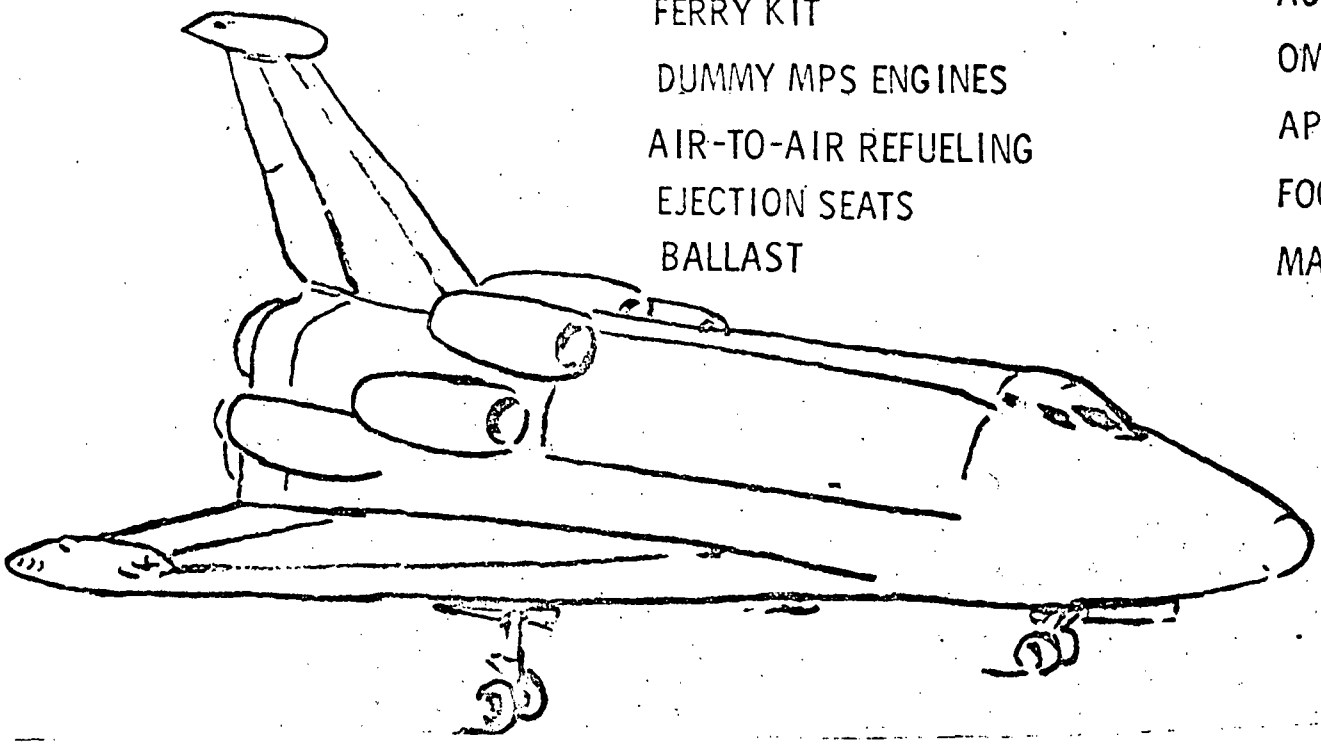

Figure 4-420. Mark I Orbiter Horizontal Flight Test Configuration

Table 4-81. Orbiter Horizontal Flight Test, Mark I

Test Objective	Estimated Developmental Flight Test Hours (Dedicated)	
	ØB'	ØB
Preliminary evaluation	20	
Stability and control	75	60
Air vehicle performance	20	20
ABES propulsion	29	10
GN&C-fly-by-wire, SAS, Tacan	33	45
Structures	28	17
Unpowered landings	10	2
Subsystems	20	25
Factor for malfunctions, retest, buildups, weather, etc., included	235	180
Air-to-air refuel	5	
Total	240	

In the flight duration analysis, the types of flights considered were—high fuel consumption, normal fuel consumption, and long-duration flight (AAR refueling). This analysis determined that approximately 35 percent of the flights could not effectively use refueling because of the nature of the tests. The remaining flights were extended by one refueling. The result was a total of 138 flights required. Historical data on test flight hours for several aircraft of varying complexity and performance were considered in establishing a predicted availability of the orbiter during the flight test phase. This flying time was considered to be compatible with ground turnaround requirements and results in an average of nine flights per month, which, in turn, identifies a need for 15.5 flight months.

An additional 1.5 months is included for vehicle modification or configuration updating for a total of 17 flight-test months. The 17 months, coupled with a preflight ground activity period of four months, results in a total time of 21 months. These data are included as Figure 4-421.

The flight test program is to be conducted at Edwards Air Force Base, California. Because the size of the orbiter has been reduced as a result of the external propellant tank, the vehicle can be moved over the highways if

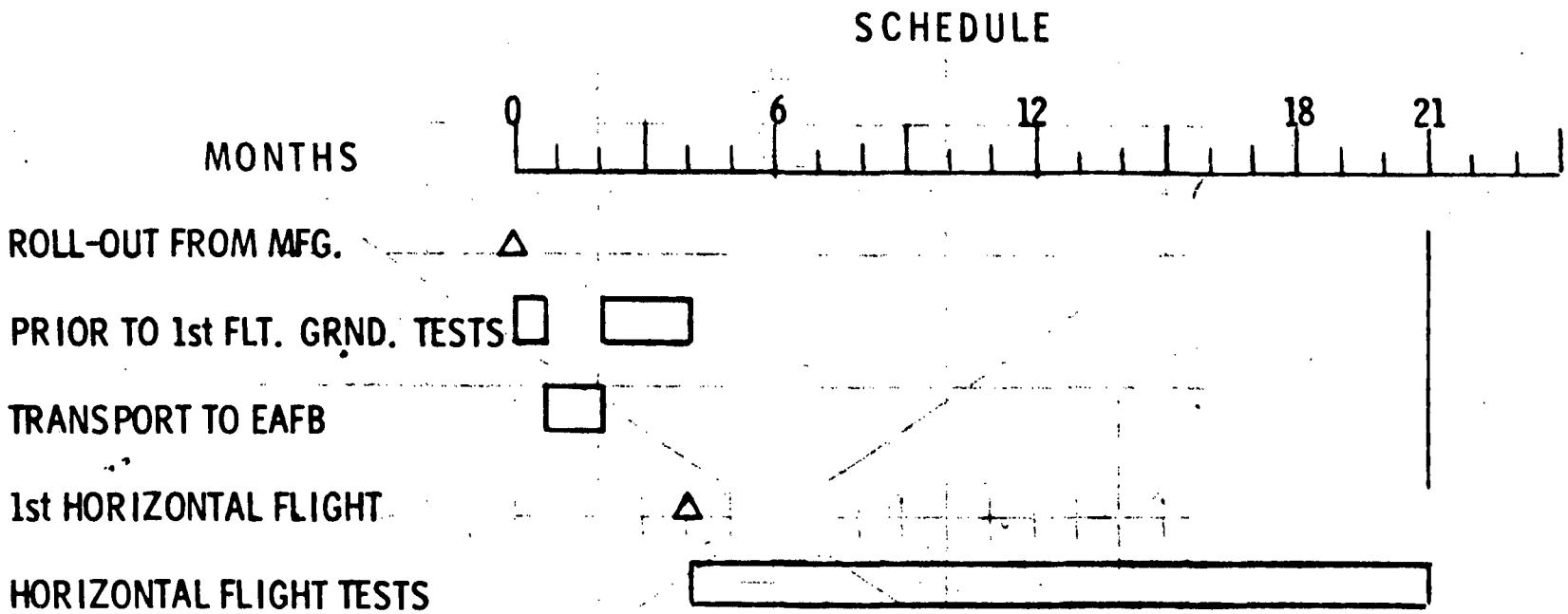

Figure 4-421. Mark I Orbiter Horizontal Flight Test Program

Table 4-82. Rationale for Phase B and B' Flight Test Hour Differences

Test	Hours	Reason
Preliminary evaluation	+20	Early verification in limited envelope to uncover any gross airworthiness problems
Stability and control	+15	Reassessment - Mil Spec 8785 supplemented by historical data
ABES propulsion	+19	Reassessment - Inadequate time allotted previously. Deployment, air starts, and inlet pressure recovery.
GN&C	-12	Inertial navigation, precision ranging, radar altimeter system deleted.
Structures	+11	Reassessment - Mil Spec 8871 added several maneuvers, better definition of structural test requirements
Unpowered landing	+8	Reassessment - Inadequate dedicated time allotted previously. More emphasis on technique and procedure developed for critical phase with only two engines.
Subsystems	-5	Reduced cabin pressure, hydraulic and electrical test requirements; transponder and VHF - FM deleted.

the wings and vertical stabilizer are removed. This has allowed deletion of the intermediate base, Pt. Mugu, and first flight of the orbiter is now scheduled for takeoff and landing at Edwards Air Force Base. The four-month ground activity includes 24 working days required to transport the vehicle from Seal Beach to Edwards and to reinstall the wings and vertical stabilizer before ground testing.

Vertical Flight Test. The vertical-flight-test program represents the final step in the overall development and demonstration of the shuttle system. This phase of the flight test activity extends the orbiter flight envelope to mated orbiter/booster launch operations through separation, flight through earth orbit injection, deorbit and entry, and final transition for the terminal subsonic flight and landing. Those requirements associated with hypersonic flight regime, performance under space environment, thermal control and protection during entry, and orbiter flight characteristics employing ACPS and aerodynamic surface control are to be satisfied by vertical flight tests. The basic concept will be the flying of conservative mission profiles such that exposure to space environment and entry conditions can be evaluated

incrementally. Although primary objectives of the vertical flight test program are evaluation and demonstration of vehicle capabilities, limited support of operational missions was established as an additional objective.

The Mark I orbital test missions are a series of flights to demonstrate orbiter system and subsystem operational capability and to validate the capability of the shuttle to conduct orbital operations. The initial flights will have the primary objective of demonstrating the operational capability of systems and subsystems. The later flights will validate the capability of the shuttle to conduct orbital operations.

The first six missions, which are primarily shuttle development flights, are designed to verify the crew and shuttle capability to operate in a space environment, to deploy and retrieve satellites, to support extra-vehicular activity, and to conduct rendezvous operations of varying complexity.

The next five missions are designed to develop and improve on-orbit satellite staging techniques to permit geosynchronous missions, to develop the shuttle sortie capability, and to verify the shuttle capability to accommodate non-astronaut passengers. The last mission, the first fully operational Mark I flight, is a mission to launch a cosmic ray module for use by the international scientific community.

The Mark II orbital test missions are a series of four flights to demonstrate orbiter system and revised TPS and MPS subsystem operational capability. Vehicle capabilities not fully validated by Mark I flights, such as maximum cross range, will be demonstrated. These flights, while primarily for achievement of test objectives, will be joint test-operational missions as in the Mark I program.

The vertical-flight-test program provides, in addition to flight test, the refinement and demonstration of the facilities and ground systems at the launch site to support the operational program. The ground tests consist of (1) flight readiness firing of the orbiter MPS, (2) interface compatibility checks of the orbiter and mated orbiter/booster with launch site facilities and support equipment, (3) orbiter prelaunch checkout, and (4) orbiter ground turnaround operations.

The ground tests and operations during the orbiter vertical flight test program will consist of the operational turnaround activities augmented by specific activities peculiar to the test program. These test activities will be incrementally phased out as the test program progresses. Cluster static firing of Orbiter No. 2 at the operational site is planned as a flight-readiness

demonstration of the main propulsion subsystem. This static firing is not unique to the flight test vehicle performing the first manned orbital launch, but is scheduled to be conducted prior to first flight on each orbiter.

Interface checks with the support equipment and facility at each launch site checkout area will be required for the orbiter. These areas include maintenance and repair, launch pad used for static firing, mated vehicle launch complex, and post-mission safing area. At each checkout area, the support equipment/facility interfaces will be checked and the support equipment functionally verified before connecting with the vehicle for interface checks. These checks will be repeated as each new orbiter is cycled through the checkout areas for the first time. Subsequent cycles of the same vehicle will require only a support equipment hookup verification check.

A schedule presenting the overall activities associated with the vertical test program is presented as Figure 4-422.

4.4.7.2 Booster

Two booster configurations are being considered as part of the Phase B' studies. The first is a LO_2/RP reusable flyback booster of a Mark I/II configuration using existing F-1 engines; the second is a pressure-fed, recoverable booster. The recoverable booster does not have flyback capability.

Horizontal Flight Test. The flight test program objectives and requirements for the LO_2/RP reusable booster are essentially the same as for the B9U booster, which is the Phase B baseline. One of the facts brought forth during the Phase B' study is that the orbiter configuration has no impact on the booster horizontal flight test program. Other factors that were identified as different from Phase B were a reduction in the number of air-breathing engines, which could permit a slight decrease in the program; avionics complexity reduction, which would have essentially no effect on the overall program; and other system changes in the proposed vehicle, which would cause negligible change to the proposed Phase B flight test program.

The Phase B' test program is based on a success-oriented concept in that minimum development testing will be required; the primary task will be to evaluate and/or demonstrate vehicle capability to satisfy mission requirements in the subsonic flight regime.

Vehicles Nos. 1 and 2 will have similar development flight instrumentation systems. The system will consist of S-band telemetry, onboard magnetic tape recording for analog and PCM, video camera transmitting

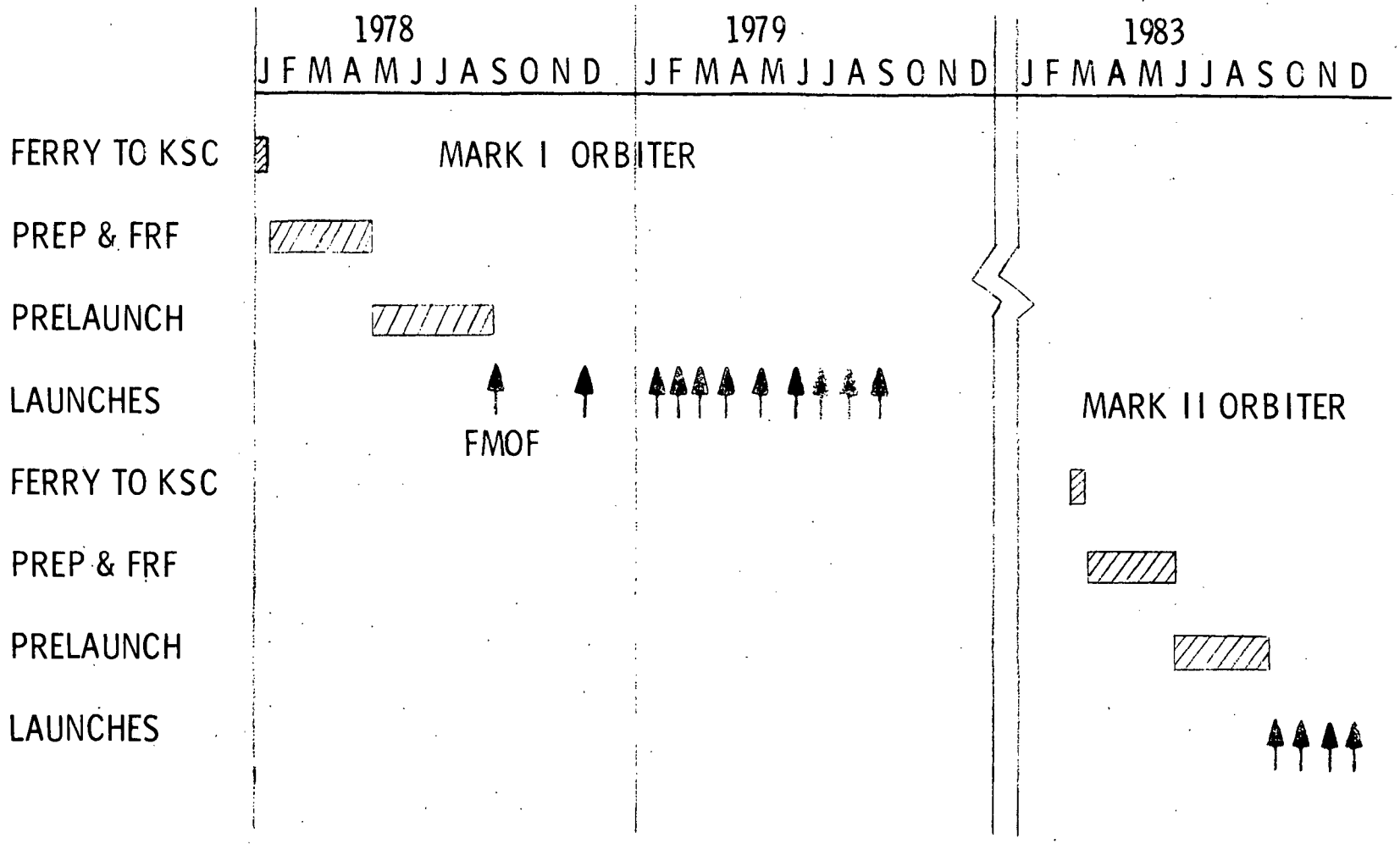

Figure 4-422. Orbiter Vertical Flight Test Program Schedule

system, and onboard photo cameras. Inaccessible sensors will be redundant for reliability and the overall system will be designed to allow integration of all test data requirements at any time on a flight.

The ground test program proposed for the vehicles prior to first flight is identified in Table 4-83.

The flight test program is broken into four main areas of interest with the percent of total flying hours allocated to each shown in Table 4-84. More emphasis is placed on overall vehicle performance and stability than subsystem performance in Phase B' as compared to the Phase B flying time allocation. Table 4-85 presents the schedules for Boosters Nos. 1 and 2 from delivery to completion of horizontal flight testing.

No differences have been identified in support or facilities requirements from the Phase B study effort.

Vertical Flight Test Program. Vertical flight test programs for both the LO_2/RP reusable booster and the pressure-fed expendable Mark I booster were prepared and are summarized below.

The vertical flight test program for the LO_2/RP reusable booster (Mark I and II) has as its objectives man-rating the booster and demonstrating that it will satisfy mission requirements. This program is felt necessary although contrary to the present traffic model, which indicates operational capability at FMOF.

The requirements that must be satisfied prior to vertical flight are completion of ground-testing of the vehicle and major subsystems, completion of wind tunnel and scale model testing, certification of airborne and ground hardware, and demonstration of flyback and landing capability.

The plan is to use one test vehicle for five launches to demonstrate the booster. All launches will be manned and mated with a manned orbiter. The initial launch trajectories will be conservative and favorable to booster and orbiter missions. The crew would have escape provisions in the booster and the vehicle would have a complete development flight instrumentation system. The schedule for such a program is presented as Figure 4-423 with additional details for turnaround operations between flights presented as Figure 4-424.

The differences between Mark I and II boosters is minimal; no additional vertical test flights are proposed for the Mark II configuration.

Table 4-83. LO_2/RP-1 Ground Test Program
(Vehicle Level)

Site	Test	Special Facilities
Michoud	Integrated system checkout Weight and balance EMI/EMC	Scales
KSC	JP fuel system Jet engine runs Systems operation with airplane power Ground vibration survey (horizontal) EMI/EMC Aerial refueling system APU Taxi	Soft ground suspension system Ramp to obtain correct tanker-receiver position Scales

Table 4-84. LO_2/RP-1 Flight Test Program

Test	Vehicle	Percent of Total Flight Hours
S & C	#1	30
Perf	#1 #2	35
Prop	#1	25
Mech. subsystem Navigation Electrical subsystem Hydraulic Avionics Structures	#1 #2	10
Total flight hours -- 180 hours #1 ≈ 160 Hrs #2 ≈ 20 Hrs		Total flight months -- 25 months #1 ≈ 22.2 months #2 ≈ 2.8 months

Table 4-85. Horizontal Flight Test Program LO_2/RP Flyback Booster

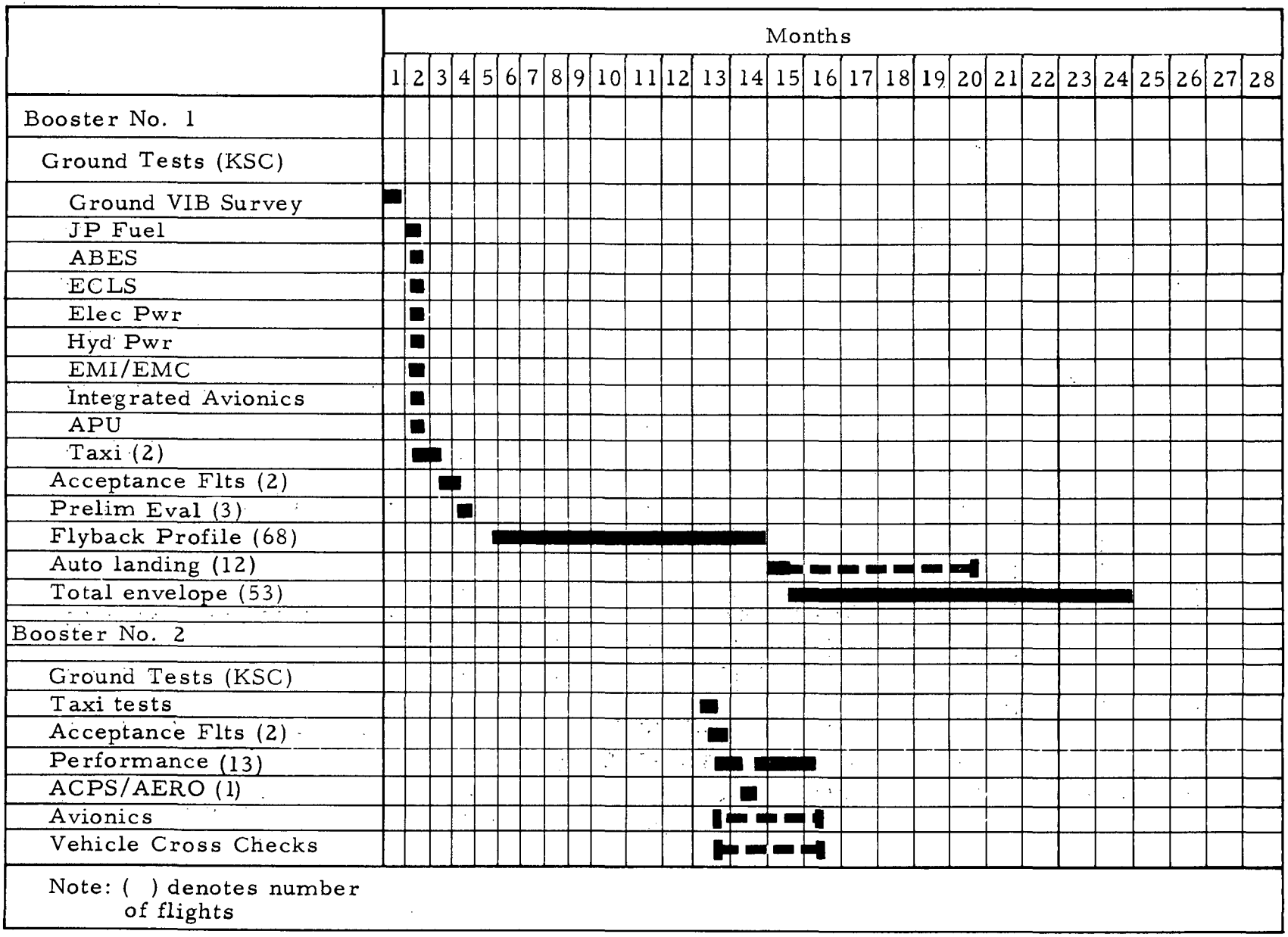

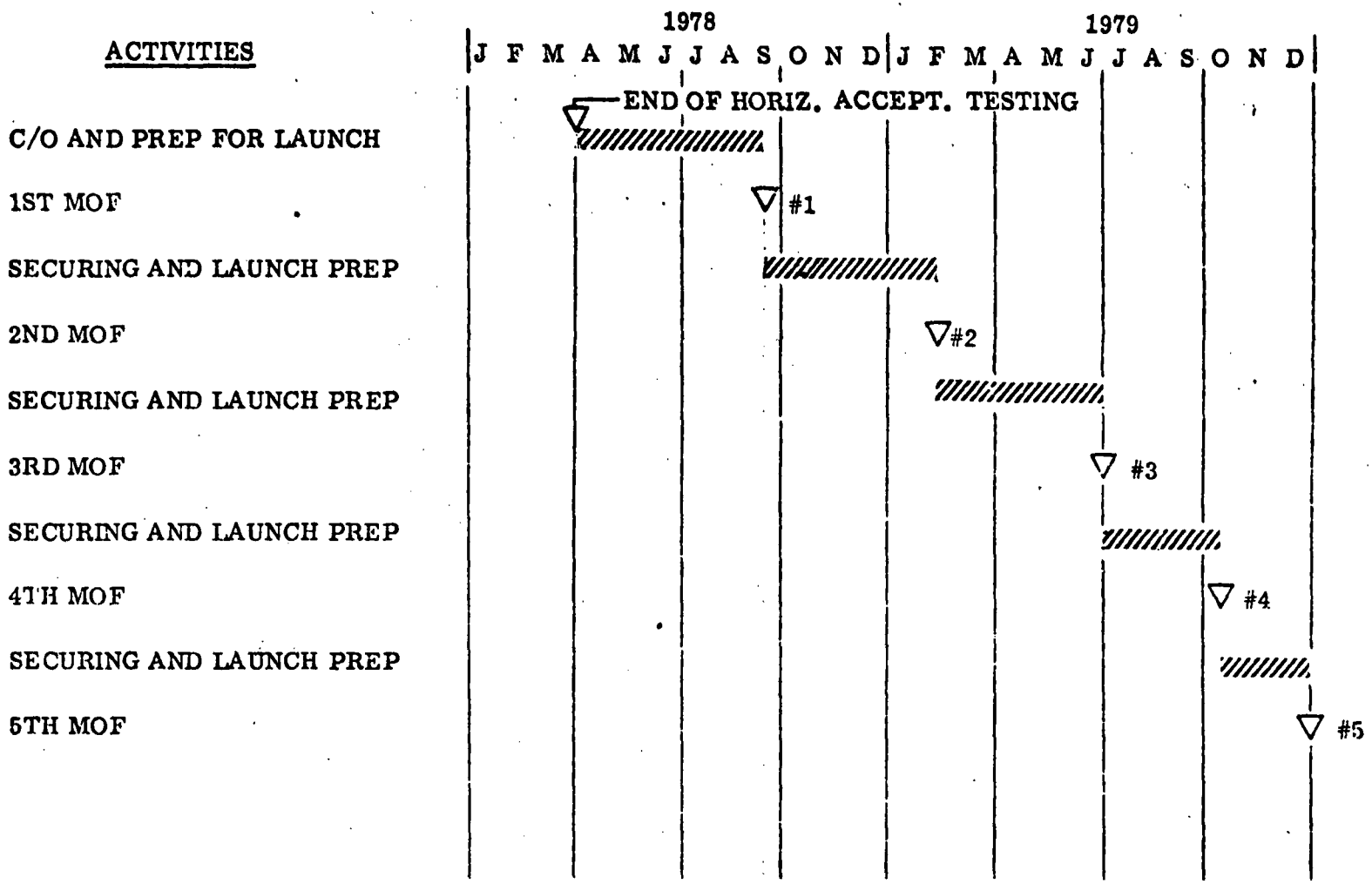

Figure 4-423. Vertical Flight Test Program Schedule

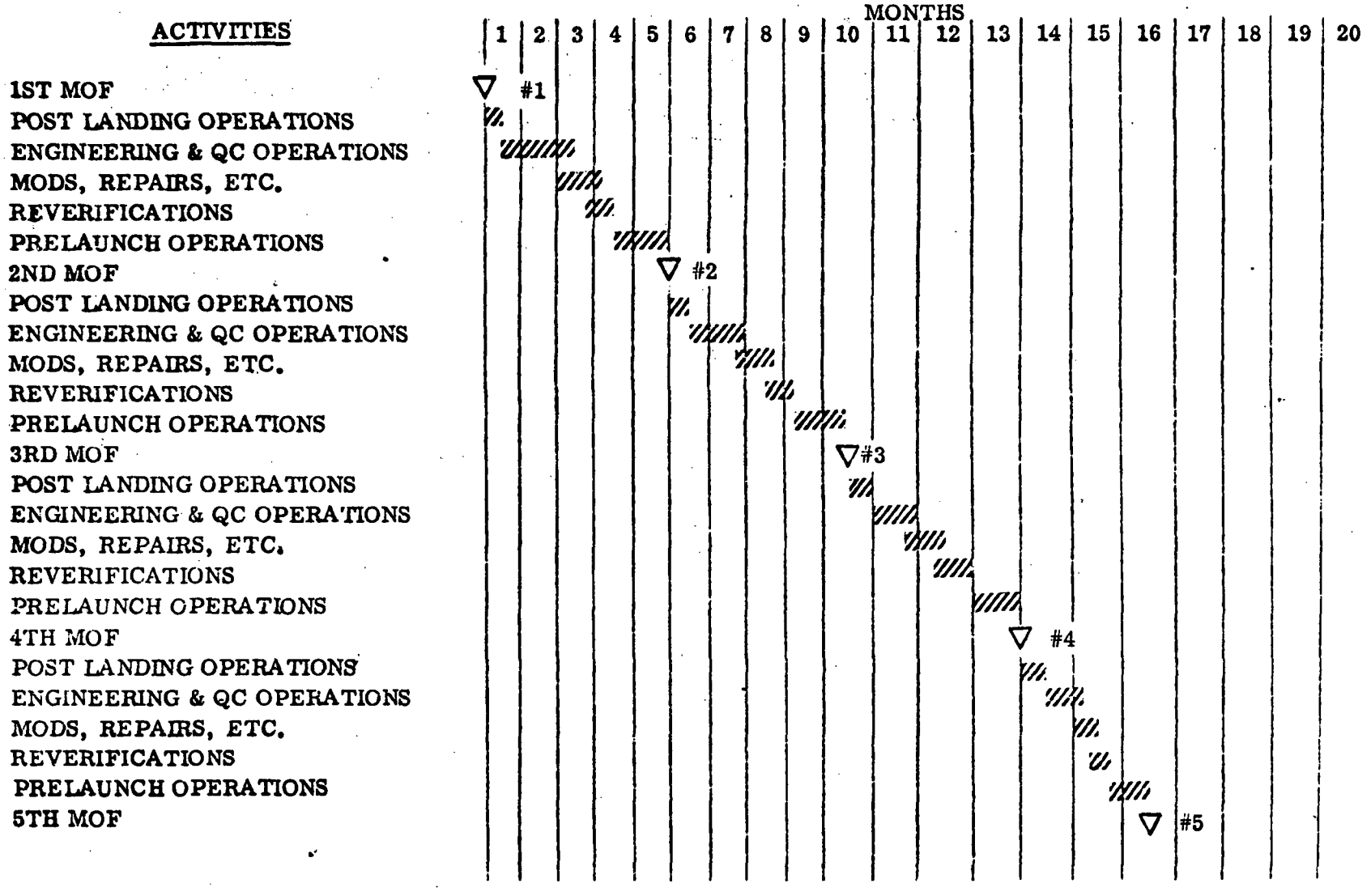

Figure 4-424. Turnaround Operations Schedule

The LO_2/RP vehicle would use the same facilities as identified for the B9U booster except that LH_2 would not be required at the launch complex; RP fuel would be. An RP storage and transfer system presently exists at the launch complexes.

The objectives of the pressure-fed expendable Mark I booster test program, assuming a pressure-fed expendable booster is used, will be to man-rate the boosters and demonstrate it will satisfy mission requirements.

Completion of ground testing, wind tunnel and scale model testing, and certification of airborne and ground equipment will be required prior to first vertical flight.

The first vertical test flight will be with a simulated orbiter. Provisions will be made for a second launch of the same basic configuration, if the first is not successful. If the first launch is successful, the second, and subsequent, launches will be with manned orbiters. Five of the 15 Mark I launches will be used to evaluate the recovery system performance. No Mark I to Mark II deltas are identified; no additional testing is planned.

No additional launch facilities would be required for the pressure-fed booster; however, a recovery system that would include a naval vessel for retrieval and a dock-side transfer system to get the booster on a barge for movement to the VAB dock would be required.

4.4.8 Operations

4.4.8.1 ABES Propulsion

The following represents delta operational requirements to the Phase B baseline.

The ABES will be a B-1 bomber version engine capable of installation and removal as a package. The package includes:

1. Two engines
2. Truss structure
3. Fuel tank and distribution system

The ABES will be installed only for some missions. Based upon the requirement to periodically remove and install the ABES, the ground turnaround work effort will be increased to accommodate the following ABES peculiar tasks.

1. Removal: 16 hours
2. Installation: 16 hours
3. Post-installation checkout: 4 hours
4. Door(s) removal/installation: 4 hours

The work activity associated with the above operations will be imposed on the vehicle post-flight maintenance period. Current planning permits 55 hours to be available for the total maintenance period. The first 22 hours of this period represent the planned maintenance period; the remaining time is available for unscheduled maintenance activities. The ABES removal operations represents a potential impact since ABES removal would represent a serial operation to payload removal.

4.4.8.2 RCS/OMS Propulsion

The OMS/RCS subsystems has been redesigned from an LO_2/LH_2 system in Phase B to a storable propellant system. The reaction control subsystem employs 32 $N_2O_4/A50$ thrusters located in three pods; each pod is self-contained and includes a pressurizing system, propellant tanks, controls, and thrusters. Two pods are wing-mounted and contain 13 thrusters

each. The third pod is mounted on the vertical stabilizer and contains six thrusters.

The orbital maneuvering subsystem employs two lunar ascent engines, which produce 3500 pounds of vacuum thrust each. Each engine system is packaged in a pod arrangement with each pod containing a pressurization system, propellant tanks, propellant distribution lines, controls, and engine.

The following represents Phase B' RCS/OMS delta operational requirements for the pod concept OMS/RCS subsystems.

The RCS pods will be preserviced with propellant at a hypergolic facility, transported to the VAB, and installed on the orbiter immediately subsequent to orbiter premate checkout. Deservicing of the RCS pods will be conducted postflight in the safing area and the RCS pods will be removed in the hangar. The orbiter will be in the horizontal attitude for pod installation or removal.

The OMS pods will also be delivered preserviced and will be installed immediately subsequent to orbiter premate checkout. OMS pod deservicing will be conducted postflight in the safing area with pod removal conducted in the maintenance hangar. The orbiter will be in the horizontal attitude for installation or removal.

The ground turnaround operations will incur the following additional work effort:

Postflight pod deservicing: 4 hours (RCS/OMS)

Postflight pod removal: 7 hours (all pods)

Pod installation: 5 hours

Post-installation checkout: 2 hours

A hypergolic servicing and decontamination process analysis was conducted during Phase B' to develop a concept for orbiter hypergolic servicing, decontamination, and safing. The evaluation included a survey of existing sytems utilized on Apollo, Titan IIIC, Agena, and Delta vehicles. The primary conclusions and recommendations are:

1. Any propellant servicing, offloading, and decontamination equipment should be remotely controllable, ideally with a flexible software system, to enable routines to be generated for all equipment control loops as well as sequential automation.

2. Orbiter hypergolic systems with onboard quantity measurement systems should utilize the measurement system for primary load determinations during servicing (OMS).

3. The primary RCS hypergolic load measurement technique employed during servicing as well as load verification following servicing should utilize a pressure/volume relationship technique, which involves determining tank ullage volumn via expanding for compressing) a known gas volume and pressure into a new volumn, containing the ullage volume, at a final, measurable pressure.

4. Hypergolic bulk storage, pumping, thermal conditioning, and toxic vapor venting facilities must be sufficiently remote from the pad and safing areas to enable maintenance/repair without impact on the work effort.

5. The propellant decontamination process should employ a portable vapor phase solvent cleaning unit and a fixed bulk propellant disposal area.

6. The helium servicing sytem should utilize a liquid nitrogen chiller heat exchanger. A technique to prechill the helium distribution system to the orbiter with no helium waste should be incorporated.

4.4.8.3 Mate/Erect and Transport

The Phase B' study effort has produced four new mate-and-erect concepts which are delta to the baseline. Concept A, horizontal belly tank mate - High Bay 4, is the prime candidate (see Figure 4-425). The new space shuttle configuration will require three mating operations as opposed to one for the baseline configuration. In Concept A, the orbiter cargo will be loaded prior to premate checkout. Subsequent to premate checkout, the hypergolic APS will be installed, the TPS closed out, and the orbiter will be transferred to High Bay 4. The external tank assembly will parallel the orbiter flow. The external tank assembly and verification will require 42 hours. The external tank will be transferred to High Bay 4 prior to orbiter arrival and prepared for mating operations.

The orbiter will then be hoisted by the overhead crane, lowered to the external tank mating surface, and structurally mated to the external tank. Electrical and mechanical systems will then be mated and verified.

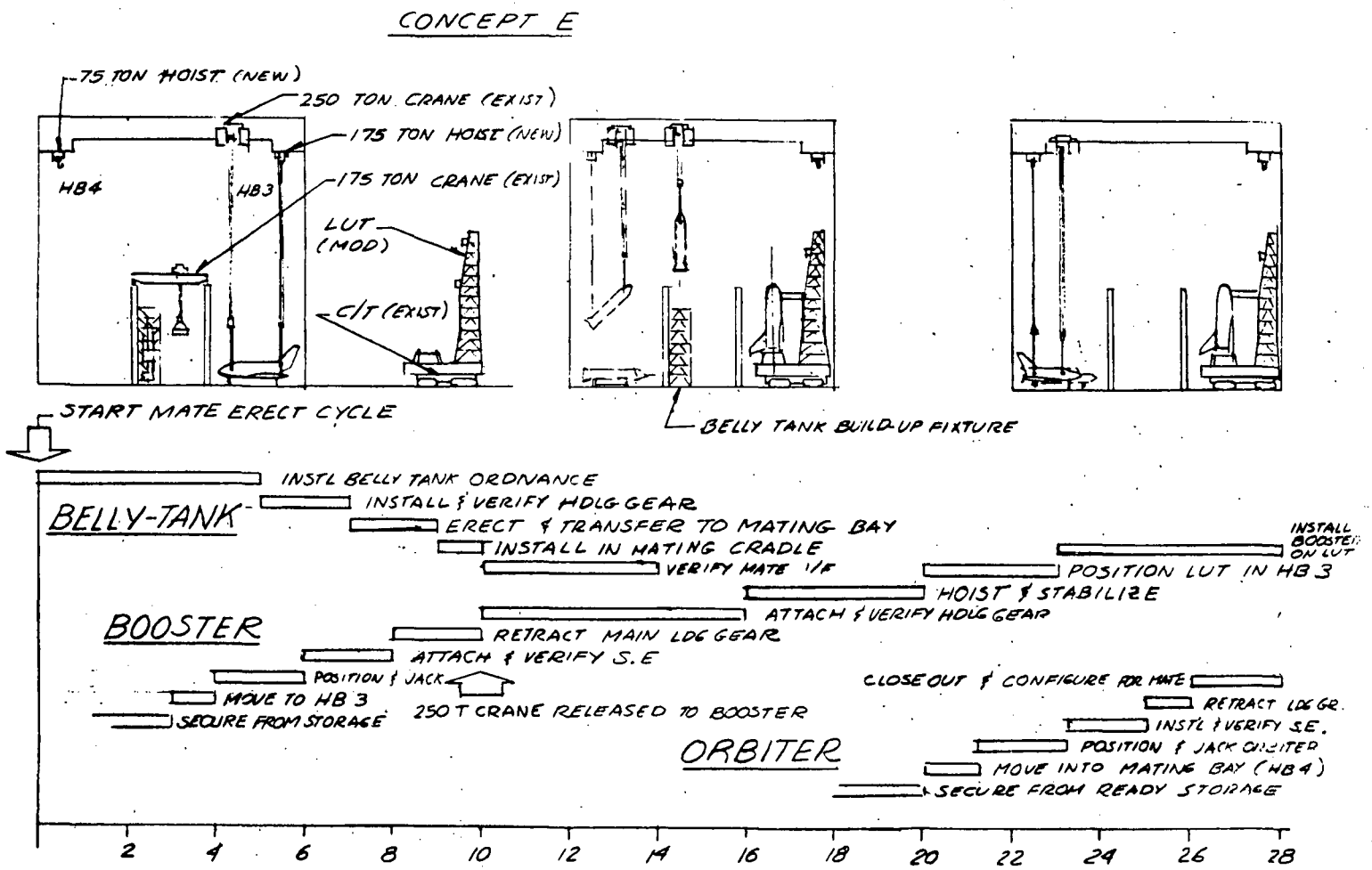

Figure 4-425. Mate-Erect Cycle, Horizontal Belly Tank Mate, High Bay 4
(Sheet 1 of 2)

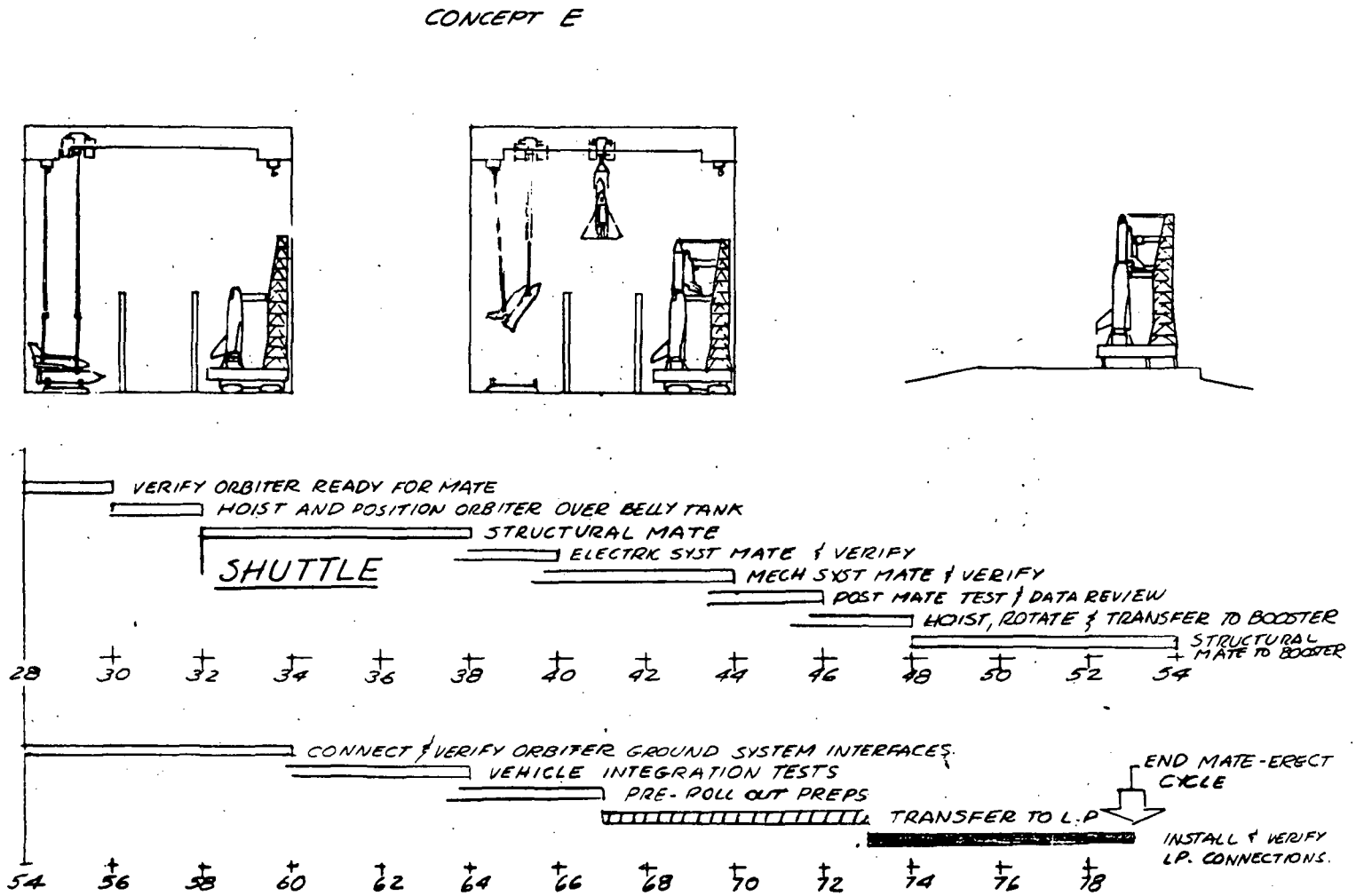

Figure 4-425. Mate-Erect Cycle, Horizontal Belly Tank Mate, High Bay 4
(Sheet 2 of 2)

Following orbiter/external tank verification testing, the orbiter and tank assembly will be mated to the booster. Subsequent to mating, an integrated orbiter/booster electrical and flight control verification test will be conducted including an umbilical ejection test. The space shuttle vehicle (SSV) will be readied for rollout to the pad subsequent to the completion of the postmating activities.

The SSV/launcher will be emplaced on the pad, interfaces will be connected, and the orbiter electromechanical/pneumatic test and launch readiness checkout tests conducted; JP and RP-1 will be loaded and the external hydrogen tank conditioned. Upon completion of the prelaunch servicing activities, the SSV is placed in a standby mode if immediate launch is not imminent. The SSV will be capable of "holding" in the standby mode for an indefinite period. Upon receipt of an "OK to proceed with launch," the cryogenic propellants will be loaded, the crew placed aboard, and prepared for launch.

Based upon the current Phase B' Mark I configuration definition for the orbiter, the activities and work effort required to be accomplished during the attainment of "standby" will increase 30 hours over the Phase B baseline.

4.4.8.4 Main Propulsion Subsystem

The main propulsion system has been redefined into two different generations of rocket engines for main propulsion. The Mark I orbiter will utilize the J2-S rocket engine system. The servicing, maintenance, and deservicing requirements of the J2-S will require more attention during ground turnaround operations than the Mark II HiPc space shuttle main rocket engine. The major delta operational requirements to the Phase B baseline for the J2-S are:

1. An electromechanical test must be conducted within 72 hours of launch.

2. The J2-S thrust chamber and LO_2 dome must be purged for 30 minutes prior to propellant loading.

3. The turbopump must be purged 15 minutes prior to propellant loading.

4. Propellants must be at the engine interface 60 minutes prior to engine start.

5. Solid propellant gas generators are required to start the engines. The estimated installation time for the gas generators is two hours.

6. A complete single engine changeout will be required after the sixth flight and the subsequent three flights to ensure replacement of the last engine of the cluster prior to expiration of its service life. Thereafter, engine changeout will be scheduled at interval of nine flights. The engine changeout cycle is based upon an engine life expectancy of 3000 seconds after delivery and an average of 330 seconds burn time per engine per mission. The estimated single engine removal and installation time is 22 hours. An option to cyclic engine changeout would be multiple or complete cluster changeout based upon engine life expectancy.

7. A gross leak check of the propulsion system will be required prior to mating and will require approximately 18 hours to complete.

4.4.8.5 Thermal Protection System

The Mark I orbiter thermal protection system has been redefined as an ablator-type installation. The orbiter will contain approximately 11,000 square feet of ablator installation, which must be removed and replaced after each mission. It is estimated that 12 shifts will be required for 100 percent ablator removal and 16 shifts for ablator installation.

4.4.8.6 Turnaround Timelines

Timelines were developed primarily for the Mark I orbiter during Phase B'. Table 4-86 illustrates the time flow comparison between the baseline 161C orbiter configuration and the Mark I orbiter configurations.

Figure 4-426 represents the Mark I external hydrogen tank/ablative TPS orbiter ground turnaround timeline. The booster timeline in Figure 4-427 represents the B18E General Dynamics booster flow. Table 4-87 illustrates a time flow comparison between the B9U baseline booster and the B18E Phase B' booster.

The assembly, checkout, mating timeline, and functional flow diagram for the orbiter external propellant tank is shown in Figures 4-428 and 4-429, respectively.

Table 4-86. Orbiter Time Flow Comparison
(161C vs. Mark I Orbiter)

Areas of Time Differences		Baseline 161C Orbiter	Mark I Orbiter	Delta Ground Operations Time
Postflight Checkout and Evaluation		None Scheduled	12	12
Turnaround Maintenance		60	198	138
External Tank Buildup and Checkout		None Required	56	56
Premate Preparations (Belly Tank/Orbiter)		None Required	31	31
Erect/Mate	Belly Tank/Orbiter	None Required	5	5
	Orbiter to Booster	3	8	5
Postmate Verification	Belly Tank/Orbiter	None Required	8	8
	Orbiter to Booster	7	91	84
Launch Readiness Test		2	4	2
Vehicle Servicing		11	40	29
Countdown Preparations		3	5	2
Countdown		2	4	2

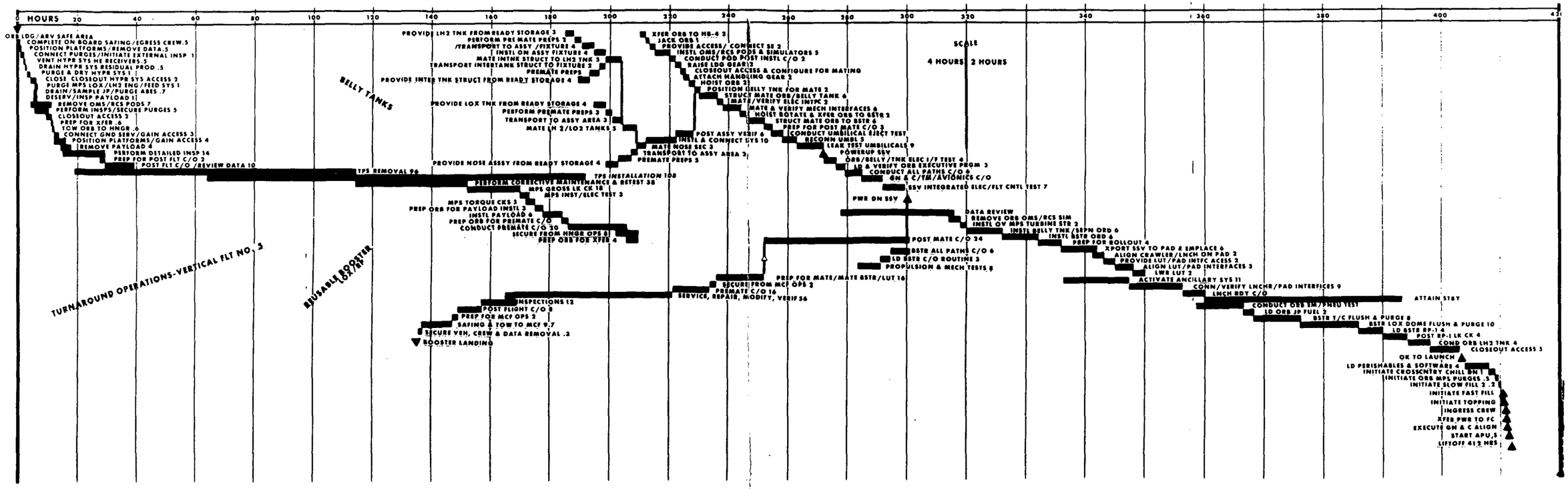

Figure 4-426. Mark I Orbiter/LO_2-RP Booster

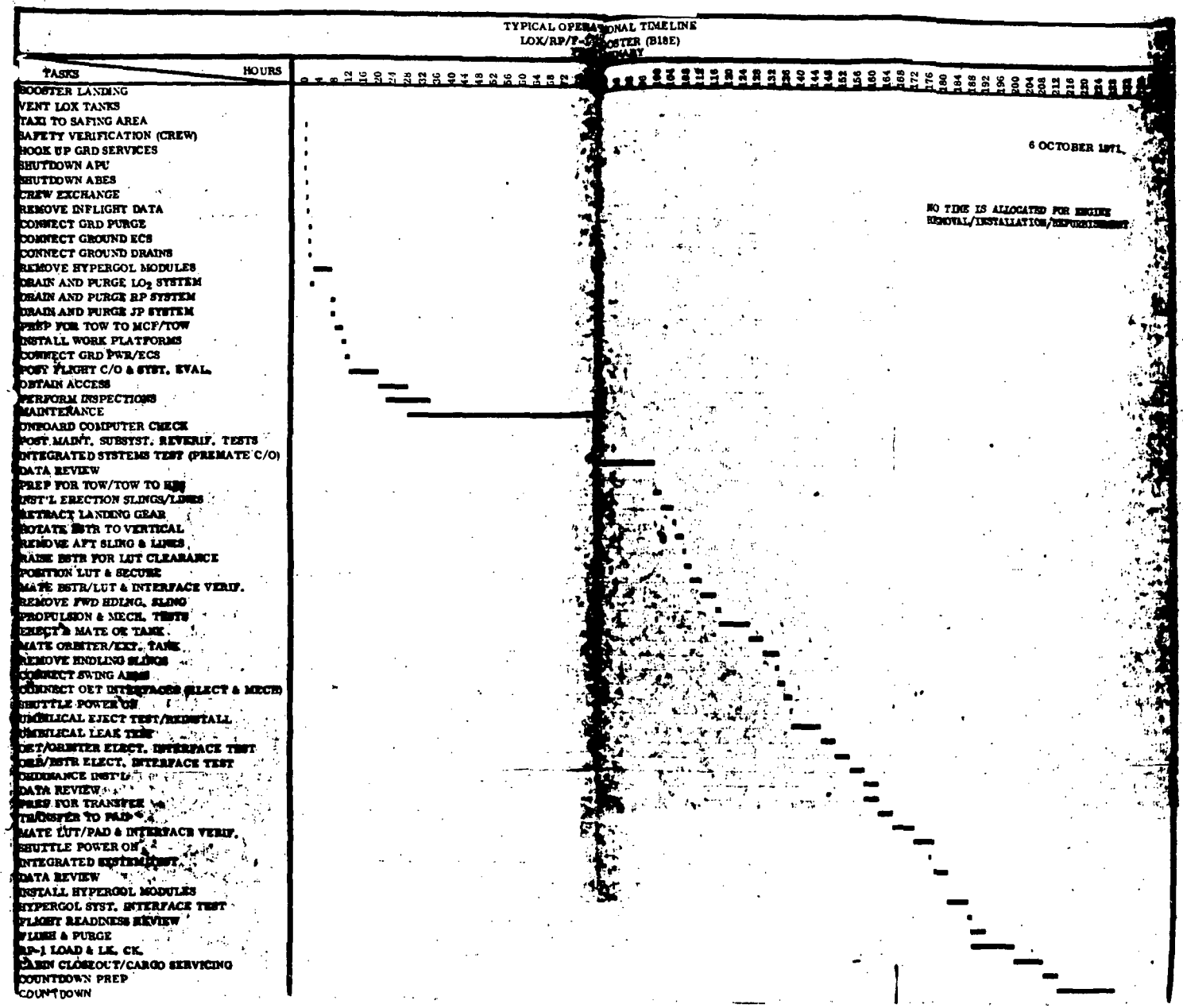

Figure 4-427. Typical Operational Timeline LO_2/RP/F-1 Booster (B18E) Preliminary

Table 4-87. Booster Time Flow Comparison (B9U vs. B18E)

Areas of Time Differences	Baseline B9U Booster (Hours)	Phase B' B18E Booster (Hours)	Delta Ground Operations Time
Postlanding and Safing	4	7	3
Postflight Checkout and Evaluation	None Scheduled	8	8
Turnaround Maintenance (F-1 Engines)	40	65	25
Premate Checkout	8	16	8
Propulsion and Mechanical Tests	None Scheduled	8	8
Postmate Checkout	None Scheduled	24	24
Launch Readiness Test	2	4	2
Vehicle Servicing	None Scheduled	30	30
Countdown Preparations	6	16	10
Countdown	2	4	2

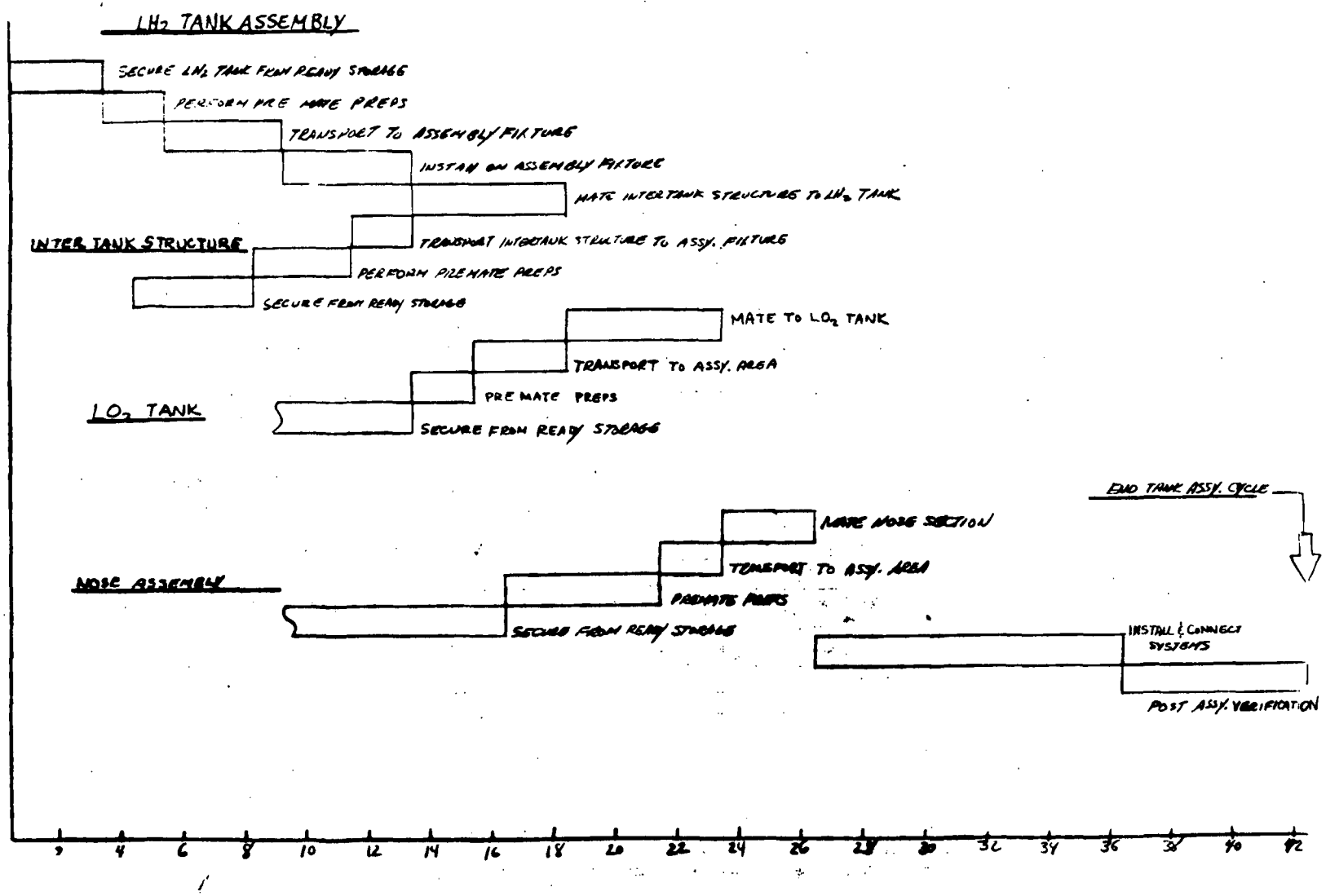

Figure 4-428. Belly Tank Assembly Timeline

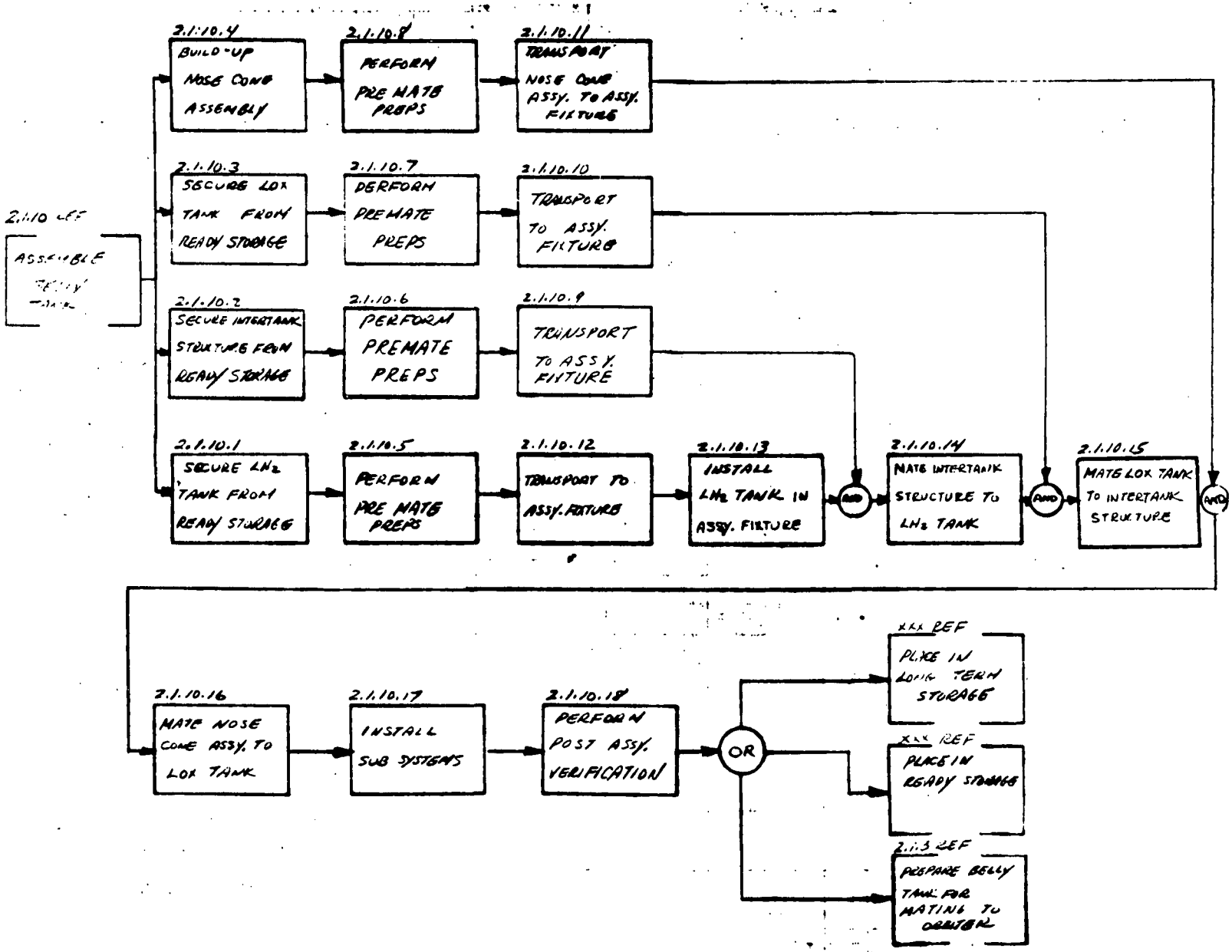

Figure 4-429. Assemble Belly Tank

The B18E booster will require approximately 120 additional hours of turnaround processing time when compared to the baseline. This delta effort is primarily attributed to F-1 engine processing, propellant loading ground equipment, avionics capability, and concept changes.

The Mark I orbiter will require approximately 374 additional hours of turnaround processing time when compared to the 161C orbiter. This delta effort is primarily attributed to external tank buildup, mate and checkout, more comprehensive post-mating booster and orbiter verifications, vehicle servicing (main propulsion engines); and design concept changes (i.e., disposable tank, hypergolic systems).

The timelines included do not allow for booster F-1 or orbiter J2-S engine removal installation, or refurbishment.

The combined B18E booster and Mark I orbiter ground turnaround operations flow is shown in Figure 4-426.